EPA/600/R-02/099
December 2002

Assessment and Recommendations for Improving the Performance of Waste Containment Systems

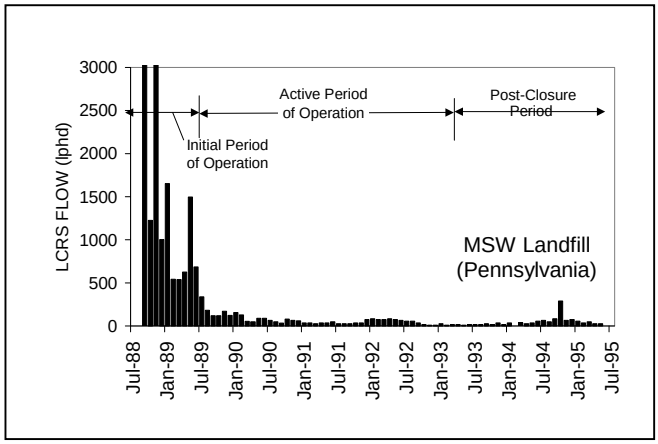

by

Rudolph Bonaparte, Ph.D., P.E.
GeoSyntec Consultants
Atlanta, GA 30342

David E. Daniel, Ph.D., P.E.
University of Illinois
Urbana, IL 61801

Robert M. Koerner, Ph.D., P.E.
Drexel University
Philadelphia, PA 19104

performed under

EPA Cooperative Agreement Number
CR-821448-01-0

Project Officer

Mr. David A. Carson
United States Environmental Protection Agency
Office of Research and Development
National Risk Management Research Laboratory
Cincinnati, OH 45268

DISCLAIMER

This publication was developed under Cooperative Agreement Number CR-821448-01-0 awarded by the United States Environmental Protection Agency (EPA). EPA made comments and suggestions on the document intended to improve the scientific analysis and technical accuracy of the document. However, the views expressed in this document are those of GeoSyntec Consultants, the University of Illinois, and Drexel University. EPA does not endorse any products or commercial services mentioned in this publication.

FOREWORD

The United States Environmental Protection Agency (EPA) is charged by Congress with protecting the Nation's land, air, and water resources. Under a mandate of national environmental laws, the Agency strives to formulate and implement actions leading to a compatible balance between human activities and the ability of natural systems to support and nurture life. To meet this mandate, EPA's research program is providing data and technical support for solving environmental problems today and building a science knowledge base necessary to manage our ecological resources wisely, understand how pollutants affect our health, and prevent or reduce environmental risks in the future.

The National Risk Management Research Laboratory is the Agency's center for investigation of technological and management approaches for preventing and reducing risks from pollution that threatens human health and the environment. The focus of the Laboratory's research program is on methods and their cost-effectiveness for prevention and control of pollution to air, land, water, and subsurface resources; protection of water quality in public water systems; remediation of contaminated sites, sediments and ground water; prevention and control of indoor air pollution; and restoration of ecosystems. NRMRL collaborates with both public and private sector partners to foster technologies that reduce the cost of compliance and to anticipate emerging problems. NRMRL's research provides solutions to environmental problems by: developing and promoting technologies that protect and improve the environment; advancing scientific and engineering information to support regulatory and policy decisions; and providing the technical support and information transfer to ensure implementation of environmental regulations and strategies at the national, state, and community levels.

This publication has been produced as part of the Laboratory's strategic long-term research plan. It is published and made available by EPA's Office of Research and Development to assist the user community and to link researchers with their clients.

E. Timothy Oppelt, Director
National Risk Management Research Laboratory

ABSTRACT

This broad-based study addressed three categories of issues related to the design, construction, and performance of waste containment systems used at landfills, surface impoundments, and waste piles, and in the remediation of contaminated sites. The categories of issues, the locations in this report where each category is addressed, and the principal investigator for the study of each category are as follows:

- geosynthetic tasks are described in Chapter 2 and Appendices A and B; the principal investigator for these tasks was Professor Robert M. Koerner, P.E.;
- natural soil tasks are described in Chapters 3 and 4 and Appendices C and D; the principal investigator for these tasks was Professor David E. Daniel, P.E.; and
- field performance tasks are described in Chapter 5 and Appendices E and F; the principal investigator for these tasks was Dr. Rudolph Bonaparte, P.E.

Each portion of the report was authored by the identified principal investigator, and individuals working with the principal investigator. However, each principal investigator provided input and recommendations to the entire study and peer-reviewed and contributed to the entire report.

Geosynthetic materials (e.g., geomembranes (GMs), geotextiles (GTs), geonets (GNs), and plastic pipe) have been used as essential components of waste containment systems since at least the early 1980's. Five separate laboratory and/or analytical tasks were undertaken to address technical issues related to the use of these materials in waste containment systems. The technical issues related to geosynthetics are: (1) protection of GMs from puncture using needlepunched nonwoven GTs; (2) behavior of waves in high density polyethylene (HDPE) GMs when subjected to overburden stress; (3) plastic pipe stress-deformation behavior under high overburden stress; and (4) service life prediction of GTs and GMs. Conclusions are: (1) needlepunched nonwoven GTs can provide adequate protection of GMs against puncture by adjacent granular soils; a design methodology for GM puncture protection was developed from the results of laboratory tests and is presented; (2) temperature-induced waves (wrinkles) in GMs do not disappear when the GM is subjected to overburden stress (i.e., when the GM is covered with soil), rather the wave height decreases somewhat, the width of the wave decreases even more, and the void space beneath the wave becomes smaller; (3) waves may induce significant residual stresses in GMs, which may reduce the GM's service life; residual stresses induced in HDPE GMs by waves may be on the order of 1 to 22% of the GM's short-term yield strength; (4) if GM waves after backfilling are to be avoided, light-colored GMs can be used, GMs can be deployed and seamed without intentional slack, GMs can be covered with an overlying light colored temporary GT until backfilling occurs, and backfilling can be performed only in the coolest part of the day or even at night; (5) based on finite element modeling results, use of the Iowa State

formula for predicting plastic pipe deflection under high overburden stress is reasonable; (6) polypropylene GTs are slightly more susceptible to ultraviolet (UV) light degradation than polyester GTs, and lighter weight GTs degrade faster than heavier GTs; (7) GTs that are partially degraded by UV light do not continue to degrade when covered with soil, i.e., the degradation process is not auto-catalytic; (8) buried HDPE GMs have an estimated service life that is measured in terms of at least hundreds of years; the three stages of degradation and approximate associated durations for each as obtained from the laboratory testing program described in this report are: (i) antioxidant depletion (≈ 200 years), (ii) induction (≈ 20 years), and (iii) half-life (50% degradation) of an engineering property (≈ 750 years); these durations were obtained from the extrapolation of a number of laboratory tests performed under a limited range of conditions; it is recommended that additional testing be performed under a broader range of conditions to develop additional insight into the ultimate service life of HDPE GMs, and other types of GMs as well.

Geosynthetic clay liners (GCLs) are a relatively new type of liner material, having first been used in a landfill in 1986. One of the key issues with respect to field performance of GCLs is their stability on permanent slopes, such as found on landfill final cover systems. Fourteen test plots, designed to replicate typical final cover systems for solid waste landfills, were constructed to evaluate the internal and interface shear strength of GCLs under full-scale field conditions on 2H:1V and 3H:1V slopes. Five different types of GCLs were evaluated, and performance was observed for over four years. All test plots were initially stable, but over time, as the bentonite in the GCLs became hydrated, three slides (all on 2H:1V slopes) that involved the GCLs have occurred. One slide involved an unreinforced GCL in which bentonite that was encased between two GMs unexpectedly became hydrated. The other two slides occurred at the interface between the woven GTs of the GCLs and the overlying textured HDPE GM. Conclusions are: (1) at the low normal stresses associated with landfill final cover systems, the interface shear strength is generally lower than the internal shear strength of internally-reinforced GCLs; (2) interfaces between a woven GT component of the GCL and the adjacent material should always be evaluated for stability; these interfaces may often be critical; (3) significantly higher interface shear strengths were observed when the GT component of a GCL in contact with a textured HDPE GM was a nonwoven GT, rather than a woven GT; (4) if bentonite sandwiched between two GMs has access to water (e.g., via penetrations or at exposed edges), water may spread laterally through waves or wrinkles in the GM and hydrate the bentonite over a large area; (5) if the bentonite sandwiched between two GMs does not have access to water, it was found that the bentonite did not hydrate over a large area; (6) current engineering procedures for evaluating the stability of GCLs on slopes (based on laboratory direct shear tests and limit-equilibrium methods of slope stability analysis) correctly predicted which test plots would remain stable and which would undergo sliding, thus validating current design practices; and (7) based on the experiences of this study, landfill final cover systems with 2H:1V sideslopes may be too steep to be stable with the desired factor of safety

due to limitations with respect to the interface shear strengths of the currently available geosynthetic products.

To evaluate the field performance of compacted clay liners (CCLs), a database of 89 large-scale field hydraulic conductivity tests was assembled and analyzed. A separate database for 12 soil-bentonite admixed CCLs was also assembled and analyzed. In addition, case histories on the field performance of CCLs in final cover test sections were collected and evaluated. Conclusions are: (1) 25% of the 89 natural soil CCLs failed to achieve the desired large-scale hydraulic conductivity of 1×10^{-7} cm/s or less; (2) all of the 12 soil-bentonite admixed CCLs achieved a large-scale hydraulic conductivity of less than 1×10^{-7} cm/s; however, all of these CCLs contained a relatively large amount (more than 6%) of bentonite; soil-bentonite admixed CCLs will not be discussed further; (3) the single most common problem in achieving the desired low level of hydraulic conductivity in CCLs was failure to compact the soil in the zone of moisture and dry density that will yield low hydraulic conductivity; (4) the most significant control parameter of CCLs was found to be a parameter denoted "P_o", which represents the percentage of field-measured water content-density points that lie on or above the line of optimums; when P_o was high (80% to 100%) nearly all the CCLs achieved the desired field hydraulic conductivity, but when P_o was low (0 to 40%), fewer than half the CCLs achieved the desired field hydraulic conductivity; (5) practically no correlation was found between field hydraulic conductivity and frequently measured soil characterization parameters, such as plasticity index and percentage of clay, indicating that CCLs can be successfully constructed with a relatively broad range of soil materials; (6) hydraulic conductivity decreased with increasing CCL thickness, up to a thickness of about 1 m; and (7) analysis of CCLs constructed in the final cover test sections generally showed that CCLs placed without a GM overlain by soil tended to desiccate and lose their low hydraulic conductivity within a few years.

Liquids management data were evaluated for 187 double-lined cells at 54 landfills to better understand the field performance of landfill primary liners, leachate generation rates, and leachate chemistry. Conclusions are: (1) average monthly active-period leak detection system (LDS) flow rates for cells with HDPE GM primary liners constructed with construction quality assurance (CQA) (but without ponding tests or electrical leak location surveys) will often be less than 50 lphd, but occasionally in excess of 200 lphd; these flows are attributable primarily to liner leakage and, for cells with sand LDSs, possibly construction water; (2) average monthly active-period LDS flow rates attributable to leakage through GM/GCL primary liners constructed with CQA will often be less than 2 lphd, but occasionally in excess of 10 lphd; (3) available data suggest that average monthly active-period LDS flow rates attributable to leakage through GM/CCL and GM/GCL/CCL primary liners constructed with CQA are probably similar to those for GM/GCL primary liners constructed with CQA; (4) GM liners can achieve true hydraulic efficiencies in the 90 to 99% range, with higher efficiencies occasionally being achievable; (5) GM/GCL, GM/CCL, and GM/GCL/CCL composite liners can achieve

true hydraulic efficiencies of 99% to more than 99.9%; (6) GMs should not be used alone in applications where a hydraulic efficiency above 90% must be reliably achieved, even if a thorough CQA program is employed, except perhaps in situations where electrical leak location surveys or ponding tests are used to identify GM defects and the defects are repaired; (7) GM/CCL and GM/GCL/CCL composite liners are capable of substantially preventing leachate migration over the entire period of significant leachate generation for typical landfill operations scenarios without leachate recirculation or disposal or liquid wastes of sludges; (8) leachate collection and removal system (LCRS) flow rates were highest at the beginning of cell operations and decreased as waste thickness increased and daily and intermediate covers were applied to the waste; leachate generation rates decreased on average by a factor of four within one year after closure and by one order of magnitude two to four years after closure; within nine years of closure, leachate generation rates were negligible for the landfill cells evaluated in this study; (9) municipal solid waste (MSW) cells produced, on average, less leachate than industrial solid waste (ISW) and hazardous waste (HW) cells; for cells of a given waste type, rainfall fractions were highest in the northeast and lowest in the west; the differences in leachate generation rates are a function of type of waste, geographic location, and operational practices; (10) in general, HW landfills produced the strongest leachates and coal ash landfills produced the weakest leachates; MSW ash leachate was more mineralized than MSW leachate and the other ISW leachates; (11) the solid waste regulations of the 1980s and 1990s have resulted in the improved quality of MSW and HW landfill leachates; and (12) the EPA Hydrologic Evaluation of Landfill Performance (HELP) computer model, when applied using an appropriate simulation methodology and an appropriate level of conservatism, provides a reasonable basis for designing LCRSs and sizing leachate management system components; due to the complexity and variability of landfill systems, however, the model will generally not be adequate for use in a predictive or simulation mode, unless calibration is performed using site-specific measured (not default) material properties and actual leachate generation data.

Waste containment system problems were identified at 74 modern landfill and surface impoundment facilities located throughout the U.S. The purpose of this aspect of the project was to better understand the identified problems and to develop recommendations to reduce the future occurrence of problems. Conclusions are: (1) the number of facilities with identified problems is relatively small in comparison to the total number of modern facilities nationwide; however, the search for problems was by no means exhaustive; (2) the investigation focused on landfill facilities: 94% of the identified problems described herein occurred at landfills; (3) among the landfill problems, 70% were liner system related and 30% were cover system related; however, the ratio of liner system problems to cover system problems is probably exaggerated by the fact that a number of the facilities surveyed were active and did not have a cover system; (4) based on a waste containment system component or attribute criterion, the identified problems can be grouped into the following general categories: (i) slope

instability of liner systems or cover systems or excessive deformation of these systems (44%); (ii) defectively constructed liners, leachate collection and removal systems (LCRSs) or LDSs, or cover systems (29%); (iii) degraded liners, LCRSs or LDSs, or cover systems (18%); and (iv) malfunction of LCRSs or LDSs or operational problems with these systems (9%); (5) considering a principal human factor contributing to the problem criterion, the identified problems are classified as follows: (i) design (48%); (ii) construction (38%); and (iii) operation (14%); (6) the main impacts of the problems were: (i) interruption of facility construction and operation; (ii) increased maintenance; and (iii) increased costs; (7) problems detected at facilities were typically remedied before adverse environmental impacts occurred; (8) impact to groundwater or surface water was only identified at one facility, where landfill gas migrated beyond the edge of the liner system and to groundwater; (9) all of the identified problems can be prevented using available design approaches, construction materials and procedures, and operation practices; (10) although the environmental impact of problems has generally been negligible thus far, the landfill industry should do more to avoid future problems in order to: (i) reduce the potential risk of future environmental impact; (ii) reduce the potential health and safety risk to facility workers, visitors, and neighbors; (iii) increase public confidence in the performance of waste containment systems; (iv) decrease potential impacts to construction, operation, and maintenance; and (v) reduce costs associated with the investigation and repair of problems.

ACRONYMS AND ABBREVIATIONS

ALCD	Alternative Landfill Cover Demonstration
ALR	action leakage rate
AOS	apparent opening size (of geotextile)
ARAR	applicable or relevant and appropriate requirements
ASTM	American Society for Testing and Materials
AZ	acceptable zone
BAT	commercial term for a type of porous probe
BNA	base neutral extractable
BOD	biological oxygen demand
BTEX	benzene, toluene, ethylbenzene, and xylenes
BuRec	U.S. Bureau of Reclamation
C&DW	construction and demolition waste
CAT	Caterpillar construction equipment
CCL	compacted clay liner
CERCLA	Comprehensive Environmental Response, Compensation, and Liability Act (aka Superfund Act)
CFR	U.S. Code of Federal Regulations
CH	soil classification symbol for a high plasticity clay soil
CL	soil classification symbol for a low plasticity clay soil
COD	chemical oxygen demand
CQA	construction quality assurance
CQC	construction quality control
CSPE	chlorosulfonated polyethylene
DSC	differential scanning calorimeter
EPA	U.S. Environmental Protection Agency
EPDM	ethylene propylene diene monomer
ET	evapotranspiration
FDEP	Florida Department of Environmental Protection
FEM	finite element model
fPP	flexible polypropylene

FOS	filtration opening size (of geotextile)
FS	factor of safety
GC	geocomposite
GCL	geosynthetic clay liner
GDL	geocomposite drainage layer
GEC	geosynthetic erosion control (material)
GM	GM
GN	geonet
GT	geotextile
HDPE	high density polyethylene
HELP	Hydrologic Evaluation of Landfill Performance (computer program)
HLR	high level radioactive (waste)
HP-OIT	high-pressure oxidative induction time
HSWA	Hazardous and Solid Waste Amendments
H/W	height/width ratio (of GM waves)
HW	hazardous waste
ISW	industrial solid waste
k	hydraulic conductivity
k_{field}	hydraulic conductivity measured in the field
k_{lab}	hydraulic conductivity measured in the laboratory
LCRS	leachate collection and removal system
LDLPE	low density linear polyethylene
LDR	land disposal restrictions
LDS	leak detection system
LL	liquid limit
LLDPE	linear low density polyethylene
LLRM	low level radioactive mixed (waste)
LLR	low level radioactive (waste)
LMDPE	linear medium density polyethylene
lphd	liters/hectare/day (1.0 lphd = 9.35 gallon/acre/day (gpad))
LYS	lysimeter

MCL	maximum containment level
MF	modification factor
MP	modified Proctor (compaction test)
MSW	municipal solid waste
NCP	National Contingency Plan
NE	northeast
NW	nonwoven (geotextile)
OD	outside diameter
OH	original height (of GM waves)
OIT	oxidative induction time
OWC	optimum water content
PCB	polychlorinated biphenyl
PCDD	polychlorinated dibenzo-p-dioxins
PCDF	polychlorinated dibenzo-furans
PE	polyethylene
PET	polyester
PI	plasticity index
PP	polypropylene
PPL	priority pollutant list
PVC	polyvinyl chloride
QA	quality assurance
RC	relative compaction
RCRA	Resource Conservation and Recovery Act
RF	reduction factor
RP	reduced Proctor (compaction test)
SARA	Superfund Amendments and Reauthorization Act
SC	soil classification symbol for a sandy clay
SDR	standard dimension ratio (of pipe)
SDRI	sealed double ring infiltrometer
SE	southeast
SMCL	secondary maximum containment level

SP	standard Proctor (compaction test)
Std-OIT	standard oxidative induction time
SVOC	semivolatile organic compound
TCLP	toxicity characteristics leaching procedure
TDS	total dissolved solids
TOC	total organic carbon
TSB	two-stage borehole test
TSCA	Toxic Substances Control Act
TSDF	treatment, storage and disposal facility
TSS	total suspended solids
UMTRCA	Uranium Mill Tailings Radiation Control Act
UV	ultraviolet
VFPE	very flexible polyethylene (includes LLDPE, LDLPE and VLDPE)
VLDPE	very low density polyethylene
VOC	volatile organic compound
W	west

ACKNOWLEDGEMENTS

The authors express appreciation to the U.S. Environmental Protection Agency for the funding that enabled this project to be performed. In particular, the authors recognize Robert E. Landreth (retired) for initiating the project and David A. Carson for providing the continuity throughout the activity.

The project involved tasks divided into three broad categories: (i) geosynthetics; (ii) natural soils; and (iii) field performance. Professor Robert M. Koerner, P.E. was the principal investigator (PI) for the geosynthetics tasks. Professor David E. Daniel, P.E. was the PI for the natural soils tasks. Dr. Rudolph Bonaparte, P.E. was the PI for the field performance tasks. The PIs and the members of each PI's project team authored their respective sections of the report. However, each PI provided input to the entire study and each provided peer-review and contributions to the entire project.

With respect to the geosynthetics tasks, the financial contributions made by the Geosynthetic Research Institute (GRI) and its membership is recognized and appreciated. Several of the geosynthetic tasks described in this report are ongoing under the continuing financial support of the GRI. Y. (Grace) Hsuan, George R. Koerner, and Te-Yang Soong were involved in many of the individual geosynthetic tasks, including preparation of Appendices A and B. Marilyn Ashley typed Chapters 1 and 2, and Appendices A and B. She also capably assembled all of the information during the entire project. Her work is sincerely appreciated by the entire team of principal investigators.

With respect to the natural soils tasks, numerous organizations assisted with the construction of the geosynthetic clay liner (GCL) field test plots in Cincinnati. Supplemental financial support was provided by CETCO, Claymax Corp. (now CETCO), Gundle (now GSE) Lining Systems, and National Seal Co. (now Serrot International). Fluid Systems, Inc. (now Serrot International), provided the geonet/GT drainage geocomposites material, Akzo (now Colbond), Synthetic Industries, and Tensar provided erosion control materials. Waste Management of North America and the staff of the Elda Landfill in Cincinnati, Ohio provided space at the Elda Landfill for the test plots and provided personnel and equipment to assist with construction and maintenance. James Anderson, John Bowders, David Bower, Richard Carriker, Mark Cadwallader, Ted Dzierzbicki, Richard Erickson, John Fuller, George Koerner, Larry Lydick, Majdi Othman, Heather Scranton, John Stark, Fred Struve, and Robert Trauger made major contributions to the program.

A database on performance of CCLs was assembled from published literature and from unpublished data obtained from the files of Craig H. Benson and Gordon P. Boutwell. Stephen J. Trautwein provided information on where in-situ hydraulic conductivity tests had been performed in CCLs. John J. Bowders assisted with the development of the

database and analysis of data. Owen Michaelis also helped with assembling data and preliminary analysis of the database.

With respect to the field performance tasks, the task manager for Appendix E was Majdi A. Othman. The authors of Appendix E were Majdi Othman, Rudolph Bonaparte, Beth A. Gross, and Dave Warren, all of GeoSyntec Consultants. The authors would like to acknowledge the following landfill owners and operators and state regulatory agencies for providing the data and information presented in Appendix E on the performance of waste containment facilities: Broward County (FL) Office of Environmental Services; Browning-Ferris Industries; Camp Dresses & McKee, Inc.; Cape May County (NJ) Municipal Utilities Authority; Chemical Waste Management; Chester County (PA) Solid Waste Authority; Cumberland County (NJ) Improvement Authority; Indiana Department of Environmental Management; Laidlaw Waste Systems; Michigan Department of Natural Resources; New Jersey Department of Environmental Protection and Energy; New York State Department of Environmental Conservation; New York State Electric and Gas Corporation; Phillips Petroleum Company; Rollins Environmental Services, Inc; USA Waste Services, Inc.; Utah Department of Environmental Quality; Waste Management, Inc.; WM J. Huff Engineering; and others.

The task manager for Appendix F was Beth A. Gross. The authors of Appendix F are Beth A. Gross, J. P. Giroud, and Rudolph Bonaparte, all of GeoSyntec Consultants. The authors would like to acknowledge the following individuals and organizations for providing information on some of the waste containment system problems described herein: California Regional Water Quality Control Board (Greg Vaughn); Florida Department of Environmental Protection (Kathy Anderson, Robert Butera, Joe Lurix, Jack McMelty, Susan Pelz, Richard Tedder); New York State Department of Environmental Conservation (Papa Chan Daniel, Matthew Eapen, Robert Phaneuf, Thomas Reynolds, Melissa Treers); Ohio Environmental Protection Agency (Doug Evans, Chuck Hull, Virginia Wilson); Metropolitan Dade County Department of Solid Waste (Lee Casey); Yolo County, California (Ramin Yazdani); GeoSyntec Consultants (Jeff Dunn, Scott Luettich, Neven Matasovic, Bert Palmer, Jeffrey Palutis, Dennis Vander Linde); Geosynthetic Research Institute (George Koerner, Robert Koerner); Golder Construction Services, Inc. (Frank Adams); Hazen and Sawyer (John Bove); I-CORP International, Inc. (Ian Peggs); Strata Systems (John Paulson); and others.

CONTENTS

Chapter 6 Summary and Recommendations

Appendix A – Behavior of Waves in High Density Polyethylene Geomembranes

Appendix B – Antioxidant Depletion Time in High Density Polyethylene Geomembranes

Appendix E – Evaluation of Liquids Management Data for Double-Lined Landfills

Chapter 1
Introduction

The environmentally safe and secure containment of wastes in landfills, waste piles, and surface impoundments has been a major goal of the United States Environmental Protection Agency (EPA) since the Agency's founding in 1970. To bring about a systematic and effective approach to the design and installation of liner systems and final cover systems, as integral components of modern waste containment systems, the Agency has developed regulations, supporting guidance, and numerous reports on this subject. The agency has likewise known that proper facility operation and maintenance are as important as design and construction in achieving satisfactory long-term containment system performance. This research report provides the results of the evaluation of field performance data for existing waste containment systems across the U.S. Based on this evaluation, it is concluded that environmentally safe and effective containment of waste is attainable. This research report also presents the results of a number of technical tasks that have led to recommendations for further improving the performance of waste containment systems in comparison to the current state-of-practice.

This first chapter of this report presents an overview of the goals of waste containment, the regulatory framework for waste containment, and the various components that make up typical waste containment systems. The chapter concludes with a description of the specific performance-related issues and technical tasks addressed by the studies described in this research report.

1.1 Goals of Waste Containment

An EPA estimate of the amount of municipal solid waste (MSW) generated in the U.S. for select years between 1960 and 1999 is presented in Table 1-1. This table does not include construction and demolition waste (C&DW), incinerator ash, sludges, and nonhazardous industrial waste, all of which add to the quantities shown in the table.

It should be recognized that waste reduction and recycling programs are having a positive impact on reducing the quantities of waste generated and disposed, respectively. Nevertheless, disposal in landfills containing engineered waste containment systems continues to be the most widely used method in the U.S. for the disposal of MSW and many other types of waste.

The following classes of waste materials, listed in descending order of approximate degree of hazard, constitute the majority of solid waste material requiring management and/or disposal in the United States today:

- low-level radioactive waste;
- hazardous waste;

Table 1-1. Generation, Materials Recovery, Composting, Combustion, and Discard of MSW, 1960 to 1999 (In millions of tons and percent of total generation) (from *Municipal Solid Waste in the United States: 1999 Final Report*, downloaded from EPA website at http://www.epa.gov/epaoswer/non-hw/muncpl/pubs/mswfinal.pdf).

Criteria	1960	1970	1980	1990	1995	1999
			Millions of Tons[e]			
Generation	88.1	121.1	151.6	205.2	211.4	229.9
Recovery for recycling	5.6	8.0	14.5	29.0	45.3	50.8
Recovery for composting[a]	0.0	0.0	0.0	4.2	9.6	13.1
Total materials recovery	5.6	8.0	14.5	33.2	54.9	63.9
Discards after recovery[b]	82.5	113.0	137.1	172.0	156.5	166.0
Combustion[c]	27.0	25.1	13.7	31.9	35.5	34.0
Discards to landfill, other disposal[d]	55.5	87.9	123.4	140.1	120.9	131.9
			Percent of Total Generation[e]			
Generation	100.0%	100.0%	100.0%	100.0%	100.0%	100.0%
Recovery for recycling	6.4%	6.6%	7.1%	7.7%	9.6%	9.9%
Recovery for composting[a]	0.0%	0.0%	0.0%	0.0%	0.0%	0.0%
Total materials recovery	6.4%	6.6%	7.1%	7.7%	9.6%	9.9%
Discards after recovery[b]	93.6%	93.4%	92.9%	92.3%	90.4%	90.1%
Combustion[c]	30.6%	26.1%	20.6%	14.4%	9.0%	7.1%
Discards to landfill, other disposal[d]	63.0%	67.3%	72.4%	77.8%	81.4%	82.9%

[a]Composting of yard trimmings and food wastes. Does not include mixed MSW composting or backyard composting.

[b]Does not include residues from recycling or composting processes.

[c]Does not include residues from recycling, composting, or combustion processes.

[d]Includes combustion of MSW in mass burn or refuse-derived fuel-form, and combustion with energy recovery of source separated materials in MSW (e.g., wood pallets and tire-derived fuel).

[e]Details may not add to totals due to rounding.

- heap leach residual waste;
- hospital/research waste;
- MSW;
- incinerator ash;
- sewage treatment sludge;
- contaminated dredge soil;
- electric power-generation ash;
- mine spoil; and
- C&DW.

A primary performance goal for waste containment systems used at all of these types of facilities is protection of groundwater quality. Historically, the use of liners to protect groundwater quality has been practiced for some types of landfills in some parts of the country from about the mid 1970s. Since that time, the use of waste containment systems has become more and more widespread, and the capabilities of these systems have progressively improved.

The need for waste containment systems in landfills is driven in large part by the need to contain liquids and gases generated in the landfill. Leachate generated in landfills flows downward by gravity and, if not for the liner system, would continue its migration out of the unit. Given a sufficient volume of leachate, this liquid would eventually migrate through the vadose zone, ultimately posing a threat to groundwater quality and, at some locations, nearby surface-water quality. Both the quantity and quality of leachate are of concern. In addition, for MSW landfills, the biodegradation of putrescible organics in the waste creates landfill gas. This gas can be an added source of groundwater contamination if not contained in the landfill and then removed by appropriate means. The gas can also create explosion hazards and contribute to air pollution.

Liquid containment is also an important consideration for surface impoundments that contain various process liquids and liquid wastes. As with landfills, the function of the liner system beneath a surface impoundment is to contain impounded liquid and prevent it from migrating through the subsurface and into the groundwater at a rate that would cause an adverse impact to groundwater quality (or surface-water quality), or at a rate that would not comply with a regulatory performance criterion. The potential for liquid migration can be particularly significant for surface impoundments, due to the relatively high liquid heads that may exist in these facilities.

With respect to abandoned dumps and remediation sites, the situation is different than for a modern landfill because these types of sites already exist and often were operated without benefit of an engineered liner system and other environmental controls. One way to remediate these types of sites is to install a final cover system over the waste. At some locations, a cover system by itself will be adequate to achieve the desired

performance levels. Other locations will require additional components, such as subsurface barriers (e.g., soil-bentonite cutoff wall) or liquid/gas extraction systems.

1.2 Regulations

In the U.S., MSW, hazardous waste, and certain other wastes are regulated under the Resource Conservation and Recovery Act (RCRA), including the Hazardous and Solid Waste Amendments (HSWA) to RCRA. As used by EPA, the term hazardous waste has a very specific, legal definition. As defined in Title 40 of the Code of Federal Regulations (CFR), Part 261 (40 CFR 261), waste is hazardous if:

1. it is listed as a hazardous waste (listed hazardous wastes are specifically identified in 40 CFR 261, Subpart D);
2. it is mixed with or derived from a hazardous waste as defined by EPA;
3. it is not excluded (some wastes, such as MSW, are specifically identified and excluded as hazardous waste); and
4. it possesses any one of four characteristics described in 40 CFR 261, Subpart C: (i) ignitability; (ii) corrosivity; (iii) reactivity; or (iv) toxicity as determined by the Toxicity Characteristic Leaching Procedure (TCLP) test.

Federal legislation applicable to MSW is contained in Subtitle D of RCRA. Federal regulations applicable to MSW landfills (and nonhazardous MSW combustor ash landfills (MSW ash landfills) are set forth in 40 CFR 258. The basic regulations were published on October 9, 1991. These regulations are implemented by states and territories with landfill regulations or laws that have been approved by the EPA. Forty-nine of the 50 states have an approved program. Federal regulations specify that a MSW or MSW ash landfill liner system meet the minimum design standard in 40 CFR 258.40(a)(2) or meet the performance standard in 40 CFR 258.40(a)(1). The design standard requires a single-composite liner system that consists of the following, from top to bottom:

- leachate collection and removal system (LCRS) that limits the head of leachate on the composite liner to 0.3 m or less;
- 0.75-mm thick geomembrane (GM) (1.5-mm thick if the GM is made of high density polyethylene (HDPE)) upper component of composite liner; and
- 0.6-m thick compacted clay liner (CCL) lower component of composite liner, with the CCL having a maximum hydraulic conductivity of 1×10^{-7} cm/s.

While the federal minimum design standard was adopted by many states, a few states require that MSW landfills or MSW ash landfills have a double-liner system.

The performance standard requires a liner system design that is demonstrated to achieve certain groundwater compliance standards (i.e., maximum contaminant levels (MCLs)) at a specified distance from the landfill (i.e., a point of compliance). This distance cannot exceed 150 m. Only the Director of an approved State can approve a

design that meets the performance standard. The technical demonstration that a certain liner system meets the performance standard is often made using the EPA HELP and MULTIMED computer models. The modeling methods must be acceptable to the Director.

Regardless of whether an MSW landfill has a liner system that meets the minimum design standard or the performance standard, groundwater monitoring and compliance in accordance with 40 CFR 258.50-58 is required for the facility. If the liner system does not meet the minimum design standard, leachate recirculation on the liner systems is not allowed as specified in 40 CFR 258.28(a)(2).

An example of a single-composite liner system for a MSW landfill is shown in Figure 1-1(a). The LCRS will often include a pipe network that drains to a sump at the low elevation of the landfill cell. From the sump, leachate is removed by a submersible pump or gravity drainage pipe. Where pumps are used, the pump is lowered in vertical manholes that extend up through the waste mass or, more commonly, in riser pipes that extend up the sideslope of the landfill. Generally, leachate generated by a landfill will need to be collected for the active life of the landfill plus a 30-year post-closure period. However, the 30-year period has yet to be reached for any landfill constructed under current EPA regulations. Longer periods of leachate removal may be required for at least some sites, while for many modern sites, leachate generation should essentially cease prior to the end of the 30-year period.

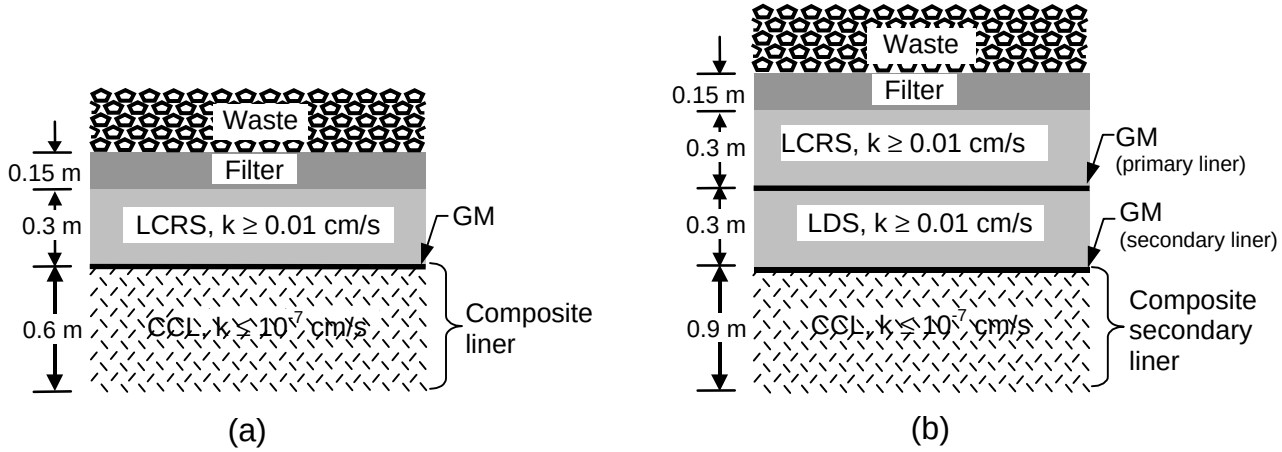

Figure 1-1. Example of liner systems for: (a) MSW landfills; and (b) hazardous waste landfills.

For waste materials considered to be hazardous as previously defined, the applicable legislation is contained in Subtitle C of RCRA. Specific EPA regulations for waste containment systems at RCRA Subtitle C landfills, surface impoundments, and waste piles are published in 40 CFR 264. These regulations require hazardous waste landfills to have two independent liners with a leak detection system (LDS) between them and LCRS above the primary (or top) liner. The purpose of the LDS is to allow monitoring of the primary liner (i.e., to identify whether, and to what extent, leakage is occurring through the primary liner) and to provide a mechanism for removing liquids that enter this system. A double-liner system with an LDS is a hallmark of hazardous waste landfill regulations in the United States. A major task of the project described in this report was to evaluate the field effectiveness of landfills underlain by double-liner systems with respect to leachate containment.

Regulatory requirements for hazardous waste landfill double-liner systems are given in 40 CFR 264.301. The minimum liner system design standard generally considered to meet these requirements includes, from top to bottom:

- LCRS that limits the head of leachate on the primary liner to 0.3 m or less;
- GM primary liner;
- 0.3-m thick granular LDS drainage layer with a minimum hydraulic conductivity of 1×10^{-2} cm/s or a geosynthetic LDS drainage layer with a minimum hydraulic transmissivity of 3×10^{-5} m^2/s;
- GM upper component of a composite secondary liner; and
- 0.9-m thick CCL lower component of the composite secondary liner, with the CCL having a maximum hydraulic conductivity of 1×10^{-7} cm/s.

An example of a double-liner system for a hazardous waste landfill is shown in Figure 1-1(b).

Federal regulatory requirements exist for the disposal of waste types other than MSW and hazardous waste. While this report is not intended to provide an exhaustive survey of these requirements, it is noted that requirements for landfill disposal of polychlorinated biphenyls (PCBs) and PCB items under the Toxic Substances Control Act (TSCA) are contained in 40 CFR 761.65, while requirements for land disposal of uranium mill tailings under the Uranium Mill Tailings Radiation Control Act (UMTRCA) are contained in 40 CFR 192.02.

Final cover systems are another important component of waste containment systems used at landfills. While liner systems are installed beneath the waste, final cover (or closure) systems are installed over the completed solid waste mass. For MSW, Subtitle D regulations require that the final cover must be placed over the landfill within one year after the waste reaches its final permitted height. In terms of long-term landfill performance and management, final cover systems are as important, and in some ways

more so, than the liner system (Bonaparte, 1995). The design, construction, and maintenance of final cover systems should be practiced to the same level of care as for liner systems.

Requirements for final cover systems for MSW and hazardous waste landfills are also addressed in federal regulations. For liner systems of the type shown in Figures 1-1(a) and (b), minimum final cover system requirements are illustrated in Figure 1-2. MSW landfills must meet federal design criteria or performance-based design requirements (40 CFR 258.60). The minimum design for a MSW landfill (which is underlain by a composite liner) cover system includes the following components, from top to bottom:

- 0.15-m thick soil surface layer;
- 0.5-mm thick GM upper component of composite barrier; and
- 0.45-m thick CCL lower component of composite barrier, with the CCL having a maximum hydraulic conductivity of 1×10^{-5} cm/s.

Under Subtitle D, alternative cover system designs are allowed, however, these designs must, at a minimum, be shown to perform equivalently to the federal design cover system with respect to reduction in percolation and erosion resistance.

It should be noted that the federal requirements for final cover systems at MSW landfills are only minimum requirements and do not represent “complete” designs for most landfills since they do not address all important design criteria. Some of these criteria are addressed in EPA (1991), which is currently being updated. For example, the minimum requirements do not include a drainage layer above the composite barrier or an adequate thickness of cover soil to allow sufficient water storage for healthy surface vegetation. As another example, the requirements do not include an adequate thickness of soil above the CCL component of the final cover system to protect the CCL from freeze-thaw damage for sites located in northern climates. As a final example, the requirements do not address the important matter of landfill gas transmission beneath the final cover system.

For hazardous waste landfills, 40 CFR 264.310 requires that the landfill be closed with a final cover system that meets certain performance criteria, most notably, “*Have a permeability less than or equal to the permeability of any bottom liner system or natural subsoils present*.” The regulations do not contain minimum design requirements for final cover systems analogous to those for liner systems. However, EPA guidance (EPA, 1989) recommends that final cover systems for hazardous waste landfills consist of at least the following, from top to bottom:

- a top layer containing two components: (i) either a vegetated or armored surface layer; and (ii) a 0.6-m thick protection layer, comprising topsoil and/or fill soil, as appropriate;
- a 0.3-m thick granular drainage layer with a minimum hydraulic conductivity of 1 x 10^{-2} cm/s; and
- a composite hydraulic barrier, consisting of (i) a 0.5-mm thick GM upper component; and (ii) a 0.6-m thick CCL lower component, with the CCL having a minimum hydraulic conductivity of 1 x 10^{-7} cm/s.

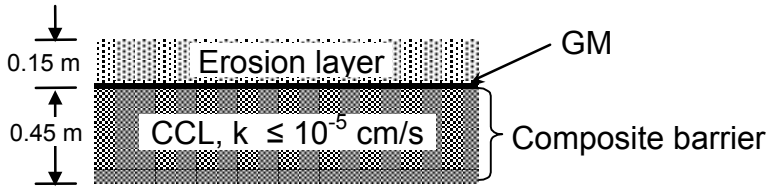

(a)

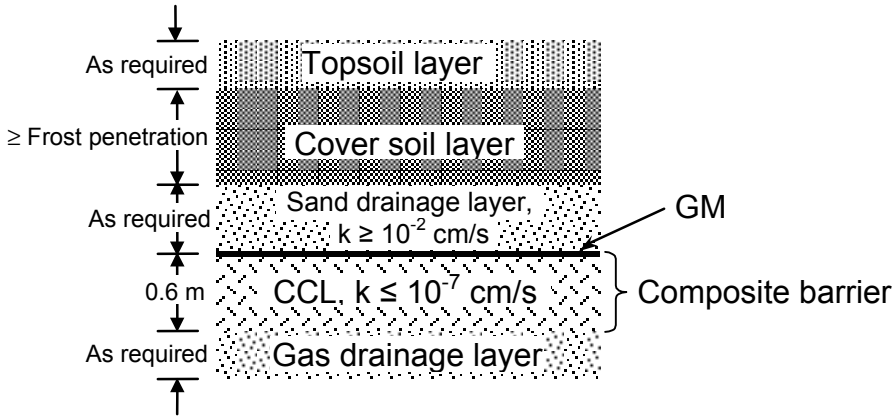

(b)

Figure 1-2. Examples of final cover systems for: (a) MSW landfills; and (b) hazardous waste landfills.

It is noted that at the time of publication of this report, EPA is concurrently completing a new technical guidance document titled, "*Technical Guidance for RCRA/CERCLA Final Covers*" (Bonaparte et al., 2002). The reader is referred to this guidance document for more detailed information on final cover systems for landfills and remediation sites.

With respect to abandoned dumps and remediation sites, the Superfund Amendments and Reauthorization Act of 1986 (SARA) adopts and expands a provision in the

Comprehensive Environmental Response, Compensation, and Liability Act (CERCLA) of 1982 to require that remedial actions at sites being remediated under the Act must at least attain applicable or relevant and appropriate requirements (ARARs). These requirements for ARARs may derive from federal or state regulations. ARARs may be location-specific, action-specific, or chemical-specific.

RCRA Subtitle C or D requirements for treatment, storage, and disposal facilities (TSDFs) will frequently be considered ARARs for CERCLA actions, because RCRA regulates the same or similar wastes or constituents as found at many CERCLA sites, covers many of the same activities, and addresses releases and threatened releases similar to those found at CERCLA sites. When RCRA requirements are ARARs, only the substantive requirements of RCRA must be met if a CERCLA action is to be conducted on site. Substantive requirements are those requirements that pertain directly to actions or conditions in the environment. Examples include performance standards for incinerators (40 CFR 264.343), treatment standards for land disposal of restricted waste (40 CFR 268), and concentration limits, such as maximum contaminant levels (MCLs). On-site actions do not require RCRA permits or compliance with administrative requirements. Administrative requirements are those mechanisms that facilitate the implementation of the substantive requirements of a statue or regulation. Examples include the requirements for preparing a contingency plan, submitting a petition to delist a listed hazardous waste, recordkeeping, and consultations. CERCLA actions to be conducted off site must comply with both substantive and administrative RCRA requirements. CERCLA MSW landfills represent a particular subset of CERCLA sites for which EPA has established presumptive remedy guidance (EPA, 1993).

RCRA and CERCLA regulatory requirements provide flexibility for innovation and alternatives by limiting the use of specific minimum design specifications in the regulations, by providing performance criteria in lieu of design specifications, and/or by providing administrative procedures for gaining approval of waivers from RCRA mandatory requirements or CERCLA ARARs. When proposing an alternative design to the performance-based and/or federal minimum design requirements contained in the applicable regulation, the proposal for the alternative design must often be supported with a demonstration that the alternate is "technically equivalent" to a design meeting the basic regulatory requirements. Alternative design approaches may be used for any one of a number of different waste containment system components or group of components, including liner systems, final cover systems, LCRSs, and LDSs.

1.3 Waste Containment System Components

Waste containment systems are generally considered to included liner systems, final cover systems, subsurface barriers, and subsurface interceptors constructed of a range of materials including soil, geosynthetics, cement, and/or metals. This report addresses liner systems and final cover systems constructed of soils and geosynthetics. The

following material choices may be considered for the design of these types waste containment systems:

- drainage layer: geonet (GN), geocomposite (GC), or granular soil;
- filter layer: geotextile (GT) or granular soil;
- hydraulic barrier: GM, geosynthetic clay liner (GCL), or CCL, or a combination of the three;
- gas transmission layer: GT, GC, or granular soil;
- protection layer: GT or soil, and;
- erosion control: geosynthetic erosion control (GEC) materials, natural jute, gravel, asphalt, riprap, or other materials.

An example of a liner system and final cover system for a landfill that incorporates some of these materials (primarily geosynthetics) is illustrated in Figure 1-3. It is of interest to compare this figure to the liner and cover systems of Figures 1-1(b) and 1-2(b). The liner system shown in Figure 1-3 incorporates a double-liner system consisting of a GM/GCL composite primary liner and a GM/CCL composite secondary liner. The LDS consists of a GT/GN/GT GC. The LCRS is gravel with a perforated pipe network contained therein. A GT filter layer covers the entire LCRS and is intended to inhibit clogging of the LCRS. A GT cushion beneath the gravel LCRS protects the primary GM from puncture by the overlying gravel. On the sideslopes, the LCRS is constructed of a GT/GN/GT GC, which transitions, at the sideslope toe, into the gravel LCRS on the base.

The final cover system illustrated in Figure 1-3 contains a GM/GCL composite hydraulic barrier. A GT gas transmission layer is shown beneath the barrier and a GT/GN/GT GC (or other type of geosynthetic composite) is shown above it. A GEC is installed on the surface of the topsoil layer. Both temporary and permanent types of GECs are commercially available.

Additional information regarding each of the natural soil and geosynthetic components of the waste containment systems illustrated in Figures 1-1, 1-2, and 1-3 are presented in the next section.

1.4 Liner System and Final Cover System Components

This section presents relevant details on liner/barrier, drainage, filtration, and ancillary materials typically used in the liner system and final cover system of waste containment facilities.

1.4.1 Liner/Barrier Materials

The types of hydraulic liner/barrier materials considered in this report are CCLs, GMs, and GCLs.

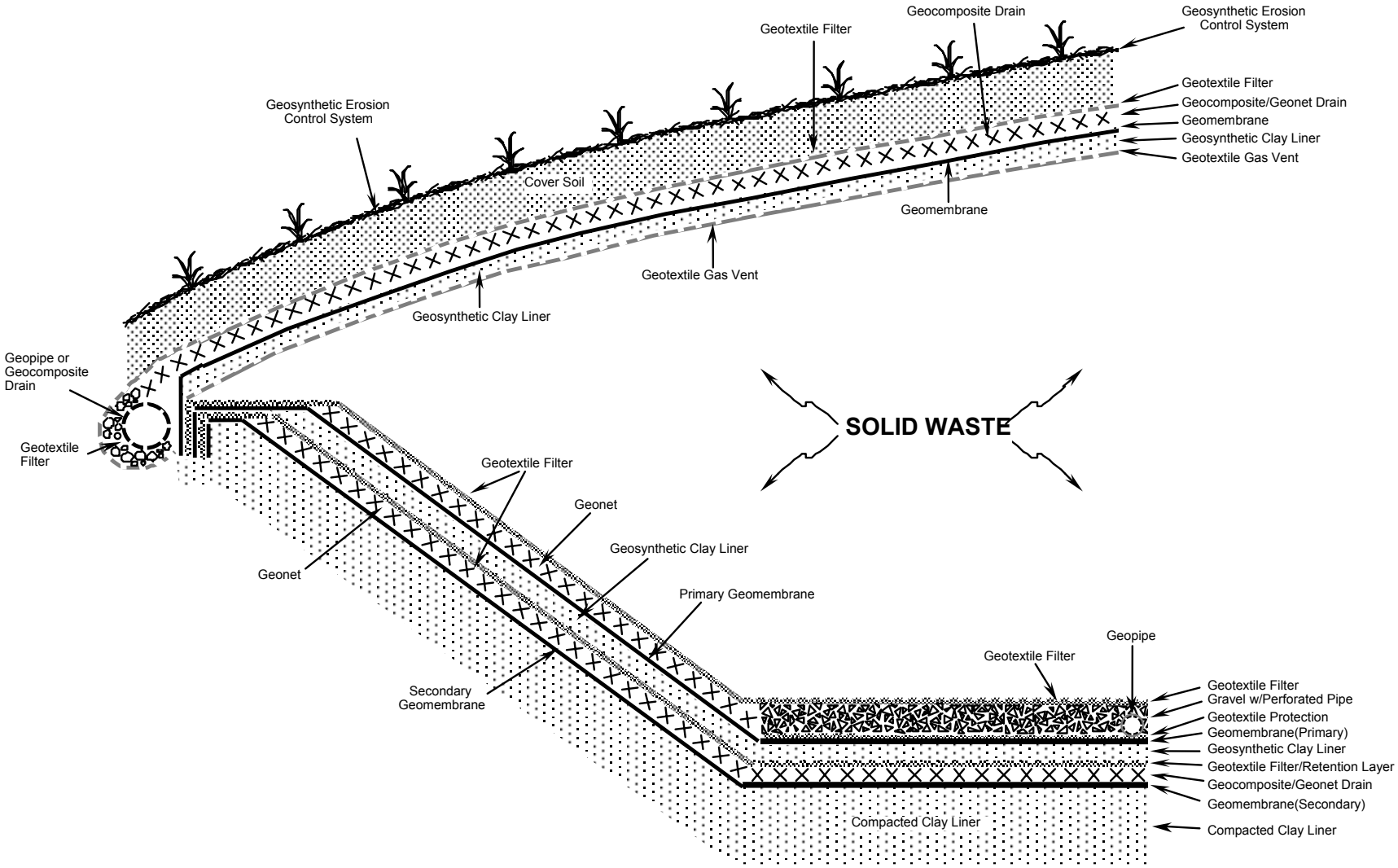

Figure 1-3. Idealized solid waste containment system (with emphasis on geosynthetic material utilization) for a solid waste landfill.

1.4.1.1 Compacted Clay Liners

CCLs are constructed primarily from natural soil materials that are rich in natural clay, although the CCL may contain processed natural clay such as bentonite. CCLs are constructed in layers called lifts that typically have a thickness after compaction of 0.15 m. On sideslopes equal to or flatter than about 3 horizontal : 1 vertical (3H:1V) lifts are placed parallel to the slope. However, parallel lifts are very difficult or impossible to construct on sideslopes steeper than about 2.5H:1V. On steeper sideslopes, CCLs are constructed using horizontal lifts.

For CCLs that must have a saturated hydraulic conductivity of not more than 1×10^{-7} cm/s, it is recommended that the CCL material have the following characteristics:

- minimum percentage of fines: from 30 to 50%
- minimum plasticity index: from 7 to 15%
- maximum percentage of gravel: from 20 to 50%
- maximum particle size: from 25 to 50 mm (less for a lift placed in direct contact with a CCL)

The percentage of fines is defined as the percent by dry weight of particles passing the No. 200 sieve, which has 0.074-mm wide square openings. Percentage of fines is typically determined by ASTM D422. Plasticity index, which is defined as the liquid limit minus the plastic limit, may be determined by ASTM D4318. Percentage of gravel is defined as the percent by dry weight retained on a No. 4 sieve (4.76 mm wide square openings). Local experience may dictate more stringent requirements and, for some soils, more restrictive criteria may be appropriate. However, if the criteria tabulated above are not met, it is unlikely that a natural soil liner material will be suitable without additives such as bentonite.

CCLs must be ductile, particularly when used in final cover systems (to accommodate possible differential settlement), and must be resistant to cracking from moisture variations, e.g., desiccation. Sand-clay mixtures are ideal materials if resistance to shrinkage and desiccation induced cracking are important (Daniel and Wu, 1993). Ductility is achieved by avoiding use of dense, dry soils, which tend to be brittle.

If suitable materials are unavailable, local soils can be blended with commercial clays, e.g., bentonite, to achieve low hydraulic conductivity. A relatively small amount of sodium bentonite (typically 2 to 6% by weight) can lower hydraulic conductivity as much as several orders of magnitude. Such liners are usually called amended clay liners and, in this report, are included in the CCL category. The percent bentonite is usually defined as the dry weight of bentonite divided by the dry weight of soil to which bentonite is added. Soils with a broad range of grain sizes usually require a relatively small amount of bentonite (less or equal to 6%). Uniform sized soils, such as concrete sand, usually require more bentonite (up to 10 to 15%). Sometimes materials are

blended to provide a material with a broad range of grain sizes, thus minimizing the amount of bentonite amendment needed.

Some of the significant issues for CCLs are: (i) the accuracy of field hydraulic conductivity assessment using laboratory tests on small undisturbed sample of the constructed CCL; (ii) the compaction criteria to achieve the required CCL hydraulic conductivity; and (iii) the long-term hydraulic performance of CCLs in final cover systems. A major task of this project focused on these topics.

1.4.1.2 Geomembranes

GMs are thin, factory-manufactured polymeric materials that are widely used as hydraulic barriers in liner and final cover systems due to their non-porous structure, flexibility, and ease of installation. GMs have the advantages of extremely low rates of water and gas permeation through intact GMs and, depending on the material, the ability to stretch and deform without tearing. They also protect underlying CCLs from desiccation. Disadvantages of GMs include leakage through occasional GM imperfections, relatively high diffusion potential by certain concentrated organic liquids, potential for slippage along interfaces between GMs and adjacent materials, and material embrittlement over time.

GMs form an essential component of most liner/barrier layers. Of the factory manufactured polymeric GMs that are commercially available, the types most commonly used in waste containment systems are:

- HDPE;
- very flexible polyethylene (VFPE) [this classification includes linear low density polyethylene (LLDPE), low density linear polyethylene (LDLPE), and very low density polyethylene (VLDPE)];
- polyvinyl chloride (PVC);
- flexible polypropylene (fPP); and
- ethylene propylene diene monomer (EPDM).

Most of these GMs are available with textured surfaces on one or both sides for increased frictional resistance when needed to achieve slope stability design criteria. Additionally, spray-on elastomeric GMs are available, as are bituminous GMs. However, these materials are rarely used in waste containment applications in comparison to those previously itemized.

GMs are most often used as liquid and gas barriers, both in liner systems and final cover systems. The mechanism for liquid or gas mass transfer through an intact GM is one of molecular diffusion. Water vapor transmission rates for several typical GMs based on testing performed in accordance with ASTM E96 are as follows:

- for 1.0-mm thick HDPE: water vapor transmission rate ≈ 0.020 g/m^2/day;
- for 0.75-mm thick PVC: water vapor transmission rate ≈ 1.8 g/m^2/day;
- for 1.0-mm thick HDPE: solvent vapor transmission rate ≈ 0.20 to 20 g/m^2/day (depends on the solvent type).

Note that 1.0 g/m^2/day ≈ 10 liter/ha/day; thus the rate for water diffusion is extremely low. In contrast, the rate of diffusion for some chemicals, particularly certain volatile organic compounds (VOCs) can be quite high. Fortunately, leachate from modern landfills typically contains only trace concentrations of VOCs and, as a consequence, VOC diffusive mass transfer rates will typically be low. A second mechanism for liquid transport through GMs, is flow through GM holes causes by punctures, tears, flawed seams, etc. The rate of flow through a given size GM hole is dependent on the hydraulic head acting on top of the hole, the permeability of the soil material underlying the GM, and other factors. The leakage rate through a GM hole where the GM is underlain by a relatively permeable soil (e.g., sand) will be much larger than for a GM hole where the GM is underlain by a CCL, all other factors being equal.

Regarding the shearing resistance of the interfaces between GMs and adjacent materials, interface strengths can be very low when smooth, relatively rigid GMs are used. Strengths can be significantly increased through the use of textured GMs. There are a number of manufacturing methods available to provide texturing:

- co-extrusion for blown film manufacturing;
- impingement for flat die manufacturing;
- lamination for flat die manufacturing; and
- structuring via a heated calendar for flat die manufacturing.

The texturing processes result in an increase in peak interface shear strength compared to the interface shear strength for a smooth GM. This increase may be in the range of 10 to 20 degrees for GM/GT interfaces. The difference may be of the same magnitude, or less, for GM/soil interfaces, depending largely on the characteristics of the soil. The difference in interface strength is typically smaller when large displacement interface strengths are considered. Testing and experience has shown that the behavior of geosynthetic/geosynthetic and soil/geosynthetic interfaces can be complex. Product-specific and project-specific interface shear tests are always recommended. Interface shear testing of geosynthetics is usually carried out in a direct shear testing apparatus in accordance with ASTM D5321.

1.4.1.3 Geosynthetic Clay Liners

GCLs consist of factory-manufactured rolls of bentonite placed between GTs or bonded to a GM. The bentonite is the low hydraulic conductivity (or permeability) component of this composite material. The geosynthetics are stitch bonded, needlepunched, or adhesively bonded to the bentonite to create self-contained products suitable for

handling, transportation, and placement as a barrier material. The fibrous structuring of needlepunched and stitchbonded materials also results in increased internal shear strength for use of GCLs on sideslopes. The application of GCLs as a barrier by itself, or as a composite barrier with an overlying GM, is rapidly growing in its use and acceptance. Three EPA workshop reports are available on GCLs (see Daniel and Scranton, 1996)).

Bentonite is the critical component of GCLs and gives rise to the material's very low hydraulic conductivity (permeability). Bentonite is a naturally occurring, mined clay mineral that is extremely hydrophilic. When placed in the vicinity of water (or even water vapor), the bentonite attracts water molecules into a complex configuration that leaves little free water space in the voids. This significantly decreases the hydraulic conductivity of the bentonite. The hydraulic conductivity of most sodium bentonite GCLs is in the vicinity of 1×10^{-9} to 5×10^{-9} cm/s (Estornell and Daniel, 1992).

The various GCL products are manufactured such that the following types are most commonly used:

- bentonite adhesively bonded between two GTs;
- bentonite stitch bonded between two GTs;
- bentonite needlepunched between two GTs; and
- bentonite adhesively bonded onto a GM.

While the low hydraulic conductivity of GCLs gives rise to its' favorable comparison to CCLs on the basis of a flow rate or (flux) calculation, the assessment of full technical equivalency is much more complicated. Koerner and Daniel (1994) have proposed a comparative assessment of GCLs to CCLs to be made on the basis of numerous hydraulic, physical/mechanical, and construction criteria.

Using the above mentioned criteria, GCL's are generally equivalent or superior to CCLs with the exception of certain field installation issues, e.g., subgrade preparation, puncturing, and direct contact by construction vehicles; with respect to certain hydraulic issues such as time-of-travel and degradation due to cation exchange; and with respect to mass transport issues, such as diffusion and retardation. It is suggested that with proper subgrade preparation and soil covering in a timely manner and of sufficient thickness, GCLs can be adequately installed. Equivalency with respect to the hydraulic and other design criteria must be determined on a project-by-project basis. The issue of the cation exchange potential of GCLs has recently received much attention and the reader is referred to Shackelford et al. (2000) and Jo et al. (2001) for additional information.

One of the more significant issues associated with the use of GCLs is that of adequate shear strength when GCLs are installed on sideslopes. A major task of this project

focused on this topic. Constructability issues involving GCLs are also important with respect to composite liners, i.e., GM/GCL intimate contact.

1.4.1.4 Composite Liners

While any of the three liner materials just described (CCL, GM, and GCL) can be used as a barrier material by itself, it is the combination of two or more of the components that has proven to be most effective in terms of liquid and gas containment. In each case of a composite liner, the GM forms the upper component, with the soil or GCL being the lower component(s). From practical experience, most composite liners fall into one of the following categories:

- GM over CCL (GM/CCL);
- GM over GCL (GM/GCL); or
- GM over GCL over CCL (GM/GCL/CCL).

In all cases, the basic premise of using a composite liner is that leakage through a hole or defect in the GM is impeded by the presence of the CCL or GCL. Figure 1-4 illustrates the concept. If a CCL or GCL is used alone, liquid migration can occur over the entire area of the liner that is subject to a hydraulic head. If a GM is used alone and is placed on a permeable substrate, the rate of flow through a hole in the GM can approach the rate of flow through a similarly-sized orifice. In a composite liner, leakage will only occur at the location of the GM hole, but it will be much slower than flow through an orifice due to the hydraulic impedance provided by the CCL or GCL. The level of impedance provided by the CCL or GCL is a function of the hydraulic conductivity of that material, and the amount of lateral flow at the interface between the GM and CCL or GCL. The amount of interface flow is a function of the "intimacy" of the contact between the GM and CCL or GCL components (Giroud and Bonaparte, 1989; Gross et al., 1990). Both theoretical investigations and field performance studies have shown that leakage through composite liners is much less than leakage through GMs alone or soil liners alone (Bonaparte and Othman, 1995). Due to their superior performance capabilities, in comparison to GMs, CCLs, or GCLs alone, composite liners have been incorporated into federal minimum requirements for both MSW and hazardous waste landfills, and they are being increasingly used in a wide variety of waste containment system applications.

In considering the use of composite liners, design engineers are often faced with evaluating the relative merits of using a GM/CCL composite liner versus a GM/GCL composite liner. Technical, cost, constructability, and disposal capacity (i.e., airspace) considerations will govern liner selection on a project-by-project basis. An important concept in comparing GM/CCL and GM/GCL composite liners is “technical equivalency.” Establishing the technical equivalency of a GM/GCL barrier to a GM/CCL barrier on a specific project requires consideration of a number of design and performance criteria. In some cases, it may be advantageous to consider a three-

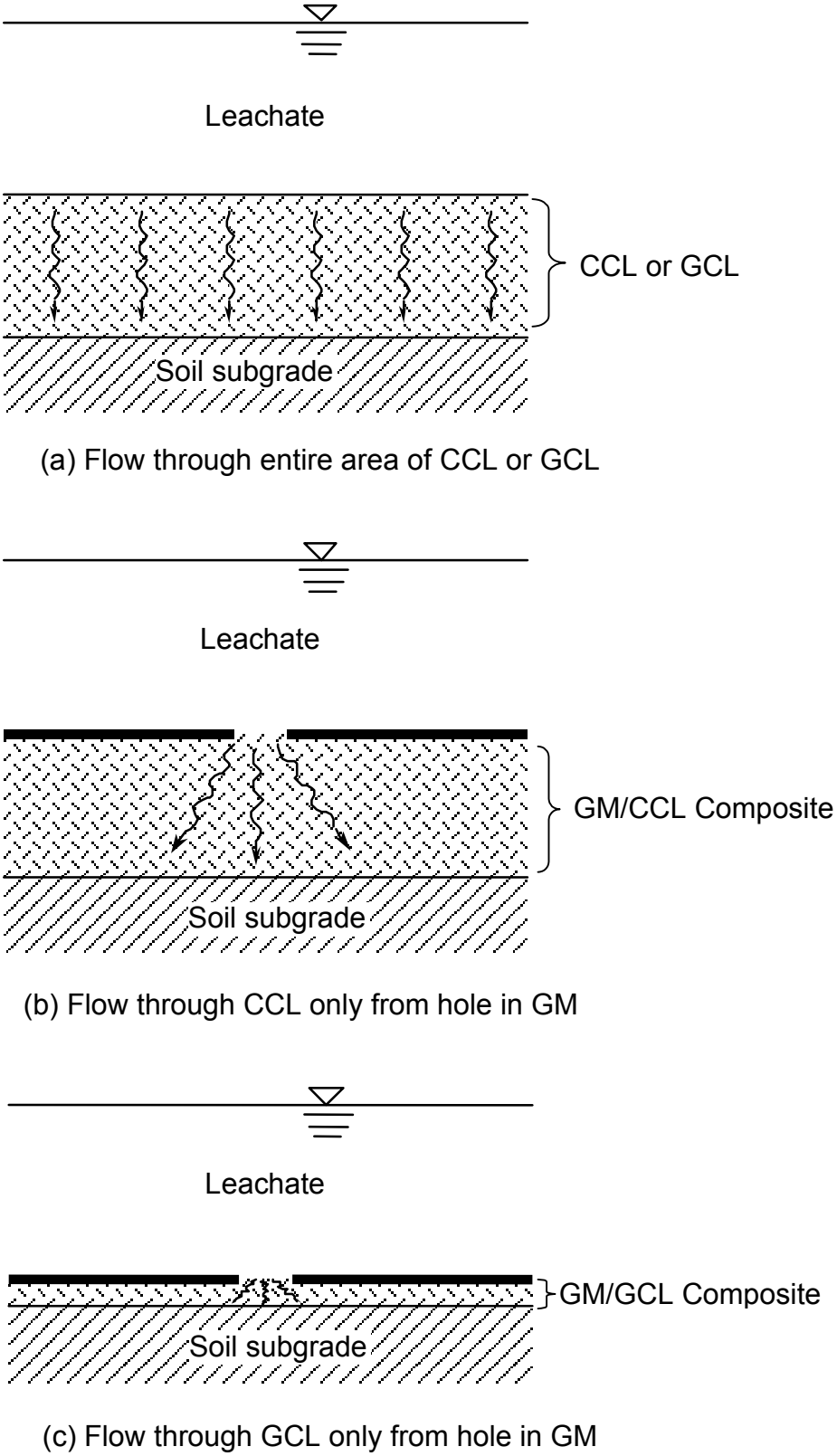

Figure 1-4. Composite liner flow minimization concept.

component composite liner. A three-component composite liner may be appropriate, for example, where clay material capable of achieving the required hydraulic conductivity performance criterion is not available, but use of a GCL by itself is not adequate for the lower component of the composite liner (due to, for example, the need for a CCL component to address issues related to time-of-travel, cation exchange, or puncture potential).

With respect to liquid migration through a GM hole in a GM/GCL composite liner, concern has been expressed with respect to the potential magnitude of interface flow within the GT that covers the GCL. This concern, however, has been shown experimentally to be of only minor consequence (Wilson-Fahmy and Koerner, 1995). The reason behind this finding is that the bentonite of the GCL hydrates and either extrudes or intrudes into the covering GT. A more significant issue than high transmissivity within the covering GT is one of possible lower interface shear strength with the material above. The same issue holds for materials that are beneath the GCL.

GMs undergo expansion and contraction in response to exposure to sunlight and temperature when placed and seamed together in the field. If seaming occurs with the GM taut, tensile stresses are induced in the GM when the temperature decreases (e.g., after the GM is covered with soil) and the GM contracts. GMs transitioning from sideslopes to the flat interior of a landfill cell have lifted off the ground in a trampoline-like manner due to contractive stresses. To avoid trampolining, a GM may be placed with some slack such that during subsequent contraction at cooler temperatures, the material will lie flat with essentially no internal tensile stress. Slack is incorporated in the form of waves, or wrinkles. However, with this approach there is always a concern that soil will be placed over the GM at a time when the waves still exist. The issue of the disposition of these waves after backfilling has been investigated, and the results of the investigation are presented in this report. It should be mentioned that all GM types (except reinforced GMs) have similar thermal coefficients of expansion. However, stiffer and thicker GMs, such as the polyethylene GMs, concentrate the waves and hence the waves are more pronounced and visible. Polyethylene GMs were the focus of the investigation described herein.

1.4.2 Drainage Materials

Fluid collection, conveyance, and removal represent another critical function of waste containment systems for landfills, surface impoundments, and waste piles. The fluid to be collected, conveyed, and removed will be leachate, water, impounded wastewater, industrial liquid, or landfill gas. There are five typical locations where drainage materials may be required within a waste containment system:

- LCRS beneath solid waste;
- LDS between primary and secondary liners of a double-liner system;
- internal drainage layer above the barrier in a final cover system;

- gas transmission layer beneath the barrier in a final cover system; and
- pore pressure relief system in areas of high groundwater.

Candidate drainage materials include soils, GNs, GTs, and/or GCs, and alternative materials, such as tire chips. Granular soil and geosynthetic (i.e., GN, GC, and GT) drainage layers are described below.

1.4.2.1 Granular Soils

Granular drainage materials are normally composed of relatively clean sand or gravel. Gravel is material that does not pass through the 4.74-mm wide openings of a No. 4 sieve. Sand consists of material that passes through the No. 4 sieve but not through the 0.075-mm wide openings of a No. 200 sieve. "Clean" sand or gravel refers to sand or gravel that contains very little or no material that passes through the openings of a No. 200 sieve. Clean sands and gravels are often produced by washing natural sands and gravels to remove any "fines," which are particles that pass through the openings of a No. 200 sieve.

The drainage layer should meet filter criteria with the overlying layer of soil or waste. If the drainage layer material does not meet these criteria, a granular soil or GT filter will be required.

Specifications for granular materials often require:

- no more than 2 to 5% (dry-weight basis) of material passing the No. 200 sieve; a "fines" content at the lower end of this range is usually preferable;
- a maximum particle size on the order of 25 to 50 mm; however, smaller particles will typically be required if a GM will underlie the drainage layer; alternatively, a GT cushion layer can be used;
- restrictions on gradation, stated in terms of allowable percentages for specified sieve sizes (these restrictions may exist for various purposes, including filtration considerations);
- limitations on mineralogy (often the drainage material is required to be a non-carbonaceous material, with a limit on the amount of calcium carbonate in the material, although hard evidence that carbonaceous materials are truly unsuitable is lacking);
- restrictions on the angularity of the material, if the material will be in contact with geosynthetics, which are vulnerable to puncture by large, sharp objects (or, alternatively, a GT cushion may be employed);
- that no deleterious material be present; and
- a minimum acceptable saturated hydraulic conductivity.

The specified material requirements attempt to ensure that the materials will not puncture adjacent geosynthetics, will be chemically stable, and will provide adequate drainage.

The required thickness and hydraulic conductivity of natural soil drainage layers should always be established on the basis of site-specific and material-specific considerations. It is not recommended that regulatory-suggested minimum values be used without verifying by calculations that such values are adequate. For example, regulatory minimum hydraulic conductivity values of 1×10^{-2} cm/s (and in some states 1×10^{-3} cm/s) are often too low to satisfy rationally-based design criteria. The use of granular drainage layers with permeabilities that are too low can lead to hydraulic head buildup on liners or barriers and, in some cases, result in seepage-induced slope instability. Lower permeability lateral drainage layers are also more prone to clogging and result in longer leak detection times when used in an LDS. Higher hydraulic heads associated with lower permeability drainage materials also increase the potential for liquid migration out of the waste management unit.

The required flow capacity, q_c ($m^3/s/m$), of a granular drainage layer must be equal to or greater than the product of the maximum flow rate, q_m ($m^3/s/m$), obtained from the design analyses and the factor of safety, FS (dimensionless):

$$q_c \geq q_m \, FS \qquad \text{(Eq. 1-1)}$$

The maximum flow rate for design should be established by appropriate analysis as discussed below. The FS selected for design should be based on the level of uncertainly inherent in the design input parameters and the consequences of failure. A minimum FS value of 2.5 is recommended for cases where the uncertainly in input parameters is low and the consequences of failure are small (e.g., no slope instability for a final cover system, little potential for increased percolation or leakage). For some situations, a larger FS may be appropriate. Koerner and Daniel (1997) have recommended using a FS value of at least 5 to 10 to account for the uncertainties typically inherent in the assessment of waste containment system hydraulic conditions.

For granular drainage layers, the drainage layer hydraulic conductivity is selected to provide adequate flow capacity and unconfined flow conditions. For geosynthetic drainage layers (discussed below), the drainage layer hydraulic transmissivity is selected to provide adequate flow capacity and unconfined flow conditions. For all drainage layer materials, the required field hydraulic properties for design are evaluated considering the material properties measured in the laboratory and reduction factors that consider the potential for reduction in the property over time due to long-term clogging, deformation, etc., in the field.

For granular drainage layers, the field hydraulic conductivity can be computed as:

$$k_f = k_l \left(\frac{1}{RF_{CC} RF_{BC}} \right) \qquad \text{(Eq. 1-2)}$$

where: k_{field} = long-term field hydraulic conductivity of granular drainage layer (m/s); k_l = hydraulic conductivity of granular drainage layer (m/s) measured in the laboratory; RF_{CC} = reduction factor for chemical clogging (dimensionless); and RF_{BC} = reduction factor for biological clogging (dimensionless).

For geosynthetic drainage layers (discussed below), the field hydraulic transmissivity can be computed as:

$$\theta_f = \theta_l \left(\frac{1}{RF_{IN} RF_{CR} RF_{CC} RF_{BC}} \right) \qquad \text{(Eq. 1-3)}$$

where: θ_f = long-term field hydraulic transmissivity of geosynthetic drainage layer ($m^3/s/m$); θ_l = hydraulic transmissivity of geosynthetic drainage layer ($m^3/s/m$) measured in the laboratory; RF_{IN} = reduction factor for elastic deformation and/or or intrusion of the adjacent geosynthetics into the drainage layer (dimensionless); RF_{CR} = reduction factor for creep deformation of the drainage layer and/or creep deformation of adjacent materials into the drainage layer (dimensionless); and all other variables are as defined previously.

It may occasionally be necessary to consider other reduction factors, such as factors for installation damage or elevated temperature effects. If necessary, they can be included on a site-specific basis. On the other hand, if the reduction factor has been included some way in the test procedure for measuring the hydraulic property, the reduction factor would appear in the foregoing formulation as a value of unity.

For design of LCRSs, the EPA Hydrologic Evaluation of Landfill Performance (HELP) water balance model (Schroeder et al., 1994) is widely employed to obtain a leachate generation rate for use in establishing an LCRS design flow rate (i.e., to establish q_m). The authors believe that the HELP model is useful for this purpose and as a design tool for comparing different design scenarios. Limitations of the model as a predictive tool are discussed subsequently in this report. To establish the design maximum flow rate for LDSs, a primary liner leakage rate must be assumed. Maximum primary liner leakage rates are sometimes taken as regulatory action leakage rates (ALRs) or are established using an arbitrary conservative value (e.g., 1000 liters/ha-day) for purposes of hydraulic design. A more rational approach has been presented by Giroud et al. (1997). The 2002 update to the EPA technical guidance document for RCRA/CERCLA final cover systems (i.e., Bonaparte et al., 2002) provides a detailed discussion of procedures to obtain the design maximum flow rate for internal drainage layers in final cover systems.

1.4.2.2 Geosynthetics

A number of different types of geosynthetics have been used as drainage layers in waste containment systems. Geosynthetic drainage materials that have been used in

these applications include:

- GNs of solid ribs with diamond-shaped apertures;
- GN of foamed ribs with diamond-shaped apertures;
- “high flow” GNs of solid ribs in a parallel orientation;
- drainage cores of single cuspations or dimples;
- drainage cores of double cuspations or dimples;
- drainage cores of built-up columns;
- drainage cores of stiff three-dimensional entangled mesh;
- needlepunched nonwoven GTs; and
- resin-bonded nonwoven GTs.

Like granular drainage layers, a geosynthetic drainage layer should meet filter criteria with the overlying protection layer. Unless a GN or other core drainage material is sandwiched between GMs, drainage cores require a GT filter to keep the overlying material from directly clogging the apertures of the drain. Furthermore, if a GM hydraulic barrier underlies a GN or core drainage layer, as is often the case, a GT may be required between the drain and GM to provide higher interface shear resistance on sideslopes and, possibly, reduce deformation-related intrusion of the GM into the drain and/or protect the GM from puncture or other damage by the drain. Often the GT is heat bonded or glued to the GN or drainage core, creating a GC, to enhance interface shear strength, decrease the potential for fugitive soil particles to enter the drain during construction, and facilitate installation. If a GT drainage layer is used, it should be selected to meet filter criteria with the overlying material.

Specifications for geosynthetic drainage layers often require:

- resin and additive requirements;
- minimum thickness;
- minimum mass per unit area;
- minimum hydraulic transmissivity at a specified normal stress and hydraulic gradient;
- minimum strength requirements to survive installation;
- if the drainage material is a GN or core, inclusion of a GT filter above the drain; and
- if the drainage material is a GN or core, inclusion of a GT beneath the drain, if necessary, to increase interface shear resistance, reduce deformation-related intrusion of an underlying hydraulic barrier material into the drain, and/or protect the hydraulic barrier from puncture or other damage by the drain.

As with the hydraulic conductivity of a granular drainage layer, no specific minimum hydraulic transmissivity can be recommended for a geosynthetic drainage material because the required value is site dependent. To minimize the potential for excessive

erosion and slope instability, however, the drainage layer should be able to convey the maximum flow rate entirely in the layer without buildup of excess head. It is noted that a geosynthetic drainage layer is generally required to have a higher transmissivity than that for a granular drainage layer to convey the required design flow rate under unconfined flow conditions. As discussed by Giroud et al. (2000), the geosynthetic drainage layer hydraulic transmissivity that is equivalent to a granular drainage layer hydraulic transmissivity for these conditions can be calculated as:

$$\theta_{dg} = E\theta_{ds} = Ek_{ds}\, t_{ds} \qquad \text{(Eq. 1-4)}$$

where: θ_{dg} = geosynthetic drainage layer transmissivity ($m^3/s/m$); E = equivalency factor (dimensionless); θ_{ds} = granular drainage layer transmissivity ($m^3/s/m$); k_{ds} = granular drainage layer hydraulic conductivity (m/s); and t_{ds} = granular drainage layer thickness (m). The equivalency factor can be approximated as (Giroud et al., 2000):

$$E = \frac{1}{0.88}\left[1 + \left(\frac{t_{ds}}{0.88L_d}\right)\left(\frac{\cos\beta}{\tan\beta}\right)\right] \qquad \text{(Eq. 1-5)}$$

where: L_d = length of drainage layer flow path (m), and all other terms are as defined previously.

The hydraulic transmissivity of geosynthetic drainage layers can be measured in the laboratory using ASTM D4716. The test setup should simulate the actual field conditions as closely as possible in terms of boundary conditions, stresses, and gradient.

1.4.3 Filtration Materials

To prevent clogging of drainage layers, it is often necessary to install a granular or GT filter layer directly over the drainage layer material. The function of the filter is to limit the migration of fines from the overlying soil into the underlying drainage layer, while allowing unimpeded flow of liquid through the filter and into to the drainage layer. If gravel is used as the drainage material, a filter is generally needed as a transition between the overlying waste or soil and the gravel due to dissimilar particle sizes of the respective soils. The filter can be either sand or a GT. If a geosynthetic is used as the drainage material, the filter will always be a GT.

Filter criteria establish the relationship of grain sizes necessary to retain adjacent materials and prevent clogging of a drainage layer, while allowing unimpeded percolation.

1.4.3.1 Granular Soils

Soil filters usually consist of fine to medium sand when placed over coarse sand or gravel drainage layers. The filter particle size distribution must be carefully selected. Fortunately, there is a considerable body of information available to use in selecting a filter particle size distribution (see Koerner and Daniel (1997)). Typically, the criteria described in Cedergren (1989) are used.

To prevent piping from the overlying soil or waste layer into the filter, and from the filter into the drainage layer, these criteria require, respectively:

$$D_{15} \text{ (filter)} / D_{85} \text{ (cover soil)} < 4 \text{ to } 5, \text{ and} \qquad \text{(Eq. 1-6)}$$

$$D_{15} \text{ (drainage layer)} / D_{85} \text{ (filter)} < 4 \text{ to } 5 \qquad \text{(Eq. 1-7)}$$

To maintain adequate permeability of the filter layer and drainage layer, respectively:

$$D_{15} \text{ (filter)} / D_{15} \text{ (cover soil)} > 4 \text{ to } 5, \text{ and} \qquad \text{(Eq. 1-8)}$$

$$D_{15} \text{ (drainage layer)} / D_{15} \text{ (filter)} > 4 \text{ to } 5 \qquad \text{(Eq. 1-9)}$$

where: D_{85} = particle size at which 85% by dry weight of the soil particles are smaller (mm); and D_{15} = particle size at which 15% by dry weight of the soil particles are smaller (mm). The criteria should be satisfied for all layers or media in the drainage system, including protection soil, filter material, and drainage material.

1.4.3.2 Geotextiles

A GT filter must be installed over a GN or GC drainage core when the adjacent material is soil or waste. GT filters are also commonly placed over granular soil drainage layers. As with soil filter layers, GT filters must allow water or leachate to pass unimpeded into the drainage layer while retaining the overlying material and limiting the migration of fines into the drainage material. As with soil filter layers, the design of GT filters involves a two-step process: first to assess permeability (or permittivity); and second to evaluate soil retention (or apparent opening size).

The first step in design of a GT filter is to establish the GT permittivity criterion. The approach to defining this criterion involves first obtaining the permittivity required to achieve unimpeded flow from the material overlying the GT (ψ_{req}) and then applying a factor of safety to obtain the minimum acceptable GT permittivity for the purpose of establishing the construction specification requirement (ψ_{min}). The following equations may be used:

$$\psi_{req} = \frac{k_o}{t} \qquad \text{(Eq.1-10)}$$

$$\psi_{min} = FS\ \psi_{req} \qquad \text{(Eq. 1-11)}$$

where: ψ = GT permittivity (s^{-1}); k_o = GT saturated hydraulic conductivity of overlying material (m/s); t = thickness of GT at a specified normal pressure (m); and FS = factor of safety. A minimum factor of safety of 5 is recommended.

The testing of a GT for permittivity is conceptually similar to the testing of granular soils permeability. In the U.S., the testing is usually performed using the permittivity test, ASTM D4491. Alternatively, some design engineers prefer to work directly with permeability and require the GT's permeability to be some multiple of the adjacent soil's permeability (e.g., a minimum of 5 times higher).

The second step of the design of a GT filter is intended to assure adequate retention of the upgradient soil. There are several methods available for establishing the soil retention requirements of GT filters. Most of the available approaches involve a comparison of the upstream material particle size characteristics and compare them to the 95% opening size of the GT (i.e., defined as O_{95} of the GT). The O_{95} is the approximate largest soil particle size that can pass through the GT. Various test methods are used to estimate O_{95}: (i) in the U.S., wet sieving is used and the value thus obtained is called the apparent opening size (AOS), ASTM D4751; (ii) in Canada and some European countries, hydrodynamic sieving is used and the value thus obtained is called the Filtration Opening Size (FOS); and (iii) in other European countries, wet sieving is used.

The simplest of the design methods compares the GT AOS to standard soil particle sizes as follows (Koerner, 1998):

- for soil with $\leq$ 50% passing the No. 200 sieve (0.074 mm): O_{95} < 0.59 mm (i.e., AOS of the GT $\geq$ No. 30 sieve); and
- for soil with > 50% passing the No. 200 sieve: O_{95} < 0.33 mm (i.e., AOS of the GT $\geq$ No. 50 sieve).

Alternatively, a series of direct comparisons of GT opening size (O_{95} , O_{50} , or O_{15}) can be made to some soil particle size to be retained (D_{90}, D_{85} , or D_{15}). The numeric value depends on the GT type, soil type, flow regime, etc. For example, Carroll (1983) recommends the following relationship:

$$O_{95} < (2 \text{ or } 3)\ D_{85} \qquad \text{(Eq. 1-12)}$$

where: D_{85} = particle size at which 85% by dry weight of the soil particles are smaller (mm); and O_{95} = the 95% opening size of the GT (mm).

However, as shown by Giroud (1982, 1996), this relationship should only be used if the coefficient of uniformity of the soil to be protected is less than four. General procedures, applicable for all values of the coefficient of uniformity of the soil to be protected, are available, see Giroud (1982), Lafleur et al. (1989), and Luettich et al. (1992).

Occasionally, a drainage layer is placed directly against a GCL. For GT-encased GCLs, the GT components may not be adequate to prevent migration of bentonite into the drainage layer. The required filter criteria for this condition are under study, and the manufacturer's and technical literature should be consulted. One study indicated that a 350 g/m^2 nonwoven, needlepunched GT provided adequate protection from bentonite migration for all GCLs investigated (Estornell and Daniel, 1992).

1.4.4 Ancillary Materials and Components

There are a number of other geosynthetic materials that are occasionally or sometimes used in waste containment systems. These other materials are briefly described below.

1.4.4.1 Plastic Pipe (aka Geopipe)

Plastic drainage pipe may be used for a variety of purposes in a waste containment system:

- leachate conveyance and removal within the LCRS;
- liquid conveyance and removal within the LDS;
- percolation water removal within the final cover system internal drainage layer;
- landfill gas transmission and removal within a final cover system gas transmission layer;
- gas extraction wells in a waste mass; and
- leachate injection into a waste mass where leachate recirculation is practiced.

The locations in a landfill where pipes are subjected to the highest compressive stresses are in the LCRS and LDS. These collection systems typically underlie the deepest parts of a landfill, and the compressive strength of the pipe may not be adequate in landfills having large depths of waste.

The allowable overburden stress that can be applied to a given plastic pipe is usually governed by a limiting deflection criterion which design engineers often evaluate using the Iowa State formula (Moser, 1990). This formula uses the full prism weight of the height of overburden and is believed to be conservative (i.e., the formula does not account for soil arching). The subject of plastic pipe capacity will be addressed in this report.

The potential for pipe clogging must also be considered by landfill design engineers. Several states require annual pipe inspection and cleanout as a means to demonstrate that a landfill piping system (or at least part of it) remains functional. While pipe inspections provide information on conditions within the pipe, they do not provide

information on the condition of the pipe backfill or the condition of any filter layer surrounding the pipe backfill. The long-term performance of these waste containment system components with respect to clogging is a subject that merits further investigation.

For piping systems above or within the solid waste (e.g., pipes in the final cover system and pipes used for gas removal or leachate injection), a key design criterion is pipe flexibility. This flexibility is required to accommodate waste settlement (both total and differential) and, in seismic impact zones, seismically-induced deformations. Corrugated or profiled drainage pipe exhibits a high degree of flexibility compared to rigid wall plastic pipe. Corrugated pipe is, however, less strong than rigid wall pipe, and the performance of connections and outlet details must be adequately considered.

1.4.4.2 GM Protection

When granular soil is used to construct an LCRS, it is placed directly above the hydraulic barrier layer, as shown in Figures 1-1 and 1-3. If the soil consists of a coarse sand or gravel, and if the hydraulic barrier includes a GM, the possibility of puncturing of the GM exists. For this situation, a cushion layer may need to be placed between the granular soil and GM. Needlepunched nonwoven GTs are typically used in this application. The key design parameter for GT cushions is the required mass per unit area. An investigation of GM puncture protection was undertaken during the course of this study, and a design methodology was developed for calculating the required mass per unit area of GT needed to prevent puncture. The results of this study are presented in Chapter 2.

1.4.4.3 Erosion Control

For many final cover systems, the establishment of plant species may be aided by placing a natural or GEC layer on the surface before, during, or after seeding. The fact that the final cover system construction is often completed late in the year (i.e., often occurs at the end of the growing season) adds to the need for proactive erosion control measures. Erosion can be harmful in more ways than simply adding to maintenance costs. For example, erosion can lead to clogging of toe drains and exposure of the final cover system internal drainage and/or barrier to unanticipated physical and climatic stresses.

The selection of erosion control materials is based upon the slope angle, slope length, hydrology, time of year, etc. Indeed, there are many such materials to fulfill site-specific needs. Theisen (1992) categorizes the materials, and each is further described in Koerner and Daniel (1997). The field performance of several GEC materials was evaluated as a component of the GCL test plot program described in this report.

1.5 Issues Evaluated in This Study

During the course of this four-year study, various concerns regarding the design construction, and performance of waste containment systems were investigated. By

association with the different principal investigators, these concerns were divided into three broad areas: (i) geosynthetic materials; (ii) natural soil materials; and (iii) field performance. Each area will be described briefly in this section and will then be elaborated upon in the individual chapters and appendices of this report. The remainder of this report is structured as follows:

- geosynthetic material studies are described in Chapter 2 along with Appendices A and B; the principal investigator for these studies was Professor Robert M. Koerner, P.E.;
- natural soil material studies are described in Chapters 3 and 4 along with Appendices C and D; the principal investigator for these studies was Professor David E. Daniel, P.E.;
- field performance studies are described in Chapter 5 along with Appendices E and F; the principal investigator for these studies was Dr. Rudy Bonaparte, P.E.;
- a summary of the project is presented in Chapter 6; and
- long-term landfill management strategies are presented in Appendix G.

1.5.1 Geosynthetic Materials Tasks

Since at least 1982, when the EPA first promulgated regulations requiring the use of GMs in hazardous waste landfill liner systems, a number of different geosynthetic materials have been used in waste containment systems. While geosynthetic materials and design methods have advanced greatly since that time, a number of important technical issues remain. The geosynthetic tasks were undertaken to address five such issues.

1.5.1.1 Puncture Protection of GMs

The possible puncture of GMs from underlying stones in the soil subgrade or from overlying granular drainage materials was experimentally evaluated. The focus of the evaluation was on HDPE GMs since this type of GM is widely used as a liner material beneath the waste mass (where stresses are the highest).

Based on the results of the experimental investigation, a design methodology was developed that can be used to calculate the mass per unit area required for a needlepunched nonwoven GT to prevent puncture of an adjacent GM by a certain size particle.

1.5.1.2 Wave Behavior in HDPE GMs

An experimental evaluation of the fate and disposition of waves, or wrinkles, in HDPE GMs was undertaken. As previously discussed, waves can prevent intimate contact between the GM and natural soil or GCL components of a composite liner and disrupt LCRS and/or LDS flow paths. If severe, waves could also produce unacceptable residual stresses in the GM, which can adversely impact GM service life. The disposition of waves when subsequently covered with soil was evaluated through a large-scale laboratory-testing program. The effects of wave height, applied stress, GM

thickness, and ambient temperature on wave disposition were assessed. All of the tests incorporated strain gaging on the GMs so as to evaluate residual stresses in the test specimens.

All tests were conducted for 1,000 hours, except for one test performed for 10,000 hours. A viscoelastic model was used to extrapolate GM tensile strains measured during the 1,000 hour tests out to 10,000 hours. A second model was used to convert the resulting strains into residual stresses. The results are informative and lead to improved recommendations for GM installation.

1.5.1.3 Plastic Pipe Behavior Under High Overburden Stresses

With the current tendency toward large regional landfills, the height of landfilled wastes is steadily increasing. Fifty-meter high landfills are commonplace, and 100-m high landfills are known to exist. Pipes within the LCRS and LDS beneath such high landfills must be able to function under the high imposed overburden stresses, or, alternatively, the performance limits of these materials (in terms of maximum allowable overburden stress) must be defined.

In this study, the behavior of plastic pipe with respect to excessive deformation was evaluated. A finite element model (FEM) was developed to model the stress-deformation behavior of plastic pipe under high overburden stress. A number of pipe and bedding configurations, including different pipe wall thicknesses, were evaluated. Graphs of waste height versus deformation under both short-term and long-term conditions were developed and calibrated against available test data. Design recommendations are provided.

1.5.1.4 Prediction of GT Service Life

An experimental study to provide data to predict the service life of polypropylene (PP) GTs, polyethylene (PE) geogrids, and polyester (PET) GTs was initiated and is ongoing. The study involves incubation in forced air ovens (oxidation) for the PP GTs and PE geogrids, and in water baths (hydrolysis) for the PET GTs. All incubations are at elevated temperatures, i.e., 50°C to 85°C. The data resulting from post-immersion tests will be extrapolated to site-specific temperatures to estimate the time for 50% degradation of some engineering property (i.e., the halflife) for each material.

As part of this task, a side issue was investigated. This side issue had to do with the potential for auto-catalytic degradation of GTs that had already been partially-degraded by exposure to sunlight after the GTs were backfilled and protected from further exposure to ultraviolet light. The result of the experiments indicates that degradation does not continue after the GT is buried, i.e., the mechanism is not auto-catalytic.

1.5.1.5 Prediction of GM Service Life

An experimental and analytical program was undertaken to develop estimates of the service life of HDPE GMs. As a first step in this effort, three stages in the degradation process were identified:

- antioxidant depletion;
- induction; and
- half-life (i.e., 50% degradation) of an engineering property.

Laboratory incubation chambers, designed to simulate oxidizing conditions below the GM and liquid exposure above the BM and a compressive stress equivalent to a 30 m high landfill, were used to obtain data to estimate the time durations of the first two stages of the degradation process. Work is still ongoing to further define the duration of the third stage under the test condition. Also, several additional incubation scenarios are still under investigation, i.e., exposure of the GM to moving water, exposure in air, and exposure under simulated sunlight.

1.5.2 Natural Materials Tasks

Natural materials (clays and granular soils) are widely used for a variety of functions in waste containment systems. A number of tasks were undertaken to address issues and questions remaining with respect to the use of these natural materials in waste containment systems.

1.5.2.1 GCL Test Plots in Cincinnati, Ohio

This task involved design, construction, and performance monitoring of 14 full-scale final cover system test plots, all containing a GCL hydraulic barrier component. The test plots were constructed on both 3H:1V slopes and 2H:1V slopes. The goal of this task was to evaluate the internal shear strength of three of the four types of commercially-available GCLs (see Section 1.4.1.3), namely:

- needlepunched reinforced GCL;
- stitch-bonded reinforced GCL; and
- unreinforced GM/bentonite composite GCL.

Four different commercially-available products were evaluated. The test plot slopes were constructed in November of 1994, and internal stresses were mobilized by cutting the overlying geosynthetics in the spring of 1995. Monitoring (using subgrade moisture sensors, bentonite moisture sensors, and deformation gages on the upper and lower surfaces of the GCLs) has been ongoing. This has resulted in a number of important technical findings, recommendations regarding the design of GCLs for final cover system applications, and recommendations for using GCL materials on sideslopes.

1.5.2.2 CCL Test Pad Analysis

This task involved collecting and analyzing data on the field performance of CCL test pads that had been constructed and monitored. The test pads were located throughout the U.S. In all, data from 102 test pad projects were obtained and analyzed. Eighty-seven of the test pads were constructed to verify that a hydraulic conductivity of 1×10^{-7} cm/s or less could be achieved using the proposed project soil material and construction methods. Test pad results were correlated to a number of different variables, including:

- index properties;
- particle-size distribution;
- compaction moisture content;
- degree of saturation;
- compaction density; and
- total thickness.

This task also involved the analysis of laboratory hydraulic conductivity testing of soils from the test pad sites (whenever available) to establish correlation between results from laboratory and field hydraulic conductivity tests.

1.5.2.3 Admixed Liners

This task focused on the use of soil-bentonite mixtures in admixed natural soil liners to achieve a hydraulic conductivity of 1×10^{-7} cm/s or less. Admixtures are often used when local borrow soil alone is not capable of meeting the hydraulic conductivity criterion. In many cases, the addition of bentonite into the soil, typically at a dry weight application rate of 2 to 12%, will produce an admixed soil liner capable of meeting the hydraulic conductivity criterion.

For this task, a database of 12 case studies was developed. The case study information is presented and analyzed. Comparisons to the findings for CCL liners are also presented.

1.5.2.4 CCLs in Final Covers

Federal regulations and most state regulations allow the use of CCLs either alone, or in combination with a GM, as a component of landfill final cover systems. Concerns associated with the use of CCLs in final cover systems include:

- degradation due to freeze-thaw;
- degradation due to shrink-swell;
- cracking from differential settlement; and
- deformations when placed on steep sideslopes.

For this task a number of field case histories were collected and analyzed. Results of the analysis are presented and recommendations with respect to the use of CCLs in final cover systems are presented.

1.5.3 Field Performance Tasks

Solid waste containment facility regulations have been in place for a number of years and assessment of the field performance of facilities meeting these regulations and especially the more recent regulations (e.g., land disposal restrictions of 40 CFR 268, which were progressively implemented from 1986 to 1994), is both timely and essential. These tasks are focused on providing information and insight into the field performance of waste containment systems, particularly liner and final cover systems for landfills. The four field performance tasks performed for this project are described below.

1.5.3.1 Review of Published Information

Available published information on the field performance of modern waste containment systems generally designed and constructed to current standards was collected and reviewed. The collected information, including approximately 100 technical papers and reports, is related to the performance of liner systems, final cover systems, LCRSs, and entire waste management units. The state of knowledge with respect to the field performance of these systems has been assessed and is included in the following field performance tasks.

1.5.3.2 Data Collection and Analysis

Data related to the performance of liner systems for double-lined waste management facilities designed and constructed to current standards have been collected and analyzed for 54 landfill facilities, representing a total of 189 landfill cells. The data cover more than an eight-year monitoring period for some facilities. The data was assembled into a database that includes: (i) general facility information (e.g., location, average annual rainfall, and subsurface soil type); (ii) general cell information (e.g., waste type, cell area, dates of construction, operation, and closure); (iii) details of the liner system and final cover system (e.g., material type, thickness, and hydraulic conductivity of each layer); (iv) LCRS flow quantities and chemical constituent concentrations; and (v) LDS flow quantities and chemical constituent concentrations. The results of this task are summarized and analyzed, and conclusions are drawn with respect to leachate generation rates, GM and composite liner performance capabilities, and leachate chemical constituents.

1.5.3.3 Assessment of Problem Facilities

Through the work conducted as part of the previous two tasks, as well as a supplemental survey of the technical literature and interviews with regulatory personnel, waste containment system problems were identified at 66 landfill and five surface impoundment facilities. The problems generally deal with the following areas; (i) slope instability or excessive deformation of liner systems or cover systems; (ii) defective as-

built components of liner systems or final cover systems; (iii) degraded components of liner systems or final cover systems; and (iv) malfunction of LCRSs or LDSs, or operational problems with these systems. The primary human factor contributing to the problem is classified as design, construction, or operation related. Case histories of the problems are provided. The case histories document the observed problem, the design, construction, and/or operational factors that led to the problem, and any implemented solution and present specific lessons that can be learned from the problem. Based on an evaluation of the data for the facilities, recommendations are developed for reducing such problems in the future.

1.5.3.4 Comparison of Actual and HELP Model Predicted LCRS Flow Rates

Measured LCRS flow rates for eight landfill cells are compared to flow rates predicted using Version 3.04a of the EPA HELP computer code. Cells were selected for evaluation based on: (i) the completeness of design, operation, and LCRS flow rate data for the cells; and (ii) waste type and geographic location of the cells. The measured LCRS flow rates are compared to flow rates simulated using the HELP model to assess whether the observed trends in measured flows from cells with different waste types and in different geographic locations are reasonably predicted. The HELP model simulations were performed using estimated hydraulic properties for the landfill liner system components and waste and either: (i) synthetic solar radiation, rainfall, and temperature data generated for the site using the HELP model, or (ii) synthetic solar radiation data and actual rainfall and temperature data recorded in the vicinity of the site. A parametric analysis is also performed to develop general guidelines on the selection of HELP model input parameters to better predict LCRS flow rates.

1.6 References

ASTM D422 - Test Method for Particle-Size Analysis of Soils.

ASTM D4318 – Test Methods for Liquid Limit, Plastic Limit, and Plasticity Index of Soils

ASTM D4491 - Test Methods for Water Permeability of Geotextiles by Permittivity.

ASTM D4716 - Test Method for Constant Head Hydraulic Transmissivity (In-Plane Flow) of Geotextiles and Geotextile Related Products.

ASTM D4751 - Test Method for Determining Apparent Opening Size of a Geotextile.

ASTM D5321 - Test Method for Determining the Coefficient of Soil and Geosynthetic or Geosynthetic and Geosynthetic Friction by the Direct Shear Method.

ASTM E96 - Test Methods for Water Vapor Transmission of Materials.

Bonaparte, R., Gross, B. A., Daniel, D. E., Koerner, R. M., and Dwyer, S. F. (2002), "*Technical Guidance for RCRA/CERCLA Final Covers*," U.S. EPA Office of Solid Waste and Emergency Response, Washington, D.C. (in final review)

Bonaparte, R. (1995), "Long-Term Performance of Landfills," *Proceedings of the ASCE Specialty Conference Geoenvironment 2000,* ASCE Geotechnical Special Publication No. 46, Vol. 1, pp. 415-553.

Bonaparte, R. and Othman, M. A. (1995), "Characteristics of Modern MSW Landfill Performance," *Geotechnical News,* Vol. 13, No. 1, pp. 25-30.

Carroll, R. G., Jr. (1983), "Geotextile Filter Criteria," Transportation Research Record 916, Transportation Research Board, Washington, DC, pp. 46-53.
Cedergren, H. R. (1989), *Seepage, Drainage, and Flow Nets*, 3rd Edition, John Wiley & Sons, Inc., New York, NY, 464 pgs.
Daniel, D. E. and Scranton, H. G. (1996), *Report of 1995 Workshop on Geosynthetic Clay Liners*, EPA/600/R-96/149, June, 93 pgs.
Daniel, D. E. and Wu, Y. K. (1993), "Compacted Clay Liners and Covers for Arid Sites," *Journal of Geotechnical Engineering*, Vol. 119, No. 2, pp. 223-227.
EPA (1989), *Final Covers on Hazardous Waste Landfills and Surface Impoundments*, Technical Guidance Document, EPA/530/SW-89/047, U.S. EPA, Office of Solid Waste and Emergency Response, Washington, D.C., 39 pgs.
EPA (1991), *Design and Construction of RCRA/CERCLA Final Covers*, Seminar Publication, EPA/625/4-91/025, U.S. EPA, Office of Research and Development, Washington, D.C., 145 pgs.
EPA (1993), *Presumptive Remedy for CERCLA Municipal Landfill Sites*, OSWER Directive No. 9355.0-49FS, EPA/540/F-93/035, U.S. EPA, Office of Solid Waste and Emergency Response, Washington, D.C., 14 pgs.
Estornell, P. M. and Daniel, D. E. (1992), "Hydraulic Conductivity of Three Geosynthetic Clay Liners," *Journal of Geotechnical Engineering*, Vol. 118, No. 10, pp. 1592-1606.
Giroud, J. P. (1982), "Filter Criteria for Geotextiles," *Proceedings of the Second International Conference on Geotextiles*, Las Vegas, NV, Vol. 1, Industrial Fabrics Association International, St. Paul, MN, pp. 103-108.
Giroud, J. P. (1996), "Granular Filters and Geotextile Filters," *Proceedings of GeoFilters '96*, Lafleur, J. and Rollin, A. L., Editors, Montréal, Canada, May 1996, pp. 565-680.
Giroud, J. P. and Bonaparte, R. (1989), "Leakage Through Liners Constructed with Geomembranes. Part II: Composite Liners," *Geotextiles and Geomembranes*, Vol. 8, No. 2, pp. 77-111.
Giroud, J. P., Gross, B. A., Bonaparte, R. and McKelvey, J. A. (1997), "Leachate Flow in Leakage Collection Layers Due to Defects in Geomembrane Liners," *Geosynthetics International*, Vol. 4, Nos. 3 and 4, pp. 215-292.
Giroud, J.P., Zhao, A., and Bonaparte, R.B. (2000), “The Myth of Hydraulic Transmissivity Equivalency Between Geosynthetic and Granular Liquid Collection Layers”, *Geosynthetics International*, Vol. 7, Nos. 4-6, pp. 381-401.
Gross, B. A., Bonaparte, R. and Giroud, J. P. (1990), "Evaluation of Flow from Landfill Leakage Detection Layers," *Proceedings of the 4th International Conference on Geotextiles and Geomembranes and Related Products,* The Hague, Netherlands, May 28 - June 1, 1990, pp. 481-486.
Jo, H. Y., Katsumi, T., Benson, C. H., Edil, T. B. (2001), “Hydraulic Conductivity and Swelling of Nonprehydrated GCLs Permeated with Single-Species Salt Solutions”, *Journal of Geotechnical and Geoenvironmental Engineering*, ASCE, Vol. 127, No. 7, pp. 557-567.
Koerner, R. M. (1998), *Designing with Geosynthetics*, 4th Edition, Prentice Hall, Englewood Cliffs, NJ, 761 pgs.

Koerner, R. M. and Daniel, D. E. (1994), "A suggested methodology for assessing the technical equivalency of GCLs to CCLs", *Proceedings of Geosynthetics Research International-7 Conference on Geosynthetic Liner Systems,* IFAI, St. Paul, MN, pp. 255-275.

Koerner, R. M. and Daniel, D. E. (1997), *Final Covers for Solid Waste Landfills and Abandoned Dumps*, ASCE Press, Reston, VA, 321 pgs.

Lafleur, J., Mlynarek, J. and Rollin, A. L. (1989), "Filtration of Broadly Graded Cohesionless Soils," *Journal of Geotechnical Engineering*, ASCE, Vol. 115, No. 12, pp. 1747-1768.

Luettich, S. M., Giroud, J. P. and Bachus, R. C. (1992), "Geotextile Filter Design Guide," *Geotextiles and Geomembranes*, Vol. 11, pp. 355-370.

Moser, A. P. (1990), *Buried Pipe Design*, McGraw-Hill, New York, NY.

Schroeder, P. R., Dozier, T. S., Zappi, P. A., McEnroe, B. M., Sjostrom, J. W. and Peyton R. L., (1994) *The Hydrologic Evaluation of Landfill Performance (HELP) Model: Engineering Documentation for Version 3*, EPA/600/R-94/168b, U. S. EPA, Risk Reduction Engineering Laboratory, Cincinnati, OH.

Shackelford, C. D., Benson, C. H., Katsumi, T., Edil, T. B., and Lin, L. (2000), "Evaluating the Hydraulic Conductivity of GCLs Permeated with Non-standard Liquids", *Geotextiles and Geomembranes*, Elsevier, Amsterdam, Vol. 18 Nos. 2-4, pp. 133-161.

Theisen, M.S. (1992), "The Role of Geosynthetics in Erosion and Sediment Control: An Overview," *Journal of Geotextiles and Geomembranes*, Vol. 11, Nos. 4-6, pp. 199-214.

Wilson-Fahmy, R. and Koerner, R. M. (1995), "Leakage Rates Through a Hole in a GM Overlying a Geosynthetic Clay Liner," *Proceedings of Geosynthetics '95*, IFAI, St. Paul, MN, pp. 655-668.

Chapter 2
Geosynthetic Tasks

This chapter presents the results of tasks that were directed specifically toward geosynthetics. Five different topics were investigated on the basis of concerns shared by the Agency and the principal investigators. The five topics are the following:

- puncture protection of GMs;
- wave behavior in HDPE GMs (with additional detail in Appendix A);
- plastic pipe behavior under high vertical stresses;
- lifetime prediction of GTs; and
- lifetime prediction of GMs (with additional detail in Appendix B).

2.1 Puncture Protection of GMs

GMs are used as barrier layers in various applications such as, in liner systems and cover systems for landfills, waste piles, and surface impoundments; as liners for oil and gas tank secondary containment systems; and for other environmental applications. Because GMs are located at the base of these contained materials, remediation of a puncture failure would generally be very difficult and expensive. This, in addition to the fact that detection of failure is not easily accomplished and, in some cases, may not even be possible, emphasizes the need to adequately protect GMs against puncture. Leakage through the GM in many of these applications may pose a risk to human health and the environment.

2.1.1 Overview

One of the mechanisms by which the hydraulic barrier function of a GM may be compromised is puncture. Puncture holes in a GM will increase the potential for leakage through it, whether the GM is the entire hydraulic barrier or part of a composite liner (Giroud and Bonaparte, 1989).

In GM applications, the puncturing object may be a stone in the subgrade or leachate collection soil placed above the GM. Because of a lack of a rational design method, puncture design is currently considered in a rather arbitrary manner. For example, the current state-of-practice for landfill liner system applications in the U.S. involves the use of a needlepunched nonwoven GT with a mass per unit area in the range of 250 to 600 g/m^2 as a protection material depending upon the maximum size of material in contact with the GM. On the other hand, significantly heavier needlepunched nonwoven GTs (mass per unit area of 1000 to 3000 g/m^2) are used in Germany despite the fact that only rounded gravel is allowed above the GM. The discrepancy between these two practices emphasizes the need for a rational design method capable of providing a puncture free GM as cost effective as possible.

In this chapter, a theoretical framework for evaluating the puncture behavior of GMs is presented first. The framework is applicable to unprotected GMs as well as GMs protected using needlepunched nonwoven GTs. The puncturing object is characterized by its shape and height above a firm subgrade. The GM behavior is considered in terms of its tensile load-elongation behavior. The protection material is characterized by both its thickness and its load-elongation behavior.

Following development of the theoretical framework, the results of an experimental study are presented in which the performance of a variety of protection materials is evaluated. The tested materials included nonwoven and woven GTs (both virgin and recycled), GCLs, used carpets (both industrial and domestic), and shredded tire rubber mats. The main focus is, however, on virgin needlepunched nonwoven GTs since these are the most commonly used materials for GM puncture protection. The GM used in most of the study is a 1.5-mm thick HDPE GM.

Based on the data obtained from the experimental investigation and supplemented by predictions using the theoretical analysis, a design methodology, with examples, is presented for use with needlepunched nonwoven GTs used as protection layers under a variety of possible field conditions.

2.1.2 Theoretical Aspects of GM Puncture

A framework for considering GM puncture has been developed by considering axisymmetric conditions on a single isolated protrusion (Figure 2-1). The loading is assumed to be hydrostatic allowing for the deformed catenary shape of the GM to gradually decrease into the underlying void space. Simultaneously, a larger portion of the GM conforms to the tip of the protrusion. To obtain a solution, several assumptions are necessary:

- the GM possesses no bending stiffness;
- the load-extension behavior of the GM is linear elastic;
- the GM in contact with the protrusion tip is assumed to be in a state of equal stress by analogy with membrane theory for a GM subjected to hydrostatic pressure;
- the contact between the GM and the protrusion tip is frictionless;
- tensile strains cease to occur in the GM after it conforms to the subgrade, i.e., the portion of the GM in contact with the subgrade becomes fixed in its position;
- the suspended portion of the GM is in a state of equal tension, i.e., the force per unit width at any radius multiplied by the circumference at that radius is constant; and
- Poisson's ratio effect is neglected.

From the equilibrium of an infinitesimal element, the following equation results:

$$2\pi(R_i - x)p_i ds = 2F_i \sin\left(\frac{d\psi}{2}\right) \qquad \text{(Eq. 2-1)}$$

where:

(R_i-x) = radius from protrusion center to an infinitesimal element;
ds = chord length of the element;
i = subscript referring to the instantaneous position of the GM;
p_i = pressure applied from overlying material;
F_i = total force in GM, i.e., force/unit width at any radius multiplied by the circumference at that radius; and
$d\psi$ = change in tangent slope angle.

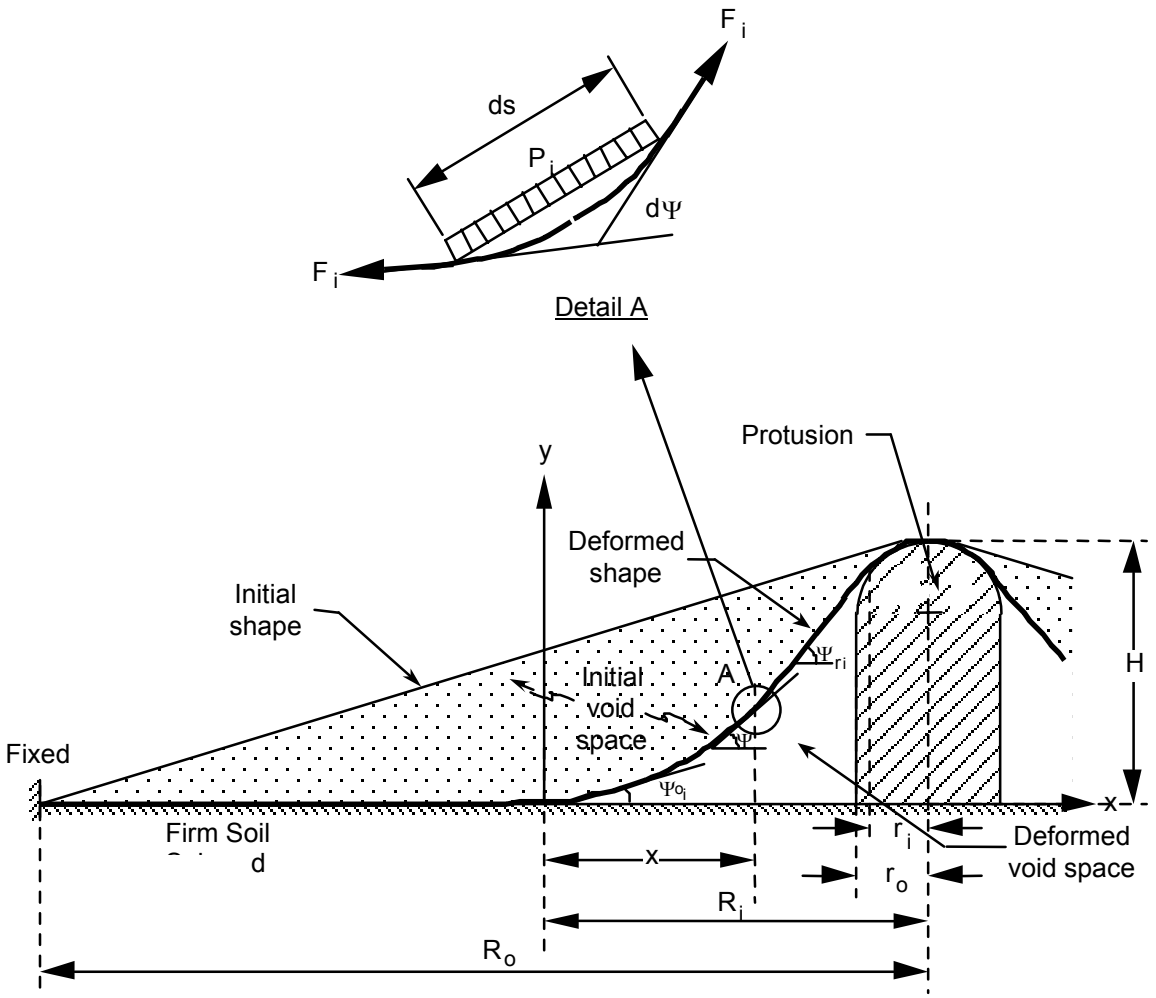

Figure 2-1. Geometry used in theoretical analysis for GM puncture.

As part of this research study, Equation 2-1 was solved with various boundary conditions and material (GM and GT) properties. From the result of this study, the following conclusions were reached by Wilson-Fahmy et al. (1996):

- The protrusion height simulates an isolated stone on a soil subgrade.
- Decreasing the tip radius is indicative of sharper stones or other puncturing objects.
- R_O/H ratios greater than 4.0 are representative of an isolated stone case.
- For a closely spaced assemblage of cones, e.g., a gravel drainage layer, a protrusion height equal to one-half of the maximum stone size is a reasonable approximation.
- The required puncture resistance is decreased for smaller stones rather than large ones, rounded stones rather than angular ones, and a bed of stones as compared to isolated stones.
- The puncture strength of a GM is improved with greater thickness, use of a GT, use of relatively thick GTs, and increased tensile strength of the GT.

2.1.3 Experimental Aspects of GM Puncture

A truncated cone arrangement was used to simulate a worst-case field condition. An array of three such cones was placed in a pressure vessel and backfilled with sand, leaving a protrusion height of a given amount (Figure 2-2). Using this device, approximately 200 tests were conducted for a range of conditions to evaluate the effects of GM puncture behavior. These tests consisted of the following material variations:

- HDPE GMs - 1.0 to 2.5 mm thick;
- PP and PET needlepunched nonwoven GTs - mass per unit area of 130 to 1350 g/m^2;
- continuous filament and staple fiber GTs;
- an assortment of other GTs made from virgin and post consumer plastics;
- discarded carpets; and
- rubber tire mats.

The test results demonstrated the improved puncture resistance of GMs protected by needlepunched nonwoven GTs compared to GMs alone. Both PP and PET, comprised of either continuous or staple fibers, produced a set of curves with very uniform trends (Figure 2-3). The test results for these materials were used to develop an equation that forms the basis of the design method:

$$p_{allow} = 450 \frac{M}{H^2} \qquad \text{(Eq. 2-2)}$$

where:

p_{allow} = allowable bearing pressure for GT-protected 1.5-mm thick HDPE GM (kPa);
M = mass per unit area of the protection GT (g/m^2); and
H = effective height of the protruding object (mm).

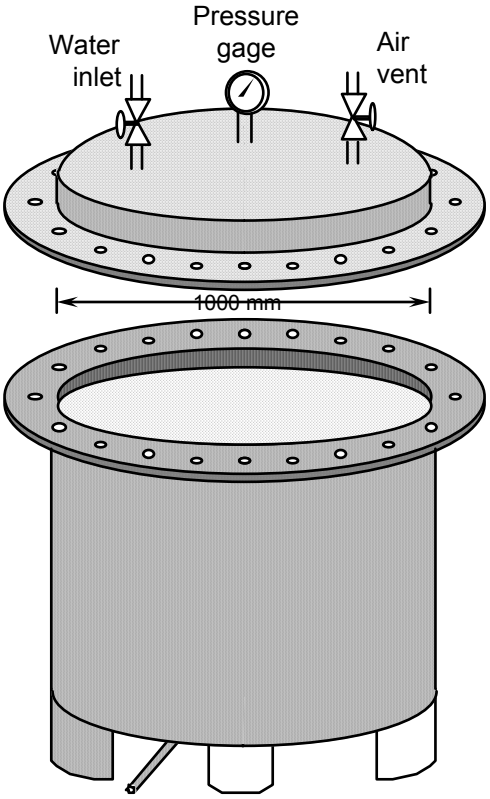

(a) Pressure vessel

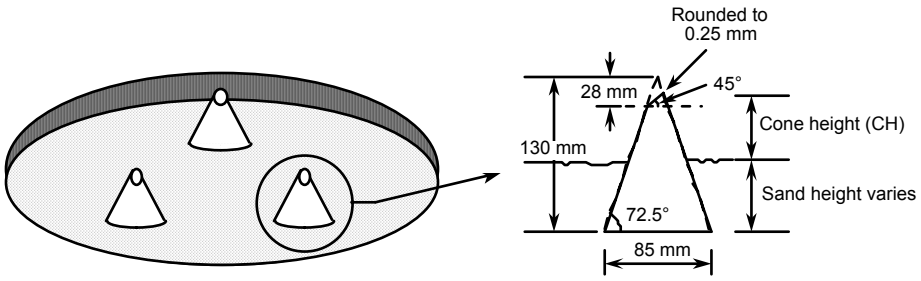

(b) Details of truncated cones

Figure 2-2. Details of the hydraulic pressure vessel and truncated cones for geomembrane puncture evaluation tests.

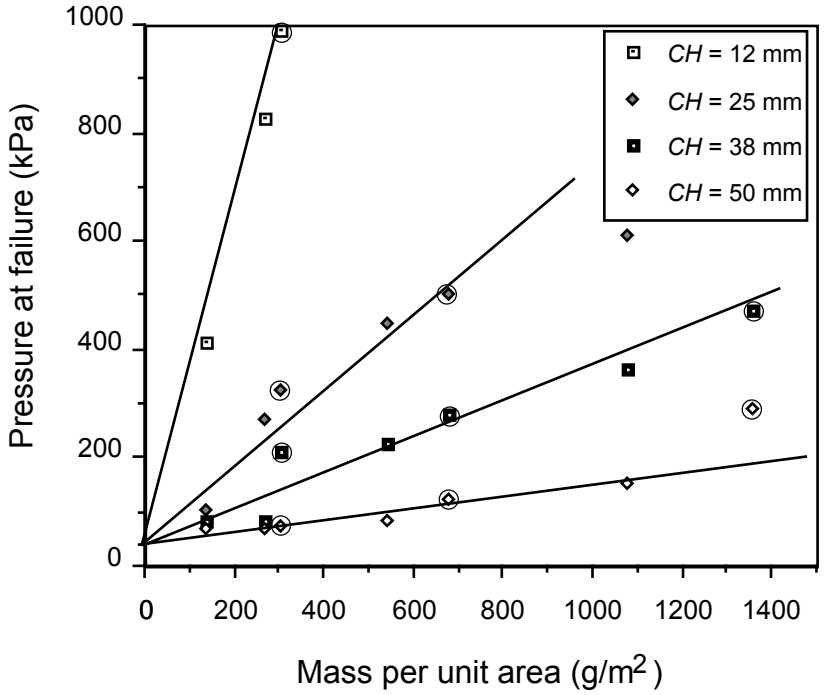

Figure 2-3. Failure pressure versus mass per unit area for nonwoven needle punched GTs at different cone heights. Data includes both PET continuous filament (not encircled) and PP staple fiber (encircled) GTs.

The failure pressures predicted using Equation 2-2 are plotted against the actual failure pressures from the laboratory tests in Figure 2-4, which is seen to result in a correlation coefficient of 0.973.

Equation 2-2 was then adjusted from the worst-case truncated cones used in the experiments to actual soils through introduction of a number of different experimentally-obtained modification factors to account for particle shape, packing density, arching, and reduction factors to account for GT creep and long-term degradation. The final form of the equation, as presented by Narejo et al. (1996), is:

$$p'_{allow} = \left(450\frac{M}{H^2}\right)\left(\frac{1}{MF_S \times MF_{PD} \times MF_A}\right)\left(\frac{1}{RF_{CR} \times RF_{CBD}}\right) \qquad \text{(Eq. 2-3)}$$

where:

p'_{allow} = modified allowable pressure for GT-protected 1.5-mm thick HDPE GM (kPa);
M = mass per unit area of the protection GT (g/m^2);
H = effective height of the protruding object (mm);
MF_S = modification factor for protrusion shape (≥ 1.0);
MF_{PD} = modification factor for packing density (≥ 1.0);

MF_A = modification factor for arching (≥ 1.0);
RF_{CR} = reduction factor for creep (≤ 1.0); and
RF_{CBD} = reduction factor for chemical/biological degradation (≤1.0).

Finally, the factor of safety is formulated in the traditional manner:

$$FS = \frac{p'_{allow}}{p_{applied}} \qquad \text{(Eq. 2-4)}$$

where:

FS = factor of safety; and
$p_{applied}$ = applied pressure (kPa) (i.e., the maximum pressure exerted on the GM).

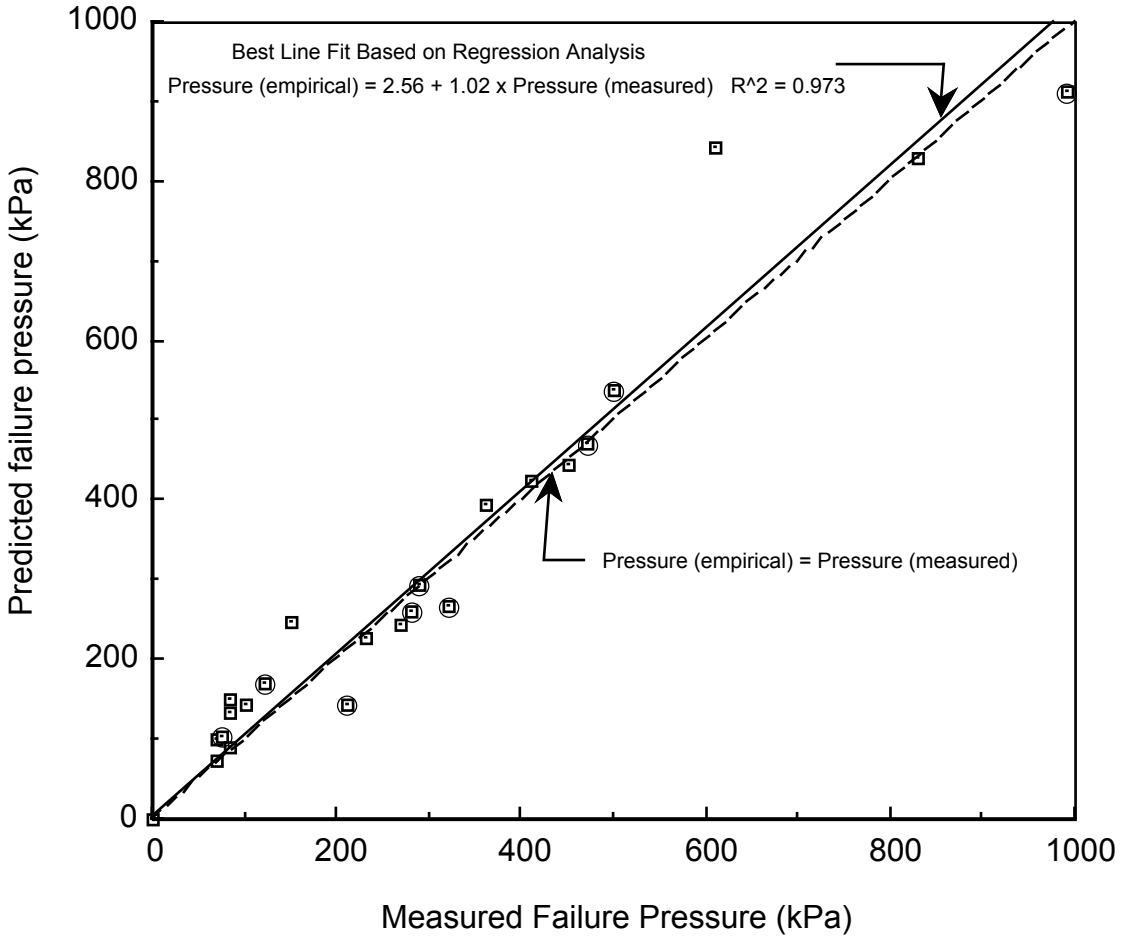

Figure 2-4. Measured values versus empirically predicted failure pressures for all nonwoven needle punched GTs evaluated in association with 1.5 mm HDPE GMs. Data includes both PET continuous filament (not encircled) and PP staple fiber (encircled) GTs.

2.1.4 Puncture Protection Design Methodology

Equations 2-3 and 2-4 provide the basis for a puncture protection design methodology. If the protection GT mass per unit area is known, the two equations are solved to obtain a factor of safety against puncture. If the protection GT is not known (as is usually the case in design), a factor of safety is selected and the equations are solved for the unknown, M, the required mass per unit area of the GT. For purposes of the design examples in this chapter, a factor of safety of 3.0 has been used. This factor of safety value is arbitrary, and the design engineer will need to select a value considering project specific criteria. Given the uncertainties associated with any real design case, a minimum factor of safety of 2.5 is recommended.

2.1.5 Examples

The following illustrative examples are taken from Koerner et al. (1996).

(a) A 30-m high landfill using 25 to 38-mm size gravel as a leachate collection layer on a 1.5-mm thick HDPE GM requires a protective cushion consisting of a GT protection layer having a mass per unit area of 590 g/m^2 to achieve a FS = 3.0.
(b) The same problem, but now for 100 m of waste, requires a protective cushion consisting of a GT protection layer having a mass unit area of 1,600 g/m^2 to achieve a FS = 3.0.
(c) Using a 2000 g/m^2 GT under 16 to 32 mm rounded leachate collection stone (as required in Germany) for a 30-m high landfill results in FS ≈ 15.
(d) A 10-m deep surface impoundment with 12-mm size stones in the soil subgrade under the GM requires a 330 g/m^2 GT, while the same conditions but 25-mm size stones requires a 550 g/m^2 GT. Both examples use a FS = 3.0.

Using the available design methodology and a site-specific FS, the required mass per unit area of a needlepunched nonwoven protection GT over or under an HDPE GM can be obtained. It should be noted that puncture during installation is not addressed by this method. GTs require a minimum mass per unit area based on installation considerations alone (Richardson, 1996).

2.2 Wave Behavior in GMs

It is a frequent occurrence to see thermally-induced waves in seamed GMs after installation and prior to covering or backfilling. The fate and disposition of these waves after backfilling were studied in this task. The study involved laboratory modeling under controlled conditions. Due to their relative stiffness and thickness, waves are of more concern for HDPE GMs than for most other commercially-available products. Thus, HDPE GMs were the focus of the study. It should be noted, however, that all GMs in commercial use have coefficients of expansion/contraction within an order of magnitude of one another, and the problem of excess slack is common to all types of GM products.

2.2.1 Large-Scale Experiments

A large-scale (1.8 m by 1.0 m by 1.0 m) experimental test box was constructed in the laboratory to evaluate the behavior of HDPE GM waves. Smooth HDPE GM specimens, 1.5 mm thick, of different lengths were placed in the box to create waves of different sizes, and sand was placed over the specimens (Figure 2-5). The box had plastic front and rear windows for visual monitoring of wave deformation under normal stress. The results for the initial series of tests on large, moderate and small waves, as quantified by the height-to-width (H/W) ratio, are given in Figure 2-6. Note that even under the highest normal stress that could be exerted by the box (e.g., 70 kPa), the waves remained and the H/W ratios increased considerably over the original H/W ratios.

By adjusting the ends of the waves to be located at the edges of the viewing windows and applying normal stress, it was seen that the wave end points did not move, irrespective of the amount of GM lying horizontally beyond the wave. It was concluded that as normal stress is applied to the entire GM, the flat GM surfaces are held in position by mobilized frictional forces between the GM and overlying and underlying sand layers. This was the case for all tests. Thus, the only wave movement possible is in decreasing the void space beneath the original size wave. There is no meaningful lateral deformation beyond the wave itself. One consequence of this observation is that the frictional forces on the upper and lower GM surfaces restrict the ability of GM waves to dissipate laterally as normal stresses are applied in the field. A second consequence, applicable to laboratory testing, is that smaller laboratory test boxes can be used with full sized waves as the GM lengths beyond the wave end points need not be large. It is easier to apply high normal stresses (e.g., greater than 1,000 kPa) to a smaller box. In addition, the smaller setups could be housed in an environmental room. As a result, four steel boxes measuring 300 mm by 300 mm by 300 mm were assembled with thick plastic faces for visual observation. The large box was subsequently used for a 10,000 hour control test.

2.2.2 Small-Scale Experiments and Results

Using the smaller boxes, a number of variables were investigated (Table 2-1). In all of these tests, at least six electrical resistance strain gages were bonded to the surfaces of the smooth HDPE GM near the crest and inflection points. The gages were bonded onto the side of the GM subject to extensional deformations. All tests were conducted for 1,000 hours. The results of these tests are summarized below:

Regarding the original wave heights (which varied from 14 to 80 mm):

- wave height decreased with increasing normal stress;
- an average reduction in wave heights of 40% was observed after 1,000 hours;
- GM thickness had a negligible effect on the decrease of wave height with normal stress;
- there was a slight decrease in wave height with increasing temperature;
- final wave heights were 5 to 47 mm; and
- intimate contact with the soil subgrade was never achieved.

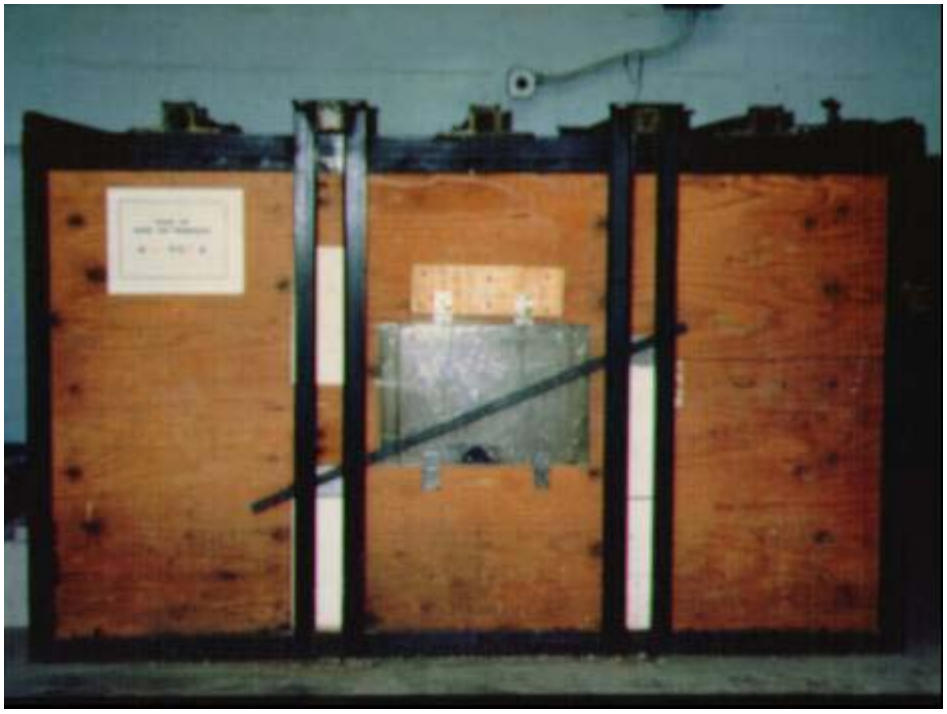

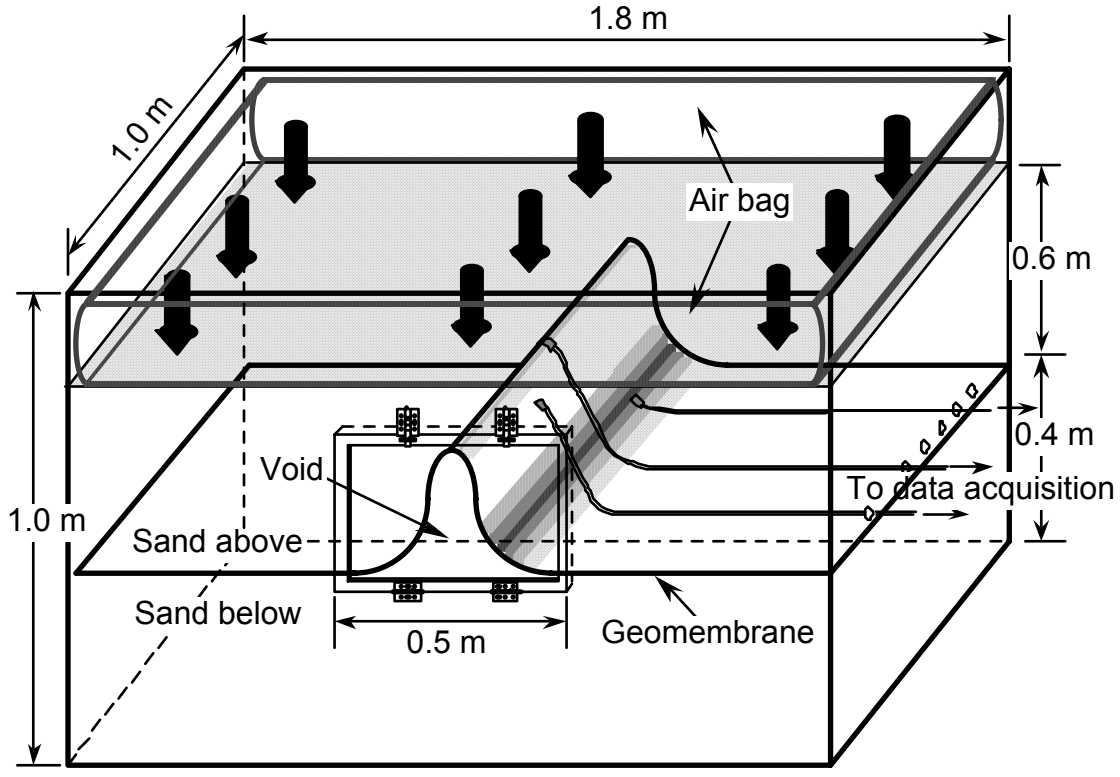

Figure 2-5. Photograph and schematic illustration of the large-scale experimental test box used in wave study.

(a) Relatively Large Wave

	Ht.	H/W
Original (0 kPa)	240 mm	0.5
Final (70 kPa)	125 mm	2.0

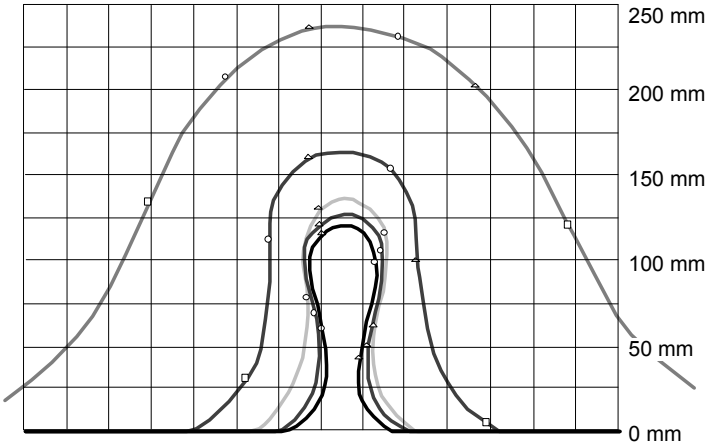

(b) Moderate Wave

	Ht.	H/W
Original (0 kPa)	130 mm	0.4
Final (70 kPa)	70 mm	0.9

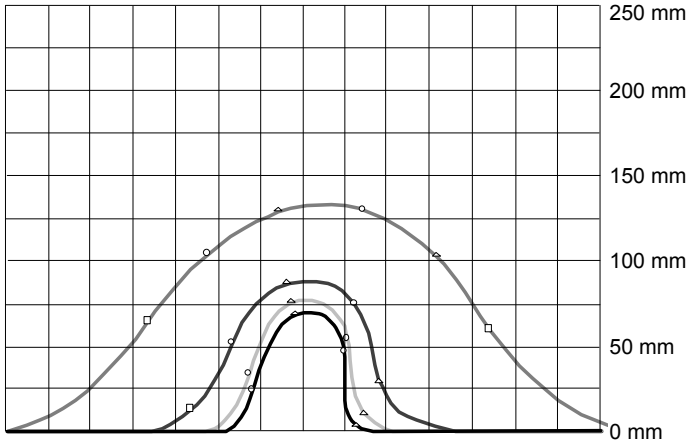

(c) Relatively Small Wave

	Ht.	H/W
Original (0 kPa)	80 mm	0.25
Final (70 kPa)	35 mm	0.4

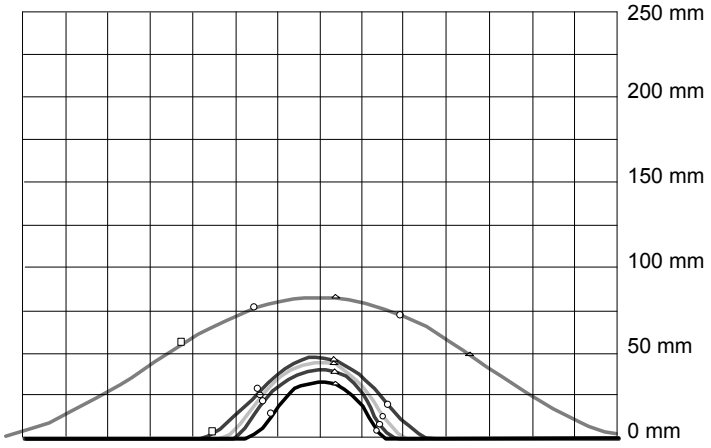

Figure 2-6. Results of profile-tracing of three preliminary tests on different size waves in 1.5 mm thick HDPE GMs subjected to increasing vertical pressures.

Table 2-1. Experiments Conducted Using Small-Scale Test Boxes.

Experimental Parameter Evaluated	Experimental Conditions			
	Normal Stress (kPa)	Original Height of Wave, (mm)	GM Thickness (mm)	Temperature (°C)
Normal Stress (kPa)	180 360 700 1,100	60	1.5	23
Height of Wave (mm)	700	14 20 40 60 80	1.5	23
GM Thickness (mm)	700	60	1.0 1.5 2.0 2.5	23
Testing Temperature (°C)	700	14 20 40 60	1.5	23 42 55

Regarding the original H/W values for the waves (which varied from 0.17 to 0.33):

- H/W increased with increasing normal stress;
- H/W increased approximately linearly with increasing original wave height;
- H/W decreased approximately linearly with increasing GM thickness;
- H/W decreased slightly with increasing temperature; and
- final H/W values varied from 0.14 to 0.65.

Regarding the tensile strains measured along the top of the GM near the crest of the wave and the bottom of the GM near the inflection points of the wave at its sides:

- strains increased with increasing normal stress;
- strains increased with increasing original wave height;
- strains increased with increasing GM thickness;
- strains increased slightly with increasing temperature; and
- maximum strains within each test series varied from 3.2% to 4.9%.

2.2.3 Data Extrapolation and Analysis

The results of a 10,000-hour control test performed in the large box were compared to predicted results extrapolated using experimental data up to 1,000 hours and the Kelvin-chain model. This model has been shown to be applicable for extrapolating physical property test results for a wide range of polymeric geosynthetic materials,

Soong and Koerner (1998). The extrapolated data showed good agreement with the experimental data. Therefore, it was considered reasonable to extrapolate all of the data from the 1,000-hour experiments to 10,000 hours using the Kelvin-chain model. The resulting values of maximum tensile strains were converted to stresses using temperature adjusted moduli values. The resulting tensile stresses were adjusted downward to account for stress relaxation using a Maxwell-Weichert model, see Soong and Lord (1998). The effect of stress relaxation was to significantly decrease the residual stress values compared to the non-adjusted values. However, the residual stresses were still significant. Table 2-2 gives the residual stresses remaining in the waves after 10,000 hours, and the corresponding percentage of short-term yield stress values.

2.2.4 Discussion

These laboratory tests appear to indicate that waves remaining in field-seamed HDPE GMs at the time of covering or backfilling do not disappear. Even the smallest wave (14 mm), at the highest normal stress (1100 kPa), for the thinnest GM (1.0 mm), at the highest temperature (55°C), remained elevated above the soil subgrade. The authors' conclusions with respect to the possible significance of these findings are as follows:

- intimate contact with the soil subgrade is not achieved when even only small waves remain in an HDPE GM upon backfilling, and even when the GM is subjected to relatively high normal stresses;
- all waves not in contact with the subgrade have some amount of residual tensile stress, the amount depending primarily on the size and shape of the wave in its final configuration;
- the waves probably form some retardation to flow of leachate on top of the GM, the implications of which have not been evaluated; and
- possible long-term implications of trapped waves in HDPE (and other types) GMs have not been evaluated and are beyond the scope of this project.

It is the authors' belief that the results of this task may have important ramifications for the way in which GM liners are installed, see Eith and Koerner (1997). The complete results of this study are given in Appendix A along with some of the possible recommendations for minimizing GM waves during installation.

2.3 Plastic Pipe Behavior Under High Vertical Stresses

A network of perforated pipes is generally required for the transmission of leachate in the leachate collection and removal system (LCRS) of waste containment facilities. HDPE or PVC pipes are normally used. The performance of plastic pipes under the stresses imposed by large heights of waste in landfills is relatively unknown due to the fact that experience with plastic pipes under high overburden stresses is limited. The problem is further complicated by the fact that the behavior of plastics is time dependent and their adequate performance is required as long as there is a possibility of generation of leachate within the landfill, which can be for a considerable number of

years. This is in contrast to the use of plastic pipes in transportation or agriculture applications where the design lifetime is relatively short, the live loads exerted on the pipe are mainly of temporary nature, and the depth of burial is relatively small. For this reason, the applicability of classical design methods for flexible pipes in landfill applications can be questioned. One of the limitations in applying classical design methods is that the effect of arching in alleviating the loads on pipes is probably underestimated (or ignored completely). Hence design according to classical theories may be overconservative. The response of plastic pipes under simulated conditions was investigated as a task of this study using a finite element modeling approach.

Table 2-2. Residual Stresses (after 10,000 hours) in the HDPE GM Test Specimens for the Various Experiments Performed in this Study.

Experimental Variables and Conditions		Residual Stress (kPa)	Residual Stress (% of yield)
Normal Stress	180 kPa	1200	8.5
	360 kPa	1300	9.2
	700 kPa	2000	13.7
	1100 kPa	2100	14.4
Original Height of Wave	14 mm	130	0.9
	20 mm	740	5.1
	40 mm	1500	9.8
	60 mm	2000	13.7
	80 mm	2300	15.7
Thickness of GM	1.0 mm	1600	10.5
	1.5 mm	2000	13.7
	2.0 mm	1600	13.7
	2.5 mm	1800	11.8
Testing Temperature	23°C	130	0.8
	14 mm - 42°C	250	2.1
	55°C	440	4.5
	23°C	740	4.9
	20 mm - 42°C	850	7.3
	55°C	750	8.0
	23°C	1500	9.5
	40 mm - 42°C	1600	13.7
	55°C	690	7.4
	23°C	2000	13.2
	60 mm - 42°C	2600	22.0
	55°C	1600	17.5

2.3.1 Leachate Removal Configurations

As shown in Figure 1-3, the leachate removal system at the bottom of a landfill usually consists of a layer of sand or gravel (0.3 to 0.6 m thick) in which a perforated pipe

removal system is embedded. There are a number of possible configurations for the pipe and its embedment, three of which are illustrated in Figure 2-7. The pipes are arranged in a variety of patterns, e.g., a header pipe in the center of the landfill with a series of feeder pipes located at right angles or at acute angles in a herringbone fashion. The spacing is such that the mounded head on the liner is no more than the regulatory maximum, 0.3 m. Giroud and Houlihan (1997) describe the analytic behavior of this leachate mound. Critical in this regard is the minimum slope of the base of the landfill, which should be larger than 0.5% after settlement or consolidation, since the entire system drains by gravity to the low point of the cell. At this location, a sump is installed and the leachate is removed as required, recall Figure 1-5. The leachate collection pipes are typically 150 to 200 mm in diameter.

2.3.2 Characteristics of Plastic Pipe

There are many candidate pipe materials for use in a leachate removal system beneath a solid waste landfill. However, HDPE or PVC plastic pipe, also known as geopipe, has emerged as the material of choice. There are a number of advantages to geopipe, but also several disadvantages.

Advantages of Plastic Pipe

- good flow characteristics;
- no corrosion;
- good resistance in chemically and biologically active environments;
- light weight, which facilitates handling, storage, and installation;
- pipe can bend along longitudinal axis; and
- economical compared to other types of pipe.

Disadvantages of Plastic Pipe

- low resistance to circumferential distortion;
- due to their visco-elastic nature, creep and/or stress relaxation may constitute a problem under long-term conditions;
- strength and stiffness are temperature dependent; and
- potentially susceptible to stress cracking if proper choice of resin and processing is not carefully considered.

Pipes from all thermoplastic materials are manufactured to the standard outside diameters of traditional pipe sizes. For waste containment applications, PVC pipe is often specified to have a wall thickness corresponding to that of Schedule 80 pipe. The dimensioning system often used with HDPE pipe is that in accordance with the standard dimension ratio (SDR) which is equal to the ratio of the outside diameter to the minimum wall thickness. An SDR of 11 is often specified for HDPE pipes in landfills. An SDR of 9 is the thickest wall section commonly used in the USA, however, some German landfills use HDPE pipe with an SDR of 6.

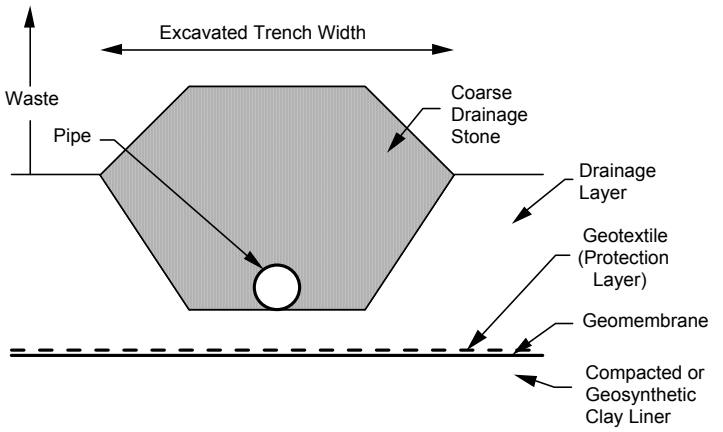

(a) Trench Type of Installation

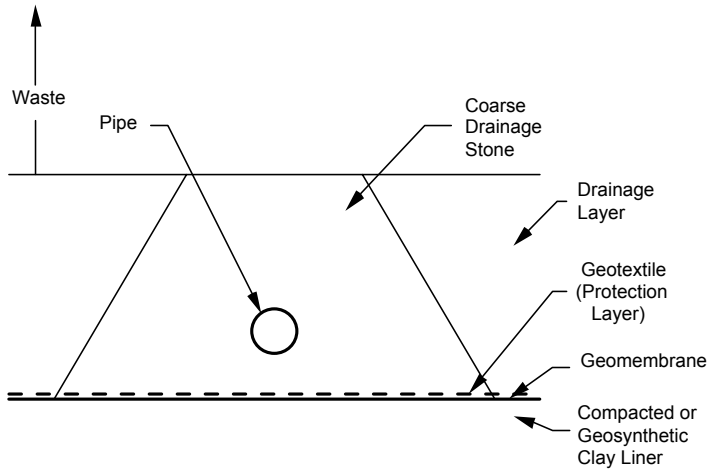

(b) Embankment Type of Installation

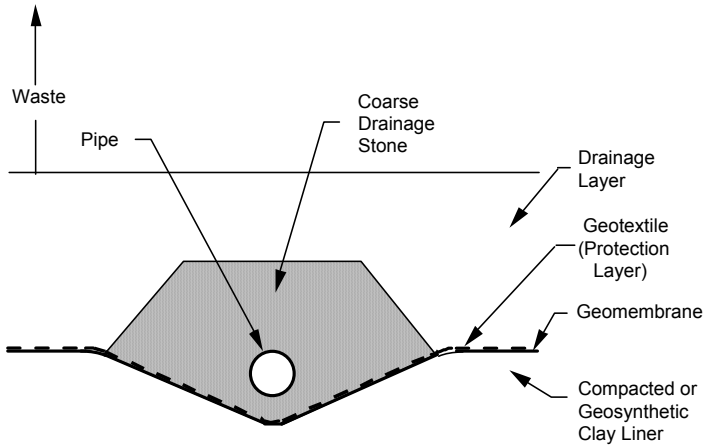

(c) Embankment with V-Trench Type of Installation

Figure 2-7. Various pipe removal schemes within leachate collection layers.

Figure 2-7. Various pipe removal schemes within leachate collection layers.

When perforated, the perforations are either in the form of slots or circular holes. General practice is to use circular perforations for smooth walled pipes and slotted

perforations for corrugated pipes. The pattern of perforations consists of two or more rows of holes of diameters ranging between 10 to 15 mm and spaced at distances between 100 and 300 mm. The rows of holes are located symmetrically though offset from each other in the lower 180 degrees or less of the pipe circumference. With perforated pipes, the slots are located at the valleys of the corrugations.

Various methods are used for joining of pipes. They can be grouped into three categories: butt fusion or seaming, overlap connections, and special couplings.

In general, butt fusion or seaming is used for thick-walled HDPE pipe (either solid or perforated). The ends of the pipe are brought together with a heated plate placed between them. A small force brings the ends of each pipe against opposite sides of the plate. When adequate thermal energy is realized and the pipe ends become viscous, the heat plate is removed and the pipe ends are quickly brought together. Adequate force is applied to the opposing pipes to extrude a slight amount of the molten material out of the seam area. After cooling, the force is released and the seam is completed. PVC pipe, on the other hand, is usually chemically seamed using a solvent on the pipe ends before the pipe ends are drawn together.

The overlap type of connections can only be made if the pipe thickness is adequate to machine the pipe ends so as to accept one another. To make a tight connection, gaskets are sometimes used which reside in slotted seats of the thicker section of the connection. Extrusion seaming can be used from the outside of small diameter pipes or from the inside of large diameter pipes to make a leak-free connection.

Special couplings are used to connect the ends of profile-wall (i.e., corrugated) pipes. Each of these couplings must be mated to the type of pipe for which they were designed. It is not acceptable practice to use couplings made for one style of profiled pipe on a different style. Electro-fusion couplings are also used with smooth HDPE pipe.

It should be noted that the influence of holes (perforations or slots) and connections (of all types) are not routinely accounted for as part of the design process. Design engineers sometimes attempt to account for holes by assuming that the normal force on the pipe is applied over an area reduced by the size of the holes (i.e., an increased normal stress is considered). The design method to follow is based on the pipe itself, not holes or connections, which represent an area of future research activity.

2.3.3 Design by the Iowa State Formula

Design of plastic pipes (i.e., the calculation of pipe deflection) in most applications is based on the modified Iowa State formula, which was originally developed in 1941, see Spangler (1971). It was later modified by Watkins and Spangler (1958). Variations to the Iowa State formula as well as other analytical approaches have been proposed for

predicting pipe deflection. However, such methods have not been generally accepted in practice and hence only the Iowa State formula is presented herein. The formula takes one of the following two forms:

$$\Delta = \frac{D_L K W}{\frac{EI}{R^3} + 0.061\, E'} \qquad \text{(Eq. 2-5)}$$

or

$$\frac{\Delta}{D} = \frac{D_L K W_s}{\frac{EI}{R^3} + 0.061\, E'} \qquad \text{(Eq. 2-6)}$$

where:

Δ = change in pipe diameter, m (Δ is used interchangeably in design for the horizontal and vertical deflections, Δx and Δy respectively as per ASTM D2412; in the derivation of the formula, Δ is the horizontal deflection and the deflected pipe is assumed to take an elliptic shape);
D_L = deflection lag factor (dimensionless);
K = bedding constant (dimensionless);
W = load per unit length of pipe (kN/m);
W_s = load per unit area (kPa);
R = mean radius of pipe (m);
D = mean diameter of pipe (m);
Δ/D = deflection ratio (dimensionless);
E = modulus of elasticity of pipe material (kPa);
I = moment of inertia of pipe wall per unit length (m^4/m); and
E' = modulus of soil reaction (kPa).

The deflection lag factor "D_L" is a result of soil compression at the sides of the pipe whereby additional load may be exerted on the pipe with time. A value of 1.5 for the deflection lag factor was originally proposed. However, due to the inherent conservatism in the formula, it has more recently been suggested that a value of 1.0 be used (Moser, 1990). Note that in design, the load W is taken as the full prism load over the pipe which, in the case of no variation of unit weight with height above the pipe, will be equal to unit weight times the pipe diameter times the full height above pipe. Accordingly, the load per unit area "W_s", will be equal to the overburden pressure above the pipe. Thus, in using this approach, the effect of arching in relieving pipe stress is not addressed, nor considered. It has been pointed out by Moser (1990) that the long term load will never exceed the prism load.

The bedding constant "K" varies with the bedding angle. However, a value of 0.1 is often assumed in calculations since other parameters are much more significant.

Howard (1977) gives various values of E' for different soil types under different compaction efforts which range between 3500 kPa (for poor quality fine grained backfill soils) to 20,000 kPa (for good quality granular backfill soils). These values are commonly used in design and are often referred to as U.S. Bureau of Reclamation (BuRec) values.

A maximum deflection, which is generally limited to 10%, is usually specified for flexible pipes. Excessive deflection of pipes can lead to reversal of curvature of the pipe ring and substantial loss in flow capacity. Once reversal of curvature occurs, fluctuations in soil pressures can cause progressive ring deformation, which could lead to eventual collapse (Watkins, 1987).

A parametric evaluation of the modified Iowa State formula under an overburden pressure of 1100 kPa is given in Figure 2-8 in which the deflection ratio $\Delta y/D$ is plotted against pipe stiffness for various values of the modulus of soil reaction. For a municipal waste unit weight of 11.8 kN/m^3, the chosen overburden pressure corresponds to a waste height of about 90 m, and for a hazardous waste unit weight of 16.5 kN/m^3 it corresponds to a height of about 67 m. Figure 2-8 indicates that the deflection ratio is more sensitive to pipe stiffness at low values of the modulus of soil reaction than at high values. This emphasizes the importance of soil type and compaction effort in the zone around the pipe. Note that the pipe stiffness for HDPE pipes of SDR 11, 9 and 6 are approximately equal to 3400, 6600 and 26,400 kPa, respectively. As already mentioned, pipe of SDR 11 is commonly used in the U.S. and pipe of SDR 6 has been used in Germany.

2.3.4 Design by Finite Element Model

The finite element method has proven to be a versatile tool for many types of geotechnical and structural analyses. The methods can be adapted to soil-pipe interaction problems.

Figure 2-9 shows the discretization scheme used in this particular finite element analysis. Because of symmetry, only half the geometry needs to be considered in the analysis. In order to reduce the amount of input data, a mesh generation subroutine is incorporated in the program. The user specifies the number and lengths of the vertical and horizontal subdivisions around the pipe. The numbering and coordinates of the nodal points and the numbering of the elements are then automatically determined.

The soil and waste are modeled using quadrilateral and triangular continuum elements. The quadrilateral elements are four-node isoparametric elements, and the triangular elements are constant strain elements. Both elements have two degrees of freedom per node and are compatible with each other. The pipe section is represented by twelve frame elements with three degrees of freedom per node. The derivation of the stiffness matrices of the frame elements and the triangular and quadrilateral elements

can be found in most finite element textbooks. The soil-pipe interface is represented by twelve quadrilateral elements of zero thickness, which allow relative displacement only in a direction parallel to the soil-pipe interface.

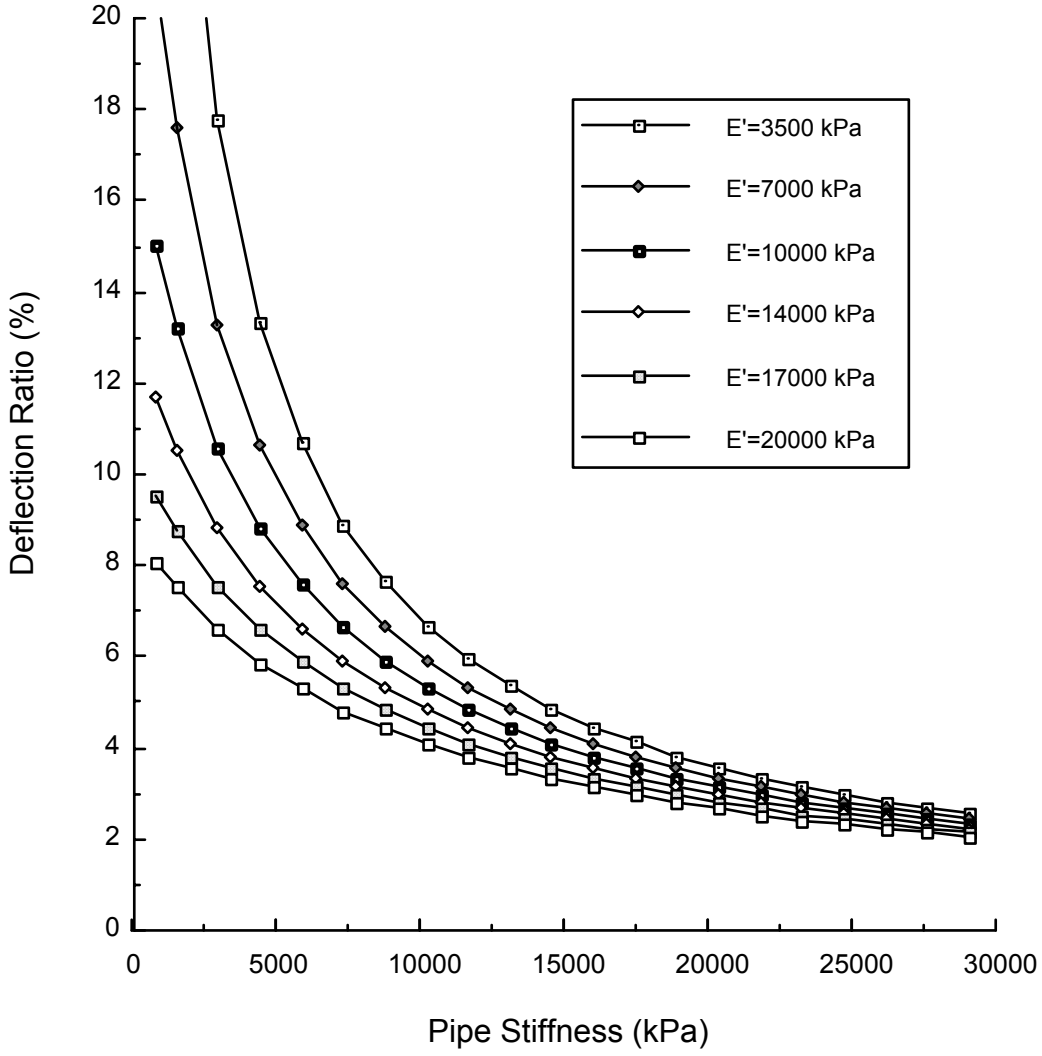

Figure 2-8. Relationships between deflection ratio and pipe stiffness for various moduli of soil reaction using the Iowa State formula.

The boundary conditions are automatically set in order to minimize the size of the input data. The nodes lying on the bottom horizontal boundary are restricted from movement in both the horizontal and vertical directions. Symmetry is simulated by allowing only vertical movement for the nodes lying on the pipe centerline with the exception of the nodal point at the intersection with the bottom boundary, which is also restricted from movement in the vertical direction. Also, no rotation is allowed at the two pipe nodes at

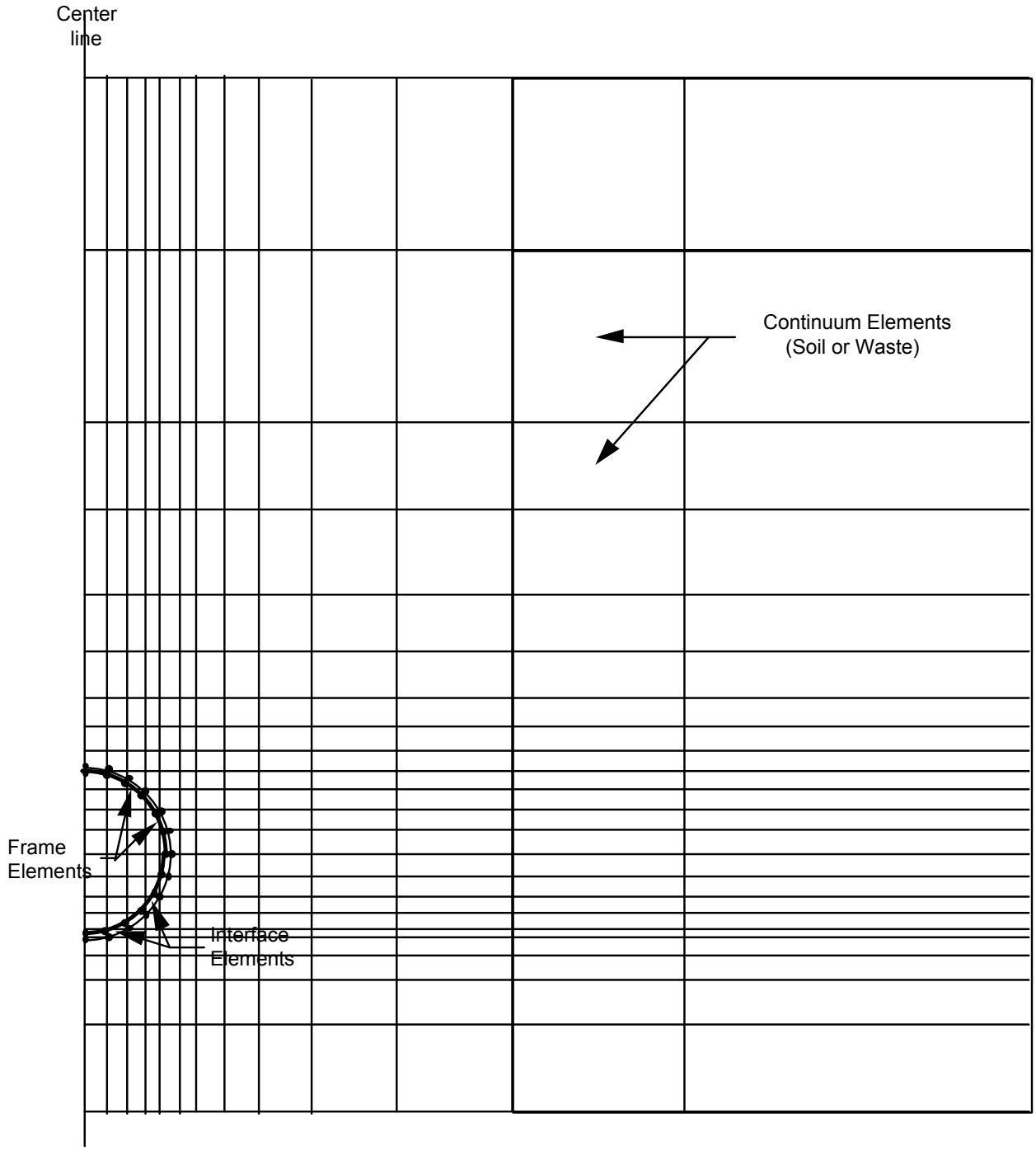

Figure 2-9. Finite element mesh developed and used in this study.

the invert and crown. The nodes lying on the vertical boundary on the right hand side of the mesh are restricted from movement in the horizontal direction.

The stress-strain properties of the pipe, soil, solid waste and soil-pipe interface are idealized in the finite element program using various available models. A brief description follows:

- The plastic pipe is modeled as in a linear elastic material. Thus, the modulus is critical in assessing both short-term and long-term deflection behavior.
- The soil around the pipe is modeled using the hyperbolic model developed by Duncan and Chang (1970).
- The solid waste is also reproduced with a hyperbolic model, but with different modulus and strength parameters.
- The soil-pipe interface is represented using a shear stress versus relative displacement relationship presented by Clough and Duncan (1971).
- The program sequence, along with the many details involved in the analysis, is given in Wilson-Fahmy and Koerner (1994).

2.3.5 Comparison of Design Methods

In order to illustrate the difference in pipe deflection behavior as calculated by the Iowa State formula versus this particular version of a FEM approach, a numeric example is presented.

This example simulates the trench type of installation of Figure 2-7 (a). Two different HDPE pipes of 150 mm nominal diameter (external diameter = 168 mm) are considered in the analysis. One has an SDR of 11 and the other has an SDR of 9. The pipe modulus is taken equal to 750 MPa to represent short-term conditions and 150 MPa to represent long-term conditions. The pipe stiffness under short-term conditions is equal to 3400 kPa for the SDR 11 pipe and 6600 kPa for the SDR 9 pipe. Other details are given in Wilson-Fahmy and Koerner (1994).

Figure 2-10 shows the relationship between overburden stress and the diameter changes in the vertical and horizontal directions under short and long-term conditions using the FEM approach. As expected, the SDR 9 pipe deflects less than the SDR 11 pipe, the difference being larger under short-term conditions.

For comparison with the modified Iowa State formula, Table 2-3 gives the deflection ratios predicted using both the FEM and the Iowa State formula at 1100 kPa overburden stress under both short-term and long-term conditions. In applying the Iowa State formula, the value of E' was taken equal to 21,000 kPa as representative of a coarse stone of the type often used around plastic pipe in landfills.

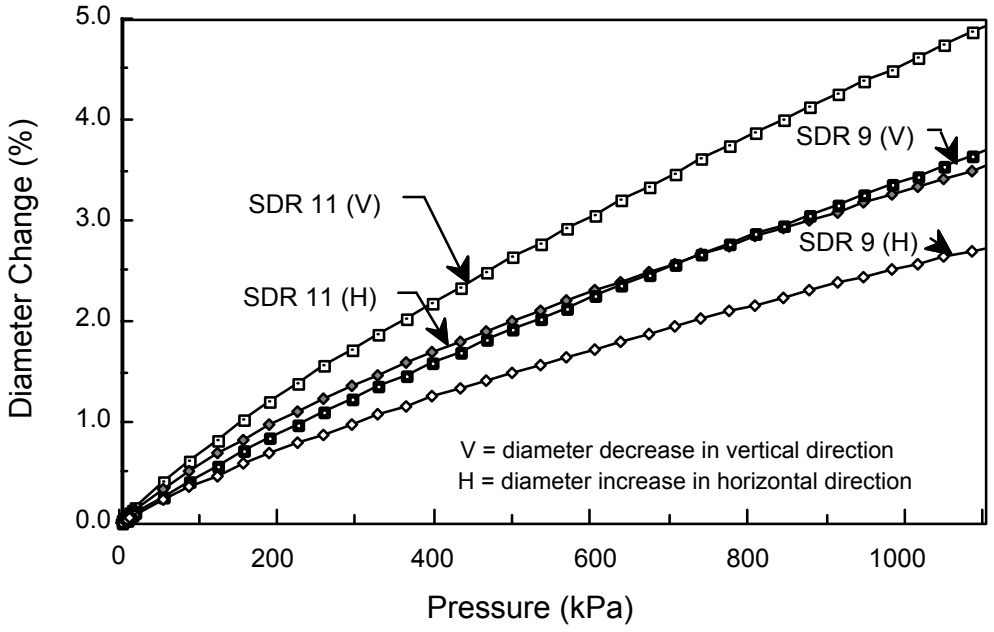

(a) Short-term pipe modulus = 750,000 kPa

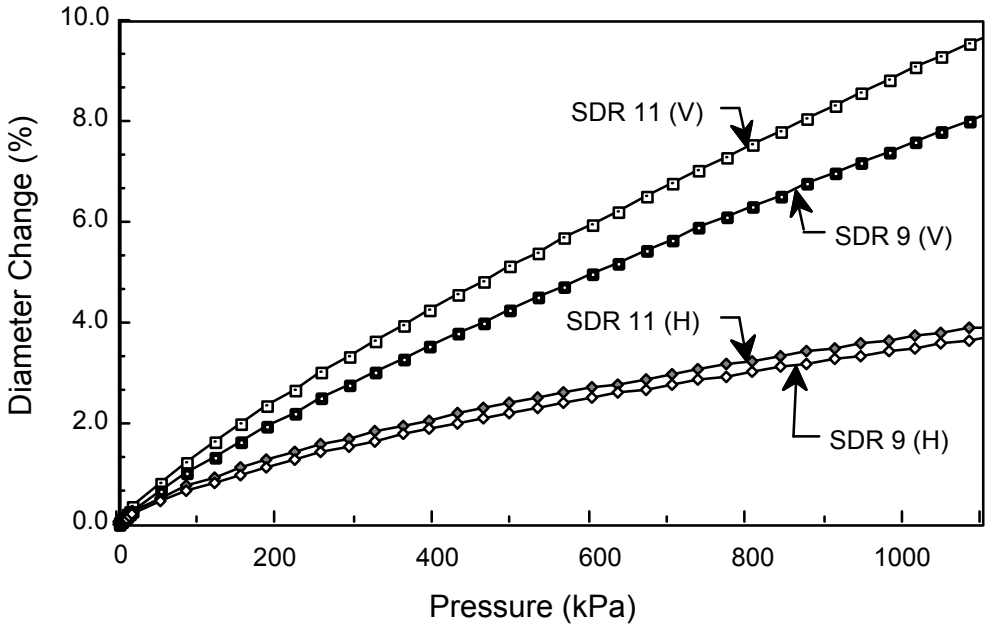

(b) Long-term pipe modulus = 150,000 kPa

Figure 2-10. Relationships between overburden stress and vertical and horizontal diameter changes using the FEM approach.

Table 2-3. Deflection Ratios Predicted Using Iowa State Formula and Finite Element Analysis.

Method of Analysis	SDR	E' (psi)	Deflection Ratio (%) Short-Term	Long-Term
Iowa State Formula	11	21,000 kPa	6.3	8.1
Finite Element	11	N/A	4.9	9.7
Iowa State Formula	9	21,000 kPa	4.9	7.6
Finite Element	9	N/A	3.7	8.2

where N/A = not applicable

The values in Table 2-3 indicate that, in comparison to FEM predictions, the Iowa State formula overestimated the deflection ratio under short-term conditions (which is conservative). Conversely, the formula slightly underestimated the vertical deflection ratio under long-term conditions (which is slightly unconservative, but typically accommodated in design by the incorporation of a factor of safety). In all cases, the deflection ratio does not exceed 10% with the short-term deflection being less than 7.5%. Note that the short-term deflection predicted using the FEM is less than 5%.

The effect of arching of the soil above the pipe is clearly shown in Figure 2-11 where it can be seen that under short term conditions (E_S = 750,000 kPa) the effect is quite small, i.e., the overburden stress on the pipe is approximately 80 to 90% of that predicted using the Iowa State formula. However, under long-term conditions (E_S = 150,000 kPa), it is significant amounting to a decrease in overburden stress of the order of 50%. Furthermore, Figure 2-11 suggests that increasing the pipe stiffness by increasing the modulus and/or increasing thickness (using low SDR) results in less potential effects of arching.

2.4 Prediction of GT Service Lifetime

A frequently asked question involving GTs is "how long will they last"? A study task was developed to provide insight into this question. The task was subdivided into three subtasks:

- behavior of partially ultraviolet-degraded GTs;
- oxidative degradation of PP and PE GT yarns and PE geogrid ribs; and
- hydrolytic degradation of PET GT yarns.

Each subtask is briefly described in this report. At the time of report preparation, however, only the first subtask has been completed.

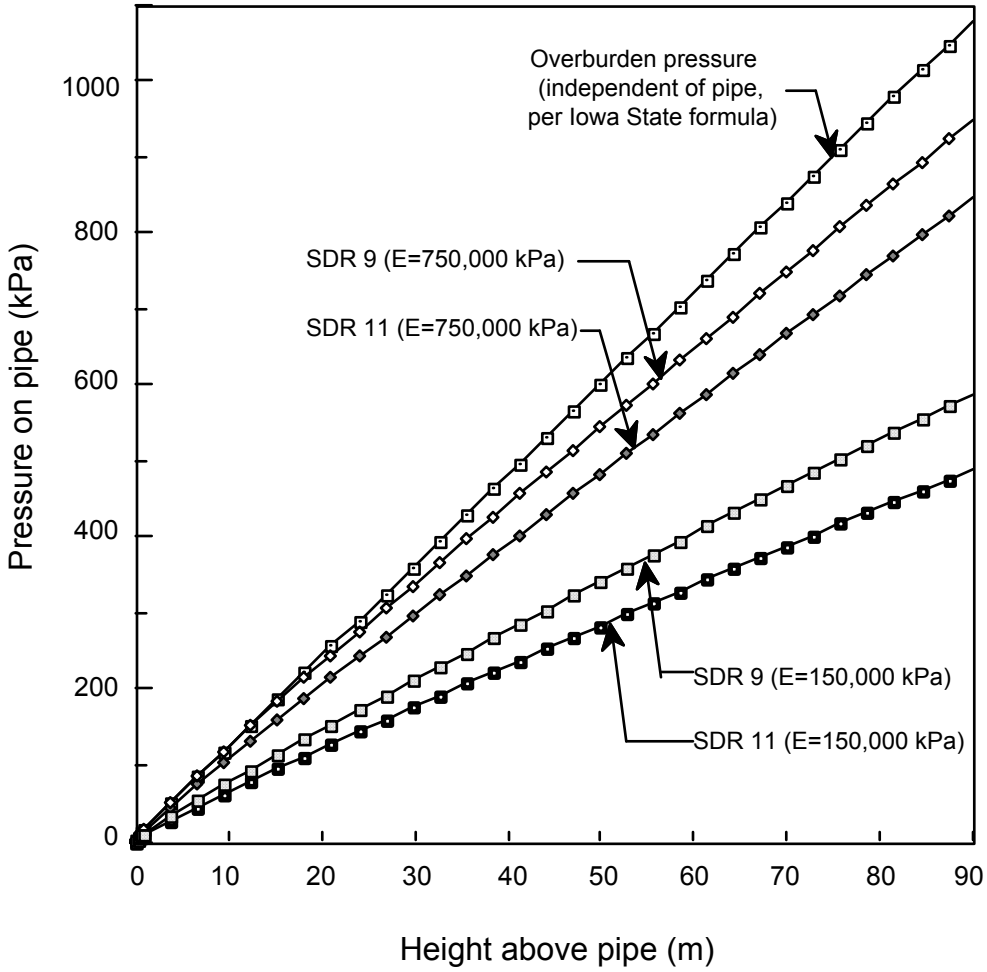

Figure 2-11. Reduction in overburden stress using FEM as compared to Iowa State formula, i.e., the effect of arching.

2.4.1 Behavior of Partially Ultraviolet Degraded GTs (PP and PET)

During any type of construction that involves the use of GTs, there will generally be the potential for exposure to sunlight. Within the sunlight spectrum, the ultraviolet (UV) portion is most harmful to polymers used in the manufacture of GTs, causing a photo-oxidative reaction to occur. Thus it is necessary to cover or backfill GTs intended for long-term service in a landfill in a timely manner. If not covered promptly, UV-degradation will begin to occur. A concern has been expressed that if such degradation is initiated, the reaction may continue to propagate within the GT even after covering or backfilling. This subtask was directed at addressing this issue, i.e., whether or not UV-initiated degradation is auto-catalytic. The subtask involved incubation of GT specimens in a laboratory UV fluorescent acceleration device per ASTM D 5208. This method was selected since the laboratory device provides for an economical approach for providing UV exposures. It also can be correlated to field exposure in the usual manner, see Hsuan and Koerner (1993).

Twelve different types of GTs were included in the experimental program. Nine were PP and three were PET. Figure 2-12 illustrates the overall experimental procedure, with incubation, removal, and testing of the various samples. Details of the experimental program are available in Hsuan et al. (1994). Results for one of the PP GTs is given in Figure 2-13(a) and for one of the PET GTs in Figure 2-13(b).

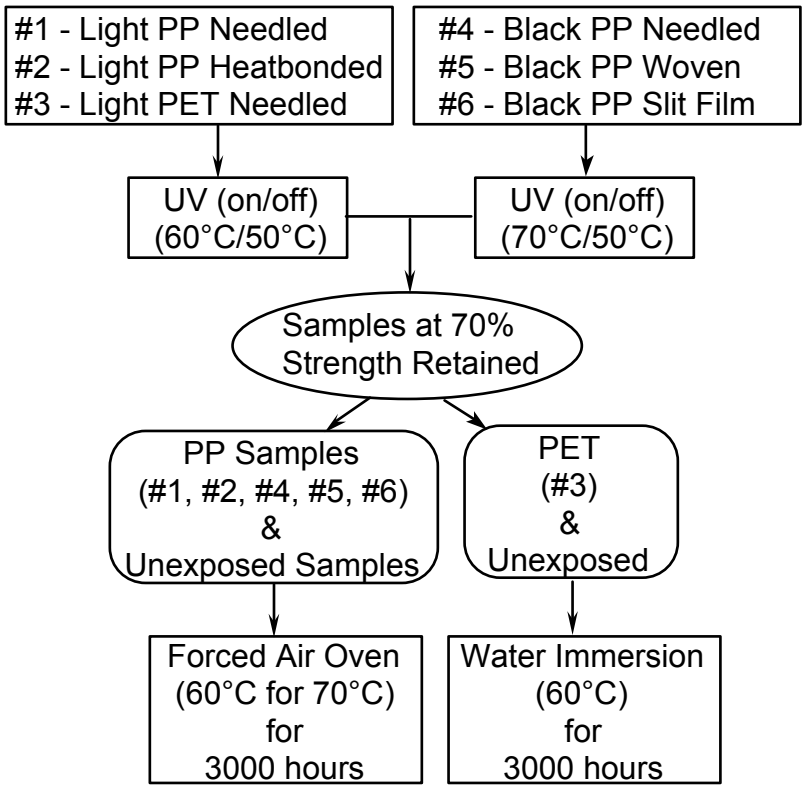

Figure 2.12. Design flow chart of the complete study (after Hsuan et al., 1994).

The results of the UV exposure tests can be summarized as follows:

- UV exposure is the major contributor to the degradation of exposed GTs as opposed to thermal-oxidative or hydrolytic degradation. PP GTs were found to be slightly more susceptible to UV degradation than PET GTs.
- The rate of tensile strength reduction due to UV exposure (as a fraction of the original strength) is inversely proportional to the mass per unit area of the GT. This is due to the degradation mechanism, which involves the initiation of photo-oxidation on the exposed surface of the GT, which moves progressively inwards as the duration of the exposure increases.
- The 70% UV-degraded GTs show similar trends as those unexposed GTs regarding the strength retained property within 3000 hours at 60°C.

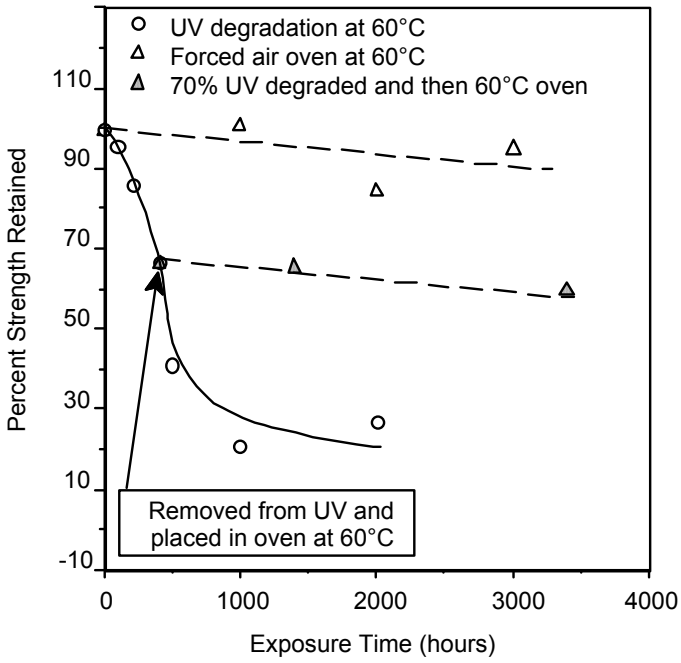

(a) Polypropylene geotextiles

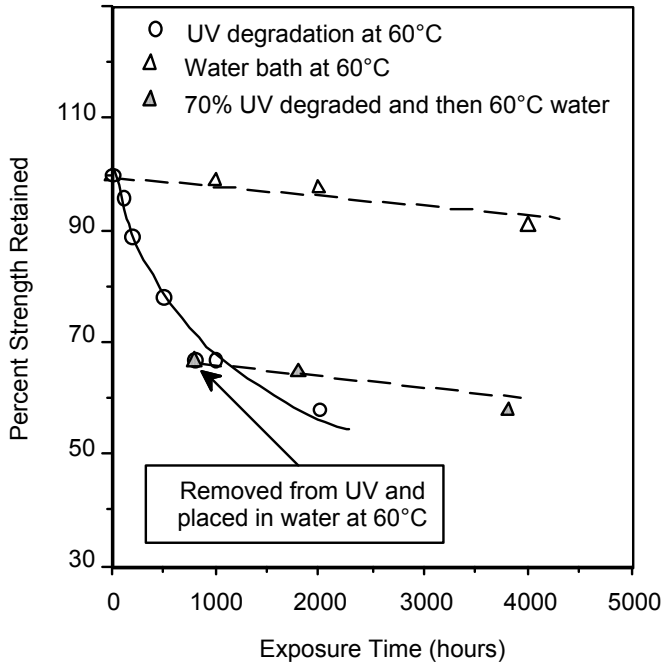

(b) Polyester geotextiles

Figure 2-13. Strength retained graphs from geotextile incubated under three different test conditions.

- Photo-oxidative degradation ceased in all of the tested GTs (PP and PET) once the UV source was removed.

While the above findings are of technical interest, it is well known that "timely cover" is necessary. Even a thin, 150-mm thick layer of soil is adequate to eliminate the potential for UV degradation. In this regard, specifications may require that the GT to be covered within two to four weeks after placement unless the GT has been shown to resist degradation for a longer time period. Pending further research, the results of the testing presented herein indicate that this maximum time frame is reasonable.

2.4.2 Oxidative Degradation of PP GT Yarns and PE Geogrid Ribs

This subtask is being used to evaluate the oxidative degradation of two types of PP GT yarns and two types of HDPE geogrid ribs. The incubation uses forced air ovens at elevated temperatures for varying times. Samples are periodically removed and tested for their retained strength and elongation. These values are then compared to the unaged strength and elongation for a percent retained value, thereby indicating the degree of degradation.

Furthermore, by incubating at several elevated temperatures (75, 65 and 55°C are used in this study), an Arrhenius plot can be developed. Using the slope of the resulting curve, extrapolation down to site-specific temperature can be made, resulting in an estimate of the service lifetime for these materials based on a thermal oxidation failure criterion.

A separate oven is required for each incubation temperature. Samples are periodically removed and tested in tension. Several of the resulting data available at the time of the preparation of this report are presented in Figure 2-14 for PP GT yarns and Figure 2-15 for PE geogrid ribs, respectively. Each point is the average of five replicate tests.

This project is projected to continue for an additional three-year period, thereby achieving an estimated five-year maximum incubation time. The reason for this lengthy duration of incubation is that shorter tests would require excessively high incubation temperatures that would unrealistically bias the predicted service lifetime, i.e., temperatures that are too high may significantly underpredict the service lifetime.

2.4.3 Hydrolytic Degradation of PET GT Yarns

This subtask is being used to evaluate the hydrolytic degradation of eight types of PET GT yarns in water baths at elevated temperatures for varying times. Immersed samples are periodically removed and tested for their retained strengths and elongation. These values are then compared to the unaged strength and elongation for a percent retained value, thereby indicating the degree of degradation.

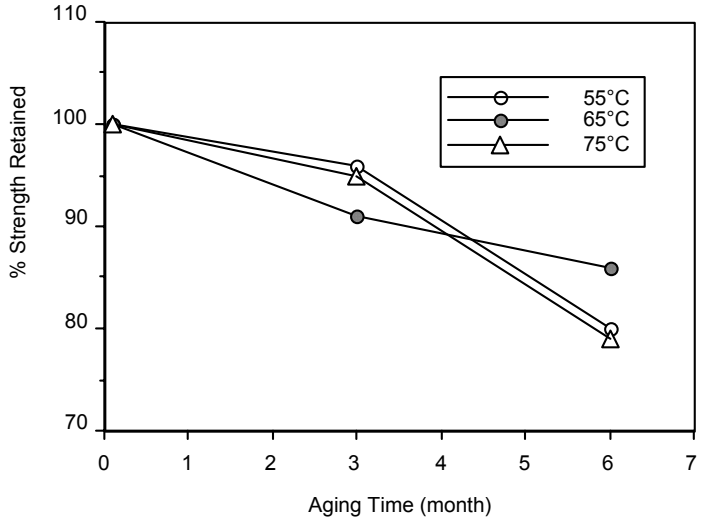

(a) PP Geotextile #1

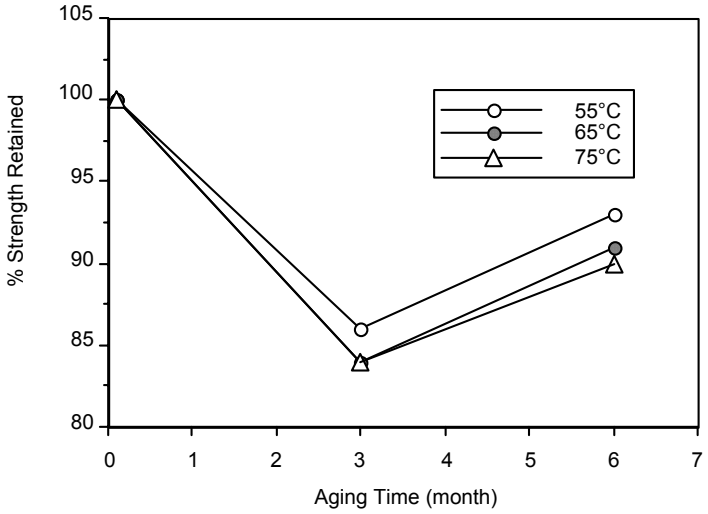

(d) PP Geotextile #2

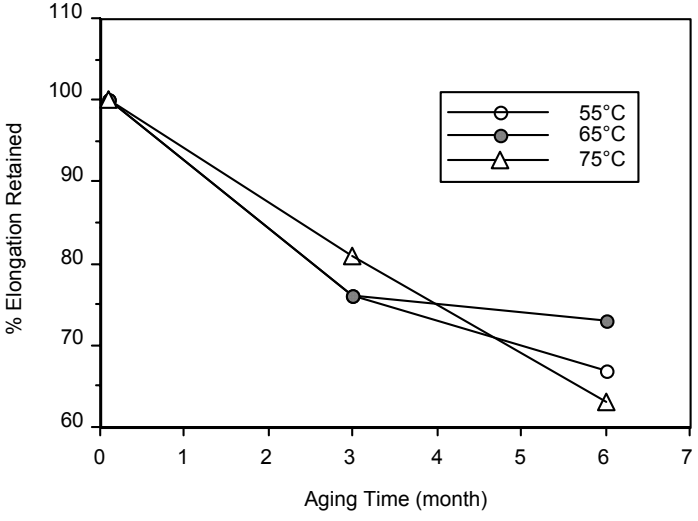

(b) PP Geotextile #1

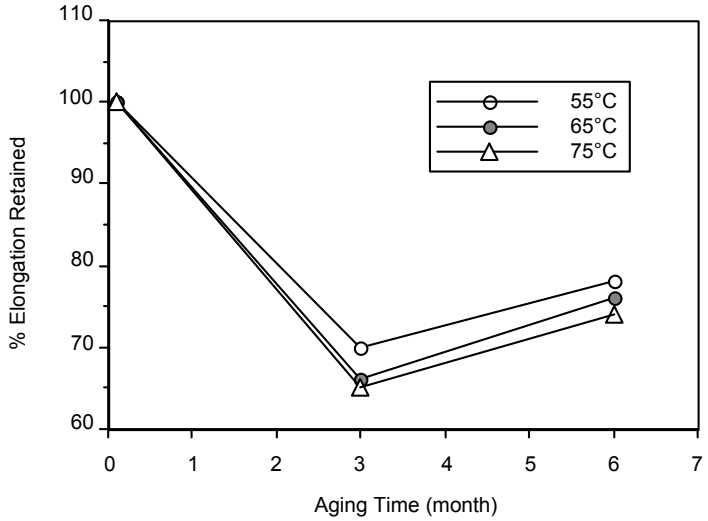

(c) PP Geotextile #2

Figure 2-14. Behavior of PP GT yarns after forced air oven incubation.

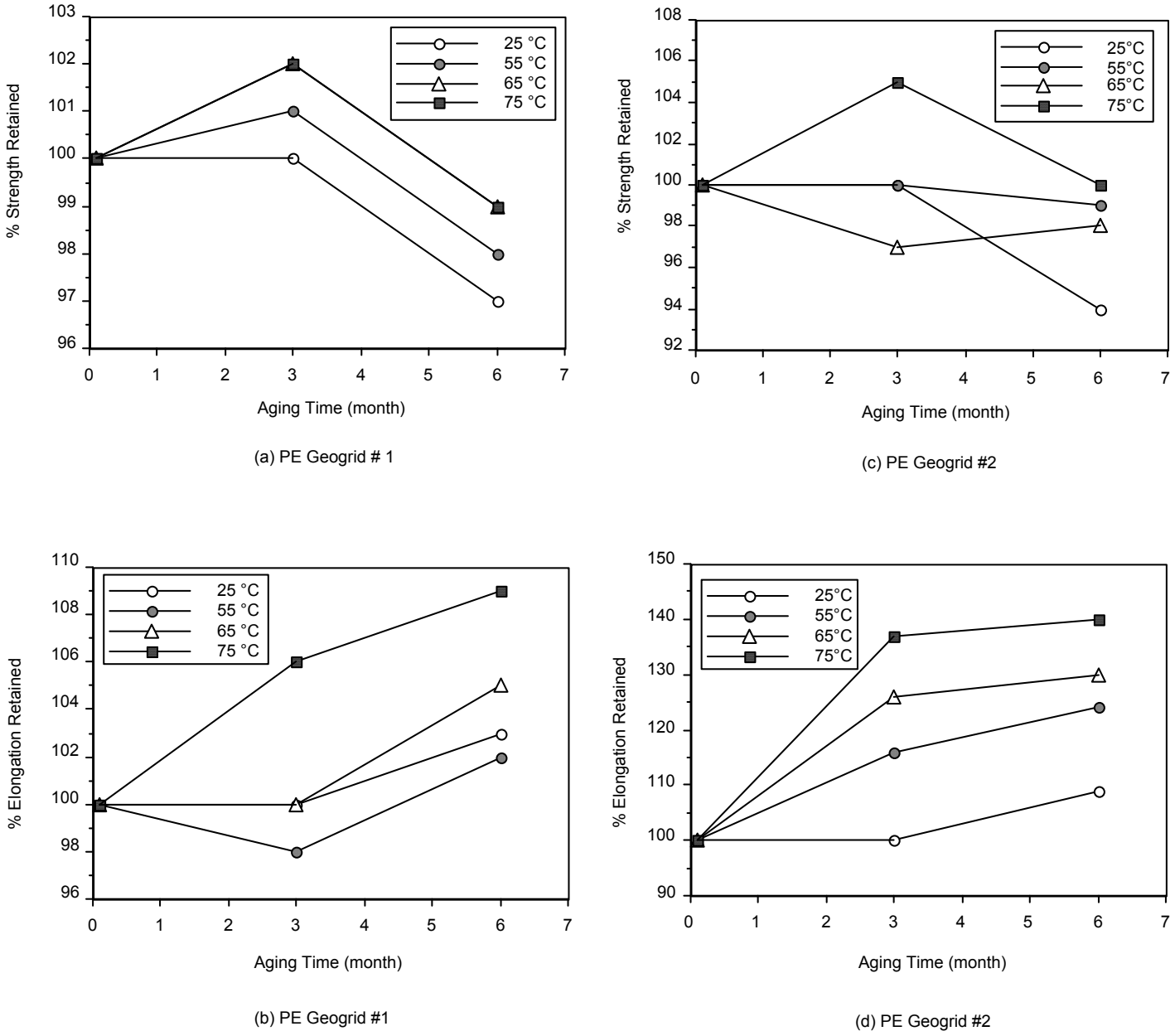

Figure 2-15. Behavior of PE geogrid ribs after forced air oven incubation.

Furthermore, by incubation at several elevated temperatures (65, 55 and 45°C are used in this study), an Arrhenius plot can be developed. Using the slope of the resulting curve, extrapolation down to site-specific temperature can be made resulting in an estimate of the service lifetime of these materials based upon a hydrolytic degradation criterion.

A separate bath is required for each temperature incubation. Samples are periodically removed and tested in tension. Some of the resulting data are presented in Figure 2-16. Each point is the average of five replicate tests.

This project is projected to continue for an additional three-year period, thereby achieving an estimated five-year maximum incubation time. As with the oxidation study previously described, the reason for the lengthy duration is that excessively high incubation temperatures may unrealistically bias the predicted service lifetime.

2.5 Prediction of GM Service Lifetime

One of the most frequently asked question involving any type of GM is, “how long will it last”? Since HDPE is the type of GM most commonly used in waste containment systems, it is the focus of this task. The steps involved in the task are as follows:

- understand the mechanisms that are involved in the degradation process;
- simulate the application(s) in the laboratory as closely as possible;
- perform the incubations under the simulated conditions at elevated temperatures (at least three and preferably four temperatures);
- remove the samples periodically and test them for changes from their as-received properties; and
- perform Arrhenius modeling to arrive at an estimated lifetime for the site specific temperature.

A detailed discussion of this task is presented in Appendix B of the report. A brief summary is given below.

2.5.1 Degradation of HDPE GMs

HDPE GMs are formulations consisting of PE resin (≈ 97%), carbon black (≈ 2%), and antioxidants (≈ 1%). The long-term aging process involves three discrete stages, see Figure 2-17(a):

- depletion time of antioxidants;
- induction time; and
- time to reach a specified reduction in the value of a significant engineering property, e.g., elongation, modulus, strength, etc.; for the purposes of this task, the numeric value of the specified property reduction is taken as 50%.

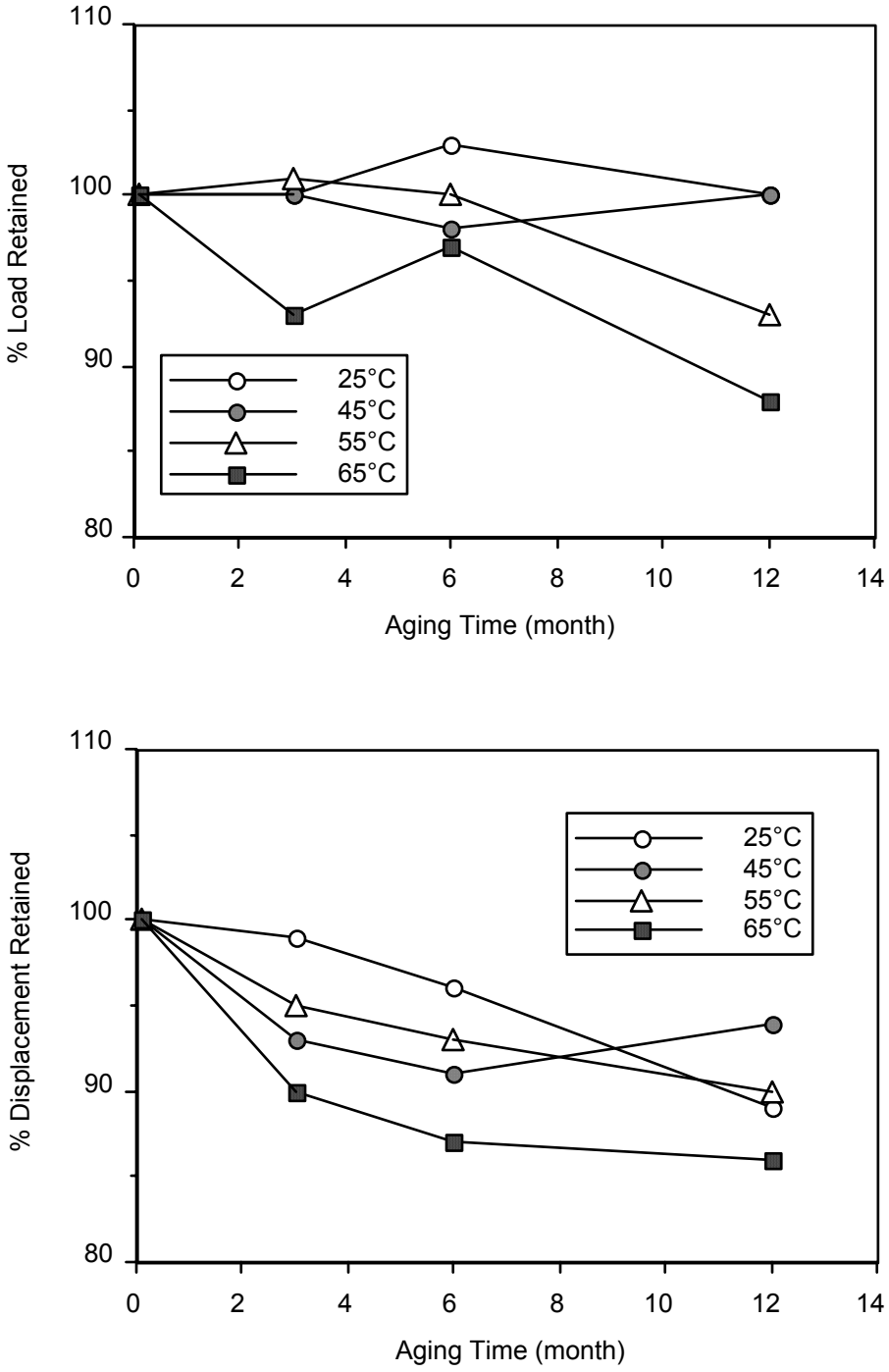

Figure 2-16. Behavior of PET yarns, sample A, after water incubation.

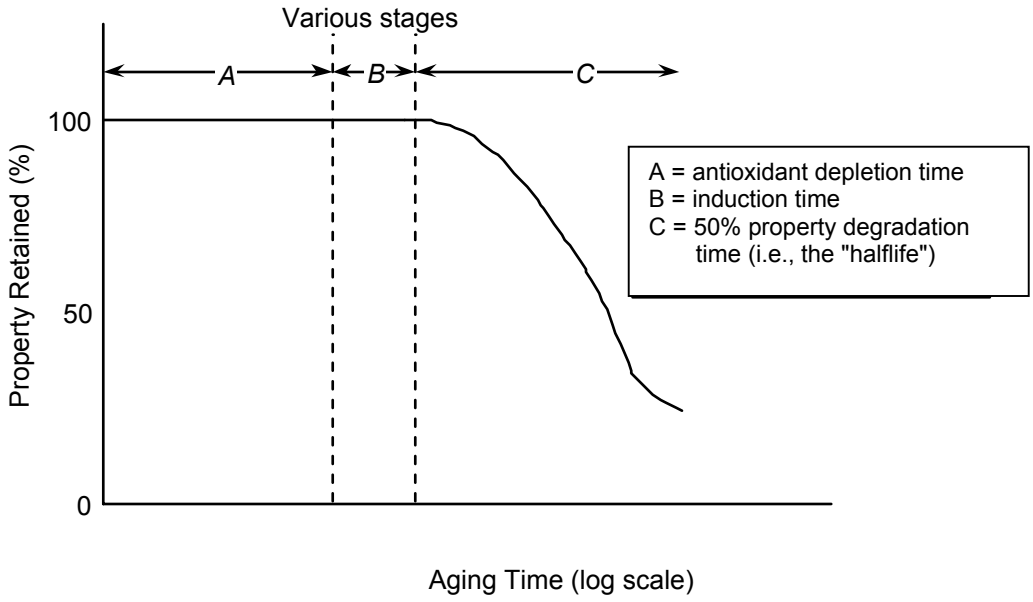

(a) The various stages of HDPE geomembrane aging

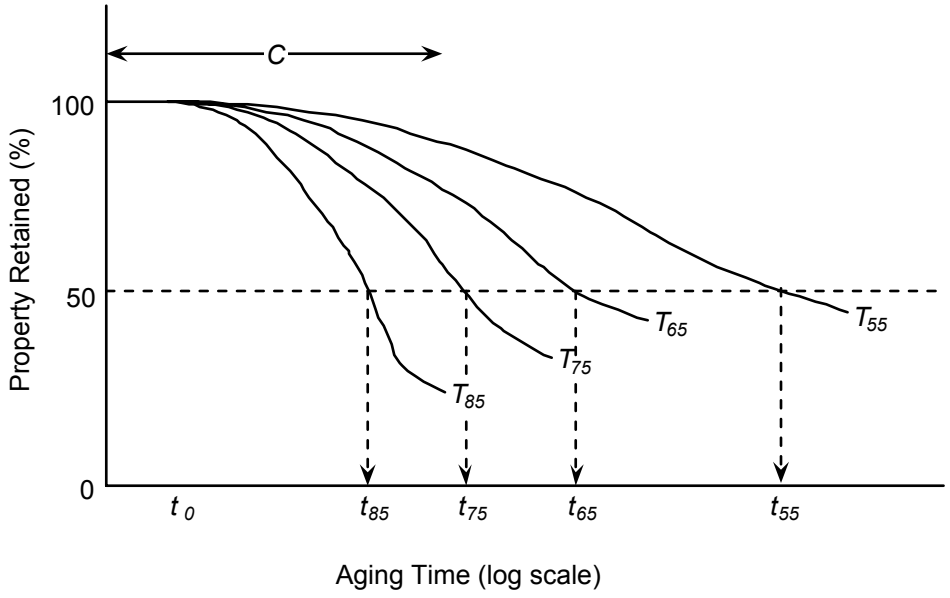

(b) Degradation with stage "C" under varying temperature (T_i)

Figure 2-17. Aging and degradation behavior of HDPE (and other polyolefins) over time under elevated temperature incubation.

These three stages of degradation are shown conceptually on Figure 2-17(a). Although not evaluated herein, this type of generalized behavior is also characteristic of low density PE and flexible PP GMs.

The antioxidants are extremely important to the aging process, since they react with oxygen diffusing into the polymer structure and thereby inhibit oxidation from occurring. When depleted at the end of Stage A (as indicated by zero oxidative induction time (OIT) using a differential scanning calorimetry test), the induction time stage begins.

The induction time represents a time period required to initiate a measurable amount of oxidation-induced chain scission of the polymer structure, i.e., Stage B. It is the least understood of the three degradation mechanisms but it is clearly present. For example, polymers (like milk jugs) with no long-term antioxidants will not begin to degrade immediately. While the relative induction time may be short, its quantification should be included in a lifetime assessment.

The oxidation process continues into Stage C such that engineering properties begin to change. Typically, the break elongation will decrease, the modulus will increase, and the break strength will slightly increase, then decrease. In general, the yield elongation and strength of HDPE will not show signs of change since these values are small in comparison to the break properties. The above events, of course, signify that the polymer is transitioning from a ductile to a brittle material. Embrittlement represents a physical manifestation of the degradation process. As shown in Figure 2-17(b), the response is strongly temperature dependent. A 50% change in properties is usually taken by polymer engineers as being a significant change and is called the “halflife”. It is arbitrarily assumed in this report to signify the end of the service life of the material.

2.5.2 Simulated Applications

There are a large number of GM applications that could be simulated in the incubation process. The applications targeted in this study are:

- landfill liners;
- surface impoundment liners; and
- landfill covers.

Each application is modeled in the simulation through selection of an incubation medium, an applied stress (if any), and specific values of elevated temperatures for the exposures. Table 2-4 provides the various simulation series that are ongoing in this particular task. This report will focus only on Series No. III, which is the most important series for the purposes of this project since it simulates the base liner of a landfill. A series using leachate as the incubation medium was started, but was subsequently terminated due to leachate variation.

Table 2-4. HDPE GM Simulation Series.

Incubation Series	Incubation Method	Applied Stress	Simulated GM Application
I	water (both sides)	none	surface impoundments below liquid level
II	air (both sides)	none	landfill covers and waste pile covers
III	water above/air beneath	260 kPa (compression)	landfills liners beneath waste
IV	water (both sides)	30% yield stress (tension)	surface impoundments along side slopes below liquid level

The incubations for Series No. III are performed in 20 identical chambers as shown in Figure 2-18. Five chambers are maintained at each of four temperatures, i.e., 85, 75, 65 and 55°C. Samples are periodically removed and tested.

2.5.3 Antioxidant Depletion Time

Upon removal of the incubated samples from the chambers shown in Figure 2-18, the samples are tested for their OIT. Two options are available: (i) standard OIT per ASTM D3895; and (ii) high pressure OIT per ASTM D5885. Both of these OIT methods utilize a calorimeter to evaluate the length of time the polymer melt can sustain an oxygen environment. The OIT (time in minutes) is related to the amount and type of antioxidants that are used in the formulation to protect the resin from degradation. The curves of Figure 2-19(a) were generated using data obtained over a period of 24-months. Note the strong influence of elevated temperature on the OIT depletion times. As shown in Figure 2-19(b), semi-logarithmic plots of the data result in straight line relationships between OIT and incubation period. The slopes of these straight lines (for extrapolation to site-specific temperature) for both OIT-tests are shown in Figure 2-20.

Using these slopes and extrapolating down to site-specific temperature results in Table 2-5. The selection of the actual value is obviously site-specific. However, data from MSW landfill monitoring in Pennsylvania, California, and Florida are now becoming available. These data indicate that 20°C is a typical value for the in-situ temperature of HDPE GMs in liner systems for MSW landfills. As seen in Table 2-5, a value of 20°C results in antioxidant depletion times for the type of GM evaluated herein of 192 years based on standard OIT (Std OIT) tests and 196 years based on HP-OIT tests.

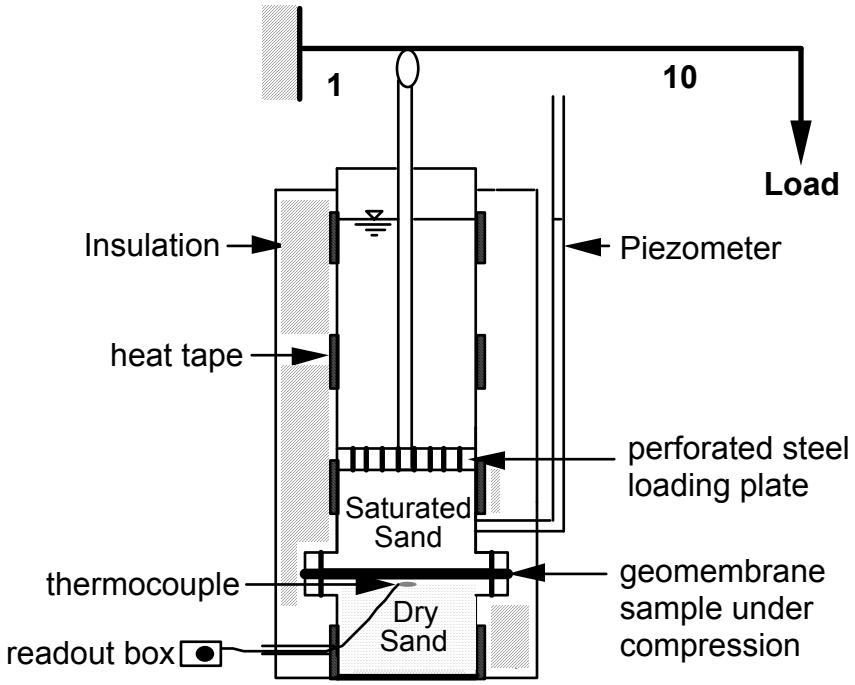

Figure 2-18. Photograph and schematic diagram of a typical compression column for incubation Series No. III.

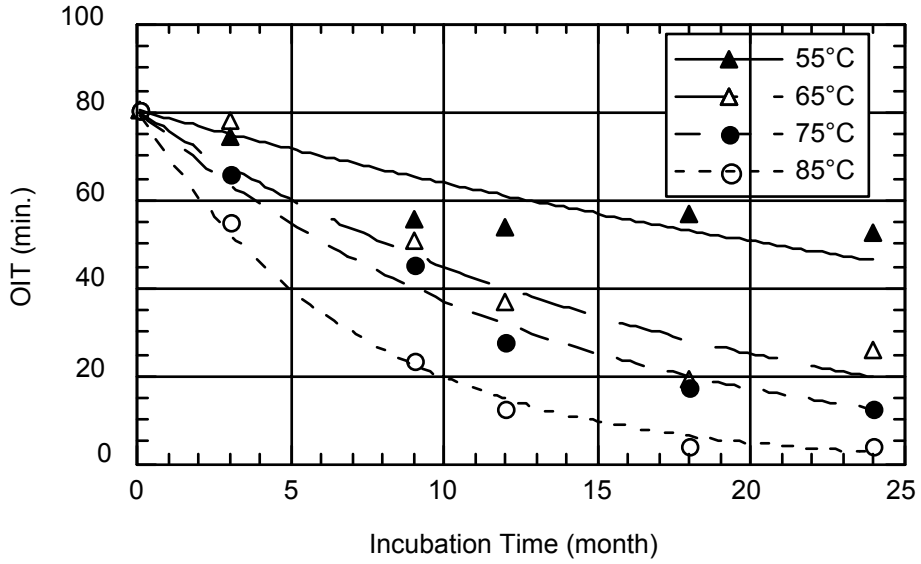

(a) Arithmetic response curves

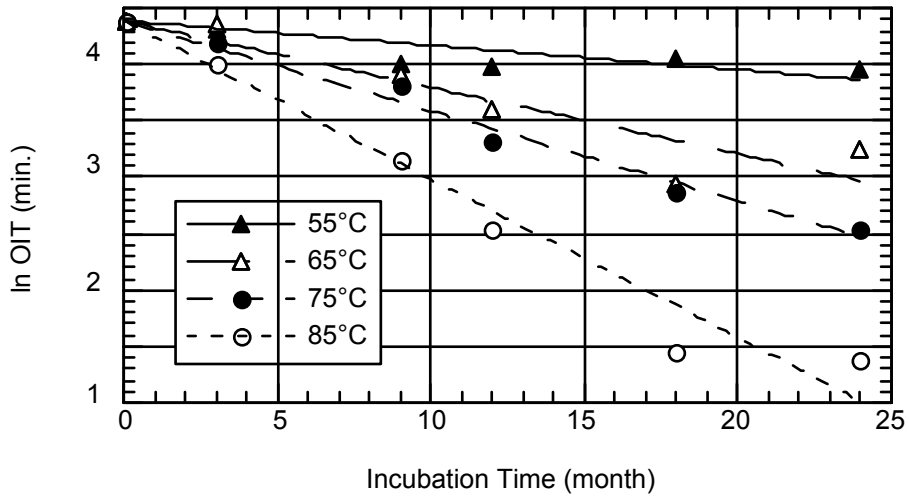

(b) Semi-log plotting of above curves

Figure 2-19. Standard oxidative induction time test results for Series No. III incubations on HDPE GM samples.

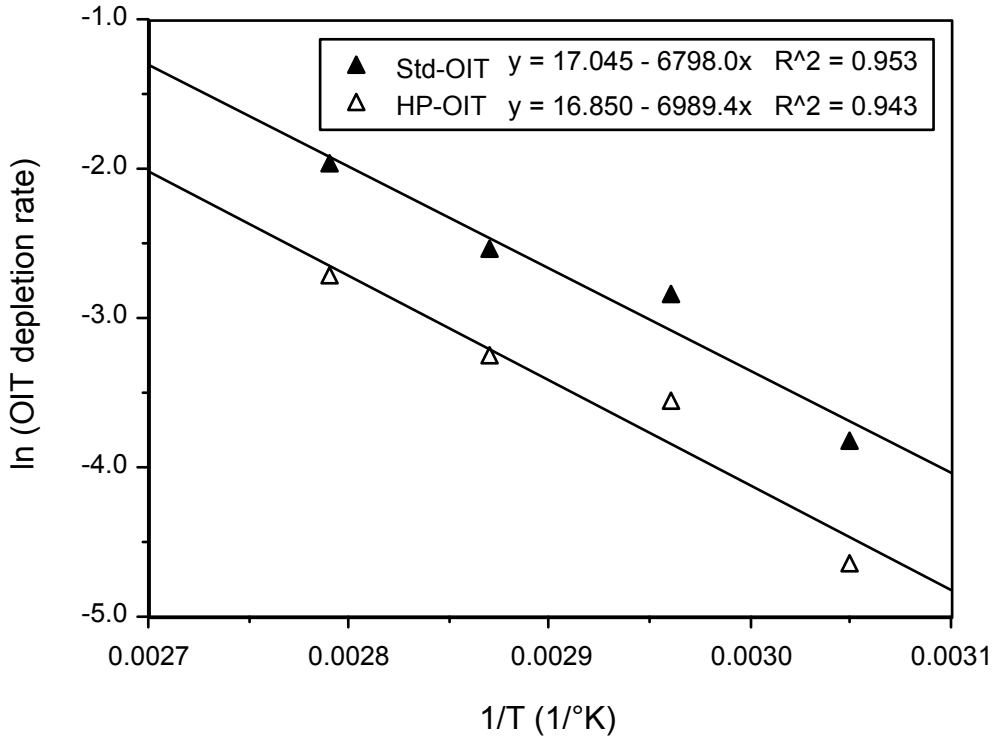

Figure 2-20. Arrhenius plot for incubation Series No. III (water above/air beneath-compression stress).

Table 2-5. Extrapolation of Depletion of Antioxidants Trends to Various In-Situ Temperatures.

In-Situ Temp.	Std OIT	HP OIT
30°C	90 yrs.	89 yrs.
25	130	131
20	192	196
15	286	296
10	432	455
5	663	709

2.5.4 Induction Time

Stage B in Figure 2-17(a) represents the time that it takes an unstabilized polymer (i.e., one with no antioxidants) to manifest a measurable amount of chain scisson. Hence, to evaluate this stage it would be appropriate to select a PE material with a minimum antioxidant content and monitor its engineering properties over time to determine the induction time.

Milk and water containers represent commercial HDPE products that do not contain antioxidants because of their limited shelf life. Some aged milk and water containers

were retrieved from the waste mass of a MSW landfill. The age of these retrieved containers was approximately 25 years based on the dates shown on newspaper and canceled checks that were retrieved at the same location of the landfill. The oxidative induction time and tensile properties of the aged samples were evaluated. The results were compared to those obtained from unaged containers, i.e., purchased at a grocery store prior to the test. The data are shown in Table 2-6(a) and (b) for water and milk containers, respectively. For this comparison, it was assumed that the aged and unaged containers were made using the same polymer resins and manufacturing processes. This may or may not be the case.

Table 2-6(a). Properties of Aged and Unaged Water Containers.

Property	Unaged Container	Aged Container	% Change
Modulus (MPa)	650	580	nil
Yield Stress (MPa)	25	24	nil
Yield Elongation (%)	11	11	nil
Break Strength (MPa)	35	22	-37%
Break Elongation (%)	1700	879	-43%

Table 2-6(b). Properties of Aged and Unaged Milk Containers.

Property	Unaged Container	Aged Container	% Change
Modulus (MPa)	550	507	nil
Yield Elongation (MPa)	24	22	nil
Yield Strain (%)	11	11	nil
Break Strength (MPa)	22	14	-36%
Break Elongation (%)	990	730	-26%

Based on this limited data for 25-year old HDPE containers, and assuming the aged and unaged containers had the same initial properties, it is seen that yield stress, yield elongation, and modulus have essentially remained unchanged in a landfill atmosphere. Only the break properties (strength and elongation) have begun to decrease. Thus, it is estimated that the induction time for HDPE is on the order of 20-years.

2.5.5 Halflife of Engineering Properties

Stage C in Figure 2-17(a) represents the time for a HDPE GM to reach 50% change in its engineering properties after depletion of antioxidants and induction time occurs. The material properties that are being monitored in this part of the study are listed in Table 2-7.

Table 2-7. Engineering Properties Being Evaluated.

Test	ASTM Method	Property
Density	D 1505	Crystallinity
Melt Index	D 1238	Molecular Weight
Tensile	D 638	Yield, Modulus, Break

The methodology used to estimate the halflife of properties is similar to that used to predict the lifetime of antioxidants in the HDPE GMs, i.e., the Arrhenius model. The properties listed in Table 2-7 were monitored over increasing incubation times at incubation temperatures of 85, 75, 65, and 55°C. The monitoring results are evaluated by plotting percentage of the original engineering property remaining at a given incubation time against that time, as shown in Figure 2-17(b). The incubation time corresponding to a percent retained of 50% is the halflife of the material at that particular incubation temperature. The inverse of the lifetime is the reaction rate. Once the reaction rates at the four elevated temperatures are obtained, the data is extrapolated by utilizing an Arrhenius plot, as shown in Figure 2-21. Subsequently, the reaction rate at a lower site-specific temperature, such as 20°C, can be predicted. The estimated time to reach halflife of the property can be calculated as the inverse of the reaction rate at this temperature.

Since the current test results of the incubations in Table 2-4 have not shown reduction in material properties in the majority of the incubated samples, the halflife of the GMs cannot be evaluated based on actual test data generated in the course of this study. Thus, Figure 2-21 presents no actual data. In order to estimate the potential halflife, data from published literature are utilized. Viebke et al. (1994) found that the activation energy of the degradation mechanism of a unstabilized PE pipe is 80 kJ/mol. (This represents the slope of the Arrhenius plot shown in Figure 2-21). During the incubation process, the pipe was exposed to water inside and circulating air outside at constant temperatures ranging from 70 to 105°C.

Using the Viebke et al. (1994) data, halflife can be estimated using Equation 2-7. (Note that the gas constant R = 8.314 J/mol and R_r represents the reaction rate from Figure 2-21 at the temperature indicated).

$$\frac{R_{r@115}}{R_{r@20}} = e^{\frac{-E_{act}}{R}\left[\frac{1}{115+273}-\frac{1}{20+273}\right]}$$

$$\frac{R_{r@115}}{R_{r@20}} = e^{\frac{-80{,}000}{8.314}\left[\frac{1}{388}-\frac{1}{293}\right]}$$

$$\frac{R_{r@115}}{R_{r@20}} = e^{8.04} = 3027$$

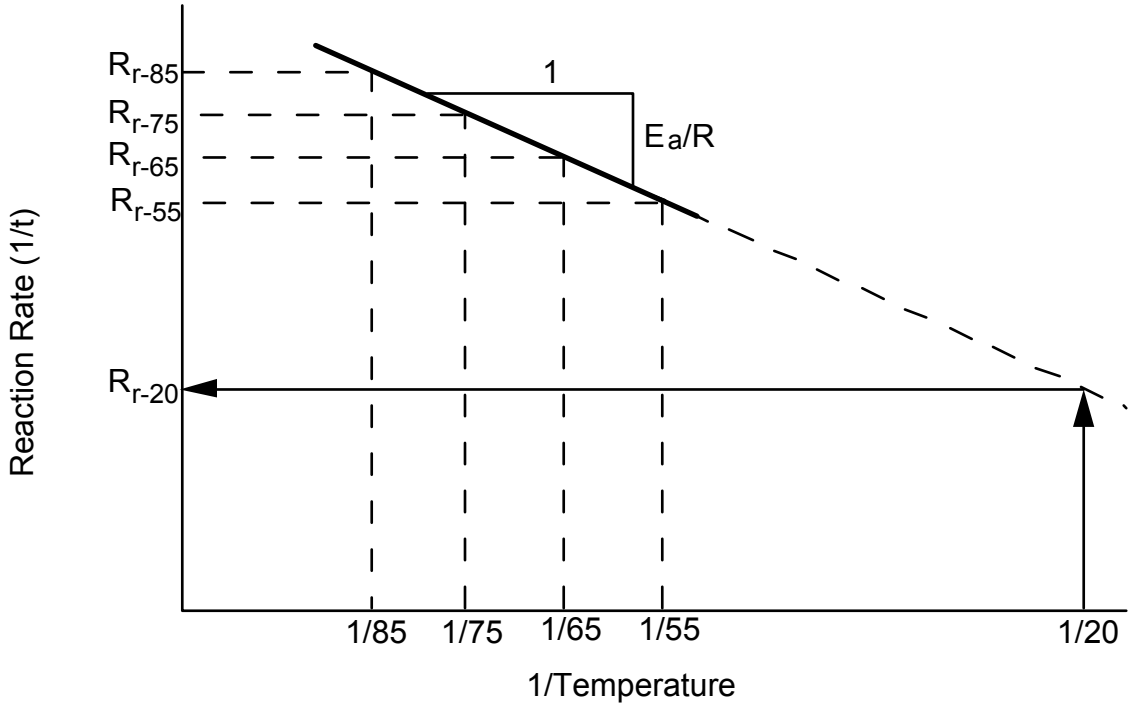

Figure 2-21. Arrhenius plot to analyze data and extrapolate to site-specific temperature.

Since halflife at 115°C is 90 days which is 3027 times faster than the incubation temperature at 20°C, the halflife at 20°C will be:

$$R_{r@20} = (90)(3027) \qquad \text{(Eq. 2-8)}$$
$$= 272{,}000 \text{ days}$$
$$= 746 \text{ years}$$

This value represents the halflife of the engineering property monitored within Stage C of the overall lifetime as illustrated in Figure 2-17.

2.5.6 Summary of Lifetime Prediction

Using the conceptual behavior model shown in Figure 2-17(a), the lifetime of a GM consists of three-stages; antioxidant depletion, induction time, and halflife of engineering properties. For the 1.5-mm thick HDPE GM being evaluated in this study

under simulated landfill conditions, Table 2-8 represents the current best-estimate of the lifetime prediction value.

Table 2-8. Estimated Lifetime of HDPE GM Being Evaluated in this Study.

Stage	Description	Duration (years)
A	Antioxidant Depletion	200
B	Induction Time	20
C	Halflife of Engineering Property	750
Total	Lifetime Estimate	970

Based on the methodology presented herein, the estimated service lifetime of a 1.5-mm thick HDPE GM under the simulated test conditions is on the order of 1,000 years. Note that the existence of wrinkles will reduce this estimated service lifetime. No attempt has been made for this report to estimate the degree to which wrinkles will reduce the service lifetime. The amount remains for further research. Also remaining for further research is an investigation as to the lifetime of GMs other than HDPE.

2.6 References

ASTM D638, Test Method for Tensile Properties of Plastics.

ASTM D1238, Test Method for Flow Rates of Thermoplastics by Extrusion Plastometer.

ASTM D1505, Test Method for Density of Plastics by the Density-Gradient Technique.

ASTM D2412, Determination of External Loading Characteristics of Plastic Pipe by Parallel-Plate Loading.

ASTM D3895, Test Method for Oxidative-Induction Time of Polyolefins by Differential Scanning Calorimetry.

ASTM D5208, Practice for Operating Fluorescent UV and Condensation Apparatus for Exposure of Photodegradable Plastics.

ASTM D5885, Test Method for Oxidative Induction Time of Polyolefin Geosynthetics by High Pressure Differential Calorimetry.

Clough, R. W. and Duncan, J. M. (1971), "Finite Element Analysis of Retaining Wall Behavior, " *Journal of Soil Mechanics and Foundation Engineering Division,* ASCE, Vol. 97, SM12, pp. 1657-1673.

Duncan, J. M. and Chang, C. Y. (1970), "Non-Linear Analysis of Stress and Strain in Soils, " *Journal of Soil Mechanics and Foundation Engineering Division,* ASCE, Vol. 96, SM5, pp. 1629-1653.

Eith, T. A. and Koerner, G. R. (1997), "HDPE GM Waves in the Field," *Proceedings GRI-11 on Field Installation of GMs*, Geosynthetic Research Institute, Philadelphia, PA, pp. 101-114.

Giroud, J. P. and Bonaparte, R. (1989), "Leakage Through Liners Constructed with Geomembranes. Part II: Composite Liners," *Geotextiles and Geomembranes*, Vol. 8, No. 2, pp. 77-111.

Giroud, J. P. and Houlihan, M. F. (1997), "Design of Leachate Collection Layers, " *Proceedings Sardinia '95*, CISA, Cagliari, Italy, pp. 613-640.
Howard, A. K. (1977), "Soil Reaction for Buried Flexible Pipe, " *Journal of Geotechnical. Engineering Division,* ASCE, Vol. 103, No. GT1, January, pp. 33-43.
Hsuan, Y. G. and Koerner, R. M. (1993), "Can Outdoor Degradation be Predicted by Laboratory Accelerated Weathering?" *Geotechnical Fabrics Report*, Vol. 11, No. 8, pp. 12-16.
Hsuan, Y. G., Koerner, R. M. and Soong, T.-Y. (1994), "Behavior of Partially Ultraviolet Degraded Geotextiles," *Proceedings 5th International Conference on Geosynthetics*, Singapore, Vol. 3, pp. 1209-1212.
Koerner, G. R. and Koerner, R. M. (1995), "Temperature Behavior of Field Deployed HDPE Geomembranes," *Proceedings Geosynthetics '95*, IFAI, pp. 921-937.
Koerner, R. M., Wilson-Fahmy, R. F. and Narejo, D. (1996), "Puncture Protection of Geomembranes Part III: Examples, " *Geosynthetics International*, Vol. 3, No. 5, pp. 655-676.
Moser, A. P. (1990), *Buried Pipe Design*, McGraw-Hill, New York, NY.
Narejo, D., Koerner, R. M. and Wilson-Fahmy, R. F. (1996), "Puncture Protection of Geomembranes Part II: Experimental," *Geosynthetics International*, Vol. 3, No. 5, pp. 629-653.
Richardson, G. N. (1996), "Field Evaluation of Geosynthetic Protection Cushions," *Geotechnical Fabrics Report*, Vol. 14, No. 2, pp. 20-25.
Soong, T.-Y. and Koerner, R. M. (1998), "Modeling and Extrapolation of Creep Behavior of Geosynthetics, " *Proceedings 6th International Conference on Geosynthetics,* IFAI, St. Paul, MN, pp. 707-710.
Soong, T. -Y. and Lord, A. E., Jr. (1998), "Slow Strain Rate Modulus via Stress Relaxation Experiments, " *Proceedings 6th International Conference on Geosynthetics,* IFAI, St. Paul, MN, pp. 711-714..
Spangler, M. G. (1971), *Soil Engineering*, 2nd Ed., International Textbook Co., Scranton, PA.
Viebke, J., Ifwarson, M. and Gedde, U. W. (1994), "Degradation of Unstabilized Medium-Density Polyethylene Pipes in Hot-Water Applications, " *Polymer Engineering and Science*, Vol. 34, No. 17, pp. 1354-1361.
Watkins, R. K. (1987), *Structural Performance of Perforated and Slotted HDPE Pipes under High Soil Cover*, Report to King County Solid Waste, Seattle, WA.
Watkins, R. K. and Spangler, M. G. (1958), "Some Characteristics of the Modulus of Passive Resistance of Soil - A Study in Similitude, " *Highway Research Board Proceedings*, Vol. 37, pp. 576-583.
Wilson-Fahmy, R. F. and Koerner, R. M. (1994), *Finite Element Analysis of Plastic Pipe Behavior in Leachate Collection and Removal System*, GRI Report #12, Geosynthetic Research Institute, Drexel Univ., Philadelphia, PA.
Wilson-Fahmy, R. F., Narejo, D. and Koerner, R. M. (1996), "Puncture Protection of Geomembranes Part I: Theory," *Geosynthetics International*, Vol. 3, No. 5, pp. 605-628.

Chapter 3
Slope Stability of Full-Scale Field Test Plots Containing GCLs to Simulate Final Cover Systems

3.1 Introduction

GCLs consist of a thin layer of bentonite encased between two GTs or mixed with an adhesive and attached to a GM. GCLs are a relatively new type of liner material, having first been used in a landfill in 1986 (Schubert, 1987). Although GCLs are relatively new, their use in waste containment facilities has increased steadily because of the extremely low hydraulic conductivity of bentonite, the low cost of GCLs, the ease and speed of installation compared to CCLs, and the low volume occupied by GCLs compared to much thicker CCLs.

GCLs enjoy several favorable hydraulic characteristics, including self-healing properties (Shan and Daniel, 1991; Estornell and Daniel, 1992), ability to withstand differential settlement (Koerner et al., 1996; Lagatta et al., 1997), ability to self-heal after desiccation (Boardman and Daniel, 1996), and resistance to the potentially damaging effects of freezing temperatures (Hewitt and Daniel, 1997; Kraus et al., 1997). Bentonite is subject to increases in hydraulic conductivity caused by chemical alterations, particularly when calcium is leached from cover soils under conditions of low overburden stress, such as in secondary containment linings (Dobras and Elzea, 1993) or final cover systems (James et al., 1997). In liner systems, where the overburden stress on the GCL is much greater, alterations in hydraulic conductivity, if any, tend to be small for GCLs permeated with actual landfill leachate (Ruhl and Daniel, 1997).

The favorable hydraulic properties of GCLs are tempered by the low shear strength of hydrated bentonite (Mesri and Olson, 1970; Olson, 1974; Gilbert et al., 1996; Stark and Eid, 1997; Stark et al., 1998; Fox et al., 1998) and low bearing capacity of hydrated GCLs (Koerner and Narejo, 1995; Fox et al., 1996). When bentonite is hydrated and sheared, angles of internal friction as low as 5 to 10° may result. Because bentonite is so well known for its low shear strength, caution is appropriate when employing materials such as GCLs that contain bentonite on slopes.

A shearing failure involving a GCL can occur at three possible locations (Figure 3-1): (1) the external interface between the top of the GCL and the overlying material (soil or geosynthetic); (2) internally within the GCL; and (3) the external interface between the bottom of the GCL and the underlying material (soil or geosynthetic). If failure is internal, the failure may be bentonite-to-bentonite (e.g., at the mid-plane of the GCL), or it may be at the internal interface between the bentonite and either the upper or lower geosynthetic component (if present).

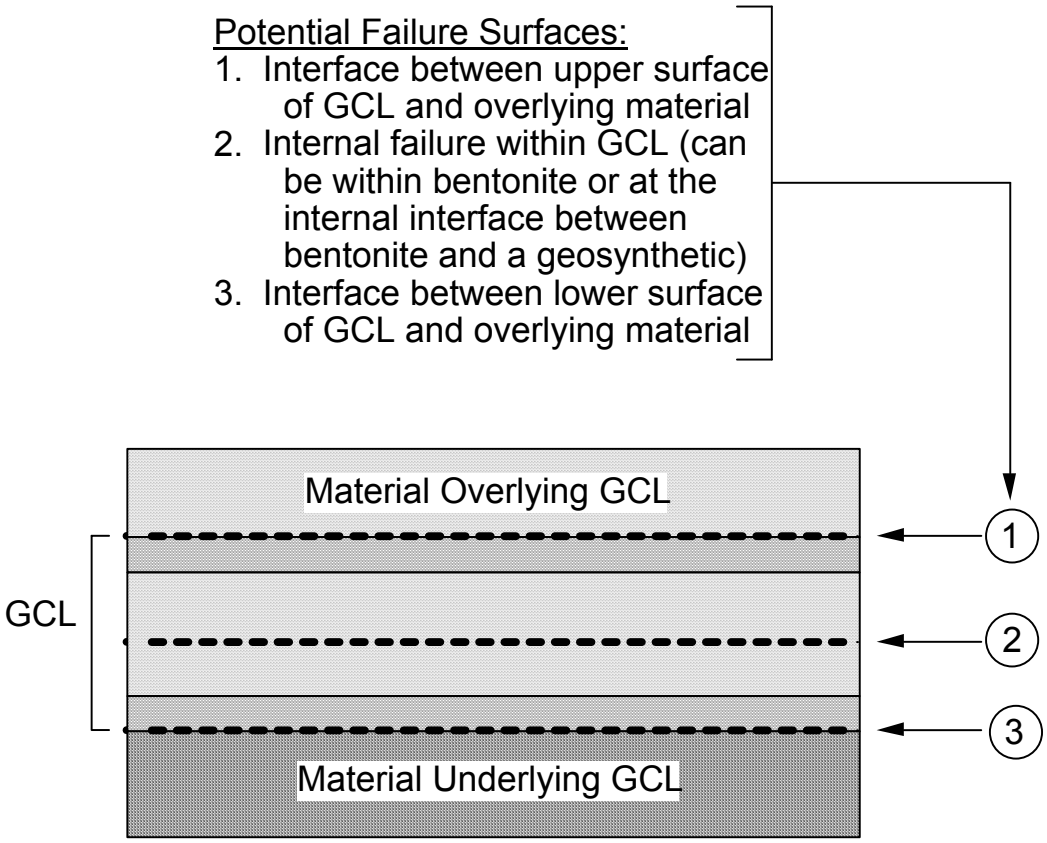

Figure 3-1. Potential failure surfaces for a GCL.

Current engineering design practice is to establish appropriate internal and interface shear strength parameters for design of GCLs on slopes using direct shear tests on 300-mm square test specimens, and to employ traditional limit equilibrium techniques for analyzing slope stability. However, the low shear strength of bentonite, the limited number of laboratory test results available, the inherent limitations of laboratory direct shear tests, the uncertainty over use of peak versus residual shear strength, the relative newness of GCLs, and the lack of field experience with GCLs all lead to questions about the long-term stability of GCLs on relatively steep slopes.

To provide field-scale data on the stability of GCLs on slopes, field test plots were constructed. It was recognized that it would not be possible to construct and instrument a full-scale landfill lined with GCLs, but it was possible to construct and instrument prototype landfill covers. Therefore, test plots were constructed to evaluate the stability of field test plots containing GCLs.

This chapter summarizes the test plots, data collected from the test plots, and conclusions from the test plots. Appendix D provides additional details.

3.2 Background on GCLs

3.2.1 Introduction

A GCL consists of approximately 5 kg/m^2 of sodium bentonite sandwiched between two GTs or attached to a GM with an adhesive. Figure 3-2 shows two general types of GCLs. Both types were used for this research.

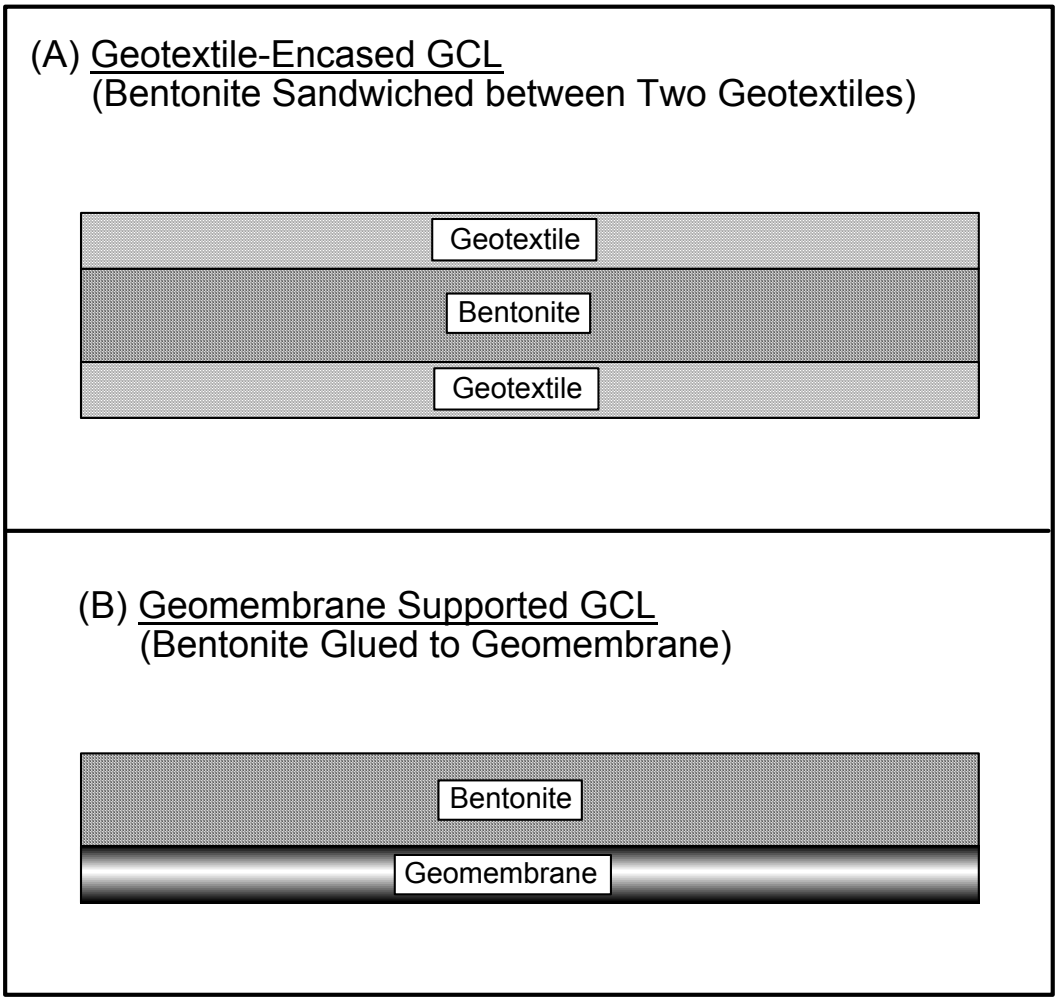

Figure 3-2. Two general types of GCLs.

The specific types of GCLs that were available when this project was initiated in 1994 are shown in Figure 3-3. Only the unreinforced, GT-encased, GCL was not included in the field test plots (all the others were included). The unreinforced, GT-encased GCL was omitted because this type of GCL is not intended for relatively steep slopes -- a reinforced, GT-encased GCL would be recommended instead.

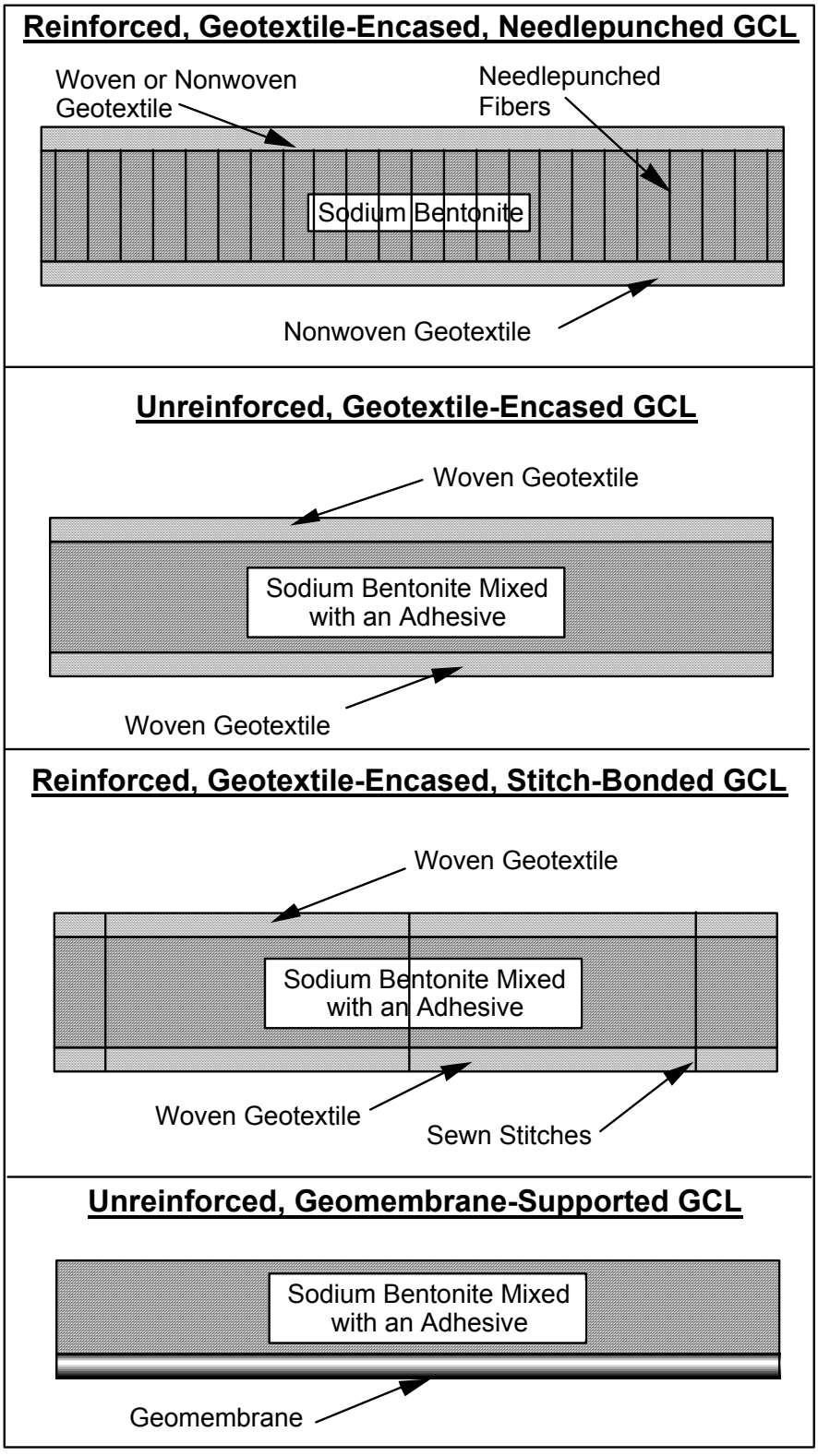

Figure 3-3. Cross sections of GCLs available at the time of this study.

The specific product types included in this testing program were as follows. Bentomat® and Bentofix® are reinforced, GT-encased, needlepunched GCLs that consist of dry sodium bentonite sandwiched between two GTs. One GT is nonwoven while the other GT can be either woven or nonwoven. The entire assembly is needle punched together. Bentomat ST, which contains nonwoven and woven GTs on the two surfaces of the GCL, was used in the research program. Bentofix NS (also with nonwoven and woven GT components on the two surfaces of the GCL) and Bentofix NW (nonwoven GTs on both surfaces) were also used in the research program. Claymax® 5000SP was the GT-encased, stitch-bonded GCL used in the test plots. Gundseal® was the GM-supported GCL employed in the testing program.

3.2.2 Advantages and Disadvantages of GCLs

GCLs enjoy numerous advantages and disadvantages (Daniel and Boardman, 1993), which are summarized here. The principal advantages of GCLs (as compared with CCLs) are favorable cost, convenience of installation, and outstanding hydraulic properties.

The installed cost of GCLs is typically equal to or less than that of CCLs, particularly if clay must be shipped from off site or if bentonite must be blended with soil to form the clay liner material. In addition, a GCL occupies less volume than a CCL, which can result in more landfill volume becoming available for waste disposal when a GCL is used. Because GCLs can be installed far more rapidly than CCLs, construction time is less with GCLs, which can significantly reduce overall construction costs.

GCLs are convenient for owners of waste containment facilities because they can be bid with the other geosynthetic components and installed by the same organization that installs the other geosynthetics. The cost of a GCL is more predictable than that of CCLs, and the much more rapid installation time of GCLs is usually attractive to the project owner.

The other major advantage of GCLs is their favorable hydraulic characteristics. The hydraulic conductivity of GCLs is typically in the range of 1 to 5 x 10^{-9} cm/s, which is one to two orders of magnitude lower than the typical hydraulic conductivities assumed for CCLs. This makes the hydraulic performance of GCLs potentially superior to CCLs. In addition, GCLs have excellent self-healing properties (Shan and Daniel, 1991; Estornell and Daniel, 1992), excellent ability to withstand differential settlement (Koerner et al., 1996; Lagatta et al., 1997), ability to self-heal after desiccation (Boardman and Daniel, 1996), and resistance to the potentially damaging effects of freezing temperatures (Hewitt and Daniel, 1997; Kraus et al., 1997).

GCLs also suffer from several disadvantages. Perhaps the three most significant disadvantages of GCLs are the low shear strength of hydrated bentonite, vulnerability to chemical alterations, and the thinness of GCLs.

Bentonite is famous among geotechnical engineers and geologists for its very low strength when hydrated. Potential problems arise when GCLs are placed on slopes. Also, bentonite may be for locally squeezed (thus thinning the GCL) by sharp stones or an uneven subgrade. It is generally accepted that GCLs can be safely placed on landfill cover slopes inclined at 10H:1V (5.7°) or flatter without any need for internal reinforcement or slope stability analysis. Steeper slopes may or may not be stable, depending on the type of GCL and specific conditions relevant to the slope.

The second disadvantage of GCLs relates to potential chemical alterations that could increase hydraulic conductivity (Ruhl and Daniel, 1997). Particular concern exists for landfill covers containing calcium-rich soils (James et al., 1997).

A third concern about GCLs is related to the thinness of GCLs. GCLs are nominally about 10 mm thick. Like any thin liner, GCLs are vulnerable to puncture, e.g., as described for a case involving accidental puncture of a GM/GCL composite liner by a piece of maintenance equipment (Daniel and Gilbert, 1996). The thinness of GCLs also makes them less able to adsorb and attenuate chemicals than much thicker CCLs, and less resistant to chemical diffusion than much thicker CCLs (Foose et al., 1996; 1999).

3.2.3 Shear Strength of GCLs

One disadvantage of GCLs is the low shear strength of hydrated bentonite. Shear test data on unreinforced, hydrated GCLs result in friction angles of about 10° at intermediate normal stress. In EPA workshops on GCLs, the shear strength of the bentonite in GCLs, which controls the internal shear strength of unreinforced GCLs, was cited as a primary technical concern in the use of GCLs in waste containment systems (Daniel and Boardman, 1993). The main factors affecting the internal shear strength of GCLs include the magnitude of normal stress, water content of the bentonite, type of hydrating liquid, rate of shearing, reinforcement, amount of deformation, and effects of seismic loading. These factors are reviewed below.

3.2.3.1 Magnitude of Normal Stress

The classical Mohr-Coulomb failure criterion for the shear strength of soil is:

$$\tau = c + \sigma \tan \phi \qquad \text{(Eq. 3-1)}$$

where: τ is the shear stress (Pa), c is the cohesion (Pa), σ is the normal stress (Pa), and ϕ is the angle of internal friction (degrees). The concept is illustrated in Figure 3-4. The

ideal Mohr-Coulomb failure envelope is linear. However, the relationship between shear stress and normal stress for bentonite is not always linear (Figure 3-5).

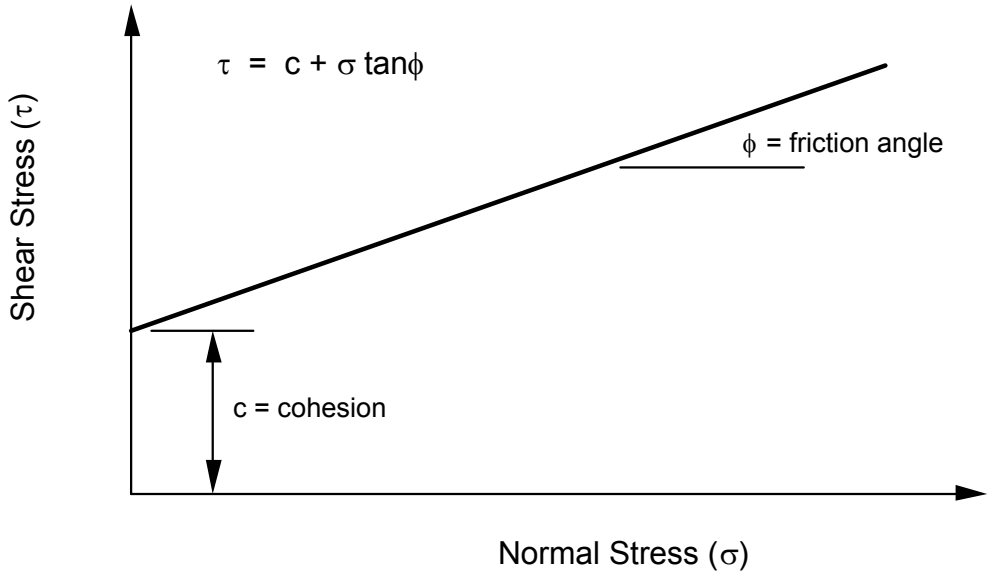

Figure 3-4. Mohr-Coulomb failure envelope.

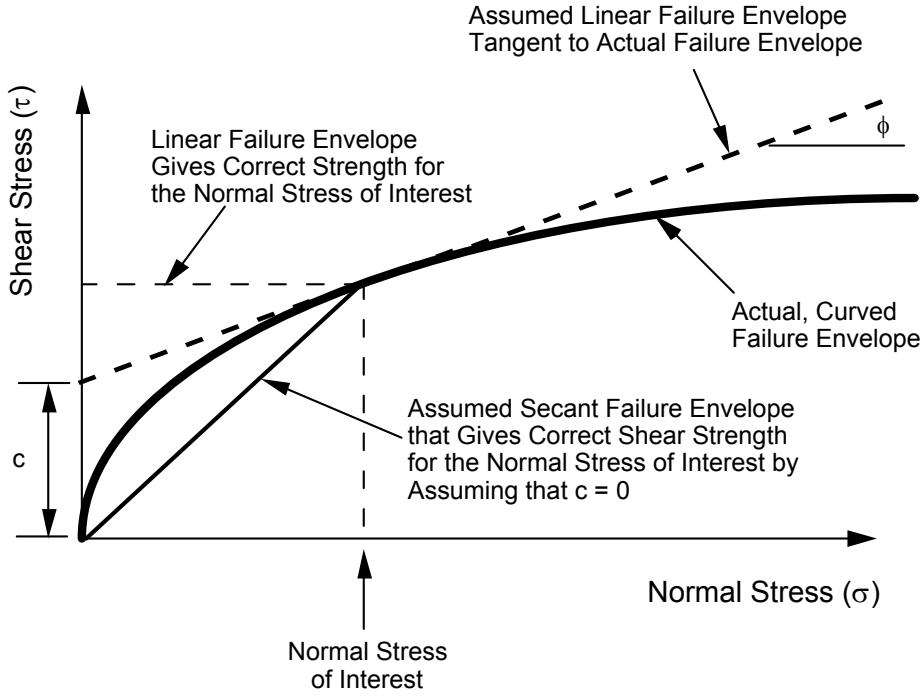

Figure 3-5. Curved Mohr-Coulomb failure envelope.

The cohesion of the GCL can be very important, particularly for internally reinforced GCLs (i.e., needlepunched or stitch-bonded GCLs) employed in situations with low normal stress, such as landfill covers. Work is underway to correlate peel strength with cohesion in the hope of identifying a relatively simple index test that will correlate with cohesion.

3.2.3.2 Water Content

The shear strength of bentonite is sensitive to water content. The angle of internal friction decreases with increasing water content. For example, shear tests that were performed on an unreinforced GCL at The University of Texas showed that at a water content of 20%, the angle of internal friction was 22°, but when the water content was increased to 50%, the friction angle of the unreinforced GCL decreased to 7° (Daniel et al., 1993). Hydrated bentonite is significantly weaker than dry bentonite.

When hydrated GCLs are tested in direct shear boxes, the GCL may either be hydrated at low normal stress and then consolidated in the shear box to the desired normal stress for shear testing, or the GCL may be immediately subjected to the final normal stress and hydrated under that stress. The recommended procedure is normally to apply stresses and hydration water in a manner that will simulate the conditions in the field. However, the procedure is also impacted by the practicality of testing. Because 300 mm by 300 mm shear boxes are very expensive, it is customary practice to minimize the amount of time that the boxes are committed to any one test. To accomplish this, the GCL is often hydrated in a separate apparatus at a comparatively low normal stress of about 12 kPa, and then transferred to the shear box for consolidation and shearing.

3.2.3.3 Type of Hydrating Liquid

The type of hydrating liquid relates to the bentonite particle's adsorption capability. This is evidenced by both hydraulic conductivity and shear strength, the latter being the focus of this study. The greater the adsorptive capability of the hydrating liquid, the lower the shear strength of the bentonite. The GCL's shear strength should be evaluated with the site-specific liquid that will hydrate the bentonite.

3.2.3.4 Rate of Loading

The rate of loading of GCLs affects the shear strength of the GCL. The general experience with bentonite is the slower the loading, the lower the internal shear strength of the GCL (Daniel et al., 1993). Thus, care should be taken in testing GCLs so as not to shear the GCL too quickly.

3.2.3.5 Reinforcement

Many commercial GCLs are reinforced to enhance the internal shear strength of the GCL. The reinforced GCLs used in the field test plots included Bentomat, Claymax

500SP, and Bentofix. When a reinforced GCL is sheared internally, the needlepunched fibers or sewn stitches are put into tension as shearing occurs, which enhances internal shear strength. However, there are limitations on the benefits of this reinforcing, as discussed below in the next subsection.

3.2.3.6 Amount of Deformation

The peak shear strength is the maximum shear strength measured during shear. Typically, however, many materials "strain soften" after the peak strength is reached. The residual shear strength is the minimum post-peak shear stress, which typically occurs at a very large displacement compared to the displacement at which the peak strength is generated. Figure 3-6 illustrates the difference between peak and residual shear strength.

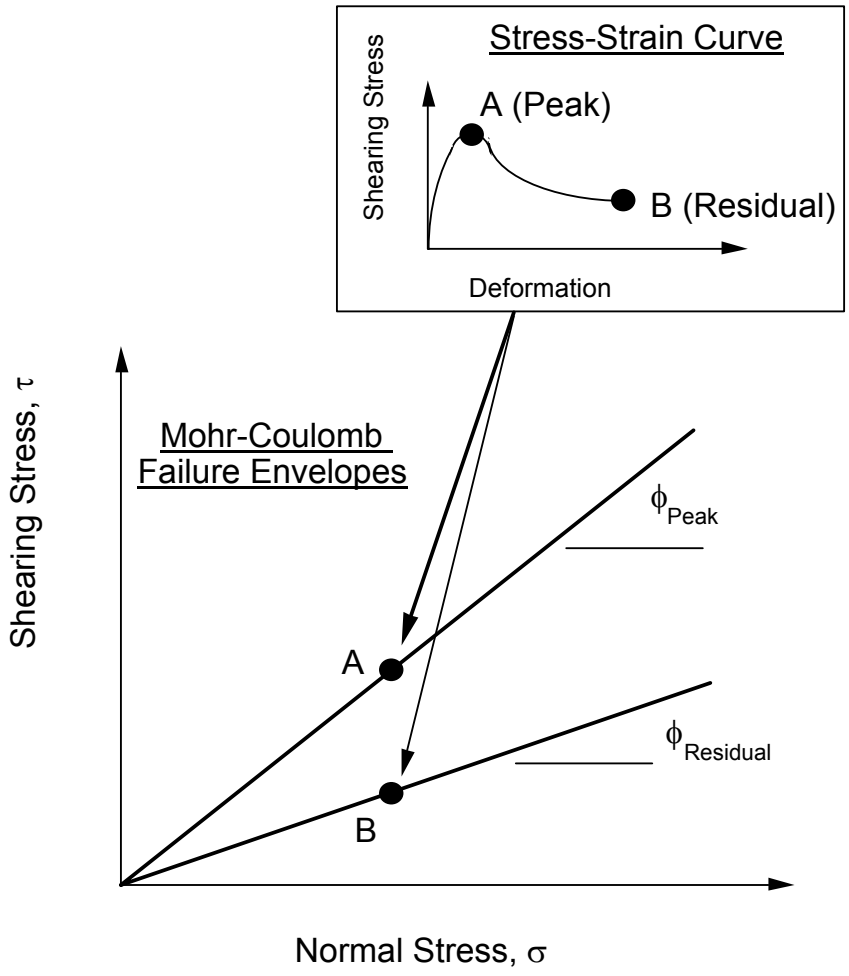

Figure 3-6. Peak and residual shear strength.

If a reinforced GCL is loaded to very large shearing displacements, reinforcing fibers may pullout from one or both of the GTs, break, or creep. If the reinforcing fibers fail, the strength of the reinforced GCL may be about the same as that of an unreinforced GCL. The key issue is how much deformation will actually occur in the field, and whether there is a risk of residual conditions actually developing.

3.2.3.7 Seismic Loading

Data on effects of cyclic loading on the internal shear strength of GCLs is very limited. The tests indicate that cyclic loading causes a slight increase in the internal shear strength of dry, unreinforced GCLs. The increase in strength is the result of a slight densification of the dry bentonite during cyclic loading. However, the tests indicate that unreinforced, saturated bentonite undergoes a reduction in strength from cyclic loading. The reduction increases with increasing number of cycles of loading. Results are described by Lai et al. (1998).

3.2.4 Interface Shear Strength

The interface shear strength of the GCL with an adjacent material can be the most critical (i.e., lowest) shear strength. The shear strength of GCLs at interfaces can be affected by several factors. One factor is the interfacing materials. For example, the friction angle between a GCL and subsoil will be different from the friction angle between a GCL and a GM. Also, a textured GM will typically have a higher interface friction angle with a GCL than a smooth GM.

Another factor affecting the interface shear strength of GT-encased GCLs is the different types of GTs used in making GCLs. An interface involving a woven GT may have a lower shear strength than an interface involving a nonwoven GT. A third factor is the degree of hydration of the bentonite and its potential mobility through the GT components of the GCL. If hydrated bentonite can swell through the GTs, the hydrated bentonite may “lubricate” the interface with an adjacent material. In addition, the level of normal stress and amount of deformation can influence interface shear strengths. Distortion before or during deformation could also be a factor. Finally, the amount of deformation can influence interface shear strength. The large-displacement interface shear strength is generally less than the peak value.

3.3 Field Test Plots

Fourteen field test plots were constructed in Cincinnati, Ohio. The layout of the plots is shown in Figure 3-7. Five plots (plots A-E) were constructed on a 3H:1V slope, and nine plots (plots F to L, N, and P) were built on a 2H:1V slope. The 3H:1V slopes were part of an actual final cover system over a closed section of the landfill, and the 2H:1V slopes were along an excavated slope on one side of a large pit located adjacent to the landfill. Plot P was built where plot G had originally been located, after a slide

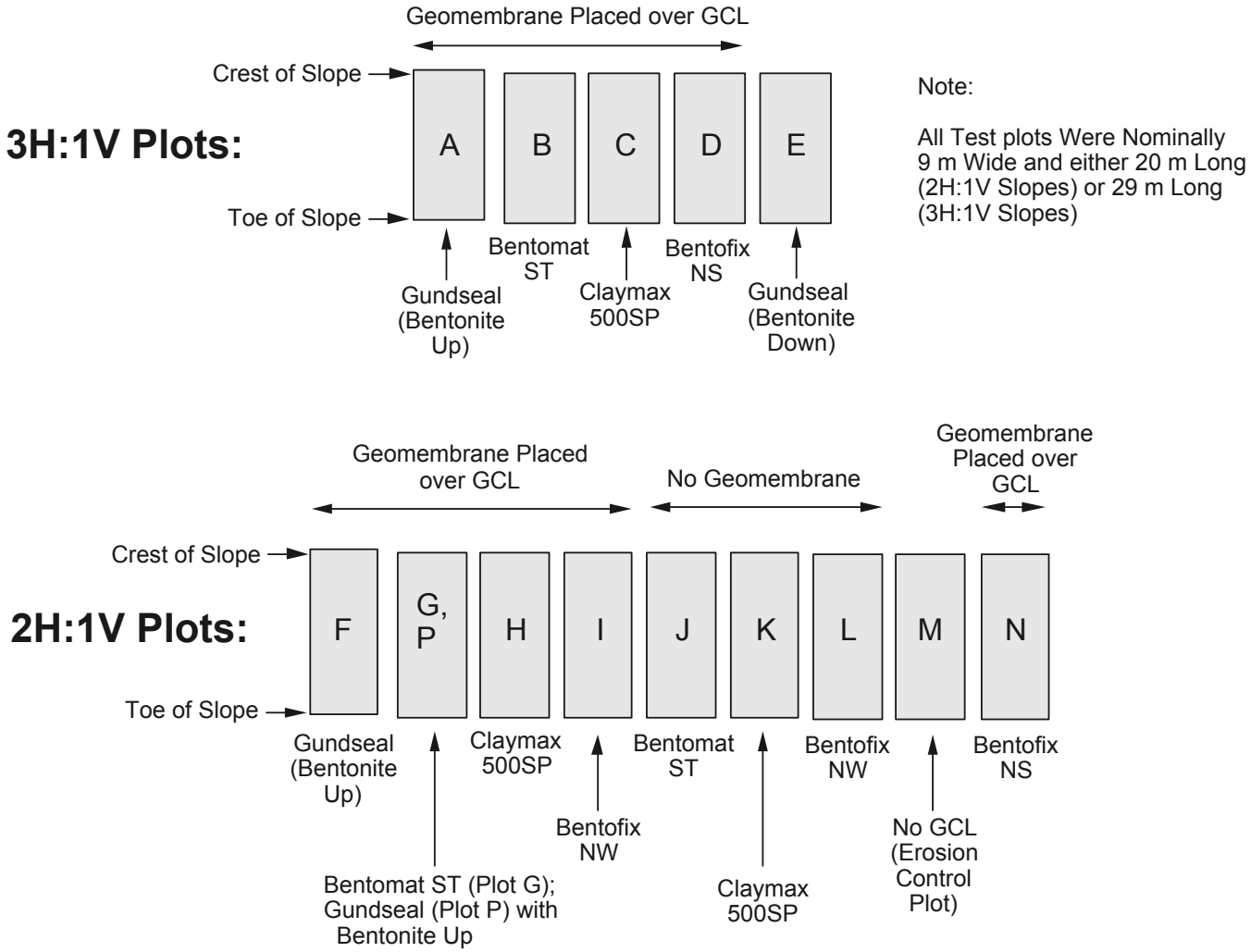

Figure 3-7. Layout of field test plots.

occurred at plot G. An additional plot (M) did not contain a GCL; this plot was constructed to study erosion of surface soils. Plots on the 2H:1V slope were nominally 20 m long while those on the 3H:1V slope were 29 m long. All plots were two GCL panel widths (≈ 9 m) wide and were 0.9 m thick.

A typical cross section of a test plot is shown in Figure 3-8. Most of the test plots were constructed with a GM overlying the GCL, which would be typical of a final cover system for a landfill. However, GCLs are also used in final cover systems without GMs. Hence, three plots were constructed with no GM. The plots were drained internally using either a GC drainage layer (GT/GN/GT system) or, for the three plots that did not contain a GM, a sand drainage layer. The drainage layer was included to limit build-up of water pressure in the overlying soils and, by doing so, to enhance the stability of the cover soils.

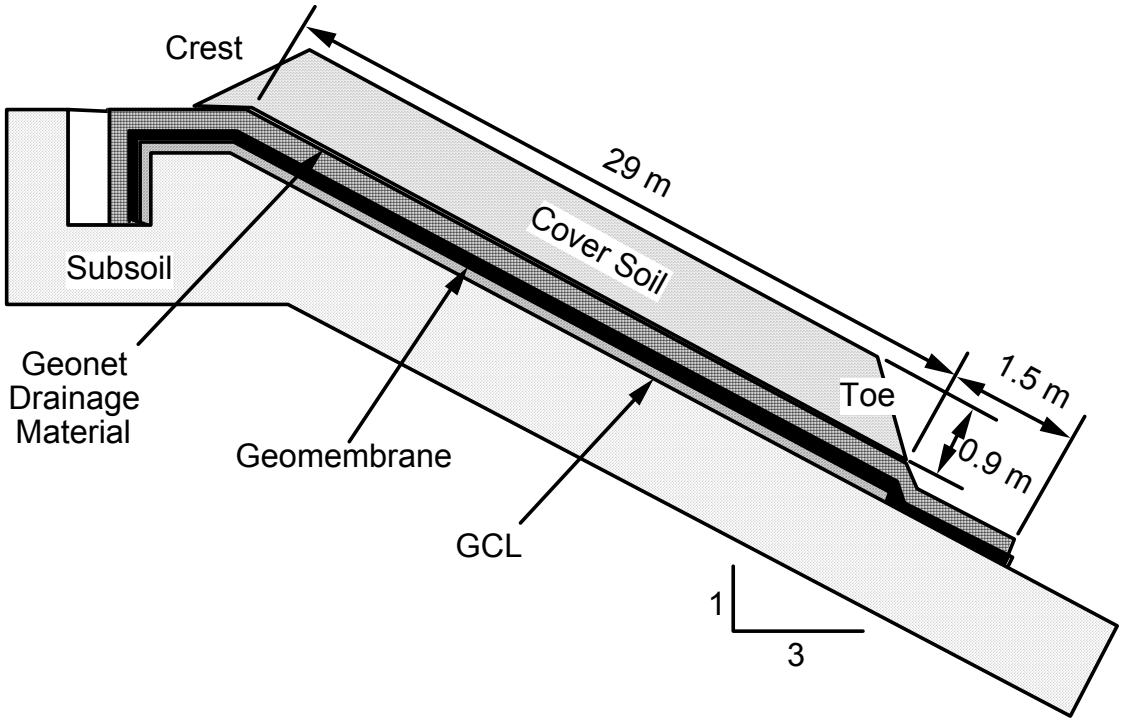

Figure 3-8. Typical cross-section for 3H:1V test plot.

Most of the GCLs were intentionally placed with bentonite in direct contact with the subgrade soil on the assumption that the bentonite would absorb water from the subgrade soils and hydrate in this manner. Laboratory experiments have shown that GCLs placed on damp or moist soils will hydrate in this fashion (Daniel et al., 1993). It

was desired that the bentonite hydrate in the test plots so that the most critical condition (i.e., hydrated bentonite) could be investigated.

3.3.1 Rationale for 2H:1V and 3H:1V Slopes

The rationale for selecting the 2H:1V and 3H:1V slope inclinations was as follows. The 3H:1V slope was selected to be representative of typical final cover systems for landfills in use at the time the study was initiated (1994). In order to confirm that GCLs are safe against internal failure on 3H:1V slopes, it must be shown that they are not only stable, but are stable with an adequate factor of safety. For an infinite slope consisting of cohesionless interfaces with no seepage, the factor of safety (FS) is:

$$FS = \tan(\phi) / \tan(\beta) \qquad \text{(Eq. 3-2)}$$

where: ϕ = the angle of internal friction (degrees); and β = the slope angle. Engineers typically design permanent slopes for landfills to have a minimum factor of safety for static loading of about 1.5. The ratio of tan β for a 2H:1V slope to tan β of a 3H:1V slope is 1.5. Subject to the assumptions listed above, if a GCL is theoretically stable on a 2H:1V slope (i.e., FS > 1.0), the same GCL is demonstrated to be stable on a 3H:1V slope with FS > 1.5. Therefore, the 2H:1V slopes were chosen to demonstrate internal stability of GCLs on in 3H:1V slopes with FS > 1.5. However, it was recognized that constructing 2H:1V slopes was pushing the GCLs to (and possibly beyond) their limits of stability, if not with respect to the internal shear strength the GCLs, then certainly with respect to the various interfaces within the system.

3.3.2 **GCLs**

Table 3-1 summarizes the type of GCL installed in each plot, the targeted and actual inclinations of the slopes, and the dimensions and cross section of each test plot. Bentofix and Bentomat are GT-encased, needle-punched GCLs. Bentofix NS and Bentomat ST consist of bentonite sandwiched between nonwoven and woven GTs. Bentofix NW consists of bentonite sandwiched between two nonwoven GTs. One surface of Bentofix is heat burnished (the side with the woven GT for Bentofix NS and one of the sides with a nonwoven GT for Bentofix NW). As indicated in Table 3-1, either the woven or nonwoven GT faced upward, depending on the GCL and test plot. Which GT component (woven or nonwoven) was in contact with a textured GM turned out to be very important. Figure 3-9A depicts the cross section for the two test plots (B and G) in which the woven GT component of the GCL faced upward. Figure 3-9B illustrates the cross section in Plots D and N with the nonwoven GT component facing upward. Plots I and L, which contained Bentofix NW, also had a nonwoven GT component of the GCL facing upward, but the lower GT component of this GCL was also a nonwoven GT.

Table 3-1. Information on Test Plots.

Test Plot	Type of GCL	Nominal Slope (H:V)	Target Slope Angle (deg)	Actual Slope Angle (deg)	Actual Slope Length (m)	Actual Plot Width (m)	Cross Section (Top to Bottom)	GCL Side Facing Upward	GCL Side Facing Downward
A	Gundseal	3:1	18.4	16.9	28.9	10.5	Soil/GDL/GM/GCL	Bentonite	GM
B	Bentomat ST	3:1		17.8	28.9	9.0	Soil/GDL/GM/GCL	Woven GT	Nonwoven GT
C	Claymax 500SP	3:1	18.4	17.6	28.9	8.1	Soil/GDL/GM/GCL	Woven GT	Woven GT
D	Bentofix NS	3:1	18.4	17.5	28.9	9.1	Soil/GDL/GM/GCL	Nonwoven GT	Woven GT
E	Gundseal	3:1	18.4	17.7	28.9	10.5	Soil/GDL/GCL	GM	Bentonite
F	Gundseal	2:1	26.6	23.6	20.5	10.5	Soil/GDL/GM/GCL	Bentonite	GM
G	Bentomat ST	2:1	26.6	23.5	20.5	9.0	Soil/GDL/GM/GCL	Woven GT	Nonwoven GT
H	Claymax 500SP	2:1	26.6	24.7	20.5	8.1	Soil/GDL/GM/GCL	Woven GT	Woven GT
I	Bentofix NW	2:1	26.6	24.8	20.5	9.1	Soil/GDL/GM/GCL	Nonwoven GT	Nonwoven GT
J	Bentomat ST	2:1	26.6	24.8	20.5	9.0	Soil/GT/Sand/GCL	Woven GT	Nonwoven GT
K	Claymax 500SP	2:1	26.6	25.5	20.5	8.1	Soil/GT/Sand/GCL	Woven GT	Woven Gt
L	Bentofix NW	2:1	26.6	24.9	20.5	9.1	Soil/GT/Sand/GCL	Nonwoven GT	Nonwoven GT
M	Erosion Control	2:1	26.6	23.5	20.5	7.6	Soil	No GCL	No GCL
N	Bentofix NS	2:1	26.6	22.9	20.5	9.1	Soil/GDL/GM/GCL	Nonwoven GT	Woven GT
P	Gundseal	2:1	26.6	24.7	20.5	9.0	Soil/GDL/GM/GCL	Bentonite	GM

Key: GDL = geocomposite (geotextile/geonet/geotextile) drainage layer; GM = textured GM; GT = geotextile; GCL = geosynthetic clay liner.

Claymax 500SP consists of bentonite mixed with an adhesive and encased between two woven slit-film GTs that are stitched together. Lines of stitching are spaced 100 mm apart. The two GT components are identical in this type of GCL.

Gundseal is an unreinforced GCL consisting of bentonite mixed with an adhesive and bonded to a GM. The GM component was a textured, 0.8-mm thick, HDPE material. With this product, the exposed surface of the bentonite component was covered with a thin GT called a "spider net," which is used to help prevent loss or dislodgment of loose particles of bentonite from the GCL during storage, transportation, and installation. The spider net was incorporated in all plots with Gundseal, except for plot P, which did not contain the spider net. Figure 3-10 shows the two uses of this type of GCL, with the bentonite component either facing upward or downward. When the bentonite was facing upward (as in plots A, F, and P), the bentonite was encased between two GMs. In this condition, the bentonite was expected to remain essentially dry, except for spot hydration along the overlap or near any imperfections in the overlying GM or GM seams. When the bentonite faced downward (as in plot E), the bentonite was expected to hydrate by absorbing moisture from the subsoil.

3.3.3 Other Materials

A 1.5-mm-thick textured HDPE GM was used for the GM component that was placed on top of the GCL in all test plots except J, K, and L (which contained no GM). The GC drainage layer consisted of two nonwoven GTs heat-bonded to both sides of a GN. The cover soil was a silty, clayey sand obtained from an on-site borrow source.

3.3.4 Construction

Construction of the test plots began on November 15, 1994 and was completed on November 23, 1994. However, plot P was constructed on June 15, 1995.

The test plots were first graded to provide a smooth subgrade, as shown in Figure 3-11. Next, geosynthetics were installed by pulling them down from the crest of the slope (Figure 3-12). Cover soil was placed by starting at the bottom of the slope and working upslope (Figure 3-13). All test plots, except plot M, were then covered with an erosion control material. The 3H:1V test plots are shown in Figure 3-14, and the 2H:1V test plots are shown in Figure 3-15.

In plots incorporating a GC drainage layer, the GM and GC were extended beyond the GCL at the toe of the slope and 1.5 m past the end of the cover soil (Figure 3-8). For plots constructed with a sand drainage layer (plots J, K, and L), a piece of geosynthetic drainage material was embedded in the sand at the toe of the slope and then extended 1.5 m beyond the end of the cover soil.

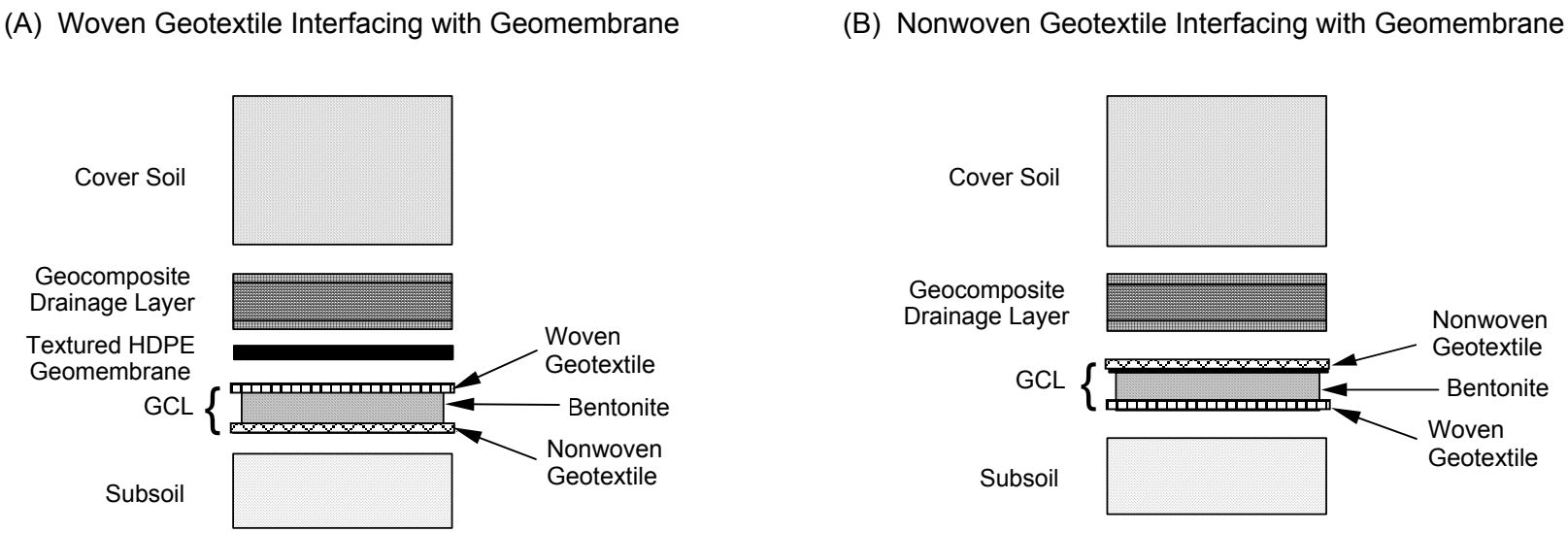

Figure 3-9. Orientation of GCL with either woven or nonwoven GT facing upward.

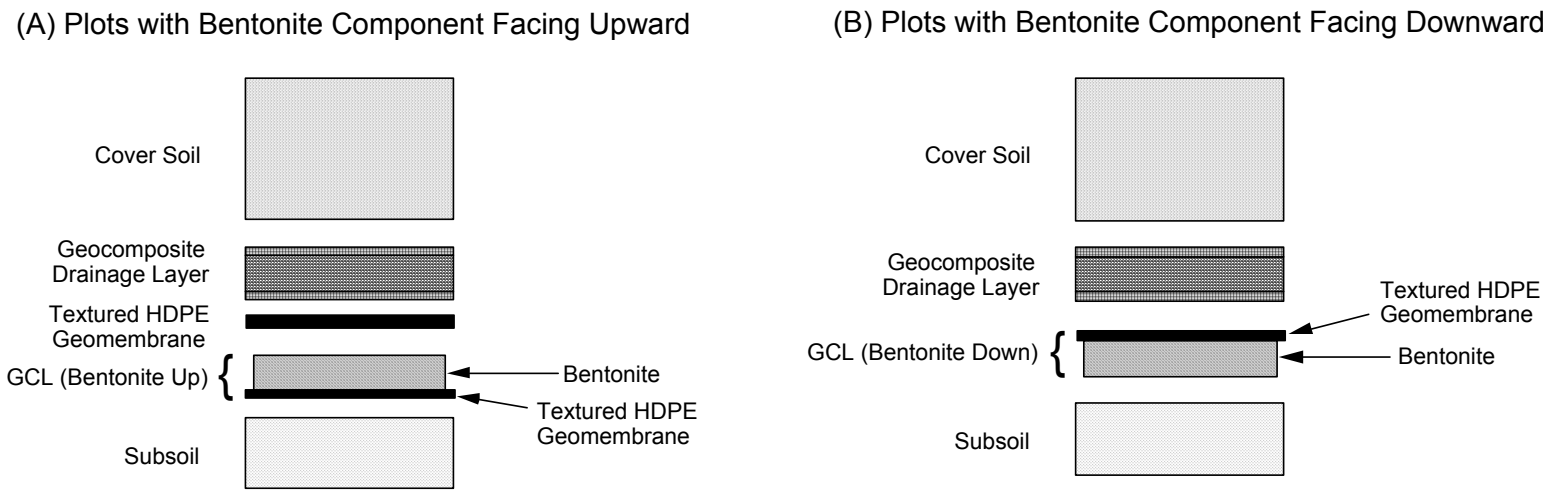

Figure 3-10. Placement of Gundseal with bentonite facing upward or downward.

Figure 3-11. Prepared surface on which 2H:1V test plots were constructed.

Figure 3-12. Typical installation of geosynthetics.

Figure 3-13. Placement of cover soil near top of slope.

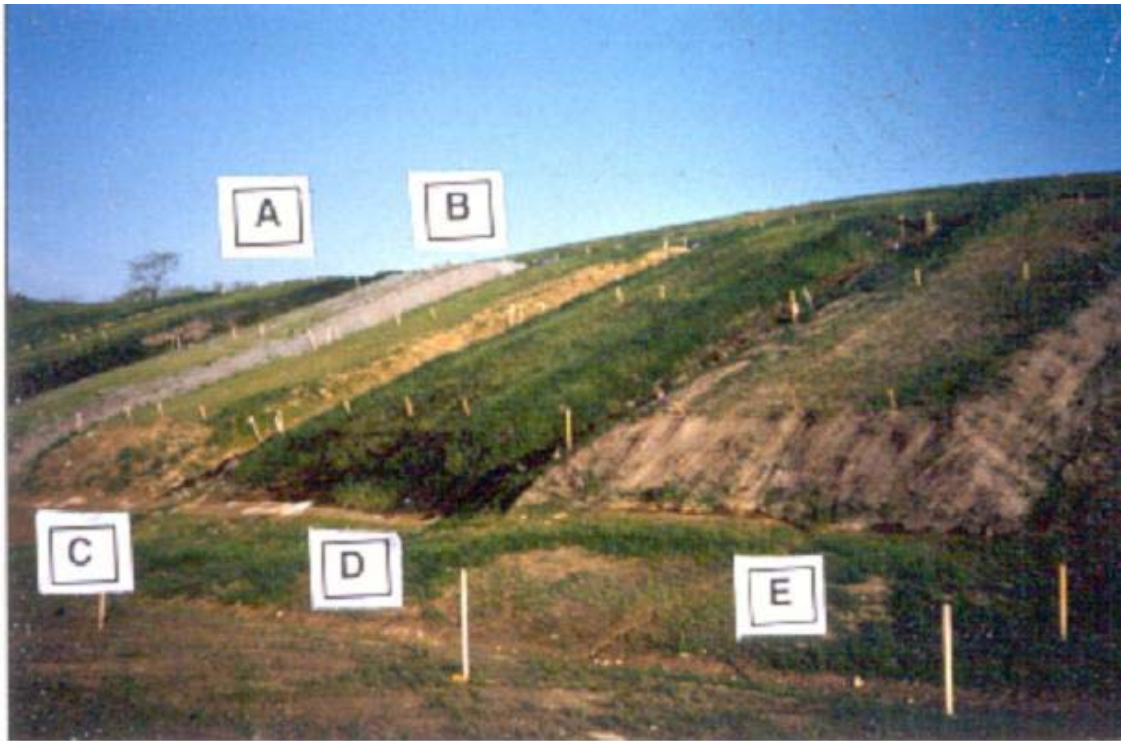

Figure 3-14. View of 3H:1V test plots.

Figure 3-15. View of 2H:1V test plots.

All of the geosynthetic materials in each test plot were brought into their respective anchor trenches (Figure 3-3), which were then backfilled. Because the purpose of each test plot was to test the internal shear strength of a particular GCL, the toe of each test plot was excavated at the completion of construction to the shape shown in Figure 3-8 so that no buttressing (i.e., passive) force could be mobilized at the toe of the slope. Similarly, any tension in the geosynthetic components located above the GCL would reduce the shearing stress to be carried by the internal structure of the GCL.

To prevent the development of tension in the geosynthetic components above the mid-plane of the GCL, components above the mid-plane of the GCL were cut as shown in Figure 3-16. Cutting occurred in the spring of 1995, about 5 months after construction of the test plots. However, the geosynthetics were not cut in plot P, which was constructed later in the program for the sole purpose of evaluating hydration of bentonite encased between two GMs (cutting the geosynthetics would have provided a pathway for water to enter the bentonite near the crest of Plot P).

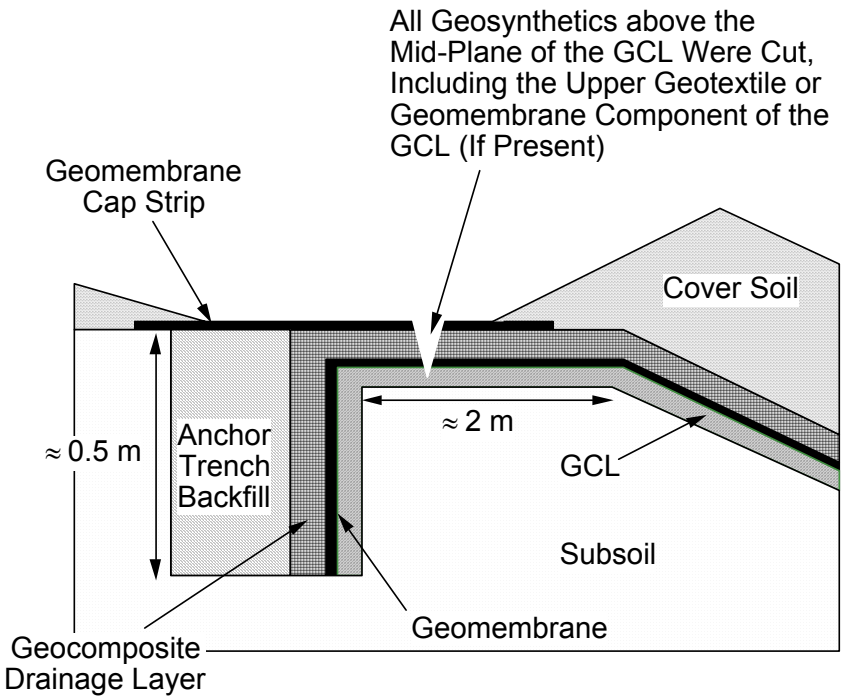

Figure 3-16. Cut in anchor trench above mid-plane of GCL

3.4 Instrumentation

The field test plots were instrumented, but limited funds available for instrumentation dictated that a simple, robust, cost-effective instrumentation program be implemented quickly and easily. The instrumentation program had two objectives: (1) provide an indication of the moisture conditions in the bentonite component of the GCL to verify that hydration had occurred; and (2) provide data on the downslope displacements occurring within the GCL. With respect to displacement, the objective was to monitor the shearing displacement, defined as the difference in displacement between the top and bottom surfaces of the GCL.

3.4.1 Moisture Sensors

It was expected that GCLs placed in contact with subgrade soils would hydrate by absorbing moisture from the subgrade. Project-specific testing indicated that substantial hydration of GCLs occurred within 10 to 20 days for GCLs placed in contact with the subgrade soils from the test site, even for subgrade soils compacted at a moisture content 4 percentage points dry of the standard Proctor optimum moisture content. Moisture sensors were installed to verify that the bentonite did indeed become hydrated. However, in the case of plots A, F, and P, the bentonite component of Gundseal was sandwiched between two GMs (see Figure 3-10A) with the expectation

that the bentonite would remain dry. For plots A, F, and P, moisture sensors were installed to verify that the bentonite remained unhydrated.

Gypsum blocks and fiberglass moisture sensors, shown schematically in Figure 3-17, were used to monitor in-situ moisture contents. These instruments were selected based on low cost and the ability to use multiple instruments to provide redundancy. Gypsum blocks were placed in subgrade soils about 50 mm below the GCL. Fiberglass sensors were placed in contact with the GCL, either at the interface between the GCL and subsoil or (for bentonite sandwiched between two GMs) between the GCL and GM. Typically, three fiberglass sensors were deployed at each test plot, near the crest, middle, and toe of the slope, and monitored every 1 to 4 weeks. However, 16 sensors were installed in Plot P.

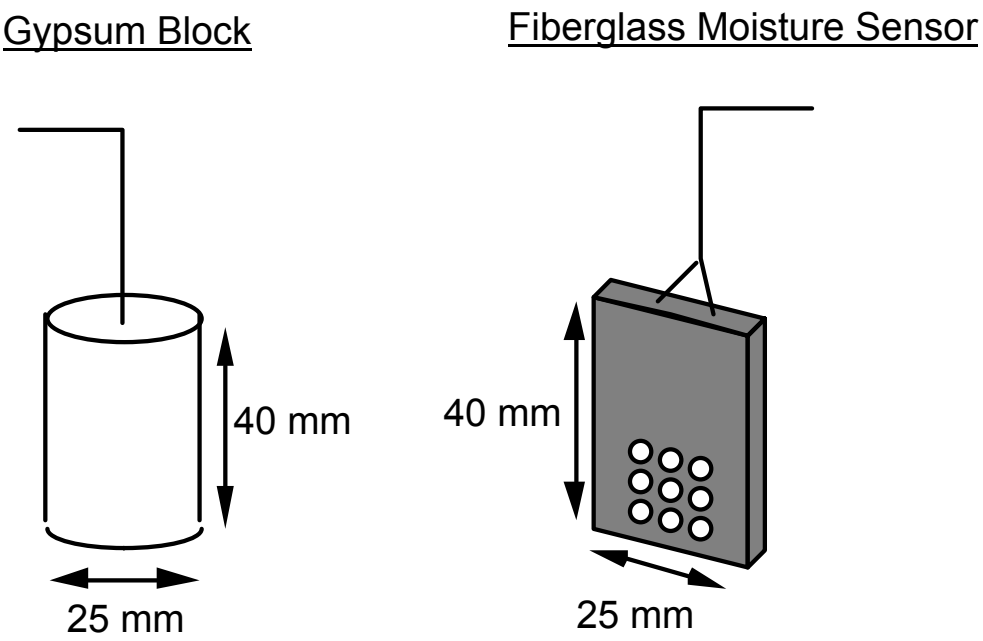

Figure 3-17. Schematic diagram of moisture sensors.

3.4.2 Displacement Gauges

Displacement gauges (extensometers) were installed in each test plot (except plot P, which was constructed only to monitor the moisture content of the bentonite) to measure total and differential displacements in the GCL at multiple locations along the slope. Pairs of stainless steel fish hooks were embedded into either the upper or lower geosynthetic component of a GCL and then glued with epoxy as shown in Figure 3-18.

A stainless steel wire was attached to the fish hooks and threaded through 6-mm outside-diameter plastic tubing, which protected the wire and minimized friction between the wire and overlying soil. Each wire extended from the fish hook to a monitoring point about 1.5 m beyond the crest of the slope. During construction, the monitoring point consisted of wooden stakes driven into the soil above the crest of the slope. After construction, the extensometer wires were connected to a more permanent table (Figure 3-19) at the crest of the slope, where the displacements were monitored for 3-1/2 years.

Fish hooks were attached to the upper and lower surfaces of each GCL panel at five equally-spaced locations along the length of the slope (Figure 3-19), resulting in 20 extensometer monitoring points per test section. The accuracy of the extensometers was estimated to be approximately 10 mm, based on experience with their use in the field. Displacements were typically measured every 1 to 4 weeks.

3.5 Laboratory Direct Shear Tests

The project schedule did not permit performing laboratory shear tests prior to construction. Instead, internal shear strength data from Shan and Daniel (1991), Daniel et al. (1993), and Shan (1993) were used for design of the test plots. Additional information on internal shear strength of GCLs is provided by Gilbert et al. (1996) and Well (1997). As initial data on the performance of the test plots became available, it became apparent that certain GM/GCL interfaces were more critical with respect to slope stability than the internal shear strength of the GCLs. Thus, the laboratory testing program focused on interfaces.

Interface direct shear tests were conducted to evaluate textured GM/GCL interfaces and the sand/GCL interface for one GCL. The tests were performed using 300 mm by 300 mm specimens per ASTM D5321, with samples taken from the same lots of materials deployed in the field. The GCLs were subjected to a normal stress of 17 kPa (equivalent to the field value in the test plots) and then hydrated for 10 days. However, Gundseal with bentonite encased between two GMs was not hydrated because the bentonite in the field was not expected to become hydrated. The rate of shear was 1 mm/min per ASTM D5321. All tests were single-point tests (i.e., one normal load of 17 kPa). For simplicity of presentation, the test results were interpreted in terms of a secant friction angle (ϕ_s). Peak and large-displacement (50 mm) secant friction angles are summarized in Table 3-2. The term “large displacement” is used rather than “residual” because the tests were carried out to displacements of about 25 mm and may not have reached true residual conditions.

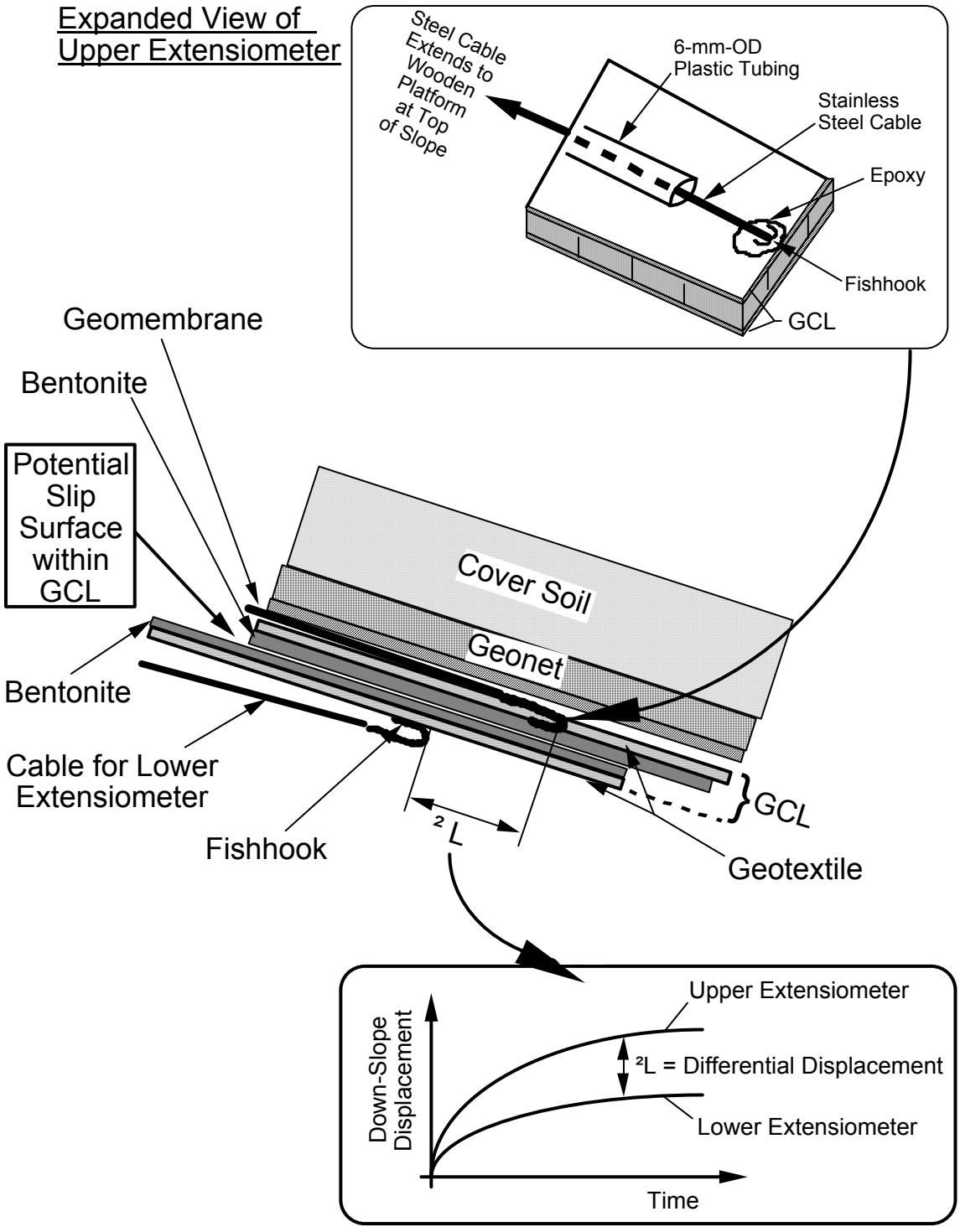

Figure 3-18. Displacement sensors attached to GCL.

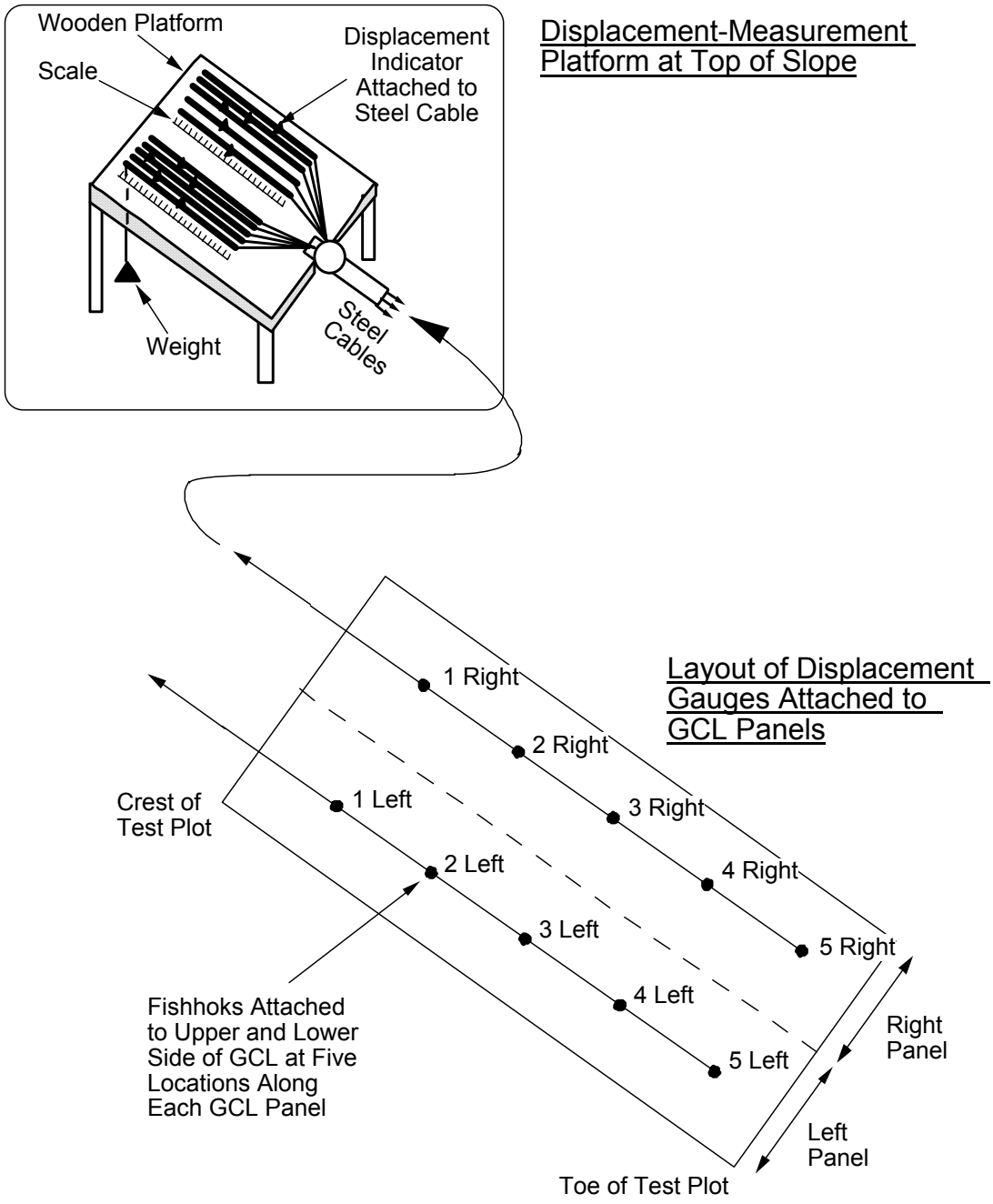

Figure 3-19. Displacement monitoring system.

Table 3-2. Summary of Results of Interface Direct Shear Tests.

Test Plot	Type of GCL	GCL Interface	Opposing Interface	Peak Secant Friction Angle (º)	Large-Displacement Secant Friction Angle (º)
A,E,F, & P	Gundseal	Dry Bentonite (Internal Shear)	Textured HDPE GM	37	35
B & G	Bentomat ST	Woven Slit-Film GT	Textured HDPE GM	23	21
C & H	Claymax 500SP	Woven Slit-Film GT	Textured HDPE GM	20	20
I	Bentofix NW	Nonwoven Needlepunched GT	Textured HDPE GM	37	24
K	Claymax 500SP	Woven Slit-Film GT	Drainage Sand	31	31
D & N	Bentofix NS	Nonwoven Needlepunched GT	Textured HDPE GM	29	22

Note: Plots J and L (plots with drainage sand and no GM) were not specifically evaluated because a relatively high friction angle (31º) was measured for plot K, which like plots J and L also had drainage sand and no GM. It was assumed that the friction angle between the drainage sand and either Bentomat ST (plot J) or Bentofix NW (plot L) was no less than the 31º value measured for Claymax 500SP.

3.6 Performance of Test Plots

3.6.1 Construction Displacements

The displacements that occurred in the GCLs were divided into construction and post-construction displacements. Displacements were usually largest for the displacement sensors located closest to the toes of the slopes (gauges 5-left and 5-right in Figure 3-19) and least for monitoring points located closest to the crests of the slopes (gauges 1-left and 1-right in Figure 3-19), indicating that the GCL panels were stretching.

Maximum downslope displacements measured during construction are summarized in Figure 3-20. The measurements shown in the plot represent the average of the maximum downslope movement of the left and right displacement gauges above and below the GCL (i.e., gauges 5-left above, 5-left below 5-right above, and 5-right below in Figure 3-19). Maximum displacements were generally 10 to 40 mm for the 3H:1V slopes and 40 to 200 mm for the 2H:1V slopes. Differential displacements between the upper and lower surfaces of the GCLs were less than the resolution of the extensometers (i.e., < 10 mm).

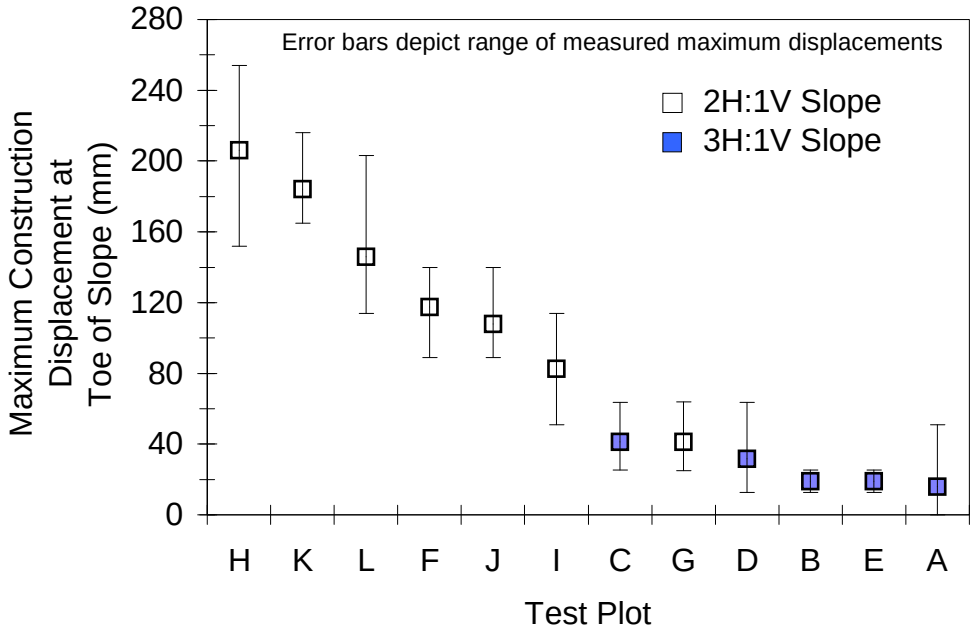

Figure 3-20. Maximum construction displacements measured at toe of slope.

Construction displacements were caused by mobilization of shear resistance at various interfaces within the system and development of tension in the geosynthetic components. The test plots with the largest movements during construction were plot C (3H:1V slope) and plots H and K (2H:1V slope). All three of these plots contained Claymax 500SP which, with woven slit-film GTs on both surfaces, had the lowest interface shear resistances of the GCLs and interfaces tested.

Test plot G (Bentomat ST) had the lowest displacement of the 2H:1V test plots, probably because the soil at this test plot was less clayey than some of the others and because the component of the GCL in contact with the subsoil was a nonwoven GT (nonwoven GTs generally have better interface shear resistances with soils than do woven slit-film GTs). Plot A had the smallest movement of the 3H:1V plots, probably because the textured GM component of Gundseal interfaced with the subgrade soil. In general, a textured GM also has comparatively good interface shear resistance (more than a woven slit-film GT).

3.6.2 Post-Construction Performance of 3H:1V Slopes

Post-construction displacements are summarized in Table 3-3. All 3H:1V slopes have remained stable. Total downslope displacements have been less than 50 mm, and differential displacements have been less than 40 mm. There has been no visual evidence of movement or surface cracking.

3.6.2.1 Test Plot A (Bentonite Between Two GMs)

The bentonite component of Gundseal was expected to remain dry because the bentonite was encased between two GMs. As indicated in Table 3-2, measured peak and large-displacement interface secant friction angles between dry bentonite and textured HDPE were 37º and 35º, respectively. Since the slope angle was 16.9º, the slope should be stable so long as the bentonite remains dry.

Fiberglass moisture sensors in plot A have provided variable results: two of the three moisture sensors have indicated that the bentonite is dry, but one sensor near the crest of the slope indicated some hydration (Appendix D). Two borings were drilled by hand near the crest and toe of the test plot in March 1995, and 100-mm-diameter samples of the GCL were removed. The water contents of the bentonite in the GCL at the crest and toe were 27% and 24%, respectively. These values are essentially identical to the water content at the time of installation, confirming that the bentonite had not hydrated. Individual fiberglass moisture sensors have been found during calibration to have relatively large scatter (Appendix D); however, the general trend indicated by the majority of sensors has proven to be correct in all test plots.

3.6.2.2 Test Plots B, C, and D (GT-Encased GCLs)

Test plots B, C, and D contain GT-encased GCLs. The bentonite in the GCL was expected to hydrate by absorbing moisture from subgrade soils. Most of the fiberglass moisture sensors have indicated that the bentonite has hydrated, although less than expected. One factor inhibiting hydration may have been the relatively dry, sandy subsoils on the 3H:1V test plots, compared to the 2H:1V test plots, which had more clayey, wetter subsoils.

Experience has shown that GCL interface shear strengths are typically less than internal shear strengths for internally-reinforced GCLs such as those used in test plots B, C, and D, when tested at low normal stress (Gilbert et al., 1996). Peak interface secant friction angles between the upward-facing GT component of the GCLs and the textured HDPE GM are 20º to 29º**,** and large-displacement friction angles are 20º to 22º degrees for essentially full hydration of the GCLs (Table 3-2).

Table 3-3. Summary of Post-Construction Performance of Test Plots.

Plot	Slope	Type of GCL	Stability of Test Plot As of June, 1997	Total Displacement (mm)	Differential Displacement (mm)
A	3H:1V	Gundseal	Stable	20	10
B	3H:1V	Bentomat ST	Stable	30	40
C	3H:1V	Claymax 500SP	Stable	25	30
D	3H:1V	Bentofix NS	Stable	50	25
E	3H:1V	Gundseal	Stable	30	30
F	2H:1V	Gundseal	Internal Slide within the GCL Occurred 495 Days after Construction of Test Plot	-	750
G	2H:1V	Bentomat ST	Interface Slide between Lower Side of GM and Upper Woven GT of GCL 20 days after Construction of Test Plot	-	25
H	2H:1V	Claymax 500 SP	Interface Slide between Lower Side of GM and Upper Woven GT of GCL 50 days after Construction of Test Plot	-	130
I	2H:1V	Bentofix NW	Slumps and Surface Cracks Developed about 900 Days after Construction of Test Plot	500	25
J	2H:1V	Bentomat ST	Slumps and Surface Cracks Developed about 900 Days after Construction of Test Plot	800	75
K	2H:1V	Claymax 500SP	Slumps and Surface Cracks Developed about 900 Days after Construction of Test Plot	1200	900
L	2H:1V	Bentofix NW	Slumps and Surface Cracks Developed about 900 Days after Construction of Test Plot	500	180
N	2H:1V	Bentofix NS	Stable	30	10
P	2H:1V	Gundseal	Stable	NA	NA

Note: Total displacement is the total amount of downslope movement measured after construction was complete; differential displacement is the difference between downslope movement of the upper and lower surfaces of the GCL that occurred after construction.

3.6.2.3 Test Plot E (Unreinforced GCL)

Test plot E was constructed with the bentonite portion of Gundseal facing downward. Interface shear tests were not performed on the hydrated GCL because the internal shear strength under consolidated-drained conditions had already been studied. Consolidated-drained conditions were used because the GCLs in the test plots were installed dry and hydrated slowly under conditions most appropriately simulated consolidated-drained conditions. Although consolidated-drained conditions were thought to be most appropriate for these test plots, it is conceivable that unconsolidated-undrained or consolidated-undrained conditions may be more critical for other conditions, e.g., seismic loading. The designer should consider the most appropriate and critical condition for any particular application. The consolidated-drained direct shear tests performed previously employed fully hydrated samples that had water contents of approximately 150%. Resulting interface shear strengths were found to vary with normal stress (Figure 3-21). For the normal stress acting on the GCL in plot E (17 kPa), the drained angle of internal friction for fully hydrated bentonite is about 20º. The slope angle at plot E was 17.7º; thus, the test plot is expected to be stable if the bentonite is hydrated, but only with FS = tan (20º)/tan (17.7º) = 1.14 for an infinite slope.

As with most of the other test plots, the fiberglass moisture sensors for test plot E have yielded variable results, with some sensors indicating that the bentonite has become hydrated and others indicating that it has not become hydrated. Experience showed that when the sensors indicated that the GCLs were dry, the GCLs were indeed dry, and that when the sensors indicated that the GCLs had become very wet, they were indeed nearly fully hydrated. However, for the broad range of moisture sensor readings between dry and fully hydrated, the moisture sensors were not found to be particularly useful for indicating the degree of partial hydration.

To verify actual moisture conditions, a boring was drilled and a sample was taken near the crest of the slope (the driest area) in March 1995, and the water content of the bentonite was found to be 46%. Eight more borings were drilled in April 1996, at various locations along the full length of the slope. The water content varied between 54% and 79%, and averaged 60%. Daniel et al. (1993) previously measured the shear strength of the bentonite component of Gundseal as a function of water content using a direct shear apparatus and a slow rate of shear that allowed excess pore water pressures to fully dissipate. The range of normal stress used in the testing program was 27 to 139 kPa. The highest water content (≈145%) was achieved by fully hydrating the bentonite. Results, plotted in Figure 3-22, show that once the water content of the bentonite reaches 50% or more, the shear strength declines to a value approximately equal to the strength of fully hydrated bentonite. In other words, the bentonite does not have to be fully hydrated for its strength to be greatly reduced. This phenomenon is observed from handling a GCL; at 50% water content, the bentonite feels hydrated and

very slick. Thus, the average water content of 60% in test plot E should be sufficiently large to replicate the strength reduction associated with full hydration of the bentonite.

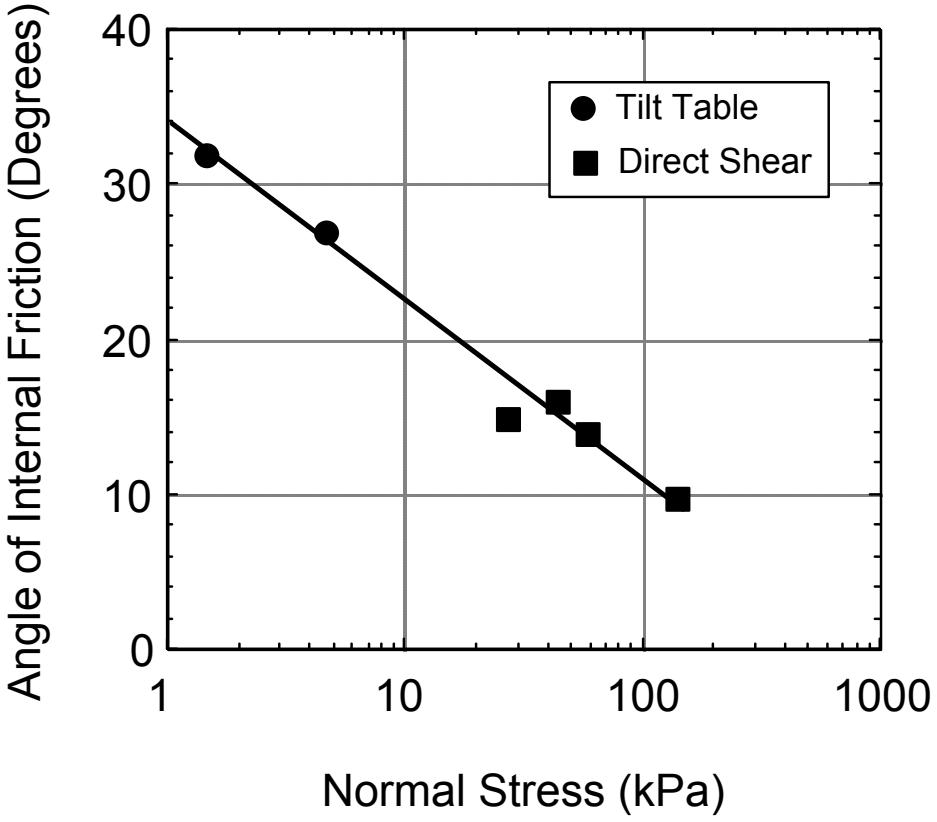

Figure 3-21. Influence of normal stress on secant angle of internal friction for internal shear of an unreinforced GCL (after Shan, 1993).

3.6.3 Post-Construction Performance of 2H:1V Plots

Slides have occurred at many of the 2H:1V test plots for different reasons. Two slides occurred at plots G and H a few weeks after construction was complete. These two slides are shown in Figure 3-23. Both involved slippage at the interface between the upper surface of the GCL (a woven GT in both cases) and the lower surface of the textured HDPE GM. The next slide occurred in plot F about a year and a half after construction. In this case, the bentonite (which was encased between two GMs) in this GCL unexpectedly became hydrated, and a slide resulted. The other test plots remained stable for the next two years, but then several slides occurred in the subsoils beneath other test plots. The subsoils were plastic clays, and the subsoil slides (which occurred at the end of a wet spring season) were presumed to be the result of hydration of the subsoil clays and possibly the buildup of excess pore water pressure in the subsoils, as well.

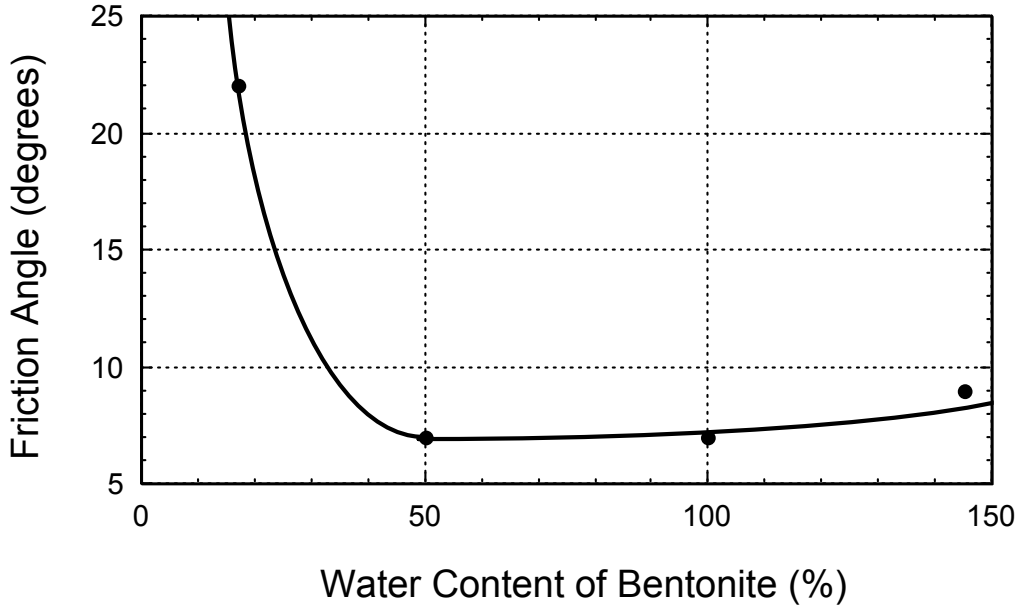

Figure 3-22. Effect of water content on the secant friction angle of an unreinforced GCL sheared internally (Daniel et al., 1993).

3.6.3.1 Test Plots G and H

Test plots G and H consisted of Bentomat ST and Claymax 500SP, respectively. Both plots slid at the interface between the upper GT (a woven, slit-film GT in both cases) and the lower surface of the overlying textured HDPE GM. Plot H slid 20 days after construction, and plot G slid 50 days after construction. Pre-slide displacements were small (< 25 to 130 mm). There was no warning of either slide. Both slides occurred at night, and the slides apparently occurred quickly.

Test Plot H, which incorporated Claymax 500SP, was constructed on a 24.7º slope, but the measured peak and large-displacement interface friction angles for the relevant materials under hydrated conditions were only 20º (Table 3-2). Test plot H did not slide immediately because the interfacial shear strength of the dry GCL was sufficient to maintain a stable slope. The slope slid when the bentonite hydrated. Tests summarized in Appendix D showed that bentonite in the GCLs hydrated in a period of 10 to 20 days when placed in contact with the subgrade soils from the test plots. Tests reported by Daniel et al. (1993) showed similar results for other soils. Thus, the sliding time of 20 days after construction is consistent with the expected period to achieve nearly full hydration of the bentonite.

Figure 3-23. Photograph of slides in plot G (left) and H (right) taken approximately 2 months after construction and several days after the slide in plot G.

When GCLs containing a woven GT component become hydrated, bentonite can extrude through the openings of the GT and lubricate the GCL/GM interface (Gilbert et al., 1996). After the slide, the surface of the GCL was very slick. The tendency of bentonite to lubricate the GM/GCL interface may be related to the thinness of the woven slit-film GT and to differences in apparent opening size between woven and nonwoven GTs.

Test plot G, which was constructed using Bentomat ST, was slower to slide, but the slope angle (23.5^{o} peak) was 1.2^{o} flatter than for plot H, and the interface shear strength between the GCL and overlying GM (23^{o} peak and 21^{o} large-displacement) was 1° to 3° higher. Also, a nonwoven GT faced downward in plot G, but a woven slit-film GT faced downward in Plot H. GCLs are expected to absorb water more slowly from subgrade soils when the GT separating the bentonite from the subsoil is a thicker nonwoven GT. Thus, the reason why plot G slid 30 days later than plot H appears to be that the

bentonite in the GCL at plot G was separated from wet subgrade soils by a thicker, nonwoven GT, which slowed hydration.

3.6.3.2 Test Plots F and P (Bentonite Encased Between Two GMs)

Plots F and P (both 2H:1V slopes), like plot A (3H:1V slope), contained bentonite sandwiched between two GMs. The bentonite in these test plots was expected to remain dry. However, within three months after plot F was constructed, two of the three moisture sensors indicated that the bentonite had become hydrated.

To evaluate the condition of the bentonite, 17 borings were drilled into Plot F in March 1995, and 100-mm-diameter samples of the GCL were recovered. The water content of the bentonite samples varied from 10% to 188%, and the data showed that the right panel was much more hydrated than the left panel. In contrast to this field data, Estornell and Daniel (1992) reported laboratory test results for Gundseal in which water migrated laterally through the GM-encased bentonite less than 100 mm over a test duration of 6 months.

Water may have entered the bentonite at plot F through cuts made in the GM liner overlying the GCL to allow insertion of the extensometer cables. Plot F was located at a point where surface water at the crest of the slope was channeled directly to the anchor trench area where the penetrations were made. The mechanism for lateral movement of water is probably waves in the overlying GM, which would allow water to spread. Alternatively, the source of water could have come from the V-shaped trough between plots F and G, and spread through waves in the GM. Unfortunately, the plot slid before a complete forensic study could be performed.

Displacement sensors showed large movements in the right panel of plot F throughout the first year of observation, but significant movement was not initiated in the left panel until later (Figure 3-24). Starting on about day 275 (August 1995), the left panel began to move downslope, suggesting that the bentonite in the left panel was finally becoming hydrated over a significant percentage of the total area of the panel.

Plot F slid on March 24, 1996, 495 days after construction. The cause of the slide is hydration of the bentonite; the peak angle of internal friction for hydrated bentonite at the normal stress existing in the field was 20º, but the slope angle was 23.6º. In contrast, the peak interface friction angle for dry bentonite was 37º. Had the bentonite not hydrated, the slope should have remained stable.

In response to the unexpected hydration, plot P was constructed on June 15, 1995. The extensometers were not installed in plot P to eliminate all penetrations in the overlying GM. The number of fiberglass moisture sensors in the bentonite was

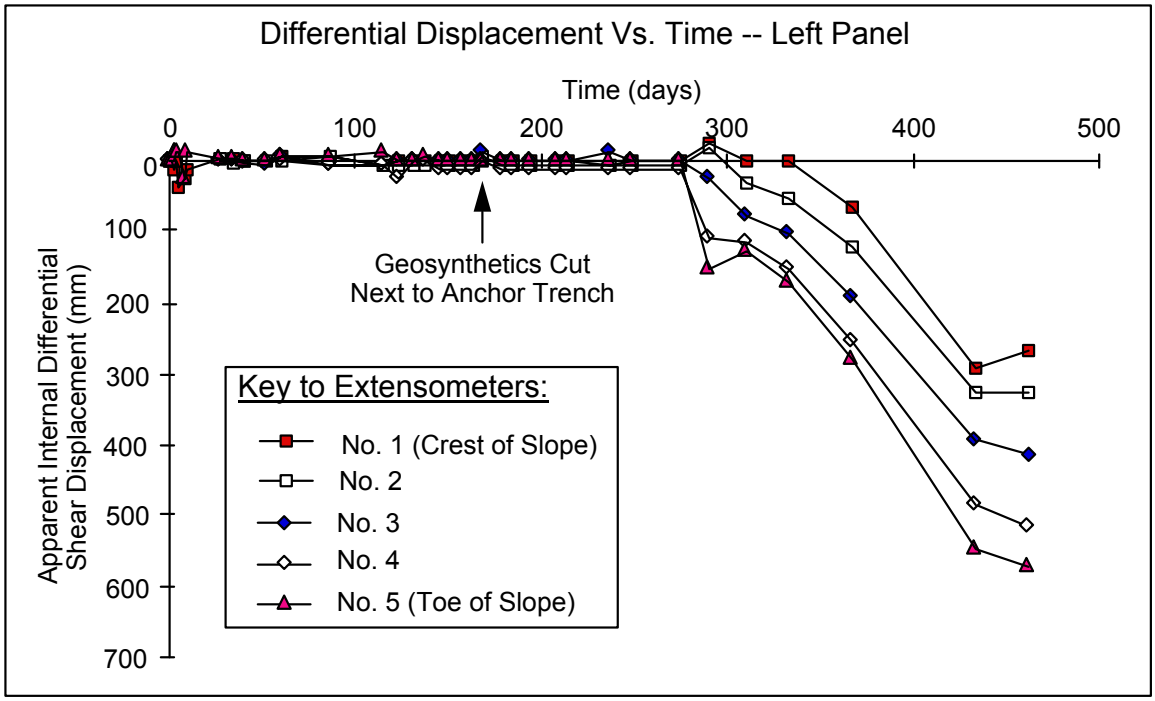

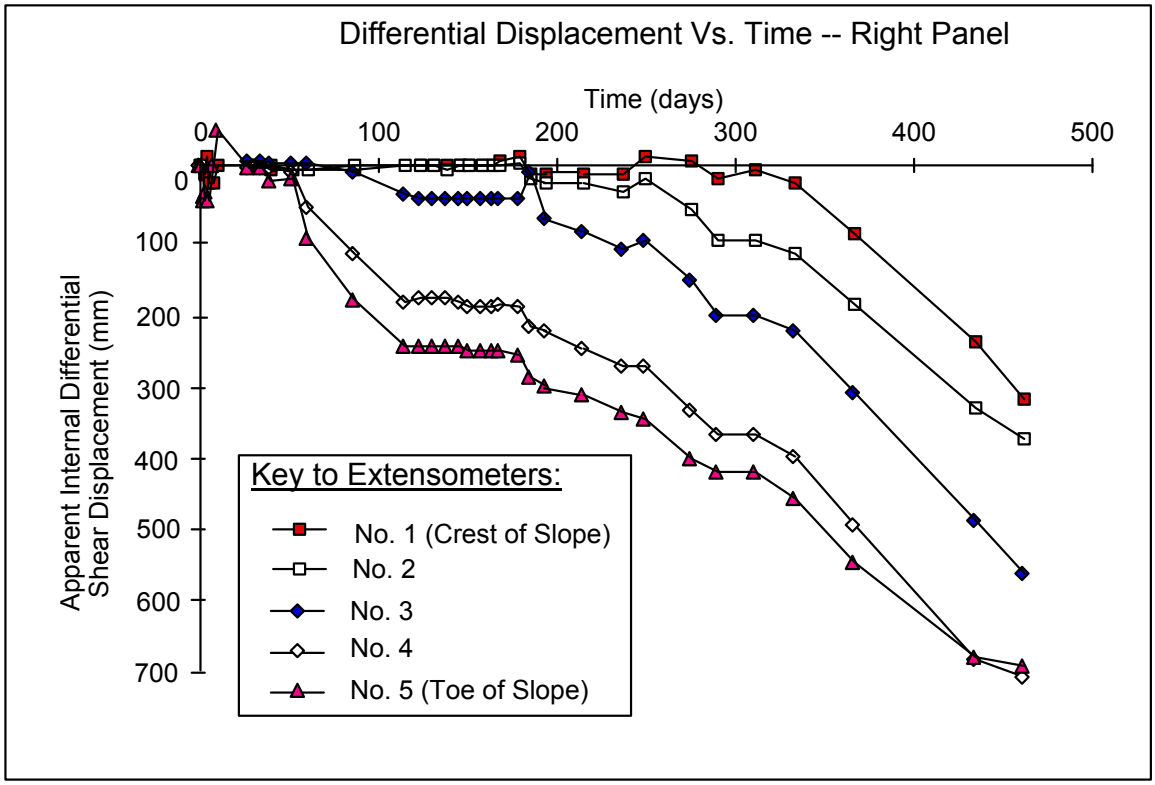

Figure 3-24. Differential displacement versus time for left and right panels of plot F.

increased from 3 in the other test plots to 16 in plot P to provide additional documentation of moisture conditions. All but one of the 16 moisture sensors have indicated that the bentonite has remained dry in the 18 months of monitoring plot P. There is, however, some indication of slight hydration near the toe of plot P, perhaps due to edge effects near the toe.

There has been no indication of any displacement in plot P, although displacements are not being monitored (other than to observe for gross and obvious movements, of which there have been none). It is apparent from the moisture sensors and stability of plot P over a period of more than four years that the bentonite has not become hydrated over a significant area of plot P. This plot confirms that if moisture is not allowed access to bentonite sandwiched between GCLs through penetrations or other sources, the bentonite can remain dry for at least several years.

All 3H:1V slopes with unreinforced bentonite (including plot A with bentonite encased between two GMs and plot E with bentonite in contact with moist subgrade) have remained stable with minimal displacement.

3.6.3.3 Plots I and N with Nonwoven GT Component Facing Upward

Plots I and N are similar to plot G, except that the GCL contained either one nonwoven GT with the nonwoven GT facing upward (plot N) or two nonwoven GTs (plot I). The slope angles at plots I and N were similar to the other 2H:1V plots. However, the interface friction angle between the nonwoven GT component of Bentofix and the textured HDPE (37º peak and 24º large-displacement) was much greater than for the woven slit-film GT component of the GCLs that slid. The geosynthetic components of plots I and N have remained stable because of the better interface shear resistance between a nonwoven GT component of a GCL compared to a woven GT component. The greater interface shear resistance from the nonwoven GT is attributed to: (1) larger shear resistance developed between nonwoven GTs and textured GMs in general; and (2) less hydrated bentonite extrusion to the interface for the thicker nonwoven GT.

Large displacements began to develop in plot I and the adjacent test plots J, K, and L about 3-1/2 years (900 days) after construction. Several small slumps with downward displacement of up to about 100 mm along scarps, and associated surface cracking, were observed. The slumps and cracks appearing in the lower half of the test plot. The subsoils in the area of the slides are CL and CH clays, with the liquid limit and plasticity index of the subsoil next to plot I averaging 48% and 24%, respectively. The average moisture content of the clay at the time of sliding was approximately 40%, or just slightly below the liquid limit. The displacements occurred at the end of the wet spring season in 1997. Examination of plot I and adjacent test plots, coupled with excavation into the subsoils, showed that sliding was occurring 0.5 to 1 m beneath the

GCL, in the clay subsoil. It is assumed that the buildup of pore water pressure behind the test plots helped to trigger the slides in the subsoils. There was no indication of movement within the GCL or either interface with the GCL. Plot N showed no signs of slumping or cracking, but plot N was at the end of the 2H:1V test plots and likely was at a location where excess pore water pressures were not as likely to develop.

3.6.3.4 Plots J, K, and L with No GM

These test plots were constructed by placing drainage sand directly above the GCL. All three test plots remained stable for about 900 days after construction, and then all three underwent significant downslope displacement (0.5 to 1.2 m, as shown in Table 3-3). All three exhibited slumping in the lower half to two-thirds of the test plots. Scarps could be observed at several locations within each test plot. Observation of the depth of slumping clearly showed that displacement was occurring entirely beneath the GCLs. Excavation into the subsoils showed that a layer of more plastic clay was located just beneath the bottom of the GCLs. The sliding mechanism was related to the subsoils and not to the GCLs or GCL interfaces. Buildup of pore water pressure in the clays following the wet spring season was assumed to be the triggering mechanism. The large differential displacements indicated for plots K and L in Table 3-3 are not representative of actual shearing of the GCLs (physical examination of the GCLs showed that they were intact and not sheared) -- the large displacements apparently rendered the differential displacement between top and bottom sensors meaningless.

The peak secant interface friction angle between the sand drainage material and GCL was 31^{o} for a woven-slit film component (Table 3-2) and, although not measured, presumably more for a nonwoven component. An interface friction angle of 31^{o} is significantly greater than the slope angle (~ 25^{o}), which explains the stability of the test plots up until the point of sliding in the subsoil.

3.6.4 Comments on Adequacy of Current Engineering Practice

Current engineering practice for evaluation of the stability of slopes such as those constructed for the test plots involves three steps: (1) measurement of the internal and interfacial shear strength, typically using direct shear apparatus to shear 300 mm by 300 mm test specimens and interfaces; (2) calculation of the factor of safety using limit equilibrium analysis; and (3) reconfiguration of the slope or use of different materials if the factor of safety is not found to be adequate. In this project, the shearing tests were performed after the slopes were constructed (due to time constraints). A critical question is: would the usual testing/design process have correctly predicted which slopes would be stable and which would undergo sliding?

The calculated FS based on both peak and large-displacement shear strength measurements is tabulated in Table 3-4. The column labeled “Peak FS” indicates factor

of safety based on peak shear strength. The column labeled "Large Displ. FS" refers to the factor of safety calculated from the shear strength measured at large displacement (50 mm).

Table 3-4. Summary of Calculated Factor of Safety (FS) and Actual Slope Stability.

Test Plot	Slope Angle (°)	Peak Friction Angle (°)	Large-Displ. Friction Angle (°)	Peak FS	Large Displ. FS	Test Plot Performance
A	16.9	37[2(D)]	35[2(D)]	2.5[2(D)]	2.3[2(D)]	Stable
B	17.8	23[1]	21[1]	1.3[1]	1.2[1]	Stable
C	17.6	20[1]	20[1]	1.1[1]	1.1[1]	Stable
D	17.5	29[1]	22[1]	1.8[1]	1.3[1]	Stable
E	17.7	20[2(H)]	20[2(H)]	1.1[2(H)]	1.1[2(H)]	Stable
F	23.6	20[2(H)]	20[2(H)]	0.8[2(H)]	0.8[2(H)]	Internal Slide
G	23.5	23[1]	21[1]	1.0[1]	0.9[1]	Interface Slide
H	24.7	20[1]	20[1]	0.8[1]	0.8[1]	Interface Slide
I	24.8	37[1]	24[1]	1.6[1]	1.0[1]	Stable[4]
J	24.8	~31[1]	~31[1]	1.3[1]	1.3[1]	Stable[4]
K	25.5	31[3]	31[3]	1.3[1]	1.3[1]	Stable[4]
L	24.9	~31[1]	~31[1]	1.3[1]	1.3[1]	Stable[4]
N	22.9	~37[1]	~24[1]	1.8[1]	1.1[1]	Stable

[1]GCL/GM interface
[2] Internal GCL strength for dry (D) or hydrated (H) bentonite
[3] GCL/drainage sand interface
[4] Large displacement occurred in subsoil below GCL, but not in or at the interface with GCL

From these data, the following conclusions are drawn: (1) all test plots with a factor of safety > 1.0 based on peak shear strengths remained stable with respect to the critical material or interface tested; (2) all test plots with a factor of safety $\geq$ 1.0 with respect to the large-displacement shear strength remained stable with respect to the critical

material or interface tested; (3) all test plots with a factor of safety $\leq$ 1.0 based on peak shear strength underwent a slope failure; and (4) all test plots with a factor of safety < 1.0 based on residual shear strength underwent a failure. Although there are no firm rules on what designers should and should not assume for the relationship between factor of safety and stability of a slope, the following comments are offered:

1. All designers would likely assume that a slope with F < 1 based on peak strengths would be at great risk of failure and would not be acceptable (and, indeed, all such test plots did undergo failure).
2. Many designers assume that slopes with a factor of safety of about 1.5 or better, based on peak shear strengths, will remain stable under static loading (and all plots with F $\geq$ 1.5 were stable).
3. Many designers assume that slopes with a factor of safety of about 1.2 to 1.5 calculated from peak shear strengths may remain stable, particularly in the short term, under static loading conditions but might not feel comfortable with factors of safety between 1.2 and 1.5 for long-term stability of critical slopes (all test plots with F between 1.2 and 1.5 remained stable in the GCL or at a critical interface for the 4-1/2 years in which the test plots have been observed).
4. Many designers consider the residual shear strength of a material or interface, and a common assumption is that if the factor of safety based on peak strength is acceptable and the factor of safety based on large-displacement shear strength is at least 1.0, then the design is acceptable (all test plots with F $\geq$ 1.0 based on large-displacement shear strength were indeed stable).

It appears that the observations from this test plot program are entirely consistent with current design practice. Had current design practices been employed for the materials and slopes used in these test plots, stable slopes would have resulted for the 4-1/2 year period of this test program. The observations from the test plots are consistent with and serve to validate current design methodology.

3.7 Erosion Control Materials

The GEC materials that were employed for the test plots are summarized in Table 3-5. The erosion control materials were installed in an overlapping manner and stapled together. Ground anchors per the manufacturer's installation recommendations were used throughout. Some plots were seeded prior to placement of the erosion control material, and others were seeded after the placement of the erosion control material (depending on the manufacturer's recommendation). The owner of the landfill site provided the seeding in December 1994.

The materials were all fully effective in preventing the development of erosion over the 4-1/2 years in which the condition of the test plots was observed. In contrast, erosion gullies and rills formed in the control plot M, which did not contain any erosion control material.

Table 3-5. Geosynthetic Erosion Control Products.

Plot	Manufacturer	Product	Color	Material
A	Tensar	TB 1000	Green	Polyolefin
B	Synthetic Industries	Polyjute	Beige	Degradable Polypropylene
C	Synthetic Industries	Polyjute	Beige	Degradable Polypropylene
D	Akzo	Enkamat 7010	Black	Nylon
E	Akzo	Enkamat 7010	Black	Nylon (with Excelsior)
F	Tensar	TM 3000	Black	Polyethylene
G	Tensar	TM 3000	Black	Polyethylene
H	Tensar	TM 3000	Black	Polyethylene
I	Synthetic Industries	Landlok 450	Green	Polyolefin
J	Synthetic Industries	Landlok 450	Green	Polyolefin
K	Akzo	Enkamat 7010	Black	Nylon (with Excelsior)
L	Akzo	Enkamat 7010	Black	Nylon
M	None	Control Plot	-	-
N	Akzo	Enkamat 7010	Black	Nylon (with Excelsior)
P	Akzo	Enkamat 7220	Black	Nylon

3.8 Summary and Conclusions

Fourteen test plots, designed to replicate typical final cover systems for solid waste landfills, were constructed to evaluate the internal and interface shear strength of GCLs under full-scale field conditions on 2H:1V and 3H:1V slopes. Five different types of GCLs were evaluated. The test plots have been observed for 4-1/2 years. All test plots were initially stable, but over time as the bentonite in the GCLs became hydrated, three slides (all on 2H:1V slopes) that involved the GCLs have occurred. One slide involved an unreinforced GCL in which bentonite that was encased between two GMs unexpectedly became hydrated. The other two slides occurred at the interface between the woven GTs of the GCLs and the overlying textured HDPE GM. Several slides (none involving GCLs) occurred in the subsoils of 2H:1V test plots following a wet spring about 3-1/2 years into the project.

Conclusions from the project may be summarized as follows: (1) at the low normal stresses associated with landfill cover systems, the interface shear strength is generally

lower than the internal shear strength of internally-reinforced GCLs; (2) interfaces between a woven GT component of the GCL and the adjacent material (e.g., textured or smooth HDPE GM) should always be evaluated for stability; these interfaces may often be critical; (3) significantly higher interface shear strengths were observed when the GT component of a GCL in contact with a textured HDPE GM was a nonwoven GT, rather than a woven GT; (4) if bentonite sandwiched between two GMs has access to water (e.g., via penetrations or at exposed edges), water may spread laterally through waves or wrinkles in the GM and hydrate the bentonite over a large area; (5) if the bentonite sandwiched between two GMs does not have access to water, it was found that the bentonite did not hydrate over a large area; (6) current engineering procedures for evaluating the stability of GCLs on slopes (based on laboratory direct shear tests and limit-equilibrium methods of slope stability analysis) correctly predicted which test plots would remain stable and which would undergo sliding, thus validating current design practices; and (7) based on the experiences of this study, 2H:1V slopes involving landfill cover situations may be too steep to be stable with the desirable factor of safety due to limitations with respect to the interface shear strengths of the currently available geosynthetic products.

The results from the test plot were consistent with the current design practice involving measuring the shear strength of critical materials and interfaces in laboratory direct shear tests, calculating the factor of safety against a slope failure using limit equilibrium analysis, and adjusting the slope cross section or materials until a satisfactory factor of safety is achieved. The test plots served to validate the current design methodology. All test plots with a factor of safety > 1 based on peak shear strength were found to be stable in the critical material or along the critical interface during the 4-1/2 years that the test plots have been observed. All test plots with a factor of safety $\geq$ 1.0 based on large-displacement shear strengths were stable. Slides that did occur along GCL/GM interfaces occurred at plots where the factor of safety using peak shear strength was $\leq$ 1.0 (and in such cases, the factor of safety based on large-displacement shear strengths was < 1.0).

3.9 References

Boardman, B.T. and D.E. Daniel (1996), "Hydraulic Conductivity of Desiccated Geosynthetic Clay Liners," *Journal of Geotechnical Engineering*, 122(3): 204-208.

Daniel, D.E., and Boardman, B.T. (1993), *Report of Workshop on Geosynthetic Clay Liners,* U.S. Environmental Protection Agency, Cincinnati, Ohio, EPA/600/R-93/171, 106 p.

Daniel, D.E., Shan, H.Y., and Anderson, J.D. (1993), "Effects of Partial Wetting on the Performance of the Bentonite Component of a Geosynthetic Clay Liner," *Geosynthetics '93,* Industrial Fabrics Association International, St. Paul, Minnesota, 3: 1483-1496.

Daniel, D.E., and Gilbert, R.B. (1996), "Practical Methods for Managing Uncertainties for Geosynthetic Clay Liners," *Uncertainty in the Geologic Environment: From Theory to Practice*, American Society of Civil Engineers, New York.

Dobras, T.N., and Elzea, J.M. (1993), "In-Situ Soda Ash Treatment for Contaminated Geosynthetic Clay Liners," *Geosynthetics '93*, Industrial Fabrics Association International, 3: 1145-1160.

Estornell, P. M. and Daniel, D.E. (1992), "Hydraulic Conductivity of Three Geosynthetic Clay Liners," *Journal of Geotechnical Engineering*, 118(10): 1592-1606.

Foose, G.J., Benson, C.H., and Edil, T.B. (1996), "Evaluating the Effectiveness of Landfill Liners," *Environmental Geotechnics*, M. Kamon (Ed.), Balkema, Rotterdam, 1: 217-221.

Foose, G.J., Benson, C.H., and Edil, T.B. (1999), "Equivalency of Composite Geosynthetic Clay Liners as a Barrier to Volatile Organic Compounds," *Geosynthetics '99*, 1: 335-344.

Fox, P.J., De Battista, D.J., and Chen, S.J. (1996), "Bearing Capacity of Geosynthetic Clay Liners for Cover Soils of Varying Particle Size," *Geosynthetics International*, 3(4): 447-461.

Fox, P.J., Rowland, M.G., and Scheithe, J.R. (1998), "Internal Shear Strength of Three Geosynthetic Clay Liners," *Journal of Geotechnical and Geoenvironmental Engineering*, 124(10): 933-944.

Gilbert, R.B., Fernandez, F., and Horsfield, D.W. (1996), "Shear Strength of Reinforced Geosynthetic Clay Liner," *Journal of Geotechnical Engineering*, 122(4): 259-266.

Hewitt, R.D., and D.E. Daniel (1997), "Hydraulic Conductivity of Geosynthetic Clay Liners after Freeze-Thaw," *Journal of Geotechnical and Geoenvironmental Engineering,* 123(4): 305-313.

James, A.N., Fullerton, D., and Drake, R. (1997), "Field Performance of GCL under Ion Exchange Conditions," *Journal of Geotechnical and Geoenvironmental Engineering*, 123(10): 897-902.

Koerner, R.M., and Narejo, D. (1995), "Bearing Capacity of Hydrated Geosynthetic Clay Liners," *Journal of Geotechnical Engineering*, 121(1): 82-85.

Koerner, R.J., Koerner, G.R., and Eberle, M.A. (1996), "Out-of-Plane Tensile Behavior of Geosynthetic Clay Liners," *Geosynthetics International*, 3(2): 277-296.

Kraus, J.F., Benson, C.H., Erickson, A.E., and Chamberlain, E.J. (1997), "Freeze-Thaw Cycling and Hydraulic Conductivity of Bentonitic Barriers, " *Journal of Geotechnical and Geoenvironmental Engineering,* 123(3): 229-238.

Lagatta, M.D. Boardman, B.T., Cooley, B.H., and D.E. Daniel (1997), "Geosynthetic Clay Liners Subjected to Differential Settlement," *Journal of Geotechnical and Geoenvironmental Engineering*, 123(5): 402-411.

Lai, J., Daniel, D.E., and Wright, S.G. (1998), "Effect of Cyclic Loading on Shear Strength of Unreinforced Geosynthetic Clay Liner," *Journal of Geotechnical and Geoenvironmental Engineering,* 124(1): 45-52.

Mesri, G., and Olson, R.E. (1970), "Shear Strength of Montmorillonite," *Geotechnique*, 20(3): 261-270.

Olson, R.E. (1974), "Shearing Strengths of Kaolinite, Illite, and Montmorillonite," *Journal of the Geotechnical Engineering Division*, ASCE, 100(GT11): 1215-1229.

Ruhl, J.L., and D.E. Daniel (1997), "Geosynthetic Clay Liners Permeated with Chemical Solutions and Leachates," *Journal of Geotechnical and Geoenvironmental Engineering*, 123(4): 369-381.

Schubert, W.R. (1987), "Bentonite Matting in Composite Lining Systems," *Geotechnical Practice for Waste Disposal '87*, American Society of Civil Engineers, New York, 784-796.

Shan, H.Y. (1993), "Stability of Final Covers Placed on Slopes Containing Geosynthetic Clay Liners," Ph.D. Dissertation, Univ. of Texas, Austin, TX, 296 p.

Shan, H.Y., and D.E. Daniel (1991), "Results of Laboratory Tests on a Geotextile/Bentonite Liner Material," *Geosynthetics 91*, Industrial Fabrics Association International, St. Paul, MN, 2: 517-535.

Stark, T.D., and Eid, H.T. (1997), "Shear Behavior of Geosynthetic Clay Liners," *Geosynthetics International*, 3(6): 771-786.

Stark, T.D., Arellano, D., Evans, W.D., Wilson, V.L., and Gonda, J.M. (1998), "Unreinforced Geosynthetic Clay Liner Case History," *Geosynthetics International*, 5(5):521-544.

Well, L.W. (1997), *Testing and Acceptance Criteria for Geosynthetic Clay Liners, ASTM STP 1308*, American Society for Testing and Materials, Philadelphia, 268 p.

Chapter 4
Summary of Natural Materials Tasks

The natural materials tasks were designed to collect information on field performance of natural materials in landfills and focused on documenting the performance of CCLs. Although drainage materials were included, it was recognized that this could be better evaluated from case histories, discussed later in this report. The work on CCLs included: (1) documenting the field hydraulic conductivity (k_{field}) of CCLs, including CCLs constructed from natural soil materials and those constructed from soil-bentonite mixtures; and (2) documenting the performance of CCLs used in landfill covers.

The rationale for focusing attention on these two topics is as follows. CCLs are an important component of many liner systems for waste containment facilities. The key performance parameter (embodied in regulatory compliance) is the hydraulic conductivity of the CCL. Although hydraulic conductivity is routinely measured on small-sized laboratory samples, it is not commonly measured at a large scale on field test pads. To provide an adequate database, this task focused on the large-scale hydraulic conductivity of CCLs in the field to provide information on how CCLs are meeting the regulatory requirement and design objective and to relate the performance of CCLs with critical design and construction variables.

Although CCLs are commonly used in landfill cover systems, data published in recent years have cast doubt on how survivable CCLs are in landfill cover systems. Desiccation, for example, can lead to cracking in CCLs and to permanent and significant increases in hydraulic conductivity. In addition, MSW landfills are known to undergo significant amounts of settlement upon closure. Such settlement can adversely affect a CCL's performance by inducing stress-related fractures in the CCL barrier that, under low compressive stress, can increase the CCL's hydraulic conductivity. The available information is summarized in order to provide information on the field performance of CCLs in landfill covers.

4.1 CCLs Constructed from Natural Soil Liner Material

4.1.1 Introduction

One of the most important components of many liner and cover systems for landfills is a low-permeability, CCL. In the past decade, dozens of papers have been written on the factors that influence the hydraulic conductivity (k) of compacted clay, the compatibility of clay liners with chemicals and leachates, laboratory and field hydraulic conductivity testing methods, the correlation of laboratory and field hydraulic conductivity, and methods of construction and CQA.

Despite the wealth of information that has been recently developed, the performance of CCLs in the field is largely undocumented. There are two principal reasons for the lack of performance data. First, compacted clays are usually used in combination with GM liners, and in such applications it is impossible to separate the performance of the compacted clay component from that of the GM component. Second, few landfills have lysimeters or other instrumentation that would enable documentation of field performance installed directly beneath the lining system. Although lysimeters have been used to document the field performance of several CCLs in actual landfills (Gordon et al., 1990; Reades et al., 1990), only a handful of CCLs are documented in this manner. Future opportunities to document field performance of CCLs with lysimeters will be very limited because CCLs are rarely used in lining systems without a GM.

The purpose of this task was to collect as much information as possible on the field performance of CCLs. In view of the dearth of information on actual performance of in-service CCLs, the next best source of data was used: large-scale field hydraulic conductivity tests on full-scale field test pads. The test pads were constructed with materials, methods of construction, and quality assurance (QA) procedures that vary from project to project but are typical of current industry practices. Any test pads that were constructed for research purposes were excluded from the database. Only those test pads that were constructed for the purpose of verifying that the field-constructed CCL had a hydraulic conductivity of 1×10^{-7} cm/s or less were included in the database presented and analyzed here.

4.1.2 Database

4.1.2.1 Source of Data

The database described herein was assembled partially from data in the literature but primarily from unpublished data contained in various engineering reports. Information on more than 120 sites was collected and screened. The data collection process is thought to have captured the results of perhaps 50% to 75% of all the CCL test pads that have been constructed in North America for the purpose of demonstrating compliance with the hydraulic conductivity requirement of $k \leq 1 \times 10^{-7}$ cm/s as measured by large-scale field testing equipment.

Although data on more than 120 CCLs were obtained, some of the sites were not included in the final database. The requirements for inclusion of a full-scale CCL or a CCL test pad in the database were: (1) construction in general accord with industry practices for full-sized liners; (2) CQA in general accord with industry practices; (3) construction with the objective of demonstrating that large-scale k_{field} did not exceed 1×10^{-7} m/s; (4) reasonably complete documentation of test results; and (5) availability of results from large-scale kfield tests such as the sealed double-ring infiltrometer, or SDRI

(Daniel, 1989; Trautwein and Boutwell, 1994). Of the CCLs eliminated from the database, the main reason for doing so was the construction of a test pad to meet a hydraulic conductivity objective other than 1 x 10^{-7} cm/s. Approximately 20 test pads constructed in California with a hydraulic conductivity objective of 1 x 10^{-6} cm/s or less were eliminated for this reason. Several test pads were constructed for research purposes using construction practices that are not consistent with industry practice for full-sized liners, and were not included in the database for this reason.

4.1.2.2 The Database

The database consists of 89 CCLs. Of the 89 CCLs in the database, 8 are actual in-service liners for landfills and 81 are test pads. The geographic distribution of CCLs in the database is shown in Figure 4-1. Data for the 89 CCLs are compiled in four tables presented in Appendix C. Specific site locations are not provided due to potential sensitivities for some sites.

The database is summarized in Tables 4-1 and 4-2. Many of the numbers in Tables 4-1 and 4-2 are averages of multiple measurements (geometric mean for k, arithmetic mean for all others). The statistics on the mean and standard deviation are summarized in Tables C-1 through C-4 in Appendix C.

Figure 4-1. Locations of sites in database for clay liners constructed of natural clay material.

Table 4-1. Field Hydraulic Conductivity, Soil Characteristics, and Compaction Data for Natural Clay Liner Materials.

Site	Field Hydraulic Conductivity (cm/s) Value	Method	Liquid Limit (%)	Plasticity Index (%)	Percent Fines	Percent Clay	Standard Proctor w_{opt} (%)	Standard Proctor $(\gamma_d)_{max}$ kN/m^3	Modified Proctor w_{opt} (%)	Modified Proctor $(\gamma_d)_{max}$ kN/m^3	Compaction Criterion
1	2.8E-07	SDRI	24	10	65	37	10.2	20.1	9	21.3	$w > w_{opt}$; $\gamma_d > 90\%$ MP
2	1.5E-07	SDRI	58	29							
3	9.0E-09	LYS	25	10	85	22	12.3	19			$w > w_{opt}$; $\gamma_d > 95\%$ SP
4	1.1E-08	SDRI	50	34	95	47	17.9	16.8			$w_{opt}+2\% < w < w_{opt}+8\%$; $\gamma_d > 90\%$ MP
5	9.0E-08	SDRI	43	26	87	32			14.3	18.6	$w > w_{opt}$; $\gamma_d > 90\%$ MP
6	2.7E-07	SDRI	32	19	88	35			13.5	19.5	$w > w_{opt}$; $\gamma_d > 90\%$ MP
7	5.8E-08	SDRI	33	13	77	27	14.1	18.6			$w > w_{opt}+2\%$; $\gamma_d > 90\%$ MP
8	1.2E-07	SDRI	35	22	75	45			14.5	18.8	$w_{opt}-2\% < w < w_{opt}+4\%$; $\gamma_d > 90\%$ MP
9	7.0E-09	LYS	55	31		45			12.7	18.6	$w > w_{opt}$; $\gamma_d > 90\%$ MP
10	3.0E-08	LYS	43	21		29			16.6	18.7	$w > w_{opt}$; $\gamma_d > 90\%$ MP
11	3.0E-09	LYS	57	30		39			21.7	17.3	$w > w_{opt}$; $\gamma_d > 90\%$ MP
12	2.0E-09	LYS	55	28		33			23	16.6	$w > w_{opt}$; $\gamma_d > 90\%$ MP
13	1.3E-08	SDRI	37	15	78	37	18	17			$w_{opt}+2\% < w < w_{opt}+5\%$; $\gamma_d > 90\%$ MP
14	2.0E-08	SDRI	40	20	70	25	16.2	16.7			$w > w_{opt}+4\%$; $\gamma_d > 98\%$ SP
15	3.3E-09	SDRI	85	58	99	57	25.8	14.6			$w > w_{opt}$; $\gamma_d > 100\%$ SP
16	3.0E-08	SDRI	41	22	77	38	15.8	17			$w_{opt}+2\% < w < w_{opt}+5\%$; $\gamma_d > 90\%$ MP
17	6.0E-09	LYS	50	34	95	47	20.3	16.4			$w_{opt}+2\% < w < w_{opt}+6\%$; $\gamma_d > 90\%$ SP
18	9.8E-09	SDRI	30	18	52	16	13	18.7			$S_i > 78.5\%$; $\gamma_d > 90\%$ MP
19	4.4E-08	LYS	32	14	85	44			10.5	20.1	$w > w_{opt}$; $\gamma_d > 90\%$ MP
20	8.0E-07	SDRI	49	23	94	43	18.5	17.2			$S_i > 82\%$
21	2.5E-07	SDRI	51	26	90	36	18	17	11.8	18.5	$w > w_{opt}$; $\gamma_d > 95\%$ SP

Table 4-1. Field Hydraulic Conductivity, Soil Characteristics, and Compaction Data for Natural Clay ... (Cont.).

Site	Field Hydraulic Conductivity (cm/s) Value	Field Hydraulic Conductivity (cm/s) Method	Liquid Limit (%)	Plasticity Index (%)	Percent Fines	Percent Clay	Standard Proctor w_{opt} (%)	Standard Proctor $(\gamma_d)_{max}$ kN/m^3	Modified Proctor w_{opt} (%)	Modified Proctor $(\gamma_d)_{max}$ kN/m^3	Compaction Criterion
22	2.0E-08	SDRI	63	42	96		20.5	16.3			S_i > 85%
23	1.4E-08	LYS	39	18	73	30	20	16.5			$w > w_{opt}$; γ_d > 90% MP
24	1.5E-08	SDRI	67	46	94	53	21.5	16.3	16	18.4	$w > w_{opt}$; γ_d > 90% MP
25	8.0E-09	SDRI	53	41	88	36	16.1	18	11.5	19.8	$w > w_{opt}$; γ_d > 90% MP
26	2.0E-07	SDRI	33	19	85	37	17.5	17.7	12.2	19.3	$w > w_{opt}$; γ_d > 90% MP
27	1.8E-07	SDRI	31	18	74	26	16.5	17.8	12.5	19.4	$w > w_{opt}$; γ_d > 90% MP
28	9.0E-08	SDRI	35	19	89	41	16.6	17.5	11.5	19.4	$w > w_{opt}$; γ_d > 90% MP
29	1.7E-08	SDRI	27	10	76	28	13	19.1	9	20.5	w_{opt}-2%<w<w_{opt}+5%; γ_d>90% MP
30	1.1E-07	SDRI	32	19					14	18.6	
31	6.0E-08	SDRI	40	24	58	23	12.4	19.3			$w > w_{opt}$; γ_d > 95% SP
32	3.9E-08	SDRI	45	27	99	42			11	19.9	w_{opt}<w<w_{opt}+6%; γ_d>90% MP
33	3.9E-08	SDRI	29	15	87	40			13.3	18.9	$w > w_{opt}$; γ_d > 90% MP
34	4.0E-07	SDRI	44	16	96		17.3	17.1			$w > w_{opt}$; γ_d > 95% SP
35	3.7E-08	SDRI	39	19	97		22.2	16.4			$w > w_{opt}$; γ_d > 95% SP
36	3.0E-08	SDRI	36	17	74	30	13.2	18.3			w_{opt}<w<w_{opt}+6%; γ_d>95% SP
37	1.3E-08	SDRI	36	17	48	16	12.4	19			$w > w_{opt}$; γ_d > 95% SP
38	3.6E-08	SDRI	21	7	60		10.3	20.4			$w > w_{opt}$; γ_d > 90% MP
39	3.5E-09	SDRI	21	7	60		10.3	20.4			11%<w<12%; γ_d > 90% SP
40	2.2E-08	SDRI	101	71	98	49	31.6	13.4			w_{opt}+1%<w<w_{opt}+5%; γ_d>92% SP
41	1.0E-07	SDRI	47	30	66		19.5	16.3			γ_d > 95% SP
42	8.0E-08	SDRI	69	45	79	49	23.4	15.1			

Table 4-1. Field Hydraulic Conductivity, Soil Characteristics, and Compaction Data for Natural Clay ... (Cont.).

Site	Field Hydraulic Conductivity (cm/s) Value	Field Hydraulic Conductivity (cm/s) Method	Liquid Limit (%)	Plasticity Index (%)	Percent Fines	Percent Clay	Standard Proctor w_{opt} (%)	Standard Proctor $(\gamma_d)_{max}$ kN/m^3	Modified Proctor w_{opt} (%)	Modified Proctor $(\gamma_d)_{max}$ kN/m^3	Compaction Criterion
43	7.0E-08	SDRI	62	42	86		22.4	15.4			$w > w_{opt}+1\%$; $\gamma_d > 95\%$ SP
44	2.0E-07	SDRI	62	42	86		22.4	15.4			$w > w_{opt}+1\%$; $\gamma_d > 90\%$ SP
45	3.7E-08	SDRI	44	28	70		19.5	16.4			$w_{opt}<w<w_{opt}+2\%$; $\gamma_d>95\%$ SP
46	2.0E-08	SDRI	35	16	98	22	23.3	15.4			$w_{opt}+1\%<w<w_{opt}+3\%$; $\gamma_d>95\%$ SP
47	5.0E-08	SDRI	39	24	69		14.6	17.7			$w_{opt}+1\%<w<w_{opt}+5\%$; $\gamma_d>90\%$ SP
48	4.0E-08	SDRI	41	23	86		18	16.7	13.3	18.7	$w_{opt}<w<w_{opt}+3\%$; $\gamma_d>95\%$ SP
49	5.0E-08	SDRI	42	22	86		18	16.7	13.3	18.7	$w_{opt}<w<w_{opt}+3\%$; $\gamma_d>95\%$ SP
50	2.6E-07	SDRI	43	24	86		18	16.7	13.3	18.7	$w_{opt}<w<w_{opt}+3\%$; $\gamma_d > 95\%$ SP
51	3.0E-07	SDRI	40	22	86		18	16.7	13.3	18.7	$w > w_{opt}+3\%$; $\gamma_d > 95\%$ SP
52	1.1E-07	SDRI	37	18	73	38	19.9	16.5			$w > w_{opt}+3\%$; $\gamma_d > 95\%$ SP
53	2.2E-08	SDRI	54	31		40	19.9	16.4			
54	7.0E-08	SDRI									
55	1.3E-07	SDRI	66	35	93		27.4	14.5			
56	2.4E-08	SDRI	66	35	93				27.4	14.5	
57	5.6E-08	SDRI	69	38	98		26.8	14.6			
58	5.0E-08	SDRI	69	38	98		26.8	14.6			
59	9.4E-08	SDRI	69	38	98		26.8	14.6			
60	1.2E-07	SDRI	68	35	95		26.6	14.6			
61	3.7E-08	SDRI	68	35	95		26.6	14.6			
62	3.1E-07	SDRI	51	20	73		20.2	15.9			
63	3.9E-07	SDRI	51	20	73		20.2	15.9			

Table 4-1. Field Hydraulic Conductivity, Soil Characteristics, and Compaction Data for Natural Clay ... (Cont.).

Site	Field Hydraulic Conductivity (cm/s) Value	Field Hydraulic Conductivity (cm/s) Method	Liquid Limit (%)	Plasticity Index (%)	Percent Fines	Percent Clay	Standard Proctor w_{opt} (%)	Standard Proctor $(\gamma_d)_{max}$ kN/m^3	Modified Proctor w_{opt} (%)	Modified Proctor $(\gamma_d)_{max}$ kN/m^3	Compaction Criterion
64	2.3E-07	SDRI	47	30	66		19.5	16.3			γ_d > 95% SP
65	1.8E-07	SDRI	47	31	66				13.5	19.2	γ_d > 91% MP
66	1.2E-08	SDRI	50	29	75		19	16.1			w_{opt}+1%<w<w_{opt}+5%; γ_d>95% SP
67	8.3E-08	SDRI	49	27	62		19.3	16.1			w_{opt}+1%<w<w_{opt}+5%; γ_d>95% SP
68	2.3E-08	SDRI	35	17	67	22	14.8	17.7	11.5	19	w_{opt}+1%<w<w_{opt}+5%; γ_d>95% SP
69	1.3E-08	SDRI	22	9	50	16	10	19.9	8.5	21.4	w_{opt}+1%<w<w_{opt}+5%; γ_d>95% SP
70	4.0E-08	SDRI	42	26	88	45			14.9	18.7	w_{opt}-2%<w<w_{opt}+4%; γ_d>90% MP
71	8.3E-08	SDRI	29	19	83	34			12.2	19.6	w_{opt-2}%<w<w_{opt}+4%; γ_d>90% MP
72	2.0E-08	SDRI	36	20	85	35	18	16.5			w_{opt}+1%<w<w_{opt}+6%; γ_d>95% SP
73	8.0E-08	SDRI	76	53			21	15.5			w > w_{opt}; γ_d > 95% SP
74	1.0E-09	SDRI	56	40	64		18	16.9			w > w_{opt}; γ_d > 95% SP
75	5.0E-08	SDRI					21	15.6			w_{opt}+3%<w<w_{opt}+6%; γ_d>95% SP
76	2.0E-08	SDRI	37	17	92		19.2	16.6			w_{opt}+3%<w<w_{opt}+5%; γ_d>95% SP
77	2.0E-08	SDRI	32	13		19	9.9	19.7			w > w_{opt}; γ_d > 98% SP
78	2.0E-08	SDRI	32	16		25	11.5	19.6			w > w_{opt}+1.5%; γ_d>94% SP
79	4.5E-08	SDRI	62	41	82		25	14.9	17.8	16.5	w > w_{opt}; γ_d > 95% SP
80	4.0E-08	SDRI	52	35	84		19.6	15.9	14.4	18	w > w_{opt}; γ_d > 95% SP
81	1.5E-07	SDRI	47	22			25	15.3			w > w_{opt}+4%
82	3.0E-08	SDRI			84	54					γ_d > 96% SP
83	4.5E-08	SDRI	39	16	81	48	18.2	17.6			γ_d > 96% SP

Table 4-1. Field Hydraulic Conductivity, Soil Characteristics, and Compaction Data for Natural Clay ... (Cont.).

Site	Field Hydraulic Conductivity (cm/s) Value	Field Hydraulic Conductivity (cm/s) Method	Liquid Limit (%)	Plasticity Index (%)	Percent Fines	Percent Clay	Standard Proctor w_{opt} (%)	Standard Proctor $(\gamma_d)_{max}$ kN/m^3	Modified Proctor w_{opt} (%)	Modified Proctor $(\gamma_d)_{max}$ kN/m^3	Compaction Criterion
84	1.3E-07	SDRI									γ_d > 90% MP
85	2.8E-08	SDRI									γ_d > 90% MP
86	1.5E-08	SDRI	43	24	84	37	17.7	17.1			$w_{opt}<w<w_{opt}+4\%$; γ_d>95% SP
87	1.4E-08	SDRI	43	24	84	37	17.7	17.1			$w_{opt}<w<w_{opt}+4\%$; γ_d>95% SP
88	2.3E-08	SDRI	25	14	70	29	11.6	19.1			$w_{opt}<w<w_{opt}+4\%$; γ_d>95% SP
89	2.1E-08	SDRI	25	14	70	29	11.6	19.1			$w_{opt}<w<w_{opt}+4\%$; γ_d>95% SP

Notes:

SDRI = Sealed Double Ring Infiltrometer
LYS = Lysimeter (Underdrain beneath Liner)
w_{opt} = Optimum Water Content
$(\gamma_d)_{max}$ = Maximum Dry Unit Weight
w = Water Content
γ_d = Dry Unit Weight
SP = Standard Proctor
MP = Modified Proctor
Percent Fines = percent passing the No. 200 (0.075 mm) sieve
Percent Clay = percent finer than 0.002 mm

Table 4-2. Summary of Construction and Additional Hydraulic Conductivity Data.

Site	Compactor Mass (kg)	Number of Passes Per Lift	Lift Thickness (mm)	Number of Lifts	Avg. Water Content (%)	Avg. Dry Density (kN/m^3)	P_o (%)	Lab. Hydraulic Conductivity (cm/s)	Field Hyd. Cond. from TSB Test (cm/s)	Lab. Hyd. Cond. from 300 mm Diameter Samples (cm/s)
1	32,400	6	150	6	10.3	19.8	44	3.2E-09		2.6E-7
2										
3	30,000	4	150	8	13.8	19.4	98	8.0E-09		
4	19,800		150	4	21.3	16	80	5.0E-09		
5	36,000	6	150	10	17.3	17.3	95	8.8E-09		4E-08
6	32,400	5	150	6	13.8	19	32	2.4E-08		
7	32,400	4	150	8	17.2	17.7	88	8.4E-08	4.3E-08	
8	12,600	4	150	6	15.3	17.7	8	9.0E-09		
9			150	10	19.6	17	90	1.0E-08		
10			150	10	17.8	16.9	50	8.0E-09		
11			150	10	25.4	16	75	2.0E-09		
12			150	10	26	16.1	78	3.0E-09		
13	32,400	4	150	8	20.7	16.7	100	1.3E-08		1.4E-08
14			170	6	17	16.8	78	4.8E-08		
15			200	7	30.8	14.1	98	4.4E-09		1.6E-08
16	39,000		170	5	19.8	16.1	91	3.7E-08		
17	19,800	6	150	4	23.3	15.7	100	3.0E-09		5.0E-09
18	25,000	4	150	5	16.6	17.4	85	1.5E-08	9.2E-09	1.4E-08
19	32,400	5	150	10	13.6	19	81	1.9E-08		
20	32,400	8	150	6	17.6	16.9	8	3.0E-08		
21	32,400	6	150	6	19.5	16.9	80	3.1E-07		2.2E-07

Table 4-2. Summary of Construction and Additional Hydraulic Conductivity Data (Cont.).

Site	Compactor Mass (kg)	Number of Passes Per Lift	Lift Thickness (mm)	Number of Lifts	Avg. Water Content (%)	Avg. Dry Density (kN/m^3)	P_o (%)	Lab. Hydraulic Conductivity (cm/s)	Field Hyd. Cond. from TSB Test (cm/s)	Lab. Hyd. Cond. from 300 mm Diameter Samples (cm/s)
22								2.4E-08		
23			150	10	22	16.4	89	1.5E-08		
24	18,900		150	5	23.6	15.8	81	9.0E-09		1.1E-08
25	18,900		150	5	18.9	16.9	71	2.3E-09		6.0E-09
26	18,900		150	6	15.5	17.6	17	2.9E-09		1.8E-07
27	18,900		150	6	13.5	18	6	3.0E-08		1.5E-07
28	18,900		150	6	16.2	17.7	57	1.9E-08		1.7E-07
29	32,400	6	170	9	13.9	18.8	84	2.2E-08		1.7E-08
30	27,000		150	6	16.2	18.6	65	3.0E-08		
31			300	2	13.1	19.1	75	1.6E-08	4.7E-08	
32	32,400		150	8	13.9	19.2	92	3.0E-08		
33	19,800		150	8	13.4	18.7	80	1.3E-08		
34	19,800	4	150	3	17.8	17.1	45	1.5E-08		3.5E-07
35	32,400	6	150	6	20.7	16.8	78	3.0E-08		
36	17,100	8	150	6	15.5	17.6	77	9.1E-09		
37		4	150	5	14.1	18.2	45	4.9E-08		
38		12	150	6	11.5	20.4				
39	19,800	12	130	6	11.6	17.9	10	2.6E-08		
40	59 kg/lin. cm		150	6	35.5	12.8	100	3.5E-09	1.6E-08	
41	19,800	40	150	4	21.9	16	92	5.5E-09		4.1E-09

Table 4-2. Summary of Construction and Additional Hydraulic Conductivity Data (Cont.).

Site	Compactor Mass (kg)	Number of Passes Per Lift	Lift Thickness (mm)	Number of Lifts	Avg. Water Content (%)	Avg. Dry Density (kN/m^3)	P_o (%)	Lab. Hydraulic Conductivity (cm/s)	Field Hyd. Cond. from TSB Test (cm/s)	Lab. Hyd. Cond. from 300 mm Diameter Samples (cm/s)
42			150	4	25	15.1	81			
43	7,200	16	150	5	23.4	15.4	63	2.4E-09		
44	7,200	8	150	5	24.2	15	47	2.4E-09		
45	19,800	42	150	4	19.8	16.3	71	5.8E-09		
46	10,900	8	225	5	27.3	15.4	100	1.5E-08		
47	19,800		85	10	16.5	17.7	100			
48	19,800		150	4	17.8	17	75	1.1E-08	2.1E-08	4.8E-08
49	19,800	3	150	4	18.9	16.7	86	5.1E-08	3.2E-07	7.7E-08
50	19,800	3	150	4	18.6	16.9	84	7.4E-08	7.5E-08	3.1E-06
51	19,800		150	4	17.8	17	73	4.1E-08	1.1E-09	5.3E-07
52					21.2	16.1	67			
53		4		4	21.6	15.5		1.7E-08	1.2E-08	
54			150	4						
55	19,800	12	160	4	27	15	100	8.1E-08		
56	19,800	10	130	4	30.6	14.2	100	2.8E-08		
57	19,800	6	140	4	29.6	14	100	3.4E-08		
58	19,800	12	150	4	30.7	14.3	100	2.5E-08		
59	19,800	12	170	4	29.4	14.4	100	2.7E-08		
60	19,800	12	170	4	26.8	15.1	100	3.4E-08		
61	19,800	12	190	4	29.8	14.4	100	4.3E-08		
62	19,800	12	150	4	24.6	15.4	100	1.6E-07		

Table 4-2. Summary of Construction and Additional Hydraulic Conductivity Data (Cont.).

Site	Compactor Mass (kg)	Number of Passes Per Lift	Lift Thickness (mm)	Number of Lifts	Avg. Water Content (%)	Avg. Dry Density (kN/m^3)	P_o (%)	Lab. Hydraulic Conductivity (cm/s)	Field Hyd. Cond. from TSB Test (cm/s)	Lab. Hyd. Cond. from 300 mm Diameter Samples (cm/s)
63	19,800	12	230	4	22.7	15.4	100	1.7E-07		
64	19,800	40	150	4	21.6	16	88	5.5E-09		4.1E-09
65	19,800	80	150	4	17.2	17.4	0			
66	19,800	2	100	10	21.7	17.2	95	3.7E-08	1.1E-08	
67	19,800	2	100	11	21.4	17.2	98	3.0E-08	8.5E-08	
68	19,800	6	150	4	17.6	18	100	7.8E-09	2.6E-08	
69	19,800	6	150	4	11.5	19.4	75	2.1E-08	5.6E-08	
70		7	150	6	20.6	16.1	60	2.0E-08		
71		7	150	6	14.3	18	64	2.0E-08		
72	32,400	8	150	4	23.7	15.5	100	1.4E-08		
73	19,800	22	100	7	25.2	14.8	97			
74	19,800	22	100	7	19.6	16.1	47			
75	19,800		150	4	25.4	15.2	100			
76	19,800	6	150	4	21.8	15.9	86	4.7E-08		
77	10,200	10	100	9	11	19.2	37			
78	10,200	4	100	9	12.4	18.8	2			
79	19,800	8	150	8	28.2	16.2		3.3E-09		
80	19,800	8	150	8	23.1	14.9		1.8E-09		
81	16,200	4	150	4	28	14.2		4.2E-08		
82	32,400-	62	150	4	17.8	17.1		1.5E-08		

Table 4-2. Summary of Construction and Additional Hydraulic Conductivity Data (Cont.).

Site	Compactor Mass (kg)	Number of Passes Per Lift	Lift Thickness (mm)	Number of Lifts	Avg. Water Content (%)	Avg. Dry Density (kN/m^3)	P_o (%)	Lab. Hydraulic Conductivity (cm/s)	Field Hyd. Cond. from TSB Test (cm/s)	Lab. Hyd. Cond. from 300 mm Diameter Samples (cm/s)
83	32,400-	62	150	4	19.3	17.3		1.7E-08		
84	19,800		200	20						
85	19,800		200	20						
86	19,800	4	150	6	20.5	16.6	100	2.2E-08		
87	19,800	7	150	6	20.4	16.6	95	2.6E-08		
88	19,800	4	150	6	13.2	19.2	100	3.9E-08		
89	19,800	6	150	6	13.2	19.1	100	3.1E-08		

Notes:

P_o = Percent of Moisture-Density Points on or Above the Line of Optimums
TSB = Two-Stage Borehole Permeability Test

The soils included in the database covered a broad spectrum of material types (Fig. 4-2). Nearly all the soils used were classified as either CL or CH soils.

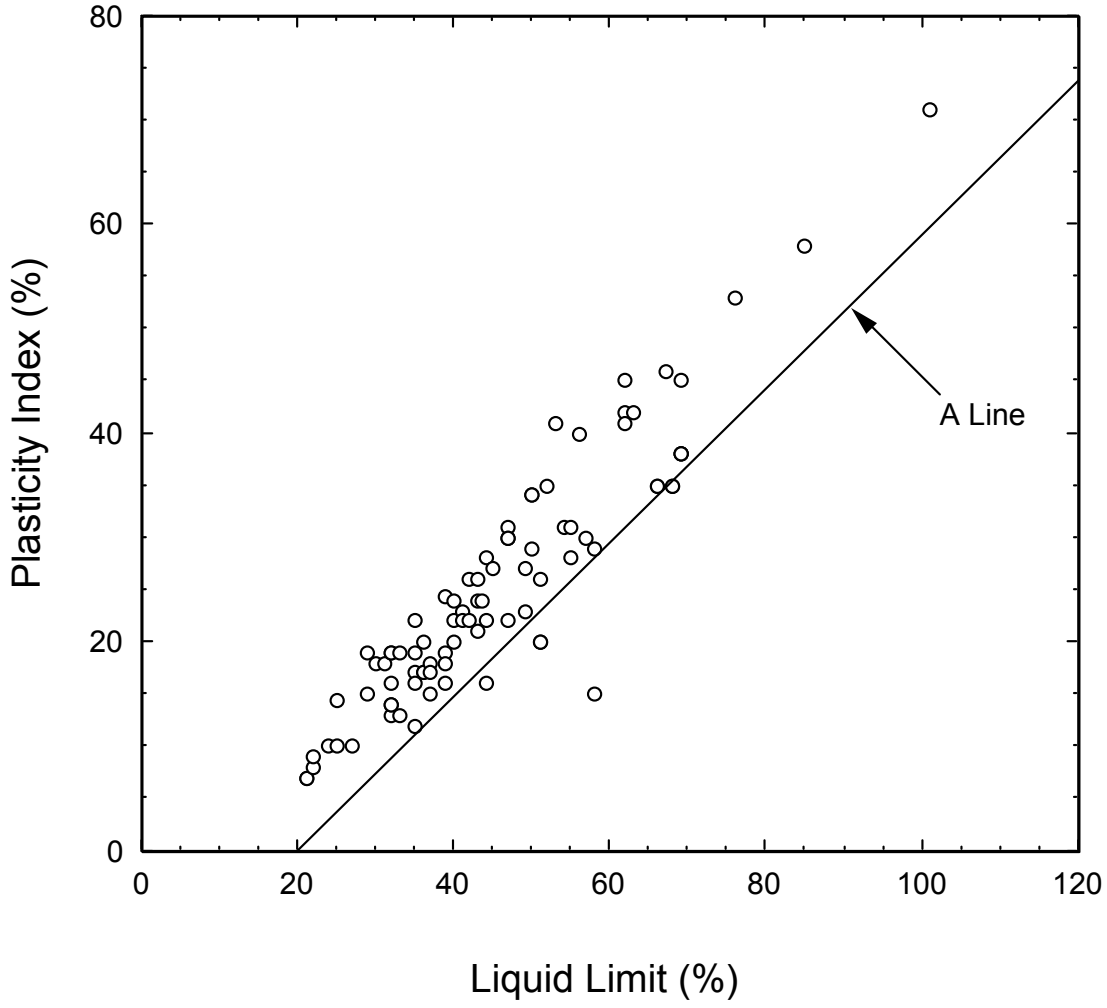

Figure 4-2. Atterberg limits of natural clay liner materials in database.

4.1.2.3 Field Hydraulic Conductivity

Open single- or double-ring infiltrometers, sealed double-ring infiltrometers (SDRIs), air entry permeameters, two-stage borehole (TSB or Boutwell) tests, and BAT probes (BAT is a commercial name for a particular type of porous probe device) have been used to measure the hydraulic conductivity of CCL test pads in situ. Information on these tests is provided by Daniel (1989), Sai and Anderson (1990), and Trautwein and Boutwell (1994). In addition, large lysimeters have been installed beneath CCLs at several actual landfills (e.g., Gordon et al., 1990).

Work by Benson et al. (1994) indicates that an area of approximately 0.1 m^2 is the minimum required to obtain a representative hydraulic conductivity measurement with field infiltrometers or laboratory tests on "undisturbed" samples from the field. For practically all of the CCL test pads in the database, only the SDRI test met this criterion. Thus, the SDRI test was selected as the test that would be used to define field k for the 81 CCL test pads that were included in the database. Most SDRIs permeated an area of 2.3 m^2, but a few were as small as 1.4 m^2.

For the 8 actual in-service CCLs beneath landfills, lysimeters were used to determine k_{Field}. One lysimeter covered an area of 0.37 m^2, but the rest covered 64 to 225 m^2.

Hydraulic conductivity was calculated from SDRI tests using the wetting-front method with a wetting-front suction of zero (Trautwein and Boutwell, 1994). No correction was made for swelling of the soil. These assumptions theoretically result in a computed k that is slightly larger than the actual k.

It is important to note that hydraulic conductivity is sensitive to the effective vertical stress acting on the CCL at the time the hydraulic conductivity is measured. For test pads, there is very little effective overburden pressure acting on the CCL. For actual in-service liners overlain by solid waste, the effective stress is relatively large. There is a tendency for decreasing hydraulic conductivity with increasing effective compressive stress because compression causes a reduction in porosity and, hence, a reduction in hydraulic conductivity.

Because increasing overburden stresses tends to reduce hydraulic conductivity, it would be expected that, on average, k_{Field} determined from lysimeters would tend to be lower than values determined from SDRI tests on test pads. It should be noted, however, that even though a CCL in a landfill liner system will be subjected to significant overburden stress as waste is placed, the overburden stress is low during the period of initial waste placement. Also, the effective vertical stress is low permanently in liquid waste impoundments and final cover systems.

4.1.3 Hydraulic Conductivity Results

4.1.3.1 Field Hydraulic Conductivity

A histogram of the logarithms of hydraulic conductivity is plotted in Fig. 4-3. Hydraulic conductivity is log normally distributed.

For the 89 CCLs in the database, the average k_{Field} is 4.0×10^{-8} cm/s. The highest k_{Field} is 8×10^{-7} cm/s and the lowest is 1.0×10^{-9} cm/s. All averages for hydraulic conductivity are the geometric mean (i.e., based on log average). For the 81 CCL test pads whose k_{Field} was determined by SDRI testing, the average k_{Field} was 5×10^{-8} cm/s. For the 8 in-place liners monitored with lysimeters, the average k_{Field} was 9×10^{-9} cm/s. The lower

k_{Field} for the in-place liners was probably affected by three factors: (1) all but one of the in-place liners had a thickness > 1 m, which is thicker than most test pads; (2) the compressive stress was much higher on the in-place liners compared to test pads; and (3) the in-place liners were all from the northeastern section of the U.S. or Canada, where the clays tend to be wet.

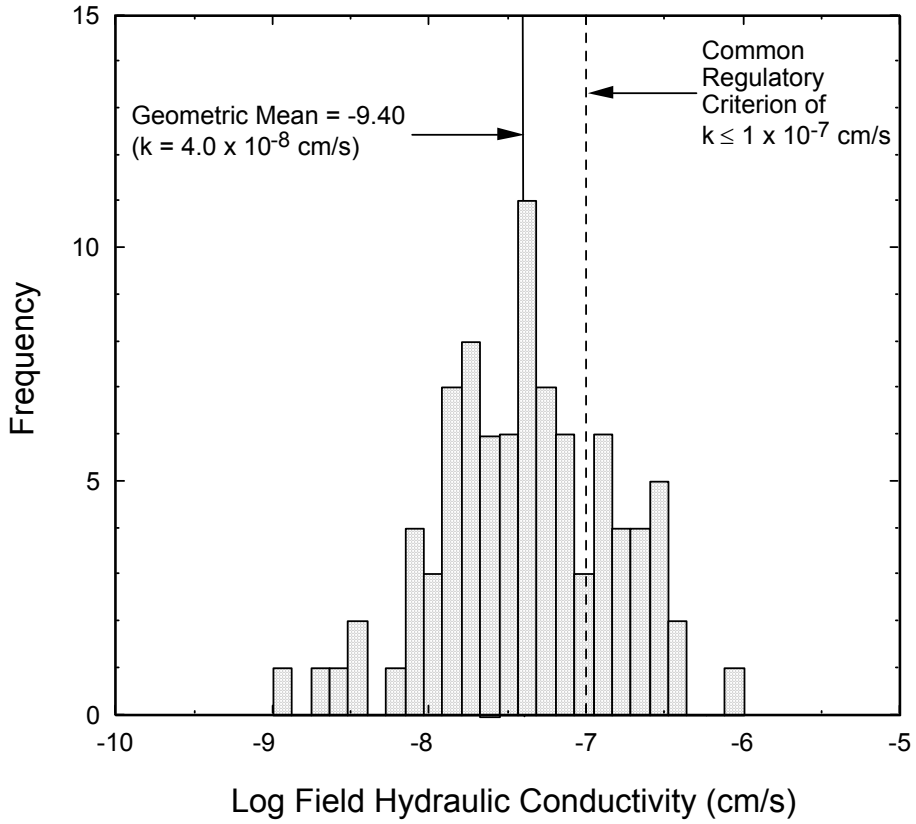

Figure 4-3. Histogram of field hydraulic conductivities for CCLs constructed from natural clay materials.

All of the full-scale clay liners and test pads in the database were constructed with the expectation that the k_{Field} would be no greater than 1 x 10^{-7} cm/s. However, while 67 of the CCLs in the database (or 75% of the total) did achieve the objective of $k \leq 1 \times 10^{-7}$ cm/s, 22 test pads (or 25% of the total) did not. A histogram of k_{Field} for the failing test pads is presented in Figure 4-4. Most of the test pads that failed just barely failed. Of the 22 test pads that failed to achieve field $k \leq 1 \times 10^{-7}$ cm/s, 12 had a $k \leq 2 \times 10^{-7}$ cm/s and 18 had $k \leq 3 \times 10^{-7}$ cm/s. Nevertheless, a hydraulic conductivity of 1 x 10^{-7} cm/s is the maximum typically allowed by regulation, and failure to meet this requirement is usually grounds for denying a construction permit. The causes for so many of the clay

liners failing to meet the 1 x 10^{-7} cm/s design objective are discussed later, but to summarize, the soils were unsuitable in a few cases, but in most cases, the compaction conditions were inadequate.

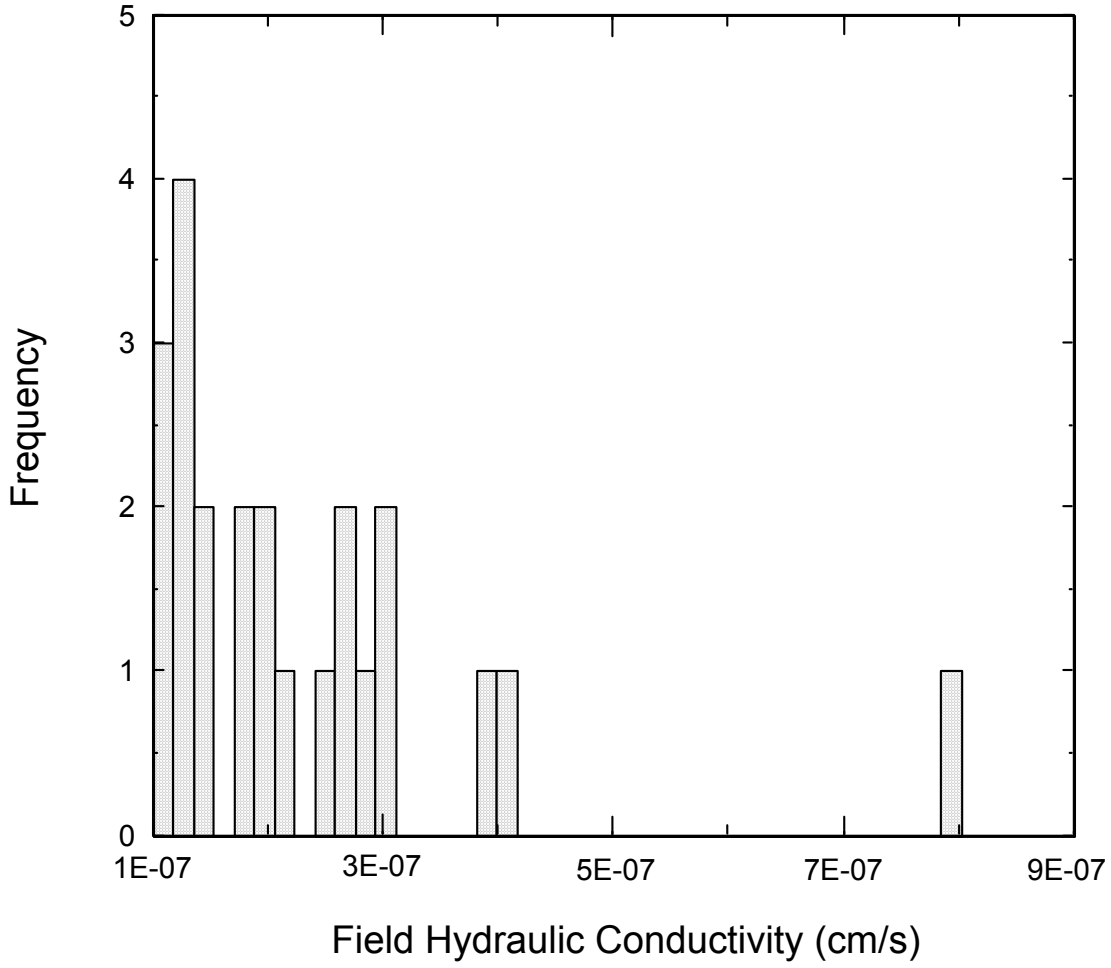

Figure 4-4. Histogram of field hydraulic conductivities that failed to achieve the desired k ≤ 1 x 10^{-7} cm/s for CCLs constructed from natural clay materials.

The database includes information from 8 lysimeters that were located beneath actual landfill liners. The average k_{Field} from the 8 lysimeters is 9 x 10^{-9} cm/s. The average k_{Field} from the 81 test pads is significantly larger (5 x 10^{-8} cm/s). Of the factors that might tend to cause k_{Field} from an SDRI test on a test pad to be larger than k_{Field} of an in-service liner at a landfill, the larger compressive stress acting on the CCL in an actual landfill liner is probably the most important one. However, CCLs in the field are

challenged to perform well at low compressive stress in final cover applications and in liner systems during the initial placement of waste in a landfill cell.

4.1.3.2 Hydraulic Conductivity from Small-Diameter Samples

One of the most contentious issues in clay liner testing is the degree to which laboratory hydraulic conductivity tests performed on relatively undisturbed, 75-mm-diameter samples obtained from the field provide an accurate indication of the large-scale k_{Field}. For poorly built liners, the laboratory hydraulic conductivity (k_{Lab}) can be orders of magnitude lower than k_{Field}. Figure 4-5 shows the relationship between k_{Lab} and k_{Field}, and Figure 4-6 relates the hydraulic conductivity ratio k_{Lab}/k_{Field} to k_{Field}. The linear regression in Figure 4-6 and some subsequent figures is shown for informational purposes only and does not imply that there is or should be a linear correlation. In general, k_{Lab} tends to be less than k_{Field}, The average k_{Lab}/k_{Field} is 0.4, but the ratio is as low as 0.0038 and as high as 7.8.

The reasons for differences between k_{Lab} and k_{Field} are many, as discussed in the literature (e.g., Benson and Boutwell, 1992; Benson et al., 1994). It is generally believed that small-scale measurements will yield the same k as large-scale measurements if the clay liner is well constructed and reasonably homogeneous. On the other hand, a poorly built liner will be heterogeneous and will contain hydraulic defects on a scale that is too large to be properly represented in a 75-mm-diameter sample. As indicated in Figure 4-6, there is a tendency for better correlation between k_{Lab} and k_{Field} (i.e., $k_{Lab}/k_{Field} \approx 1$) for small values of k_{Field}. Small values of k_{Field} are presumably achieved when good construction specifications, materials, construction procedures, and QA practices are used. In other words, there is good correlation between k_{Lab} and k_{Field} for good-quality liners with a very low k_{Field}, and a tendency for the k_{Lab} to be significantly smaller than k_{Field} as k_{Field} increases. Not surprisingly, the worst correlation between k_{Lab} and k_{Field} (i.e., lowest value of k_{Lab}/k_{Field}) is for the highest value of k_{Field} in the database (Figure 4-6).

Laboratory k tests on 75-mm-diameter samples obtained from the field-compacted clay liner are a routine part of many CQA programs, and the results often form the principal basis for pass/fail decisions. Of the 89 CCLs in the database, laboratory-measured hydraulic conductivity's were reported for 75 CCLs. Twenty-two CCLs in the database failed to achieve a k_{Field} of 1×10^{-7} cm/s or less. Of the 18 failing CCLs for which k_{Lab} data are available, laboratory k tests incorrectly indicated that 15 of the CCLs passed the 1×10^{-7} cm/s requirement. The laboratory measurements of hydraulic conductivity provided a false positive (pass) in 15 of 18 (83%) of the failing test pads. The k_{Lab} values correctly predicted failing k_{Field} in just 3 of the 18 (17%) test pads. The database clearly shows that k_{Lab} tests have a strong tendency to yield unconservative (passing) values for failing CCLs. On the other hand, of the 67 instances in which k_{Field} was $\leq 1 \times 10^{-7}$ cm/s, all the laboratory-measured hydraulic conductivity's were $\leq 1 \times 10^{-7}$ cm/s.

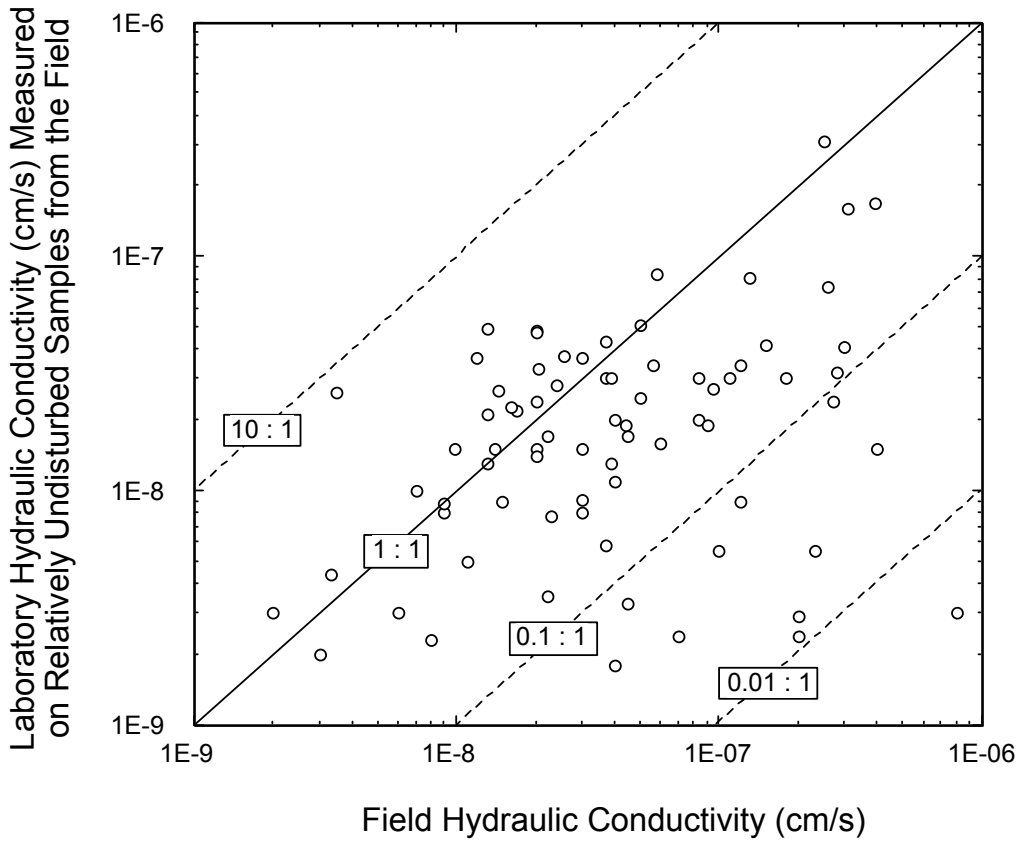

Figure 4-5. Relationship between field hydraulic conductivity (k_{Field}) and the hydraulic conductivity measured in the laboratory (k_{Lab}

Thus, the database shows:

- If k_{Lab} is $\leq 1 \times 10^{-7}$ cm/s, the k_{Field} may or may not be $\leq 1 \times 10^{-7}$ cm/s. Of the 72 CCLs with $k_{Lab} \leq 1 \times 10^{-7}$ cm/s, 57 had k_{Field} values that achieved the hydraulic conductivity criterion of 1×10^{-7} cm/s or less. Based on this database, if $k_{Lab} \leq 1 \times 10^{-7}$ cm/s, there is a 57/72 = 79% probability that k_{Field} will also be $\leq 1 \times 10^{-7}$ cm/s.
- If the k_{Lab} is $> 1 \times 10^{-7}$ cm/s, this database shows that 100% of the time k_{Field} was also $> 1 \times 10^{-7}$ cm/s.
- Laboratory hydraulic conductivity tests are not that useful for discriminating between well and poorly built liners.

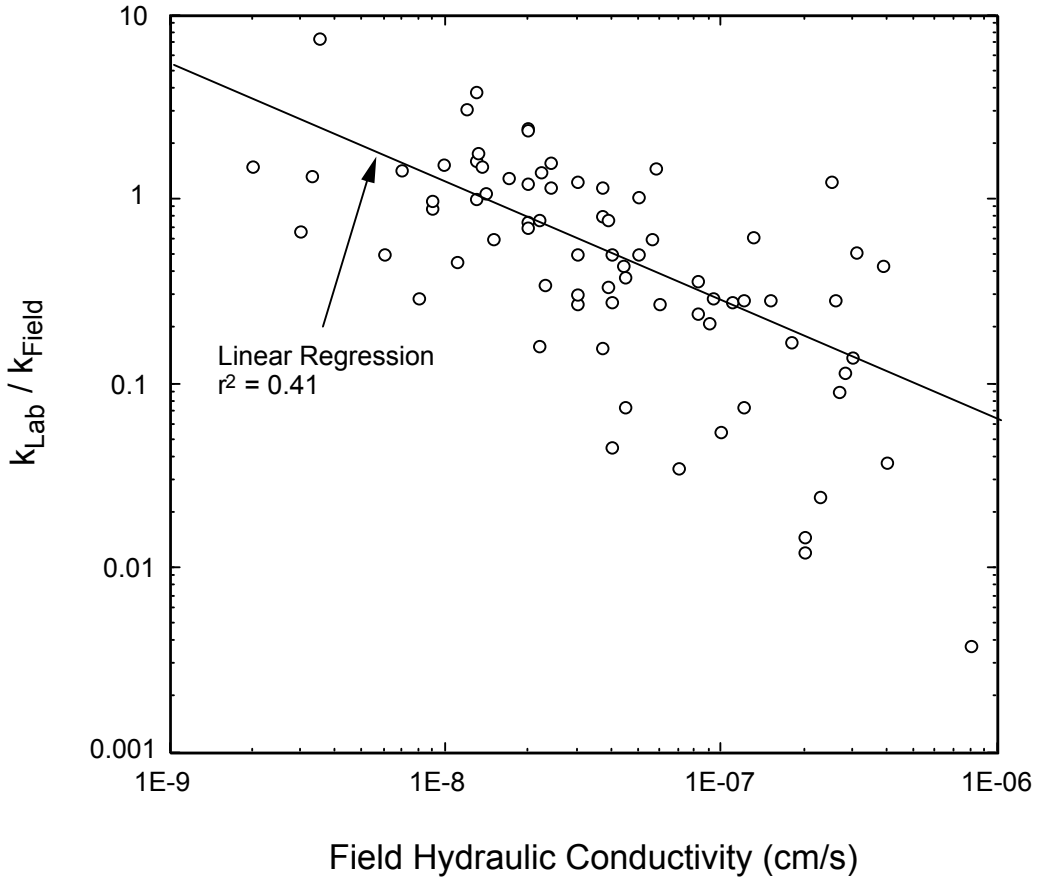

Figure 4-6. Ratio of field hydraulic conductivity to laboratory-measured hydraulic conductivity (k_{Field}/k_{Lab}) versus field hydraulic conductivity for clay liners constructed from natural clay material.

4.1.4 Soil Characteristics

Construction of a CCL with a hydraulic conductivity $\leq 1 \times 10^{-7}$ cm/s requires the use of suitable soils. The engineer usually specifies a minimum plasticity index (PI) for the soil (PI typically $\geq$ 12 to 15%) and a minimum percentage of fines (typically $\geq$ 50% passing the No. 200 sieve). A minimum percentage of clay (fraction finer than 2 μm) is also sometimes required (e.g., $\geq$ 20 to 25% clay). Values are also sometimes specified for the liquid limit (LL) of the soil. The succeeding subsections present an assessment of the significance of LL, PI, percentage of fine material, and percentage of clay.

4.1.4.1 Liquid Limit (LL)

The relationship between k_{Field} and LL is shown in Figure 4-7. Linear regression indicates an essentially flat best-fit curve, and $r^2 = 0.00$ confirms the obvious observation that there is no correlation between k_{Field} and the LL of the soil. All linear

regression analyses presented herein were calculated using the software package Cricket Graph.

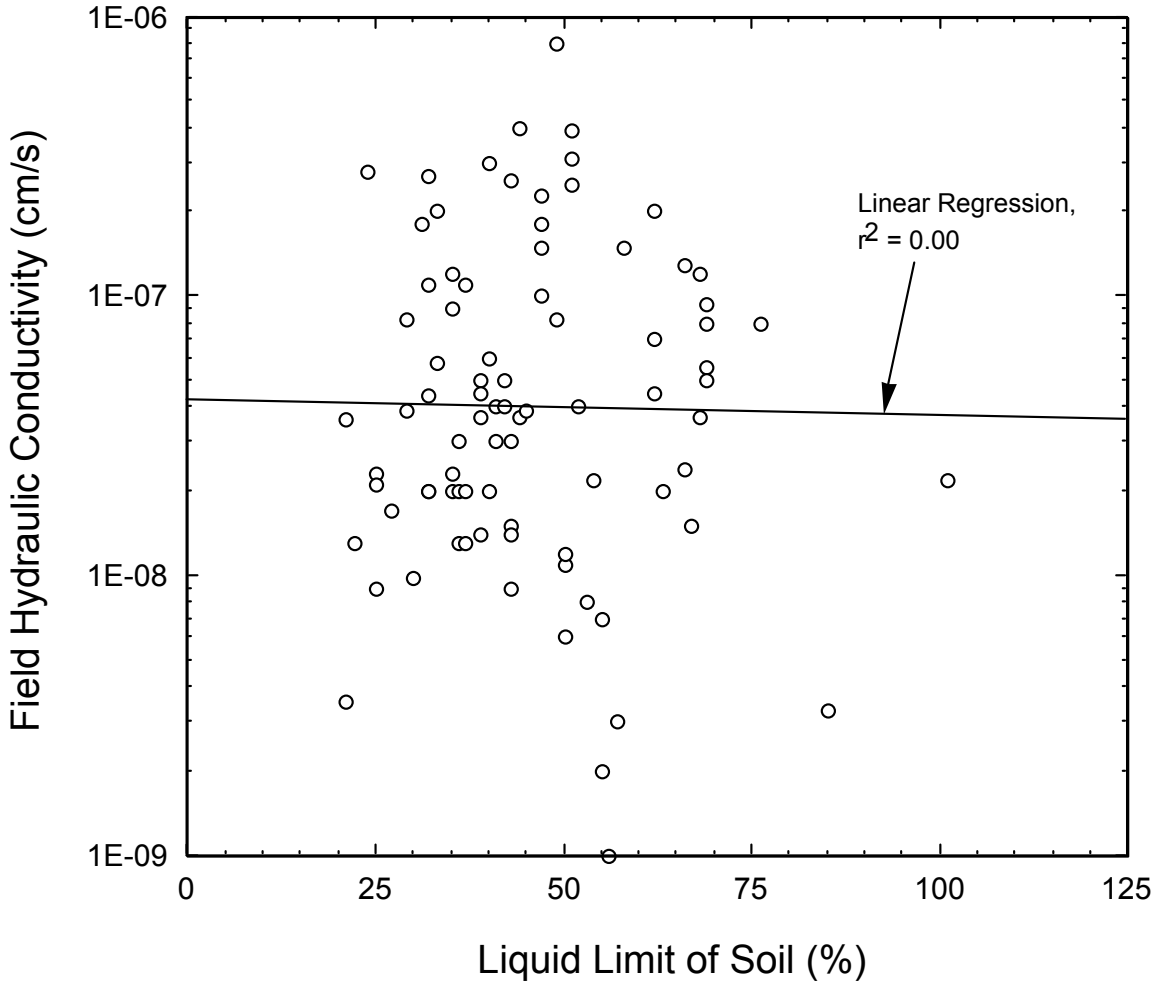

Figure 4-7. Field-measured hydraulic conductivity versus liquid limit of the soil for CCLs constructed from natural clay material.

4.1.4.2 Plasticity Index (PI)

The relationship between k_{Field} and PI is shown in Figure 4-8. There is a slight tendency for decreasing k_{Field} with increasing PI, but the correlation is very weak.

Because the PI of the soil is perhaps the single most frequently used indicator of the quality of a natural soil material for use in a CCL, it is useful to consider whether some minimum value of PI provides a good indication of the suitability of a soil for use in a CCL. Figure 4-9 shows the percentage of CCLs that attained a $k_{Field} \leq 1 \times 10^{-7}$ cm/s as a function of PI. Soils with PI's greater than 30 to 40% have a higher probability of

achieving $k_{Field} \leq 1 \times 10^{-7}$ cm/s than soils of lower PI. However, of the 11 CCLs for which the PI was lower than 15%, 8 had $k_{Field} \leq 1 \times 10^{-7}$ cm/s, confirming that clays of low plasticity can be used successfully. The database does not support the concept that there is a minimum PI that should be specified for clay liner materials, although no liners with PI's < 7 are included in the database.

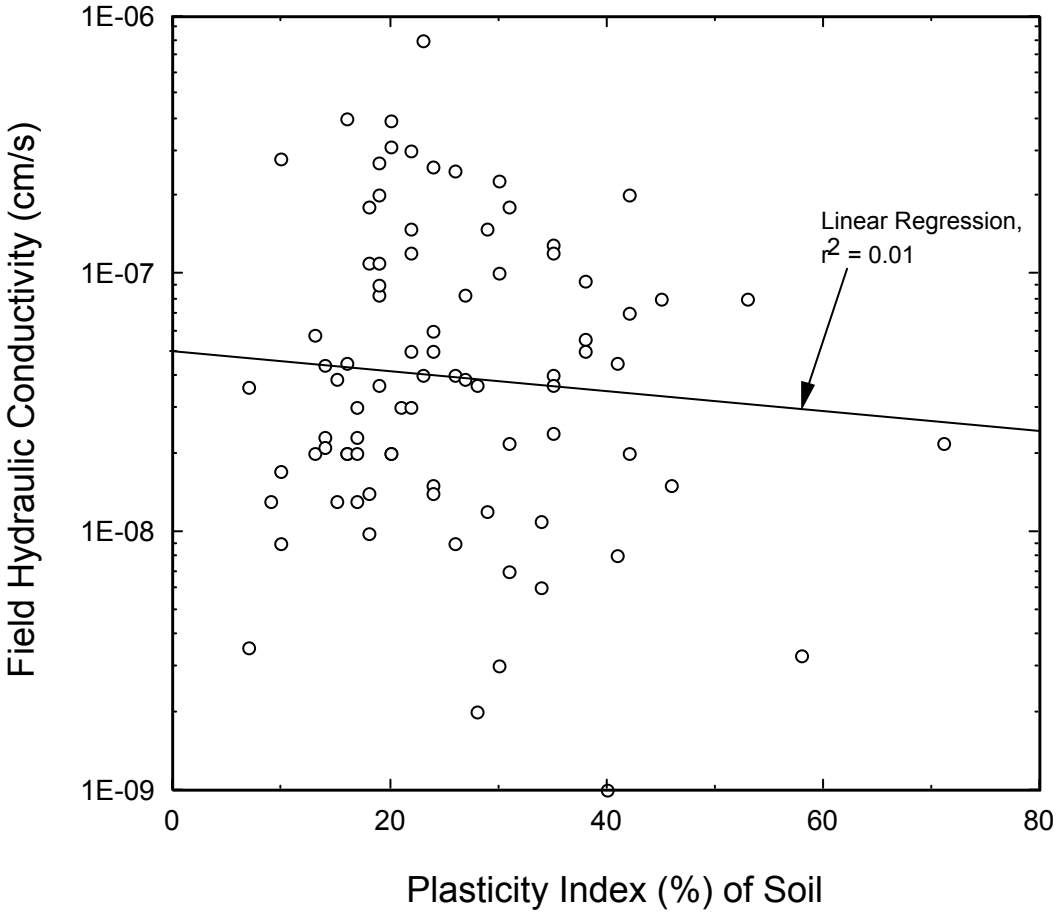

Figure 4-8. Field-measured hydraulic conductivity versus plasticity index of the soil for CCLs constructed from natural clay material.

There have been correlations published between k_{Lab} and PI of the soil (e.g., Benson et al., 1992). Figure 4-10 presents the relationship between k_{Lab} and PI for this database. There is a much stronger correlation between k_{Lab} and PI, compared to k_{Field} and PI. Because it is k_{Field} that counts, and because k_{Field} does not correlate well with PI (Figure 4-8), the value of plots such as the one shown in Figure 4-10, which shows a slight trend of decreasing k_{Lab} with increasing PI, is questionable.

4.1.4.3 Percent Fines

As shown in Figure 4-11, no correlation was observed between k_{Field} and the percentage of fines in the soil (defined as the percent on a dry weight basis passing through a No. 200 sieve, which has openings of 0.075 mm). However, all but one soil in the database had at least 50% fines, which is a minimum value that is commonly specified or required. The data support the current approach of specifying a minimum percentage fines but providing no preference over the amount of fines in the soil, other than to ensure that the specified minimum is met.

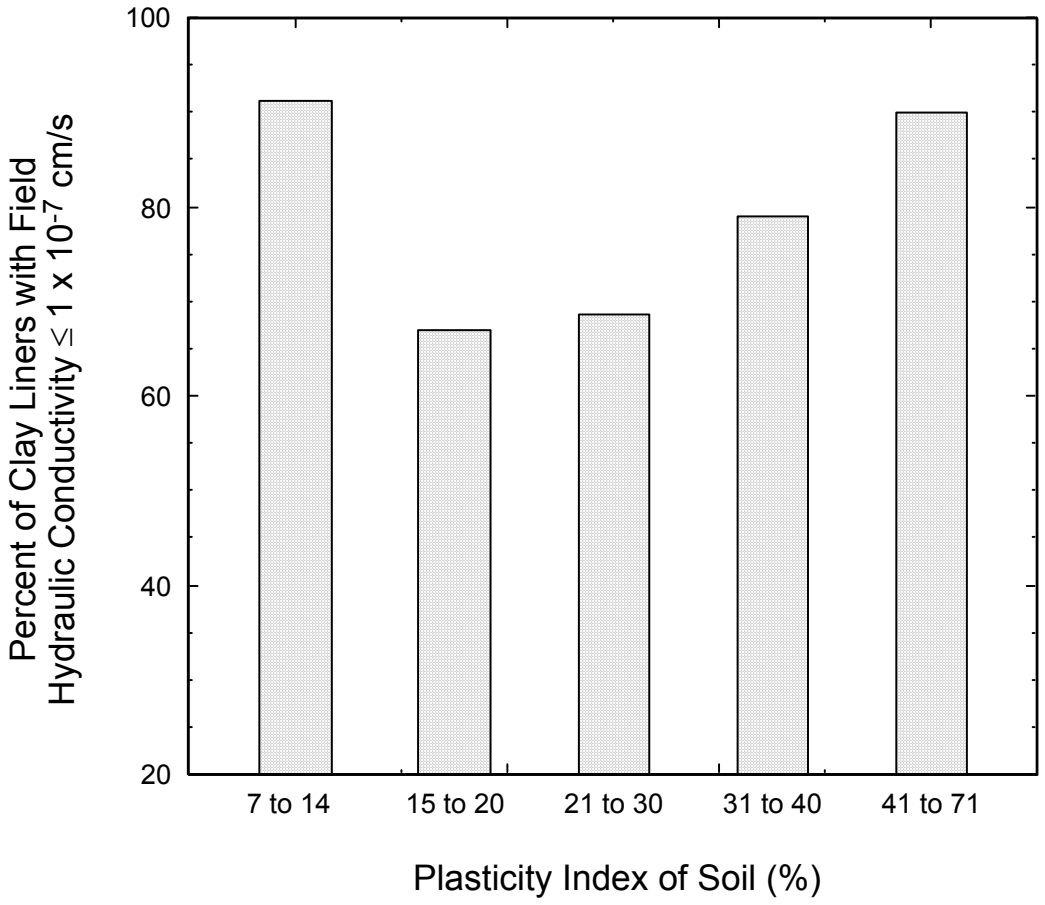

Figure 4-9. Percent of clay liners with a field hydraulic conductivity less than or equal to 1 x 10^{-7} cm/s as a function of the plasticity index of the soil.

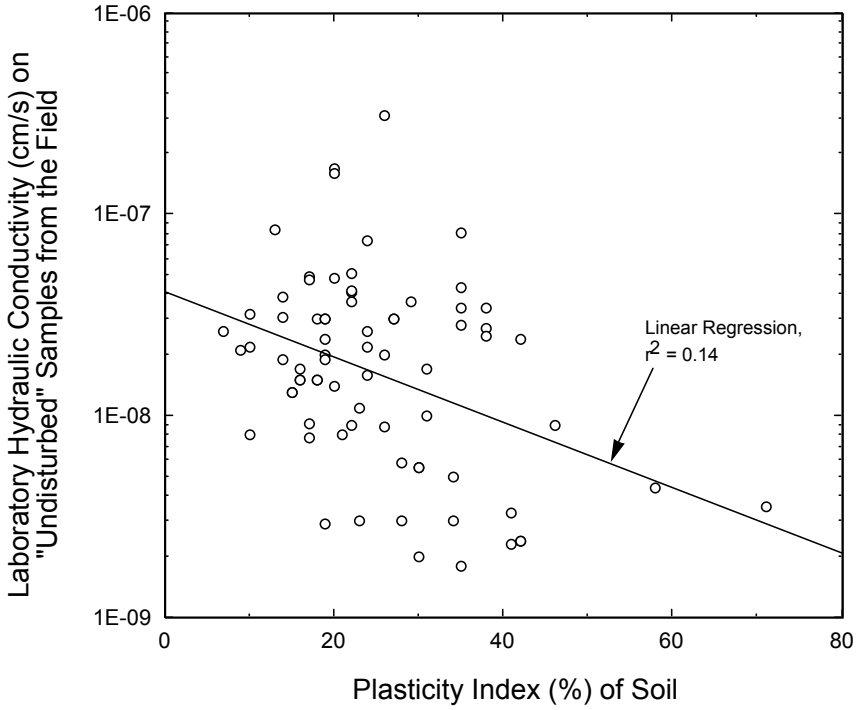

Figure 4-10. Laboratory-measured hydraulic conductivity versus plasticity index of the soil for CCLs constructed from natural clay material.

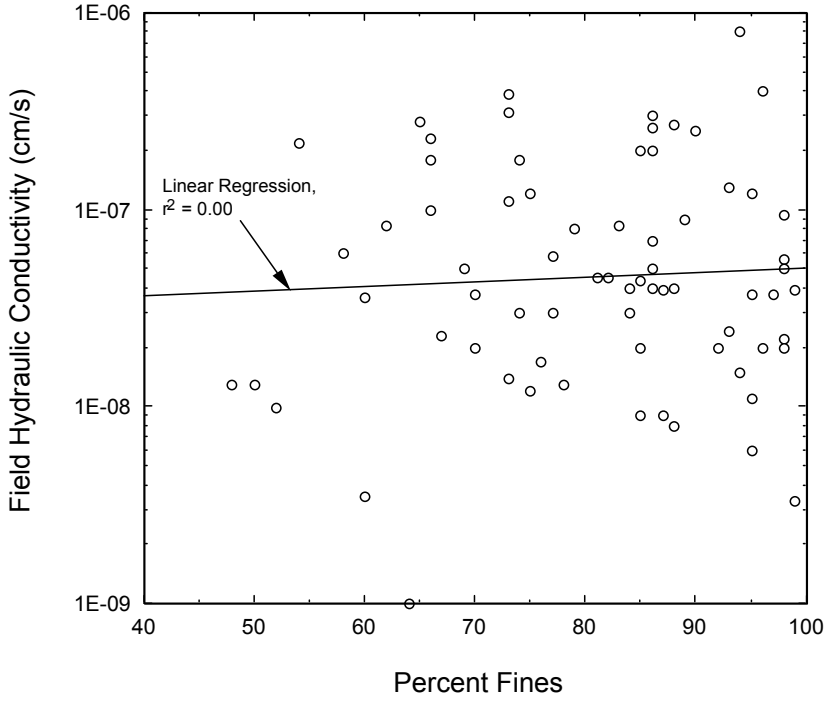

Figure 4-11. Field-measured hydraulic conductivity versus percentage of fines in the soil for CCLs constructed from natural clay material.

4.1.4.4 Clay Fraction

As shown in Figure 4-12, there is no relationship between k_{Field} and the percentage of clay (defined as the fraction finer than 2 μm) in the soil. Because clay content is relatively difficult and expensive to determine, the value of clay content tests for CQA programs is questioned. Other factors overshadow the clay content in terms of impact on k_{Field}.

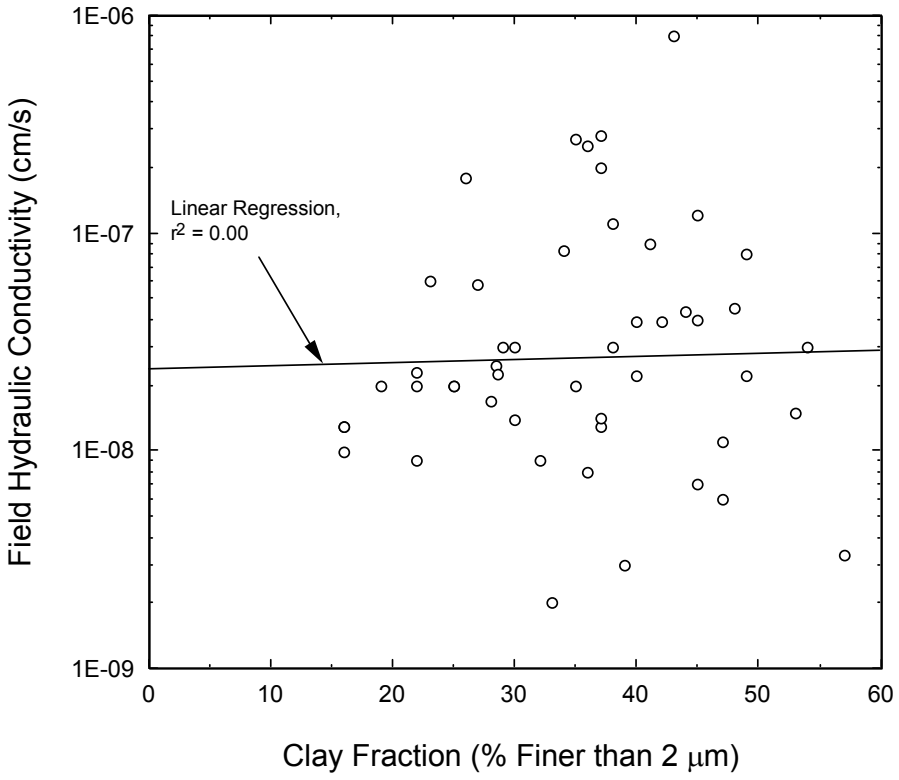

Figure 4-12. Field-measured hydraulic conductivity versus percentage of clay in the soil for CCLs constructed from natural clay material.

Figure 4-13 shows the relationship between k_{Lab} and clay content. A better correlation was found for k_{Lab} than for k_{Field}. The k_{Lab} values may be more dependent on clay content than k_{Field} values because construction variables play a more important role for k_{Field} than k_{Lab}. As will be seen later, moisture-density conditions have a dominant effect on the k_{Field} of CCLs and probably mask the comparatively subtle effects of soil characteristics, such as clay fraction.

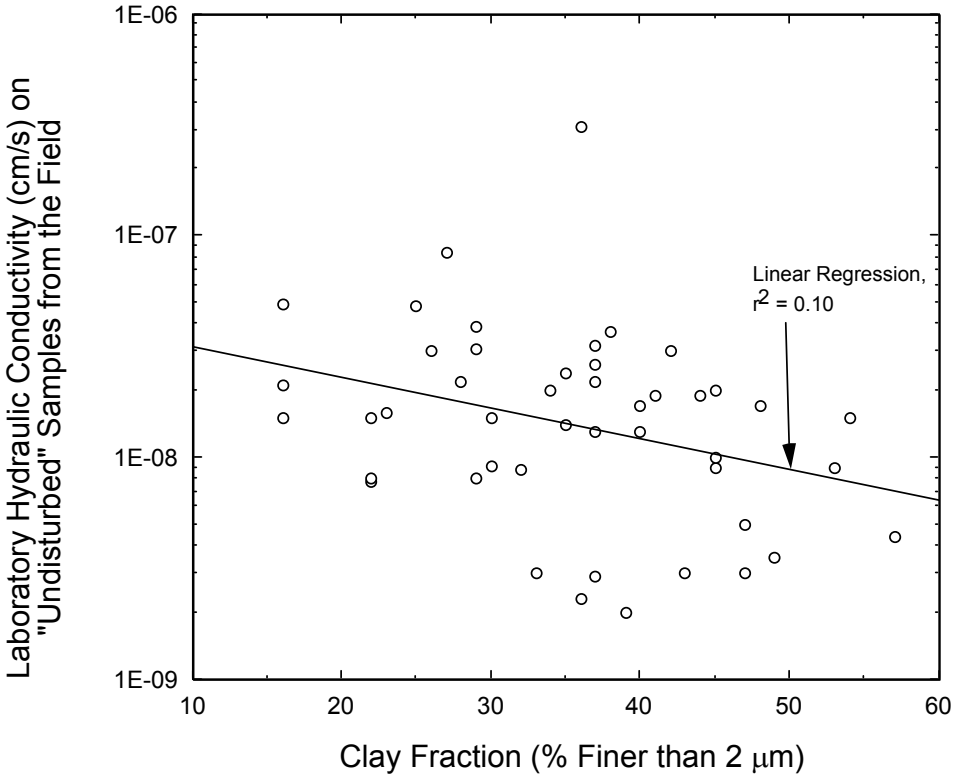

Figure 4-13. Laboratory-measured hydraulic conductivity versus percentage of clay in the soil for CCLs constructed from natural clay material.

4.1.5 Compaction Conditions

The results of standard Proctor and/or modified Proctor compaction tests were reported for most test pads. The maximum dry unit weights are plotted as a function of optimum water content in Fig. 4-14. The standard Proctor optimum water content averaged 4.0 percentage points higher than the modified Proctor optimum, and the maximum dry unit weight averaged 1.7 kN/m^3 more for modified Proctor.

Construction specifications for CCLs typically require that the water content fall within a specified range and that the percent compaction (defined as the dry unit weight divided by the maximum dry unit weight from a specified compaction test, times 100%) equal or exceed a specified minimum value. The concept is illustrated in Fig. 4-15. However, the recommended procedure (e.g., Daniel and Koerner, 1995) involves testing the soil to determine the appropriate range of water content and dry unit weight to achieve the desired hydraulic conductivity (Fig. 4-16). However, when the data are plotted as recommended in Fig. 4-16C, no single acceptable zone of water content-density is observed (Fig. 4-17). It appears that each material should be evaluated on its own merits.

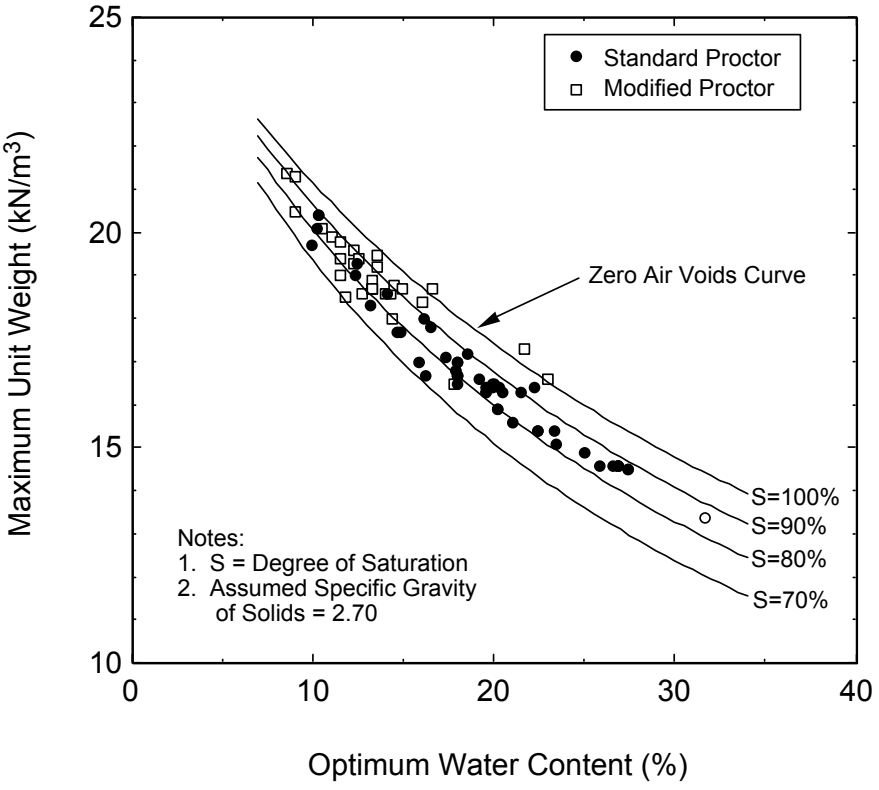

Figure 4-14. Results of laboratory compaction tests.

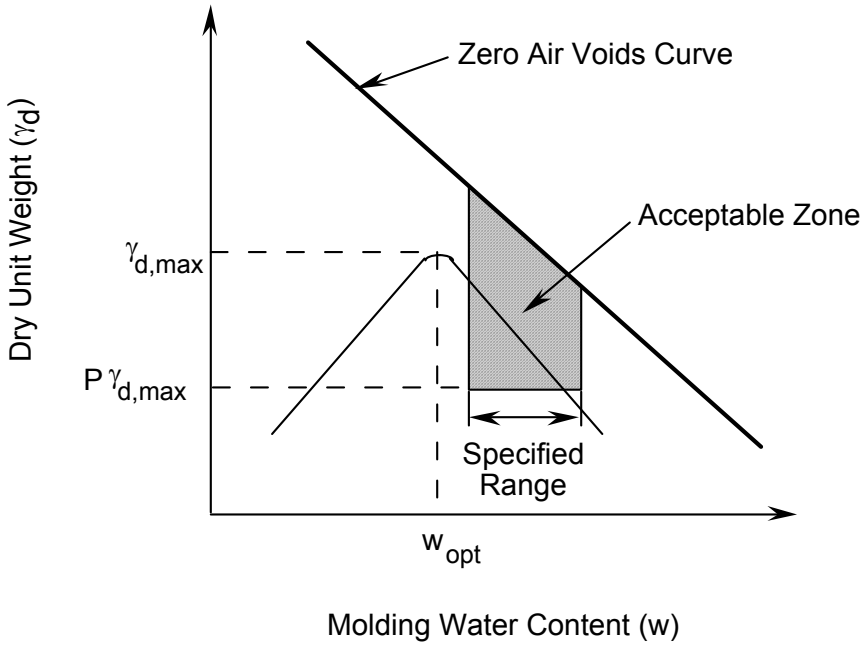

Figure 4-15. Typical water content-density specification relying on water content and percent compaction (P).

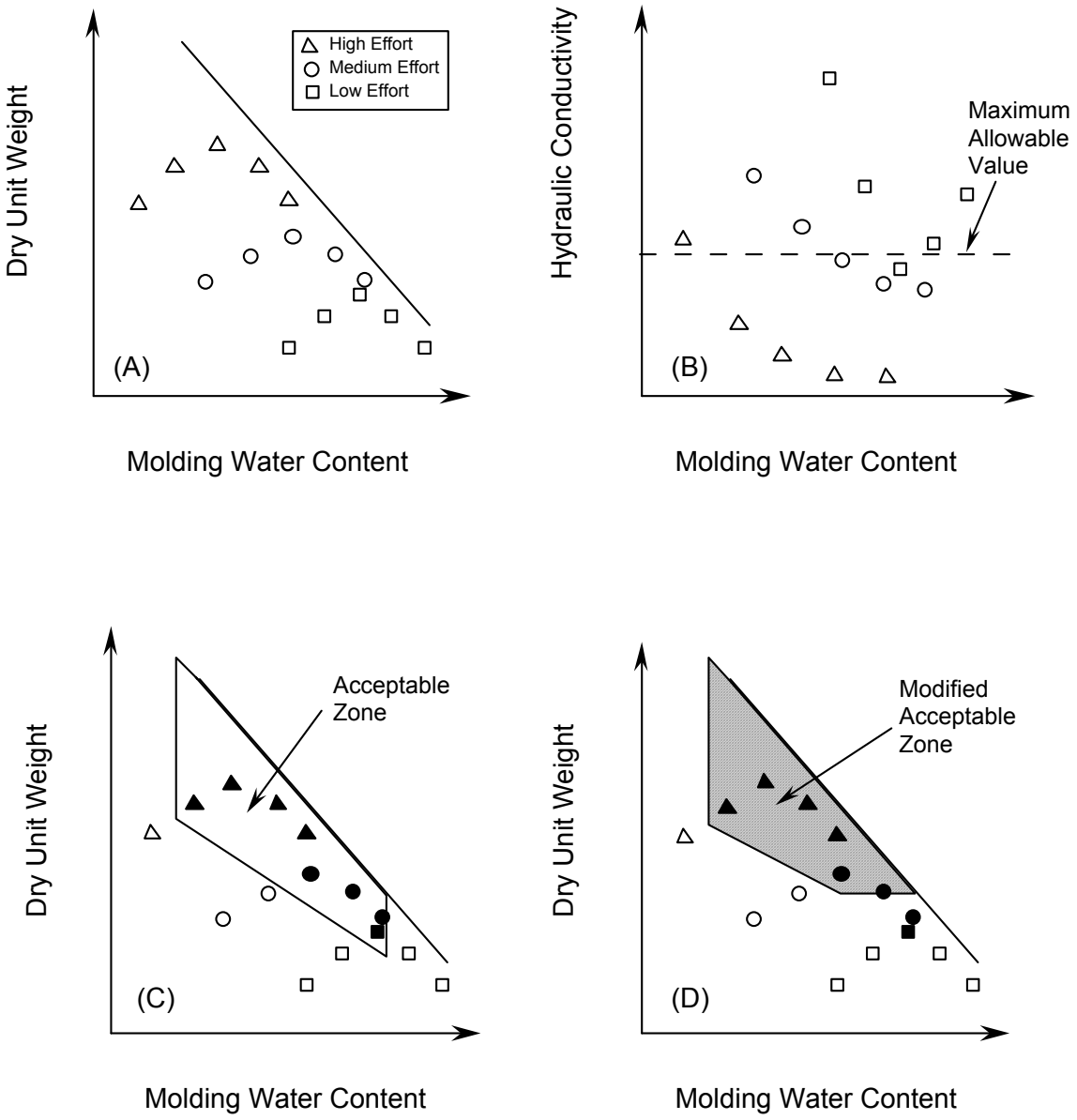

Figure 4-16. Recommended procedure for determining acceptable compaction zone for low hydraulic conductivity: (A) compact soil over range of compactive energy; (B) permeate compacted specimens; (C) determine acceptable water content-density zone; and (D) modify acceptable zone to account for other factors such as shear strength.

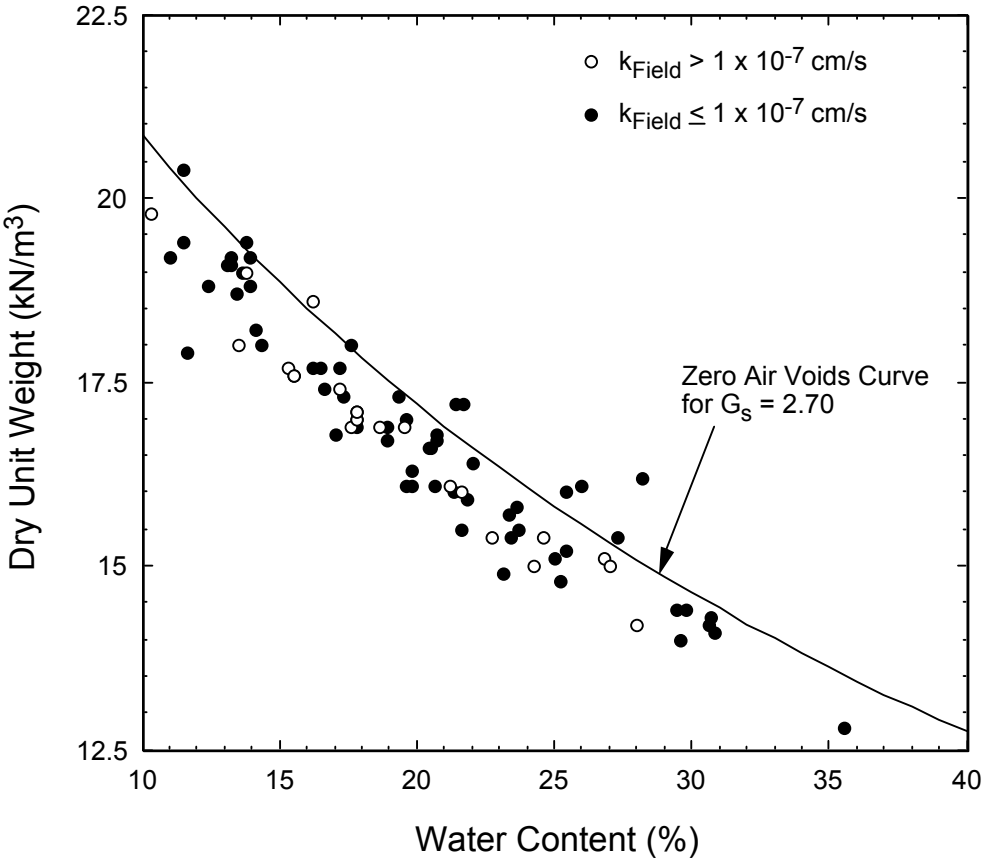

Figure 4-17. Dry unit weight vs. water content for CCLs with hydraulic conductivity's that did or did not meet the hydraulic conductivity objective of 1 x 10^{-7} cm/s.

Hydraulic conductivity was found to be a function of the amount by which the water content of the soil exceeds optimum. Engineers have known for decades that clays must be compacted wet of optimum in the laboratory to achieve low k. Figure 4-18 quantifies the trend for decreasing k_{Field} with increasing amount wet of optimum. Even more significant is the relationship between how wet the soil is at the time of compaction and the probability of achieving $k \leq 1 \times 10^{-7}$ cm/s. This relationship, shown in Fig. 4-19, shows a very low probability (≈40%) of success when the soil is compacted dry or at optimum, increasing to a 100% probability of success for soils compacted 6 to 8 percentage points wet of optimum. It should be noted that many soils cannot be compacted so wet of optimum with heavy field equipment, and that for soils compacted substantially wet of optimum the low shear strength of the soil should be considered. Indeed, achieving a sufficiently wet soil to achieve low k, but not too wet (to preserve shear strength), is an essential trade-off in clay liner design.

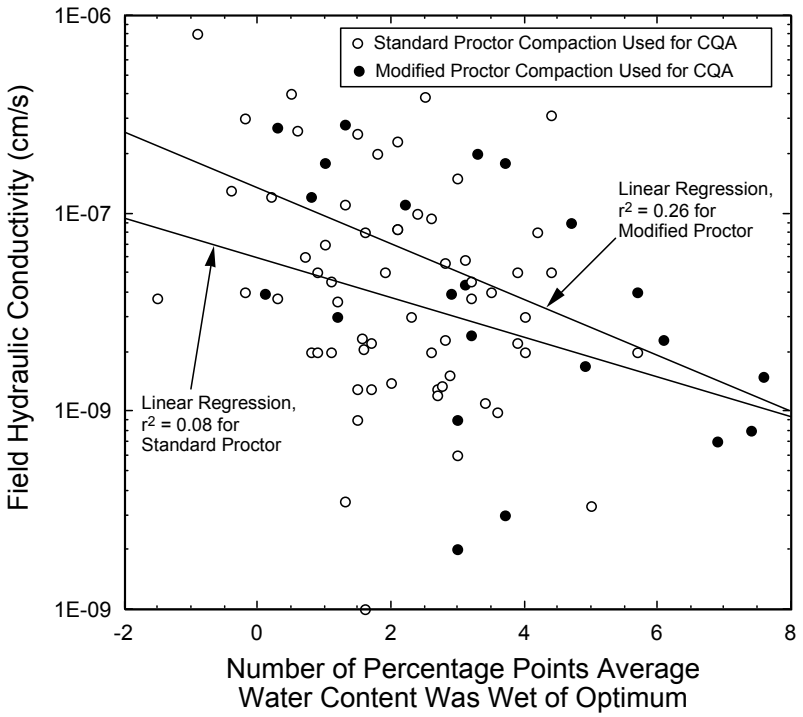

Figure 4-18. Field hydraulic conductivity vs. number of percentage points above the optimum water content.

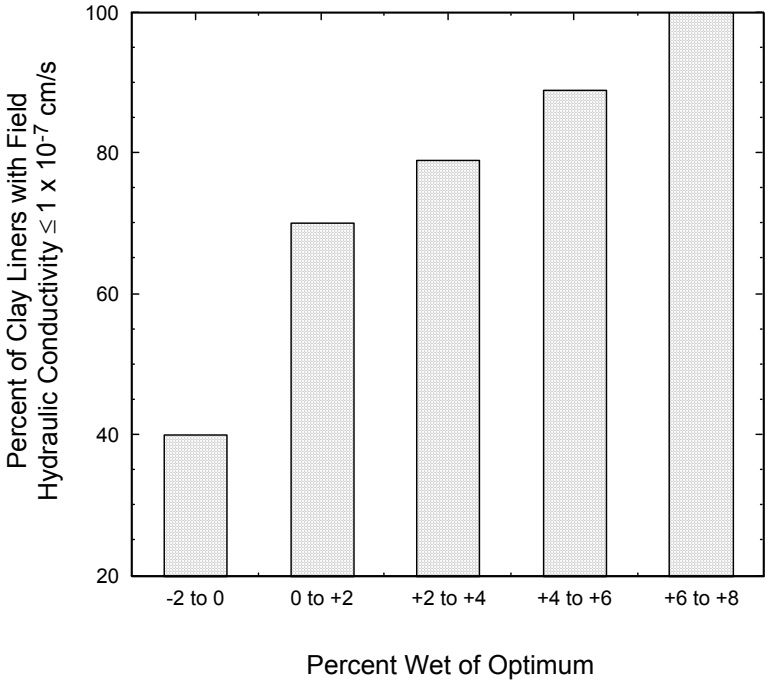

Figure 4-19. Percent of CCLs with field hydraulic conductivity ≤1 x 10^{-7} cm/s as a function of the percent wet of optimum water content.

Percent compaction is a critical field construction control parameter for structural fills. The percent compaction is often specified in clay liner construction, as well (e.g., Table 4-1). As shown in Fig. 4-20, there was no significant correlation between k_{Field} and percent compaction. The data actually show a counter-intuitive trend of increasing k_{Field} with increasing percent compaction. This trend is probably just a reflection of the high degree of scatter ($r^2 = 0.03$) and is not a real trend. Compaction is important (it reduces the porosity of the soil and kneads the soil into a homogeneous mass), but percent compaction is a poor indicator of k_{Field} for CCLs.

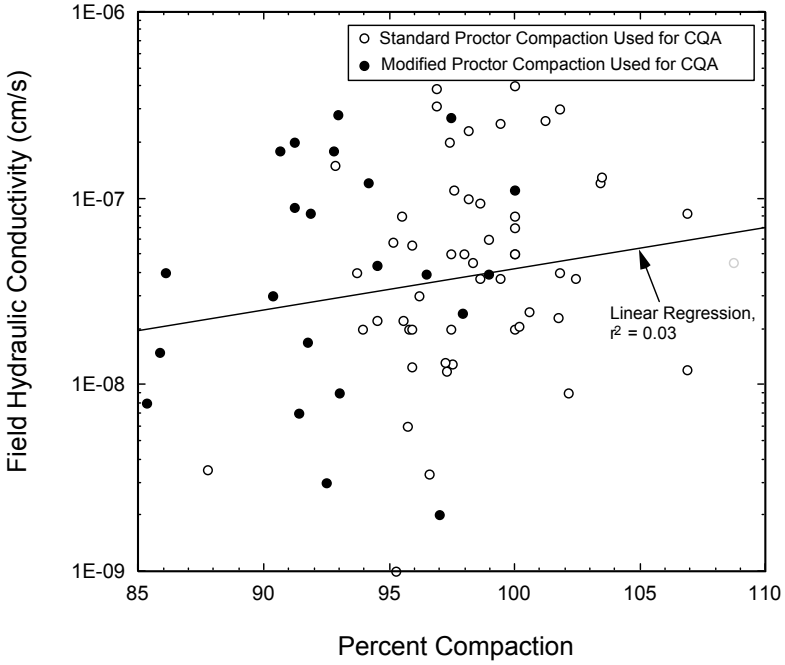

Figure 4-20. Field hydraulic conductivity vs. percent compaction.

Some engineers prefer to use degree of saturation as the specification requirement rather than water content and dry density (e.g., Benson and Boutwell, 1992). There is a tendency for k_{Field} to decrease with increasing degree of saturation (Fig. 4-21), but the trend is not as strong as that shown in Fig. 4-18 for water content relative to optimum. Values of degrees of saturation greater than 100% are the result of normal variability in water content and density measurements, and (probably more significantly) uncertainties in the specific gravity of the soil solids, which was assumed to be 2.7 but which probably varied from soil to soil within the normal range of 2.65 to 2.8. The relationship between the probability of achieving $k_{Field} \leq 1 \times 10^{-7}$ cm/s and the average degree of saturation immediately after compaction is shown in Fig. 4-22. While there is a trend, it is not an especially strong one.

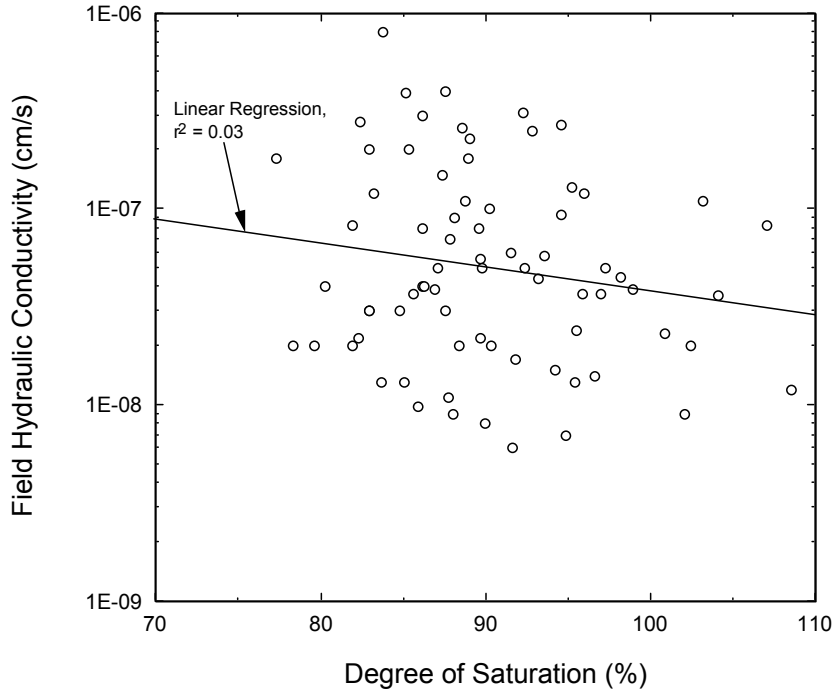

Figure 4-21. Field hydraulic conductivity vs. degree of saturation at the time of compaction of a CCL.

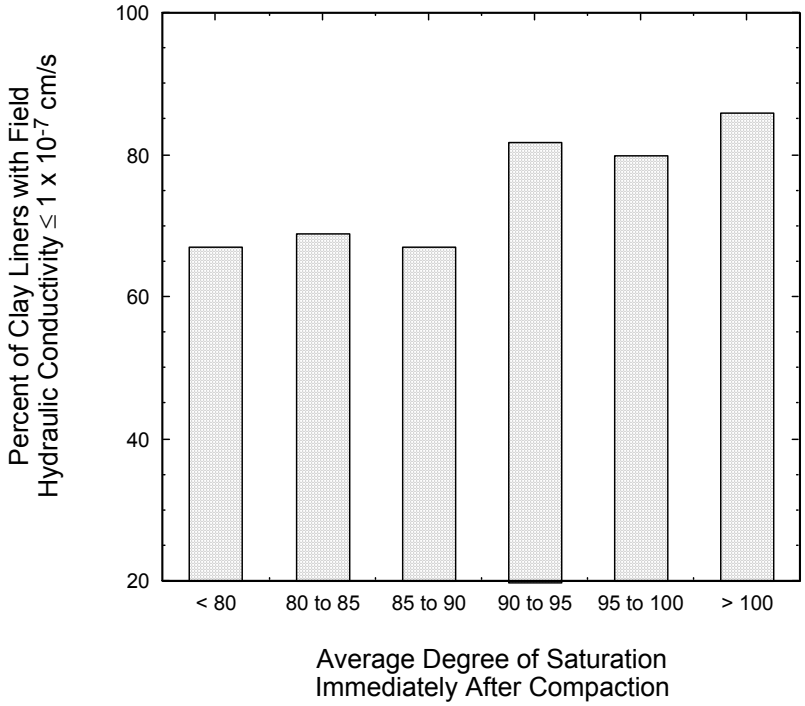

Figure 4-22. Percent of CCLs with field hydraulic conductivity ≤1 x 10^{-7} cm/s as a function of the degree of saturation at the time of compaction.

One reason why the correlation in Fig. 4-21 is not stronger is that the average degree of saturation fails to capture the degree of scatter in the compaction data. Benson and Boutwell (1992) found that an important factor in CCL performance is the percent of water content-dry density (w-γ_d) points (determined from the CQA program) that lie on or above the line of optimums. This percentage is termed "P_o." The "line of optimums" is a line (the "line" is actually slightly curved in most cases) connecting the peaks of compaction curves developed using a range of compactive energy. The concept is illustrated in Fig. 4-23. The value of P_o is calculated as illustrated in Fig. 4-24. Hydraulic conductivity should decrease as the percentage of the measured (w-γ_d) points that line on or above the line of optimums increases. Indeed, a very strong correlation between hydraulic conductivity and P_o was observed, as shown in Fig. 4-25. Of all the variables that were examined, P_o is the single best indicator of the probability of achieving $k_{Field} \leq 1 \times 10^{-7}$ cm/s. The obvious implication is that specification writers should consider requiring a minimum P_o. A suggested minimum P_o is 70% to 80%, but the engineer should recognize that as P_o increases, shear strength (including interface shear strength with geosynthetics) often decreases. Thus, it is critical that the P_o not be arbitrarily raised without careful consideration given to the effects of reduced internal shear strength of the CCL or interface strength with adjacent components. Of the liners that failed to achieve $k_{Field} \leq 1 \times 10^{-7}$ cm/s, half were specified using standard Proctor compaction (ASTM D698) as the reference, and half were specified using modified Proctor compaction (ASTM D1557) as the reference. Thus, there was no relationship between the tendency of a liner to achieve the desired low hydraulic conductivity and the method of specification. Instead, the key factor appears to be the percentage of (w, γ_d) points that lie on or above the line of optimums, i.e., P_o.

4.1.6 Construction Parameters

The construction parameters that were evaluated were the thickness of lifts, mass of the compactor, and number of passes of the compactor. The relationship between k_{Field} and thickness of individual lifts is shown in Fig. 4-26. Although there is a trend for increasing k_{Field} with increasing lift thickness, the scatter is so large ($r^2 = 0.02$) that the trend cannot be viewed as statistically significant. Further, the vast majority of lifts had a nominal compacted thickness of 150 mm, and there are relatively few data points for other lift thicknesses. Nevertheless, for a given mass of compactor and number of passes of the compactor over the soil, the compactive energy per unit volume of compacted soil decreases as the thickness of the lift increases. Thus, it is to be expected that hydraulic conductivity would tend to increase with increasing lift thickness. However, the data do not suggest any particular minimum lift thickness. Other factors (rather than lift thickness) appear to be dominant in terms of determining the field hydraulic conductivity.

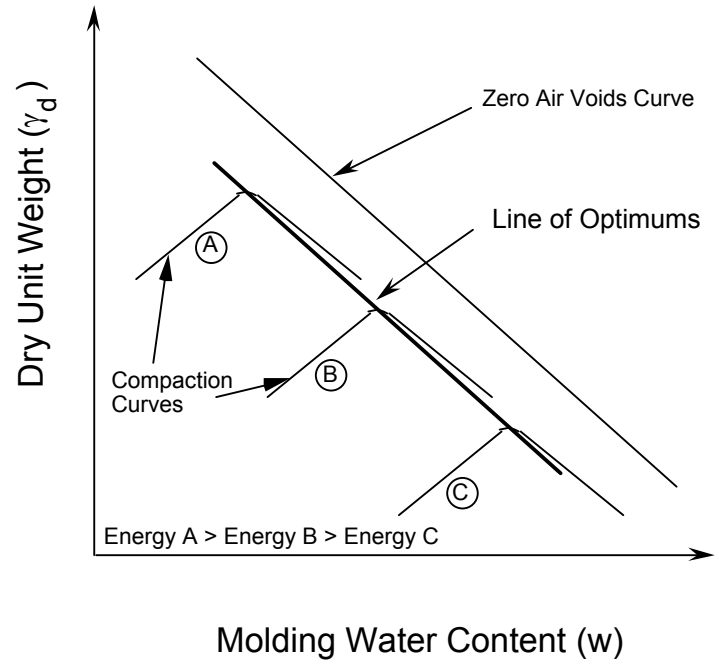

Figure 4-23. Determination of the line of optimums.

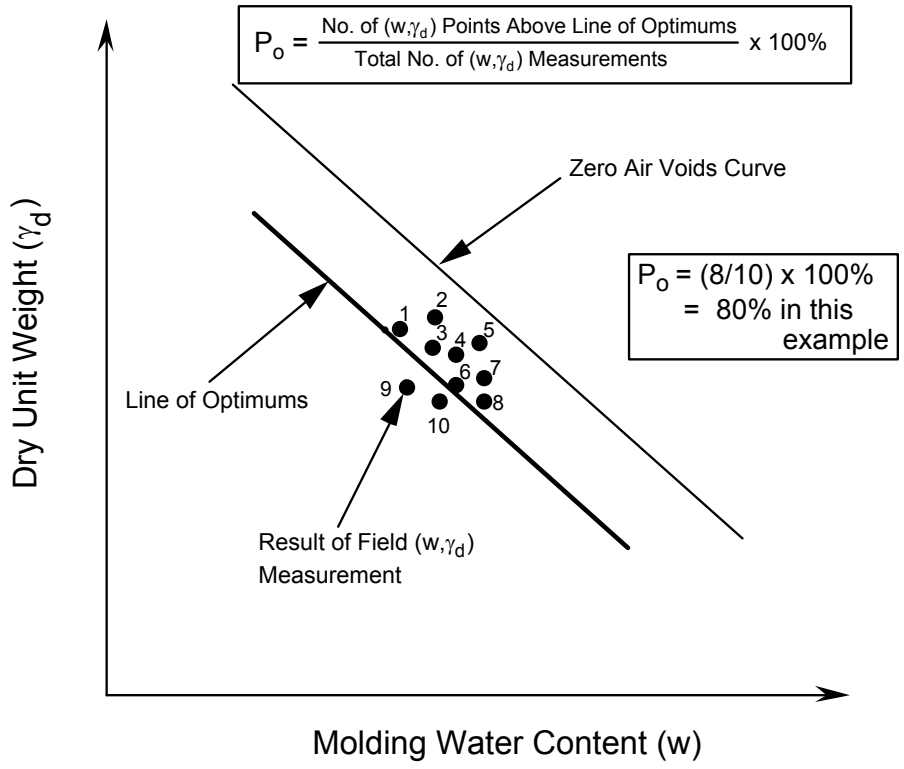

Figure 4-24. Definition of percent of points wet of optimums (P_o).

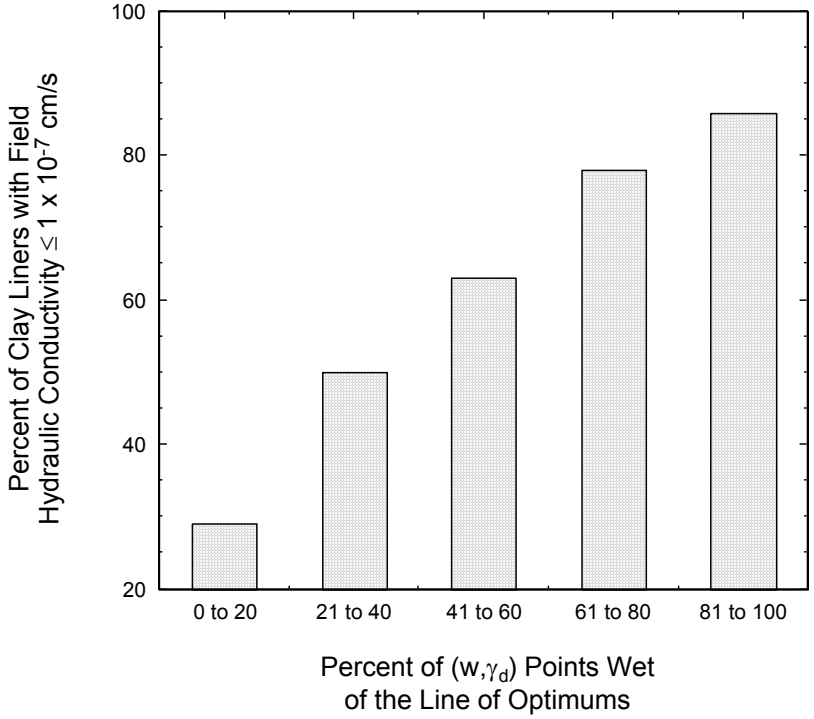

Figure 4-25. Percent of CCLs with field hydraulic conductivity ≤1 x 10^{-7} cm/s as a function of the percent of water content-density points measured during field construction quality assurance that lie on or above the line of optimums.

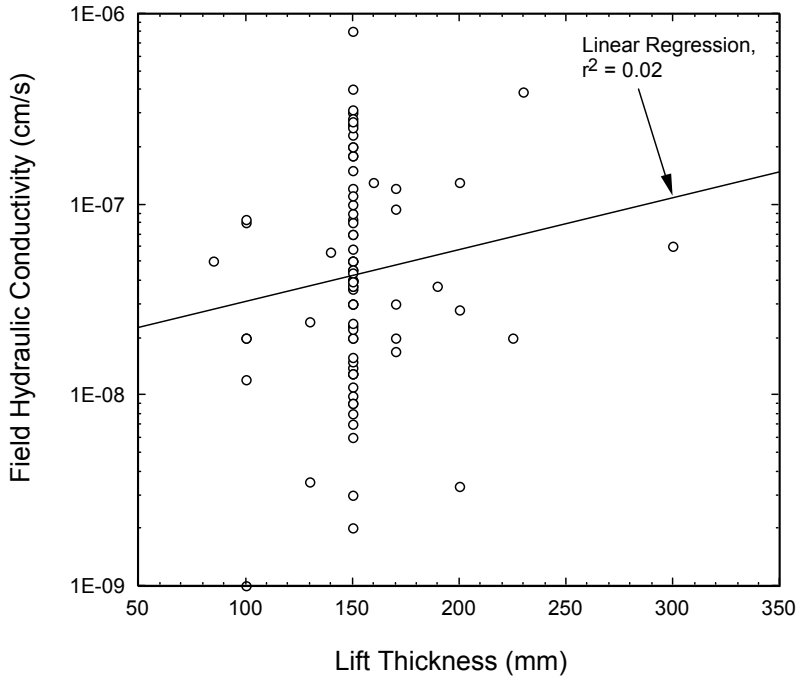

Figure 4-26. Field hydraulic conductivity versus thickness of lifts.

The relationship between k_{Field} and mass of compactor is shown in Fig. 4-27. Linear regression showed that the data are very scattered ($r^2 = 0.00$), and that the regression line is nearly horizontal. Thus, there is no relationship between mass of compactor and k_{Field}. This observation comes as a surprise because laboratory tests have consistently shown that the energy of compaction of the soil is a very significant variable, with a strong trend of decreasing hydraulic conductivity with increasing compactive energy (e.g., as discussed in Daniel and Koerner, 1995). However, the compactive energy is a function of the mass of the compactor, the number of passes, and thickness of lifts. The relationship between number of passes of the compactor per lift and the mass of the compactor for the CCLs in the database is shown in Fig. 4-28. One would expect that perhaps the heavier the compactor, the fewer the number of passes of the compactor on the assumption that fewer passes would be required to achieve the required dry density for a heavier compactor. However, Fig. 4-28 shows large scatter and practically no trend -- the data do not suggest that heavier compactors are typically associated with fewer passes of the compactor over a given lift of soil.

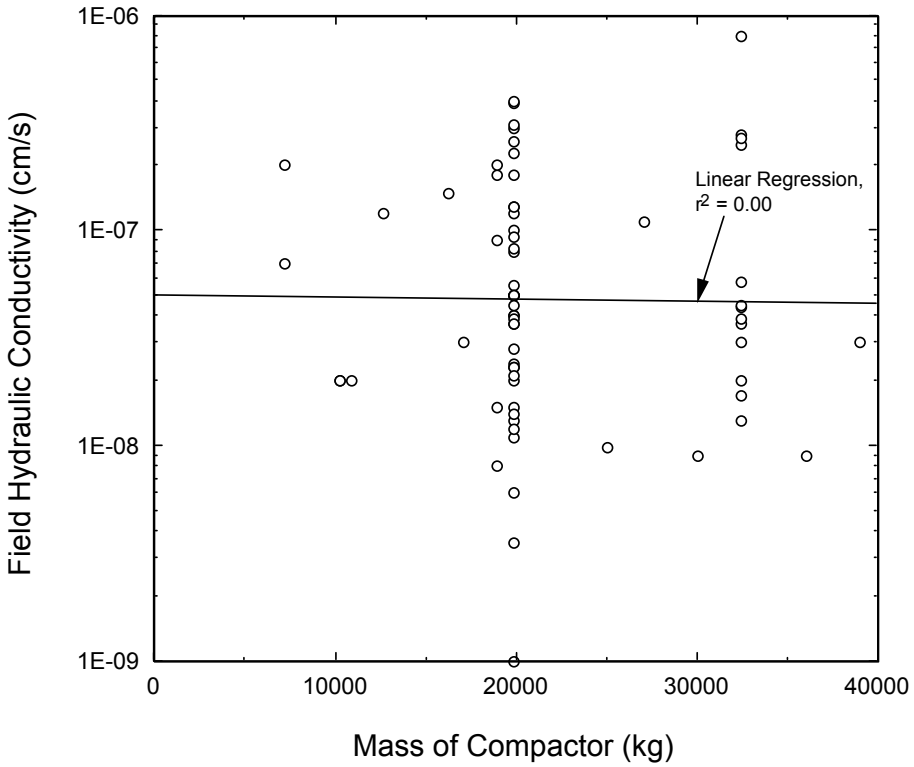

Figure 4-27. Field hydraulic conductivity versus mass of compactor.

The relationship between k_{Field} and number of passes of the compactor per lift is shown in Fig. 4-29. The expected trend is decreasing hydraulic conductivity with increasing number of passes, but the data do not support this expectation. The data are very scattered, and there are very few data points for more than 20 passes of the compactor

per lift. As discussed in 4.1.5, the data do indicate that percentage of (w, γ_d) points lying on or above the line of optimums (P_o) is a critical parameter. The relationship between P_o and mass of compactor and number of passes of the compactor is shown in Figs. 4-30 and 4-31, respectively. There is a trend for increasing P_o with increasing mass of the compactor (Fig. 4-30), but the scatter is large. Similarly, the relationship between P_o and number of passes of the compactor is weak (Fig. 4-31). The trend line in Fig. 4-31 is significantly influenced by a single point at a very large number of passes (80) for Site 65. Despite the very large number of passes, P_o was zero, probably as a result of the low water content of the soil. Compactor mass and number of passes alone do not capture all of the critical factors that influence P_o.

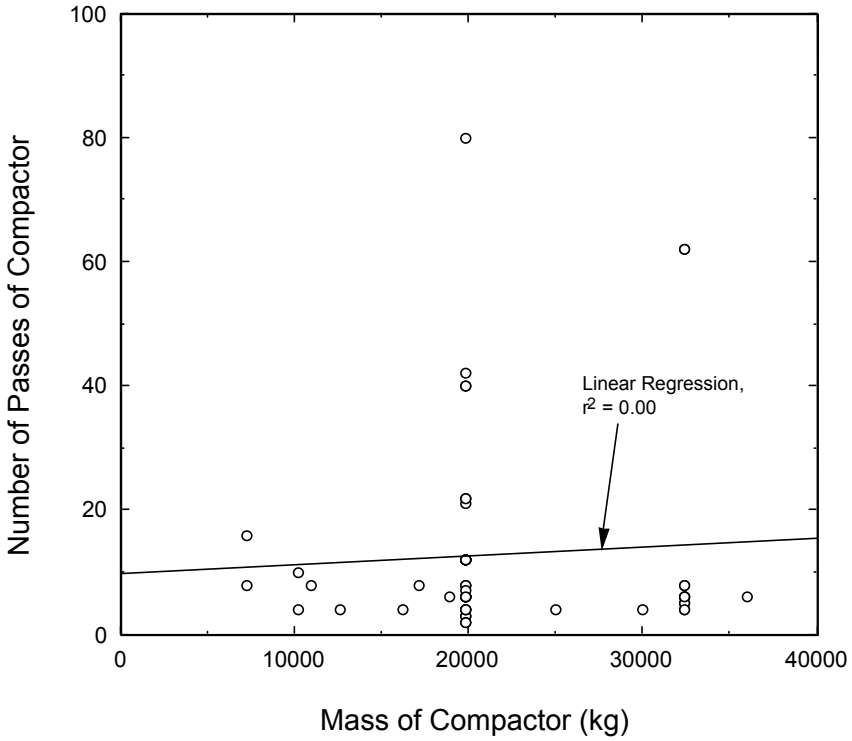

Figure 4-28. Number of passes of compactor per lift of soil versus mass of compactor.

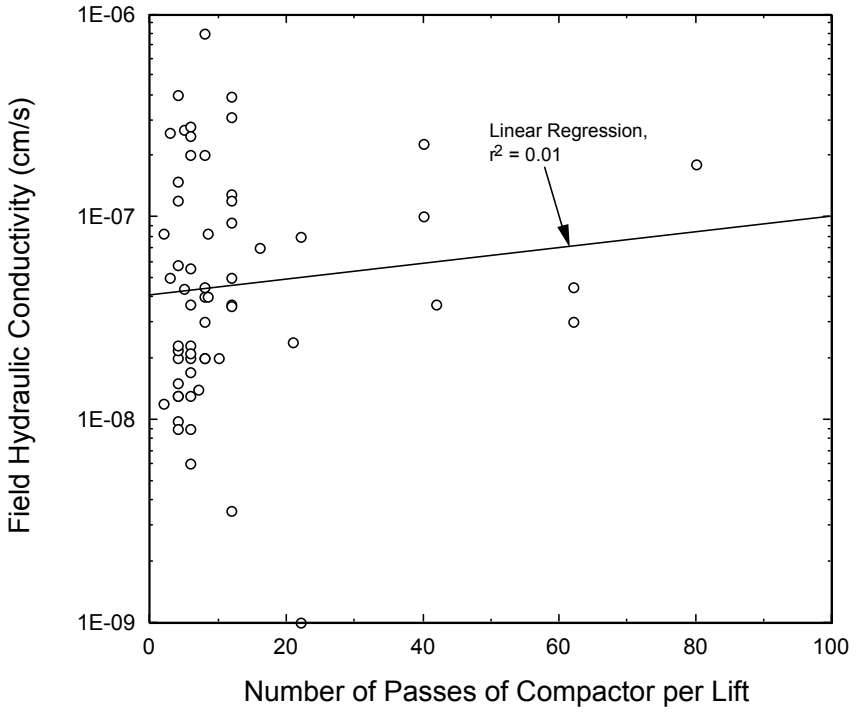

Figure 4-29. Field hydraulic conductivity versus number of passes of compactor per lift of compacted soil.

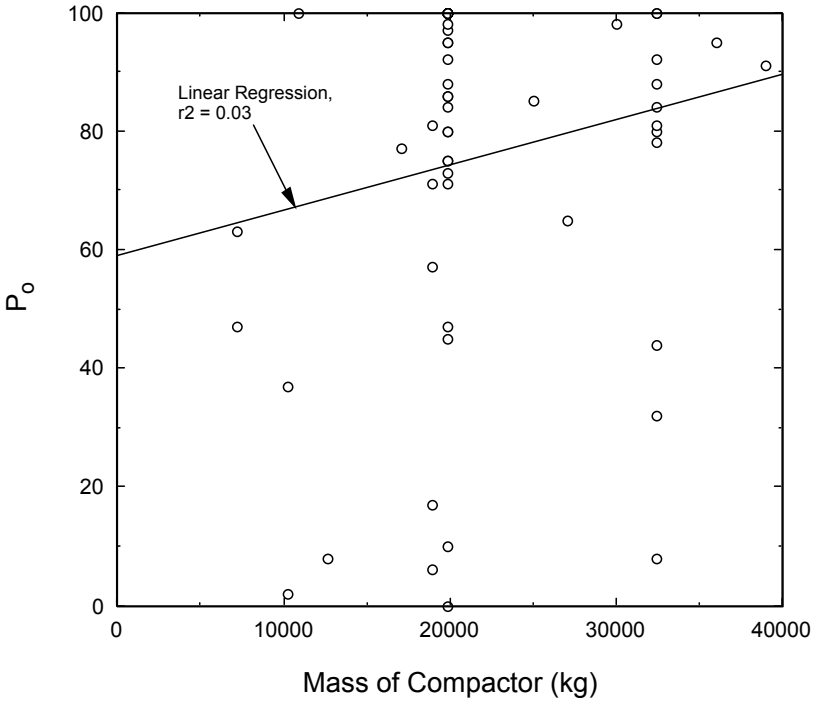

Figure 4-30. Percent of (w, γ_d) points lying on or above the line of optimums (P_o) versus mass of compactor.

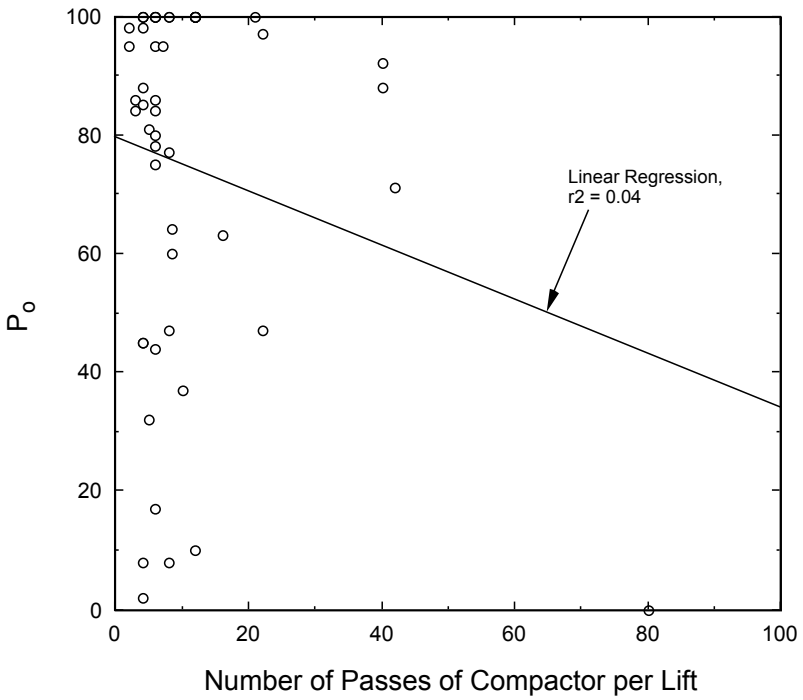

Figure 4-31. Percent of (w, γ_d) points lying on or above the line of optimums (P_o) versus number of passes of compactor per lift.

4.1.7 Thickness of Liner

The relationship between k_{Field} and the thickness of the clay liner is shown in Fig. 4-32. Although the scatter is large (r^2=0.13), there appears to be a trend for decreasing hydraulic conductivity with increasing thickness. As shown in Fig. 4-33, there is a relationship between the probability that the k_{Field} will be $\leq 1 \times 10^{-7}$ cm/s and the thickness of the liner. It appears from the data that liners with a thickness of 1 m or more have a significantly better chance of attaining a $k_{Field} \leq 1 \times 10^{-7}$ cm/s.

There are 21 CCLs in the database with thicknesses > 1 m. These 21 sites are not uniformly distributed in terms of geography or data type. The thickest liners in the U.S. tend to be constructed in Wisconsin, whose state regulations require CCLs with thicknesses of typically $\geq$ 1.2 m. Clays in Wisconsin tend to be very wet. Also, of the 89 CCLs in the database, k_{Field} was obtained by lysimeters at 8 sites and by SDRIs at 81 sites. Of the 8 in-place liners where k_{Field} was obtained by lysimeter, 7 of these CCLs had thicknesses > 1 m.

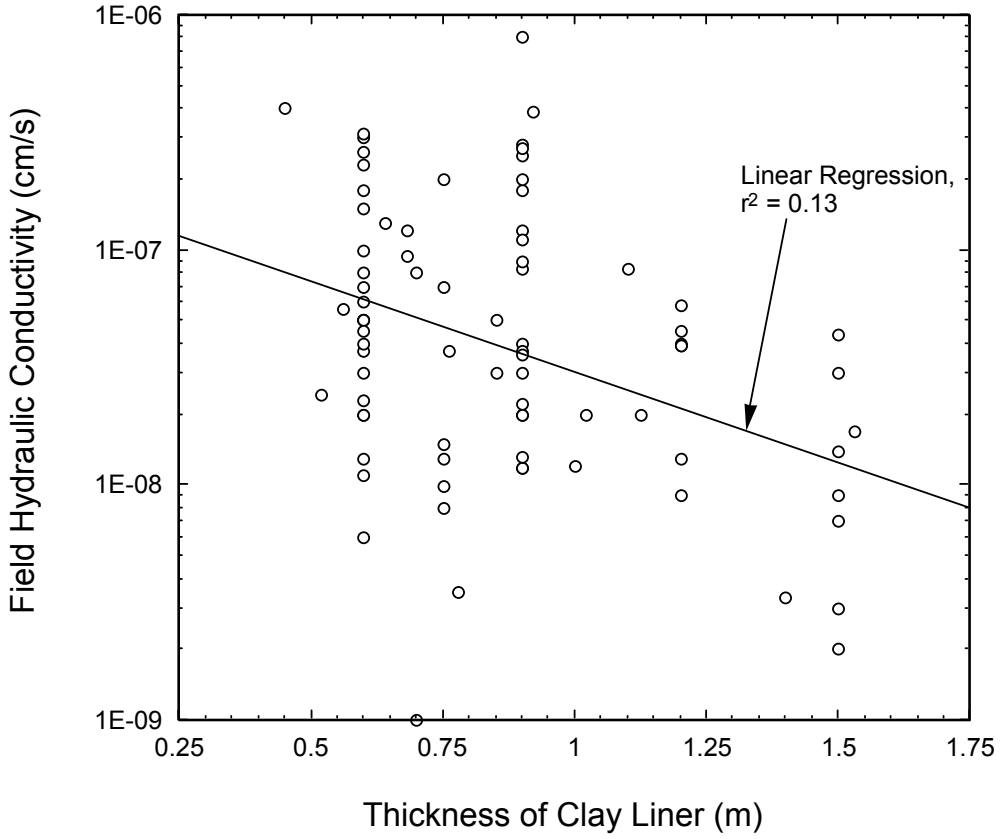

Figure 4-32. Field hydraulic conductivity versus thickness of clay liner.

Thus, the tendency seen in Fig. 4-33 for lower k_{Field} for liners with thicknesses > 1 m may simply reflect the fact that the thick liners were wetter than average or were subjected to greater effective overburden stress. Construction with a high percentage of data points on or above the line of optimums appears to be more important than thickness, at least for liners with thicknesses in the range of 0.6 to 1.5 m.

Benson and Daniel (1994) found that k_{Field} decreases with increasing thickness of the liner but that little benefit is gained by increasing the thickness beyond 0.6 to 0.9 m. In the U.S., the minimum thickness of CCLs is typically 0.6 to 0.9 m, although, as mentioned earlier, some states require thicker liners. The database does indicate a trend of decreasing k_{Field} with increasing thickness (Fig. 4-33), but for liners with thickness of 0.6 to 0.9 m or more, construction variables (especially P_o) appear to be more important than thickness. There may, however, be justification for increasing the thickness to 1 m or more for critical facilities or for situations in which added redundancy is desired.

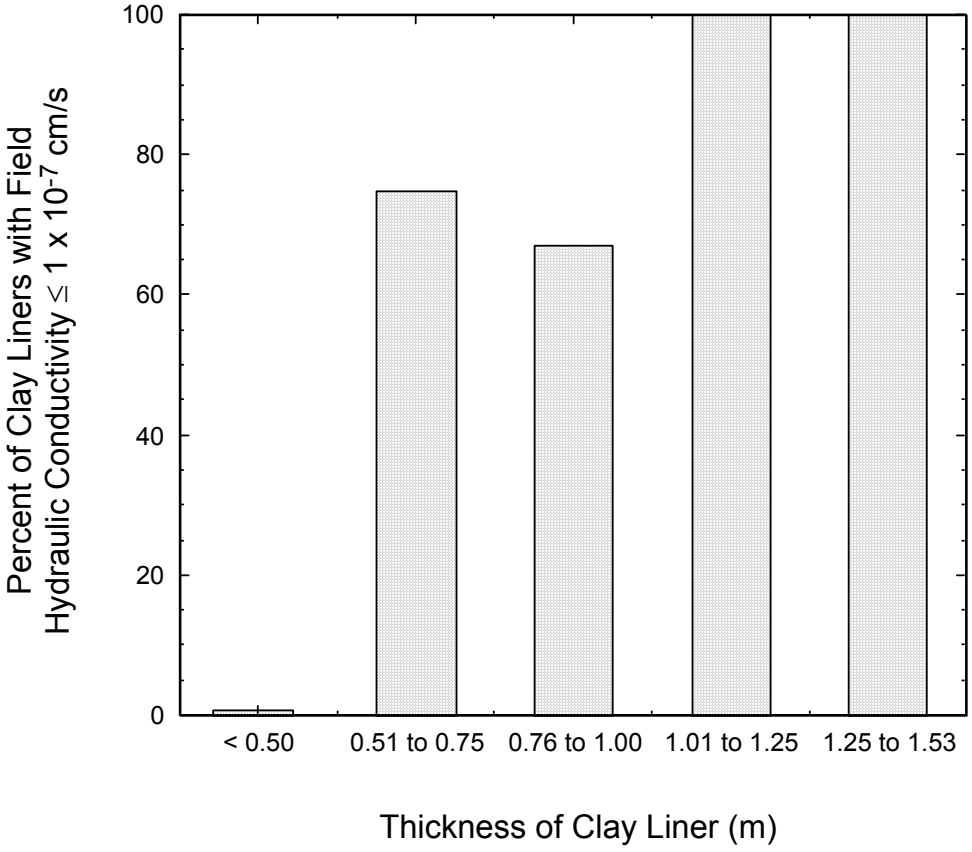

Figure 4-33. Percentage of clay liners with a hydraulic conductivity ≤ 1 x 10^{-7} cm/s versus thickness of the CCL.

4.1.8 Field Hydraulic Conductivity Testing Method

Information was collected on the hydraulic conductivity measured with the TSB test, which is experiencing expanded use for k_{Field} measurements on test pads because of the lower cost, faster testing time, and greater information on variability of k_{Field} provided by multiple TSB tests compared to a single SDRI test. As shown in Fig. 4-34, the k_{Field} from the TSB test correlates well with that of the SDRI test. However, for the four test pads in Fig. 4-34 for which the SDRI test indicated that the test pad failed to meet the k ≤ 1 x 10^{-7} cm/s criterion, the TSB test indicated that the test pads had met the hydraulic conductivity criterion, thus providing four false positives (passing hydraulic conductivity's when, based on SDRI tests, the hydraulic conductivity was not satisfactory). Also, in one case, the TSB test indicated that k_{Field} was > 1 x 10^{-7} cm/s, but the SDRI test indicated it was < 1 x 10^{-7} cm/s, thus providing a false negative. It should be emphasized that both the SDRI test and two-stage borehole test have limitations, and the natural range of scatter in hydraulic conductivity and the testing methods may account for much of the differences noted.

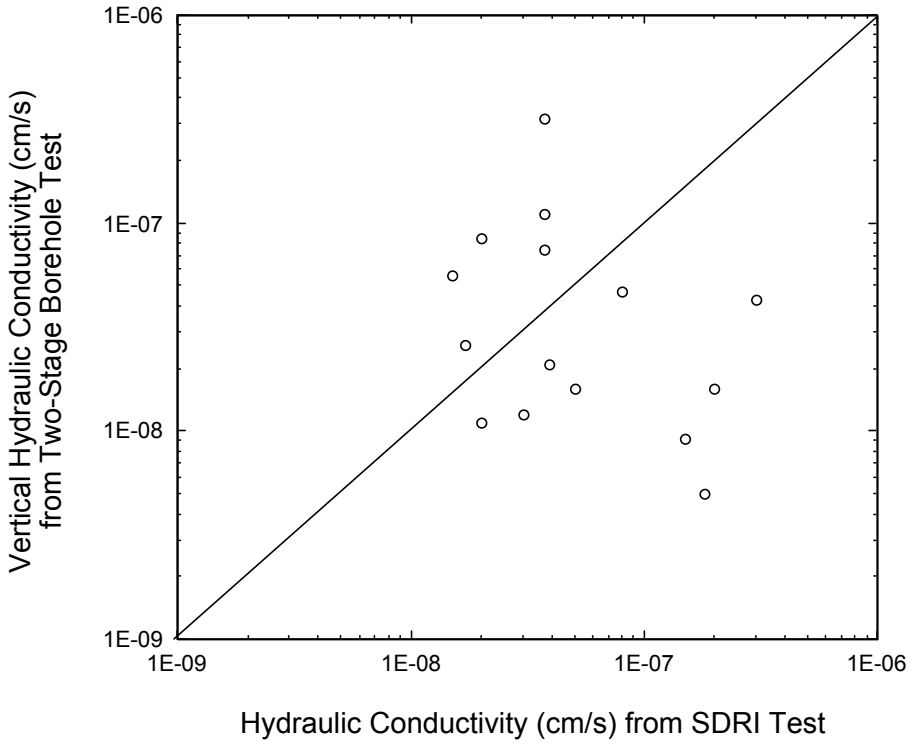

Figure 4-34. Vertical hydraulic conductivity from two-stage borehole test versus field hydraulic conductivity from the sealed double ring infiltrometer (SDRI) test.

Benson (e.g., Benson et al., 1994) has pioneered the investigation of the possibility of using large-scale k_{Lab} tests on 300-mm-diameter samples collected in the field as a substitute for k_{Field} tests. Figure 4-35 shows the relationship between k_{Lab} measured on 300-mm-diameter samples and k_{Field} measured with the SDRI test. For all but a few laboratory tests, the correlation between k_{Lab} and k_{Field} is excellent. Of the 8 test pads for which the SDRI indicated a failing k_{Field}, the laboratory tests also indicated failing hydraulic conductivity (i.e., $k > 1 \times 10^{-7}$ cm/s) in 7 of the 8 test pads. Thus, the database supports the use of laboratory tests on 300-mm-diameter samples from the field as an alternative to SDRI tests.

4.1.9 Case Histories

This section focuses on an analysis of test pads that failed to achieve a hydraulic conductivity of 1×10^{-7} cm/s or less. The reasons why the test pads failed to meet design objectives are identified and compared.

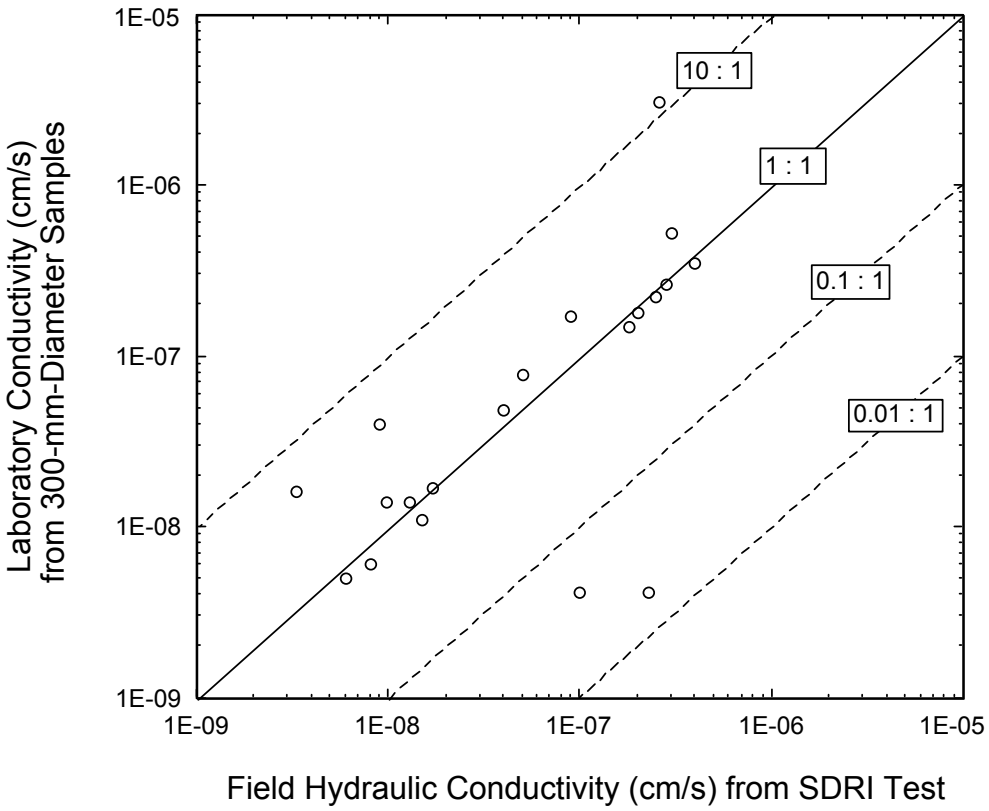

Figure 4-35. Laboratory-measured hydraulic conductivity on 300-mm-diameter samples versus field hydraulic conductivity from the sealed double ring infiltrometer (SDRI) test.

4.1.9.1 Test Pads at Sites 26 and 27

These test pads were constructed for the purpose of verifying that the hydraulic conductivity of two compacted glacial tills would be $\leq 1 \times 10^{-7}$ cm/s. The specifications for both test pads were the same: (1) compact wet-of-optimum, as determined by modified Proctor, and (2) compact to a minimum dry density equal to 90% of the maximum dry density based on modified Proctor.

For test pad 26, 75% of field water content and 100% of dry density measurements were met the specifications. However, only 17% of the field water content and dry density measurements fell on or above the line of optimums, i.e. P_o = 17%. Thus, the low P_o value indicates that a large portion of the test pad was compacted dry of the line of optimums despite the fact that most of the water content-density data met the project specifications.

The test pad at Site 27 had a similar problem. At Site 27, 100% of the field data met the density criterion and 90% of the field data met the water content criterion. The P_o value was only 6%, however. Compaction below the line of optimums was the problem at both of these sites.

Analysis of the case histories in the database shows that compaction dry-of-optimum is the most common cause for field hydraulic conductivity values > 1 x 10^{-7} cm/s. The fundamental flaw of many compaction criteria is that they allow compaction to occur dry of the line of optimums. However, the recommended procedure, as described by Daniel and Benson (1990) and as illustrated in Fig. 4-16, will prevent the development of a specification that allows excessive compaction dry of the line of optimums.

4.1.9.2 Test Pad at Site 21

The SDRI test performed at this site achieved a k_{Field} of 2.5 x 10^{-7} cm/s, whereas the k_{Lab} was 3.0 x 10^{-7} cm/s. The soil was a western loess that contained 90% fines and 36% clay. The compaction criteria for the test pad were as follows: the as-compacted water content must be wet of standard Proctor optimum and the dry density must be greater than 95% of the standard Proctor maximum. The field water content and dry density measurements indicate that P_o at this site was 80%.

Laboratory compaction curves for a reduced Proctor sample indicate a four-order-of-magnitude decrease in hydraulic conductivity between water contents of 15% and 21%. The reduced Proctor compaction test uses the same equipment as the standard Proctor compaction test but only fifteen blows from the hammer are applied to each lift. The reduced Proctor test was not performed until after the SDRI test failed to assist with identification of the causes for the high SDRI result.

Maximum reduced Proctor density was approximately 16.5 kN/m^3 and maximum standard Proctor density was 17.2 kN/m^3. The density specification allowed compaction to occur within the reduced Proctor density range (i.e. 95% of 17.2 = 16.3 kN/m^3). Field density measurements indicate that although all of the field-measured dry density values met the density specification, approximately 40% of the dry density values were less than or equal to the maximum density from reduced Proctor tests. Therefore, an inadequate density specification was the major reason this site had a k_{Field} greater than 1 x 10^{-7} cm/s.

From the investigation of this test pad, the usefulness of the reduced Proctor compaction test is evident. It is especially important to use the reduced Proctor test as a lower bound when standard Proctor density is a compaction criterion. In this case, a density lower than standard Proctor was allowed, but the hydraulic conductivity of the soil was never determined at that density. The soil at this site was very sensitive to changes in compactive energy. If the soil had been tested at a density below standard Proctor, the compaction criteria most likely would have been changed.

Another problem with this test pad, not evident in the database information, is the lower boundary condition. The SDRI test requires a known lower boundary condition in order to calculate k_{Field} accurately if the wetting front from the infiltrating water penetrates to the bottom of the test pad. Sometimes a sand drainage layer is placed beneath the compacted clay test pad to provide free drainage at the lower boundary of the test pad. At this site, no sand drainage layer was installed and the subbase material had a hydraulic conductivity of approximately 1×10^{-9} cm/s. As a result, after thirty days of testing, the hydraulic conductivity was 2.5×10^{-7} cm/s, until it abruptly decreased to 1×10^{-9} cm/s a short period later. It is believed that after thirty days the wetting front reached the subbase, and then the hydraulic conductivity was misinterpreted as 1×10^{-9} cm/s. Therefore, the drainage layer can provide a critical boundary condition for the SDRI test.

4.1.9.3 Test Pads at Sites 55-63

Nine test pads were constructed at one site using four different clays and various water contents. Three of the four soils were suitable for use as a liner with field hydraulic conductivity $\leq 1 \times 10^{-7}$ cm/s. For these sites, the test pads consistently showed that whether or not the soil met the hydraulic conductivity criterion of 1×10^{-7} cm/s or less was dependent almost entirely upon the water content of the soil. When the soil was compacted near optimum water content, the soil failed to meet the hydraulic conductivity criterion. When the soil was typically 2 to 4% wet of optimum, the objective was met.

One of the soils in this series of field tests, however, was simply unsuitable. The soil was compacted 2% to 6% wet of optimum at Sites 61 and 62, and despite the high water content the soil still failed to achieve a hydraulic conductivity $\leq 1 \times 10^{-7}$ cm/s. All of the soils were kaolin clays obtained from commercial clay pits. The clay that was not suitable was from a different geologic formation than the other kaolin clays that were suitable.

One lesson learned from these tests is that, in retrospect, a comprehensive program of laboratory hydraulic conductivity testing prior to field testing would have been desirable for two reasons: (1) to define the appropriate range of water content for field compaction, and (2) to verify that the soil was suitable. The soil at Sites 61 and 62 probably would have been found to be unsuitable had it first been tested in the laboratory.

4.1.9.4 Test Pads at Sites 64 and 65

Sites 64 and 65 provide an excellent example of the futility of conventional compaction specifications. Test pads were constructed of the same material but with a minimum dry unit weight of 95% of standard Proctor (Site 64) or 91% of modified Proctor (Site 65). Both test pads were compacted several percentage points wet of optimum.

Neither achieved the desired k_{Field} of 1 x 10^{-7} cm/s. Site 65 is particularly interesting because it was compacted 3.7% wet of optimum to a density greater than 91% of the maximum from modified Proctor using an astonishing 80 passes per lift of a heavy, footed compactor. Despite all this, the liner failed to achieve the desired k_{Field} apparently because not a single (w, γ_d) point was on or above the line of optimums.

4.1.9.5 Test Pads at Sites 43 and 44

Although there was no statistically significant correlation between field hydraulic conductivity and either weight of compactor or number of passes of the compactor, there were examples in which the number of passes of the compactor was the only variable between two test pads. For example, Sites 43 and 44 represent two test pads that were constructed from the same soil at essentially the same water content, and compacted with the same compactor. The only variable was number of passes of the compactor: 16 passes for Site 43 and 8 passes for Site 44. The k_{Field} for Sites 43 and 44 were 7 x 10^{-8} and 2 x 10^{-7} cm/s, respectively, illustrating that increasing the compactive effort can have a significant impact on field hydraulic conductivity. The soil compacted with 16 passes of the compactor achieved 63% of the (w, γ_d) points on or above the line of optimums, whereas P_o was only 47% when 8 passes were used.

4.1.10 Practical Findings from Database

CCLs are almost always constructed with the objective of achieving a hydraulic conductivity of 1 x 10^{-7} cm/s or less. All of the 89 liners and test pads in this database were constructed for the purpose of demonstrating that the k_{Field} would meet this requirement. Despite all that has been written and learned about CCLs in the past 15 years, the hydraulic conductivity objective of $k_{Field} \leq 1 \times 10^{-7}$ cm/s was not met at more than one-fourth (26%) of the sites in the database. Why such poor success?

The soil was unsuitable at a few sites. It appears that in all cases involving unsuitable soils, test pads were built without the benefit of a comprehensive laboratory testing program prior to construction. No simple way of identifying unsuitable soils (based on plasticity information or other index properties) was identified. The database reinforces the recommendation that k_{Lab} tests be performed on representative samples of soil prior to construction, e.g., following the procedures recommended by Daniel and Benson (1990).

Perhaps the single biggest problem identified from the database is failure to recognize that conventional specification of water content and dry unit weight based on a minimum percent compaction often leads to difficulty. The problem is that this procedure does not guarantee that any of the (w, γ_d) points will lie on or above the line of optimums. Despite widespread publication of procedures that will avoid this problem (e.g., Daniel and Benson, 1990; Daniel and Koerner, 1995), many design professionals and specification writers continue to repeat the mistake. The type of specification that is not

generally recommended (but which is still commonly used) is shown in Fig. 4-36A; the more appropriate and recommended approach is shown in Fig. 4-36B.

A conclusion from analysis of the database is that P_o is the single most important CQA parameter. The definition of P_o is summarized in Fig. 4-24: P_o is the percent of water content-dry density (w, γ_d) points lying on or above the line of optimums. The line of optimums is the locus of peaks of compaction curves developed employing different compaction energies (Fig. 4-23). The key to success in achieving a $k_{Field} \leq 1 \times 10^{-7}$ cm/s is to ensure that a high percentage (the data indicate a minimum of 70% to 80%) of the field-measured (w, γ_d) points lie on or above the line of optimums, i.e., in the shaded zone shown in Fig. 4-36B. It should be emphasized that it is practical to compact soil in the shaded zone in Fig. 4-36B, particularly in the shaded area above the line of optimums but below the compaction curve (compaction in this zone could be achieved with a smaller compactive effort than used to develop the compaction curve indicated in the figure). The data in Fig. 4-25 provides confirmation that it is possible and practical to achieve a large value for P_o, i.e., to compact within the shaded zone shown in Fig. 4-36B.

Although this analysis has focused on hydraulic conductivity, the authors emphasize that other factors (such as bearing capacity, internal shear strength of a clay liner, and interfacial shear strength with geosynthetics) are equally important considerations. The engineer must give proper consideration to these factors and avoid the temptation to add too much water to the clay (in order to drive down hydraulic conductivity), at the expense of compromising other critical engineering properties of the clay liner. As the value of P_o is increased, the shear strength of the soil tends to decrease. The designer must ensure that all criteria, and not just hydraulic conductivity, are satisfied.

4.2 Soil-Bentonite Mixtures

Even though the most common type of CCL is one that is made from natural soils that contain a significant quantity of clay, if the soils found near the waste disposal facility are not sufficiently clayey to be suitable for direct use as a liner material, a common alternative is to blend natural soils available on or near a site with sodium bentonite. Soil-bentonite liners are discussed by Daniel and Koerner (1995).

4.2.1 Database

A database of 12 test pads that had bentonite added to the natural clay soils was developed. The database is summarized in Tables C-5 through C-8 in Appendix C. All test pads were constructed for the purpose of demonstrating that $k_{Field} \leq 1 \times 10^{-7}$ cm/s.

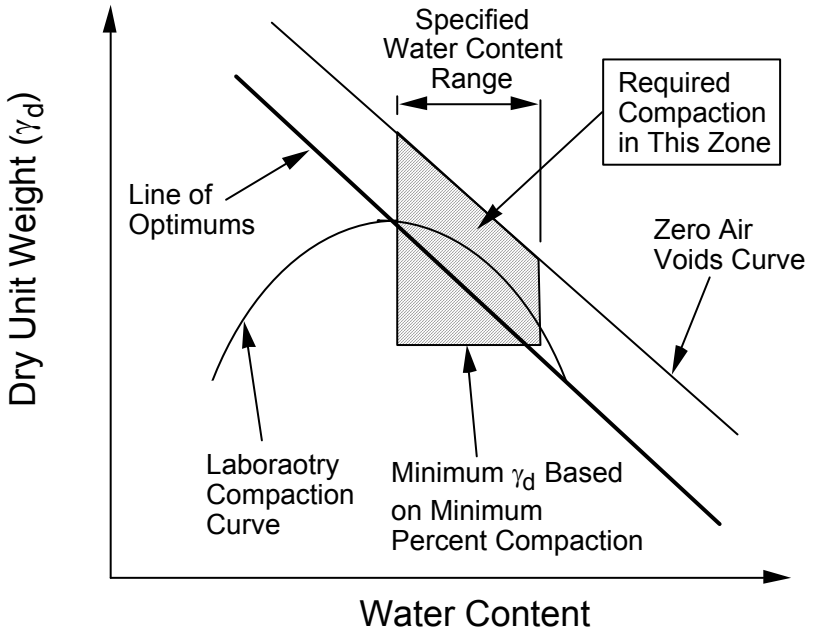

(A) Typical Type of Specification Currently Used

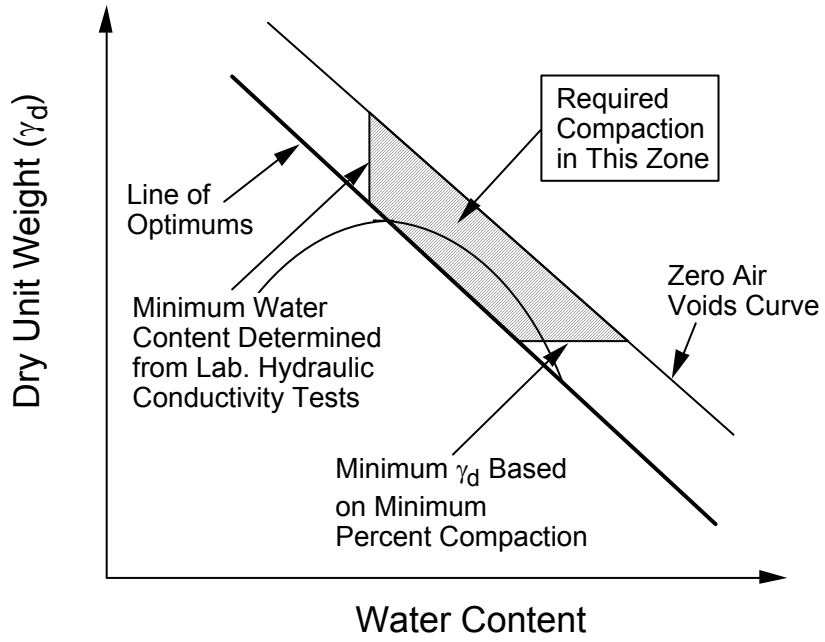

(B) Recommended Compaction Specification

Figure 4-36. Water content-density specifications indicating: (A) the traditional (but not recommended) type of specification, and (B) the recommended type of specification emphasizing compaction to water content-density values on or above the line of optimums.

In all cases, the large-scale hydraulic conductivity tests were the SDRI test. The SDRI test results are referred to as k_{Field}. Additionally, the results of k_{Lab} tests obtained on thin-walled sampling tubes were documented at several sites. Finally, one large block sample test was performed for k_{Lab}.

There is a basic limitation of the database associated with that fact that only 12 test pads comprise the database. Further, the information is not complete for all 12 tests pads. Although this is the most complete database of its type assembled to date, there remain relatively few well-documented cases in which the large-scale performance of soil-bentonite clay liners is documented.

4.2.2 Hydraulic Conductivity Results

k_{Field} covered a comparatively narrow range of 2×10^{-9} cm/s to 1×10^{-7} cm/s. All liners in the database met the objective of $k_{Field} \leq 1 \times 10^{-7}$ cm/s. The geometric mean k_{Field} was 1.9×10^{-8} cm/s.

The most important parameter in soil-bentonite mixtures is the amount of bentonite added to the mixture. k_{Field} is plotted as a function of percent bentonite in Fig. 4-37. As expected, there is a tendency for k_{Field} to decrease when the amount of bentonite is increased. However, the scatter in the data is significant ($r^2 = 0.28$), and there are relatively few data points in the database.

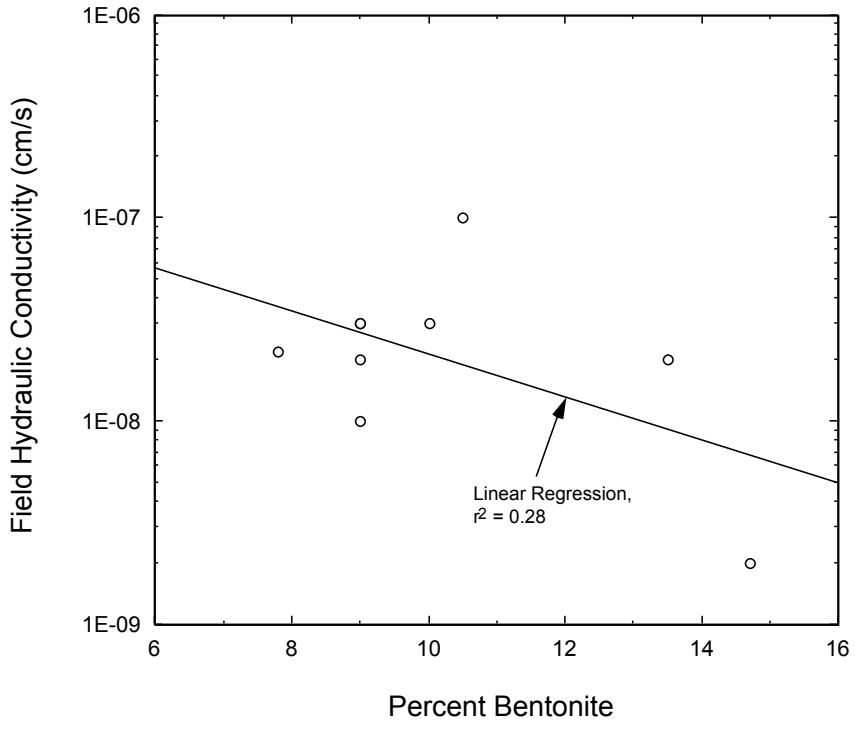

Figure 4-37. Field hydraulic conductivity versus percent bentonite in soil.

The results of k_{Lab} tests are compared to the results of k_{Field} tests in Fig. 4-38. There is good agreement between k_{Lab} and k_{Field}. This suggests that all liners were reasonably homogeneous and free of large-scale features that would tend to lead to large differences between the results of k_{Lab} and k_{Field} tests.

It was found that for natural soil liner materials, the percent wet of optimum was a significant variable. For soil-bentonite liners, this was not found to be the case (Fig. 4-39). Instead, percent compaction (Fig. 4-40) was found to be more significant. Experience in the laboratory has shown that water content is much less important for soil-bentonite admixtures than for natural soil materials, perhaps because of the high swelling that occurs in bentonite regardless of the initial water content. It does appear, however, that the more compact the soil (i.e., the higher the percent compaction), the lower the k_{Field}.

The masses of the compactors used to compact the liners in the database were nearly all identical. However, the number of passes of the compactor did vary. k_{Field} was found to slightly increase with number of passes within the very small range of number of passes used to construct the liners that comprise the database (Fig. 4-41). Unfortunately, the projects that comprise the database were not sufficiently well documented to permit determination of P_o.

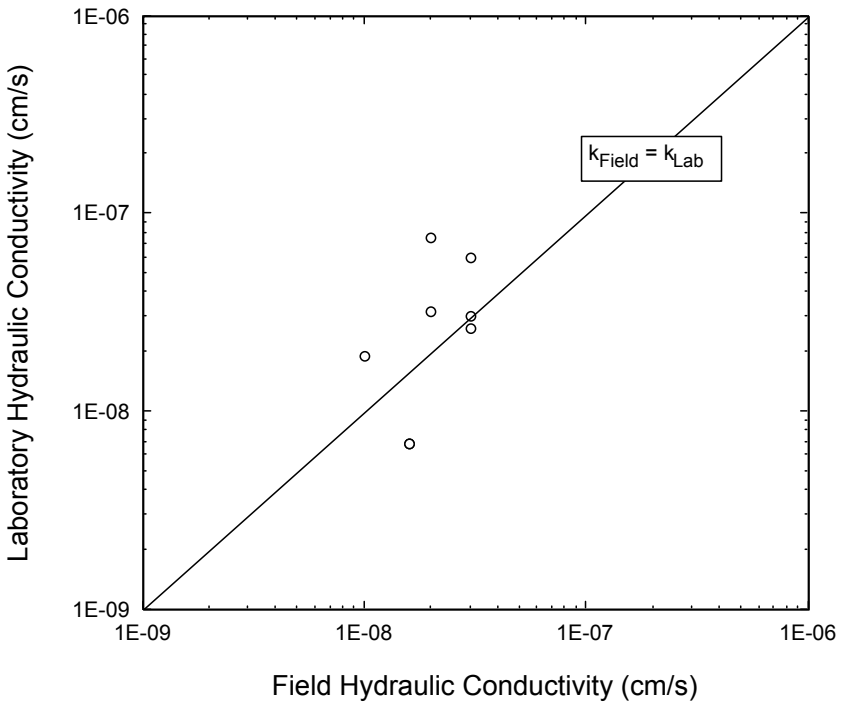

Figure 4-38. Laboratory-measured hydraulic conductivity vs. field-measured hydraulic conductivity for soil-bentonite liners.

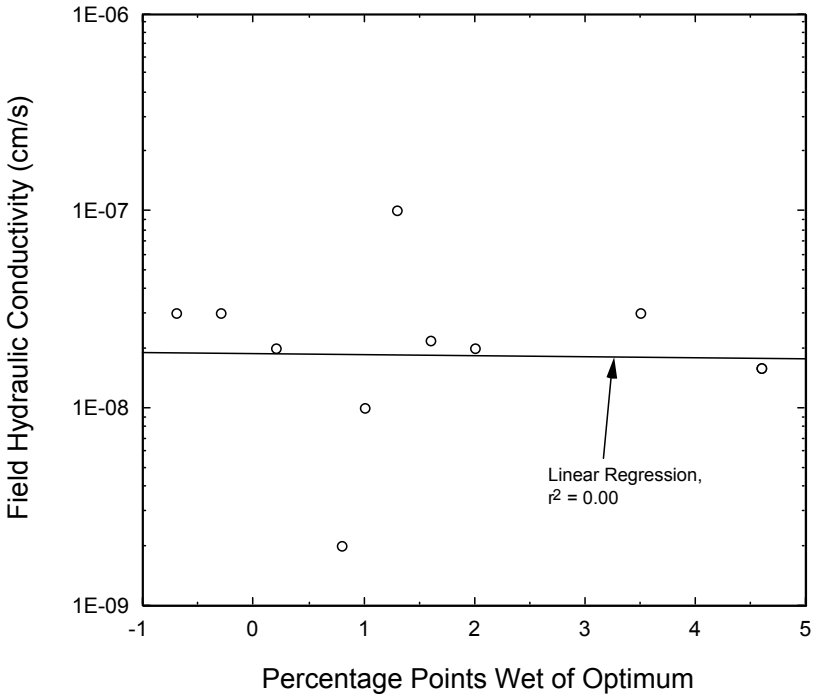

Figure 4-39. Field hydraulic conductivity versus percentage points wet of optimum for soil-bentonite liners.

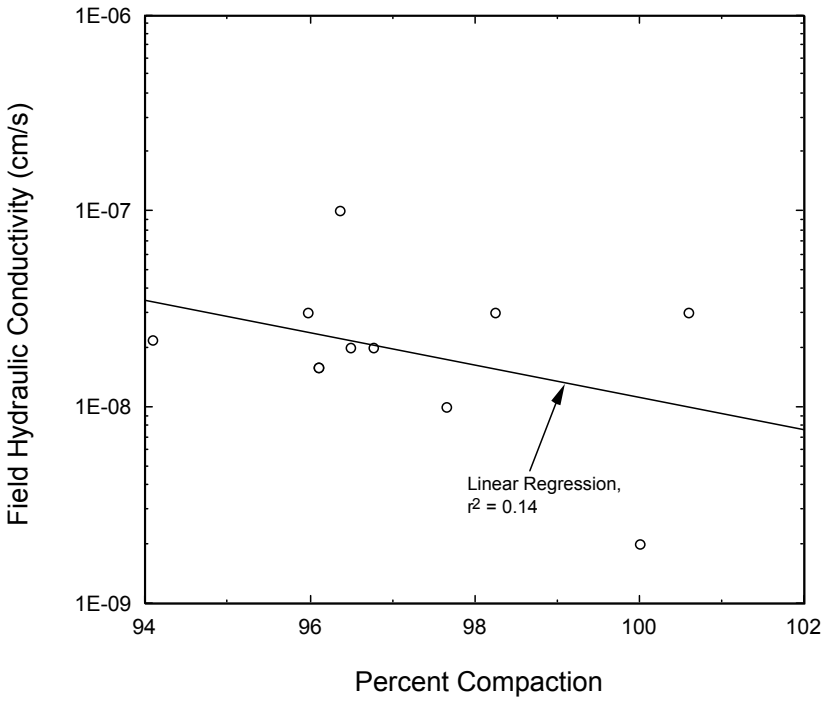

Figure 4-40. Field hydraulic conductivity vs. percent compaction for soil-bentonite liners.

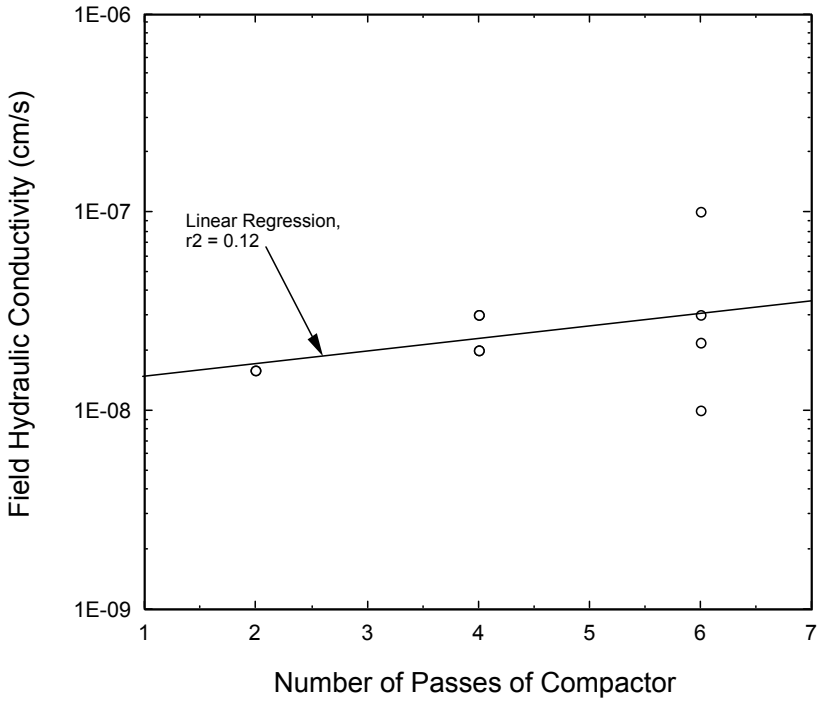

Figure 4-41. Field hydraulic conductivity vs. number of passes of compactor for soil-bentonite liners.

4.2.3 Conclusions

Relatively little information could be gleaned from the database for soil-bentonite liners, primarily because so few liners (12) comprise the database. It is significant, perhaps, that the desired k_{Field} of $\leq 1 \times 10^{-7}$ cm/s was achieved in all cases. However, it should be noted that all the liners contained a relatively large amount of bentonite (more than 6% for sites with reliable field hydraulic conductivity measurements). The data suggest that there is justification for focusing attention on a high percent compaction for soil-bentonite liners rather than a high water content. More data are needed to be able to draw more definitive conclusions about soil-bentonite liners.

4.3 Compacted Clays in Final Cover Systems

One of the tasks for this project was to evaluate available information concerning the performance of CCLs in final cover systems. No new information, beyond that already published in the literature or in reports, could be identified concerning the specific performance of the CCL component of final cover systems. The literature, however, is consistent, and is summarized below.

4.3.1 Omega Hills Final Cover Test Plots

The first detailed information to be presented on the performance of CCLs in landfill covers was described by Montgomery and Parsons (1989). The study involved the construction of three large test pads on the top of a closed municipal solid waste landfill, the Omega Hills landfill, which is located approximately 30 km northwest of Milwaukee, Wisconsin. The test plots were constructed to evaluate the performance of alternative final cover designs.

The cross sections of the three test plots are shown in Fig. 4-42. Test plot 1, consisting of 150 mm of topsoil overlying 1.2 m of CCL, represented the existing final cover system design at the time that the study was initiated. Test plot 2 involved the same thickness of CCL, but a thicker topsoil layer that was intended to promote better vegetative growth and thereby enhance evapotranspiration. Test plot 3 involved the use of a layer of coarse-grained soil (sand) sandwiched between two CCLs. The idea for the third plot was to take advantage of the so-called capillary barrier effect in which the coarse-grained soil (sand) remains unsaturated and thereby serves as a barrier to downward infiltration of water. With test plot 3, the intention was for the sand layer to promote retention of water in the upper CCL, where the water could be returned to the atmosphere via evapotranspiration. The use of this alternative design is consistent with the research nature of these test plots. All test plots were constructed on 3H:1V sideslopes of the actual landfill surface.

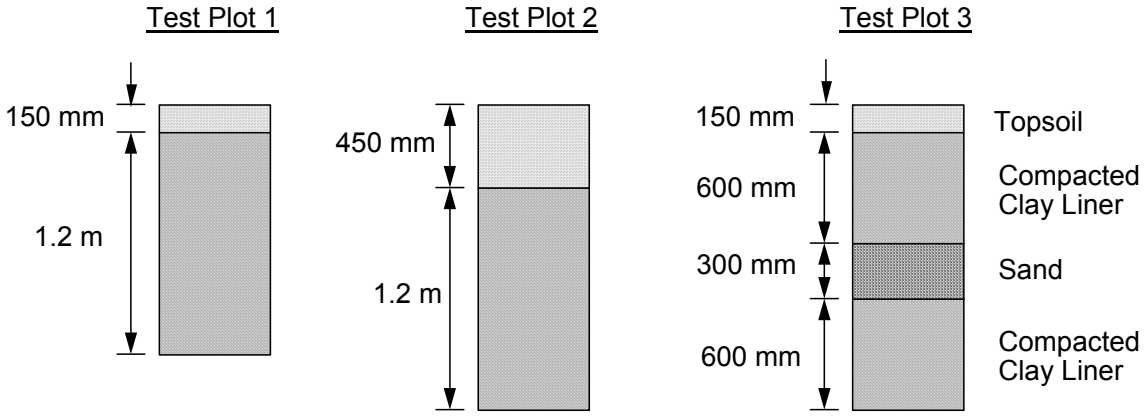

Figure 4-42. Cross-sectional view of test plot arrangement at Omega Hills landfill (after Montgomery and Parsons, 1989).

The CCL material consisted of CL soil with a high silt content. The soil was placed and compacted in 150-mm-thick lifts to a hydraulic conductivity $\leq 1 \times 10^{-7}$ cm/s, based on laboratory hydraulic conductivity tests on "undisturbed" samples of the compacted soil. The topsoil was an uncompacted clay loam to silty clay loam. The intermediate sand in

test plot 3 was a clean, washed, medium sand. The topsoil was seeded with a mixture of grasses.

The test plots contain two principal data collection systems. The first was a lysimeter located beneath the test plot to collect water that percolated through the cover soils and permit quantification of the rate of percolation. Figure 4-43 shows the plan location of the lysimeter system, and Fig. 4-44 shows the location in profile. The lysimeter consisted, from top to bottom, of a GT filter, a GC drainage layer, and a GM. The second data collection system was designed to collect and measure surface runoff (Figs. 4-43 and 4-44).

The test plots were constructed in 1986. Data collection and analysis started in September, 1986. Measurements were obtained of precipitation, runoff, percolation, and other parameters such as temperature. Soil moisture content was monitored with neutron access probes.

The 12-month period September 1986 through August 1987 was near normal. The period of September 1987 through August 1988 was dominated by a severe drought in 1988. The summer months in 1988 were characterized by substantially below-average rainfall and temperatures that averaged 6°C above normal. The drought reduced the cover vegetation to a dry, dormant state, and cracking of the surface of the cover soils was obvious. The third and final year of data collection saw a return to moist conditions.

At the end of three years, test pits were excavated in each test plot, outside the area of the lysimeters. The test pits measured 3 m in length, 1.2 m in width, and 2 m in depth. A summary of data collected is presented in Table 4-3. The key parameter is the quantity of percolation, i.e., rate of flow of water into the lysimeter. In test plots 1 and 2, the percolation in the first year was 2 to 7 mm/year (6×10^{-9} to 2×10^{-8} cm/s, respectively). However, by the third year, these values had increased to a range of 56 to 98 mm/year (2×10^{-7} and 3×10^{-7} cm/s, respectively). The test pits showed that the CCLs in test plots 1 and 2 were in a similar condition after three years:

- the upper 200 to 250 mm of CCL was weathered and blocky (probably from desiccation and/or freeze-thaw;
- cracks 6 to 12 mm wide extended 0.9 to 1 m into the CCL;
- roots penetrated 200 to 250 mm into the CCL in a continuous mat, and some roots extended into crack planes as deep as 750 mm into the CCL; and
- the base of the CCL appeared to be undamaged.

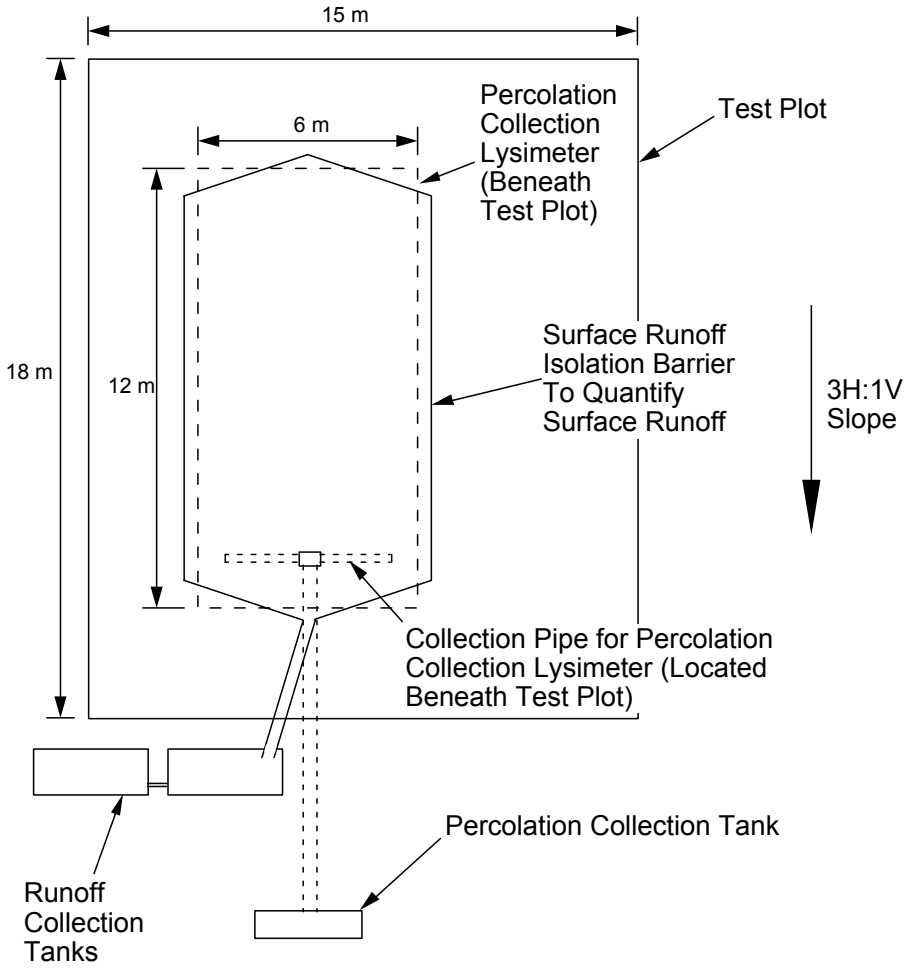

Figure 4-43. Plan view of test plot arrangement at Omega Hills landfill (after Montgomery and Parsons, 1989).

The drought conditions in the second year of the study period apparently caused severe desiccation of the CCL, which led to the significantly increased hydraulic conductivity in subsequent years. Although the CCL may have initially had a hydraulic conductivity of 1×10^{-7} cm/s or less, after three years, the desiccation damage caused the CCLs in test plots to no longer have this low level of hydraulic conductivity.

Test plot 3 was designed with the intention of maintaining moisture in the upper CCL. The percolation rate through test pad 3 remained more consistent and was found to range from 22 to 41 mm/year (7×10^{-8} to 1.3×10^{-7} cm/s). At the end of the three-year study period, the upper 200 to 250 mm of the uppermost CCL was weathered and blocky, and cracks extended through the entire thickness of the uppermost CCL. Cracking of the uppermost CCL allowed significant amounts of water to enter the sand drainage layer. Discharge of water from the sand layer was found to occur within hours of the start of precipitation events, suggesting rapid transmission of water through the

upper CCL due to flow through cracks. Moisture in the sand drainage layer probably helped to protect the underlying CCL from damage. The multi-component cap in test plot 3 did not function as anticipated. It was expected that the sand drainage layer would help the overlying CCL retain moisture, but the uppermost CCL quickly cracked.

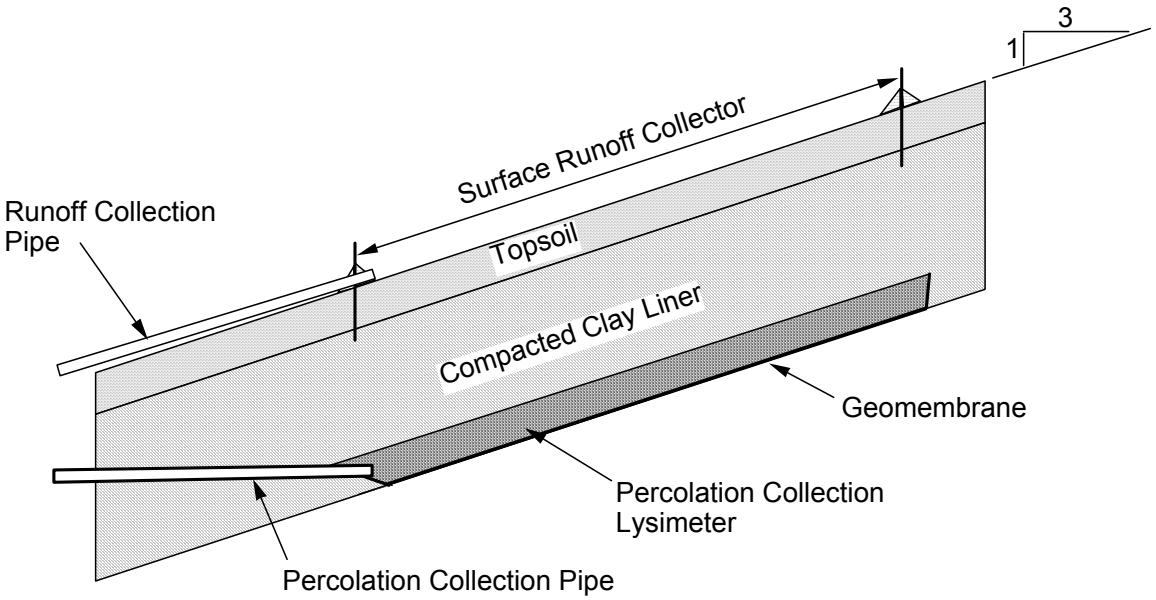

Figure 4-44. Cross section of underdrain system at Omega Hills landfill (after Montgomery and Parsons, 1989).

Table 4-3. Summary of information concerning performance of field test plots at Omega Hills landfill (data from Corser and Cranston, 1991).

Test Plot	Year	Precipitation (mm)	Runoff (mm)	Percolation (mm)
1	1986-87	896	180	2
	1987-88	579	38	5
	1988-89	823	56	56
2	1986-87	896	109	7
	1987-88	579	38	30
	1988-89	823	51	98
3	1986-87	896	97	40
	1987-88	579	38	22
	1988-89	823	66	41

The principal lesson learned from the Omega Hills study was that in a fairly short period of time (3 years), CCLs overlain by 150 to 450 mm of topsoil are subject to major desiccation, cracking, and increases in hydraulic conductivity. The CCL was not "survivable" with a hydraulic conductivity of 1 x 10^{-7} cm/s or less under these conditions.

4.3.2 Test Plots in Kettleman City, California

Corser and Cranston (1991) and Corser et al. (1992) describe test plots constructed at a waste disposal facility located in Kettleman City, California. Three test plots were constructed as shown in Fig. 4-45. Test plot 1 consisted of a 900-mm-thick CCL overlain by an exposed HDPE GM. Test plot 2 consisted of the same profile as test plot 1, except that 600 mm of topsoil covered the GM. Test plot 3 contained 450 mm of topsoil covering the CCL, with no GM covering the CCL. A portion of the test plots was flat, and a portion that sloped at 3H:1V. The test plots were constructed to study the factors that influence desiccation in a CCL placed in a final cover system profile.

The CCL was a high-plasticity clay that was expected to be used to construct final cover systems for approximately 30 ha of landfill at the site. The clay had an average liquid limit of 66% and plasticity index of 48%. The instrumentation consisted of thermistors to monitor temperature in the soil and CCL, and tensiometers to measure soil suction. Corser and Cranston (1991) summarize the first 6 months of data collection. At the end of the six month period, the surfaces of the CCLs were exposed over an area of 1.5 m by 1.5 m to observe and document cracking patterns.

Test plot 1 did not represent a final cover situation but is representative of a bottom liner with an exposed HDPE GM during the construction or operations phase. The clay exhibited some drying and cracking in areas where the HDPE was not in contact with the CCL. In other areas where the HDPE was in contact with the CCL, the moisture content of the CCL at the surface increased. It appears that the high temperature of the exposed HDPE GM caused heating and drying of the underlying CCL. In some areas (e.g., around wrinkles in the GM), moisture could migrate away via vapor transport. In other areas, the moisture could condense during cooler periods, causing moistening of the soil. In any case, there clearly was desiccation of the CCL beneath some portions of the exposed GM.

Test plot 3 did not perform well during the summer season. The CCL dried, and cracking was observed at the surface when a test pit was excavated in the fall. In contrast, was no evidence of drying or cracking of the CCL at test plot 2.

Although the test plots were observed for only six months, significant deterioration of the CCL was observed in test plots 1 and 3. Only test plot 2, in which the CCL was covered with a GM and 450 mm of top soil, performed well. The observations from Kettleman City are consistent with those of Omega Hills and suggest that perhaps the only practical way to protect a CCL from desiccation damage in typical final cover system

cross sections is to incorporate a GM and sufficiently thick cover soil over the GM/CCL composite barrier.

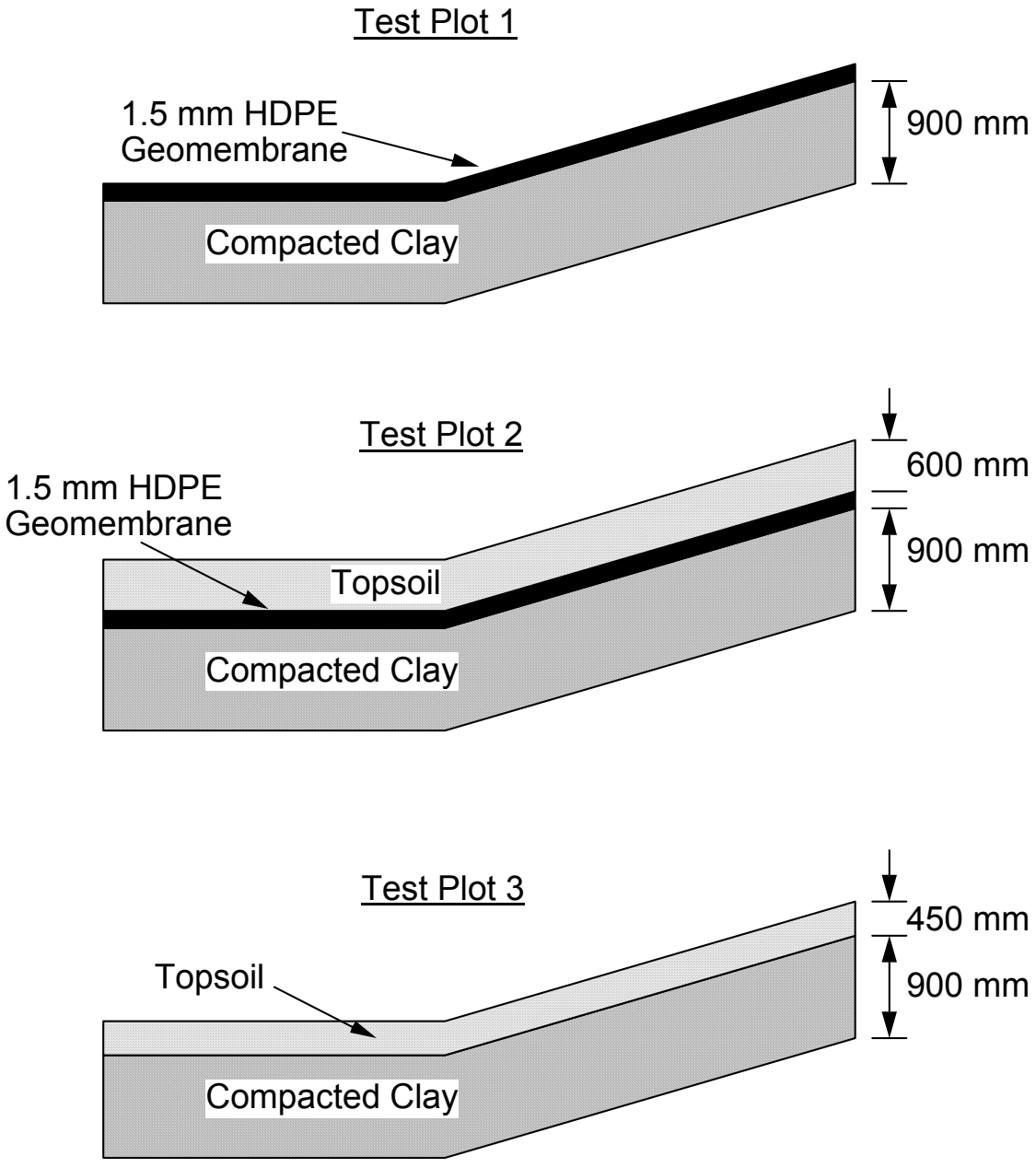

Figure 4-45. Cross sections of test plots at Kettleman City facility (after Corser and Cranston, 1991).

4.3.3 Test Plots in Hamburg, Germany

Melchior et al. (1994) describe what may be the most extensive test plot program of any constructed to date involving CCLs. Three test plots were constructed, as shown in Fig. 4-46. All test plots were constructed on top of an existing MSW landfill. There were two sections for each test plot. The upper section was located on the relatively flat portion near the top of the landfill and sloped at 4%. The lower half sloped more steeply at an inclination of 5H:1V (20%). The test plots were underlain with a lysimeter, much like the Omega Hills facility (Fig. 4-44).

The CCLs at the Hamburg site were constructed in three lifts, each 200 mm thick. The material consisted of 17% clay, 26% silt, 52% sand, and 5% gravel. The principal clay minerals in the clay fraction were (in decreasing abundance) illite, smectite, and kaolinite. The liquid limit was 20%, and the plasticity index was 9%. The soil was compacted 2% wet of optimum at an average degree of compaction of 96%. The CCL at the Hamburg site was significantly different from that at Omega Hills and Kettleman City. At Omega Hills, the low-plasticity (CL) clay contained a large amount of silt, which can make the material vulnerable to shrinkage cracking. The Kettleman City clay was a highly plastic (CH) clay. At Hamburg, the soil contained more than 50% sand- and gravel-sized particles and would therefore be classified as a clayey sand (SC). Clayey sands tend to be less vulnerable to shrinkage cracking than clays (especially highly plastic clays) that contain relatively little coarse-grained particles.

The percolation rates through the CCLs and into the lysimeters are summarized in Table 4-4. Also shown are the drainage rates in the sand drainage layer that overlies the CCL. The last column in Table 4-4 expresses the leakage through the CCL as a percentage of the drainage from the sand drainage layer. The leakage as a function of drainage is plotted vs. time in Fig. 4-47.

Test plots 1 and 3, which did not have a GM overlying the CCL, underwent a very large increase in leakage in 1992. The summer of 1992 was extremely dry in Hamburg, and the subsequent fall season was very wet. Excavations made in 1993 confirmed that the clay liner was cracked. Barely visible fissures were observed between soil aggregates (around 50 mm in diameter). Plant roots were observed to have reached the upper parts of the CCLs. Under the conditions of a hydraulic conductivity of 1×10^{-7} cm/s for the CCL and a unit hydraulic gradient, the calculated percolation rate through the CCL is approximately 30 mm/year. The actual leakage rates through the CCLs at test plots 1 and 3 exceeded 30 mm/year in 1992. The apparent problem was gradual deterioration of the CCL caused by desiccation during a particularly dry summer.

Test plot 2, on the other hand, has maintained a very low leakage rate. This test plot contains a GM overlying the CCL (Fig. 4-46).

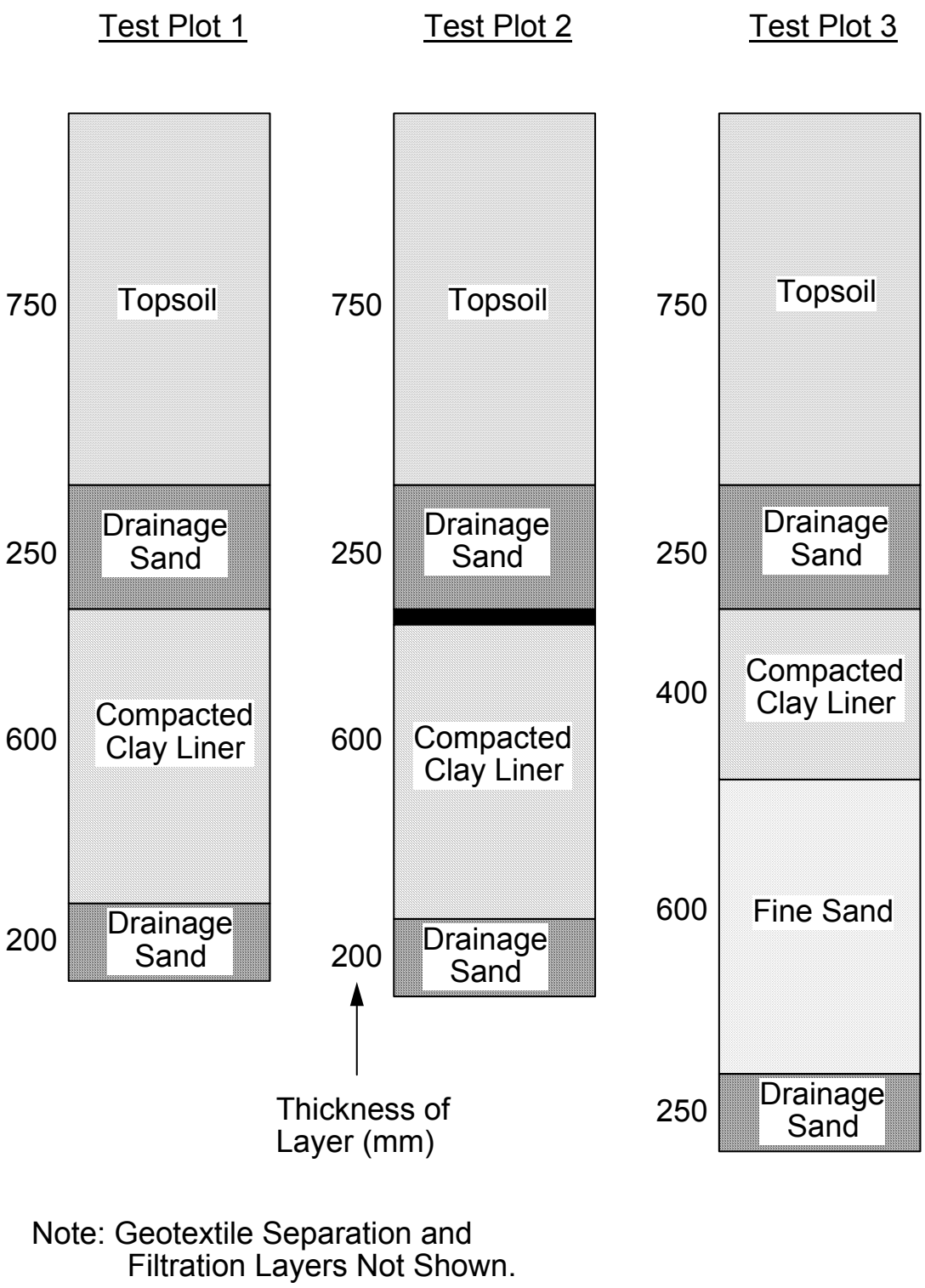

Figure 4-46. Cross sections of test plots in Hamburg, Germany (after Melchior et al., 1994).

Table 4-4. Summary of information concerning performance of field test plots at Hamburg, Germany (data from Melchior et al., 1994).

Test Plot	Year	Drainage (mm)	CCL Leakage (mm)	Leakage / Drainage (%)
1	1988	371	7	2
	1989	181	8	4
	1990	291	18	5
	1991	184	9	5
	1992	225	103	31
2	1988	296	3	1
	1989	155	0.6	0.4
	1990	269	0.4	0.1
	1991	164	0.5	0.3
	1992	311	0.8	0.3
3	1988	390	8	2
	1989	233	14	6
	1990	321	31	10
	1991	198	32	16
	1992	278	116	42

The results from Hamburg are consistent with those from Omega Hills and Kettleman City, even though the CCL material was very different. It appears that a CCL placed in a final cover system without a GM and soil covering the GM is likely to fail to maintain a hydraulic conductivity $\leq 1 \times 10^{-7}$ cm/s. If the CCL is to have a chance of maintaining this level of hydraulic conductivity for extended periods, it appears that the CCL must be protected with both a GM and a sufficiently thick layer of cover soil above the GM.

Melchior (1997) describes additional work performed at the Hamburg site in which two additional test covers were constructed and monitored. The two additional test covers both consisted of 300 mm of topsoil underlain by 150 mm of drainage sand, which in turn was underlain by a GCL. Two different GT-encased, needlepunched GCLs were used for the two different test plots. As with the first three test covers, the two additional test covers with GCLs were underlain by drainage sand and a GM to collect any water that percolated through the test cover. Both GCLs performed well for about a year, with almost no liquid appearing in the drainage layers beneath the test covers. However, about a year after construction (in the fall, following a dry summer), percolation began to occur and was closely linked with rainfall events. Peak percolation rates were on the order of 0.4 mm per hour (about 1×10^{-5} cm/s). Melchior (1997) states that research on the causes for high percolation rate is on-going, but indications are that the causes for the increase in hydraulic conductivity of the GCLs may have been related to: (1) penetration of the GCL by plant roots; (2) desiccation of the GCL, leading to high initial seepage rates following major rainfall events; and (3) ion exchange (calcium was

apparently leached from cover soils, and replacement of sodium in the bentonite with calcium is expected to cause an increase in hydraulic conductivity).

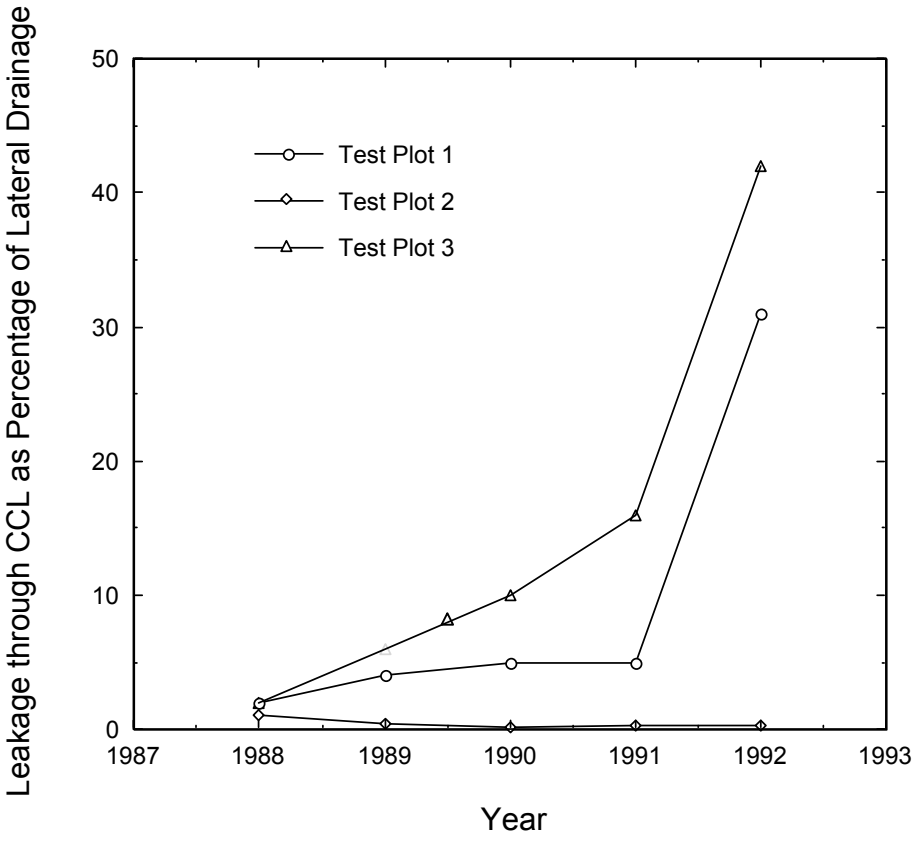

Figure 4-47. Leakage through CCL as a percentage of the drainage from the overlying sand drainage layer plotted vs. time.

4.3.4 Final Covers in Maine

The Maine Bureau of Remediation and Waste Management (1997) reported the results of field measurements of percolation rates through four CCLs in actual municipal solid waste landfill covers. All liners appear to have been constructed using methods of construction and construction quality assurance practices that are typical of the landfill industry.

4.3.4.1 Cumberland Site

The 2-ha Cumberland Municipal Solid Waste Landfill was closed in 1992 with a cover system that consisted of 150 mm of vegetated topsoil that was underlain by 450 mm of compacted silty clay, which in turn was underlain by sand-filled trenches that served to collect gases. k_{Lab} tests were performed during construction and in post-construction

investigation programs conducted in 1994 and 1996. An SDRI test was performed in 1994.

At the time of construction, the average k_{Lab} was 5 x 10^{-8} cm/s. In the 1994 investigation, k_{Lab} was 1 to 2 x 10^{-7} cm/s. k_{Field}, measured with the SDRI, was 6 x 10^{-6} cm/s. It is not certain whether the liner originally had a k_{Field} < 1 x 10^{-7} cm/s (since no field testing was performed at the time of construction).

4.3.4.2 Vassalboro Site

The Vassalboro Municipal Solid Waste Landfill consists of one 1.6 ha site that was closed in 1990. The final cover consists of 150 mm of vegetated cover (sludge amended topsoil) overlying 450 mm of compacted glacial till CCL, which in turn was underlain by a gas collection layer. k_{Lab} tests were performed at the time of construction (1990) and again in 1994 and 1996. An SDRI test was performed in 1994.

k_{Lab} at time of construction averaged 2 x 10^{-7} cm/s. In 1994, k_{Lab} ranged from 9 x 10^{-7} to 5 x 10^{-6} cm/s. The k_{Field} measured by SDRI test in 1994 was 2 x 10^{-6} cm/s. It appears that the hydraulic conductivity of the CCL increased about an order of magnitude from 1990 to 1994.

4.3.4.3 Yarmouth Site

The Yarmouth Municipal Solid Waste Landfill covers 2.5 ha and was closed in 1990 using a cover system consisting of 150 mm of sludge-amended topsoil overlying 450 mm of compacted silty clay, which was underlain by a gas collection layer.

k_{Lab} tests performed at the time of construction (1990) indicated an average k_{Lab} of 8 x 10^{-8} cm/s. In a 1994 investigation, k_{Lab} was approximately 3 x 10^{-7} cm/s, and in 1996, k_{Lab} was found to be 2 x 10^{-6} to 2 x 10^{-5} cm/s, or about 20 to 100 times larger than in 1990. k_{Field} was measured with the SDRI in 1994 and again in 1996. k_{Field} was 2 x 10^{-7} cm/s in 1994 and 2 x 10^{-6} cm/s in 1996. There is a clear trend of increasing hydraulic conductivity over time, with the magnitude of increase being one to two orders of magnitude over the six-year study period.

4.3.4.4 Waldoboro Site

The Waldoboro Municipal Solid Waste Landfill covers 1.6 ha and was closed in 1991 with a cover system consisting of 150 mm of sludge-amended topsoil overlying 450 mm of compacted silty clay, which in turn was underlain by a gas collection layer.

k_{Lab} tests indicated that k_{Lab} increased over time from an initial average value of about 5 x 10^{-8} cm/s (1991) to 1 x 10^{-6} cm/s (1993) and to 3 x 10^{-6} cm/s (1996). k_{Field} measured with SDRI tests was 1 x 10^{-6} cm/s in 1993 and 4 x 10^{-6} cm/s in 1996. Thus, the data indicate that the hydraulic conductivity increased about two orders of magnitude over a five year period.

4.3.4.5 Discussion

The observations from these four actual cover systems are consistent with those of the other sites mentioned previously in this section of the report. All of the available field performance data indicate that a CCL overlain by a relatively thin layer of topsoil (150 to 450 mm thick), and without a GM above the CCL, cannot maintain a hydraulic conductivity of 1 x 10^{-7} cm/s or less. From analysis of the condition of the four CCLs at these sites, it appeared that desiccation was the most significant factor leading to an increase in k_{Field}. Freeze/thaw may also have contributed significantly to damage. Penetration of plant roots into the CCL was also observed.

4.3.5 Alternative Cover Demonstration at Sandia National Laboratory

A major field demonstration project, initiated in the mid 1990s, is underway at Sandia National Laboratories and, although only preliminary data were available at the time of preparation of this report, the project bears mentioning here. The project is known as the Alternative Landfill Cover Demonstration (ALCD), and is a large-scale field test conducted at Sandia National Laboratories, located on Kirtland Air Force Base in Albuquerque, New Mexico. The climate at the test site is semi-arid. The goal of the ALCD is to field test, compare, and document the performance of alternative landfill cover technologies, of various complexities and costs, with emphasis on arid and semi-arid environments (Dwyer, 1997). The purpose of the ALCD is to provide information on cost, construction, and performance, so that design engineers and regulatory agency officials will have data on alternatives to conventional cover design.

The test plots are each 13 m wide by 100 m long (Dwyer, 1997). All covers were constructed with a 5% slope in all layers. Slope lengths are 50m (the test covers are crowned at the middle half of the length). The western slopes are maintained and monitored under natural conditions while a sprinkler system was installed on the eastern slopes to facilitate stress testing of the covers. Two conventional covers and four alternative covers comprise the six test covers, with cross sections as follows:

1. Baseline Test Cover 1 is a “RCRA Subtitle D” conventional cover, consisting of 150 mm of topsoil underlain by 450 mm of compacted “barrier layer soil” with a maximum hydraulic conductivity of 1 x 10^{-5} cm/s (actual hydraulic conductivity measured on laboratory samples recovered from the constructed barrier layer were in the range of 5 x 10^{-7} cm/s to 6 x 10^{-6} cm/s, and an in situ hydraulic conductivity test yielded a hydraulic conductivity of 5 x 10^{-7} cm/s).
2. Baseline Test Cover 2 is a “RCRA Subtitle C” conventional cover, consisting (from top to bottom) of 600 mm of topsoil, a GT separator/filter, 300 mm of sand drainage material, a 1-mm-thick linear low density polyethylene GM, and 600 mm of compacted clay with a design hydraulic conductivity less than or equal to 1 x 10^{-7} cm/s (although an in situ hydraulic conductivity test indicated a hydraulic

conductivity of 8 x 10^{-7} cm/s, with the comparatively large hydraulic conductivity thought to have been caused by desiccation cracking during construction).

3. Alternative Test Cover 1 is essentially identical to the RCRA Subtitle C cover, except that it incorporates a GCL rather than CCL and (very significantly), the GM component was punctured with 8 holes, each measuring 1 cm^2, to simulate defects in the GM.
4. Alternative Test Cover 2 is a capillary barrier, which makes use of a clean, granular layer below a topsoil layer to provide a capillary break between the topsoil and underlying soils, thus promoting moisture retention in the topsoil layer. So long as the granular layer beneath the topsoil remains relatively dry, the downward movement of moisture should be minimal. The capillary barrier test cover consists (from top to bottom) of 300 mm of topsoil, an upper lateral drainage layer comprised of 80 mm of sand underlain by 220 mm of clean pea gravel (the sand serves as a filter that prevents the overlying topsoil from migrating downward into the gravel), a barrier layer consisting of 450 mm of compacted soil, and a lower drainage layer comprised of 300 mm of sand. The "barrier layer" was compacted dry of optimum and was not intended to have a hydraulic conductivity comparable to a traditional CCL.
5. Alternative Test Cover 3 is referred to as the anisotropic barrier and attempts to limit downward movement of water with a layering of capillary barriers. The various layers are enhanced by varying soil properties and techniques that lead to the anisotropic properties of the cover. The anisotropic barrier consists (from top to bottom) of 150 mm of vegetative material (a mixture of 75% topsoil and 25% pea gravel by weight), 600 mm of native soil to allow for water storage, a 150-mm-thick interface layer consisting of fine sand that serves as a filter between the overlying native soil and underlying gravel, and 150 mm of pea gravel. The fine sand layer was intended to create one capillary break, and the gravel was intended to create a second capillary break.
6. Alternative Test Cover 4 is referred to as the evapotranspiration (ET) cover. The ET cover consists of a single, 900-mm-thick layer of native soil. The bottom 750 mm of soil was placed in lifts and compacted, while the top 150 mm was not compacted. The cover material was seeded with native species that contained a mix of cool and warm weather plants (primarily native grasses).

Preliminary results have indicated that all six test covers are performing well, although there are significant differences in percolation rates. Dwyer (personal communication) provided a summary of the first year of percolation, as indicated in Table 4-5. Cost data are also summarized in Table 4-5. The test cover program will provide valuable insights into conventional and alternative cover designs as data are developed, analyzed, and published.

Table 4-5. Summary of Preliminary Data from ALCD Project.

Test Cover	Construction Cost ($/m^2)	Percolation (L) after One Year
RCRA Subtitle D Cover	$51	6724
RCRA Subtitle C Cover	$158	46
Alternative RCRA Subtitle C Cover with GCL (GM with 8 Defects)	$90	572
Capillary Barrier	$93	804
Anisotropic Barrier	$75	63
Evapotranspiration Cover	$74	80

4.3.6 Test Covers in East Wenatchee, Washington

Khire et al. (1997) describe a project at the Greater Wenatchee Regional Landfill in East Wenatchee, Washington (a semi-arid region), in which two test covers were constructed and monitored. The test covers measured 30 m by 30 and were constructed on a 2.7H:1V slope. The test covers were instrumented to measure runoff and percolation, as well as to monitor moisture conditions within the various layers of the test covers.

Test Cover 1 was referred to as a "resistive barrier" and was a RCRA Subtitle D type cap. Test Cover 1 consisted of 150 of topsoil underlain by a 450-mm-thick barrier layer constructed from low plasticity silty clay that was compacted to achieve a hydraulic conductivity of 2 x 10^{-7} cm/s. The low-permeability barrier layer was intended to provide resistance to infiltration of water, and thus the use of the term "resistive barrier." Test Cover 2 was a capillary barrier consisting of 150 mm of vegetated silt topsoil, underlain by a 750-mm-thick layer of medium, uniformly graded sand that served as the capillary break layer.

Performance of the test covers has been documented for a 3-year period (Khire et al., 1997). For the first three years, Test Cover 1 allowed percolation of a total of 33 mm of water (equal to 5.1% of precipitation) through the cover, while Test Cover 2 allowed only 5 mm (equal to 0.8% of precipitation) to percolate through the cover. Significant percolation through the capillary barrier occurred only during the winter of 1993, when record snow fall occurred. If the surface layer of the capillary barrier cover had been increased, it is anticipated that percolation through the capillary barrier would have been nearly zero. In the resistive barrier cap, percolation occurred only when the wetting front reached the base of the low-permeability barrier layer. Percolation increased significantly in 1995. The primary reason for this increase appeared to be preferential flow through vertical cracks in the barrier layer, which apparently formed from desiccation during the previous summer. Animal burrows, found during field reconnaissance in the spring of 1995, may have also contributed to increase in percolation.

The data indicating an increase in percolation through the low-permeability clay layer is consistent with observations at Omega Hills, Kettleman City, and Hamburg.

4.3.7 Test Covers at Los Alamos National Laboratory

Nyhan et al. (1997) describe the performance of four test covers constructed at Los Alamos National Laboratory for the Protective Barrier Landfill Cover Demonstration. The four test plots were each constructed on slopes of 5, 10, 15, and 25%, making a total of 16 test plots. None of the plots was vegetated, apparently to simulate extreme conditions in which plants provided no evapotranspiration. Precipitation, runoff, drainage, and percolation were measured for each plot. The moisture content of the soils was also monitored. Performance for the first four years is documented by Nyhan et al. (1997).

The four test plots contained the following cross sections:

1. Test Cover 1 was termed the "conventional design" for Los Alamos, and consisted of 150 mm of loam topsoil underlain by 760 mm of crushed Los Alamos tuff (an angular, silty sand), underlain by 300 mm of gravel.
2. Test Cover 2 was termed the "EPA design" and consisted (from top to bottom) of 610 mm of loam topsoil, a GT separator/filter, 300 mm of sand drainage material, and 610 mm of low-permeability clay-sand material. The GM component that usually overlies compacted clay in "EPA designs" was intentionally omitted because it was thought when the design was conceived in the late 1980s that the GM would not have a sufficiently long service life for radioactive waste disposal units.
3. Test Cover 3 was termed the "loam capillary barrier design" and consisted of 610 mm of loam topsoil underlain by 760 mm of fine sand, which served as the capillary break.
4. Test Cover 4 was termed the "clay loam capillary barrier design" and consisted of 610 mm of clay loam topsoil underlain by 760 mm of fine sand.

Performance data showed that 86% to 91% of all precipitation that fell on the covers was evaporated from the unvegetated test covers, which was not unexpected in the semi-arid climate of Los Alamos. Of the four test covers, the EPA design provided the least amount of percolation through the test plots (zero percolation on all four test plots employing the EPA design). The bentonitic clay mixed in with sand to form the barrier layer apparently helped with the water balance at this semi-arid site. Test Cover 1 (conventional design for Los Alamos) allowed the greatest amount of seepage, varying from 174 mm of percolation for the 5% slope to 31 mm for the 25% slope over a 4.5 year period. Test Cover 3 (loam capillary barrier design) allowed 76 mm of percolation for the 5% slope, 36 mm of percolation for the 10% slope, and no percolation for the 15% and 25% slopes over the same 4.5 year period. Test Cover 4 (clay loam capillary

barrier design) allowed 48 mm of percolation for the 5% slope, and no percolation for test plots on steeper slopes for the 4.5-year observation period.

The Los Alamos test plots appear to be the only documented cases in which a compacted clay placed in a test cover without a protective GM worked well over a period of several years of observation.

4.3.8 Other Studies

Other papers have been published on the performance of CCLs in final covers, but none is as comprehensive as the studies discussed in the preceding sections. Questions have been raised about the long-term survivability of CCLs, even if the CCL is covered by a GM. Suter et al. (1993) discuss the factors that might cause long-term degradation of CCLs. The primary mechanisms of concern are desiccation, freeze-thaw, thermally induced moisture movement leading to desiccation, root penetration, subsidence, and animal intrusion.

It appears that the best way to document the field performance of CCLs in landfill final cover systems is with the use of lysimeters installed at the base of the cover system. Lysimeters consist of a barrier (typically GM) overlain by a drainage material (typically sand or gravel, but possibly GN or other geosynthetic drainage material), and drained by gravity at the low point. Few, if any, such systems have been installed, except in test plots. Until performance data are collected over a period of many years on actual covers, the long-term performance of CCLs will remain the subject of speculation. However, the admittedly sparse data that are available points to the likelihood (if not certainty) of desiccation and subsequent flow rates well in excess of those associated with a CCL having a hydraulic conductivity of 1×10^{-7} cm/s or less for cover systems employing a layer of topsoil overlying a CCL (with no GM separating the CCL and topsoil). Although the monitoring of leachate production rates can be very useful in indicating whether or not the cover is working reasonably well, a careful analysis of actual flow rates through the cover system may be difficult with such a global measurement as leachate production rate. Scientists and engineers are encouraged to collect percolation data with lysimeters whenever possible.

4.4 Summary and Conclusions

The objective of this component of the study was to document the field performance of CCLs, and particularly to address the question of whether CCLs are meeting the objective of having a hydraulic conductivity of 1×10^{-7} cm/s or less. Field performance data on CCLs employed as liners for actual landfills are very limited (only 8 such cases are documented), and even fewer data are available on CCLs in landfill cover systems. Therefore, the approach taken was: (1) document large-scale hydraulic conductivity measurements obtained from test pads (with the 8 cases of documented field performance), and (2) document information available on test covers used to evaluate CCL performance in landfill cover systems.

A database consisting of 89 CCLs (81 test pads plus 8 actual bottom liners) constructed from natural soils was assembled and analyzed for large-scale field hydraulic conductivity. The cases covered a broad range of soil types, construction methods, and regions. All CCLs were constructed using construction and CQA procedures that appear to be consistent with the current state of practice, and only those CCLs that were constructed for the explicit purpose of achieving a field hydraulic conductivity (k_{Field}) $\leq 1 \times 10^{-7}$ cm/s were included in the database. Conclusions may be summarized as follows: (1) 25% of the 89 CCLs failed to achieve the desired large-scale hydraulic conductivity of 1×10^{-7} cm/s or less, confirming the difficulty that is often encountered in achieving the required low hydraulic conductivity and indicating that achieving this level of impermeability requires careful planning, use of appropriate materials, specification of suitable compaction requirements, and thorough CQA; (2) a few of the CCLs failed to meet the desired hydraulic conductivity because the soil materials turned out not to be suitable; (3) for soils that were found to be unsuitable, a comprehensive laboratory testing program had not preceded construction of the test pad -- thorough laboratory testing is recommended for all CCLs prior to construction to verify the suitability of the soil and the proposed compaction specification; (4) the single most common problem in achieving the desired low level of hydraulic conductivity was failure to compact the soil in the zone of moisture and dry density that will yield low hydraulic conductivity; (5) the most significant control parameter was not found to be water content or density, but rather a parameter denoted "P_o", which represents the percentage of field-measured water content-density points that lie on or above the line of optimums -- when P_o was high (80% to 100%) nearly all the CCLs achieved the desired field hydraulic conductivity, but when P_o was low (0 to 40%), fewer than half the CCLs achieved the desired field hydraulic conductivity; (6) practically no correlation was found between hydraulic conductivity and frequently measured soil characterization parameters, such as liquid limit, plasticity index, percentage of clay, percentage of fine material, indicating that natural soil CCLs can be constructed with a relatively broad range of soil materials; (7) good agreement was obtained between k_{Field} and k_{Lab} on small samples for well constructed liners with $k_{Field} \leq 1 \times 10^{-7}$ cm/s, but poor agreement was found for poorly constructed liners with $k_{Field} > 1 \times 10^{-7}$ cm/s (with laboratory measurements often yielding significantly lower hydraulic conductivities); and (8) hydraulic conductivity decreased with increasing thickness of CCLs, up to a thickness of about 1 m, at which point all CCLs in the database achieved $k_{Field} \leq 1 \times 10^{-7}$ cm/s.

A database on soil-bentonite CCLs was also assembled, but only contained 12 field-measured hydraulic conductivities on test pads. Relatively little information could be gleaned from the database for soil-bentonite liners. The desired hydraulic conductivity of $\leq 1 \times 10^{-7}$ cm/s was achieved in all 12 cases. However, all the CCLs in the database contained a relatively large amount of bentonite (more than 6%). The data suggest that there is justification for focusing attention on a high percent compaction for soil-

bentonite liners rather than a high water content. More data are needed to be able to draw more definitive conclusions about soil-bentonite liners.

Finally, data were assembled from the literature on performance of CCLs in landfill final cover systems. Most of the field data indicate that CCLs tend to desiccate over time, and if not covered with a GM overlain by soil, are likely to undergo significant increases in hydraulic conductivity within five years after construction as a result of desiccation cracking. If the CCL is protected from desiccation by a GM and covering soil, it appears that water percolation through the composite barrier will be extremely small, and that the CCL probably be protected from desiccation for at least several years, if not longer. Of the data analyzed from final cover systems, only the Omega Hills and Hamburg test sites were situated on an actual landfill cover, where differential settlement was a possibility. MSW landfills are known to undergo significant settlement, which can produce stress-induced cracking that increases hydraulic conductivity. Although the discussion herein focused primarily on the desiccation issue, this was because the test covers themselves were impacted far more by desiccation than by settlement, due to the nature of the test arrangements. Settlement-induced cracking may be a far more significant effect than indicated by this collection of information from performance of cover system test sections.

4.5 References

Benson, C.H. and Boutwell, G. (1992). "Compaction Control and Scale-Dependent Hydraulic Conductivity of Clay Liners," *Proceedings of the 15th Annual Madison Waste Conference*, University of Wisconsin, Madison, Wisconsin, 62-83.

Benson, C.H., Zhai, H., and Rashad, S.M. (1992), "Assessment of Construction Quality Control Measurements and Sampling Frequencies for Compacted Soil Liners," *Environmental Geotechnics Report No. 92-6*, Univ. of Wisconsin, Dept. of Civil and Environmental Engineering Madison, Wisconsin.

Benson, C.H., Hardianto, F.S., and Motan, E.S. (1994), "Representative Specimen Size for Hydraulic Conductivity Assessment of Compacted Soil Liners," *Hydraulic Conductivity and Waste Contaminant Transport in Soils, ASTM STP 1142*, D.E. Daniel and S.J. Trautwein (Eds.), American Society for Testing and Materials, Philadelphia, 3-29.

Benson, C.H., and Daniel, D.E. (1994), "Minimum Thickness of Compacted Soil Liners: II. Analysis and Case Histories." *Journal of Geotechnical Engineering*, 120 (1): 153-172.

Corser, P., and Cranston, P. (1991), "Observations on Long-Term Performance of Composite Clay Liners and Covers," *Proceedings, Geosynthetic Design and Performance*, Vancouver Geotechnical Society, Vancouver, BC.

Corser, P., Pellicer, J., and Cranston, M. (1992), "Observation on Long-Term Performance of Composite Clay Liners and Covers," *Geotechnical Fabrics Report*, November, pp. 6-16.

Daniel, D.E. (1989), "In Situ Hydraulic Conductivity Tests for Compacted Clays," *Journal of Geotechnical Engineering*, 115(9): 1205-1227.
Daniel, D.E., and Benson, C.H. (1990), "Water Content-Density Criteria for Compacted Soil Liners," *Journal of Geotechnical Engineering*, 116(12): 1811-1830.
Daniel, D.E., and Koerner, R.M. (1995), *Waste Containment Systems: Guidance for Construction, Quality Assurance, and Quality Control of Liner and Cover Systems*, ASCE Press, New York, 354 p.
Dwyer, S.F. (1997), "Large-Scale Field Study of Landfill Covers at Sandia National Laboratories," *Proceedings, Landfill Capping in the Semi-Arid West: Problems, Perspectives, and Solutions*, Environmental Science and Research Foundation, Idaho, Falls, ID, ESRF-019, 87-108.
Gordon, M.E., Huebner, P.M., and Mitchell, G.R. (1990), "Regulation, Construction and Performance of Clay Lined Landfills in Wisconsin," *Waste Containment Systems*, R. Bonaparte (Ed.), American Society of Civil Engineers, New York, 14-27.
Khire, M.V., Benson, C.H., and Bosscher, P.J. (1997), "Water Balance of Two Earthen Landfill Caps in a Semi-Arid Climate," *Proceedings, International Containment Technology Conference*, St. Petersburg, Florida, 252-261.
Maine Bureau of Remediation and Waste Management (1997), *An Assessment of Landfill Cover System Barrier Layer Hydraulic Performance*, Augusta, Maine.
Melchior, S., Berger, K., Vielhaver, B., and Miehlich, G. (1994), "Multilayered Landfill Covers: Field Data on the Water Balance and Liner Performance," *In-Situ Remediation: Scientific Basis for Current and Future Technologies*, G.W. Gee and N.R. Wing (Eds.), Battelle Press, Columbus, Ohio, Part 1, pp. 4111-425.
Melchior, S. (1997), "In-Situ Studies of the Performance of Landfill Caps," *Proceedings, International Containment Technology Conference*, St. Petersburg, Florida, 365-373.
Montgomery, R.J., and Parsons, L.J. (1989), "The Omega Hills Final Cover Test Plot Study: Three-Year Data Summary," Presented at the Annual Meeting of the National Solid Waste Management Association, Washington, DC.
Nyhan, J.W., Schofield, T.G., and Salazar, J.A. (1997), "A Water Balance Study of Four Landfill Cover Designs Varying in Slope for Semiarid Regions," *Proceedings, International Containment Technology Conference*, St. Petersburg, Florida, 262-269.
Reades, D.W., Lahti, L.R., Quigley, R.M., and Bacopoulos, A. (1990), "Detailed Case History of Clay Liner Performance," *Waste Containment Systems: Construction, Regulation, and Performance*, R. Bonaparte (Ed.), American Society of Civil Engineers, New York, 156-174.
Sai, J.O., and Anderson, D.C. (1990), "Field Hydraulic Conductivity Tests for Compacted Soil Liners," *Geotechnical Testing Journal*, 13(3): 215-225.
Suter, G.W., Luxmoore, R.J., and Smith, E.D. (1993), "Compacted Soil Barriers at Abandoned Landfill Sites Are Likely to Fail in the Long Term," *Journal of Environmental Quality*, Vol. 22, pp. 217-226.
Trautwein, S.J., and Boutwell, G.P. (1994), "In-Situ Hydraulic Conductivity Tests for Compacted Soil Liners and Caps," *Hydraulic Conductivity and Waste Contaminant*

Transport in Soils, ASTM STP 1142, D.E. Daniel and S.J. Trautwein (Eds.), American Society for Testing and Materials, Philadelphia, 184-223.

Chapter 5
Detailed Summary of Field Performance Tasks

5.1 Introduction

5.1.1 Scope of Work

This portion of the project involved four tasks designed to evaluate the field performance of liner systems and final cover systems (referred to as cover systems in this chapter) for modern landfills in the U.S. The term "modern landfill" refers to a landfill designed with components substantially meeting current federal regulations and constructed and operated to the U.S. state of practice from the mid-1980's forward. The four tasks are:

- evaluation of available published information on the field performance of modern landfills;
- collection and analysis of liquids management data for double-lined landfills;
- evaluation of problems that have occurred in waste containment systems (i.e., liner systems and cover systems) for waste management facilities; and
- assessment of the adequacy of the EPA HELP computer model as a tool for LCRS design.

The purpose of performing these tasks is to develop an improved understanding of the actual field performance of modern landfill liner systems and cover systems and, to the extent possible, provide data that allow answers to be developed for the following questions:

1. What conclusions can be drawn from available LCRS and LDS data regarding leakage rates through primary liners and hydraulic efficiencies of liners?
2. How much leachate is generated in modern landfills, both during active operations and after closure, and what is the effect of site location (climatic region) and waste type on leachate generation rates?
3. What is the chemistry of modern landfill leachate and what is the effect of site location, waste type, and operation conditions on leachate chemistry?
4. What is the effect of the federal solid waste regulations of the 1980's and early 1990's, which limit the disposal of certain types of wastes to HW facilities and prohibit the disposal of certain types of waste in any facility, on landfill leachate chemistry?
5. How do leachate generation rates estimated using the EPA HELP computer model compare to actual leachate generation rates at modern operating facilities?
6. Do the HELP model simulations predict the same effects of site location and waste type on leachate generation rates as observed from the actual data?
7. What is the nature, frequency, and significance of identified problems in liner systems and cover systems for modern waste management facilities?
8. How can the identified problems be prevented in the future?

9. What overall conclusions can be drawn regarding the likely long-term performance of landfills?

Complete results from the first three tasks were incorporated into two appendices to this report. These appendices are:

- "Appendix E: Evaluation of Liquids Management Data for Double-Lined Landfills"; and
- "Appendix F: Waste Containment System Problems and Lessons Learned".

Summaries of Appendices E and F are presented below in Sections 5.2 and 5.3, respectively, of this report. Section 5.4 presents the results of the fourth task, an assessment of the appropriateness of the HELP model as a design tool. The HELP model is evaluated by comparing LCRS flow rate data for six landfill cells to leachate generation rates predicted for these cells from HELP model simulations with typical input parameters. Sections 5.2 through 5.4 also present the findings of the project with respect to the questions listed above. References are presented in Section 5.5.

5.1.2 Terminology

Waste containment systems for landfills consist of liner systems that underlay the wastes placed in them and cover systems constructed over the wastes (Figure 5-1). A liner system consists of a combination of one or more drainage layers and low-permeability barriers (liners). The functions of liners and drainage layers are complementary. Liners impede leachate percolation and gas migration out of a landfill and improve the collection capability of overlying drainage layers. Drainage layers collect and convey liquids on underlying liners to controlled collection points (sumps) and limit the buildup of hydraulic head on the liners. Most liner systems installed beneath modern landfills are classified as single-composite liner systems or double-liner systems and include the components illustrated in Figure 5-1. A single-composite liner system consists of a composite liner overlain by an LCRS drainage layer. A double-liner system consists of a primary liner and a secondary liner with an LDS drainage layer between the two liners and an LCRS drainage layer above the primary liner. The LCRS and LDS may also contain networks of perforated pipes, sumps, pumps, flowmeters, and other flow conveyance and monitoring components. A liner system may also include a protection layer over the LCRS drainage layer to further isolate the liner from the environment (e.g., freezing temperature, stresses from equipment).

Once an area of a landfill is filled to final grade, a cover system is constructed over the area to contain the waste, minimize the infiltration of water into the waste, and control the emissions of gases produced by waste decomposition or other mechanisms. A cover system consists of up to six basic components, from top to bottom: (i) surface layer; (ii) protection layer; (iii) drainage layer; (iv) barrier; (v) gas collection layer; and (vi) foundation layer. In some cases, the functions of several adjacent components can be

provided by one soil layer. For example, a sand gas collection layer may also serve as a foundation layer. Many modern landfills have a cover system consisting of a soil surface and protection layer, drainage layer, barrier, and gas collection layer.

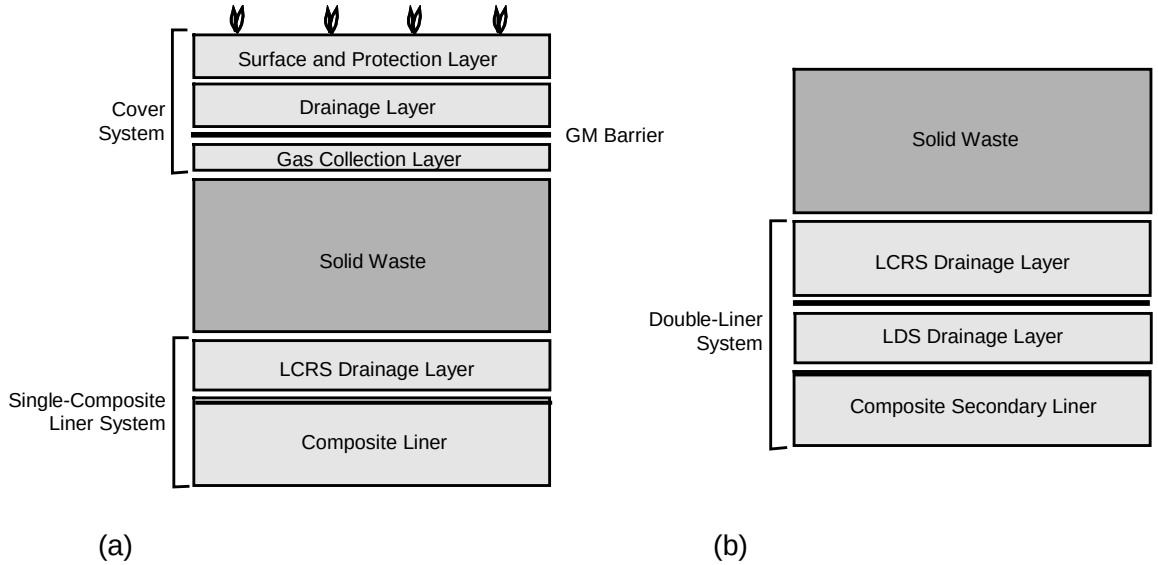

Figure 5-1. Typical waste containment system components for landfills: (a) single-composite liner system and cover system for a closed landfill; and (b) double-liner system for an active landfill.

In general, the materials used to construct liners and barriers in modern landfills are GMs alone and composites consisting of GMs overlying CCLs or GCLs (i.e., GM/CCL or GM/GCL composites). Drainage layers and gas collection layers are typically constructed with sand, gravel, GNs, or GCs. Protection layers typically consist of soil or thick GTs. The protection layer over the LCRS drainage layer sometimes consists of select waste. Surface layers for cover systems are typically constructed with vegetated topsoil.

Liner systems for modern MSW landfills and nonhazardous MSW combustor ash (MSW ash) landfills must, based on state-specific implementation of RCRA Subtitle D requirements, meet federal minimum design criteria or performance-based design requirements (40 CFR 258.40) as described in Section 1.2. Federal minimum design criteria require a single-composite liner system for new MSW landfills and MSW ash landfills. While the federal minimum design criteria were adopted by many states, a few states require that MSW landfills or MSW ash landfills have a double-liner system. For RCRA HW landfills, federal regulations (40 CFR 264.301) require a double-liner system with at least a GM primary liner and a GM/CCL secondary liner, as described in Section 1.2.

Cover systems for modern lined MSW landfills and MSW ash landfills (40 CFR 258.40) must meet federal minimum design criteria or performance-based design requirements (40 CFR 258.60), as described in Section 1.2. The cover system meeting federal minimum design criteria consists of a soil surface layer over a composite barrier. Cover systems for RCRA HW landfills must meet federal performance-based design requirements (40 CFR 264.310). There is not a federal minimum design criteria cover system for HW landfills; however, EPA guidance (EPA, 1989) recommends that the cover system for these landfills contain a soil surface and protection layer, drainage layer, and composite barrier, as described in Section 1.2.

There are currently no federal minimum design requirements for liner systems or cover systems for ISW landfills. ISW landfills contain such wastes as papermill sludge, coal ash, and construction and demolition waste (C&DW).

5.1.3 Data Collection Methodology

The landfill performance data presented in Appendices E and F and summarized in this chapter were obtained from the technical literature, engineering drawings, project specifications, as-built records, and operation records, and from discussions with facility owners, facility operators, design engineers, and federal and state regulators throughout the U.S. The data were collected in accordance with a quality assurance plan, which was reviewed and approved by the EPA. Efforts were made to obtain data from a wide variety of facilities with different waste types (i.e., MSW, MSW ash, HW, and ISW), site conditions, and waste containment system components. The study focused on landfills, and only information on landfills is summarized in this chapter. Based on the broad-based method of data collection for this study, it is believed that the data in this report are generally representative of landfills nationwide.

5.2 Evaluation of Liquids Management Data for Double-Lined Landfills

5.2.1 Scope of Work

The scope of work for this portion of the project consisted of the collection and analysis of liquids management data for 187 active or closed double-lined cells at 54 modern landfills located throughout the U.S. These data are typically required to be collected and reported to regulatory agencies as part of the permit conditions for a landfill. The data were used to evaluate: (i) leakage rates and hydraulic efficiencies of landfill primary liners; (ii) landfill leachate generation rates (LCRS flow rates), including how these flow rates vary with waste type, site location, and presence of cover system; and (iii) landfill leachate chemistry (LCRS flow chemistry), including how leachate chemistry varies with waste type, site location, and operation conditions, and whether federal solid waste regulations promulgated in the 1980's and early 1990's have had an effect on the quantity of potentially-toxic trace chemicals found in leachate.

5.2.2 Description of Database

The liquids management data and related data collected for the 187 landfill cells include: (i) general facility information (including location, average annual rainfall, subsurface soil types, groundwater separation distance from bottom of landfill); (ii) general cell information (including cell area, type of waste, height of waste, dates of construction, operation, and closure); (iii) double-liner system and cover system design details (including type, thickness, and hydraulic conductivity of each layer); (iv) LCRS flow rate and chemical constituent data; and (v) LDS flow rate and chemical constituent data. For comparison purposes, the data are sorted according to liner system type, waste type, and site geographic location (which is indicative of site climate). The full database is presented in Appendix E. The reader is referred to the following figures and tables in Appendix E for specific information:

- double-liner system types: Table E-1.1 and Figure E-1.1;
- geographic regions and site locations: Figure E-1.3;
- general facility information: Table E-3.1;
- general cell information: Table E-3.2;
- double-liner system design details: Table E-3.3;
- cover system design details: Table E-3.4;
- LCRS flow rate data: Table E-3.5;
- LDS flow rate data: Table E-3.6; and
- LCRS and LDS flow chemistry data: Table E-3.7.

The distributions of the landfill facilities and cells in the database by waste type and geographic region and by primary liner and LDS types are shown in Tables 5-1(a) and (b), respectively. From Table 5-1(a), most of the landfills in the database are located in the northeast (NE). This is not surprising because: (i) the NE has a relatively dense population; and (ii) double-liner systems are required for MSW landfills in several states in the NE. In addition, the majority of the landfills in the database are used for disposal of MSW. Based on the extent of the database and comparisons of these data with published data, discussed in Section E-2 of Appendix E, the database appears to adequately characterize conditions for MSW landfills in the NE and southeast (SE), HW landfills in the NE and SE, and MSW ash landfills in the NE. The database is quite sparse for landfills in the west (W), coal ash landfills, and C&DW landfills. Additional data from these facilities should be collected and evaluated.

From Table 5-1(b), most of the cells at most of the landfills have either a GM primary liner (37% of all cells) or GM/CCL or GM/GCL/CCL primary liner (48%). Fewer cells (15%) have a GM/GCL primary liner. About 48% of the cells have a sand or gravel LDS and 52% have a GN LDS. Based on the distribution of the data, the database appears to be representative of typical double-liner system designs in landfills.

Table 5-1(a). Distribution of Database by Waste Type and Geographic Region.

	Geographic Region		
Waste Type	*Northeast U.S.*	*Southeast U.S.*	*West U.S.*
MSW	24 landfills 71 cells	8 landfills 26 cells	1 landfill 2 cells
HW	5 landfills 26 cells	5 landfills 31 cells	3 landfills 10 cells
MSW Ash	5 landfills 12 cells	2 landfills 4 cells	0 landfills
Coal Ash	1 landfills 1 cell	0 landfills	0 landfills
C&DW	2 landfills 4 cells	0 landfills	0 landfills

Table 5-1(b). Distribution of Database by Primary Liner and LDS Types.

	LDS Type	
Primary Liner Type	*Sand or Gravel*	*GN*
GM	13 landfills 41 cells	11 landfills 28 cells
GM/GCL Composite	3 landfills 19 cells	4 landfills 9 cells
GM/CCL or GM/GCL/CCL Composite	13 landfills 31 cells	16 landfills 57 cells

Most of the liquids management data are for open cells; only about 23% of the cells in the database had received a cover system.

5.2.3 Data Interpretation

5.2.3.1 Landfill Development Stages

In evaluating LCRS and LDS flow rate and chemical constituent data for this report, three distinct landfill development stages were considered: (i) the “initial period of operation”; (ii) the “active period of operation”; and (iii) the “post-closure period”. These stages are defined by the waste filling and capping rates of a landfill cell and are described below. The *initial period of operation* occurs during the first few months after the start of waste disposal in a cell. During this stage, there is not sufficient waste in a cell to significantly impede the flow of rainfall into the LCRS. To the extent rainfall occurs during this stage, it will rapidly find its way into the LCRS. LCRS flow rates during this stage are usually controlled by rainfall and can be directly correlated to local climatic conditions. LCRS flow rates are higher at landfills in wetter climates than at those in arid climates. During the *active period of operation*, the cell is progressively

filled with waste and daily and intermediate layers of cover soil. As waste placement continues, more of the rainfall occurring during this stage falls onto the waste and cover soils rather than directly onto the liner system. As a consequence, the LCRS flow rates decrease and eventually stabilize. LCRS flow rates during this stage are generally dependent on rainfall, waste thickness, waste properties (i.e., initial moisture content, field capacity, and permeability), and storm-water management practices. During the *post-closure period*, the cell has been closed with a cover system that further reduces infiltration of rainfall into the waste, resulting in further reduction in LCRS flow rates. LCRS and LDS flows associated with these three development stages are illustrated for a MSW landfill in Pennsylvania in Figure 5-2.

5.2.3.2 Primary Liner Leakage Rates and Hydraulic Efficiencies

LCRS and LDS flow data were interpreted to assess primary liner leakage rates and/or apparent efficiencies for the following:

- GM primary liners by development stage, LDS type, and use of CQA;
- GM/GCL primary liners by development stage and LDS type; and
- GM/CCL primary liners by development stage.

The data were first assessed using a methodology presented by Gross et al. (1990) for using LCRS and LDS flow data to evaluate the performance of primary liners in terms of primary liner leakage. The basic approach involves the evaluation of LCRS and LDS flow rate and chemical constituent data to quantify that portion of LDS flow that is attributable to primary liner leakage as opposed to other sources. Other sources of LDS flow include: (i) water (mostly rainwater) that infiltrates the LDS during construction and continues to drain to the LDS sump after the start of facility operation ("construction water"); (ii) water that infiltrates the LDS during construction, is held in the LDS by capillary tension, and is expelled from the LDS during waste placement as a result of LDS compression under the weight of the waste ("compression water"); (iii) water expelled into the LDS from any CCL and/or GCL components of a composite primary liner as a result of clay consolidation under the weight of the waste ("consolidation water"); and (iv) water that percolates through the secondary liner and infiltrates the LDS ("infiltration water"). The sources of LDS flow are illustrated in Figure 5-3. Evaluation of the potential flow rates and times of occurrence of each of these potential sources of flow were made using the calculations procedures contained in Gross et al. (1990). That portion of LDS flow attributable to leakage through the composite primary liner of a double-liner system would be leakage into the ground for a single-composite liner system if the two composite liners have similar characteristics. Extrapolation of primary liner performance levels to the secondary liner of a double-liner system enables inferences to be drawn regarding performance of the entire double-liner system.

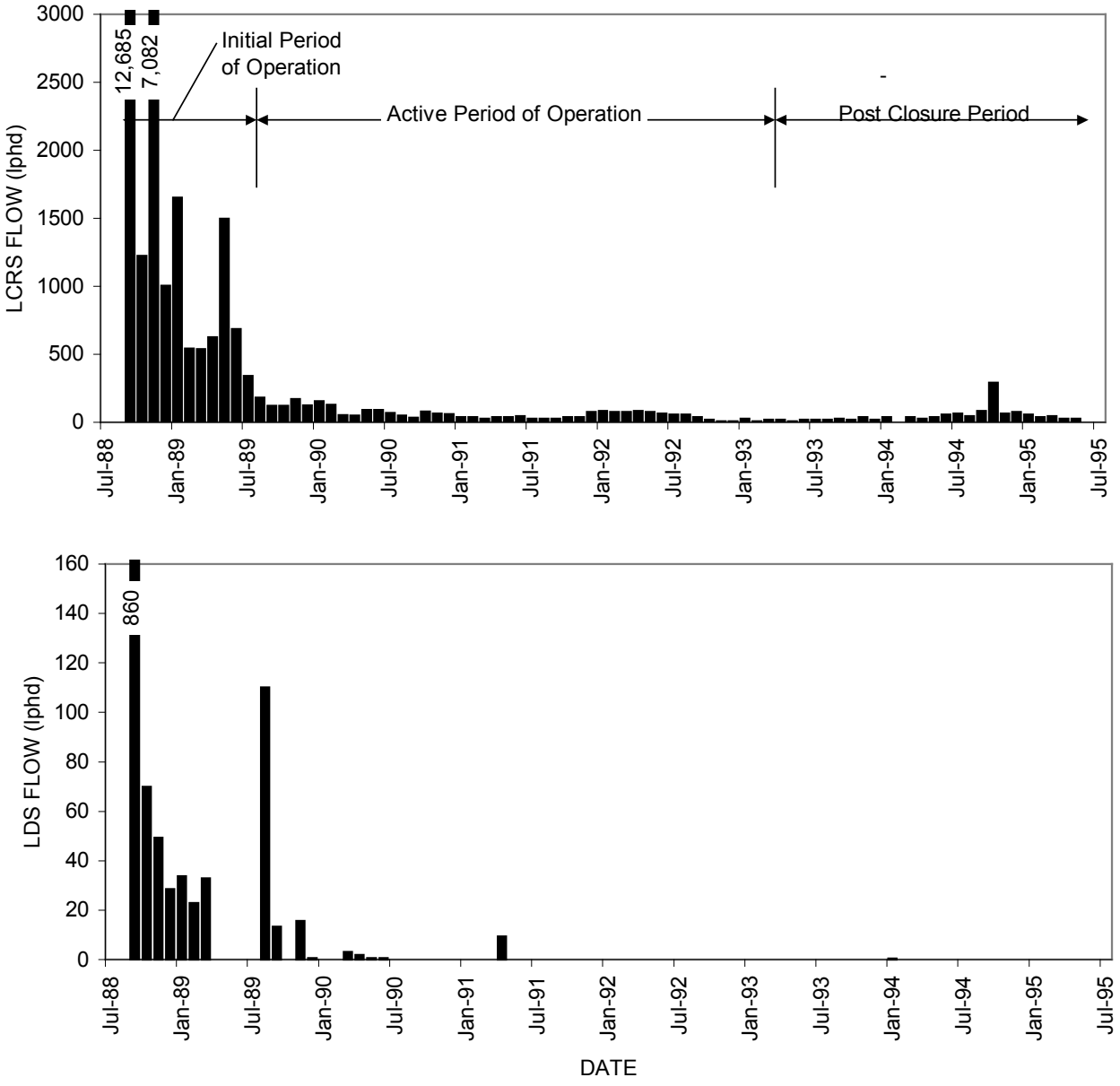

Figure 5-2. LCRS and LDS flow rates over time at a MSW landfill in Pennsylvania. (Flow rates are given in liters/hectare/day (lphd).)

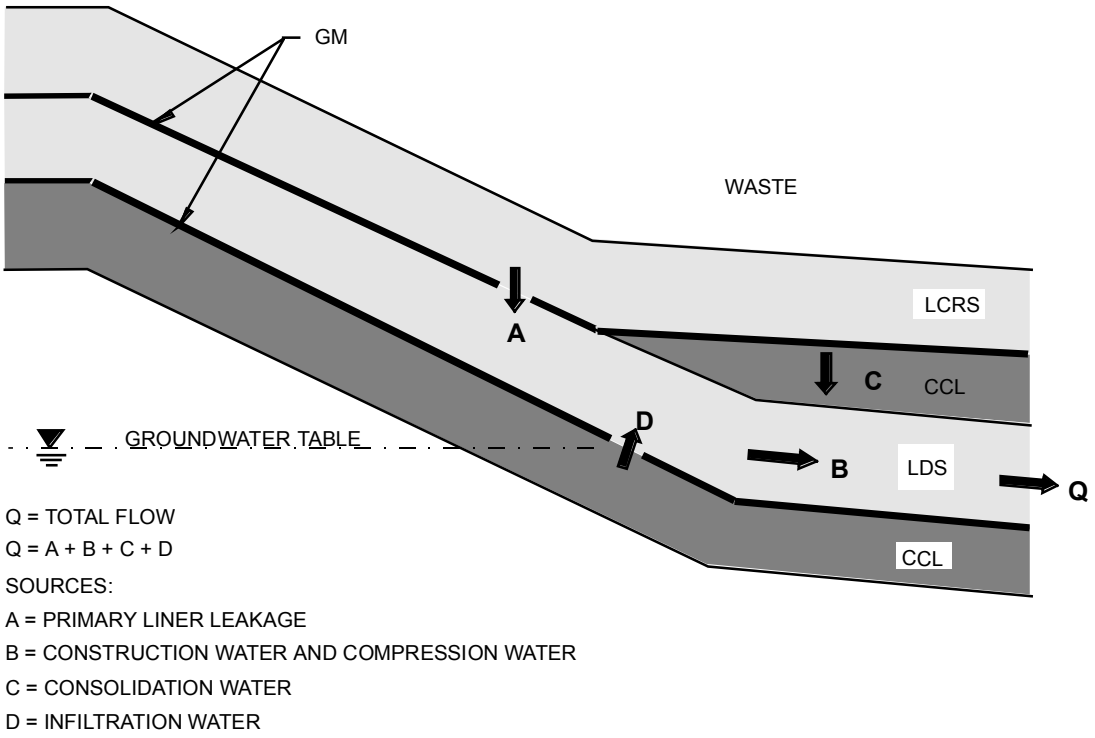

Figure 5-3. Sources of flow from LDSs (from Bonaparte and Gross, 1990).

The relative performances of the different types of primary liners were then evaluated using the “apparent liner hydraulic efficiency” parameter, E_a, introduced by Bonaparte et al. (1996) and defined as:

$$E_a\,(\%) = (1 - \text{LDS Flow Rate/LCRS Flow Rate}) \times 100 \qquad \text{(Eq. 5-1)}$$

The higher the value of E_a, the smaller the flow rate from an LDS compared to the flow rate from an LCRS. The value of E_a may range from 0 to 100%, with a value of zero corresponding to an LDS flow rate equal to the LCRS flow rate and a value of 100% indicating no flow from the LDS. The parameter E_a is referred to as an "apparent" hydraulic efficiency because, as described above, flow into the LDS sump of a landfill may be due to sources other than primary liner leakage (Figure 5-3). The value of E_a is calculated using total flow into the LDS, regardless of source. If the only source of flow into the LDS sump is primary liner leakage, then Equation 5-1 provides the "true" liner hydraulic efficiency, E_t. True liner efficiency provides a measure of the effectiveness of a particular liner in limiting or preventing advective transport across the liner. For example, if a liner is estimated to have an E_t value of 99%, the rate of leakage through the primary liner would be assumed to be 1% of the LCRS flow rate. The true efficiency of a liner is not constant but rather a function of the hydraulic head in the LCRS and size of the area over which LCRS flow is occurring (the area is larger at high flow rates

compared to low flow rates). The true efficiency of a liner is also a function of design: identical liners overlain by different LCRSs or placed on different slopes will exhibit different E_t values. Also, the efficiency of a liner for a given set of hydraulic conditions could change over time if the physical condition of the liner changes. For example, time-dependent changes in GMs could result from chemical degradation or stress cracking under certain conditions. Time-dependent changes in CCLs or GCLs could result from chemical degradation, consolidation, or other factors. Notwithstanding all of these limitations, the hydraulic efficiency concept has been found useful in characterizing liner hydraulic performance.

The methodology described above was used to evaluate the hydraulic performance of GM primary liners and GM/GCL composite primary liners. Chemical constituent data were not utilized in the evaluation of these types of liners because the initial hydraulic assessment (i.e., comparing LCRS and LDS flow rates) yielded significant insight into these liners' true hydraulic efficiencies. However, the situation was found to be more complicated for GM/CCL and GM/GCL/CCL composite primary liners due the generation of consolidation water by these liners not only during the initial period of operation, but also during the active and post-closure periods. The performance evaluation of these liners included the additional step of comparing the chemistry of LCRS and LDS liquids to assess whether the liquids had different primary sources (i.e., leachate for LCRS liquids and CCL pore water for LDS liquids). The concentrations of five key chemical constituents (i.e., the inorganic anions sulfate and chloride and the aromatic hydrocarbons benzene, toluene, and xylene) in the LCRS and LDS flows were compared in more detail to further assess whether primary liner leakage had contributed to LDS flows.

It is noted that the presence of chemical constituents in the LDS was evaluated empirically. Therefore, the concentrations of chemicals collected in the LDS were directly compared to concentrations of the same chemicals collected in the LCRS. No fate and transport analysis was performed that accounts for attenuation of the LCRS chemicals migrating through the primary liner CCL. However, to overcome the need to perform such an analysis, the five key chemical constituents were selected based on their high solubility in water, low octanol-water coefficient, high resistance to hydrolization, and high resistance to anaerobic biodegradation in soil.

5.2.3.3 Leachate Generation Rates

LCRS flow rate data were interpreted in terms of average and peak monthly leachate generation rates for the following:

- MSW landfills by geographic region and development stage;
- HW landfills by geographic region and development stage;
- ash (i.e., coal ash and MSW ash) landfills by geographic region and development stage; and

- C&DW landfills by development stage.

The data were also used to evaluate the ratios of average LCRS flow rates to historical average annual rainfalls by waste type, geographic region, and development stage.

5.2.3.4 Leachate Chemistry

Data on leachate chemical constituents were interpreted in terms of the average concentrations and detection frequencies (i.e., were the chemicals detected in 50% or less of the samples or more than 50% of the samples) of 30 representative chemical parameters. These data were then used to assess the following:

- effect of waste type on leachate chemistry; and
- effect of federal solid waste regulations of the 1980's and early 1990's on leachate chemistry (i.e., has the amount of trace toxic inorganic and synthetic organic chemicals in leachate decreased).

The 30 representative chemical parameters consist of water quality indicator parameters (e.g., pH, specific conductance, total dissolved solids (TDS), etc.), major inorganic cations and anions (e.g., calcium, chloride, sulfate, etc.), trace metals (e.g., arsenic, chromium, lead, etc.), and volatile organic compounds (VOCs) (e.g., benzene, methylene chloride, trichloroethylene, etc.). The specific trace metals and VOCs were chosen for this study because these metals and VOCs are sometimes found in leachates from MSW, HW, and ISW landfills. They were also selected based on availability of parameters between landfills, frequency of detection, and concentration.

It is recognized that the leachate chemistry database is limited in terms of completeness and duration of monitoring. In addition, key MSW and HW leachate constituents, such as alcohols and ketones, are poorly represented in the database and, thus, could not be included in the list of select parameters. It is important that these additional data be collected so that our understanding of leachate chemistry can continue to improve. The chemical data presented herein are intended to be representative, not comprehensive. The data should not be considered complete for purposes of evaluating potential human health or ecological impacts.

5.2.4 Evaluation Results

5.2.4.1 Primary Liner Leakage Rates and Hydraulic Efficiencies

GM Liners

The performance of 31 of the 69 cells with GM primary liners was assessed. The remaining 38 cells with GM primary liners were excluded from the assessment primarily because they do not have continuous LCRS and LDS flow rate data available for an individual cell from the start of operation and for a significant monitoring period. Flow rate data are available for the considered 31 cells at 14 landfills with monitoring periods

of up to 114 months. Twenty-five cells have a HDPE GM primary liner, and the remaining six cells have a chlorosulfonated polyethylene (CSPE) GM primary liner. A formal CQA program was used in the construction of 23 of the 25 cells with an HDPE GM primary liner. To the best of the authors' knowledge, none of the cells received electrical leak location surveys or ponding tests as part of the CQA program. The remaining two cells with an HDPE GM primary liner (i.e., F1 and K1) and the six cells with a CSPE GM primary liner (i.e., B1, B2, and E1 to E4) were all constructed without CQA. A summary of the LCRS and LDS flow rate data for the 31 cells is provided in Table 5-2, and detailed results are given in Figure E-4.1 and Tables E-4.3 through E-4.5 of Appendix E. The major findings from the data evaluation of cells with GM primary liners are given below:

- LDS flows during the initial period of operation are attributed primarily to construction water and primary liner leakage. LDS flows during the active and post-closure periods are attributed primarily to primary liner leakage.
- Average monthly LDS flow rates for cells constructed with a formal CQA program ranged from about 5 to 440 lphd during the initial period of operation, 1 to 360 lphd during the active period, and 2 to 60 lphd during the post-closure period. Peak monthly flow rates for these cells were typically below 500 lphd and exceeded 1,000 lphd in only two of the 23 cells.
- Based on an analysis of the available data, average monthly active-period LDS flow rates for cells with HDPE GM primary liners constructed with CQA will often be less than 50 lphd, but occasionally in excess of 200 lphd. These flows are attributable primarily to liner leakage and, for cells with sand LDSs, possible construction water.
- The eight cells constructed without a formal CQA program exhibited average monthly LDS flow rates about one to two orders of magnitude greater than LDS flow rates for cells constructed with CQA. The average flow rates from the eight cells ranged from 120 to 2,140 during the initial period of operation, 70 to 1,600 lphd during the active period, and, for the two cells for which post-closure data are available, 210 to 240 lphd during the post-closure period. The large differences in LDS flow rates between cells constructed with CQA and cells constructed without CQA are partly attributed to the benefits of CQA and partly due to differences in the GM materials and construction (i.e., seaming) methods. The two cells that had HDPE GM primary liners and no formal CQA had average LDS flow rates that are about two to seven times greater than the mean LDS flow rate for all cells constructed with a formal CQA program. In contrast, the cells with CSPE GM primary liners and no formal CQA exhibited average LDS flow rates that are about one to two orders of magnitude greater than the mean LDS flow rate for all cells that had CQA. There are not sufficient data in this appendix, however, to accurately separate the effects of CQA and GM type (i.e., HDPE vs. CSPE) and construction methods on leakage rates through GM liners.
- Based on an analysis of the available data, GM liners can be constructed to achieve very good hydraulic performance (i.e. E_t values greater than 99%). However, even when constructed with a CQA program, GM liners sometimes

Table 5-2. Summary of LCRS and LDS Flow Rate Data for Landfill Cells with GM Top Liners.

Cell No.	Cell Area (hectare)	Start of Waste Place. (month-year)	End of Final Closure (month-year)	Initial Period of Operation[1]						Active Period of Operation[2]						Post-Closure Period[3]					
				Time Period (months)	LCRS Flow[4] Avg. (lphd)	LCRS Flow Peak (lphd)	LDS Flow Avg. (lphd)	LDS Flow Peak (lphd)	E_{am} (%)	Time Period (months)	LCRS Flow Avg. (lphd)	LCRS Flow Peak (lphd)	LDS Flow Avg. (lphd)	LDS Flow Peak (lphd)	E_{am} (%)	Time Period (months)	LCRS Flow Avg. (lphd)	LCRS Flow Peak (lphd)	LDS Flow Avg. (lphd)	LDS Flow Peak (lphd)	E_{am} (%)
B1	3.3	5-84	11-88	1-19	ND[5]	ND	ND	ND		20-31	2,245	5,754	266	499	88.14	55-66	317	670	106	222	66.48
										32-43	5,223	6,845	424	808	91.87	67-78	703	1,877	267	1,134	62.02
										44-54	3,975	7,464	892	1,426	77.55	79-90	1,146	1,956	279	451	75.64
																91-102	1,306	1,943	326	612	75.01
																103-114	510	718	74	97	85.41
B2	3.5	5-84	11-88	1-19	ND	ND	ND	ND		20-31	2,732	5,393	404	605	85.20	55-66	493	1,040	154	393	68.83
										32-43	3,740	5,707	996	1,690	73.36	67-78	337	654	328	514	2.80
										44-54	2,337	3,982	665	1,102	71.54						
C1	3.2	5-90	NA[5]	1-9	ND	ND	ND	ND		10-21	789	1,419	123	304	84.40	NA	NA	NA	NA	NA	
										22-33	259	780	89	170	65.52						
										34-45	159	286	27	128	83.08						
										46-56	103	200	40	227	61.27						
C2	3.7	4-91	NA	1-12	1,475	2,585	92	398	93.74	13-24	435	859	9	31	98.03	NA	NA	NA	NA	NA	
										25-36	300	610	22	125	92.71						
										37-45	161	464	7	14	95.40						
C3	3.6	8-91	NA	1-8	3,417	9,558	63	268	98.16	9-20	311	671	2	9	99.49	NA	NA	NA	NA	NA	
										21-32	314	752	33	276	89.56						
										33-41	268	987	16	103	94.02						
C4	3.7	2-92	NA	1-4	14,828	41,331	178	265	98.80	5-16	937	2,055	70	147	92.52	NA	NA	NA	NA	NA	
										17-28	438	622	51	92	88.39						
										29-35	407	686	26	29	93.71						
C5	2.6	11-92	NA	1-12	6,419	12,528	23	40	99.64	13-26	2,513	10,440	28	115	98.88	NA	NA	NA	NA	NA	
D1	0.4	10-85	5-86	1-7	ND	ND	32	80		NA	NA	NA	NA	NA		8-19	ND	ND	102	886	
																20-26	ND	ND	1	10	
																27-38	376	1,455	5	70	98.58
																39-50	715	1,352	64	156	91.05
D3	0.3	7-87	NA	1-12	20,292	51,265	12	56	99.94	13-24	13,003	44,895	7	73	99.95	NA	NA	NA	NA	NA	
										25-28	1,010	2,413	283	341	71.97						
D4	0.4	1-89	NA	1-11	31,281	120,527	233	801	99.25	NA	NA	NA	NA	NA		NA	NA	NA	NA	NA	

Table 5-2. Summary of LCRS and LDS Flow Rate Data for Landfill Cells with GM Top Liners (cont.).

Cell No.	Cell Area	Start of Waste Place.	End of Final Closure	Initial Period of Operation[1]						Active Period of Operation[2]						Post-Closure Period[3]					
				Time	LCRS Flow[4]		LDS Flow		E_{am}	Time	LCRS Flow		LDS Flow		E_{am}	Time	LCRS Flow		LDS Flow		E_{am}
				Period	Avg.	Peak	Avg.	Peak	(%)	Period	Avg.	Peak	Avg.	Peak	(%)	Period	Avg.	Peak	Avg.	Peak	(%)
	(hectare)	(month-year)	(month-year)	(months)	(lphd)	(lphd)	(lphd)	(lphd)		(months)	(lphd)	(lphd)	(lphd)	(lphd)		(months)	(lphd)	(lphd)	(lphd)	(lphd)	
E1	2.4	3-88	NA	1-7	ND	ND	2,144	5,026		8-19	8,432	19,614	1,436	3,069	82.97	NA	NA	NA	NA	NA	
										20-31	11,521	36,164	1,051	1,915	90.88						
										32-40	6,525	13,075	743	1,015	88.61						
E2	2.4	10-87	NA	1-12	ND	ND	483	3,518		13-24	5,821	10,445	802	2,447	86.22	NA	NA	NA	NA	NA	
										25-36	4,547	11,014	685	1,404	84.93						
										37-45	4,434	6,830	596	999	86.56						
E3	1.2	5-90	NA	1-12	9,425	25,394	1,595	1,951	83.08	13-14	6,062	9,038	1,603	1,758	73.56	NA	NA	NA	NA	NA	
E4	1.2	7-90	NA	1-12	20,148	55,785	996	2,362	95.06	NA	NA	NA	NA	NA		NA	NA	NA	NA	NA	
F1	1.8	7-92	NA	1-12	14,472	45,010	124	479	99.14	13-24	9,000	25,450	66	83	99.27	NA	NA	NA	NA	NA	
										25-30	7,826	10,932	67	77	99.15						
G1	3.0	6-89	NA	1-12	22,371	46,120	ND	ND		13-24	12,893	23,485	ND	ND		NA	NA	NA	NA	NA	
										25-36	3,438	11,652	156	238	95.47						
										37-42	8,356	10,303	101	116	98.79						
										43-51	ND	ND	121	384							
										52-63	ND	ND	74	139							
										64-67	ND	ND	49	64							
G2	1.6	6-89	NA	1-12	22,371	46,120	197	645	99.12	13-24	12,893	23,485	37	65	99.71	NA	NA	NA	NA	NA	
										25-36	3,438	11,652	35	42	98.98						
										37-42	8,356	10,303	60	100	99.28						
I1[6]	3.2/2.7[7]	8-87	10-94	1-5	ND	ND	234	508		9-15	16,224	48,932	5	18	99.97	85-93	800	1,794	62	119	92.25
				6-8	ND	ND	ND	ND		16-32	ND	ND	ND	ND							
										33-44	7,167	22,020	10	44	99.86						
										45-48	231	332	4	10	98.49						
										49-54	ND	ND	ND	ND							
										55-66	624	1,580	2	5	99.68						
										67-78	541	752	13	42	97.60						
										79-84	904	1,827	79	157	91.26						
I2[6]	4.2/2.3[7]	10-87	10-94	1-7	6,627	13,959	31	77	99.53	8-24	ND	ND	ND	ND		77-85	800	1,794	2	4	99.71
										25-36	1,030	3,241	5	35	99.52						
										37-40	427	1,054	6	11	98.67						
										41-46	ND	ND	ND	ND							
										47-58	624	1,580	8	37	98.67						
										59-70	541	752	8	23	98.54						
										71-76	904	1,827	5	6	99.49						

Table 5-2. Summary of LCRS and LDS Flow Rate Data for Landfill Cells with GM Top Liners (cont.).

Cell No.	Cell Area	Start of Waste Place.	End of Final Closure	Initial Period of Operation[1]						Active Period of Operation[2]						Post-Closure Period[3]					
				Time Period	LCRS Flow[4]		LDS Flow		E_{am}	Time Period	LCRS Flow		LDS Flow		E_{am}	Time Period	LCRS Flow		LDS Flow		E_{am}
					Avg.	Peak	Avg.	Peak			Avg.	Peak	Avg.	Peak			Avg.	Peak	Avg.	Peak	
	(hectare)	(month-year)	(month-year)	(months)	(lphd)	(lphd)	(lphd)	(lphd)	(%)	(months)	(lphd)	(lphd)	(lphd)	(lphd)	(%)	(months)	(lphd)	(lphd)	(lphd)	(lphd)	(%)
I3[6]	3.4/1.8[7]	4-88	10-94	1-7	11,559	21,081	37	87	99.68	8-24	ND	ND	ND	ND		77-85	800	1,794	3	12	99.57
										25-36	11,684	26,339	7	23	99.94						
										37-40	2,464	4,666	5	8	99.80						
										41-46	ND	ND	ND	ND							
										47-58	624	1,580	4	17	99.39						
										59-70	541	752	13	55	97.64						
										71-76	904	1,827	17	53	98.14						
K1	2.7	12-89	NA	1-12	17,808	24,832	122	163	99.31	13-24	12,929	27,663	88	180	99.32	NA	NA	NA	NA	NA	
										25-36	10,879	17,683	76	104	99.30						
										37-48	6,155	11,331	514	892	91.64						
										49-60	5,952	8,024	349	495	94.14						
										61-66	9,494	12,245	282	378	97.03						
N2	6.3	1-92	NA	1-12	ND	ND	ND	ND		13-19	4,547	5,741	113	468	97.52	NA	NA	NA	NA	NA	
										20-31	2,561	3,460	203	669	92.08						
										32-34	6,399	7,274	786	1,058	87.72						
										35-39	2,741	3,170	201	406	92.65						
O1[8]	4.2	9-88	NA	1-6	ND	ND	293	620		7-18	4,407	9,826	0	3	99.99	NA	NA	NA	NA	NA	
										19-30	4,023	13,231	3	7	99.93						
										31-42	7,089	16,467	0	5	99.99						
										43-54	6,201	12,561	1	6	99.98						
										55-64	8,661	15,327	3	9	99.97						
O2[8]	4.9	3-89	NA	1-12	4,407	9,826	6	24	99.86	13-24	4,023	13,231	2	5	99.95	NA	NA	NA	NA	NA	
										25-36	7,089	16,467	1	4	99.98						
										37-48	6,201	12,561	3	11	99.96						
										49-59	8,661	15,327	1	5	99.99						
S1	2.0	9-90	NA	1-10	2,226	5,081	12	39	99.45	11-22	653	1,220	38	68	94.18	NA	NA	NA	NA	NA	
										23-28	ND	ND	ND	ND							
										29-40	1,571	4,074	8	26	99.51						
										41-45	1,086	2,067	4	7	99.64						
S2	1.6	8-90	NA	1-9	2,185	4,650	5	24	99.78	10-17	654	1,135	5	24	99.20	NA	NA	NA	NA	NA	
										18-33	ND	ND	ND	ND							
										34-46	1,255	3,638	5	8	99.63						

Table 5-2. Summary of LCRS and LDS Flow Rate Data for Landfill Cells with GM Top Liners (cont.).

Cell No.	Cell Area	Start of Waste Place.	End of Final Closure	Initial Period of Operation[1]						Active Period of Operation[2]						Post-Closure Period[3]					
				Time	LCRS Flow[4]		LDS Flow		E_{am}	Time	LCRS Flow		LDS Flow		E_{am}	Time	LCRS Flow		LDS Flow		E_{am}
				Period	Avg.	Peak	Avg.	Peak	(%)	Period	Avg.	Peak	Avg.	Peak	(%)	Period	Avg.	Peak	Avg.	Peak	(%)
	(hectare)	(month-year)	(month-year)	(months)	(lphd)	(lphd)	(lphd)	(lphd)		(months)	(lphd)	(lphd)	(lphd)	(lphd)		(months)	(lphd)	(lphd)	(lphd)	(lphd)	
V1[8]	4.2	1-90	NA	1-10	13,622	49,828	117	153	99.14	NA	NA	NA	NA	NA		NA	NA	NA	NA	NA	
V2[8]	3.9	1-90	NA	1-10	13,622	49,828	135	256	99.01	NA	NA	NA	NA	NA		NA	NA	NA	NA	NA	
W1	15.4	5-92	NA	1-8	ND	ND	ND	ND		13-24	2,693	6,365	34	109	98.72	NA	NA	NA	NA	NA	
				9-12	7,492	8,799	439	765	94.14	25-35	943	1,572	19	44	97.98						
W2	15.4	5-92	NA	1-8	ND	ND	ND	ND		9-20	4,288	9,389	594	1,826	86.15	NA	NA	NA	NA	NA	
										21-32	4,813	10,524	204	1,217	95.76						
										33-35	719	2,141	32	52	95.50						
X1	3.0	8-92	NA	1	111,031	111,031	364	364	99.67	8-19	5,926	14,315	5	45	99.92	NA	NA	NA	NA	NA	
				2-7	32,469	104,645	4	25	99.99	20-33	2,188	5,376	0	2	99.99						

Notes:

(1) "Initial Period of Operation" represents period after waste placement has started and not more than a few lifts of waste and daily cover have been placed in the cell (i.e., no intermediate cover).

(2) "Active Period of Operation" represents period when waste thickness in cell is significant and/or an effective intermediate cover is placed on the waste.

(3) "Post-Closure Period" represents period after final cover system has been placed on the entire cell.

(4) Flow rates are given in liter/hectare/day.

(5) NA = not applicable; ND = not determined.

(6) LCRS for Cells I1, I2, and I3 are combined after February 1992. The measure average flow rates are assumed to represent flow rates for the three cells.

(7) Values given represent LCRS and LDS areas, respectively.

(8) LCRS flows are combined for Cells O1 and O2 and for Cells V1 and V2. Measured average flow rates are assumed to represent flows for the two cells at each landfill.

will not achieve this performance level and lower E_t values, in the range of about 90 to 99%, will occur. This relatively broad range of E_t values is a consequence of the potential for even appropriately installed GMs to have an occasional small hole, typically due to an imperfect seam, but also potentially due to a manufacturing or construction-induced defect not identified by the CQA program. Leakage can occur, relatively unimpeded, through a GM hole if the GM is not underlain by a low-permeability material such as a CCL or GCL. If a hole occurs at a critical location where a hydraulic head exists, such as in a landfill sump, the leakage rate through the hole can be significant. In contrast, the GCL or CCL component of a composite liner can impede flow through a GM hole, even if it occurs at a critical location.

- The conclusion to be drawn from the above data evaluation is that single liner systems with GM liners (installed on top of a relatively permeable subgrade) should not be used in applications where E_t values as low as 90% would be unacceptable, even if a thorough CQA program is employed. In these cases, single-composite liner systems or double-liner systems should be utilized. An exception to this conclusion may be made for certain facilities, such as surface impoundments or small, shallow landfill cells, with GM primary liners that can be field tested over the GM sheet and seams using electrical leak location surveys, ponding tests, or other methods. For these facilities, higher efficiencies (i.e., greater than 99%) may be achieved with GM liners by identifying and repairing the GM holes during construction and, especially for surface impoundments, during operation. In all cases, GM liners should be manufactured and installed using formal quality assurance programs.

GM/GCL Composite Liners

The performance of all 28 cells with GM/GCL composite primary liners was assessed. Flow rate data are available for the 28 cells at seven landfills with monitoring periods of up to 83 months. All of these cells were constructed with formal CQA programs. A summary of the LCRS and LDS flow rate data for the cells is provided in Table 5-3 and detailed results are given in Table E-4.10 of Appendix E. The major findings from the data evaluation of cells with GM/GCL primary liners (excluding cell I4, which may have surface-water infiltration into the LDS at the anchor trench) are given below:

- LDS flows during the initial period of operation are attributed primarily to construction water. LDS flows during the active and post-closure periods are attributed primarily to primary liner leakage and compression water.
- Average monthly LDS flow rates ranged from about 0 to 290 lphd during the initial period of operation, 0 to 11 lphd during the active period, and 0 to 2 lphd (with many values reported as zero) during the post-closure period. Peak monthly flow rates were typically below 200 lphd and exceeded 500 lphd in only four of the 28 cells.
- Based on the above data, average monthly active-period LDS flow rates attributable to leakage through GM/GCL primary liners constructed with CQA will often be less than 2 lphd, but occasionally in excess of 10 lphd.

Table 5-3. Summary of LCRS and LDS Flow Rate Data for Landfill Cells with GM/GCL Composite Primary Liners.

Cell No.	Cell Area	Waste Place. Start Date	Final Closure Date	Initial Period of Operation[1]						Active Period of Operation[2]						Post-Closure Period[3]					
				Time Period[6]	LCRS Flow[4]		LDS Flow		Ea	Time Period[6]	LCRS Flow		LDS Flow		Ea	Time Period[6]	LCRS Flow		LDS Flow		Ea
	(ha)			(months)	Avg. (lphd)	Peak (lphd)	Avg. (lphd)	Peak (lphd)		(months)	Avg. (lphd)	Peak (lphd)	Avg. (lphd)	Peak (lphd)		(months)	Avg. (lphd)	Peak (lphd)	Avg. (lphd)	Peak (lphd)	
C6	3.6	Aug-93	NA	1-10	3,273	12,155	178	823	94.57	11-17	393	1,403	3	15	99.29						
I4	4.7	May-92	Jul-94	1-12	4,494	17,251	24	70	99.47	13-26	2,041	4,282	26	142	98.73	27-36	567	1389	59	133	89.59
I5	4.7	Jul-92	May-94	1-12	3,938	7,985	2	11	99.95	13-21	3,108	11,669	11	54	99.65	22-34	189	779	2	8	98.78
AW1	2.4	May-93	NA	1-12	6,358	20,570	131	524	97.94												
AW2	2.4	Aug-93	NA	1-10	3,553	7,480	290	514	91.84												
AX1	2.0	Jul-88	Feb-91	1-2	16,718	19,738	0	0	100	3-33	540	2,383	0	0	100	34-83	66	94	0	0	100
AX2	2.0	Jul-88	Feb-91	1-5	15,521	58,671	15	45	99.90	6-33	281	570	2	21	99.33	34-83	178	421	0	0	100
AX3	1.7	Sep-88	Apr-93	1-5	3,366	7,985	35	151	98.97	6-56	307	1,075	4	47	98.78	57-81	206	458	1	10	99.55
AX4	1.7	Sep-88	Apr-93	1-12	2,534	12,688	101	860	96.01	13-56	75	187	1	13	98.75	57-81	47	84	0	0	100
AX5	2.8	Oct-88	NA[5]	1-11	1,384	3,394	37	92	97.30	12-80	56	191	2	37	96.67						
AX6	3.9	Dec-88	NA	1-9	3,759	7,171	53	93	98.58	10-80	168	655	0	0	100						
AX7	2.6	Feb-89	NA	1-10	5,376	12,155	34	47	99.37	11-76	234	851	2	9	99.20						
AX8	3.8	Jul-89	NA	1-14	4,881	21,038	48	189	99.02	15-71	439	1,384	0	0	100						
AX9	3.3	Dec-89	NA	1-9	1,047	3,478	1	7	99.91	10-65	41	159	0	0	100						
AX10	3.9	Jul-90	NA	1-7	2,786	13,698	0	0	100	8-59	374	645	0	0	100						
AX11	3.0	Feb-90	NA	1-16	4,675	14,586	0	0	100	17-62	150	337	0	0	100						
AX12	4.0	Oct-90	NA	1-12	3,494	8,836	0	0	100	13-56	803	3,029	0	0	100						
AX13	3.0	Jan-91	NA	1-7	6,683	14,343	0	0	100	8-53	1,408	9,294	0	0	100						
AX14	2.8	Apr-91	NA	1-11	2,777	6,582	0	0	100	12-38	281	449	0	0	100						
AX15	2.8	May-92	NA	1-12	5,573	11,809	0	0	100	13-37	299	561	0	0	100						
AX16	4.5	Jan-93	NA	1-10	8,601	17,756	0	0	100	11-29	819	5,096	0	0	100						
AY1	1.3	Oct-94	NA	1-9	6,803	12,439	0	0	100												
AY2	1.0	Aug-94	NA	1-11	10,964	23,914	3	12	99.97												
AY3	1.0	Aug-94	NA	1-11	12,198	32,326	6	28	99.95												
AZ1	3.8	Dec-92	NA	2-12	4,093	5,219	0	0	100	13-31	3,473	5,054	2	22	99.94						
BB1	4.0	Feb-91	NA	1-6	10,378	22,130	15	65	99.86	7-47	2,494	8,983	6	25	99.78						
BB2	2.4	Jan-93	NA	1-11	ND[5]	ND	1	12		12-23	5,422	14,042	0	0	100						
BB3	2.8	Jan-93	NA	1-11	ND	ND	0	0		12-23	2,284	7,945	0	1	100						

Notes:

(1) "Initial Period of Operation" represents period after waste placement has started and only a small amount of waste has been placed in the cell.

(2) "Active Period of Operation" represents period when waste thickness in cell is significant and/or an effective intermediate cover is placed on the waste.

(3) "Post Closure Period" represents period after final cover system has been placed on the entire cell.

(4) Flow rates are given in liter/hectare/day.

(5) NA = not applicable; ND = not determined.

(6) Breakthrough time for steady-state saturated flow through GCL component of composite liner is estimated to be 2 months based on a calculation using Darcy's equation and a saturated hydraulic conductivity of 5×10^{-11} m/s, hydraulic gradient of 5, and effective porosity of 0.2. For this calculation, it is assumed that flow through the GM component of the composite liner occurs through small holes and is instantaneous.

The above data indicate that GM/GCL composite liners can be constructed to achieve E_t values of 99.9% or more. However, E_t values in the range of 99 to 99.9% will also occur. These high efficiencies demonstrate that the GCL component of a GM/GCL composite liner is effective in impeding leakage through holes in the GM component of the liner.

GM/CCL and GM/GCL/CCL Composite Liners

The performance of 13 of the 88 cells with GM/CCL or GM/GCL/CCL primary liners was assessed. The remaining 75 cells with GM/CCL or GM/GCL/CCL primary liners were generally excluded from the assessment because: (i) they did not have continuous LCRS and LDS flow rate data available for an individual cell from the start of operation; or (ii) there were insufficient LCRS and LDS chemical constituent data to evaluate whether primary liner leakage did or did not occur. Flow rate data are available for 13 cells at nine landfills with monitoring periods of up to 121 months. All of these cells were constructed with CQA. A summary of the LCRS and LDS flow rate data for the cells is provided in Table 5-4. The main findings from the evaluation of flow rate data for cells with GM/CCL or GM/GCL/CCL primary liners are given below:

- LDS flows during the initial period of operation are attributed primarily to construction water. LDS flows during the active and post-closure periods are attributed primarily to consolidation water.
- Average monthly LDS flow rates ranged from about 10 to 1,400 lphd during the initial period of operation, 0 to 370 lphd during the active period, and 5 to 210 lphd during the post-closure period.

Given the "masking" effects of consolidation water, chemical constituent data must be used to assess the hydraulic performance of composite primary liners having a CCL or GCL/CCL lower component, as described in Section 5.2.3.2. This approach was applied to the 13 landfill cells. Concentrations of chemical constituents in LDS liquids were compared to concentrations of the same constituents in LCRS liquids. These chemical data are reported in Table E-4.9 of Appendix E. The general water quality characteristics of LDS liquids were found to be different than the corresponding characteristics for the LCRS liquids. This is due to the different origins of the primary sources of the two liquids: leachate for LCRS liquids and CCL pore water for LDS liquids. The different origins of the two liquids are reflected in different major ion chemistries, as well as differences in chemical oxygen demand (COD), biological oxygen demand (BOD), and total organic carbon (TOC) concentrations.

To further evaluate whether primary liner leakage had contributed to the LDS flows, the concentrations of the previously mentioned five key chemical constituents (i.e., sulfate, chloride, benzene, toluene, and xylene) in LCRS and LDS liquids were investigated. The results of the comparison of key constituents are presented in Tables 5-5 and 5-6. Table 5-5 presents the concentrations of the five key constituents as a function of time

Table 5-4. Summary of LCRS and LDS Flow Rate Data for Landfill Cells with GM/CCL or GM/GCL/CCL Composite Primary Liners.

Cell No.	Cell Area (ha)	Waste Place. Start Date	Final Closure Date	Initial Period of Operation[1]					Active Period of Operation[2]					E_a	Post-Closure Period[3]					E_a
				Time Period (months)	LCRS Flow[4] Avg. (lphd)	LCRS Flow Peak (lphd)	LDS Flow Avg. (lphd)	LDS Flow Peak (lphd)	Time Period (months)	LCRS Flow Avg. (lphd)	LCRS Flow Peak (lphd)	LDS Flow Avg. (lphd)	LDS Flow Peak (lphd)	(%)	Time Period (months)	LCRS Flow Avg. (lphd)	LCRS Flow Peak (lphd)	LDS Flow Avg. (lphd)	LDS Flow Peak (lphd)	(%)
B3[5]	6.4	Jul-87	NA[6]	1-4	15,304	24,858	1,394	4,250	5-16	5,700	8,935	124	266	97.8						
									17-28	9,272	22,444	101	168	98.9						
									29-40	7,575	13,978	262	803	96.5						
									41-52	2,859	6,043	231	713	91.9						
									53-64	1,189	2,280	45	152	96.2						
									65-76	403	490	92	133	77.3						
									77-88	560	919	102	193	81.8						
									89-93	578	648	98	109	83.0						
Y2	3.0	Jan-91	NA	1-10	23,368	36,791	655	1,768	11-22	10,353	19,204	370	1,993	96.4						
									23-34	11,344	25,309	90	168	99.2						
									35-46	4,404	6,380	70	248	98.4						
									47-54	4,397	5,199	48	56	98.9						
AD1	0.6	May-85	Jul-88	1-12	ND[6]	ND	ND	ND	13-20	ND	ND	ND	ND		33-44	145	652	24	42	83.4
									21-32	373	892	107	603	71.4	45-51	85	130	26	31	69.5
															52-63	3	22	28	45	-833
															64-75	3	42	42	103	-1300
															76-87	3	21	23	68	-667
															88-99	1	4	8	46	-700
															100-111	1	2	5	43	-400
															112-121	2	9	6	24	-200
AD7	1.5	Sep-87	Oct-93	1-12	12,597	26,492	135	1,101	13-24	2,212	2,857	71	291	96.8	70-81	375	533	73	157	80.5
									25-36	1,539	2,755	96	393	93.8	82-87	165	334	105	172	36.3
									37-48	1,429	2,813	17	21	98.8						
									49-60	249	629	33	74	87.0						
									61-69	480	614	64	112	86.6						
AK1	1.4	Oct-93	NA	1-12	9,867	17,986	206	804												
AL1	14.9	1990	NA	1-29	ND	ND	ND	ND	30-41	934	2,085	231	367	75.3						
									42-54	1,349	5,885	103	183	92.4						
AM1	3.2/2.4[7]	Oct-90	NA	1-9	ND	ND	ND	ND	10-21	270	533	15	64	94.4						
									22-33	236	329	10	15	95.8						
									34-45	111	283	3	14	97.3						
									46-57	20	77	1	1	95.0						
									58-69	18	21	1	1	94.4						

Table 5-4. Summary of LCRS and LDS Flow Rate Data for Landfill Cells with GM/CCL or GM/GCL/CCL Composite Primary Liners (Continued).

Cell No.	Cell Area (ha)	Waste Place. Start Date	Final Closure Date	Initial Period of Operation[1]					Active Period of Operation[2]					E_a	Post-Closure Period[3]					E_a
				Time Period (months)	LCRS Flow[4] Avg. (lphd)	LCRS Flow[4] Peak (lphd)	LDS Flow Avg. (lphd)	LDS Flow Peak (lphd)	Time Period (months)	LCRS Flow Avg. (lphd)	LCRS Flow Peak (lphd)	LDS Flow Avg. (lphd)	LDS Flow Peak (lphd)	(%)	Time Period (months)	LCRS Flow Avg. (lphd)	LCRS Flow Peak (lphd)	LDS Flow Avg. (lphd)	LDS Flow Peak (lphd)	(%)
AM1									70-81	11	18	5	8	54.4						
AM2	4.8/2.4[7]	Oct-90	NA	1-9	ND	ND	ND	ND	10-21	32	154	9	42	71.9						
									22-33	35	51	9	29	74.3						
									34-45	17	45	3	26	82.4						
									46-57	67	274	0	0	100						
									58-69	64	181	8	13	87.5						
									70-81	112	136	9	13	92.0						
AO1	1.8	Jan-92	NA	1-5	ND	ND	ND	ND	6-17	1,984	4,130	184	353	90.7						
									18-29	1,299	1,577	96	126	92.6						
									30-37	1,144	1,371	60	102	94.8						
AO2	1.8	Jul-92	NA	1-5	15,881	24,541	149	191	6-17	3,027	5,266	110	158	96.4						
									18-31	1,688	2,383	33	64	98.1						
AQ1	0.6	Mar-86	early 90	1-6	10,203	18,944	352	569	7-25	ND	ND	255	1239		59-65	5,835	11,244	215	246	96.3
									26-34	ND	ND	ND	ND		66-77	644	1,011	117	165	81.8
									35-46	ND	ND	197	435		78-89	1,367	3,264	98	132	92.8
									47-58	4,530	10,531	116	143	97.4	90-97	1,615	3,575	51	118	96.8
AQ10	0.9	Jan-89	mid 91	1-9	ND	ND	14	32	10-14	ND	ND	26	32		27-38	682	2,251	29	48	95.7
									15-26	15,933	38,751	48	250	99.7	39-50	300	1,709	18	63	94.0
															51-63	852	1,588	24	75	97.2
AR1	9.7	Mar-92	NA	1-11	27,042	65,871	292	705	12-23	11,251	23,384	181	470	98.4						
									24-36	9,668	26,274	155	442	98.4						

Notes:

(1) "Initial Period of Operation" represents period after waste placement has started and only a small amount of waste has been placed in the cell.

(2) "Active Period of Operation" represents period when waste thickness in cell is significant and/or an effective intermediate cover is placed on the waste.

(3) "Post-Closure Period" represents period after final cover system has been placed on the entire cell.

(4) Flow rates are given in liter/hectare/day.

(5) 65 percent of Cell B3 received final cover at 60 months after start of waste placement.

(6) NA = not applicable; ND = not determined.

(7) Values given represent LCRS and LDS areas, respectively.

(8) Breakthrough times for steady-state saturated flow through CCL or GCL/CCL component of composite liners are estimated to be 2 to 145 months based on a calculation using Darcy's equation and specified hydraulic conductivities, hydraulic gradient of 5 for GCLs and 1 for CCLs, and effective porosity of 0.2. For this calculation, it is assumed that flow through the GM component of the composite liner occurs through small holes and is instantaneous.

Table 5-5. Average Concentrations of Five Key Chemicals in LCRS and LDS Flows from Landfill Cells with GM/CCL and GM/GCL/CCL Composite Primary Liners.

Cell No.	Time Period (months)	Chemical[1]									
		Sulfate (mg/l)		Chloride (mg/l)		Benzene (μg/l)		Toluene (μg/l)		Xylene (μg/l)	
		LCRS	LDS	LCRS	LDS	LCRS	LDS	LCRS	LDS	LCRS	LDS
B3	1-4	282	95	25	19	<11[2]	<25	150	<25		
	5-16	105	1,286	207	173	<1	<1	<1	<1		
	17-28	348		352	241	<1		<1			
	29-40	104	500	580	118	<5	<5	354	<6		
	41-52	47	14	355		8	6	233	24		
	53-64	28	123	899	59	7	<1	101	<1		
	65-76	<127	90	203	58	<5	<5	14	<6		
	77-88	<6	301	998		<5	<5	<5	<4		
	89-93		48	1,383		<2	<5	<1	<1		
Y2	1-10	108	231	349	60						
	11-22	108	299	590	25	10		720	7		
	23-34	52	326	876	89						
	35-46										
	47-54										
AD1	1-12	6,353		3,930		492		305			
	13-20	5,830		24,300	289	429	<4	292	<6		
	21-32	5,470	480	10,763	210	33	<4	133	<6		
	33-44	4,455	498	11,590	185	5	<4	60	<6		
	45-51	2,223	308	13,960	217	35	<4	108	<6		
	52-63		443		240		<4	<300	<6		
	64-75		338		131		<4		<6		
	76-87	1,785	456	13,900	377		<4		<6		
	88-99	4,488	339	14,550	137	26	<4	186	<6		
	100-111	3,633	296	14,075	114	18	<1	<30	<1		
	112-121	3,870	369	14,800	138	<25	<1	<25	<1		

Table 5-5. Average Concentrations of Five Key Chemicals in LCRS and LDS Flows from Landfill Cells with GM/CCL and GM/GCL/CCL Composite Top Liners (Continued).

Cell No.	Time Period (months)	Chemical									
		Sulfate (mg/l)		Chloride (mg/l)		Benzene (µg/l)		Toluene (µg/l)		Xylene (µg/l)	
		LCRS	LDS	LCRS	LDS	LCRS	LDS	LCRS	LDS	LCRS	LDS
AD7	1-12	2,818	340	3,214	109	140	<4	317	<6		
	13-24	3,620	683	9,550	216	612	<4	892	<6		
	25-36	7,361	586	10,720	219	1168	<4	1,859	<6		
	37-48	8,213	954	11,535	469	644	<4	2,960	<6		
	49-60	6,867	1,050	14,400	418	778	<4	1,660	<6		
	61-69	5,740	1,148	15,775	387	687		1,288	<6		
	70-81	6,998	1,168	12,875	387	540	<4	906	<1		
	82-87	7,480	1,132	14,267	357	<240	<1	450	<1		
AK1	1-12	47	16	104	2	<5	<1	88	<1	30	<3
AL1	1-29	300	1,030	330	89	<4	<2	133	<1[3]	540	<1
	30-41	225	900	273	203	1	<1	5	<1	<3	
	42-54	247	1,375	400	215	2	<1	2	<1	<3	<1
AM1	1-9	51		77		<21		219		150	
	10-21	<2		120		18	<1	160	2	90	<1
	22-33	<16	1,341	159	2,260	<19	<1	336	<1	121	<1
	34-45	<27	1,200	219	2,600	18	<1	290	<1	122	<3
	46-57	<12		265		14		199		90	
	58-69	<3		240		13		56		82	
AM2	1-9	96		140		11		22		34	
	10-21	<2		290		17	<1	89	<1	57	<2
	22-33	<13	1,032	353	2,175	19	<1	266	<1	95	<1
	34-45	<7	1,300	326	2,600	18	<1	286	<1	94	<3
	46-57	<2	1,730	368	2,700	15	<1	148	<1	115	<2
	58-69	<3	2,405	262	2,635	7	<1	65	<1	50	<2
AO1	1-5										
	6-17	49	88	930	58	6	<1	230	<1	59	<3
	18-29	35	41	988	27	10	<1	288	44	45	<3
	30-37	69	2	570	46	<5	<5	77	<5	21	<10

Table 5-5. Average Concentrations of Five Key Chemicals in LCRS and LDS Flows from Landfill Cells with GM/CCL and GM/GCL/CCL Composite Top Liners (Continued).

Cell No.	Time Period (months)	Chemical									
		Sulfate (mg/l)		Chloride (mg/l)		Benzene (μg/l)		Toluene (μg/l)		Xylene (μg/l)	
		LCRS	LDS	LCRS	LDS	LCRS	LDS	LCRS	LDS	LCRS	LDS
AO2	1-5										
	6-17	49	89	930	16	6	<1	230	<1	59	<3
	18-31	35	93	988	24	10	<1	288	<1	45	<4
AR1	1-11	180	600	1,000	49						
	12-23	440	170	2,200	8		<1		<2		<4
	24-36	520	265	1,650	41	<100	<50	<100	<50	<100	<50
AQ1	1-58										
	59-65					<5	<4	<5	<10		
	66-77					<8	<4	<5	<6	<5	
	78-89					<12	<4	<5	<14	<8	
	90-97					<5	<4	<5	<5	<5	
AQ10	1-15										
	15-26					<10	<4	<12	<5		
	27-38					<10	<4	<30	<5	190	
	39-50					<6	<4	<6	<5	<7	
	51-63					<5	<4	5	<5	10	

Notes:

(1) Reported concentrations represent average of 1 to 17 individual analysis results (typically on the order of 5) during incremental reporting period.

(2) Data preceded by "<" indicates more than half of analysis results for parameter were reported as non-detects; in calculating average values, half of the test detection limit was conservatively used for all results reported as non-detects.

(3) For Cell AL1, toluene was not detected in nine of ten LDS flow samples obtained during the 1-41 months time period. Toluene was detected at a concentration of 91 μg/l in month 30. This one detection is attributed to sampling or analysis error and is not included in the average.

Table 5-6. Evaluation of Chemical Constituent Migration Through Landfill GM/CCL and GM/GCL/CCL Composite Primary Liners.

Cell No.	Monitor. Period (months)	Estimated Advective Breakthr. Time for GCL/CCL (months)[1]	Chemical					Summary of Observations for Five Key Constituents
			Sulfate	Chloride	Benzene	Toluene	Xylene	
B3	93	46	not diagnostic due to fluctuating C_o[2] in both LCRS and LDS	lower C_o in LDS than in LCRS and trend of decreasing LDS C_o with time not indicative of chloride breakthrough	not diagnostic due to very low C_o in both LCRS and LDS (i.e., C_o almost always below DL[3] of 5 μg/l)	in LCRS, C_o up to 700 μg/l; in LDS, C_o typically below DL of 1 to 10 μg/l; no indication of toluene breakthrough	no data available	no evidence of significant leachate migration into LDS after almost 8 years of cell operation, twice the estimated CCL breakthrough time
Y2	54 (no key chemical data after 34 months)	35	not diagnostic due to high C_o in LDS consolidation water	in LCRS, C_o = 170 to 1,160 mg/l with m[2] = 628 mg/l; in LDS, C_o = 8 to 140 mg/l with m = 58 mg/l; no indication of chloride breakthrough	no LDS data available	only one C_o available from each system (at 11-22 months): LCRS C_o = 720 μg/l and LDS C_o = 7 μg/l	no data available	data are insufficient to draw conclusions; monitoring period is about equal to estimated CCL breakthrough time; more chemical data are needed

Table 5-6. Evaluation of Chemical Constituent Migration Through Landfill GM/CCL and GM/GCL/CCL Composite Primary Liners.

Cell No.	Monitor. Period (months)	Estimated Advective Breakthr. Time for GCL/CCL (months)[1]	Chemical					Summary of Observations for Five Key Constituents
			Sulfate	Chloride	Benzene	Toluene	Xylene	
AD1	121	70	in LCRS, C_o = 1,785 to 6,353 mg/l with m = 4,234 mg/l; in LDS, C_o = 296 to 498 mg/l with m = 392 mg/l; no indication of sulfate breakthrough	in LCRS, C_o = 3,930 to 24,300 mg/l, with m = 13,450 mg/l; in LDS, C_o = 114 to 337 mg/l, with m = 204 mg/l; no indication of chloride breakthrough	in LCRS, C_o = <25 to 492 μg/l; in LDS, C_o below DL of 1 to 4 μg/l; no indication of benzene breakthrough	in LCRS, C_o = <25 to 305 μg/l; in LDS, C_o below DL of 1 to 6 μg/l; no indication of toluene breakthrough	no data available	no evidence of significant leachate migration into LDS after 10 years of cell operation and closure, 1.7 times more than the estimated CCL breakthrough time
AD7	87	70	in LCRS, C_o=2,818 to 8,213 mg/l with m=6,137 mg/l; in LDS, C_o=340 to 1,168 mg/l with m=882 mg/l; increasing LDS C_o after 36 months attributed to decreasing dilution of consol. water by construct. water	in LCRS, C_o=3,214 to 15,775 mg/l with m=11,547 mg/l; in LDS, C_o=109 to 469 mg/l with m=320 mg/l; increasing LDS C_o after 36 months attributed to decreasing dilution of consol. water by construct. water	in LCRS, C_o = <240 to 1,168 μg/l; in LDS, C_o below DL of 1 to 4 μg/l; no indication of benzene breakthrough	in LCRS, C_o = 317 to 2,960 μg/l; in LDS, C_o below DL of 1 to 6 μg/l; no indication of toluene breakthrough	no data available	evidence of possible breakthrough for sulfate & chloride at 12 36 months; authors attribute trend to decreased dilution of consolidation water by construction water; no evidence of organic constituent breakthrough; more chemical data are needed

Table 5-6. Evaluation of Chemical Constituent Migration Through Landfill GM/CCL and GM/GCL/CCL Composite Primary Liners.

Cell No.	Monitor. Period (months)	Estimated Advective Breakthr. Time for GCL/CCL (months)[1]	Chemical					Summary of Observations for Five Key Constituents
			Sulfate	Chloride	Benzene	Toluene	Xylene	
AK1	12	48	in LCRS, C_o = 7 to 110 mg/l with m = 47 mg/l; in LDS, C_o = 10 to 51 mg/l with m = 16 mg/l; no indication of sulfate breakthrough	in LCRS, C_o = 2 to 230 mg/l with m = 104 mg/l; in LDS, C_o = 2 to 6 mg/l with m = 4 mg/l; no indication of chloride breakthrough	not diagnostic because C_o is below DL in both LCRS and LDS	in LCRS, C_o = 5 to 300 μg/l with m = 88 μg/l; in LDS, C_o below DL of 1 μg/l; no indication of toluene breakthrough	in LCRS, xylene detected in half of sampling events at C_o up to 79 μg/l; in LDS, C_o below DL of 3 μg/l; no indication of xylene breakthrough	no evidence of significant leachate migration into LDS; however, monitoring period is only about 1/4th of the estimated GCL/CCL breakthrough time; more chemical data are needed
AL1	54	70	not diagnostic due to high C_o in LDS consolidation water	increasing LDS C_o with time likely due to decreasing dilution of consolidation water by construction water	not diagnostic because C_o is below DL in both LCRS and LDS	in LCRS, C_o = up to 600 μg/l; in LDS, toluene below DL of 1 μg/l; no indication of toluene breakthrough	not diagnostic because C_o is below DL in LDS and, after 29 months, also in LCRS	no evidence of significant leachate migration in to LDS; monitoring period somewhat less than estimated CCL breakthrough time; more chemical data are needed

Table 5-6. Evaluation of Chemical Constituent Migration Through Landfill GM/CCL and GM/GCL/CCL Composite Primary Liners.

Cell No.	Monitor. Period (months)	Estimated Advective Breakthr. Time for GCL/CCL (months)[1]	Chemical					Summary of Observations for Five Key Constituents
			Sulfate	Chloride	Benzene	Toluene	Xylene	
AM1	58	4	not diagnostic due to high C_o in LDS consolidation water	not diagnostic due to high C_o in LDS consolidation water	in LCRS, C_o = 12 to 20 μg/l; in LDS, C_o below DL of 1 μg/l; no indication of benzene breakthrough	in LCRS, C_o = 40 to 420 μg/l with m = 267 μg/l; in LDS, C_o below DL of 1 μg/l; no indication of toluene breakthrough	in LCRS, C_o = 71 to 150 μg/l with m = 122 μg/l; in LDS, C_o below DL of 1 to 3 μg/l; no indication of xylene breakthrough	no evidence of significant leachate migration into LDS after almost 5 years of cell operation; monitoring period more than 12 times longer than estimated CCL breakthrough time
AM2	58	4	not diagnostic due to high C_o in LDS consolidation water	not diagnostic due to high C_o in LDS consolidation water	in LCRS, C_o = 5 to 20 μg/l; in LDS, C_o below DL of 1 μg/l; no indication of benzene breakthrough	in LCRS, C_o = 10 to 400 μg/l with m = 146 μg/l; in LDS, C_o below DL of 1 μg/l; no indication of toluene breakthrough	in LCRS, C_o = 2 to 130 μg/l with m = 71 mg/l; in LDS, C_o below DL of 1 to 3 mg/l; no indication of xylene breakthrough	no evidence of significant leachate migration into LDS after almost 5 years of cell operation; monitoring period more than 12 times longer than estimated CCL breakthrough time

Table 5-6. Evaluation of Chemical Constituent Migration Through Landfill GM/CCL and GM/GCL/CCL Composite Primary Liners.

Cell No.	Monitor. Period (months)	Estimated Advective Breakthr. Time for GCL/CCL (months)[1]	Chemical					Summary of Observations for Five Key Constituents
			Sulfate	Chloride	Benzene	Toluene	Xylene	
AO1[4]	37	140	not diagnostic due to similar LCRS and LDS C_o ranges	in LCRS, C_o = 320 to 1300 mg/l with m = 860 mg/l; in LDS, C_o = 7 to 100 mg/l with m = 40 mg/l; no indication of chloride breakthrough	in LCRS, benzene detected in half of the sampling events at C_o = 7 to 12 μg/l; in LDS, C_o below DL of 1 μg/l; no indication of benzene breakthrough	in LCRS, C_o = 10 to 550 μg/l with m = 167 μg/l; in LDS, C_o below DL of 1 μg/l in 2/3 of sampling events; no indication of toluene breakthrough	in LCRS, C_o = 12 to 76 μg/l with m = 34 μg/l; in LDS, C_o below DL of 3 μg/l; no indication of xylene breakthrough	no evidence of significant leachate migration into LDS after 3 years of cell operation; however, monitoring period is only 1/4th of estimated CCL breakthrough time; more chemical data are needed
AO2[4]	31	145	not diagnostic due to similar LCRS and LDS C_o ranges	in LCRS, C_o = 320 to 1,300 mg/l with m = 862 mg/l; in LDS, C_o = 3 to 34 mg/l with m = 24 mg/l; no indication of chloride breakthrough	in LCRS, benzene detected in half of the sampling events at C_o = 7 to 12 μg/l; in LDS, C_o below DL of 1 μg/l; no indication of benzene breakthrough	in LCRS, C_o = 10 to 550 μg/l with m = 167 μg/l; in LDS, C_o below DL of 1 μg/l; no indication of toluene breakthrough	in LCRS, C_o = 12 to 76 μg/l with m = 34 μg/l; in LDS, C_o below DL of 3 μg/l; no indication of xylene breakthrough	no evidence of significant leachate migration into LDS after 3 years of cell operation; however, monitoring period is only 1/4th of estimated CCL breakthrough time; more chemical data are needed

Table 5-6. Evaluation of Chemical Constituent Migration Through Landfill GM/CCL and GM/GCL/CCL Composite Primary Liners.

Cell No.	Monitor. Period (months)	Estimated Advective Breakthr. Time for GCL/CCL (months)[1]	Chemical					Summary of Observations for Five Key Constituents
			Sulfate	Chloride	Benzene	Toluene	Xylene	
AQ1	97	35	no data available	no data available	not diagnostic because C_o is below DL in both LCRS and LDS	not diagnostic because C_o is below DL in both LCRS and LDS	no LDS data available	data are insufficient to draw conclusions; more data are needed
AQ10	63	35	no data available	no data available	not diagnostic because C_o is below DL in both LCRS and LDS	not diagnostic because C_o is below DL in both LCRS and LDS	no LDS data available	data are insufficient to draw conclusions; more data are needed
AR1	36	2	not diagnostic due to similar LCRS and LDS C_o ranges	in LCRS, C_o = 600 to 2700 mg/l with m = 1625 mg/l; in LDS, C_o = 8 to 74 mg/l with m = 35 mg/l; no indication of chloride breakthrough	not diagnostic because C_o is below DL in both LCRS and LDS	not diagnostic because C_o is below DL in both LCRS and LDS	not diagnostic because C_o is below DL in both LCRS and LDS	no evidence of significant leachate migration into LDS; monitoring period is more than 10 times the estimated GCL/CCL breakthr. time; data are not diagnostic; more data are needed

Notes:

(1) Advective breakthrough times for steady-state saturated flow through CCL or GCL/CCL component of composite liners were calculated using Darcy's equation and specified hydraulic conductivities, hydraulic gradient of 5 for GCLs and 1 for CCLs, and effective porosity of 0.2. For this calculation, it is assumed that flow through the GM component of the composite liner occurs through small holes and is instantaneous.

(2) C_o = average concentration during incremental reporting period; m = mean concentration for the entire reporting period.

(3) DL = detection limit.

(4) Composite liquid quality samples from the LCRSs of Cells AO1 and AO2 were assumed to represent average conditions at the two cells.

period after the start of landfill cell operation. Table 5-6 presents the results of the authors' assessment of the occurrence of key constituent migration through the composite primary liners. This assessment is based on a qualitative comparison of the five key chemical constituents. Table 5-6 also presents an estimate of the advective breakthrough time for the CCL or GCL/CCL component of each composite primary liner. The estimated breakthrough times were calculated assuming that the GM component of the composite primary liner has one or more holes through which leachate instantaneously migrates and that leachate migration through the CCL or GCL/CCL component of the composite liner is governed by Darcy's equation assuming one-dimensional steady-state saturated flow. Other assumptions used in the calculations are given in the table. The effect of chemical retardation was not considered in calculating the advective breakthrough times. Retardation of chloride and sulfate should be negligible. Retardation characteristics for benzene, toluene, and xylene will depend on the organic carbon content of the CCL or GCL, redox conditions, and other factors. It is expected, however, that the effective retardation coefficient for these constituents would have been 2 or more. These organic compounds were chosen for analysis notwithstanding their retardation characteristics for a combination of reasons, including relatively widespread occurrence in leachate, and relatively higher concentrations in leachate than other organic compounds. In addition, these three constituents are not known as laboratory contaminants, in contrast to methylene chloride, a constituent that is more mobile but is also a common laboratory contaminant.

The current database is not sufficient to draw definitive conclusions on the performance of GM/CCL and GM/GCL/CCL composite primary liners. However, using the data and comparisons in Tables 5-5 and 5-6, the following observations can be offered with respect to key chemical constituent migration through the composite primary liners of the 13 considered cells:

- There were insufficient data for three cells (i.e., Y2, AQ1, and AQ2) to draw any conclusions on primary liner leakage rates based on key chemical constituent data.
- For the remaining ten cells, key chemical constituent data did not reveal obvious indications of primary liner leakage.
- One of the ten cells (i.e., AD7) exhibited a potential indication of primary liner leakage when sulfate and chloride concentrations in LDS flows increased between 12 and 36 months after construction. However, the concentrations of other chemicals did not increase over time. The estimated breakthrough time for the composite primary liner in this cell is 70 months, several times greater than the time when sulfate and chloride concentrations increased. The reason for the increase in the anion concentrations in the LDS flow from Cell AD7 is unclear.
- Five of the ten cells (i.e., B3, AD1, AD7, AM1, and AM2) have key chemical constituent data of sufficient completeness and duration to conclude that leachate migration into the LDS at a rate of any engineering significance has not

occurred for a time period exceeding the estimated breakthrough time for the CCL component of the composite liner.

- Et values were estimated for cells B3, AD1, AD7, AM1, and AM2 using Equation 5-1, presented in Section 5.2.3, with constituent mass fluxes from the LCRS and LDS. Mass fluxes were calculated using average flow rates and chemical concentrations for benzene, toluene, and xylene during the active operation and post-closure periods. With this approach, Et values for these cells were found to range from 99.1 to more than 99.9%.
- Based on the above data and similar to GM/GCL composite liners, GM/CCL and GM/GCL/CCL composite liners of the type evaluated in this study can be constructed to achieve Et values of 99.9% or more. However, Et values in the range of 99 to 99.9% will also occur.
- Available leakage rate calculation methods for composite liners give leakage rates in the same range as the rates estimated from the data for composite primary liners presented in Appendix E. Notwithstanding the uncertainties in both the assumptions used in the calculations and the estimated leakage rates, this is a useful finding.
- In the U.S., landfill cells are typically operated for periods of one to five years, occasionally longer, and they are promptly covered with a GM or other low-permeability barrier after filling. This operations sequence defines the timeframe for significant leachate generation in a landfill cell that does not contain liquid wastes or sludges and that does not undergo leachate recirculation or moisture addition. For the cells in this study, estimated advective breakthrough times through CCLs, assuming no chemical retardation, were generally calculated to range from about 3 to 12 years (see Table 5-6). It thus appears that GM/CCL and GM/GCL/CCL composite liners are capable of substantially preventing leachate migration over the entire period of significant leachate generation for typical modern landfills.
- The conclusions given above for GM/CCL composite liners should be considered preliminary. Additional analyses are recommended using a larger database representing a larger time period of operation to confirm or modify these preliminary conclusions. The additional analyses should include a more thorough analysis of the transport characteristics of a wider array of key chemical constituents than considered in this study.

5.2.4.2 Leachate Generation Rates

Average and peak monthly LCRS flow rate data were evaluated for 73 MSW cells at 32 landfills, 56 HW cells at 12 landfills, eight MSW ash or coal ash cells at six landfills, and three C&DW cells at two landfills. Most of these landfills are located in the northeast and southeast; only four of the landfills are located in the west. The LCRS flow rate data are presented in Table E-3.5 of Appendix E for monitoring periods up to about ten years. Almost half of the cells have more than four years of LCRS flow rate data available. Post-closure data are available for eleven MSW cells at three landfills and 22 HW cells at five landfills. Detailed results of the data analysis are given in Tables E-5.1 to E-5.5 of Appendix E and are summarized in Tables 5-7 and 5-8 below. The range of

average LCRS flow rates for the cells and the mean average LCRS flow rates are presented in Table 5-7 as a function of waste type, landfill operational stage, and geographical region of the U.S. Figure 5-4 illustrates the effects of geographic region and waste type on LCRS flow rate. Table 5-8 presents the range of average rainfall fractions (RFs) for the cells and the mean average RFs as a function of the same variables. In this report, RF (in percent) is the ratio of average LCRS flow rate to historical average annual rainfall.

Table 5-7. Summary of Average LCRS Flow Rates (in lphd).

Waste Type	U.S. Region	Initial Period of Operation		Active Period of Operation		Post-Closure Period	
		Range	*Mean*	*Range*	*Mean*	*Range*	*Mean*
MSW	*NE*	1,050-39,900	10,200	41-17,700	3,530	55-680	400
	SE	1,480-43,700	10,400	300-10,900	2,930		
	W			55-110	83(1)		
HW	*NE*	4,980-18,800	11,000	1,050-21,300	5,380	340-1,130	780
	SE	480-31,300	15,500	270-37,100	4,890	36-1,580	370
	W	42-3,090	480	1-4,280	990	56(1)	56(1)
Ash	*NE*	2,190-28,600	18,700	1,030-35,300	17,700		
	SE			8,940-24,490	17,800		
C&DW	*NE*	15,600-19,600	17,600	3,570-16,200	10,600		

Notes: (1) Values are based on only one or two cells from one landfill.

The major findings from the evaluation of leachate generation rates are given below:

- LCRS flow rates during operations (i.e., the initial and active periods of operation) can vary significantly between landfills located in the same geographic region and accepting similar wastes. Large variations in flow rates (e.g., one order of magnitude difference) can even occur between cells at the same landfill. Differences in waste placement practices may be responsible for these significant variations. Limiting the size of the active disposal area and using effective measures to minimize rainfall infiltration into the waste and to divert surface-water runoff away from the waste will significantly decrease leachate generation rates compared to the rates observed under less controlled conditions.

Table 5-8. Summary of Average Rainfall Fractions (in percent).

Waste Type	U.S. Region	Initial Period of Operation		Active Period of Operation		Post-Closure Period	
		Range	*Mean*	*Range*	*Mean*	*Range*	*Mean*
MSW	*NE*	4-160	39	0.1-54	13	0.2-3	1
	SE	5-157	33	1-23	8		
	W			0.5-1	0.7(1)		
HW	*NE*	21-87	46	4-81	21	1-4	3
	SE	1-73	33	1-74	11	0.08-3	0.8
	W	1-30	5	0.01-41	10	0.3(1)	0.3(1)
Ash	*NE*	8-84	58	4-104	55		
	SE			22-60	43		
C&DW	*NE*	50-63	56(1)	12-52	34		

Notes: (1) Values are based on only one or two cells from one landfill.

- The MSW cells produced, on average, less leachate than the HW and ISW cells. Average LCRS flow rates for MSW cells located in the NE and SE ranged from 1,000 to 44,000 lphd during the initial period of operation and 40 to 18,000 lphd during the active period of operation. For this group of cells during the initial period of operation, 60% exhibited average LCRS flow rates less than 10,000 lphd and 87% had rates less than 20,000 lphd. For the same group of cells during the active period of operation, 52% had average LCRS flow rates less than 5,000 lphd and 95% had flow rates less than 10,000 lphd. Only two MSW cells are located in the W. These two MSW cells had very low average LCRS flow rates (i.e., 55 and 110 lphd).
- RF values calculated for the MSW cells in the NE (means of 39% and 13% for the initial and active periods of operation, respectively) were higher than RF values for the SE cells (means of 33% and 8% for the initial and active periods of operation, respectively). It is possible that the higher water evaporation rates and the higher runoff occurring with shorter duration, more intense rainfalls associated with the SE offset any potential increases in leachate generation rates caused by the higher total amount of rainfall in the SE as compared to the NE. RF values for the two MSW cells that are located at an arid site (average annual rainfall of about 430 mm) in the W were less than 1%.
- Average LCRS flow rates for HW cells located in the NE and SE ranged from 500 to 31,000 lphd during the initial period of operation and 300 to 37,000 lphd

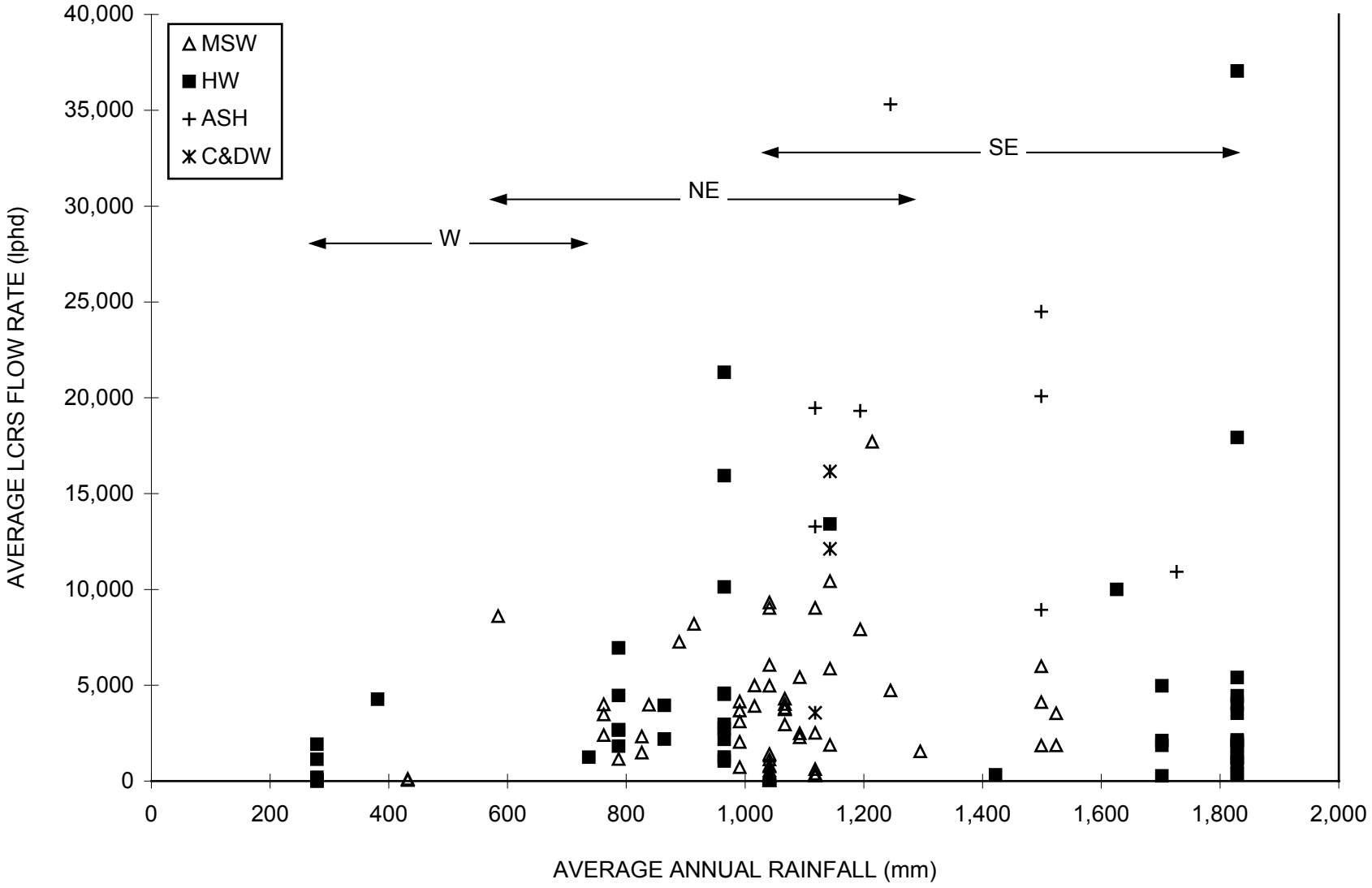

Figure 5-4. Average LCRS flow rate versus average annual rainfall during the active period of operation.

during the active period of operation. About 69% of these cells exhibited average LCRS flow rates greater than 10,000 lphd during the initial period of operation and 21% exhibited average LCRS flow rates greater than 5,000 lphd during the active period of operation. Average LCRS flow rates from HW cells during the active period of operation were 50 to 70% higher than flow rates from MSW cells. The reason for the higher leachate generation rates at the HW cells in this study is unclear, but may, in part, be due to differences in waste characteristics (e.g., initial moisture content, porosity, and permeability) and operational practices (e.g., waste placement and covering procedures). The ten HW cells located in the W had low average flow rates, ranging from about 1 to 4,000 lphd during operations.

- RF values calculated for the HW cells in the NE (means of 46% and 21% for the initial and active periods of operation, respectively) were higher than RF values for the SE cells (means of 33% and 11% for the initial and active periods of operation, respectively). Similar to the MSW cells, the HW cells in the SE had lower RF values than cells in the NE. For most of the HW cells in the W, RF values were less than 10% during operations.
- Average flow rates during operations ranged from 1,000 to 35,000 lphd for ash cells (1,000 to 25,000 lphd for the seven MSW ash cells and 35,000 lphd for the coal ash cell) and from 4,000 to 20,000 lphd for the C&DW cells. The limited number of MSW ash, coal ash, and C&DW cells considered in this study exhibited average LCRS flow rates during the active period of operation that were 300 to 600% higher than average LCRS flow rates from MSW cells during the same period. It is possible that the higher leachate generation rates at the MSW ash, coal ash, and C&D waste landfills may, in part, be due to differences in waste characteristics and operational practices.
- Mean RF values were 53% for ash cells and 43% for C&DW cells.
- Peak monthly LCRS flow rates were typically two to three times the average monthly flow rates for all types of waste and regions of the U.S.
- Landfill geographic region has a major impact on LCRS flow rates. For landfill sites with historical average annual rainfall less than 500 mm, average LCRS flow rates were low, typically less than 2,000 lphd. LCRS flow rates increased with increasing rainfall up to a point. In general, for landfills with historical average annual rainfall greater than 1,100 to 1,200 lphd, an increase in rainfall did not appear to cause a corresponding increase in leachate generation rate.
- LCRS flow rates were typically two to three times smaller during the active period of operation than during the initial period of operation.
- Leachate generation rates for the closed landfills in this study typically decreased by a factor of four within one year after closure and by one order of magnitude within two to four years after closure, as shown in Figure 5-5. Six years after closure, LCRS flow rates were between 5 and 1,200 lphd (mean of 180 lphd). Nine years after closure, LCRS flow rates were negligible. These data show that well designed and constructed cover systems can be very effective in minimizing infiltration of rainfall into the waste, thus reducing leachate generation rates to near-zero values.

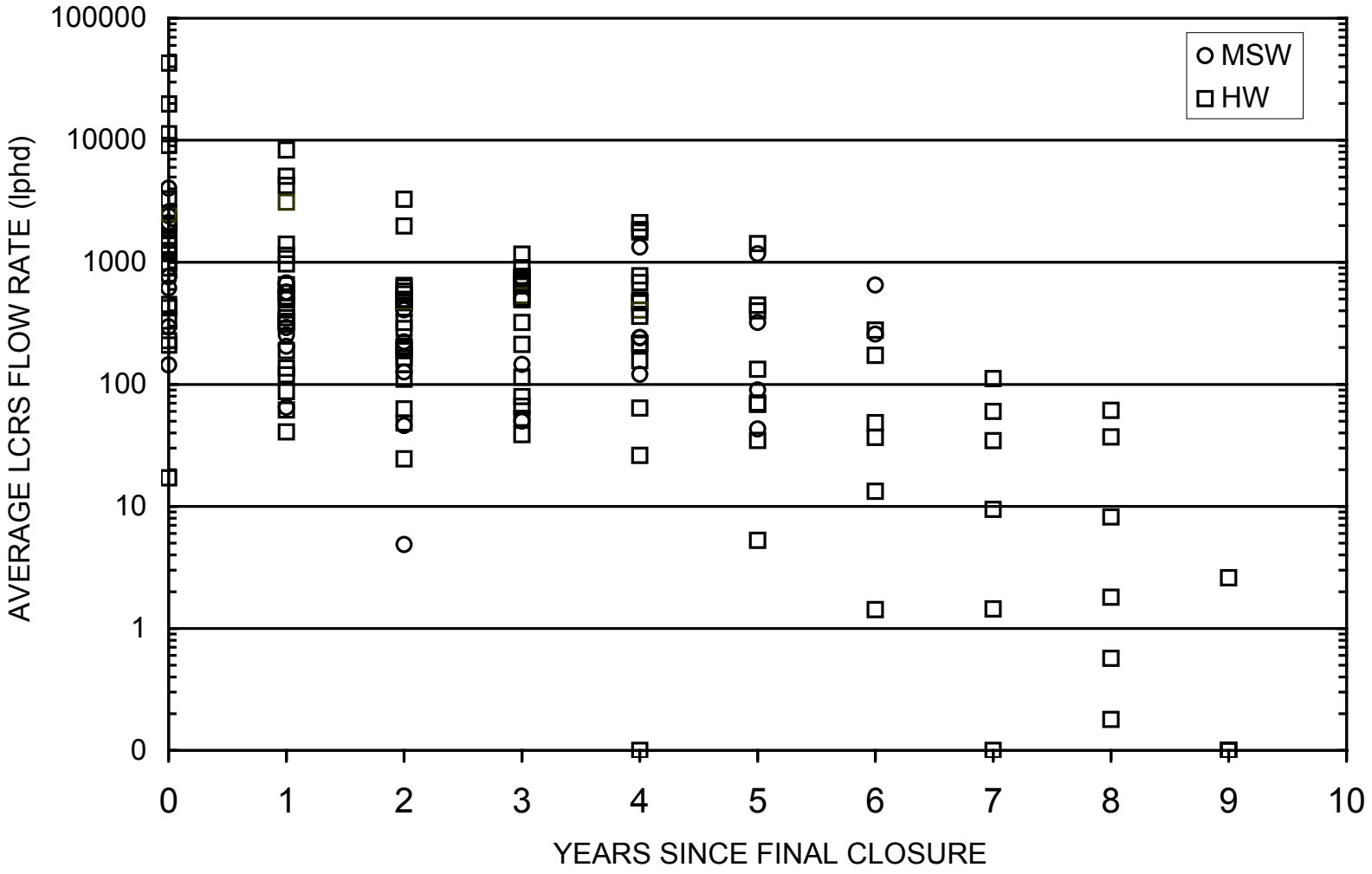

Figure 5-5. Average LCRS flow rates after closure for eleven MSW cells and 22 HW cells.

5.2.4.3 Leachate Chemistry

Select leachate chemistry data for 59 cells at 50 double-lined landfills were evaluated in terms of average constituent concentrations and relative detection frequencies. The distribution of leachate chemistry data by waste type and start of operation date is presented in Table 5-9. For the purposes of the discussions on leachate chemistry in this chapter, MSW ash landfill leachate is grouped with leachate from ISW landfills. This grouping is considered appropriate because MSW ash landfill leachate is typically nonhazardous and has chemical characteristics more similar to leachate from ISW landfills than to leachates from MSW or HW landfills. The MSW leachate chemistry data are from 36 landfills located in all geographic regions of the U.S. Based on the extent of the leachate chemistry data, the data are believed to be representative of modern MSW landfills in the U.S operated without leachate recirculation or other special activities (e.g., special waste disposal, induced aerobic degradation). About 70% of these landfills began operating in the 1990's. While the data for modern MSW landfills are extensive, they should not be considered to reflect the full range of leachate chemistry associated with the anaerobic decomposition process, from the acid stage to the methane fermentation stage. Moreover, differences will exist from facility to facility based on a variety of climate, site, waste, and operational factors. Additional data are needed from more facilities over a longer time period to better identify the potential range of leachate chemistry characteristics throughout the initial, active, and post-closure operational periods of a facility.

Table 5-9. Distribution of LCRS Chemistry Database by Waste Type and Start of Operation Date.

Waste Type	Pre-1990 Start of Operation	Post-1990 Start of Operation
MSW	11 landfills 13 cells	25 landfills 28 cells
HW	3 landfills 5 cells	1 landfill 1 cell
MSW Ash	1 landfill 1 cell	6 landfills 6 cells
Coal Ash	1 landfill 1 cell	1 landfill 1 cell
C&DW	1 landfill 2 cells	1 landfill 1 cell

Fewer data are available for HW and ISW landfills than for MSW landfills. In addition, the types of wastes placed in HW and ISW landfills are generally more variable between landfills than wastes placed in MSW landfills. With the exception of the leachate chemistry data for MSW ash landfills, it is likely that the data presented in this report do not characterize the variation in leachate chemistry for HW and ISW landfills. The

chemistry data for MSW ash landfill leachate may be representative of modern MSW ash landfills in the U.S. because seven landfills are included in the database and the chemistry of MSW ash is less variable than that of HW.

The leachate chemistry data are presented in Table E-3.7 of Appendix E and summarized in Table 5-10. Federal MCLs, which are available for two of the heavy metals and ten of the VOCs considered in this study, are also listed in Table 5-10. The distributions of select chemistry data for MSW, HW, and MSW ash cells are shown in Figures E-6.1 to E-6.3 of Appendix E. For MSW landfills, the chemical data for older landfills that started operating before 1990 (pre-1990 cells) and newer landfills that started operating during 1990 or later (post-1990 cells) are compared (Figure E-6.4 of Appendix E). The major findings from the evaluation of leachate chemistry data are given below:

- For a given waste type, many of the leachate constituents exhibited significant concentration variations (e.g., several orders of magnitude difference) between landfill cells and, sometimes, for a given cell.
- For the leachate types for which data are available for more than two landfills, the average value of pH (pH units), specific conductance (μmhos), COD (mg/l), BOD_5 (mg/l), TOC (mg/l), and chloride (mg/l) were, respectively:
    - MSW leachate: 6.7, 4,470, 2,500, 1,440, 380, and 560;
    - HW leachate: 8.2, 22,100, not available, not available, 1,620, and 7,760; and
    - MSW ash leachate: 7.1, 22,100, 1,670, 55, 62, and 10,400.

  The MSW landfill leachates were mineralized, biologically-active liquids with relatively low concentrations of heavy metals and VOCs. On average, the leachates were slightly acidic (i.e., average pH of 6.7), which is expected because carbon dioxide and organic acids are the primary by-products of the first stage (i.e., the acid stage) of anaerobic degradation of organic compounds in MSW landfills. The chemistry of these leachates changed with time as the organic compounds degraded (see for example, Table E-6.2 of Appendix E). In general, the leachate characteristics for cells receiving waste were more indicative of the acid phase of degradation than the second stage (i.e., the methane fermentation phase) of anaerobic degradation. For closed cells, the leachate pH typically increased with time and the BOD/COD ratio decreased with time, which is expected as the landfill is more fully in the methane fermentation phase of degradation. Of the heavy metals and VOCs considered in Table 5-10, chromium, nickel, methylene chloride, and toluene were detected at the highest concentrations in MSW leachates. Average concentrations of cadmium, benzene, 1,2-dichloroethane, trichloroethylene, and vinyl chloride in MSW landfills leachates exceeded federal maximum contaminant levels (MCLs) (40 CFR 141.11, 141.61, and 141.62) for community drinking water systems. None of the landfills had leachate with average chemical concentrations exceeding the MCLs for ethylbenzene, toluene, or xylenes.

Table 5-10. Summary of Landfill Leachate Chemistry Data.

Waste Type / Number of Landfills			MSW							
			10 Pre-1990				26 Post-1990			
Parameter	Units	MCLs	Average	Minimum	Maximum	No. of Landfills	Average	Minimum	Maximum	No. of Landfills
pH	pH units		6.62	6.30	7.20	8	6.79	5.90	8.09	22
Specific conductance	µmhos/cm		6,588	3,438	8,983	8	3,693	597	13,548	22
TDS	mg/l		5,487	2,740	8,640	9	2,758	480	8,621	21
COD	mg/l		3,878	804	8,267	9	1,939	< 10	6,800	22
BOD_5	mg/l		2,281	< 2	4,510	10	976	< 2	4,700	18
TOC	mg/l		1,509	4	2,852	8	527	24	2,609	21
Alkalinity	mg/l		2,295	1,508	3,278	7	1,536	203	5,800	22
Chloride	mg/l		801	199	2,263	10	463	5	1,625	25
Sulfate	mg/l		274	< 23	1,943	10	205	< 7	1,376	24
Calcium	mg/l		444	261	610	6	398	66	1,994	22
Magnesium	mg/l		153	84	279	6	83	10	191	21
Sodium	mg/l		532	225	1,115	8	282	3	1,219	23
Arsenic	µg/l	50	19	< 4	78	10	23	< 2	236	21
Cadmium	µg/l	5	< 8	< 1	< 17	8	< 7	< 1	< 20	22
Chromium	µg/l	100	68	5	320	10	38	3	90	21
Lead	µg/l		36	1	90	7	15	1	50	22
Nickel	µg/l		56	27	98	9	82	10	220	20
Benzene	µg/l	5	< 17	< 3	< 36	7	< 19	< 2	< 100	21
1,1-Dichloroethane	µg/l		88	< 5	294	8	66	< 2	260	22
1,2-Dichloroethane	µg/l	5	< 33	< 4	< 100	6	< 16	< 1	< 100	20
cis-1,2-Dichloroethylene	µg/l	70	< 64	< 53	< 75	2	< 57	< 1	436	13
trans-1,2-Dichloroethylene	µg/l	100	< 51	< 32	< 100	4	< 18	< 1	< 110	16
Ethylbenzene	µg/l	700	40	< 5	87	7	35	< 1	118	22
Methylene chloride	µg/l		435	< 5	1,303	8	334	< 1	4,150	22
1,1,1-Trichloroethane	µg/l	200	< 68	< 5	100	6	< 55	< 1	270	20
Trichloroethylene	µg/l	5	< 56	< 5	114	7	< 24	< 1	100	19
Toluene	µg/l	1,000	491	< 5	959	7	228	< 1	740	22
Vinyl chloride	µg/l	2	< 49	< 7	< 100	6	< 34	< 3	< 300	20
Xylenes	µg/l	10,000	117	< 5	277	6	83	< 5	220	20

Note: (1) " " = not analyzed; < = more than 50% of measurements reported as non-detect.

Table 5-10. Summary of Landfill Leachate Chemistry Data (Continued).

			HW				MSW ASH			
Waste Type										
Number of Landfills			4				7			
Parameter	Units	MCLs	Average	Minimum	Maximum	No. of Landfills	Average	Minimum	Maximum	No. of Landfills
pH	pH units		8.17	7.55	9.36	3	7.06	6.54	7.44	5
Specific conductance	µmhos/cm		22,096	12,302	39,598	3	22,083	10,732	43,383	4
TDS	mg/l						24,493	6,067	46,733	6
COD	mg/l						1,670	304	5,607	4
BOD_5	mg/l						55	15	84	4
TOC	mg/l		1,623	7	3,239	2	62	39	109	3
Alkalinity	mg/l						1,942	99	5,010	4
Chloride	mg/l		7,758	3,783	11,734	2	10,426	2,940	22,400	4
Sulfate	mg/l		2,985	704	5,267	2	881	85	3,430	5
Calcium	mg/l						900	96	1,332	3
Magnesium	mg/l						267	113	420	2
Sodium	mg/l		5,243	2,514	7,972	2	1,181	684	1,994	5
Arsenic	µg/l	50	26,710	30	79,912	3	9	5	17	6
Cadmium	µg/l	5	< 119	< 5	< 233	2	< 12	< 2	49	6
Chromium	µg/l	100	124	22	226	2	< 30	< 1	84	6
Lead	µg/l		109	24	249	3	23	3	74	6
Nickel	µg/l		738	285	1,190	2	< 40	< 24	48	4
Benzene	µg/l	5	< 131	< 7	370	3	< 3	< 1	< 5	3
1,1-Dichloroethane	µg/l		123	< 14	< 371	4	< 12	< 1	< 33	3
1,2-Dichloroethane	µg/l	5	< 382	5	< 1,124	3	< 3	< 1	< 5	3
cis-1,2-Dichloroethylene	µg/l	70					< 2	< 1	< 3	2
trans-1,2-Dichloroethylene	µg/l	100	< 79	< 14	< 143	2	< 3	< 1	< 5	3
Ethylbenzene	µg/l	700	< 133	< 5	< 512	4	< 4	< 2	< 7	3
Methylene chloride	µg/l		161	4	< 447	4	< 3	< 1	< 6	3
1,1,1-Trichloroethane	µg/l	200	< 99	8	< 347	4	< 7	< 1	< 16	3
Trichloroethylene	µg/l	5	< 76	33	< 146	3	< 3	< 1	< 5	3
Toluene	µg/l	1,000	< 173	< 9	616	4	< 10	< 1	< 25	3
Vinyl chloride	µg/l	2	< 1,475	< 10	< 4,405	3	< 5	< 1	< 10	3
Xylenes	µg/l	10,000	14	9	18	2	< 2	< 1	< 3	2

Note: (1) " " = not analyzed; < = more than 50% of measurements reported as non-detect.

Table 5-10. Summary of Landfill Leachate Chemistry Data (Continued).

Waste Type			COAL ASH				C&DW			
Number of Landfills			2				2			
Parameter	Units	MCLs	Average	Minimum	Maximum	No. of Landfills	Average	Minimum	Maximum	No. of Landfills
pH	pH units		7.70	7.66	7.74	2	6.43	6.43	6.43	1
Specific conductance	µmhos/cm		884	623	1144	2	4815	4815	4815	1
TDS	mg/l		723	347	1098	2	3553	2880	4225	2
COD	mg/l		11	11	11	1	2414	1139	3688	2
BOD_5	mg/l		< 3	< 3	< 3	1	1126	1126	1126	1
TOC	mg/l		6	6	6	1	839	443	1235	2
Alkalinity	mg/l		190	160	220	2	2450	2450	2450	1
Chloride	mg/l		21	21	21	1	681	671	690	2
Sulfate	mg/l		383	178	587	2	255	48	463	2
Calcium	mg/l		190	190	190	1	292	203	382	2
Magnesium	mg/l		22	15	30	2	202	202	202	1
Sodium	mg/l		46	46	46	1	304	284	324	2
Arsenic	µg/l	50	36	< 9	62	2	15	15	15	1
Cadmium	µg/l	5	< 7	< 5	< 9	2	< 3	< 1	< 5	2
Chromium	µg/l	100	< 16	< 9	22	2	39	39	39	1
Lead	µg/l		< 19	< 4	< 34	2	7	3	10	2
Nickel	µg/l		38	38	38	1	< 56	< 56	< 56	1
Benzene	µg/l	5	< 4	< 4	< 4	1	17	17	17	1
1,1-Dichloroethane	µg/l		< 4	< 4	< 4	1	92	92	92	1
1,2-Dichloroethane	µg/l	5	< 4	< 4	< 4	1	3	3	3	1
cis-1,2-Dichloroethylene	µg/l	70								
trans-1,2-Dichloroethylene	µg/l	100	< 1	< 1	< 1	1				
Ethylbenzene	µg/l	700	< 3	< 3	< 3	1	66	66	66	1
Methylene chloride	µg/l		< 4	< 4	< 4	1	417	417	417	1
1,1,1-Trichloroethane	µg/l	200	< 4	< 4	< 4	1	51	51	51	1
Trichloroethylene	µg/l	5	< 4	< 4	< 4	1	< 11	< 11	< 11	1
Toluene	µg/l	1,000	< 2	< 2	< 2	1	613	613	613	1
Vinyl chloride	µg/l	2	< 7	< 7	< 7	1	8	8	8	1
Xylenes	µg/l	10,000	< 4	< 4	< 4	1	210	210	210	1

Note: (1) " " = not analyzed; < = more than 50% of measurements reported as non-detect.

- The HW landfill leachates were more mineralized and had a higher organic content than MSW leachates. All of the HW leachates were alkaline, with pH values ranging from 7.5 to 9.4. One possible explanation for the alkaline pH values is the relatively common practice of solidifying hazardous waste with pozzolonic additives prior to disposal. These relatively high pHs decrease the mobility of metals. Even so, the average heavy metals concentrations were generally several times to several orders of magnitude higher in HW leachates as compared to MSW leachates. The HW leachates also had higher average concentrations of all VOCs, except methylene chloride, toluene, and xylenes. Of the heavy metals and VOCs considered in Table 5-10, arsenic, nickel, 1,2-dichloroethane, and vinyl chloride were detected at the highest concentrations in HW leachates. Average concentrations of arsenic, cadmium, chromium, benzene, 1,2-dichloroethane, trichloroethylene, and vinyl chloride in HW landfill leachates exceeded MCLs. None of the landfills had leachate with average chemical concentrations exceeding the MCLs for ethylbenzene, toluene, or xylenes.
- The chemistry of the ISW landfill leachates was highly variable due to the wide variety of wastes disposed in ISW landfills. The pH values for these leachates ranged from 6.4 to 7.7. The MSW ash leachates, the most mineralized of the ISW landfill leachates, were even more mineralized than the MSW leachates in this study, as evidenced by the high specific conductance, TDS, sulfate, and chloride levels of the MSW ash leachates. Coal ash leachates were the least mineralized. Both the MSW ash and coal ash leachates had low BOD values that were several orders of magnitude less than the BOD values for MSW leachate because most of the organic materials originally in the MSW and coal had been combusted. The average BOD value for C&DW leachate, however, was within range of values reported for MSW leachate. Heavy metals concentrations in MSW ash and C&DW leachates were similar to those for MSW leachates. Metals concentrations in coal ash leachate were lower, generally at the lower end of the concentration range for MSW leachates. As expected, the MSW ash and coal ash leachates did not contain VOCs. However, published data show that MSW ash leachates can contain trace amounts of base neutral extractables (BNAs), polychlorinated dibenzo-p-dioxins (PCDDs), and polychlorinated dibenzo-furans (PCDFs). The one C&DW landfill for which organic chemistry data are available produced leachate containing VOCs. Average concentrations of cadmium in MSW ash and coal ash landfill leachates and benzene, trichloroethylene, and vinyl chloride concentrations in C&DW landfill leachates exceeded MCLs.
- In general, the leachate chemistry data collected for the study fall within the range of published data.
- With the federal solid waste regulations promulgated in the 1980's and early 1990's (e.g., 1980 RCRA Subtitle C regulations for HW in 40 CFR 261 and Land Disposal Restrictions in 40 CFR 268), it is expected that the quality of MSW and HW landfill leachates would have improved over time. No statistically significant differences in concentrations of the considered trace metals or VOCs in leachates from older modern MSW landfills constructed prior to 1990 (pre-1990

landfills) and leachates from newer MSW landfills constructed after 1990 (post-1990 landfills) were observed at the 90% confidence level. However, average VOC concentrations were generally lower in leachate from the post-1990 landfills (Table 5-10). The statistical analysis findings were limited by the data. The limited number of landfills contributing to each dataset and the wide range of chemical concentrations led to large confidence intervals for each parameter in the datasets. To further evaluate the differences in leachate chemistry between older and newer MSW landfills, the data for the post-1990 MSW landfills were compared to published leachate chemistry data for 61 older MSW landfills (i.e., pre-1980 landfills in NUS (1988) and pre-1985 landfills in Gibbons et al. (1992)). The distributions of the leachate chemistry data for the older MSW landfills were not known, so the two data sets could not be compared statistically. However, the average concentrations of trace metals and VOCs in leachate from the newer landfills were almost always less than the average concentrations in leachate from the older landfills. Based on the above, it appears that the solid waste regulations have resulted in improved MSW landfill leachate quality. However, more data are needed to quantify this improvement. From the published information summarized in this report, the regulations may have also reduced the occurrence of certain chemicals. For example, acetonitrile, cyanide, and naphthalene were detected more frequently in leachate from older landfills than in leachate from newer landfills.

- Published leachate chemistry data for 33 older HW landfills (i.e., pre-1984 landfills in Bramlett et al. (1987), pre-1983 landfills in NUS (1988), and pre-1987 landfills in Gibbons et al. (1992)) were compared to the data presented for HW landfills in this report (i.e., newer HW landfills). The dataset for newer HW landfills is small; only leachate chemistry data for four landfills are available. The concentrations of chemicals in leachate from the newer landfills were found to be within the range of published values for the older landfills. The distribution of the leachate chemistry data for the older HW landfills was not known, so the two datasets could not be compared statistically. However, on average, most heavy metal concentrations and almost all VOC concentrations were lower in leachate from the newer landfills. This reduction in leachate strength is likely a result of the Subtitle C regulations and the Land Disposal Restrictions.

5.3 Lessons Learned from Waste Containment System Problems at Landfills

5.3.1 Scope of Work

The scope of work for this portion of the project involved an investigation into problems that have occurred in waste containment systems for 69 modern landfill facilities and five modern surface impoundment facilities located throughout the U.S. The investigation focused on landfills, and only landfill-related problems are discussed in this section. The purpose of the investigation is twofold: (i) to better understand the nature, frequency, and significance of identified problems; and (ii) to develop recommendations to reduce the future occurrence of problems.

The scope of work specifically excluded consideration of problems in older waste containment systems not designed and constructed to current standards and practices. These problems include, for example, the LCRS and cover system internal drainage layer failures described by Bass (1986), Ghassemi et al. (1986), and Kmet et al. (1988). The scope of work also excluded foundation stability problems at older landfills, such as the problems described by Oweis (1985), Dvirnoff and Munion (1986), Richardson and Reynolds (1991), Kenter et al. (1997), Stark and Evans (1997), and Schmucker and Hendron (1997). Problems at older facilities are often not relevant to current standards and practices.

5.3.2 Description of Database

The 80 landfill problems identified during the investigation for this report are categorized on the basis of two criteria. The first criterion addresses the component or attribute of the landfill liner system or cover system affected by the problem. The specific landfill components and attributes considered in this study are: (i) liner construction; (ii) liner degradation; (iii) LCRS or LDS construction; (iv) LCRS or LDS degradation; (v) LCRS or LDS malfunction; (vi) LCRS or LDS operation; (vii) liner system stability; (viii) liner system displacement; (ix) cover system as built; (x) cover system degradation; (xi) cover system stability; and (xii) cover system displacement. Specific problems that may affect these components and attributes are listed in Tables F-4.1 to F-4.3 in Appendix F. Other components or attributes not specifically associated with landfill integrity were not considered in the investigation. These include landfill daily and intermediate cover components (except for cracking of the soil intermediate cover during the Northridge earthquake), leachate transmission and treatment components beyond the leachate collection sumps or manholes, and landfill gas extraction and management components.

The second criterion used to categorize the problem addresses the principal human factor contributing to the problem. The principal human factors considered are: (i) design; (ii) construction; and (iii) operation. While a principal human factor has been assigned to each problem, it should be recognized that most problems have complex causes and several contributing factors. Hereafter, the problem classifications are shown as “component or attribute criterion”/”principal human factor criterion” (e.g., liner system stability/design).

Detailed case histories of the problems are presented in Attachment F-A of Appendix F. The information sources for the problems are listed in Table F-2.1 of Appendix F. Summaries of the identified problems are presented in Table F-2.2 and are repeated in Table 5-11 below. The problems are grouped according to the above two criteria in Table F-2.3 of Appendix F.

Table 5-11. Summary of Identified Problems at Landfills.

Problem Classification[(1)]	Facility Designation/ Appendix Section	Problem Summary
liner construction/ construction	L-1/F-A.2.1	leakage through holes in HDPE GM primary liner
liner construction/ construction	L-3/F-A.2.2	leakage through holes in HDPE GM liners
liner construction/ construction	L-5/F-A.2.3	leakage through holes in HDPE GM primary liner
liner construction/ operation	L-6/F-A.2.4	leakage through holes in HDPE GM primary liner
liner construction/ operation	L-7/F-A.2.5	leakage though HDPE GM/CCL composite primary liner at pipe penetration
liner construction/ design	L-8/F-A.2.6	landfill gas migrated beyond liner system and into vadose zone resulting in groundwater contamination
liner construction/ construction	L-9/F-A.2.7	leakage though HDPE GM primary liner at pipe penetration
liner construction/ construction	L-11/F-A.2.8	construction debris in CCL with initially smooth surface protruded from CCL after CCL was left exposed and subsequently eroded
liner construction/ construction	L-11/F-A.2.9	leakage though HDPE GM primary liner at pipe penetration
liner construction/ construction	L-15/F-A.2.10	sand bag under installed GM liner approved by CQA consultant
liner construction/ construction	L-17/F-A.2.11	leakage through holes in HDPE GM primary liner
liner construction/ construction	L-19/F-A.2.12	wind uplifted and tore HDPE GM liner during construction
liner construction/ construction	L-19/F-A.2.13	severe wrinkling of HDPE GM due to thermal expansion during construction
liner construction/ construction	L-29/F-A.2.14	large folded wrinkles in HDPE GM primary liner at two exhumed leachate sumps
liner degradation/design	L-2/F-A.3.1	desiccation cracking of CCL in exposed HDPE GM/CCL composite liner
landfill liner degradation/operation	L-4/F-A.3.2	HDPE GM/CCL composite liner damaged by waste fire
liner degradation/ design	L-12/F-A.3.3	leachate extraction well installed in landfill appeared to puncture GM primary liner
liner degradation/ construction	L-14/F-A.3.4	HDPE GM liner damaged by fire believed to be started by lightning strike
liner degradation/ construction	L-20/F-A.3.5	saturation of GCL beneath GM liner when rainwater ponded on tack-seamed patch over GM hole
liner degradation/ construction	L-43/F-A.3.6	water ponded between HDPE GM and CCL components of composite secondary liner and was contaminated from a source other than the landfill
liner degradation/ design	L-44/F-A.3.7	landfill gas well punctured GM component of composite liner and extended into CCL

Table 5-11. Summary of Identified Problems at Landfills (Continued).

Problem Classification	Facility Designation/ Appendix Section	Problem Summary
LCRS or LDS construction/construction	L-10/F-A.4.1	rainwater entered LDS through anchor trench
LCRS or LDS construction/construction	L-15/F-A.4.2	sand bags in LCRS drainage layer and debris in LCRS pipe trench approved by CQA consultant
LCRS or LDS construction/construction	L-16/F-A.4.3	rainwater entered LDS through anchor trench
LCRS or LDS construction/construction	L-28/F-A.4.4	excessive needle fragments in manufactured needlepunched nonwoven GT
LCRS or LDS construction/construction	L-32/F-A.4.5	HDPE LCRS pipe separated at joints
LCRS or LDS construction/construction	L-33/F-A.4.6	HDPE LCRS pipe separated at joints
LCRS or LDS degradation/ design	L-9/F-A.5.1	erosion of sand LCRS drainage layer on liner system side slopes
LCRS or LDS degradation/ design	L-11/F-A.5.2	erosion of sand protection layer on liner system side slopes
LCRS or LDS degradation/ construction	L-13/F-A.5.3	polypropylene continuous filament nonwoven GT filter degraded due to outdoor exposure
LCRS or LDS degradation/ construction	L-18/F-A.5.4	polypropylene staple-fiber needlepunched nonwoven GT filter degraded due to outdoor exposure
LCRS or LDS degradation/ construction	L-30/F-A.5.5	HDPE LCRS pipe crushed during construction
LCRS or LDS malfunction/ operation	L-12/F-A.6.1	LCRS pipes were not regularly cleaned and became clogged, and LCRS drainage layer may be partially clogged
LCRS or LDS malfunction/ design	L-22/F-A.6.2	waste fines clogged needlepunched nonwoven GT filter wrapped around perforated LCRS pipes
LCRS or LDS malfunction/ design	L-36/F-A.6.3	waste fines clogged needlepunched nonwoven GT filter around LCRS pipe bedding gravel
LCRS or LDS malfunction/ operation	L-37/F-A.6.4	leachate seeped out landfill side slopes in the vicinity of chipped tire layers
LCRS or LDS operation/ operation	L-5/F-A.7.1	overestimation of LDS flow quantities due to problems (e.g., clogging) with automated LDS flow measuring and removal equipment
LCRS or LDS operation/ operation	L-23/F-A.7.2	valves on LCRS pipes were not opened and leachate could not drain, and waste and leachate flowed over a berm into a new unapproved cell
LCRS or LDS operation/ operation	L-34/F-A.7.3	LCRS leachate pump moved air and liquid causing pump airlock and underestimation of leachate quantities
LCRS or LDS operation/ design	L-35/F-A.7.4	LCRS leachate pumps and flowmeters continually clogged and LDS leachate pumps turned on too frequently and burned out prematurely

Table 5-11. Summary of Identified Problems at Landfills (Continued).

Problem Classification	Facility Designation/ Appendix Section	Problem Summary
liner system stability/ design	L-21/F-A.8.1	sliding along PVC GM/CCL interface during construction
liner system stability/ operation	L-24/F-A.8.2	sliding along GN/GCL (HDPE GM side) and GCL(bentonite side)/CCL interfaces during operation
liner system stability/ design	L-25/F-A.8.3	sliding along HDPE GM/ polyester needlepunched nonwoven GT and HDPE GM/CCL interfaces during operation
liner system stability/ design	L-26/F-A.8.4	two tears in HDPE GM liner and cracks in soil intermediate cover from Northridge earthquake
liner system stability/ design	L-27/F-A.8.5	extensive cracks in soil intermediate cover and further tearing of GT cushion from Northridge earthquake
liner system stability/ design	L-38/F-A.8.6	sliding along needlepunched nonwoven GT/HDPE GM primary liner interface after rainfall
liner system stability/ design	L-39/F-A.8.7	sliding along needlepunched nonwoven GT/HDPE GM liner interface after rainfall
liner system stability/ design	L-40/F-A.8.8	sliding along gravel/HDPE GM liner interface after rainfall
liner system stability/ design	L-41/F-A.8.9	sliding along very flexible GM liner/needlepunched nonwoven GT interface after rainfall
liner system stability/ operation	L-42/F-A.8.10	sliding along needlepunched nonwoven GT/PVC GM liner interface after a thaw
liner system stability/ operation	L-45/F-A.8.11	sliding along needlepunched nonwoven GT/HDPE GM liner interface after erosion of soil anchoring geosynthetics
liner system stability/ design	L-46/F-A.8.12	sliding along GN/HDPE GM primary liner interface during construction
liner system displacement/design	L-9/F-A.9.1	uplift of GM by landfill gas after erosion of overlying sand LCRS drainage layer
liner system displacement/design	L-11/F-A.9.2	uplift of geosynthetics by landfill gas after erosion of overlying sand protection layer
liner system displacement/design	L-25/F-A.9.3	uplift of composite liner by surface-water infiltration during construction
liner system displacement/design	L-31/F-A.9.4	uplift of composite liner by surface-water infiltration during construction
cover system construction/ construction	C-2/F-A.10.1	portion of topsoil from off-site source was contaminated with chemicals
cover system construction/ construction	C-16/F-A.10.2	high failure rate of HDPE GM seam samples during destructive testing
cover system degradation/ design	C-1/F-A.11.1	failure of geosynthetic erosion mat-lined downchute on 3H:1V side slope
cover system degradation/ design	C-12/F-A.11.2	erosion of topsoil layer on 60 m long, 3H:1V side slope

Table 5-11. Summary of Identified Problems at Landfills (Continued).

Problem Classification	Facility Designation/ Appendix Section	Problem Summary
cover system stability/ construction	C-3/F-A.12.1	sliding along nonwoven GT/GM interface during construction
cover system stability/ design	C-4/F-A.12.2	sliding along topsoil/GCL interface after rainfall
cover system stability/ design	C-5/F-A.12.3	sliding along sand/woven GT interface after rainfall
cover system stability/ design	C-6/F-A.12.4	sliding along sand/GM interface after rainfall
cover system stability/ design	C-7/F-A.12.5	sliding along gap-graded sand/GM interface after rainfall
cover system stability/ design	C-8/F-A.12.6	sliding along gravel/GT interface during construction
cover system stability/ design	C-9/F-A.12.7	sliding along sand/calendered nonwoven GT interface after rainfall
cover system stability/ design	C-10/F-A.12.8	sliding along sand/GM interface after rainfall
cover system stability/ design	C-11/F-A.12.9	sliding along topsoil/nonwoven GT interface during construction
cover system stability/ design	C-13/F-A.12.10	sliding along PVC GM/CCL interface after a thaw
cover system stability/ construction	C-14/F-A.12.11	sliding along geogrid/HDPE GM interface during construction
cover system stability/ design	C-17/F-A.12.12	sliding along sand/CCL interface during rainfall
cover system stability/ design	C-18/F-A.12.13	sliding along sand/CCL interface immediately after rainfall
cover system stability/ design	C-19/F-A.12.14	sliding along sand/CCL interface after rainfall
cover system stability/ design	C-20/F-A.12.15	sliding along sand/CCL interface after rainfall
cover system stability/ design	C-21/F-A.12.16	minor cracks in soil intermediate cover from Northridge Earthquake
cover system stability/ design	C-22/F-A.12.17	215-m long cracks in soil intermediate cover from Northridge Earthquake
cover system stability/ design	C-23/F-A.12.18	minor cracks in soil intermediate cover from Northridge Earthquake
cover system displacement/design	C-12/F-A.13.1	cover system settlement caused tearing of HDPE GM boots around gas well penetrations of GM barrier
cover system displacement/construction	C-15/F-A.13.2	localized cover system settlement during construction stretched, but did not damage, PVC GM barrier and opened GCL joints

Note: (1) Each problem classification has two parts: (i) the component or attribute of the landfill that experienced the problem; and (ii) the principal human factor contributing to the problem.

5.3.3 Study Findings

Based on the results of the investigation into waste containment system problems presented in Appendix F, the following conclusions are drawn:

- This investigation identified 69 modern landfill facilities that had experienced a total of 80 waste containment system problems. This number of facilities is relatively small in comparison to the over 1,000 modern landfills nationwide. The search for problem facilities for this study was not exhaustive, and it is certain that there are other facilities with problems similar to those described in this report.
- About 72% of the landfill problems were liner system related and 28% were cover system related. The ratio of liner system problems to cover system problems is probably exaggerated by the fact that a number of the facilities surveyed were active and did not have a cover system.
- Based on the waste containment system component or attribute criterion, the identified landfill problems were classified as follows, in order of decreasing frequency:
    - cover system stability: 23%;
    - liner construction: 18%;
    - liner system stability: 15%;
    - liner degradation: 9%;
    - LCRS or LDS construction: 8%;
    - LCRS or LDS degradation: 6%;
    - LCRS or LDS malfunction: 5%;
    - LCRS or LDS operation: 5%;
    - liner system displacement: 5%;
    - cover system construction: 2%;
    - cover system degradation: 2%; and
    - cover system displacement: 2%.
- Using this criterion, these problems can also be grouped into the following general categories (Figure 5-6):
    - liner system or cover system slope stability or displacement: 45%
    - liner, LCRS or LDS, or cover system construction: 28%;
    - liner, LCRS or LDS, or cover system degradation: 17%; and
    - LCRS or LDS malfunction or operation: 10%.
- Based on the principal human factor contributing to the problem criterion, the identified landfill problems were classified as follows (Figure 5-7):
    - design: 51%;
    - construction: 35%; and
    - operation: 14%.

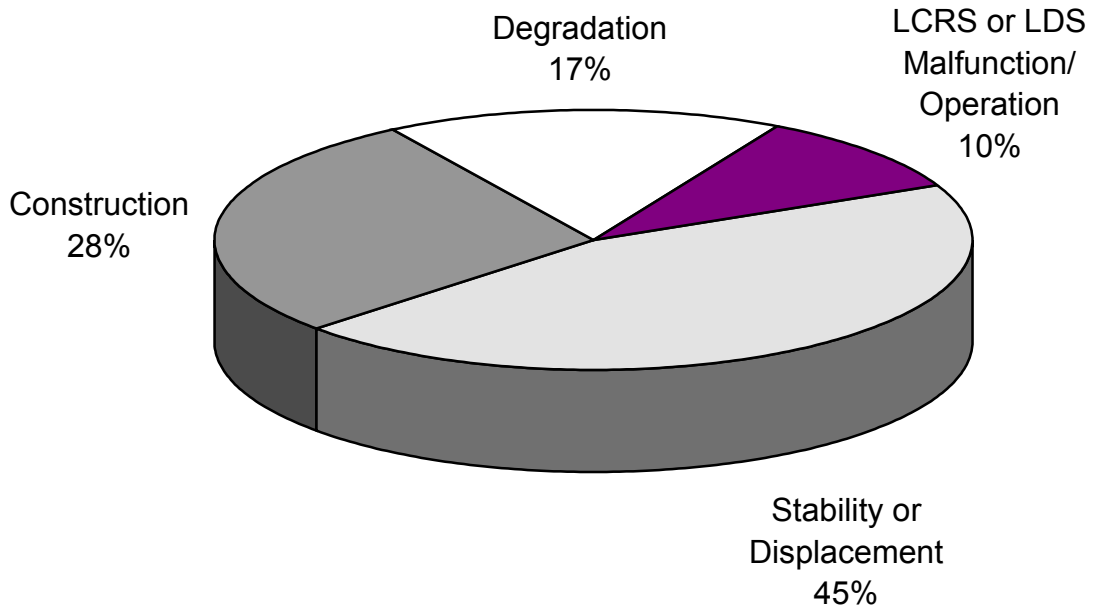

Figure 5-6. General distribution of problems by waste containment system component or attribute criterion.

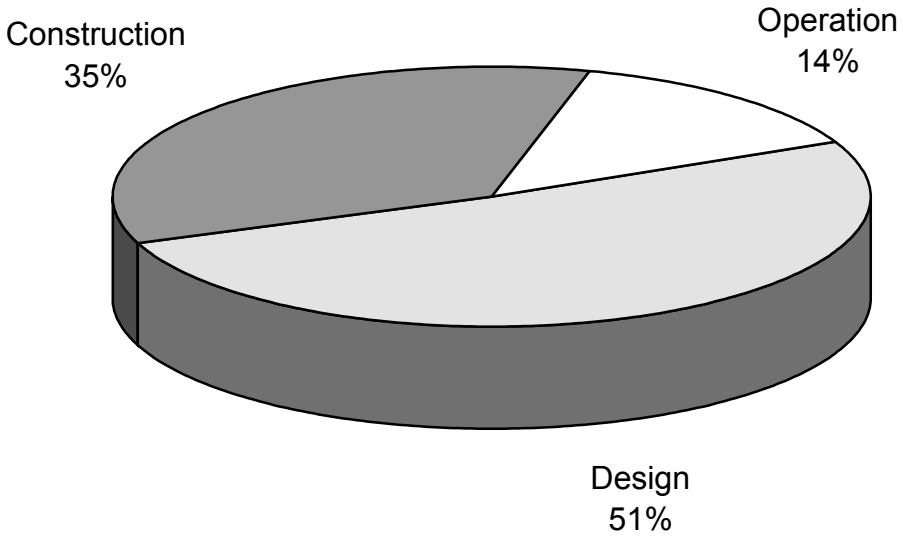

Figure 5-7. Distribution of problems by principal human factor contributing to the problem criterion.

- Problems that occurred at two or more landfills and the number of landfills at which they occurred are as follows, in order of presentation in Chapter F-3 of Appendix F:
    - leakage through holes (construction- or operation-related) in an HDPE GM primary liner (5 landfills);
    - leakage through an HDPE GM primary liner or HDPE GM/CCL composite primary liner at the LCRS pipe penetration of the liner (3 landfills);
    - severe wrinkling of an HDPE GM liner during construction (2 landfills);
    - liner damage by fire (2 landfills);
    - liner damage during well installation (2 landfills);
    - rainwater entered the LDS through the anchor trench (2 landfills);
    - HDPE LCRS pipe was separated at joints (2 landfills);
    - erosion of the sand layer on liner system side slopes (2 landfills);
    - degradation of polypropylene nonwoven GT filters due to outdoor exposure (2 landfills);
    - waste fines clogged the needlepunched nonwoven GT filter in the LCRS piping system (2 landfills);
    - clogging and other problems with the leachate pump or flow rate measuring system (3 landfills);
    - liner system slope failure due to static loading (10 landfills);
    - liner system damage due to earthquakes (2 landfills);
    - uplift of liner system geosynthetics by landfill gas after erosion of the overlying sand layer (2 landfills);
    - uplift of composite liner by surface-water infiltration during construction (2 landfills);
    - cover system slope failure during construction (4 landfills);
    - cover system slope failure after rainfall or a thaw (11 landfills); and
    - soil cover damage due to earthquakes (3 landfills).
- For problems that occurred at three or more landfills, the principal human factor contributing to the problem criterion, detection of the problem, causes of the problem, and remedy of the problem are described below:
    - *Leakage through holes in an HDPE GM primary liner* occurred at five landfills. In each case, the holes were attributed to construction or, at one landfill, possibly operation factors. At two of the landfills, leakage was first detected during electrical leak location surveys performed as part of CQA and by the relatively high LDS flow rates that occurred after rainwater ponded in a landfill. At the remaining three landfills, leakage was first detected during operation by the relatively high LDS flow rates and the color of and chemical constituents in the LDS liquid. The cause of the leakage was attributed to construction-related holes in the GM. However, at one landfill, where waste was placed directly on liner system geosynthetics (i.e., there is no soil protection layer), the GM may have been damaged during waste placement. The leakage problem was resolved at four landfills by repairing the GM holes; at the remaining landfill, the problem, clearly identified only

after the cell had been covered with waste, was partially remedied by lowering the “pump on” liquid level in the LCRS sump.

- *Leakage through an HDPE GM primary liner or HDPE GM/CCL composite primary liner at the LCRS pipe penetration of the liner* occurred at three landfills. This leakage was attributed to construction factors at two of the landfills and operation factors at the third landfill. At two of the landfills, leakage at the pipe penetration was detected during construction after rainwater ponded over the penetration and LDS flow rates increased. The cause of the leakage was construction defects in the pipe penetration; it is difficult to construct a defect-free pipe penetration, even when extra measures are taken to enhance the integrity of the connection. At the remaining landfill, leakage was detected during operation when the average LDS flow rate increased significantly. For this landfill, the pipe penetration was damaged during operation when a rubber-tired loader trafficked over it. The pipe penetrations were repaired; however, at one landfill where the problem was detected during construction, the repairs did not significantly decrease LDS flow rates; thus there must have existed a penetration defect that was not located.
- *Clogging and other problems with the leachate pumps or flow rate measuring system* occurred at three landfills. These problems were attributed to design factors at one of the landfills and operation factors at the other two landfills. The problems, which were identified during routine operations, included: (i) clogging of the air lines and failure of the compressor for the control system; (ii) drift of the leachate level measurement system; (iii) drift of the “pump on” time setting; (iv) burn out of pumps due to control system problems; (v) clogging of pumps; (vi) clogging of mechanical flowmeters; (vii) damage to electrical equipment by electrical storms; (viii) check valve failure; and (ix) inaccurate measurement of LCRS or LDS flow rates due to the above equipment problems. These problems appear to have been primarily caused by: (i) inadequate overall mechanical system design; (ii) using equipment that was less reliable than was needed; (iii) using equipment that was not compatible with the landfill leachate; and (iv) not performing equipment maintenance often enough. These problems were primarily remedied by equipment maintenance, repair, and replacement.
- *Liner system slope failure due to static loading* occurred at ten landfills. These problems were attributed to design factors at seven of the landfills and operation factors at the remaining three landfills. Slope failure occurred during construction at two of the landfills and during operation at the remaining eight landfills. The problem was detected by visual observation of mass movement of the liner system, cracking of soil layers near the slope crest, and tearing, tensioning, or wrinkling of geosynthetics. The primary causes of failure were: (i) using unconservative presumed values for the critical interface shear

strength; (ii) not evaluating the critical condition for slope stability (e.g., liner system with waste at intermediate grades); (iii) not accounting for, or underestimating, seepage pressures; (iv) not accounting for moisture at the GM/CCL interface (which weakens the interface) due to spraying of the CCL and thermal effects; and (v) not maintaining the drainage layer outlets free of snow and ice, which can lead to increased seepage pressures. The slope failures were remedied by reconstructing the damaged liner systems, sometimes with different materials, and developing new construction procedures to reduce moisture at the GM/CCL interface.

- *Cover system slope failure during construction* occurred at four landfills. These problems were attributed to design factors at two of the landfills and construction factors at the remaining two landfills. Slope failure was detected by visual observation of mass movement of the cover system, cracking of soil layers near the slope crest, and wrinkling of geosynthetics at the toe of the cover system slope. The primary causes of failure were: (i) placing soil over the side slope geosynthetics from the top of the slope downward, rather from the toe of the slope upward; (ii) not considering the effects of variation in the tested geosynthetics, accuracy of test methods, and test conditions on the interface shear strength to use in design; and (iii) using unconservative presumed values for the critical interface shear strength. The problems were remedied by reconstructing the cover systems using different cover system materials that result in higher interface shear strengths and placing soil over side slope geosynthetics from the toe of the slope upward.
- *Cover system slope failure after rainfall or a thaw* occurred at eleven landfills. At all of these landfills, the failures were attributed to design factors. Slope failure occurred during the post-closure period and was detected by visual observation of mass movement of the cover system, cracking of soil layers near the slope crest, and wrinkling of geosynthetics at the toe of the cover system slope. The primary causes of failure appeared to be: (i) not accounting for, or underestimating, seepage pressures; (ii) clogging of the drainage system, which can lead to increased seepage pressures; and (iii) not accounting for moisture at the GM/CCL interface (which weakens the interface) due to rain falling on the CCL surface during construction and freeze-thaw effects. In general, the problems were remedied by reconstructing the cover systems with new drainage systems or different materials.
- *Soil cover damage due to earthquakes* occurred at three landfills. These problems all occurred during operation and were attributed to design factors. The damage, which was detected by visual inspection, consisted of surficial cracking of soil intermediate cover occurring primarily near locations with contrast in seismic response characteristics (e.g., top of waste by canyon walls). The damage was

expected and dealt with as an operation issue through post-earthquake inspection and repair (i.e., regrading and revegetating the cracked soil layers).

- Almost all of the problems identified in this investigation were detected shortly after they occurred by visual observation or evaluation of monitoring data.
- Of the problems in this study for which the remedy was identified, six problems were not completely repaired because their environmental impacts were not expected to be significant and because: (i) the source of the problem could not be identified; (ii) the problem was not worsening; (iii) repair of liner systems or LCRS pipes after waste placement would be extremely difficult and expensive; and/or (iv) additional liner system damage could occur in any attempt to excavate the waste and repair the liner system.
- The problems only resulted in an identified environmental impact to groundwater or surface-water quality by leachate or landfill gas at one facility, landfill L-8. At this MSW landfill, groundwater impact by VOCs was attributed to gas migration through a relatively permeable soil layer that secured the edge of the GM liner and extended from the crest of the liner system side slope to beyond the liner system. The problem was resolved by installing additional gas extraction wells in the landfill. Without the measures taken to correct the problems at some of the other facilities, however, adverse environmental impacts could have eventually occurred at these facilities.
- The main impacts of the problems identified in this investigation are interruption of waste containment system construction and operation, increased maintenance, and increased costs.
- The identified problems that most often disrupted construction and were required to be repaired before construction proceeded were related to:
    - holes in GM liners and at pipe penetrations of liners;
    - large wrinkles in HDPE GM liners;
    - degradation of exposed geosynthetics;
    - uplift of constructed liners by groundwater or infiltrating surface water; and
    - erosion of unprotected soil layers (CCLs, sand drainage layers, soil protection layers).
- Problems that disrupt operation are generally more severe in terms of required repairs than those that interfere with construction and may require waste relocation. Consequently, problems that disrupt operation generally require more time to remedy than problems that are identified and repaired during construction. Problems that involve major breaches of liner systems or cover systems (e.g., failure of landfill liner system slopes) may require months to repair. The identified problems that most often disrupted operation and were required to be repaired before operation proceeded were related to:
    - holes in GM liners and at pipe penetrations of liners;
    - failure of one or more components of a liner system or cover system on landfill slopes; and
    - clogging of GTs in LCRSs.

- Problems that require maintenance may be more severe in terms of required repairs than those that interfere with construction, but are generally less severe than those that interfere with operation. In addition, problems that require maintenance are more likely to be reoccurring. The identified problems that most often required maintenance were related to:
    - erosion of soil layers (sand drainage layers, soil protection layers);
    - repair of LCRS or LDS flow rate measuring and removal systems; and
    - cracking of soil intermediate cover after earthquakes.
- The costs of remedying the problems can be significant. For the identified problems, the costs at the times the remedies were implemented ranged from less than $10,000 for repairs of GM holes identified by leak location surveys during construction to more than several million dollars for repair of a liner system slope failure that occurred during cell operation. In general, problems that impacted operation were more expensive than those that impacted construction or maintenance. However, certain problems that impact maintenance, such as erosion of soil layers, may ultimately be more costly than other problems if these problems reoccur.
- Even though there was only evidence of environmental impact at one of the waste containment systems in this study, the landfill industry should do more to avoid future problems in order to: (i) reduce the potential risk of future environmental impact; (ii) reduce the potential health and safety risk to facility workers, visitors, and neighbors; (iii) increase public confidence in the performance of waste containment systems; (iv) decrease potential impacts to construction, operation, and maintenance; and (v) reduce costs associated with the investigation and repair of problems.
- Importantly, all of the design, construction, and operation problems identified in this investigation can be prevented using available design approaches, construction materials and procedures, and operation practices. It is the responsibility of all professionals involved in the design, construction, operation, and closure of waste containment systems to improve the practice of waste containment system engineering. Owners must be prepared to adequately fund the levels of design and CQA activity necessary to properly design and construct waste containment systems. Design engineers must improve their practice to avoid the types of problems identified herein. Earthwork contractors, geosynthetics installers, and landfill operators all must be properly trained, supervised, and committed to the "quality goals" necessary to eliminate problems.

5.3.4 Recommendations

Based on an evaluation of the identified waste containment system problems, the following general and specific design, construction, and operation recommendations are made to reduce the incidence of these problems. These measures are not new; they have been used extensively for other engineered structures, such as dams. The measures include widely available design approaches, construction procedures, and operation practices. Many recommendations for landfill liner systems also apply to

cover systems, and vice versa. Because of this, the recommendations are grouped to apply to the following broad categories:

- general;
- liners and barriers;
- drainage systems;
- surface layers and protection layers;
- liner system and cover system stability; and
- liner system and cover system displacements.

Recommendations for each of these categories are presented below.

General recommendations intended to reduce the occurrence of problems include:

- information dissemination (e.g., this report);
- training of design engineers to better understand waste containment system design fundamentals and to avoid the types of design problems described in this report;
- training of design engineers to be better prepared to develop waste containment system specifications and CQA plans that are complete and precise, that include the construction-related assumptions made during design, and that require construction and CQA procedures to identify and prevent the kinds of construction problems identified in this report;
- training of CQA personnel in standard CQA procedures to avoid the types of construction problems identified in this report; for engineering technicians, this training can be demonstrated through the National Institute for Training in Engineering Technologies (NICET) certification program;
- training of contractors to avoid the types of construction problems identified in this report;
- development of better construction materials, techniques, and quality control/quality assurance procedures to prevent the kinds of construction problems identified in this report;
- development of better operations manuals to describe and provide controls for procedures to be followed by landfill operations personnel;
- training of facility operators to better avoid the types of operation problems identified in this report;
- training of facility operators to better detect and quickly report problems occurring during operation; and
- performing periodic independent audits to verify that the specified operation procedures are being practiced.

Specific recommendations are presented below in Table 5-12.

Table 5-12. Specific Recommendations to Reduce Landfill Problems.

	Recommendations		
Category	*Design*	*Construction*	*Operation*
Liners and Barriers	• Resin used to manufacture HDPE GM should be resistant to stress cracking. This is currently evaluated using the notched constant tensile load test (ASTM D 5397). This test should be required in project specifications. • Project specifications should require that both the inner and outer tracks of GM fusion seam samples taken for destructive testing meet the project seam requirements. Failure of one track is generally indicative of overall seaming problems and can result in increased stress concentrations in the adjacent track. In addition, testing both tracks may allow seaming problems to be identified and corrected quicker. • The potential for GM damage during placement of a soil layer over a GM can be reduced by protecting the GM. Measures for GM protection should be incorporated into the design and specifications. Measures include placing a protection layer (e.g., thick GT cushion or GC drainage layer) over the GM, using a greater initial lift thickness of soil above the GM, and using construction equipment with low ground pressure to place soils over the GM. The protection measures should be selected based on the characteristics of the soil to be placed (e.g., angularity, maximum particle size), the thickness of the soil layer, the type of equipment placing the soil, and whether CQA will be performed during soil placement. If the soil layer is placed during operation without CQA, extra GM protection is necessary. • GMs located in areas subjected to high static and dynamic stresses from construction equipment, such as beneath temporary access roads, require an even higher level of protection than GMs	• Construction equipment should be inspected for fuel and oil leaks, and those leaks should be repaired prior to using the equipment in liner construction to avoid liner and LDS contamination. • Liners and barriers should be constructed in manageable increments that ensure protection of the liner and barrier materials under seasonal weather changes. • CCLs should not be constructed with materials containing construction debris or large particles, even if prior to GM installation the CCL has a smooth surface and meets the hydraulic conductivity criterion. The debris may adversely impact the hydraulic conductivity of the CCL and/or damage an overlying GM. • CCLs should not be left unprotected for an extended period of time. They can desiccate and crack due to evaporation of water in the CCL, degrade when exposed to freezing and thawing actions, and be eroded by wind and water. • Prior to deploying a GM, all extraneous objects (e.g., tools, sand bags) should be removed from the surface on which the GM is to be placed to avoid GM damage and, for composite liners, promote good contact between the GM and underlying GCL or GCL. • HDPE GMs should be installed so that they are essentially stress-free at their lowest expected temperatures to avoid GM straining and, potentially, rupture. • GMs should be covered with thermal insulation layers at very low temperatures since GM strain at break decreases with decreasing temperature. • The leading edge of an uncovered GM should be secured to prevent wind from flowing beneath the GM and uplifting it. This is typically	• Landfill operations manuals should include limitations on the types of equipment that may traffic over the liner system before the first lift of waste is placed to prevent liner damage. • Landfill operations personnel should be aware of sensitive areas of a liner system, such as at pipe penetrations or sumps, and should protect these areas from damage. Sensitive areas can be identified with cones, flags, or other markers. They can also be isolated from traffic by berms, bollards, or other means. • Landfills should be operated to minimize the potential for waste fires. Measures to be taken could include not depositing loads of hot waste in a landfill and covering waste with a soil cover to decrease waste access to oxygen. • Care should be taken to not damage the liner system components when drilling into landfilled waste. Settlement of the waste surface must be taken into account when selecting the depth of drilling, and boreholes should not extend close (e.g., within 1 m) to the primary liner. Also, the limits of waste containment systems should be identified with markers or other means to reduce the potential for liner system or cover system damage by drilling or other invasive activities.

Table 5-12. Specific Recommendations to Reduce Landfill Problems (Continued).

	Recommendations		
Category	*Design*	*Construction*	*Operation*
Liners and Barriers (continued)	not subjected to high stresses. These protection measures should be incorporated into the design and specifications. • GM should be protected during waste placement over the GM. Protection measures should be incorporated into the design and specifications. Measures include installing a protection layer (e.g., thick GT cushion, GC drainage layer, or soil layer) over the GM, using spotters to direct equipment operators during waste placement over the GM, and placing only select waste over the GM. Protection measures should be selected with consideration of waste characteristics and the equipment placing the waste. • Sensitive areas of a liner system (e.g., at pipe penetrations) should be designed to be untraffickable by berms, bollards, or other means to decrease the potential for damage to these areas. • It is difficult to construct pipe penetrations of liners to be defect free. Until new methods for constructing better connections between GMs and ancillary structures have been developed and tested, designs without pipe penetrations (i.e., designs with internal sumps) should be preferred. • Internal sumps typically have sustained leachate heads at greater depths than other locations within the landfill and have seamed corners, which may contain holes. To decrease the rate of leakage through GM holes at sumps, the sump design should include additional liner components, such as a GCL, beneath the GM liner in the sump area, even if the GM is already underlain by a CCL. A design with a prefabricated GM sump may also be considered. • The potential for landfill gas to migrate over the geosynthetics	accomplished by seaming adjacent panels of GM shortly after deployment and placing a row of sandbags along the edge of the GM. • If sand bags are used to secure GM panels, the installer should ensure that the sand bags, and all other extraneous objects, are not trapped beneath the GM after seaming to avoid GM damage and, for composite liners, promote good contact between the GM and underlying CCL or GCL. • For HDPE GMs, fusion seams are preferred over extrusion seams because fusion seams have higher seam integrity and lower stress concentrations at seams. Extrusion seams should be minimized in the field by using prefabricated pipe boots, careful GM installation, etc. • HDPE GMs must be cleaned along the seam path before the seam is constructed since dirt in the seam adversely impacts seam integrity. To minimize the potential for dirt to collect in the seam path, GM should be seamed shortly after deployment. A temporary protective plastic film may also be placed on the GM edges at the factory and removed from the GM just prior to seaming. • In general, holes in HDPE GM seams should not be repaired by reseaming. This reheating of seams can embrittle the HDPE at the repair and make it more susceptible to stress cracking. • To the extent practicable, holes in GMs liners installed over GCLs should be repaired as soon as possible to avoid swelling of the GCL in case of hydration. GCL swelling results in a decrease in GCL shear strength and may impact landfill slope stability. Holes located in areas where rainwater may pond should be patched first. The patches should be sealed with a	

Table 5-12. Specific Recommendations to Reduce Landfill Problems (Continued).

	Recommendations		
Category	*Design*	*Construction*	*Operation*
Liners and Barriers (continued)	at the edge of the liner system must be considered in design. The potential for gas migration into the subsurface can be reduced by collecting gas generated in the landfill, using low-permeability soils over the edge of the liner system, and modifying the edge of the liner system so that the liner extends back up to the ground surface (like a reverse anchor trench).	permanent seam and not only tack welded. • When a GM is placed over a GCL, the GM should be covered with soils as soon as possible to minimize swelling of the GCL in case of hydration. GCL swelling results in a decrease in GCL shear strength and may impact landfill slope stability. • Connections between GMs and ancillary structures should be carefully constructed and inspected to decrease the potential for construction-related GM defects. • To decrease the potential for construction-related GM defects in sumps, the GM panel layout should be configured to minimize seams in sumps or prefabricated sumps should be used. • With respect to the potential for leakage, pipe penetrations are generally the most critical locations in landfills without internal sumps. If pipe penetrations are used, they should be carefully constructed and inspected. • Sumps and pipe penetrations of liners should be leak tested by ponding tests, leak location surveys, gas tracer tests, or pressure tests of double pipe boots as part of liner system CQA. Leak testing of the liner on the landfill base (where leachate heads are the highest) may also be considered. Identified holes should be repaired. • The entire installed GM should be inspected for damage and any damage should be repaired prior to placement of overlying materials. • GM should be covered with a soil layer as soon as practicable after installation, but not during the hottest time of the day if the GM is significantly wrinkled, to reduce GM wrinkles, prevent GM uplift by wind, and protect the GM from damage.	

Table 5-12. Specific Recommendations to Reduce Landfill Problems (Continued).

	Recommendations		
Category	*Design*	*Construction*	*Operation*
Liners and Barriers (continued)		• Prior to placing soil over a GM, the GM should be inspected for wrinkles. Excessive GM wrinkles and wrinkles that may fold over should be removed by waiting to backfill until the GM cools and contracts during the cooler nighttime and early morning hours, pulling the wrinkles out, or cutting the wrinkles out. The latter method is less desirable than the former methods because it requires intact GM to be cut, and it results in more GM seaming and testing. • On long side slopes, it may be preferable to use textured GM rather than smooth GM to decrease the size of GM wrinkles that develop, especially near the slope toe. • Composite liners and barriers constructed with a CCL should be covered with an insulation layer as soon as practicable to prevent CCL desiccation related to heating or freeze-thaw action.	
Drainage Systems	• Adjacent materials conveying water should be designed to decrease the clogging potential of the downgradient material using filter criteria calculations and/or laboratory testing. • If gap-graded soils are used as drainage materials, the effect of particle migration should be evaluated during design using filter criteria calculations and/or laboratory testing. In fact, the effect of particle migration from all granular drainage materials should be evaluated since these materials have fines. • Perforated pipes bedded in gravel should not be wrapped with a GT because the GT is useless, and, in some cases, even detrimental because the GT in this location is prone to clogging. Instead, the design should include a GT between the gravel and the surrounding soil or, possibly, no GT. • Geosynthetic anchor trenches should be backfilled with low-permeability soil and the soil	• The drainage system should be kept free of debris that may impede the flow of liquid. In general, all sandbags should be removed from the drainage system. However, if the sand in the bags meets the project specifications for the overlying drainage layer material, the bags can be cut and removed and the sand left in place. • GTs and GCs should be covered as soon as possible after installation to protect them from the environment (e.g., ultraviolet light, water, high temperature, animals). • The CQA consultant should verify that all connections required for adjacent drainage system pipes have been made. When pipe is connected by butt fusion seaming, the seam should be inspected for defects. • Care should be taken to not damage drainage system pipes during construction. The contractor should maintain	• Leachate may seep from landfill side slopes if the leachate can perch on layers of less permeable materials (e.g., daily and intermediate cover materials) within the waste or drain from layers of more permeable materials (e.g., tires) in the waste that are located relatively close to the side slope. The potential for seepage can be decreased by: (i) not placing layers of the more permeable materials near the side slopes; (ii) sloping layers of the less and more permeable materials away from the side slopes; (iii) distributing the more permeable materials throughout the waste; (iv) constructing leachate chimney drains to the LCRS around these layers; (v) removing perched leachate from wells installed to these layers; and (vi) using alternate daily covers (e.g., foams, tarps) that do not result in layers of less

Table 5-12. Specific Recommendations to Reduce Landfill Problems (Continued).

	Recommendations		
Category	*Design*	*Construction*	*Operation*
Drainage Systems (continued)	should be well compacted to reduce the potential for water to infiltrate into the trenches and flow into LCRSs or LDSs. If this is not practicable, the anchor trenches should be designed to drain freely and/or covered with a barrier, such as a GM. In addition, the ground surface should be graded away from the trenches to reduce runon from infiltrating into the trenches. • Project specifications for needlepunched nonwoven GTs should require that the GTs be needle-free and should require a certification from the manufacturer attesting to this. Needles, if present, may damage a nearby GM. • The CQA Plan should require that deployed GTs near GMs be inspected for needles before the GTs are covered with overlying materials. If needles are found, the GT should be rejected. • If a GT is to be exposed to the environment for an extended time period after installation, the potential for degradation of the GT should be evaluated under all the anticipated environmental conditions. EPA recommends that the effect of ultraviolet light on GT properties be evaluated using ASTM D 4355 (Daniel and Koerner, 1993). This test is typically run for 500 hours; however, it can be run for longer time periods to meet project-specific conditions. In any case, prior to covering the exposed GT, the condition of the GT should be evaluated by laboratory testing to verify that the GT is still satisfactory. • If test results indicate that the GT will not have the required properties after exposure (typically a specified strength retention), the GT should be protected with a sacrificial opaque waterproof plastic tarp, soil layer, or other means. • When the waste in a	sufficient soil cover between construction equipment and the pipes during construction. Equipment operators should be aware of pipe locations, since pipes can be crushed by trafficking equipment. Also, soil around pipes should be compacted using hand operated or walk-behind compaction equipment. • After construction of a cell with an external sump, the pipe from the cell to the sump should be inspected to verify that the pipe is functioning as designed. The inspection may be performed by surveying the pipe with a video camera, pulling a mandrel through the pipe, flushing the pipe with water, or other means.	permeable materials in the waste. • Drainage system pipes should be maintained by cleaning the pipes at least annually and more frequently, if warranted. • Landfills with external sumps may also include riser pipes at the low point of LCRSs as a precautionary measure to allow for leachate removal from the landfill, if necessary. • Leachate flow measurement systems should be calibrated and adjusted as needed at least annually to ensure that the quantities measured are accurate. • Due to the potential for problems in automated leachate metering and pumping equipment, landfill operations plans should include a verification program and contingency method for estimating the quantities of liquid removed from the LCRS and LDS. • Leachate sump pumps should be self priming so the pumps will not become airlocked and shut down if air is pulled into the pumps. • Leachate sump pumps should be selected to be compatible with sump geometries and anticipated leachate recharge rates so pump cycles are appropriate (e.g., not so short that the pumps turn on and off too frequently and burn out prematurely). • The “pump on” levels in internal sumps should be kept as low as practicable to reduce leakage if there are holes in the GM liner in the sump, especially if the GM is not underlain by a GCL. It is recognized, however, that "pump on" liquid levels in internal sumps may need to be larger than 0.3 m to achieve efficient sump pump operation. • The potential for clogging of water-level indicators, pumps, and flowmeters must be considered when selecting the

Table 5-12. Specific Recommendations to Reduce Landfill Problems (Continued).

	Recommendations		
Category	*Design*	*Construction*	*Operation*
Drainage Systems (continued)	containment system contains some fine particles that may migrate to the LCRS, the potential for LCRS clogging may be reduced by allowing those fine particles to pass though the drainage system to the LCRS pipes, which can subsequently be cleaned. The fine particles will pass more easily through the LCRS if no GTs are used in the LCRS or if the LCRS contains relatively thin open nonwoven GTs rather than thicker nonwoven GTs with a smaller apparent opening size. Note that the above does not apply to an LCRS with only a GN drainage layer. Though a GN drainage layer has a high transmissivity, it is thin and is, therefore, generally more susceptible to clogging by sedimentation than a granular drainage layer.		types of equipment to use at a facility. • Outlets of cover system drainage layers should be kept free of snow and ice so that these layers can drain freely.
Surface Layers and Protection Layers	• Erosion of soil protection layers on liner system side slopes should be anticipated and dealt with in design. The potential for erosion can be reduced by grading the liner system to avoid concentrated runoff and using a relatively permeable soil in the protection layer. In areas where the potential for erosion is relatively high, erosion control structures (e.g., silt fence) can be used to reduce the need for intensive maintenance of soil protection layers. Protection layers can also be covered with a tarp or temporary erosion control mat. • When a landfill is constructed on top of an existing landfill (vertical expansion), an exposed GM liner can be uplifted by gases from the underlying landfill. Therefore, in the case of a vertical expansion, unless gases from the underlying landfill are well controlled, GMs must be covered by a soil layer to prevent GM uplift and precautions must be taken to prevent erosion of this soil.	• Though it may be less costly for the owner to construct several landfill cells at once, this can leave new cells exposed to the environment for a significant time period. These cells will experience more erosion than cells filled sooner and will have more opportunity for liner damage. Additionally, every time an eroded soil layer is pushed back up the side slopes there is an opportunity for the underlying liner system materials to be damaged by construction equipment.	

Table 5-12. Specific Recommendations to Reduce Landfill Problems (Continued).

	Recommendations		
Category	*Design*	*Construction*	*Operation*
Surface Layers and Protection Layers (continued)	• Better methods for protecting exposed soil layers on liner system side slopes from erosion or alternatives to soil layers (e.g., sand filled mats, Styrofoam sheets) are needed. • Post-construction plans should be developed for portions of landfills that may sit idle for an extended period of time. The plans should include procedures describing how the liner systems should be maintained prior to operation. • For liner systems where soil protection layers are placed incrementally during landfill operation, a geosynthetic cushion (supercushion) better than the usual thick nonwoven GT needs to be developed to protect the liner system during soil placement. • Erosion of surface layers on cover system side slopes should be anticipated and dealt with in design. In areas where the potential for erosion is relatively high, erosion control measures (e.g., silt fence, turf reinforcement and revegetation mat) can be specified to reduce the need for intensive maintenance of soil layers. However, the erosion control measures themselves require maintenance. • The length of cover system slopes between ditches or swales where runoff is collected should be selected to limit erosion to acceptable amounts (e.g., 5 tonnes/ha/yr). At a minimum, the potential for erosion should be evaluated using the universal soil loss equation. Cover system slopes may need to be 4H:1V or less and intercepted by swales at 6-m vertical intervals to meet acceptable erosion levels (EPA, 1994). • Design flow velocities in drainage channels should be calculated so the appropriate channel lining can be selected.		

Table 5-12. Specific Recommendations to Reduce Landfill Problems (Continued).

	Recommendations		
Category	*Design*	*Construction*	*Operation*
Liner System and Cover System Stability	• The stability of liner system and cover system slopes should always be evaluated using rigorous slope stability analysis methods that consider actual shear strengths of materials, anticipated seepage pressures, and anticipated loadings. • The majority of the slides described herein occurred along geosynthetic/ geosynthetic interfaces. For a number of these cases, the interface shear strengths were estimated on the basis of published test data. This approach should be avoided because there may be significant differences in interface shear strengths between similar materials from different manufacturers and even identical materials in different production lots from the same manufacturer. Because of this, geosynthetic interface shear strengths should be measured and not estimated. • Interface shear strength test conditions (moisture, stresses, displacement rate, and displacement magnitude) should be representative of field conditions. • The effects of variation in the tested geosynthetics, accuracy of test methods, and test conditions must be considered when selecting the design interface shear strength. • Freeze-thaw of CCLs can have a significantly detrimental impact on GM/CCL interface shear strength and should be considered when selecting the interface shear strength to use in slope stability analyses. However, freeze-thaw effects on interface strength should not actually be a design consideration, since CCLs should be protected from freezing in the first place. • The effect of construction on moisture conditions at the GM/CCL interface should be	• Soils should be placed over geosynthetics from the toe of slope upward to avoid tensioning the geosynthetics. Methods of soil placement that are not toe to top should be pre-approved by the engineer who analyzed the stability. • Geosynthetic reinforcement should be anchored prior to placing the soil layer to be reinforced.	• Outlets of drainage layers should be kept free of snow and ice so these layers can drain freely and prevent the buildup of seepage pressures. • Soils or waste should be placed over geosynthetics from the toe of slope upward to avoid tensioning the geosynthetics. Methods of waste placement that are not toe to top should be pre-approved by the engineer who analyzed the stability. • Surficial cracking of soil cover layers during seismic loading, especially near locations with contrast in seismic response characteristics (e.g., top of waste by rock canyon walls), should be anticipated and dealt with as an operation issue through post-earthquake inspection and repair. • Proposed changes to the landfill filling sequence should be reviewed by the design engineer to ensure that these changes will not adversely impact slope stability. • Soil layers anchoring geosynthetics should be maintained during landfill construction and operation.

Table 5-12. Specific Recommendations to Reduce Landfill Problems (Continued).

	Recommendations		
Category	*Design*	*Construction*	*Operation*
Liner System and Cover System Stability (continued)	considered when developing the specification for CCL construction and selecting the strength of liner system interfaces for slope stability analyses. The CCL construction specification should generally include limitations on maximum compacted moisture content, restrictions on applying supplemental moisture, and requirements for covering the CCL and overlying GM as soon as practical to minimize moisture migration to the GM/CCL interface. If a CCL on a slope becomes desiccated, it should be reworked and not just moistened. • Cover systems incorporating a low-permeability barrier layer should include a drainage layer above the barrier when the cover system side slopes are steeper than 5H:1V (EPA, 1994). The purpose of this drainage layer is to prevent the buildup of seepage pressures in the cover system soil layer(s) overlying the barrier layer. • When liner systems or cover systems are constructed over wastes, the potential for the wastes to generate gases that uplift the liners or barriers must be considered. The gas pressures decrease the shear strength along the bottom interface of the uplifted layer and may lead to slope instability. Gas collection systems, therefore, may be required to prevent the buildup of gas pressures. • Cover system drainage layers should be designed to handle the total anticipated flow to the drainage layer calculated using a water balance or other appropriate analysis (e.g., Giroud and Houlihan, 1995). Soong and Koerner (1997) recommend using a short-duration intensive storm in the water balance and do not		

Table 5-12. Specific Recommendations to Reduce Landfill Problems (Continued).

	Recommendations		
Category	*Design*	*Construction*	*Operation*
Liner System and Cover System Stability (continued)	recommend the EPA HELP computer model for this purpose. The drainage layer flow rates output from the HELP model are an average for a 24-hour period and may be much less than the peak flow rates calculated using other methods if the precipitation data used in the HELP model are not carefully selected. • Water collected in the drainage layer must be allowed to outlet to prevent the buildup of seepage pressures. • Containment systems should be designed to limit seismic displacements to tolerable amounts. To do this, designs may incorporate predetermined slip surfaces to confine movements to locations where they will cause the least damage (i.e., above the GM liner) and inverted liner system keyways to provide more resistance to movement. For example, a GM with a smooth top surface and a textured bottom surface could be used in certain liner systems to create a predetermined slip surface above the GM. • Liner system anchor trenches should be designed to secure geosynthetics during construction, but release the geosynthetics before they are damaged by displacements during earthquakes. An alternative is to unanchor the liner system after construction and secure it on a bench with an overlying soil layer. • Stress concentrations at or near the liner system side slope crest should be avoided. Areas with stress concentrations are more problematic when subjected to seismic displacements. In particular, GM seams should generally not be sampled near the slope crest.		

Table 5-12. Specific Recommendations to Reduce Landfill Problems (Continued).

	Recommendations		
Category	*Design*	*Construction*	*Operation*
Liner System and Cover System Displacements	• When liner systems or cover systems are constructed over existing wastes, the potential for the wastes to generate gases must be considered. The gases may uplift GMs, causing excessive stresses in the GMs and may impact slope stability. Some landfills may be generating little or no gas at the time of construction and may not need a gas collection system. Other landfills may be generating significant amounts of gas and may require a gas collection system beneath the entire liner system. • Surface-water runoff should be managed to reduce foundation uplift problems during and after construction. Temporary and permanent surface-water diversion structures located near a cell may need to be lined to reduce infiltration, especially if the structures are located on relatively permeable soils and convey relatively large amounts of water. Runoff should not be allowed to pond near the cell, where it can infiltrate into the cell. • Liner systems constructed over compressible, low shear strength waste materials should be designed to accommodate the anticipated settlements. When GCL is used, seam overlaps should be wider than normal. • Gas extraction well boots should be designed to accommodate the anticipated landfill settlements.	• Cover systems with soil layers placed over compressible, low shear strength waste should use lightweight construction equipment and have good control of the thickness of soil placed over the waste so as not to cause bearing capacity failure of the waste and excessive displacement of the cover system.	

5.4 Assessment of EPA HELP Model Using Leachate Generation Data

5.4.1 Introduction

The HELP model was developed by the U.S. Army Engineer Waterways Experiment Station for the EPA Risk Reduction Engineering Laboratory, Cincinnati, OH, to help landfill designers compare the hydraulic performance of alternative waste containment system designs. However, the HELP model has increasingly been used to design LCRS drainage layers and to estimate leachate generation rates in order to size leachate storage tanks. There is little published information on the adequacy of the HELP model for these purposes. In this section of the report, the HELP model is assessed by comparing LCRS flow rate data from six landfill cells to leachate

generation rates predicted for these cells from HELP model simulations with typical input parameters. The cells were selected to represent different waste types and geographical regions of the U.S. General data for the six landfill cells are included in the landfill performance database described in Section 5.2.2.

The HELP model theoretical development and data requirements are described in Section 5.4.2. A review of published literature on leachate generation rate predictions by the HELP model is presented in Section 5.4.3. The evaluation of the HELP model as a design tool is described in Section 5.4.4, and results of this evaluation are presented in Section 5.4.5.

5.4.2 Description of HELP Model

The HELP model simulates hydrologic processes for a landfill by performing daily, sequential water budget analyses using a quasi-two-dimensional, deterministic approach (Schroeder et al., 1994a, 1994b). The hydrologic processes considered in the HELP model include precipitation, surface-water storage (i.e., storage as snow), interception of precipitation by foliage, surface-water evaporation, runoff, snow melt, infiltration, plant transpiration, soil water evaporation, soil water storage, vertical drainage (saturated and unsaturated) through non-barrier soil layers, vertical percolation (saturated) through soil barriers, vertical percolation through GM and GM/soil composite barriers, and lateral drainage (saturated).

Five main routines are used in the HELP model to estimate runoff, evapotranspiration, vertical drainage, vertical percolation, and lateral drainage. Several other routines interact with the main routines to generate daily precipitation, temperature, and solar radiation values and simulate snow accumulation and melt, vegetative growth, interception, and leakage through GM and GM/soil composite barriers. Runoff is computed using the runoff curve-number method of the U.S. Department of Agriculture Soil Conservation Service (USDA-SCS) (USDA-SCS, 1985). Evapotranspiration is computed using a two-stage modified Penman energy balance method developed by Ritchie (1972). Vertical drainage is computed using Darcy's equation, modified to allow drainage under unsaturated conditions using an unsaturated soil hydraulic conductivity calculated using an equation by Campbell (1974). Percolation through a soil liner or barrier is also evaluated using Darcy's equation, but under saturated conditions. Lateral drainage is modeled by an analytical approximation to the steady-state solution of the Boussinesq equation. Leakage through GMs and GM/soil composite liners or barriers is evaluated based on the work of Giroud and Bonaparte (1989a, 1989b) and Giroud et al. (1992).

Version 1 of the HELP model was issued in 1984, and the model has been updated several times since then. At the time this report was prepared, Version 3 was the most current. Data requirements for Version 3 of the HELP model are summarized in Table 5-13. HELP requires daily and general climatic data, material properties data for the landfill components being modeled, and landfill design data. Required daily weather

data are precipitation, mean temperature, and total global solar radiation. Daily precipitation may be input manually, selected from a historical database (e.g., 1974-1977 data in HELP database, NOAA Tape, or Climatedata™), or generated stochastically using a weather generation model developed by the U.S. Department of Agriculture-Agricultural Research Service (USDA-ARS) (Richardson and Wright, 1984) with simulation parameters available for 139 U.S. cities. Other daily climatologic data are generated stochastically using the USDA-ARS routine. Required general weather data include average annual wind speed and latitude. Default general weather data for 183 U.S. cities are used by the model. The material properties of each layer being modeled are either selected from the HELP model database of default material properties or are specified by the model user. Landfill design data, including landfill general information and layer configuration, are user specified.

Table 5-13. Data Requirements for the EPA HELP Model, Version 3.

WEATHER DATA REQUIREMENTS

Evapotranspiration Data
- Default evapotranspiration option
  - Location
  - Evaporation zone depth
  - Maximum leaf area index
- Manual evapotranspiration option
  - Location
  - Evaporation zone depth
  - Maximum leaf area index
  - Dates starting and ending the growing season
  - Normal average annual wind speed
  - Normal average quarterly relative humidity

Precipitation Data
- Default precipitation option
  - Location
- Synthetic precipitation option
  - Location
  - Number of years of data to be generated
  - Normal mean monthly precipitation
- Create/Edit precipitation option
  - Location
  - One or more years of daily precipitation data
- NOAA Tape precipitation option
  - Location
  - NOAA ASCII print file of Summary of Day daily precipitation data in as-on-tape format
- Climatedata™ precipitation option
  - Location
  - Climatedata™ prepared file containing daily precipitation data
- ASCII precipitation option
  - Location
  - Files containing ASCII data
  - Years

Table 5-13. Data Requirements for the EPA HELP Model, Version 3 (Continued).

Precipitation Data (continued)
- HELP Version 2 data option
  - Location
  - File containing HELP Version 2 data

Temperature Data
- Synthetic temperature option
  - Location
  - Number of years of data to be generated
  - Years of daily temperature values
  - Normal mean monthly temperature
- Create/Edit temperature option
  - Location
  - One or more years of daily temperature data
- NOAA Tape temperature option
  - Location
  - NOAA ASCII print file of Summary of Day data file containing years of daily maximum temperature values or daily mean temperature values in as-on-tape format
  - NOAA ASCII print file of Summary of Day data file containing years of daily minimum temperature values or daily mean temperature values in as-on-tape format
- Climatedata™ temperature option
  - Location
  - Climatedata™ prepared file containing daily maximum temperature data
  - Climatedata™ prepared file containing daily minimum temperature data
- ASCII temperature option
  - Location
  - Files containing ASCII data
  - Years
- HELP Version 2 data option
  - Location
  - File containing HELP Version 2 data

Solar Radiation Data
- Synthetic solar radiation option
  - Location
  - Number of years of data to be generated
  - Years of daily solar radiation values
  - Latitude
- Create/Edit solar radiation option
  - Location
- One or more years of daily solar radiation data
- NOAA Tape solar radiation option
  - Location
  - NOAA ASCII print file of Surface Airways Hourly solar radiation data in as-on-tape format
- Climatedata™ solar radiation option
  - Location
  - Climatedata™ Surface Airways prepared file containing years of daily solar radiation data
- ASCII Solar Radiation Option
  - Location
  - Files containing ASCII data
  - Years

Table 5-13. Data Requirements for the EPA HELP Model, Version 3 (Continued).

Solar Radiation Data (continued)
- HELP Version 2 Data Option
  - Location
- File containing HELP Version 2 data

MATERIAL PROPERTY AND DESIGN DATA REQUIREMENTS

Landfill General Information
- Project title
- Landfill area
- Percentage of landfill area where runoff is possible
- Method of initialization of moisture storage
- Initial snow water storage

Layer Data
- Layer type
- Layer thickness
- Soil texture (Default, User-built, or manual options)
  - Porosity
  - Field capacity
  - Wilting point
  - Saturated hydraulic conductivity
- Initial volumetric soil water content
- Rate of subsurface inflow to layer

Lateral Drainage Layer Design Data
- Maximum drainage length
- Drain slope
- Percentage of leachate collected from drainage layer that is recirculated
- Layer to receive recirculated leachate from drainage layer

GM Liner Data
- Pinhole density in GM liner
- GM liner installation defects
- GM liner installation quality
- GM liner saturated hydraulic conductivity (vapor diffusivity)
- GT transmissivity

Runoff Curve Number Information
- User-specified runoff curve number used without modification
- User-specified runoff curve number modified for surface slope and slope length
- Curve number calculated by HELP

5.4.3 Literature Review

A number of researchers have performed field studies and analytical assessments to evaluate the HELP model (EPRI, 1984; Thompson and Tyler, 1984; Peters et al., 1986; Peyton and Schroeder, 1988; Barnes and Rodgers, 1988; Udoh, 1991; Lane et al., 1992; Benson et al., 1993; Peyton and Schroeder, 1993; Field and Nangunoori, 1994; Khire et al., 1994; Lange et al., 1997). In particular, the studies evaluated the reliability of the HELP model as a tool to predict trends and magnitudes of the different landfill water balance

components (i.e., infiltration, runoff, etc.). The conclusions of these studies are not always in agreement. For example, some of these studies found that HELP over-predicted infiltration in humid climates and under-predicted infiltration in arid climates, but other studies concluded just the opposite. In some cases, the HELP model was not able to predict short-term trends. However, for a number of cases the HELP model analysis was shown to give reasonable predictions of cumulative longer-term water balances. Despite the wide use of the HELP model to predict landfill leachate generation rates, to the author's knowledge, there are very few published studies comparing leachate generation rates for modern landfills predicted with HELP model to actual leachate generation rates measured at these landfills. Two such studies were performed by Field and Nangunoori (1994) and Lange et al. (1997). Results from these two studies are summarized below.

Field and Nangunoori (1994) used the HELP model, Version 2 to predict leachate generation rates at an active, modern double-lined HW landfill in New York. They compared the predicted rates to measured leachate generation rates at the landfill during 1992. Site-specific and default data were used in the model simulations. Actual site rainfall data during 1992 were input manually. The HELP model default values for a city near the site were used for all other required weather data (i.e., evapotranspiration, temperature, and solar radiation data). The waste and liner system geometries used in the model were selected to represent the actual landfill conditions in 1992. Data for the intermediate and daily covers, waste, LCRS, and liner system layers (i.e., porosity, field capacity, wilting point, and saturate hydraulic conductivity) were selected from the HELP model database of default material characteristics. The permeabilities of the liner system drainage layers (i.e., a 0.3-m thick sand layer and a GN) were modified to match laboratory results or manufacturer's data. The authors did not provide modeling data related to the runoff curve number or the percentage of the landfill area where runoff is possible. The average annual leachate generation rate predicted by HELP was 36% of the measured average annual LCRS flow rate. Field and Nangunoori (1994) reported that increasing the default hydraulic conductivity of the waste from $2x10^{-6}$ to $2x10^{-5}$ m/s caused the predicted leachate generation rate to be within 17% of the measured rate. It is noted that the HELP model does not contain default properties for HWs, and Field and Nangunoori used the default properties for MSW in their simulations.

Lange et al. (1997) presented a case study of the use of the HELP model to predict leachate generation rates at a modern MSW landfill in northeastern Ohio. The liner system for the landfill consisted of a GM/GCL/CCL composite liner and a GN drainage layer. At the landfill permitting stage, the landfill designer used Version 2.05 of the HELP model to estimate leachate generation rates. The designer used the model's default weather data for a nearby city and default material property data. The designer assumed intermediate covers would be bare (i.e., unvegetated) and no surface water runoff would leave the modeled landfill area. The average annual leachate generation rate estimated using the HELP model was 12,200 lphd. The landfill began waste placement operations in December 1992 on a 5-ha portion of the landfill. Additional

areas were utilized with time, up to 25 ha by October 1995. Actual leachate generation rates were measured between December 1992 and February 1997. Rates were highest, up to 15,000 lphd, during the first few months of operations and decreased with time. By July 1996, LCRS flow rates had reached relatively steady levels of 800 to 900 lphd. In this case, the leachate generation rate estimated during the design phase was in the range of measured rates during the first few months of the landfill operation, but was not representative of rates measured in the following years.

Lange et al. (1997) evaluated the ability of the HELP model, Version 3.05 to predict leachate generation rates that occurred at different times in the life of the landfill by using input data that model the conditions of the landfill at these times. In particular, actual precipitation and temperature data recorded at a nearby city between 1992 and 1996 were used in the HELP model. For comparison, one-year and five-year simulations were performed. Furthermore, the landfill was modeled in terms of five areas with different cover, slope, and vegetation conditions. The extent of these areas varied during the operation of the landfill. The leachate generation rate for the landfill at a certain time was estimated as the area-weighted average of the average leachate generation rates for the five areas during the considered simulation period (i.e., one year or five years). The landfill geometry was modeled based on aerial topographic maps obtained at different times in the life of the landfill. The fraction of runoff that could exit the landfill areas was assumed to be zero for the active area (i.e., working face) and areas with no waste, 75% for areas covered with daily cover, and 100% for all other areas. Good vegetation was assumed for intermediate cover placed over areas that reached final grades. The material property data were, for the most part, selected from the HELP default values. The predicted leachate generation rates at the five different times in the life of the landfill were between 90 and 230% of the measured rates. It is noted that the length of the simulation period had limited effect on the predicted average leachate generation rates.

5.4.4 Evaluation of HELP Model

The performance of the HELP model was evaluated as a “design tool” to estimate landfill leachate generation rates using a specific simulation methodology (i.e., specific procedures for selecting simulation period and model input parameter values). The evaluation was conducted by comparing leachate generation rates estimated by HELP Version 3.04a when used with the specific simulation methodology for six landfill cells to measured LCRS flow rates at these cells. Table 5-14 presents operation information and LCRS and liner system details for the six cells. Four of the cells contain MSW, one contains HW, and one contains MSW ash. All of the MSW cells and the ash cell are located in the NE; the HW cell is located in the W. The cells varied in area between 2.2 and 6.4 ha and varied in maximum waste height between 21 and 46 m. Average annual rainfall at the landfill sites was lowest (i.e., 280 mm) for Cell AC2 located in the W and highest (i.e., 1,190 mm) for Cells Y1 and Y2, located in the NE. As shown in Table 5-14, all of the cells, except for Cell AC2, have a sand LCRS drainage layer. Cell

Table 5-14. Operation Information and Liner System Details for Six Landfill Cells Modeled Using EPA HELP Model.

Cell No.	U.S. Region[1]	Avg. Annual Rainfall (mm)	Waste Type[2]	Cell Area (ha)	Max. Waste Height (m)	Avg. Liner Base Slope (%)	LCRS Material			LCRS Collector Pipe		Primary Liner				
							Type[4]	Thick. (mm)	Hydraulic Cond.[5] (m/s)	Size (mm) & Material[6]	Spacing (m)	Liner Type[7]	GM		CCL	
													Material[6]	Thick. (mm)	Thick. (mm)	Hydraulic Cond.[5] (m/s)
B1	NE	1,070	MSW	3.3	21	2.0	S	450	$1X10^{-4}$	152 PVC	38	GM	CSPE	0.9	NA[3]	NA
B3	NE	1,070	MSW	6.4	25	2.0	S	450	$1X10^{-4}$	152 PVC	30	GM/CCL	CSPE	0.9	600	$1X10^{-9}$
I2	NE	990	MSW	2.4	46	2.5	S	600	$1X10^{-4}$	ND[3]	30	GM	HDPE	1.5	NA	NA
Y1	NE	1,190	ASH	2.2	10	5.5	S	600	$5X10^{-5}$	152 PVC	30	GM/CCL	HDPE	2.0	450	$1X10^{-9}$
Y2	NE	1,190	MSW	3.0	15	5.5	S	600	$5X10^{-5}$	152 PVC	30	GM/CCL	HDPE	2.0	450	$1X10^{-9}$
AC2	W	280	HW	4.2	30	2.0	G/GN	300/5	$5X10^{-3}/0.1$	ND	30	GM/CCL	HDPE	1.5	450	$1X10^{-9}$

Notes:

(1) Regions of the U.S. are: NE = northeast, SE = southeast, W = west

(2) Waste types are: MSW = municipal solid waste, HW = hazardous waste, ASH = MSW ash

(3) ND = not determined; NA = not applicable

(4) LCRS material types are: S = sand, G = gravel, GN = geonet

(5) Hydraulic conductivity values shown represent minimum values for the LCRS drainage layer and maximum values for the CCL, as required in the project material specifications.

(6) Collector pipe and primary liner GM materials are: PVC = polyvinyl chloride, HDPE = high-density polyethylene, CSPE = chlorosulfonated polyethylene

(7) Liner types are: GM = geomembrane, CCL = compacted clay liner

AC2 has a gravel drainage layer underlain by a GN. LCRS collector pipes were used at all of the cells and were spaced 30 to 38 m apart.

The simulation methodology used herein involved modeling four landfill scenarios representing conditions that typically occur at different times and in different areas within a cell during landfill operations. The first scenario assumes that essentially no waste has been placed on the liner system and no measures have been implemented to prevent direct infiltration of rainwater into the LCRS. This scenario may occur during the first few months of cell operation. The second scenario assumes waste has been placed in the cell, and either no daily cover has been placed on the waste or no measures have been implemented to divert clean rainwater from the cell. The third scenario models an area of the cell that has received waste and has been covered with daily cover. It was assumed that the daily cover can shed away 50% of the storm-water runoff in the cell. The fourth scenario assumes an intermediate cover has been placed on waste that has almost reached final grades. The intermediate cover is assumed to be vegetated with good grass and capable of diverting 100% of storm-water runoff.

The simulation methodology used herein utilized average annual (not peak) HELP model results calculated over a 100-year simulation period. Other methodologies could also be used, although no other methodologies were used in the preparation of this report. Weather data for the simulation (i.e., daily precipitation, temperature, and solar radiation values) were generated stochastically by the HELP program for the closest city to the landfill site for which HELP has built-in weather parameters. One hundred years of data were generated and used in the HELP simulation to represent a wide range of weather conditions that the landfill may experience. The normal mean monthly precipitation values were modified to match the historical average annual precipitation at the site. Table 5-15 summarizes HELP soil and design parameter values used for the four different scenarios modeled at the six landfill cells. Daily and intermediate covers and waste were modeled as vertical percolation layers. The LCRS drainage material was modeled as a lateral drainage layer, and the CCL component of the primary liner was modeled as a barrier soil liner. The layer material properties were selected from the HELP model database of default material properties to represent material properties described in the landfill design plans and specifications. LCRS material hydraulic conductivity was modified in some cases to reflect values required by the project specifications. The cell geometry parameters (i.e., drainage length and slope, waste height, and surface slope and length) were selected based on the cell design plans and on anticipated waste placement sequence and practices.

5.4.5 Study Findings

The results of the HELP model simulations are summarized in Table 5-16. Reported for each cell are actual average LCRS flow rates measured at the cell during the initial and active periods of operation, as well as average flow rates obtained using HELP with the four cell modeling scenarios. Average annual LCRS flow rates over the 100-year

Table 5-15. HELP Model Soil and Design Input Parameters for Select Cells.

Landfill General Information						
- Project title	MSW Cell **B1** located in the NE					
- Area of modeled portion of landfill (ha)	1					
- Percentage of landfill area where runoff is possible (percent) (1)	0 for no waste and uncovered areas, 50 for areas with daily cover, and 100 for areas with an intermediate cover					
- Moisture storage initialization method	Program initialized to near steady state					
- Initial snow water storage (cm)	0					
Layer Data	Daily Cover (1)	Intermed. Cover (1)	Waste	Drainage Material	GM	CCL
- Layer type	1	1	1	2	4	NA
- Layer thickness (cm)	15	30	varies (1)	45	0.09	NA
- Material texture default number	5	10	18	1	40	NA
Porosity (vol./vol.)	0.457	0.398	0.671	0.417	NA	NA
Field capacity (vol./vol.)	0.131	0.244	0.292	0.045	NA	NA
Wilting point (vol./vol.)	0.058	0.136	0.077	0.018	NA	NA
Saturated hydraulic conductivity (cm/s)	$1x10^{-3}$	$1.2x10^{-4}$	$1x10^{-3}$	$1x10^{-2}$	$3x10^{-12}$	NA
- Rate of subsurface inflow to layer	0	0	0	0	0	NA
Lateral Drainage Layer Design Data						
- Maximum drainage length (m)	20					
- Drain slope (%)	2					
- Percentage of leachate collected from drainage layer that is recirculated (%)	0					
- Layer to receive recirculated leachate from drainage layer	NA					
Geomembrane Liner Data						
- Pinhole density per hectare	1					
- Installation defects per hectare	5					
- Geomembrane liner installation quality	Good					
- Geotextile transmissivity (m^2/sec)	NA					
Runoff Curve Number Calculated by HELP	No Waste (1)	No Cover (1)	Daily Cover (1)	Intermed. Cover (1)		
- Surface slope (%)	2	5	5	25		
- Slope length (m)	20	20	20	45		
- Default soil texture	1	18	5	10		
- Quantity of vegetative cover	Bare	Bare	Bare	Good		
- Runoff curve number calculated by HELP	75	82	85	82		

Notes:

(1) Four scenarios are analyzed which model different conditions at different areas of the cell: (i) the no waste scenario models conditions at an area which has not received waste and where measures have not been implemented to prevent rainwater from entering the LCRS; (ii) the no cover scenario models an active waste disposal area which has not received daily or intermediate covers, and therefore, no runoff is allowed (waste thickness assumed at 3 m); (iii) the daily cover scenario models an area which received daily cover and allows rainwater runoff from 50% of the area (waste thickness assumed at 6 m); and (iv) the intermediate cover scenario models an area which received an intermediate cover and allows rainwater runoff from the entire area (waste thickness assumed at 12 m).

Table 5-15. HELP Model Soil and Design Input Parameters for Select Cells (Continued).

Landfill General Information						
- Project title	MSW Cell **B3** located in the NE					
- Area of modeled portion of landfill (ha)	1					
- Percentage of landfill area where runoff is possible (percent) [(1)]	0 for no waste and uncovered areas, 50 for areas with daily cover, and 100 for areas with an intermediate cover					
- Moisture storage initialization method	Program initialized to near steady state					
- Initial snow water storage (cm)	0					
Layer Data	**Daily Cover [(1)]**	**Intermed. Cover [(1)]**	**Waste**	**Drainage Material**	**GM**	**CCL**
- Layer type	1	1	1	2	4	3
- Layer thickness (cm)	15	30	varies [(1)]	45	0.09	60
- Material texture default number	5	10	18	1	40	16
Porosity (vol./vol.)	0.457	0.398	0.671	0.417	NA	0.427
Field capacity (vol./vol.)	0.131	0.244	0.292	0.045	NA	0.418
Wilting point (vol./vol.)	0.058	0.136	0.077	0.018	NA	0.367
Saturated hydraulic conductivity (cm/s)	$1x10^{-3}$	$1.2x10^{-4}$	$1x10^{-3}$	$1x10^{-2}$	$3x10^{-12}$	$1x10^{-7}$
- Rate of subsurface inflow to layer	0	0	0	0	0	0
Lateral Drainage Layer Design Data						
- Maximum drainage length (m)	17					
- Drain slope (%)	2					
- Percentage of leachate collected from drainage layer that is recirculated (%)	0					
- Layer to receive recirculated leachate from drainage layer	NA					
Geomembrane Liner Data						
- Pinhole density per hectare	1					
- Installation defects per hectare	5					
- Geomembrane liner installation quality	Good					
- Geotextile transmissivity (m^2/sec)	NA					
Runoff Curve Number Calculated by HELP	**No Waste [(1)]**	**No Cover [(1)]**	**Daily Cover [(1)]**	**Intermed. Cover [(1)]**		
- Surface slope (%)	2	5	5	25		
- Slope length (m)	17	17	17	60		
- Default soil texture	1	18	5	10		
- Quantity of vegetative cover	Bare	Bare	Bare	Good		
- Runoff curve number calculated by HELP	76	82	85	82		

Notes:

(1) Four scenarios are analyzed which model different conditions at different areas of the cell: (i) the no waste scenario models conditions at an area which has not received waste and where measures have not been implemented to prevent rainwater from entering the LCRS; (ii) the no cover scenario models an active waste disposal area which has not received daily or intermediate covers, and therefore, no runoff is allowed (waste thickness assumed at 3 m); (iii) the daily cover scenario models an area which received daily cover and allows rainwater runoff from 50% of the area (waste thickness assumed at 6 m); and (iv) the intermediate cover scenario models an area which received an intermediate cover and allows rainwater runoff from the entire area (waste thickness assumed at 12 m).

Table 5-15. HELP Model Soil and Design Input Parameters for Select Cells (Continued).

Landfill General Information						
- Project title	MSW Cell **I2** located in the NE					
- Area of modeled portion of landfill (ha)	1					
- Percentage of landfill area where runoff is possible (percent) [(1)]	0 for no waste and uncovered areas, 50 for areas with daily cover, and 100 for areas with an intermediate cover					
- Moisture storage initialization method	Program initialized to near steady state					
- Initial snow water storage (cm)	0					
Layer Data	**Daily Cover [(1)]**	**Intermed. Cover [(1)]**	**Waste**	**Drainage Material**	**GM**	**CCL**
- Layer type	1	1	1	2	4	NA
- Layer thickness (cm)	15	30	varies [(1)]	60	0.15	NA
- Material texture default number	5	10	18	1	35	NA
Porosity (vol./vol.)	0.457	0.398	0.671	0.417	NA	NA
Field capacity (vol./vol.)	0.131	0.244	0.292	0.045	NA	NA
Wilting point (vol./vol.)	0.058	0.136	0.077	0.018	NA	NA
Saturated hydraulic conductivity (cm/s)	$1x10^{-3}$	$1.2x10^{-4}$	$1x10^{-3}$	$1x10^{-2}$	$2x10^{-13}$	NA
- Rate of subsurface inflow to layer	0	0	0	0	0	NA
Lateral Drainage Layer Design Data						
- Maximum drainage length (m)	76					
- Drain slope (%)	2.5					
- Percentage of leachate collected from drainage layer that is recirculated (%)	0					
- Layer to receive recirculated leachate from drainage layer	NA					
Geomembrane Liner Data						
- Pinhole density per hectare	1					
- Installation defects per hectare	3					
- Geomembrane liner installation quality	Good					
- Geotextile transmissivity (m^2/sec)	NA					
Runoff Curve Number Calculated by HELP	**No Waste [(1)]**	**No Cover [(1)]**	**Daily Cover [(1)]**	**Intermed. Cover [(1)]**		
- Surface slope (%)	2.5	5	5	20		
- Slope length (m)	76	20	25	35		
- Default soil texture	1	18	5	10		
- Quantity of vegetative cover	Bare	Bare	Bare	Good		
- Runoff curve number calculated by HELP	74	82	85	83		

Notes:

(1) Four scenarios are analyzed which model different conditions at different areas of the cell: (i) the no waste scenario models conditions at an area which has not received waste and where measures have not been implemented to prevent rainwater from entering the LCRS; (ii) the no cover scenario models an active waste disposal area which has not received daily or intermediate covers, and therefore, no runoff is allowed (waste thickness assumed at 3 m); (iii) the daily cover scenario models an area which received daily cover and allows rainwater runoff from 50% of the area (waste thickness assumed at 6 m); and (iv) the intermediate cover scenario models an area which received an intermediate cover and allows rainwater runoff from the entire area (waste thickness assumed at 12 m).

Table 5-15. HELP Model Soil and Design Input Parameters for Select Cells (Continued).

Landfill General Information						
- Project title	MSW Ash Cell **Y1** located in the NE					
- Area of modeled portion of landfill (ha)	1					
- Percentage of landfill area where runoff is possible (percent) [(1)]	0 for no waste and uncovered areas and for areas with daily cover; 100 for areas with an intermediate cover					
- Moisture storage initialization method	Program initialized to near steady state					
- Initial snow water storage (cm)	0					
Layer Data	Daily Cover [(1)]	Intermed. Cover [(1)]	Waste	Drainage Material	GM	CCL
- Layer type	1		1	2	4	3
- Layer thickness (cm)	15	Not	varies [(1)]	60	0.2	45
- Material texture default number	5	Applicable	32	1	35	16
Porosity (vol./vol.)	0.457		0.450	0.417	NA	0.427
Field capacity (vol./vol.)	0.131		0.116	0.045	NA	0.418
Wilting point (vol./vol.)	0.058		0.049	0.018	NA	0.367
Saturated hydraulic conductivity (cm/s)	$1x10^{-3}$		$1x10^{-2}$	$5x10^{-3}$	$2x10^{-13}$	$1x10^{-7}$
- Rate of subsurface inflow to layer	0		0	0	0	0
Lateral Drainage Layer Design Data						
- Maximum drainage length (m)	17					
- Drain slope (%)	5.5					
- Percentage of leachate collected from drainage layer that is recirculated (%)	0					
- Layer to receive recirculated leachate from drainage layer	NA					
Geomembrane Liner Data						
- Pinhole density per hectare	1					
- Installation defects per hectare	3					
- Geomembrane liner installation quality	Good					
- Geotextile transmissivity (m^2/sec)	NA					
Runoff Curve Number Calculated by HELP	No Waste [(1)]	No Cover [(1)]	Daily Cover [(1)]	Intermed. Cover [(1)]		
- Surface slope (%)	5.5	5	5			
- Slope length (m)	17	17	17	Not		
- Default soil texture	1	32	5	Applicable		
- Quantity of vegetative cover	Bare	Bare	Bare			
- Runoff curve number calculated by HELP	76	97	85			

Notes:

(1) Four scenarios are analyzed which model different conditions at different areas of the cell: (i) the no waste scenario models conditions at an area which has not received waste and where measures have not been implemented to prevent rainwater from entering the LCRS; (ii) the no cover scenario models an active waste disposal area which has not received daily or intermediate covers, and therefore, no runoff is allowed (waste thickness assumed at 3 m); (iii) the daily cover scenario models an area which received daily cover and allows rainwater runoff from 50% of the area (waste thickness assumed at 6 m); and (iv) the intermediate cover scenario models an area which received an intermediate cover and allows rainwater runoff from the entire area (waste thickness assumed at 12 m).

Table 5-15. HELP Model Soil and Design Input Parameters for Select Cells (Continued).

Landfill General Information						
- Project title	MSW Cell **Y2** located in the NE					
- Area of modeled portion of landfill (ha)	1					
- Percentage of landfill area where runoff is possible (percent) [(1)]	0 for no waste and uncovered areas, 50 for areas with daily cover, and 100 for areas with an intermediate cover					
- Moisture storage initialization method	Program initialized to near steady state					
- Initial snow water storage (cm)	0					
Layer Data	**Daily Cover [(1)]**	**Intermed. Cover [(1)]**	**Waste**	**Drainage Material**	**GM**	**CCL**
- Layer type	1	1	1	2	4	3
- Layer thickness (cm)	15	30	varies [(1)]	60	0.2	45
- Material texture default number	5	10	18	1	35	16
Porosity (vol./vol.)	0.457	0.398	0.671	0.417	NA	0.427
Field capacity (vol./vol.)	0.131	0.244	0.292	0.045	NA	0.418
Wilting point (vol./vol.)	0.058	0.136	0.077	0.018	NA	0.367
Saturated hydraulic conductivity (cm/s)	$1x10^{-3}$	$1.2x10^{-4}$	$1x10^{-3}$	$5x10^{-3}$	$2x10^{-13}$	$1x10^{-7}$
- Rate of subsurface inflow to layer	0	0	0	0	0	0
Lateral Drainage Layer Design Data						
- Maximum drainage length (m)	17					
- Drain slope (%)	5.5					
- Percentage of leachate collected from drainage layer that is recirculated (%)	0					
- Layer to receive recirculated leachate from drainage layer	NA					
Geomembrane Liner Data						
- Pinhole density per hectare	1					
- Installation defects per hectare	3					
- Geomembrane liner installation quality	Good					
- Geotextile transmissivity (m^2/sec)	NA					
Runoff Curve Number Calculated by HELP	**No Waste [(1)]**	**No Cover [(1)]**	**Daily Cover [(1)]**	**Intermed. Cover [(1)]**		
- Surface slope (%)	5.5	5	5	30		
- Slope length (m)	17	17	17	30		
- Default soil texture	1	18	5	10		
- Quantity of vegetative cover	Bare	Bare	Bare	Good		
- Runoff curve number calculated by HELP	76	82	85	83		

Notes:

(1) Four scenarios are analyzed which model different conditions at different areas of the cell: (i) the no waste scenario models conditions at an area which has not received waste and where measures have not been implemented to prevent rainwater from entering the LCRS; (ii) the no cover scenario models an active waste disposal area which has not received daily or intermediate covers, and therefore, no runoff is allowed (waste thickness assumed at 3 m); (iii) the daily cover scenario models an area which received daily cover and allows rainwater runoff from 50% of the area (waste thickness assumed at 6 m); and (iv) the intermediate cover scenario models an area which received an intermediate cover and allows rainwater runoff from the entire area (waste thickness assumed at 12 m).

Table 5-15. HELP Model Soil and Design Input Parameters for Select Cells (Continued).

Landfill General Information							
- Project title	HW Cell **AC2** located in the W						
- Area of modeled portion of landfill (ha)	1						
- Percentage of landfill area where runoff is possible (percent) [(1)]	0 for no waste and uncovered areas, 50 for areas with daily cover, and 100 for areas with an intermediate cover						
- Moisture storage initialization method	Program initialized to near steady state						
- Initial snow water storage (cm)	0						
Layer Data	Daily Cover [(1)]	Intermed. Cover [(1)]	Waste	Protect. Material	Drainage Material	GM	CCL
- Layer type	1	1	1	1	1/2	4	3
- Layer thickness (cm)	15	30	varies [(1)]	30	30/0.5	0.15	45
- Material texture default number	5	10	18	5	1/20	35	16
Porosity (vol./vol.)	0.457	0.398	0.671	0.457	0.417/0.85	NA	0.427
Field capacity (vol./vol.)	0.131	0.244	0.292	0.131	0.045/0.01	NA	0.418
Wilting point (vol./vol.)	0.058	0.136	0.077	0.058	0.018/0.005	NA	0.367
Saturated hydraulic conductivity (cm/s)	$1x10^{-3}$	$1.2x10^{-4}$	$1x10^{-3}$	$1x10^{-3}$	0.5/10	$2x10^{-13}$	$1x10^{-7}$
- Rate of subsurface inflow to layer	0	0	0	0	0	0	0
Lateral Drainage Layer Design Data							
- Maximum drainage length (m)	40						
- Drain slope (%)	2.0						
- Percentage of leachate collected from drainage layer that is recirculated (%)	0						
- Layer to receive recirculated leachate from drainage layer	NA						
Geomembrane Liner Data							
- Pinhole density per hectare	1						
- Installation defects per hectare	3						
- Geomembrane liner installation quality	Good						
- Geotextile transmissivity (m^2/sec)	NA						
Runoff Curve Number Calculated by HELP	No Waste [(1)]	No Cover [(1)]	Daily Cover [(1)]	Interm. Cover [(1)]			
- Surface slope (%)	2	5	5	25			
- Slope length (m)	17	17	17	30			
- Default soil texture	5	18	5	10			
- Quantity of vegetative cover	Bare	Bare	Bare	Good			
- Runoff curve number calculated by HELP	76	82	85	83			

Notes:

(1) Four scenarios are analyzed which model different conditions at different areas of the cell: (i) the no waste scenario models conditions at an area which has not received waste and where measures have not been implemented to prevent rainwater from entering the LCRS; (ii) the no cover scenario models an active waste disposal area which has not received daily or intermediate covers, and therefore, no runoff is allowed (waste thickness assumed at 3 m); (iii) the daily cover scenario models an area which received daily cover and allows rainwater runoff from 50% of the area (waste thickness assumed at 6 m); and (iv) the intermediate cover scenario models an area which received an intermediate cover and allows rainwater runoff from the entire area (waste thickness assumed at 12 m).

simulation were selected for comparison with measured flow rates. As shown in Table 5-16, estimated flow rates are highest for the "no waste" scenario and decrease significantly with placement of waste and daily cover. The lowest flow rates were estimated for the "intermediate cover" scenario. Therefore, when the HELP model is used in the manner described above, it seems capable of modeling the trend of decreasing leachate generation rate with time observed at landfills. This trend is more fully investigated in Appendix E.

Table 5-16. Summary of Measured and Estimated LCRS Flow Rates for Six Landfill Cells.

Cell No.	Initial Period of Operation		Active Period of Operation		LCRS Flow Rates (lphd) Estimated Using HELP for Four Different Scenarios			
	Time Period (months)	Avg. LCRS Flow Rate (lphd)	Time Period (months)	Avg. LCRS Flow Rate (lphd)	No Waste	No Cover	Daily Cover	Intermediate Cover
B1	ND[1]	ND	20-54	3,816	14,335	9,622	9,124	4,392
B3	1-4	15,304	5-93	3,748	16,075	10,820	10,142	5,035
I2	1-7	6,627	8-76	728	11,698	7,290	7,462	3,533
Y1	ND	ND	13-78	19,319	17,685	17,066	15,504	NA [1]
Y2	1-10	23,368	11-54	7,918	17,685	12,597	12,225	6,708
AC2	1-6	272	7-88	18	1,885	1,250	1,025	130

Notes: (1) ND = not determined, NA = not applicable.
(2) Reported measurements are average values over the indicated time period. HELP simulation estimates represent average values for 100-year simulation period.

As shown in Table 5-16, the MSW ash Cell Y1 exhibited much higher measured LCRS flow rates than the MSW and HW cells. During the active period of operation, the average LCRS flow rate for Cell Y1 was about 19,300 lphd and the average flow rates for the other cells ranged from about 20 to 7,900 lphd. The higher flow rate in this range is for MSW Cell Y2, located at the same site and having the same liner system details and cell geometry as Cell Y1. The higher LCRS flow rate for Cell Y1 than for Cell Y2 may be attributed to the slow placement rate of ash, the high hydraulic conductivity of the ash, and lack of storm-water diversion from the ash cell. The small thickness of waste, high ash hydraulic conductivity, and lack of storm-water diversion allow for relatively unimpeded infiltration of rainwater through the waste into the LCRS, and, therefore, result in high leachate flow rates. The lowest measured flow rate during the active period of about 20 lphd occurred for HW cell AC2, located in the W at a site with an average annual rainfall of only 280 mm.

LCRS flow rates estimated using the HELP simulation methodology exhibited similar trends as the measured flow rates. The MSW ash cell Y1 had the highest estimated flow rates; the HW cell in the W had the lowest estimated flow rates. Leachate generation rates of approximately 17,100 lphd and 12,600 lphd were estimated for the MSW ash Cell Y1 and MSW Cell Y2, respectively, for the "no cover" scenario, demonstrating that, at least for the considered cells, the HELP simulation methodology is capable of predicting relative differences in LCRS flow rates for different waste types.

Figure 5-8 presents a comparison of average measured LCRS flow rates for the six cells and the LCRS flow rates estimated for these cells using the HELP simulation methodology. In this figure, the ranges of estimated LCRS flow rates given in Table 5-16 are plotted against the average measured LCRS flow rates given in the same table. In particular, estimated LCRS flow rates for the "no waste" and "no cover" scenarios are directly compared to average measured flow rates during the initial period of operation and estimated LCRS flow rates for the "daily cover" and "intermediate cover" scenarios are directly compared to average measured flow rates during the active period of operation. Each complete data set is represented by a box when the data points are connected as done in the figure. As shown in Figure 5-8, except for HW Cell AC2 located in the W, the estimated leachate generation rates using the HELP simulation methodology are generally of the same order of magnitude. The estimated LCRS flow rates were somewhat higher than measured flow rates for MSW cells and somewhat lower than the measured flow rate for the MSW ash cell. For MSW Cells B1 and B3, the estimated flow rates were somewhat higher than measured flow rates. For example, for Cell B3, estimated LCRS flow rates were in the range of 5,000 to 16,100 lphd, while average measured flow rates were 15,300 lphd during the initial period of operation and 3,700 lphd during the active period of operation. For MSW ash Cell Y1, the HELP methodology somewhat underpredicted leachate generation rates. Average measured flow rates were 19,300 lphd during the active period of operation; the estimated flow rates using the HELP simulation methodology were in the range of 15,500 to 17,700 lphd. For MSW Cell I2 and especially for HW Cell AC2, the estimated rates were significantly higher than measured rates. Average measured LCRS flow rates for Cell AC2 were about 270 lphd during the initial period of operation and 20 lphd during the active period of operation; the estimated flow rates using the HELP simulation methodology were in the range of 130 to 1,000 lphd.

For the evaluations performed in this section, the HELP model responded as expected to changes in waste type and site climate. When used with default parameters, the HELP model may generally overpredict LCRS flow rates for MSW landfills and landfills in arid climates; however, too few sites were evaluated to draw definitive conclusions. Part of the conservatism of the HELP model in predicting LCRS flow rates, especially as waste is placed, may lie in the default moisture content value for the waste. In the HELP model, the waste is assumed to be at field capacity. However, MSW is typically placed at moisture contents less than field capacity. The moisture storage capacity of waste is particularly important in arid climates since this storage capacity, if utilized, may hold essentially all the rainwater infiltrating the waste, and little leachate will be generated. Also, some landfill cells, and especially HW cells, have special methods of handling rainwater that may not be taken into account in the HELP model. For example, in some HW cells, part of the waste is covered with a GM during cell operation. Rainwater collected on the GM is removed from the cell separate from leachate, and, if clean, is discharged.

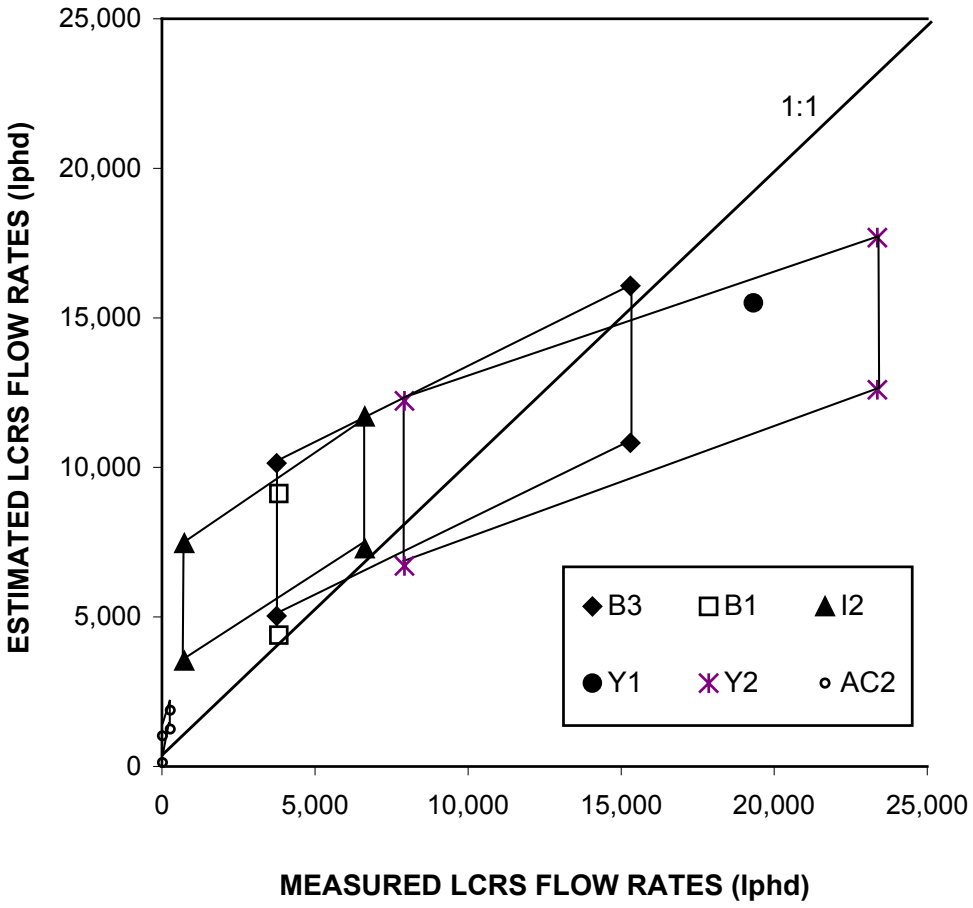

Figure 5-8. LCRS flow rates estimated using HELP versus measured LCRS flow rates for six landfill cells.

The authors believe that the HELP model can appropriately be employed as a tool to estimate long-term *average* leachate generation rates to use with an appropriate level of conservatism in the design of LCRS drainage layers and the sizing of leachate management system components. The authors recommend that users develop a consistent simulation methodology (analogous to the methodology used herein, with the same or different underlying assumptions) for the HELP model and that they evaluate the simulations, similar to the evaluations in Table 5-16 and Figure 5-8, using data from existing local landfills. These simulations can be enhanced by performing parametric analyses for key input parameters, such as initial waste moisture content. With this consistent, locally calibrated approach, the usefulness of the HELP model as a design tool can be improved.

5.5 References

Barnes, F. J. and Rodgers, J. E. (1988), "*Evaluation of Hydrologic Models in the Design of Stable Landfill Final Covers*", U.S. Environmental Protection Agency, Office of Research and Development, Cincinnati, OH, EPA Project Summary, Report No. EPA/600/S-88/048.

Bass, J. M. (1986), "*Avoiding Failure of Leachate Collection and Cap Drainage Layers*", EPA/600/2-86/058, U.S. Environmental Protection Agency, Hazardous Waste Engineering Research Laboratory, Cincinnati, OH, 142 p.

Benson, C. H., Khire, M. V., and Bosscher, P. J. (1993), "*Final Cover Hydrologic Evaluation, Final Cover-Phase II*", Environmental Geotechnics Report No. 93-4, University of Wisconsin, Madison, WI, 151 p.

Bonaparte, R. and Gross B. A. (1990), "Field Behavior of Double-Liner Systems", *Waste Containment Systems: Construction, Regulation, and Performance*, ASCE Geotechnical Special Publication No. 26, R. Bonaparte ed., New York, pp. 52-83.

Bonaparte, R., Othman, M. A., Rad, N. S., Swan, R. H., and Vander Linde, D. L. (1996), "Evaluation of Various Aspects of GCL Performance", Appendix F in *Report of 1995 Workshop on Geosynthetic Clay Liners*, D.E. Daniel and H.E. Scranton, authors, EPA/600/R-96/149, EPA National Risk Management Research Laboratory, Cincinnati, OH, pp. F1-F34.

Bramlett, J., Furman, C., Johnson, A., Ellis, W. D., Nelson, H. and Vick, W. H. (1987), "*Composition of Leachates from Actual Hazardous Waste Sites*", U.S. Environmental Protection Agency, Office of Research and Development, Cincinnati, OH, EPA/600/2-87/043, 113 p.

Campbell, G. S. (1974), "A Simple Method for Determining Unsaturated Hydraulic Conductivity from Moisture Retention Data", *Soil Science*, 117(6), pp. 311-314.

Daniel, D. E. and Koerner, R. M. (1993), "*Technical Guidance Document: Quality Assurance and Quality Control for Waste Containment Facilities*", EPA/600/R-93/182, EPA Risk Reduction Research Laboratory, Cincinnati, OH, 305 p.

Dvirnoff, A. H. and Munion, D. W. (1986), "Stability Failure of a Sanitary Landfill", *International Symposium on Environmental Geotechnology*, Lehigh, Pennsylvania, pp. 25-35.

EPA (1989), "*Technical Guidance Document: Final Covers on Hazardous Waste Landfills and Surface Impoundments*", EPA/530/SW-89/047, U.S. Environmental Protection Agency, Office of Solid Waste and Emergency Response, Washington, D.C., 39 p.

EPA (1994), "*Seminar Publication Design, Operation, and Closure of Municipal Solid Waste Landfills*", EPA/625/R-94/008, U.S. Environmental Protection Agency, Center for Environmental Research Information, Cincinnati, Ohio, 86 p.

EPRI (1984), "*Comparison of Two Groundwater Flow Models-UNSAT1D and HELP*", Electric Power Research Institute, Topical Report, EPRI CS-3695, Project 1406-1.

Field, C. R. and Nangunoori, R. K. (1994), "Case Study-Efficacy of the HELP Model: A Myth or Reality?", *Proceedings of the Waste Tech '94 Conference*, National Solid Wastes Management Association, Charleston, SC., 9 p.

Ghassemi, M., Crawford, K., and Haro, M. (1986), "*Leachate Collection and Gas Migration and Emission Problems at Landfills and Surface Impoundments*",

EPA/600/2-86/017, U.S. Environmental Protection Agency, Hazardous Waste Engineering Research Laboratory, Cincinnati, Ohio, 206 p.

Gibbons, R. D., Dolan, D., Keough, H., O'Leary, K., and O'Hara, R. (1992), "A Comparison of Chemical Constituents in Leachate From Industrial Hazardous Waste & Municipal Solid Waste Landfills", *Proceeding of Fifteenth Annual Madison Waste Conference*, University of Wisconsin - Madison, Sep, pp. 251-276.

Giroud, J. P. and Bonaparte, R. (1989a), "Leakage Through Liners Constructed with Geomembranes - Part I. Geomembrane Liners", *Geotextile and Geomembranes*, Vol. 8, No. 1, pp. 27-67.

Giroud, J. P. and Bonaparte, R. (1989b), "Leakage Through Liners Constructed with Geomembranes - Part II. Composite Liners", *Geotextile and Geomembranes*, Vol. 8, No. 2, pp. 77-111.

Giroud, J. P., Badu-Tweneboah, K., and Bonaparte, R. (1992), "Rate of Leakage Through a Composite Liner Due to Geomembrane Defects", *Geotextile and Geomembranes*, Vol. 11, No. 1, pp. 1-28.

Gross, B. A., Bonaparte, R., and Giroud, J.P. (1990), "Evaluation of Flow From Landfill Leakage Detection Layers", *Proceedings of Fourth International Conference on Geotextiles*, Vol. 2, The Hague, pp. 481-486.

Kenter, R. J., Schmucker, B. O., and Miller, K. R. (1997), "The Day the Earth Didn't Stand Still: The Rumpke Landfill", *Waste Age*, Mar, pp. 66-81.

Khire, M. V., Benson, C. H., and Bosscher, P. J. (1994), "*Final Cover Hydrologic Evaluation-Phase III*", Environmental Geotechnics Report No. 94-4, University of Wisconsin-Madison, WI, 142 p.

Kmet, P., Mitchell, G., and Gordon, M. (1988), "Leachate Collection System Design and Performance - Wisconsin's Experience", Proceedings of *ASTSWMO National Solid Waste Forum on Integrated Municipal Waste Management*, Lake Buena Vista, Florida.

Lane, D. T., Benson, C. H., and Bosscher, P. J. (1992), "*Hydrologic Observations and Modeling Assessments of Landfill Covers*", Final report No. 92-10, University of Wisconsin-Madison, 406 p.

Lange, D. A., Cellier, B. F., and Dunchak, T. (1997), "A Case Study of the HELP Model: Actual Versus Predicted Leachate Production Rates at a MSW Landfill in North-eastern Ohio", *Proceedings of the SWANA Conference*, Sacramento, CA, 18 p.

NUS (1988), "*Draft Background Document Summary of Data on Municipal Solid Waste Landfill Leachate Characteristics "Criteria for Municipal Solid Waste Landfills" (40 CFR Part 258) Subtitle D of Resource Conservation and Recovery Act (RCRA)*", U.S. Environmental Protection Agency, Office of Solid Waste, Washington, D.C., EPA/530-SW-88-038, Jul.

Oweis, I. S. (1985), "Stability of Sanitary Landfills", *Geotechnical Aspects of Waste Management*, seminar sponsored by ASCE Metropolitan Section, New York.

Peters, N., Warner, R. S., Coates, A. L., Logsdon, D. S., and Grube, W. E. (1986), "Applicability of the HELP Model in Multilayer Cover Design: A Field Verification and Modeling Assessment", *Land Disposal of Hazardous Waste-Proceedings of the 1986 Research Symposium*, U.S. Environmental Protection Agency, Cincinnati, OH.

Peyton, R. L. and Schroeder, P. R. (1988), "Field Verification of HELP Model for Landfills", *Journal of Environmental Engineering*, ASCE, Vol. 114, No. 2, pp. 247-269.

Peyton, R. L. and Schroeder, P. R. (1993), "Water Balance for Landfills", *Geotechnical Practice for Waste Disposal*, D.E. Daniel, Ed., Chapman & Hall, London, pp. 214-243.

Richardson, G. and Reynolds, D. (1991), "Geosynthetic Considerations in a Landfill on Compressible Clays", *Proceedings of Geosynthetics '91*, Atlanta, Georgia, 1991, Vol. 2, pp. 507-516.

Richardson, C. W. and Wright, D. A. (1984), "*WGEN: A Model for Generating Daily Weather Variables*", ARS-8, U.S. Department of Agriculture, Agricultural Research Service, 83 p.

Ritchie, J. T. (1972), "A Model for Predicting Evaporation from a Row Crop with Incomplete Cover", *Water Resources Research*, 8(5), pp. 1204-1213.

Schmucker, B. O. and Hendron, D. M. (1997), "Forensic Analysis of 9 March 1996 Landslide at the Rumpke Sanitary Landfill, Hamilton County, Ohio", *Slope Stability in Waste Systems*, seminar sponsored by ASCE Cincinnati and Toledo Sections, Ohio.

Schroeder, P. R., Lloyd, C. M., and Zappi, P. A. (1994a), "*The Hydrologic Evaluation of Landfill Performance (HELP) Model, User's Guide for Version 3*", U.S. Environmental Protection Agency, Office of Research and Development, Washington, D.C., Report No. EPA/600/R-94/168a.

Schroeder, P. R., Dozier, T. S., Zappi, P. A., McEnroe, B. M., Sjostrom, J. W., and Peyton, R. L. (1994b), "*The Hydrologic Evaluation of Landfill Performance (HELP) Model Engineering Documentation for Version 3*", U.S. Environmental Protection Agency, Office of Research and Development, Washington, D.C., Report No. EPA/600/R-94/168b, 116 p.

Soong, T. Y. and Koerner, R. M. (1997), "*The Design of Drainage Systems Over Geosynthetically Lined Slopes*", GRI Report #19, Geosynthetic Research Institute, Philadelphia, Pennsylvania, 88 p.

Stark, T. D. and Evans, W. D. (1997), "Balancing Act", *Civil Engineering*, Aug, pp. 8A-11A.

Thompson, F. and Tyler S. (1984), "*Comparison of Two Groundwater Flow Models (UNSAT1D and HELP) and their Application to Covered Fly Ash Disposal Sites*", EPRI Document Series, Electric Power Research Institute, Palo Alto, California, Aug.

Udoh, F. D. (1991), "*Minimization of Infiltration Into Mining Stockpiles Using Low Permeability Covers*", Dissertation Proposal, Dept. of Materials Science and Engineering, Mining Engineering Program, University of Wisconsin-Madison.

UDSA-SCS (1985), "Hydrology", Section 4 in *National Engineering Handbook*, U.S. Government Printing Office, Washington, D.C.

Chapter 6
Summary and Recommendations

6.1 Rationale and Scope of Chapter

The study discussed in this research report addressed three important areas of waste containment system design and performance, namely:

- geosynthetic materials (puncture protection of GMs using GTs, wave behavior in HDPE GMs, plastic pipe behavior under high overburden stresses, and service life prediction of GTs and GMs);
- natural soil materials (slope stability of final cover systems with GCLs, k_{field} of natural soil CCLs and soil-bentonite admixed CCLs, and hydraulic performance of CCLs in final cover systems); and
- field performance (LCRS and LDS flow quantities and chemical quality at landfills, assessment of EPA HELP computer code as a design tool using LCRS flow rate data, and lessons learned from waste containment problems at landfills).

All three areas were addressed through multiple tasks, each important in its' own right, but also complementary to the other tasks because of the interrelationships between waste containment system components. The ultimate goals of this study were to assess the field performance of waste containment systems and to develop recommendations for further improving the performance of these systems in comparison to the current state-of-practice.

This chapter presents a summary of the tasks conducted for this study and provides recommendations on practices to further improve the performance of waste containment systems. These recommendations were developed, in part, using the results of the various tasks. Some, however, go beyond the scope of this study and are offered by the authors with the understanding that the current level of "good" field performance can be further improved within current material, design, testing, and installation technology and practices.

6.1.1 Geosynthetics

As discussed in Chapter 1, geosynthetics, including GMs, GTs, GNs, GCs, plastic pipe, and GCLs, are used in waste containment systems for a variety of functions. Most modern waste containment systems contain one or more geosynthetic components. Notwithstanding their broad use, issues related to geosynthetic materials persist. Indeed, the relative newness of these materials compared to natural soil construction materials requires that they continue to be studied and evaluated. Chapter 2 of this report described the results of the geosynthetic-related tasks of this research project. These tasks addressed:

- protection of GMs from puncture using needlepunched nonwoven GTs;
- behavior of waves in HDPE GMs when subjected to overburden stress;
- plastic pipe stress-deformation behavior under high overburden stress;
- service life prediction of GTs; and
- service life prediction of GMs.

Key findings of the geosynthetic-related tasks are given below:

- Needlepunched nonwoven GTs can provide adequate protection of GMs against puncture by adjacent granular soils. A design methodology for GM puncture protection was developed from the results of laboratory tests and was presented.
- Temperature-induced waves (wrinkles) in GMs do not disappear when the GM is subjected to overburden stress (i.e., when the GM is covered with soil), rather the wave height decreases somewhat, the width of the wave decreases even more (i.e., the height-to-width ratio (H/W) of the wave increases), and the void space beneath the wave becomes smaller. Residual stresses in HDPE GMs installed in the field may be on the order of about 1% to 22% of the GM's short-term yield strength in the vicinity of GM waves, with higher residual stresses associated with higher H/W values. Significant residual stresses can reduce the GM service life. The relationship between GM type, residual stress magnitude, and service life requires further investigation.
- If GM waves after backfilling are to be avoided, light-colored (e.g., white) GMs can be used, GMs can be deployed and seamed without intentional slack, GMs can be covered with an overlying light colored temporary GT until backfilling occurs, and backfilling can be performed only in the coolest part of the day or even at night.
- Based on finite element modeling results, use of the Iowa State formula for predicting plastic pipe deflection under high overburden stress is reasonable. In comparison to the FEM predictions, the Iowa State formula overestimated pipe vertical deflection under short-term conditions (which is conservative) and slightly underestimated pipe vertical deflection under long-term conditions (which is slightly unconservative, but typically accommodated by the incorporation of a factor of safety).
- PP GTs are slightly more susceptible to UV degradation than PET GTs, and lighter weight GTs degrade faster than heavier GTs.
- GTs that are partially degraded by UV light do not continue to degrade when covered with soil, i.e., the degradation process is not auto-catalytic. Nonetheless, good practice dictates that GTs be covered with overlying protective materials in a timely manner to minimize exposure. Also, GTs should be protected from exposure prior to installation (i.e., by keeping the GT rolls in opaque bags).

- Buried HDPE GMs have an estimated service life that is measured in terms of at least hundreds of years. The three stages of degradation and approximate associated times for each as obtained from the laboratory testing program described in this report are: (i) antioxidant depletion (≈ 200 years), (ii) induction (≈ 20 years), and (iii) half-life (50% degradation) of an engineering property (≈ 750 years). It is noted that these durations were obtained from the extrapolation of a number of laboratory tests performed under a limited range of conditions. It is recommended that additional testing be performed under a broader range of conditions to develop additional insight into the ultimate service life of HDPE GMs, and other types of GMs as well.

6.1.2 Natural Soils

CCLs, including those constructed from natural clay soils and those constructed from soil-bentonite mixtures, have long been used in waste containment systems as hydraulic barriers to inhibit liquid migration from the waste management unit. Either used alone, or with a GM component in the form of a GM/CCL composite liner, CCLs form an essential part of many liner systems and final cover systems. Other natural soil materials used in liner and final cover systems include sands and gravels used for gas conveyance systems or liquid drainage and collection systems, and soil layers used for filtration, separation, or protection. Notwithstanding the widespread use of natural soil materials in liner systems and final cover systems, questions and issues persist relative to their use. Several of these questions and issues were investigated, and the results were reported in Chapters 3 and 4 of this report. The subject areas that were addressed are:

- slope stability of GCLs in final cover systems, as assessed from field test plots;
- k_{field} of low-permeability natural soil CCLs;
- k_{field} of admixed (soil-bentonite) CCLs; and
- CCL hydraulic performance in final cover systems;

These topics were selected on the basis of past research indicating areas where additional insight was required, or on the basis of concerns developed from relatively recent field experience. Key findings of the natural soils related tasks are given below:

- Slope stability monitoring of final cover system test plots incorporating GCLs demonstrated acceptable performance for test plots constructed on 3H:1V slopes, but several of the test plots constructed on 2H:1V slopes failed. Importantly, for internally-reinforced GCLs, these failures were not due to inadequate internal strength, but inadequate interface strength. Clearly, proper characterization of GCL interface shear strength is an important design step.
- The key to achieving low k_{field} for natural soil CCLs is to ensure that 70 to 80%, or more, of the field-measured compaction (w vs. γ_d) points lie on or above the line of optimums for the particular CCL being placed.

- Practically no correlation was found between k_{field} and frequently measured soil characterization parameters, such as plasticity index and percentage of clay, indicating that natural soil CCLs can be constructed with a relatively broad range of soil materials.
- Compaction density appears to be more significant than water content for achieving low k_{field} in soil-bentonite liners.
- The long-term hydraulic performance of low-permeability (i.e., $k_{field} \leq 10^{-7}$ cm/s) CCLs in final cover systems may not be good in light of the effects of desiccation, freeze-thaw, root penetration, animal intrusion, and subsidence.

6.1.3 Field Performance

The premise of this portion of the study was that "modern" waste containment systems have been installed for up to a decade or more allowing for an assessment of their field performance. Information on actual field performance can be used to evaluate how waste containment systems are performing now, and for extrapolation of their long-term performance. Chapter 5 presented a discussion of the following specific topics related to the performance of waste containment systems for modern landfills:

- evaluation of published information on field performance;
- collection and analysis of liquids management data;
- identification and assessment of problems; and
- assessment of the EPA HELP model as a tool for LCRS design.

These topics were selected to develop an improved understanding of the actual field performance of modern landfill liner systems, and, to the extent possible, to develop answers to the questions identified in Section 5.1.1 of this report. Key findings of the field performance tasks are:

- LDSs from double-lined landfills will almost always exhibit flow. Much of this flow may be from sources other than primary liner leakage, particularly in the time frame just after construction when construction water can be a significant source, and for GM/CCL composite liners, following waste placement when consolidation water from the CCL can be a major source.
- Average monthly active-period LDS flow rates for cells with HDPE GM primary liners constructed with CQA (but without ponding tests or electrical leak location surveys) will often be less than 50 lphd, but occasionally in excess of 200 lphd. These flows are attributable primarily to liner leakage and, for cells with sand LDSs, possibly construction water. Average monthly active-period LDS flow rates attributable to leakage through GM/GCL primary liners constructed with CQA will often be less than 2 lphd, but occasionally in excess of 10 lphd. Available data suggest that average monthly active-period LDS flow rates attributable to leakage through GM/CCL and GM/GCL/CCL primary liners constructed with CQA are probably similar to those for GM/GCL primary liners constructed with CQA.

- Single liner systems with GM liners (installed on top of a relatively permeable subgrade) should not be used in applications where a true hydraulic efficiency above 90% must be reliably achieved, even if a thorough CQA program is employed. In these cases, single-composite liner systems or double-liner systems should be used. An exception to this may be made for certain facilities where electrical leak location surveys or ponding tests are used to identify GM defects and the defects are repaired. Higher true hydraulic efficiencies of 99% to more than 99.9% can be achieved by GM/GCL, GM/CCL, and GM/GCL/CCL composite liners constructed with good CQA.
- Based on the existing data, GM/CCL and GM/GCL/CCL composite liners are capable of substantially preventing leachate migration over the entire period of significant leachate generation for typical landfill operation scenarios (i.e., for a landfill cell filled over a number of years, that does not undergo leachate recirculation or disposal of liquid wastes or sludges, and that is capped with a final cover system designed to minimize percolation into the landfill; based on our existing understanding of their performance capabilities, these types of composite liners are capable of substantially preventing leachate migration for a much longer period, although field performance data of the type presented in this report do not yet exist for this longer period.
- LCRS flow rates during operations (i.e., the initial and active periods of operation) can vary significantly between landfills located in the same geographic region and accepting similar wastes. Large variations in flow rates (e.g., one order of magnitude difference) can even occur between cells at the same landfill.
- LCRS flow rates were highest at the beginning of cell operations and decreased as waste thickness increased and daily and intermediate covers were applied to the waste. Leachate generation rates decreased, on average, by a factor of four within one year after closure and by one order of magnitude two to four years after closure. Within nine years of closure, LCRS flow rates were negligible for the landfill cells evaluated in this study.
- MSW cells produced, on average, less leachate than HW and ISW cells.
- For cells of a given waste type, rainfall fraction (RF) values were highest in the northeast U.S. and lowest in the west.
- In general, HW landfills produced the strongest leachates and coal ash landfills produced the weakest leachates. MSW ash leachate was more mineralized than MSW leachate and the other ISW leachates.
- The solid waste regulations of the 1980s and 1990s have resulted in the improved quality of MSW and HW landfill leachates.
- The EPA HELP computer model, when applied using an appropriate simulation methodology and an appropriate level of conservatism, provides a reasonable basis for designing LCRSs and sizing leachate management system components. Use of the HELP model for these purposes can be enhanced through calibration to leachate generation rates at other landfills in the region and through parametric analyses that consider the potential range of values for key input parameters (e.g., initial moisture contents of waste). Due to the

complexity and variability of landfill systems, however, the model will generally not be adequate for use in a predictive or simulation mode, unless calibration is performed using site-specific measured (not default) material properties and actual leachate generation data.

- The frequency of occurrence of design, construction, and operational problems at landfills is significant. The most common types of problems encountered involved liner system and final cover system slope stability. Almost all of the problems were detected shortly after they occurred, and environmental impact due to the problems was only identified at one facility, which has since been remediated. The main impacts of the problems were interruption of waste containment system construction and operation, increased maintenance, and increased costs. Importantly, all of the problems identified in this investigation could have been prevented using available design approaches, construction materials and procedures, and operation practices.

In light of the significant findings in each of the three areas of investigation, it is obvious that landfills are complex structures that require careful and thorough design, testing, construction and operation/maintenance. Procedures exist to avoid the types of issues and problems identified in this report. Unfortunately, as most clearly demonstrated by Appendix F of this report, landfill industry personnel do not always utilize adequate design, testing, construction, and operation/maintenance practices. The authors feel strongly that current practices can and should be improved. In the next four sections of this report, the authors highlight a number of areas related to landfill design, construction, and operation where they believe practice improvement can be achieved using readily available technology.

6.2 Liner Systems

Liner systems for the containment of solid waste consist of at least a low-permeability barrier (liner) and an overlying LCRS. Depending on the nature of the waste (and obviously the pertinent regulations) a single-liner system or a double-liner system with a LDS between the two liners may be required. In all cases, geosynthetics and/or natural soils are typically utilized for the liners, drainage layers, or both. The design of these multi-component and multilayered systems (see Figures 1-1 and 1-3) requires the application of sophisticated engineering analysis methods. These systems also require careful construction methods and CQA if they are to function as intended. This section of the report is intended to highlight several of the more important challenges faced by engineers and contractors in designing and constructing these systems. It is noted that some of these challenges go beyond the tasks directly evaluated in this project; however, these challenges are identified because they are important to waste containment system performance.

6.2.1 Construction Quality Assurance

CQA has been shown to be of direct benefit in minimizing the potential leakage through liner systems. This finding was originally put forth by Bonaparte and Gross (1990) on the basis of sparse data and has been reinforced with the considerable additional data generated since that time, including data presented in this study. Considerable guidance exists for the development and implementation of liner system and cover system CQA plans. Among the many requirements for such plans, the authors make note of the following:

- soil and geosynthetic material conformance with the project specifications;
- proper pre-conditioning and placement of CCL lifts;
- proper compaction moisture content and density of CCLs;
- protection of CCLs from desiccation and freezing;
- placement of GMs without excessive waves and covering or backfilling the GMs in a manner that minimizes the trapping of waves; the goal of these measures is intimate contact between the GM and the underlying CCL or GCL;
- prevention of premature GCL hydration;
- inspection of GM seams, including nondestructive and destructive testing; and
- protection of GMs from puncture by adjacent materials or equipment.

6.2.2 Liner System Stability

This category of stability involves the liner system prior to waste placement. The main concern regarding liner system stability is for natural soils (particularly sand and gravel drainage soils) or geosynthetics (particularly GTs and GNs) to slide on underlying geosynthetic surfaces. Sliding of drainage soils or sliding of drainage soils and GT cushions on underlying GMs is unfortunately too common. The instability is induced by low shear strength interfaces, steep and/or long slopes, equipment loads, seepage forces, and/or seismic forces. An area requiring particular attention is at access ramps into below-grade landfills. These ramps are needed for operations, but are sometimes overlooked in the assessment of landfill cell slope stability. In some cases, ramps have been installed by landfill operations personnel, without an evaluation of their effect on liner system stability. Another type of liner system stability problem that requires careful attention is sliding of GM layers on underlying CCLs or GCLs prior to waste placement.

Design of liner systems for adequate slope stability is well within the design state-of-practice. The available technical literature contains more than adequate information to design liner systems to be stable (see for example, Giroud and Beech, 1989; Koerner and Hwu, 1991; Giroud et al., 1995; and Koerner and Soong, 1998). However, in the authors' experience, the available methods are often not adequately utilized in design. For example, it is not uncommon for seepage forces to be inadequately addressed during the design process. Another significant design issue involves the inadequate characterization of interface shear strengths, apparently due to insufficient effort

expended in the laboratory evaluation of these strengths. Testing must be performed under both project-specific and material-specific conditions, with considerable attention given to the many variables that can influence the interface shear test results (e.g., boundary conditions, normal stresses, hydration times, moisture conditions, and displacement rates). A number of papers, including those by Dove et al. (1997), Eid and Stark (1997), Gilbert et al. (1997), Sharma et al. (1997), Sabatini et al. (1998), Breitenbach and Swan (1999), and Sabatini et al. (2001), discuss variables that can influence test results.

It is somewhat fortunate that many liner system slope stability problems can be repaired at relatively small cost and with no environmental impact. This is particularly true of slides that occur above the GM component of the liner system. However, these facts certainly do not justify a less rigorous or careful design approach, and overall improvement in the rigor with which some owners and engineers address this design issue is warranted.

6.2.3 Waste Stability

Of potentially greater significance than instability of the liner system before waste is placed is a failure that occurs after waste has been deposited on top of the liner system. The Kettleman Hills landfill failure (Byrne et al., 1992) is perhaps the best known of this type of occurrence. Design to resist this type of instability requires that the design engineer specify acceptable waste configuration (e.g., intermediate slope angles) and waste placement procedures, in addition to appropriately using slope stability analysis methods and selecting liner system interface shear strengths. For many facilities, waste placement operations will need to be carefully sequenced. Canyon-type landfills and landfills built on soft foundation soils represent two classes of facilities for which waste mass stability deserves particular attention.

As with liner system stability, the technical analysis for waste mass stability is within the state-of-practice, relying principally on limit equilibrium slope stability methods developed in geotechnical engineering. The validity of the analysis is dependent on the choice of analysis methods, waste geometry and properties, interface shear strengths, and moisture conditions in the landfill. Particularly important with respect to waste placement operations are the slope of the exposed surface of the waste, distance of this exposed surface from the liner system sideslopes, height of the waste, waste density, and waste shear strength. Discussion of solid waste shear strengths to use in design can be found in Kavazanjian et al. (1995). To help assure waste stability, the authors recommend that the operations plans developed for landfills provide detailed criteria for waste placement so that the landfill operator does not unknowingly fill the facility in a potentially unstable manner.

Of particular importance in choosing waste and interface shear strengths is deformation compatibility. It must be recognized that the amounts of deformation needed to generate peak shear strengths in waste and along geosynthetic interfaces are very different. As discussed by Byrne (1994), Stark and Poeppel (1994), Gilbert et al. (1997), and Sabatini et al. (2001), careful consideration must be given to the shear strength deformation conditions used in design (i.e., peak, large displacement, or residual).

It is interesting to note that several of the larger waste failures reported in the literature occurred after periods of high rainfall, which had the effect of temporarily increasing the density of the waste (Reynolds, 1991). High rainfall can also impose seepage forces, which will decrease stability accordingly.

Also important in some cases is seismic stability of the waste mass. While the performance of several lined earthquakes in the 1994 California Northridge earthquake was very good (Matasovic et al., 1995; Matasovic and Kavazanjian, 1996) more needs to be learned about this subject, particularly with respect to the seismic response of the landfill and the determination of the acceptable magnitude of seismically-induced liner system deformation. With respect to this latter criterion, it is the authors' experience that design engineers often select a seismic deformation criterion of 150 to 300 mm based on Seed and Bonaparte (1992). However, these values may not be appropriate in all applications. Careful consideration should be given to selection of an acceptable level of deformation for design. For example, all other factors being equal, a lower allowable deformation should be used if the critical interface is below the GM component of the liner system (because excessive deformation would cause the GM to rupture) than above it. Guidance on the seismic design of landfills can be found in Richardson et al. (1995), Anderson and Kavazanjian (1995), and Kavazanjian (1998).

6.2.4 Performance of Composite Liner

For over a decade it has been known through theoretical analyses, laboratory tests, and limited field data that composite liners are superior to either GMs alone or CCLs alone for the containment of leachate or other liquids (Brown et al., 1987; EPA, 1987; Giroud and Bonaparte, 1989a,b; Bonaparte and Gross, 1990; Bonaparte and Othman, 1995). This report has presented significant new field data that confirms the very good performance characteristics of GM/GCL, GM/CCL, and GM/GCL/CCL composite liners versus current types of single liner materials.

As discussed in Section 1.4.1.4, the basic premise of using a composite liner is that leakage through a hole or defect in the GM upper component is impeded by the presence of a CCL or GCL lower component. The GM improves the performance of the composite liner relative to that for a CCL or GCL alone by greatly limiting the portion of the CCL or GCL exposed to leachate, and, for CCLs, lowering the potential for

desiccation cracking. Another benefit derived by using a composite liner is reduced potential for diffusive transport through the liner. Diffusion is not an important transport mechanism for inorganic ions through GMs. However, as shown by Rowe (1998) and others, diffusion rates of certain organic contaminants through GMs can be significant when the concentrations of these contaminants are relatively high (i.e., diffusion through GMs is generally not a concern at MSW landfills, but may be a concern at landfills or impoundments where the liquid above the liner has relatively high concentrations of volatile organic compounds). A CCL, and to a lesser extent GCL, component of a composite liner will help retard organics that diffuse through the GM. Analysis methods to design composite liners to account for diffusive transport are given by Rowe (1998). If diffusion is the primary concern for a specific project, a CCL is preferred to a GCL as the soil component of the composite liner. To maximize retardation potential, adequate thickness of CCLs is more important than low permeability. One approach to achieve a composite liner with both low advective transport and low diffusive transport potential is to specify a GM/GCL/CCL composite liner. Giroud et al. (1997) present equations to evaluate advective leakage rates through composite liners containing GCLs. While a GM/GCL/CCL composite liner has advantages with respect to minimizing contaminant transport potential, it may also create challenges with respect to slope stability factors of safety. Shear strengths for both the GM/GCL interface and GCL/CCL interface require careful evaluation.

6.2.5 Single vs. Double Liner System

As discussed in Section 1.2, federal regulations under Subtitle C of RCRA require permitted HW facilities to be underlain by double-liner systems with leak detection capability. Also as discussed in Section 1.2, federal minimum design criteria for MSW landfills include a single composite liner system. Several states have gone beyond these minimum criteria for MSW landfills by requiring double-liner systems. A 1998 survey of 43 states has shown that for MSW landfills:

- 31 (72%) states require single liner systems;
- 6 (14%) states require double liner systems; and
- 6 (14%) states provide options for the use of either a single liner or double liner system.

This survey highlights the differences in perspective (due to regional political differences, population attitudes, hydrogeology, climate, drinking water resources, and other factors) between states as to the minimum requirements for liner systems at RCRA Subtitle D landfills. These differences are even greater when it is realized that the federal Subtitle D regulations contain both federal minimum design criteria and performance-based criteria. The performance-based critera require technical demonstrations that are often made using the EPA HELP and MULTIMED computer models, which do not address the potential for the migration of any landfill-generated

gas through the liner system. With respect to selection of the type of liner system for a specific project, the authors offer the following thoughts:

- Caution should be exercised in using the EPA HELP model to make a technical demonstration that the Subtitle D performance standard can be achieved with a liner system less (e.g., without a GM) than the federal minimum design criteria. Input parameters to the model can be selected to demonstrate a lesser potential for leachate generation than actually exists. For example, the discussion in Chapter 5 of this report indicated that modeled leachate generation rates are sensitive to the assumed initial moisture content of the waste. Because of the sensitivity of the HELP model results to the input parameters, when the model is used to make a technical performance demonstration, the model should be calibrated against data (i.e., LCRS flow rates) from lined landfills in the same geographic area. In addition, the potential for landfill gas impacts to groundwater should also be considered as part of the technical demonstration.
- Based on the landfill operation data presented in this report, Subtitle D single-composite liner systems meeting federal minimum design criteria can achieve a very high hydraulic efficiency and are capable of preventing adverse impacts to groundwater. This conclusion is consistent with the previous conclusion reached by EPA regarding the performance capabilities of liner systems meeting federal minimum design criteria.
- Caution should be exercised in substituting a GCL alone for the CCL as the low-permeability soil component of a Subtitle D single-composite liner on the base of a landfill. While the hydraulic efficiency of a GM/GCL composite liner is as good, or better, than a GM/CCL composite liner, the GM/GCL composite liner is more susceptible to diffusive transport (Rowe, 1998) and puncture than the GM/CCL composite liner. These concerns are less important for sideslope areas of the landfill where leachate heads are lower; thus, a GM/GCL composite liner is more likely be appropriate for sideslopes than for base areas from a hydraulic perspective. Also, a GM/GCL/CCL composite liner may be an effective low-permeability soil component for a single-composite liner. In this case, it may be acceptable to specify a maximum hydraulic conductivity on the order of 1×10^{-5} cm/s for the CCL of a three-component composite liner used at MSW landfills.
- There may exist situations for MSW landfills where a double-liner system would be preferred to a liner system meeting the federal minimum design criteria. In addition to the obvious situation where a state regulation requires use of a double-liner system, the project conditions favoring selection of a double-liner system include: (i) sites with especially vulnerable hydrogeology; (ii) sites where groundwater cannot be reliably monitored due to the presence of complex hydrogeology, karst, or other factors; and (iii) sites where, for whatever reason, a higher degree of reliability/redundancy is required of the liner system than can be achieved by the Subtitle D federal design criteria. In some cases, it may be desirable to use a double-liner system beneath the base of the landfill, and, for cost-effectiveness, a single-composite liner system beneath the sideslopes.

- The authors endorse a design strategy of providing additional protection at critical locations in the landfill. For a landfill underlain by a single-composite liner system, this strategy might take the form of installing a GM/GCL/CCL liner beneath each landfill sump. This design feature adds little cost to the overall project, but significant benefit in terms of design reliability and redundancy at the project's most critical location.
- Where double-liner systems are used, the authors prefer that the secondary liner be a GM/CCL or GM/GCL/CCL composite to a GM alone or a GM/GCL alone. Furthermore, the authors prefer a GM/GCL composite liner to either a GM alone or GM/CCL composite liner as the primary liner component of the double-liner system. The preferred type of composite primary liner is much easier to construct on top of the LDS and secondary liner than is a GM/CCL composite primary liner and it minimizes LDS flow rates compared to the rates associated with the other types of primary liners considered in this report.
- Notwithstanding the specificity of the recommendations given above, the authors do endorse the use of creative thinking and good engineering to develop better-performing, more cost-effective liner systems. The key to this approach, however, should be good engineering, and not, for example, manipulation of the HELP model or any other data or design tool to achieve a pre-conceived desired outcome.

6.2.6 Fate of Liner Systems

Of critical importance to the long-term performance of a liner system is the service life of the GM component of the system. Both CCLs and GCLs consist of geologic materials. These materials can be expected to have service lives in excess of the design lives that have been defined for MSW, HW, and LLRW disposal facilities constructed in the United States. This conclusion is only valid, however, if these materials stay hydrated and stable, are adequately protected, and, for GCLs, are not subjected to unacceptable chemical interactions (i.e., an increase in hydraulic conductivity of bentonite may result if sodium in the bentonite is replaced by other cations present in the permeant). For the CCL or GCL component of a composite liner beneath a waste mass these conditions will often be met.

Perhaps the most important factor governing the service life of GMs is the polymer type, and resin formulation. Of the variety of choices, HDPE is the most widely used polymer and the resin formulation includes carbon black and an antioxidant package. As described in this report and in Hsuan and Koerner (1998), lifetime predictions are measured in terms of hundreds of years (but not "forever"). However, this report has also pointed out that additional research in this area is warranted.

Perhaps the most significant issue related to the use of HDPE GMs is the potential for premature stress cracking before the end of its design life. Currently, the notched constant tensile load (NCTL) test is used with a minimum onset of brittle behavior of 100

hours. (This is equivalent to a single point value, per ASTM D5397, of 200 hours). At the designer's discretion, these values can be increased, and, depending on site-specific conditions, this is encouraged. Regarding HDPE formulations, the antioxidant package included in the formulation is critically important, and specifications should include a minimum OIT along with a minimum OIT retained value after oven aging and laboratory simulated UV exposure.

6.3 Liquids Management

The liquids management strategy for a landfill generally refers to all liquids including:

- leachate collection and removal at the bottom of the waste mass, above the primary liner system;
- leakage collection and removal at the bottom of the waste mass between the primary and secondary liners;
- rainwater collection and removal via the final cover system drainage layer above the barrier material;
- gas condensate collection and removal via the gas collection piping system; and
- groundwater collection and control via the pore pressure relief system in areas of high groundwater.

For the first three systems, drainage layers transmit liquid by gravity to a low point where the liquid empties into a sump or gravity drain or is discharged from the waste containment system, in the case of a final cover system drainage layer. In the case of a sump, the liquid is withdrawn using submersible pumps or bailers. For a gravity drain, the liquid flows by gravity through a pipe that penetrates the liner system and discharges to a storage or treatment system outside the limits of the landfill. From final cover system drains, the liquid flows by gravity either as sheet flow to the surrounding land, or, more typically, into a perimeter stormwater collection and conveyance structure. For gas condensate collection and removal systems, liquids collected in gas collection piping systems typically drain to a low point in the piping system. From this location, condensate is usually introduced back into the waste; however, sometimes condensate is removed from the waste containment system and treated. With respect to pore pressure relief system, these systems may consist of a series of wells or perimeter trenches that are pumped to lower the groundwater table or may include a drainage layer and sump installed beneath the liner system.

These liquid collection and removal systems were discussed in Section 1.4.2 of this report. That discussion is not repeated in this chapter.

6.3.1 Construction Quality Assurance

The authors provide the following commentary on CQA of liquids management systems:

- Placement of natural drainage soils on previously placed geosynthetics should be done with great care. Minimum thicknesses of soil should be maintained between construction equipment and the underlying geosynthetics. Only low ground pressure equipment should be allowed to spread the soil. Particular attention should be focused on preventing accumulation of excess slack and the propagation of waves in the underlying GM.
- When shallow trenching is conducted within a natural drainage soil in order to place plastic pipes above the previously installed GM, the trenching should be conducted by hand, with special lightweight backhoes equipped with rubber bucket tips, or by an alternate method that will not damage the GM.
- Pipe fittings and joints need careful observation during installation to confirm that the fittings are mated with one another and are fabricated by the same manufacturer.
- Sumps, sideslope or vertical riser pipes, and pipe penetrations through GMs should be carefully constructed since they are located in areas with the highest sustained hydraulic head on the liner. To this end, GM seams in sumps should be limited to the extent possible. The placement of an enhanced liner in the sump (e.g., GM/GCL/CCL instead of a GM/CCL) should also be considered. In addition, extra care should be taken to protect the liner around these features by ensuring that required cushion layers are properly placed and that construction equipment maintains adequate separation from the GM.
- GN placement should be observed to ensure that no gaps exist between roll ends and edges and that sufficient plastic ties are used per the specifications.
- GNs must be carefully inspected for excess soil particles, fugitive bentonite from GCLs, vegetative growth, or other foreign matter, and these materials should be removed. Flushing of water through the installed GN could be considered .
- Full coverage of required GT filters over drainage layers should be provided whether the drain is natural soil or a GN.
- If select waste is to be placed directly over the drainage stone (with no intervening filter layer), its placement should have full-time inspection by a CQA monitor to assure that the underlying materials are not disturbed.

6.3.2 Potential for Clogging and Reduction of Flow Capacity

An important question regarding drainage systems is whether or not the system will clog excessively. The phrase "excessively" is used because all drainage systems will, over time, undergo a decrease in their flow capability from the original installation or manufacture; the issue is to what degree. The authors provide the following commentary and recommendations on this topic:

- For LCRSs, the authors believe that the often cited regulatory value for drainage layer hydraulic conductivity of 1×10^{-2} cm/s for natural soil is too low in many

applications. Furthermore, a value of 1 x 10^{-3} cm/s, which is sometimes specified, will almost always be too low. Hydraulic conductivities at these values result in drainage layers with substantial liquid storage (capillary) capacity and slow drainage rates. These conditions result in increased hydraulic head on the liner and, consequently, increased potential for clogging and leakage. Design of LCRSs should be performed on a site specific basis, using an adequate factor of safety. The soil should be free draining, with few fines, and little or no capillarity.

- For design of LCRSs, the HELP model can be an appropriate design tool for estimating leachate generation rates (see Chapter 5). As previously indicated, however, HELP model results are sensitive to the input parameters provided. The authors believe design engineers can do much more to calibrate their HELP model runs using data from already active landfills in the region. In this regard, design engineers and landfill operators are encouraged to collect and disseminate this information.
- Landfill LCRS design should include not only an evaluation of leachate quantity, but also leachate quality. This report presents considerable new data on landfill leachate characteristics. From a design perspective, it is important to identify conditions (e.g., sludge co-disposal, special waste disposal) that would create a leachate with more than usual potential to clog a drainage layer. For example, Koerner et al. (1994) identified leachate with high TSS and/or BOD_5 values (e.g., above 10,000 to 15,000 mg/l) as a condition requiring special design consideration. Interestingly, in the study of liquids management data described in Chapter 5, none of the landfill cells for which leachate chemistry data are available had average BOD_5 values greater than 5,000 mg/l.
- For the internal drainage layer in a final cover system, water is the medium being transmitted and clogging of the drainage layer by water is generally not considered. The primary issue for this layer is inadequate drainage capacity and the buildup of seepage forces in the final cover system, leading to slope instability. A significant number of seepage-induced final cover system failures were identified in Chapter 5. The HELP model must be used with caution to calculate liquid heads in the final cover system drainage layer, as experience has shown that these heads may be underpredicted if the peak daily rainfall used in the model is too low. Guidance on using the HELP model for this purpose is given in the upcoming EPA technical guidance document titled, "*Technical Guidance for RCRA/CERCLA Final Covers*" (Bonaparte et al., 2002). Also, the manual procedure in Koerner and Daniel (1997) can be used to estimate liquid heads in the final cover system drainage layer.

6.3.3 Perched Leachate

Perched leachate (which does not have full hydraulic connection to the underlying LCRS) can occur as a result of a number of conditions in a landfill. Excessively clogged filters above the drainage layer, low-permeability buffer (or protection) soils placed above the LCRS, low-permeability daily cover, and high moisture content sludges (industrial or sewage) within the waste mass all can lead to the trapping of moisture in

pockets within the waste. The perched leachate can increase the unit weight of the waste and impact waste stability. Saturated conditions within the zone of perched leachate will inhibit the generation of landfill gas and reduce the effectiveness of gas extraction wells in the area. In addition, the "breakout" of perched leachate as seeps has contaminated nearby surface waters, created odor problems, and killed vegetation.

6.3.4 Fate of Liquids Management Systems

Data in Chapter 5 and Appendix E indicate that in modern landfills, within a few years to a decade after a final cover system with a GM is placed, LCRS flow rates become very low to negligible. At a minimum, an LCRS should be designed for the anticipated peak leachate flows during the facility's active life assuming that some amount of clogging will occur (the amount being specific to the anticipated leachate and the details of the design). The authors recommend, however, that the system also be designed to retain a significant flow capacity even after closure. The rationale for this recommendation is that it provides the ability to continue to collect and remove leachate at some future date, should that need ever become necessary. The future need could arrive out of an unforeseen, even if improbable, future event such as undetected damage to the final cover system that allows significant new infiltration into the landfill. The need could also arrive out of a planned future event, such as the future use of a closed landfill cell as a bioreactor or the placement of additional waste as in "piggybacking" operations. Finally, the authors encourage the increasing tendency of design engineers to design LCRSs to performance levels better than those required by regulatory minimums. Examples include specifying higher permeability natural drainage materials (e.g., materials having hydraulic conductivities of at least five to ten times larger than the regulatory minimum of 1×10^{-2} cm/s specified by some states for MSW landfills), and designing to a lower maximum leachate head than the maximum allowed by regulation (e.g., designing to a maximum leachate head of 0.03 or 0.1 m, rather than the maximum value of 0.3 m allowed by Subtitle C and Subtitle D regulations).

The internal drainage layer above the hydraulic barrier in a final cover system must function for as long as the final cover system is required. Thus, the design must result in a stable hydraulic condition within the final cover system over its' design life. This will typically require careful selection of the protection soil above a filter or drainage layer so that hydraulic equilibrium can be established (i.e., so that particles of the protection soil are retained by the filter or drainage layer without clogging the layer).

6.4 Final Cover Systems

Conventional final cover systems placed over solid waste typically consist of a barrier material, internal drainage layer, cover soil, and surface material. Regulatory requirements for these conventional systems were discussed in Section 1.2 of this report. Increasingly, alternative design concepts are being applied to final cover systems. These alternative concepts include evapotranspiration (ET) or capillary

barriers, rather than low-permeability hydraulic barriers such as GMs, CCLs, and GCLs. ET and capillary barrier cover systems are finding increasing use at arid and semi-arid sites. These alternative cover systems are discussed in detail in the upcoming EPA technical guidance document titled, "*Technical Guidance for RCRA/CERCLA Final Covers*" (Bonaparte et al., 2002).

Both geosynthetics and natural soils are commonly used in final cover systems. Great care is required during both design and construction in order to achieve adequate performance. While many of the authors' comments in Section 6.2 of this report on liner systems also apply to the final cover systems, there are several differences between the two. For cover systems in comparison to liner systems:

- the barrier is meant to keep liquid out of the waste mass, rather than containing liquid within;
- the liquid to be managed is infiltrating rainwater (and snow melt) which percolates through the cover soil rather than leachate;
- upward rising gases from the waste may need to be captured beneath the barrier and effectively transmitted for proper management;
- the upward rising gases usually contain volatile constituents from the leachate, albeit at low concentrations for landfills (though potentially at higher concentrations at remediation sites), thus chemical mass transport and chemical compatibility of systems in contact with the gas should be considered;
- final cover systems slopes may be relatively steep and long, resulting in significant slope stability design issues;
- final cover systems are subjected to different environmental stresses than liner systems; these stresses include freeze-thaw and desiccation-wetting cycles; and
- the impact of waste settlements, both total and differential, on final cover system integrity should be considered for proper design of all system components.

Several of the more important issues with respect to design, construction, and maintenance of landfill final cover systems are discussed below.

6.4.1 Construction Quality Assurance

It seems intuitive that if proper CQA produces improved performance for liner systems, the same will be true for final cover systems. The authors believe that in addition to the CQA items for liner systems mentioned in Section 6.2.1 of this report, the following items require special attention when performing CQA of final cover systems:

- evaluation of the subgrade upon which the final cover system is to be placed to assure adequate bearing capacity and that buried waste will not damage overlying final cover system components;
- careful construction according to the design details for connections of GMs and GCLs to pipe vents;

- attention to construction details of the gas drainage layer (beneath the barrier) connection to the vent system to prevent GM blowouts;
- careful construction for connections of cover system internal drainage layers to their outlets;
- attention to proper location of haul roads and access roads according to lines and grades of the plans; and
- inspection of the erosion control features to verify that measures have been taken to obtain a healthy vegetative cover before the conclusion of construction activities.

6.4.2 Compacted Clay Barriers

There are serious concerns with respect to the use of CCLs in final cover systems, particularly when used alone. These concerns are as follows:

- based on the case histories presented in Section 4.3 of this report, desiccation of CCLs is a distinct long-term possibility in almost every final cover system application where the CCL is not covered by a GM; it has been shown that upon rewetting, a desiccated CCL does not return to its original low hydraulic conductivity;
- the freeze-thaw sensitivity of CCLs has been demonstrated in laboratory studies whereby the CCL hydraulic conductivity is increased significantly and self-healing of the thawed CCL is not likely (Othman et al., 1994);
- as discussed in Section 4.3 of this report, there are documented cases of moisture migration through some CCLs used in final cover systems due to CCL degradation;
- depending upon the thickness and properties of the final cover system materials above the CCL, root penetration of CCLs may occur; these roots can cause the development of channels for water migration into the underlying waste;
- again depending upon the thickness and properties of the final cover system materials above the CCL, burrowing animal intrusion into CCLs is a possibility; animal intrusion could lead to relatively large pathways for water migration into the underlying waste mass; and
- distortion of CCLs due to total and (more importantly) differential settlement of the underlying waste may lead to CCL tensile strains that exceed the ultimate tensile strain by orders of magnitude; based on studies by Leonards and Narain (1963), Ajaz and Parry (1975a,b, 1976), and others, most CCLs tested under unconfined or low confinement conditions exhibit failure at extensional strains of 0.5% or less.

For these reasons, it is felt that CCL barriers should typically not be used alone in the final cover systems of landfills (particularly MSW landfills, which contain wastes that undergo significant settlement) and that GMs or GCLs, by themselves, or as part of a composite cap, will typically be preferable.

6.4.3 Final Cover System Stability

Notwithstanding the availability of proven slope stability design methods (e.g., Koerner and Hwu, 1991; Giroud et al., 1995), the sliding of cover soils on underlying soil/geosynthetic and geosynthetic/geosynthetic interfaces has been a relatively common problem for landfill final cover systems. In evaluating final cover system stability, consideration must be given to a variety of potential destabilizing forces (i.e., the gravitational mass of the cover soil, equipment loadings, seepage forces, and seismic forces). As for liner systems, attention to detail by a qualified design engineer has sometimes been lacking. This attention to detail should apply to the selection of the input parameters to the slope stability analysis, to the evaluation of seepage, seismic, and/or equipment forces to be applied to the cover system, the factor of safety used in the analysis, and the analysis itself. As for the evaluation of liner system stability, it is recommended that the shear strengths of cover system materials and interfaces be evaluated using the results of project-specific laboratory shear tests conducted in a manner to simulate the anticipated field conditions.

In the experience of the authors, factors that contribute to the observed high frequency of final cover system slope failures include:

- relatively steep slopes with long uninterrupted surfaces; these conditions can be mitigated by using flatter slopes, benches, intermediate berms, and/or tapered cover soil thicknesses;
- equipment loadings, which can be minimized by limiting the ground pressure of equipment and orienting the equipment in predetermined (and properly designed) paths; the effect of even low ground pressure equipment on cover system stability should be checked by the design engineer;
- build-up of seepage forces within the drainage layer and/or cover soils due to inadequate drainage capacity, which is often the result of not performing a water balance for the internal drainage layer and evaluating the potential for seepage forces; if the HELP model is used to estimate seepage forces, considerable care is needed in selecting a design storm event and other input parameters that do not lead to an underestimate of liquid head buildup in the drainage layer; as previously noted, the manual calculation method of Koerner and Daniel (1997) can also be used to estimate liquid heads;
- inadequate design of drain transitions and outlets, such that water backs up in the drain and causes a buildup of pore pressure within the cover soil mass; and
- instability caused by seismic forces, which is clearly a site-specific situation and one requiring careful design and interpretation; paradoxically, current regulations require seismic design of many MSW landfills but do not do so for HW landfills or abandoned landfills.

6.4.4 Cover Soil Erosion

The evaluation of cover soil erosion is also an important step in the design of a landfill cover system. A possible design strategy to avoid seepage forces within a cover soil is

to use low permeability materials thereby preventing infiltration. Steep slopes, long uninterrupted slope lengths, and/or poor vegetative cover all tend to increase runoff and the potential for erosion of cover soils. The authors would like to highlight the following design considerations with respect to cover soil erosion:

- temporary erosion control materials should be used more widely than current practice so as to minimize erosion until a healthy stand of vegetation is obtained;
- cover system construction projects often conclude in the late fall, with little time to establish vegetation before the end of the growing season; this condition should be avoided, if possible; it is critical to have a good stand of surface vegetation prior to the end of the growing season if the potential for severe winter erosion is to be avoided;
- a careful choice of vegetation is critical in providing year-round protection of topsoil; a diverse mixture of native vegetation that closely emulate a selected local "climax" community is preferred;
- channelization of runoff is critical, and the design of soft or hard armor surface drainage swales and channels is necessary; let-down chutes represent a particular design challenge due to the high water velocities that occur on steep slopes; and
- erosion control in arid and semi-arid sites takes a completely different strategy than just described; the use of hard armor surfaces, particularly rock riprap, is common, with the selection of rock size being an important design output.

6.4.5 Fate of Final Cover Systems

Final cover systems play a critical long-term role at landfills. A properly functioning final cover system will largely eliminate the long-term post-closure leachate generation potential at solid waste landfills where there is no other input source for liquid (which is usually the case). If liquids are prevented from entering the waste mass, there is, in the long term after the waste has biodegraded and/or stabilized, no significant potential for continuing leachate and/or gas generation. Thus, the barrier component of the final cover system should be as durable as the liner component of the liner system. Current regulations call for a 30-year post-closure care period, and many design engineers assume that this time frame represents the required design life for the final cover system barrier. The authors of this report recommend that the barrier in the final cover system generally be designed for a longer design life, for example, a 100-year design life. The authors also offer the following observations:

- The choice of GM resin in a final cover system is influenced by a number of factors. For MSW landfills where settlement potential is significant, high out-of-plane deformation capability is a desirable characteristic. This design criterion favors VFPE, fPP and PVC GMs. Long-term durability considerations favor HDPE (recall Sections 2.5 and 6.2.6), which does not perform well above the pressure rate of 7 kPa/min given in the out-of-place deformation test ASTM

D5617. At lower pressure rates, where stress relaxation can occur, the situation is different but the test is rarely conducted in a slow strain rate or creep mode.

- In the current state-of-practice, chemical compatibility is rarely considered for final cover system GMs since the upper surface of the GM is only exposed to water infiltrating the cover soil. However, the lower surface of the GM may be exposed to landfill gas, which invariably contains low concentrations of volatile components present in the leachate. Thus, chemical resistance is an issue that should be considered based on site-specific conditions.
- Both durability and chemical compatibility are issues with respect to the reinforcing fibers or yarns of reinforced GCLs placed on sideslopes. While the GCL test plots described in Chapter 3 go far to show the validity of such GCL reinforcement, GCLs have not been installed for a long enough time to demonstrate the adequacy of this reinforcement over a 30 or 100-year time frame.
- The design of internal drainage layers in final cover systems is too often inadequate, i.e., the flow capacity is too low and outlets and transitions do not have adequate flow capacity. The potential for fines migration through the drainage layer filter is not always considered. The potential for freezing or other blockage of the drainage layer outlets is sometimes not assessed.
- The design of final cover systems in seismic impact zones requires careful consideration. The potential for amplification of free-field ground motions by the waste mass combined with low shear strength geosynthetic interfaces makes seismic performance an important consideration. EPA guidance (Richardson et al. 1995) and Anderson and Kavazanjian (1995) provide procedures for evaluating the potential for seismically-induced final cover systems deformations. Considerations applicable to seismically-induced deformations of liner systems (discussed in Section 6.2.3) are also applicable to final cover systems. An additional consideration for final cover systems is that in high seismic zones (e.g., near major active faults in California), it may not be feasible to design sloping final cover systems containing geosynthetics to sustain non-damaging deformations during major earthquakes. As discussed by Kavazanjian (1998), in these circumstances, it may be appropriate to design the final cover system to an acceptable damage criterion. Acceptable damage levels would be based on preventing adverse environmental impact, cost of repair, ease of repair, and any other impacts associated with the damage (e.g., loss of serviceability). This approach would necessitate development of a detailed post-earthquake response action plan coupled with financial assurances to provide the required funds to make the repairs at the time when they are needed.
- The fact that the waste mass is subsiding over time means that sideslope angles are progressively decreasing. The amount is waste-dependent, but the mechanism is one that tends to progressively increase final cover system slope stability factors of safety.

6.5 Gas Management

The degradation of any putrescible organic fraction of the solid waste in a landfill produces a number of gases. The condition is mostly applicable to MSW, but other types of waste may also produce some type of gas by biological or chemical means. The anaerobic decomposition of MSW produces two principal gases, methane and carbon dioxide, in roughly equal quantities (i.e., 40 to 50% each of total gas volume) and much smaller quantities of other gases. The gases produced in a MSW landfill is generated over a relatively long period of time, especially for landfills at arid sites. Using the EPA LandGEM computer program with Clean Air Act (CAA) default parameters for gas generation at a temperate site and considering an increment of waste placed in one year, 10% of the gas from this waste is produced within two years of waste placement, 40% is produced within 10 years of waste placement, and 80% is produced within 30 years. For an arid site, 20% of the gas from the waste is produced within 10 years of waste placement, 45% is produced within 30 years, and 80% is produced within 80 years. The gases move within and from the landfill primarily by convection, but also by diffusion. Gas emissions from MSW landfills are currently governed by the RCRA Subtitle D regulations, which address the personal and fire/explosion aspects of landfill gas, and the CAA regulations, which regulate emissions of non-methane organic compounds as a surrogate to total landfill gas emissions. Under the CAA, MSW landfills greater than a certain size must collect and combust their landfill gas.

Some design engineers collect and vent or extract MSW landfill gases with vertical, perforated collection wells (typically 5 wells per 2 hectares) without a continuous gas transmission layer beneath the barrier system. This approach can be justified if the waste itself is sufficiently permeable to gas, if the gas wells are relatively closely spaced, or, perhaps, at arid sites, where gas is generated relatively slowly. With gas wells, the gas moves within the waste to the perforations in the pipe and then flows or is drawn out of the system. Another approach to venting or extracting gas from a landfill involves installing a continuous gas transmission layer beneath the final cover system barrier layer. Shallow gas venting or extraction pipes will tie into the gas transmission layer. Gas collection trenches with periodic vent or extraction pipes represents a third approach to gas collection beneath the final cover system. Also, a combination of these three gas venting/extraction systems can be used.

In any case (deep wells penetrating the waste, a continuous gas transmission layer beneath the final cover barrier layer, and/or collection trenches), the system outlets are typically plastic pipes extending up through the final cover system. Gas flow through the pipes can be either passive (vented to the atmosphere or flared) or active (collected through a header using a blower system to create a small vacuum). Without a gas management system, gas pressure will build up in the landfill. Note that with a GM in the final cover system and relatively small cover soil thicknesses, gas pressures can

cause GM uplift. Even if the GM is not physically lifted, positive gas pressure beneath the GM can lower the effective stress at the interface between the GM and underlying material (e.g., GCL), thereby reducing interface shear strength and potentially contributing to a slope failure.

6.5.1 Construction Quality Assurance

As with all aspects of a waste containment system, CQA plays an important role in achieving acceptable performance of a gas management system. For deep wells, the number, location and extent of the pipe perforations are important. Also, the wells must be kept safely above the liner system beneath the waste. Several examples exist where gas well borings have extended into the liner system because of inadequate survey control and not accounting for landfill settlement. For continuous gas transmission layers beneath the barrier, continuity is important for either soil or geosynthetic gas transmission layers. If the latter, the material is often a GN with GTs bonded to both sides. The overlapping of the GN along its edges and ends is important as well as its joining with plastic ties per the specifications. Both upper and lower GTs need to be continuous with generous overlaps (often 300 mm) or sewn together to prevent soil from entering and clogging the GN.

Lastly, the penetration of gas wells or vents through a GM barrier should have tightly fitting prefabricated boots. Unlike boots for liner penetrations at the bottom of the landfill, boots for the final cover system GM must be designed to function while accommodating the anticipated landfill settlement. GCL tie-ins have similar considerations.

6.5.2 Gas Uplift

As indicated above, when using a GM in an MSW landfill final cover system, gas uplift pressures will be exerted on the GM unless the gas is efficiently conveyed to the wells, vents, or collection trenches. If gas is not adequately managed, uplift pressure will either cause GM bubbles (or "wales") to occur displacing the cover soil and appearing at the surface, or it will decrease the normal stress between the GM and the underlying material. At several facilities, this latter effect has led to slippage of the GM and overlying cover materials creating high tensile stresses as evidenced by compression ridges in the cover soil and folding of the GM at the slope toe and tension cracks in the cover soil near the slope crest. Three situations need careful design consideration:

- if gas removal is by deep wells, the uppermost pipe perforations should be effective in capturing gas in the upper layers of waste;
- if gas removal is by a gas transmission layer beneath the GM and vents, the gas transmission layer should be designed with adequate long-term transmissivity; and

- if gas is removed by horizontal collection trenches, some of the trenches should be placed in close proximity to the bottom of the final cover system to prevent gas accumulation and uplift pressure on the cover system GM.

6.5.3 Landfill Settlement

The design of final cover system drainage systems and gas collection systems (including the gas wells, vents, and/or collection trenches, and the network of piping for gas and condensate transmission systems) is complicated by the magnitude of waste settlement that typically occurs at solid waste landfills. Post-closure total settlement may equal 10 to 20% of the landfill height for MSW landfills and up to 20 to 30% of the waste height for some abandoned dumps. The design, construction, and maintenance of both the final cover system and gas management system must take these settlements into account. Figure 6-1 illustrates the magnitude of post-closure settlements that can occur at MSW landfills. The settlement magnitudes given in this figure should be considered to represent the upper range of values potentially applicable to modern landfills because the database used to develop the figures includes data for not only MSW landfills, but also abandoned dumps. Of equal concern (but largely unquantified) is the differential settlement that may occur in isolated areas of the landfill.

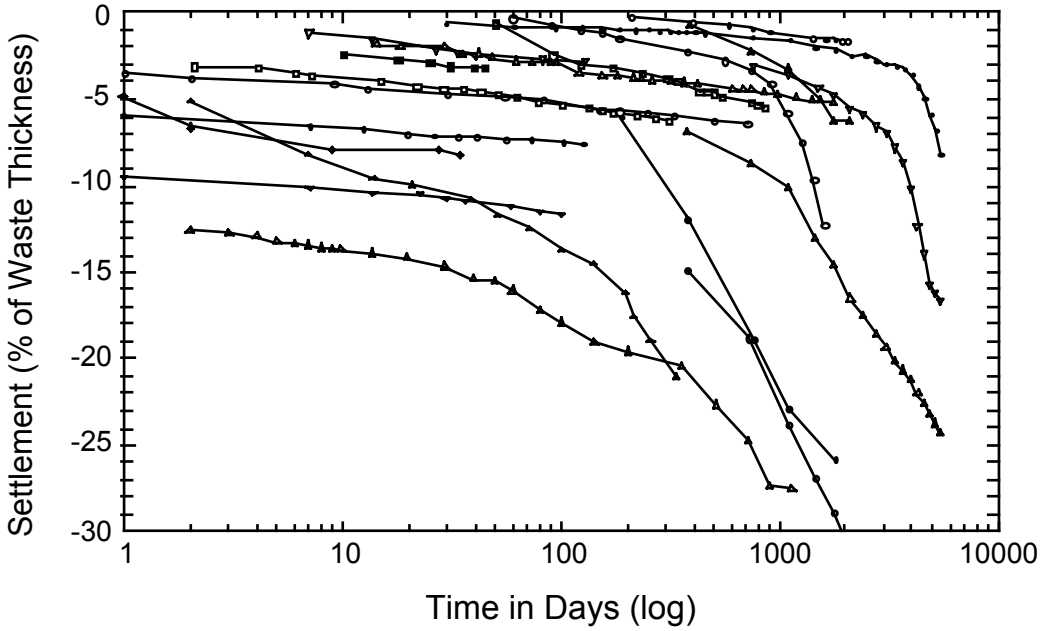

Figure 6-1. Total post closure settlement data for MSW landfills and abandoned dumps [after Edgers et al. (1990); König et al. (1996); Spikula (1996)].

The time frames over which both total and differential settlement may occur are quite long and depend on the many factors including the liquids management strategy practiced at the site. Table 6-1 presents a framework for evaluating likely post-closure total and differential settlements at MSW landfills and abandoned dumps.

Table 6-1. Impact of Liquids Management Practice on Final Cover System Settlement at MSW Landfills and Abandoned Dumps[1,2] (Koerner and Daniel, 1997).

Leachate	Total Settlement		Differential Settlement[3,4]	
Management Practice	Amount	Time	Amount	Time
Standard leachate withdrawal	10-20%	≤ 30 yrs.	Little to moderate	≤ 20 yrs.
Leachate recirculation	10-20%	≤ 15 yrs.	Moderate to major	≤ 10 yrs.
None, e.g., at abandoned landfills or dumps	Up to 30%	> 30 yrs.	Unknown	> 20 yrs.

[1]HW landfills, ISW landfills, and MSW ash monofills usually have much less settlement than the amounts listed in this table.

[2]The estimates in this table regarding the impact of the liquids management practice on settlement of landfill final cover systems are based on sparse data. They are meant to be a guide only, and site-specific estimates are required to develop more appropriate figures for any particular final cover system project.

[3]The estimates in this table regarding differential settlement amount and time are also based on very sparse data. Clearly, field monitored data is needed in this regard.

[4]These qualitative assessment terms are also affected by the density of the waste; well-compacted waste produces less differential settlement than poorly-compacted waste.

6.5.4 Landfill Fires

While the incidence of landfill fires in MSW landfills has greatly diminished since the days of the "open dump", they still sometimes occur. Air-to-methane mixture ratios of 20 to 50% have given rise to at least one fire, which damaged a geosynthetic final cover system. The vulnerable time frame of a facility with respect to landfill fires appears to be after the GM is seamed and before cover soil is placed. Wind uplift of the GM can draw air in through vents providing the oxygen necessary to create ignitable conditions.

Fires at depth within a waste mass may occasionally occur. The origin of such fires is apparently spontaneous combustion and an air source is required for sustenance. The key to preventing such a fire is to block air entry. Identifying and blocking all potential sources of air entry can sometimes be difficult.

6.5.5 Fate of Gas Management Systems

For large regionalized landfills where energy is utilized there is an incentive to maintain the gas management system in good working order. When the energy conversion becomes inefficient, however, the wells or vents may be decoupled from their external piping systems and be allowed to vent to the atmosphere. It is important, at that time, to show the amount of gas being vented is below regulatory limits and does not present a health or an environmental hazard. It is also important to show that gas emissions through the final cover system in the vicinity of the decoupled well or vent are below regulatory limits.

6.6 Long-Term Landfill Management

The performance data for operating landfills presented in this report demonstrate that landfills can be designed, constructed, and operated/maintained to achieve very high levels of leachate and landfill gas containment and collection. The report has also demonstrated that design, construction, and operation/maintenance issues and problems persist at many landfills. In the preceding part of this chapter, the authors have attempted to provide guidance to design engineers on how to avoid the most significant issues and problems that may typically arise. Information on the anticipated service lives of the various engineered components of a landfill waste containment system was also given.

The ultimate degradation of any individual waste containment system component of a landfill after the completion of that component's useful service life may or may not lead to a release of leachate or gas and contamination of groundwater. Furthermore, a release may, or may not, result in a significant environmental impact. In evaluating the consequences of ultimate degradation, the design engineer must consider a wide range of factors including: the climatological and hydrogeologic setting; the composition, age, and level of degradation of the waste; the potential for leachate and gas generation after the component has completed its service life; the potential to maintain, rehabilitate, or install other systems to achieve leachate and gas containment; and collection, cost, and social and institutional factors. These various factors should be considered within an overall decision-making framework that addresses long-term landfill management. Long-term landfill management strategies are discussed in Appendix G.

6.7 References

Anderson, D.G. and Kavazanjian, E., Jr. (1995), "Performance of Landfills Under Seismic Loading," *Proceedings of the 3rd International Conference on Recent Advances in Geotechnical Earthquake Engineering and Soil Dynamics,* St. Louis, Missouri, pp. 1557-1587.

Ajaz, A. and Parry, R. H. G. (1975a), "Stress-Strain Behavior of Two Compacted Clays in Tension and Compression," *Geotechnique*, Vol. 25, No. 3, pp. 495-512.

Ajaz, A. and Parry, R. H. G. (1975b), "Analysis of Bending Stresses in Soil Beams, " *Geotechnique*, Vol. 25, No. 3, pp. 586-591.

Ajaz, A. and Parry, R. H. G. (1976). "Bending Test for Compacted Clays," *Journal of the Geotechnical Engineering Division*, Vol. 102, No. 9, pp. 929-943.

Bonaparte, R. and Gross, B.A. (1990), "Field Behavior of Double-Liner Systems," *Proceedings of the Symposium on Waste Containment Systems*, ASCE Geotechnical Special Publication No. 26, pp. 52-83.

Bonaparte, R., Gross, B. A., Daniel, D. E., Koerner, R. M., and Dwyer, S. F. (2002), "*Technical Guidance for RCRA/CERCLA Final Covers*," U.S. EPA Office of Solid Waste and Emergency Response, Washington, D.C. (in final review)

Bonaparte, R. and Othman, M. A. (1995), "Characteristics of Modern MSW Landfill Performance," *Geotechnical News,* Vol. 13, No. 1, pp. 25-30.

Breitenbach, A. J. and Swan, R. H. (1999), "Influence of High Load Deformations on Geomembrane Liner Interface Strengths," *Geosynthetics '99 Conference Proceedings*, Industrial Fabrics Association International, St. Paul, MN, Vol. 1, pp. 517-529

Brown, K. W., Thomas, J. C., Lytton, R. L., Jayawickarama, P. and Bahrt, S. C. (1987), "*Quantification of Leak Rates Through Holes in Landfill Liners*," report for cooperative agreement CR-810940, EPA Risk Reduction Engineering Research Laboratory, Cincinnati, 147 p.

Byrne, J. (1994), "Design Issues with Strain-Softening Interfaces in Landfill Liners," *Proceedings, Waste Tech '94,* National Solid Waste Management Association, Charleston, 26 p.

Byrne, R. J., Kendall, J. and Brown, S, (1992), "Cause and Mechanism of Failure, Kettleman Hills Landfill B-19, Unit 1A," *Stability and Performance of Slopes and Embankments-II*, ASCE Geotechnical Special Publication No. 31, R. B. Seed and R. W. Boulanger, eds., pp. 1188-1215.

Dove, J. E., Frost, D. J., Bachus, R. C. and Han, J. (1997), "The Influence of Geomembrane Surface Roughness on Interface Strength," *Proceedings, Geosynthetics '97 Conference,* Long Beach, CA, Mar., Vol. 2, pp. 863-876.

Edgers, L., Noble, J. J. and Williams, E. (1990), "*A Biologic Model for Long Term Settlement in Landfills*, " Tufts University, Medford, MA.

Eid, H. T. and Stark, T. D. (1997), "Shear Behavior of an Unreinforced Geosynthetic Clay Liner," *Geosynthetics International*, Vol. 4, No. 6, pp. 645-659.

EPA (1987), Proposed Rulemaking, 40 CFR Parts 260, 264, 265, 270 and 271, "Liners and Leak Detection for Hazardous Waste Land Disposal Units," *Federal Register*, Vol. 52, No. 103, pp. 20218-20311.

Gilbert, R. B., Scranton, H. D. and Daniel, D. E. (1997), "Shear Strength Testing for Geosynthetic Clay Liners," *Testing and Acceptance Criteria for Geosynthetic Clay Liners,* ASTM STP 1308, Larry W. Well, Ed., American Society for Testing and Materials.

Giroud, J. P., Bachus, R. C. and Bonaparte, R. (1995), "Influence of Water Flow on the Stability of Geosynthetic-Soil Layered Systems on Slopes," *Geosynthetics International,* Vol. 2, No. 6, pp. 1149-1180.

Giroud, J. P., Badu-Tweneboah, K. and Soderman, K. L. (1997), "Comparison of Leachate Flow Through Compacted Clay and Geosynthetic Clay Liners in Landfill Liner Systems," *Geosynthetics International,* Vol. 4, Nos. 3 and 4, September, pp. 391-431.

Giroud, J. P. and Beech, J. F. (1989), "Stability of Soil Layers on Geosynthetic Lining Systems," *Proceedings, Geosynthetics '89 Conference,* Vol. 1, San Diego, pp. 35-46.

Giroud, J. P. and Bonaparte, R. (1989a), "Leakage Through Liners Constructed with Geomembranes, Part I: Geomembrane Liners," *Geotextiles and Geomembranes,* Vol. 8, No. 1, pp. 26-67.

Giroud, J. P. and Bonaparte, R. (1989b), "Leakage Through Liners Constructed with Geomembranes, Part II: Composite Liners," *Geotextiles and Geomembranes,* Vol. 8, No. 2, pp. 77-111.

Hsuan, Y. G. and Koerner, R. M. (1998), "Antioxidant Depletion Lifetime in High Density Polyethylene Geomembranes," *Journal of Geotechnical and Geoenvironmental Engineering,* ASCE, Vol. 124, No. 6, pp. 532-541.

Kavazanjian, E., Jr. (1998), "Current Issues in Seismic Design of Geosynthetic Cover Systems," *Proceedings of the 6th International Conference on Geosynthetics,* Atlanta, pp. 219-226.

Kavazanjian, E., Jr., Matasovic, N., Bonaparte, R. and Schmertmann, G. R. (1995), "Evaluation of MSW Properties for Seismic Analyses," *Proceedings of the ASCE Specialty Conference Geoenvironment 2000,* ASCE Geotechnical Special Publication No. 46, Y.B. Acar and D.E. Daniel, eds., Vol. 2, pp. 1126-1141.

Koerner, G. R., Koerner, R. M. and Martin, J. P. (1994), "Geotextile Filters Used for Leachate Collection Systems: Testing, Design of Field Behavior", *Journal of Geotechnical Engineering,* ASCE, Vol. 120, No. 10, pp. 1792-1803.

Koerner, R. M. and Daniel, D. E. (1997), "*Final Covers for Solid Waste Landfill and Abandoned Dumps*," ASCE Press, 256 pgs.

Koerner, R. M. and Hwu, B. L. (1991), "Stability and Tension Considerations Regarding Cover Soils in Geomembrane Lined Slopes," *Geotextiles and Geomembranes,* Vol. 10, No. 4, pp. 335-355.

Koerner, R. M. and Soong, T. Y. (1998), "Analysis and Design of Veneer Cover Soils," *Proceedings, Sixth International Conference on Geosynthetics*," Industrial Fabrics Association International, St. Paul, MN, Vol. 1, pp. 1-26.

König, D., Kockel, R. and Jessberger, H. L. (1996), "Zur Beurteilung der Standsicherhert und zur Prognose der Setzungen von Mischabfalldeponien," *Proceedings 12th Nürnberg Deponieseminar,* Vol. 75, Eigenverlag LGA, Nürnberg, Germany, pp. 95-117.

Leonards, G. A. and Narain, J. (1963), "Flexibility of Clay and Cracking of Earth Dams," *Journal of the Soil Mechanics and Foundations Division*, Vol. 89, No. 2, pp. 47-98.

Matasovic, N., Kavazanjian, E., Jr., Augello, A. J., Bray, J. D. and Seed, R. B. (1995), "Solid Waste Landfill Drainage Caused by 17 January 1994 Northridge Earthquake," *The Northridge, California Earthquake of 17 January 1994,* California Department of Conservation, Division of Mines and Geology Special Publication No. 116, M.C. Woods and R.W. Sieple, eds., pp. 221-229.

Matasovic, N. and Kavazanjian, E., Jr. (1996), "Observations of the Performance of Solid Waste Landfills During Earthquakes," *Proceedings of the 11th World Conference on Earthquake Engineering,* Elsevier Science Ltd. Paper No. 341, 8 p. (on CD ROM).

Othman, M. A., Benson, C. H., Chamberlain, E. J., and Zimmie, T. F. (1994), "Laboratory Testing to Evaluate Changes in Hydraulic Conductivity of Compacted Clays Caused by Freeze-Thaw: State-of-the-Art," *Hydraulic Conductivity and Waste Containment Transport in Soils*, STP 1142, D.E. Daniel and S.J. Trautwein (eds.), American Society for Testing and Materials, Philadelphia, PA, pp. 227-254.

Reynolds, R. T. (1991), "Geotechnical Field Techniques Used in Monitoring Slope Stability at a Landfill," *Proceedings Field Measurements in Geotechnics,* ed. G. Sorum, Rotterdam: A. A. Balkema, pp. 883-891.

Richardson, G. N., Kavazanjian, E., Jr. and Matasovic, N. (1995), "RCRA Subtitle D (258) Seismic Design Guidance for Municipal Solid Waste Landfill Facilities," U.S. Environmental Protection Agency Report No. 600/R-95/051, 143 p.

Rowe, R. K. (1998), "Geosynthetics and the Minimization of Contaminant Migration through Barrier Systems Beneath Solid Waste," *Proceedings, 6th International Conference on Geosynthetics,* Atlanta, pp. 27-102.

Sabatini, P. J., Schmertmann, G. R. and Swan, R. H. (1998), "Issues in Clay/Geomembrane Interface Testing," *Proceedings of the 6th International Conference on Geosynthetics,* Atlanta, pp. 423-426.

Sabatini, P. J., Griffin, L. M., Bonaparte, R., Espinoza, R. D., Giroud, J. P. (2001), "Reliability of State-of-Practice for Selection of Shear Strength Parameters for Waste Containment System Stability Analysis, " *Proceedings, GRI-15 Conference on Hot Topics in Geosynthetics – II (Peak/Residual; RECMs; Installation Concerns)*, Geosynthetic Research Institute, pp 86-109.

Seed, R. B. and Bonaparte, R. (1992), "Seismic Analysis and Design of Lined Waste Fills: Current Practice," *Stability and Performance of Slopes and Embankments - II*, ASCE Geotechnical Special Publication No. 31, pp. 1521-1545.

Sharma, H. D., Hullings, D. E., and Greguras, F. D. (1997), "Interface Strength Tests and Application to Landfill Design, " *Geosynthetics '97 Conference Proceedings*, Industrial Fabrics Association International, St. Paul, MN, Vol. 2, pp. 913-926.

Spikula, D. (1996), "Subsidence Performance of Landfills: A 7-Year Review," *Proceedings GRI-10 Conference on Field Performance of Geosynthetics and Geosynthetic Related Systems,* Geosynthetic Research Institute, Philadelphia, pp. 237-244.

Stark, T. D. and Poeppel, A. R. (1994), "Landfill Liner Interface Strengths from Torsional-Ring Shear Tests," *Journal of Geotechnical Engineering*, Vol. 120, No. 3, pp. 597-615.

Appendix A
Behavior of Waves in High Density Polyethylene Geomembranes

by

Robert M. Koerner, Ph.D., P.E.
Drexel University
Philadelphia, PA 19104

performed under

EPA Cooperative Agreement Number
CR-821448-01-0

Project Officer

Mr. David A. Carson
United States Environmental Protection Agency
Office of Research and Development
National Risk Management Research Laboratory
Cincinnati, OH 45268

Appendix A
Behavior of Waves in
High Density Polyethylene Geomembranes

A-1 Overview and Focus

Geomembranes (GMs) form the essential material component in many liner systems which require a liquid or vapor barrier. Such applications are landfill liners, landfill covers, liquid impoundment liners, and other waste pile liners. The usual assumption in the placement of such liners is that they lay flat on the subgrade beneath them, e.g., on the underlying compacted clay liner, geosynthetic clay liner, etc. This is sometimes not the case. Waves, or wrinkles, of different sizes can occur in the as-placed and seamed GMs, see Figures A-1 and A-2. These waves have given design engineers a certain amount of concern as to the behavior of GMs after soil backfilling or covering. The research study described in this appendix was developed to shed insight into the issue of GM wrinkles.

Figure A-1. Relatively small waves, or wrinkles, in a field deployed GM.

Figure A-2. Relatively large waves, or wrinkles, in a field deployed GM.

The approach to this study of the behavior of GM waves involved an extensive series of laboratory tasks. It is important to note that the purpose of the tests was to evaluate the behavior of GM waves under field stresses. The tests were not designed to try to quantify the effects of waves on hydraulic containment performance. The scope of the laboratory testing program involved an assessment of the effects of the following four variables on wave behavior:

(a) normal stress;
(b) original wave height;
(c) thickness of GM; and
(d) temperature.

Due to its common use in a variety of waste containment systems, high density polyethylene (HDPE) GMs were used throughout the study. In particular, one manufacturer's commercially available GM was used. The only GM variable considered was thickness. In all other cases, the thickness was maintained at 1.5 mm, which is a commonly used HDPE GM thickness in many applications.

GM waves, such as seen in Figures A-1 and A-2, can be classified as two different types: thermally-induced GM waves and construction induced GM waves.

Thermally-induced waves in GMs are created due to the thermal expansion characteristics of GMs after they are seamed together and before backfilling occurs. These types of waves have been observed in GMs for many years (Schultz and Miklas, 1980). The height and/or width of the wave depends on the GM type (e.g., modulus, thickness, surface texture, surface color), temperature difference after seaming and before backfilling, and distance between points of fixity, e.g., previously backfilled locations.

As an illustration of a thermally induced wave, a 30 m long section of 1.5 mm thick HDPE GM (with a thermal expansion coefficient of 15×10^{-5}/°C) undergoing a temperature change from 15°C installation temperature to 50°C (sheet surface) under a summer sun, will expand the following amount:

$$\Delta L = \Delta T\ (\alpha)\ L = (50 - 15)\ (15 \times 10^{-5})\ (30) = 0.158\ m = 158\ mm$$

Obviously, such thermally induced GM waves can be created in the field via the local ambient conditions.

Alternatively, construction induced GM waves are sometimes created purposely. In North America, an adequate amount of slack is sometimes left in the GM liner to compensate for the coldest temperatures envisioned (EPA, 1993). The philosophy is that the majority of the slack will be removed when the GM is covered and the sheet temperature is reduced. Ultimately, when the envisioned coldest temperature is reached, the rest of the built-in slack will be completely removed, therefore, intimate contact to the underlying soil will be achieved.

In order to estimate the wave dimensions that can be created by a given amount of slack in GMs, Figure A-3 was developed. In the figure, the slack in the GM which results in the creation of waves with various height-to-width ratios is plotted as a function of wave height.

As seen in Figure A-3, a slack of 158 mm, as calculated in the earlier example, can create the following different wave patterns:

- a 120 mm high wave with height-to-width ratio of 1.0;
- a 165 mm high wave with height-to-width ratio of 0.5;
- a 215 mm high wave with height-to-width ratio of 0.33; or
- a 265 mm high wave with height-to-width ratio of 0.2

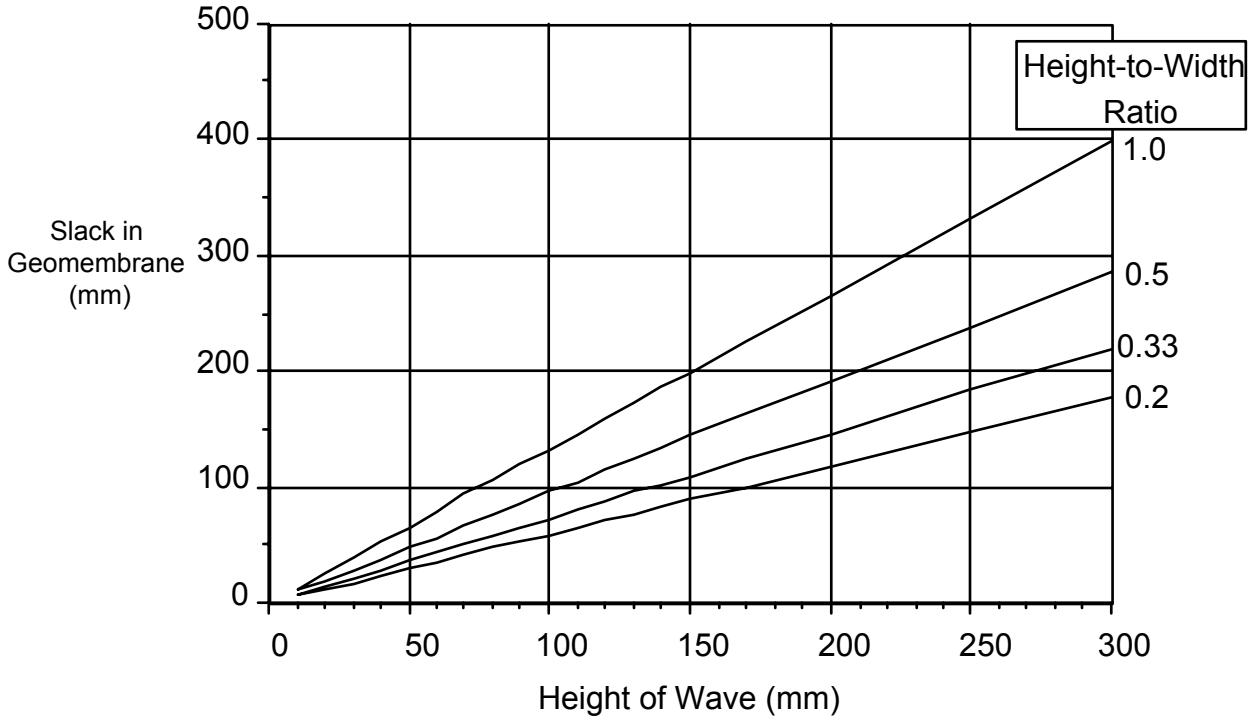

Figure A-3. Slack in GM resulting in the creation of waves with various height-to-width ratios.

Alternatively, if the GM is relatively flexible or thinner than in the previous example, two or even more smaller waves can be created within the same slack in the GM. Table A-1 summarizes the types of multiple waves that can be produced by a 158 mm expansion of a GM. In an actual facility, an expansion of this magnitude can certainly create waves of the type seen in the photographs of Figures A-1 and A-2. While this example is based on the coefficient of thermal expansion/contraction of 1.5 mm thick HDPE GMs, it should be noted that all types of GMs currently used in the waste containment industry have similar values of coefficient of thermal expansion/contraction (Koerner, 1998).

Table A-1. Types of Waves Produced by a Slack of 158 mm in a GM in a Distance of 30 m with a Temperature Difference of 35°C

Height-to-Width Ratio (H/W)	Single Wave Height (mm)	Two Waves Height (mm)	Three Waves Height (mm)
1.00	120	60	40
0.50	165	80	55
0.33	215	105	70
0.20	265	130	90

However, such an ideal situation of a perfectly flat GM is very difficult to achieve. The reasons are as follows:

- it is very difficult to quantify the actual difference between the two extreme temperatures, i.e., the installation temperature and the coldest temperature envisioned;
- the focus of concern is the sheet temperature, not the ambient temperature;
- the sheet temperature is a complicated function of ambient temperature, surface color and texture, incidence of sun, weather, etc.;
- accurate measurement of the coefficient of thermal expansion is difficult;
- frictional forces mobilized between the interfaces can retard, or even constrain, the reduction of slack; and
- it is extremely difficult to build into an installed and seamed GM, a prescribed amount of slack.

As a result, relatively large waves of the type seen in Figure A-2 are commonly seen in the field.

It has been observed both in the field and in the laboratory that the installed wave greatly distorts from its original shape under increasing normal stress. However, the deformation pattern depends on the GM type (e.g., thickness, modulus, flexural rigidity, etc.), the original wave shape (e.g., height, height-to-width ratio, etc.), and the surrounding environment (e.g., stress level, duration, temperature, etc.).

Figure A-4 illustrates some possible deformation scenarios. Figure A-4a shows how the wave distorts under relatively low normal stress. Figure A-4b shows that the profile of the wave remains almost unchanged when higher normal stress is applied. This could possibly be the case for waves in relatively thick and/or stiff GMs. When normal stress is applied nonuniformly (e.g., with a horizontal component), the waves may roll over towards one side as seen in Figure A-4c. When normal stress is applied to waves in relatively thinner or more flexible GMs, they may become vertically flattened as seen in Figure A-4d. For extremely flexible GMs, they may even be flattened in a pancake manner as seen in Figure A-4e. Note that conditions as shown in Figure A-4d and e are also possible when the service temperature is relatively high.

The concern as to the ultimate fate of GM waves should certainly receive attention as to a rigorous understanding of the problem. However, to date, all analyses and investigations into GM waves have been semi-qualitative, see Giroud and Morel (1992) and Giroud (1995). Quantitative approaches which evaluate the ultimate fate of GM waves in a more rigorous manner are needed. For instance, there could be a maximum wave height, for a given set of conditions, where the GM wave will eventually

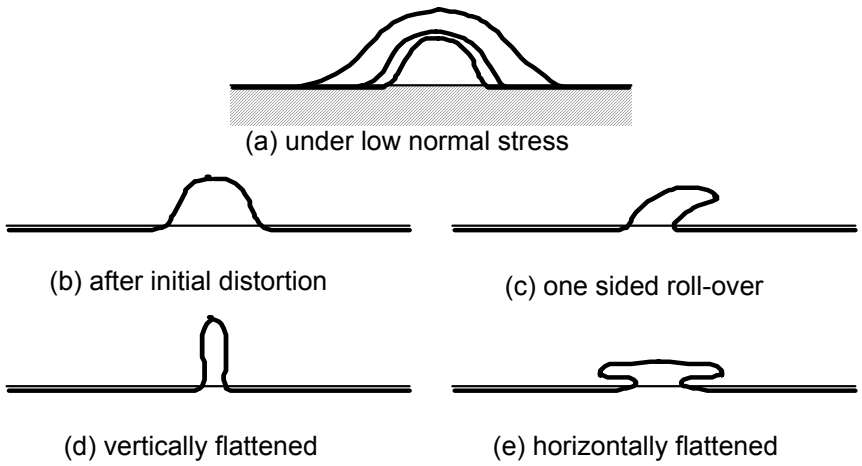

Figure A-4. Possible deformation scenarios in GM waves.

lay flat on the soil. Given a maximum wave height, which could be specified in the installation contract, the optimal fate of GM waves might be as follows:

1. The installer seams the GM with waves up to a maximum specified amount.
2. Typically a geotextile (GT) will cover the GM and the temperature of the GM will decrease. Thus, the wave(s) will decrease in size (Koerner and Koerner, 1995).
3. Upon backfilling over the GT covered GM, the waves are fixed in position and contained by friction from further size reduction stemming from future decreasing temperature.
4. Under increasing normal stress, due to soil, solid waste or liquids, the wave distorts from its original shape. As seen in Figure A-5, from results of this study, the wave becomes narrower in width at its base and only marginally shorter in its height. Thus, the wave's height-to-width ratio is actually accentuated from its initial condition (from approximately 0.33 to 0.44 for this particular GM).
5. Over time, creep and/or stress relaxation in the polymer structure occurs and the wave height decreases in size thus reducing the H/W ratio.
6. Ultimately, it is hoped that the wave flattens to a H/W ratio of zero, so as to achieve contact with the underlying soil subgrade.

From the above description it is suggested that creep and stress relaxation play a key (and essentially unknown) role in the ultimate elimination of GM waves. Furthermore, by knowing the characteristics of the "entombed" wave, one can possibly back-calculate to the originally allowable maximum wave height.

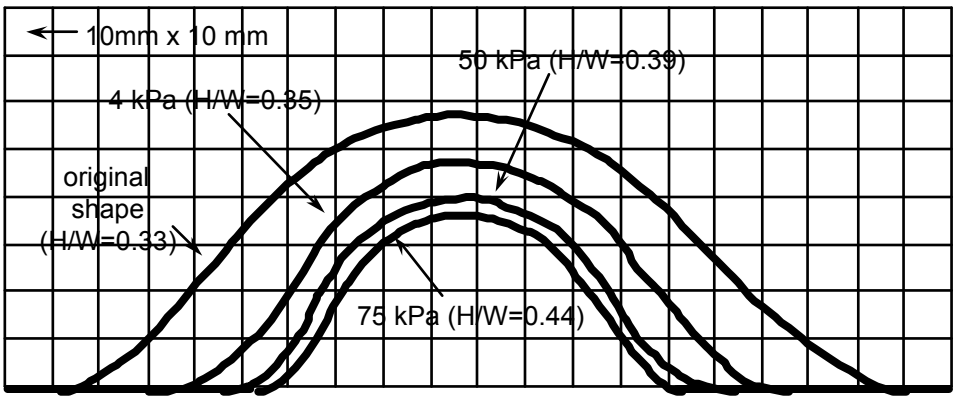

Figure A-5. Wave distortion under increasing normal stress from large-scale laboratory experiments conducted in this study.

These issues then frame the essence of this study. It is focused completely on GM waves which exist in the GM at the point of backfilling and are caused by elevated temperature above that which existed when the GM rolls were seamed. In this study, only GMs made from HDPE are evaluated. This is felt to be justified since HDPE represents approximately 70% of the landfill liner market in North America. In other countries, e.g., Germany, it is the only type of GM that is allowed.

A-2 Experimental Setup and Monitoring

A large-size experimental test box was constructed in the laboratory for the evaluation of the behavior of HDPE GM waves. Initially, the test box was utilized to conduct preliminary tests to gain a better understanding of the problem to be investigated. It was then used for the justification of performing smaller scale experiments. Finally, it was designated for conducting a 10,000-hour control test. Details regarding each of the these items will be presented after a description of the test box.

A photograph and schematic illustration of the test box is shown in Figure A-6. The basic components of the setup include a rigid box and a data acquisition system. The box has dimensions of 1.8 m long by 1.0 m wide by 1.0 m high. On the front panel, there is a 0.5 m-wide plexiglass window for the purpose of visual observations. An air bag which provides a uniform normal pressure up to 70 kPa is placed on top of the soil and the reaction is transmitted through a 25 mm thick wooden board to five steel reaction cross beams connected at the top of the box. Also, a number of electrical resistance strain gages are bonded on the test specimen at various locations with wires extended out of the box and connected to a data acquisition system.

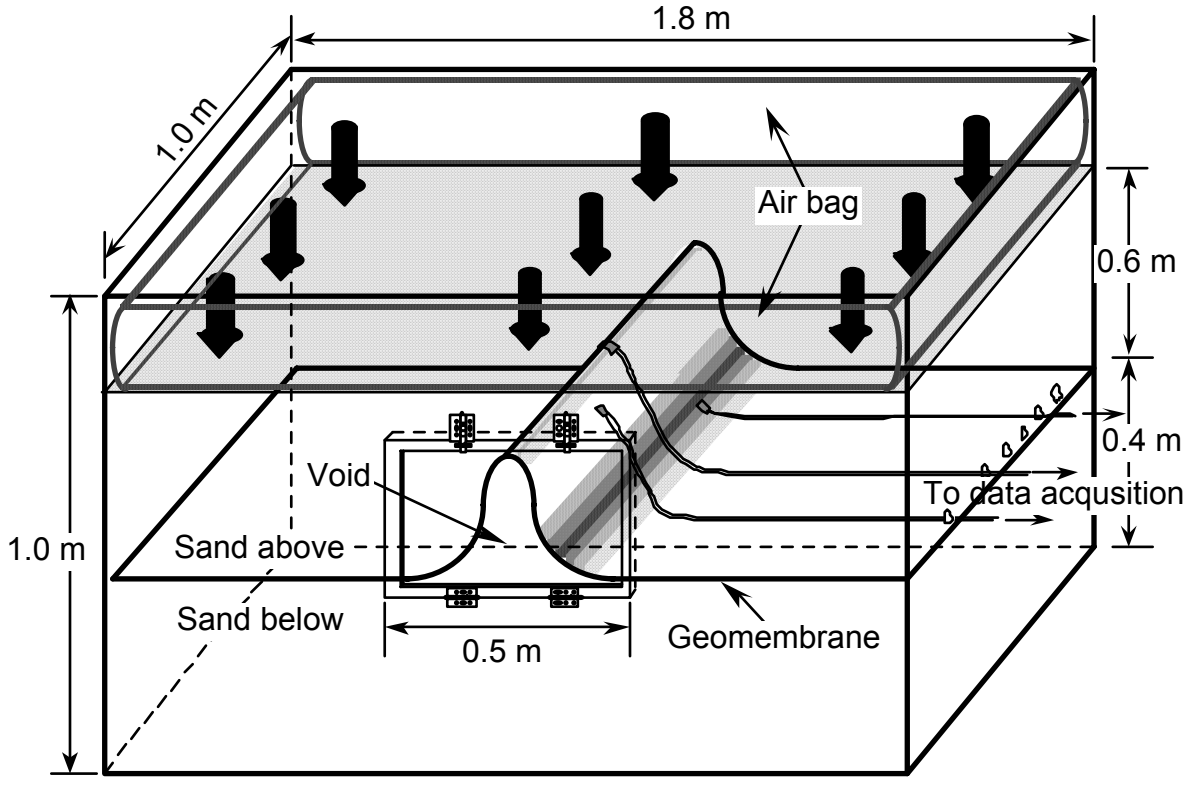

Figure A-6. Photograph and schematic illustration of the large-scale experimental test box used in this study.

The experimental monitoring of the behavior of HDPE GM waves includes two parts: profile-tracing of the actual wave and strain gage monitoring. The profile-tracing provides the opportunity of visual observation and recording the distortion of GM waves under various experimental conditions. Important information such as the final configuration, the final height-to-width ratio, and the locations of stress concentrations can be obtained using this type of monitoring. Tracing the profile of GM waves is done via the window on the front panel of the test box. An example of profile-tracing was shown in Figure A-5. This type of monitoring was also performed routinely on trial runs before the actual experiments began to determine the layout pattern of the other type of experimental monitoring, i.e., the strain gage monitoring.

Strain gage monitoring quantifies the actual strain induced at different locations of the GM wave under various experimental conditions. When used in conjunction with a data acquisition system, this type of monitoring provides reliable information on the experiment over the duration of the test. The strain gages used in this study are electrical resistance (foil-type) strain gages having resistance of 120-ohms and gage length of 12.7 mm. With proper configuration, this particular type of gage measures strain within the range of ±5%. The installation procedure recommended by the gage manufacturer was precisely followed. The surface cleaning and preparation was considered most critical in this regard. The photograph of an installed strain gage is shown in Figure A-7. Note that a bondable terminal along with two curved “jumper wires” are also used in the gage installation to prevent the gage from being subjected to any unexpected stresses.

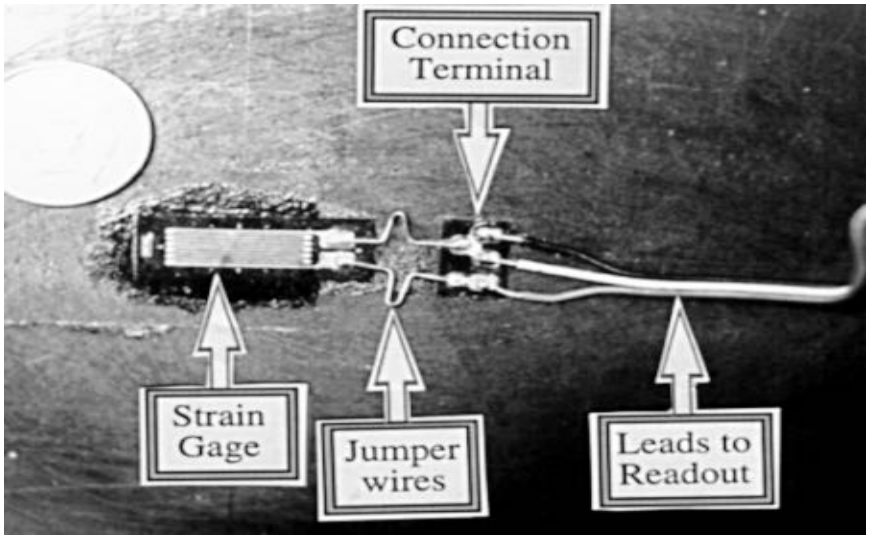

Figure A-7. Strain gage with soldered connection installed on GM specimen.

Sets of preliminary tests were conducted using the large-scale experimental setup. These tests were performed at an early stage of the task and were designed to gain further understanding of the GM wave, as well as to evaluate the possibility of transferring the large-scale tests to a small-scale experimental setup. The material used in these tests was a 1.5-mm thick smooth HDPE GM. Details of the preliminary tests are presented as follows.

The first series of preliminary tests consisted of three separate experiments. Namely, a 1.5-mm thick GM with relatively large, moderate, and relatively small waves. The waves were created by using specimens longer than the inner length of the test box. After each specimen was placed in the box, sand backfilling was started from the end to the center of the box in a symmetrical manner. Consequently, the “slack” of specimen was “pushed” toward the center and, as a result, a wave was formed. The “original” configuration of waves was defined as the wave profile under approximately 100 mm of sand backfill. Using profile-tracing as previously described, the shape of the original wave was recorded. The same type of monitoring was repeated at various stages of the backfilling and progressed until the maximum normal pressure provided by the experimental setup, i.e., 70 kPa, was reached.

The results of the profile-tracing monitoring of these tests are shown in Figure A-8. In the figure, the outermost curves of all tests represent the original wave configuration and the innermost curves correspond to the final wave profiles under 70 kPa. As seen in the figure, under increasing normal stress, the waves greatly distort from their original shapes. The waves become narrower in width at the base but only marginally shorter in height. A quantitative parameter was devised by calculating a ratio of the wave height to its base width, i.e., a H/W ratio. For purposes of gaining perspective with field installations, a somewhat accepted rule-of-thumb in the field deployment of GMs is that the height-to-width (H/W) ratio should not be greater than 0.5. This being the case, the “relatively large” and “moderate” waves in this study were already marginal from the outset. The accentuated H/W ratios upon backfilling, 2.0, 0.9 and 0.4 as seen in Figure A-8, were already considered as a valuable finding in the course of this study.

Even further, with respect to the empirical field guide, the drastic increase in the H/W ratio for the “relatively large” and “moderate” waves indicated locations of high curvature and therefore the possibility of high stress concentrations under even higher normal stresses. Such waves should clearly be removed before the placing of backfill. As a result, the rest of this task focused on waves with an original height smaller than the height of the relatively small wave shown in Figure A-8.

Also seen in Figure A-8 are the reference marks located at various portions of the waves. These marks are very helpful in tracking the critical locations of a wave under normal pressure with respect to the undeformed test specimen. Therefore, the information will be used to establish the layout pattern of strain gage installation.

(a) Relatively Large Wave

	Ht.	H/W
Original	240 mm	0.5
Final	125 mm	2.0

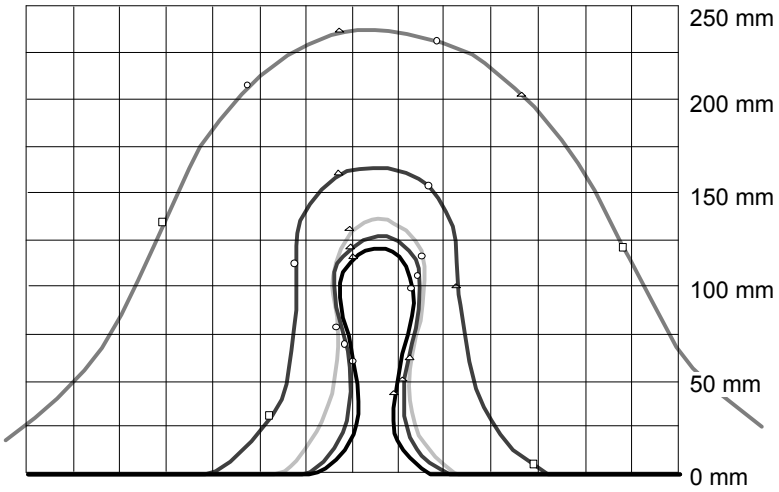

(b) Moderate Wave

	Ht.	H/W
Original	130 mm	0.4
Final	70 mm	0.9

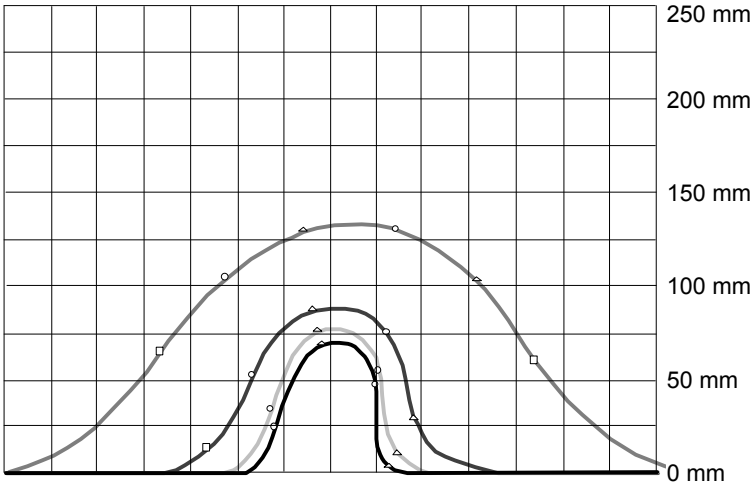

(c) Relatively Small Wave

	Ht.	H/W
Original	80 mm	0.25
Final	35 mm	0.4

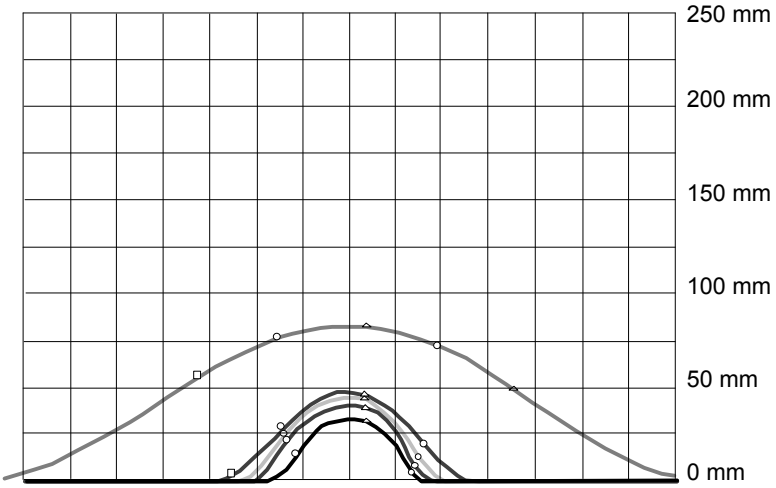

Figure A-8. Results of the profile-tracing monitoring of three preliminary tests.

As mentioned earlier, the pressurizing mechanism (i.e., the air bag and reaction beams) in the large-scale test box can only provide a uniform normal pressure up to 70 kPa. If the average unit weight of typical solid waste is assumed as 12 kN/m^3, such a normal pressure is approximately equivalent to solid waste of 6 m in height. This is relatively low for a typical landfill. In order to evaluate the behavior of GM waves under high normal pressures, e.g., greater than 1,000 kPa, transferring the experiments to smaller setups which allow the application of higher normal pressures is necessary. Moreover, smaller setups which can be housed in a environmental room will be especially beneficial since the effect of temperature on the behavior of GM waves can then be investigated. However, such smaller tests must be justified on the basis of this larger test setup.

A small-scale setup justification test was designed and conducted to examine the behavior of the wave itself. A wave, identical to the relatively small wave shown in Figure A-8, was created in the large-scale test box. However, instead of being supported by the side walls of the test box, both ends of the specimen were held by metal sticks 50 mm away from the walls of the box. In addition, both ends of the test specimen were covered by 75 mm-wide smooth HDPE GM strips acting as protective slip-sheets. The experimental setup is shown in Figure A-9.

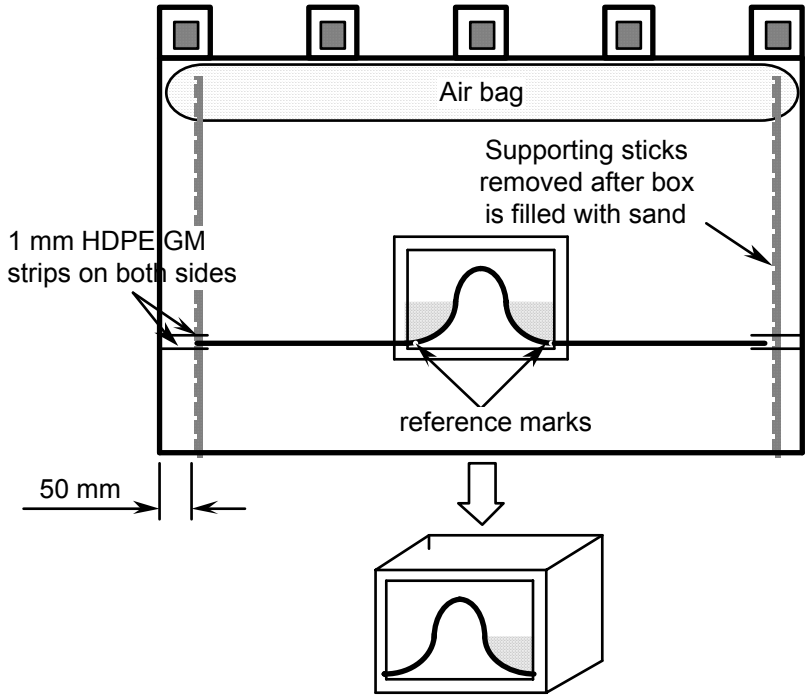

Figure A-9. Justification experiment for small-scale experimental setups.

Before the backfilling process was started, a 300 mm by 300 mm square region was marked on the window of the test box. It was used as a virtual image of a smaller test box in which the GM wave could be housed. Two reference marks, immediately adjacent to the square region, were made on the front edge of the wave, as seen in Figure A-9. With the supporting sticks on both ends of the test specimen, backfilling was carefully carried out until the test box was filled. The supporting sticks were then removed, leaving two horizontal spaces of 50 mm each on both ends of the specimen (protected by the slip sheets) for possible lateral movement.

The GM wave was then pressurized using the air bag against the reaction beams. It was observed that under a normal pressure of 70 kPa, the wave distorted in a manner exactly like the relatively small wave shown in Figure A-8. Moreover, the two reference marks remained completely stationary, i.e., there was no lateral movement of the GM. This observation suggests that the frictional forces, mobilized between the GM specimen and the adjacent sand fill, were sufficient to restrict the horizontal portions of the GM from any lateral movement and decrease in wave height.

In other words, the mobilized friction forces on the horizontal extensions of the wave offered the same reaction as would a smaller test box simulated by the 300 mm by 300 mm square region. This important finding not only provided the justification of using a smaller scale test box, it also justified the use of both experimental setups, large and small scale, to simulate situations in the field where the HDPE GMs waves are normally much further apart.

Based on the above findings, four rigid boxes having dimensions of 300 mm long by 300 mm wide by 300 mm high were built. Along with steel reaction frames and a hydraulic pressurizing system, these boxes allow a application of normal pressure higher than 1,500 kPa. This is equivalent to a solid waste landfill of approximately 125 m in height, i.e., a so-called “megafill”. In addition, all four boxes can be simultaneously housed in a environmental room where constant environmental conditions can be maintained within ranges of 0 to 55°C temperature and 0 to 98% relatively humidity. Photographs of one of four identical small scale test boxes and the environmental room used in this task are shown in Figure A-10. As seen in the figure, data acquisition is also available for strain gage measuring.

One of the objectives of the experimental part of the task is to investigate the behavior of HDPE GM waves under various conditions. As discussed earlier, the four small-scale test boxes in conjunction with the environmental room are ideal in this regard. The other objective of the experimental part of this study is to obtain actual long-term experimental data so that the validity of using rheologic models for the purpose of long-term prediction can be evaluated.

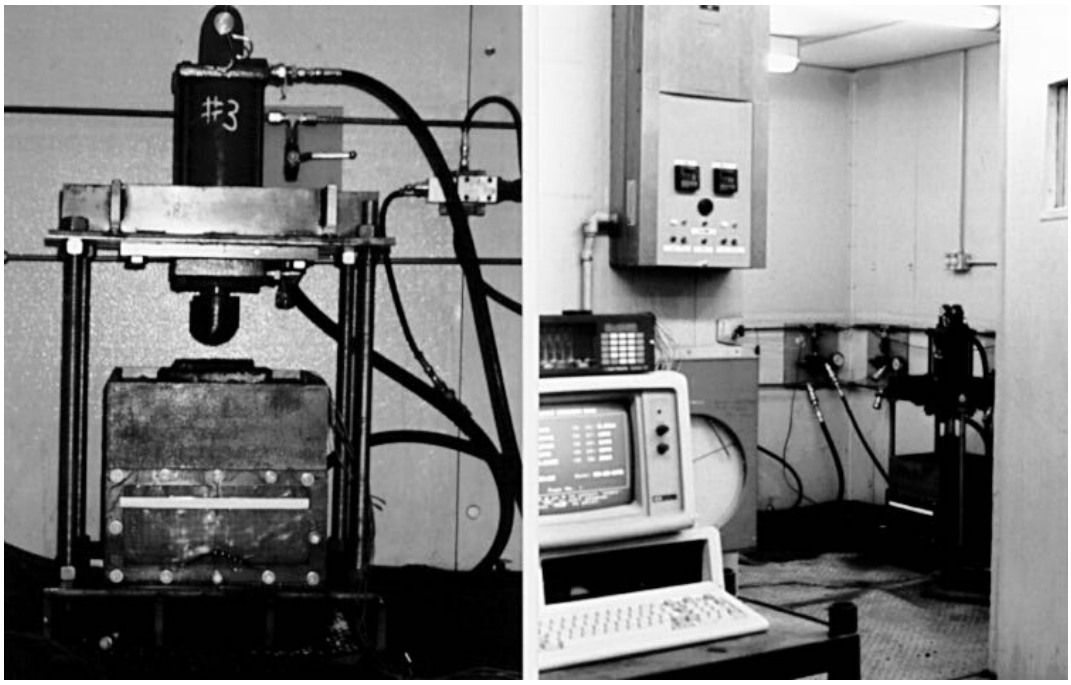

Figure A-10. Photographs of the small scale test box and the environmental room used in this study.

Four sets of 1,000 hour experiments, utilizing the small scale test boxes just described within an environmental room, were designed and conducted to evaluate the effect of four experimental parameters on the behavior of HDPE GM waves. These parameters were the normal stress, original height of wave, thickness of GM, and testing temperature. Table A-2 presents the experimental design of these tests. As seen, the effects of different variables were evaluated by varying the particular one under investigation while holding the others constant. In all cases, smooth HDPE GMs were used and strain gages were attached to the wave specimens at different locations with continuous readout over the duration of the tests. Note that all of the waves in the experiments listed in Table A-2 were created with an original height-to-width ratio of approximately 0.33. Such a ratio was found typical for most of the naturally formed HDPE GM waves in the laboratory covered by little-to-no backfill.

The large-scale test box was reserved and used for conducting a single long-term (10,000 hours) control experiment. A 1.5-mm thick smooth HDPE GM wave with original height of 60 mm and a original height-to-width ratio of 0.33 was created and it was subjected to a constant normal stress of 70 kPa at a temperature of 23±2°C. This test is considered to be the control test for subsequent comparison of the results of the small-scale tests.

Table A-2. Experiments Conducted Using Small Scale Test Boxes

Experimental Parameter Evaluated	Experimental Conditions			
	Normal Stress (kPa)	Original Height of Wave (mm)	GM Thickness (mm)	Temperature (°C)
Normal Stress	180 360 700 1,100	60	1.5	23
Original Height of Wave	700	14 20 40 60 80	1.5	23
GM Thickness	700	60	1.0 1.5 2.0 2.5	23
Testing Temperature	700	14 20 40 60	1.5	23 42 55

A-3 Experimental Results - 1,000 hour Tests

The results of all twenty five of the 1,000 hour tests, as listed in Table A-2, will be presented in this section. They will be given on a variable-by-variable basis. Both original and final (after 1,000 hours) shapes of the GM waves along with the corresponding heights and height-to-width ratios will be shown. Also, if applicable, a comparison among results generated under different test conditions will be made to evaluate the effect of that particular experimental variable.

As listed in Table A-2, four 1.5 mm thick HDPE GM wave specimens, having original heights of 60 mm, were subjected to four different normal stresses, namely, 180, 360, 700, and 1,100 kPa. The temperature was maintained at 23°C for all experiments over the entire duration of the experiments, i.e., 1,000 hours. The original (same for all specimens) and the final shapes of all test specimens, obtained via profile-tracing monitoring, are shown in Figure A-11.

Six strain gages, numbered from G1 to G6, were originally bonded at the locations shown in Figure A-11 for all specimens. Note that gages G4 to G6 (shown as darker circles in Figure A-11) were bonded on the lower side of the GM since the gages which

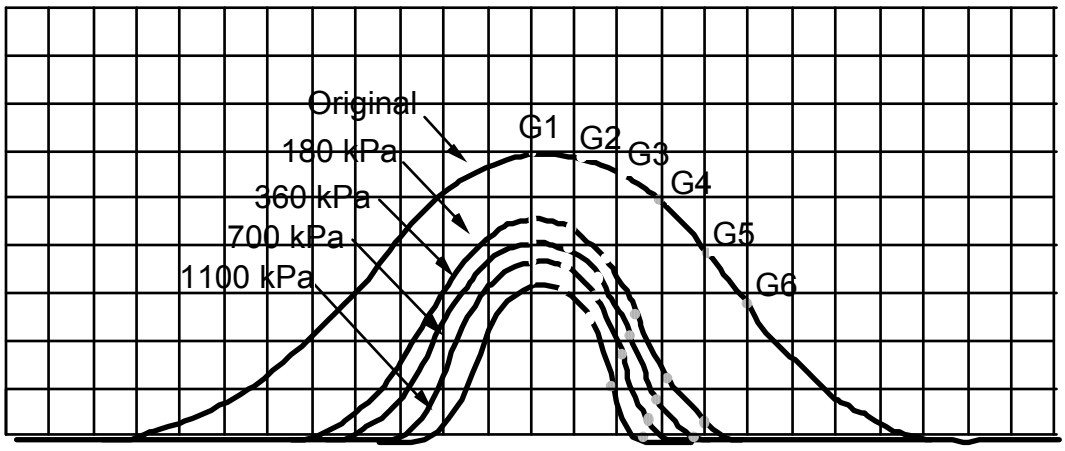

Figure A-11. Original and final shapes of HDPE GM waves under various normal stresses (grid lines have dimensions of 10 mm by 10 mm).

were used respond more accurately under tension than compression. As a result of different normal stresses, these gages measured the strains corresponding to various locations on the GM test specimens. A typical result of the test conducted under a normal stress of 700 kPa is shown in Figure A-12 where the measured strains are plotted against time. By viewing Figures A-11 and A-12 simultaneously, it is seen that the upper portion of this particular wave specimen experienced measurable strain with a maximum tensile strain of 3.4% recorded near the crest of wave.

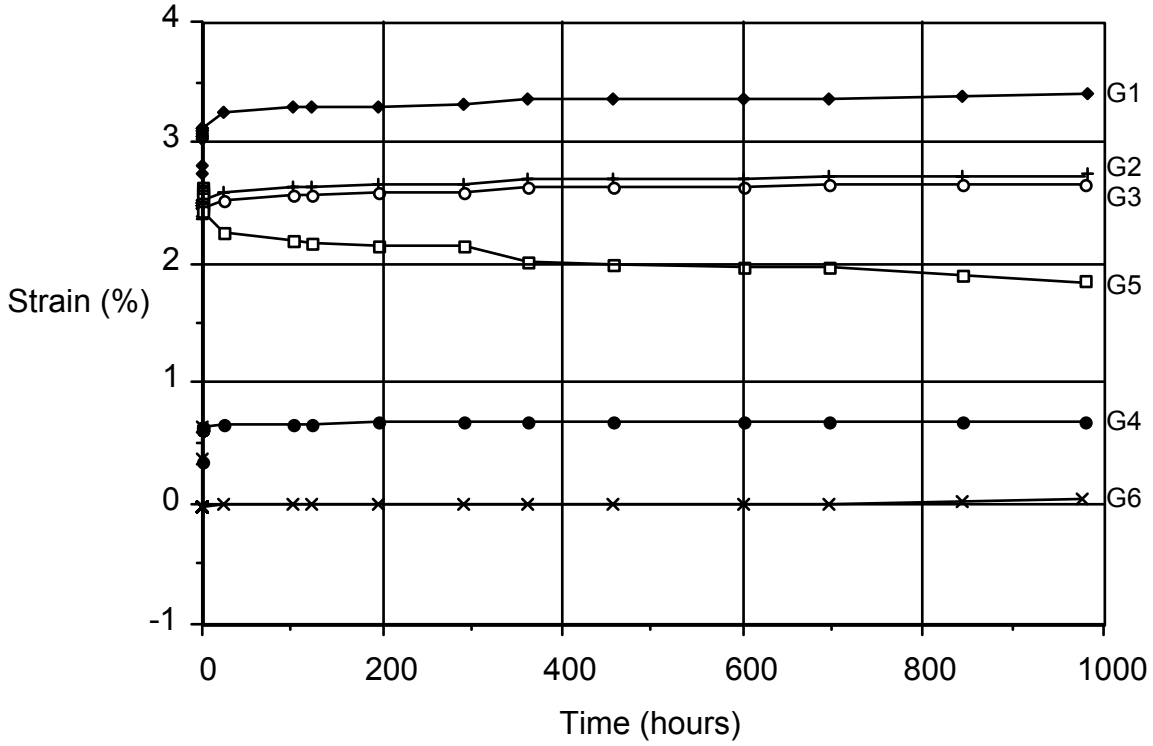

Figure A-12. Strain measurement results of experiment conducted at 700 kPa.

By investigating the results generated from both parts of the experimental monitoring, i.e., the profile-tracing illustrated in Figure A-11 and the strain gage measuring illustrated in Figure A-12, information such as final wave height, final height-to-width ratio, maximum strain recorded, and the locations of high stress concentrations were obtained. Table A-3 summarizes such information obtained from the first series of 1,000 hour experiments.

As shown in Table A-3, the final wave height decreases with increasing normal stress. However, the height-to-width ratio increases with increasing normal stress even more significantly. It was seen that the effect on the height-to-width ratio is essentially doubled in comparison with the effect on the final wave height. For example, a normal stress of 700 kPa resulted in a 37% reduction in the wave height compared to its original configuration. However, the same normal stress caused a 76% increase in the height-to-width ratio. Since high height-to-width ratios generally indicate large curvatures and locations of high stress concentration, the overall effect of high normal stress is obviously unfavorable.

Table A-3. Summarized Results of Test Series No.1 - Effect of Normal Stress

Normal Stress (kPa)	Final Wave Ht. (mm)	Final H/W Ratio	Max. Strain (%)	Actual Location(s) of Highest Stress Concentration (Strain Gage Location)
0 (original)	60 (original)	0.33 (original)	+ 1.7 (original)	Crest of wave (G1)
180	47	0.47	+ 1.8	Crest of wave (G1)
360	42	0.51	+ 2.0	Crest of wave (G1) Crest of wave (G1)
700	38	0.58	+ 3.0	Upper portion of wave (G1, G2 and G3)
1,100	34	0.62	+ 3.2	Upper portion and base of wave (G2 and G5)

The strain recorded in each experiment shows that tensile strain increases as normal stress increases. This is expected since the H/W values increase significantly with greater curvature. Nevertheless, the GM is tensioned significantly less than its yield point. (Note that the tensile yield strain for this GM is in the range of 15 to 25% depending on the temperature.) Therefore, tensile yield is not expected. However, the general design objective is to place the GM with as little stress as possible. This concern will be re-examined later where the actual stresses induced will be quantified using various rheologic models.

The second series of 1,000 hour experiments was designed to evaluate the effect of the original wave height on the behavior of HDPE GM waves. Five tests using 1.5 mm-thick

HDPE GM wave specimens were conducted. The original heights of the waves were 14, 20, 40, 60, and 80 mm, respectively. All specimens were subjected to a constant normal stress of 700 kPa and maintained at a constant temperature of 23°C over the entire duration of the experiment. The original and final (after 1,000 hours) shapes of the test specimens are shown in Figure A-13. Again, reference marks which identify the locations and movement of the bonded strain gages are also shown in Figure A-13.

By summarizing the results generated from both parts of the monitoring, Table A-4 was established.

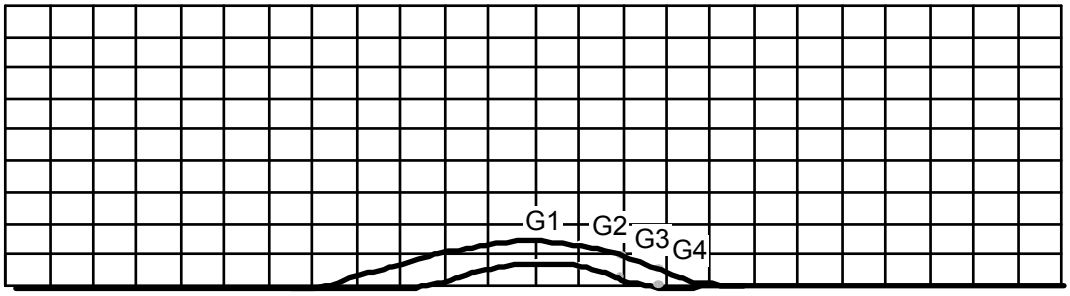

(a) GM wave with original height of 14 mm

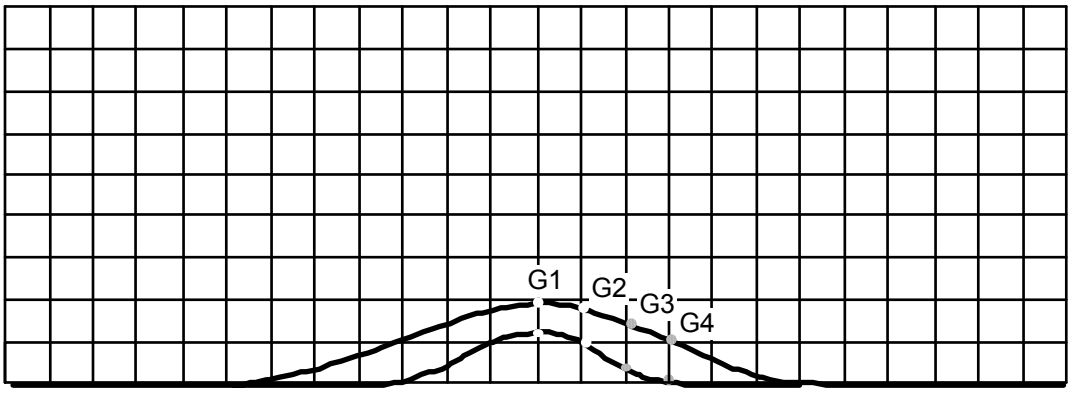

(b) GM wave with original height of 20 mm

Figure A-13. Original and final shapes of HDPE GM waves with various original wave heights (grid lines have dimensions of 10 mm by 10 mm).

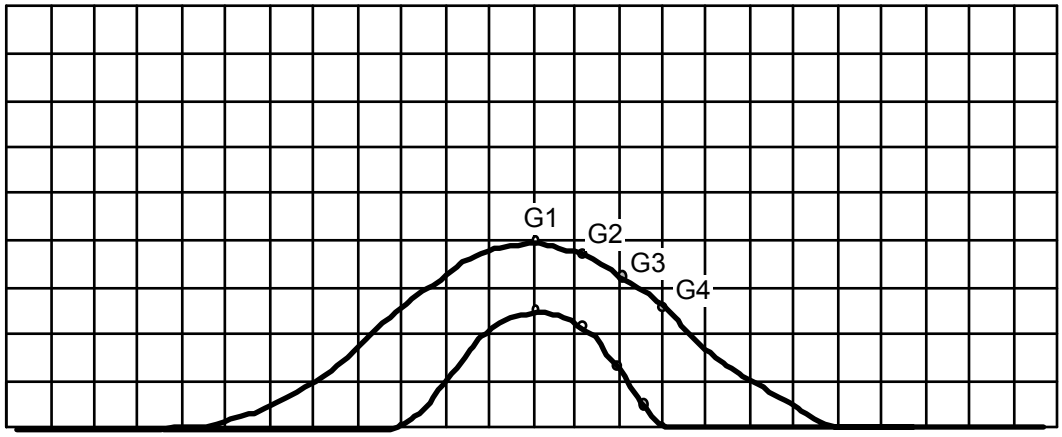

(c) GM wave with original height of 40 mm

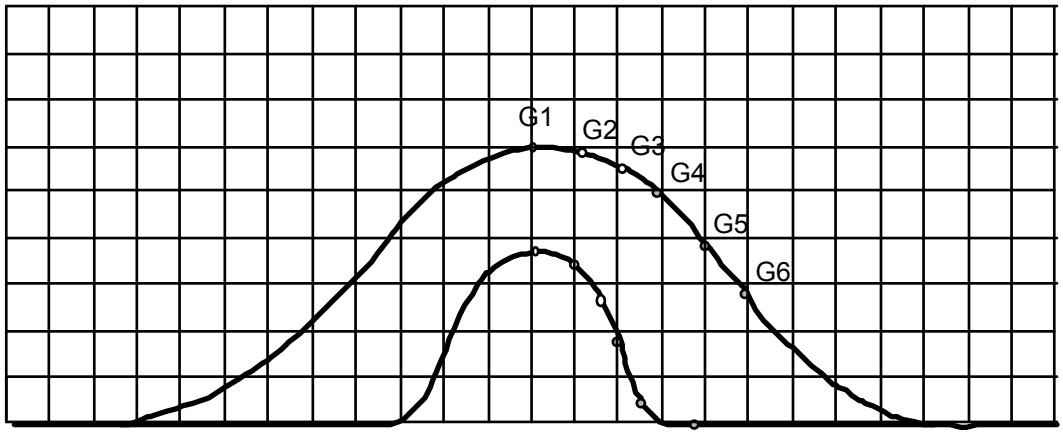

(d) GM wave with original height of 60 mm

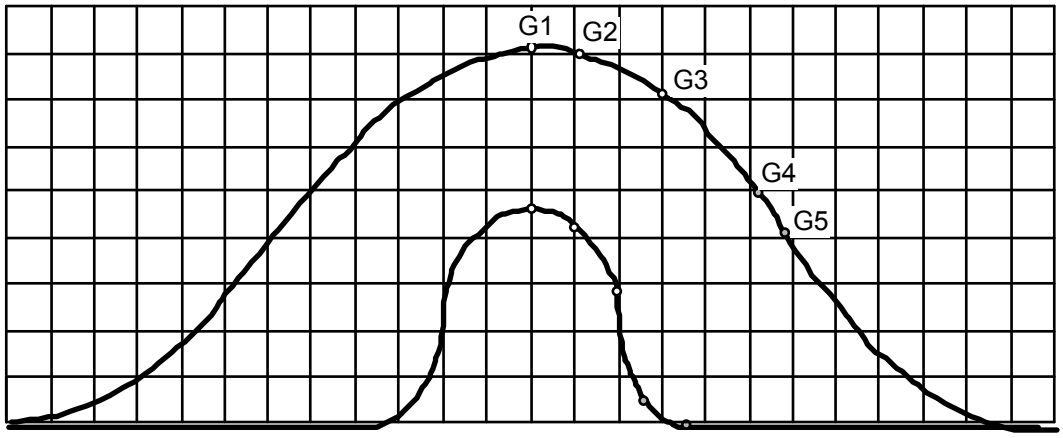

(e) GM wave with original height of 80 mm

Figure A-13 (cont.). Original and final shapes of HDPE GM waves with various original wave heights (grid lines have dimensions of 10 mm by 10 mm).

Table A-4. Summarized Results of Test Series No.2 - Effect of Original Wave Height

Original Wave Ht. (mm)	Original H/W Ratio	Final Wave Ht. (mm)	Final H/W Ratio	Max. Strain (%)	Actual Location(s) of Highest Stress Concentration (Strain Gage Location)
14	0.17	8	0.14	+ 0.2	Negligible
20	0.15	12	0.18	+ 1.2	Base of wave (G3)
40	0.27	25	0.38	+ 2.4	Upper portion and base of wave (G2 and G4)
60	0.33	38	0.58	+ 3.0	Upper portion of wave (G1, G2 and G3)
80	0.33	47	0.65	+ 3.4	Upper portion and base of wave (G2 and G4)

As seen in Table A-4, there was an approximate 40% reduction in height after 1,000 hours for all waves. As to the final H/W ratio, it increases with increasing original wave height. Note that for waves originally higher than 60 mm, the final H/W ratios exceeded a value of 0.5. With regard to the maximum strain recorded, an increasing trend is also seen with increasing original height. Moreover, there was no sign of achieving intimate contact between the specimen and the underlying subgrade after 1,000 hours, even for the wave with the smallest original height, i.e., the 14 mm wave.

The third series of 1,000 hour experiments was designed to evaluate the effect of GM thickness on the behavior of HDPE GM waves. Four tests using HDPE GM wave specimens, with thicknesses of 1.0, 1.5, 2.0, and 2.5 mm, were conducted. The original heights of all wave specimens were approximately 60 mm. Owing to the various stiffnesses of the GMs having different thicknesses, a constant value of original H/W ratio could not be maintained, see Table A-5. All specimens were subjected to a constant normal stress of 700 kPa and maintained at a constant temperature of 23°C over the entire duration of the experiments. The original and final (after 1,000 hours) shapes of the test specimens, along with reference marks which indicate the location and movement of the strain gages, are shown in Figure A-14.

As shown in Table A-5, with the only exception being the 1.0-mm-thick GM wave, the following observations are made. First, the thickness of GM has very little effect on the final height of GM waves. There was an approximate 40% reduction in height after 1,000 hours for all waves. In other words, the original height essentially determined the final height of GM waves. Second, the GM thickness did show a significant effect on the final H/W ratio of the waves. That is to say, the final H/W ratio decreases with increasing GM thickness. The latter observation can be interpreted in an alternative manner. That is, for waves with the same original height, thicker GMs resulted in wider voids beneath the wave. Third, the maximum strain recorded in each experiment shows that tensile strain slightly increases as the thickness of GM increases.

Table A-5. Summarized Results of Test Series No.3 - Effect of GM Thickness

GM Thickness (mm)	Original H/W Ratio	Final Wave Ht. (mm)	Final H/W Ratio	Max. Strain (%)	Actual Location(s) of Highest Stress Concentration (Strain Gage Location)
1.0	0.24	27	0.52	+ 2.5	Base of wave (G5)
1.5	0.34	38	0.56	+ 3.0	Upper portion and base of wave (G1, G2 and G3)
2.0	0.18	33	0.34	+ 3.1	Upper portion and base of wave (G1, G2, G4 and G5)
2.5	0.21	38	0.32	+ 3.3	Upper portion and base of wave (G2, G3, G4 and G5)

Note: Original heights of all wave specimens were approximately 60 mm

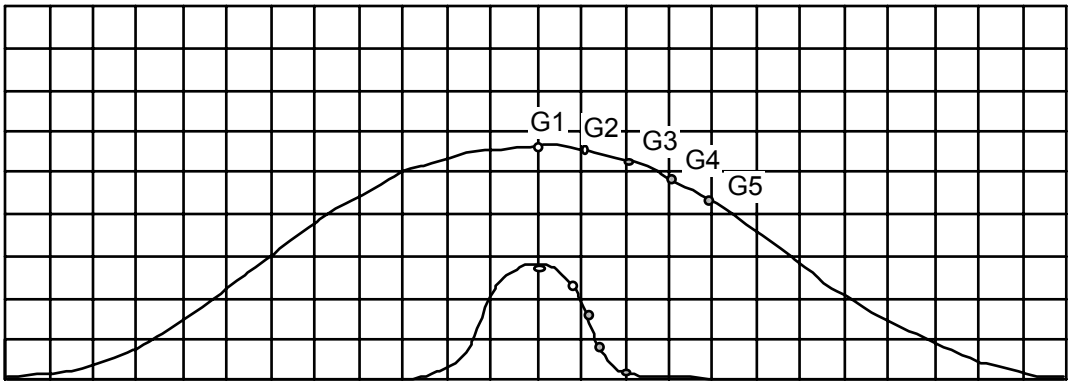

(a) GM wave with thickness of 1.0 mm

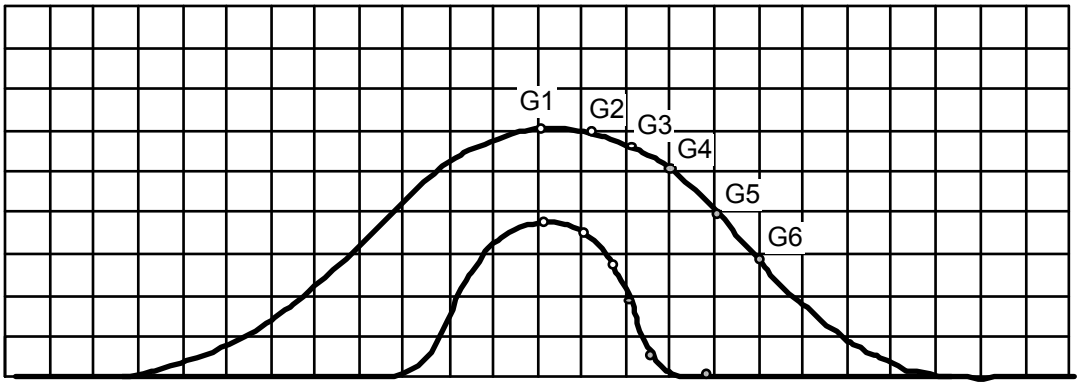

(b) GM wave with thickness of 1.5 mm

Figure A-14. Original and final shapes of HDPE GM waves with various thicknesses (grid lines have dimensions of 10 mm by 10 mm).

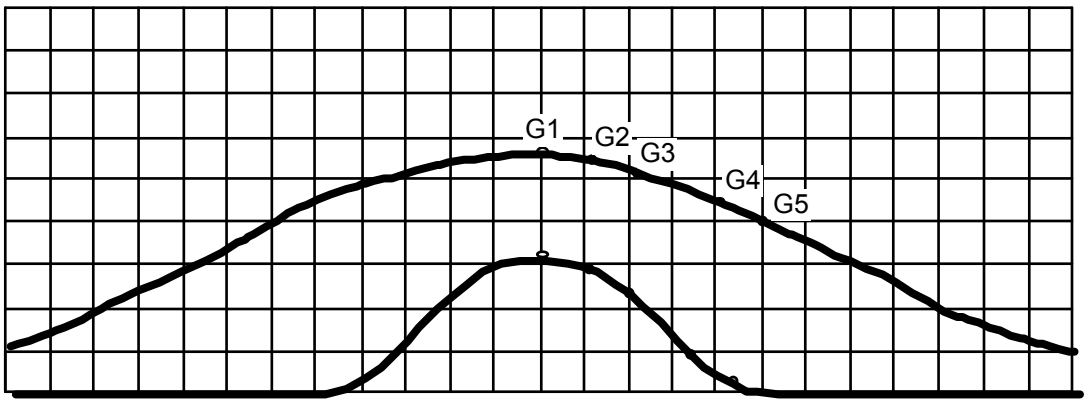

(c) GM wave with thickness of 2.0 mm

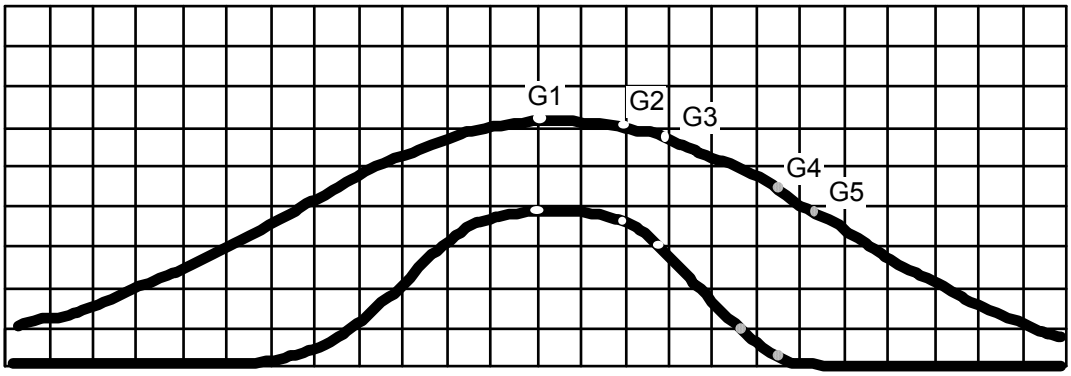

(d) GM wave with thickness of 2.5 mm

Figure A-14 (cont.). Original and final shapes of HDPE GM waves with various thicknesses (grid lines have dimensions of 10 mm by 10 mm).

The fourth series of 1,000 hour experiments were designed to evaluate the effect of temperature on the behavior of HDPE GM waves. Three sets of experiments, each consisting of 1.5 mm thick HDPE GM waves with original heights of 14, 20, 40, and 60 mm, were conducted at temperatures of 23, 42 and 55°C.

The original shapes of all wave specimens were formed at 23°C with approximately 100 mm of sand backfill over them. Temperature was then increased, as necessary, to the desired value. This was meant to replicate field situations where the exposed GMs experience an increase in temperature after placement and seaming. The test boxes were then filled with sand, followed by a decrease in temperature back to 23°C, to simulate the decreasing in the sheet temperature of the field deployed GMs after the protection and drainage layers are placed. After approximately 24 hours, a constant normal stress of 700 kPa was applied. After another hour, temperature was increased

from 23°C to the desired value and maintained for the remainder of the experiment. The last step was intended to simulate a possible increase in the sheet temperature over the entire lifetime of landfills.

The original and final shapes of the test specimens at the three temperatures, along with reference marks which indicate the location and movement of the strain gages, are shown in Figure A-15.

A typical strain measurement result of this series of experiments is shown in Figure A-16. This particular test was conducted at a temperature of 42°C using a wave specimen with an original height of 20 mm. As seen in the figure, temperature was increased from 23 to 42°C one hour after the normal stress was applied. For this particular experiment, a trend of increasing strain with increasing temperature was observed in all measurements. This is due to a combined effect of both thermal expansion and material softening with increasing temperature. Although such a trend is seen in most of the other measurements, a decreasing trend was also observed in some cases. This suggests that the change of shapes due to the material softening with increasing temperature can sometimes cause portions of the GM waves to undergo compressive stresses. When such an effect is more significant than the effect of thermal expansion, a decreasing strain with increasing temperature is seen.

The summarized results generated from this test series of the monitoring is presented in Table A-6. Note that the values of maximum strain listed in the table are corresponding to the maximum final (after 1,000 hours) strain.

A-4 Experimental Results - 10,000 hour Tests

The strain gage measurement results of the 10,000 hour test are presented graphically in Figure A-17. Experimental data up to 1,000 hours was used to establish the first set of Kelvin-Chain models for predictions out to 10,000 hours. The calculated curves using these models are shown in dashed lines. As seen in Figure A-17, they agree with the actual data measured between 1,000 and 10,000 hours very well. This encouraging finding is felt to justify the use of the Kelvin-Chain model for the purpose of long-term prediction, Soong (1996). With this in mind, the second set of Kelvin-Chain models was developed using the entire experimental strain gage measurements and another order of extrapolation, i.e., predictions out to 100,000 hours, was made. The resulting curves are also shown in Figure A-17 as solid lines.

A-5 Analysis of Test Results

The experimental results, including the profile-tracing of the actual waves and the strain gage monitoring, of the 1,000 hour tests were summarized and briefly discussed in the previous section. Complete results of all of the strain gage monitoring, along with the

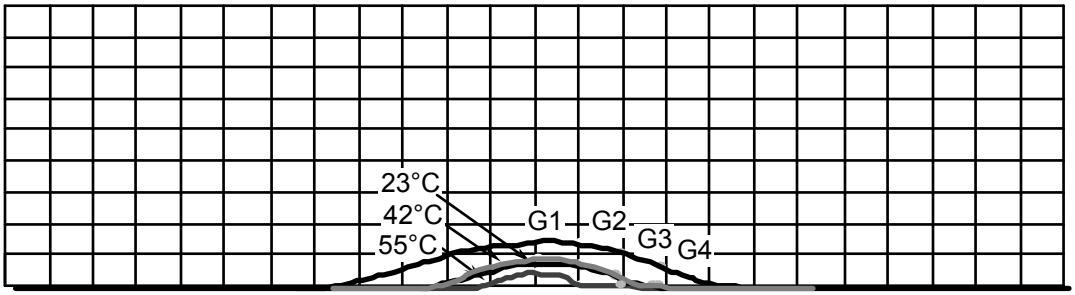

(a) GM wave with original height of 14 mm

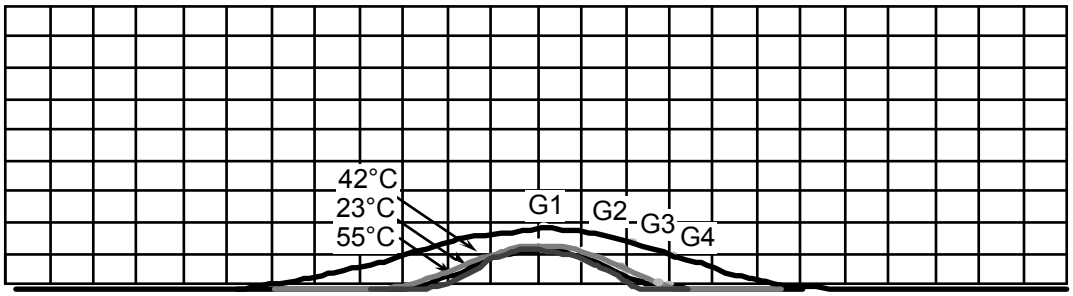

(b) GM wave with original height of 20 mm

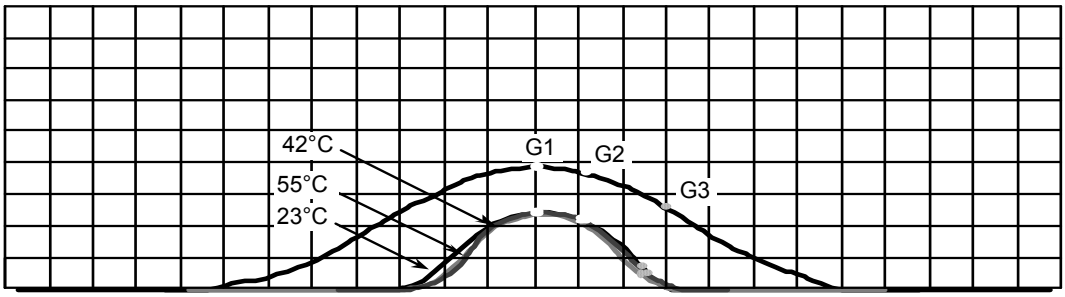

(c) GM wave with original height of 40 mm

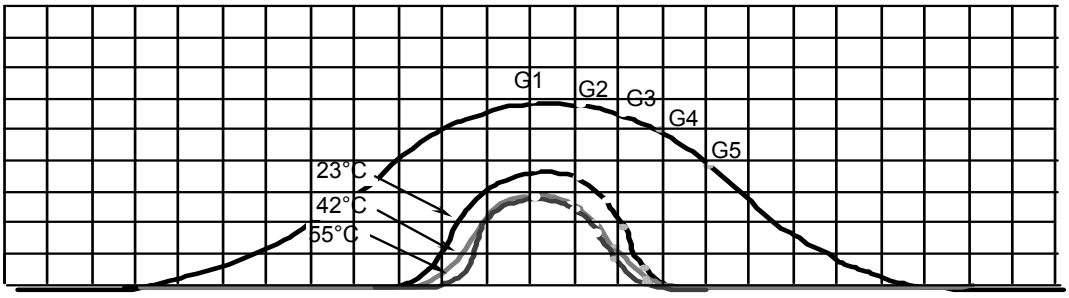

(d) GM wave with original height of 60 mm

Figure A-15. Original and final shapes of HDPE GM waves at various temperatures (grid lines have dimensions of 10 mm by 10 mm).

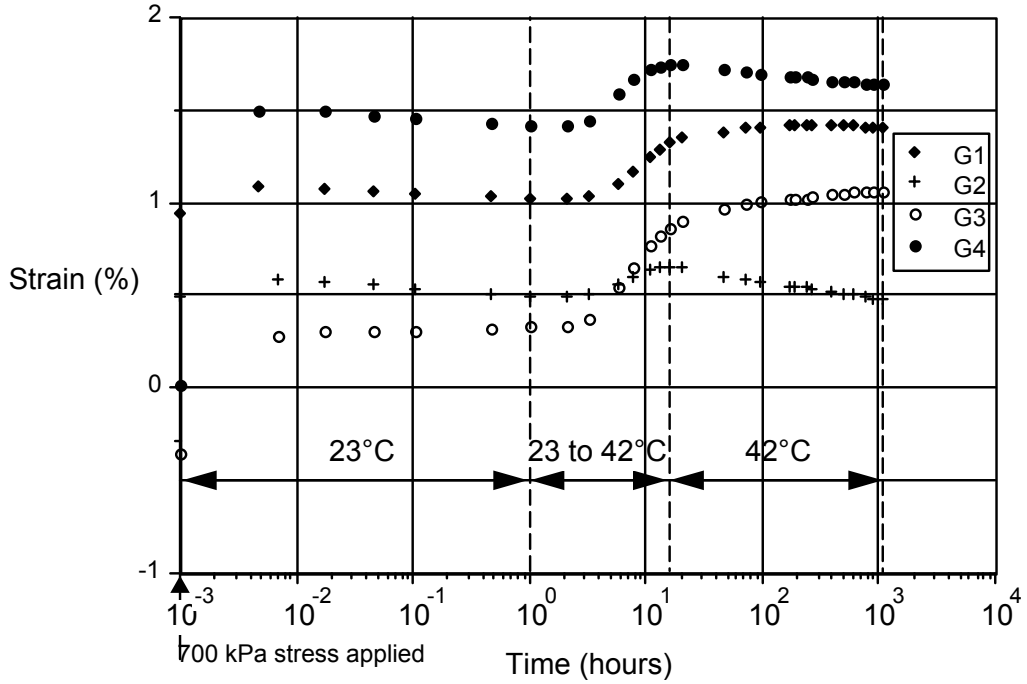

Figure A-16. Strain measurement results of test conducted on wave specimen with an original height of 20 mm and at a temperature of 42°C.

Table A-6. Summarized Results of Test Series No. 4 - Effect of Temperature

Original Height (mm)/ H/W Ratio	Temp. (°C)	Final Wave Height (mm)	Final H/W Ratio	Max. Strain (%)	Actual Location(s) of Highest Stress Concentration (Strain Gage Locations)
	23	8	0.14	+ 0.2*	Negligible
14 / 0.17	42	10	0.19	+ 0.6	Negligible
	55	5	0.20	+ 1.3	Base of wave (G2)
	23	12	0.18	+ 1.2	Base of wave (G3)
20 / 0.15	42	14	0.21	+ 1.6	Base of wave (G4)
	55	12	0.30	+2.1	Base of wave (G4)
	23	25	0.38	+ 2.4	Upper portion and base of wave (G2 and G3)
40 / 0.27	42	25	0.42	+ 3.2	Base of wave (G3)
	55	25	0.40	+ 2.1	Crest of wave (G1)
	23	38	0.58	+ 3.0	Upper portion and base of wave (G1, G2, G3 and G5)
60 / 0.33	42	30	0.52	+ 4.9	Upper portion and base of wave (G1, G2, G3 and G5)
	55	28	0.55	+ 4.9	Upper portion and base of wave (G1, G2 and G5)

Note: "+" strain=tension
"-" strain=compression

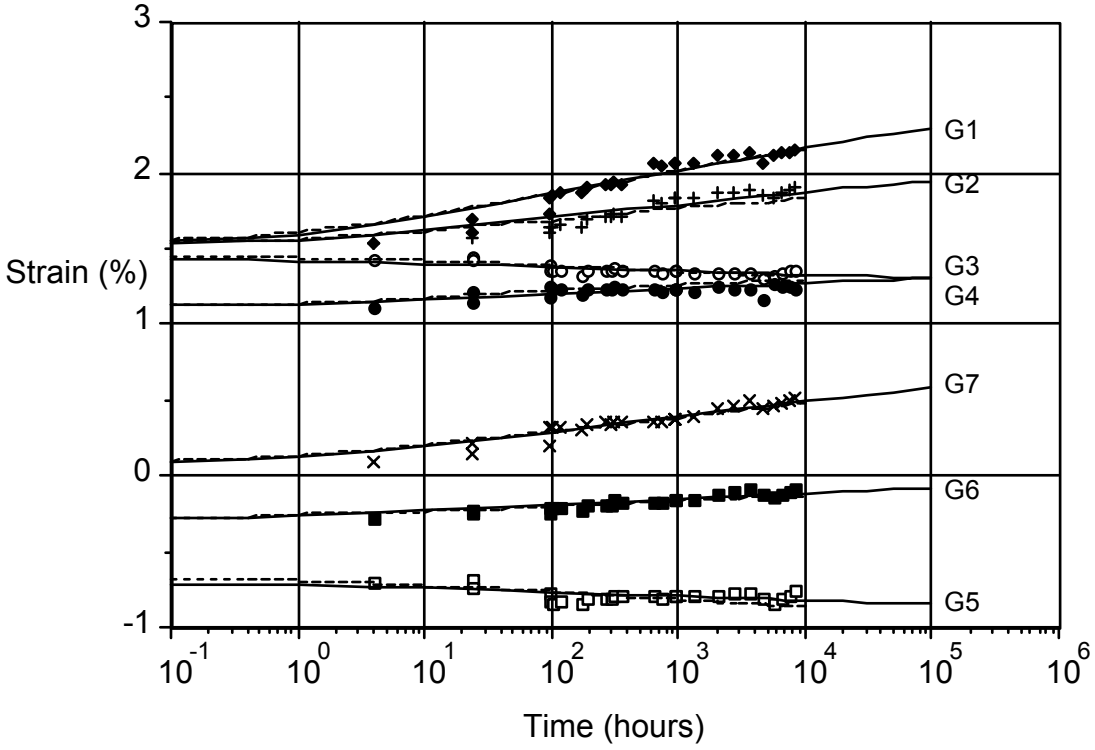

Figure A-17. Experimental and modeled results of the 10,000 hour control test.

predicted behavior up to 10,000 hours, can be found in Soong (1996). In this section, the previous test results will be analyzed further. Various aspects of the test results, including final wave height, final height-to-width ratio, and the maximum strain at the end of 1,000 hour experiments, will be utilized to quantify the effect of different experimental variables on the behavior of HDPE GM waves.

In this section, the height of HDPE GM wave specimens at the end of the 1,000 hour experiments as previously described are plotted against the relevant experimental variables. These variables include normal stress, original height of wave, thickness of GM and testing temperature. The results are shown in Figures A-18 through A-21. Some observations are made and summarized in Table A-7.

Additionally, the height-to-width (H/W) ratio of the HDPE GM wave specimens at the end of the experiments are plotted against various experimental variables, as shown in Figures A-22 through A-25. Some observations are made and summarized in Table A-8.

Lastly, the maximum tensile strain of the HDPE GM wave specimens at the end of the experiments (irrespective of their locations) are plotted against various experimental variables, as shown in Figures A-26 through A-29. Some observations are made and summarized in Table A-9.

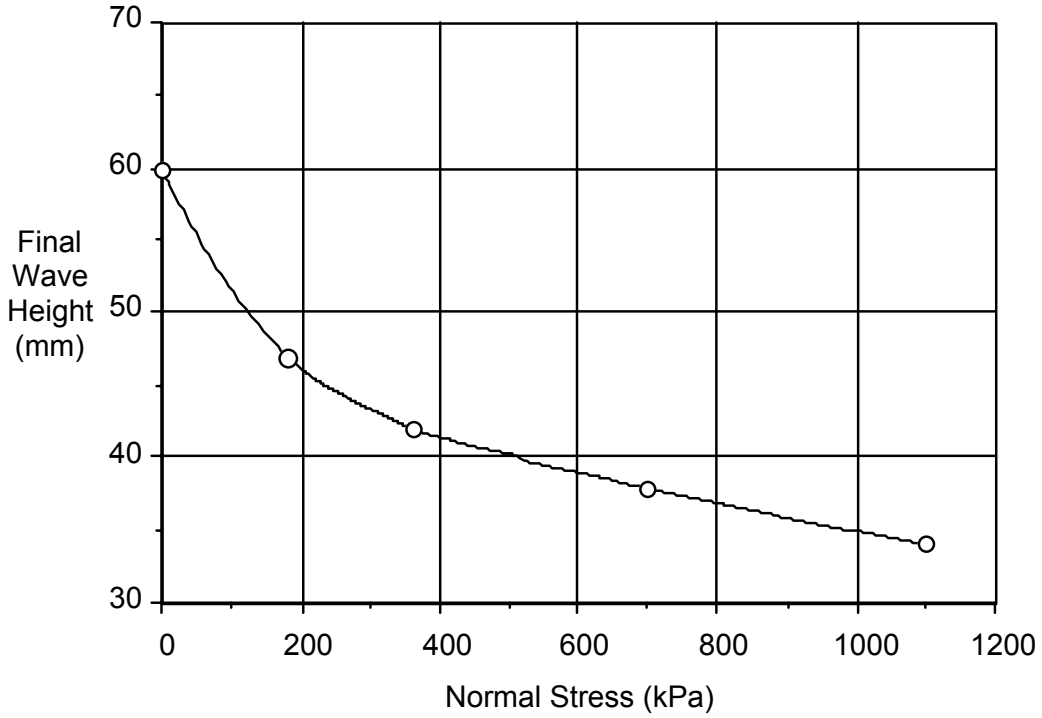

Figure A-18. Effect of normal stress on the final height of HDPE GM waves.

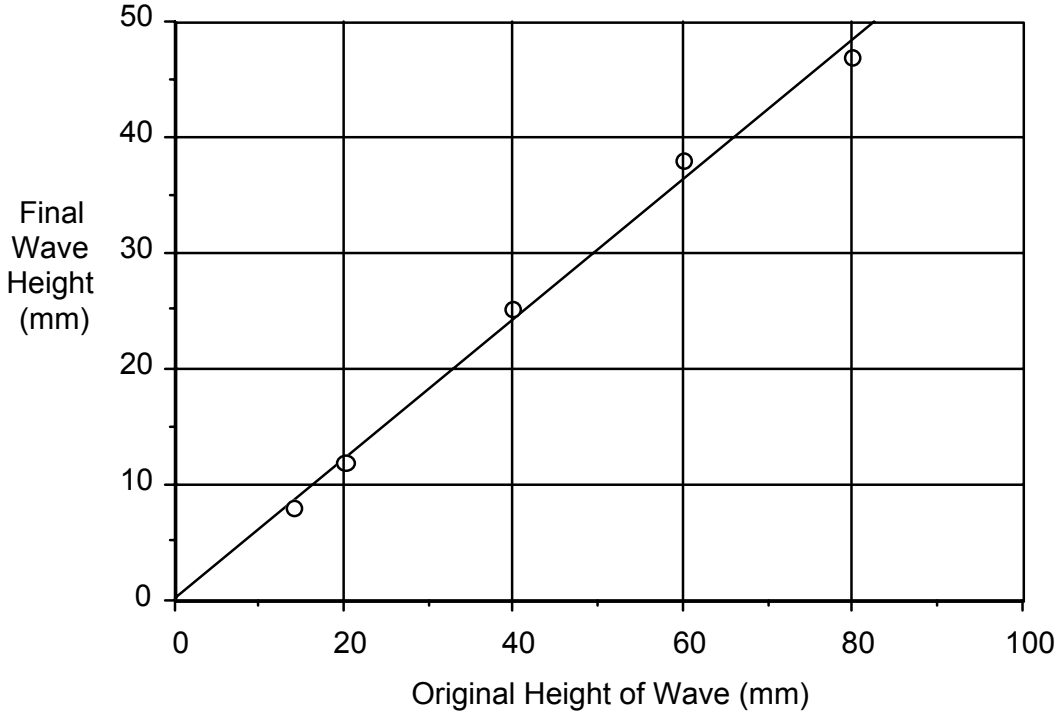

Figure A-19. Effect of original height of wave on the final height of HDPE GM waves.

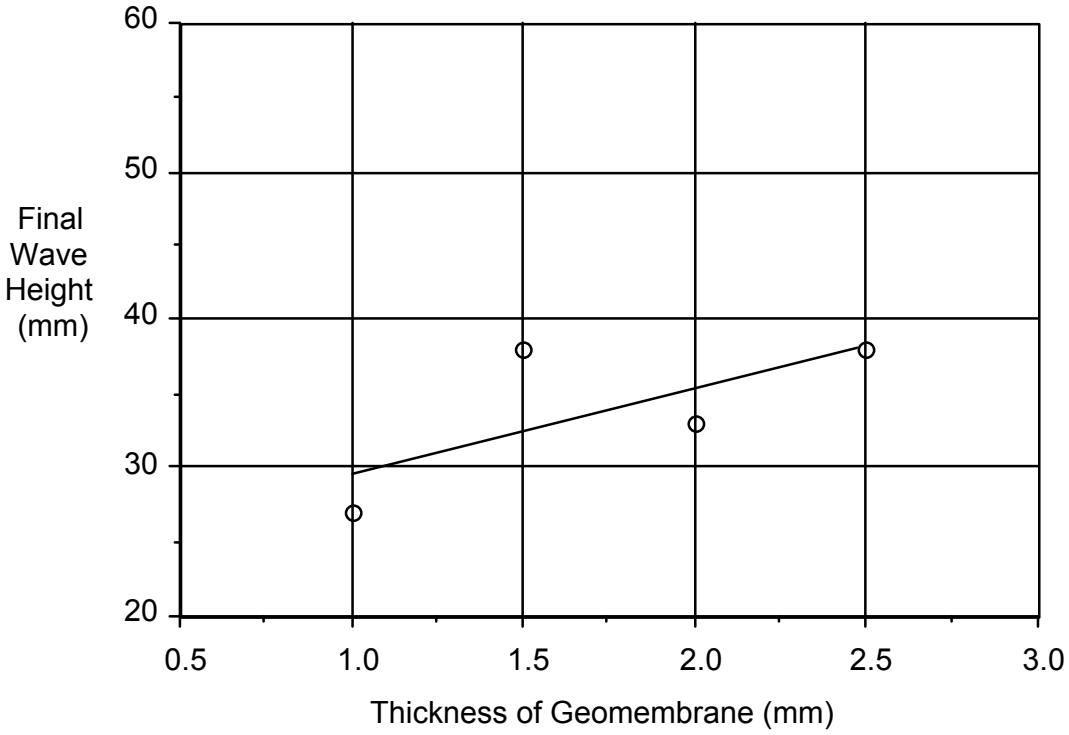

Figure A-20. Effect of GM thickness on the final height of HDPE GM waves.

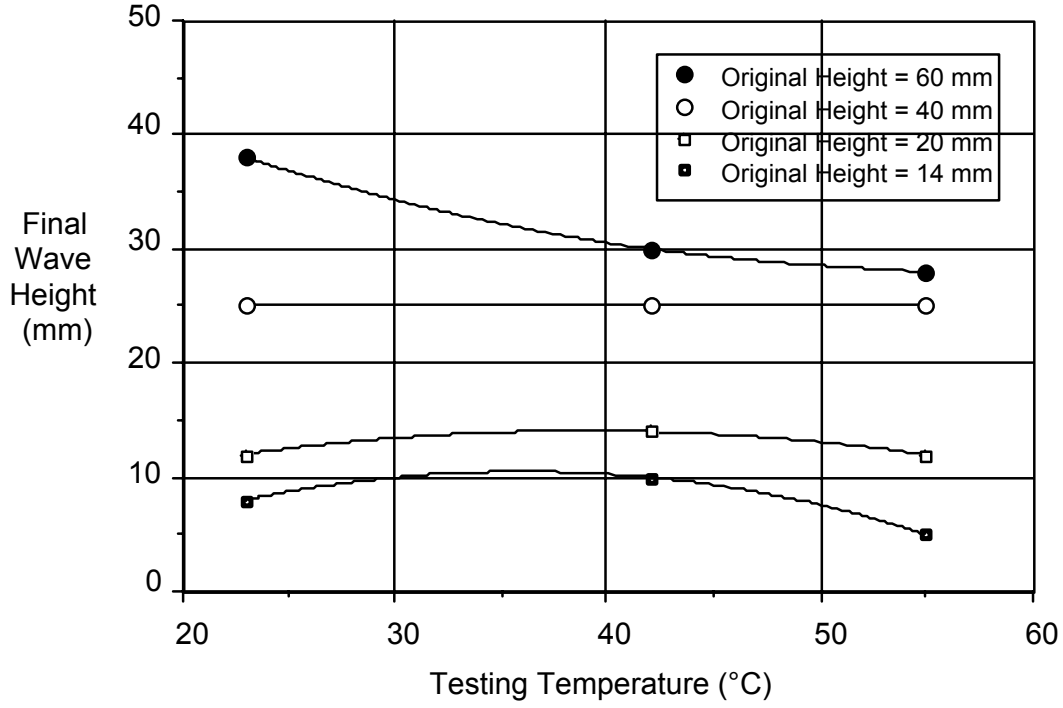

Figure A-21. Effect of testing temperature on the final height of HDPE GM waves having various original heights.

Table A-7. Effects of Different Experimental Variables on the Final Height of HDPE GM Waves

Experimental Variable	Observations
Normal Stress	• Final wave height decreases with increasing normal stress • % reduction in height $\cong$ 27 log σ_n – 40 where σ_n = normal stress in kPa
Original Height of Wave	• Final wave height increases linearly with increasing original wave height • An average of 40% reduction in height after 1,000 hours
Thickness of GM	• Thickness of GM has only a marginal effect on the final wave height • An average of 40% reduction in height after 1,000 hours • Original wave height determines the final wave height
Testing Temperature	• Testing temperature has only slight effect on the final wave height.

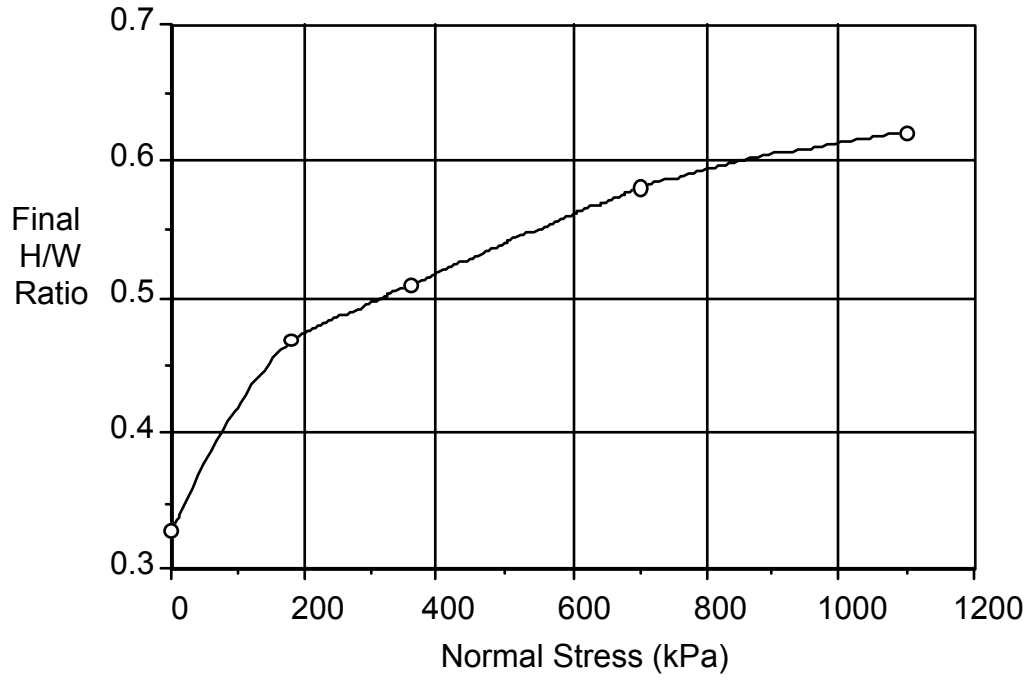

Figure A-22. Effect of normal stress on the final height-to-width ratio of HDPE GM waves.

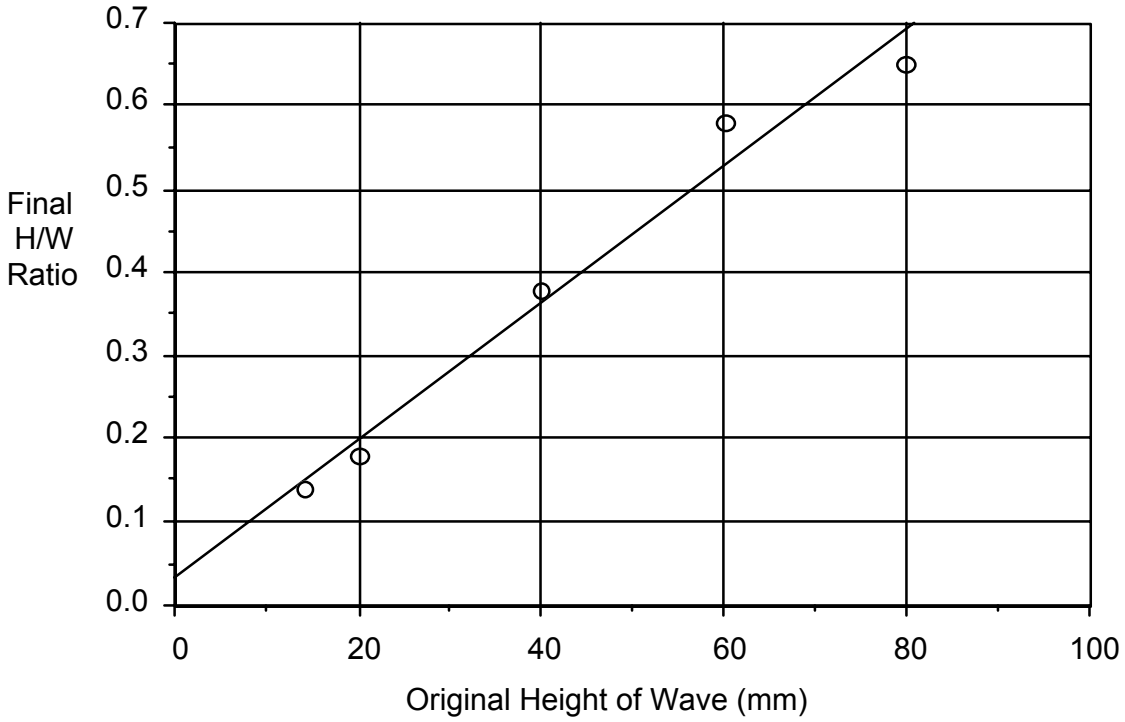

Figure A-23. Effect of original height of wave on the final height-to-width ratio of HDPE GM waves.

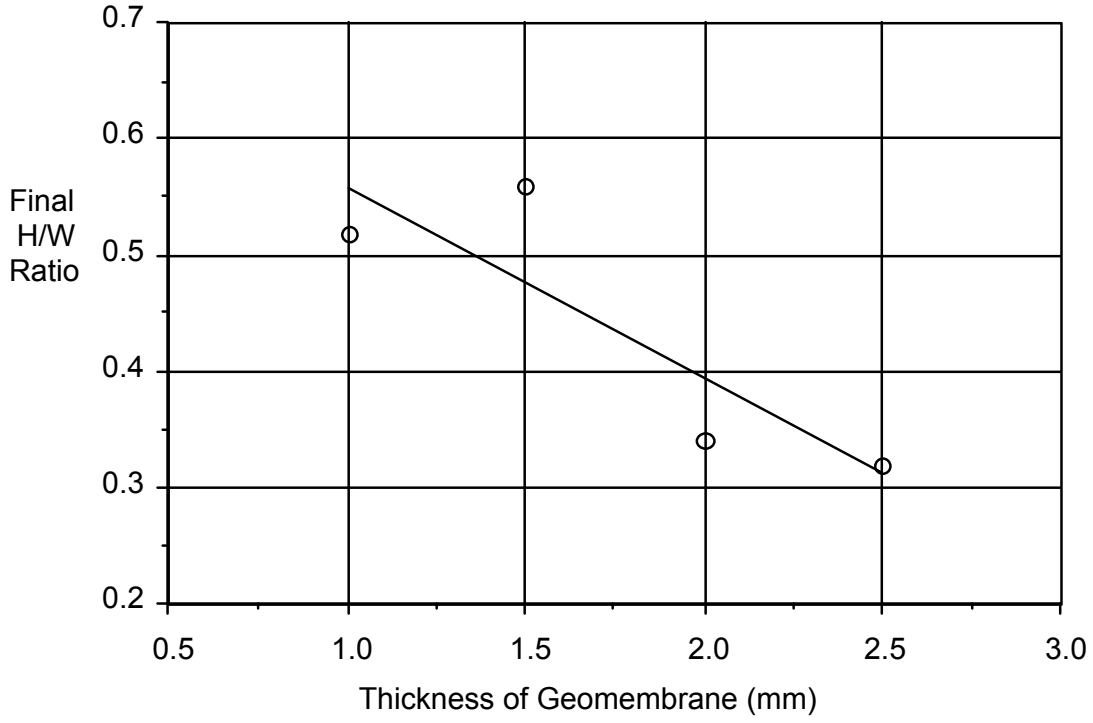

Figure A-24. Effect of GM thickness on the final height-to-width ratio of HDPE GM waves.

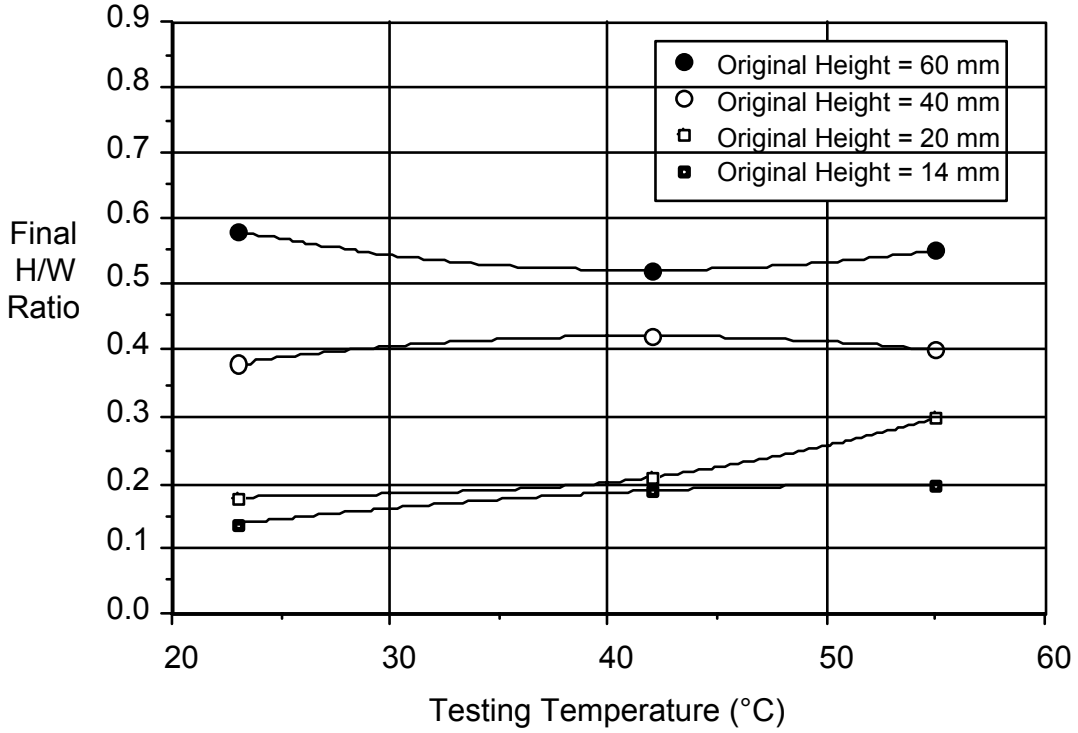

Figure A-25. Effect of testing temperature on the final height-to-width ratio of HDPE GM waves having various original heights.

Table A-8. Effects of Different Experimental Variables on the Final Height-to-Width Ratio of HDPE GM Waves

Experimental Variable	Observations
Normal Stress	• Final H/W ratio increases with increasing normal stress • % reduction in height $\cong$ 59 log σ_n - 93 where σ_n = normal stress kPa
Original Height of Wave	• Final H/W ratio increases approximately linearly with increasing original wave height • Final H/W ratio $\cong$ 0.008 (OH) + 0.03 where OH = original height in mm.
Thickness of GM	• Final H/W ratio decreases approximately linearly with increasing GM thickness • Final H/W ratio $\cong$ 0.72 - 0.16 t where t = thickness of GM in mm.
Testing Temperature	• Testing temperature has only a marginal effect on the final height-to-width ratio.

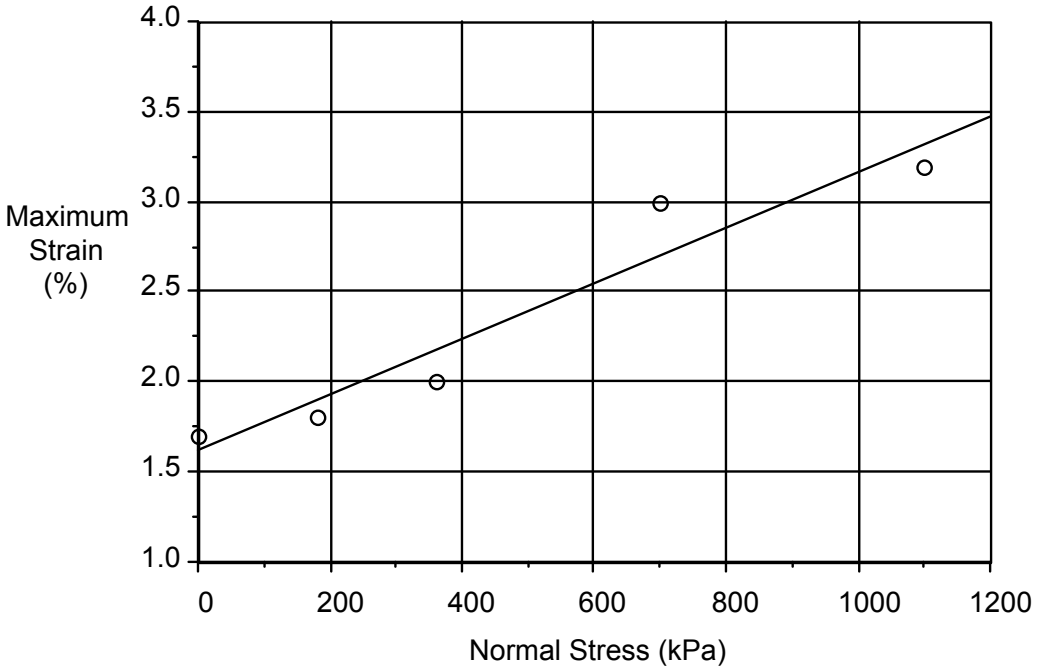

Figure A-26. Effect of normal stress on the maximum strain measured at the end of experiments of HDPE GM waves.

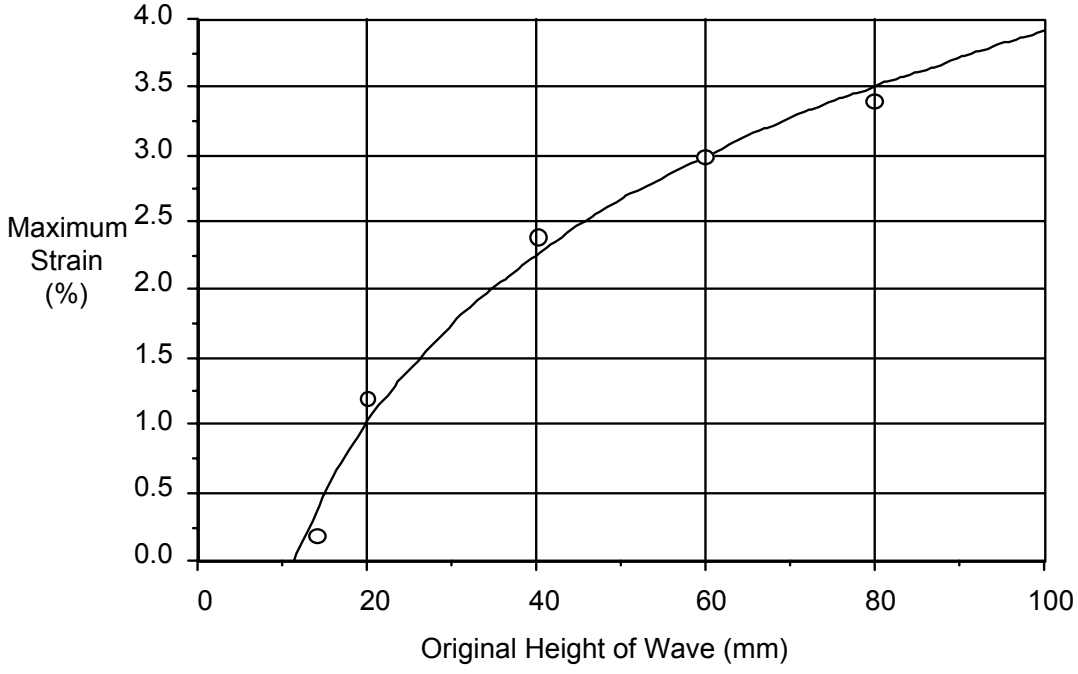

Figure A-27. Effect of original height of wave on the maximum strain measured at the end of experiments of HDPE GM waves.

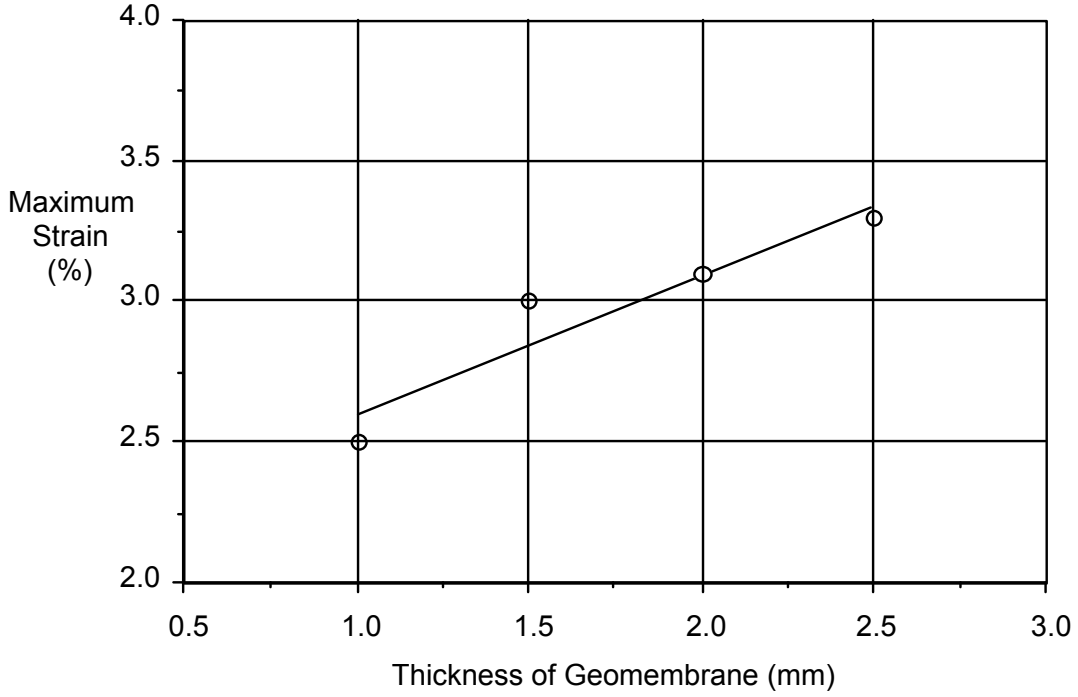

Figure A-28. Effect of GM thickness on the maximum strain measured at the end of experiments of HDPE GM waves.

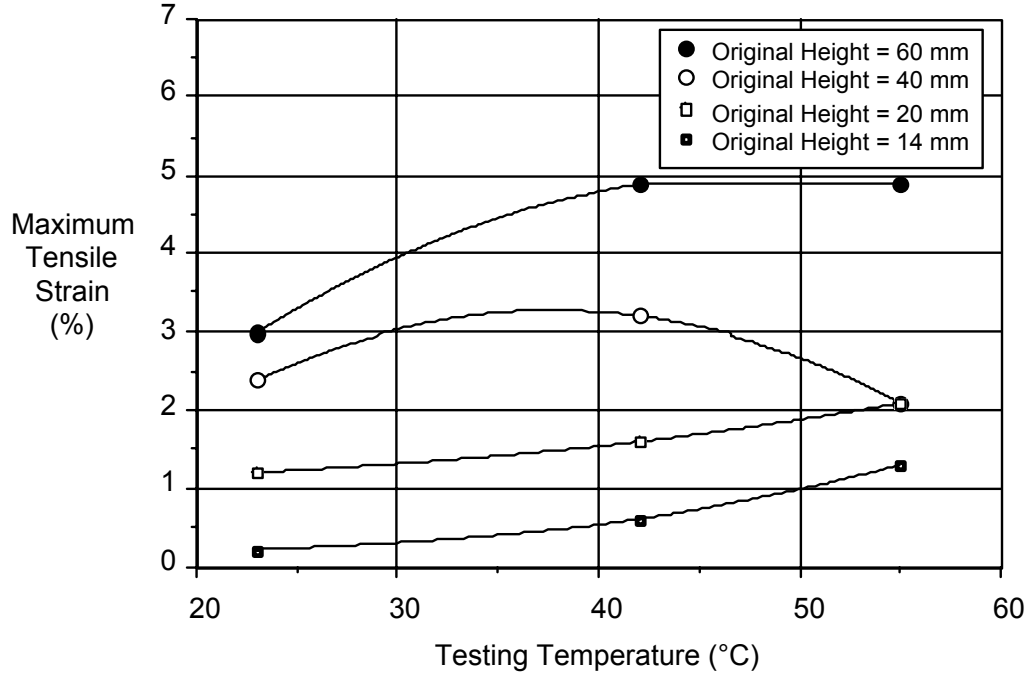

Figure A-29. Effect of testing temperature on the maximum strain measured at the end of experiments of HDPE GM waves having various original heights.

Table A-9. Effects of Different Experimental Variables on the Maximum Strain Measured at the end of Experiments of HDPE GM Waves

Experimental Variable	Observations
Normal Stress	• Maximum strain increases approximately linearly with increasing normal stress • Max. % Strain $\cong$ 0.0015 σ_n + 1.6 Where σ_n = normal stress in kPa
Original Height of Wave	• Maximum strain increases logarithmically with increasing original wave height • Max. % Strain $\cong$ 4.1 log (OH) - 4.34 Where OH = original height in mm
Thickness of GM	• Maximum strain increases approximately linearly with increasing GM thickness • Max. % Strain $\cong$ 0.5t + 2.1 Where t = thickness of GM in mm
Testing Temperature	• Maximum strain increases with increasing temperature for waves originally shorter than 40 mm • Maximum strain showed no clear trend with increasing temperature for waves originally higher than 40 mm

The Maxwell-Weichert model was seen to successfully predict the stress relaxation behavior of HDPE GMs over the temperature range of -10 to 70°C (Soong et al., 1994; Soong, 1995, 1996). This covers the range of interest in this study. Moreover, the effects of strain rate on the stress/strain relationships and the initial modulus of HDPE GMs were also successfully described by the same model. As a result, the initial modulus values of HDPE GMs at various temperatures, which are suitable for the use of design and stress analysis, were quantified. Values of the initial modulus of HDPE GMs, which will be used in the stress analysis to follow, have been assembled and summarized in Table A-10.

Table A-10. Modulus of HDPE GMs at Various Temperatures to be Used in the Stress Analysis to Follow

Temperature (°C)	Initial Modulus (MPa)
23	230
42	140
55	90

Using the modulus values presented in Table A-10, the stress induced in the GM can be calculated with any known strain at a given temperature. However, such stresses will relax over time. The stress relaxation behavior of the tested HDPE GM is dependent

upon temperature only. In addition, master curves generated via time-temperature superposition can be used for the prediction of long-term stress relaxation behavior.

As shown in Figure A-30, a normalized master curve for a 1.5 mm thick HDPE GM is plotted against time at various temperatures. Via proper curve fitting, these normalized master curves can be described using numerical expressions. The resulting expressions from the above procedure are given in Equations A-1, A-2 and A-3 for temperatures of 10, 30 and 50°C, respectively. Note that the "time" terms in these equations are in the units of hours.

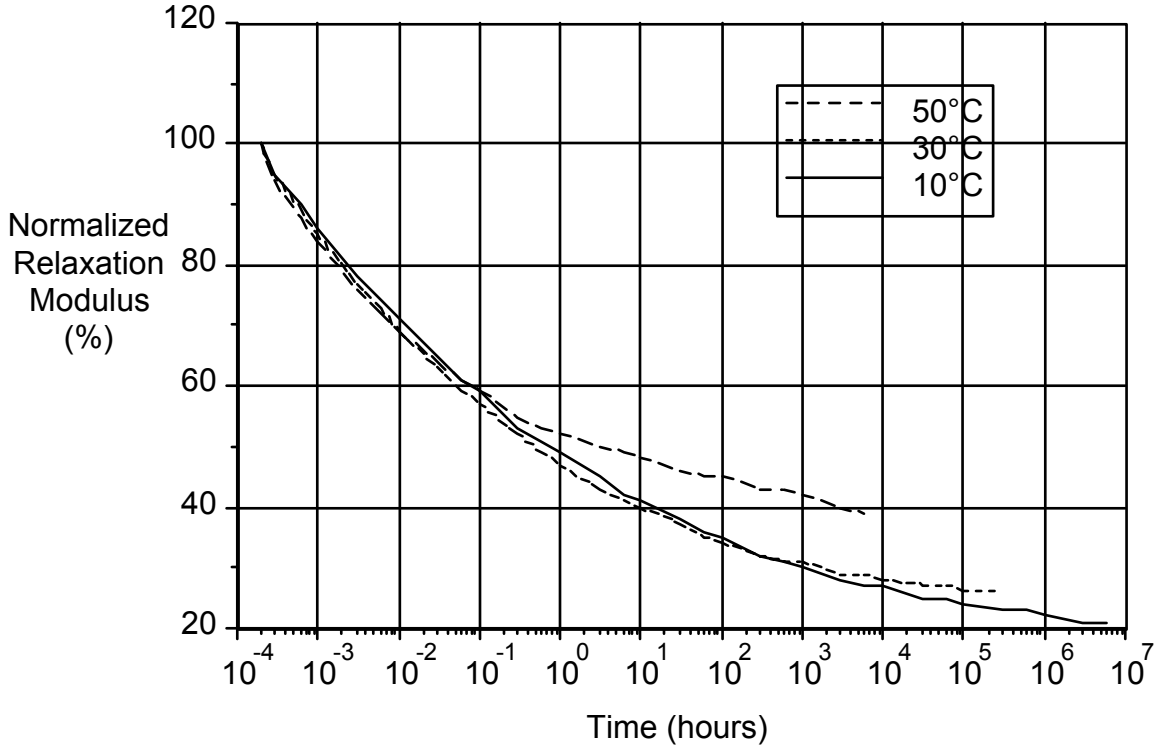

Figure A-30. Normalized master curves of the long-term stress relaxation behavior of HDPE GM at various temperatures.

Normalized stress relaxation behavior of HDPE GM at 10°C:

$$(\%\ \text{Relaxation}) = 51.4 + 8.9 \log(\text{time}) - 1.0 (\log(\text{time}))^2 + 0.05 (\log(\text{time}))^3 \quad \text{(A-1)}$$

Normalized stress relaxation behavior of HDPE GM at 30°C:

$$(\%\ \text{Relaxation}) = 53.0 + 8.4 \log(\text{time}) - 1.2 (\log(\text{time}))^2 + 0.07 (\log(\text{time}))^3 \quad \text{(A-2)}$$

Normalized stress relaxation behavior of HDPE GM at 50°C:

$$(\%\ \text{Relaxation}) = 48.0 + 5.3 \log(\text{time}) - 1.2 (\log(\text{time}))^2 + 0.19 (\log(\text{time}))^3 \quad \text{(A-3)}$$

A procedure for analyzing the stress induced in the GM wave is proposed as follows. Note that a worksheet, as shown in Table A-11, will be utilized to illustrate the procedure conceptually. Also note that the numerical expression for the stress relaxation behavior at 30°C, i.e., Equation A-2, will be used to analyze the results of experiments conducted at 23°C. As to the experiments conducted at 42 and 55°C, they will be analyzed using the expression for the behavior at 50°C, i.e., Equation A-3.

Table A-11. Elements of the Worksheet for the Stress Analysis of the Experimental Results

Time	Strain ε_I	Stress Induced During (t_i-t_{i-1}), σ_i	Relaxation Behavior of σ_{i0}	Relaxation Behavior of σ_{i1}	•••••	Residual Stress, σ_r
t_0	ε_0	$\sigma_{i0} = E^{\dagger} \times \varepsilon_0$				Summation of stress (horizontally)
t_1	ε_1	$\sigma_{i2} = E\times(\varepsilon_1-\varepsilon_0)$	$(1\text{-Eqn}^{*}(t_1-t_0)^{\S})\times\sigma_{i0}$			"
t_2	ε_2	$\sigma_{i2} = E\times(\varepsilon_2-\varepsilon_1)$	$(1\text{-Eqn}(t_2-t_0))\times\sigma_{i0}$	$(1\text{-Eqn}(t_2-t_1))\times\sigma_{i1}$		"
•	•	•	•	•	•	•
•	•	•	•	•		•
•	•	•	•	•		•
t_{n-1}	ε_{n-1}	•	•	•	••	•
		•	•	•		•
		•	•	•		•
t_n	ε_n	$\sigma_{i2} = E\times(\varepsilon_n-\varepsilon_{n-1})$	$(1\text{-Eqn}(t_n-t_0))\times\sigma_{i0}$	$(1\text{-Eqn}(t_n-t_1))\times\sigma_{i1}$	•••	"
•	•	•	•	•		•
•	•	•	•	•	••••	•
•	•	•	•	•		•
t_{f-1}	ε_{f-1}	•	•	•		•
		•	•	•	•••••	•
		•	•	•		•
t_{final}	ε_f	$\sigma_{if} = E\times(\varepsilon_f-\varepsilon_{f1})$	$(1\text{-Eqn}(t_f-t_0))\times\sigma_{i0}$	$(1\text{-Eqn}(t_f-t_1))\times\sigma_{i1}$	••••••	"

Notes: † Appropriate initial modulus value listed in Table A-10
• Equation A-3 for experiments conducted at 23°C
Equation A-4 for experiments conducted at 42 and 55°C
§ Replace the "time" terms in equations by the difference between the considered time and the corresponding stress induction time.

As seen in Table A-11, the stress induced between any two adjacent instants of time is determined via multiplying the differences in their corresponding strains by an appropriate initial modulus value, i.e., the values listed in Table A-10. Immediately after a stress is induced, the GM will start to relax according to the appropriate modeled behavior as expressed in Equations A-1, A-2 and A-3, depending on the temperature. This concept is illustrated in the fourth and subsequent columns of Table A-11. Finally, as seen in the last column of Table A-11, the instantaneous residual stress in the GM is

calculated by summing the remainder of all the discretized stresses corresponding to that particular time instant.

Three example calculations which illustrate the above stress analysis procedure are as follows. They are corresponding to the most critical strain measurements of three different 1,000 hour experiments and their extrapolations. Detailed information regarding these three experiments is summarized in Table A-12.

Table A-12. Example Used to Illustrate the Use of the Stress Analysis Procedure

Example	Thickness of GM (mm)	Original Wave Height (mm)	Normal Stress (kPa)	Temperature (°C)	Location where Strain is the Maximum
1	1.5	20	700	23	Near the base of the wave where the wave curvature changes to accommodate the horizontal subgrade
2	1.0	60	700	23	
3	1.5	60	700	55	

Example A-1

As shown in Table A-12, this particular experiment was conducted at 23°C. Hence, an initial modulus of 230 MPa and a relaxation behavior as expressed in Equation A-2 is used in this particular stress analysis. By inserting the strain data, along with the appropriate constant and expression, into a preestablished spreadsheet, the strain data is converted to stresses. The results are shown in Figure A-31, where strain and stress are plotted against time. Note that the incorrect “modulus times strain” curve is also shown in the figure to demonstrate the amount of stress relaxed over the entire duration of time.

As seen in Figure A-31, a stress of 3,700 kPa was induced immediately after the full load was applied to the wave specimen. Subsequently, through the phenomenon of stress relaxation along with the decreasing actual strain, the residual stress decreased approximately 2,000 kPa to 750 kPa after 10,000 hours.

Example A-2

As shown in Table A-12, this particular experiment was also conducted at 23°C. Hence, an initial modulus of 230 MPa and a relaxation behavior as expressed in Equation A-2 was used in this particular stress analysis. A similar procedure to that used in Example A-1 was carried out and the results are shown in Figure A-32.

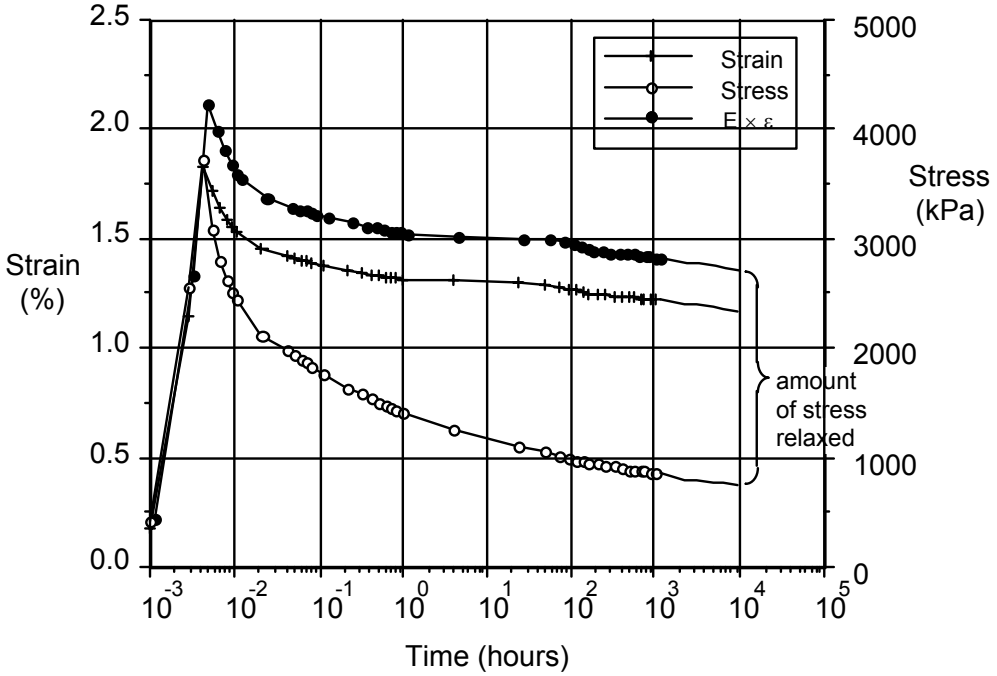

Figure A-31. Results of the stress analysis of example 1.

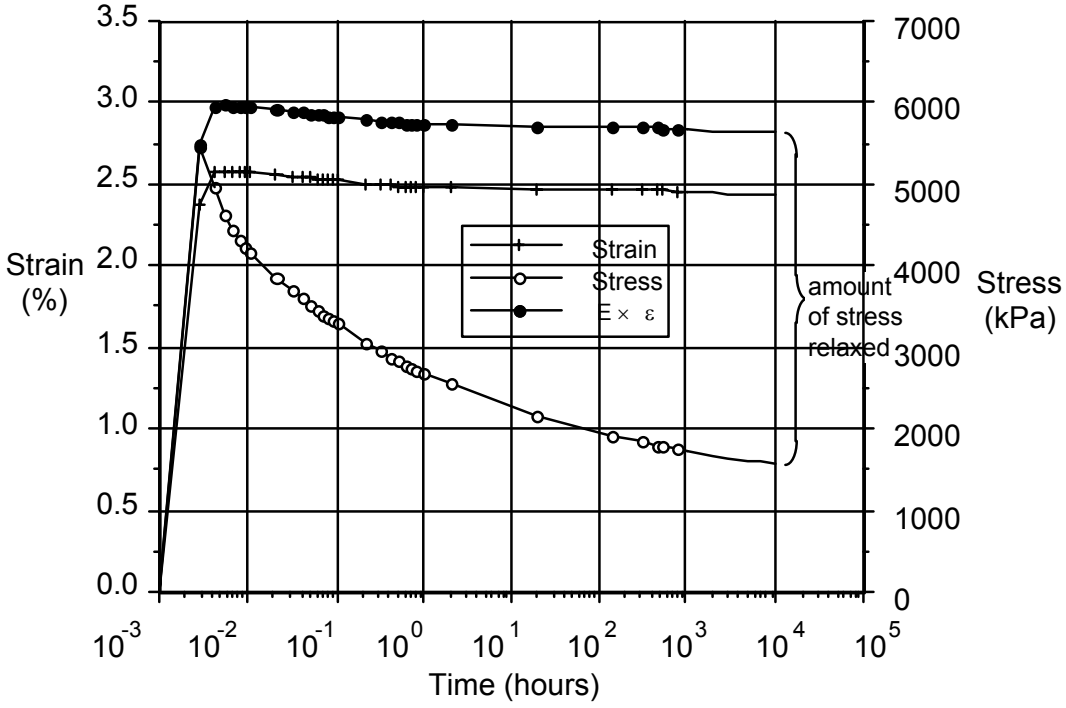

Figure A-32. Results of the stress analysis of example 2.

As seen in Figure A-32, a stress as high as 5,500 kPa was induced immediately after the full load was applied to the wave specimen. Although there was only a slight decrease in strain over the entire duration of time, a significant amount of stress was still relaxed via the general stress relaxation phenomenon. As shown in the figure, the residual stress decreased approximately 4,000 kPa to 1,500 kPa after 10,000 hours.

Example A-3

This experiment was started at 23°C and maintained at that temperature for one hour. The temperature was then increased from 23°C to 55°C. It took approximately nine hours for the entire experimental setup to reach equilibrium at 55°C. Hence, for analyzing strain data recorded during the initial one hour, an initial modulus of 230 MPa and a relaxation behavior as expressed in Equation A-2 was used. As for analyzing the strain data recorded at twelve hours and beyond, an initial modulus of 90 MPa and a relaxation behavior as expressed in Equation A-3 was used. Again, a similar procedure as that used in the previous two examples was carried out and the results are shown in Figure A-33.

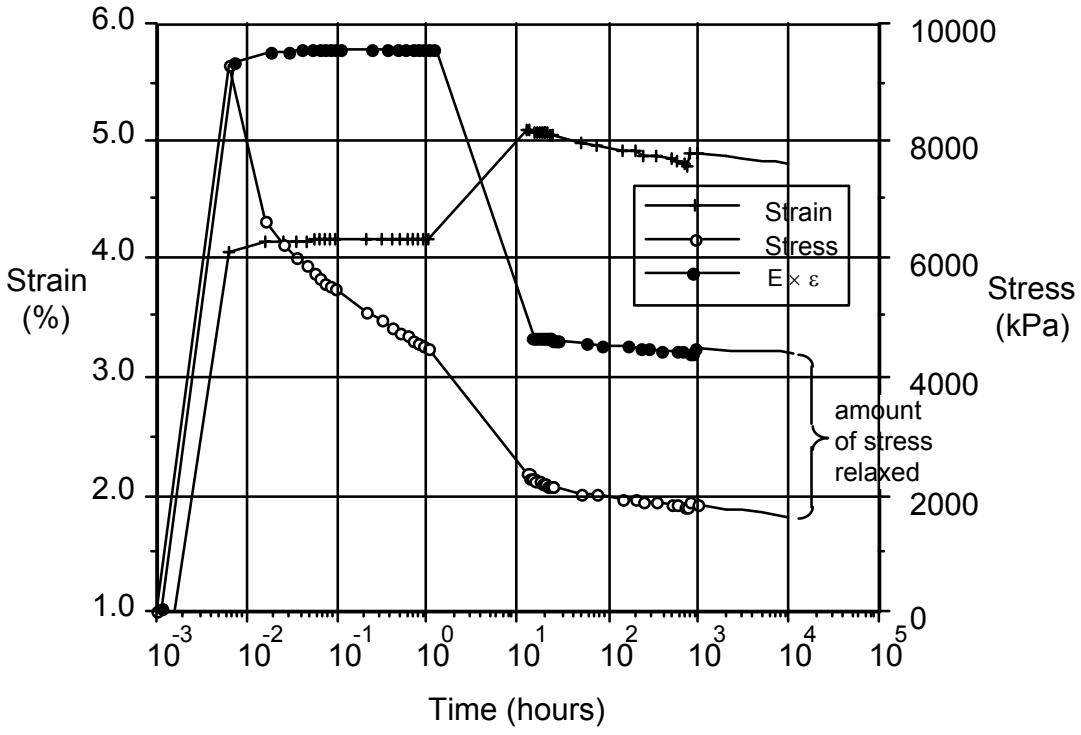

Figure A-33. Results of the stress analysis of example 3.

As seen in Figure A-33, a stress more than 9,000 kPa was induced immediately after the full load was applied to the wave specimen. During the initial one hour of the test, the stress relaxed to a residual value of approximately 4,500 kPa (i.e., 50% relaxation in

one hour). The effect of the subsequent increasing in temperature is clearly shown in both curves between one and twelve hours. Finally, at a relatively high temperature of 55°C, the residual stress decreased approximately 2,900 kPa to 1,600 kPa after 10,000 hours.

The same procedure as illustrated in these three examples was carried out for all twenty-five of the 1,000 hour experiments conducted in this study. Again, only the most critical strain measurement for each experiment was analyzed. The complete results all of analyses can be found in Soong (1996).

The residual stresses after 10,000 hours were also compared to the yield stress at the particular temperature of the respective test. The values of yield stress were obtained via tensile tests conducted at the appropriate corresponding temperatures. The test specimens were 1.5 mm thick HDPE GMs with a height of 50 mm and a width of 100 mm. The rate of extension used to conduct these tests was 12.7 mm/min (25%/min). The short-term, but temperature corrected, yield stresses of HDPE GMs were evaluated and are listed in Table A-13.

Table A-13. Yield stresses of HDPE GMs at various temperatures to be used in calculating the percent residual stresses to follow.

Temperature (°C)	Yield Stress (kPa)
23	15000
42	12000
55	9400

The entire procedure for obtaining the residual stress as a percentage of the yield stress is summarized in a flow chart format as shown in Figure A-34.

The results of the stress analysis, in terms of the residual stress after 10,000 hours, are summarized in Table A-14. Both the actual residual stress values and the percent of the yield stress are presented. Some observations are made and summarized in Table A-15.

A-6 Summary and Conclusions

In this appendix, the characteristics, fate, and behavior of waves of the type that are seen in field deployed GMs were evaluated. The entire task was laboratory oriented. However, full size waves were created, thus it is believed that scale effects did not significantly influence the test results. Due to their widespread use, the study focused on HDPE GMs. The effects of four important experimental variables on the different aspects of the behavior of the waves were evaluated. The variables are normal stress, original wave height, GM thickness, and temperature.

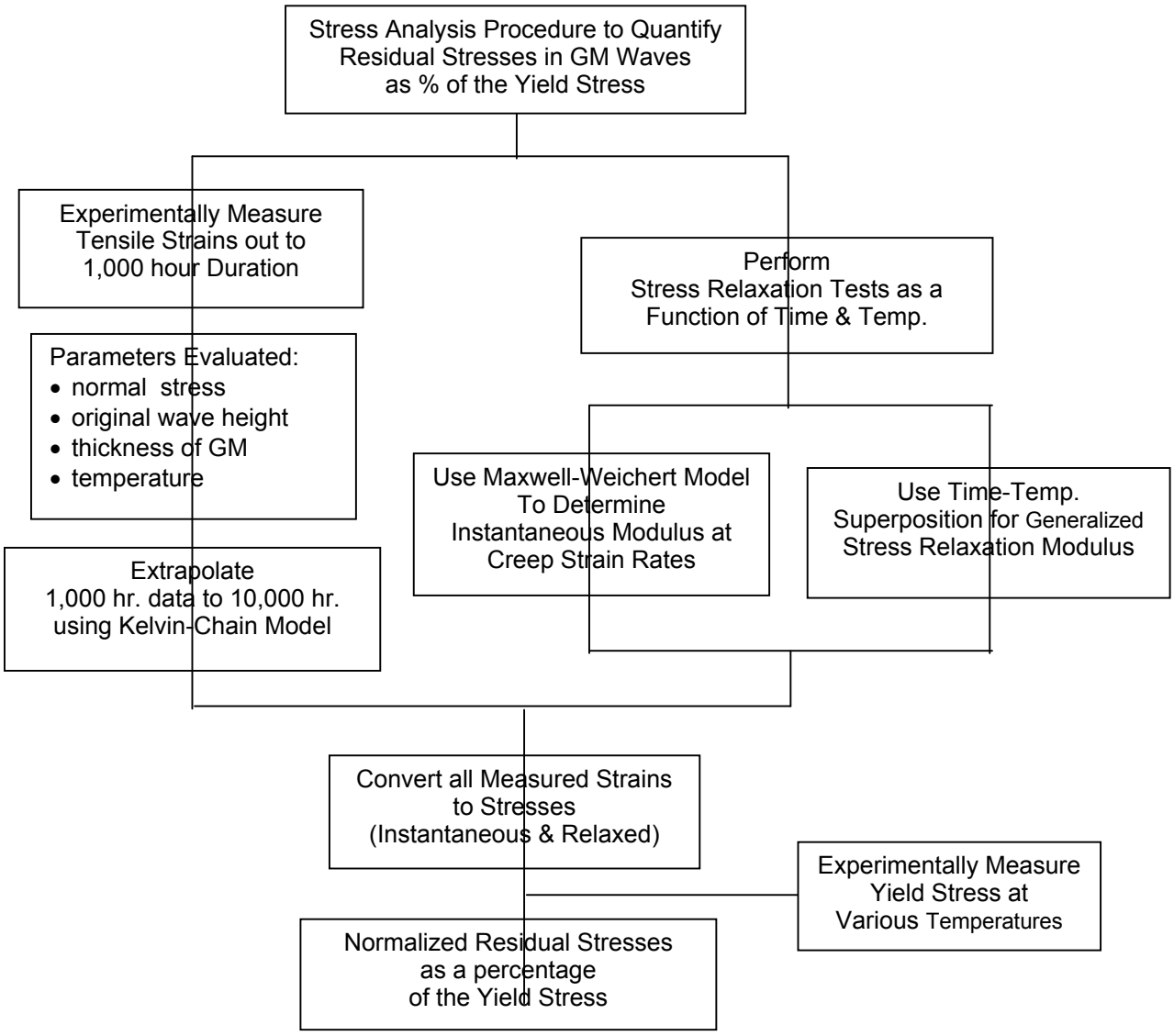

Figure A-34. Flow chart for the procedure of obtaining residual stresses in terms of percent yield stress.

The experimental design for this task represented 25 separate tests each conducted for 1,000 hours. In addition, a single control test was maintained for 10,000 hours (1.1 years). Each of the tests utilized HDPE GMs with strain gages attached at a number of critical locations. This enabled extensional strain to be monitored for the duration of the experiments. The results of the strain gage measurements on the 1,000 hour tests were then modeled and extrapolated one order of magnitude to 10,000 hours using the Kelvin-chain model. The applicability of using the Kelvin-chain model was established

on the basis of the experimental results of the 10,000 hour control test. The other important rheologic model presented in this study is the Maxwell-Weichert model. It is an analytic model that was calibrated using the results of large-scale stress relaxation experiments. The Maxwell-Weichert model was used to predict the stress relaxation behavior of the modeled material at a range of temperatures. In addition, the initial portion of the stress/strain relationships of the modeled material at slow strain rates was also predicted. As a result of combining both predictions, the design modulus of HDPE GMs at various temperatures was determined. By incorporating the generalized stress relaxation behavior with such design modulus values, the measured strains were converted into tensile stresses. These stresses were then expresses as a percent of the tensile yield stress of the GM.

Table A-14. Residual stress (after 10,000 hours) in the HDPE GM specimens of experiments conducted in this study.

Experimental Parameter and Variables		Residual Stress (kPa)	Residual Stress (% of Yield)
Normal Stress	180 kPa	1200	7.9
	360 kPa	1300	8.8
	700 kPa	2000	13.2
	1100 kPa	2100	13.8
Original Height of Wave	14 mm	130	0.8
	20 mm	740	4.9
	40 mm	1500	9.5
	60 mm	2000	13.2
	80 mm	2300	14.9
Thickness of GM	1.0 mm	1600	10.3
	1.5 mm	2000	13.2
	2.0 mm	1600	10.6
	2.5 mm	1800	11.5
Testing Temperature	23°C	130	0.8
	14 mm - 42°C	250	2.1
	55°C	440	4.5
	23°C	740	4.9
	20 mm - 42°C	850	7.3
	55°C	750	8.0
	23°C	1500	9.5
	40 mm - 42°C	1600	13.7
	55°C	690	7.4
	23°C	2000	13.2
	60 mm - 42°C	2600	22.0
	55°C	1600	17.5

Table A-15. Effects of the Variables Evaluated in this Study on Residual Stress After 10,000 hours of HDPE GM Wave Experiments

Experimental Variable	Observations
Normal Stress	• Residual stress after 10,000 hours increases approximately linearly with increasing normal stress • Residual stress (% of yield) $\cong$ 6.8 + 7 σ_n where σ_n = normal stress in MPa
Original Height of Wave	• Residual stress after 10,000 hours increases logarithmically with increasing original wave height • Residual stress (% of yield) $\cong$ 18 log (OH) - 30 where OH = original wave height in mm
Thickness of GM	• Thickness of GMs has no effect on variation of the residual stress
Testing Temperature	• Residual stress increases approximately linearly with increasing temperature - for waves originally shorter than 40 mm • Residual stress shows no clear trend with increasing temperature - for waves originally higher than 40 mm

The completed laboratory tests and the associated extrapolated results for 10,000 hours were evaluated and a number of observations were developed. These observations are subdivided according to the physical manifestation of the wave and its long-term stress condition.

<u>Regarding the original wave heights (which varied from 14 to 80 mm):</u>

- wave height decreased with increasing normal stress;
- an average reduction in wave heights of 40% was observed after 1,000 hours;
- GM thickness had a negligible effect on the decrease in wave height with normal stress;
- there was a slight decrease in wave height with increasing temperature;
- final wave heights varied from 5 to 47 mm after 1,000 hours; and
- intimate contact with the soil subgrade was not achieved after 1,000 hours, even for the smallest wave (14 mm) at the highest testing temperature.

<u>Regarding the original H/W values for the waves (which varied from 0.17 to 0.33):</u>

- H/W increased with increasing normal stress;
- H/W increased approximately linearly with increasing original wave height;
- H/W decreased approximately linearly with increasing GM thickness;

- H/W decreased slightly with increasing temperature; and
- final H/W values recorded from all experiments varied from 0.14 to 0.65 after 1,000 hours.

Regarding the tensile strains measured at the end of the 1,000 hour experiments along the top of the GM near the crest of the wave and the bottom of the GM near the inflection points of the wave at its sides:

- strains at the maximum point of curvature of the waves increased approximately linearly with increasing normal stress;
- strains at the maximum point of curvature of the waves increased logarithmically with increasing original wave height of the waves;
- strains at the maximum point of curvature of the waves increased linearly with increasing GM thickness;
- strains at the maximum point of curvature of the waves increased with increasing testing temperatures for waves originally shorter than 40 mm;
- strains at the maximum point of curvature of the waves showed no clear trend with increasing testing temperatures for waves originally higher than 40 mm;
- maximum recorded from all experiments varied from 3.2% to approximately 4.9% after 1,000 hours.

Regarding the residual tensile stresses after the 1,000 hour experiments which were then extrapolated to 10,000 hours:

- residual tensile stress at the points of maximum curvature increased with increasing normal stress;
- residual tensile stress at the points of maximum curvature increased with increasing original wave height;
- thickness of the GM had essentially no effect on the residual tensile stresses;
- residual tensile stresses increased with increasing testing temperature for waves originally shorter than 40 mm;
- residual tensile stresses showed no clear trend with increasing testing temperature for waves originally higher than 40 mm; and
- residual tensile stresses recorded from all experiments varied from 130 kPa (approximately 1% of the yield stress) to 2,600 kPa (approximately 22% of the yield stress).

Based on the test results and the observations given above the following conclusions are provided:

- GM waves, which are induced in the field during placement and seaming of GMs, distort upon the application of even a small normal stress. The distortion typically increases the height-to-width ratio of the wave.
- The maximum tensile strain measured in this series of twenty-five 1,000-hour tests was approximately 5%. Note that yield of HDPE GMs is in the range of 15

to 25% strain (depending on the temperature), thus yielding of the GM was not observed in the tests.

- The maximum tensile stresses occur at locations of maximum tensile strain. These locations are on the side of the GM that undergoes extension, i.e., along the upper surface of the wave near its crest and along the lower surface where the wave curvature changes to accommodate the horizontal subgrade beneath the wave.
- Based on an extrapolation to 10,000 hours to account for polymer stress relaxation, residual tensile stresses in the GM waves varied from 1% to 22% of the GM short-term tensile yield stress.
- Over the 1,000-hour experimental time of stress application for the main series of tests, the waves did not appear to significantly decrease, much less disappear.
- It is important to note that this study did not address the potential effects of the waves on liquid flow in lateral drainage layers above the GM, on liquid migration through the GM, or on the estimated GM service life.

A-7 Recommendations for the Field Placement of GMs

As illustrated in the Section A-1, the current practice of field placement of GMs in North America is to install the GM with a certain amount of slack. The concept is that the majority of the slack will be removed when the GM is covered and the temperature of the GM is reduced from its exposed temperature during installation and seaming. The goal is that when the long-term steady-state temperature is reached during the GM's in-situ service life, the slack will be completely removed as a result of thermal contraction and, therefore, intimate contact by the GM with the subgrade will be achieved. Many construction quality assurance (CQA) documents in current practice include statements referring to slack in the GM. For example, in EPA (1993), it states "The GM shall have adequate slack such that it does not lift up off the subgrade or substrate material at any location within the facility, i.e., no "trampolining" of the GM shall be allowed to occur at any time."

As a result of such statements, informal rules have been developed by some for the deployment of HDPE GMs. One such informal rule is that the height of GM wave must be such that it does not fold over on itself during backfilling; another informal rule is that the height-to-width ratio of the installed GM wave should not be greater than 0.5. The implicit assumption in allowing such waves is that the subsequent decrease in temperature, along with the creep and stress relaxation inherent in the GM, will eventually remove the waves and reduce residual stresses to negligible levels.

However, the experimental and analytic work presented in this study brings into question the acceptability of these informal rules. It was shown in this study that the dissipation of waves that typically occur in GM liners under current installation procedures is only nominal and much of the original wave remains over time. The implication is that contact with the subgrade material should not be expected to be

achieved, even with relatively small waves having an original height of 14 mm. This was the smallest wave evaluated in this study.

The results of this study show that if waves are to be avoided, the GM must be essentially flat on the underlying subgrade before backfilling. Waves having small heights, e.g., less than 14 mm, might be acceptable for wet clay subgrades, providing the underlying clay is soft enough so the normal stress can “deform” the adjacent wet clay into the void that is created beneath the wave. Further study in this regard is needed. Based on this task, however, the size of such waves is likely to be very small, e.g., 5 mm or less.

Even after accounting for the stress relaxation that occurs over 10,000 hours, a significant amount of tensile stress still remains in GM waves. Such tensile stress could shorten the service life of a GM in comparison to GMs that are installed flat on the subgrade. As already noted, this issue was not evaluated as part of the current study.

One possible GM installation option to mitigate the potential negative consequences of GM waves is to deploy and seam the GM without slack. This installation procedure has found increasing application in Germany. With this procedure, as the liner cools during the night, it develops tensile stress due to restrained thermal contraction. The following day, the temperature again rises and the GM is covered with soil at approximately the same temperature that it was seamed. In this way, contact with the subgrade is achieved with only nominal tensile stress in the GM. Unfortunately, subsequently induced thermal stresses, if any, will not be dissipated through the phenomenon of stress relaxation. This was shown by Lord et al. (1995). Moreover, experiments showed that going from high installation temperature, e.g., 40°C, to low final service temperature, e.g., 25°C, can induce tensile stresses as high as 1,000 kPa, see Soong (1996) for details.

It is suggested that a balance must be achieved so as to achieve contact with the subgrade while only inducing a nominal amount of tensile stress in the GM. This nominal amount of tensile stress is subjective at this time, Hsuan et al (1993). Studies are ongoing in this regard. This balance may require some, or all, of the following changes in the current practice of field deployment and seaming of GMs used in landfill liner applications.

1. GMs having light colored (e.g., white) surfaces can be used to advantage in decreasing the surface temperature of the GMs while exposed, hence the height of the waves will be smaller (Koerner and Koerner, 1995).
2. GMs should be deployed and seamed without intentional slack. However, installation should be carried out at a temperature as close to the coolest part of the day as possible. After the covering GT is placed, if one is required, the periphery of the seamed area can be ballasted with cover soil.

3. If a GT covering is not required, placement of an overlying light colored temporary GT may be necessary. This can prevent the GM from being exposed to direct sunlight before backfilling occurs.
4. Backfilling should be performed only in the coolest part of the day. Quite possibly, it might have to be placed at night.

The above procedures will help considerably in gaining contact between the GM and the underlying subgrade. Since the GMs should only experience small decreases in temperature between installation, backfilling, and in-situ service conditions, the induced tensile stresses should be able to be accommodated with a properly selected stress-crack resistant GM.

A-8 References

EPA (1993), Technical Guidance Document, "Quality Assurance and Quality Control for Waste Containment Facilities", EPA/600/R-93/182, September.

Giroud, J.P. and Morel, N. (1992), "Analysis of Geomembrane Wrinkles", *Journal of Geotextiles and Geomembranes*, Vol. 11, No. 3, pp. 255-276 (Erratum: 1993, Vol. 12, No. 4, p 378).

Giroud, J.P. (1995), "Wrinkle Management for Polyethylene Geomembranes Requires Active Approach", *Geotechnical Fabrics Report*, Vol. 13, No. 3, pp. 14-17.

Hsuan, Y.G., Koerner, R.M. and Lord, A.E. Jr. (1993), "Notched Constant Tensile Load Test (NCTL) for High Density Polyethylene Geomembranes", *Geotechnical Testing Journal*, GTJODJ, Vol. 16, No. 4, December, pp. 450-457.

Koerner, R.M. (1998), *Designing with Geosynthetics*, 4th ed. New Jersey: Prentice Hall Inc.

Koerner G.R. and Koerner R.M. (1995), "Temperature Behavior of Field Deployed HDPE Geomembranes" *Proceedings Conference on Geosynthetics*, Nashville, TN, IFAI, pp. 921-937.

Lord, A.E., Jr., Soong T.-Y. and Koerner, R.M. (1995), "Relaxation Behavior of Thermally-Induced Stress in HDPE Geomembranes", *Geosynthetics International*, Vol. 2, No. 3, pp. 626-634.

Schultz, D.W. and Miklas, M.P. Jr., (1980), *Proceedings Disposal of Hazardous Waste*, EPA-600/9-80-010, March, pp. 135-159.

Soong, T.-Y., Lord, A.E., Jr. and Koerner, R.M. (1994), " Stress Relaxation Behavior of HDPE Geomembranes", *Proceedings 5th International Conference on Geotextiles, Geomembranes and Related Products*, Singapore, pp. 1121-1124.

Soong T.-Y. (1995), "Effects of Four Experimental Variables on the Stress Relaxation Behavior of HDPE Geomembranes" *Proceedings Conference on Geosynthetics*, Nashville, TN, IFAI, pp. 1139-1147.

Soong, T.-Y. (1996), "Behavior of Waves in HDPE Geomembranes," Ph.D. Thesis, Drexel University, Philadelphia, PA.

Appendix B
Antioxidant Depletion Time in High Density Polyethylene Geomembranes

by

Robert M. Koerner, Ph.D., P.E.
Drexel University
Philadelphia, PA 19104

Grace Hsuan, Ph.D.
Geosynthetic Research Institute
Philadelphia, PA 19104

performed under

EPA Cooperative Agreement Number
CR-821448-01-0

Project Officer

Mr. David A. Carson
United States Environmental Protection Agency
Office of Research and Development
National Risk Management Research Laboratory
Cincinnati, OH 45268

Appendix B
Antioxidant Depletion Time in High Density Polyethylene Geomembranes

B-1 Introduction

High density polyethylene (HDPE) geomembranes (GMs) have been used extensively as barrier materials in waste containment applications, e.g., landfills, surface impoundments, and waste piles. The required service lifetime of such GMs varies according to the type of waste, the sensitivity of the local environment, the stipulated regulations (if any), and other factors. Service timeframes that have been considered for landfills have typically fallen into the following ranges:

- regulatory minimum (post closure) = 30 years
- typical nonhazardous waste = 50 - 200 years
- hazardous/low level radioactive waste = 200 - 1000 years

Ideally, the service life of a GM should be at least equal to the service life of the landfill structure. Thus, it is important to be able to quantify the anticipated service lifetime of GMs used in waste containment applications.

The most direct way to assess service lifetime is to use information obtained from GMs that have been installed at actual landfills. However, the first generation of HDPE GM lined waste facilities is only about 20 to 25 years old. The available information suggests that 20-year old HDPE GMs continue to perform in a manner consistent with their as-installed properties. An alternative approach is needed to estimate GM service life beyond the 20 to 25 year timeframe. In this appendix, the results of a set of laboratory tests are presented and described. The results are used to develop estimates of the service lifetime of HDPE GMs.

The laboratory testing described herein involves aging the GM samples under an environment that is designed to simulate actual field conditions. The reaction rate that causes the degradation of the samples under such test conditions is accelerated by incubating the samples at elevated test temperatures. This results in an aging of the samples in a relatively short period of time, i.e., a few years under accelerated conditions in comparison to perhaps hundreds of years under actual site conditions. The degradation data from such elevated temperature testing can then be extrapolated to predict the lifetime at a site specific ambient temperature by using the Arrhenius method.

It should be emphasized that this appendix focuses on GMs that are covered or backfilled in a "timely manner". Covering with another geosynthetic material or backfilling with soil is necessary to protect the GMs from ultraviolet (UV) degradation which is not considered in this task. Furthermore, the surface temperatures of GMs that are exposed to sunlight are invariably much higher than the applications to which this study on covered GMs is directed.

Note that this report focuses on lifetime of the antioxidants which are part of a HDPE GM formulation. Subsequent stages of the total lifetime of the GM are induction time and the onset of physical/mechanical property degradation. Due to the long term nature of the incubation processes (up to 10 years), only the first stage of antioxidant depletion time is reported in this appendix. An example of the entire sequence of the three stages of the long-term aging process of GMs was given in Section 2.5 of the main report.

B-2 Formulation, Compounding and Fabrication of HDPE GMs

Before going into a discussion on the long term aging mechanisms of HDPE GMs, the various steps of producing HDPE GMs will be explained. The components to be formulated, their compounding, and finally the manufacturing process are described in this section.

The components of an HDPE GM consist of 96 to 97.5% polyethylene (PE) resin, 2 to 3 % carbon black, and 0.5 to 1.0% antioxidants. It should be recognized that HDPE GMs are actually manufactured using PE resin with a density between 0.932 and 0.940 g/cc. This resin density is classified as medium density PE according to ASTM D 883. The addition of carbon black and antioxidants, however, increases the formulated density of the product to a range between 0.941 and 0.950 g/cc which is defined as HDPE in ASTM D 883. Therefore, the conventional term used in the industry of "HDPE" will be used.

- PE - The resin used for HDPE GMs is a linear copolymer which is produced by using ethylene and α-olefin as comonomer under low pressure and the appropriate type of catalyst. The amount of α-olefin has a direct effect on the density of the resin; a greater amount of α-olefin added in the polymerization yields a lower density PE polymer.

- Carbon black - Carbon black is added into a HDPE GM formulation mainly for UV light stabilization. The loading range of carbon black in GMs is typically 2 to 3% by weight per ASTM D 1603. Up to the level of opacity, the higher the loading of carbon black, the greater is the degree of UV light stability. However, the addition of carbon black above the opacity level (which is around 3%) will not further improve UV resistance (Accorsi and Romero, 1995).
- Antioxidants - Antioxidants are introduced to an HDPE GM formulation for the

purposes of oxidation prevention during high temperature extrusion and to improve the product long-term service life. There are a number of types of antioxidants used in GM manufacture and each of them has unique functional characteristics. Usually, synergistic mixtures of antioxidants of more than one type are used. Although the total amount of antioxidants in the GM is relatively small, less than 1%, their presence is vital to achieving the desired product service life. Note that this aspect of antioxidant depletion, and the corresponding time to depletion, is the subject of this appendix.

The compounding methods that are used to mix the three components (PE resin, carbon black and antioxidants) vary from manufacturer to manufacturer. Three different methods can be utilized. They are as follows:

- GM Manufacturers Perform Their Own Mixing:
  GM manufacturers can purchase pure PE resin that contains no carbon black nor antioxidants from resin producers. They then purchase carbon black powder and antioxidants from their respective suppliers. The appropriate amounts of these three ingredients are mixed in an extruder, forming pellets that consist of the proper proportion of each component. These stabilized pellets are then transferred to another extruder for GM production.

- Let-down From Concentrated Carbon Black Pellets:
  GM manufacturers can purchase PE resin that contains antioxidants only. Separately, they then purchase concentrated carbon black pellets consisting of approximately 25% carbon black in a PE resin carrier which is the same generic type as the parent PE resin. During the production of the GMs, the exact proportion of PE resin/antioxidant pellets and concentrated carbon black pellets are added to the extruder, resulting a product with the proper proportion of each component.

- Completely Formulated Pellets:
  GM manufacturers can purchase pellets that consist of the proper proportion of PE resin, carbon black and antioxidants. The completely formulated pellets go directly to the extruder for GM production.

Upon using a large extruder to mix, melt and filter the resin pellets into a flowing viscous mass, there are two major processes used for manufacturing HDPE GMs. Their differences are at the exit section of the extruder which is some type of die. One process is flat sheet extrusion wherein a flat die (or “coathanger die”) is utilized. The other process is blown film wherein a circular die is used. Struve (1994) explains the details of the two processes.

- Flat die extrusion:
  Flat dies used in the GM extrusion process are configured with adjustable lips from where the polymer sheet exits. By adjusting the die lips (manually or automatically),

the thickness of the GM can be accurately controlled. Figure B-1(a) is a schematic diagram of center fed flat die. The molten polymer from the extruder enters centrally into the die and spreads horizontally in both directions. On exiting, the somewhat cooled polymer sheet is deposited onto a series of chilled rolls. For the production of a very wide sheet, two side by side coathanger dies can be joined together, see Figure B-1(b). The molten polymer in each side of the die is supplied from separate extruders. The two melt streams commingle together within the die. Again, the somewhat cooled polymer sheet is deposited onto a series of chilled rolls. After further cooling, the GM sheet is rolled onto a core for shipment and placement.

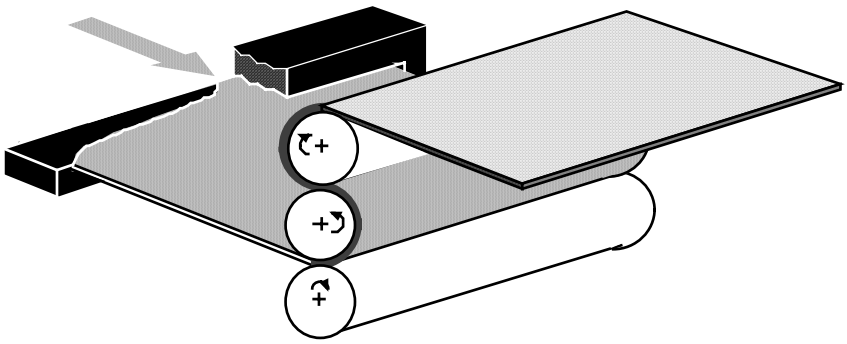

Figure B-1(a). Flat die extrusion process to manufacture GM (Struve, 1994).

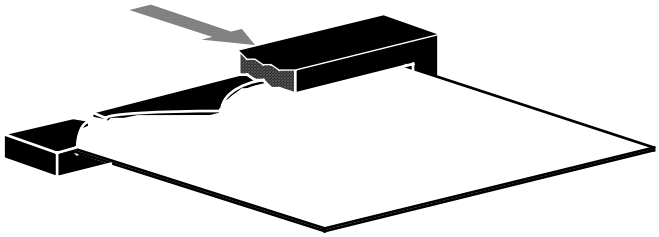

Figure B-1(b). Dual flat die extruders used to manufacture wide GMs (Struve, 1994).

- Blow film extrusion:
  Circular dies are also utilized in the extrusion process of manufacturing PE GMs. They are oriented such that the polymer exits the die vertically. The molten polymer supplied from the extruder enters into an annular chamber through a number of symmetrically radial feed ports. As the somewhat cooled polymer exits the die, a large cylinder of GM is formed, as can be seen in Figure B-2. The cylinder is closed at the top where it passes between a set of nip rollers which draws the GM up and away from the die. The dimensional stability of the cylinder is provided by internal and external air pressure. After the material passes through the nip rollers, the collapsed cylinder is cut longitudinally, opened to form a full width of GM sheet and rolled onto a core for shipment and placement.

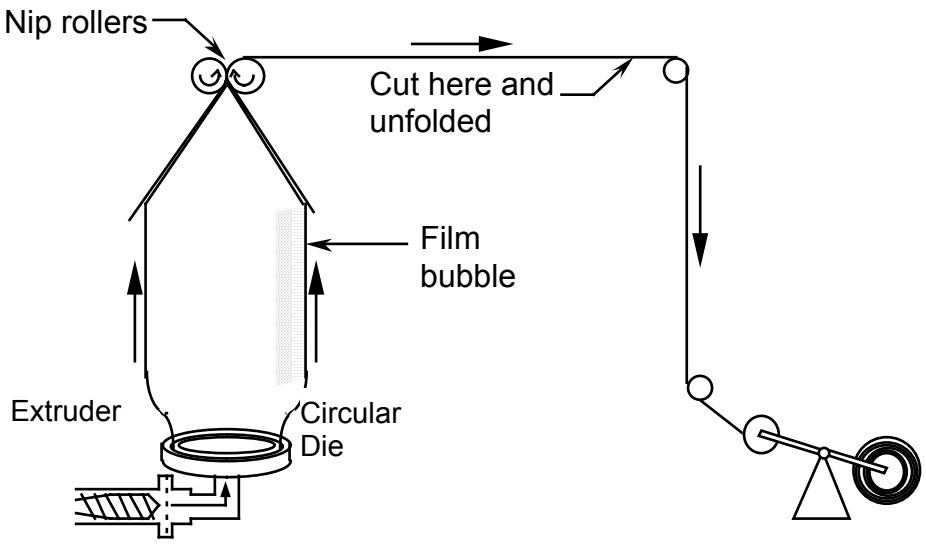

Figure B-2. Blow film extrusion process used to manufacture PE GMs.

B-3 Stages of Degradation in HDPE GMs

After proper placement of the GM sheets and seaming into a liner system, the GM will hopefully serve as a barrier for many years. During the service period, aging takes place in the GM. The aging process of HDPE GMs can be considered to be a combination of: physical aging and chemical aging. Both aging mechanisms take place simultaneously. Physical aging implies a slow processes in which the material attempts to establish equilibrium from its as-manufactured nonequilibrium state. For semi-crystalline polymers like HDPE, the process involves changes in the crystallinity of the material (Petermann et al., 1976). Under this definition of physical aging there are no primary (covalent) bonds broken.

On the other hand, chemical aging indicates some type of degradation involving the breaking of covalent bonds, e.g., thermal-oxidation, radioactive-degradation, etc., (Struik, 1978). This process eventually leads to a reduction in engineering properties. Therefore, from an applications point of view, chemical aging is the important degradation mechanism and should be studied in great detail. In the following sections the different stages of chemical aging in HDPE GMs are described.

Conceptually, the chemical aging process of a HDPE GM can be considered to consist of three distinct stages. They can be seen in Figure B-3. These three stages are designated as (a) depletion time of antioxidants, (b) induction time to the onset of polymer degradation and (c) degradation of the polymer to decrease some engineering property(s) to an arbitrary level, e.g., to 50% of its original value.

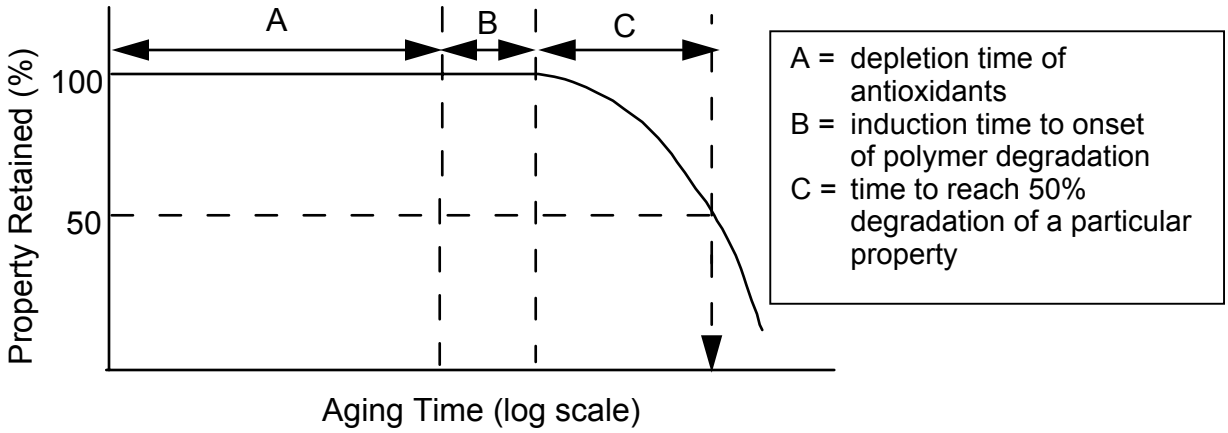

Figure B-3. The three conceptual stages in chemical aging of HDPE GMs.

B-3.1 Depletion of Antioxidants

The purpose of antioxidants in a HDPE GM formulation is to prevent degradation during processing and to prevent oxidation reactions taking place during the first stage of service life. However, there is only a limited amount of antioxidants in the formulation. Hence, the lifetime for this stage is also limited. Once the antioxidants are completely depleted, oxygen will begin to attack the polymer, leading to the induction time and subsequently the deterioration of performance properties. The duration of this antioxidant depletion stage depends strongly on the type of selected antioxidants. Since many different antioxidants can be selected, depletion time can vary from formulation to formulation, subsequently affecting the lifetime of the GM. Proper selection, however, will be seen to contribute greatly to the overall lifetime of the GM.

The depletion of antioxidants may be consequence of two processes: chemical reactions of the antioxidants, and physical loss of the antioxidants from the polymers. In addition, the rate of depletion is related to the type of antioxidants, to the service temperature, and to the nature of the site specific environment. Regarding the chemical reactions of antioxidants, two main functions are involved: the scavenging of free radicals, converting them into stable molecules, and the reaction with unstable hydroperoxide (ROOH) forming a more stable substance. Regarding their physical loss, the process involves the distribution of antioxidants in the GM and their volatility and extractability. Since antioxidants are the main subject of this appendix, a detailed investigation of these two processes will be presented in Section B-5.

B-3.2 Induction Time

In a pure PE resin, i.e., one with no carbon black and antioxidants, oxidation occurs extremely slow at the beginning; often immeasurably slow. However, at the end of this period acceleration occurs more rapidly. Eventually, the reaction decelerates and once

again becomes very slow. This progression is illustrated by the curve in Figure B-4(a). The initial portion of the curve (before measurable degradation takes place) is called the induction period (or induction time) of the polymer.

In a stabilized polymer such as one with antioxidants, the acceleration stage takes a considerably longer time to reach. The antioxidants create an additional depletion time stage prior to the onset of the induction time, as shown in Figure B-4(b).

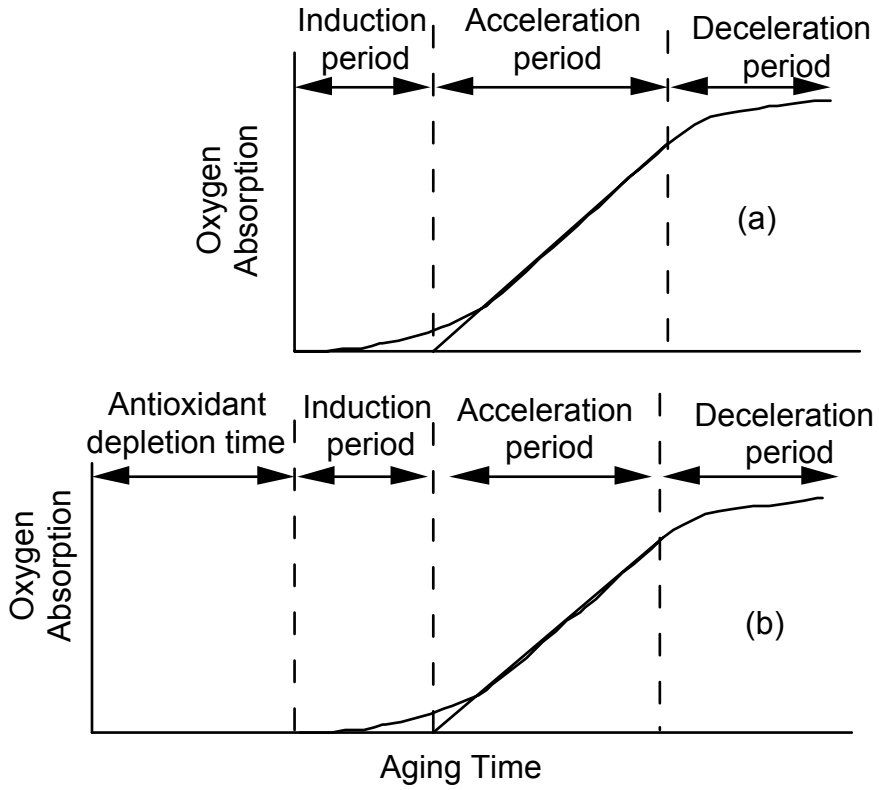

Figure B-4. Curves illustrating the various stage of oxidation: (a) unstabilized PE, (b) stabilized PE.

Regarding the chemical process, the first step of oxidation in an unstabilized PE is the formation of free radicals. The free radicals subsequently react with oxygen and start chain reactions. The reactions are described in Eqs. B-1 to B-6 (Grassie and Scott, 1985).

Initiation stage:

$$RH \rightarrow R\bullet + H\bullet \text{ (under energy or catalyst residues)} \quad \text{(B-1)}$$

$$R\bullet + O_2 \rightarrow ROO\bullet \quad \text{(B-2)}$$

Propagation stage:

$$ROO\bullet + RH \rightarrow ROOH + R\bullet \quad \text{(B-3)}$$

Acceleration stage:

$$ROOH \rightarrow RO\bullet + OH\bullet \text{ (under energy)} \quad \text{(B-4)}$$

$$RO\bullet + RH \rightarrow ROH + R\bullet \quad \text{(B-5)}$$

$$OH\bullet + RH \rightarrow H_2O + R\bullet \quad \text{(B-6)}$$

(where: RH represents the PE polymer chains, the symbol "•" represents free radicals which are highly reactive.)

In the induction period, little hydroperoxide (ROOH) is present and when formed it does not decompose. Thus, the acceleration stage of the oxidation cannot be achieved. As oxidation propagates slowly, additional ROOH molecules are formed. Once the concentration of ROOH reaches a critical level, decomposition of ROOH begins and accelerated chain reactions begin, signifying the end of the induction period (Rapoport and Zaikov, 1986). This indicates that the concentration of ROOH has a major effect on the duration of the induction period.

Viebke et al. (1994) have studied the induction time of an unstabilized medium-density PE pipe. The pipes were internally pressure tested with stagnant water and externally by circulating air at temperatures ranging from 70 to 105 °C. They found the activation energy of oxidation in the induction period to be 75 KJ/mol. Using their experimental values, an induction time of 12 years can be extrapolated at a temperature of 25°C for the material evaluated.

B-3.3 Material Property Degradation

The end of the induction period signifies the onset of relatively rapid oxidation. This is because the free radicals increase significantly via the decomposition of ROOH, as indicated in Eqs. B-4 to B-6. One of the free radicals is an alkyl radical (R•) which represents polymer chains that contain a free radical. In the early stage of acceleration, cross-linking occurs in these alkyl radicals due to oxygen deficiency. The reactions involved are expressed by Eqs. B-7 and B-8. The physical and mechanical properties of the material subsequently respond to such molecular changes. The most noticeable change is in the melt index, since it relates to the molecular weight of the polymer. In this stage, a lower melt index value is detected. In contrast, the mechanical properties do not seem to be very sensitive to cross-linking. The tensile properties generally remain unchanged or are unable to be detected.

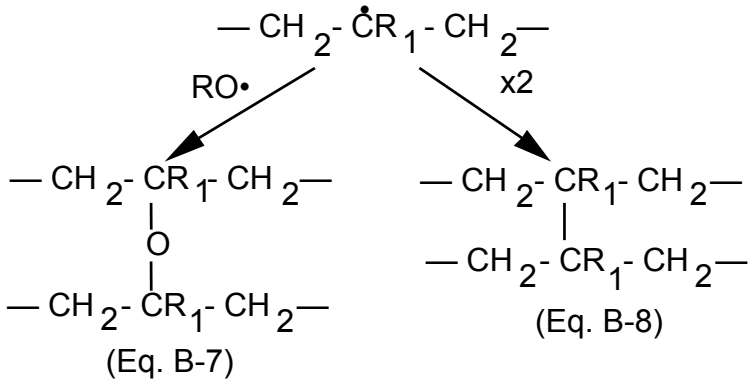

As oxidation proceeds further, and abundance of oxygen becomes available, the reactions of alkyl radicals change to chain scission. This causes a reduction in molecular weight, as shown in Eqs. B-9 and B-10. In this stage, the physical and mechanical properties of the material change according to the extent of the chain scission. The melt index value reverses from the previous low value to a value higher than the original starting value signifying a decrease in molecular weight. As for tensile properties, break stress and break strain decrease. Tensile modulus and yield stress increase and yield strain decrease, although to a lesser extent. Eventually, the GM becomes so brittle that all tensile properties change significantly and the engineering performance is jeopardized. This signifies the end of the so-called “service life” of the GM.

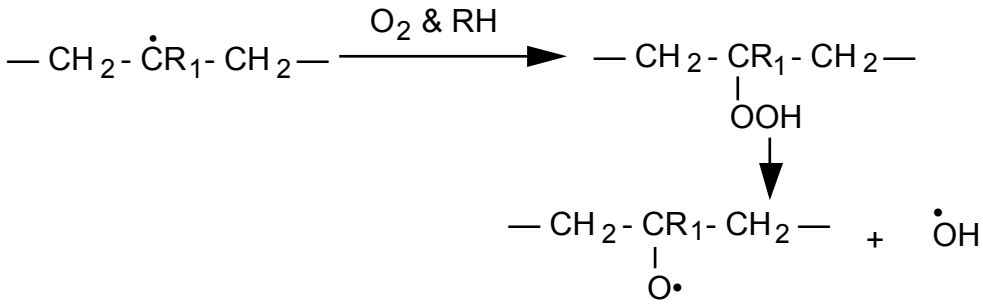

(B-9)

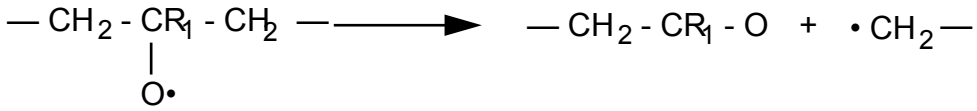

(B-10)

Although quite arbitrary, the limit of service life of a GM is often selected as a 50% reduction in a specific design property. This is commonly referred to as the half-lifetime, or simply the *halflife*. The specific property could be tensile modulus, break stress,

break strain, impact strength, etc. It should be noted that even at halflife the GM still exists and can function albeit at a decreased performance level.

Hence, the lifetime of a GM will be equal to the depletion time of antioxidants, plus induction time of the polymer, plus the time to reach a 50% reduction in a specific engineering property. Graphically this was shown in Figure B-3 as the sum of “A”, “B” and “C”.

B-4 Major Influences on Oxidation Behavior

There are many aspects of the polymer resin, its formulation, the ambient environment and its service conditions that can effect the oxidation behavior of HDPE GMs. This section describes several of them placed in two categories: internal material effects and external environmental/service effects.

B-4.1 Internal Material Effects

The chemical and physical structure of the polymer has a strong influence on the rate of oxidation. This structure controls the formation of free radicals and the diffusion of oxygen into the polymer. Three major factors will be discussed: branch density, crystallinity and transition metals.

The medium density PE used to manufacture HDPE GMs is a copolymer. Apart from the dominant ethylene monomer, a comonomer is added to the polymerization. The comonomer is some type of α-olefin such as butene, hexene, methyl pentene, or octene (Chu and Hsieh, 1992). The comonomer forms short chain branches along the backbone of the PE chain. Two examples are given in Figure B-5. The concentration of the short chains varies from 5 to 8 per 1000 carbon atoms. The particular carbon atom where the branch attaches is surrounded by three other carbon atoms and is defined as the tertiary carbon. The hydrogen atom attached to the tertiary carbon possess a lower dissociation energy than other hydrogen atoms, thus free radicals are most likely to occur at these locations. This is illustrated by Eq. B-11. In other words, PE with greater branch density concentration will generate more free radicals than those with less branches under the same conditions.

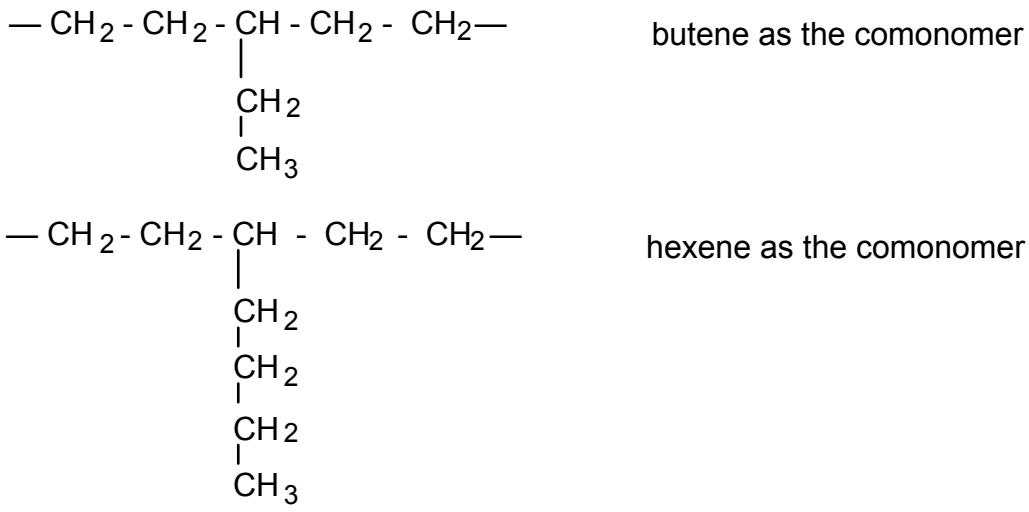

Figure B-5. PE with butene and hexene as the comonomer.

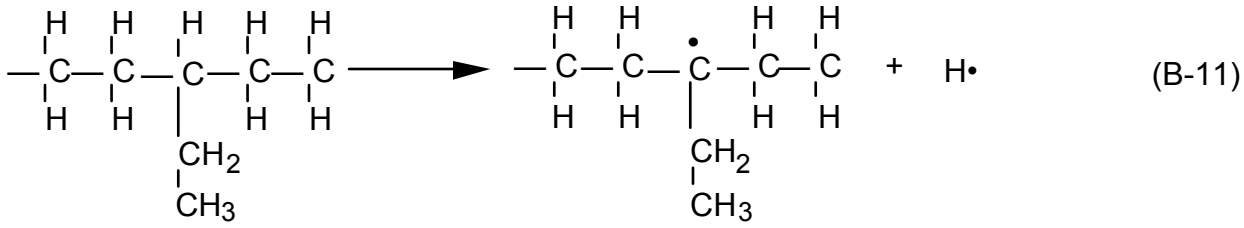

It is established (Michaels and Bixler, 1961) that the crystalline regions in PE are sufficiently dense to severely limit oxygen penetration. The result of this impermeability is that the diffusion of oxygen in the polymer is essentially controlled by the amorphous region. Hence, the diffusion coefficient increases as crystallinity decreases. During the initial stage of the oxidation, alkyl radicals are probably produced in both the crystalline and amorphous regions. As oxygen gradually diffuses into the amorphous region, it converts the radicals to alkylperoxy radicals, i.e., ROO•, starting the chain oxidation reactions. On the other hand, those alkyl radicals that are trapped in the crystalline matrix are unable to progress further (Billingham and Calvert, 1986). In addition, crystallinity relates closely to the branch density of the polymer. This is because chain branches interrupt the folding of the polymer chains, reducing the total amount of crystallinity in the polymer. Therefore, as branch density increases, the crystallinity decreases and the rate of oxidation increases.

The oxidation reaction of PE can be increased in the presence of transition metals, e.g., Co, Mn, Cu, Al and Fe (Osawa and Ishizuka, 1973). The source of these elements usually comes from residual catalyst used to polymerize the resin. Although the concentration of these elements is very low, they still can be a concern regarding the long term durability of the polymer. The transition metals break down hydroperoxides

via “redox” reactions, creating an additional amount of free radicals, as demonstrated in Eqs. B-12 and B-13.

$$ROOH + M^{n+} \rightarrow RO\bullet + M^{(n+1)} + OH^{-} \quad \text{(B-12)}$$

$$ROOH + M^{(n+1)} \rightarrow ROO\bullet + M^{n+} + H^{+} \quad \text{(B-13)}$$

B-4.2 External Environmental Effects

The oxidation reaction in PE is rather sensitive to the surrounding ambient environment. Any conditions that provide oxygen and accelerate the formation of free radicals, particularly the decomposition of hydroperoxide, increase the rate of oxidation. Three considerations are described: energy level, oxygen concentration and adjacent materials.

Sunlight, heat and radiation are three types of energy which should be considered. For an exposed GM, sunlight is the major concern. Coupled with heat there is a great potential for free radical formation. Covering in a timely manner, however, avoids photodegradation and greatly diminishes the heat from direct sunlight exposure. As mentioned previously, this study does not address sunlight exposed GMs. Heat, however, can come from other sources than direct sunlight. All other things being equal, a GM will degrade faster at higher temperature as opposed to lower temperature. In predicting lifetime, it is essential to accurately estimate the service temperature of the buried GM. For buried wastes that are radioactive there is a potential for the GM to be exposed to high energy levels depending on the type of waste. It is expected that low level radioactive (LLR) and low level radioactive mixed (LLRM) wastes are orders of magnitude too low to produce energy levels that could cause degradation. Conversely, high level radioactive (HLR) and transuranic (TRU) wastes must be assessed accordingly. They are not within the scope of this study

The concentration of available oxygen is an obvious essential component to any oxidation reaction. For exposed GMs, the availability of oxygen is high and the oxygen concentration is at its maximum. Contrary, for the liner beneath a landfill, the available oxygen will be extremely limited. In the case of a liner for municipal solid waste landfill, biodegradation of the waste will probably consume most of the available oxygen. (Poland and Harper, 1986) showed that the biodegradation of solid waste changes from aerobic and anaerobic after approximately 3 to 5 years). Under this situation, if degradation occurs in PE, it may lead to crosslinking rather than chain scission, as shown in Eqs. B-7 and B-8. In surface impoundment applications, the portion of GM that is covered by liquid is only exposed to approximately one eighth of the oxygen in comparison to that exposed in air. Unfortunately, in unsaturated soil, the percentage of oxygen present is very difficult to be defined since it is affected by the type of soil and the moisture content. Table B-1 lists an approximate ranking of GM exposure to oxygen

on the bases of various applications. This leads directly to different experimental incubation possibilities, e.g., immersed in liquid, liquid on top/air on bottom, and completely in air.

Table B-1. Oxygen Availability to GMs in Several Common Applications.

Application	Location	GM Surface	Oxygen Availability
surface impoundment	top of slope	top	high
	top of slope	bottom	moderate
Liners	base of slope	top	low
	base of slope	bottom	moderate
landfill liners	beneath waste	top	very low
		bottom	low
final covers	above waste	top	high to moderate
		bottom	very low

The type of material (soil or liquid) that makes direct contact with the GM has an influence on the oxidation rate. If the adjacent soil contains a large amount of transition metals (the amount is very subjective) and there is moisture or liquid present, the transition metals can diffuse into the GM. This action catalyzes the oxidation by accelerating the decomposition of ROOH, as explained in Eqs. B-12 and B-13. Furthermore, if the liquid that is contained by the GM consists of a relatively large amount of organic solvent, the amorphous phase of the GM can swell, increasing the oxygen diffusion coefficient and accelerating the oxidation.

B-4.3 Commentary on Various Influences

This section described some of the major influences (internal and external) on the rate of oxidation of HDPE GMs. In devising this particular long term experimental program of approximately 10 years duration, only one type of HDPE GM was selected. Thus the internal effects from the material itself such as branch density, crystallinity and transition metals are fixed to that particular GM type.

Additionally, in developing the incubation procedures, various external effects had to be considered. Three separate incubation environments were evaluated. They are water immersed, landfill simulated (water above and air below) and air immersed. It is suggested that these different types of incubation procedures cover the range of typical end uses illustrated in Table B-1.

B-5 Overview of Antioxidants

Since the subject of this appendix is the depletion of antioxidants in HDPE GMs, it is essential to explain the performance of antioxidants during their depletion period. Three properties will be discussed in this section; the function of antioxidant, the types of

antioxidants along with their individual characteristics, and the antioxidant depletion mechanisms.

B-5.1 Function of Antioxidants

The sequence of oxidation reactions in HDPE GMs indicated by Eqs. B-1 to B-6 can also be interconnected by cycles "A" and "B", as illustrated in Figure B-6. There are four important links in these two cycles, designated as (a) to (d). If any of the links are broken, the rate of oxidation of the polymer will be retarded. If all four links are broken, then oxidation will be stopped. The purpose of antioxidants in the polymer is to break such links.

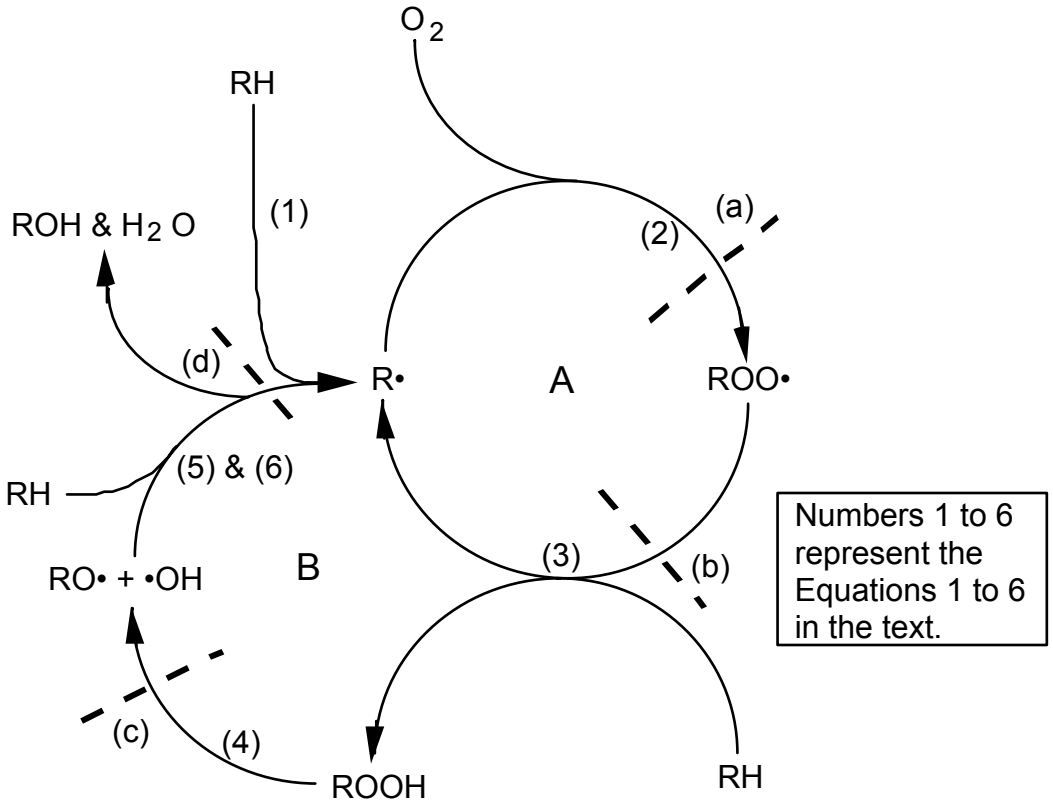

Figure B-6. Oxidation cycles in PE (Grassie and Scott, 1985).

Since the involved molecular species in each of the four cycle links are not the same, different types of antioxidants are designed to accommodate various requirements. Antioxidants can be divided into two categories; primary and secondary.

Primary Antioxidants - They provide stabilization by trapping or deactivating free radical species after they are formed, i.e., breaking links (a), (b) and (d). The antioxidants which intercept the links (b) and (d) function in that they donate an electron. The electrons react with free radicals ROO•, RO• and •OH converting them to ROOH, ROH

and H_2O, respectively. The types of antioxidants that break the link (a) are electron acceptors. They convert the alkyl free radical (R•) to form a stable polymer chain.

Secondary Antioxidants - They are designed to intercept the link (c) in the "B" cycle. Their function is to decompose hydroperoxides (ROOH), preventing them from becoming free radicals. The chemical reactions change the ROOH to a stable alcohol (ROH).

B-5.2 Types and Characteristics of Antioxidants

Apart from the two categories just described, antioxidants can be further classified into four large chemical types within which many different types are included. Table B-2 lists the chemical type and some of the commercial available antioxidants that can be used in PE GMs. To ensure long term durability, a manufacturer will use two or more types of antioxidants; typically one from each category.

Table B-2. Types of Antioxidants (after Fay and King, 1994)

Category	Chemical Type	Examples of Commercially Available Antioxidants
Primary	Hindered Phenol	Irganox® 1076, Irganox®1010, Santowhite Crystals
	Hindered Amines (HALS*)	Tinuvin® 622, Chimassorb® 922
Secondary	Phophites	Irgafos®168
	Sulfur Compounds (Thiosynergists)	distearyl thiodipropionate (DSTDP) dilauryl thiodipropionate (DLTDP),
	Hindered Amines (HALS*)	Irganox® 1076, Irganox® 1010, Santowhite Crystals

* HALS = hindered amine light stabilizers

There is another issue that needs to be considered during the selection of antioxidants. That is the effective temperature range for each of the selected antioxidants. The antioxidant formulation or "package" should protect the product at both the high temperature of the extrusion process and the significant lower temperature during its lifetime. Thus the functioning temperature range for each type of antioxidant should be recognized. For the four chemical types listed above, the effective temperature ranges are given in Figure B-7. The graph shows that phosphites have an effective temperature range above 150°C. They are considered to be process stabilizers. Either thiosynergists or hindered amines will be added to the formulation to accommodate the low temperature service protection. On the other hand, for a formulation consisting of hindered phenols, a wide range of temperatures are covered; from ambient to process temperatures. However, hindered phenols are only primary stabilizers. A secondary antioxidant is also required which can be either thiosynergists or hindered amines.

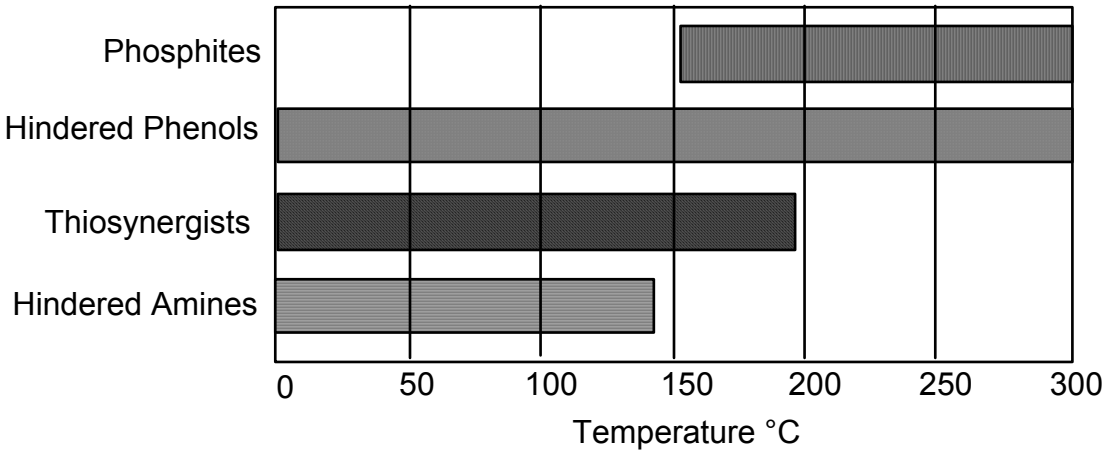

Figure B-7. Effective temperature ranges of the four antioxidant types (Fay and King, 1994).

In the mixing of the various types of antioxidants, one must beware of the possible antagonistic effects between them. For products that require long term thermal stability and light stability, a combination of phenolic and thiosynergist for thermal stability, and hindered amine for light stability could be used. Unfortunately, the oxidation product of the sulfur compound can be acidic which reacts with hindered amine, preventing its interacting with free radicals (Kikkawa et al., 1987). In HDPE GMs, the carbon black can also influence the stability of the material, in particular, the thermal stability. Materials containing carbon black absorb more heat than those without carbon black. While this discussion is seemingly complicated, it should be recognized that the polymer industry is quite advanced in the selection of antioxidants. There are many custom designed packages for each product, including GMs, in order to accommodate a wide range of processing and service requirements.

One last item to conclude this subsection is the issue of antioxidant cost. Antioxidants are comparatively much more expensive than the polymer resin. Thus cost of the final product is weighted heavily by the amount and type of antioxidants used in the formulation. A careful balance must be drawn between the required performance and economy of the final product.

B-5.3 Antioxidant Depletion Mechanisms

The amount of antioxidant in a HDPE GM decreases gradually as aging progresses. The depletion can be caused by two mechanisms; chemical reactions of the antioxidants and physical loss of antioxidants from the polymers by leaching. These mechanisms can occur simultaneously.

Chemical reactions: As discussed previously, the antioxidants are consumed by free radicals and alkylperoxides present in the material. The rate of consumption which progresses from the surfaces of the GM inward depends on the concentration of these two species. Since phenolic and phosphite types of stabilizers are utilized in the processing stage, the antioxidants that remain in GMs for longevity protection are probably a combination of residue phenolic types along with thiosynergists or hindered amines. Of these three types of antioxidants, hindered amines have a unique reactive behavior. They can be cyclical and regenerative, both leading to a long functioning time. Only undesirable side reactions can terminate their efficiency (Fay and King, 1994).

Physical loss: The two major concerns with respect to the physical stability of antioxidants in the polymer are their volatility and extractability (Luston, 1986). Research has indicated that the distribution of antioxidants in semicrystalline polymers is not uniform, owing to the presence of crystalline and amorphous phases. It appears that a greater concentration of antioxidants is found in the amorphous region which is fortunate because the amorphous region is also the most sensitive to degradation. Hence the mobility of antioxidants in the amorphous phase controls these two physical processes.

The volatility of antioxidants is a thermally activated process and temperature changes effect not only the evaporation of the stabilizers from the surface of the polymer but also their diffusion from the interior to the surface layer. For HDPE GMs, the typical operating temperature is well below 60°C. Hence volatility is probably not a major concern. Because of this, one must avoid inducing such a mechanism in accelerated laboratory aging tests. Very high testing temperatures should not be utilized. However, elevated temperature is necessarily to accelerate the laboratory aging study. Therefore a careful balance is required in the design of the experimental incubation setup. As noted previously this task is proposed to be a 10-year effort. The reason for such long time is that the selected test temperatures are relatively low so as to minimize volatility of antioxidants from occurring.

Extractability of antioxidants plays a part wherever the GMs comes into contact with liquids such as water or leachate. The rate of extraction is controlled by the dissolution of antioxidants from the surface and the diffusion from the interior structure to the surface. However, dissolution is faster than evaporation. Smith et al. (1992) performed an aging study on a medium density PE pipe material that was exposed to water internally and air externally. They monitored the antioxidant depletion across the thickness of the pipe via oxidative induction time (OIT). They found that the consumption of antioxidants was three times faster in water than in air at temperatures of 105, 95 and 80°C.

Thus in the physical loss of antioxidants, extraction takes a central role in lifetime predictions. Clearly, this is a concern if the GM contacts liquid during its service life. Unfortunately, there is no data available regarding the effect of humidity on antioxidant loss.

B-6 Experimental Design

As indicated in Table B-1, HDPE GMs can experience different levels of oxygen concentration depending on the application, its site specific location, and the materials in contact with the upper and lower surfaces. It is important that the laboratory aging tests simulate the site conditions as close as possible. In this regard, four different laboratory incubation protocols have been developed. They are described in Table B-3. A detailed description of each incubation method is presented in this section.

Table B-3. Incubation Method of HDPE GMs in this Task

Incubation Series	Incubation Method	Applied Stress	Simulated GM Application
I	water (both sides)	none	surface impoundments below liquid level
II	air (both sides)	none	landfill covers and waste pile covers
III	water above/air beneath	260 kPa (compression)	landfills liners beneath waste
IV	water (both sides)	30% yield stress (tension)	surface impoundments along side slopes below liquid level

The incubation method of Series I is designed to simulate GMs which are exposed to liquids (water or leachate) on both sides and are essentially nonstressed, e.g., shallow surface impoundments. HDPE GM samples are fully immersed in four water baths maintained at constant temperatures of 55, 65, 75 and 85°C. The dimensions of the incubated samples are 150 mm by 150 mm. Samples are retrieved at various time intervals and evaluated by a number of tests for their physical, chemical and mechanical properties.

The incubation method of Series II is designed to simulate GMs which are exposed to air on both of their surfaces, e.g., landfill covers and waste pile covers. GMs in these applications will be exposed to air from above and perhaps from beneath as well. The exact oxygen concentration that the GM will be subjected to is very difficult to define. The incubation represents the extreme condition of full oxygen exposure. Hence the lifetime predicted from this experiment will be a conservative value. In this series, GM samples are exposed to a continuous flow of air. HDPE GM samples are suspended in

five forced air ovens maintained at temperatures of 55, 65, 75, 95°C and 115°C. The dimensions of the samples are 100 mm by 150 mm. Samples are retrieved at various time intervals and are evaluated by a number of tests for their physical, chemical and mechanical properties.

The incubation method of Series III is intended to simulate GMs situated beneath solid waste landfills. Circular shaped samples of 200 mm diameter are placed in incubation columns similar to those suggested by Mitchell and Spanner (1985), as shown in Figure B-8. Twenty (20) identical units of this type are used in this incubation series. A static compressive stress of 260 kPa is applied to each sample. This is approximately equivalent to a 30 m high solid waste landfill. Above each sample is a layer of 100 mm thick sand with 300 mm of water head. Beneath each sample is dry soil with a limited amount of air. Four test temperatures of 55, 65, 75, and 85°C are being utilized. Samples are retrieved at various time intervals and evaluated by a number of tests for their physical, chemical and mechanical properties.

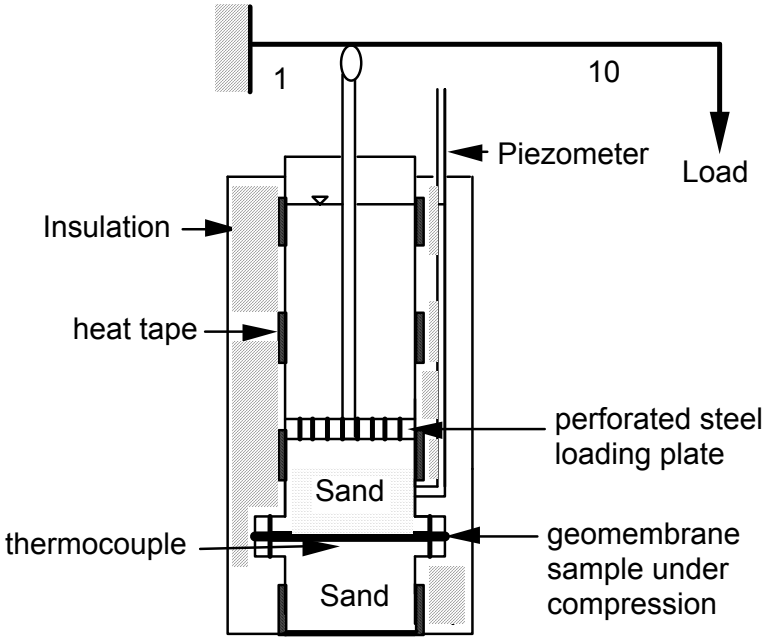

Figure B-8. A schematic diagram of the compression column for incubation series III.

The incubation method of Series IV is intended to simulate GMs located on side slopes of surface impoundments where tensile stress may be generated. GM samples of dimensions 38 mm by 150 mm are subjected to a constant tensile stress equal to 30% of their room temperature yield stress. The tensioned samples are completely immersed in four water baths maintained at constant temperatures of 55, 65, 75 and

85°C. Samples are retrieved at various time intervals and evaluated by a number of tests for their physical, chemical and mechanical properties.

The four incubation conditions used in this study are attempts at replicating the most commonly encountered site situations where GMs are being used. How the resulting predicted lifetimes compare to one another is obviously a major focus of this task. From a comparison of the results it is hoped that one can deduce effects on oxidation on GMs that are not directly studied, e.g., different types of stresses, tension effects, water extraction effects, etc.

B-7 Evaluation Tests on Incubated Samples

The HDPE GM samples in the four incubation series just described are retrieved after predetermined lengths of time. The times depend on the change in property behavior which cannot be estimated apriori. Hence the retrieval time is adjusted for each series. The progression of the aging process in each series is monitored by the results of a set of physical, chemical and mechanical tests. Table B-4 shows the tests that are used to track the behavior of the incubated GM samples. Most of tests are standard test methods commonly performed on HDPE GMs test specimens. The only necessary commentary has to do with the different types of OIT tests, since these are the test results presented and analyzed in this appendix.

Table B-4. Tests Used to Evaluate Incubated Samples

GM Property	ASTM Test Methods	Test Description
crystallinity	D 1505	density
antioxidant amount (total)	D 3895 and D5885	Standard OIT and high pressure OIT
molecular weight (indirect)	D1238	melt flow index
mechanical properties	D 638	tensile properties
stress crack resistance	D5397-appendix	single point notched constant tensile load

In this study, the total amount of antioxidant remaining in the incubated GM samples is evaluated using two slightly different OIT tests. They are the standard method and the high pressure method. Although OIT cannot identify the individual type or exact amount of each antioxidant present in the formulation, it does quantify the effectiveness of the antioxidants. OIT is the time required for the GM test specimen to be oxidized under a specific pressure and temperature. Since antioxidants protect the GM from oxidation, the length of OIT (in minutes) indicates the amount of antioxidants present in the test specimen. Howard (1973) showed that OIT is proportional to the antioxidant

concentration in the same formulation package. However, for different antioxidant packages, direct comparison between two single OIT values can be very misleading and caution must be expressed. Since we are only investigating a single GM type and its antioxidant package, this caution is not a concern in this task.

B-7.1 Standard Oxidative Induction Time (Std-OIT) Test

The Std-OIT test is performed according to ASTM D3895. The test uses a differential scanning calorimeter (DSC) with a specimen testing cell that can sustain a 35 kPa gauge pressure. A 5 mg GM specimen is heated from room temperature to 200°C at a heating rate of 20°C/min under a nitrogen atmosphere. The gas flow rate is maintained at 50 cc/min. When 200°C is reached, the cell is maintained in an isothermal condition for 5 minutes. The gas is then changed from nitrogen to oxygen. The pressure and flow rate of oxygen are 35 kPa gauge pressure and 50 cc/min, respectively. The test is terminated after an exothermal peak is detected. The exothermal peak results from the oxidation of the GM specimen. An example thermal curve with its identified OIT value is shown in Figure B-9.

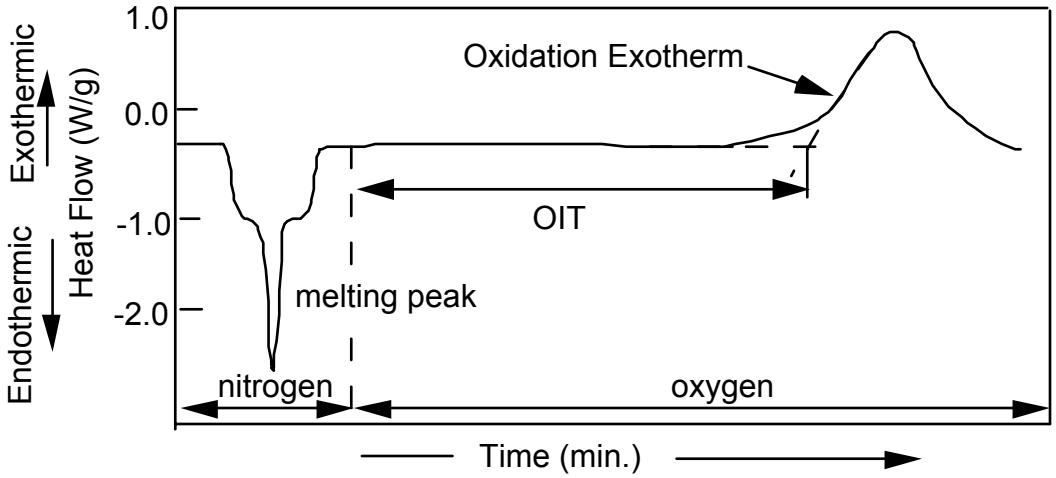

Figure B-9. Thermal curve of a standard OIT test.

B-7.2 High Pressure Oxidative Induction Time (HP-OIT)Test

The HP-OIT test is also performed using a DSC except now with a cell that can sustain a pressure of 5500 kPa. This type of cell is called a high pressure cell and consequently the test is called high pressure OIT (HP-OIT). It is performed according to ASTM D5885.

Tikuisis et al. (1993) have performed a detailed study on the effect of pressure and temperature on HP-OIT values. A series of such tests was evaluated using 8 different isothermal temperatures ranging from 150°C to 200°C under 8 different pressures, from

690 kPa to 5500 kPa. They found an Arrhenius relationship between temperature and HP-OIT values. Pressure had very little influence on the HP-OIT values at temperatures above 170 °C. At 150 °C isothermal temperature, pressure greater than 3500 kPa resulted in little change HP-OIT values. As a result of their study, the generally agreed upon pressure and isothermal temperature can be selected. In the draft ASTM standard, these values are 3500 kPa and 150°C, respectively.

The test protocol of the HP-OIT test used in this study is that a 5 mg GM specimen is heated from room temperature to 150°C at a heating rate of 20°C/min under a nitrogen atmosphere. The pressure of the cell in this nitrogen stage is maintained at 35 kPa gauge pressure. The gas flow rate is not monitored. When 150°C is reached, the cell is maintained in an isothermal condition for 5 minutes. The gas is then changed from nitrogen to oxygen. The oxygen pressure in the cell is gradually increased to 3500 kPa within 1 minute. The test is terminated after an exothermal peak is detected. The exothermal peak results from the oxidation of the GM specimen. The resulting thermal curve is similar to that shown in Figure B-9, except that the HP-OIT value is much longer than the Std-OIT value for the same material. This is due to the lower testing temperature.

B-7.3 Commentary on the Different OIT Tests

The major differences between the two OIT tests are oxygen pressure and isothermal temperature. For the standard OIT test, a low pressure and high temperature are used. For the HP-OIT test, a high pressure and low temperature are utilized. Their differences create somewhat of a dilemma insofar as the selection of a preferred test method for OIT. Table B-5 summaries the advantages and disadvantages.

The main reason behind developing the HP-OIT test is that the 200°C testing temperature used in Std-OIT test is unable to bring out the stabilization effect of thiosynergists and hindered amine types of antioxidants. As shown in Figure B-7, the maximum effective temperature of both of these antioxidants is below 150°C. At 200°C, both types of antioxidants rapidly volatilize from the GM thus losing their apparent effect. As a result, GMs with these types of antioxidants will exhibit a shorter OIT value than those without. Yet the long term performance of these GMs may be very similar, or even better than those without these types of antioxidants. In the HP-OIT test, the test temperature is lowered to 150°C. Note that 150°C is the minimum temperature to ensure complete melting of the HDPE GM specimen. The low testing temperature, however, results in an extremely long test at the standard pressure of 35 kPa, making the test somewhat unpractical. Hence a high pressure is applied. At a higher oxygen pressure, the concentration gradient of oxygen atoms across the specimen's surface becomes greater. This increases the number of oxygen atoms diffusing into the molten specimen, thereby accelerating the oxidation and reducing the testing time.

Table B-5. Differences Between the Standard and High Pressure OIT Tests

Test	Advantages	Disadvantages
Std-OIT (200°C, 35 kPa)	• existing ASTM test protocol • short testing time (~ 100 min) • standard test apparatus	• high temperature may bias the test results for certain types of antioxidants
HP-OIT (150°C, 3500 kPa)	• existing ASTM test protocol • able to distinguish the stabilization effect of different types of antioxidants in the GM • lower temperature relates closer to service conditions	• long testing time (>300 min.) • special testing cell and set up are required

B-8 Data Extrapolation Method

It is well established that chemical reactions of all types proceed more rapidly at higher temperatures than at lower temperatures. The relationship between chemical reaction rate (R_r) and temperature is usually expressed by the Arrhenius equation, Eq. B-14:

$$R_r = C \exp\left(-Q/RT\right) \tag{B-14}$$

where:

R_r = reaction rate
C = constant (independent of temperature)
Q = activation energy of the reaction
R = gas constant
T = absolute temperature

Taking the natural logarithm of both sides of Eq. B-14, Eq. B-15 is obtained.

$$\ln\left(R_r\right) = \ln C - Q/RT \tag{B-15}$$

If the log reaction rate is plotted against inverse temperature as shown in Figure B-10, the slope of the line will be -Q/R and the intercept on the vertical axis will be the constant “C”. The plot in Figure B-10 is called the “Arrhenius Plot” from which reaction rates at other temperatures (typically lower temperatures) can be extrapolated. In order to produce a reliable extrapolation, there should be a minimum of three data points, i.e., data from three different incubation temperatures, so that the experimental portion of the line can be reasonably established. In addition, the test temperatures cannot be so high that changes in material occur, thereby altering the nature of the reaction.

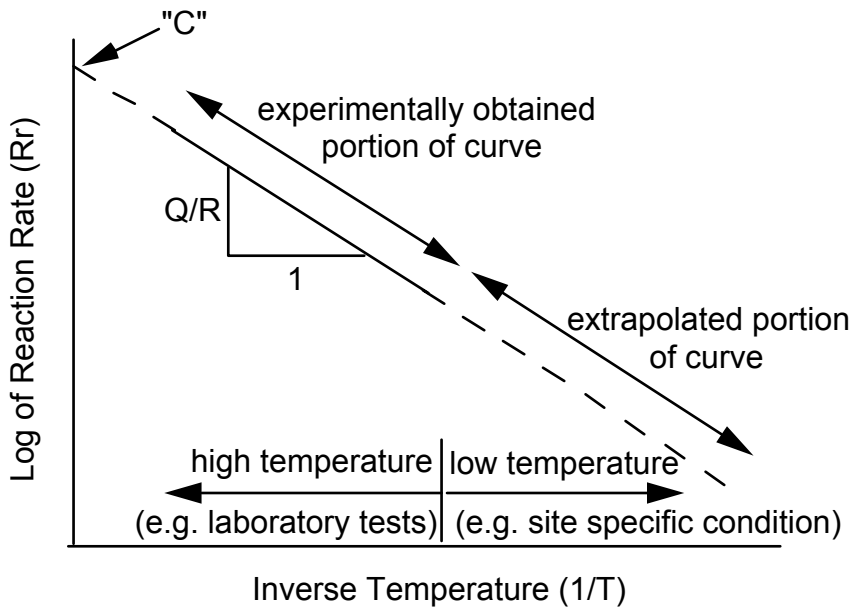

Figure B-10. Generalized Arrhenius plot for low-temperature reaction rate predictions from high-temperature laboratory experimental data.

In this aging study, the four selected testing temperatures are 55, 65, 75 and 85°C. The reaction rate being evaluated in this particular report will be the antioxidant depletion rate. Data obtained from the experimental portion will be extrapolated to a lower site specific temperature. Hence, the potential lifetime of the antioxidants in the HDPE GM can be assessed. In Figure B-3, this is Stage "A" of the overall predicted lifetime of the HDPE GM being evaluated.

B-9 Results and Data Analysis on Antioxidant Depletion

This appendix presents the results to date on antioxidant depletion rates. Incubation Series I and III are presented. Series II and IV are ongoing. As shown in Table B-4, GM test samples in Series I are incubated in water media under nonstressed conditions whereas GM test samples in Series III are exposed to water above/air beneath and under compressive stress. The antioxidant depletion rate is measured using both the Std-OIT and HP-OIT tests as explained previously.

B-9.1 Preparation of OIT Test Specimens

The incubated samples from each test series were retrieved after varying incubation periods. The retrieved samples were equilibrated at room conditions for 24 hours. They were then cleaned with tap water to remove surface contaminants. The cleaned samples were placed in a plastic bag and stored inside a cabinet until testing.

OIT test specimens weighing 5 mg each were taken from the incubated samples. They were cut from surface to surface across the thickness of the GM near the center portion

of the sample. Therefore, the resulting OIT values represent the average amount of antioxidants across the thickness of the test specimens.

For the Std-OIT tests, three replicates were performed on each incubated sample and the average value was used in the analysis. For the HP-OIT tests, a single test was performed on most of the incubated samples. Some samples were tested twice to verify the reproducibility of the test.

B-9.2 Results and Data Analysis of Incubation Series I

HDPE GM samples in incubation Series I were completely immersed in water at temperatures of 55, 65, 75 and 85°C. The average OIT value for each incubated sample was evaluated by Std-OIT and HP-OIT tests. In this subsection, the results of both tests are presented together with the step-by-step data analysis which leads to the prediction of antioxidant depletion.

The Std-OIT and HP-OIT test results are shown in Table B-6. The OIT values are presented graphically by plotting OIT value against incubation time. Figures B-11 and B-12 show Std-OIT and HP-OIT values, respectively. The curves in both figures indicate an exponential decrease in the amount of antioxidant present as incubation time increases. The curves also exhibit that the decrease in OIT values is greater for the higher incubation temperatures than for the lower temperatures.

Since OIT values decrease exponentially as incubation time increases in both tests, a linear relationship can be obtained between ln(OIT) and incubation time. Figures B-13 and B-14 show the ln(OIT) versus incubation time plots for Std-OIT and HP-OIT, respectively. The generalized equation for each of the straight lines is expressed by Eq. B-16.

$$\ln(\mathrm{OIT}) = \ln(\mathrm{P}) + (\mathrm{S})^{*}(\mathrm{t}) \qquad \text{(B-16)}$$

Table B-6. OIT Test Results of Incubation Series I

Incubation Time (months)	55°C		65°C	
	Std-OIT (min)	HP-OIT (min)	Std-OIT (min)	HP-OIT (min)
0.1	80.5	210*	80.5	210*
1.0	79.5	201	78.2	204
3	77.0	196	74.0	157
9	59.0	173	40.2	135
12	45.3	160	24.2	120
18	n/a	n/a	17.0	109
30	19.1	111	10.8	87

Incubation Time (months)	75°C		85°C	
	Std-OIT (min)	HP-OIT (min.)	Std-OIT (min)	HP-OIT (min)
0.1	80.5	210*	80.5	210*
1.0	75.2	172	70.5	181
3	69.5	154	63.4	127
9	15.1	82	12.9	72
12	9.7	87	6.2	50*
18	10.3	76	3.4	38
30	2.1	38*	0.5	28*

Notes:
All Std-OIT values are the average of three replicate tests.
All HP-OIT values are from a single test with the exception of those marked with an asterisk which are the average of two replicate tests.

where

OIT = OIT time
S = slope of the lines (i.e., OIT depletion rate)
t = incubation time
P = constant (the original value of OIT time in either the Std-OIT or HP-OIT tests)

Table B-7 lists the depletion rates that are obtained from both Std-OIT and HP-OIT tests.

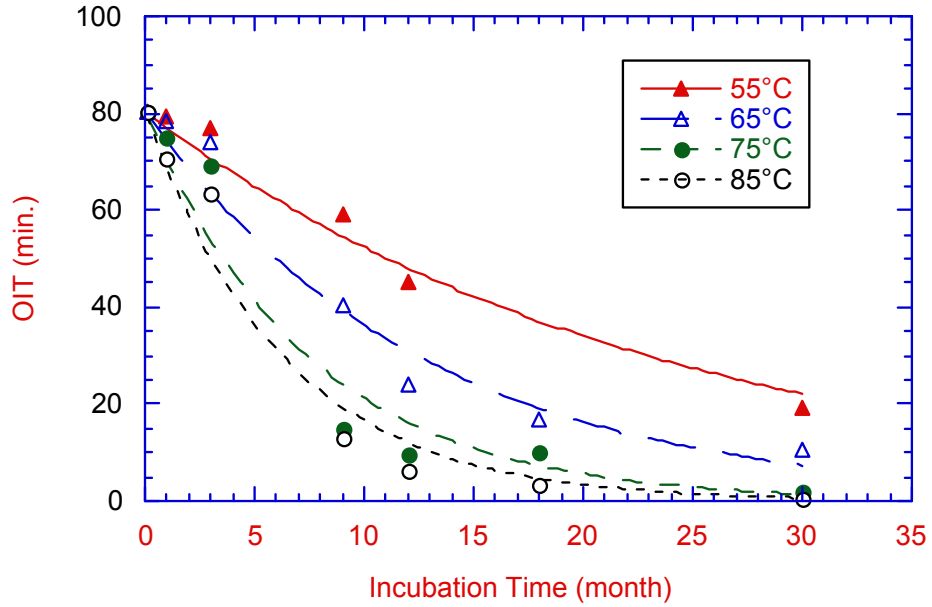

Figure B-11. Standard OIT versus incubation time plot for incubation Series I.

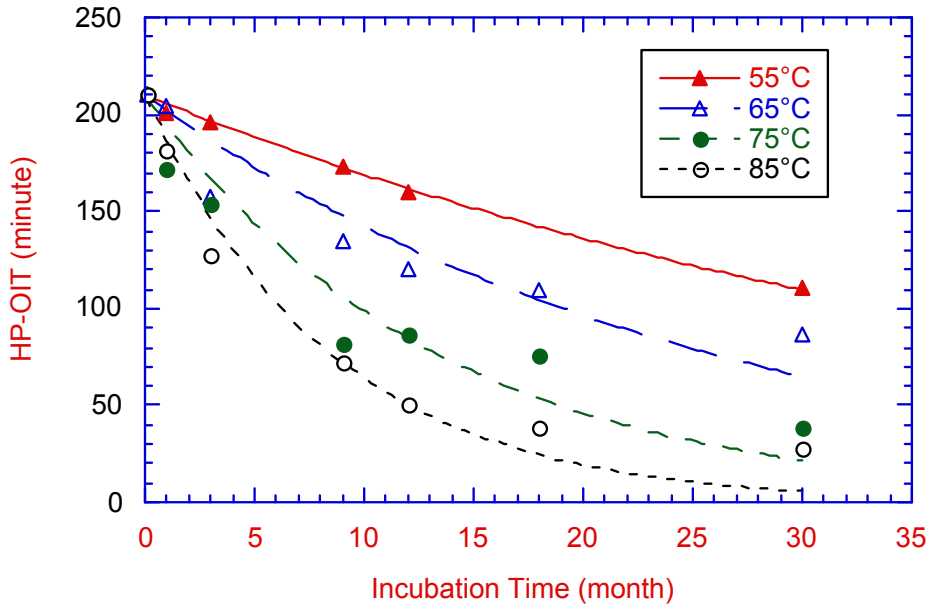

Figure B-12. HP-OIT versus incubation time plot for incubation Series I.

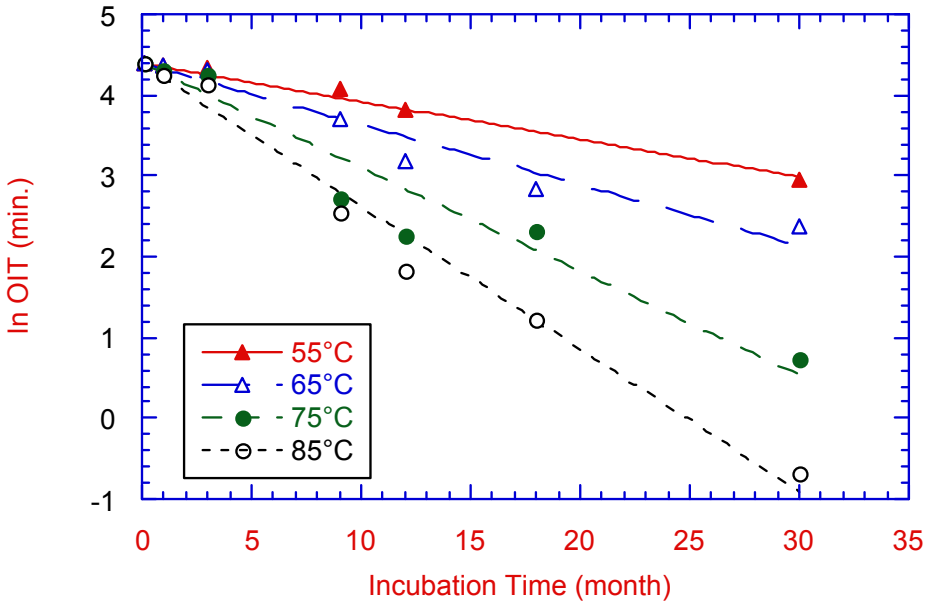

Figure B-13. Ln(OIT) versus incubation time plot for incubation Series I using Standard OIT tests.

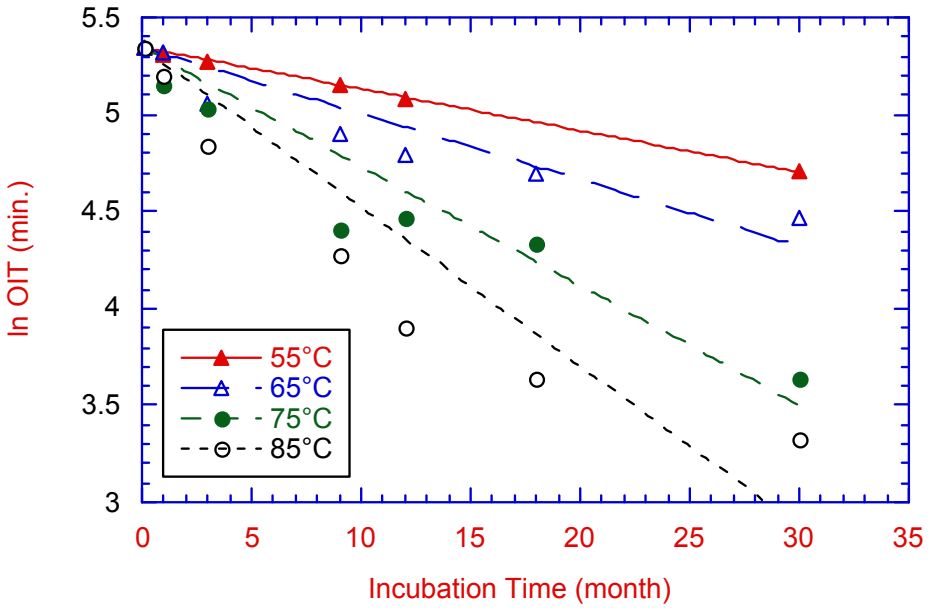

Figure B-14. Ln(OIT) versus incubation time plot for incubation series I using HP-OIT test.

Table B-7. Antioxidant Depletion Rates of Incubation Series I (i.e., the slopes of the straight lines in Figures B-13 and B-14).

Test Temperature	Std-OIT	HP-OIT
55°C	-0.0467	-0.0215
65°C	-0.0749	-0.0342
75°C	-0.1280	-0.0615
85°C	-0.1765	-0.0822

The next step in the analysis is to extrapolate the OIT depletion rate to a lower temperature, such as site specific temperature. This is performed utilizing the Arrhenius equation, as described in Eqs. B-17 and B-18.

$$S = A*Exp(-E/RT) \quad \text{(B-17)}$$

$$\ln(S) = \ln(A) + (-E/R)*(1/T) \quad \text{(B-18)}$$

where

S = OIT depletion rate (slope of the lines listed in Table B-7)
E = activation energy of the antioxidant depletion mechanism (KJ/mol)
R = gas constant (8.31 J/mol°K)
T = test temperature in absolute value (°K)
A = constant

Thus a linear relationship can be established between ln(S) and inverse temperature, as indicated in Figure B-15. The activation energy deduced from the slope of the lines is 43 KJ/mol for Std-OIT and 44 KJ/mol for HP-OIT. These two values are seen to be extremely close to one another. The corresponding Arrhenius Equation for Std-OIT and HP-OIT are expressed in Eqs. B-19 and B-20.

$$\ln(S) = 12.839 - 5210.2/T \quad \text{for Std-OIT} \quad \text{(B-19)}$$

$$\ln(S) = 12.372 - 5311.8/T \quad \text{for HP-OIT} \quad \text{(B-20)}$$

Using Eqs. B-19 and B-20, the OIT depletion rates at a site specific temperature can be obtained. Koerner and Koerner (1995) and Yazadini et al. (1995) found that the temperatures at the base of landfills in Pennsylvania and California, USA are around 25°C. Thus 25°C is used to demonstrate the extrapolation calculation. OIT depletion rates of both tests are as follows:

S = - 0.0096 for Std-OIT
S = - 0.0043 for HP-OIT

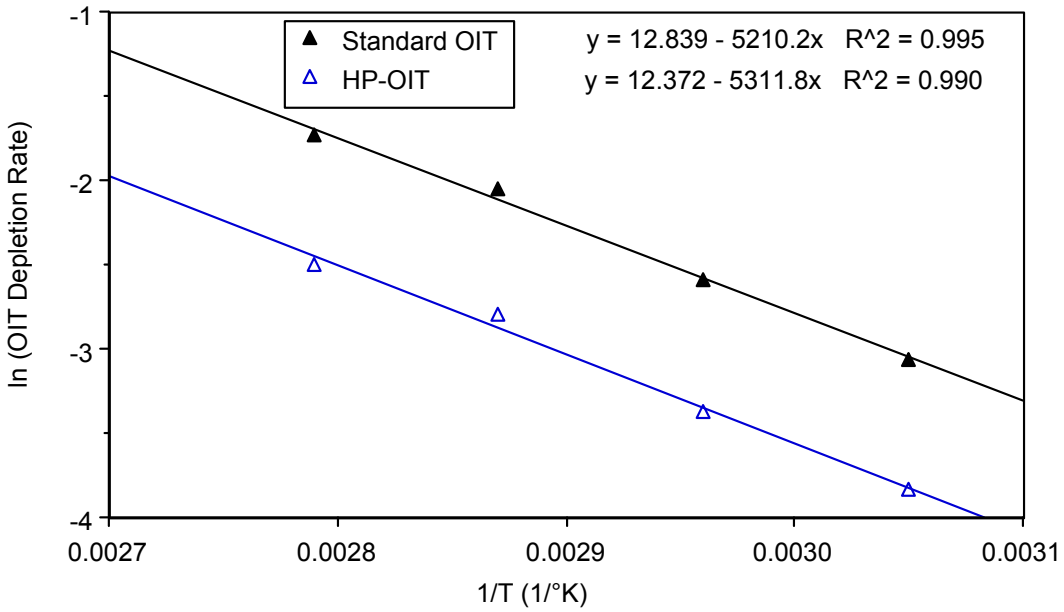

Figure B-15. Arrhenius plot for incubation Series I (water immersion-nonstressed).

In order to predict the aging time required to deplete the antioxidants in the HDPE GM evaluated, Eq. B-16 is utilized. The calculation procedure is as follows:

- For Std-OIT tests:
  The Std-OIT value for a pure unstabilized (i.e., no antioxidants) HDPE fluff was found to be 0.5 minutes. Thus 0.5 minutes is taken to be the OIT value when essentially all of antioxidants in the incubated HDPE GMs are consumed. The calculation to find the time for this depletion at a service temperature of 25°C is as follows:

  $\ln (OIT) = \ln(P) + (S) * (t)$ (B-16)
  $\ln (0.5) = \ln (80.5) + (-0.0096) (t)$
  $-0.69 = 4.39 - 0.0096 (t)$
  t = **529 months (44 years)**

- For HP- OIT tests:
  The OIT value for a pure unstabilized HDPE fluff was found to be 25 minutes. (This relatively high value is due to the low isothermal temperature and switching nitrogen to oxygen in the test method). Thus 25 minutes is taken to be the OIT value when essentially all of the antioxidants in the incubated HDPE GM consumed.

$$\ln (OIT) = \ln(P) + (S)*(t) \quad \text{(B-16)}$$

$$\ln (25) = \ln (210) + (-0.0043)*(t)$$

$$3.22 = 5.35 - 0.0043*(t)$$

$$t = \textbf{495 months (41 years)}$$

Thus it is seen that the predicted antioxidant lifetime at a service temperature of 25°C is approximately 40 years for this particular HDPE GM formulation under this set of immersion conditions.

B-9.3 Results and Data Analysis of Incubation Series III

HDPE GM samples in incubation Series III were exposed to water on top and air beneath and a compressive stress of 260 kPa. The incubation temperatures are 55, 65, 75 and 85°C. The average amount of antioxidants in each aged sample was evaluated by both Std-OIT and HP-OIT tests. In this subsection, the results of both tests are presented together with the step-by-step data analysis which leads to the prediction of antioxidant depletion.

The Std-OIT and HP-OIT values are shown in Table B-8. Also, the OIT values are presented graphically by plotting OIT value against incubation time. Figures B-16 and B-17 show the Std-OIT and HP-OIT values, respectively. Similar to Series I, the depletion of OIT decreases exponentially as incubation time increases. The curves also exhibit that the decrease in OIT values is greater for the higher incubation temperatures than for the lower temperatures.

Since OIT values in this incubation series also decrease exponentially as incubation time increases, the data extrapolation steps will follow those used in Series I. Based on Eq. B-16, a straight line can be formed by plotting ln(OIT) versus incubation time, as indicated in Figures B-18 and B-19 for Std-OIT and HP-OIT, respectively. The slope of the lines represent the OIT depletion rate at each particular temperature. Table B-9 lists the depletion rates that are obtained from both Std-OIT and HP-OIT tests.

Table B-8. OIT Test Results of Incubation Series III

Incubation	55°C		65°C	
Time (months)	Std-OIT (min)	HP-OIT (min)	Std-OIT (min)	HP-OIT (min)
0.1	80.5	210*	80.5	210*
3	74.3	221	77.9	189
9	55.5	181*	50.5	164
12	54.1	175*	36.8	135
18	57.0	186	19.0	105*
24	52.9	167	25.9	125

Table B-8 (cont.). OIT Test Results of Incubation Series III

Incubation Time (months)	75°C		85°C	
	Std-OIT (min)	HP-OIT (min)	Std-OIT (min)	HP-OIT (min)
0.1	80.5	210*	80.5	210*
3	66.2	192	55.0	181
9	45.3	143	23.5	113
12	27.9	113	12.6	94
18	17.5	103	4.3	76
24	12.6	92	4.0	38

Notes:
All Std-OIT values are the average of three replicate tests.
All HP-OIT values are from a single test with the exception of those marked with an asterisk which are the average of two replicate tests.

Table B-9. Antioxidant Depletion Rates of Incubation Series III (i.e., the slopes of the straight lines in Figures B-18 and B-19).

Test Temperature	Std-OIT	HP-OIT
55°C	-0.0217	-0.0097
65°C	-0.0589	-0.0284
75°C	-0.0798	-0.0387
85°C	-0.1404	-0.0661

The next step in the analysis is to extrapolate the OIT depletion rate to 25°C using Eq. B-18. Figure B-20 shows the Arrhenius plot for both OIT tests. The activation energy deduced from the slope of the lines is 56 KJ/mol for Std-OIT and 58 KJ/mol for HP-OIT. Again these two values are seen to be extremely similar to one another. However, they are both slightly higher than those obtained in incubation Series I. This indicates that the reaction mechanism for antioxidant depletion in Series III requires more energy than that in Series I. In other words, the OIT depletion rate in Series III is slower compared to Series I and the correspondingly lifetime prediction will be longer. The corresponding Arrhenius Equations for Std-OIT and HP-OIT are expressed in Eqs. B-21 and B-22.

$$\ln(S) = 16.885 - 6738.9/T \quad \text{for Std-OIT} \tag{B-21}$$

$$\ln(S) = 16.856 - 6991.3/T \quad \text{for HP-OIT} \tag{B-22}$$

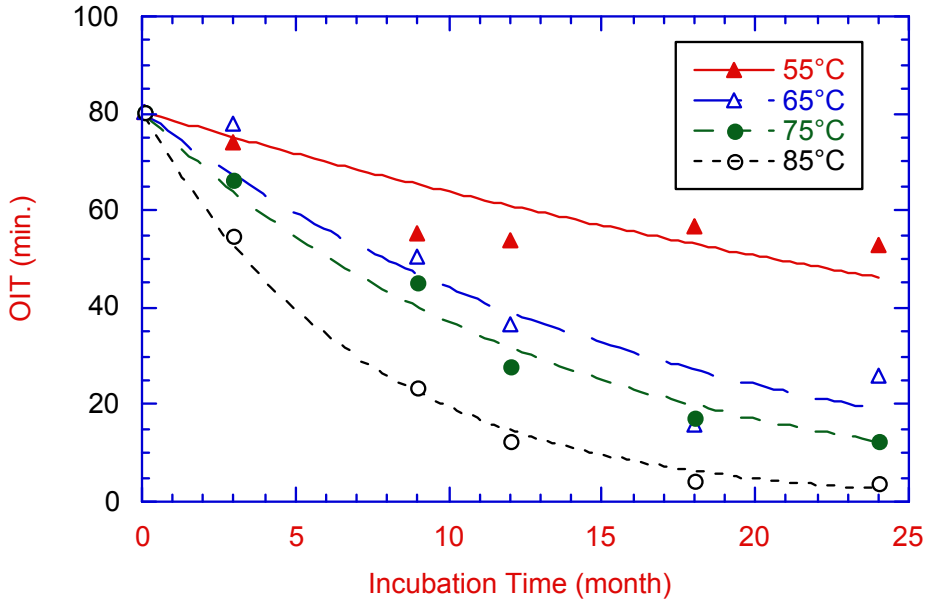

Figure B-16. Standard OIT versus incubation time plot for incubation Series III.

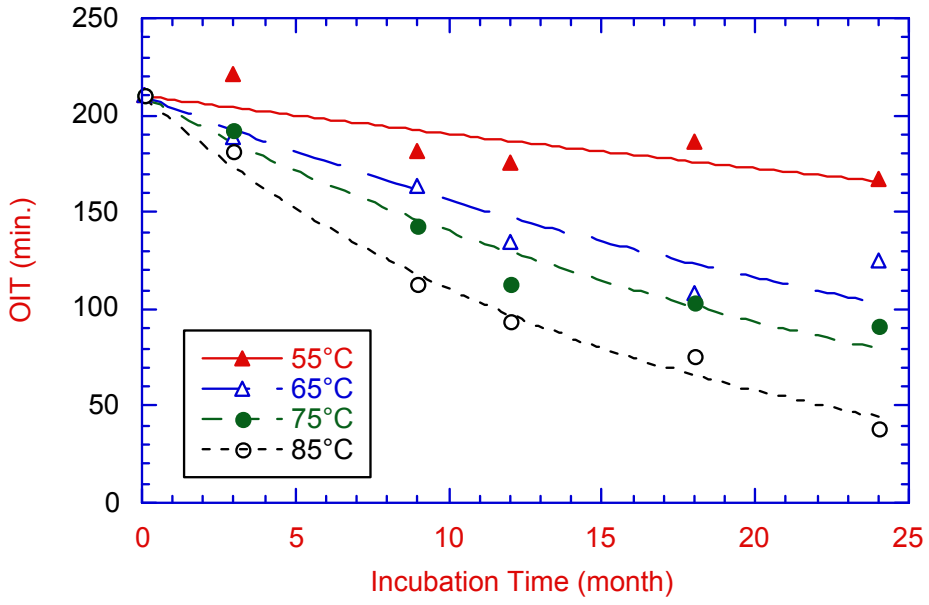

Figure B-17. HP-OIT versus incubation time plot for incubation Series III.

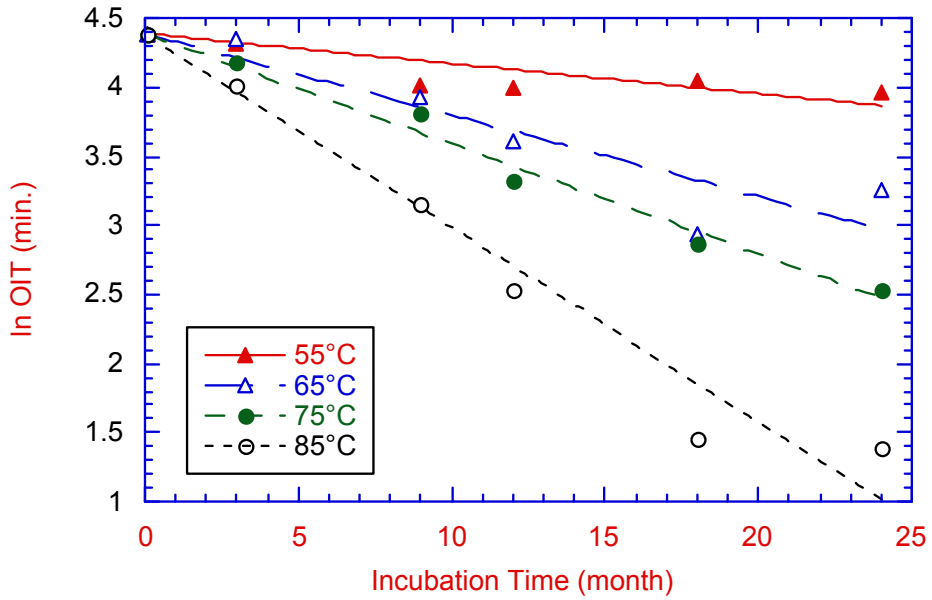

Figure B-18. Ln (OIT) versus incubation time plot for incubation Series III using Standard OIT tests.

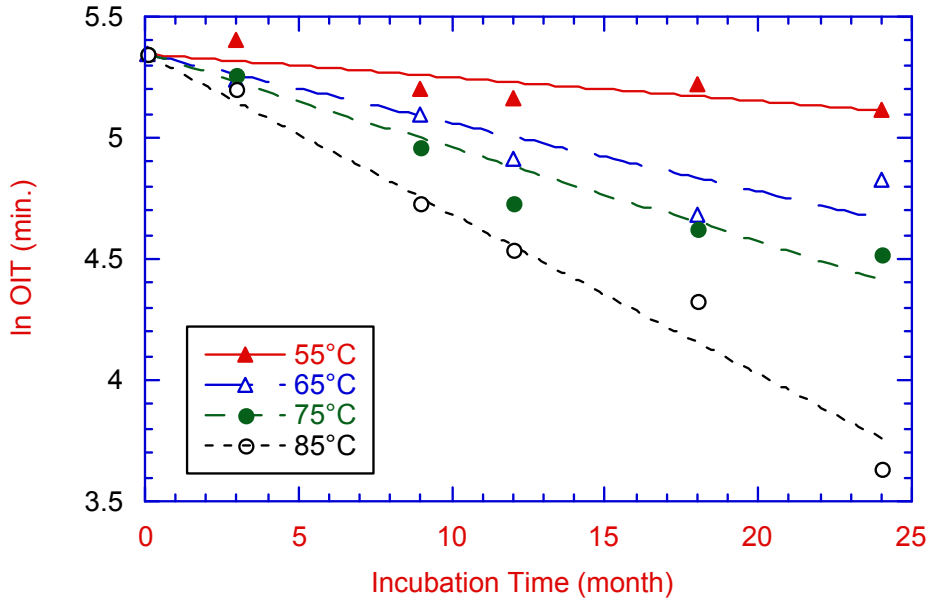

Figure B-19. Ln (OIT) versus incubation time plot for incubation Series III using HP-OIT tests.

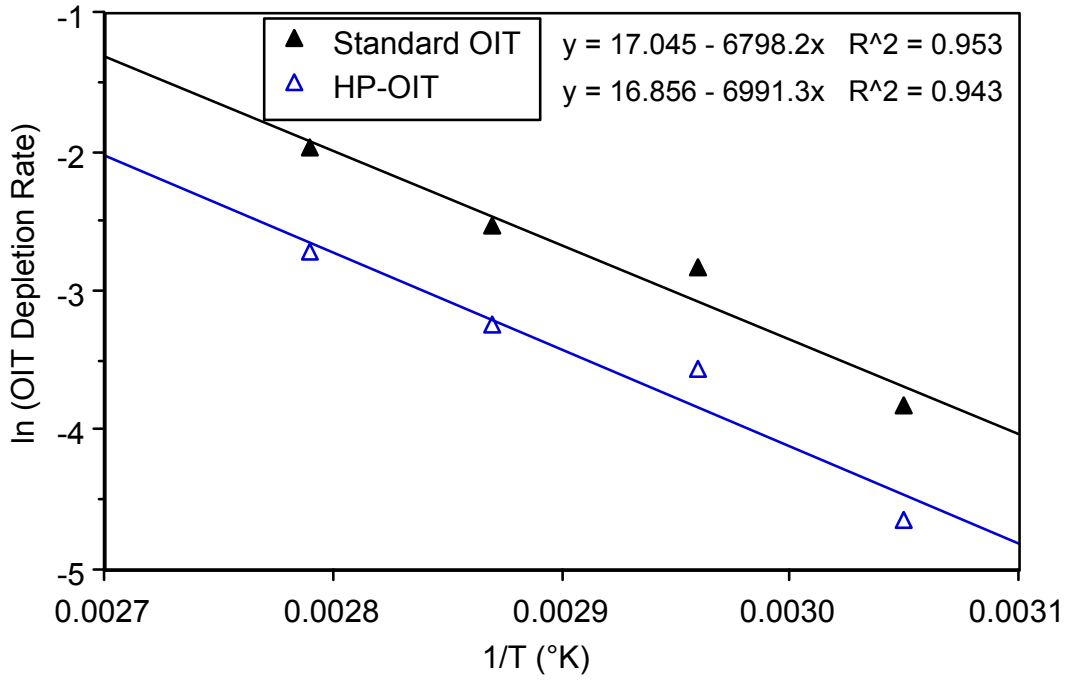

Figure B-20. Arrhenius plot for incubation Series III (water top/air beneath-compression stress).

Using Eqs. B-21 and B-22, the OIT depletion rates can be obtained.

S = - 0.0033 for Std-OIT
S = - 0.0014 for HP-OIT

In order to predict the aging time that is required to deplete the antioxidants in the HDPE GMs, Eq. B-16 is utilized. The calculation procedures to obtain the depletion times at 25°C are as follows:

- For Std-OIT tests:
  The OIT value for a pure unstabilized HDPE fluff was found to be 0.5 minutes. Thus 0.5 minutes is taken to be the OIT value when the antioxidants are consumed.

  ln (OIT) = ln(P) + (S) *(t) (B-16)
  ln (0.5) = ln (80.5) + (-0.0033)*(t)
  t = **1539 months (128 years)**

- For HP- OIT tests:
  The OIT value for a pure unstabilized HDPE fluff was found to be 25 minutes. Thus 25 minutes is taken to be the OIT value when the antioxidants are consumed.

  $\ln (OIT) = \ln(P) + (S)*(t)$ (B-16)
  $\ln (25) = \ln (210) + (-0.0014)*(t)$
  t = **1521 months (126 years)**

Thus it is seen that the predicted antioxidant lifetime at a service temperature of 25°C is approximately 120 years for this particular HDPE GM formulation under this set of simulated conditions.

B-9.4 Status of Incubation Series II and IV

Both incubation Series II and IV were started in June 1998. Thus there is only a small amount of data available and it is insufficient to perform an analysis and to generate lifetime predictions.

However, incubation Series II does require a brief discussion. Instead of using a single HDPE GM in the evaluation, eight different HDPE GMs are being evaluated. The GMs were supplied by five different manufacturers. Thus different antioxidants were most likely to have be used in the GM formulation packages. In addition, higher temperatures are being applied to this particular incubation series. The test temperatures are 55°, 65°C, 75°C, 95°C and 115°C. The purpose of experimental design is to investigate the highest possible incubation temperature for HDPE GMs without changing the antioxidant depletion mechanism. The incubation samples from the three highest test temperatures are being retrieved every month in order to monitor the rate of depletion of antioxidant content.

B-10 Summary

The three distinct stages of aging of HDPE GMs are described in this report. These stages are (A) depletion time of antioxidants, (B) induction time to the onset of polymer degradation and (C) the time to reach 50% degradation of a particular property. The lifetime of the GM is equal to the summation of these three stages. The focus of this task, however, is on the depletion time of antioxidants.

Four different incubation conditions were designed to simulate various field applications of HDPE GMs. The incubation environments involve a combination of air, water, compressive stress, and tensile stress. In addition, the aging mechanisms in each incubation condition were accelerated by elevated test temperatures which were set at 55, 65, 75 and 85°C. In this appendix, only data from two of the incubation series, Series I and Series III were presented and analyzed. Samples in Series I were completely immersed in water without any applied stress. Series III involved samples

that were exposed to water on top and air beneath, and a compressive stress of 260 kPa. Samples from both series were retrieved after specified periods of time for property evaluation. The antioxidant depletion of the incubated samples was monitored using both the Std-OIT test and HP-OIT test.

Data obtained from the elevated temperatures tests were then extrapolated to a site specific (lower) temperature using the Arrhenius model. For a site specific temperature of 25°C, the time to consume the antioxidants in this particular HDPE GM formulation will take 40 years under incubation Series I conditions. On the other hand, it will take 120 years under incubation Series III conditions. The shorter depletion time in Series I is probably due to the extraction rate of antioxidant which is higher in Series I than in Series III. The samples in Series I were exposed to moving water on all of their surfaces, whereas samples in Series III were exposed to static water on only one surface. It is known that moving water as in the Series I tests actually causes leaching of antioxidants. Hence, the depletion time for incubation Series I is likely conservative in comparison to most field situations since it is not common for both sides of the GM to be exposed to moving liquids. In this regard, the results of the Series III tests may better represent HDPE GM in-service conditions. It is noted, however, that the Series III tests were conducted with water rather than leachate. Certain strong leachates may increase the antioxidant depletion rate. Additional research of this effect is needed.

Regarding the effect of compressive stress on the antioxidant depletion rate in the Series III incubation, a definitive result has not yet been obtained. On a preliminary basis it appears that compressive stress may reduce the depletion rate, since the depletion time for Series III samples is three times greater than that of the Series I samples. One possible hypothesis is that the compressive stress may increase the density of the amorphous phase of the HDPE material, consequently reducing the diffusion rates of both antioxidants out of, and oxygen into, the GM.

Finally, it should again be emphasized that the antioxidant depletion time represents only the initial step in a three-step GM aging process, i.e., it is Stage A in Figure B-3. At the end of the antioxidant depletion time, the physical and mechanical properties of the HDPE GM still remain essentially unchanged. In order to establish the service life (i.e., the half lifetime) of an HDPE GM, the induction time plus the time to reach 50% reduction in the relevant mechanical property must be obtained. This will take longer than the current incubation time of three years, thus the time frame of this study is estimated to be ten years. The second and third parts of the study will be presented in due course.

B-11 Conclusion

Since this is only the first part in a series of three stages on the topic of HDPE lifetime prediction, this conclusion will necessarily be preliminary. Clearly though, this study establishes that the depletion of antioxidants in the HDPE GM under investigation is

quite long. Depending on the incubation method, the time for antioxidant depletion at 25°C is between 40 to 120 years.

These values, in and of themselves, are powerful indicators that HDPE GMs should last well beyond the 30-year post closure period required in many environmental regulations without any measurable degradation of mechanical properties. Clearly, a service lifetime measured in at least hundreds of years appears to be achievable. It is hoped that the results of the ongoing study will allow even better estimates of GM service lifetime in the near future.

B-12 References

Accorsi, J. and Romero, E., (1995) "Special Carbon Blacks for Plastics" *Plastics Engineering*, April 1995, pp. 29-32.

ASTM D638 - Test Method for Tensile Properties of Plastics.

ASTM D883 - Terminology Relating to Plastics.

ASTM D1238 - Test Method for Flow Rates of Thermoplastics by Extrusion Plastomer.

ASTM D1505 - Test Method for Density of Plastics by the Density-Gradient Technique.

ASTM D1603 - Test Method for Carbon Black in Olefin Plastics.

ASTM D3895 - Test Method for Oxidative Induction Time of Polyolefins by Differential Scanning Calorimetry.

ASTM D5397 - Test Method for Evaluation of Stress Crack Resistance of Polyolefin Geomembranes Using Notched Constant Tensile Load Test

ASTM D5885 - Test Method for Oxidative Induction Time for Polyolefin Geosynthetics by High Pressure Differential Calorimetry.

Billingham, N.C. and Calvert, P.D., (1986), "The Physical Chemistry of Oxidation and Stabilization of Polyolefins", *Developments in Polymer Stabilization - 3*, Chapter 5, edited by Scott, G., Published by Applied Science Publishers Ltd, London, pp. 139-190.

Chu, P.P. and Hsieh, E. T., (1992), "^{13}C and ^{1}H Nuclear Magnetic Resonance Methodologies in Industrial Polymer Research and Production", *MQC/MQA and CQC/CQA of Geosynthetics*, Edited by Koerner, R.M. and Hsuan, Y.G., GRI Conference Series, Published by IFAI, St Paul, MN., pp. 234-243.

Fay, J. J. and King R. E., (1994), "Antioxidants for Geosynthetic Resins and Applications", *Geosynthetic Resins, Formulations and Manufacturing*, Edited by Hsuan, Y.G. and Koerner, R.M., GRI Conference Series, Published by IFAI, St Paul, MN., U.S.A., pp. 77-96.

Grassie, N. and Scott, G., (1985), *Polymer Degradation and Stabilization*, Published by Cambridge University Press, New York, U.S.A.

Howard, J.B., (1973), "Data for Control of Stability in Polyolefin Wire and Cable Compounds", *Polymer Engineering Science*, Vol. 13, No. 6, pp. 429-434.

Koerner, G.R. and Koerner, R.M., (1995), "Temperature Behavior of Field Deployed HDPE Geomembranes", *Geosynthetics '95 Conference Proceedings*, Nashville, TN., pp. 921-938.

Kikkawa, K., Nakahara, Y., and Ohkatsu, Y., (1987), "Antagonism Between Hindered Amine Light Stabilizers and Sulfur-Containing Compounds", *Polymer Degradation Stabilization*, Vol. 18, pp. 237-245.

Luston, J., (1986), “Physical Loss of Stabilizers from Polymers”, *Developments in Polymer Stabilization - 2*, Chapter 5, edited by Scott, G., Published by Applied Science Publishers Ltd, London, pp. 185-240.
Mitchell, D.H. and Spanner, G.E., (1985), *Field Performance Assessment of Synthetic Liners for Uranium Tailings Ponds*, Status Report, Battelle PNL, U.S. NRC, NUREG/CR-4023, PNL-5005.
Michaels, A.S. and Bixler, H.J., (1961), “Solubility of Gases in Polyethylene”, *Journal of Polymer Science*, 50, Vol. L, pp. 393-412.
Osawa, Z. and Ishizuka, T., (1973), “Catalytic Action of Metal Salts in Autoxidation and Polymerization. (X) - The Effect of Various Methyl Stearates on the Thermal Oxidation of 2,6,10,14-Tetramethylpentadecane”, *Journal of Applied Polymer Science*, Vol. 17, pp. 2897-2907.
Petermann, J., Miles, M. and Gleiter, H., (1976), “Growth of Polymer Crystals During Annealing”, *Journal of Macromolecular Science - Physics*, B12(3), pp. 393-404.
Poland, F.G. and Harper, S.R., (1986), “Critical Review and Summary of Leachate and Gas Production from Landfills - Final Report”, U.S. EPA Cooperative Agreement, CR 908 997.
Rapoport, N.Ya. and Zaikov, G.E., (1986), “Kinetics and Mechanism of the Oxidation of Stressed Polymer”, *Developments in Polymer Stabilization - 4*, Chapter 6, edited by Scott, G., Published by Applied Science Publishers Ltd, London, pp. 207-258.
Smith, G.D., Karlsoon, K. and Gedde, U.W., (1992), “Modeling of Antioxidant Loss From Polyolefins in Hot-Water Applications. I; Model and Application to Medium Density Polyethylene Pipes”, *Polymer Engineering and Science*, Vol. 32, No.10, pp. 658-667.
Struik, L.C.E., (1978), *Physical Aging in Amorphous Polymers and Other Materials*, Elsevier Scientific Publishing Company, Amsterdam, The Netherlands.
Struve, F., (1994), “Extrusion of Geomembranes”, *Geosynthetic Resins, Formulations and Manufacturing*, Edited by Hsuan, Y.G. and Koerner, R.M., GRI Conference Series, Published by IFAI, St Paul, MN., U.S.A., pp. 77-96.
Tikuisis, T., Lam, P., and Cossar, M., (1993), “High Pressure Oxidative Induction Time Analysis by Differential Scanning Calorimetry”, *MQC/MQA and CQC/CQA of Geosynthetics*, Edited by Koerner, R.M. and Hsuan, Y.G., GRI Conference Series, Published by IFAI, St Paul, MN., pp. 191-201.
Viebke, J., Elble, E., Ifwarson, M. and Gedde, U.W. (1994), “Degradation of Unstabilized Medium-Density Polyethylene Pipes in Hot-Water Applications”, *Polymer Engineering and science*, Vol. 34, No.17, pp. 1354-1361.
Yazadini, R., Campbell, J.L. and Koerner, G.R., (1995), “Long-Term In-Situ Strain Measurements of a High Density Polyethylene Geomembrane in a Municipal Solid Waste Landfill”, *Geosynthetics ‘95 Conference Proceedings*, Nashville, TN., pp. 893-906.

B-13 Acknowledgments

Due to the nature of long-term research, which is typified by this 10-year study, financing by a number of agencies and sources is necessary. This particular task has commingled funds in the form of partnering by different organizations. The authors express their sincere appreciation to all of the following:

1. US Environmental Protection Agency, via its Risk Reduction Engineering Laboratory under Cooperative Agreement No. CR 821448. Mr. Robert Landreth (retired) and Mr. David A. Carson are the Project Officers.

2. National Science Foundation, via its Geomechanical, Geotechnical and Geo-Environmental Systems (G3S) program under Grant No. CMS-9312772. Dr. Priscilla P. Nelson is the Project Officer.

3. The consortium of Geosynthetic Research Institute (GRI) member organization via a portion of their membership fees. A listing of the current members is as follows:

GSE Lining Systems, Inc.- *William W. Walling/Melody Adams*
Earth Tech Consultants, Inc. - *Walt Studebaker/Charles P. Ballod*
U.S. Environmental Protection Agency - *David A. Carson*
Polyfelt GmbH - *Gernot Mannsbart/Philippe Delmas*
Browning-Ferris Industries - *Charles Rivette/Dan Spikula [BoD]*
E. I. duPont de Nemours & Co., Inc. - *John L. Guglielmetti/Ronald J. Winkler*
Federal Highway Administration - *Albert F. DiMillio/Jerry A. DiMaggio*
Tensar Earth Technologies, Inc. - *Peter J. Vanderzee/Donald G. Bright/Mark H. Wayne*
National Seal Co. - *Gary Kolbasuk [BoD]/George Zagorski*
Poly-Flex, Inc. - *James Nobert/George Yazdani*
Akzo Nobel Geosynthetics Co. - *Wim Voskamp/Joseph Luna*
Phillips Petroleum Co. - *Rex L. Bobsein [BoD]*
GeoSyntec Consultants Inc. - *Jean-Pierre Giroud/James A. McKelvey III/Majdi Othman*
NOVA Chemicals Ltd. - *Nolan Edmunds*
Tenax, S.p.A. - *Pietro Rimoldi [BoD]/Aigen Zhao*
Amoco Fabrics and Fibers Co. - *Gary Willibey*
U.S. Bureau of Reclamation - *Alice I. Comer/Jack Haynes*
EMCON - *Donald E. Hullings/Mark A. Swyka*
Montell USA, Inc. - *Robert G. Butala*
TC Mirafi, Inc. - *Michael M. Koutsourais/Dean Sandri*
CETCO - *James T. Olsta*
Huesker, Inc. - *Thomas G. Collins*
Solvay Polymers - *J. Michael Killough*
Naue-Fasertechnik GmbH - *Georg Heerten/Kent von Maubeuge*
Synthetic Industries, Inc. - *Marc S. Theisen/Deron N. Austin*
Mobil Chemical Co. - *Per K. Husby/Frank J. Velisek*
BBA Nonwovens - *John Matheny/Geoff Kempton*
NTH Consultants, Ltd. - *Jerome C. Neyer/Robert Sabanas*
TRI/Environmental, Inc. - *Sam R. Allen [BoD]/Richard Thomas*
U.S. Army Corps of Engineers - *David L. Jaros [BoD]*
Chevron Chemical Co. - *Pamela L. Maeger*

Serrot Corp. - *Robert A. Otto/Bill Torres [BoD]*
Union Chemical Lab (ITRI) - *Frank L. Chen*
Haley and Aldrich, Inc. - *Richard P. Stulgis [BoD]*
Westinghouse-Savannah River - *Michael Hasek*
URS/Greiner/WCC - *Pedro C. Repetto/John C. Volk*
S. D. Enterprise Co., Ltd. - *David Eakin*
Solmax Géosynthétiques - *Robert Denis*
EnviroSource Treatment & Disposal Services, Inc. - *Patrick M. McNamara*
Strata Systems, Inc. - *John N. Paulson [BoD]*
CARPI, Inc. - *Alberto M. Scuero/John A. Wilkes*
Rumpke Waste Service, Inc. - *Bruce Schmucker*
Civil & Environmental Consultants, Inc. - *Richard J. Kenter*
Firestone Building Products Co. - *H. Joseph Kalbas*
FITI (GSI-Korea) - *Han-Yong Jeon*
Waste Management Inc. - *James R. (Ron) Jones*
CETCO Europe, Ltd. - *Archie Filshill*

Appendix C
Field Performance Data for Compacted Clay Liners

by

David E. Daniel, Ph. D., P.E.
University of Illinois
Urbana, IL 61801

performed under

EPA Cooperative Agreement Number
CR-821448-01-0

Project Officer

Mr. David A. Carson
United States Environmental Protection Agency
Office of Research and Development
National Risk Management Research Laboratory
Cincinnati, OH 45268

Appendix C
Field Performance Data for Compacted Clay Liners

C-1 Introduction

The performance of compacted clay liners (CCLs) constructed from natural soil materials and soil-bentonite blends was discussed in Chapter 4. A number of graphs were presented correlating various parameters.

This appendix contains a summary of the data used in compiling the results presented in Chapter 4. The data are presented in this appendix in the form of tables of information. The intent is to provide sufficient information so that future researchers can add newly acquired data to the database and perform new analyses. Also, data on statistical variability of certain parameters was collected and is summarized in this appendix.

C-2 Data for Natural Soil Liner Materials

The data for natural soil liner materials are presented in four attached tables:

- Table C-1: Material properties
- Table C-2: Construction information
- Table C-3: Quality assurance information
- Table C-4: Hydraulic conductivity data

Each of the 89 sites is given a site number, which is shown in column 1 of all the tables. The symbols used are defined as follows:

Clay Fraction = percent on a dry weight basis finer than 2 μm
D_F = maximum depth of penetration of wetting front into soil liner
i = hydraulic gradient
k = hydraulic conductivity
L = thickness of soil liner
LL = liquid limit of the soil
MP = modified Proctor (ASTM D-1557)
OWC = optimum water content
Percent Fines = percent on a dry weight basis passing the No. 200 sieve
Percent Gravel = percent on a dry weight basis retained on the No. 4 sieve
PI = plasticity index of the soil
P_o = percent of (w,γ_d) points lying on or above the line of optimums
RC = relative compaction (dry unit weight of compacted soil divided by maximum dry unit weight from laboratory compaction test)
RP = reduced Proctor (less than the compactive effort from SP)
ΔS_i = degree of saturation of compacted soil minus degree of saturation on the line of optimum for the same dry unit weight
SP = standard Proctor (ASTM D-698)

TSB = two-stage borehole test
w = water content as a percentage
w_{opt} = optimum water content
γ_d = dry unit weight
$\gamma_{d,max}$ = maximum dry unit weight
σ' = effective stress in kPa
ψ_o = initial suction of soil liner

Some of the columns of data contain three data entries, one above the other, with the following meaning:

- Upper number is the number of data points
- Middle number is the average (geometric mean for hydraulic conductivity)
- Lower number is the standard deviation

C-3 Data for Soil-Bentonite Admixed Liners

Data for soil-bentonite admixed liners are presented in tables as follows:

- Table C-4: Material properties
- Table C-5: Construction information
- Table C-6: Quality assurance data
- Table C-7: Hydraulic conductivity data

The symbols are the same as those given in section C-2.

Table C-1. Material Properties for Natural Clay Liner Materials in Database.

Site No.	Location and Date	Source of Data	LL (%)	PI (%)	Percent Gravel	Percent Fines	Clay Fraction (%<2 μm)	w_{opt} (%)	$\gamma_{d,max}$ (kN/m^3)	Compactive Effort
1	SCA Wilsonville, IL Oct. 1992	Benson et al. 1992	- 24 -	- 10 -	- 4 -	- 65 -	- 37 -	10.2 9.0	20.1 21.3	SP MP
2	Confidential	Benson & Boutwell 1992	- 58 -	- 29 -	- - -	- 85 -	- 50 -	26.8	14.6	SP
3	Keele Valley Toronto, OT 1990	Lahti et al. 1987 Reades et al. 1990	- 25 -	- 10 -	- 2 -	- 85 -	- 22 -	12.3	19.0	SP
4	PAD B Livingston, LA 1987	Johnson et al. 1990	9 50 3	9 34 3	- 0 -	- 95 -	- 47 -	17.9	16.8	SP
5	Confidential	Benson & Boutwell 1992	- 43 -	- 26 -	- 3 -	- 87 -	- 32 -	14.3	18.6	MP
6	Confidential	Benson & Boutwell 1992	- 32 -	- 19 -	3	- 88 -	- 35 -	13.5	19.5	MP
7	Imperial, PA Dec. 1990	GeoSyntec Report	8 33 1	8 13 1	8 5 2	8 77 6	8 27 2	14.1	18.6	SP
8	Confidential	Benson & Boutwell 1992	- 35 -	- 22 -	- 1 -	- 75 -	- 45 -	14.5	18.8	MP

Table C-1. Material Properties for Natural Clay Liner Materials in Database (Continued).

Site No.	Location and Date	Source of Data	LL (%)	PI (%)	Percent Gravel	Percent Fines	Clay (%<2 μm)	w_{opt} (%)	$\gamma_{d,max}$ (kN/m^3)	Compactive Effort
9	Sauk City, WI 1988	Gordon et al. 1989	- 55 -	- 31 -	- 4 -	- - -	- 45 -	12.7	18.6	MP
10	Portage, WI 1988	Gordon et al. 1989	32 43 -	32 21 -	- 1 -	- - -	- 29 -	16.6	18.7	MP
11	Marathon, WI 1988	Gordon et al. 1989	- 57 -	- 30 -	- - -	- - -	- 39 -	21.7	17.3	MP
12	Marathon, WI 1988	Gordon et al. 1989	- 55 -	- 28 -	- - -	- - -	- 33 -	23.0	16.6	MP
13	Imperial, PA April 1991	GeoSyntec Report	8 37 1	8 15 1	8 2 1	8 78 5	8 37 4	18.0	17.0	SP
14	Test Fill 2 July 1988	Mundell & Boos 1990	3 40 8	3 20 3	6 0 -	6 70 8	6 25 11	16.2	16.7	SP
15	Confidential	Benson & Boutwell 1992	12 85 3	12 58 3	1 0 -	1 99 -	- 57 -	25.8	14.6	SP
16	Test Fill 1	Mundell & Boos 1990	24 41 9	24 22 6	20 0 -	20 77 -	20 38 8	15.8	17.0	SP
17	Livingston, LA Pad A Oct. 1988	Johnson et al. 1990	9 50 3	9 34 3	- 0 -	- 95 -	- 47 -	20.3	16.4	SP

Table C-1. Material Properties for Natural Clay Liner Materials in Database (Continued).

Site No.	Location and Date	Source of Data	LL (%)	PI (%)	Percent Gravel	Percent Fines	Clay Fraction (%<2 μm)	w_{opt} (%)	$\gamma_{d,max}$ (kN/m^3)	Compactive Effort
18	Tangipahoa Landfill Amite, LA March 1992	Boutwell & McManis 1995	10 30 6	10 18 4	5 0 -	5 52 3	5 16 1	13.0	18.7	SP
19	Confidential	Benson & Boutwell 1992	12 32 3	12 14 2	12 1 1	12 85 3	12 44 4	10.5	20.1	MP
20	Confidential	Personal Files	- 49 -	- 23 -	- 1 -	- 94 -	- 43 -	18.5	17.2	SP
21	Confidential	Trast 1993	- 51 -	- 26 -	- 1 -	- 90 -	- 36 -	11.8 18.0	18.5 17.0	MP SP
22	1993	Othman & Luettich 1994	- 63 -	- 42 -	- - -	- 96 -	- - -	20.5	16.3	SP
23	Green County, WI 1987	Krantz & Bailey 1990	20 39 4.2	20 18 3.8	- - -	- 73 -	- 30 -	20.0	16.5	SP
24	Confidential	Trast 1993	- 67 -	- 46 -	- 0 -	- 94 -	53	16.0 21.5	18.4 16.3	MP SP
25	Confidential	Trast 1993	- 53 -	- 41 -	- 0 -	- 88 -	- 36 -	11.5 16.1	19.8 18.0	MP SP

Table C-1. Material Properties for Natural Clay Liner Materials in Database (Continued).

Site No.	Location and Date	Source of Data	LL (%)	PI (%)	Percent Gravel	Percent Fines	Clay Fraction (%<2 μm)	w_{opt} (%)	$\gamma_{d,max}$ (kN/m^3)	Compactive Effort
26	Confidential	Trast	-	-	-	-	-	12.2	19.3	MP
		1993	33	19	7	85	37	17.5	17.7	SP
			-	-	-	-	-	18.5	17.1	RP
27	Confidential	Trast	-	-	-	-	-	12.5	19.4	MP
		1993	31	18	8	74	26	16.5	17.8	SP
			-	-	-	-	-	18.5	17.2	RP
28	Confidential	Trast	-	-	-	-	-	11.5	19.4	MP
		1993	35	19	3	89	41	16.6	17.5	SP
			-	-	-	-	-	18.5	17.0	RP
	ERC Facility	Bergstrom et al.	-	-	-	-	-	9.0	20.5	MP
	Milan, MI	1995	27	10	2	76	28	13.0	19.1	SP
29	1993		-	-	-	-	-	14.4	18.6	RP
30	Confidential	Personal Files	-	-	-	-	-	14.0	18.6	MP
			32	19	-	-	-			
			-	-	-	-	-			
31	Confidential	Personal Files	7	7	7	7	7	12.4	19.3	SP
			40	24	7	58	23			
			1	1	4	3	1			
32	Confidential	Personal Files	-	-	-	-	-	11.0	19.9	MP
			45	27	0	99	42			
			-	-	-	-	-			
33	Confidential	Personal Files	-	-	-	-	-	13.3	18.9	MP
			29	15	1	87	40			
			-	-	-	-	-			
34	Confidential	Personal Files	-	-	-	-	-			
			44	16	0	96	-	17.3	17.1	SP
			-	-	-	-	-			

Table C-1. Material Properties for Natural Clay Liner Materials in Database (Continued).

Site No.	Location and Date	Source of Data	LL (%)	PI (%)	Percent Gravel	Percent Fines	Clay Fraction (%<2 μm)	w_{opt} (%)	$\gamma_{d,max}$ (kN/m^3)	Compactive Effort
35	Confidential	Personal Files	- 39 -	- 19 -	- 0 -	- 97 -	- - -	22.2	17.7	SP
36	Confidential	Personal Files	9 36 2.5	9 17 1.6	9 2 1.6	9 74 2.6	9 30 3.4	13.2	18.3	SP
37	Indianapolis, IN 1994	Personal Files	3 36 3	3 17 2	3 10 5	3 48 3	3 16 1	12.4	19.0	SP
38	ISGS Prototype Urbana, IL 1986	ISGS Report	- 21 -	- 7 -	- 9 -	- 60 -	- 26 - (4 μm)	10.3	20.4	SP
39	ISGS Field-Scale Urbana, IL April 1988	ISGS Report	- 21 -	- 7 -	- 9 -	- 60 -		10.3	20.4	SP
40	Confidential	Personal Files	15 101 5	15 71 5	- 0 -	- 98 -		31.6	13.4	SP
41	BP Chemicals SDRI 1 Port Lavaca, TX Nov. 1988	McBride-Ratcliff Report	- 47 -	- 30 -	- - -	- 66 -	- - -	19.5	16.3	SP
42	Celanese Bishop, TX July 1986	Personal Files	3 69 3.6	3 45 3.0	2 0 0	3 79 3.0	2 49 4.2	23.4	15.1	SP

Table C-1. Material Properties for Natural Clay Liner Materials in Database (Continued).

Site No.	Location and Date	Source of Data	LL (%)	PI (%)	Percent Gravel	Percent Fines	Clay Fraction (%<2 μm)	w_{opt} (%)	$\gamma_{d,max}$ (kN/m^3)	Compactive Effort
43	GCWDA Test Fill A	Personal Files	119	119	-	119	-	22.4	15.4	SP
	Texas City, TX		62	42	-	86	-			
	Nov. 1988		4.1	4.3	-	6.2	-			
44	GCWDA Test Fill B	Personal Files	119	119	-	119	-	22.4	15.4	SP
	Texas City, TX		62	42	-	86	-			
	Nov. 1988		4.1	4.3	-	6.2	-			
	Texas Eastman	H.B. Zachry Co.	8	8	-	8	-	19.5	16.4	SP
	Longview, TX	Report	44	28	-	70	-			
45	1987		4.0	3.2	-	2.4	-			
46	Puckett Plant	Personal Files	31	31	-	31	2	23.3	15.4	SP
	Ft. Stockton, TX		35	16	-	98	22			
	April 1988		1.8	2.3	-	1.1	8.4			
47	Shell	Personal Files	41	41	-	41	-	14.6	17.7	SP
	Deer Park, TX		39	24.3	-	69.5	-			
	Dec. 1988		4.7	5.2	-	-	-			
48	Confidential	Personal Files	60	60	-	-	-	20.0	16.2	RP
			41	23	-	86	-	18.0	16.7	SP
			2.7	-	-	-	-	13.3	18.7	MP
49	Confidential	Personal Files	60	60	-	-	-	20.0	16.2	RP
			42	22	-	86	-	18.0	16.7	SP
			1.7	-	-	-	-	13.3	18.7	MP

Table C-1. Material Properties for Natural Clay Liner Materials in Database (Continued).

Site No.	Location and Date	Source of Data	LL (%)	PI (%)	Percent Gravel	Percent Fines	Clay Fraction (%<2 μm)	w_{opt} (%)	$\gamma_{d,max}$ (kN/m^3)	Compactive Effort
50	Confidential	Personal Files	88	88	-	-	-	20.0	16.2	RP
			43	24	-	86	-	18.0	16.7	SP
			3.4	-	-	-	-	13.3	18.7	MP
51	Confidential	Personal Files	62	62	-	-	-	20.0	16.2	RP
			40	22	-	86	-	18.0	16.7	SP
			1.9	-	-	-	-	13.3	18.7	MP
52	Emelle, AL	Golder Assoc.	2	2	3	3	3	19.9	16.5	SP
	Oct.1984	Report	37	18	10	73	38			
			1.4	2.8	8.9	15.1	9.0			
	Confidential	Personal Files	8	8	8	-	8	19.9	16.4	SP
			54	31	0	-	40			
53			2	3	0	-	3			
54	Quarantine Rd Landfill	Personal Files	-	-	-	-	-	-	-	-
			-	-	-	-	-	-	-	-
	Baltimore, MD		-	-	-	-	-	-	-	-
	Jan. 1994									
55	Savannah	Mueser-Rutledge	-	-	-	-	-	27.4	14.5	SP
	River Plant Panel A1	Report	66	35	0	93	-			
			-	-	-	-	-			
	March 1988									
56	Savannah	Mueser-Rutledge	-	-	-	-	-	27.4	14.5	SP
	River Plant Panel A2	Report	66	35	0	93	-			
			-	-	-	-	-			
	March 1988									
57	Savannah	Mueser-Rutledge	-	-	-	-	-	26.8	14.6	SP
	River Plant Panel B1	Report	69	38	0	98	-			
			-	-	-	-	-			
	March 1988									

Table C-1. Material Properties for Natural Clay Liner Materials in Database (Continued).

Site No.	Location and Date	Source of Data	LL (%)	PI (%)	Percent Gravel	Percent Fines	Clay Fraction (%<2 μm)	w_{opt} (%)	$\gamma_{d,max}$ (kN/m^3)	Compactive Effort
58	Savannah River Plant Panel B2 March 1988	Mueser-Rutledge Report	- 69 -	- 38 -	- 0 -	- 98 -	- - -	26.8	14.6	SP
59	Savannah River Plant Panel B3 March 1988	Mueser-Rutledge Report	- 69 -	- 38 -	- 0 -	- 98 -	- - -	26.8	14.6	SP
60	Savannah River Plant Panel C1 March 1988	Mueser-Rutledge Report	- 68 -	- 35 -	- 0 -	- 95 -	- - -	26.6	14.6	SP
61	Savannah River Plant Panel C2 March 1988	Mueser-Rutledge Report	- 68 -	- 35 -	- 0 -	- 95 -	- - -	26.6	14.6	SP
62	Savannah River Plant Panel D1 March 1988	Mueser-Rutledge Report	- 51 -	- 20 -	- 0 -	- 73 -	- - -	20.2	15.9	SP
63	Savannah River Plant Panel D2 March 1988	Mueser-Rutledge Report	- 51 -	- 20 -	- 0 -	- 73 -	- - -	20.2	15.9	SP
64	BP Chemicals Port Lavaca, TX SDRI 2 Dec. 1988	McBride-Ratcliff Report	- 47 -	- 30 -	- - -	- 66 -	- - -	19.5	16.3	SP

Table C-1. Material Properties for Natural Clay Liner Materials in Database (Continued).

Site No.	Location and Date	Source of Data	LL (%)	PI (%)	Percent Gravel	Percent Fines	Clay Fraction (%<2 μm)	w_{opt} (%)	$\gamma_{d,max}$ (kN/m^3)	Compactive Effort
65	BP Chemicals	McBride-Ratcliff	-	-	-	-	-	13.5	19.2	MP
	Port Lavaca, TX	Report	47	31	-	66	-			
	SDRI 3		-	-	-	-	-			
	Dec. 1988									
66	Confidential	Personal Files	-	-	-	-	-	19.0	16.1	SP
			50	29	-	75	-			
			-	-	-	-	-			
	Confidential	Personal Files	-	-	-	-	-	19.3	16.1	SP
			49	27	-	62	-			
67			-	-	-	-	-			
68	Confidential	Personal Files	4	4	4	4	4	14.8	17.7	SP
			35	17	2	67	22	11.5	19.0	MP
			1	1	2	10	4			
69	Confidential	Personal Files	4	4	4	4	4	10.0	19.9	SP
			22	9	6	50	16	8.5	21.4	MP
			1	1	3	2	1			
70	Confidential	Personal Files	-	-	-	-	-	14.9	18.7	MP
			42	26	0	88	45			
			-	-	-	-	-			
71	Confidential	Personal Files	-	-	-	-	-	12.2	19.6	MP
			29	19	4	83	34			
			-	-	-	-	-			
72	SDDS Longtree LF	S. Dakota Disposal	3	3	-	-	-	18.0	16.5	SP
	Igloo, SD	Systems Report	36	20	0	85	35			
	Feb. 1990		2.0	1.7	-	-	-			

Table C-1. Material Properties for Natural Clay Liner Materials in Database (Continued).

Site No.	Location and Date	Source of Data	LL (%)	PI (%)	Percent Gravel	Percent Fines	Clay Fraction (%<2 μm)	w_{opt} (%)	$\gamma_{d,max}$ (kN/m^3)	Compactive Effort
73	Sea Drift, TX	McClelland	4	4	-	-	-	21.0	15.5	-
	Sept. 1988	Engineers Report	76	53	-	-	-			
			6.0	6.0	-	-	-			
74	Sea Drift, TX	McClelland	4	4	-	-	-	18.0	16.9	-
	Sept. 1988	Engineers Report	56	40	-	64	-			
			6.0	5.0	-	-	-			
75	McClellandtown, PA	Cumberland Geot.,	-	-	-	-	-	21.0	15.6	SP
	Sept. 1990	Consultants Report	-	-	-	-	-			
			-	-	-	-	-			
	Confidential	Personal Files	4	4	-	-	-	19.2	16.6	SP
			37	17	1	92	-			
76			3.0	2.0	-	-	-			
77	Arnoni LF Pad 1	Personal Files	45	45	-	-	-	9.9	19.7	SP
	Pittsburgh, PA		32	13	-	-	=19			
	Feb. 1994		0.8	0.9	-	-	-			
78	Arnoni LF Pad 2	Personal Files	45	45	-	-	-	11.5	19.6	SP
	Pittsburgh PA		32	16	-	-	=25			
	Feb. 1994		1.6	1.3	-	-	-			
79	DuPont Pad 1	Engineering	12	12	-	9	-	25.0	14.9	SP
	Victoria, TX	Sciences Report	62	41	-	82	-	17.8	16.5	MP
	Jan. 1989		5.3	4.9	-	3.2	-			
80	DuPont Pad 2	Engineering	17	17	-	15	-	19.6	15.9	SP
	Victoria, TX	Science Report	52	35	-	84	-	14.4	18.0	MP
	Jan 1989		1.3	1.2	-	6.0	-			

Table C-1. Material Properties for Natural Clay Liner Materials in Database (Continued).

Site No.	Location and Date	Source of Data	LL (%)	PI (%)	Percent Gravel	Percent Fines	Clay Fraction (%<2 μm)	w_{opt} (%)	$\gamma_{d,max}$ (kN/m^3)	Compactive Effort
81	GE Waterford, NY July 1989	Clough Harbor & Assoc. Report	- 47 -	- 22 -	- - -	- - -	- - -	25	15.3	SP
82	Findlay Township, PA Aug. 1988	Paul Rizzo & Assoc. Report	- - -	- - -	- - -	4 84 5.4	4 54 6.7	-	-	-
83	Findlay Township, PA Aug. 1988	Paul Rizzo & Assoc. Report	4 39 3.6	4 16 1.9	4 10 3.3	4 81 2.7	4 48 8.6	18.2	17.6	SP
84	Montezuma Hills, CA Pad A (Dark) Feb. 1991	IT Corp. Report	- - -	- - -	- - -	- - -	- - -	-	-	-
85	Montezuma Hills, CA Pad B (Light) Feb. 1991	IT Corp. Report	- - -	- - -	- - -	- - -	- - -	-	-	-
86	Fernald, OH Pad 1 (Ln. 1) Nov. 1996	GeoSyntec Report	- 43 -	- 24 -	- - -	- 84 -	- 37 -	17.7	17.1	SP
87	Fernald, OH Pad 1 (Ln. 2) Nov. 1996	GeoSyntec Report	- 43 -	- 24 -	- - -	- 84 -	- 37 -	17.7	17.1	SP

Table C-1. Material Properties for Natural Clay Liner Materials in Database (Continued).

Site No.	Location and Date	Source of Data	LL (%)	PI (%)	Percent Gravel	Percent Fines	Clay Fraction (%<2 μm)	w_{opt} (%)	$\gamma_{d,max}$ (kN/m^3)	Compactive Effort
88	Fernald, OH	GeoSyntec Report	-	-	-	-	-	11.6	19.1	SP
	Pad 2 (Ln. 1)		25	14	-	70	29			
	Nov. 1996		-	-	-	-	-			
89	Fernald, OH	GeoSyntec Report	-	-	-	-	-	11.6	19.1	SP
	Pad 2 (Ln. 2)		25	14	-	70	29			
	Nov. 1996		-	-	-	-	-			

Table C-2. Construction Information for Natural Clay Liner Materials in Database.

Site No.	Compaction Criteria	Compactor	Compactor Mass (kg)	Passes per Lift	Lift Thickness (mm)	Number of Lifts	Pad Size (m x m or m^2)
1	w > OWC RC > 90% MP	CAT 825	32,400	6	150	6	36 x 15
2	None	Bomag 210PD	-	6	150	5	32 x 14
3	w > OWC RC > 95% SP	Rex 370	30,000	4	150	8	30 x 30
4	w > OWC + 2, <+8 RC > 90% MP	CAT 815	19,800	-	150	4	15 x 30
5	w > OWC RC > 90% MP	Rex Trashmaster	36,000	6	150	10	Liner
6	w > OWC RC > 90% MP	CAT 825	32,400	5	150	6	29 x 12
7	w > OWC + 2 RC > 90% MP	CAT 825	32,400	4	150	8	15 x 24
8	w > OWC -2 to +4 RC > 90% MP	Dynapac CT25	12,600	4	150	6	24 x 18
9	w > OWC RC > 90% MP	-	-	-	150	10	Liner
10	w > OWC RC > 90% MP	-	-	-	150	10	Liner
11	w > OWC RC > 90% MP	-	-	-	150	10	Liner
12	w > OWC RC > 90% MP	-	-	-	150	10	Liner
13	w > OWC + 2, <+5 RC > 90% MP	CAT 825	32,400	4	150	8	15 x 24

Table C-2. Construction Information for Natural Clay Liner Materials in Database (continued).

Site No.	Compaction Criteria	Compactor	Compactor Mass (kg)	Passes per Lift	Lift Thickness (mm)	Number of Lifts	Pad Size (m x m or m^2)
14	w > OWC + 2, <+5 RC > 90% MP	-	-	-	170	6	9 x 14
15	w > OWC RC > 100% SP	-	-	-	200	7	12 x 26
16	w > OWC + 2, <+5 RC > 90% MP	CAT 835	39,000	-	170	5	9 x 9
17	w > OWC + 2, <+6 RC > 90% SP	CAT 815	19,800	6	150	4	15 x 30
18	S_i >78.5 RC > 90% MP	CAT D7G bulldozer	25,000	4	150	5	30 x 12
19	w > OWC RC > 90% MP	CAT 825	32,400	5	150	10	Liner
20	S_i > 82.0	CAT 825	32,400	8	150	6	45 x 20
21	w > OWC RC > 95% SP	CAT 825	32,400	6	150	6	58 x 26
22	S_i > 85.0	-	-	-	-	-	-
23	w > OWC RC > 90% MP	-	-	-	150	10	Liner
24	w > OWC RC > 90% MP	CAT 815A	18,900	8 - 12	150	5	31 x 15
25	w > OWC RC > 90% MP	CAT 815A	18,900	8 - 12	150	5	31 x 15
26	w > OWC RC > 90% MP	Dynapac CA25	18,900	4 - 6	150	6	27 x 17
27	w > OWC RC > 90% MP	Dynapac CA25	18,900	4 - 6	150	6	27 x 17

Table C-2. Construction Information for Natural Clay Liner Materials in Database (continued).

Site No.	Compaction Criteria	Compactor	Compactor Mass (kg)	Passes per Lift	Lift Thickness (mm)	Number of Lifts	Pad Size (m x m or m^2)
28	w > OWC RC > 90% MP	Dynapac CA25	18,900	4 - 6	150	6	27 x 17
29	w > OWC-2, +5 RC > 90% MP	CAT 825	32,400	6	170	9	32 x 16
30	RC > 90% MP	Rex Trashmaster	27,000	-	150	6	-
31	w > OWC RC > 95% SP	CAT S563	-	-	300	2	13 X 26
32	w > OWC, <+6 RC > 90% MP	CAT 825	32,400	-	150	8	15 x 40
33	w > OWC RC > 90% MP	CAT 815B	19,800	-	150	8	15 x 30
34	w > OWC RC > 95% SP	IR SPF-56 & CAT 815	19,800	4 (2 each)	150	3	-
35	w > OWC RC > 95% SP	CAT 824B	32,400	6	150	6	-
36	w > OWC, <+6 RC > 95% SP	CAT 815	17,100	8	60	6	15 x 30
37	w > OWC RC > 95% SP	FWD 741	-	4	60	5	-
38	w > OWC RC > 90% MP	Hyster C852A	-	12	150	6	3 x 9
39	w: 11 to 12% RC > 90% SP	CAT 815B	19,800	12	130	6	14.6 x 7.3
40	w > OWC, +5 RC > 92% SP	sheepsfoot	59 kg/lin. cm	-	150	6	8 x 26

Table C-2. Construction Information for Natural Clay Liner Materials in Database (continued).

Site No.	Compaction Criteria	Compactor	Compactor Mass (kg)	Passes per Lifs	Lift Thickness (mm)	Number of Lifts	Pad Size (m x m or m^2)
41	RC > 95% SP	CAT 815	19,800	40	150	4	93
42	-	wedgefoot	-		150	4	30 x 15
43	w > OWC+1 RC > 95% SP	IR SPF-48	7,200	16	150	5	37 x 9
44	w > OWC+1 RC > 90% SP	IR SPF-48	7,200	8	150	5	37 x 9
45	w > OWC, <+2 RC > 95% SP	CAT 815 & Bomag BW213PD	19,800 14,000	4 2	150	4	288
46	w > OWC+1, <+3 RC > 95% SP	Dynapac CA25	10,900	8	200 - 250	5	15 x 30
47	w > OWC+1, <+5 RC > 90% SP	CAT 815B	19,800	6 - 10	85	10	46 x 24
48	w > OWC, <+3 RC > 95% SP	CAT 815B	19,800	5 - 8	150	4	46 x 15
49	w > OWC, <+3 RC > 95% SP	CAT 815B	19,800	3	150	4	46 x 15
50	w > OWC, <+3 RC > 95% SP	CAT 815B	19,800	3	150	4	46 x 15
51	w > OWC, <+3 RC > 95% SP	CAT 815B	19,800	4 - 5	150	4	46 x 15
52	w > OWC, <+3 RC > 95% SP	-	-	-	-	-	150
53	-	CAT 825C	-	4	-	4	-
54	-	-	-	-	150	4	-
55	-	CAT 815B	19,800	12	160	4	483

Table C-2. Construction Information for Natural Clay Liner Materials in Database (continued).

Site No.	Compaction Criteria	Compactor	Compactor Mass (kg)	Passes per Lift	Lift Thickness (mm)	Number of Lifts	Pad Size (m x m or m^2)
56	-	Rex 3-50A & CAT 815B	19,800	6 (Lifts 1-3) 21 (Lift 4)	130	4	483
57	-	CAT 815B	19,800	6	140	4	483
58	-	CAT 815B	19,800	12	150	4	483
59	-	CAT 815B	19,800	12	170	4	483
60	-	CAT 815B	19,800	12	170	4	483
61	-	CAT 815B	19,800	12	190	4	483
62	-	CAT 815B	19,800	12	150	4	483
63	-	CAT 815B	19,800	12	230	4	483
64	RC > 95% SP	CAT 815	19,800	40	150	4	93
65	RC > 91% MP	CAT 815	19,800	80	150	4	186
66	w > OWC+1, <+5 RC > 95% SP	CAT 815	19,800	2	100	10	12 x 26
67	w > OWC+1, <+5 RC > 95% SP	CAT 815	19,800	2	100	11	12 x 26
68	w > OWC+1, <+5 RC > 95% SP	CAT 815B	19,800	6	150	4	15 x 36
69	w > OWC+1, <+5 RC > 95% SP	CAT 815B	19,800	6	150	4	15 x 36
70	w > OWC-2, <+4 RC > 90% MP	-	-	7 to 10	150	6	24 x 18
71	w > OWC-2, <+4 RC > 90% MP	-	-	7 to 10	150	6	24 x 18
72	w > OWC, <+6 RC > 95% SP	CAT 825C	32,400	8	150	4	18 x 36

Table C-2. Construction Information for Natural Clay Liner Materials in Database (continued).

Site No.	Compaction Criteria	Compactor	Compactor Mass (kg)	Passes per Lift	Lift Thickness (mm)	Number of Lifts	Pad Size (m x m or m^2)
73	w > OWC, <SL RC > 95% SP	CAT 815B	19,800	22	1 @ 200 6 @ 100	7	12 x 23
74	w > OWC, <SL RC > 95% SP	CAT 815B	19,800	22	1 @ 200 6 @ 100	7	12 x 23
75	w > OWC+3, <+6 RC > 95% SP	CAT 815B	19,800	-	1 @ 200 3 @ 150	4	15 x 30
76	w > OWC+3, <+5 RC > 95% SP	CAT 815B	19,800	6	150	4	18 x 30
77	w > OWC+0.4 RC > 98% SP	IR SD-100D	10,200	10	100	9	15 x 30
78	w > OWC+1.5 RC > 94% SP	IR SD-100D	10,200	4	100	9	15 x 30
79	w > OWC RC > 95% SP	CAT 815B	19,800	8	150	8	465
80	w > OWC RC > 95% SP	CAT 815B	19,800	8	150	8	465
81	w > OWC+4	Dresser VOS PD84A	16,200	4	150	4	465
82	RC > 96% SP	CAT 825 & Vib. Smooth Drum	32,400 -	6 2	150	4	223
83	RC > 96% SP	CAT 825 & Vib. Smooth Drum	32,400 -	6 2	150	4	223
85	RC > 90% MP	CAT 815B	19,800	-	1 @ 300 3 @ 200	20 x 24	-

Table C-2. Construction Information for Natural Clay Liner Materials in Database (continued).

Site No.	Compaction Criteria	Compactor	Compactor Mass (kg)	Passes per Lift	Lift Thickness (mm)	Number of Lifts	Pad Size (m x m or m^2)
85	RC > 90% MP	CAT 815B	19,800	-	1 @ 300 3 @ 200	20 x 24	-
86	W > OWC, <+4; RC > 95% SP	CAT 815	19,800	4	150	6	13 x 15
87	W > OWC, <+4; RC > 95% SP	CAT 815	19,800	7	150	6	13 x 15
88	W > OWC, <+4; RC > 95% SP	CAT 815	19,800	4	150	6	13 x 15
89	W > OWC, <+4; RC > 95% SP	CAT 815	19,800	6	150	6	13 x 15

Table C-3. Quality Control/Quality Assurance Data for Natural Clay Liners in Database.

Site No.	w (%)	γ_d (kN/m^3)	P_o	ΔS_i	Distress	Purpose	Remarks
1	34 10.3 0.8	34 19.8 0.036	44	- 2.0	None	Verify k ≤ 1 x 10^{-7} cm/s	
2	57 26.6 2.2	57 14.4 4.0	28	-4.0	None	Verify k ≤ 1 x 10^{-7} cm/s	
3	- 13.8 -	- 19.4 -	98	+17.7	None	Verify k ≤ 1 x 10^{-8} cm/s	
4	4 21.3 0.5	4 16.0 0.17	80	+3.0	None	Verify k ≤ 1 x 10^{-7} cm/s ; show KF = KL using standard construction methods	Compacted slightly wet of modified Proctor optimum and wet of line of optimums
5	21 17.3 2.2	21 17.3 0.51	95	-3.0	None	Verify k ≤ 1 x 10^{-7} cm/s	
6	32 13.8 0.9	37 19.0 0.31	32	-8.2	None	Verify k ≤ 1 x 10^{-7} cm/s	Met CQA Spec, but dry of line of optimums
7	33 17.2 1.5	33 17.7 0.47	88	+1.0	None	Verify k ≤ 1 x 10^{-7} cm/s	
8	17 15.3 1.2	17 17.7 0.9	8	-12.6	None	Verify k ≤ 1 x 10^{-7} cm/s	
9	85 19.6 1.9	85 17.0 0.31	90	+5.8	None	Monitor liner performance and Verify k ≤ 1 x 10^{-7} cm/s	

Table C-3. Quality Control/Quality Assurance Data for Natural Clay Liners in Database (continued).

Site No.	w (%)	γ_d (kN/m^3)	P_o	ΔS_i	Distress	Purpose	Remarks
10	93 17.8 1.5	93 16.9 0.34	50	+3.5	None	Monitor liner performance and verify k ≤ 1 x 10^{-7} cm/s	
11	91 25.4 3.2	9100 16.0 0.66	75	-7.4	None	Monitor liner performance and verify k ≤ 1 x 10^{-7} cm/s	
12	289 26.0 2.3	289 16.1 0.50	78	+4.6	None	Monitor liner performance and verify k ≤ 1 x 10^{-7} cm/s	
13	34 20.7 0.6	34 16.7 0.24	100	+9.0	None	Verify k ≤ 1 x 10^{-7} cm/s	
14	18 17.0 0.9	18 16.8 0.16	78	+4.0	None	Verify k ≤ 1 x 10^{-7} cm/s	
15	48 30.8 0.5	48 14.1 0.27	48 98 -	48 +8.0 0.03	None	Verify k ≤ 1 x 10^{-7} cm/s	
16	11 19.8 1.2	11 16.1 0.22	91	+6.0	None	Verify k ≤ 1 x 10^{-7} cm/s	
17	16 23.3 1.2	16 15.7 0.44	100	+3.0	None	Verify k ≤ 1 x 10^{-7} cm/s; show KF = KL using standard construction methods	
18	20 16.6 0.9	20 17.35 0.25	85	+4.0	None	Verify k ≤ 1 x 10^{-7} cm/s	

Table C-3. Quality Control/Quality Assurance Data for Natural Clay Liners in Database (continued).

Site No.	w (%)	γ_d (kN/m^3)	P_o	ΔS_i	Distress	Purpose	Remarks
19	584 13.6 0.72	584 19.0 0.19	81	+3.8	None	Monitor liner performance and verify k ≤ 1 x 10^{-7} cm/s	
20	37 17.6 0.52	37 16.9 0.33	8	-6.2	None	Verify k ≤ 1 x 10^{-7} cm/s	Compacted dry of line of optimums using acceptable zone approach
21	18 19.5 0.3	18 16.9 0.15	80	+4.3	None	Veryfy Suitability of Silty Material for k ≤ 1 x 10^{-7} cm/s	
22	-	-	-	-3.0	None	Verify k ≤ 1 x 10^{-7} cm/s	Spec. required that So ≥ 90%
23	60 22.0 2.8	60 16.4 0.57	89	+7.4	None	Monitor liner performance and perify k ≤ 1 x 10^{-7} cm/s	
24	19 23.6 1.1	19 15.8 0.32	81	+0.4	None	Verify k ≤ 1 x 10^{-7} cm/s	
25	18 18.9 0.31	18 16.9 0.42	71	-0.5	None	Verify k ≤ 1 x 10^{-7} cm/s	
26	53 15.5 -	53 17.6 -	17	-8.8	None	Verify k ≤ 1 x 10^{-7} cm/s	In spec, but dry of line of optimums
27	36 13.5 -	36 18.0 -	6	-10.4	None	Verify k ≤ 1 x 10^{-7} cm/s	In spec, but dry of line of optimums

Table C-3. Quality Control/Quality Assurance Data for Natural Clay Liners in Database (continued).

Site No.	w (%)	γ_d (kN/m^3)	P_o	ΔS_i	Distress	Purpose	Remarks
28	54 16.2 -	54 17.7 -	57	-0.3	None	Verify K < 1 x 10^{-7} cm/s	In spec, but straddles line of optimums
29	92 13.9 0.71	92 18.8 0.28	84	+1.0	None	Verify K < 1 x 10^{-7} cm/s	
30	- 16.2 -	- 18.6 -	65	-2.3	None	Verify K < 1 x 10^{-7} cm/s	
31	- 13.1 -	- 19.1 -	75	-1.5	None	Verify K < 1 x 10^{-7} cm/s	
32	- 13.9 -	- 19.2 -	92	+7.5	None	Verify K < 1 x 10^{-7} cm/s	
33	- 13.4 -	- 18.7 -	80	+0.7	None	Verify K < 1 x 10^{-7} cm/s	
34	- 17.8 -	- 17.1 -	45	+2.5	None	Verify K < 1 x 10^{-7} cm/s	
35	- 20.7 -	- 16.8 -	78	+2.8	None	Verify K < 1 x 10^{-7} cm/s	
36	- 15.5 -	- 17.6 -	77	+3.4	None	Verify K < 1 x 10^{-7} cm/s	Constructed with mine spoil

Table C-3. Quality Control/Quality Assurance Data for Natural Clay Liners in Database (continued).

Site No.	w (%)	γ_d (kN/m^3)	P_o	ΔS_i	Distress	Purpose	Remarks
37	- 14.1 -	- 18.2 -	45	-1.2	None	Verify k ≤ 1 x 10^{-7} cm/s	Disturbance in tube by gravel
38	24 11.5 3.6	24 20.4 0.77	Raw Data NA	+10.2	None	Verify k ≤ 1 x 10^{-7} cm/s	
39	57 11.6 1.1	57 17.9 0.82	10	-19	None	Verify k ≤ 1 x 10^{-7} cm/s	
40	40 35.5 0.5	40 12.8 0.17	100	+0.03	Desiccation (Hot HDPE)	Verify k ≤ 1 x 10^{-7} cm/s	
41	13 21.9 0.88	13 16.0 0.22	92	+5.6	None	Verify k ≤ 1 x 10^{-7} cm/s	
42	26 25.0 1.5	26 15.1 0.36	81	+5.5	None	Verify k ≤ 1 x 10^{-7} cm/s	
43	49 23.4 1.12	49 15.4 0.28	63	+3.9	None	Verify k ≤ 1 x 10^{-7} cm/s	East Side = A, West = B; used light roller
44	49 24.2 1.5	49 15.0 0.40	47	+1.0	None	Verify k ≤ 1 x 10^{-7} cm/s	
45	31 19.8 1.03	31 103.8 2.61	71	+0.4	None	Verify k ≤ 1 x 10^{-7} cm/s	Nothing unusual

Table C-3. Quality Control/Quality Assurance Data for Natural Clay Liners in Database (continued).

Site No.	w (%)	γ_d (kN/m^3)	P_o	ΔS_i	Distress	Purpose	Remarks
46	32 27.3 3.4	32 15.4 0.22	100	+8.0	None	Verify $k \leq 1 \times 10^{-7}$ cm/s	Cell 1E had SDRI, G_s = 2.67 measured
47	51 16.5 1.25	51 17.7 0.50	100	+9.9	None	Verify $k \leq 1 \times 10^{-7}$ cm/s	
48	160 17.8 0.40	160 17.0 1.1	75	1.1	potentially desiccation or freeze-thaw damage	Verify $k \leq 1 \times 10^{-7}$ cm/s	Pads at Sites 48-51 were constructed with same material by 4 different contractors. Objective in each case to obtain KF $\leq 10^{-7}$ cm/s, with low bid/low K contractor winning job.
49	152 18.9 1.05	152 16.7 0.25	86	0.3	potentially desiccation or freeze-thaw damage	Verify $k \leq 1 \times 10^{-7}$ cm/s	
50	216 18.6 1.16	216 16.9 0.37	84	1.3	potentially desiccation or freeze-thaw damage	Verify $k \leq 1 \times 10^{-7}$ cm/s	
51	152 17.8 1.10	152 17.0 0.40	73	-0.7	potentially desiccation or freeze-thaw damage	Verify $k \leq 1 \times 10^{-7}$ cm/s	
52	9 21.2 1.08	9 16.1 0.32	67	+1.5	None	Verify $k \leq 1 \times 10^{-7}$ cm/s	
53	32 21.6 2.2	32 15.5 0.36	32 71	32 +0.02 0.04	None	Verify $k \leq 1 \times 10^{-7}$ cm/s	

Table C-3. Quality Control/Quality Assurance Data for Natural Clay Liners in Database (continued).

Site No.	w (%)	γ_d (kN/m^3)	P_o	ΔS_i	Distress	Purpose	Remarks
54	- - -	- - -	-	-	None	Verify $k \leq 1 \times 10^{-7}$ cm/s	SDRI Test on Liner
55	- 27.0 0.7	- 15.0 0.22	100*	+5.9	None	Verify suitability of soil for $k \leq 1 \times 10^{-7}$ cm/s; $w \approx w_{opt}$	k>1 x 10-7 because soil wasn't wet enough
56	- 30.6 0.7	- 14.2 0.17	100*	+6.6	None	Verify suitability of soil for $k \leq 1 \times 10^{-7}$ cm/s; $w \approx w_{opt}$+3%	Wetting soil up to opt. +3% lowered k (compared to site 55)
57	- 29.6 1.1	- 14.0 0.30	100*	+0.5	None	Verify suitability of soil for $k \leq 1 \times 10^{-7}$ cm/s	
58	- 30.7 1.3	- 14.3 0.22	100*	+8.6	None	Verify suitability of soil for $k \leq 1 \times 10^{-7}$ cm/s	
59	- 29.4 1.3	- 14.4 0.31	100*	+6.3	None	Verify suitability of soil for $k \leq 1 \times 10^{-7}$ cm/s	
60	- 26.8 0.8	- 15.1 0.20	100*	+8.4	None	Verify suitability of soil for $k \leq 1 \times 10^{-7}$ cm/s; $w \approx w_{opt}$	
61	- 29.8 0.4	- 14.4 0.14	100*	+7.6	None	Verify suitability of soil for $k \leq 1 \times 10^{-7}$ cm/s; $w \approx w_{opt}$+3%	

Table C-3. Quality Control/Quality Assurance Data for Natural Clay Liners in Database (continued).

Site No.	w (%)	γ_d (kN/m^3)	P_o	ΔS_i	Distress	Purpose	Remarks
62	- 24.6 0.6	- 15.4 0.17	100*	+10.9	None	Verify suitability of soil for $k \leq 1 \times 10^{-7}$ cm/s	
63	- 22.7 0.5	- 15.4 0.16	100*	+3.2	None	Verify suitability of soil for $k \leq 1 \times 10^{-7}$ cm/s	
64	8 21.6 0.32	8 16.0 0.22	88	+4.3	None	Verify $k \leq 1 \times 10^{-7}$ cm/s	
65	23 17.2 1.07	23 17.4 0.31	0	-6.1	None	Verify $k \leq 1 \times 10^{-7}$ cm/s	
66	39 21.7 1.3	59 17.2 0.52	95	+8.6	None	Verify $k \leq 1 \times 10^{-7}$ cm/s	
67	59 21.41.2	59 17.2 0.52	98	+8.1	None	Verify $k \leq 1 \times 10^{-7}$ cm/s	
68	13 17.6 1.0	13 18.0 0.38	100	+6.4	None	Verify $k \leq 1 \times 10^{-7}$ cm/s	
69	8 11.5 0.6	8 19.4 1.6	75	+8.0	None	Verify $k \leq 1 \times 10^{-7}$ cm/s	
70	- 20.6 -	- 16.1 -	60	-	None	Verify $k \leq 1 \times 10^{-7}$ cm/s	

Table C-3. Quality Control/Quality Assurance Data for Natural Clay Liners in Database (continued).

Site No.	w (%)	γ_d (kN/m^3)	P_o	ΔS_i	Distress	Purpose	Remarks
71	- 14.3 -	- 18.0 -	64	-	None	Verify $k \leq 1 \times 10^{-7}$ cm/s	
72	6 23.7 1.0	6 15.5 0.2	100	11.3	freeze-thaw, but upper lift re-worked before SDRI	Verify $k \leq 1 \times 10^{-7}$ cm/s	
73	36 25.2 1.2	36 14.8 0.86	97	5	None	Verify $k \leq 1 \times 10^{-7}$ cm/s	On site clay
74	30 19.6 1.6	30 16.1 0.02	47	-3.7	None	Verify $k \leq 1 \times 10^{-7}$ cm/s	Off site clay
75	7 25.4 2.0	7 15.2 0.7	100	11.1	None	Verify $k \leq 1 \times 10^{-7}$ cm/s	
76	76 21.8 0.4	76 15.9 0.3	86	1.1	None	Verify $k \leq 1 \times 10^{-7}$ cm/s	
77	111 11.0 0.6	111 19.2 0.6	37	1.1	None	Verify $k \leq 1 \times 10^{-7}$ cm/s	
78	109 12.4 1.5	109 18.8 0.5	2	-7.2	None	Verify $k \leq 1 \times 10^{-7}$ cm/s	

Table C-3. Quality Control/Quality Assurance Data for Natural Clay Liners in Database (continued).

Site No.	w (%)	γ_d (kN/m^3)	P_o	ΔS_i	Distress	Purpose	Remarks
79	39 28.2 3.1	37 16.2 0.49	-	12.6	None	Verify $k \leq 1 \times 10^{-7}$ cm/s	
80	37 23.1 2.2	39 14.9 0.46	-	11.7	None	Verify $k \leq 1 \times 10^{-7}$ cm/s	
81	8 28.0 2.5	8 14.2 0.20	-	2.7	None	Verify $k \leq 1 \times 10^{-7}$ cm/s	
82	14 17.8 2.0	14 17.1 0.44	-	2.4	None	Verify $k \leq 1 \times 10^{-7}$ cm/s	
83	16 19.3 1.5	16 17.3 0.53	-	12	None	Verify $k \leq 1 \times 10^{-7}$ cm/s	
84	-	-	-	-	None	Verify $k \leq 1 \times 10^{-7}$ cm/s	Dark clay
85	-	-	-	-	None	Verify $k \leq 1 \times 10^{-7}$ cm/s	Light clay
86	18 20.5 2.3	18 16.6 0.68	100	5.5	None	Verify $k \leq 1 \times 10^{-7}$ cm/s	
87	19 20.4 2.2	19 16.6 0.61	95	4.1	None	Verify $k \leq 1 \times 10^{-7}$ cm/s	

Table C-3. Quality Control/Quality Assurance Data for Natural Clay Liners in Database (continued).

Site No.	w (%)	γ_d (kN/m^3)	P_o	ΔS_i	Distress	Purpose	Remarks
88	24 13.2 0.8	24 19.2 0.35	100	11.7	None	Verify $k \leq 1 \times 10^{-7}$ cm/s	
89	29 13.2 1.1	29 19.1 0.45	100	10.8	None	Verify $k \leq 1 \times 10^{-7}$ cm/s	

Table C-4. Hydraulic Conductivity for Natural Clay Liner Materials in Database.

Site No.	Thin-Wall Sampling Tube		SDRI		Lysimeter		TSB	30 cm Block	D_F/L	ψ_o (kPa)
	k (cm/s)	Method, σ', i	k (cm/s)	Size (m^2)	k (cm/s)	Size (m^2)	k (cm/s)	k (cm/s)		
1	4 3.2 x 10-8 0.32	D 5084 69 10	2.8 x 10-7	1.44	-	-	-	2.6 x 10-7	1	60
2	2 3.6 x 10-9 -	- - -	1.5 x 10-7	1.82	-	-	-	-	1	70
3	109 8.0 x 10-9	Flexible-Wall 165 20	-	-	9 x 10-9	15 x 15	-	-	-	-
4	4 5.0 x 10-9 0.34	9100 - -	1.1 x 10-7	2.33	-	-	-	-	0.3	-
5	3 8.7 x 10-9 0.21	D 5084 69 10	9 x 10-9	1.49	-	-	-	4 x 10-8	0.6	80
6	4 2.4 x 10-8 0.46	Flexible-Wall - -	2.7 x 10-7	2.33	-	-	-	-	0.7	70
7	8 8.4 x 10-8 0.35	D 5084 - -	5.8 x 10-8	2.33	-	-	5 4.3 x 10-8 0.12	-	-	-
8	5 9.0 x 10-9 0.58	D 5084 - -	1.2 x 10-7	2.33	-	-	-	-	-	-

Table C-4. Hydraulic Conductivity for Natural Clay Liner Materials in Database (continued).

Site No.	Thin-Wall Sampling Tube		SDRI		Lysimeter		TSB	30 cm Block	D_F/L	ψ_o (kPa)
	k (cm/s)	Method, σ', i	k (cm/s)	Size (m^2)	k (cm/s)	Size (m^2)	k (cm/s)	k (cm/s)		
9	- 1.0 x 10-8 -	- - -	-	-	7 x 10-9	-	-	-	-	-
10	- 8.0 x 10-9 -	- - -	-	-	3 x 10-8	-	-	-	-	-
11	- 2.0 x 10-9 -	- - -	-	-	3 x 10-9	-	-	-	-	-
12	- 3.0 x 10-9 -	- - -	-	-	2 x 10-9	-	-	-	-	-
13	8 1.3 x 10-8 0.18	D 5084 69 -	1.3 x 10-8	2.33	-	-	5 1.4 x 10-8 0.16	-	0.1	-
14	4 4.8 x 10-8 0.29	- - -	2.0 x 10-8	2.33	-	-	-	-	0.2	-
15	10 4.4 x 10-9 0.48	9100 - -	3.3 x 10-9	2.33	-	-	4 1.6 x 10-8 0.21	-	0.7	-
16	7 3.7 x 10-8 0.48	D 5084 - -	3.0 x 10-8	2.33	-	-	-	-	0.1	-

Table C-4. Hydraulic Conductivity for Natural Clay Liner Materials in Database (continued).

Site No.	Thin-Wall Sampling Tube		SDRI		Lysimeter		TSB	30 cm Block	D_F/L	ψ_o (kPa)
	k	Method, σ', i	k (cm/s)	Size (m^2)	k (cm/s)	Size (m^2)	k (cm/s)	k (cm/s)		
17	7 3 x 10-9 0.19	9100 34 -			6 6 x 10-9 0.25	0.37	6 5 x 10-9 0.23	-	1.0	-
18	5 1.5 x 10-8 0.12	D 5084 34 -	9.8 x 10-9	2.33	-	-	8 9.2 x 10-9 0.26	4 1.4x10-8 0.34	-	-
19	8 1.9 x 10-8 0.46	- - -	-	-	4.4 x 10-8	8 x 8	-	-	-	-
20	9 3.0 x 10-9 0.63	D 5084 35 -	8 x 10-7	2.33	-	-	-	-	1	30
21	2 3.1 x 10-7 -	D 5084 69 10	2.5 x 10-7	2.33	-	-	-	2 2.2 x 10-7 -	1	-
22	- 2.4 x 10-8 -	- - -	2 x 10-8	2.33	-	-	-	-	-	-
23	6 1.5 x 10-8 0.45	- - -	-	-	1.4 x 10-8	-	-	-	-	-
24	2 9 x 10-9 -	D 5084 69 10	1.5 x 10-8	2.33	-	-	-	1.1 x 10-8	1	45

Table C-4. Hydraulic Conductivity for Natural Clay Liner Materials in Database (continued).

Site No.	Thin-Wall Sampling Tube		SDRI		Lysimeter		TSB	30 cm Block	D_F/L	ψ_o (kPa)
	k (cm/s)	Method, σ', i	k (cm/s)	Size (m^2)	k (cm/s)	Size (m^2)	k (cm/s)	k (cm/s		
25	2 2.3 x 10-9 -	D 5084 69 10	8 x 10-9	2.33	-	-	-	6 x 10-9	1	35
26	2 2.9 x 10-9 -	D 5084 69 10	2.0 x 10-7	2.33	-	-	-	1.8 x 10-7	1	-
27	2 3.0 x 10-8 -	D 5084 69 10	1.8 x 10-7	2.33	-	-	-	1.5 x 10-7	1	-
28	2 1.9 x 10-8 -	D 5084 69 10	9 x 10-8	2.33	-	-	-	1.7 x 10-7	1	-
29	2 2.2 x 10-8 -	D 5084 69 10	3 1.7 x 10-8 -	1.85	-	-	-	2 1.7 x 10-8 -	1	-
30	- 3.0 x 10-8 -	Flexible-Wall - 22	1.1 x 10-7	2.33	-	-	-	-	> 0.7	-
31	7 1.6 x 10-8 0.26	D 5084 - -	6.0 x 10-8	2.33	-	-	6 4.7 x 10-8 0.034	--	1	32
32	2 3.0 x 10-8 -	Flexible-Wall - -	3.9 x 10-8	2.33	-	-	-	-	1	0

Table C-4. Hydraulic Conductivity for Natural Clay Liner Materials in Database (continued).

Site	Thin-Wall Sampling Tube		SDRI		Lysimeter		TSB	30 cm Block		ψ_o
No.	k (cm/s)	Method, σ', i	k (cm/s)	Size (m^2)	k (cm/s)	Size (m^2)	K (cm/s)	k (cm/s)	D_F/L	(kPa)
33	2 1.3 x 10-8 -	- - -	3.9 x 10-8	2.33	-	-	-	-	1	0
34	6 1.5 x 10-8 0.62	D 5084 69 10	4 x 10-7	2.33	-	-	-	3 3.5 x 10-7 0.23	1	-
35	2 3.0 x 10-8 -	- - -	3.7 x 10-8	2.33	-	-	-	-	>0.7	-
36	6 9.1 x 10-9 0.58	D 5084 21 20	3.0 x 10-8	2.33	-	-	-	-	>0.7	25
37	- 4.9 x 10-8 -	Flexible-Wall - -	1.3 x 10-8	2.33	-	-	-	-	0.5	--
38	- - -	- - -	<3.6x10-8	0.16	-	-	-	-	0.1	-
39	6 2.6 x 10-8 0.14	D 5084 14 10	2.6 x 10-9 4.3 x 10-9	0.08 m^2 1.76 m^2	No Flow	-	-	-	0.5	-
40	7 3.5 x 10-9 0.35	D 5084 34 -	2.2 x 10-8		-	-	7 1.6 x 10-8 0.33	-	0.8	-
41	5.5 x 10-9	-	1.0 x 10-7	2.33	-	-	-	4.1x10-9	0.24	-

Table C-4. Hydraulic Conductivity for Natural Clay Liner Materials in Database (continued).

Site	Thin-Wall Sampling Tube		SDRI		Lysimeter		TSB	30 cm Block		ψ_o
No.	k (cm/s)	Method, σ', i	k (cm/s)	Size (m^2)	k (cm/s)	Size (m^2)	k (cm/s)	k (cm/s)	D_F/L	(kPa)
42	-	-	8 x 10-8	2.33	-	-	-	-	-	-
43	3 2.4 x 10-9 0.12	Const. Head - -	7 x 10-8	2.33	-	-	-	-	-	-
44	3 2.4 x 10-9 0.13	Const. Head - -	2 x 10-7	2.33	-	-	-	-	-	-
45	12 5.8×10^{-9} 0.63	- - -	3.7 x 10-8	2.33	-	-	-	-	0.5	-
46	9 1.5 x 10-8 0.12	- - -	2 x 10-8	2.33	-	-	-	-	-	-
47	-	-	5x10-8	2.33	-	-	-	-	0.5	20
48	3 1.1 x 10-8 0.21	D 5084 69 10	4 x 10-8	2.33	-	-	5 2.1x10-8 0.57	4.8x10-8	1	32
49	4 5.1 x 10-8 0.67	D 5084 69 10	5.0 x 10-8	2.33	-	-	5 3.2 x 10-7 1.07	7.7x10-8	1	35
50	3 7.4 x 10-8 0.31	D 5084 69 10	2.6 x 10-7	2.33	-	-	5 7.5 x 10-8 1.20	3.1x10-6	1	34
51	3 4.1 x 10-8 0.15	D 5084 69 10	3.0 x 10-7	2.33	-	-	5 1.1 x 10-7 1.08	5.3x10-7	1	22

Table C-4. Hydraulic Conductivity for Natural Clay Liner Materials in Database (continued).

Site No.	Thin-Wall Sampling Tube		SDRI		Lysimeter		TSB	30 cm Block	D_F/L	ψ_o (kPa)
	k (cm/s)	Method, σ', i	k (cm/s)	Size (m^2)	k (cm/s)	Size (m^2)	k (cm/s)	k (cm/s)		
52	- - -	- - -	2 1.1 x 10-7 0.10	7.20	-	-	-	-	-	2
53	4 1.7 x 10-8 0.21	D 5084 - -	2.2 x 10-8	2.33	-	-	5 1.2 x 10-8 0.35	-	0.2	-
54	-	-	7 x 10-8	2.33	-	-	-	-	1	70
55	- 8.1 x 10-8 -	- - -	1.3 x 10-7	2.33	-	-	-	-	0.67	-
56	- 2.8 x 10-8 -	- - -	2.4 x 10-8	2.33	-	-	-	-	0.63	-
57	- 3.4 x 10-8 -	- - -	5.6 x 10-8	2.33	-	-	-	-	0.71	-
58	- 2.5 x 10-8 -	- - -	5.0 x 10-8	2.33	-	-	-	-	0.71	-
59	- 2.7 x 10-8 -	- - -	9.4 x 10-8	2.33	-	-	-	-	0.54	-
60	- 3.4 x 10-8 -	- - -	1.2 x 10-7	2.33	-	-	-	-	0.63	-

Table C-4. Hydraulic Conductivity for Natural Clay Liner Materials in Database (continued).

Site No.	Thin-Wall Sampling Tube		SDRI		Lysimeter		TSB	30 cm Block	D_F/L	ψ_o (kPa)
	k (cm/s)	Method, σ', i	k (cm/s)	Size (m^2)	k (cm/s)	Size (m^2)	k (cm/s)	K (cm/s)		
61	- 4.3 x 10-8 -	- - -	3.7 x 10-8	2.33	-	-	-	-	0.63	-
62	- 1.6 x 10-7 -	- - -	3.1 x 10-7	2.33	-	-	-	-	0.75	-
63	- 1.7 x 10-7 -	- - -	3.9 x 10-7	2.33	-	-	-	-	0.54	-
64	- 5.5 x 10-9 -	- - -	2.3 x 10-7	2.33	-	-	-	4.1 x 10-9	0.25	-
65	-	-	1.8 x 10-7	2.33	-	-	-	-	0.80	-
66	3 3.7×10^{-8} 0.31	D 5084 - -	1.2×10^{-8}	2.33	-	-	5 1.1×10^{-8} 0.26	-	> 0.5	26
67	3 3.0×10^{-8} 0.30	D 5084 - -	8.3×10^{-8}	2.33	-	-	5 8.5×10^{-8} 0.21	-	> 0.5	34
68	4 7.8×10^{-9} 0.14	D 5084 22 34	2 2.3×10^{-8} 0.017	2.33	-	-	5 2.6×10^{-8} 0.11	-	> 0.7	60
69	4 2.1×10^{-8} 0.33	D 5084 22 34	2 1.3×10^{-8} 0.002	2.33	-	-	5 5.6×10^{-8} 0.12	-	> 0.7	46

Table C-4. Hydraulic Conductivity for Natural Clay Liner Materials in Database (continued).

Site	Thin-Wall Sampling Tube		SDRI		Lysimeter		TSB	30 cm Block		ψ_o
No.	k (cm/s)	Method, σ', i	k (cm/s)	Size (m^2)	k (cm/s)	Size (m^2)	k (cm/s)	k (cm/s)	D_F/L	(kPa)
70	- 2 x 10-8 -	Flexible-Wall - -	4 x 10-8	2.33	-	-	-	-	-	-
71	- 2 x 10-8 -	Flexible-Wall - -	8.3 x 10-8	2.33	-	-	-	-	-	-
72	2 1.4 x 10-8 0.06	- 52 -	2.0 x 10-8	2.33	-	-	-	-	0.5	-
73	-	-	8 x 10-8	2.33	-	-	-	-	0.6	-
74	-	-	1 x 10-9	2.33	-	-	-	-	0.5	-
75	-	-	5 x 10-8	2.33	-	-	-	-	1	-
76	4 4.7 x 10-8 1.1	- 52 -	3 x 10-8	2.33	-	-	-	-	1	-
77	-	-	2 x 10-8	2.33	-	-	-	-	0.5	-
78	-	-	2 x 10-8	2.33	-	-	-	-	0.5	-
79	5 3.3 x 10-9 0.22	- - -	2 4.5 x 10-8 -	2.33	-	-	-	-	-	-
80	3 1.8 x 10-9 0.15	- - -	2 4.0 x 10-8 -	2.33	-	-	-	-	0.4	-
81	2 4.2 x 10-8 0.27	- - -	1.5 x 10-7	2.33	-	-	-	-	0.8	-

Table C-4. Hydraulic Conductivity for Natural Clay Liner Materials in Data Base (continued).

Site No.	Thin-Wall Sampling Tube		SDRI		Lysimeter		TSB	30 cm Block	D_F/L	ψ_o (kPa)
	k (cm/s)	Method, σ', i	k (cm/s)	Size (m^2)	k (cm/s)	Size (m^2)	k (cm/s)	k (cm/s)		
82	4 1.5 x 10-8 0.29	Flexible-Wall 34 -	3 x 10-8	2.33	-	-	-	-	0.4	-
83	4 1.7 x 10-8 0.05	Flexible-Wall 34 -	4.5 x 10-8	2.33	-	-	-	-	0.4	-
84	-	-	1.3 x 10-7	2.33	-	-	-	-	0.8	-
85	-	-	2.8 x 10-8	2.33	-	-	-	-	0.8	-
86	2 2.2 x 10-8 -	Flexible-wall 14 -	1.5 x 10-8	2.25	-	-	-	-	-	-
87	2 2.6 x 10-8 -	Flexible-wall 14 -	1.4 x 10-8	2.25	-	-	-	-	-	-
88	2 3.9 x 10-8 -	Flexible-wall 14 -	2.3 x 10-8	2.25	-	-	-	-	-	-
89	2 3.1 x 10-8 -	Flexible-wall 14 -	2.1 x 10-8	2.25	-	-	-	-	-	-

Table C-5. Material Properties for Soil-Bentonite Liners in Database.

Site No.	Location and Date	Source of Data	LL (%)	PI (%)	Percent Gravel	Percent Fines	Percent Bentonite)	w_{opt} (%)	$\gamma_{d,max}$ (kN/m^3)	Compactive Effort
1	Oxford, NJ 1991	Golder Assoc	- - -	- - -	- - -	- - -	- 3.75 -	-	-	
2	Southern Nebraska	D.L. Osadnick	31 51 -	31 36 -	32 13 -	32 32 -	- 9.0 -	15.0	17.1	SP
3	Southern Nebraska	D.L. Osadnick	31 51 -	31 36 -	32 13 -	32 32 -	- 9.0 -	15.0	17.1	SP
4	Southern Nebraska	D.L. Osadnick	31 51 -	31 36 -	32 13 -	32 32 -	- 9.0 -	15.0	17.1	SP
5	Southern Nebraska	D.L. Osadnick	31 51 -	31 36 -	32 13 -	32 32 -	- 9.0 -	15.0	17.1	SP
6	Kettleman City, CA 1987	Golder Assoc.	- - -	- 29 -	- - -	- 81 -	-	23.8	15.4	SP
7	Kettleman City, CA 1987	Golder Assoc.	- - -	- 29 -	- - -	- 81 -	-	23.8	15.4	SP
8	Borfer, TX 1988	McBride-Ratcliff	- 56 -	- 31 -	- - -	- 55 -	7.8	18.6	16.9	SP

Table C-5. Material Properties for Soil-Bentonite Liners in Database (continued).

Site No.	Location and Date	Source of Data	LL (%)	PI (%)	Percent Gravel	Percent Fines	Percent Bentonite)	w_{opt} (%)	$\gamma_{d,max}$ (kN/m^3)	Compactive Effort
9	Borfer, TX 1988	McBride-Ratcliff	- 65 -	- 39 -	- - -	- 63 -	10.5	20.1	16.5	SP
10	San Mateo County, Ca 1993	BFI	- 51 -	- 36 -	- 2 -	- 21 -	10.0	9.0	19.9	MP
11	Lead, South Dakota 1994	Golder Assoc.	- - -	- - -	- - -	- - -	- 14.7 -	17.7	16.8	SP
12	Mobile, AZ 1990	Golder Assoc.	- 60 -	- 38 -	- - -	- 39 -	4.0	13.5	18.5	SP

Table C-6. Construction Information for Soil Bentonite Liners in Database.

Site No.	Compaction Criteria	Compactor	Compactor Mass (kg)	Passes per Lift	Lift Thickness (mm)	Number of Lifts	Pad Size (m x m or m^2)
1		Ingersol Rand S100	-	10	150	4	9 x 9
2	w > OWC, <+4 RC > 95% SP	CAT 815	20,000	6	150	6	31 x 11
3	w > OWC, <+4 RC > 95% SP	CAT 815	20,000	6	150	6	31 x 11
4	w > OWC, <+4 RC > 95% SP	CAT 815	20,000	4	150	6	31 x 11
5	w > OWC, <+4 RC > 95% SP	CAT 815	20,000	4	150	6	31 x 11
6	w > OWC RC > 90% MP	CAT 815	20,000	2	150	7	43 x 15
7	w > OWC +3 RC > 90% SP	CAT 815	20,000	2	150	7	43 x 15
8	w > OWC RC > 95% SP	CAT 815	12,600	6	150	6	13 x 28
9	w > OWC +2 RC > 92% SP	CAT 815	20,000	6	150	6	13 x 28
10	w > OWC+2, ,+5 RC > 905 MP	CAT 825	32,400	4	150	6	15 x 15
11	w > OWC, <+3 RC > 98% SP	-	-	-	150 - 230	3	11 x 11
12	w > OWC +2 RC > 95% SP	CAT 815 (1-4 lift), CAT CP433B (5^{th} lift), Sakai SV (6^{th} lift)	-	4	150	6	36 x 18

Table C-7. Quality Control/Quality Assurance Data for Soil-Bentonite Liners in Database.

Site No.	w (%)	γ_d (kN/m^3)	P_o	ΔS_i	Distress	Purpose	Remarks
1	28 12.3 1.4	28 16.0 0.3	-	-	None	Verify k ≤ 1 x 10^{-7} cm/s	
2	2 14.7 -	2 17.2 -	-	-	None	Verify k ≤ 1 x 10^{-7} cm/s	
3	2 16.0 -	2 16.7 -	-	-	None	Verify k ≤ 1 x 10^{-8} cm/s	
4	2 143 -	2 16.8 -	-	-	None	Verify k ≤ 1 x 10^{-7} cm/s	
5	2 15.2 -	2 16.5 -	-	-	None	Verify k ≤ 1 x 10^{-7} cm/s	
6	- 28.4 -	- 14.8 -	54	-	None	Verify k ≤ 1 x 10^{-7} cm/s	
7	- 28.4 -	- 14.8 -	54	-	None	Verify k ≤ 1 x 10^{-7} cm/s	
8	38 20.2 -	38 15.9 -	-	-	None	Verify k ≤ 1 x 10^{-7} cm/s	
9	38 21.4 -	38 15.9 -	-	-	None	Verify k ≤ 1 x 10^{-7} cm/s	

Table C-7. Quality Control/Quality Assurance Data for Soil-Bentonite Liners in Database (continued).

Site No.	w (%)	γ_d (kN/m^3)	P_o	ΔS_i	Distress	Purpose	Remarks
10	34 12.5 0.77	34 19.1 0.22	100	-	None	Verify k ≤ 1 x 10^{-7} cm/s	
11	8 18.5 -	8 16.8 -	75	-	None	Verify k ≤ 1 x 10^{-7} cm/s	
12	32 15.5 -	32 17.9 -	-	-	None	Verify k ≤ 1 x 10^{-7} cm/s	

Table C-8. Hydraulic Conductivity for Soil-Bentonite Liners in Database.

Site	Thin-Wall Sampling Tube		SDRI		Lysimeter		TSB	30 cm Block	D_F/L	ψ_o (kPa)
	k (cm/s)	Method, σ', i	k (cm/s)	Size (m^2)	k (cm/s)	Size (m^2)	k (cm/s)	k (cm/s)		
1	4 5.5 x 10-8 -	D5084 - -	?	-						
2	2 3.0 x 10-8 -	D5084 34 -	3.0 x 10-8	2.33						
3	2 1.9 x 10-8 -	D5084 34 -	1.0 x 10-8	2.33						
4	2 6.0 x 10-8 -	D5084 34 -	3.0 x 10-8	2.33						
5	2 7.5 x 10-8 -	D5084 34 -	2.0 x 10-8	2.33						
6	7 6.9 x 10-9 -	- - -	1.6 x 10-8	2.33						
7	7 6.9 x 10-9 0.35	- - -	6.2 x 10-8	2.33						
8	- - -	- - -	2.2 x 10-8	2.33						

Table C-8. Hydraulic Conductivity for Soil-Bentonite Liners in Database (continued).

Site	Thin-Wall Sampling Tube		SDRI		Lysimeter		TSB	30 cm Block	D_F/L	ψ_o (kPa)
	k (cm/s)	Method, σ', i	k (cm/s)	Size (m^2)	k (cm/s)	Size (m^2)	k (cm/s)	k (cm/s)		
9	- - -	- - -	1.0 x 10-7	2.33						
10	10 2.6 x 10-8 -	- - -	3.0 x 10-8	2.33						
11	- - -	- - -	2.0 x 10-9	2.33						
12	6 3.2 x 10-8 -	- - -	2.0 x 10-8	2.33						

Appendix D
Cincinnati Geosynthetic Clay Liner Test Site

by

David E. Daniel, Ph.D., P.E.
University of Illinois
Urbana, IL 61081

performed under

EPA Cooperative Agreement Number
CR-821448-01-0

Project Officer

Mr. David A. Carson
United States Environmental Protection Agency
Office of Research and Development
National Risk Management Research Laboratory
Cincinnati, OH 45268

Appendix D
Cincinnati Geosynthetic Clay Liner Test Site

D-1 Introduction

This appendix contains additional information that augments Chapter 3 in the main body of the report regarding the research program related to field test plots constructed at a site in Cincinnati, Ohio. The test plots were constructed to evaluate the internal shear resistance of geosynthetic clay liners (GCLs) that were constructed on 2H:1V and 3H:1V slopes in prototype landfill cover systems.

D-2 Test Plots

The main objective in constructing the field test plots was to investigate the internal (mid-plane) shear strength of GCLs in carefully controlled, field-scale tests. Other objectives were to verify that GCLs in landfill cover systems will remain stable on 3H:1V slopes with a factor of safety of at least 1.5, to monitor the displacement and creep of GCLs in the field for as long as possible, to develop information on erosion control materials, and to better understand the field performance of GCLs as a component in liner and cover systems.

Fourteen test plots have been constructed at the ELDA Landfill in Cincinnati, Ohio. Nine of the plots were constructed on 2H:1V slopes and five were constructed on 3H:1V slopes. Each plot is about 9 m wide by 20 or 29 m long and is covered by approximately 0.9 m of cover soil. Instrumentation was placed in each test plot (with a few exceptions) in order to monitor the moisture content of the subsoil and displacements of the GCL. An additional plot consisting only of cover soil was constructed on the 2H:1V slope. This plot did not contain geosynthetic materials and was used as a control plot to study the effect of erosion on the cover soil on a plot that did not contain any synthetic erosion control material.

Slope angles of 2H:1V and 3H:1V were selected to test the shear strength limits of the GCLs. The rationale for selecting these slope inclinations was as follows. Many landfill final covers have slopes of approximately 3H:1V. If GCLs are to be widely used in landfill covers, they will have to be stable at a slope angle of 3H:1V. Thus, the 3H:1V slope was selected to be representative of a typical landfill cover. However, it is not sufficient to demonstrate that GCLs are stable on 3H:1V slopes — it must be shown that they are stable with an adequate factor of safety. Many regulators and design engineers require that permanent slopes have a minimum factor of safety for static loading of 1.5.

For an infinite slope in a cohesionless material, with no seepage, the factor of safety (FS) is:

$$FS = \tan(\phi) / \tan(\beta) \qquad (D.1)$$

where ϕ is the friction angle and β is the slope angle. If a GCL remains stable on the 2H:1V slope, the friction angle of the GCL (assuming zero cohesion) must be at least 26.6°, and for this friction angle, the factor of safety on a 3H:1V slope must be at least 1.5. Thus, the logic was to try to demonstrate a minimum factor of safety of 1.5 on 3H:1V slopes, and in order to do this, it was necessary to test the GCLs on 2H:1V slopes. It was recognized that constructing a 2H:1V slope was pushing the test to (and possibly beyond) the limits of stability, not necessarily of the mid-plane of the GCLs but certainly at various interfaces within the system.

D-2.1 *Expectations at the Beginning of the Project*

During the conception and design of the field test plots, there were several expectations concerning the performance of the GCLs. First, it was assumed that if the GCLs were placed with the bentonite in contact with the subgrade soils that the bentonite would hydrate by absorbing water from the adjacent soils. However, it was also assumed that if a geomembrane (GM) separated the bentonite component of the GCL from the underlying subsoil, and a GM was placed over the bentonite to encase the bentonite between two GMs, that the bentonite would be isolated from adjacent soils (except at edges) and would not hydrate.

A key expectation was that none of the GCLs would fail internally on any of the field test plots. This expectation was based on the results of mid-plane laboratory shearing test on fully-hydrated GCLs. Interface shear slides were viewed as possible, but the greatest concern was with the GCL/subsoil interface. It was predicted that displacements of the GCLs would be downslope with the largest displacements on the 2H:1V slopes. Creep of the GCLs was considered possible. Differential (shear) displacements were expected to be nominal.

D-2.2 *Layout of the Test Plots*

Fourteen test plots containing a GCL as a component were constructed. The layout of the plots is shown in Figure D-1. Each plot was assigned a letter. Five plots (plots A-E) were constructed on a 3H:1V slope, and nine plots (plots F to L, N, and P) were built on a 2H:1V slope. An additional plot, plot M, which consisted of only cover soil and no geosynthetics, was an erosion control plot that was installed on a 2H:1V slope to document the degree of erosion that would occur if no synthetic erosion control material was placed over the cover soil. In all other plots, a synthetic erosion control material covered the surface of the test plot. Plots on the 2H:1V slope were about 20 m long and 9 m wide; plots on the 3H:1V slope were about 29 m long and 9 m wide.

D-2.3 *Plot Compositions*

Four different types of GCLs were placed at the site: Gundseal, Bentomat ST, Claymax 500SP, and Bentofix. Two styles of Bentofix were employed: Bentofix NW contained

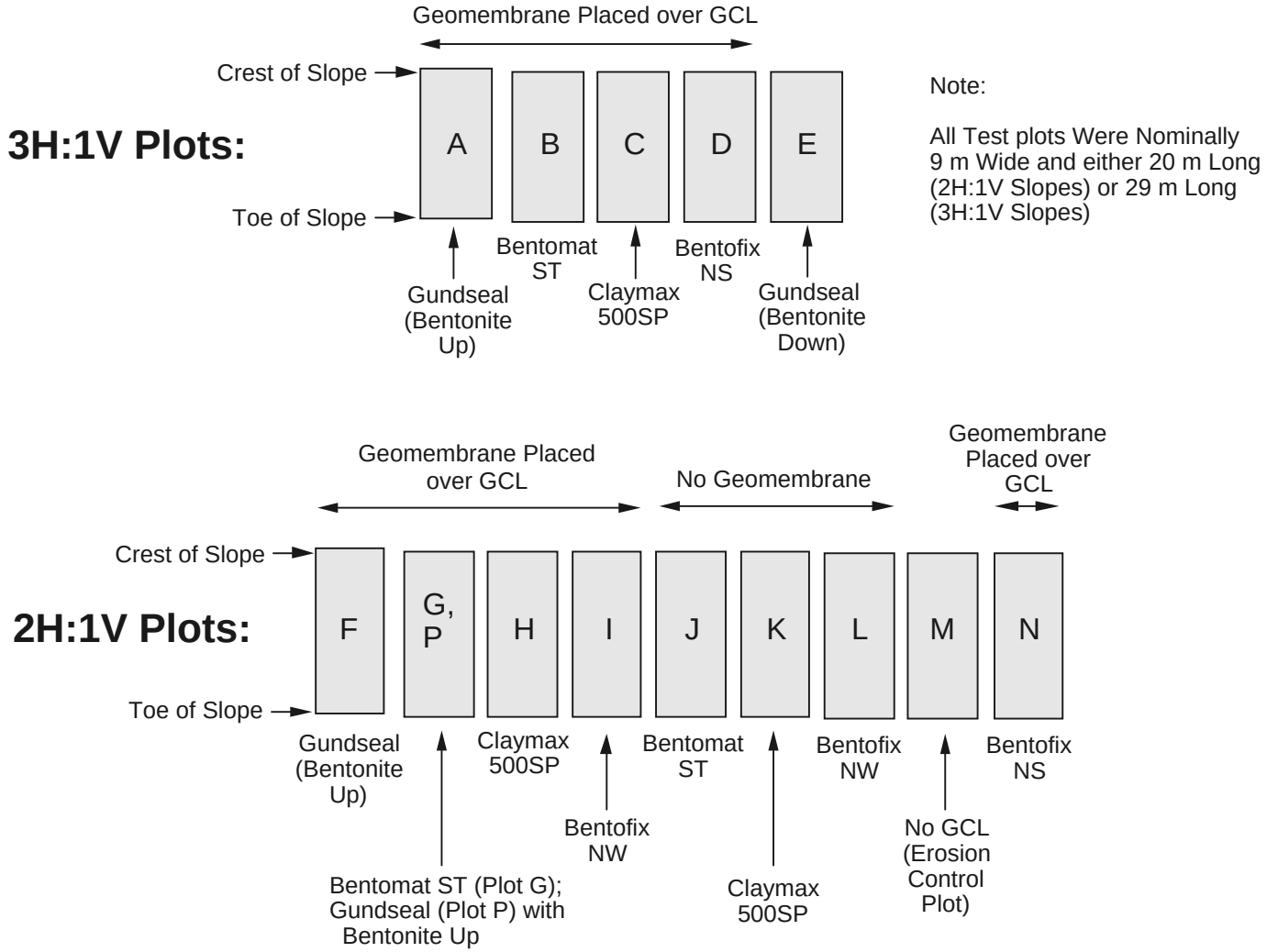

Figure D-1. Layout of field test plots.

nonwoven geotextiles (GTs) on both surfaces. Bentofix NS contained a woven GT on the side that faced downward and a nonwoven GT on the side that faced upward.

Two general designs were employed. The principal design involved a subgrade overlain by a GCL, textured GM, geotextile/geonet/geotextile drainage composite, and 0.9 m of cover soil, as shown in Figure D-2. This cross section is typical of many final cover systems for landfills being designed today. The GTs were heat-bonded to the geonet (GN). A nonwoven, needlepunched GT was used between the textured GM and GN in an effort to develop a high coefficient of friction between the GM and drainage layer.

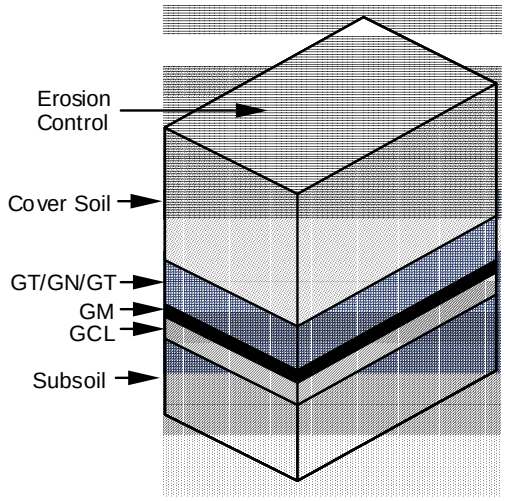

Figure D-2. Typical test plot cross section employing a composite textured HDPE GM/GCL liner system.

The second design involves a GCL overlain by 0.3 m of drainage soil, a GT, and 0.6 m of cover soil, as shown in Figure D-3. This design is also typical of current GCL designs for final cover systems in which a GM is not used.

The GM-supported GCL was employed in two configurations, i.e., with the bentonite encased between two GMs as shown in Figure D-4A, or with the bentonite in contact with the subgrade, as shown in Figure D-4B. In the former case, the bentonite was designed to stay dry. In the latter case, it was expected that the bentonite would hydrate by absorbing moisture from the subgrade.

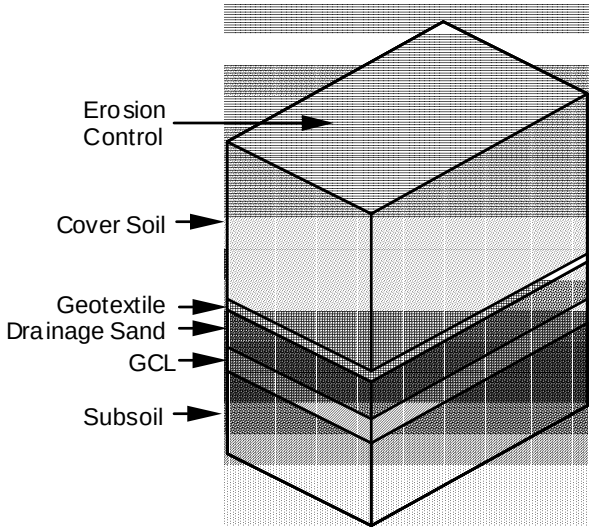

Figure D-3. Alternative test plot cross section employing a GCL with no GM.

Geotextile-encased, needlepunched GCLs consisted of materials that either had woven and nonwoven GTs on the surfaces, or two nonwoven GTs. For the GCLs containing a woven GT on one surface, the woven GT faced upward in some cases (Figure D-5A) and downward in other cases (Figure D-5B)

Plot M is an erosion control section and consisted only of 0.9 m of cover soil. There were no geosynthetic materials or instrumentation at the erosion control section. The plot was constructed to document the erosion that would occur without any geosynthetic erosion control material on the surface.

General cross sections are shown in Figure D-6 for plots constructed on the 2H:1V slope and in Figure D-7 for plots constructed on the 3H:1V slope. A cross section in the perpendicular direction is shown in Figure D-8. Each plot width was equal to two GCL panels minus a 150-mm-wide overlap. The spaces between plots on the 2H:1V slope ranged between 0 and 1.5 m, and were typically 1.5 m on the 3H:1V slope. There were graded drainage swales only on the 3H:1V slopes. Table D-1 lists the slope angles, plot, type of GCL, and a description of the plot cross-section from top to bottom. Table D-2 lists the composition, dimensions, etc., of each plot.

D-2.4 *Anchor Trenches*

Anchor trenches were constructed at the crest of each test plot. On the 3H:1V and 2H:1V slopes all of the geosynthetic materials (GCL, GM, and GN, if present) were brought into the anchor trench. A GM cap strip was placed over the GCL in the anchor trench with the purpose of preventing moisture from entering the GCL from the crest of the plot. A typical anchor trench detail is shown in Figure D-9.

Soil in the anchor trench was nominally compacted. The anchor trench was used only for the purpose of holding the geosynthetics in position during construction. As discussed later, the geosynthetics above the mid-plane of the GCLs were cut next to the anchor trenches so that the shear force from the cover would be transmitted to the internal structure of the GCL (and not simply carried by tension in the geosynthetics overlying the mid-plane and anchored in the anchor trench).

D-2.5 *Toe Detail*

At the toe of the slope the GM and GN were extended beyond the GCL in the plots on the 3H:1V and 2H:1V slopes. The extension is shown in Figures D-6 and D-7 for test plots employing a GN for the drainage layer. Both the GM and the GN were extended (daylighted) approximately 1.5 m past the end of the cover soil. For test plots in which a sand drainage layer was used, a GN was extended beyond the sand drainage material as shown in Figure D-10. The toe was designed to provide no buttressing effect for the cover soil.

D-2.6 *Instrumentation*

The objectives of the instrumentation for the field test plots were to monitor the wetting of the subsoil and the bentonite in the GCLs, and to monitor displacements of the GCLs. Moisture sensors were installed to verify that the bentonite was hydrated, or in the case of plots A, F, and P, to verify that the bentonite was dry. Extensometers were installed to document the internal shear and creep of the GCLs in each plot. As there was a limited budget, the instrumentation was selected based on simplicity, low cost, and redundancy.

D-2.6.1 Moisture Sensors. Moisture sensors were installed in each test plot in order to assess the moisture conditions impacting the bentonite within the GCLs. Two types of sensors were used in the project: a gypsum block sensor and a fiberglass mesh sensor (Figure D-16). The gypsum block sensors were placed in the subsoil beneath the GCLs; the fiberglass sensors were placed within the bentonite of the GCLs. Both sensors operate on a resistance basis. The fiberglass sensors contain a porous fiberglass mesh embedded in two wire screens . The resistance to flow of electric current between the two screens is dependent on the moisture present in the fiberglass mesh. The resistance is measured and converted to moisture content by comparison with a calibration chart. The calibration is a function of soil type and the constituents of the soil moisture. The gypsum block sensors have two concentric spirals of wire between which resistance of gypsum is determined. The electrical resistance of the gypsum is a function of the moisture content of the gypsum. The resistance is measured using a digital meter manufactured specifically to measure resistance for these sensors.

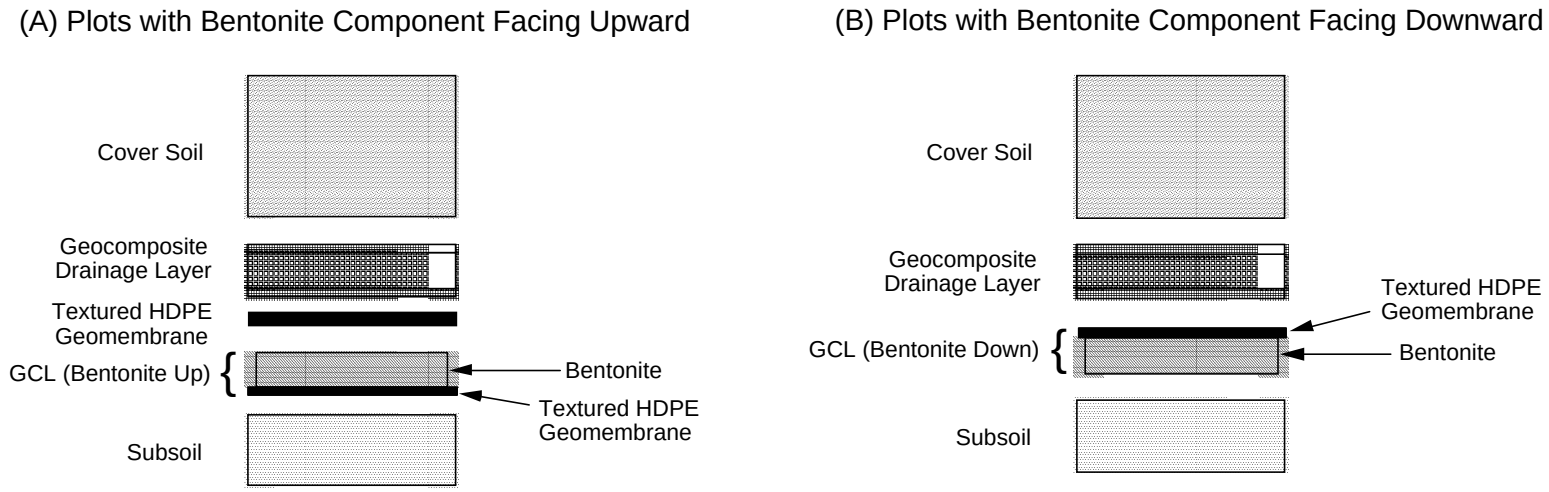

Figure D-4. Placement of Gundseal with bentonite facing upward or downward.

(A) Woven Geotextile Interfacing with Geomembrane

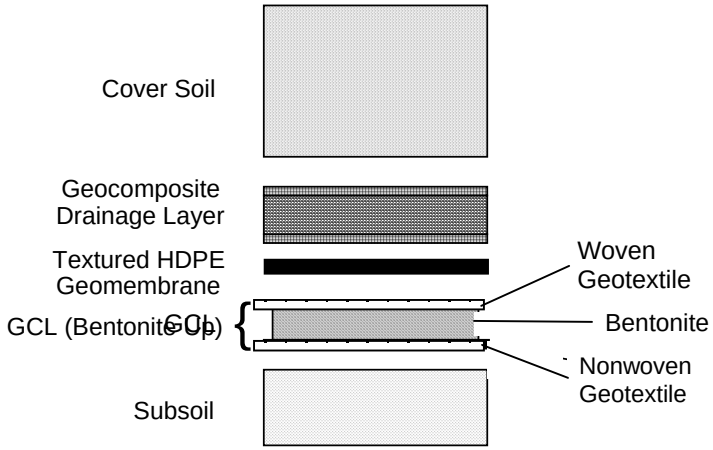

(B) Nonwoven Geotextile Interfacing with Geomembrane

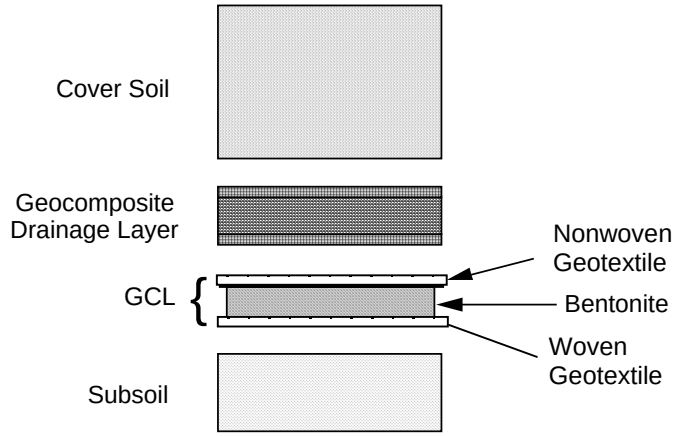

Figure D-5. Orientation of GCL with either woven or nonwoven GT facing upward.

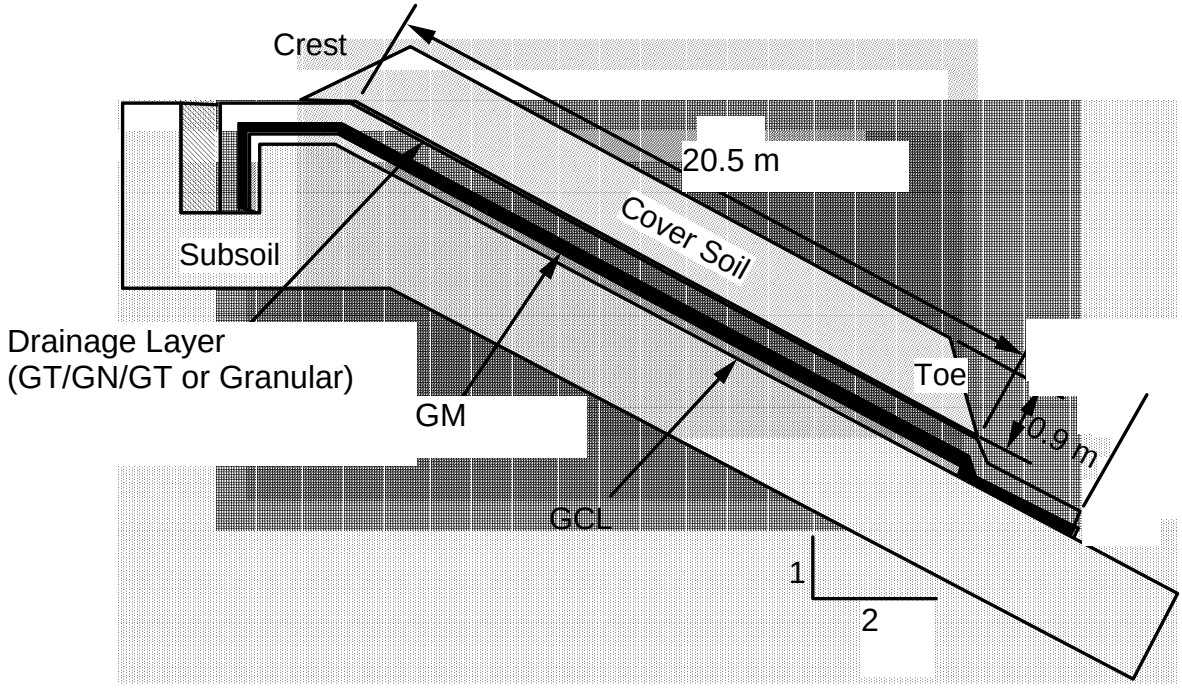

Figure D-6. General cross section of plots on a 2H:1V slope.

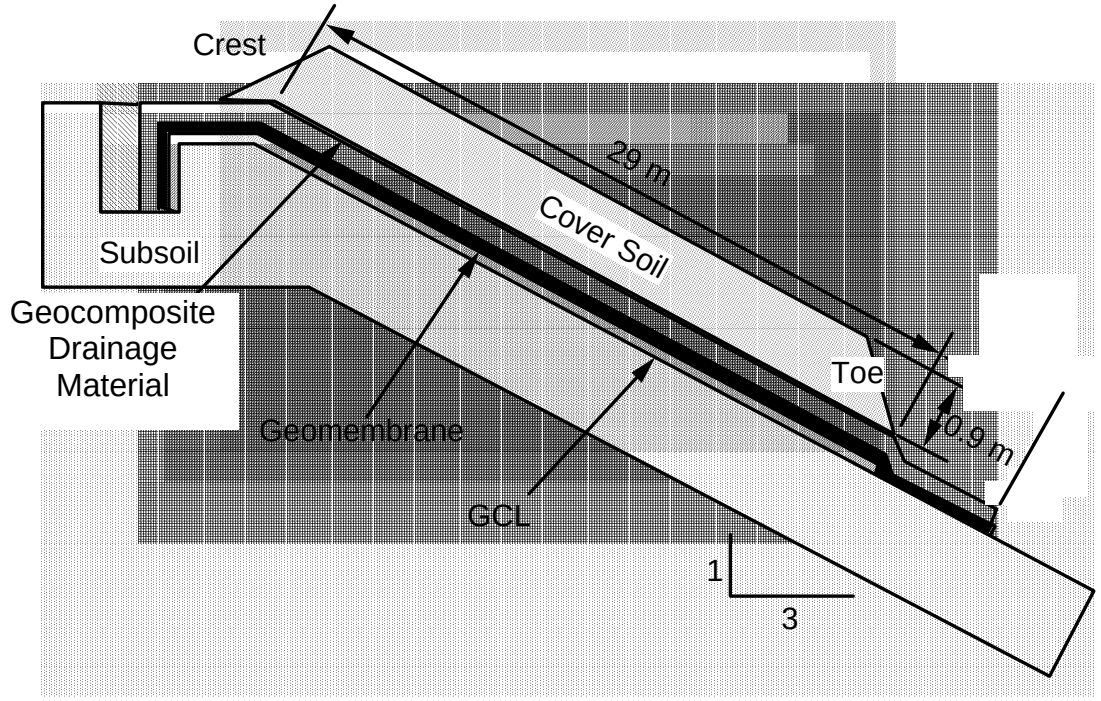

Figure D-7. General cross section of plots on a 3H:1V slope.

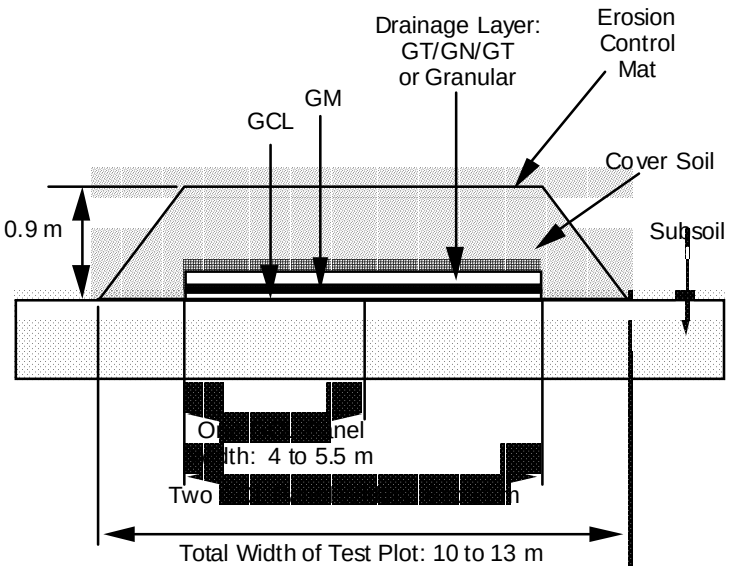

Figure D-8. Cross section along width of test plots.

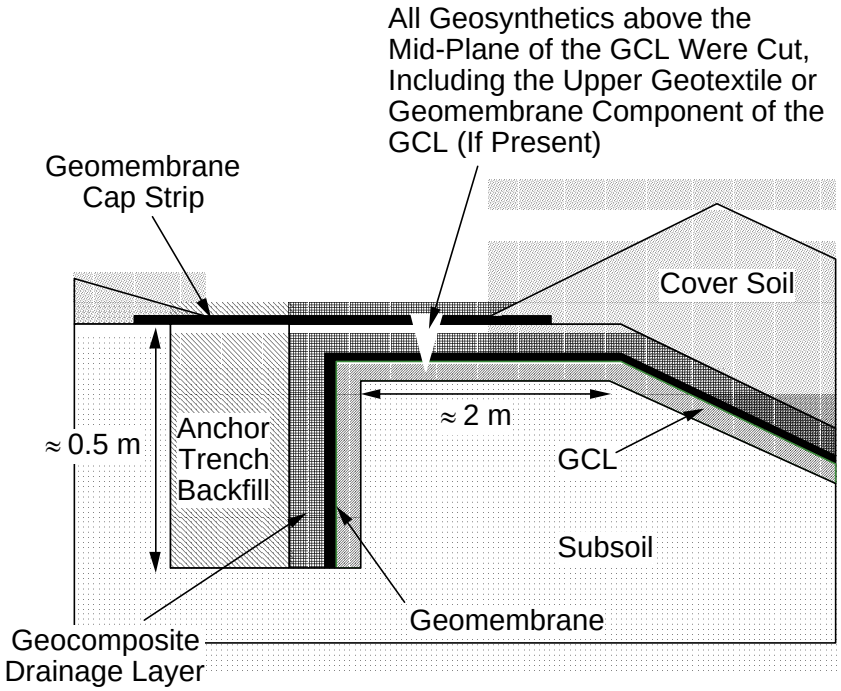

Figure D-9. Typical anchor trench detail.

Table D-1. Components of the GCL Field Test Plots.

Plot	GCL	Target Slope (deg.)	Actual Slope (deg.)	Cross-section (from top to bottom)
A	Gundseal	18.4	16.9	Soil/GN/GM/GCL (Bent. up)
B	Bentomat ST	18.4	17.8	Soil/GN/GM/GCL (W up)
C	Claymax 500SP	18.4	17.6	Soil/GN/GM/GCL (W-W)
D	Bentofix NS	18.4	17.5	Soil/GN/GM/GCL (NW up)
E	Gundseal	18.4	17.7	Soil/GN/GCL (Bent. down)
F	Gundseal	26.6	23.6	Soil/GN/GM/GCL (Bent. up)
G	Bentomat ST	26.6	23.5	Soil/GN/GM/GCL (W up)
H	Claymax 500SP	26.6	24.7	Soil/GN/GM/GCL (W-W)
I	Bentofix NW	26.6	24.8	Soil/GN/GM/GCL (NW-NW)
J	Bentomat ST	26.6	24.8	Soil/GT/Sand/GCL (W up)
K	Claymax 500SP	26.6	25.5	Soil/GT/Sand/GCL (W-W)
L	Bentofix NW	26.6	24.9	Soil/GT/Sand/GCL (NW-NW)
M	Erosion Control	26.6	23.5	Soil
N	Bentofix NS	26.6	22.9	Soil/GN/GM/GCL (NW up)
P	Gundseal	26.6	24.7	Soil/GN/GM/GCL (Bent. up)

where:

Soil = cover soil
GN = geonet
GM = textured GM
GT = geotextile
GCL = geosynthetic clay liner
Bent. up = bentonite side of Gundseal facing upward (GM against subgrade)
Bent. down = bentonite side of Gundseal against subgrade
W up = woven GT of GCL up, nonwoven side of GCL against subgrade
NW up = nonwoven GT of GCL up, woven side of GCL against subgrade
NW-NW = both sides of GCL nonwoven
Bentofix I is Bentofix NW, with a nonwoven GT on both sides
Bentofix II is Bentofix NS, with a woven GT facing upward.

Table D-2. Summary of Test Plots.

Plot	GCL Type	GM (Y/N)	Drain Type	Slope	Slope Length (m)	Crest Elev. (m)	Toe Elev. (m)	Test Plot Width (m)
A	Gundseal	Y	GN	3H:1V	28.9	179.2	170.0	10.5
B	Bentomat	Y	GN	3H:1V	28.9	179.2	170.0	9.0
C	Claymax	Y	GN	3H:1V	28.9	179.2	170.0	8.1
D	Bentofix NS	Y	GN	3H:1V	28.9	179.2	170.0	9.1
E	Gundseal	Y	GN	3H:1V	28.9	179.2	170.0	10.5
F	Gundseal	Y	GN	2H:1V	20.5	157.9	148.7	10.5
G	Bentomat	Y	GN	2H:1V	20.5	157.9	148.7	9.0
H	Claymax	Y	GN	2H:1V	20.5	157.9	148.7	8.1
I	Bentofix NW	Y	GN	2H:1V	20.5	157.9	148.7	9.1
J	Bentomat	N	Sand	2H:1V	20.5	157.9	148.7	9.0
K	Claymax	N	Sand	2H:1V	20.5	157.9	148.7	8.1
L	Bentofix NW	N	Sand	2H:1V	20.5	157.9	148.7	9.1
M	Erosion Control	N	Sand	2H:1V	20.5	157.9	148.7	7.6
N	Bentofix NS	N	Sand	2H:1V	20.5	157.9	148.7	9.1
P	Gundseal	Y	GN	2H:1V	20.5	157.9	148.3	10.5

Notes:

1. Bentofix NW contained a nonwoven GT on both sides.
2. Bentofix NS was installed with the nonwoven GT facing upward.
3. Bentomat ST was installed with the woven GT facing upward.
4. Gundseal was installed with the bentonite facing upward in plots A, F, and P, and with the bentonite facing downward at plot E.

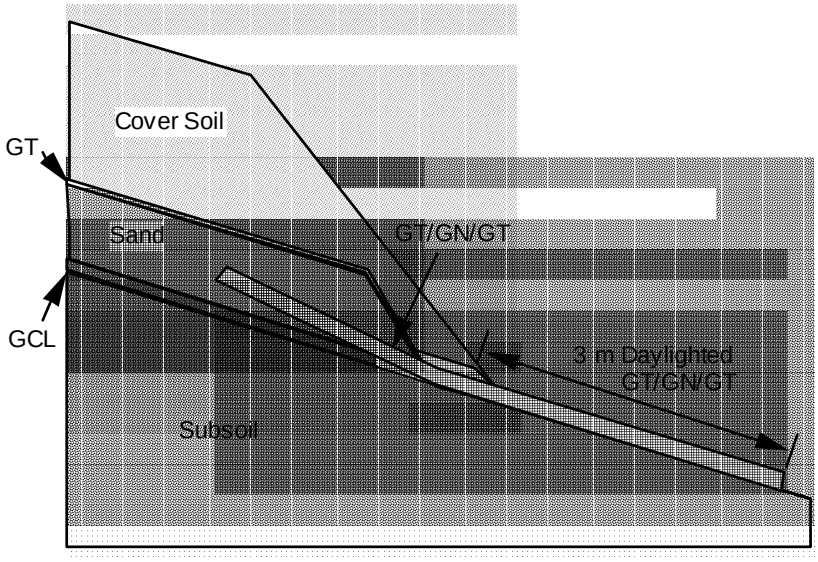

Figure D-10. Detail of drainage at toe for sections with GN drainage layer (not to scale).

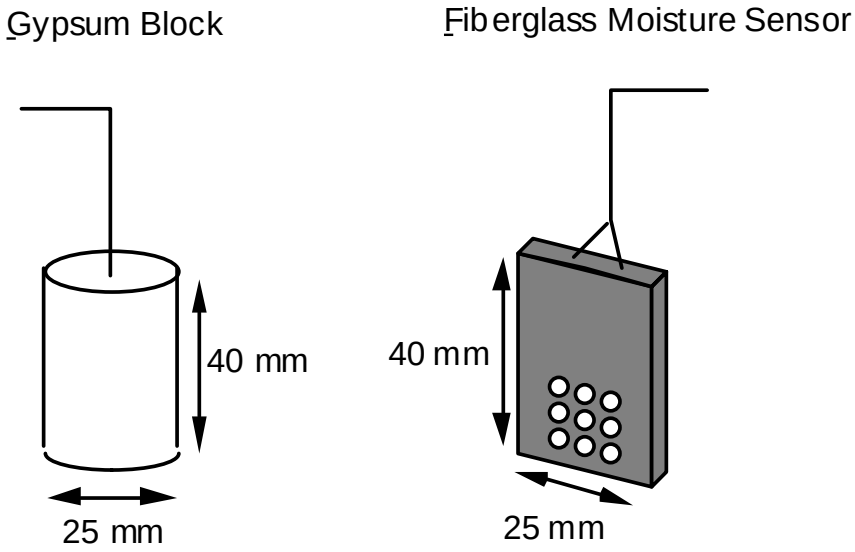

Figure D-11. Schematic diagrams of moisture sensors.

The sensors were placed on the centerline of one of the two GCL panels at three locations - top , middle, and bottom - of each plot as shown in Figure D-12. The sensors were installed 5.2 m, 10.7 m, and 16.8 m from the crest on the 2H:1V slope and 6.1 m, 15.2 m, and 24.4 m from the crest on the 3H:1V slope. At each location two, and in some cases three, moisture sensors were placed in the subsoil, at the subsoil-GCL interface, and in a few instances, above the GCL. The purpose of the sensors was to monitor the moisture content of the bentonite and soil adjacent to the bentonite. Because most plots contained a GM above the GCL, placing sensors in the cover soil would not provide information on moisture conditions within or near the GCLs. Therefore, moisture sensors were generally placed adjacent to or beneath the GCLs. A cross section of the typical moisture sensor installation in all plots except for plots A, F, and P, is shown in Figure D-13. Figure D-14 shows how the moisture sensors were installed in plots A and F.

The moisture sensors in Plot P were installed differently than the other plots. Only fiberglass moisture sensors were installed in Plot P. Sixteen moisture sensors were placed in a 4 x 4 grid on the upper side of the bentonite of the GCL but underneath the overlying GM.

The gypsum blocks and digital meter were obtained from Soil Moisture Equipment Corporation of Santa Barbara, CA. The fiberglass sensors were obtained from Techsas, Inc. of Houston, TX.

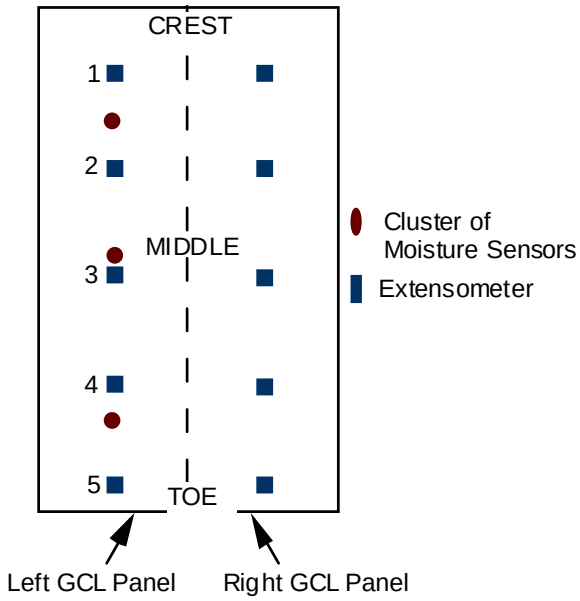

Figure D-12. Locations of moisture sensors and extensiometers.

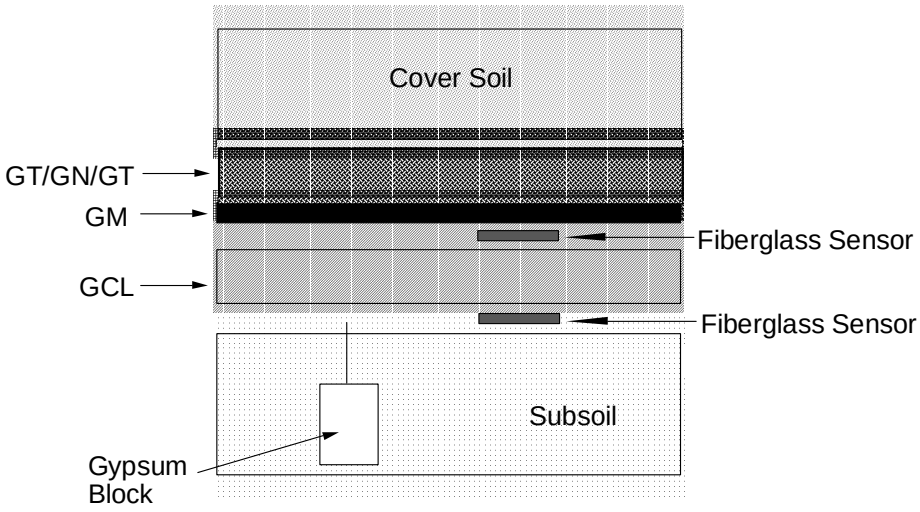

Figure D-13. Location of moisture sensors in all plots except A and F.

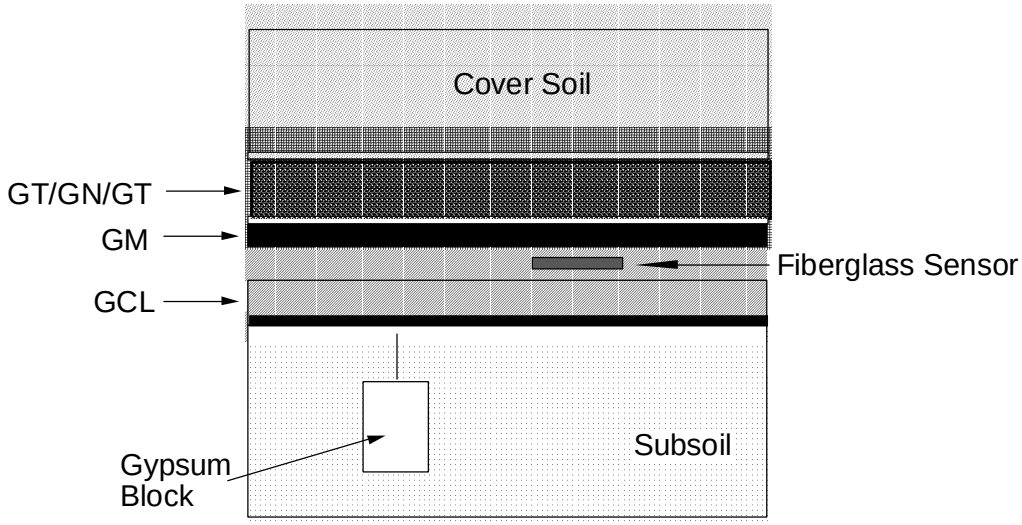

Figure D-14. Location of moisture sensors in plots A, F, and P.

As mentioned above, the electrical resistance of a moisture sensor is measured and converted to moisture content by comparison with a calibration chart. The moisture sensor readout device used on this project reads from 0 to 100, with 0 corresponding to no soil moisture and 100 corresponding to a very wet soil. However, the calibration is a

function of soil type. There are generally four different soil types at the site. Three soils are distributed generally as shown in Figure D-15 for the 2H:1V test plots. Soil A is a gray fat clay, soil B is a clayey silt, and soil C is a silty clay (field classifications). The subsoil on the 3H:1V slope is primarily a clayey silt (soil D).

Calibration tests were performed for both the gypsum block and fiberglass moisture sensors for soils A, B, C, and D. A 1000 ml beaker was filled with soil, and a circular piece of Gundseal was placed above the soil with the bentonite portion of the GCL in contact with the soil. A small layer of sand was placed over the GCL and a pressure of 18 kPa was applied to the specimen. A gypsum block was inserted within the subsoil, and a fiberglass moisture sensor was placed at the interface of the GCL and the subsoil. The subsoil was incrementally wetted, and after the moisture gauge reading had equilibrated, the resistance reading was recorded and a sample of the soil was obtained for measurement of water content. A typical calibration curve for the gypsum block in the subsoil and the fiberglass moisture gauge at the soil/GCL interface is shown for Soil A in Figure D-16.

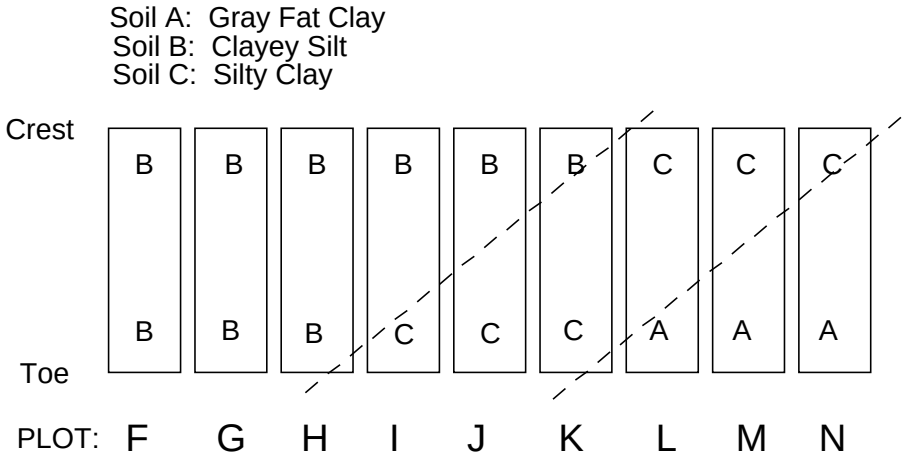

Figure D-15. Soil types at 2H:1V test plots.

The calibration of the fiberglass moisture sensor with bentonite was performed as follows. A fiberglass sensor was sandwiched between two prewetted pieces of Gundseal so that the sensor was surrounded by bentonite. Sand was placed below and above the GCLs, and a pressure of 18 kPa was applied. After the moisture gauge reading had stabilized, the moisture gauge reading was recorded.

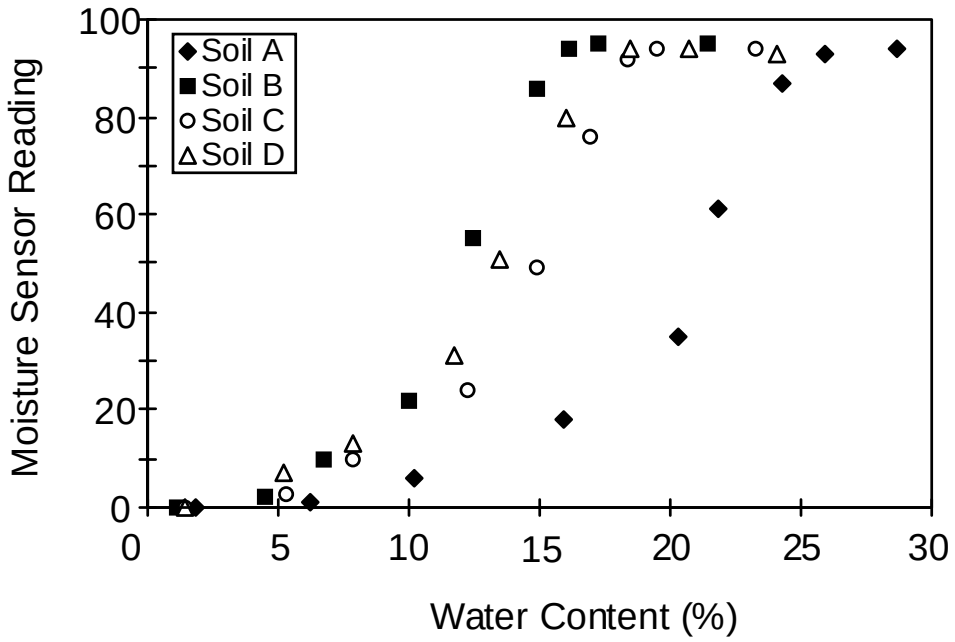

Figure D-16. Calibration of gypsum block moisture sensors (typical calibration).

The calibration curve for the fiberglass moisture sensor with bentonite is shown in Figure D-17. The scatter is due to the use of 15 different sensors in the development of the calibration curve (each moisture sensor should ideally have its own individual calibration curve). This calibration curve can be used to qualitatively distinguish whether the bentonite is relatively dry or saturated. Beyond that, however, statistical scatter limits resolution. For example, a moisture gauge reading of 20 indicates that the water content of the bentonite could range between 40 and 150%, and for a gauge reading of 80 the water content of the bentonite could range between 190 and 290%. However, a gauge reading of close to 0 clearly indicates that the bentonite is dry, and a reading close to 100 clearly indicates that it is wet.

D-2.6.2 Displacement Gauges. Displacement gauges, or extensometers, were installed in each plot to measure displacements and to assess shear strains in the GCL at multiple locations. Twenty displacement gauges were installed in each plot (10 pairs on each panel). Five gauges in each panel were attached to the upper side of the GCL Figure D-18. With gauges on the upper and lower side of the GCL, the difference in total displacement between the upper and lower gauges provides a measure of shearing displacement. Figure D-19 shows the attachment of the hooks to the upper

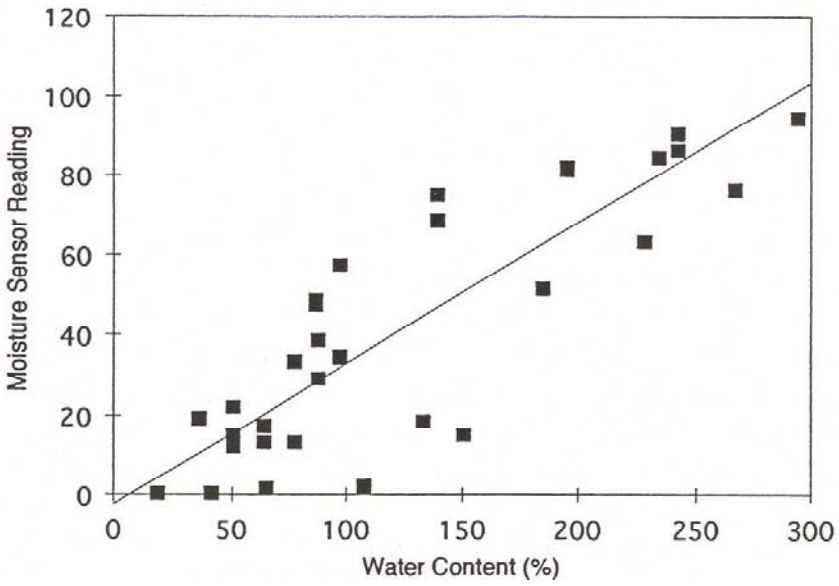

Figure D-17. Calibration of fiberglass moisture sensors with bentonite.

and lower GTs of the GCLs. Each extensometer consisted of a braided steel wire (for flexibility) running from its point of attachment to above the crest of the slope. The wire was contained within a 6-mm OD (outside diameter) plastic tubing, and was connected to a fishhook at the end of the wire (Figure D-19). The fishhook was attached by epoxy to the surface of the GT component of the GCL. Gauges on the upper and lower surfaces were used to measure differential displacement, as shown in Figure D-20. Each wire extended from the fishhook to a monitoring station, or displacement table, at the crest of the slope. A displacement table is shown in Figure D-21.

D-2.7 *Construction*

Construction of the plots began on November 15, 1994, and was completed on November 23, 1994. The construction sequence was as follows:

1. Subgrade preparation.
2. Installation of moisture sensors in the subgrade and at the surface of the subgrade.
3. Placement of GCL.
4. Installation of the extensometers and displacement cables.
5. Installation of moisture gauges within the GCL (plots A, F, P).
6. Placement of GM (not applicable to plots J, K, L, and M).
7. Placement of GN composite or granular drainage layer (plots J, K, L, M).
8. Placement of GT (plots J, K, L, M only).
9. Placement of cover soil.
10. Construction of displacement tables.

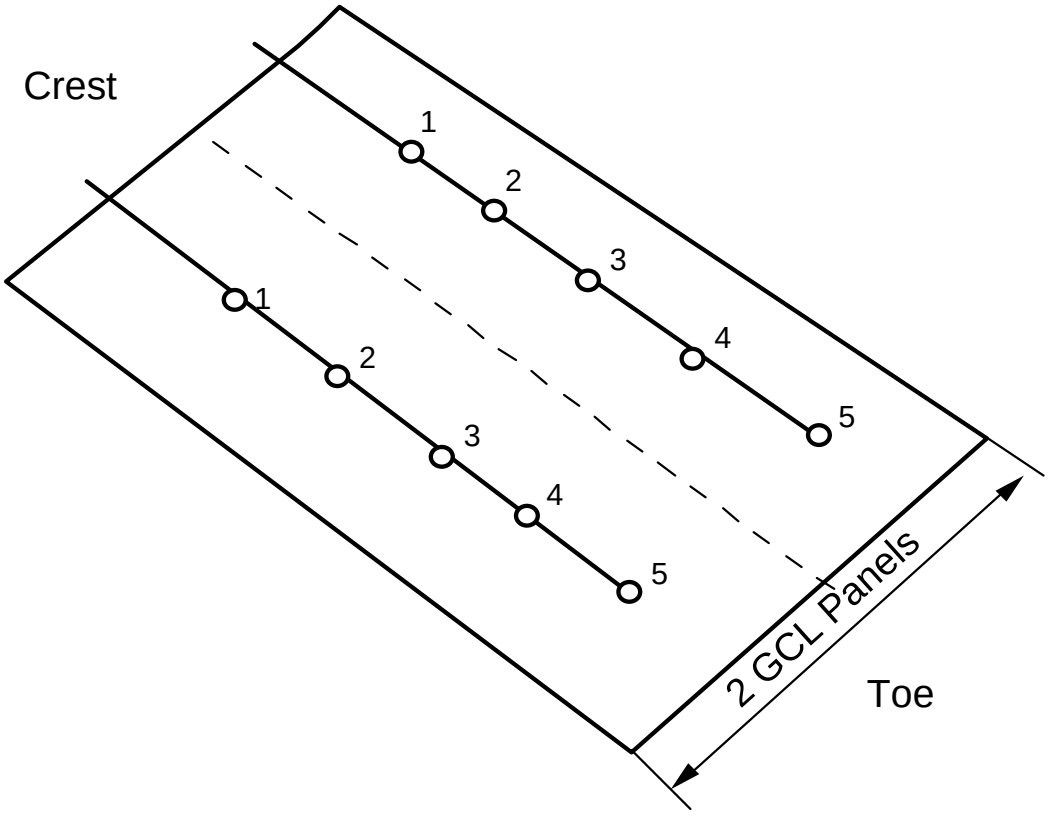

Figure D-18. Locations of displacement sensors.

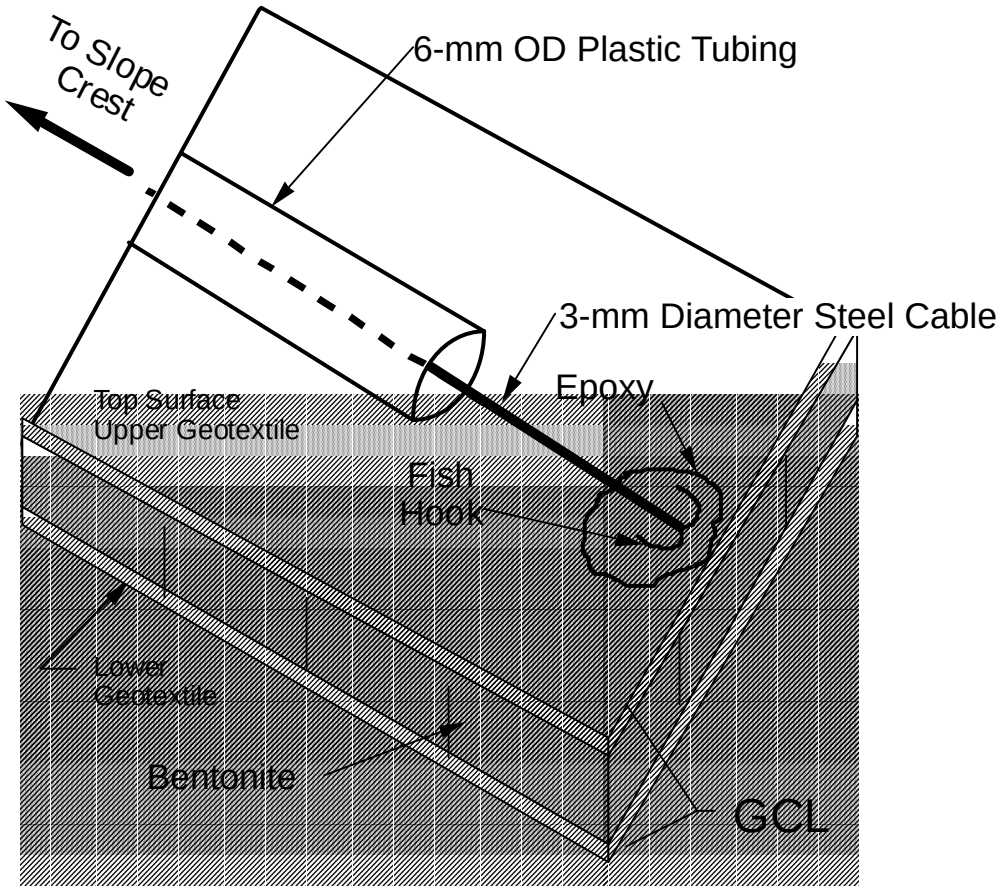

Figure D-19. Attachment of displacement monitoring hook to GCL.

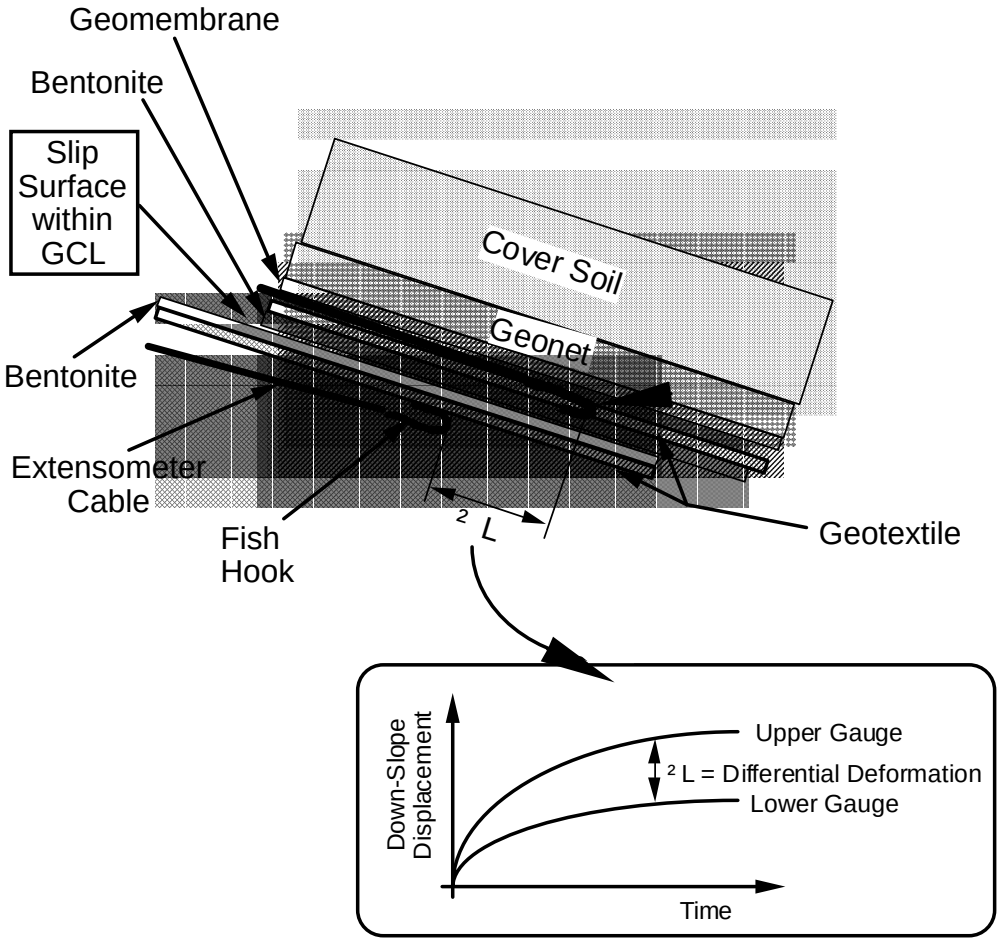

Figure D-20. Location of displacement gauges to measure differential movement.

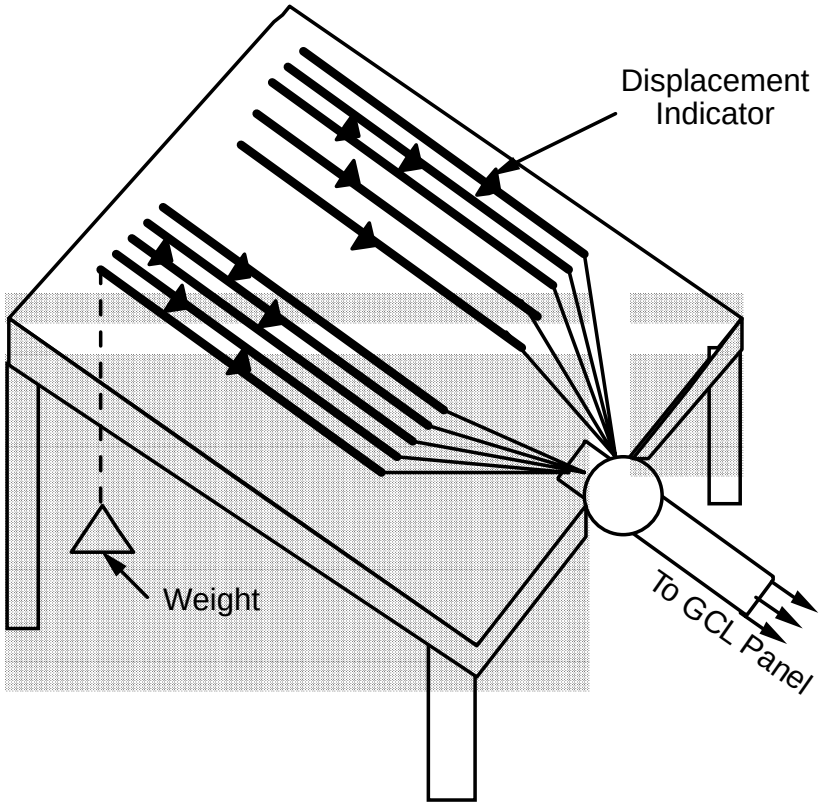

Figure D-21. Displacement table at crest of slope.

D-2.8 *Cutting of the Geosynthetics*

With other geosynthetic materials besides the GCL leading into the anchor trench, part of the down-slope component of force created by the cover soil is carried by tension in these geosynthetic materials. To concentrate all of the shear stress within the mid-plane of the GCL, the geosynthetic materials above the mid-plane of the GCL were severed. The geosynthetics above the mid-plane of the GCLs in plots A through D (3H:1V slope) were cut on April 13, 1995, and the geosynthetics above the mid-plane of the GCLs on the 2H:1V slopes and plot E (3H:1V slope) were cut on May 2, 1995.

In plots with GT-encased GCLs, the GN composite, GM, and the upper GT of the GCL were cut at the crest of the slope down to the mid-plane of the GCL as shown in Figure D-22. The geosynthetic materials in plots constructed with a granular drainage layer were cut down to the mid-plane of the GCL as shown in Figure D-23. The granular drainage material did not extend into the anchor trench, so the GT was cut as well as the upper GT in the GCL.

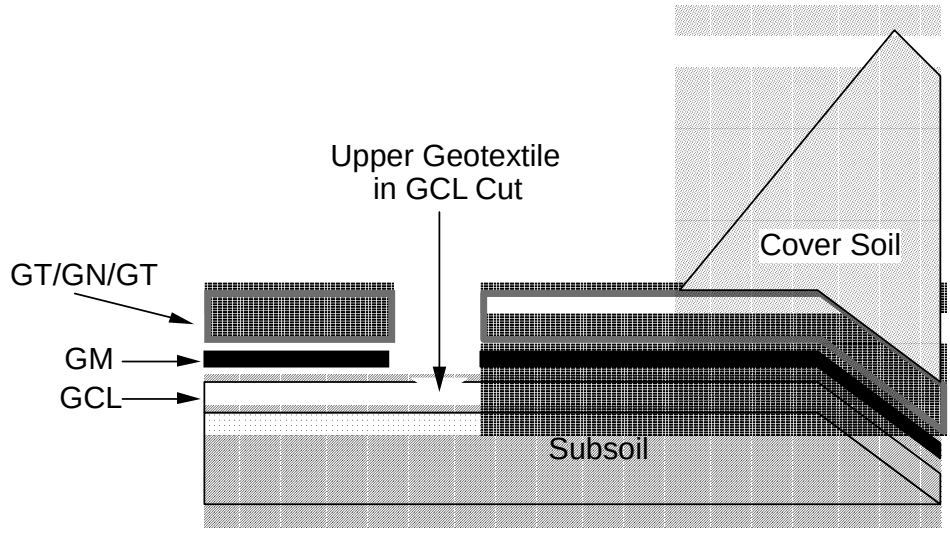

Figure D-22. Cross-section at crest of slope showing cutting of geosynthetics down to mid-plane of GCL on test plots with a GM.

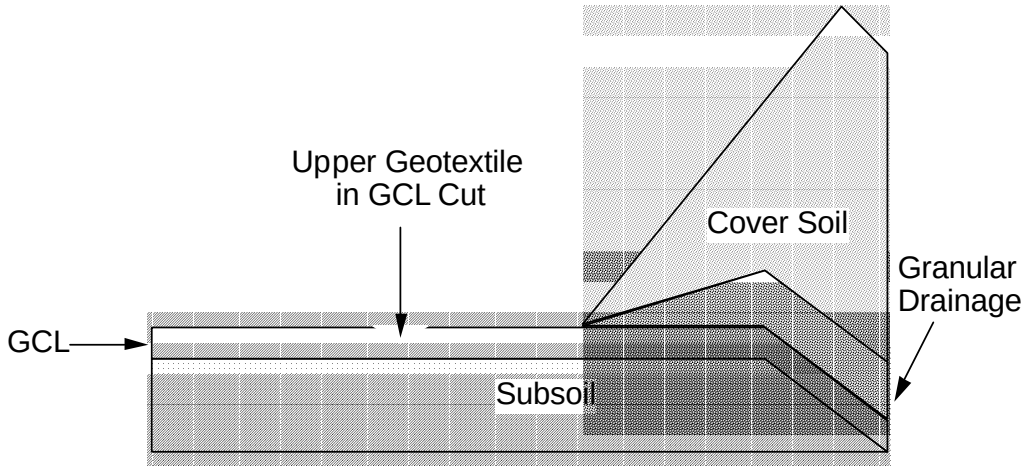

Figure D-23. Cross-section at crest of slope showing cutting of geosynthetics down to mid-plane of GCL on test plots without a GM.

The cutting of anchor trench materials in plots with Gundseal is shown in Figures D-24 and D-25. In the case with the bentonite side of the GCL facing up (Figure D-24), the GN and GM were cut leaving the entire GCL intact. In the case with the bentonite side of the GCL facing downward (Figure D-25), the GN and the GM of the GCL were cut.

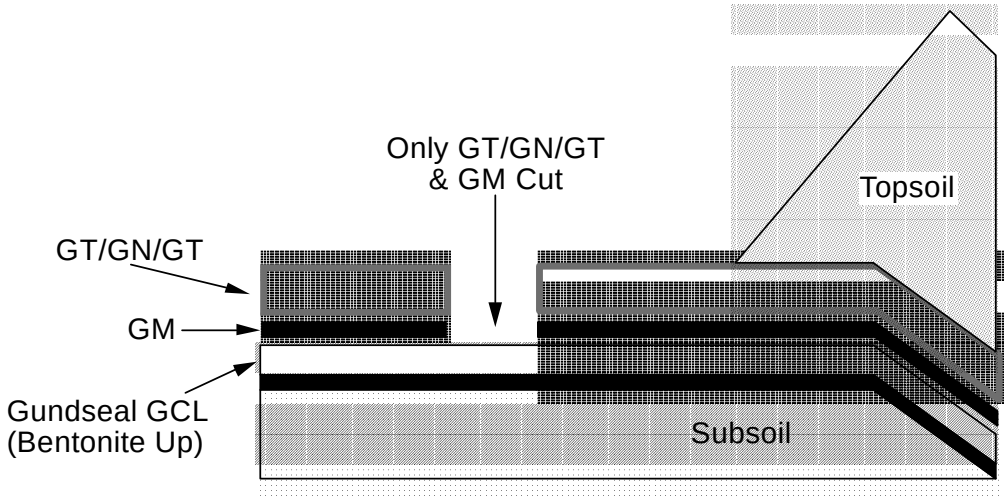

Figure D-24. Cutting of slope with Gundseal, bentonite side facing upward.

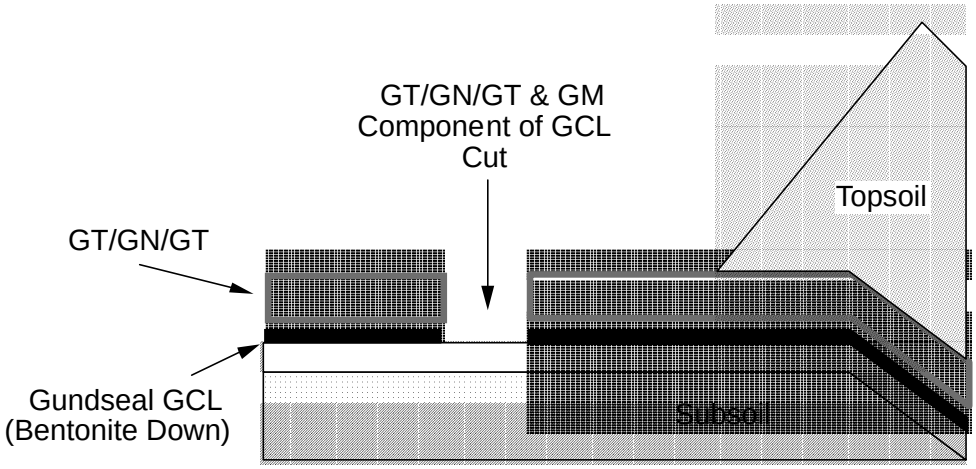

Figure D-25. Cutting of slope with Gundseal, bentonite side facing downward.

D-2.9 *Supplemental Analyses of Subsoil Characteristics*

In the summer of 1997, displacements developed in several test plots that appeared to be consistent with the soil patterns depicted in Figure D-20. The various soil

boundaries shown in Figure D-15 were determined in the field at the time of construction, based on visual observations. Cracks developed in several test plots parallel to the lines shown in Figure D-20.

In an attempt to refine Figure D-15, additional samples were obtained between the 2H:1V test plots and analyzed for liquid and plastic limits following American Society for Testing Materials (ASTM) procedure D4318. Results are summarized in Figures D-26 and D-27. There was some correlation between the originally mapped soil zones and the results of liquid limit (LL) and plasticity index (PI) determinations from the 1997 investigation, particularly in terms of the mapped location of the fat clay where it intersected with the other soils.

Several samples were also obtained from the 3H:1V test plots, and the results of LL and PI determinations are shown in Figure D-28. Little variability was noted. The soils were originally described as sandy, but it was clear that the sands were clayey because of their plasticity.

D-2.10 *Results of Water Absorption Tests*

Tests were performed by GeoSyntec Consultants to evaluate the probable hydration of GCLs placed in contact with soils from the site. Hydration tests were performed on Claymax 500SP, Bentomat ST, and Bentofix NW. Dry GCLs were placed in sealed containers and in contact with compacted soils from that site. The soil used had a LL of 41% and a PI of 19%. The optimum moisture content was 20% when the soil was compacted with standard Proctor (ASTM D698).

The soils were mixed to predetermined water contents equal to 16%, 20%, and 24%. The soils were then compacted into 75-mm-diameter molds to a depth of 150 mm. The GCL specimens were placed in contact with the soil and subjected to a nominal compressive stress of 10 kPa. The nonwoven GT component of Bentomat ST was placed against the soil. The apparatus was sealed, and GCL samples were removed at various times for a period approaching three months. At the end of 75 days of hydration, the water contents were as shown in Table D-3.

As expected, the GCLs did hydrate, and the data indicate that the bentonite was still absorbing water from the wettest soils when the tests were discontinued. The soils at the site were substantially wetter than 24% at the time of construction, and at subsequent times. For example, samples of subsoils taken in June, 1997, from the 2H:1V test plots showed that the water content of the five soil samples averaged 40%.

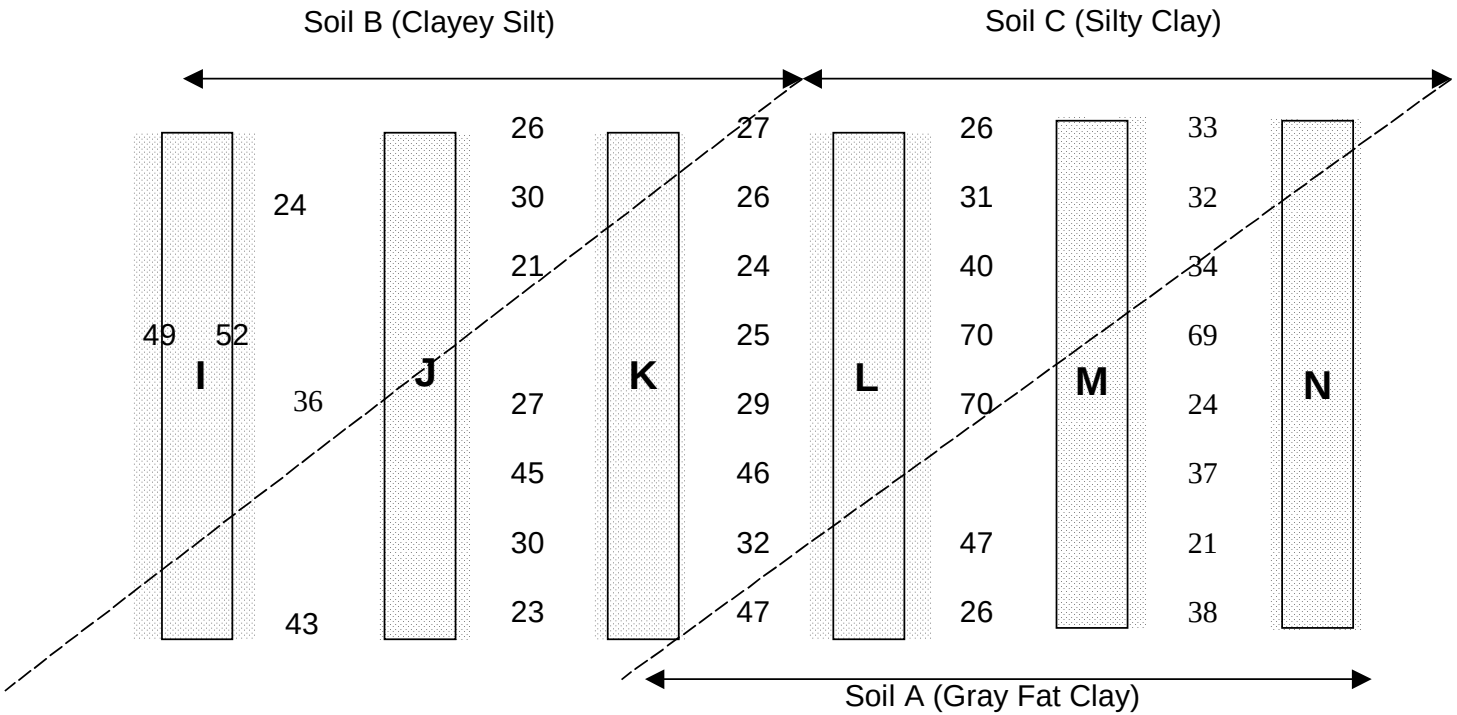

Note: Locations of soil types and descriptions of soils determined at the time of construction of the test plots in 1994 - - LL values shown were measured in 1997. The Information is shown together for purposes of comparison.

Figure D-26. LL(%) measured in 1997 at 2H:1V test plots.

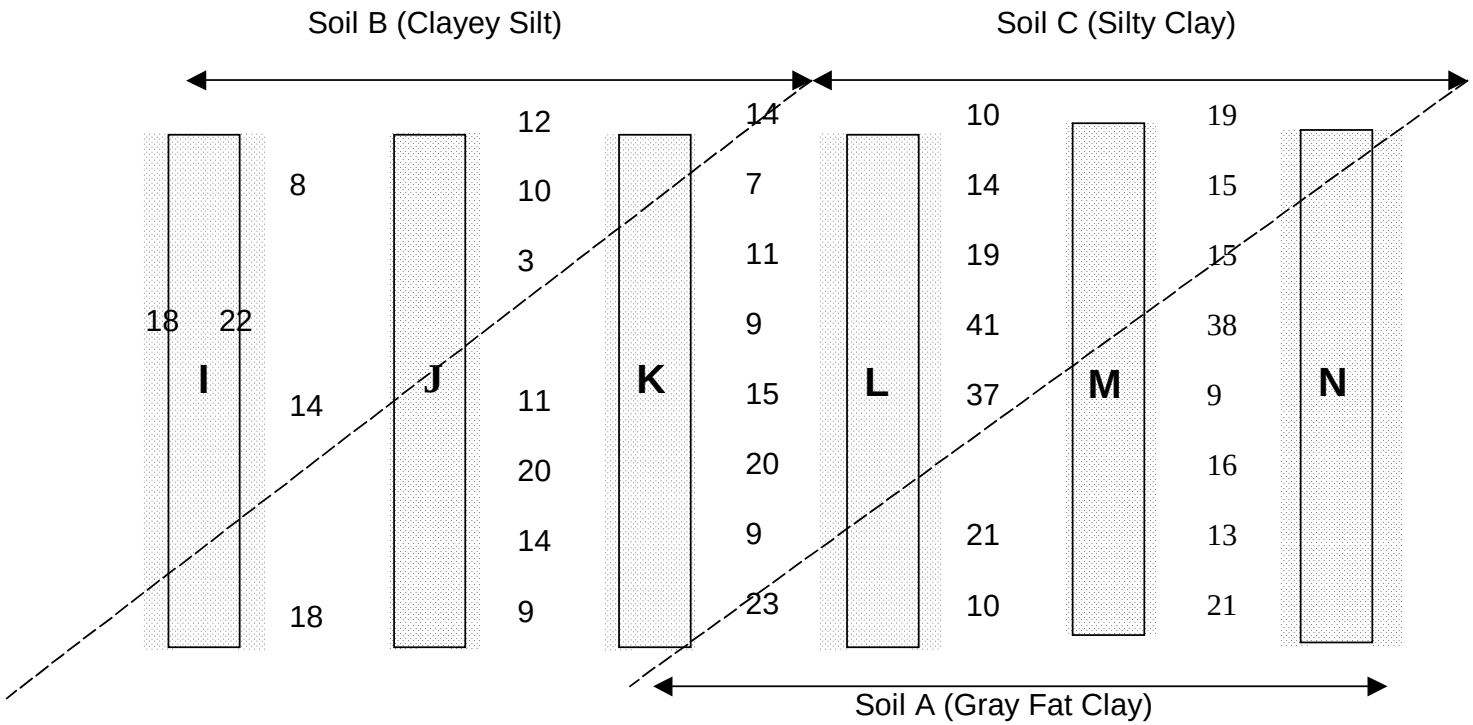

Note: Locations of soil types and descriptions of soils determined at the time of construction of the test plots in 1994 - - LL values shown were measured in 1997. The Information is shown together for purposes of comparison.

Figure D-27. PI (%) measured in 1997 at 2H:1V test plots.

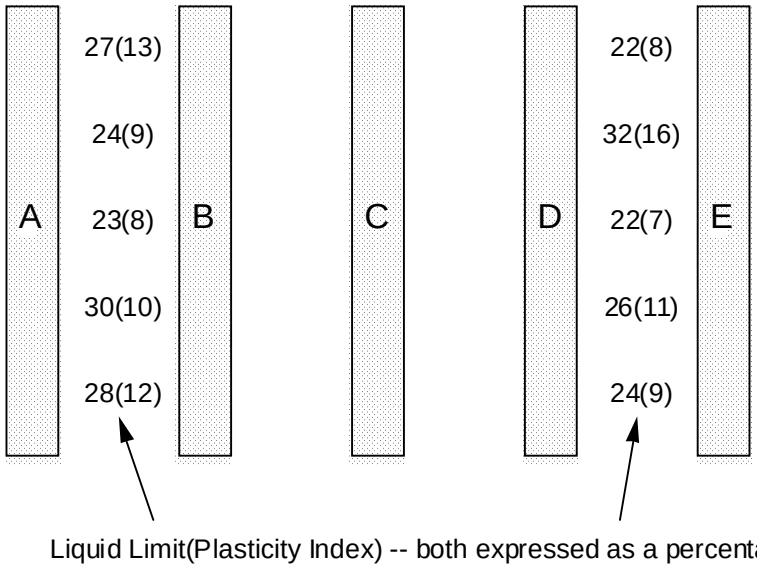

Figure D-28. Results of LL and PI tests on samples taken from subsoils in 1997 at the 3H:1V test plots.

Thus, confirmation was provided that GCLs placed against the subgrade soils at the site would be expected to hydrated to water contents in excess of 70 to 90%.

Table D-3. Water Contents of GCLs after 75 Days of Hydration when Placed Against Soils with Various Initial Water Content (w).

GCL	Soil at w=16%	Soil at w=20%	Soil at w=24%
Bentofix NW	37	58	76
Bentomat ST	40	67	94
Claymax 500SP	38	55	70

D-3 Laboratory Shear Tests

Due to scheduling constraints, it was necessary to construct the test plots before laboratory direct shear tests could be performed. Experienced gained from the test plots in the first few weeks after construction was complete indicated that the interfaces between the GCLs and adjacent materials (particularly between the GCL and overlying textured High Density Polyethylene (HDPE) GM) were the potential failure surfaces of greatest concern. To assist in evaluating if the interfaces between materials at the test site would be stable, Drexel University's Geosynthetic Research Institute (GRI) performed shear tests on critical interfaces.

At the time the shear testing was performed, thirteen plots had been constructed (all of the test plots discussed earlier except for plot P, which was constructed later. Five plots were constructed on a 3H:1V slope, and eight plots were constructed on a 2H:1V slope. The shear testing focused on the plots and interfaces installed on the 2H:1V slope because these were the more critical slopes. The interfaces of concern were:

1. The interface between the top of the GCL and the overlying textured GM.
2. The interface between the top of the GCL and the overlying sand.
3. The interface between the bottom of the GCL and the underlying subgrade (particularly the clayey subgrade soils identified as Soil A and Soil C in Figure D-20).

D-3.1 *Testing Method*

The shear tests were performed according to ASTM D5321 in a 300 mm square shear box. The specimens were hydrated for 10 days in the shear device under a normal stress of 18 kPa. This stress is the approximate normal stress acting on the GCLs in the 2H:1V test plots. The specimens were sheared at a strain rate of 1 mm/min. For each test, the peak and large-displacement strengths were reported. Single point failure envelopes were created by fitting a straight line through the origin and the failure point.

The interface between the top of the GCL and the textured GM was the main focus of the program of laboratory shear testing because of the two interface slides at the test site. To simulate the field conditions as best as possible, site-specific products were used in the tests. In order to obtain the large-displacement strengths, the specimens were sheared to displacements of 35 mm.

D-3.2 *Results*

The results of the direct shear tests are presented in Attachment 1 of this appendix. The testing results are summarized in Table D-4.

Table D-4. Summary of Results of Interface Direct Shear Tests.

Test Plot	Type of GCL	GCL Interface	Opposing Interface	Peak Secant Friction Angle (deg.)	Large-Displacement Secant Friction Angle (deg.)
A,E,F, & P	Gundseal	Dry Bentonite Surface of GCL	Textured HDPE GM	37	35
B & G	Bentomat ST	Woven Slit-Film GT	Textured HDPE GM	23	21
C & H	Claymax 500SP	Woven Slit-Film GT	Textured HDPE GM	20	20
I	Bentofix NW	Nonwoven Needlepunched GT	Textured HDPE GM	37	24
K	Claymax 500SP	Woven Slit-Film GT	Drainage Sand	31	31
-	Bentofix NS	Nonwoven Needlepunched GT	Textured HDPE GM	29	22

Note. Plots J and L (plots with drainage sand and no GM) were not specifically evaluated because a relatively high friction angle (31^o) was measured for plot K, which like plots J and L also had drainage sand and no GM. It was assumed that the friction angle between the drainage sand and either Bentomat ST (plot J) or Bentofix NW (plot L) was no less than the 31^o value measured for Claymax 500SP.

The tests performed on Gundseal and summarized in Attachment 1 and Table D-4 were performed with interface shear on dry bentonite. The testing was performed in this manner on the assumption that the bentonite encased between two GMs would remain dry. The measured angle of internal friction was 37° for peak failure conditions and 35° for large displacement, for the shearing rate of 1 mm/min. Daniel et al. (1993) performed internal shear tests on Gundseal on smaller (60-mm-diameter) samples. Results are summarized in Figure D-29. For shearing rates of 0.26 mm/min and 0.0003 mm/min, the respective angles of internal friction for the most comparable normal stress used were 41° and 35°. Considering the differences in materials and testing conditions, the published results compare favorably with the results of tests on 300x300mm samples conducted for this research project.

Shearing tests were not performed on hydrated Gundseal for this study because the shearing properties of hydrated Gundseal have been studied extensively and documented by Daniel et al. (1993) and Shan (1993). The tests described in the

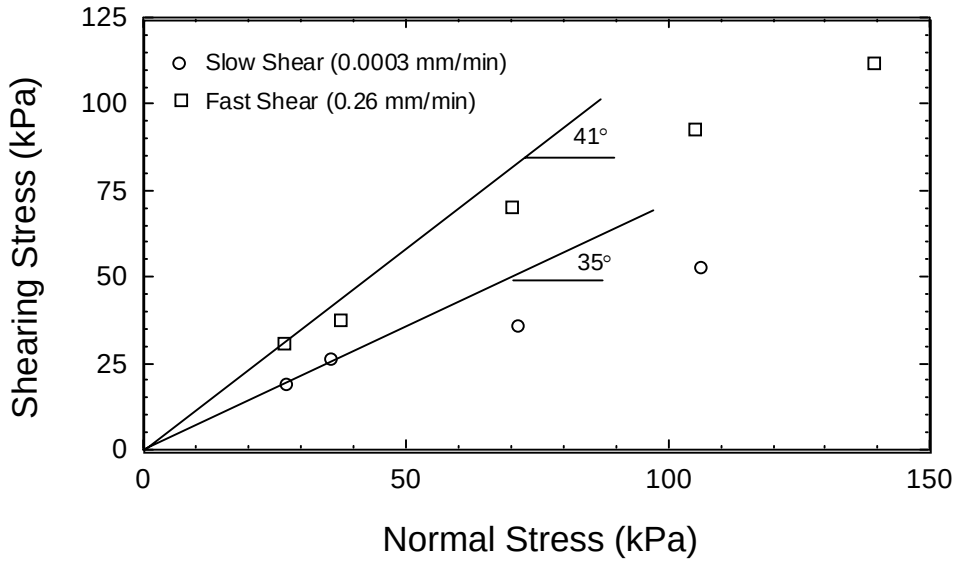

Figure D-29. Results of direct shear tests on dry Gundseal (from Daniel et al., 1993).

literature were all fully drained tests performed using either 60-mm-diameter test specimens in a direct shear apparatus or a 450x450mm test specimen in a tilt table submerged in a water bath. The direct shear tests were performed at an extremely slow speed (0.0003 mm/min), which yields a lower shear strength compared to faster shear. The tilt table tests were performed by slowly increasing the angle of tilt over a period of several weeks. The secant friction angle from the direct shear and tilt table tests is plotted versus normal stress in Figure D-30. For a normal stress of 18kPa (the estimated value at the test plots), the angle of internal friction for the hydrated Gundseal is approximately 20°.

The influence of water content on the shear strength of unreinforced bentonite in Gundseal has also been evaluated by Daniel et al. (1993). Results are summarized in Figure D-31 for a normal stress of approximately 27kPa. The water contents plotted are the average final water content determined at the end of shear. The test at a water content of 145% was for fully hydrated bentonite. The angle of internal friction was found to be comparatively high for the as-manufactured water content, but for water contents $\geq$ 50%, the friction angle was essentially independent of water content and equal to the value for fully hydrated bentonite.

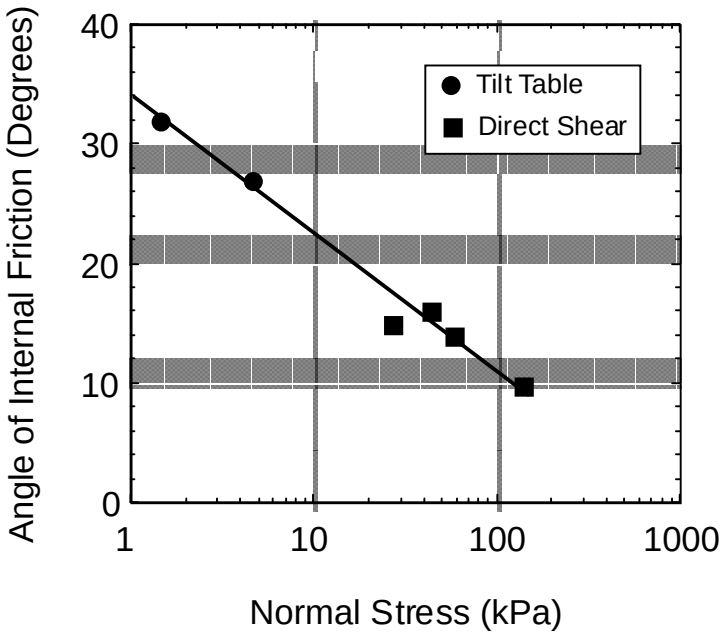

Figure D-30. Influence of normal stress on the internal shear strength of hydrated bentonite (from Shan, 1993).

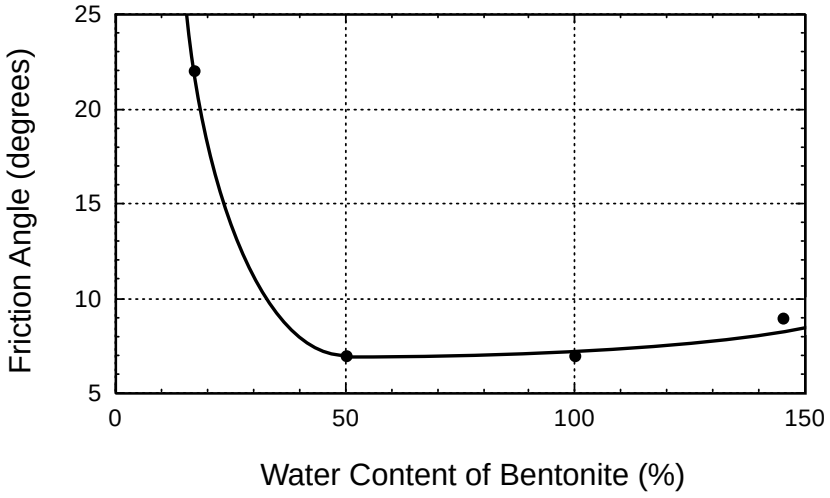

Figure D-31. Influence of water content on the internal shear strength of Gundseal (after Daniel et al., 1993).

Interface shear tests were performed on the interface between the textured HDPE GM and Bentomat ST, Bentofix NW, and Claymax 500SP. As shown in Table D-4, the peak friction angles for the GCL/HDPE interfaces varied from a low of 20° for Claymax 500SP (with a woven, slit-film GT interfacing with the GM), to a high of 37° for Bentofix NW, which had a nonwoven GT interfacing with the GM. Bentomat ST was sheared with the woven GT interfacing with the GM, and the resulting peak friction angle was 23°. Large displacement shear strengths were 0 to 2° below the peak friction angle for GCLs having a woven GT interfacing with the GM, but for the GCL with a nonwoven GT interfacing with the GM, there was a much larger (13°) difference between peak and large-displacement friction angles, probably as a result of "polishing" of the GT with large displacement. When Bentofix NS was sheared with the woven side of the GCL in contact with a GM, the peak and large-displacement friction angles were 29° and 22°, respectively. This configuration was not actually used for any of the test plots because the nonwoven side of Bentofix NS was installed in contact with the GM at plots D and N. The appropriate GM/GCL interface friction angles to assume for plots D and N are those from the results of tests on Bentofix NW, which was tested with the nonwoven GT component of Bentofix interfacing with the GM.

Plots J, K, and L were installed with sand as a drainage layer directly overlying the GCL. Placed above the sand was a nonwoven GT overlain by cover soil that was protected with an erosion control geosynthetic. A GM was not installed. The concern in plots J, K, and L was the shear strength of the interfaces between the GT component of the GCL and the overlying sand. A direct shear test was performed on this interface. The resulting peak and large-displacement interface friction angles were both 31° for tests on Claymax 500SP. The other GCL-sand interfaces were not tested because the lowest friction was expected for Claymax 500SP. The two other GT-encased GCLs should have higher interface friction angles with the drainage sand that Claymax 500SP, which contains woven slit-film GTs on both surfaces.

D-4 Performance of Test Plots

Displacement and moisture data from the test plots have been collected once every two to three weeks since installation. The post-construction data have been arranged into three different types of graphs in order to characterize how the test plots are moving and hydrating with time: 1) total down-slope displacement vs. time; 2) differential displacement between upper and lower surfaces of the GCLs vs. time; and 3) moisture gage readings vs. time. These graphs are presented in Attachments 2, 3, and 4 of this Appendix.

D-4.1 *Construction Displacement*

Construction displacements are the down-slope displacements of the GCLs observed during construction of the test plots (during placement of the overlying geosynthetics or

drainage soil, and cover soil). Post-construction displacements are displacements recorded after construction of the test plots and the associated displacement tables.

Construction displacements were measured by monitoring how far the displacement cables moved in relation to reference stakes placed at the crest of the slope. Maximum construction displacements measured from displacement gages attached to the top of the GCL (at the crest and toe of the slope) and at the bottom of the GCL (at the crest and toe of the slope) are listed in Table D-5. However, the displacements varied with time, and the maximum construction displacement did not always correspond to the last construction displacement, probably because of limitations in the resolution of the extensiometers. Figure D-32 shows the maximum construction displacements for the left and right panel at the toe of each plot. Nearly all of the construction displacements occurred when soil was placed above the GCLs.

Table D-5. Maximum Construction Displacements.

Plot	Maximum Construction Displacements(mm)			
	Above GCL		Below GCL	
	Crest	Toe	Crest	Toe
A	0	13	25	51
B	0	25	0	25
C	13	51	13	64
D	0	25	0	64
E	13	25	13	25
F	64	140	25	127
G	25	64	38	38
H	89	254	89	178
I	25	76	38	114
J	38	140	44	114
K	64	216	51	178
L	51	203	64	114
N	*	*	*	*

note: * = data not recorded

In general, the construction displacements were greater on the 2H:1V slopes than on the 3H:1V slopes and greater at the toe of the slope than at the crest. Table D-6 lists ranges of maximum construction displacements from all of the extensiometer readings on the 2H:1V and 3H:1V slopes. Construction displacements for plots on both slopes ranged from 0 to 89 mm at the crest and 13 to 254 mm at the toe. In some instances,

such as plot I, the maximum construction displacement below the GCL was greater than the maximum displacement above the GCL. This indicates the bottom of the GCL moved more than the top of the GCL at least one time during construction. However, it was expected that the top of the GCL would move more than the bottom of the GCL. It should not be possible for the bottom of the GCL to deform downslope more than the

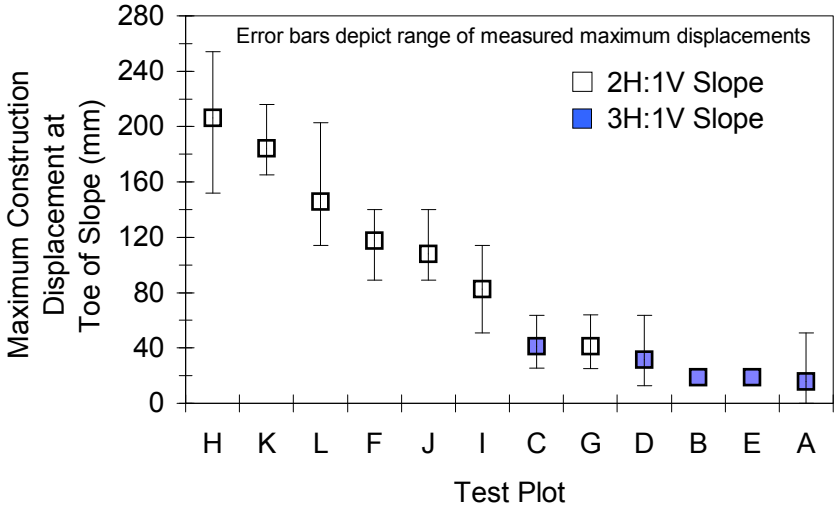

Figure D-32. Maximum construction displacements at toe of slope.

Table D-6. Range of Maximum Construction Displacements.

	2:1 Slope		3:1 Slope	
	Above GCL (mm)	Below GCL (mm)	Above GCL (mm)	Below GCL (mm)
Crest	25 - 89	25 - 89	0 - 13	0 - 25
Toe	64 - 254	38 - 178	13 - 51	25 - 64

top. It is probable that error occurred in the measurements of the construction displacements. Possible causes of error include friction between the steel cables and inside of the surrounding tubing or loss of bonding of gauges to the GCL. Maximum construction differential displacements between the upper and lower surface of the GCL were all less than the resolution of the extensiometers (10 mm).

D-4.2 *Post-Construction Displacement of 3H:1V Slopes*

Post-construction displacements (both total and differential) are summarized in Table D-7. All 3H:1V slopes have remained stable during the 3-1/2 years of observation. Total down-slope displacements have been less than 50 mm, and differential displacements have been less than 10 to 40 mm. There has been no visual evidence of movement or surface cracking.

D-4.2.1 Test Plot A (Bentonite Between Two GMs). The bentonite component of Gundseal was expected to remain dry because the bentonite was encased between two GMs. The measured peak and large-displacement interface secant friction angles between dry bentonite and textured HDPE were 37^o and 35^o, respectively. Because the slope angle was 16.9^o, the slope should be stable so long as the bentonite remains dry.

Fiberglass moisture sensors in plot A have provided variable results: two of the three moisture sensors have indicated that the bentonite is dry, but one sensor near the crest of the slope had indicated some hydration. Two borings were drilled by hand near the crest and toe of the test plot in March, 1995, and 100-mm-diameter samples of the GCL were removed. The water contents of the bentonite in the GCL at the crest and toe were 27% and 24%, respectively. These values are essentially the same as the values at the time of installation, confirming that the bentonite had not hydrated.

D-4.2.2 Test Plots B, C, and D (GT-Encased GCLs). Test plots B, C, and D contain GT-encased GCLs. The bentonite in the GCL was expected to hydrate by absorbing moisture from subgrade soils. Most of the fiberglass moisture sensors have indicated that the bentonite has hydrated, although less than expected. One factor inhibiting hydration may have been the relatively dry, sandy subsoils on the 3H:1V test plots, compared to the 2H:1V test plots, which had more clayey, wetter subsoils. The test plots have remained stable because the slope angles are 17.5^o to 17.8^o, i.e., less than the interfacial friction angles.

D-4.2.3 Test Plot E (Unreinforced GCL). Test plot E was constructed with the bentonite portion of Gundseal facing downward. The drained angle of internal friction for fully hydrated bentonite is about 20^o. The slope angle at plot E was 17.7^o; thus, the test plot is expected to be stable if the bentonite is hydrated, but only with $F = \tan(20^o)/\tan(17.7^o) = 1.14$ for an infinite slope (and possibly less, since the interface shear strength with the underside of the GM may be slightly lower than the internal strength of the bentonite).

As with most of the other test plots, the fiberglass moisture sensors for test plot E have yielded variable results, with some sensors indicating that the bentonite has become hydrated and others indicating that it has not become hydrated. A boring was drilled

and a sample was taken from near the crest of the slope (the driest area) in March, 1995, and the water content of the bentonite was found to be 46%. Eight more borings were drilled in April, 1996, at various locations along the full length of the slope. The water content varied between 54% and 79%, and averaged 60%. The average water content of 60% in test plot E should be sufficiently large to replicate the strength reduction associated with full hydration of the bentonite.

Table D-7. Summary of Post-Construction Performance of Field Test Plots.

Plot	Slope	Type of GCL	Stability of Test Plot As of February, 1998	Total Displacement (mm)	Differential Displacement (mm)
A	3H:1V	Gundseal	Stable	20	10
B	3H:1V	Bentomat ST	Stable	30	40
C	3H:1V	Claymax 500SP	Stable	25	30
D	3H:1V	Bentofix NS	Stable	50	25
E	3H:1V	Gundseal	Stable	30	30
F	2H:1V	Gundseal	Internal Slide within the GCL Occurred 495 Days after Construction of Test Plot	-	750
G	2H:1V	Bentomat ST	Interface Slide between Lower Side of GM and Upper Woven GT Surface of GCL Occurred 20 days after Construction of Test Plot	-	25
H	2H:1V	Claymax 500 SP	Interface Slide between Lower Side of GM and Upper Woven GT Surface of GCL Occurred 50 days after Construction of Test Plot	-	130
I	2H:1V	Bentofix NW	Slumps and Surface Cracks Developed about 900 Days after Construction of Test Plot	500	25
J	2H:1V	Bentomat ST	Slumps and Surface Cracks Developed about 900 Days after Construction of Test Plot	800	75
K	2H:1V	Claymax 500SP	Slumps and Surface Cracks Developed about 900 Days after Construction of Test Plot	1200	900
L	2H:1V	Bentofix NW	Slumps and Surface Cracks Developed about 900 Days after Construction of Test Plot	500	180
N	2H:1V	Bentofix NS	Stable	30	10
P	2H:1V	Gundseal	Stable	NA	NA

Note: Total displacement is the total amount of down-slope movement measured after construction was complete and displacement tables were installed; differential displacement is the difference between down-slope movement of the upper and lower surfaces of the GCL that occurred after construction.

D-4.3 *Post-Construction Performance of 2H:1V Plots*

Slides have occurred at most of the 2H:1V test plots. Two slides occurred at plots G and H a few weeks after construction was complete. Both involved slippage at the interface between the upper surface of the GCL (a woven GT in both cases) and the lower surface of the textured HDPE GM. The next slide occurred in plot F about a year and a half after construction. In this case, the bentonite (which was encased between two GMs) in this GCL unexpectedly became hydrated, and a slide resulted. The test plots remained stable for the next two years, but then several slides occurred in the subsoils beneath other test plots. The subsoils were plastic clays, and the subsoil slides (which occurred at the end of a wet spring season) were presumed to be the result of hydration of the subsoil clays and possibly the buildup of excess pore water pressure in the subsoils, as well.

D-4.3.1 Test Plots F and P (Bentonite Encased Between Two GMs). Plots F and P, like plot A, contained bentonite encased between two GMs. The bentonite in these test plots was expected to remain dry. However, within three months after plot F was constructed, two of the three moisture sensors indicated that the bentonite had become hydrated.

To evaluate the condition of the bentonite, 17 borings were drilled into Plot F in March, 1995, and 100-mm-diameter samples of the GCL were recovered. The water content of the bentonite samples varied from 10% to 188%, and the data showed that the right panel was much more hydrated than the left panel (Figure D-33). In contrast to this field data, Estornell and Daniel (1992) reported laboratory test results for Gundseal in which water migrated laterally through the GM-encased bentonite less than 100 mm over a test duration of 6 months.

Water may have entered the bentonite at plot F through cuts made in the GM liner overlying the GCL to allow insertion of the extensiometer cables. Plot F was located at a point where surface water at the crest of the slope was funneled directly to the anchor trench area where the penetrations were made. The mechanism for lateral movement of water is probably waves in the overlying GM, which would allow water to spread. Alternatively, the source of water could have come from the V-shaped trough between plots F and G, and spread through waves in the GM. Unfortunately, the plot slid before a complete forensic study could be performed. Large-scale laboratory tests, described later in this appendix, were performed to investigate the potential for lateral spreading of water in the plane of the GCL.

Displacement sensors showed large movements in the right panel of plot F during the first year of observation, but not in the left panel until later. Starting on about day 275 (August, 1995), the left panel began to move down slope, suggesting that the bentonite

in the left panel was finally becoming hydrated over a significant percentage of the total area of the panel.

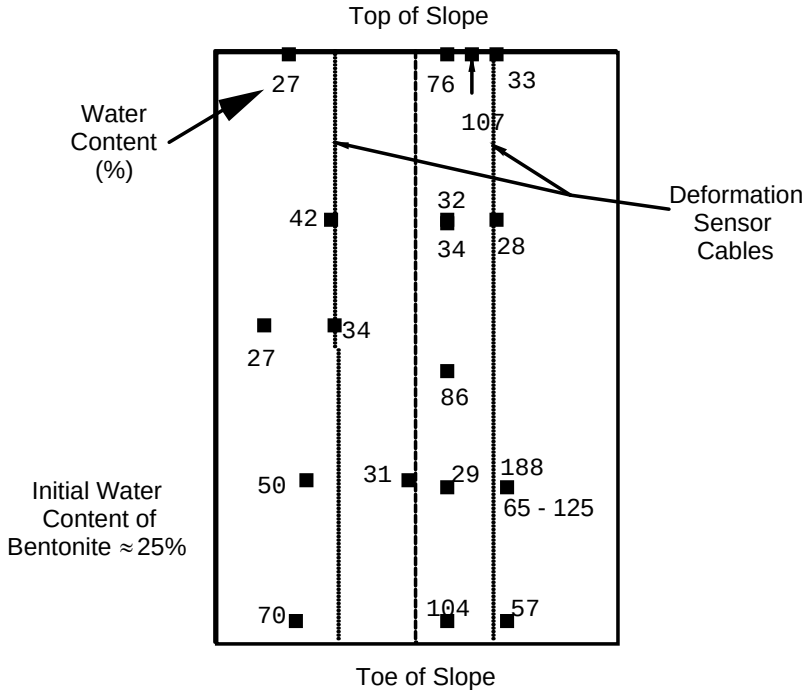

Figure D-33. Water content (%) measured in bentonite at plot F.

Plot F slid on March 24, 1996, 495 days after construction. The cause of the slide is hydration of the bentonite; the peak angle of internal friction for hydrated bentonite at the normal stress existing in the field was 20^o, but the slope angle was 23.6^o. In contrast, the peak interface friction angle for dry bentonite was 37^o. Had the bentonite not hydrated, the slope should have remained stable.

In response to the unexpected hydration, plot P was constructed on June 15, 1995. The extensiometers were not installed in plot P to eliminate all penetrations in the overlying GM. The number of fiberglass moisture sensors in the bentonite was increased from 3 in the other test plots to 16 in plot P to provide additional documentation of moisture conditions. All but one of the 16 moisture sensors have indicated that the bentonite has remained dry in the 18 months of monitoring plot P.

D-4.3.2 Test Plots G and H. Test plots G and H consisted of Bentomat ST and Claymax 500SP, respectively. Both plots slid at the interface between the upper GT (a woven, slit-film GT in both cases) and the lower surface of the overlying textured HDPE GM. Plot H slid 20 days after construction, and plot G slid 50 days after construction. Pre-slide displacements were small (< 25 to 130 mm). There was no

warning of either slide. Both slides occurred at night, and the slides apparently occurred quickly.

Test Plot H, which incorporated Claymax 500SP, was constructed on a 24.7^o slope, but the measured peak and large-displacement interface friction angles for the relevant materials under hydrated conditions were only 20^o. Test plot H did not slide immediately because the interfacial shear strength of the dry GCL was sufficient to maintain a stable slope. The slope slid when the bentonite hydrated. Tests described earlier showed that bentonite in the GCLs hydrated in a period of 10 to 20 days when placed in contact with the subgrade soils from the test plots. Tests reported by Daniel et al. (1993) showed similar results for other soils. Thus, the sliding time of 20 days after construction is consistent with the expected period to achieve nearly full hydration of the bentonite.

When GCLs containing a woven GT component become hydrated, bentonite can swell through the openings of the GT and lubricate the GCL-GM interface. After the slide, the surface of the GCL was very slick. The tendency of bentonite to lubricate the GM/GCL interface may be related to the thinness of the woven slit-film GT and to differences in apparent opening size between woven and nonwoven GTs.

Test plot G, which was constructed using Bentomat ST, was slower to slide, but the slope angle (23.5^o) was 1.2^o flatter than for plot H, and the interface shear strength between the GCL and overlying GM (23^o peak, 21^o large-displacement) was 1° to 3° higher. Also, a nonwoven GT faced downward in plot G, but a woven slit-film GT faced downward in Plot H. GCLs are expected to absorb water more slowly from subgrade soils when the GT separating the bentonite from the subsoil is a thicker nonwoven GT. Thus, the reason why plot G slid 30 days later than plot H appears to be that the bentonite in the GCL at plot G was separated from wet subgrade soils by a thicker, nonwoven GT, which slowed hydration.

D-4.3.3 Plots I and N with Nonwoven GT Component Facing Upward. Plots I and N are similar to plot G, except that the GCL contained either one nonwoven GT with the nonwoven GT facing upward (plot N) or two nonwoven GTs (plot I). The slope angles at plots I and N were similar to the other 2H:1V plots. However, the interface friction angle between the nonwoven GT component of Bentofix and the textured HDPE (37^o peak and 24^o large-displacement) was much greater than for the woven slit-film GT component of the GCLs that slid. The geosynthetic components of plots I and N have remained stable because of the better interface shear resistance between a nonwoven GT component of a GCL compared to a woven GT component. The greater interface shear resistance from the nonwoven GT is attributed to: (1) larger shear resistance developed between nonwoven GTs and textured GMs in general, and (2) less hydrated bentonite extrusion to the interface for the thicker nonwoven GT.

Large displacements began to develop in plot I and the adjacent test plots (J, K, and L) about 3-1/2 years (900 days) after construction. Several small slumps with downward displacement of up to about 100 mm along scarps, and associated surface cracking, were observed, with the slumps and cracks appearing in the lower half of the test plot. The subsoils in the area of the slides are CL and CH clays, with the LL and PI of the subsoil next to plot I averaging 45% and 18%, respectively. The displacements occurred at the end of the wet spring season in 1997. Examination of plot I and adjacent test plots, coupled with excavation into the subsoils, showed that sliding was occurring 0.5 to 1 m beneath the GCL, in the clay subsoil. It is assumed that the buildup of pore water pressure behind the test plots helped to trigger the slides in the subsoils. There was no indication of movement within the GCL or an interface with the GCL. Plot N showed no signs of slumping or cracking, but plot N was at the end of the 2H:1V test plots and likely was at a location where excess pore water pressures were not as likely to develop.

D-4.3.4 Plots J, K, and L with No GM. These test plots were constructed by placing drainage sand directly above the GCL. All three test plots remained stable for about 900 days after construction, and then all three underwent significant down-slope displacement (0.5 to 1.2 m, as shown in Table D-7). All three exhibited slumping in the lower half to two-thirds of the test plots. Scarps could be observed at several locations within each test plot. Observation of the depth of slumping clearly showed that displacement was occurring nominally 0.2 to 1 m beneath the GCLs. Excavation into the subsoils showed that a layer of plastic clay was located at about this same depth. The sliding mechanism was related to the subsoils and not to the GCLs or GCL interfaces. Buildup of pore water pressure in the clays following the wet spring season was assumed to be the triggering mechanism.

The peak secant interface friction angle between the sand drainage material and GCL was 31^o for a woven-slit film component (Table D-7) and, although not measured, presumably more for a nonwoven component. An interface friction angle of 31^o is significantly greater than the slope angle (~ 25^o), which explains the stability of the test plots up until the point of sliding in the subsoil.

D-4.4 *Moisture Gage Readings*

Graphs of moisture gage readings vs. time (attachment) provide a general indication of how and where the bentonite and subsoil is hydrated in each test plot. Each graph includes the readings of the moisture sensors installed at one location along the slope of the plot. The moisture sensors include the gypsum block in the subsoil, the fiberglass sensor at the interface of the GCL and the subsoil, and the fiberglass sensor between the GCL and the overlying GM (only in plots A, F, N, and P).

D-5 Tests to Study Lateral Spreading of Water in Bentonite

The Gundseal used in plot F contained a lightweight GT backing called “spidernet.” Because unexpected lateral spreading of water in the bentonite component occurred in plot F, tests were performed to determine if the spidernet contributed to the lateral spreading of water. Tests were performed by placing a 0.9-m-diameter piece of Gundseal (with or without the spidernet) in a large pipe with the bentonite facing up (Figure D-34). A sheet of textured HDPE GM with a 152 mm-diameter hole was placed over the sheet of Gundseal. A 152 mm-diameter standpipe was sealed to the edges of the hole in the overlying GM. The volume of the large pipe surrounding the standpipe was filled with aggregate.

Three series of lateral rate of wetting tests were performed. In the first series, two specimens of Gundseal (with textured HDPE GMs) were tested, one with a spidernet and the other without the spidernet. At the beginning of each test, water was poured rapidly into the standpipe to a height of 152 mm. In both tests (with spidernet and without spidernet) the lateral spread of water was greater than 460 mm after twenty-four hours of the application of 152 mm of head.

In the first series of tests, it was believed that the application of water in the standpipe was too rapid. Therefore, a second series of tests was performed on two specimens of Gundseal (with textured HDPE GMs), one with a spidernet and one without the spidernet. Water was introduced in 50 g increments per day for 7 days. This allowed the bentonite to “pre-hydrate” and create a seal with the standpipe. After 7 days of pre-hydration, water was added to the standpipe to a total height of 150 mm. The specimens were left for an additional 7 days under 150 mm of head. After that time, the water content of the bentonite was determined at distances from the center of the standpipe to the edge of the Gundseal specimen. Figure D-35 shows the water contents from the 7-day inundation period. The water contents were similar for the specimens with and without the spidernet.

Another series of tests was performed on two specimens of Gundseal, with and without the spidernet. The Gundseal specimens had smooth HDPE GMs. This series was performed exactly like the second series except that the specimens were allowed to sit under 152 mm of head for 21 days. After 21 days, water contents were determined at distances from the center of the standpipe to the edge of the Gundseal specimen. The water contents were similar for the specimens with and without the spidernet (Figure D-36).

The results of these tests indicate that the spidernet has little effect on the lateral rate of wetting of Gundseal for inundation periods of 21 days. However, it appears that the rate of inundation has an effect on the lateral spread of water. The initial series of tests indicate that rapid inundation of water leads to greater lateral spreading of water.

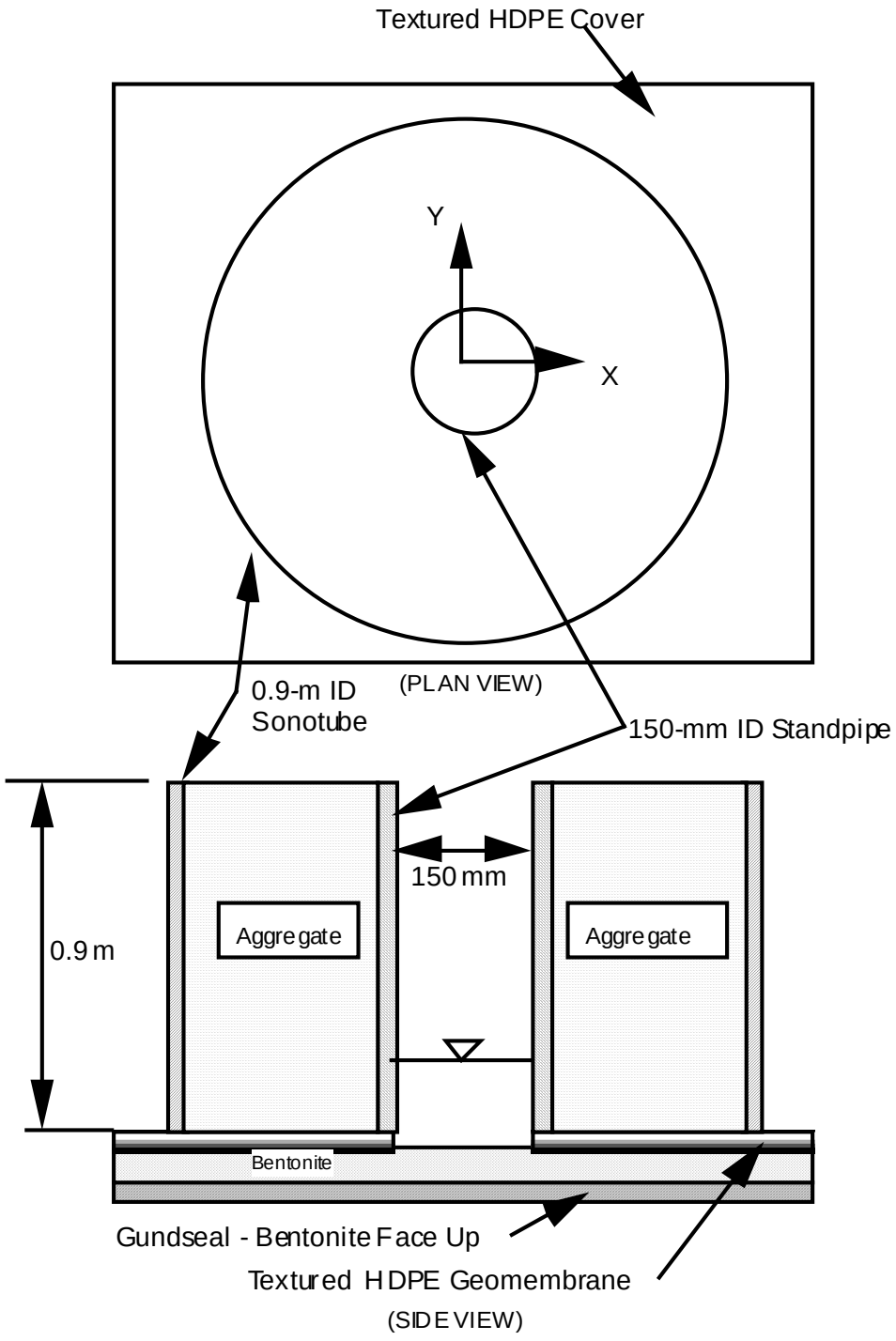

Figure D-34. Apparatus to study lateral spreading of water in bentonite.

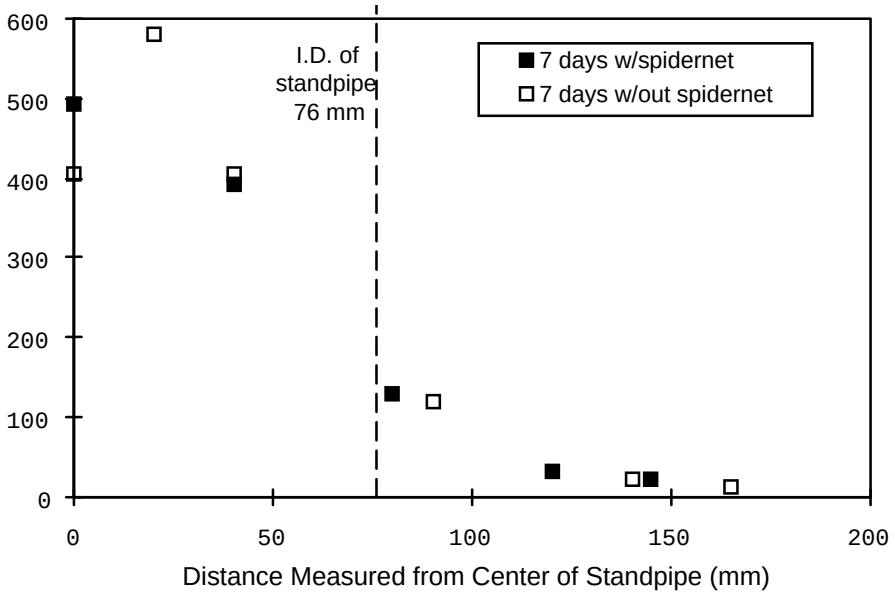

Figure D-35. Results from rate of lateral wetting tests after 7 days.

D-6 Erosion Control Materials

Erosion control materials were placed on the surfaces of all the test plots, except Plot M, which was intentionally not covered with any erosion control material as a control plot. The purpose of the erosion control materials was to stabilize the slopes rapidly and to maintain each slope's surface integrity. Erosion control materials provide for the rapid growth of seeded grass by retaining heat from the sun and limiting erosion due to overland runoff. The erosion control materials give shelter to the seeds from flowing water and winds.

Table D-8 summarizes the erosion control products that were placed on the various test plots. Three plots (E, K, and N) had a sacrificial, biodegradable woody material applied to the surface. All erosion control materials were installed according to manufacturer's specifications. The erosion control materials were installed in an overlapping manner and stapled together. They were stapled to the soil at spacings of approximately 1 m per the manufacturer's recommendations. Some plots were seeded prior to placement of the erosion control material, and others were seeded after the erosion control placement (depending on the manufacturer's recommendation). The site owner provided for the seeding of the plots in December, 1994.

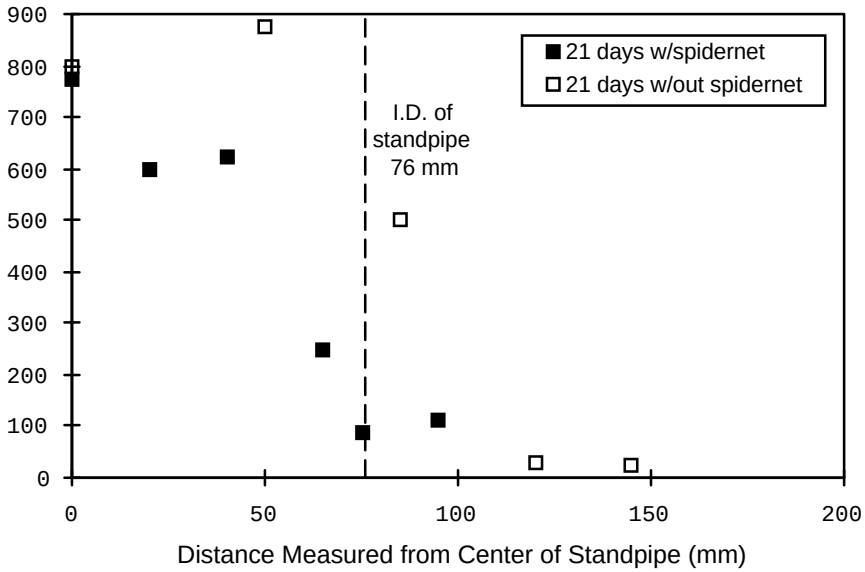

Figure D-36. Results from rate of lateral wetting tests after 21 days.

All of the erosion control materials have worked well. There were significant erosion gullies and some sloughing of the cover at the toe of the slope in the control Plot M that did not contain any erosion control material. All the erosion control materials appeared to be functioning as designed and to have maintained the integrity of the surface of the test plots.

D-7 Additional Laboratory Direct Shear Testing on an Unreinforced GCL

This section describes a laboratory-testing program designed to study the changes in internal shear strength of GCLs as a result of varying laboratory test preparations and conditions. Direct shear tests were performed on the internal portion of unreinforced GCLs. The test preparations and conditions evaluated include hydration time, shear rate, and normal stress. An unreinforced GCL was selected to focus on the strength of the bentonite itself. The following section reports on results from a one-dimensional consolidation test of an unreinforced GCL

D-7.1 *Materials Tested*

A roll of Claymax 200R was supplied by the manufacturer and used for testing. Claymax 200R is an unreinforced GCL consisting of bentonite mixed with an adhesive and sandwiched between two nonwoven GTs. Specimens of Claymax 200R were used in the direct shear and one-dimensional consolidation tests.

Table D-8 Geosynthetic Erosion Control Products.

Plot	Manufacturer	Product	Color	Material
A	Tensar	TB 1000	Green	Polyolefin
B	Synthetic Industries	Polyjute	Beige	Degradable Polypropylene
C	Synthetic Industries	Polyjute	Beige	Degradable Polypropylene
D	Akzo	Enkamat 7010	Black	Nylon
E	Akzo	Enkamat 7010	Black	Nylon (with Excelsior)
F	Tensar	TM 3000	Black	Polyethylene
G	Tensar	TM 3000	Black	Polyethylene
H	Tensar	TM 3000	Black	Polyethylene
I	Synthetic Industries	Landlok 450	Green	Polyolefin
J	Synthetic Industries	Landlok 450	Green	Polyolefin
K	Akzo	Enkamat 7010	Black	Nylon (with Excelsior)
L	Akzo	Enkamat 7010	Black	Nylon
M	None	Control Plot	-	-
N	Akzo	Enkamat 7010	Black	Nylon (with Excelsior)
P	Akzo	Enkamat 7220	Black	Nylon

D-7.2 *Direct Shear Tests*

D-7.2.1 Testing Equipment. Two different direct shear machines were utilized in the direct shear tests. A 64 mm diameter direct shear machine supplied by ELE (Engineering Laboratory Equipment, Ltd.) was used in tests involving lower normal stresses. A 63.5 mm diameter Wykeham Farrance direct shear machine was used in tests involving higher normal stresses.

D-7.2.2 Testing Variables. The testing variables evaluated include hydration time, shear rate, and normal stress. The effects of one variable on the measured shear strength was studied while the other two variables were kept constant. Table D-9 describes each test by listing the test number, hydration time before shear, normal stress, and shear rate.

D-7.2.3 Hydration Time. Direct shear tests were performed after the GCLs had been hydrated 24, 48, 72, and 152 hours. Three direct shear tests were performed for each different length of hydration, except only one shear test was performed after 152 hours of hydration. All tests were performed with a normal stress of 17 kPa and a shear rate of 1 mm/min.

Table D-9. Outline of Shearing Program.

Test No.	Hydration Period (hrs)	Shear Rate (mm/min)	Normal Stress (kPa)
1	24	1	17
2	24	1	17
3	24	1	17
4	48	1	17
5	48	1	17
6	48	1	17
7	72	1	17
8	72	1	17
9	72	1	17
23	153	1	17
14	24	0.1	17
15	24	0.1	17
19	24	0.1	17
20	24	0.02	17
21	24	0.02	17
22	24	0.02	17
24	24	0.0025	17
25	24	0.0025	17
26	24	0.0025	17
27	24	0.0005	17
29	24	0.0005	17
37	24	1	172
38	24	1	172
32	24	0.024	172
36	24	0.024	172
28	24	0.0005	172
30	24	0.0005	172

D-7.2.4. Shear Rate and Normal Stress. The effect of shear rate on the shear strength of GCLs was investigated at two normal stresses, 17 kPa and 170 kPa. At a normal stress of 17 kPa, the strengths were investigated at shear rates of 1, 0.1, 0.02, 0.0025, and 0.0005 mm/min. At a normal stress of 170 kPa, the strengths were investigated at shear rates of 1, 0.024, and 0.0005 mm/min. All shear tests were performed after 24 hrs of hydration.

The effect of normal stress on the internal shear strength was investigated at three different shear rates, 1, 0.02, and 0.0005 mm/min. At each shear rate, tests were performed at normal stresses of 17 kPa and 172 kPa. All shear tests were performed after 24 hrs of hydration.

D-7.3 *Specimen Description and Preparation*

Direct shear tests were performed according to ASTM D3080. However, the procedure was modified and is described in the following paragraphs.

Sections of 200 mm x 200 mm GCL were cut from a sheet of Claymax 200R. The direct shear specimen was trimmed to the diameter of the direct shear box from one of these sections. Trimming was carefully performed in order to minimize the escape of bentonite from the GCL. Initial water contents were obtained.

A thin layer of vacuum grease was applied to the lower surface of the upper shear box, to the upper surface of the lower shear box, and to the inside of the shear box. The GCL specimen was placed in the direct shear box in the as-received (dry) condition. Additional porous stones and thin plates of foil were used to adjust the vertical position of the specimen in the direct shear box in order to force the failure plane through the mid-plane of the hydrated GCL. The normal stresses used during shear were applied to the specimens in one increment. Water was added to the shear boxes, and the specimens were hydrated for a specific period of time. The height of the specimens was monitored during hydration.

After hydration for the designated amount of time the specimen was prepared for shear. The upper shear box was raised by turning the shear box screws a one-quarter to one-half turn. However, the shear screws were not removed. Instead, they were left in contact with the lower shear box. Shearing of the specimen commenced and the shear stress and height were monitored. Shearing was performed at a designated shear rate, and the test was terminated after the maximum shear developed. The specimen was dismantled, and the water content after shear was obtained.

D-7.4 *Correction for Shear Box Friction*

The measured shearing resistance of the GCL was adjusted for friction that developed between the shear box screws and the lower shear box. The friction of the screws against the shear box surface was measured by performing several shear tests on an “empty” direct shear box with no normal load applied and recording the maximum resistance. The maximum resistance in both shear machines was 1 kPa, and this value was used as the friction. After a GCL was sheared, the friction was deducted from the maximum recorded shear resistance of the GCL.

D-7.5 *Test Results*

Individual curves of shear stress vs. displacement for all direct shear tests are shown in Attachment 5. The shear stresses shown in Figures 1 to 11 in Attachment 5 have not been adjusted for friction.

D-7.5.1 Effect of Hydration Time. Table D-10 lists the adjusted peak shear stress and the displacement at peak stress from direct shear tests on GCL specimens after 24, 48, 72 and 153 hours of hydration. The average, standard deviation, and coefficient of variation for peak stress and peak displacement are listed in Table D-10 for the different lengths of hydration. Overall, the averages of peak stress for each hydration period are very similar. However, within each hydration period, the peak stresses are variable. The coefficient of variation for the peak shear stresses in each hydration period range between 10 and 11%.

Table D-10. Shear Results for Various Hydration Periods.

Test No.	Hydration Period (hr)	Shear Rate (mm/min)	σ_{normal} (kPa)	τ_{peak}* (kPa)	δ_{peak} (mm)
1	24	1	17	10.2	3.2
2	24	1	17	11.9	4.3
3	24	1	17	9.8	4.3
Average				10.6	3.9
Standard Deviation				1.1	0.7
Coefficient of Variation				0.11	0.17
4	48	1	17	9.6	2.3
5	48	1	17	11.9	4.3
6	48	1	17	10.6	3.6
Average				10.7	3.4
Standard Deviation				1.2	1.0
Coefficient of Variation				0.11	0.30
7	72	1	17	11	3.6
8	72	1	17	9.6	2.3
9	72	1	17	11.7	2.4
Average				10.8	2.8
Standard Deviation				1.1	0.7
Coefficient of Variation				0.10	0.25
23	153	1	17	11.3	2.9

* peak shear stress is adjusted for machine friction

σ_{normal} = normal stress; τ_{peak} = peak shear stress; δ_{peak} = displacement at τ_{peak}

Figure D-37 contains a Mohr-Coulomb diagram showing the results listed in Table D-10. Friction angles for the tests in each hydration period were determined from regression analysis forced through the origin (i.e. assuming no cohesion) and are listed in Table D-11. The results indicate that lengths of hydration between 24 and 153 hrs have little effect on the measured internal shear strength of unreinforced GCLs at normal stresses of 17 and 172 kPa.

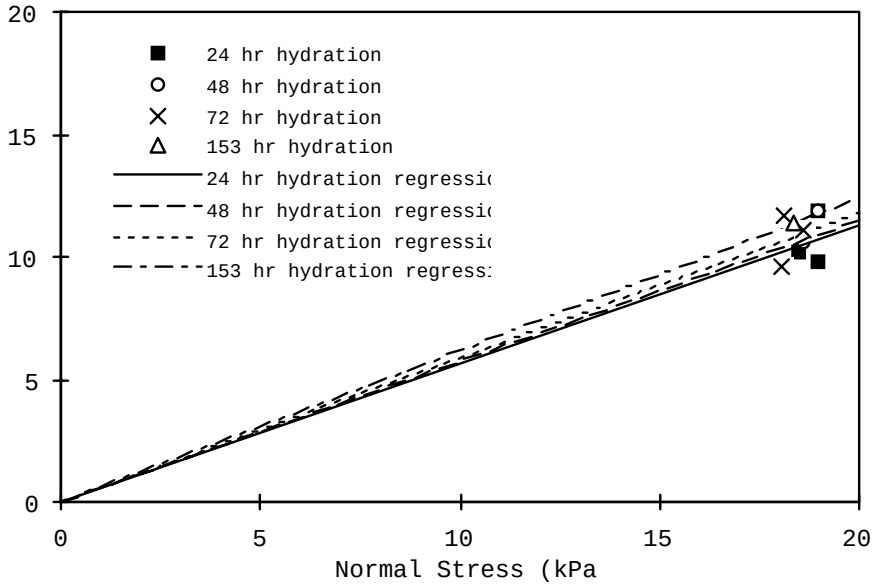

Figure D-37. Mohr-Coulomb diagram for GCLs hydrated for various durations.

Table D-11. Friction Angles of GCLs Hydrated for Various Durations.

Hydration Time (hr)	Number of Tests	Friction Angle (degrees)
24	3	29.5
48	3	30.0
72	3	30.5
153	1	31.7

D-7.5.2. Effect of Shear Rate and Normal Stress. Table D-12 lists the adjusted peak shear stress and the displacement at peak stress from direct shear tests on GCL

specimens after being sheared at rates of 1, 0.1, 0.02, 0.0025, and 0.0005 while under 17 kPa normal stress. Table D-13 lists the adjusted peak shear stress and the displacement at peak stress from direct shear tests on GCL specimens after being sheared at rates of 1, 0.024, and 0.0005 while under 170 kPa normal stress. The average, standard deviation, and coefficient of variation for peak stress and peak displacement are listed for each series of tests. Figure D-38 shows the ratio of peak strength to normal stress versus shear rate for tests conducted with 17 and 172 kPa normal stress. Table D-14 summarizes the results.

Results from the shear tests indicate that at both normal stresses, the shear strength decreases as the shear rate decreases. It appears that only after the shear rate has decreased below 0.01 to 0.0001 mm/min does the shear strength become constant. The friction angle for each group of tests (at a particular shear rate and normal stress) was determined by forcing a failure envelope through a Mohr-Coulomb diagram of the shear results where the envelope was forced through the origin. The results show that as the shear rate decreases, the friction angle decreases. At 17 kPa normal stress, the friction angle is 29.5 for shear rates of 1 mm/min and decreases to less than 22 degrees for shear rates below 0.0025 mm/min. At 172 kPa normal stress, the friction angle is 15.7 degrees for shear rates of 1 mm/min and decreases to less than 13 degrees below shear rates of 0.024 mm/min.

Results from the shear tests also indicate that the shear strength increases as normal stress increases. However, both the ratio of peak shear stress to normal stress and the friction angle decrease as the normal stress increases.

D.7.6 *One-Dimensional Consolidation Test*

The purpose of performing a consolidation test was to verify appropriate shearing rates determined from the direct shear tests of hydrated unreinforced GCLs specimens. The results from the direct shear tests (discussed in the previous section) indicate that when the GCL is sheared slower than 0.01 to 0.001 mm/min at normal stresses of 17 to 170 kPa, the measured shear strength will be independent of the shearing rate. A one-dimensional consolidation test was performed on a specimen of Claymax 200R to determine the estimated time to failure for normal stresses close to 17 and 170 kPa.

The consolidation test was performed in a Wykeham Farrance loading frame in a fixed-ring consolidation cell. The diameter of the cell was 64 mm.

The specimen for the consolidation test was obtained from the same sheet of Claymax 200R used in the direct shear specimens testing. The specimen was trimmed to minimize escape of bentonite from the GCL. The initial height of the specimen was measured, and then the specimen was placed in the consolidation cell in the as-received condition.

Table D-12. Results for GCLs Sheared at Various Rates under 17 kPa Normal Stress.

Test No.	Shear Rate (mm/min)	Normal Stress (kPa)	Hydration Period (hr)	Peak Shear Strength (kPa)	Displ. at Peak Strength (mm)
1	1	17	24	10.2	3.2
2	1	17	24	11.9	4.3
3	1	17	24	9.8	4.3
Average				10.6	3.9
Standard Deviation				1.1	0.7
Coefficient of Variation				0.11	0.17
14	0.1	17	24	10.3	2.5
15	0.1	17	24	11.9	3.4
19	0.1	17	24	12.1	3.3
Average				11.5	3.1
Standard Deviation				1.0	0.5
Coefficient of Variation				0.09	0.16
20	0.02	17	24	9.5	2.8
21	0.02	17	24	8.1	3.5
22	0.02	17	24	9.0	3.1
Average				8.9	3.1
Standard Deviation				0.7	0.4
Coefficient of Variation				0.08	0.11
24	0.0025	17	24	6.7	3.4
25	0.0025	17	24	7.2	3.4
26	0.0025	17	24	6.6	2.8
Average				6.8	3.2
Standard Deviation				0.3	0.4
Coefficient of Variation				0.04	0.11
27	0.0005	17	24	7.9	2.4
29	0.0005	17	24	6.6	2.4
Average				7.2	2.4
Standard Deviation				0.9	0.05
Coefficient of Variation				0.13	0.02

* peak shear stress is adjusted for machine friction

Table D-13. Results for Various Rates and GCLs under 170 kPa Normal Stress.

Test No.	Shear Rate (mm/min)	Normal Stress (kPa)	Hydration Period (hr)	Peak Shear Strength (kPa)	Displ. at Peak Shear Strength (mm)
37	1	172	24	50.7	2.8
38	1	172	24	59.1	4.1
Average				54.9	3.4
Standard. Deviation				6.0	0.9
Coefficient of Variation				0.11	0.26
32	0.024	172	24	43.8	2.3
36	0.024	172	24	38.7	2.1
Average				41.2	2.2
Standard. Deviation				3.6	0.2
Coefficient of Variation				0.09	0.07
28	0.0005	172	24	46.2	2.3
30	0.0005	172	24	38.9	4.2
Average				42.5	3.2
Standard. Deviation				5.2	1.4
Coefficient of Variation				0.12	0.4

* peak shear stress is adjusted for machine friction

Table D-14. Effect of Normal Stress and Shear Rate on Friction Angle.

Shear Rate (mm/min)	Number of Tests	Friction Angle (degrees)
Normal Stress = 17 kPa		
1	3	29.5
0.1	3	31.9
0.02	3	25.6
0.0025	3	20.3
0.0005	2	21.6
Normal Stress = 170 kPa		
1	2	15.7
0.024	2	12.9
0.0005	2	13.0

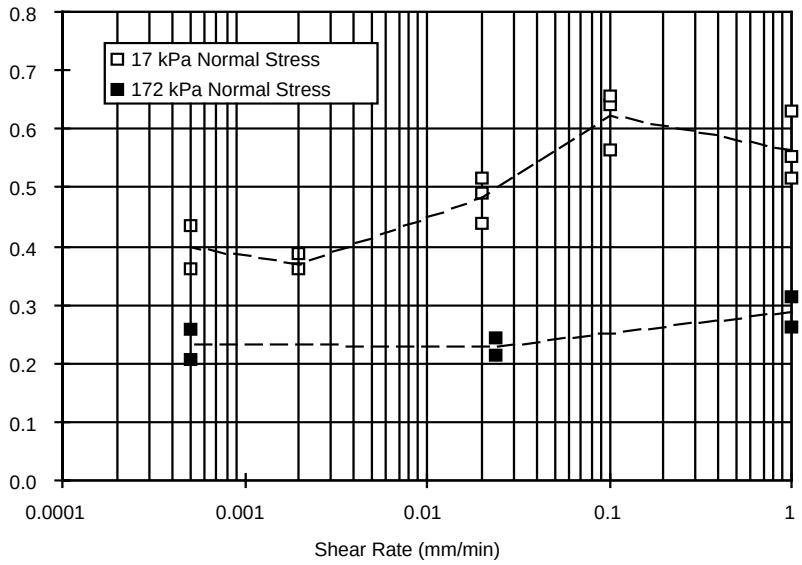

Figure D-38. Effect of Normal Stress and Shear Rate on Shear Strength.

The consolidation test was performed according to ASTM D2435. A seating load of 11 kPa was applied, and water was introduced in to the consolidation cell. The specimen was allowed to hydrate under 11 kPa normal stress until the swelling ceased or until the height of the specimen became constant. After hydration, the first load was applied. Subsequent loads were applied after the specimen had passed primary consolidation, which was longer than 24 hours in most cases. Loads were applied to a maximum of 307 kPa using a load-increment ratio of 2. Then, the specimen was unloaded using a load increment ratio of 4.

The hydration curve of the GCL in the consolidation test is shown in Figure D-39. The test lasted 48 days. Also shown in Figure D-39 are hydration curves of several GCL specimens tested in the direct shear tests. The consolidation specimen swelled from an initial thickness of 4.7 mm to a thickness of 14.6 mm under a seating load of 11 kPa. The hydrated thickness of the consolidation specimen was greater than all of the hydrated thicknesses of the direct shear specimens. However, the GCL in direct shear Test No. 7 swelled close to 12 mm. The difference in hydrated thicknesses of the consolidation and direct shear specimens may have occurred because of different hydration conditions. First, the direct shear specimens were all hydrated under 17 kPa normal stress, whereas the consolidation specimen was hydrated under 11 kPa normal stress. However, the interpolated (between load increments of 11 kPa and 20 kPa) hydrated thickness of the GCL at 17 kPa was 14.2 mm. Therefore, the difference in normal stress between 11 kPa and 17 kPa might not be a factor in the differences in

hydration thicknesses of the consolidation specimen and shear specimens. Second, most of the direct shear specimens were hydrated for only 24 hours (only seven were hydrated for durations of 2 to 7 days), whereas the consolidation specimen was allowed to hydrate for 48 days.

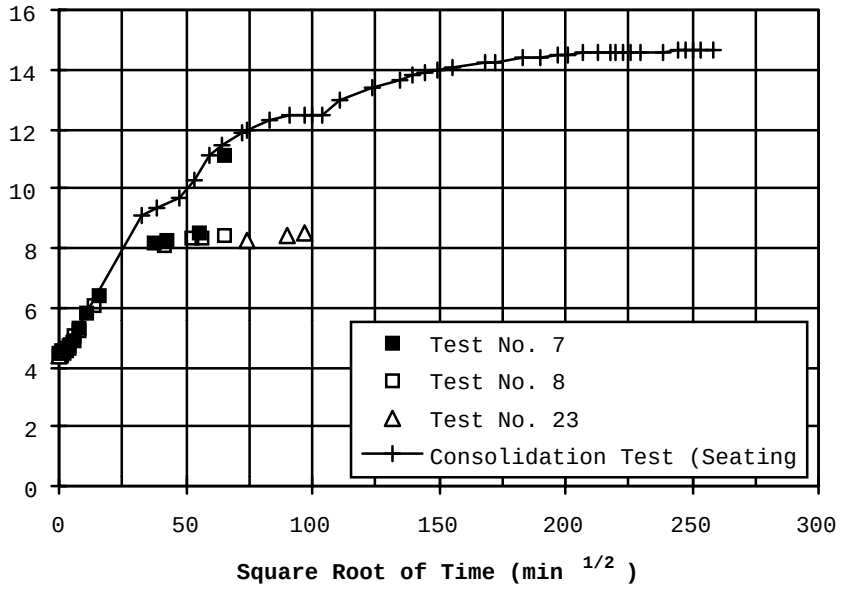

Figure D-39. Hydration curves for Claymax 200R.

The height of the specimen corresponding to the end of primary consolidation and end of loading increment was determined using the square root of time method. The end of primary consolidation height and end of loading increment heights are shown in the consolidation curve in Figure D-40.

The minimum time to failure, t_f, required for a consolidated-drained direct shear test, according to Gibson and Henkel (1954) and Terzaghi's theory of consolidation, is:

$$t_f = \frac{H^2}{2c_v(1 - U_f)} \qquad \text{(D.2)}$$

If the coefficient of consolidation, c_v , which is given by:

$$c_v = \frac{0.197H_c^{\,2}}{t_{50}} \qquad \text{(D.3)}$$

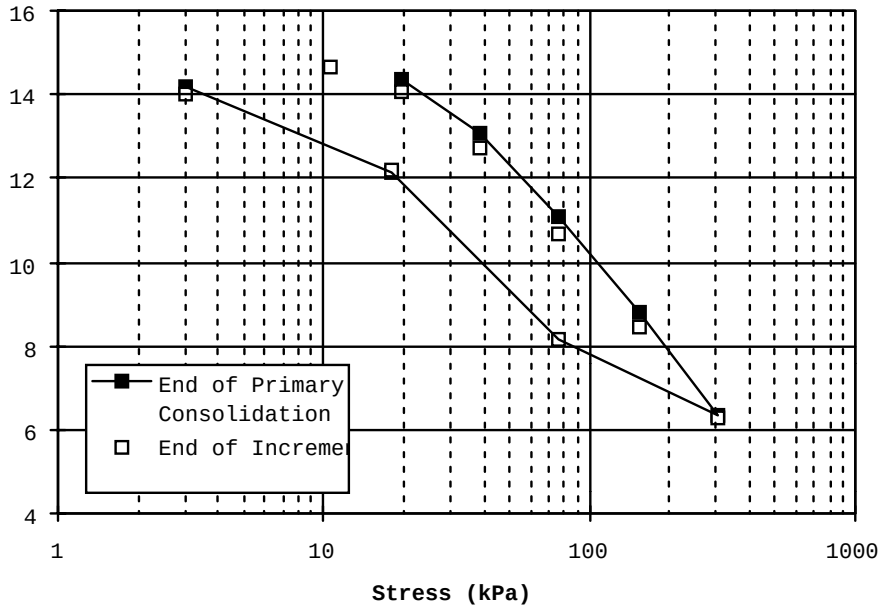

Figure D-40. Consolidation curve of Claymax 200R.

is substituted in equation D.2, where H_c is the average drainage distance during consolidation (or half the specimen height) and t_{50} is the time required for 50% consolidation, then equation D.3 becomes:

$$t_f = \frac{H_d^{\,2}}{(2)(.197)(H_c^{\,2})(1-U_f)}\, t_{50} \qquad \text{(D.4)}$$

By assuming the thickness of the specimen is the same during consolidation and shear (H_c is equal to H_d), and U_f is equal to 95%, Equation D.4 reduces to:

$$t_f = 50 t_{50} \qquad \text{(D.5)}$$

Equation D.6 is the method specified in ASTM D3080 for determining the rate of shear.

The required times to failure were calculated based on Equation D.5 for each load increment of the consolidation test and are listed in Table D-15. Maximum allowable shear rates in a consolidated drained direct shear test were calculated assuming a

displacement at failure of 2 mm. Based on times to failure calculated from consolidation results, consolidated-drained shear tests with normal stresses of 17 kPa require a shear rates less than .001 mm/min, and shear tests with normal stresses of 154 kPa require shear rates less than .0002 mm/min. The maximum shear rates that were determined from the consolidation test at normal stresses of 17 kPa and 154 kPa are consistent with the maximum shear rates determined from the direct shear tests at similar normal stresses.

Table D-15. Maximum Shear Rates.

Stress (kPa)	t_{50} (min)	Estimated Time to Failure, t_f (min)	Maximum Shear Rate (mm/min)
19.7	36	1800	0.001
38.3	132	6600	0.0003
77	149	7450	0.0003
154	210	10500	0.0002
307	272	13600	0.0001

D-8 References

Daniel, D.E., Shan, H.Y., and Anderson, J.D. (1993), "Effects of Partial Wetting on the Performance of the Bentonite Component of a Geosynthetic Clay Liner," *Geosynthetics '93,* Industrial Fabrics Association International, St. Paul, Minnesota, 3: 1483-1496.

Estornell, P. M. and Daniel, D. E. (1992), “Hydraulic Conductivity of Three Geosynthetic Clay Liners,” *Journal of Geotechnical Engineering*, 118 (10): 1592-1606.

Gibson, R.E., and Henkel, D.J. (1954), “Influence of Duration of Tests at Constant Rate of Strain on Measured ‘Drained’ Strength,” *Geotechnique*, 4: 6-15.

Shan, H.Y. (1993), “Stability of Final Covers Placed on Slopes Containing Geosynthetic Clay Liners,” Ph.D. Dissertation, Univ. of Texas, Austin, TX, 296 p.

Appendix D

Attachment 1

Results of Laboratory Direct Shear Tests on GCL Interfaces

(Tests Performed on 300 mm x 300 mm Samples in the Laboratories of the Geosynthetic Research Institute, Drexel University)

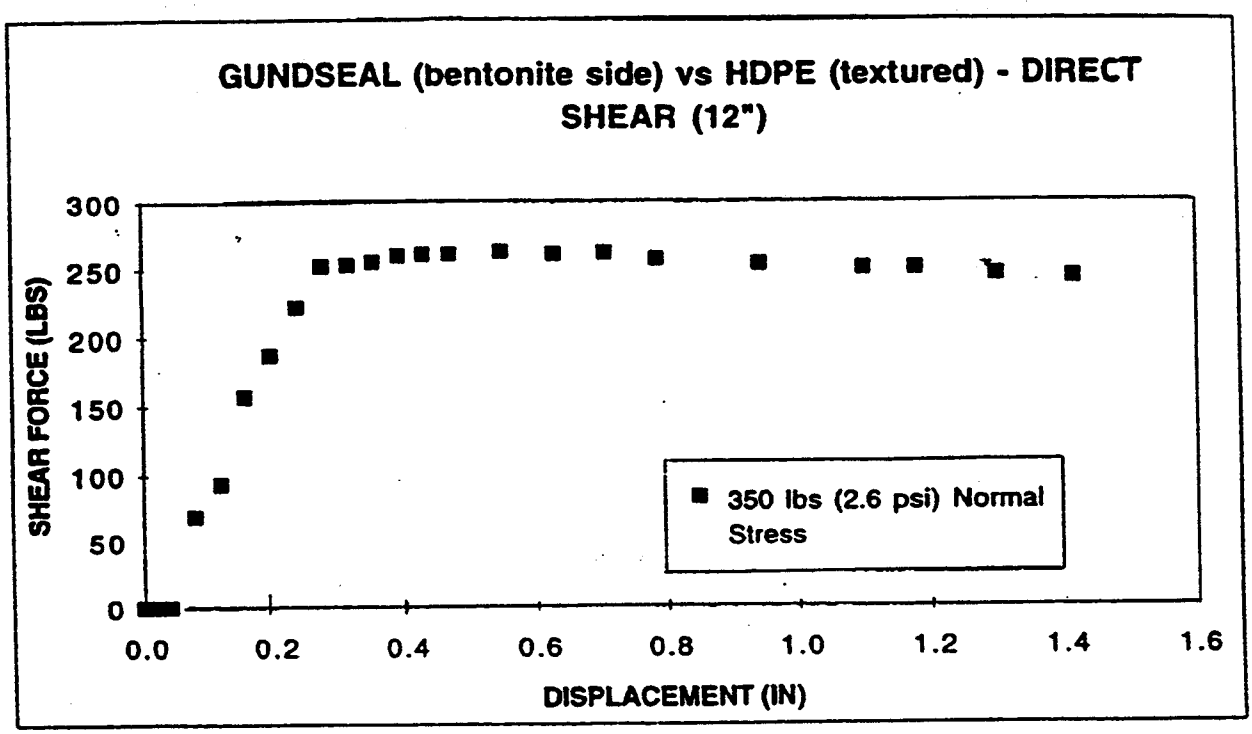
GUNDSEAL (bentonite side) vs HDPE (textured) - DIRECT SHEAR (12")
SHEAR FORCE (LBS)
300
250
200
150
100
50
0
0.0
0.2
0.4
0.6
0.8
1.0
1.2
1.4
1.6
DISPLACEMENT (IN)
350 lbs (2.6 psi) Normal Stress

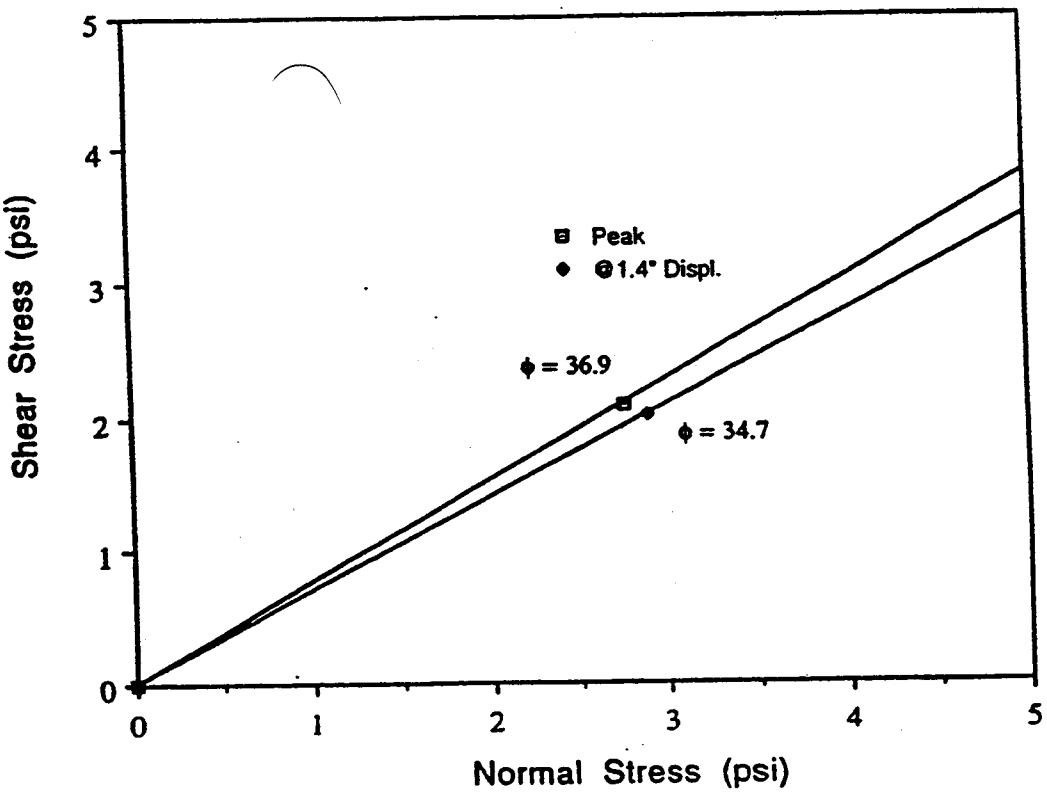
Shear Stress (psi)
5
4
3
2
1
0
0
1
2
3
4
5
Normal Stress (psi)
Peak
@1.4" Displ.
ϕ = 36.9
ϕ = 34.7

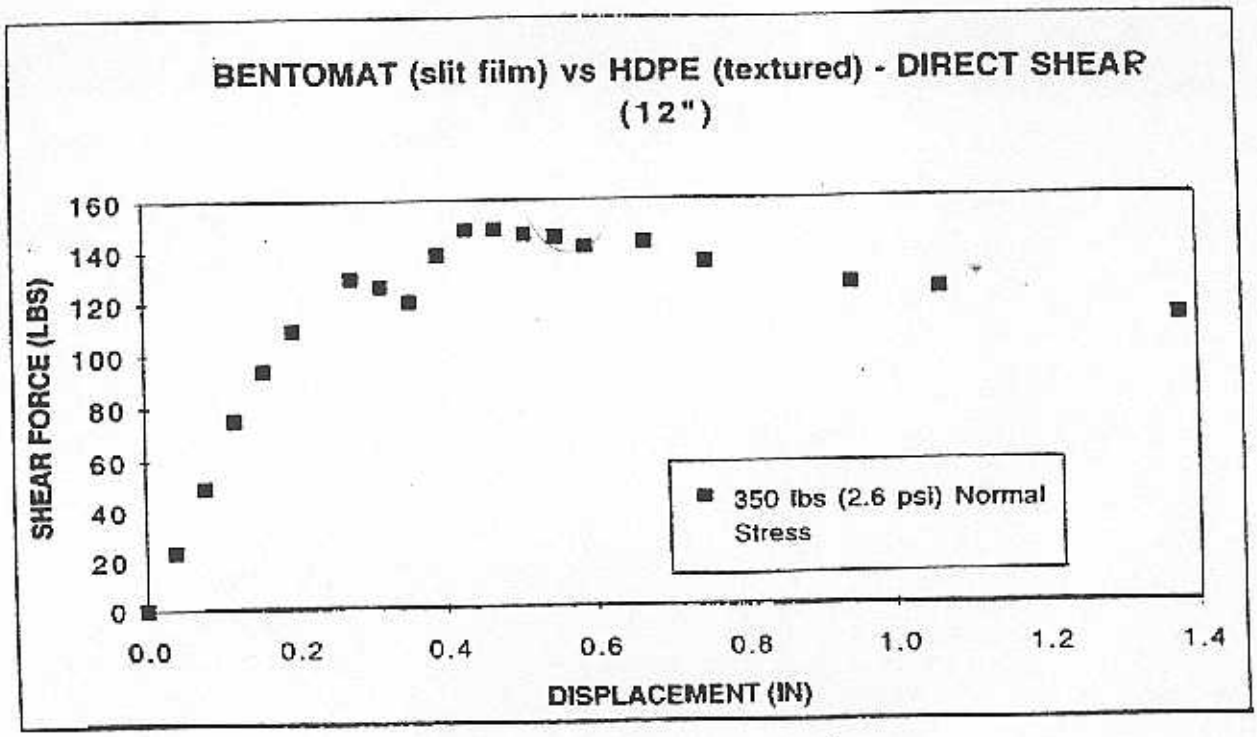
BENTOMAT (slit film) vs HDPE (textured) - DIRECT SHEAR
(12")
SHEAR FORCE (LBS)
160
140
120
100
80
60
40
20
0
0.0
0.2
0.4
0.6
0.8
1.0
1.2
1.4
DISPLACEMENT (IN)
350 lbs (2.6 psi) Normal Stress

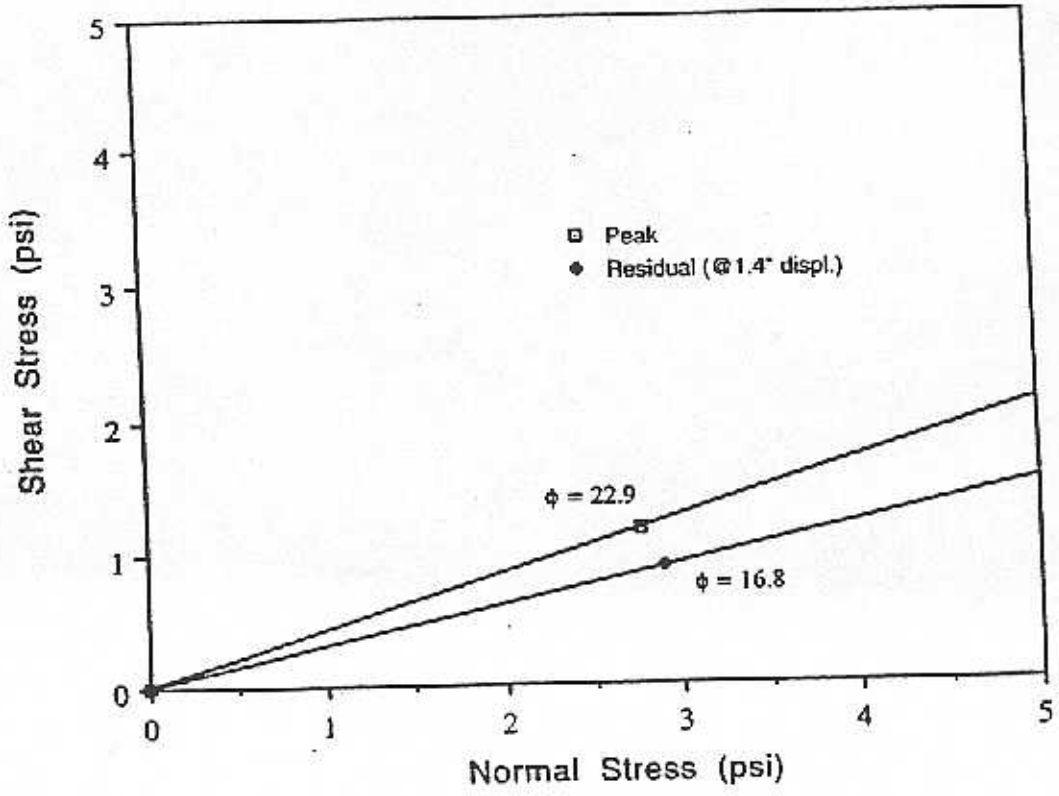
Shear Stress (psi)
5
4
3
2
1
0
0
1
2
3
4
5
Normal Stress (psi)
Peak
Residual (@1.4" displ.)
ϕ = 22.9
ϕ = 16.8

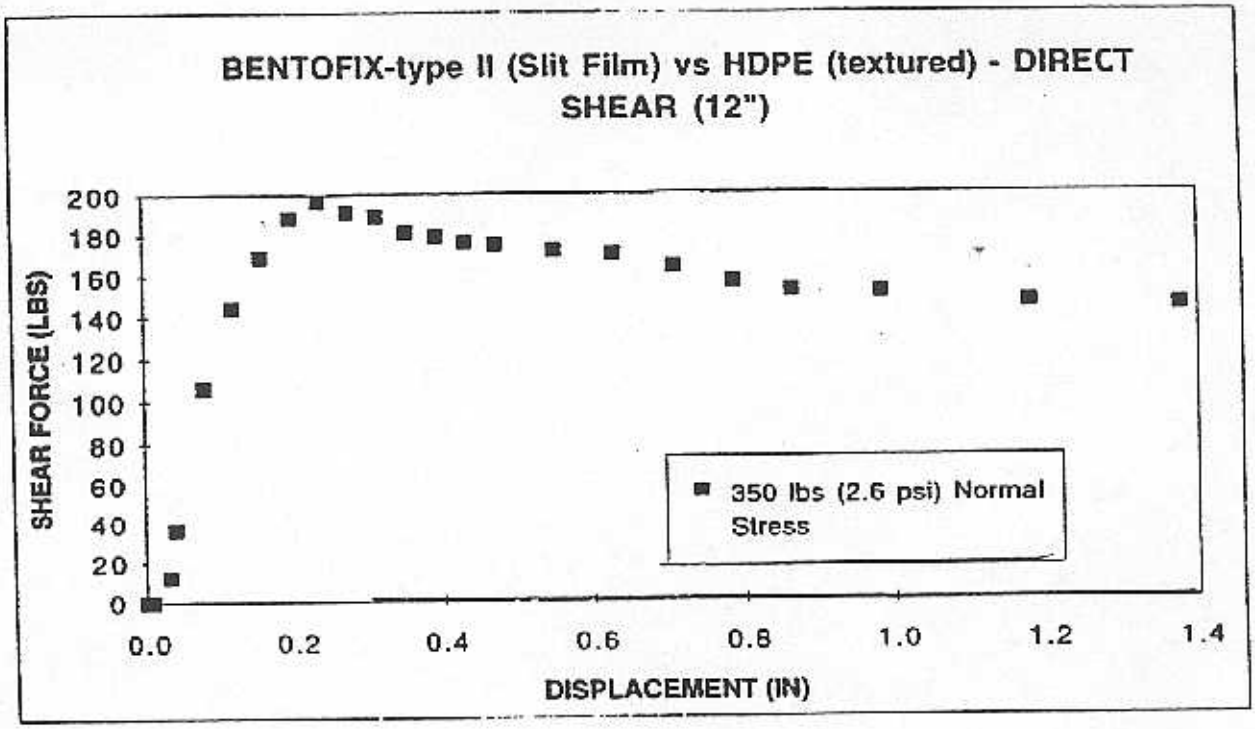
BENTOFIX-type II (Slit Film) vs HDPE (textured) - DIRECT SHEAR (12")
SHEAR FORCE (LBS)
200
180
160
140
120
100
80
60
40
20
0
0.0
0.2
0.4
0.6
0.8
1.0
1.2
1.4
DISPLACEMENT (IN)
350 lbs (2.6 psi) Normal Stress

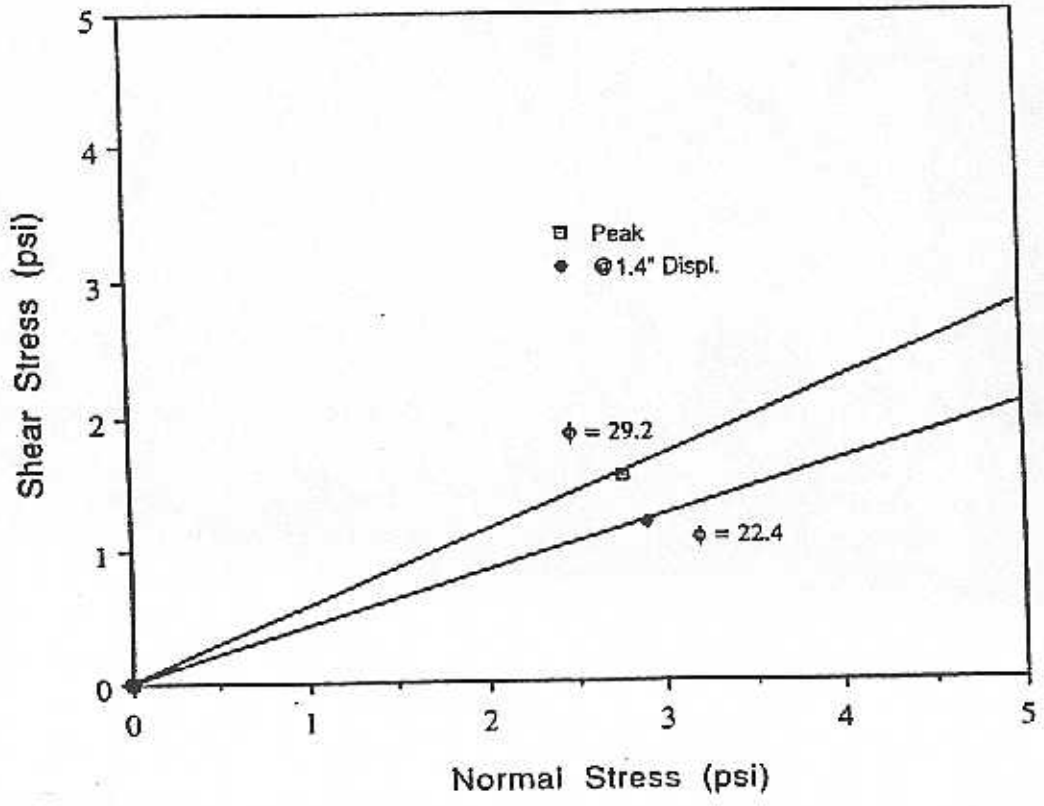
Shear Stress (psi)
5
4
3
2
1
0
0
1
2
3
4
5
Normal Stress (psi)
Peak
@1.4" Displ.
ϕ = 29.2
ϕ = 22.4

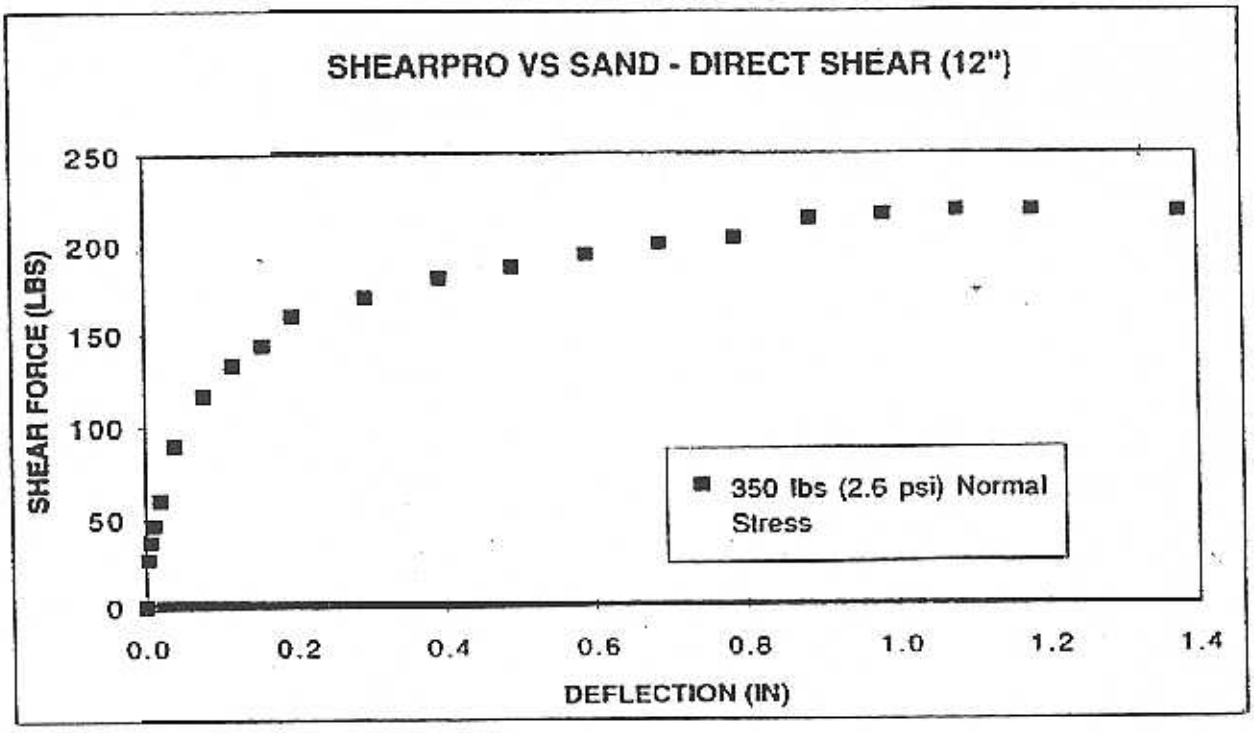
SHEARPRO VS SAND - DIRECT SHEAR (12")
SHEAR FORCE (LBS)
250
200
150
100
50
0
0.0
0.2
0.4
0.6
0.8
1.0
1.2
1.4
DEFLECTION (IN)
350 lbs (2.6 psi) Normal Stress

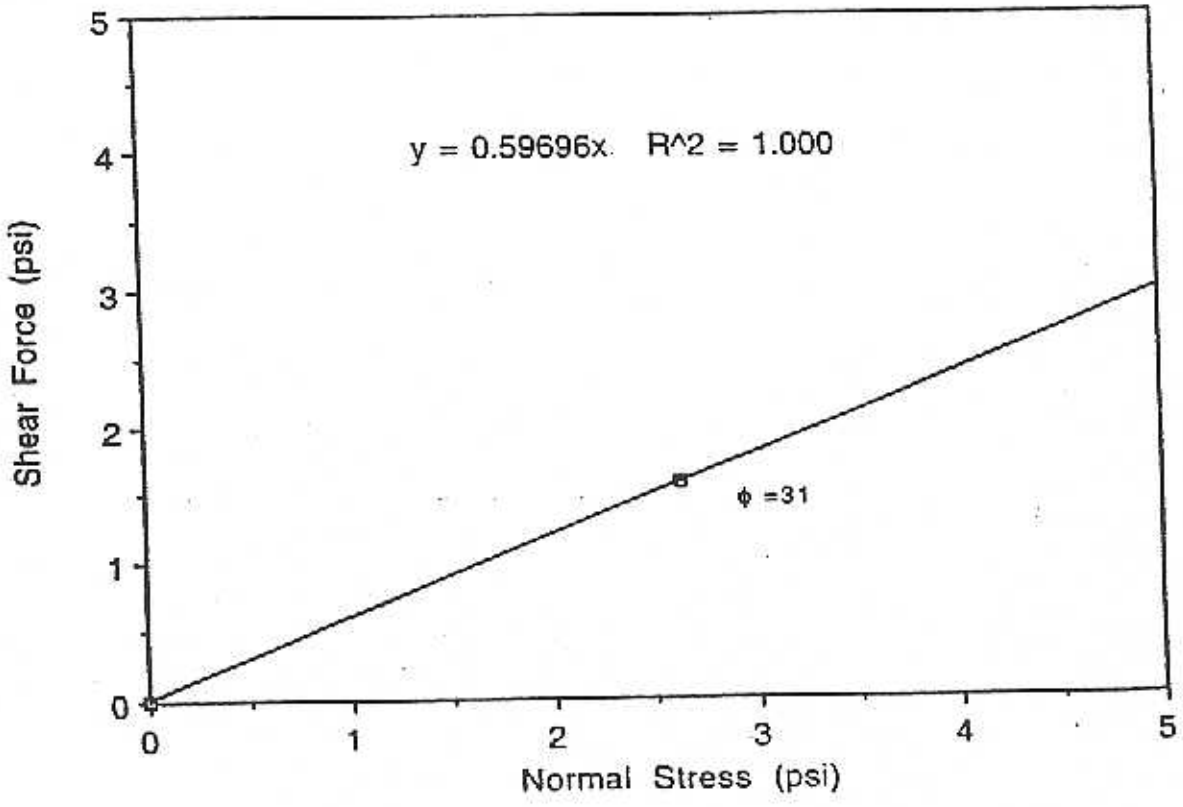
y = 0.59696x R^2 = 1.000
Shear Force (psi)
Normal Stress (psi)
ϕ =31
0
1
2
3
4
5

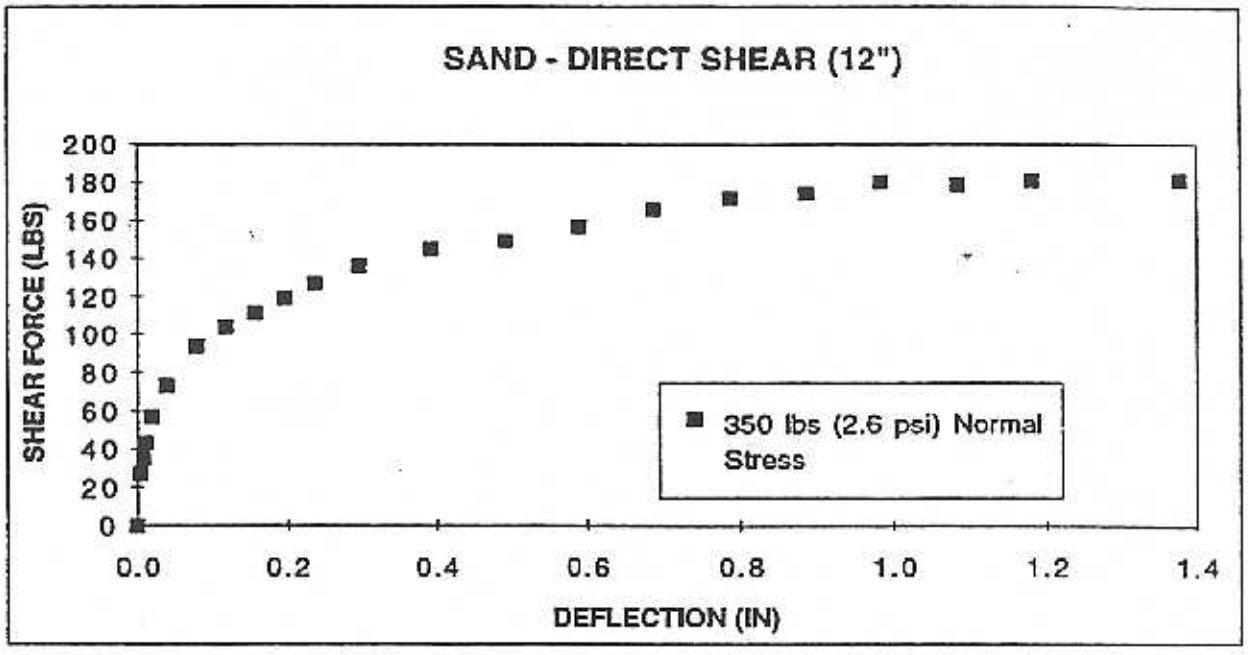
SAND - DIRECT SHEAR (12")
SHEAR FORCE (LBS)
200
180
160
140
120
100
80
60
40
20
0
0.0
0.2
0.4
0.6
0.8
1.0
1.2
1.4
DEFLECTION (IN)
350 lbs (2.6 psi) Normal Stress

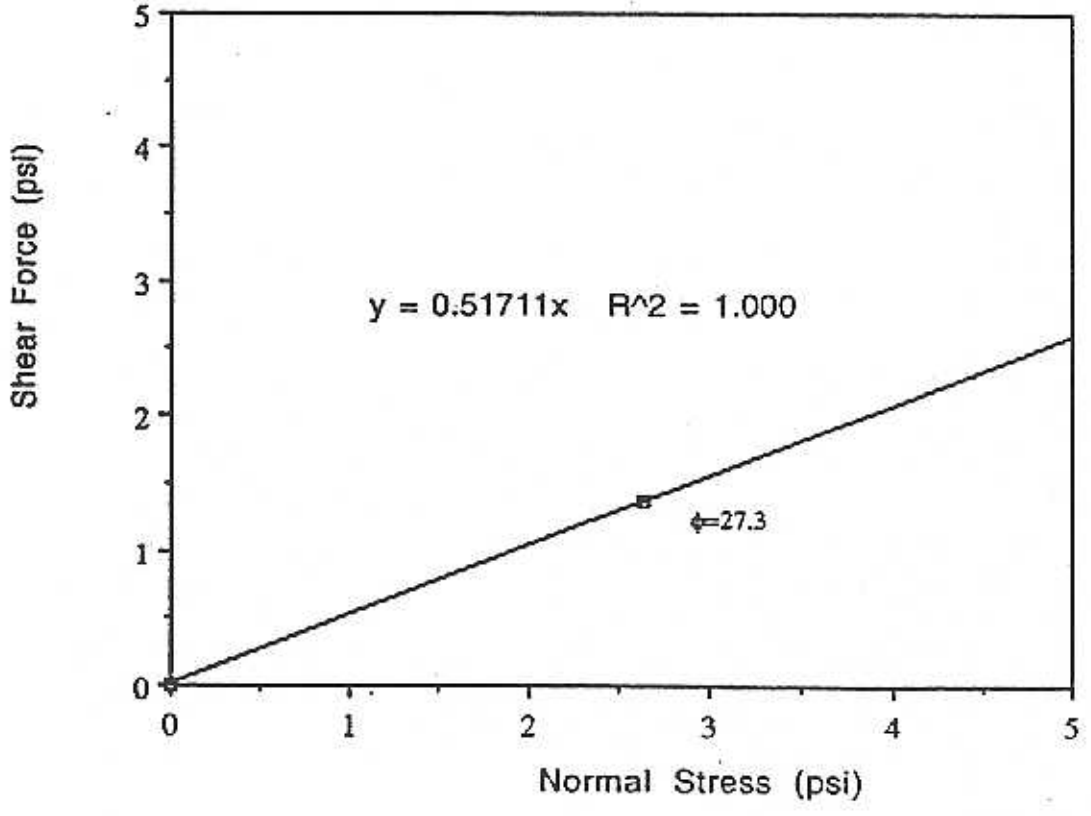
Shear Force (psi)
5
4
3
2
1
0
y = 0.51711x R^2 = 1.000
⇐27.3
0
1
2
3
4
5
Normal Stress (psi)

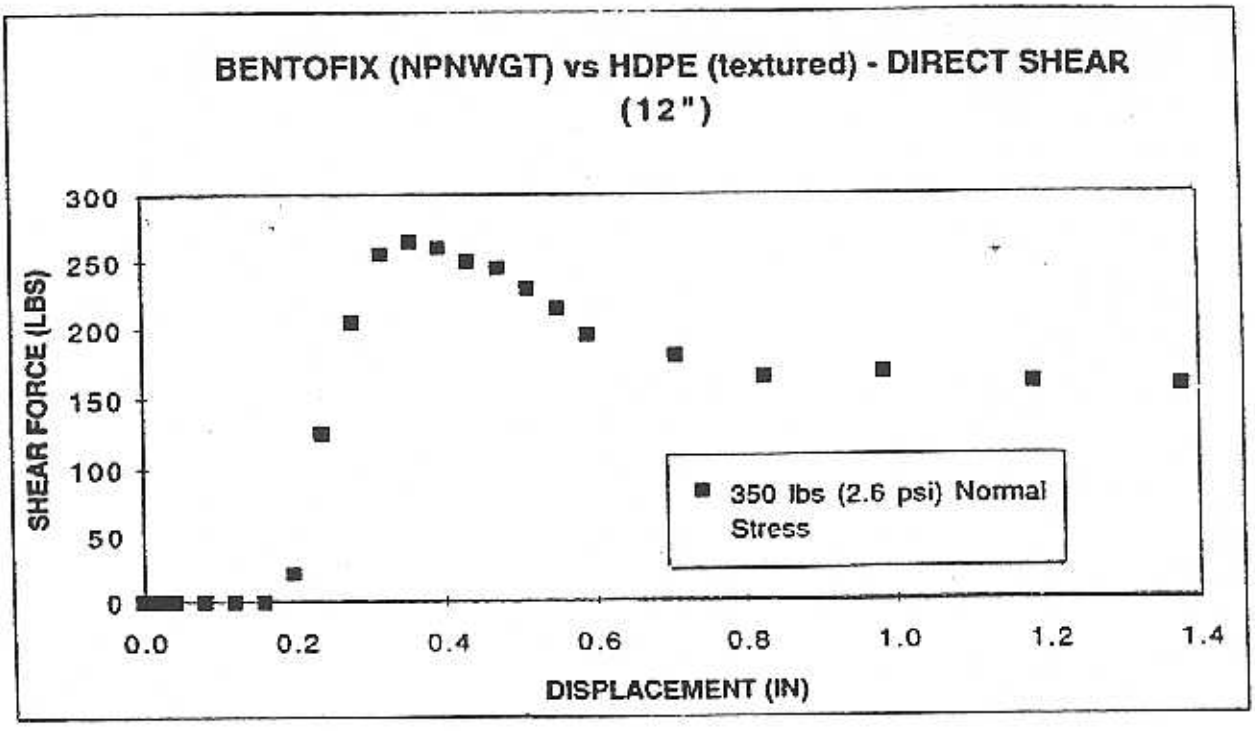
BENTOFIX (NPNWGT) vs HDPE (textured) - DIRECT SHEAR
(12")
SHEAR FORCE (LBS)
300
250
200
150
100
50
0
0.0
0.2
0.4
0.6
0.8
1.0
1.2
1.4
DISPLACEMENT (IN)
350 lbs (2.6 psi) Normal Stress

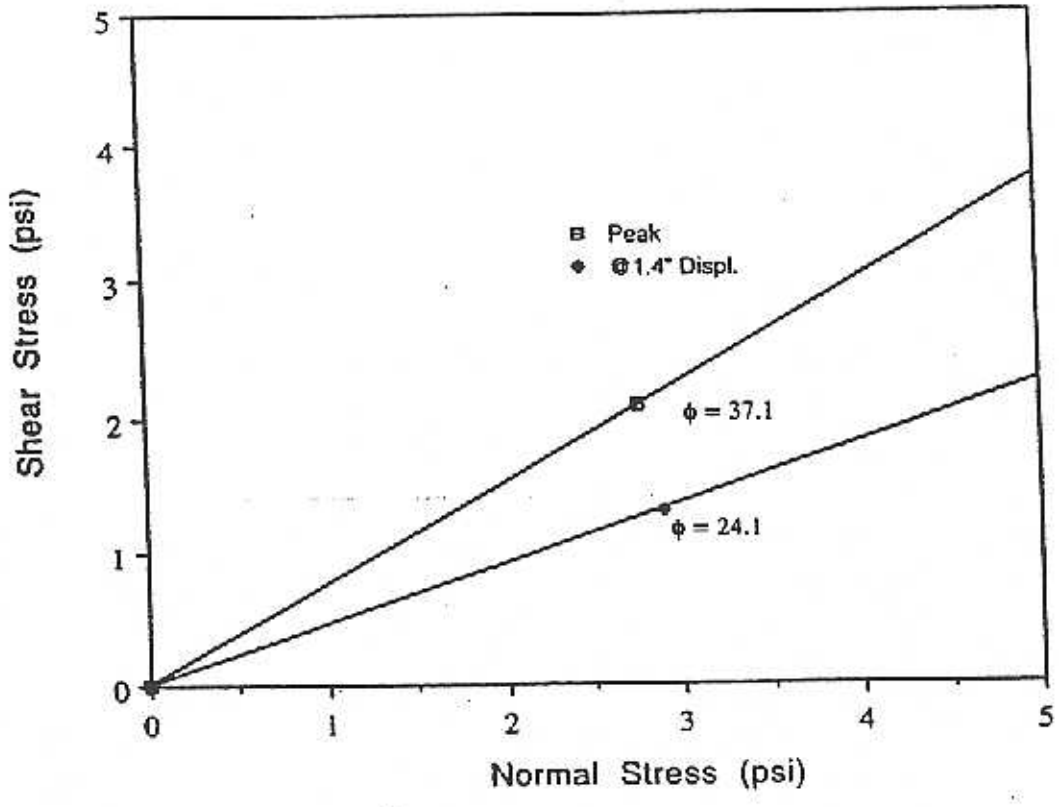
Shear Stress (psi)
5
4
3
2
1
0
0
1
2
3
4
5
Normal Stress (psi)
Peak
@1.4" Displ.
ϕ = 37.1
ϕ = 24.1

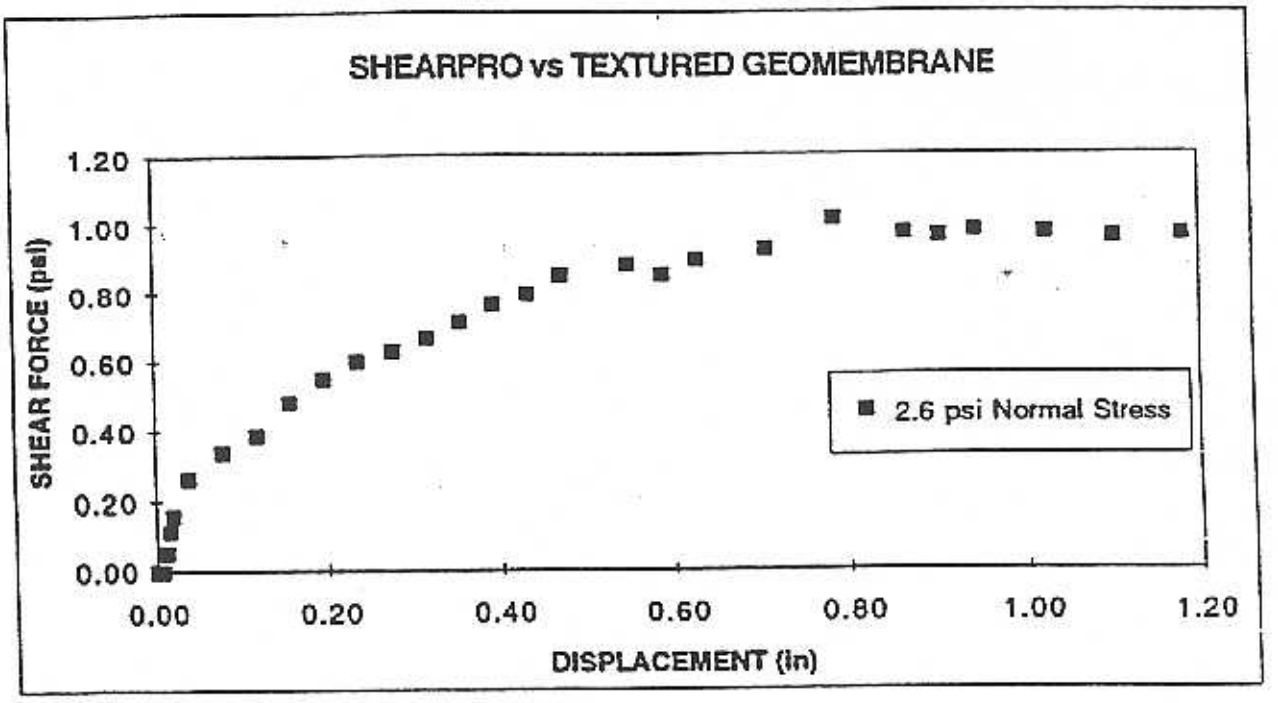
SHEARPRO vs TEXTURED GEOMEMBRANE
SHEAR FORCE (psi)
1.20
1.00
0.80
0.60
0.40
0.20
0.00
0.00
0.20
0.40
0.60
0.80
1.00
1.20
DISPLACEMENT (in)
2.6 psi Normal Stress

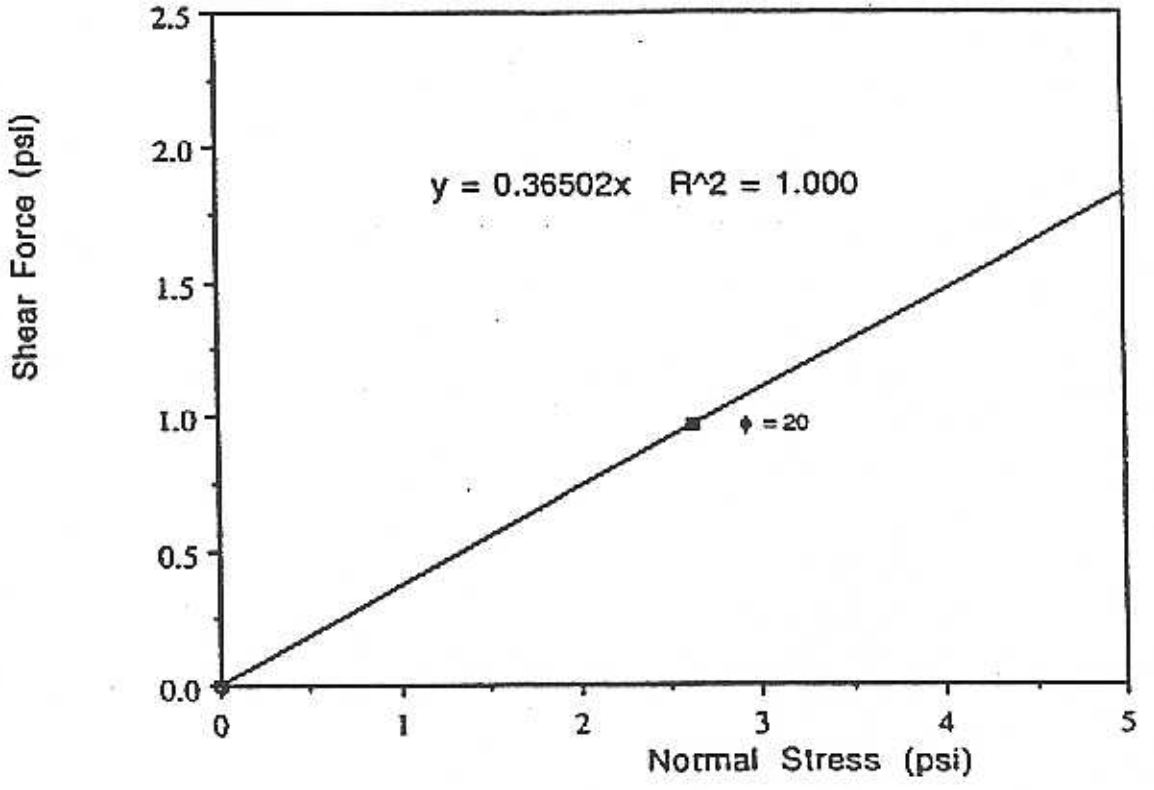
Shear Force (psi)
2.5
2.0
1.5
1.0
0.5
0.0
y = 0.36502x R^2 = 1.000
ϕ = 20
0
1
2
3
4
5
Normal Stress (psi)

Appendix D

Attachment 2

Plots of Total Down-Slope Displacements of GCLs Versus Time

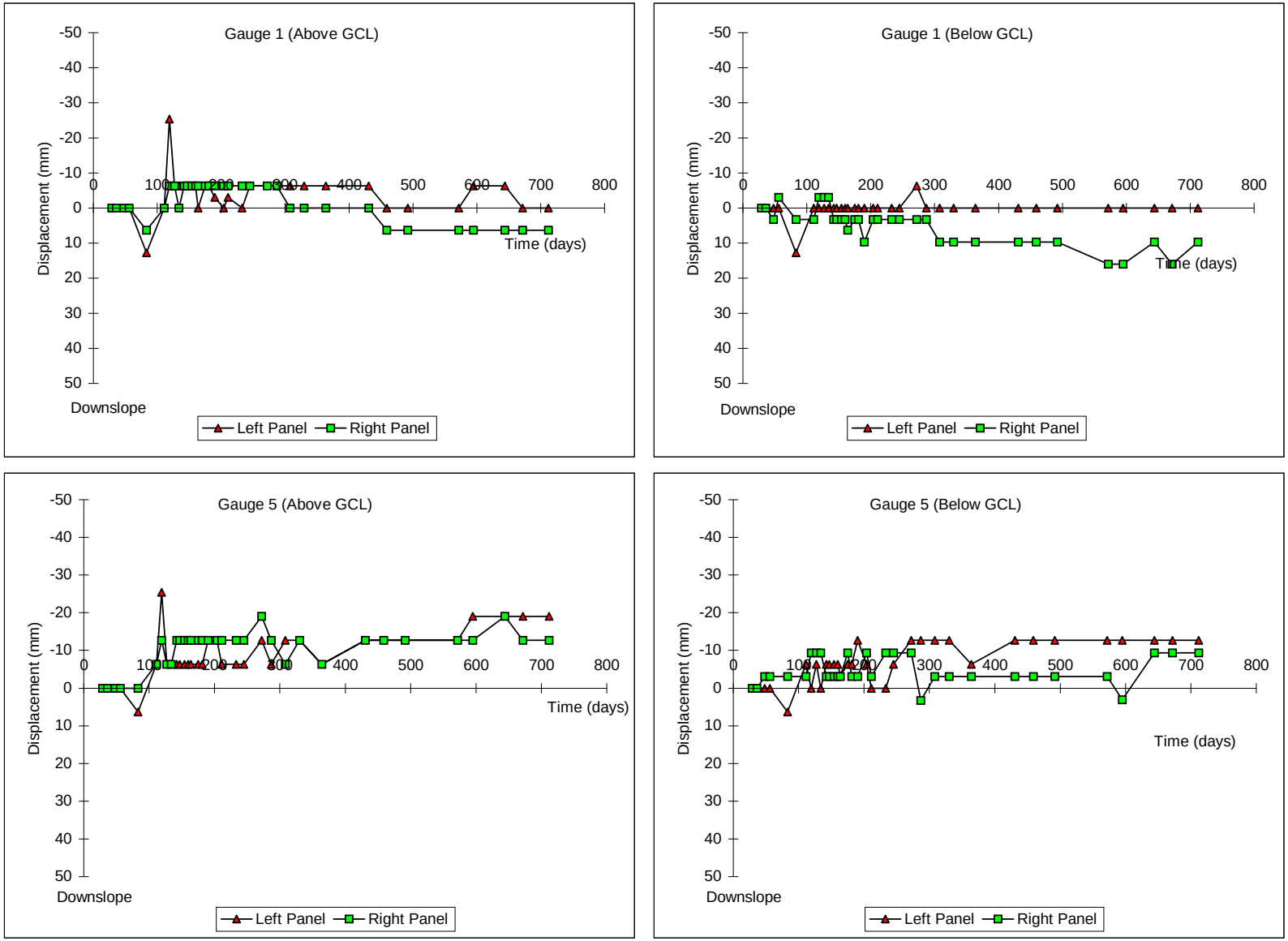

Figure A.1: POST-CONSTRUCTION DISPLACEMENT VS. TIME FOR PLOT A
(Gundseal - Bentonite Side Up - 3:1 Slope)

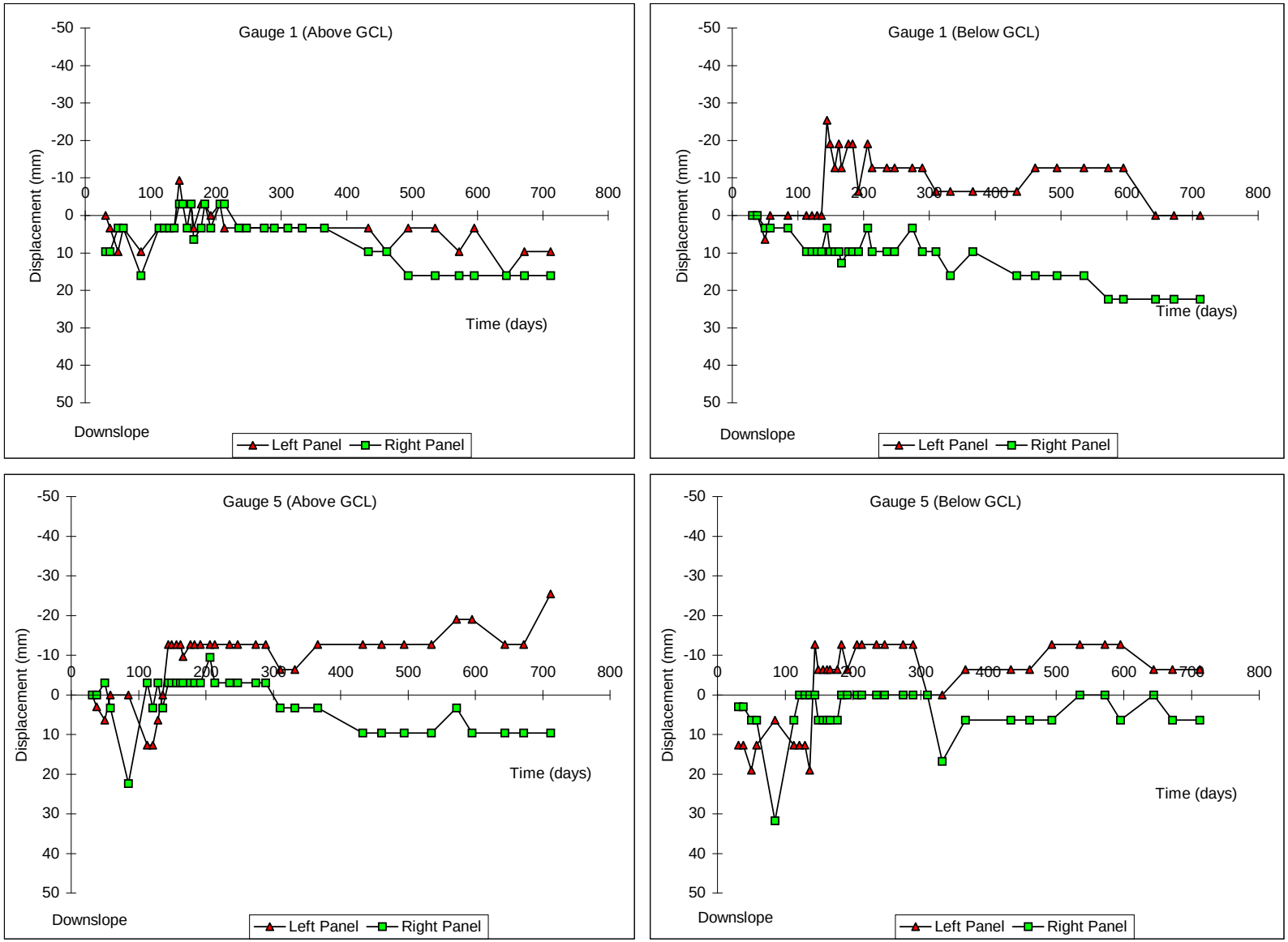

Figure A.2: POST-CONSTRUCTION DISPLACEMENT VS. TIME FOR PLOT B
(Bentomat - 3:1 Slope)

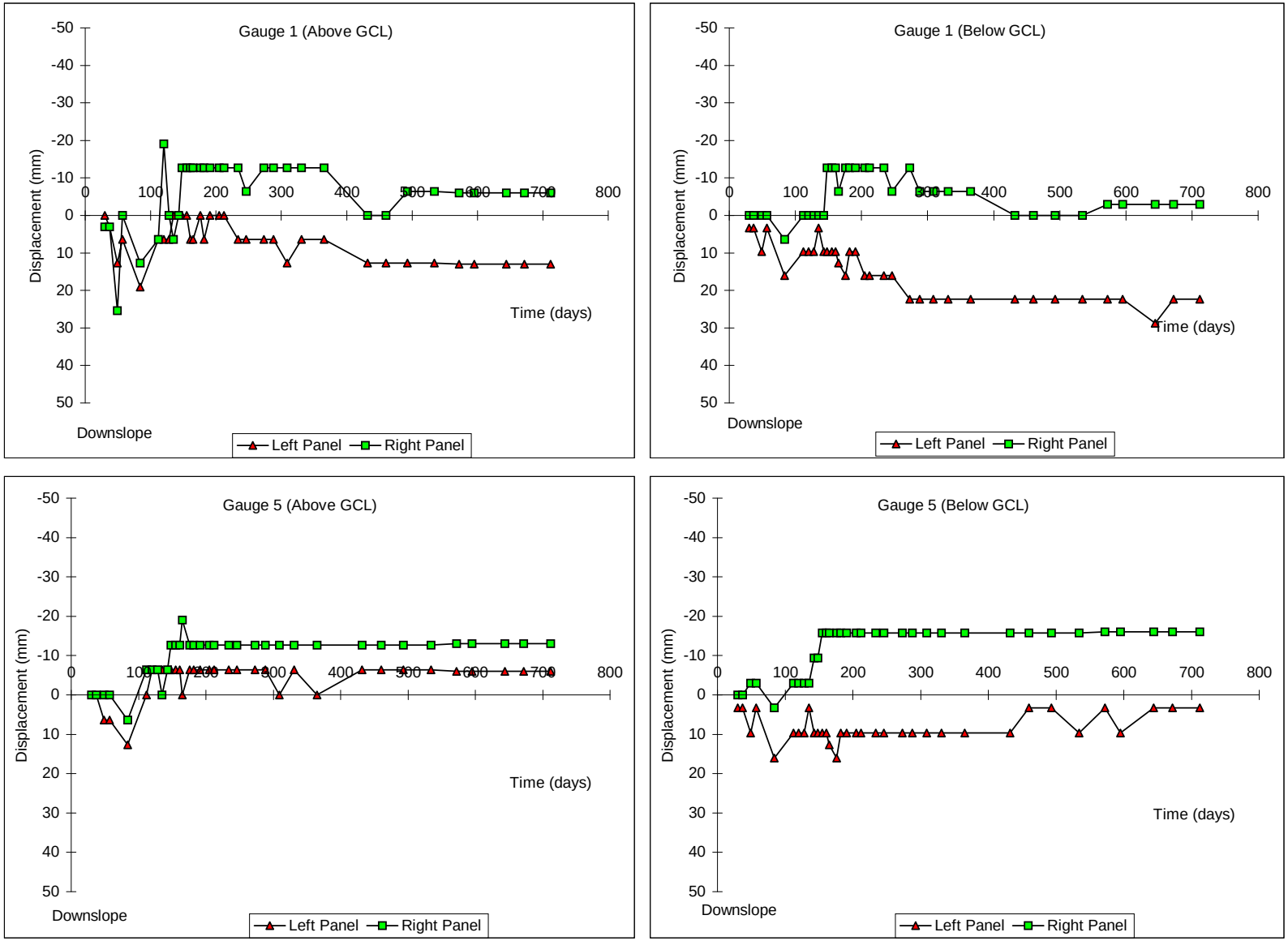

Figure A.3: POST-CONSTRUCTION DISPLACEMENT VS. TIME FOR PLOT C
(Claymax - 3:1 Slope)

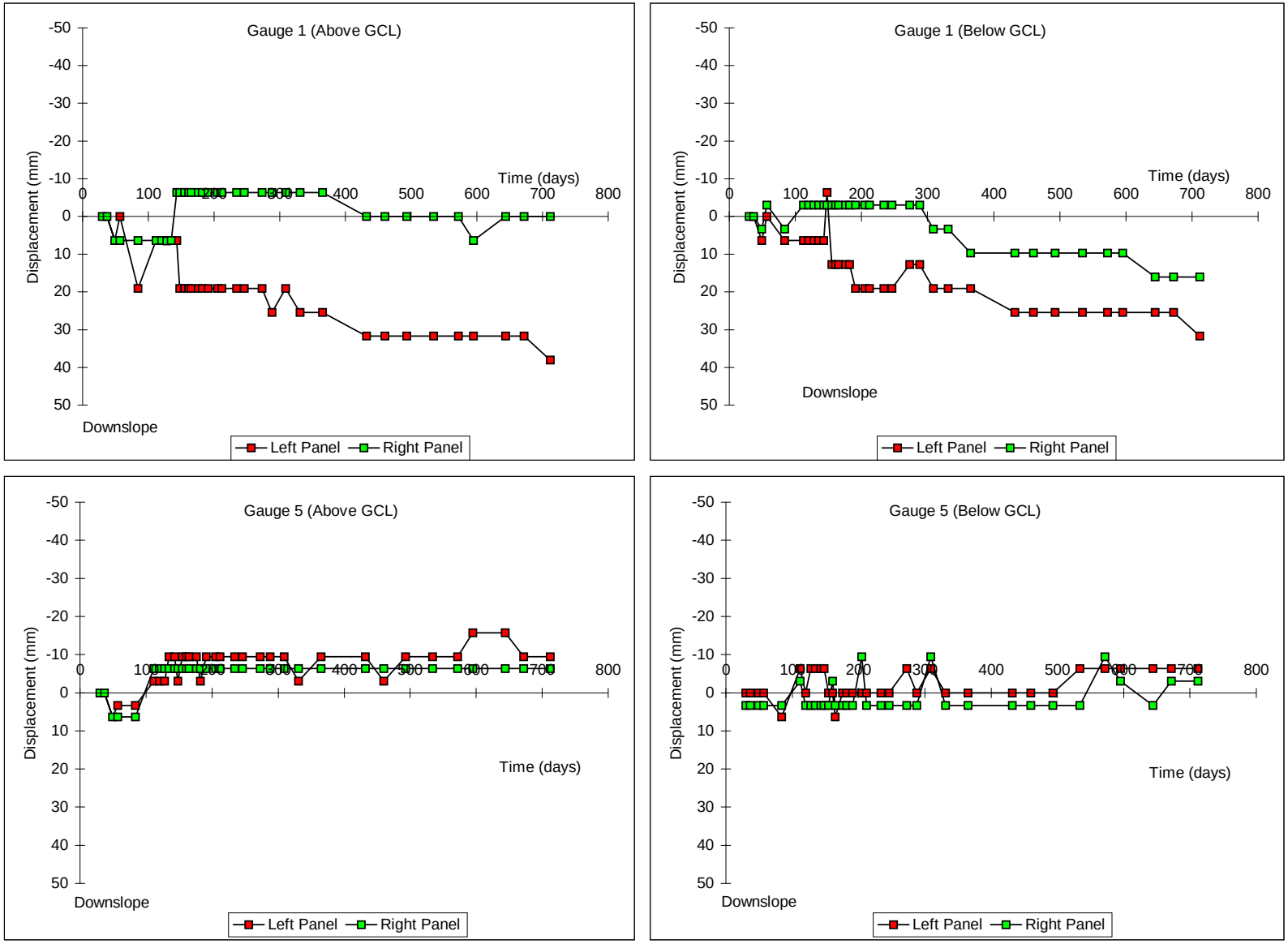

Figure A.4: POST-CONSTRUCTION DISPLACEMENT VS. TIME FOR PLOT D
(Bentofix II (NW up) - 3:1 Slope)

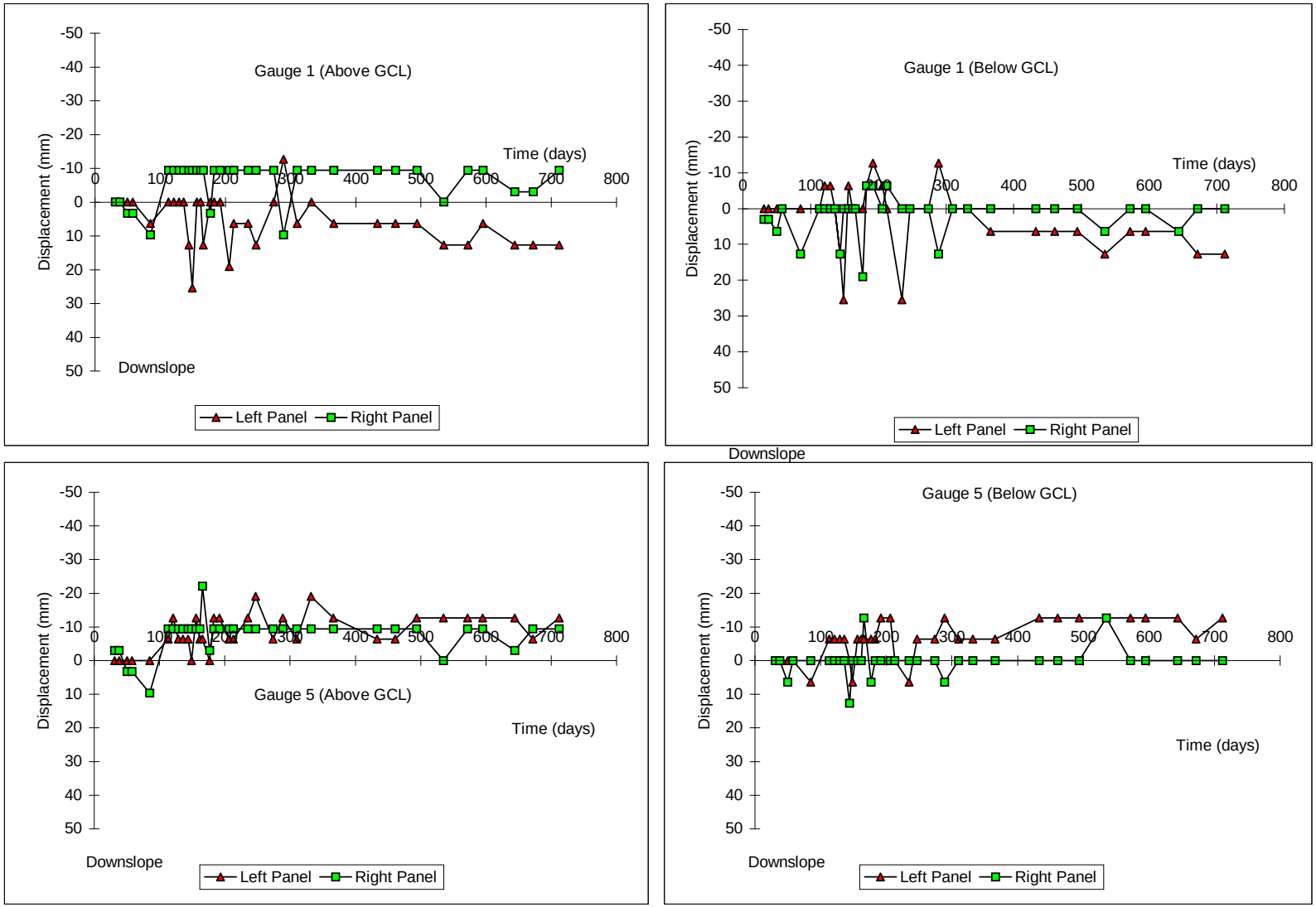

Figure A.5: POST-CONSTRUCTION DISPLACEMENT VS. TIME FOR PLOT E
(Gundseal - Bentonite Side Down - 3:1 Slope)

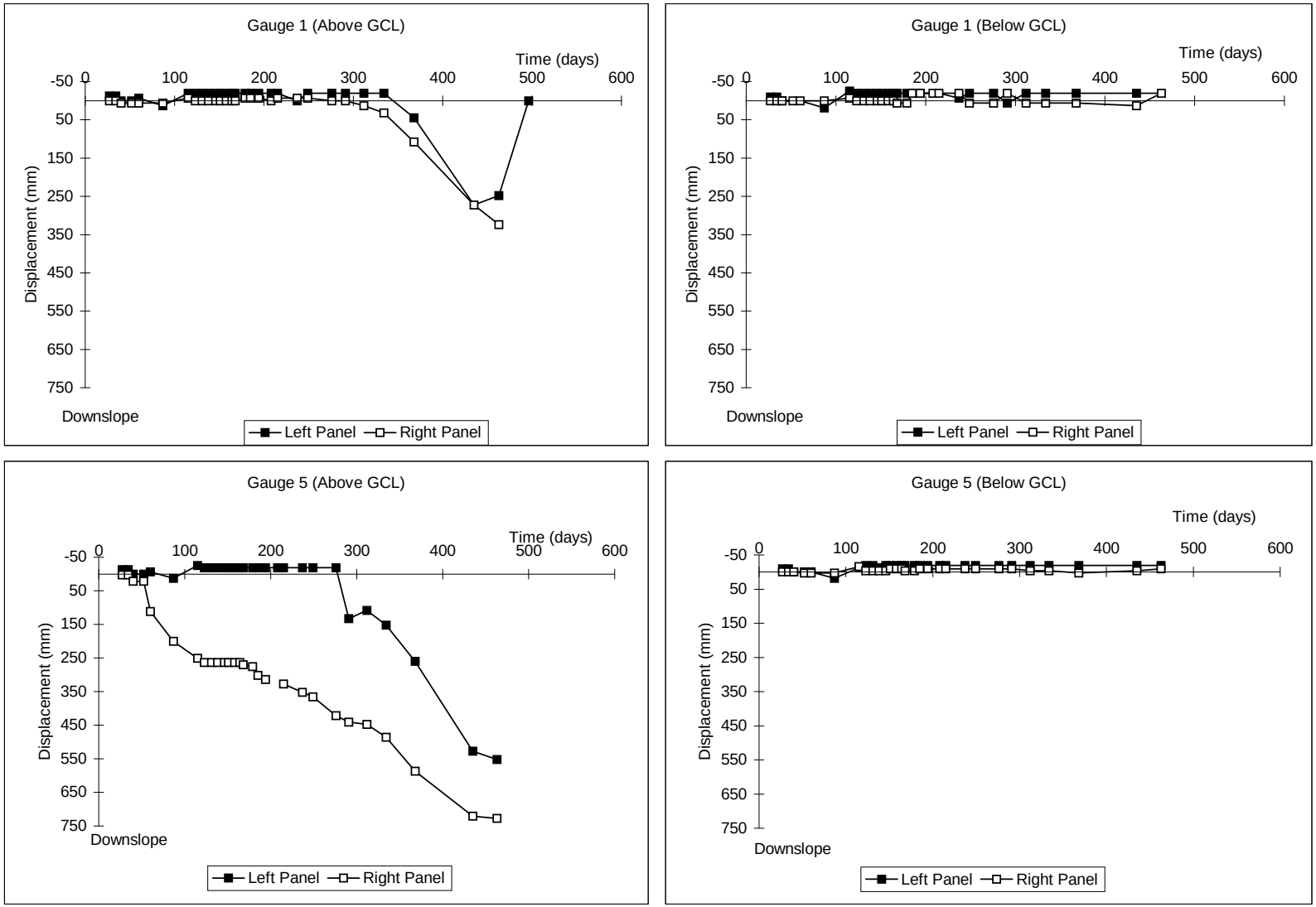

Figure A.6: POST-CONSTRUCTION DISPLACEMENT VS. TIME FOR PLOT F
(Gundseal - Bentonite Side Up - 2:1 Slope)

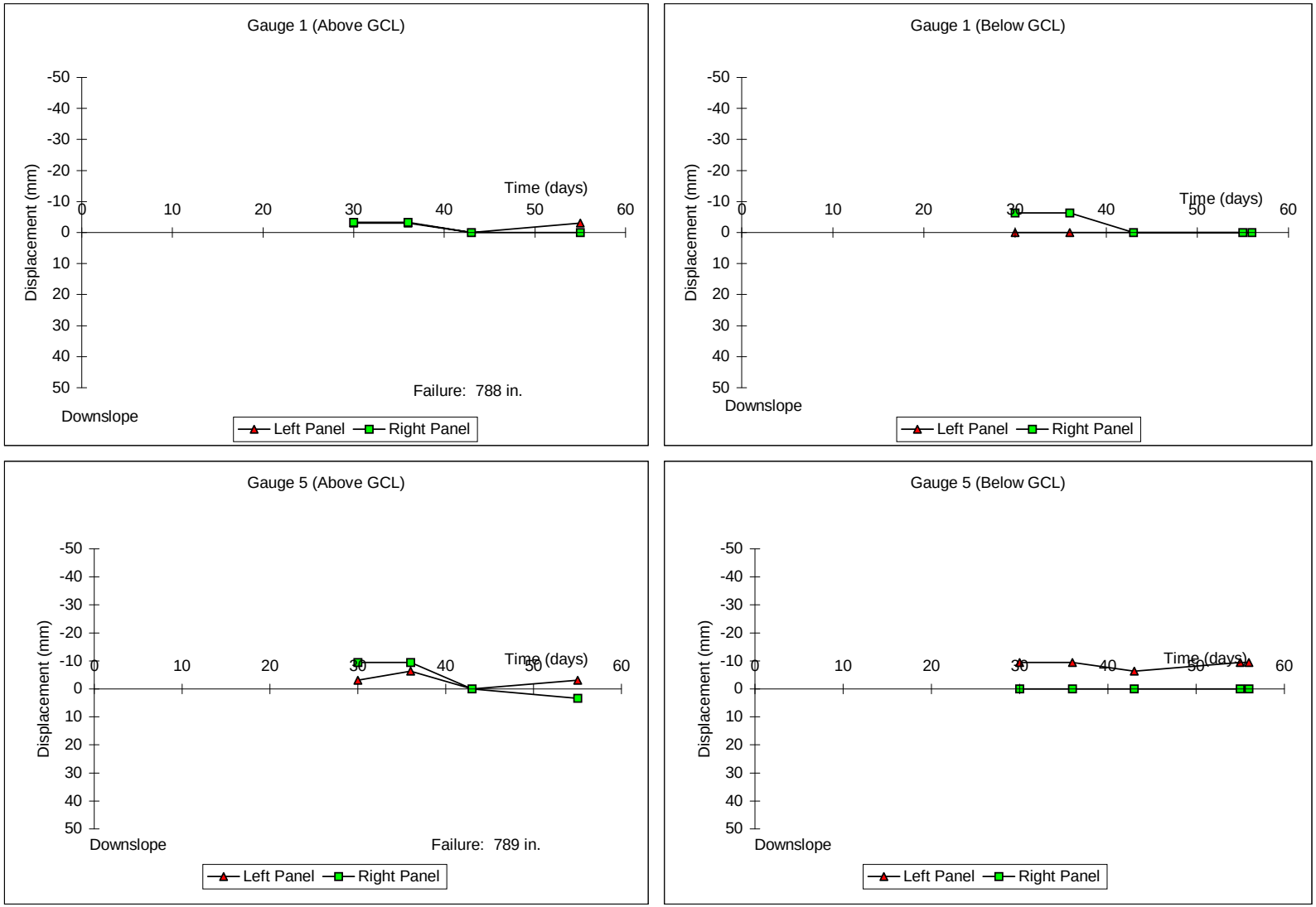

Figure A.7: POST-CONSTRUCTION DISPLACEMENT VS. TIME FOR PLOT G
(Bentomat - 2:1 Slope)

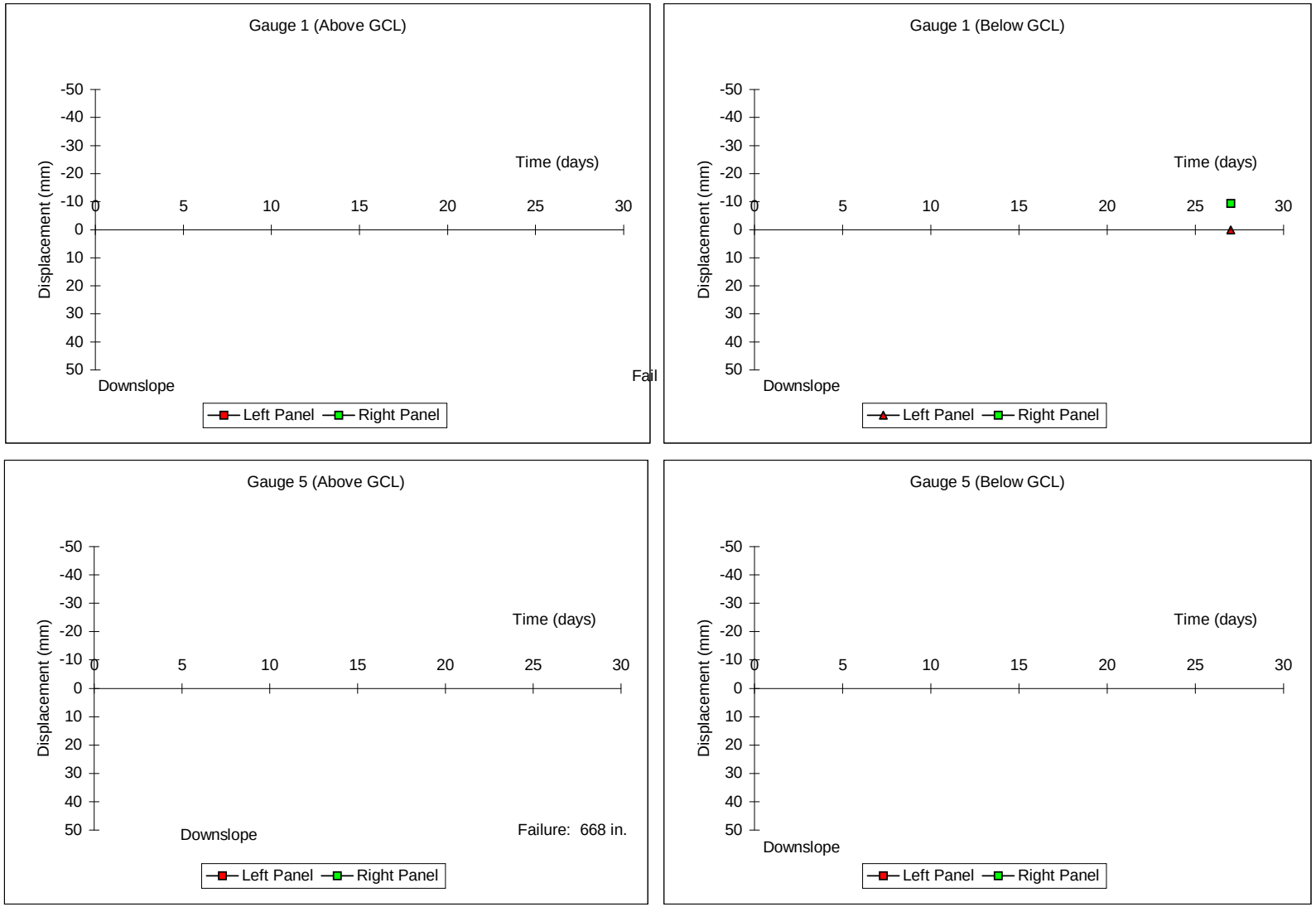

Figure A.8: POST-CONSTRUCTION DISPLACEMENT VS. TIME FOR PLOT H
(Claymax - 2:1 Slope)

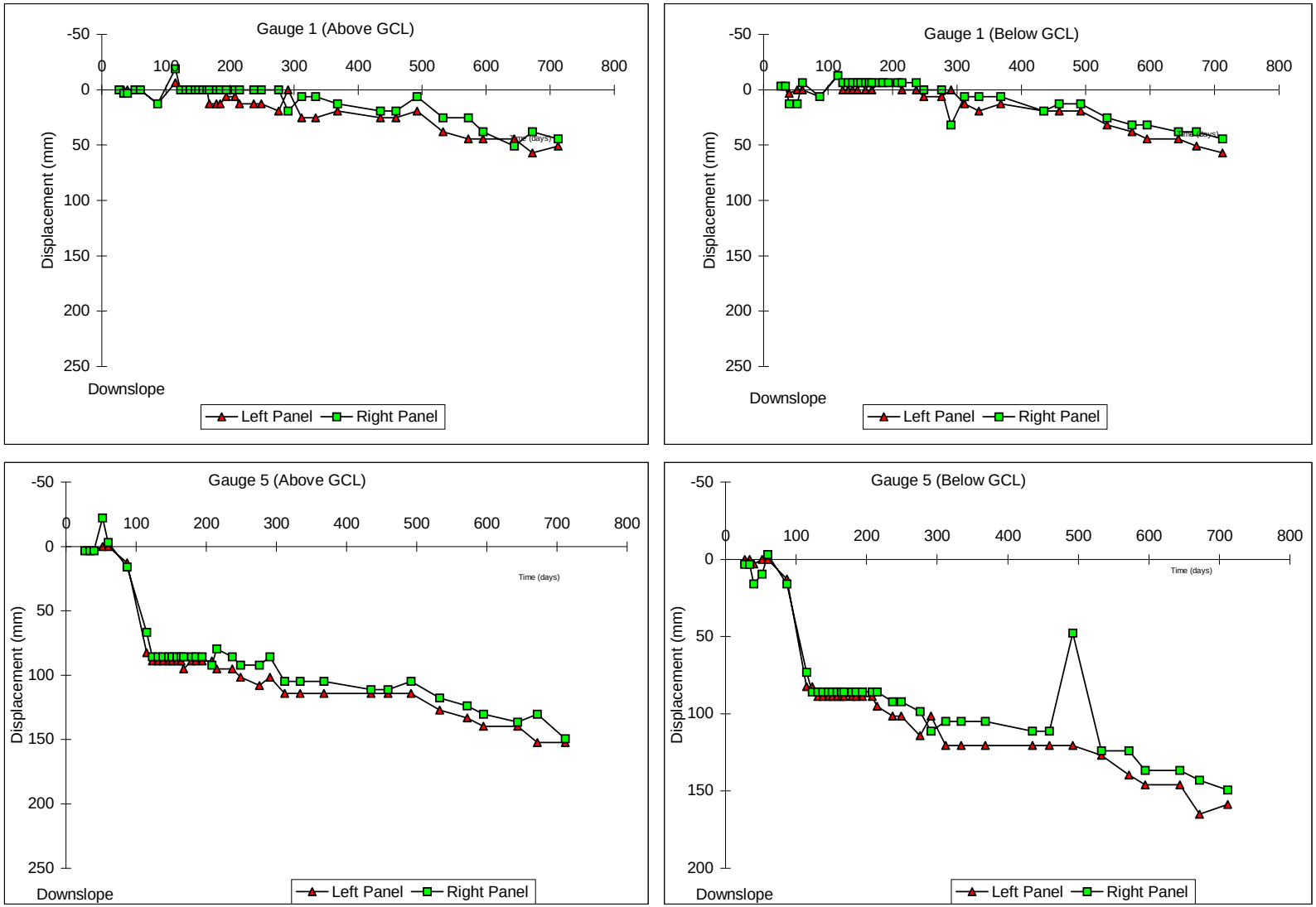

Figure A.9: POST-CONSTRUCTION DISPLACEMENT VS. TIME FOR PLOT I
(Bentofix I - 2:1 Slope)

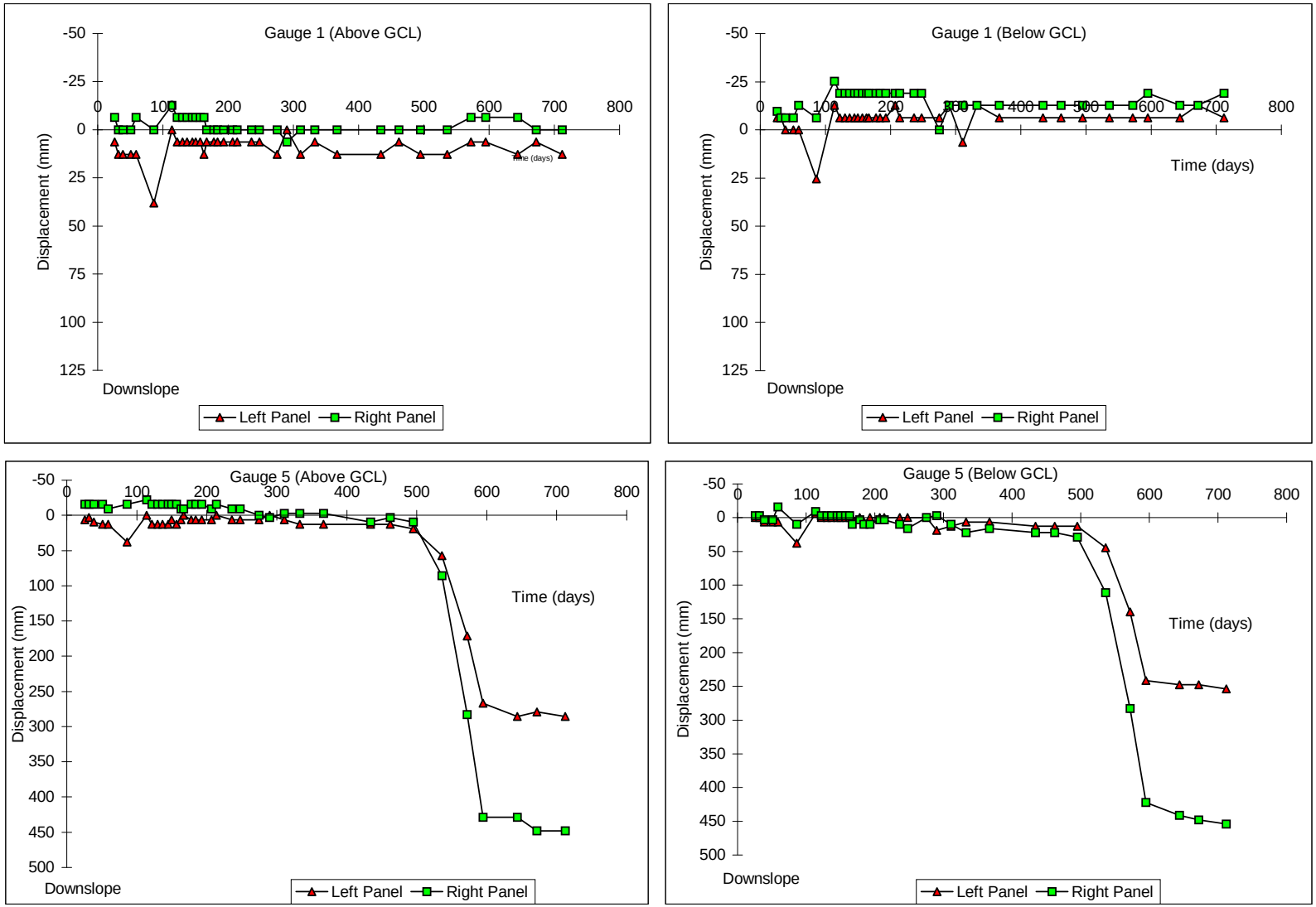

Figure A.10: POST-CONSTRUCTION DISPLACEMENT VS. TIMEFOR PLOT J
(Bentomat - Granular Drainage - 2:1 Slope)

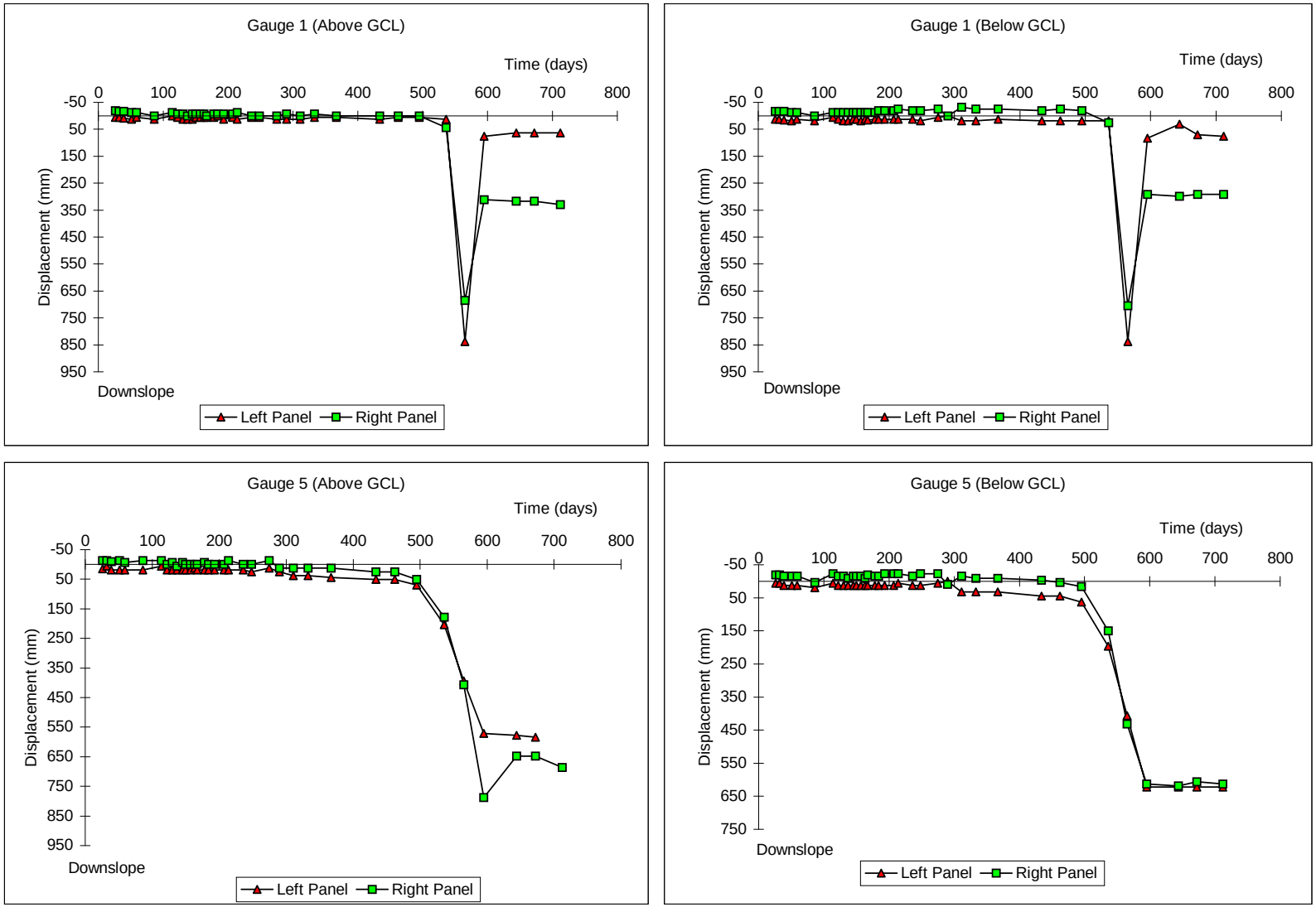

Figure A.11: POST-CONSTRUCTION DISPLACEMENT VS. TIME FOR PLOT K
(Claymax - Granular Drainage - 2:1 Slope)

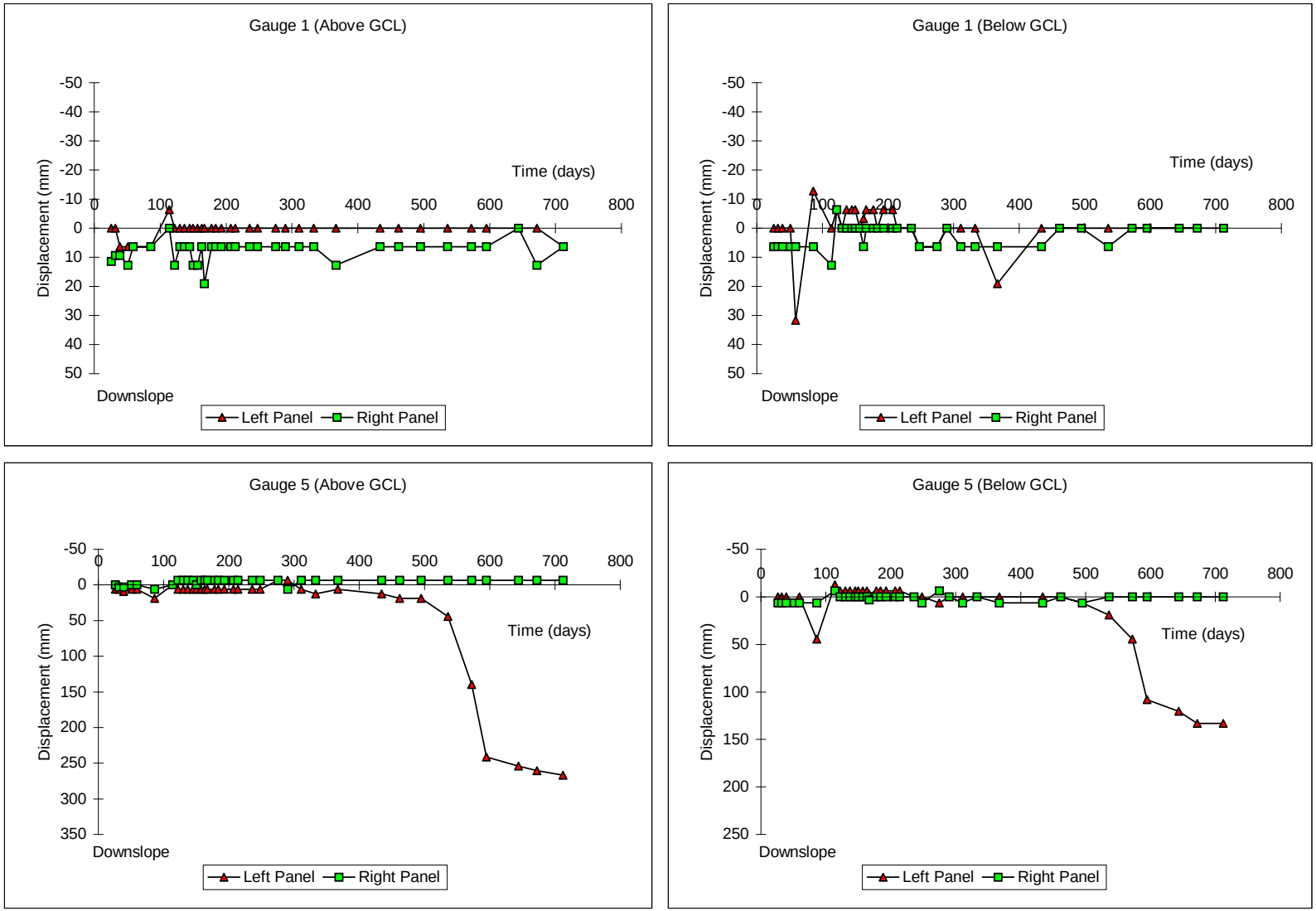

Figure A.12: POST-CONSTRUCTION DISPLACEMENT VS. TIME FOR PLOT L
(Bentofix - Granular Drainage I - 2:1 Slope)

Plot M -- Erosion control plot -- no instrumentation installed

Plot P -- Only moisture sensors were installed -- no deformation sensors

Appendix D

Attachment 3

Plots of Differential Displacement between Upper and Lower Surfaces of GCLs Versus Time

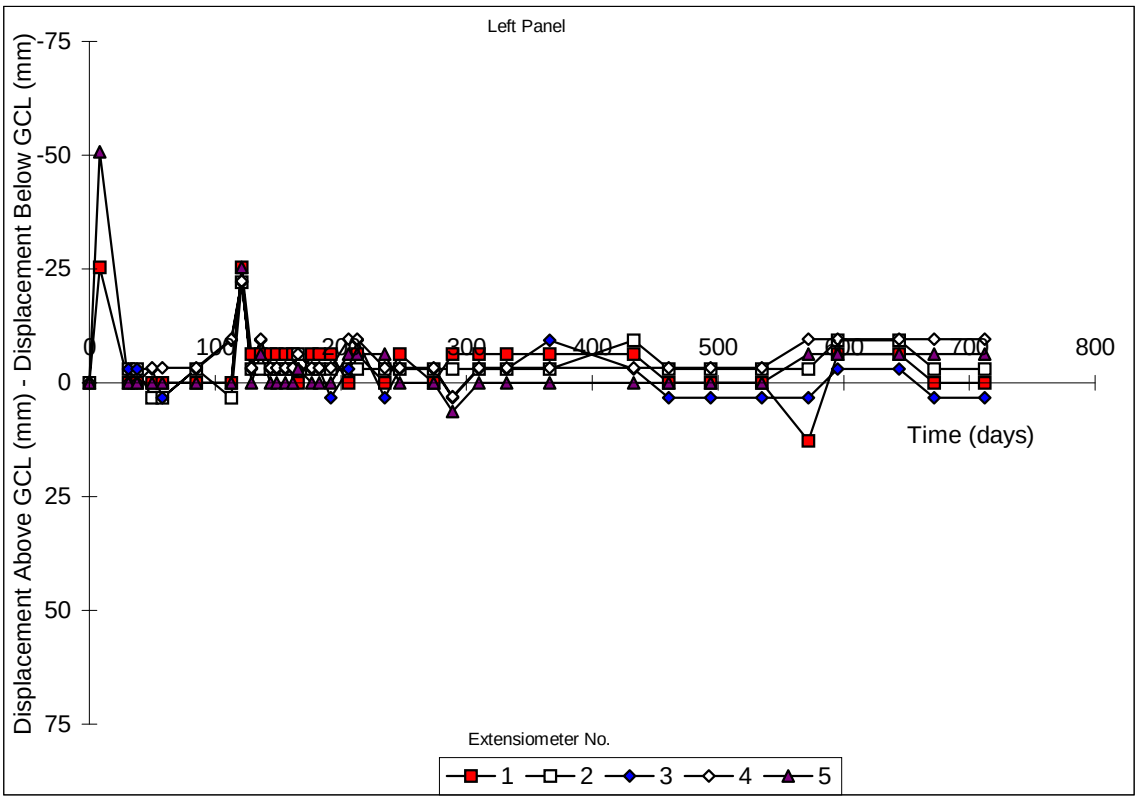

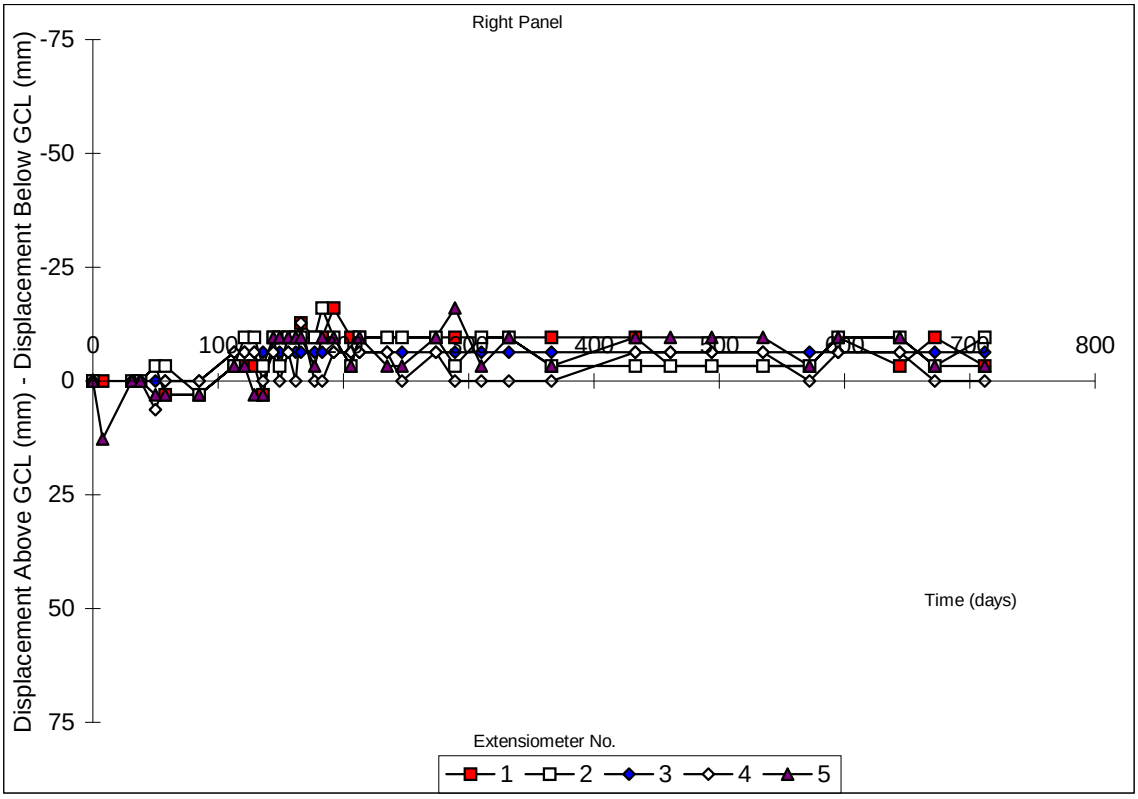

Figure C.1: RELATIVE DISPLACEMENT VS. TIME FOR PLOT A
(Gundseal - Bentonite Side Up - 3:1 Slope)

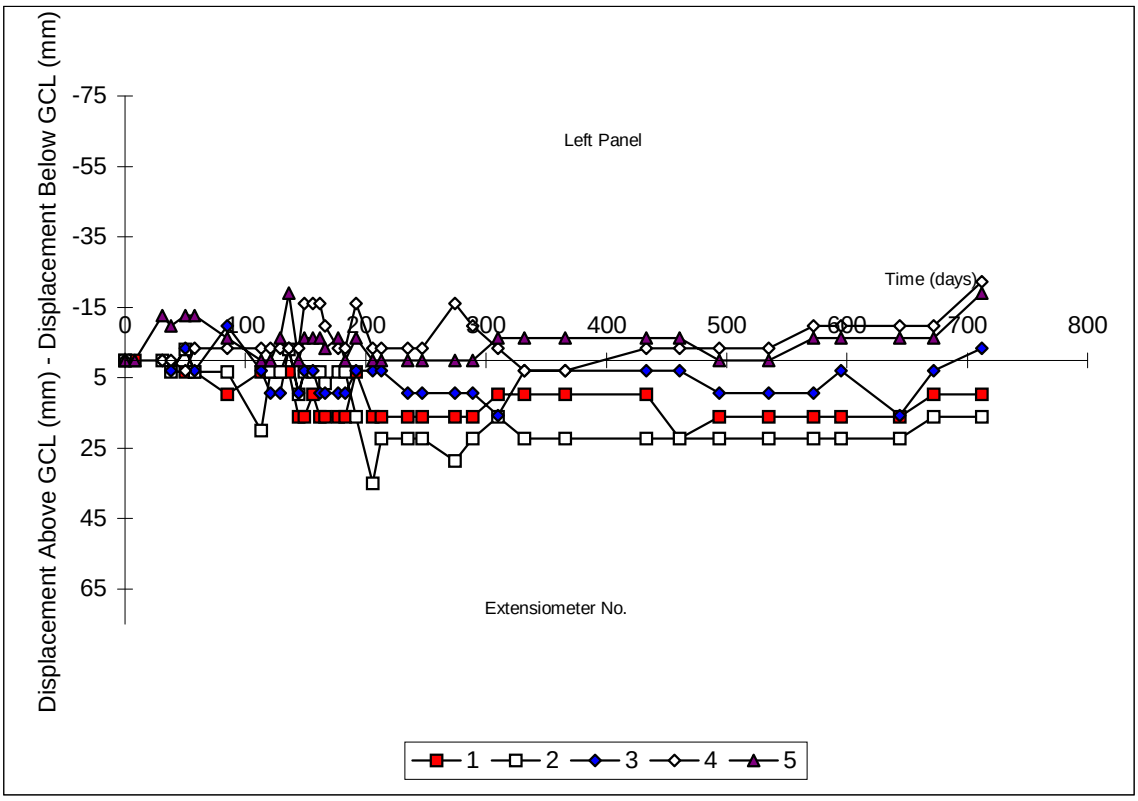

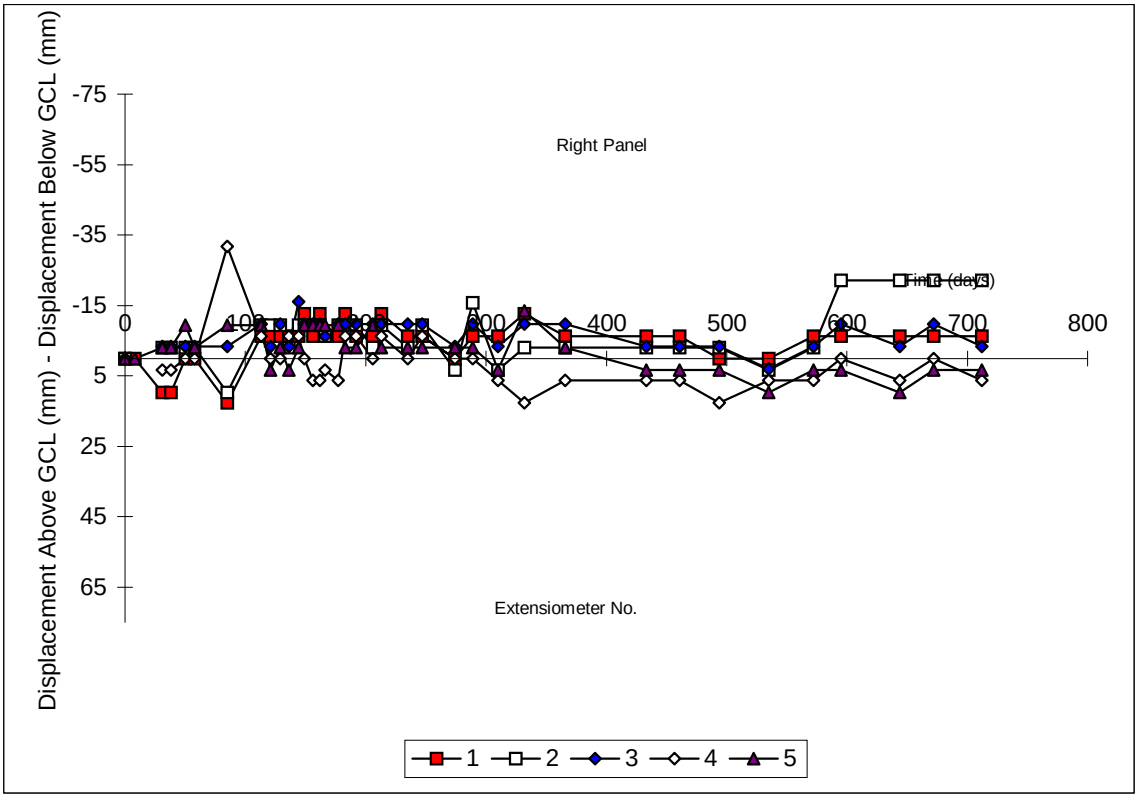

Figure C.2: RELATIVE DISPLACEMENT VS. TIME FOR PLOT B
(Bentomat - 3:1 Slope)

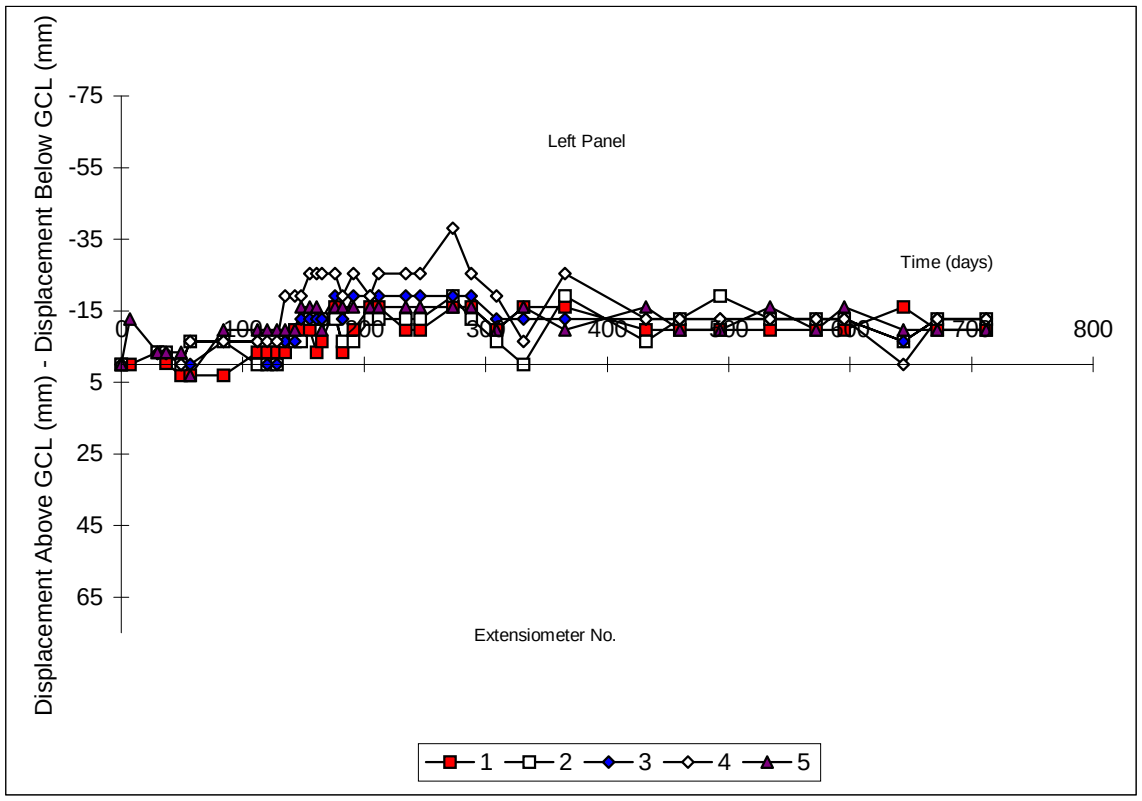

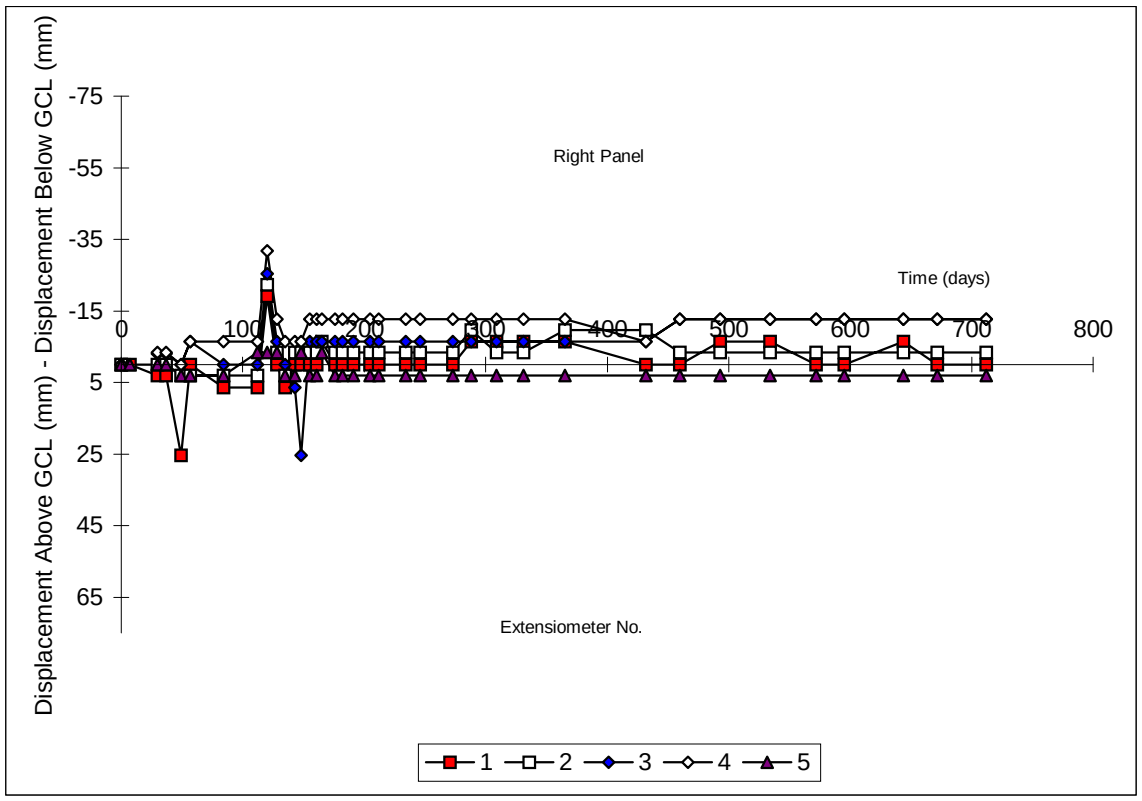

Figure C.3: RELATIVE DISPLACEMENT VS. TIME FOR PLOT C
(Claymax - 3:1 Slope)

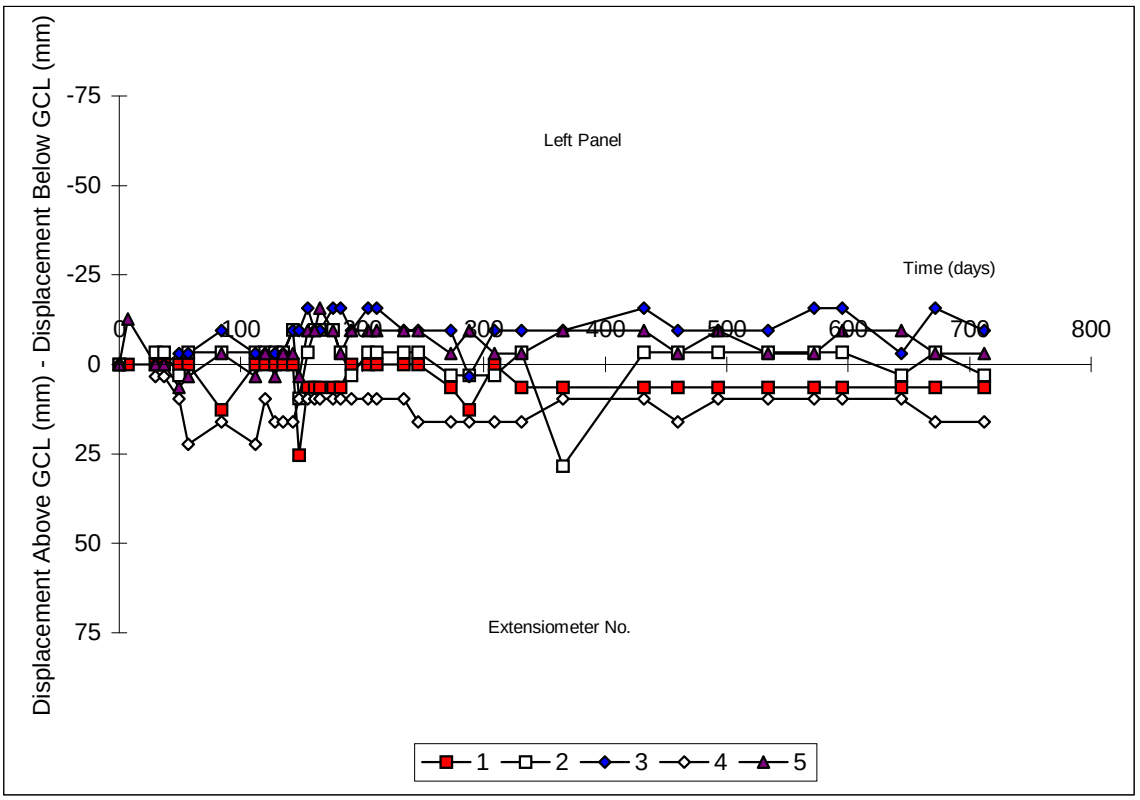

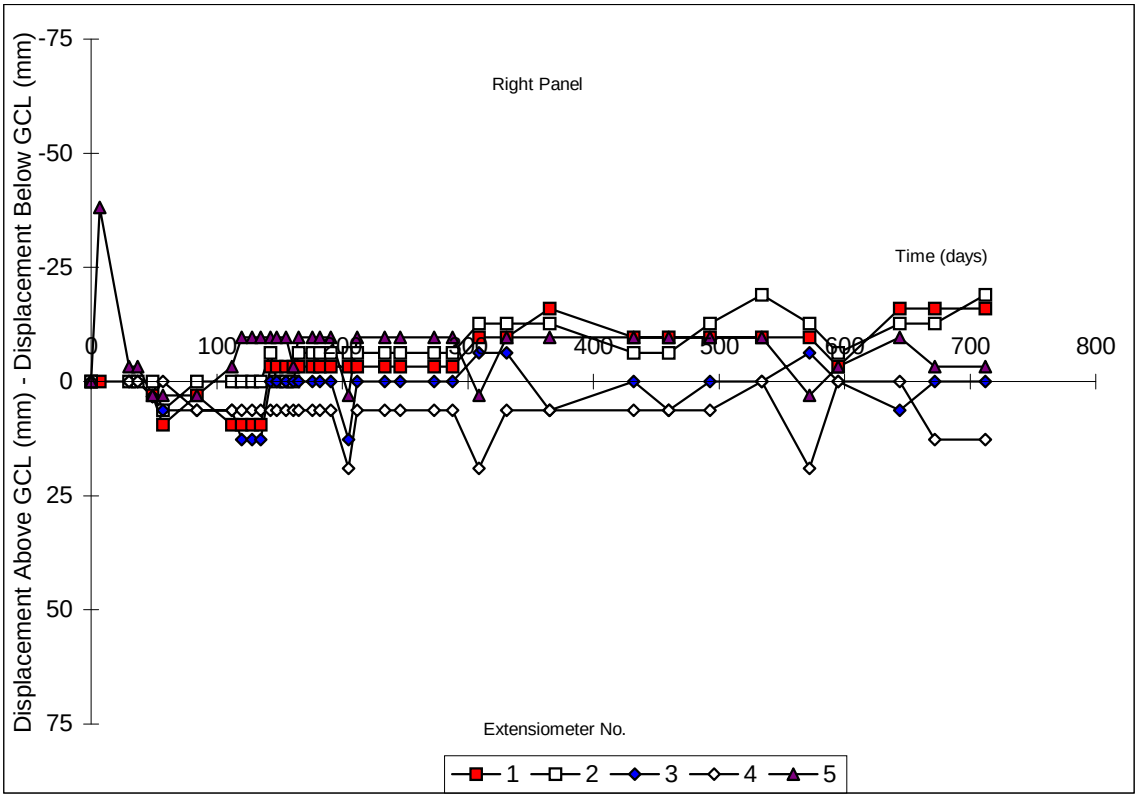

Figure C.4: RELATIVE DISPLACEMENT VS. TIME FOR PLOT D
(Bentofix NS - 3:1 Slope)

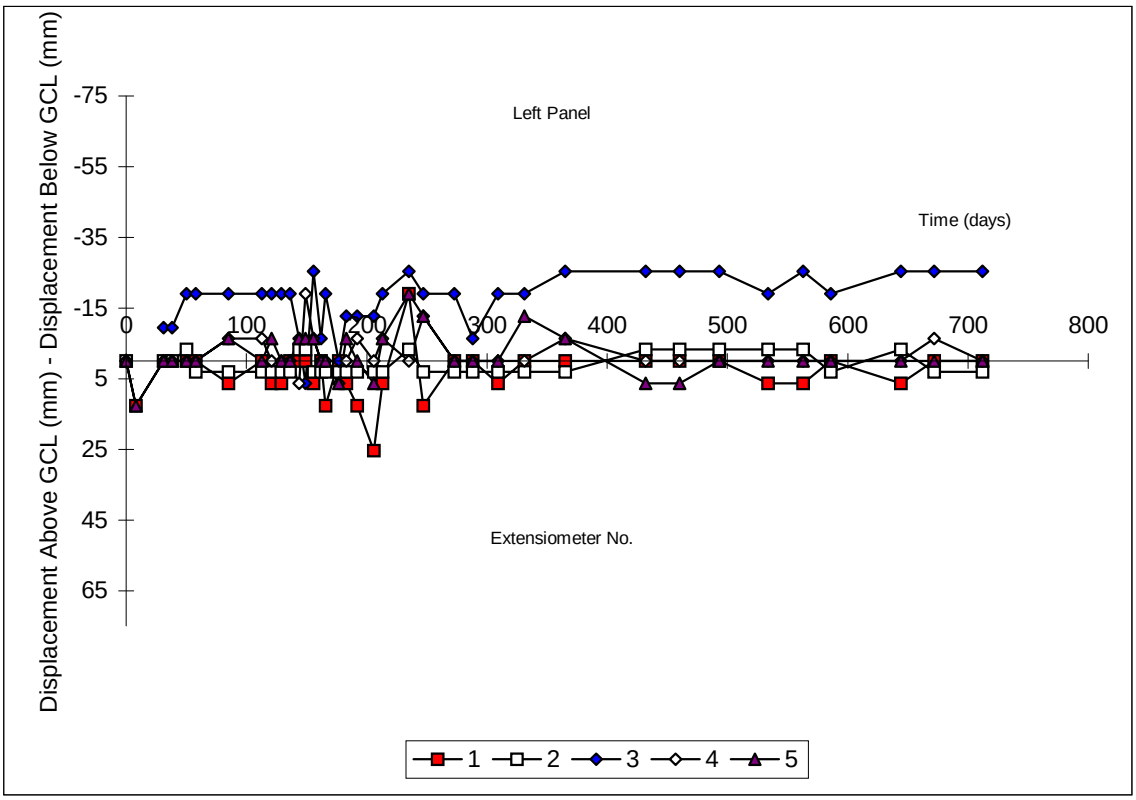

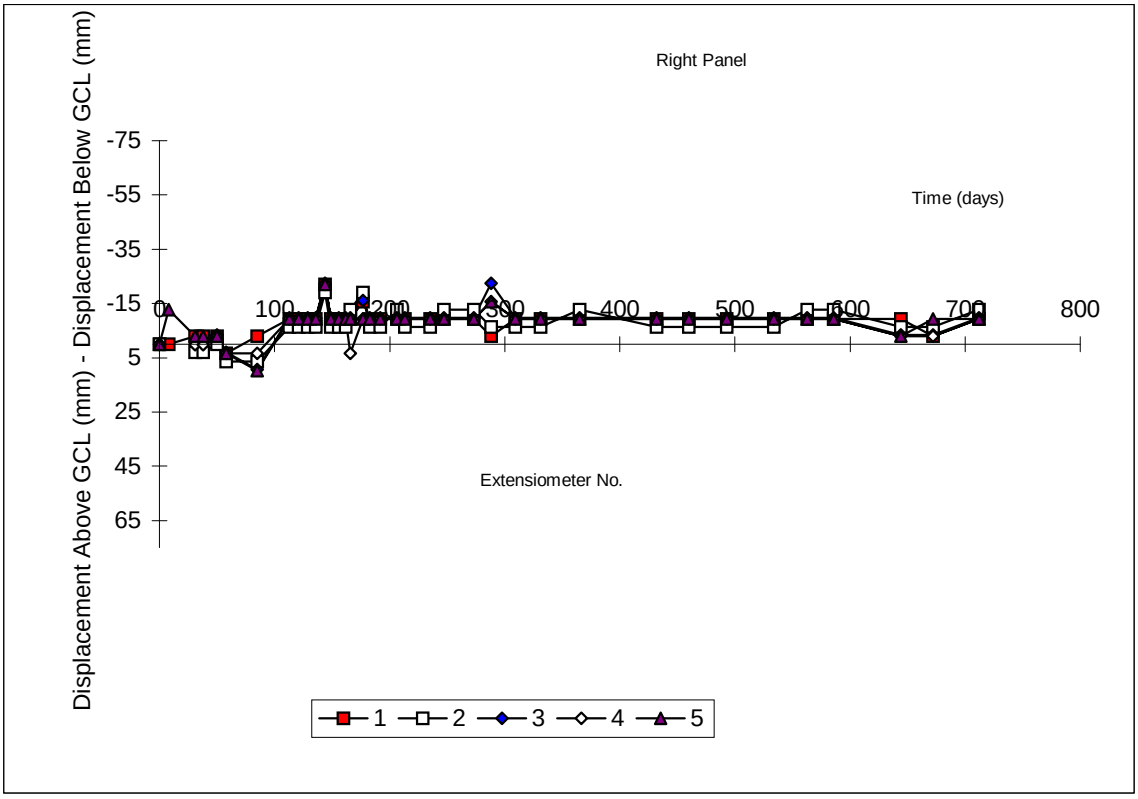

Figure C.5: RELATIVE DISPLACEMENT VS. TIME FOR PLOT E
(Gundseal - Bentonite Down - 3:1 Slope)

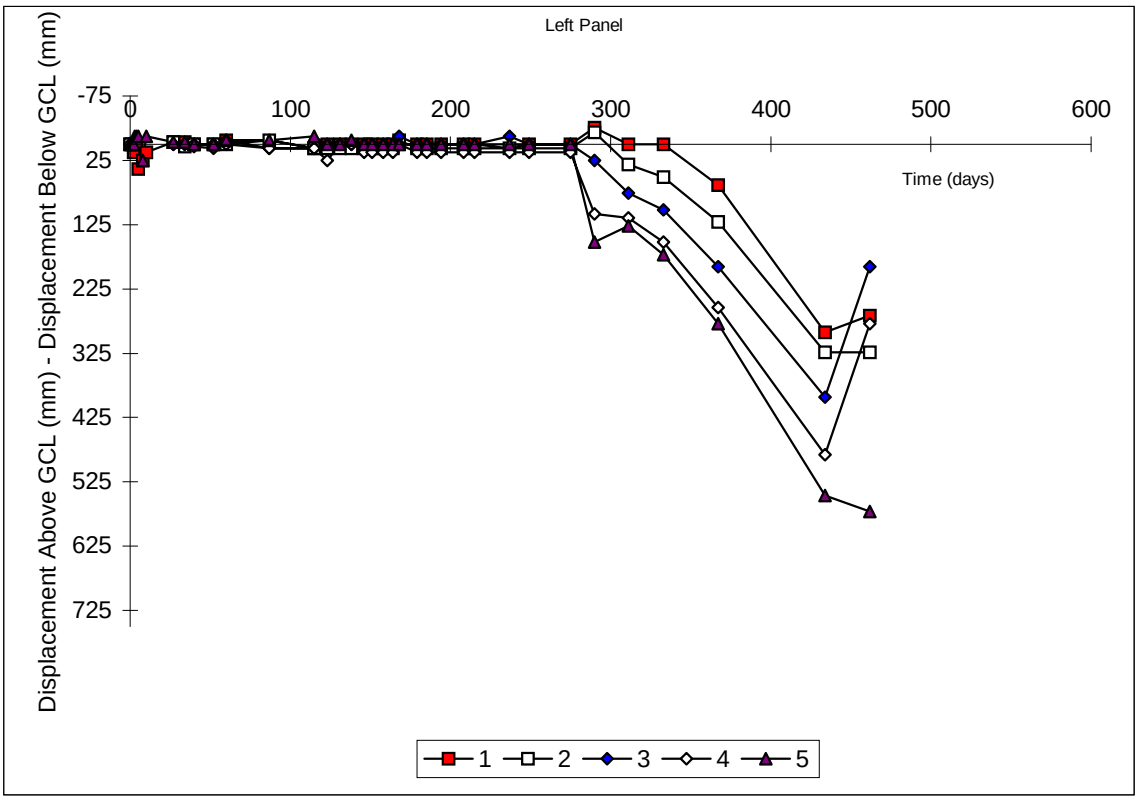

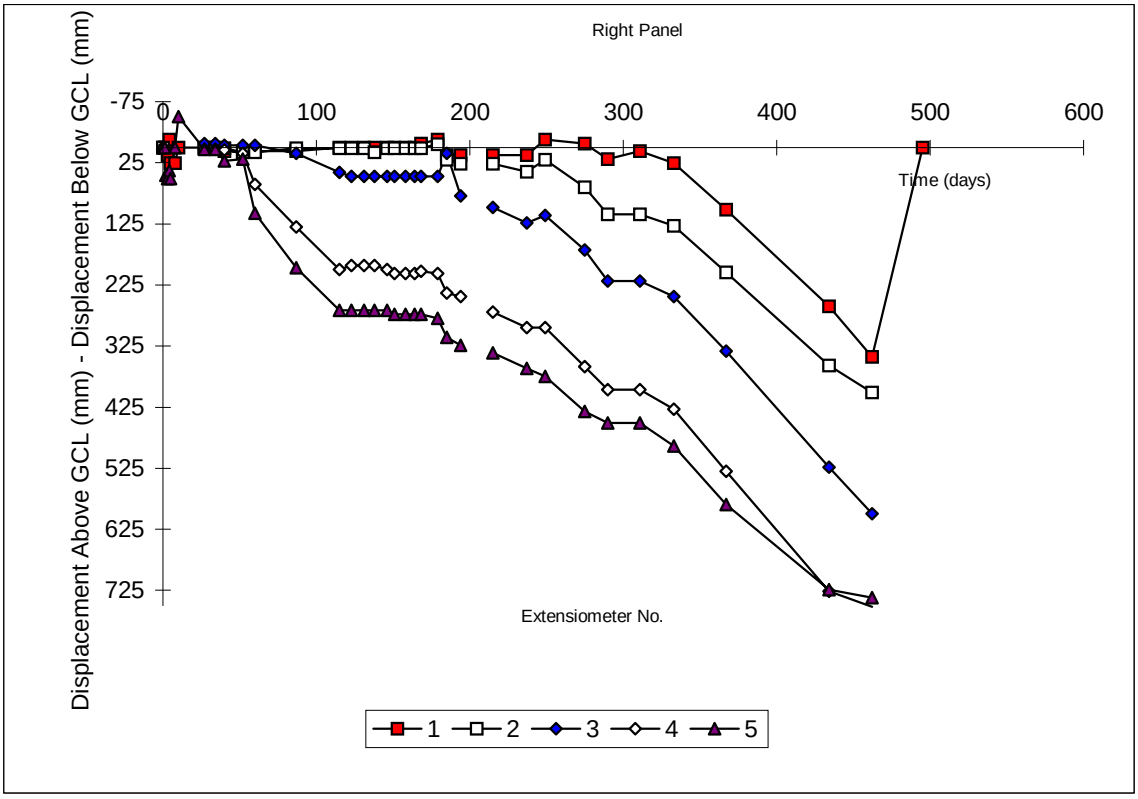

Figure C.6: RELATIVE DISPLACEMENT VS. TIME FOR PLOT F
(Gundseal - Bentonite Up - 2:1 Slope)

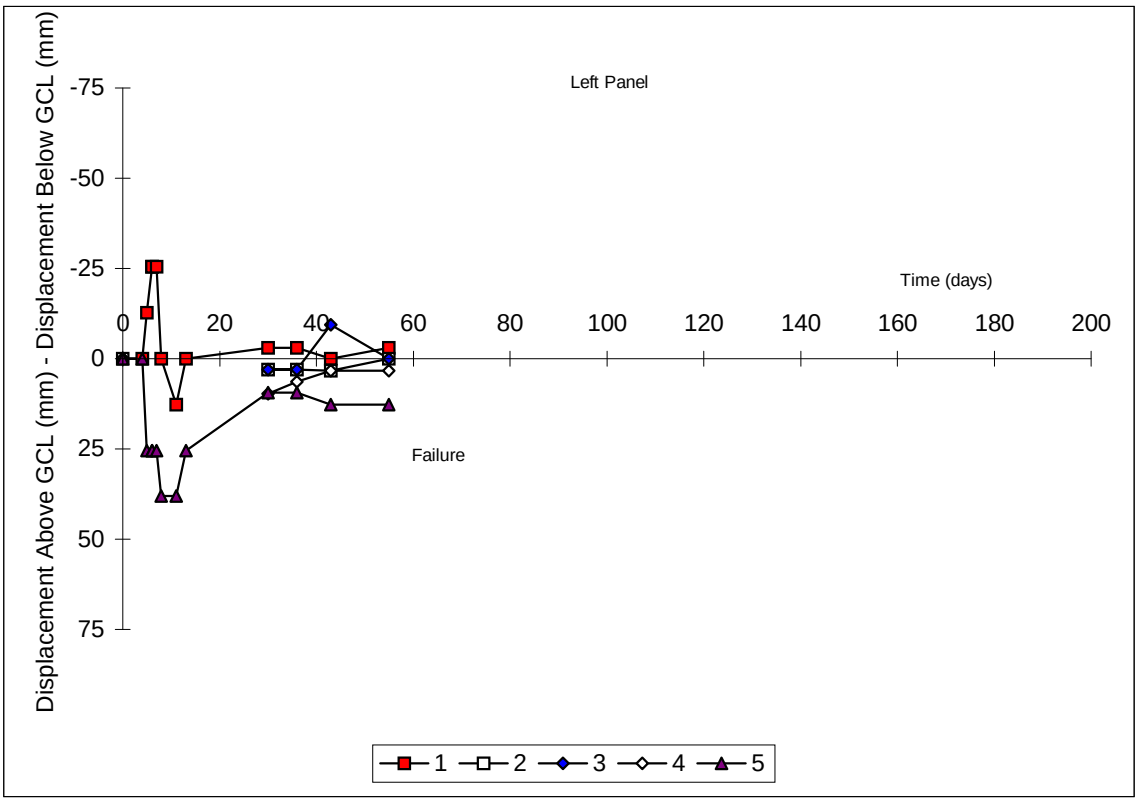

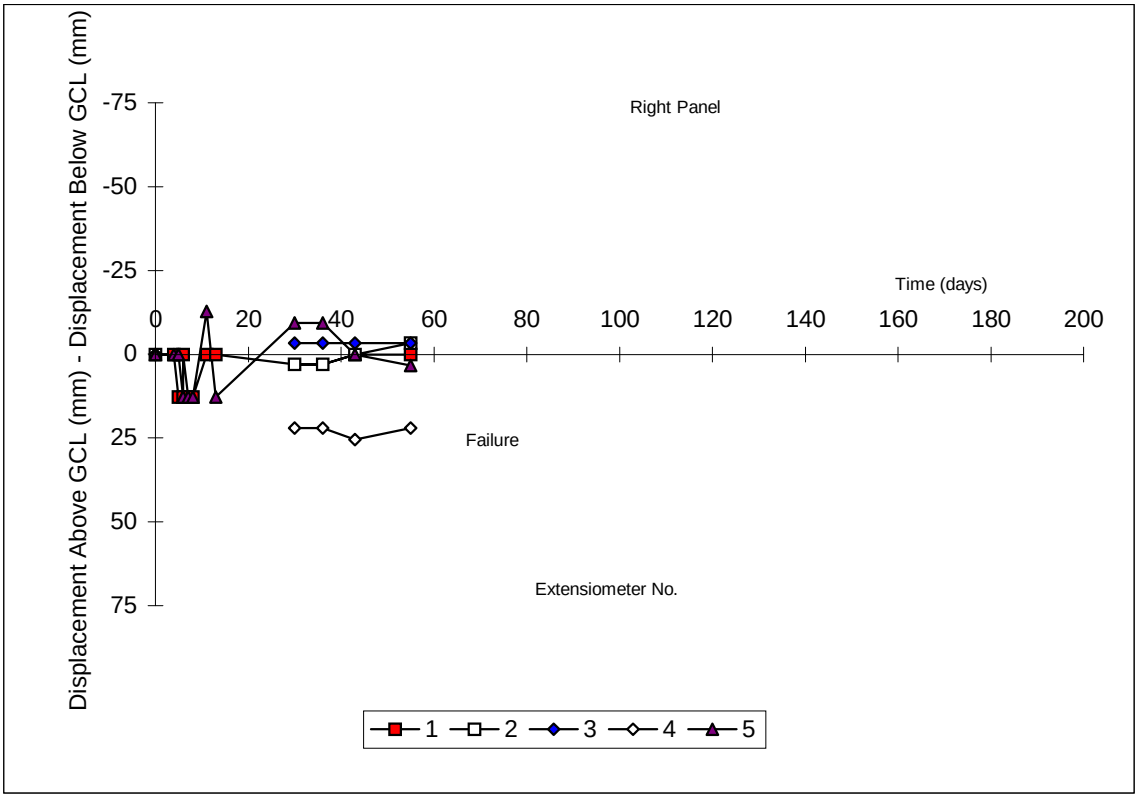

Figure C.7: RELATIVE DISPLACEMENT VS. TIME FOR PLOT G
(Bentomat - 2:1 Slope)

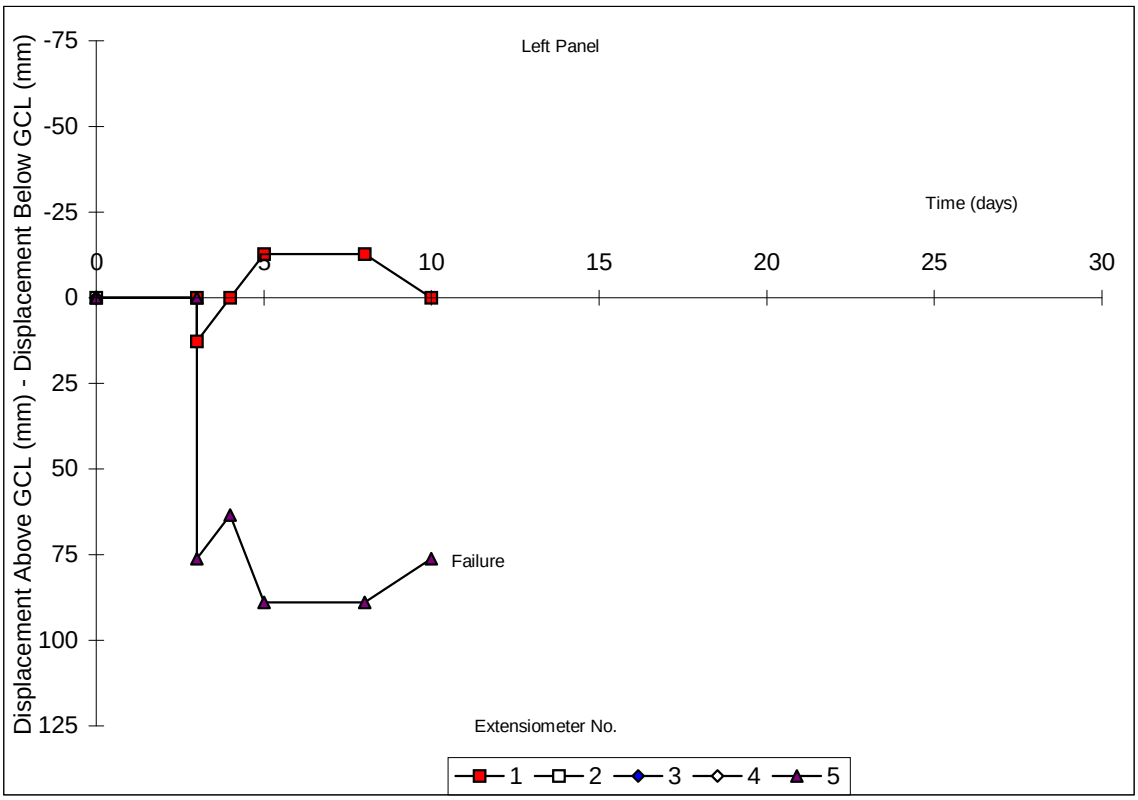

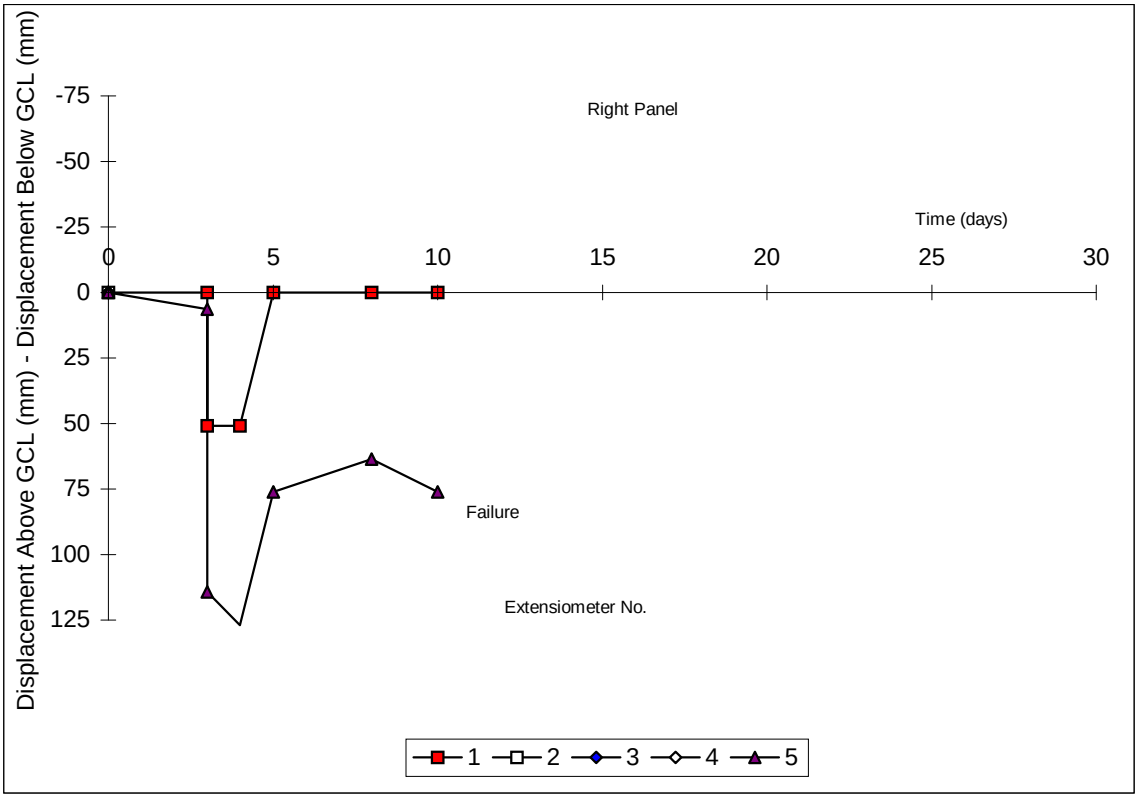

Figure C.8: RELATIVE DISPLACEMENT VS. TIME FOR PLOT H
(Claymax - 2:1 Slope)

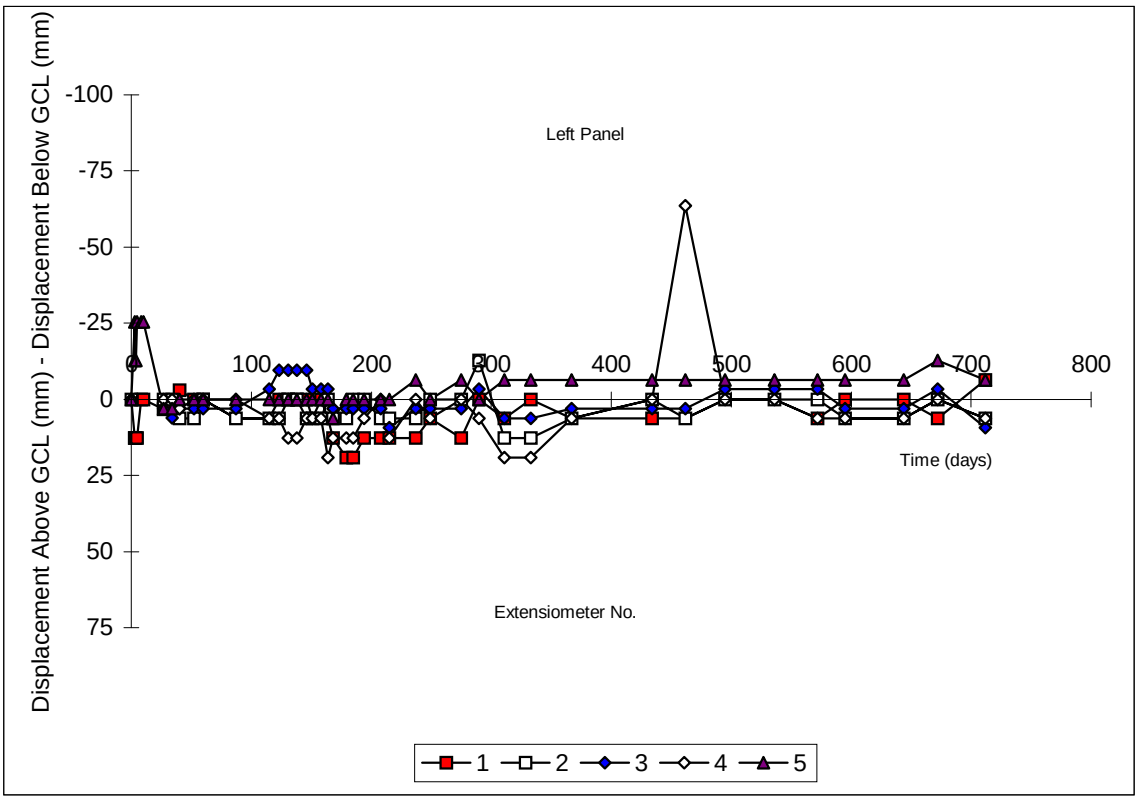

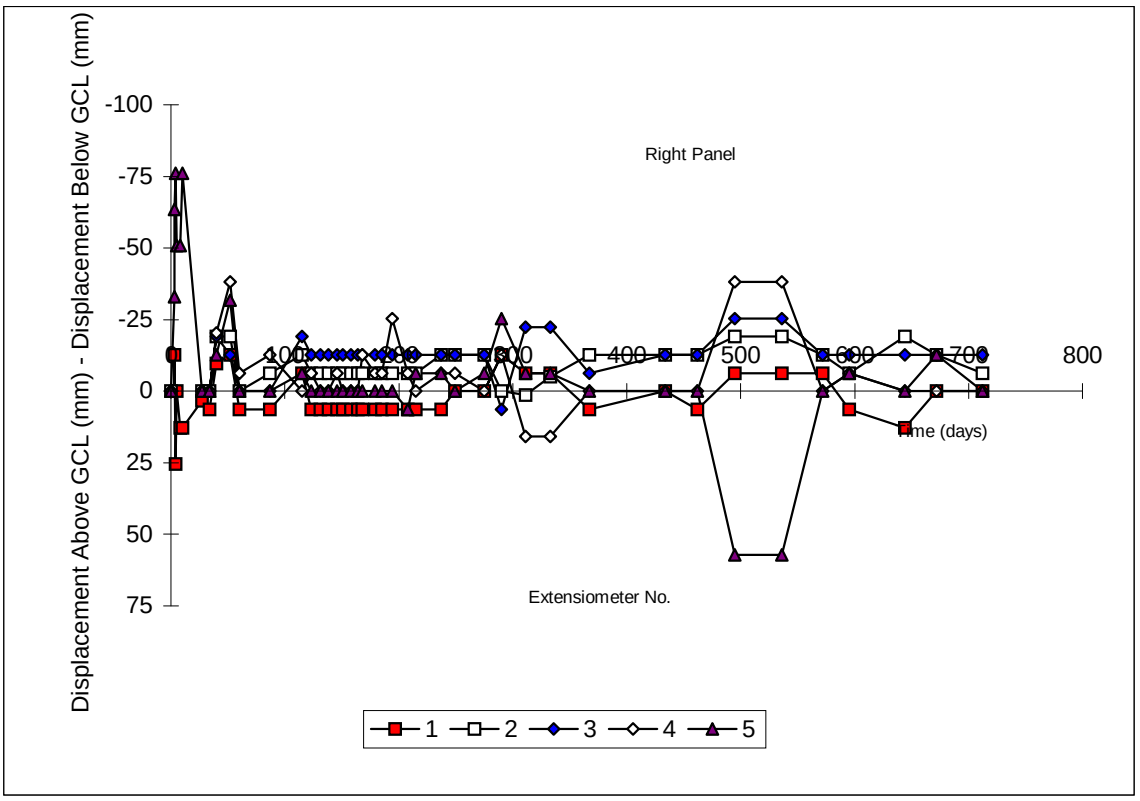

Figure C.9: RELATIVE DISPLACEMENT VS. TIME FOR PLOT I
(Bentofix NW - 2:1 Slope)

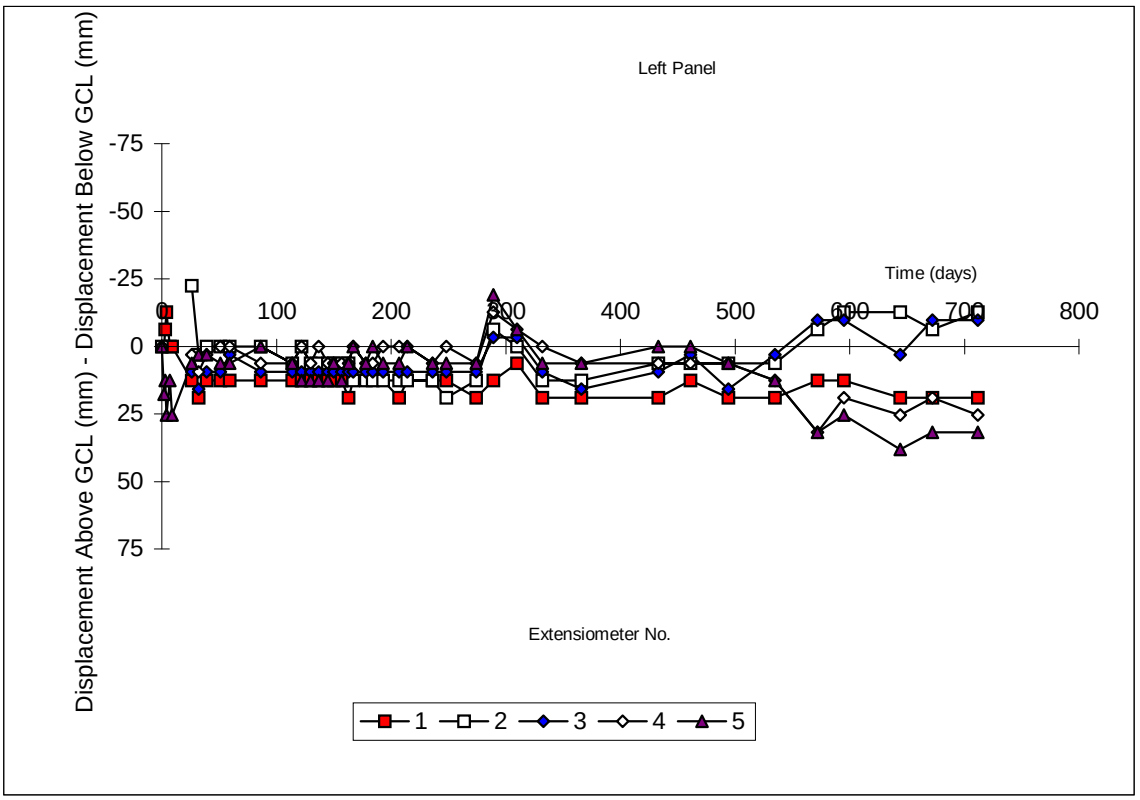

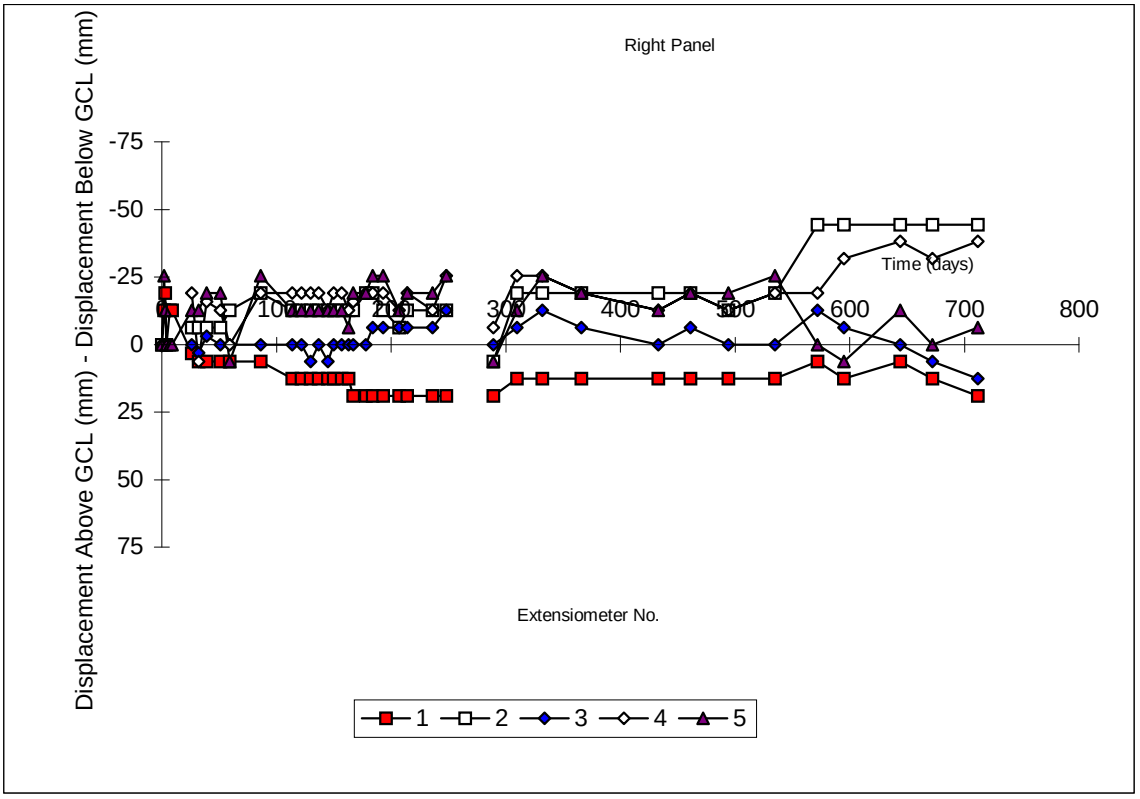

Figure C.10: RELATIVE DISPLACEMENT VS. TIME FOR PLOT J
(Bentomat - Granular Drainage - 2:1 Slope)

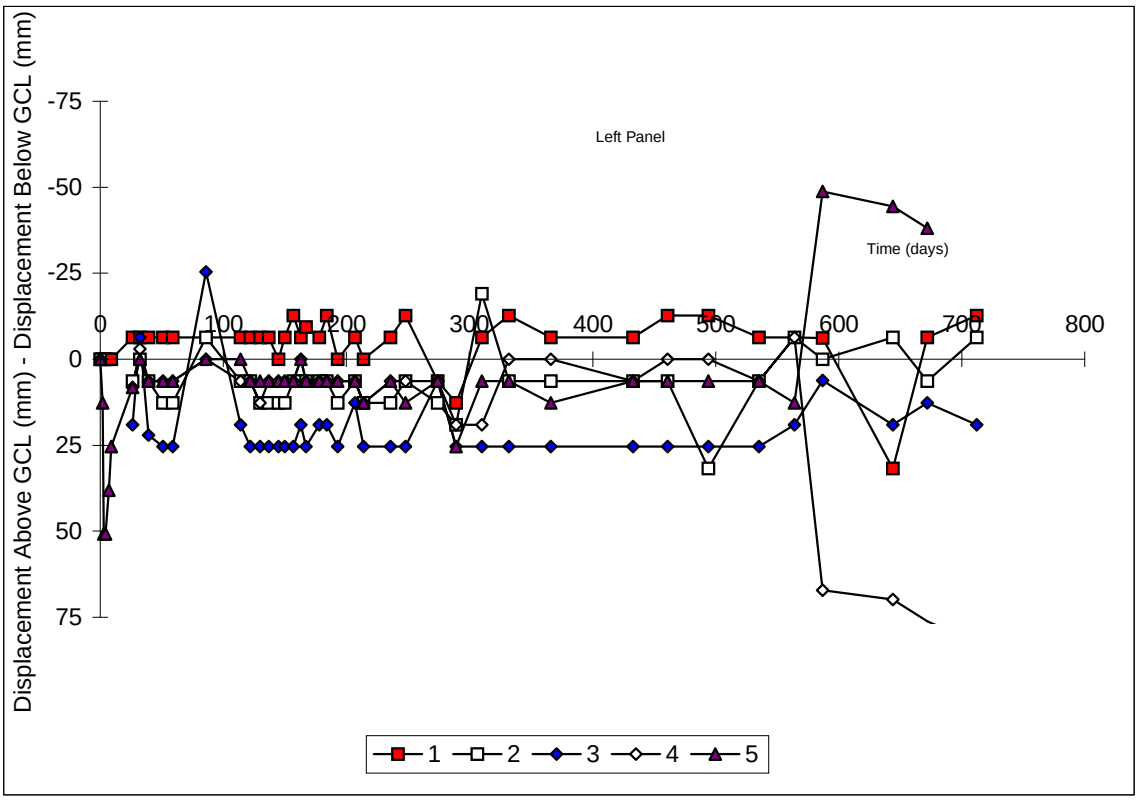

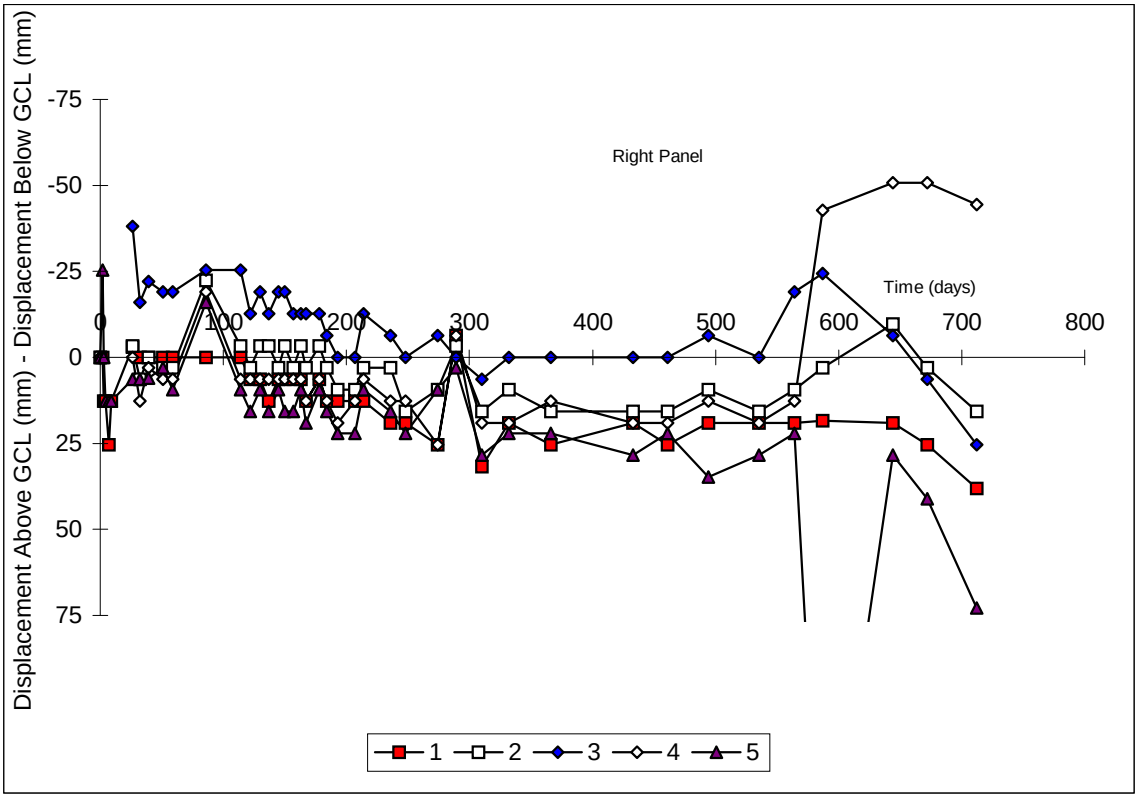

Figure C.11: RELATIVE DISPLACEMENT VS. TIME FOR PLOT K
(Claymax - Granular Drainage - 2:1 Slope)

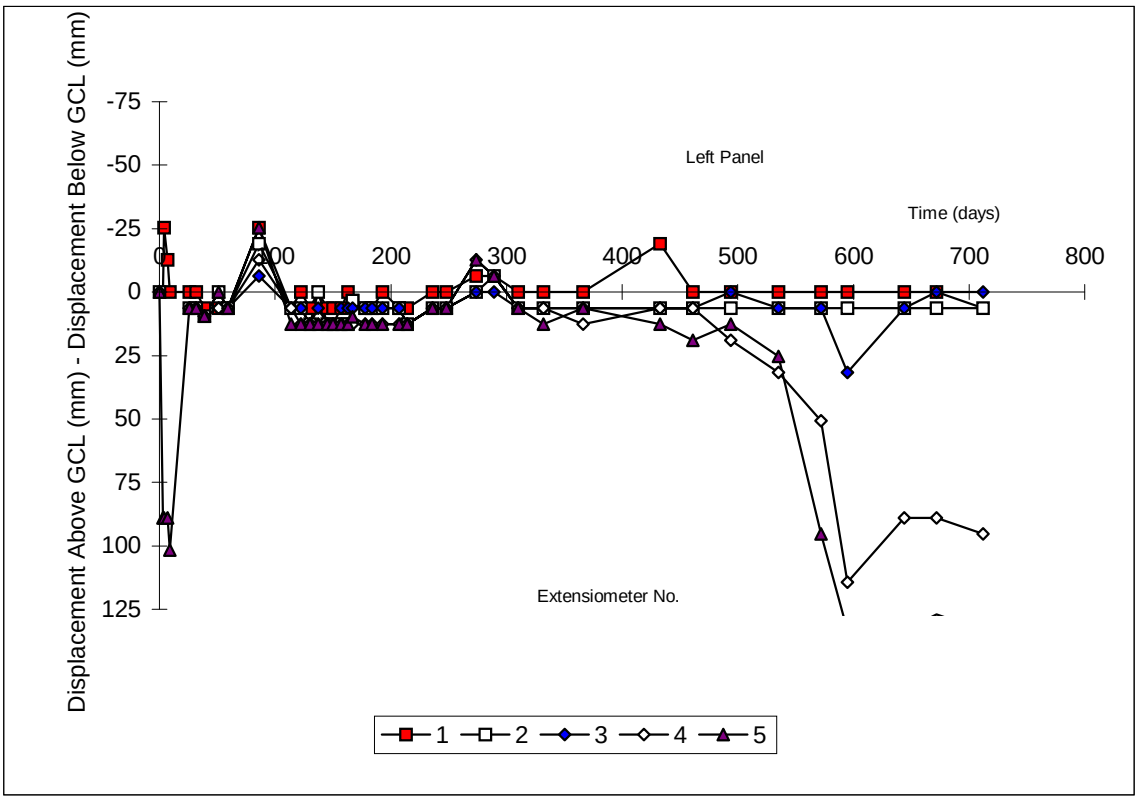

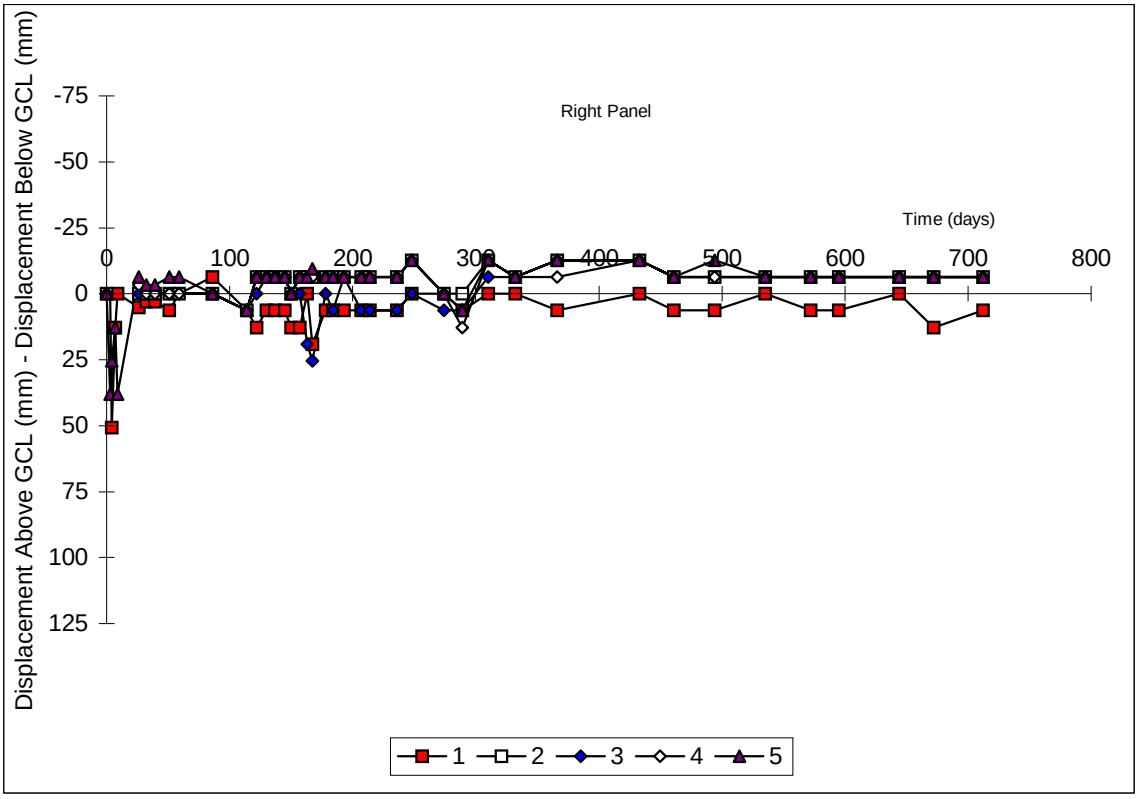

Figure C.12: RELATIVE DISPLACEMENT VS. TIME FOR PLOT L
(Bentofix NW - Granular Drainage - 2:1 Slope)

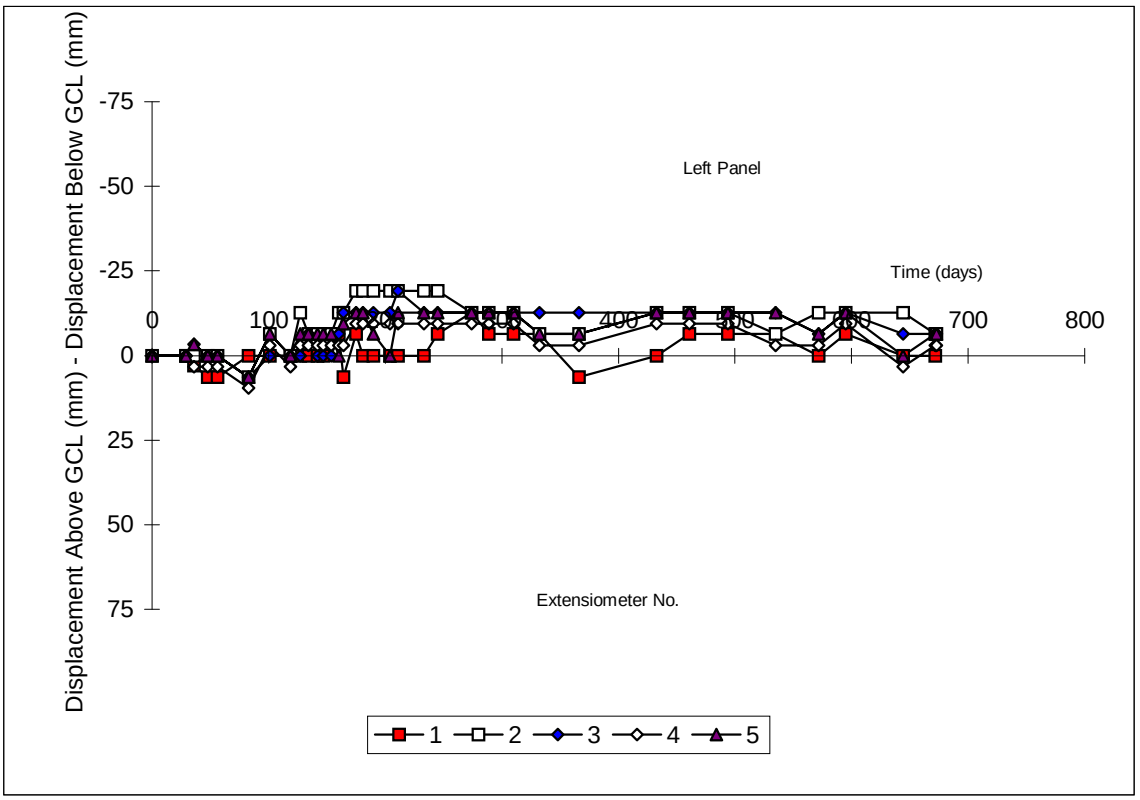

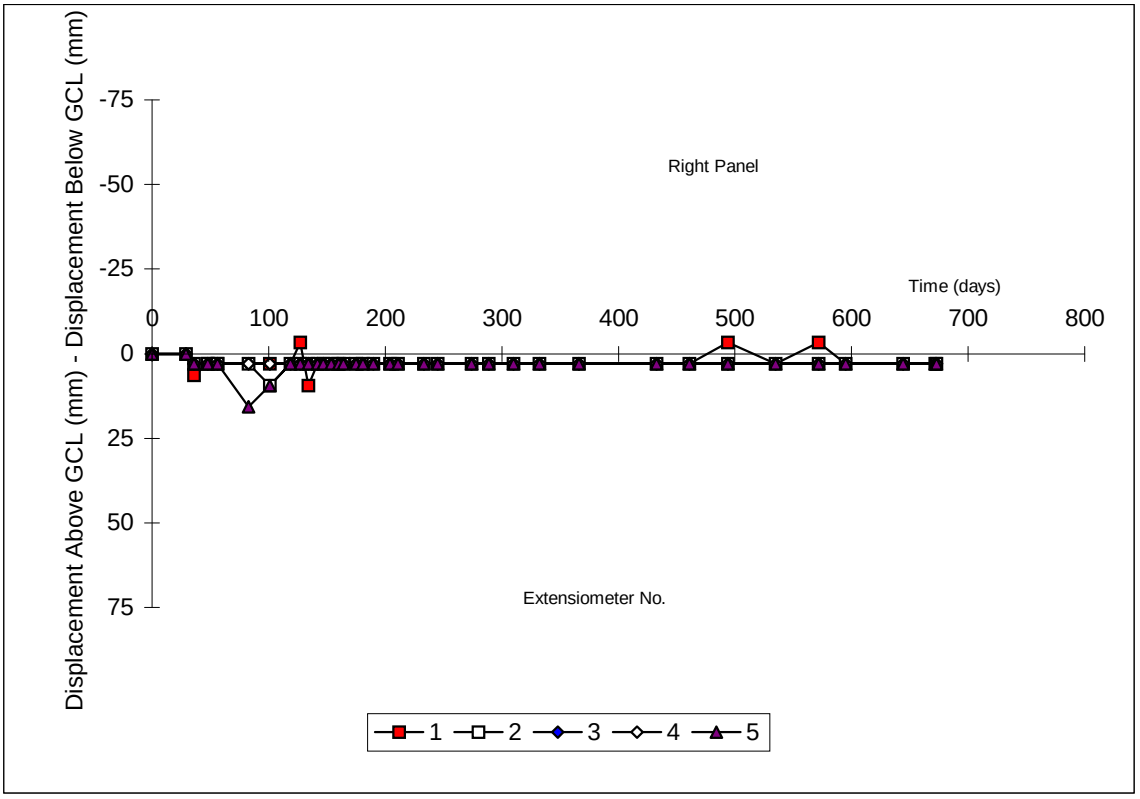

Figure C.13: RELATIVE DISPLACEMENT VS. TIME FOR PLOT N
(Bentofix NS - 2:1 Slope)

Appendix D

Attachment 4

Plots of Moisture Sensor Readings Versus Time

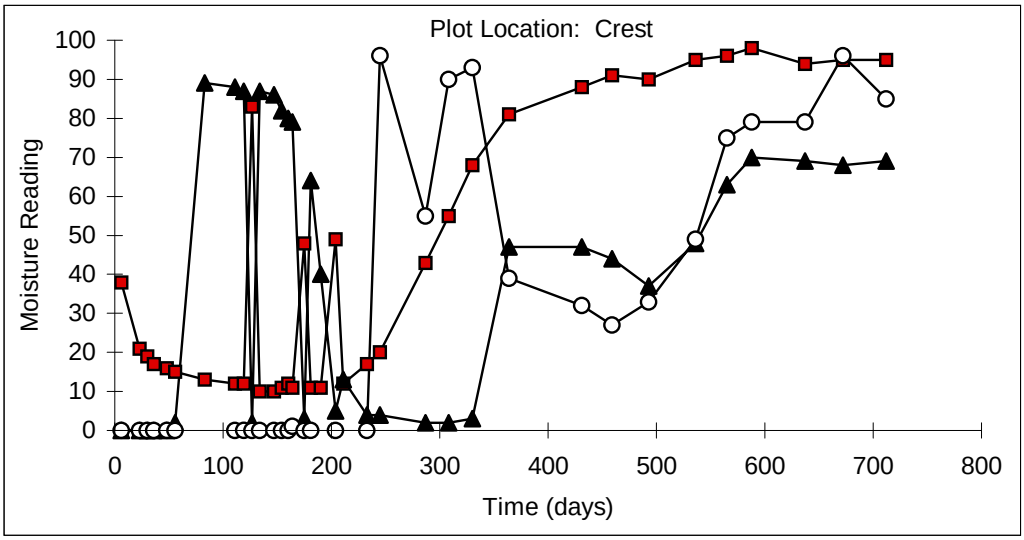

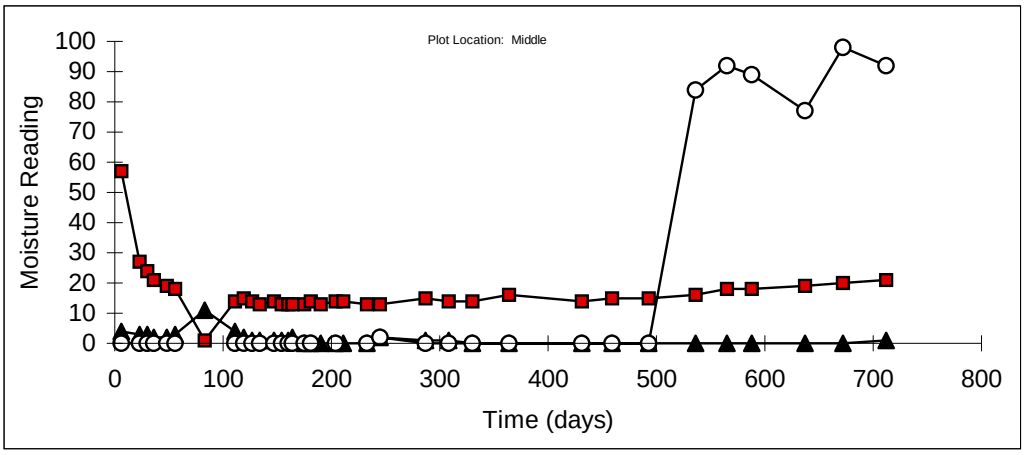

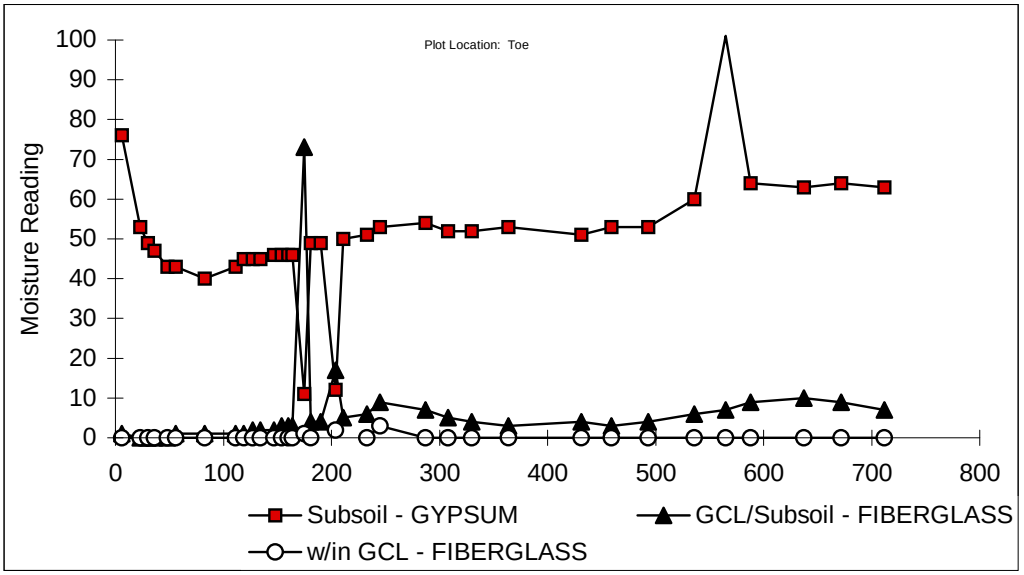

Figure D1: MOISTURE READINGS VS. TIME FOR PLOT A
(Gundseal - Bentonite up - 3:1 Slope)

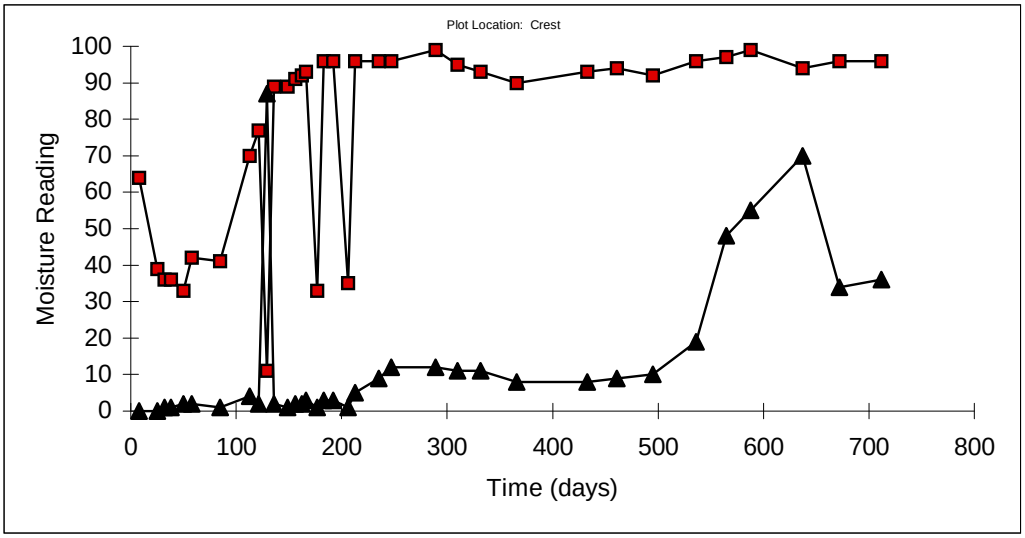

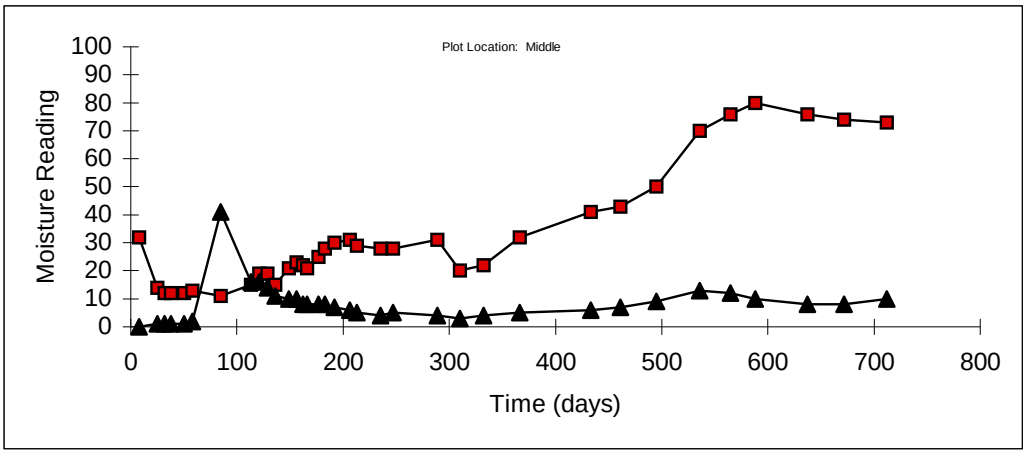

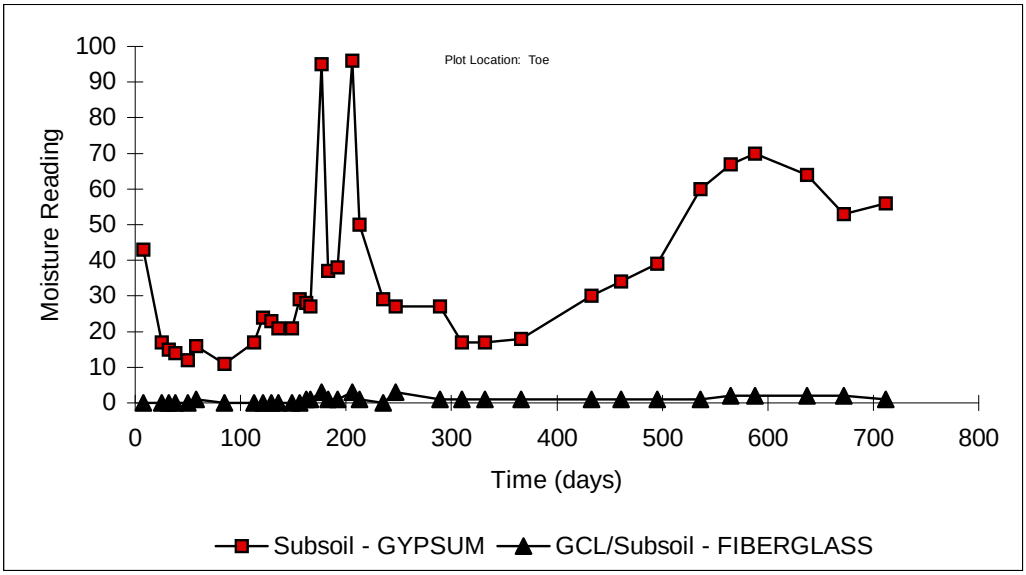

Figure D.2: MOISTURE READINGS VS. TIME FOR PLOT B
(Bentomat - 3:1 Slope)

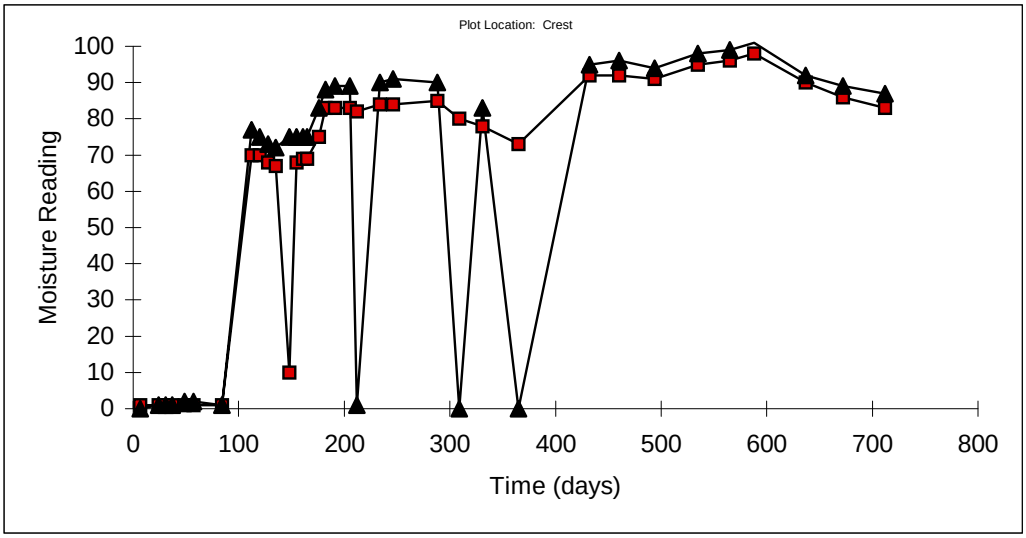

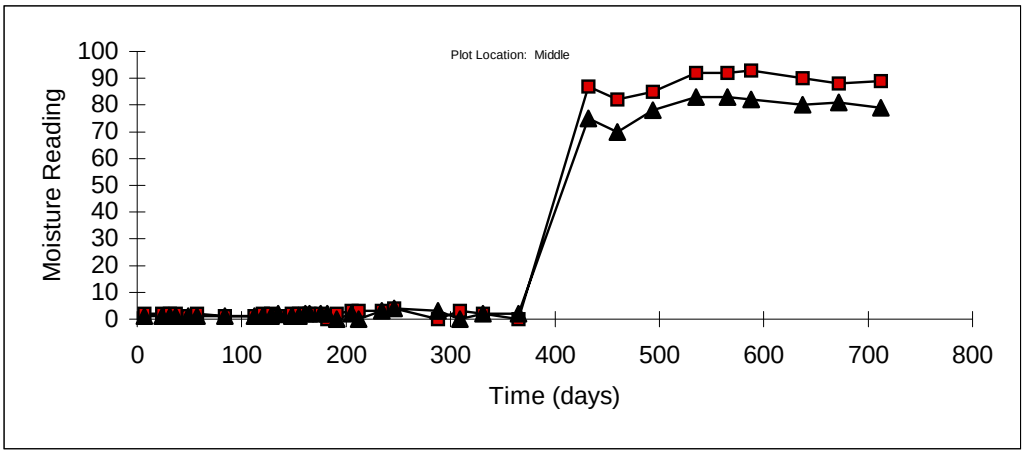

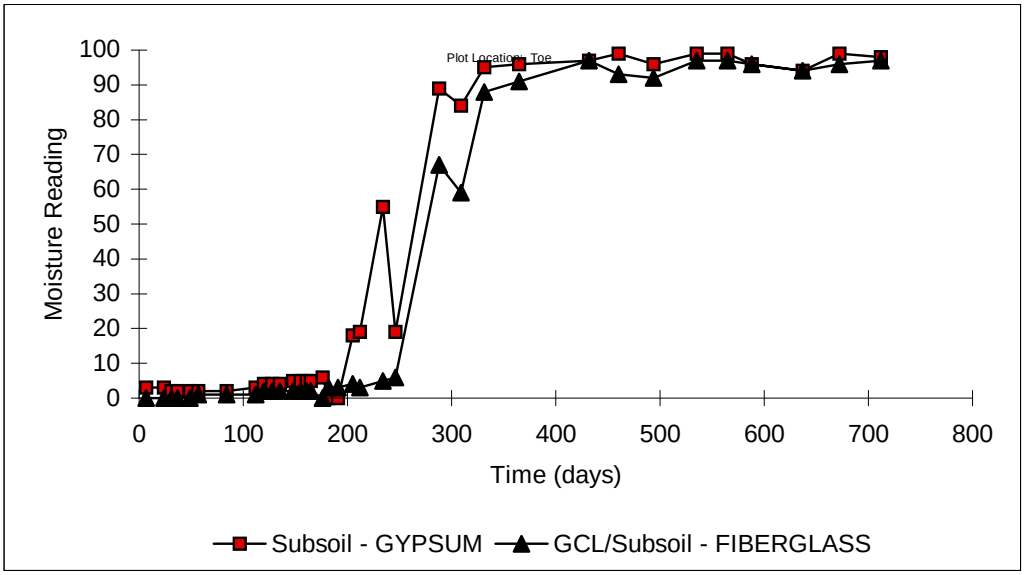

Figure D.3: MOISTURE READINGS VS. TIME FOR PLOT C
(Claymax - 3:1 Slope)

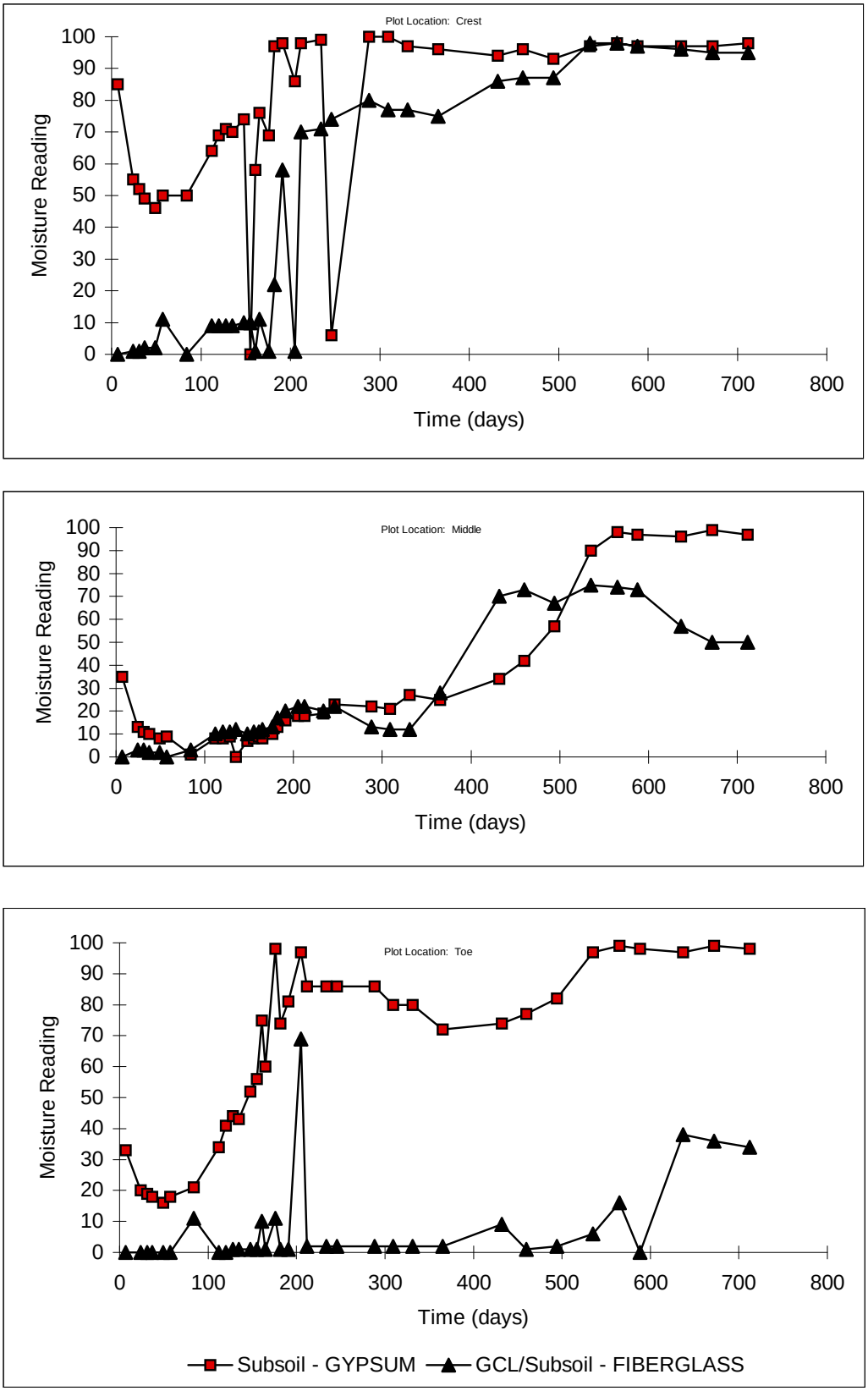

Figure D.4: MOISTURE READINGS VS. TIME FOR PLOT D
(Bentofix NS - 3:1 Slope)

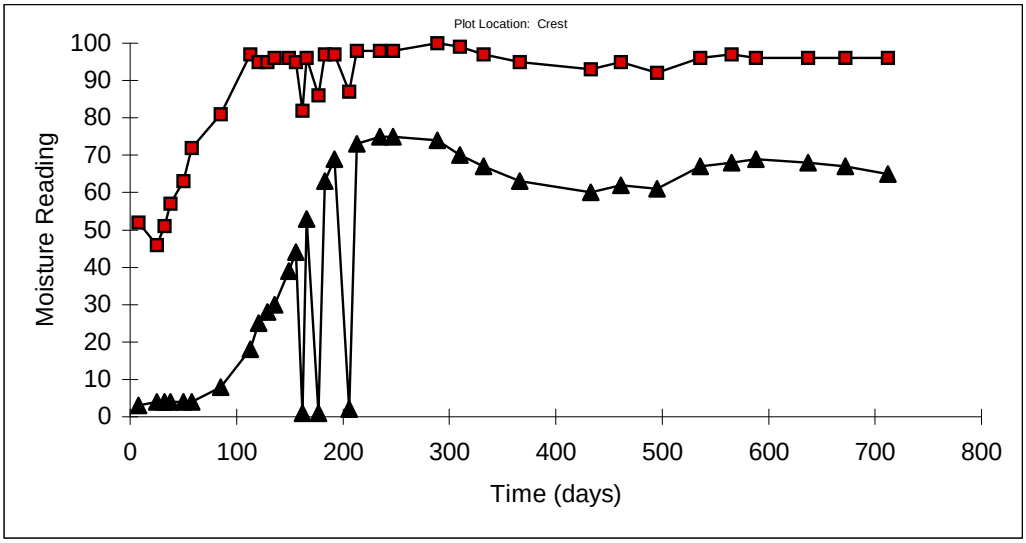

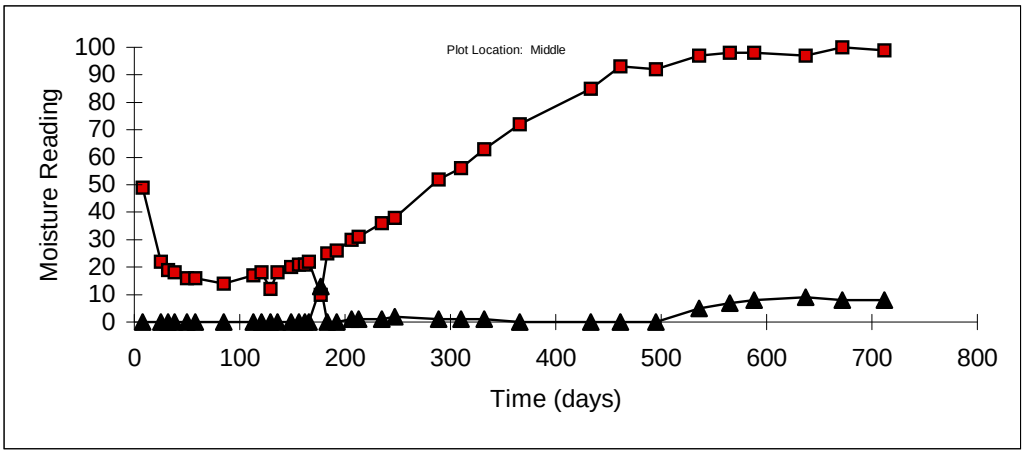

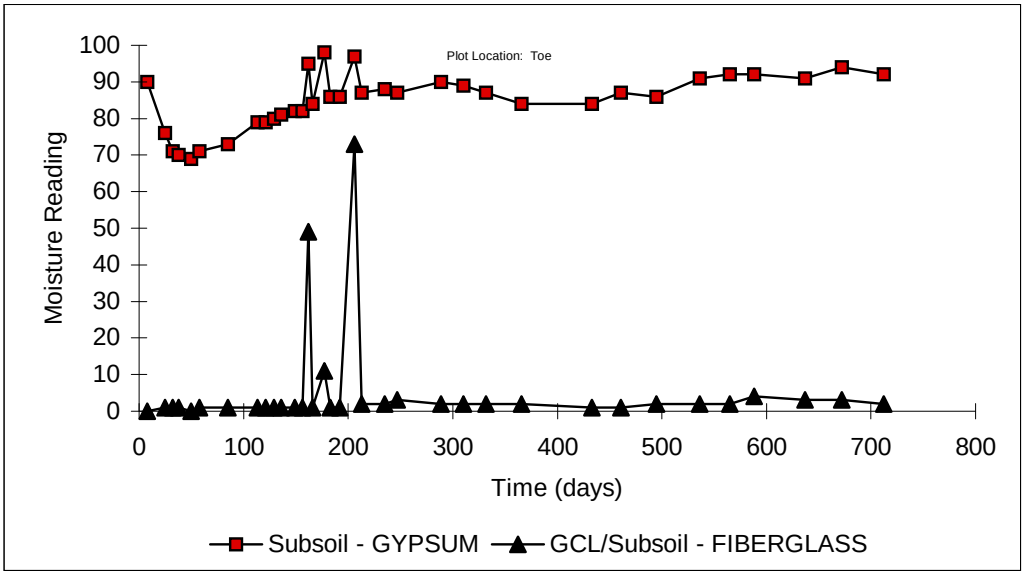

Figure D.5: MOISTURE READINGS VS. TIME FOR PLOT E
(Gundseal - Bentonite Side Down - 3:1 Slope)

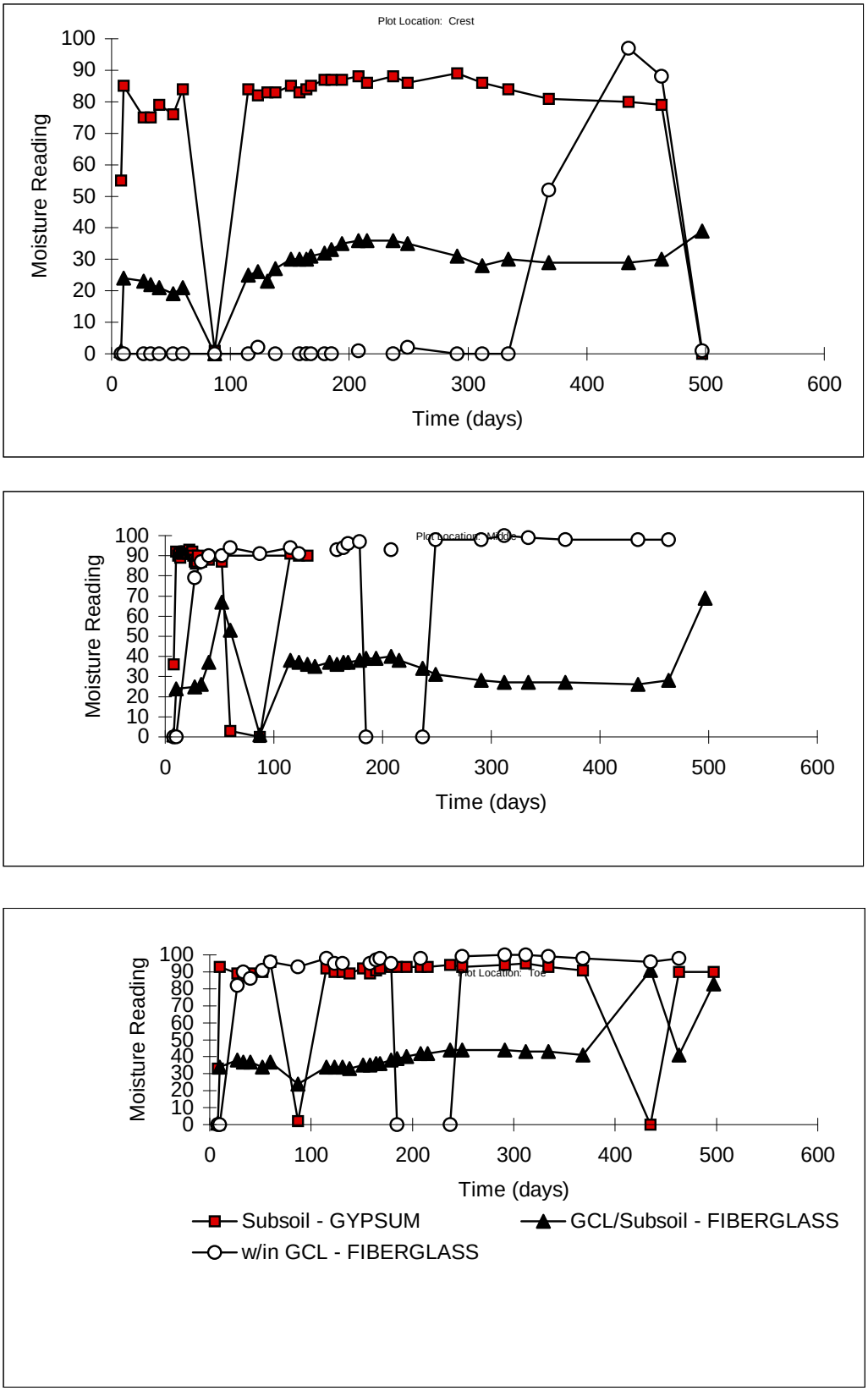

Figure D.6: MOISTURE READINGS VS. TIME FOR PLOT F
(Gundseal - Bentonite up - 2:1 Slope)

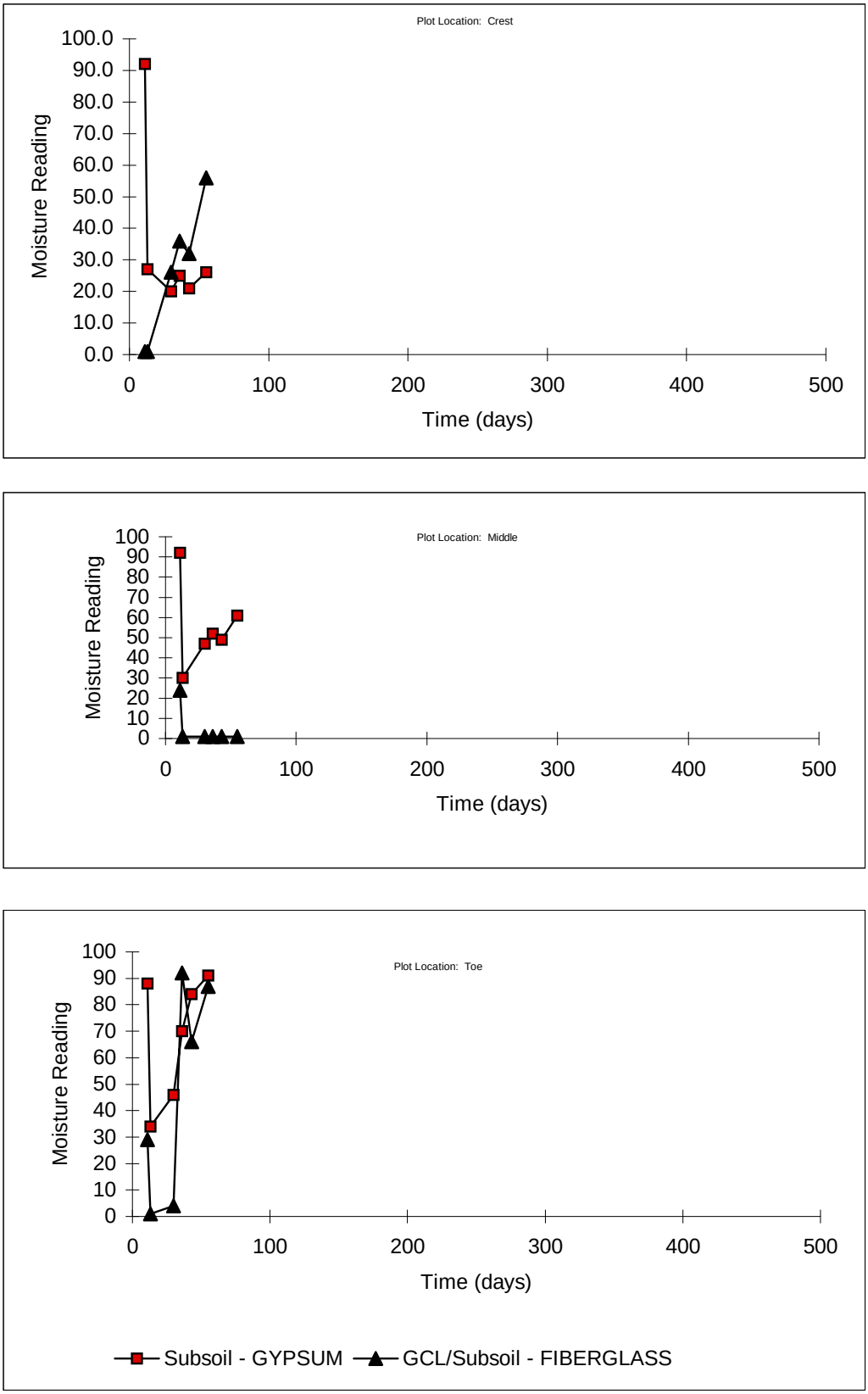

Figure D.7: MOISTURE READINGS VS. TIME FOR PLOT G
(Bentomat - 2:1 Slope)

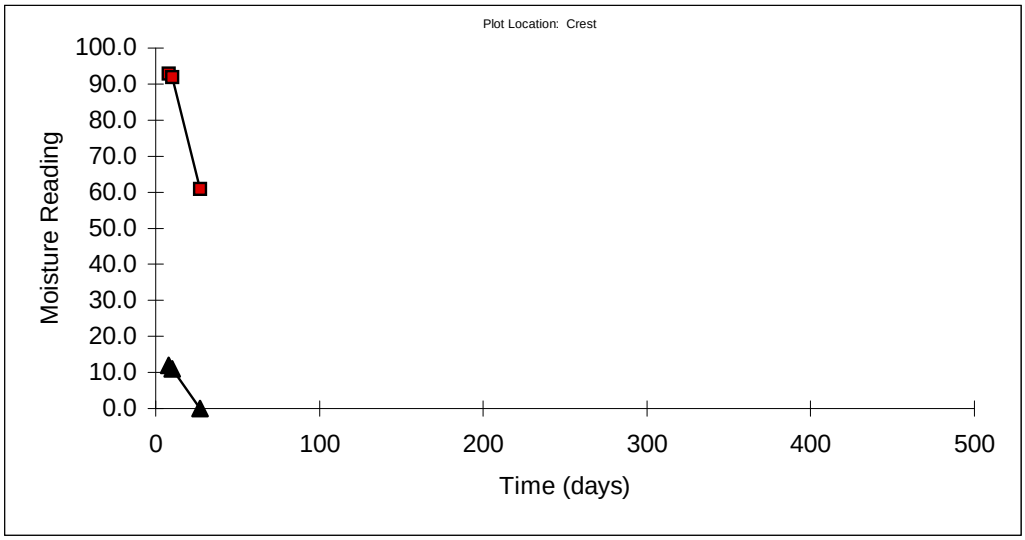

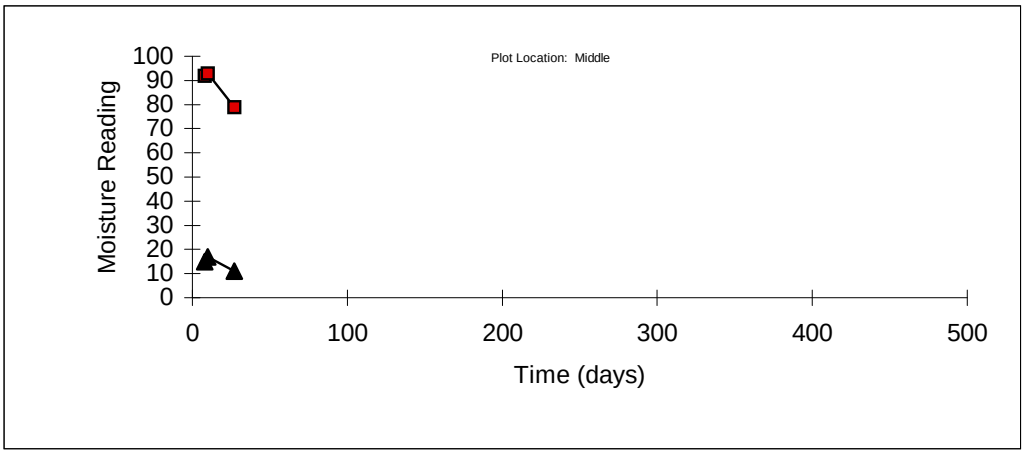

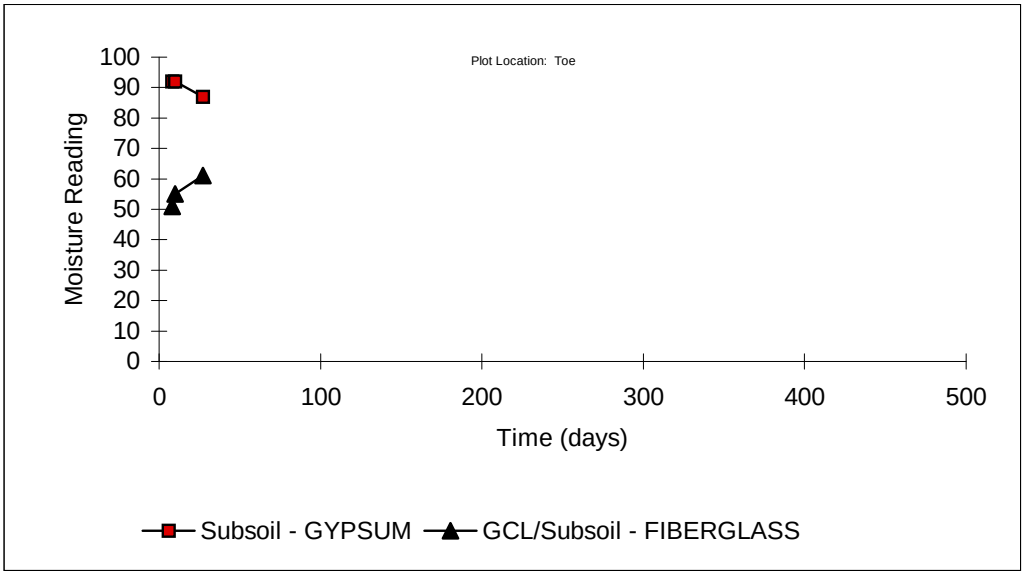

Figure D.8: MOISTURE READINGS VS. TIME FOR PLOT H
(Claymax - 2:1 Slope)

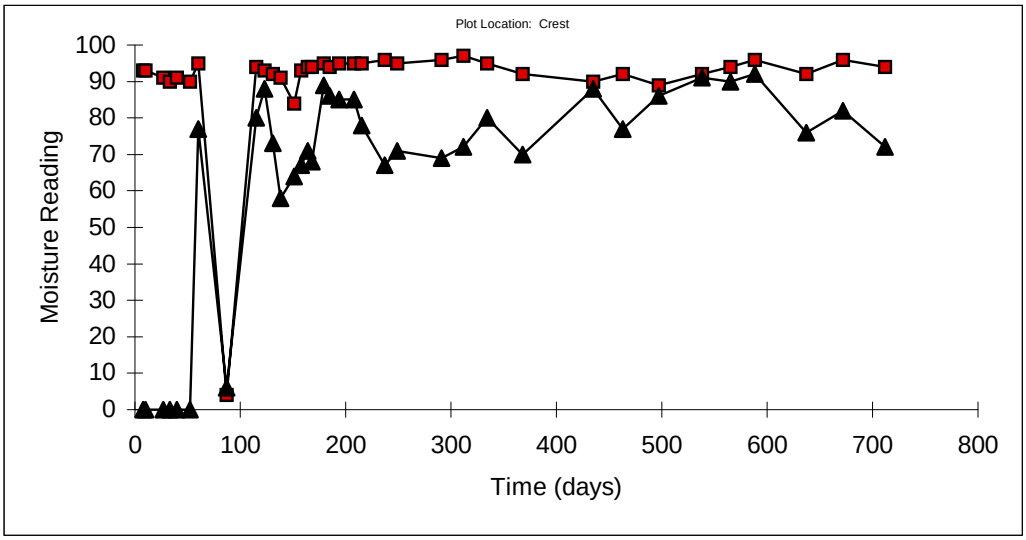

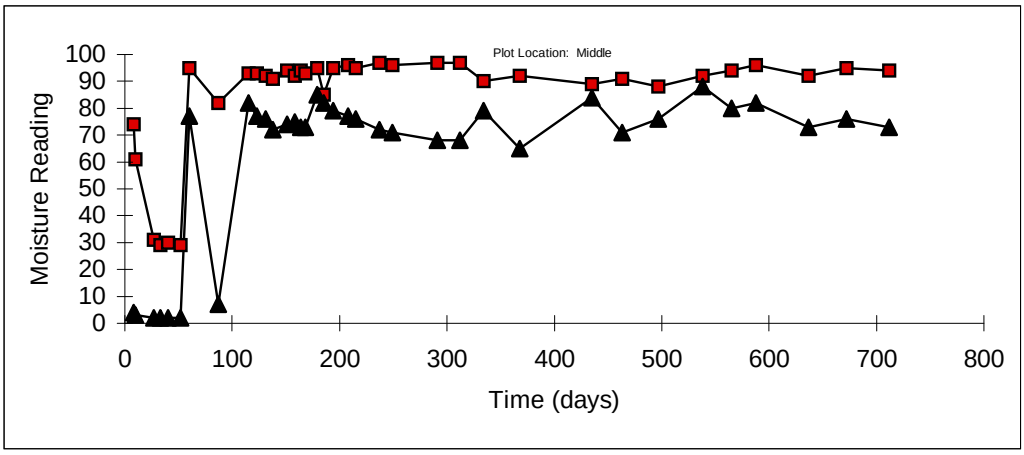

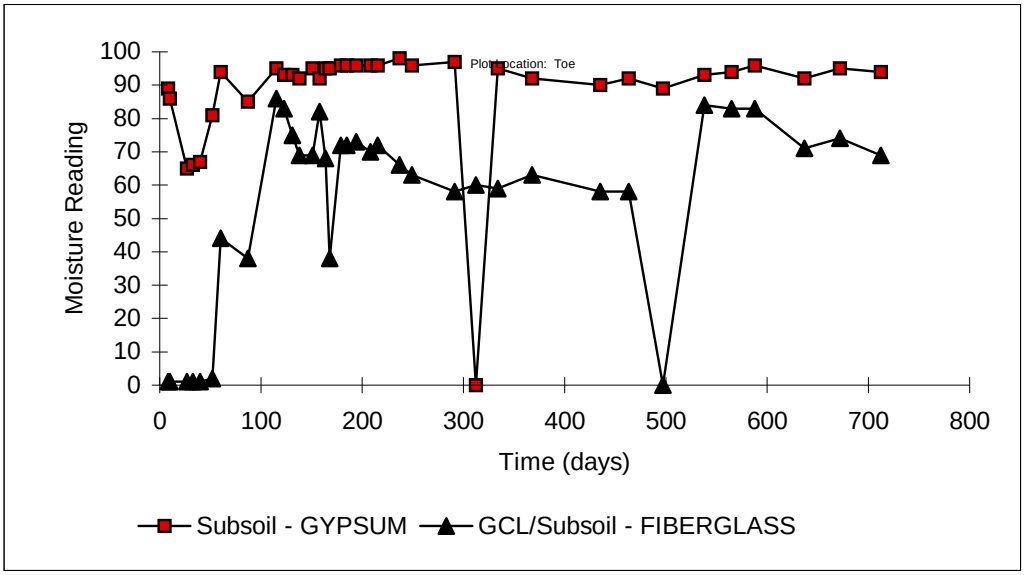

Figure D.9: MOISTURE READINGS VS. TIME FOR PLOT I
(Bentofix NW - 2:1 Slope)

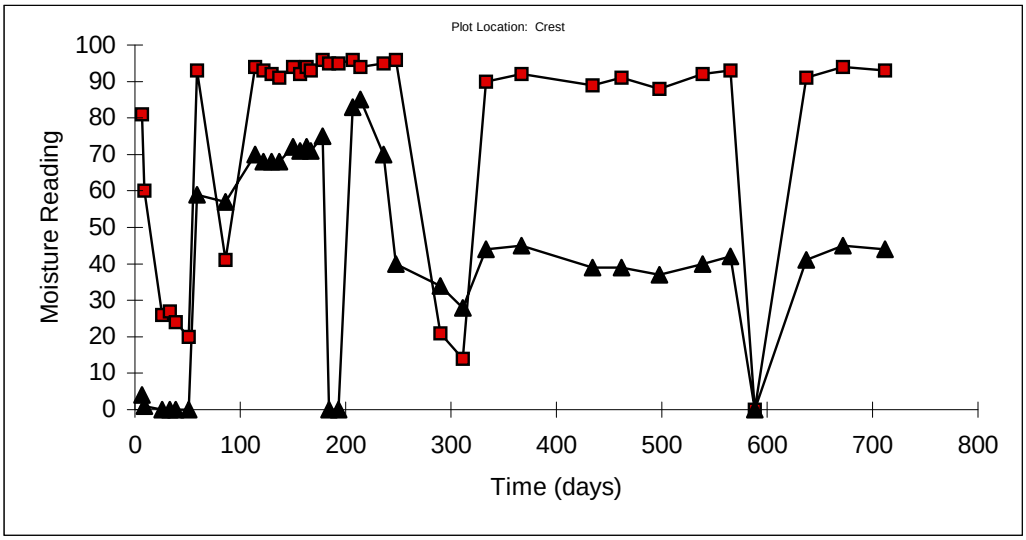

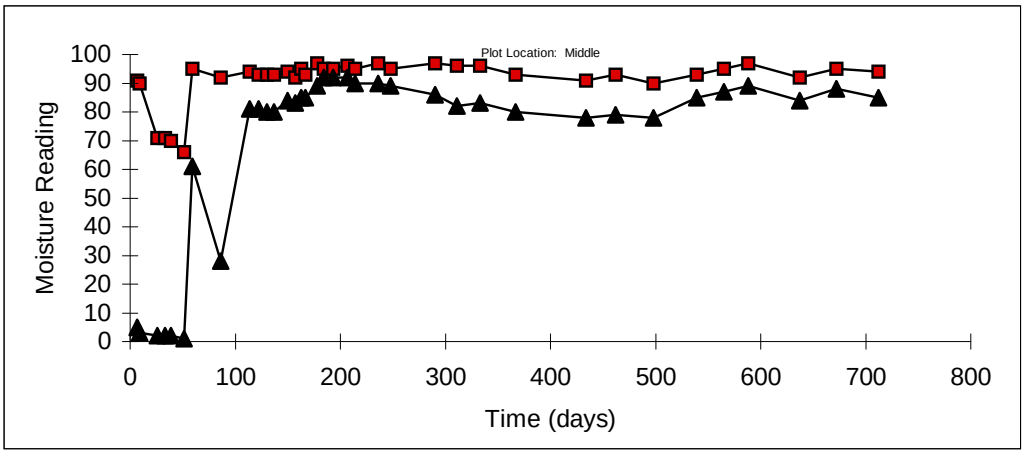

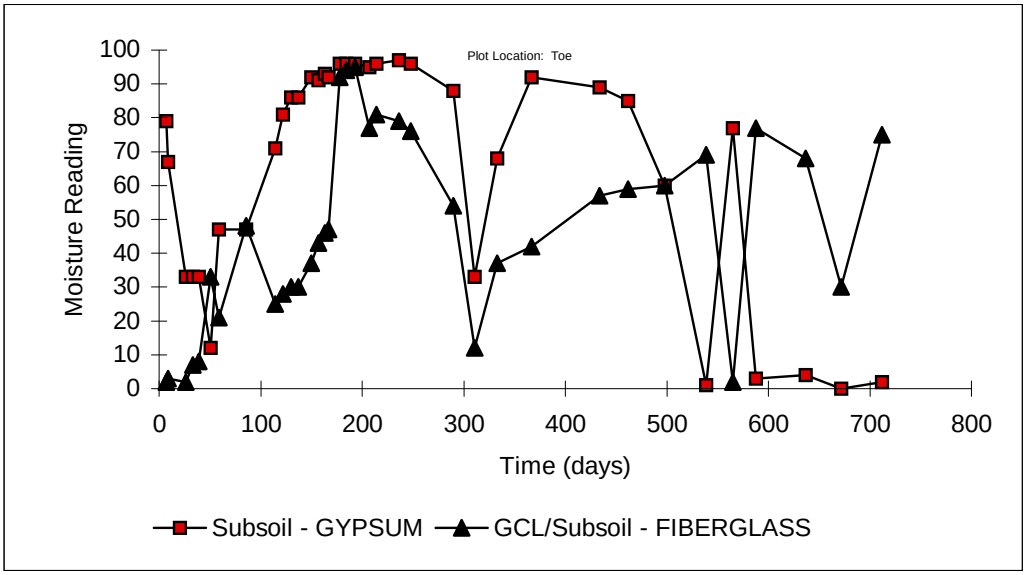

Figure D.10: MOISTURE READINGS VS. TIME FOR PLOT J
(Bentomat - Granular Drainage - 2:1 Slope)

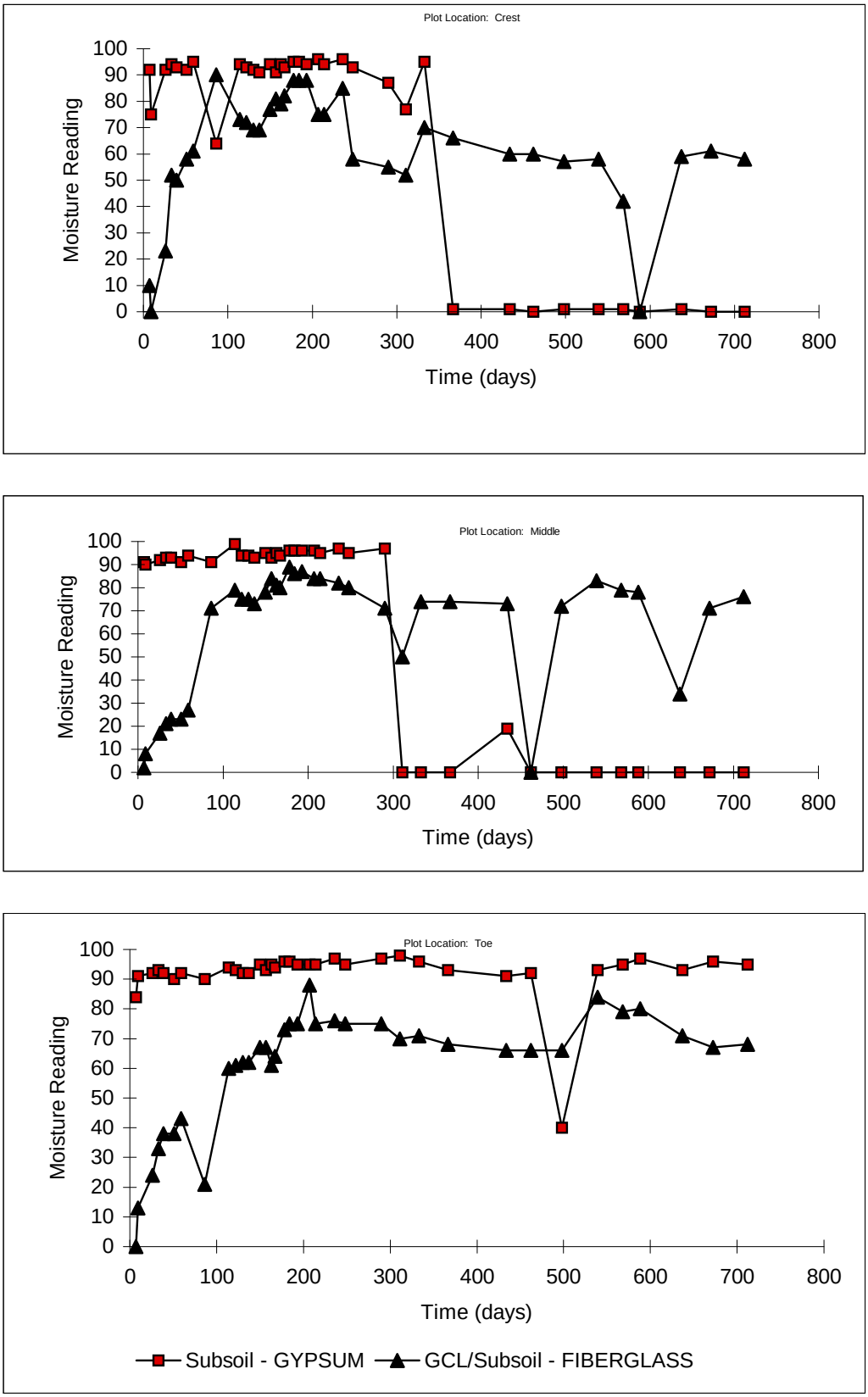

Figure D.11: MOISTURE READINGS VS. TIME FOR PLOT K
(Claymax - Granular Drainage - 2:1 Slope)

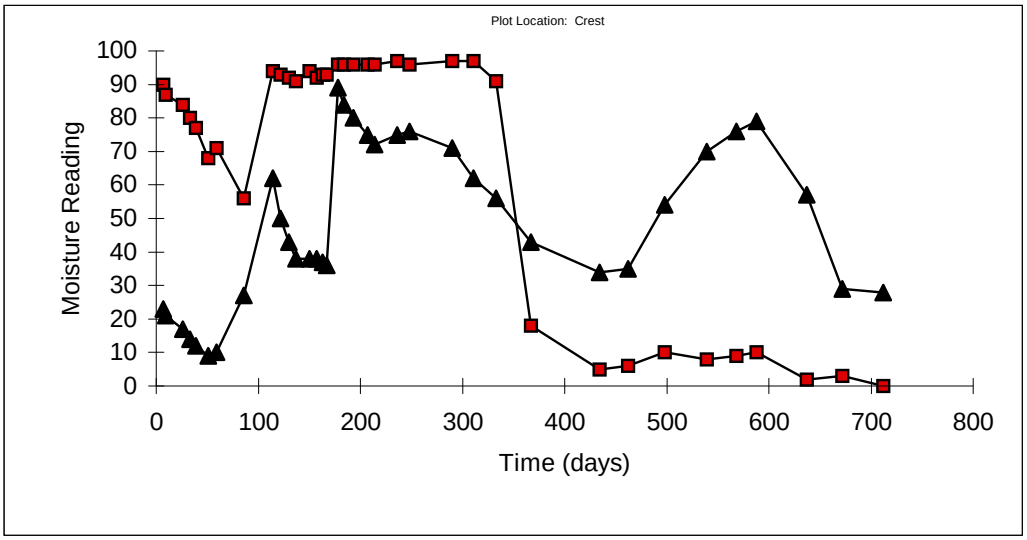

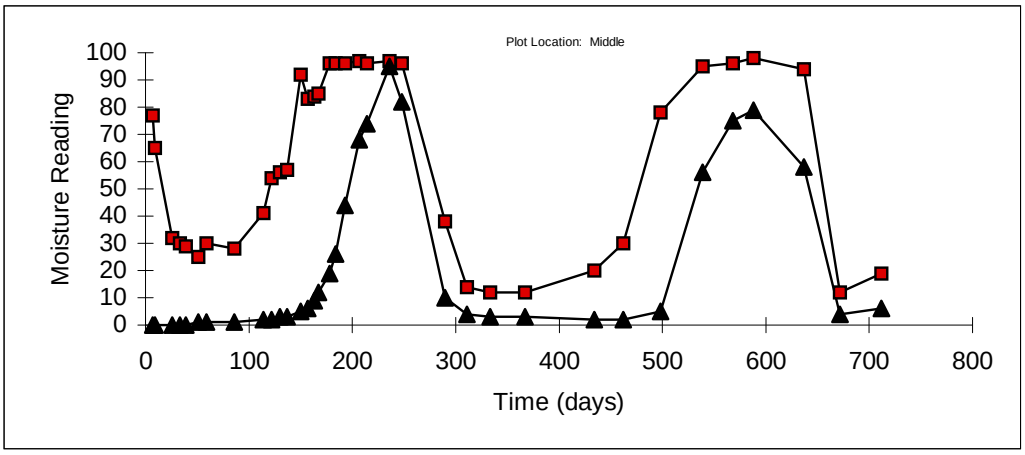

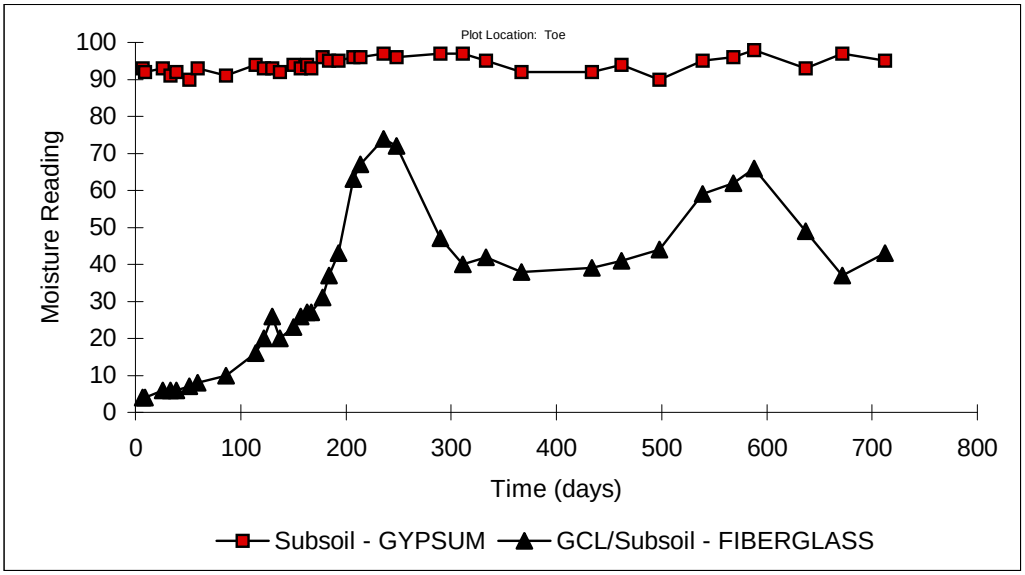

Figure D.12: MOISTURE READINGS VS. TIME FOR PLOT L
(Bentofix NW - Granular Drainage - 2:1 Slope)

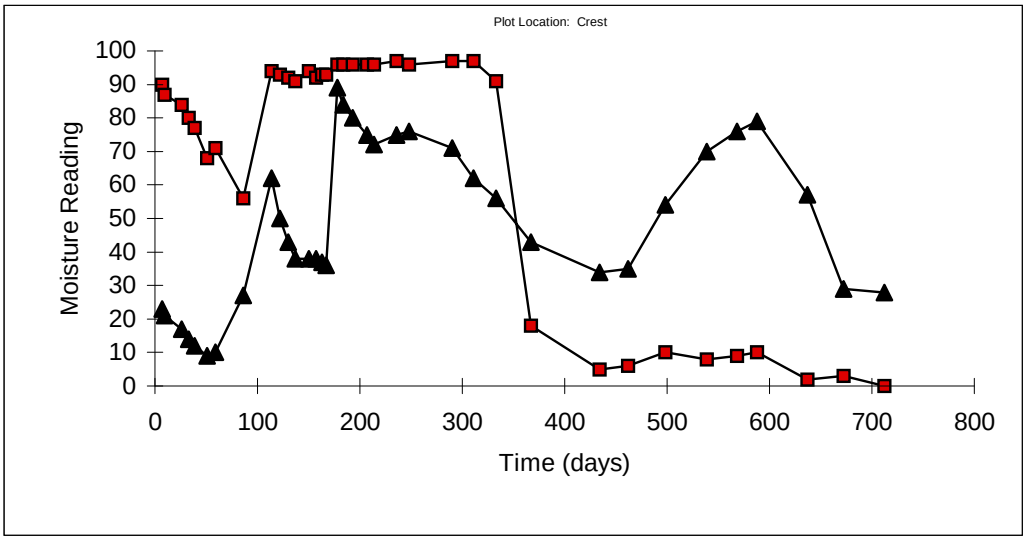

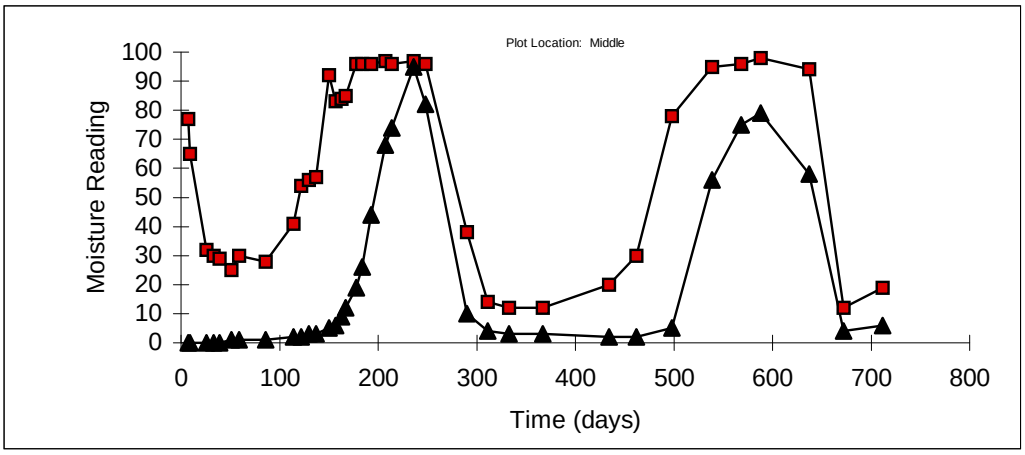

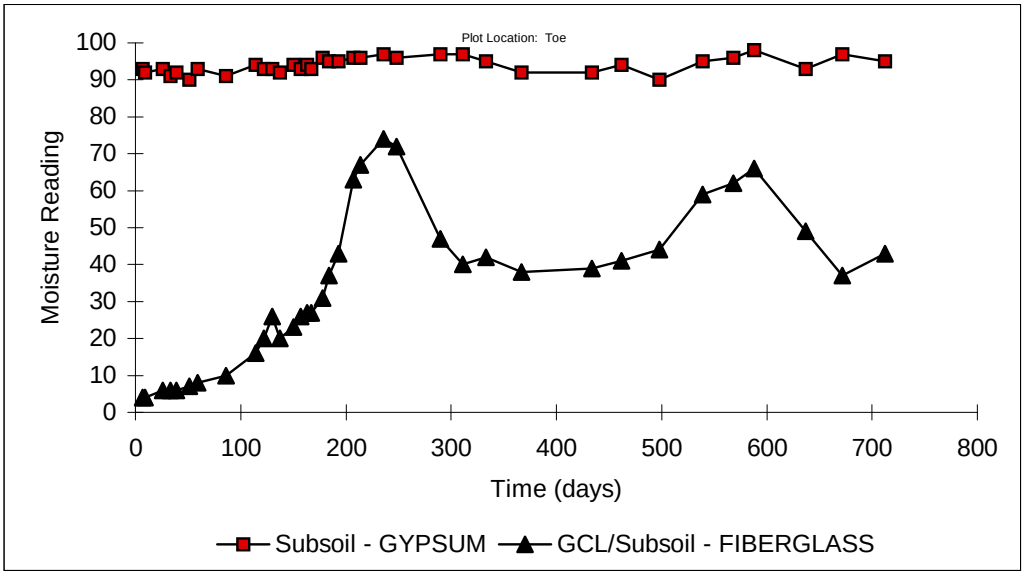

Figure D.12: MOISTURE READINGS VS. TIME FOR PLOT L
(Bentofix NW - Granular Drainage - 2:1 Slope)

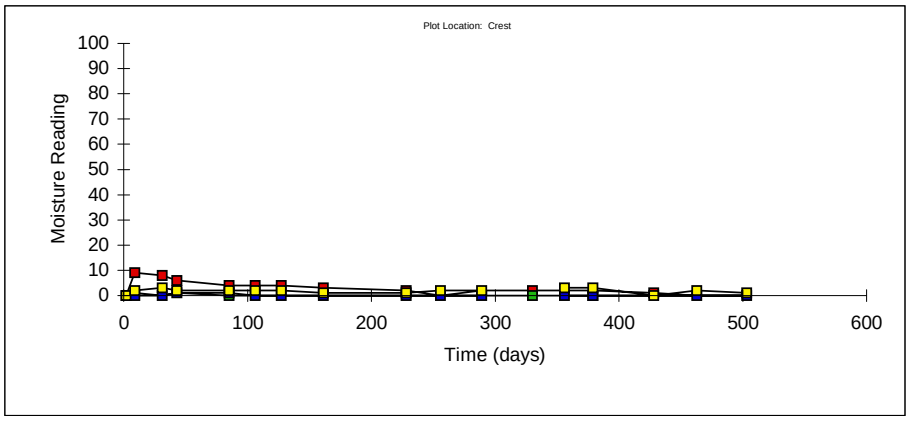

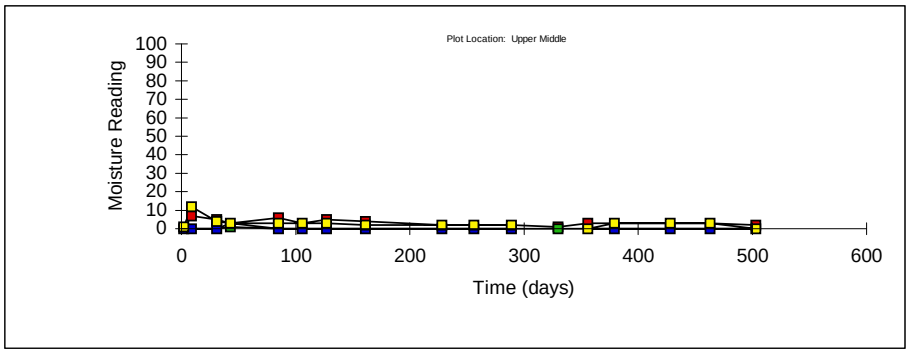

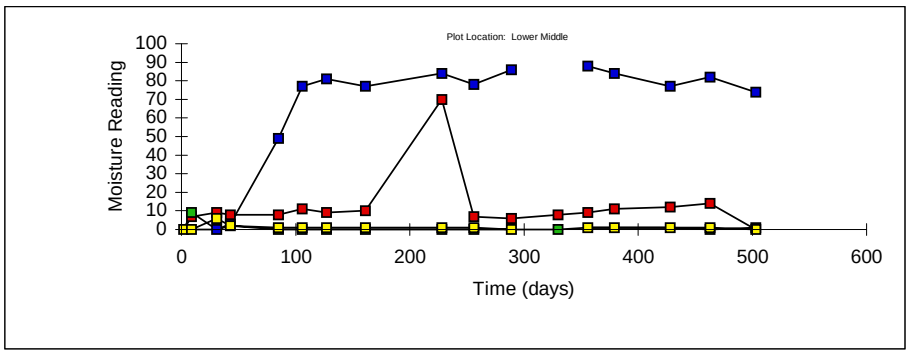

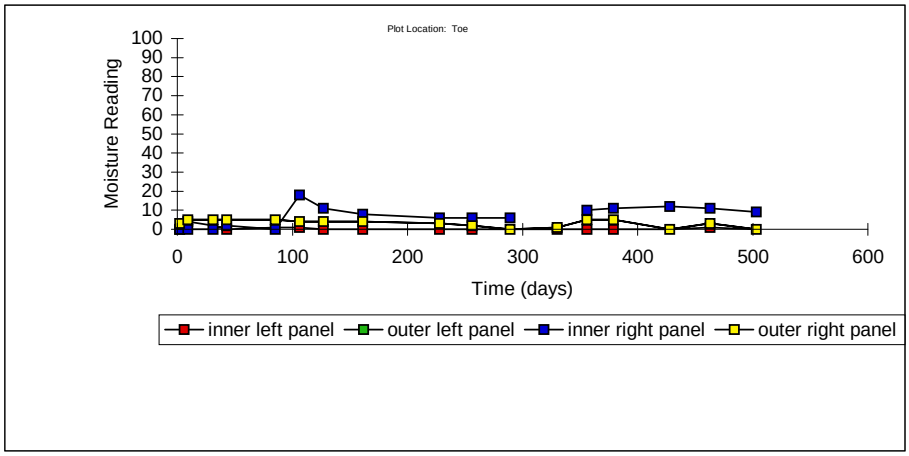

Figure D.14: MOISTURE READINGS VS. TIME FOR PLOT P
(Gundseal - Bentonite side up - 2:1 Slope)

Appendix D

Attachment 5

Results of Laboratory Direct Shear Tests Performed on 64-mm-Wide Specimens in University of Texas Laboratories

(Results Described in Section D-7)

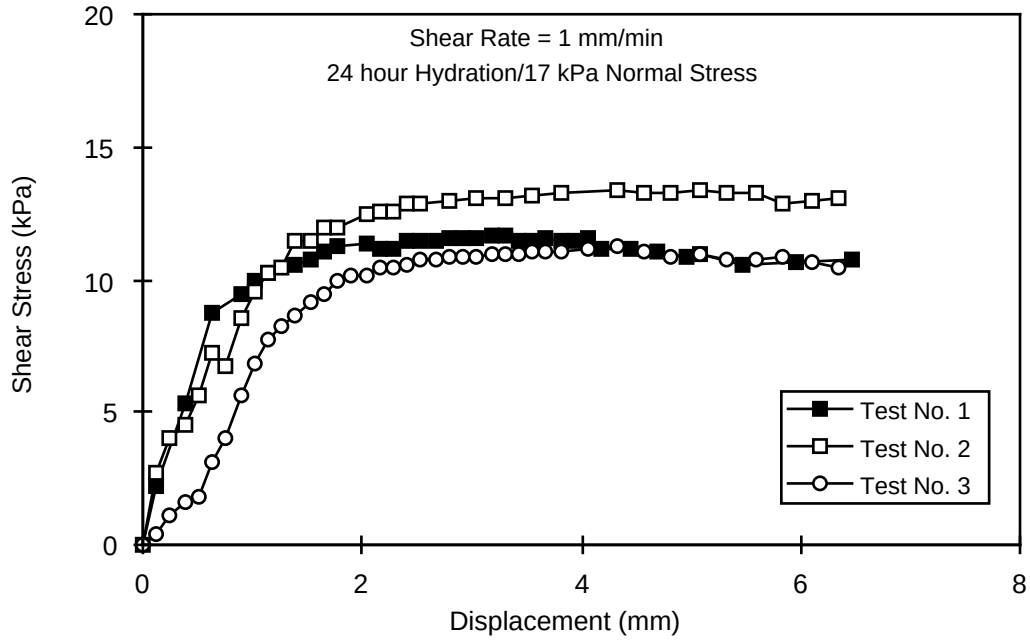

Figure 1: Shear Stress vs. Displacement for Test No. 1, 2, and 3

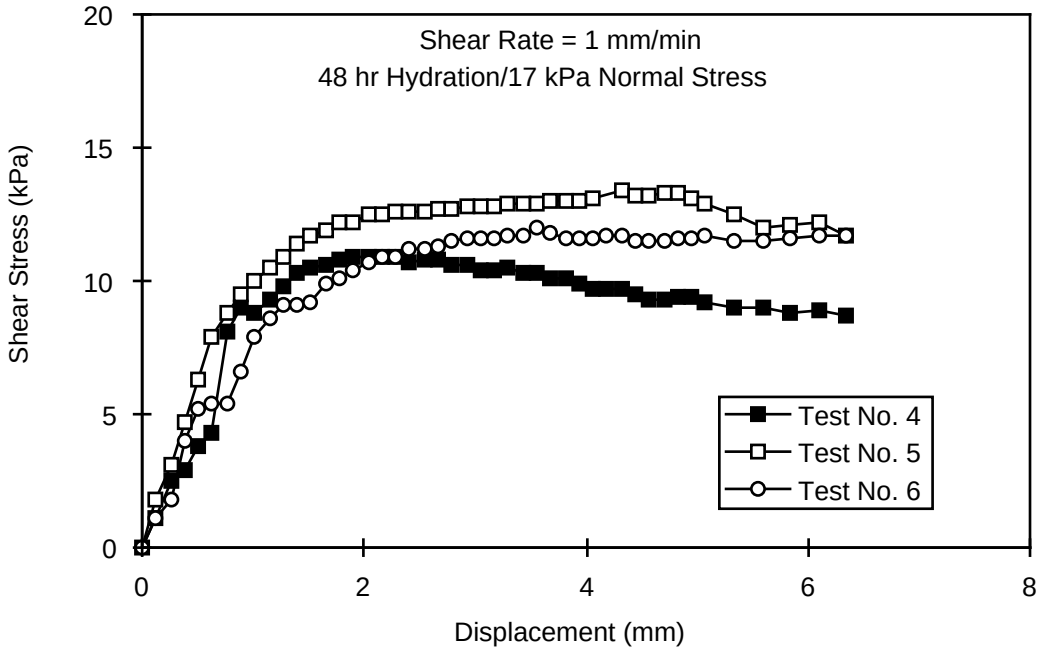

Figure 2: Shear Stress vs. Displacement for Test No. 4, 5, and 6

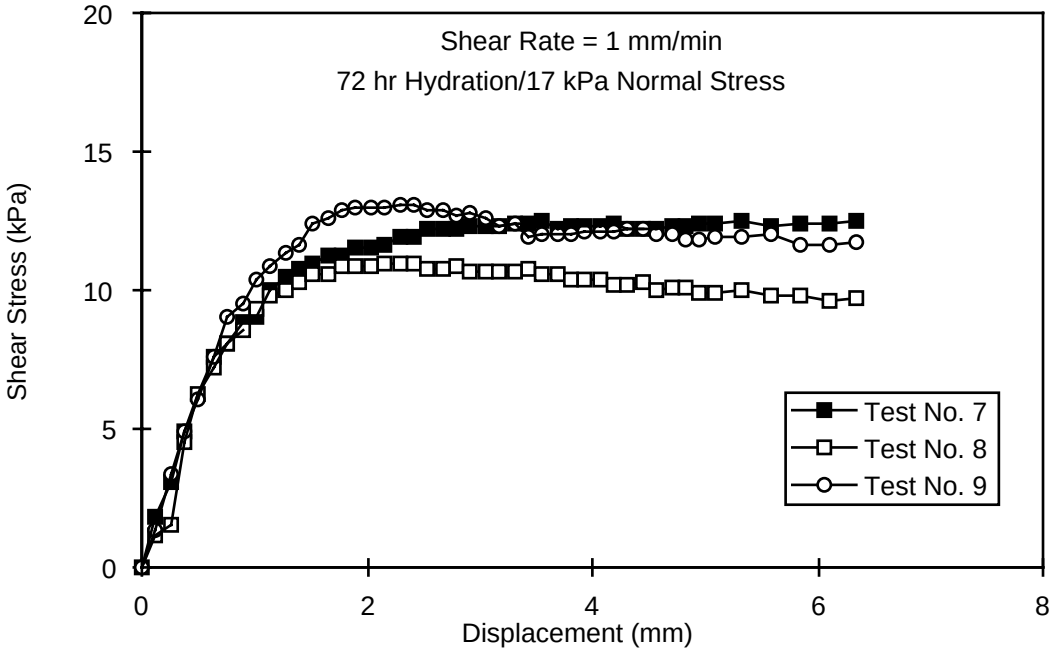

Figure 3: Shear Stress vs. Displacement for Test No. 7, 8, and 9

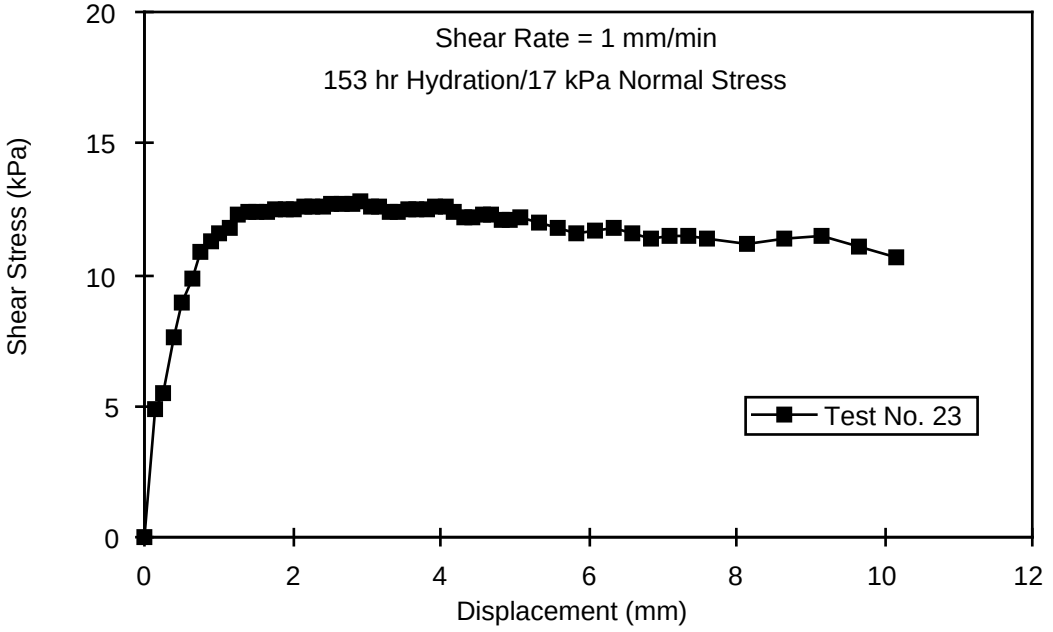

Figure 4: Shear Stress vs. Displacement for Test No. 23

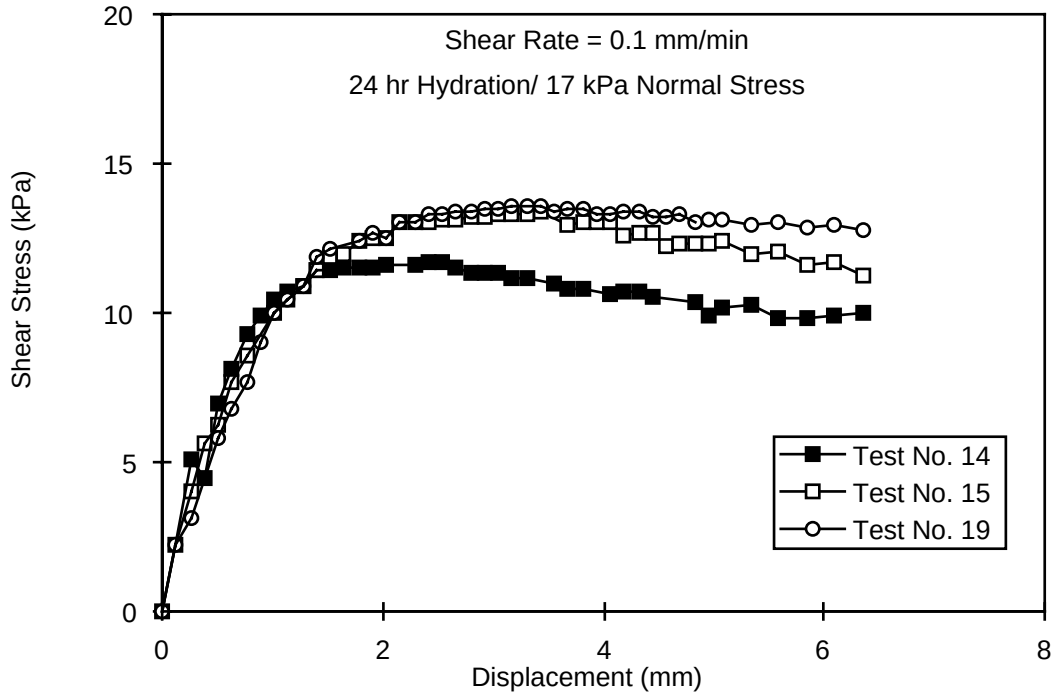

Figure 5: Shear Stress vs. Displacement for Test No. 14, 15, and 19

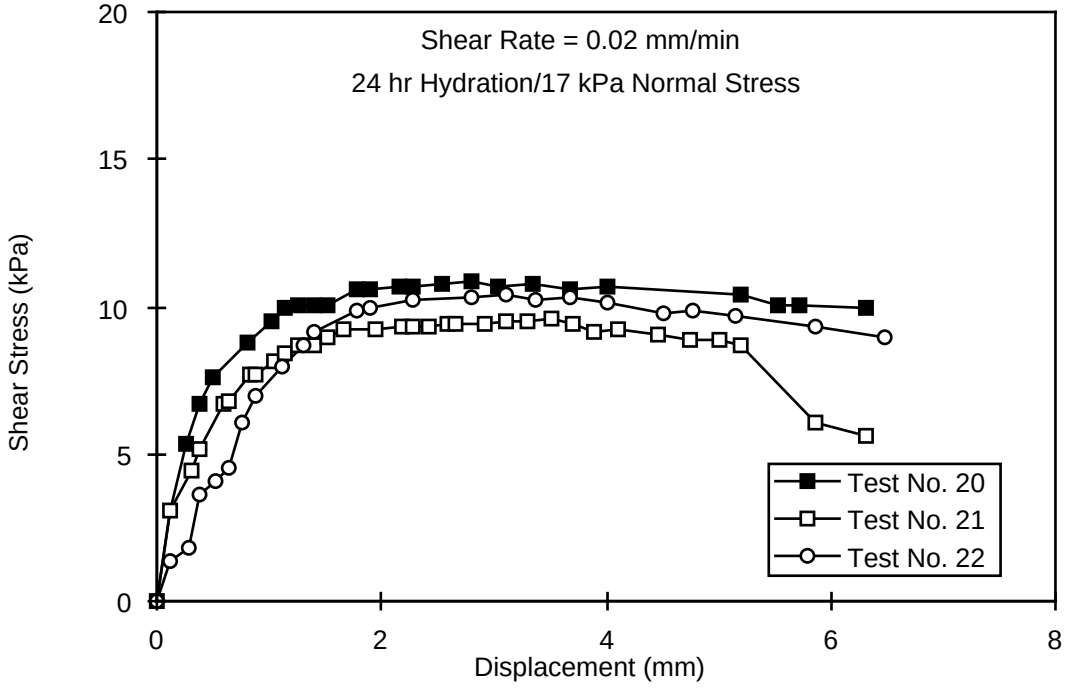

Figure 6: Shear Stress vs. Displacement for Test No. 20, 21, and 22

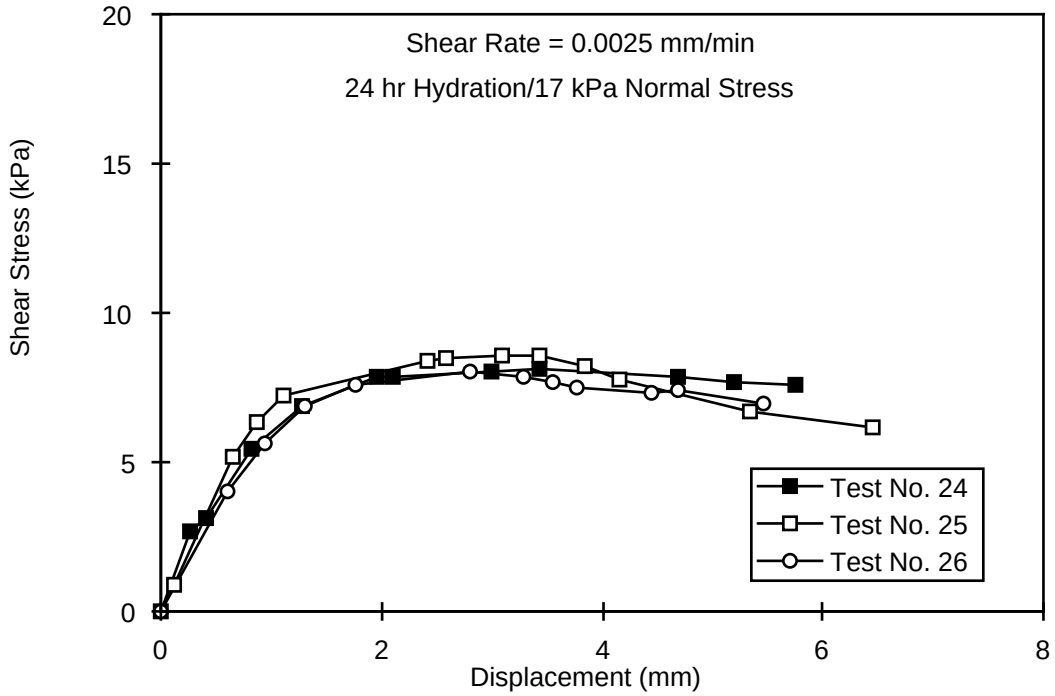

Figure 7: Shear Stress vs. Displacement for Test No. 24, 25, and 26

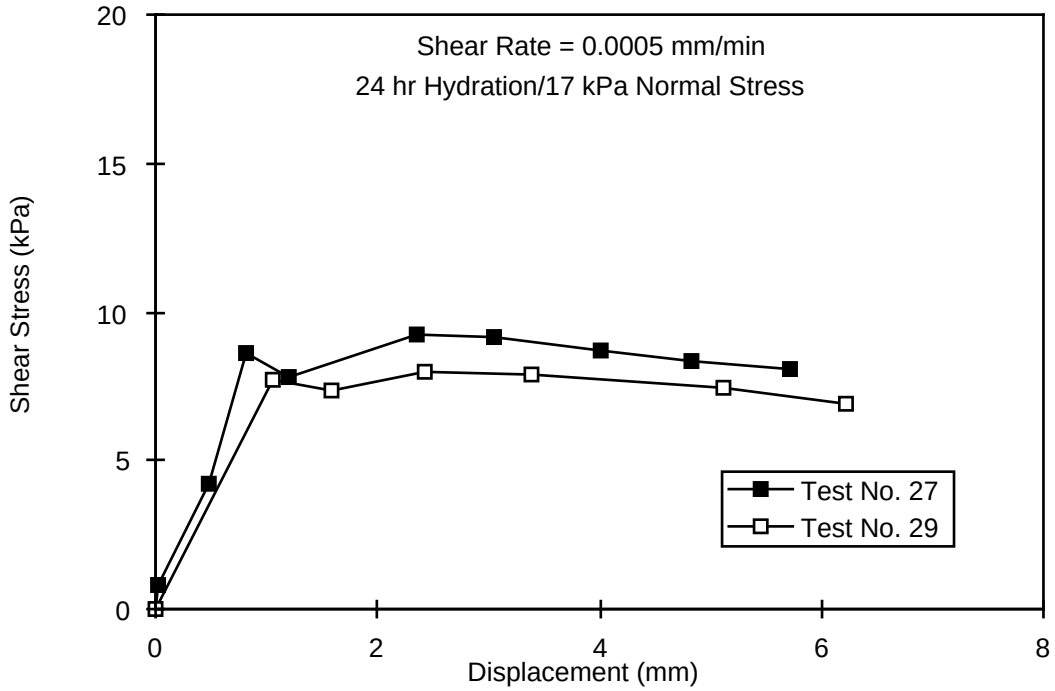

Figure 8: Shear Stress vs. Displacement for Test No. 27 and 29

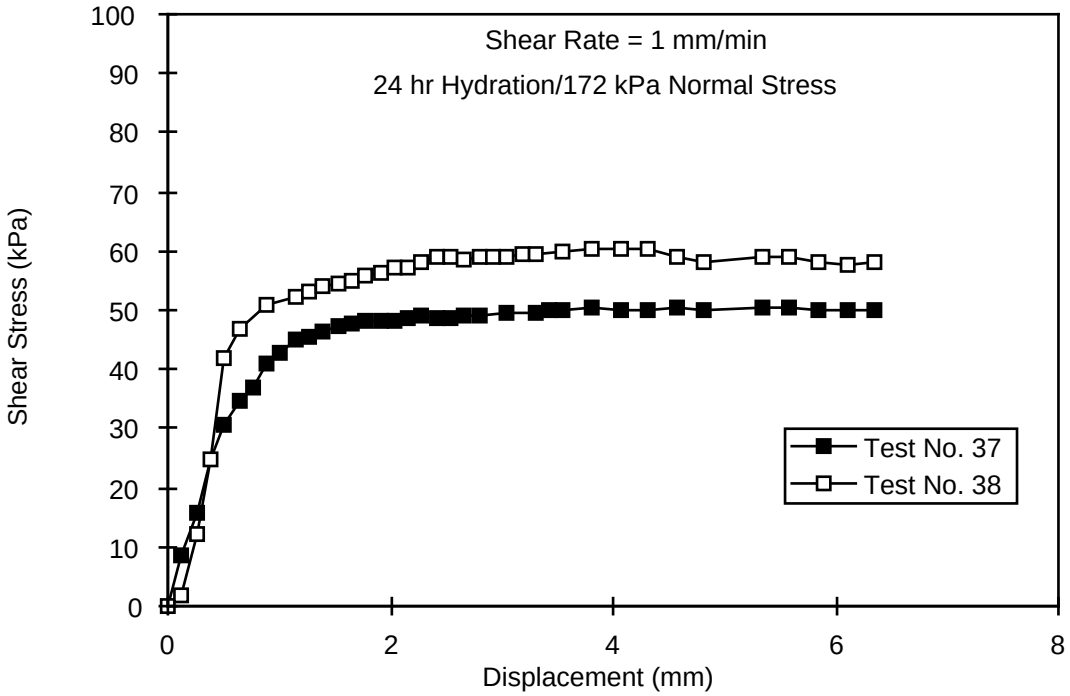

Figure 9: Shear Stress vs. Displacement for Test No. 37 and 38

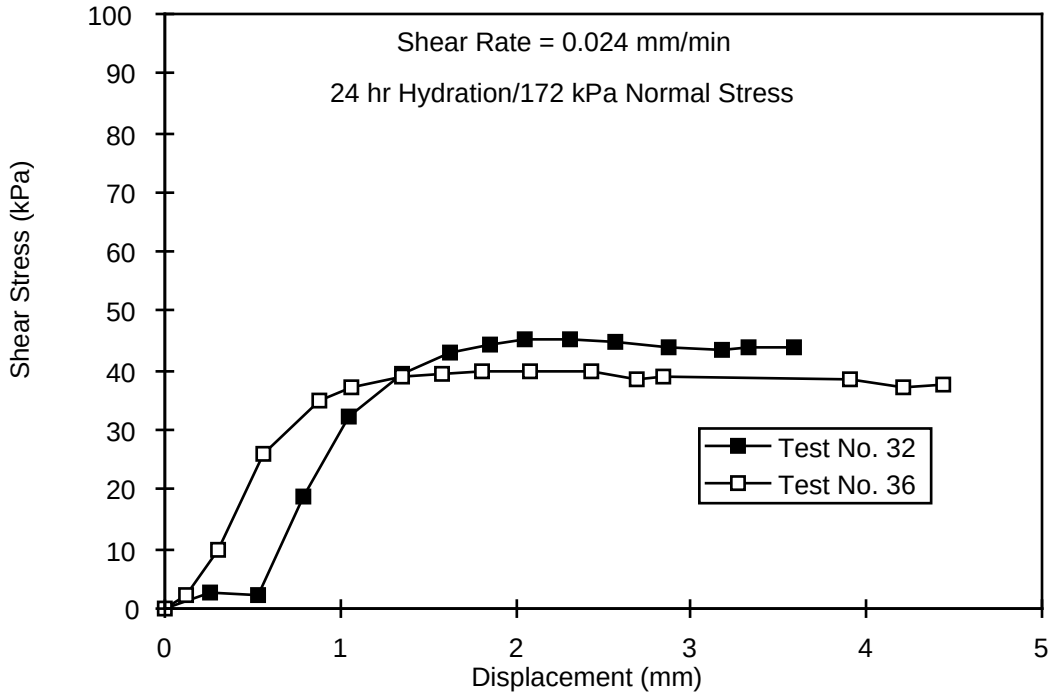

Figure 10: Shear Stress vs. Displacement for Test No. 32 and 36

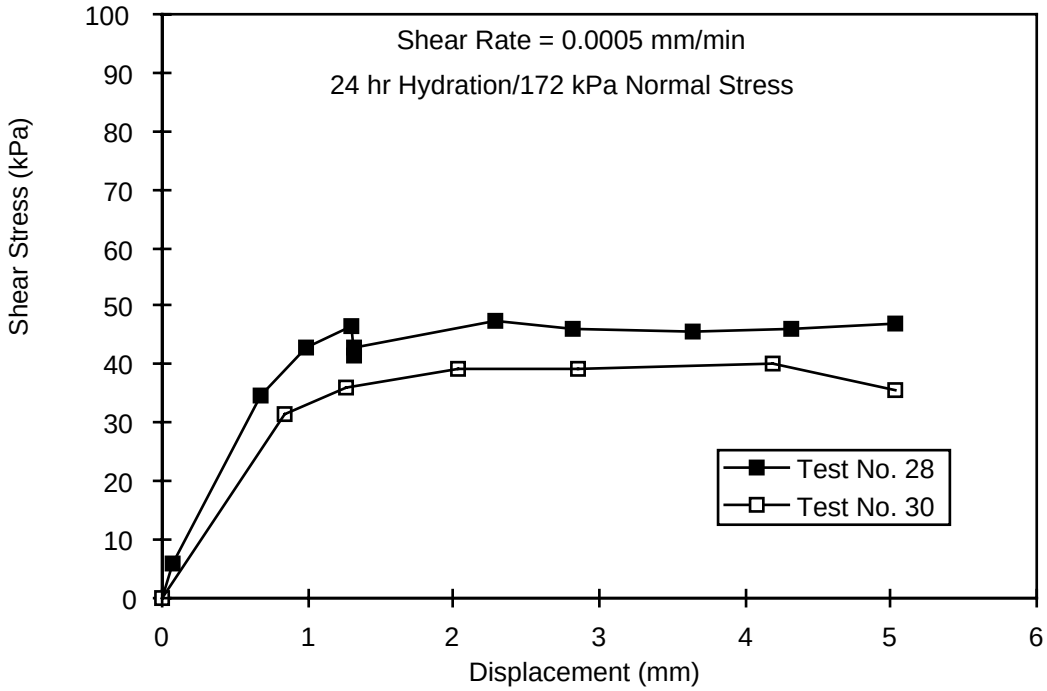

Figure 11: Shear Stress vs. Displacement for Test No. 28 and 30

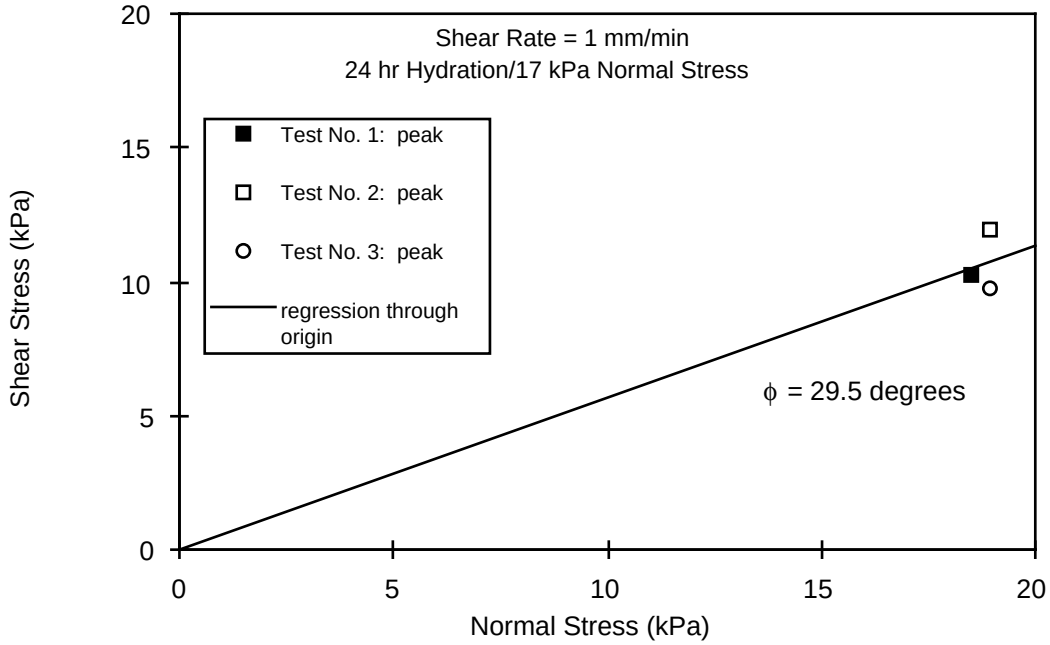

Figure 12: Mohr-Coulomb Diagram for Test No. 1, 2, and 3

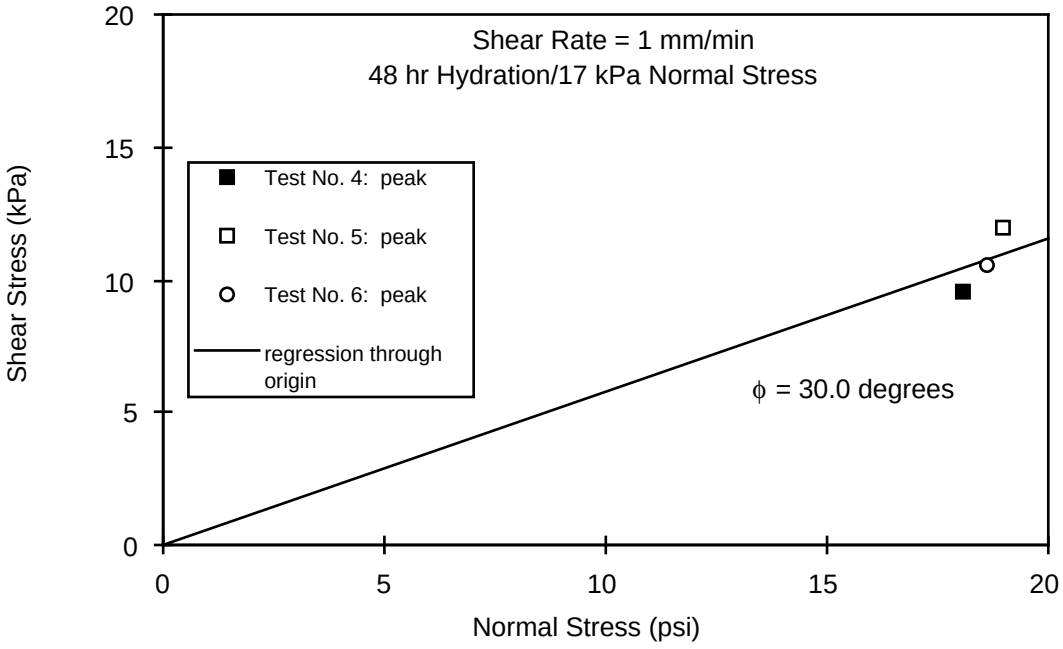

Figure 13: Mohr-Coulomb Diagram for Test No. 4, 5, and 6

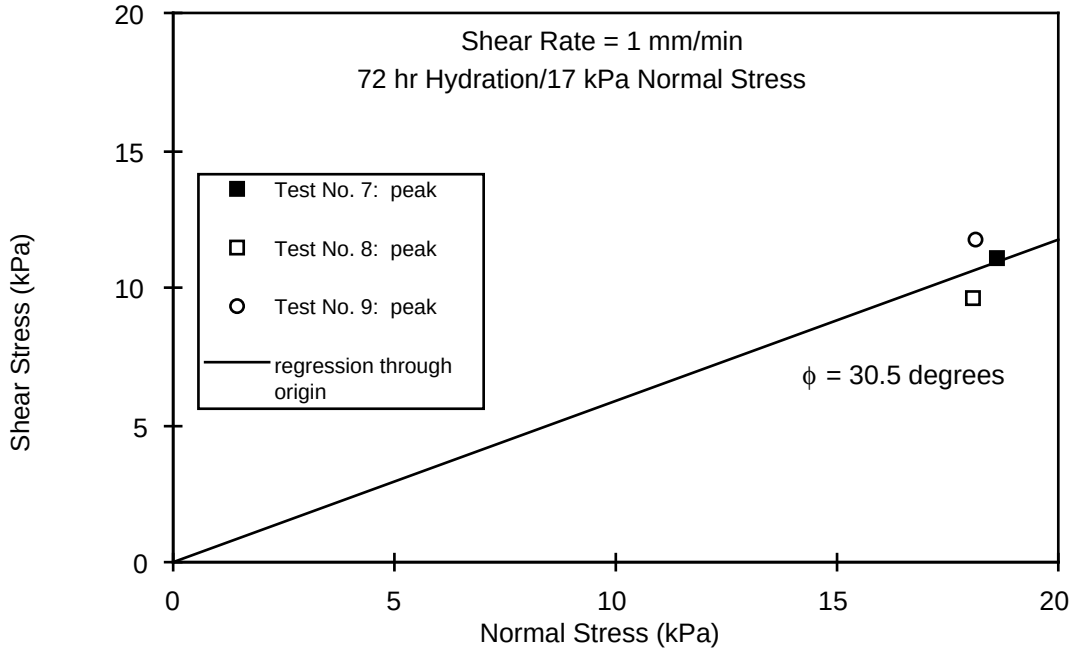

Figure 14: Mohr-Coulomb Diagram for Test No. 7, 8, and 9

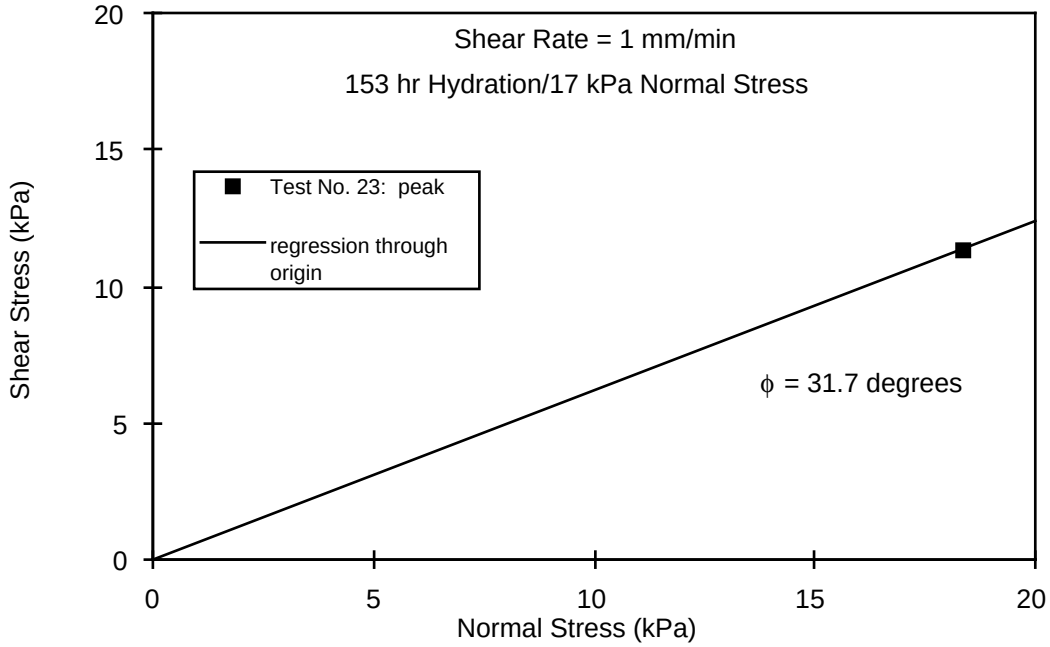

Figure 15: Mohr-Coulomb Diagram for Test No. 23

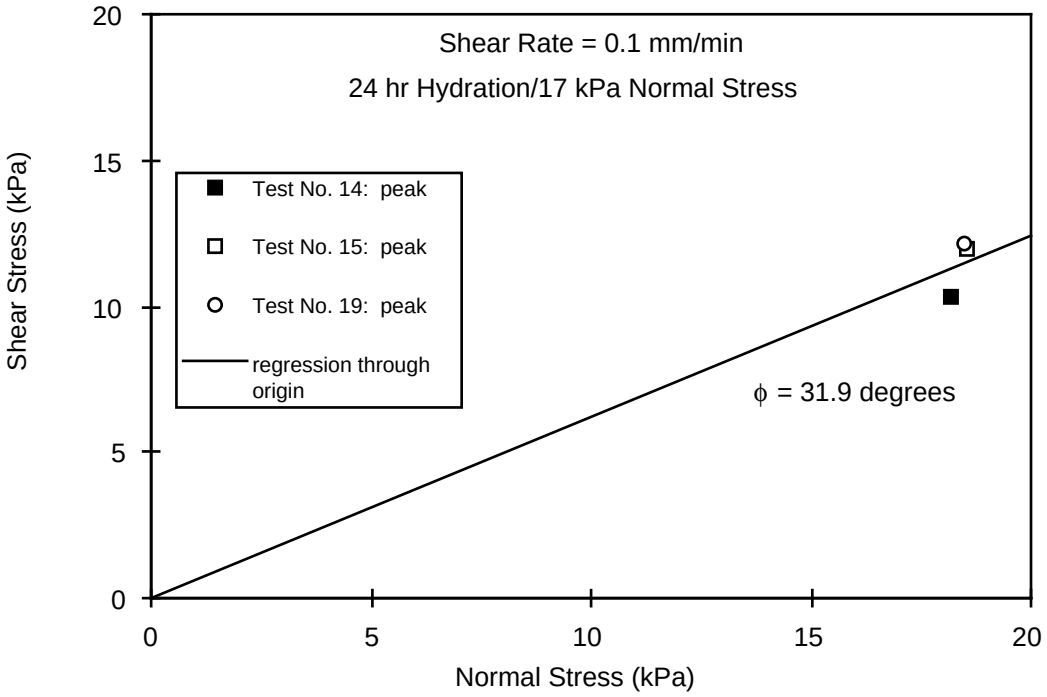

Figure 16: Mohr-Coulomb Diagram for Test No. 14, 15, and 19

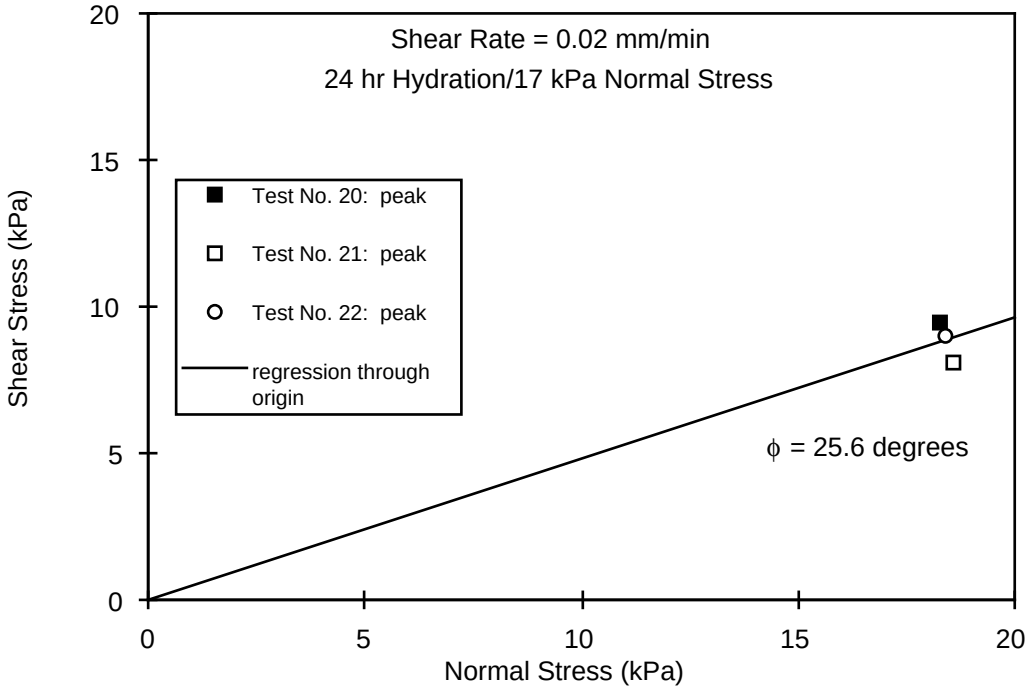

Figure 17: Mohr-Coulomb Diagram for Test No. 20, 21, and 22

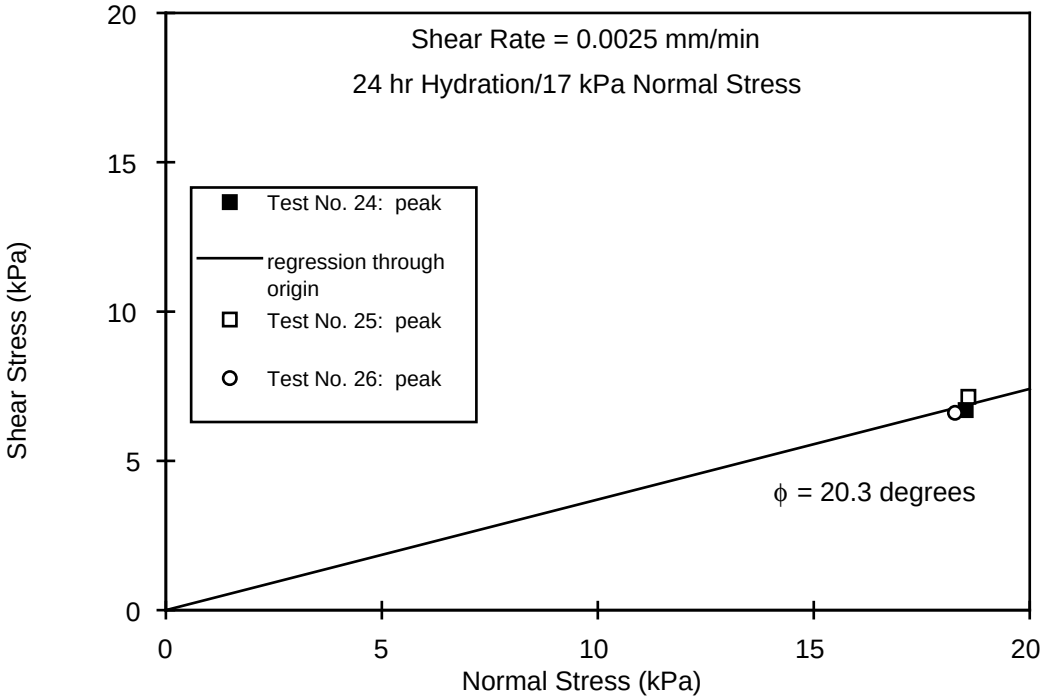

Figure 18: Mohr-Coulomb Diagram for Test No. 24, 25, and 26

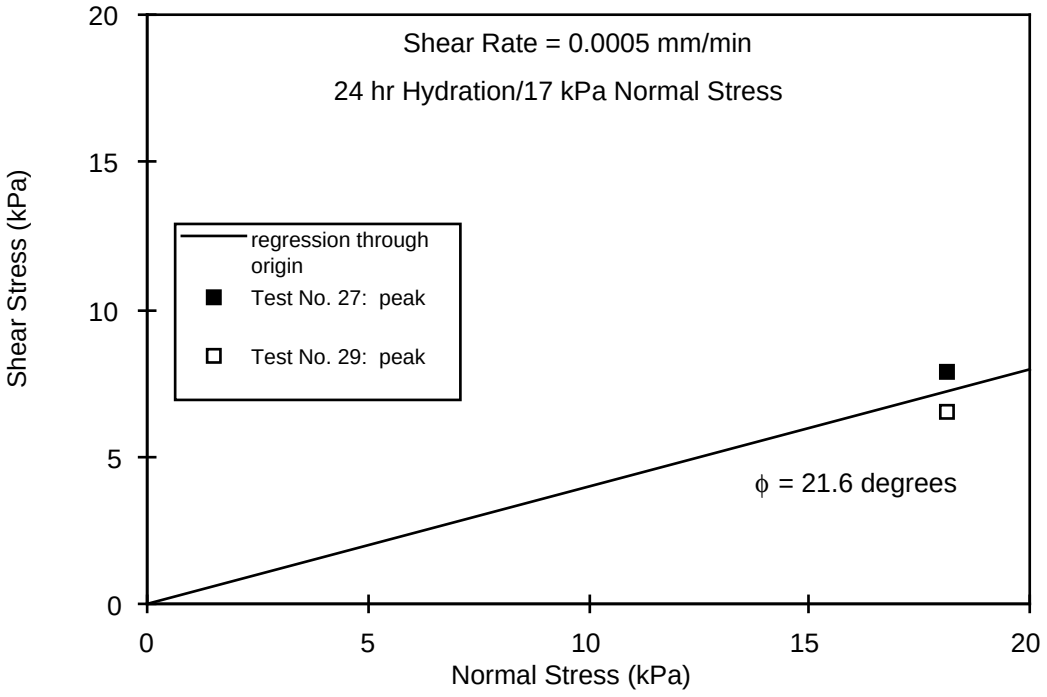

Figure 19: Mohr-Coulomb Diagram for Test No. 27 and 29

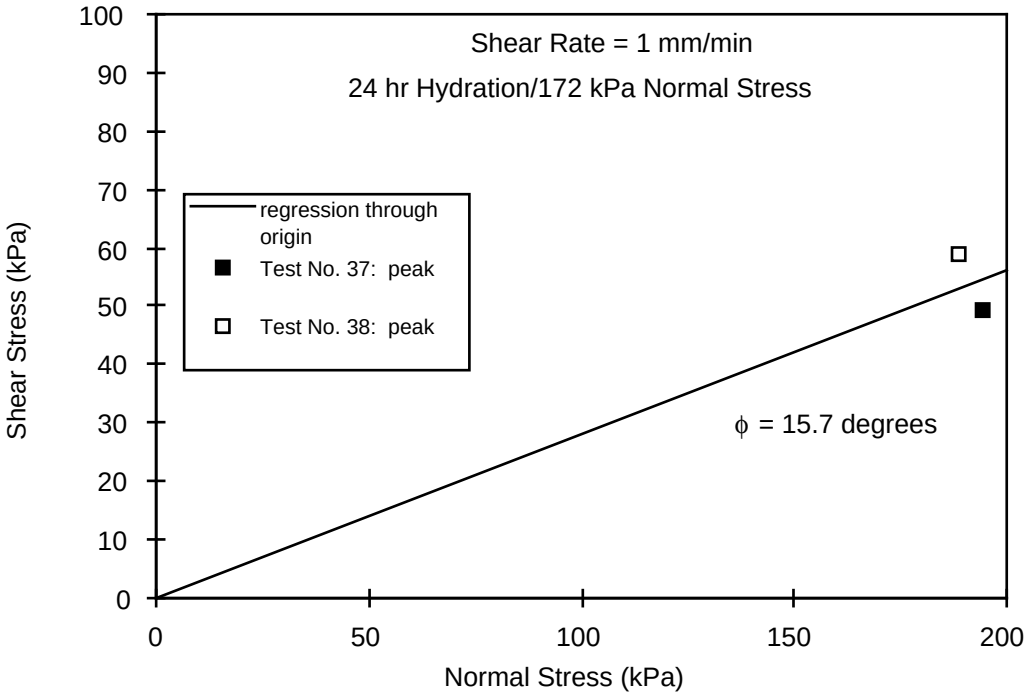

Figure 20: Mohr-Coulomb Diagram for Test No. 37 and 38

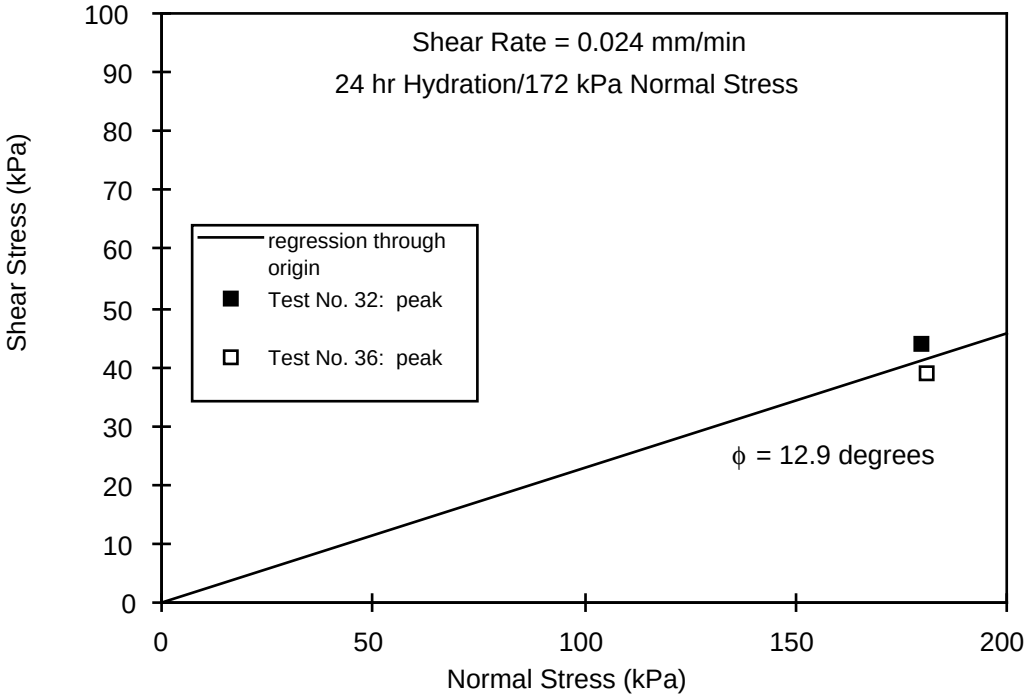

Figure 21: Mohr-Coulomb Diagram for Test No. 32 and 36

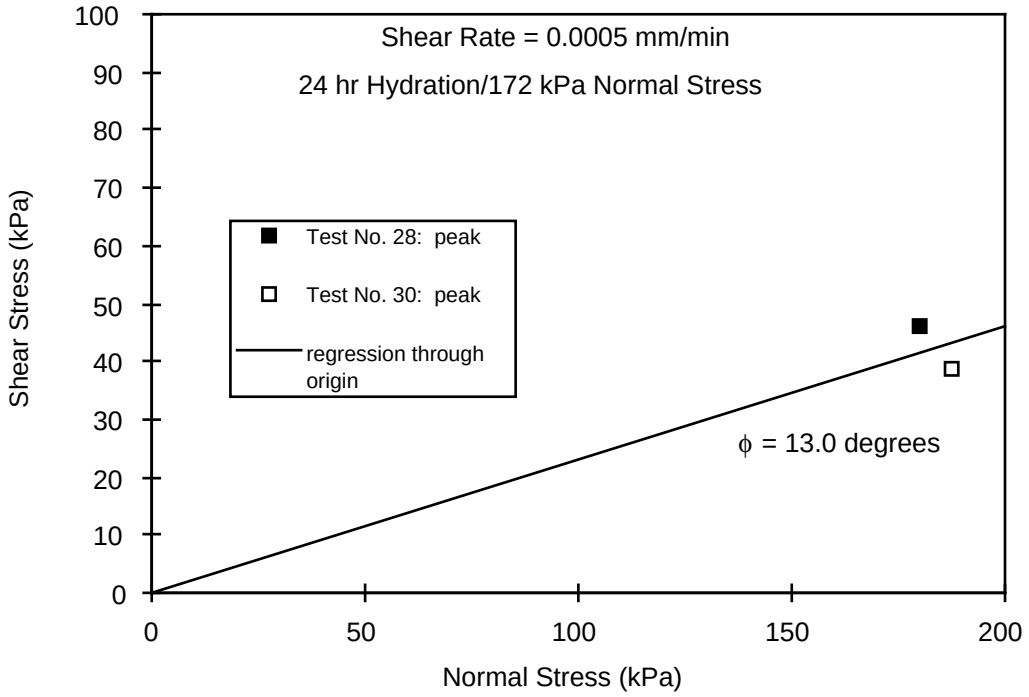

Figure 22: Mohr-Coulomb Diagram for Test No. 28 and 30

Appendix E
Evaluation of Liquids Management Data for Double-Lined Landfills

by

Majdi A. Othman, Ph.D. P.E.
GeoSyntec Consultants
Atlanta, Georgia 30342

Rudolph Bonaparte, Ph.D. P.E.
GeoSyntec Consultants
Atlanta, Georgia 30342

Beth A. Gross, P.E.
GeoSyntec Consultants
Austin, Texas 70748

Dave Warren
GeoSyntec Consultants
Atlanta, Georgia 30342

performed under

EPA Cooperative Agreement Number
CR-821448-01-0

Project Officer

Mr. David A. Carson
United States Environmental Protection Agency
Office of Research and Development
National Risk Management Research Laboratory
Cincinnati, OH 45268

Appendix E
Evaluation of Liquids Management Data for Double-Lined Landfills

E-1 Introduction

E-1.1 Purpose and Scope of Appendix

The purpose of this appendix is to summarize and analyze liquids management data for modern double-lined landfills located throughout the United States (U.S.). Specifically, leachate collection and removal system (LCRS) and leak detection system (LDS) flow rate and flow chemistry data are presented for 189 cells at 54 municipal solid waste (MSW), hazardous waste (HW), and industrial solid waste (ISW) landfills. These data are used to evaluate:

- leakage rates and hydraulic efficiencies of landfill primary liners;
- landfill leachate generation rates (LCRS flow rates), including how leachate generation rates vary with waste type, geographic location (climate), and presence of final cover system; and
- landfill leachate chemistry (LCRS flow chemistry), including how leachate chemistry varies with waste type, geographic location, and operation conditions, and whether federal solid waste regulations promulgated in the 1980's and early 1990's have had an effect on the quantity of potentially-toxic trace chemicals found in leachate.

In addition to the field data presented herein, this appendix presents a literature review summarizing significant previous work related to this study.

E-1.2 Organization of Appendix

The organization of this appendix is as follows:

- a review of significant previously published work on primary liner performance and landfill leachate generation rates and chemistry is presented in Subsection E-2;
- a description of the data collected for this study and data reduction methods are presented in Subsection E-3;
- a summary and evaluation of data on leakage through landfill primary liners are presented in Subsection E-4;
- a summary and evaluation of landfill leachate generation rate data are presented in Subsection E-5;
- a summary and evaluation of landfill leachate chemistry data are presented in Subsection E-6; and
- general conclusions are presented in Subsection E-7.

E-1.3 Definitions

E-1.3.1 Landfills

Landfills are land-based waste management cells that contain solid wastes. Waste containment systems for landfills consist of liner systems that underlay the wastes placed on them and final cover systems constructed over the wastes. The goal of the liner systems is to minimize, to the extent achievable, the migration of waste constituents out of the landfills. The goal of the final cover systems is to contain the wastes, minimize, to the extent achievable, the percolation of water into the landfills, and control the migration of gases, if any, from the wastes.

E-1.3.2 Liner, Liner System, and Double-Liner System

A *liner* is a low-permeability barrier used to impede liquid or gas flow. As discussed in Giroud (1984) and U.S. Environmental Protection Agency (EPA) (1987a), no currently available liner is totally impermeable. Since no liner is impermeable, liquid containment within a landfill cell can only result from a combination of liners and drainage layers performing complementary functions. Liners impede leachate percolation and gas migration out of the cell and improve the collection capability of overlying drainage layers. Drainage layers collect and convey liquids on liners towards controlled collection points (sumps) where the liquids can be removed from the cell. Drainage layers limit the build up of hydraulic head on underlying liners. Combinations of liners and drainage layers in the cells are called *liner systems*.

A *double-liner* system consists of a primary liner and a secondary liner with an LDS between the primary and secondary liners and an LCRS above the primary liner. Essentially all landfill double-liner systems being constructed today have liners that include geomembranes (GMs). These liners can consist of a GM alone, GM on top of a compacted clay liner (CCL), or GM on top of a geosynthetic clay liner (GCL). The latter two liners are both referred to as “composite” liners. Only landfills with GM, GM/CCL composite, or GM/GCL composite primary liners were considered in this appendix. In addition, with the exception of six cells, all of the landfills considered herein have GM or composite secondary liners. Older liner systems constructed with CCL primary liners were not considered.

E-1.3.3 Double-Liner System Components and Groups

Figure E-1.1 illustrates the double-liner system types considered in this appendix. The two main differences between the double-liner systems shown in Figure E-1.1 are the primary liner type (GM, GM/CCL composite, or GM/GCL composite) and LDS drainage layer type (granular material or geonet (GN)). The types of liners and drainage materials used in double-liner systems significantly influence the frequencies of occurrence, sources, and rates of flow from LDSs. For purposes of this appendix, the considered liner systems are grouped into “Type I” through “Type VI” based on primary liner and LDS materials, as defined in Table E-1.1 and illustrated in Figure E-1.1.

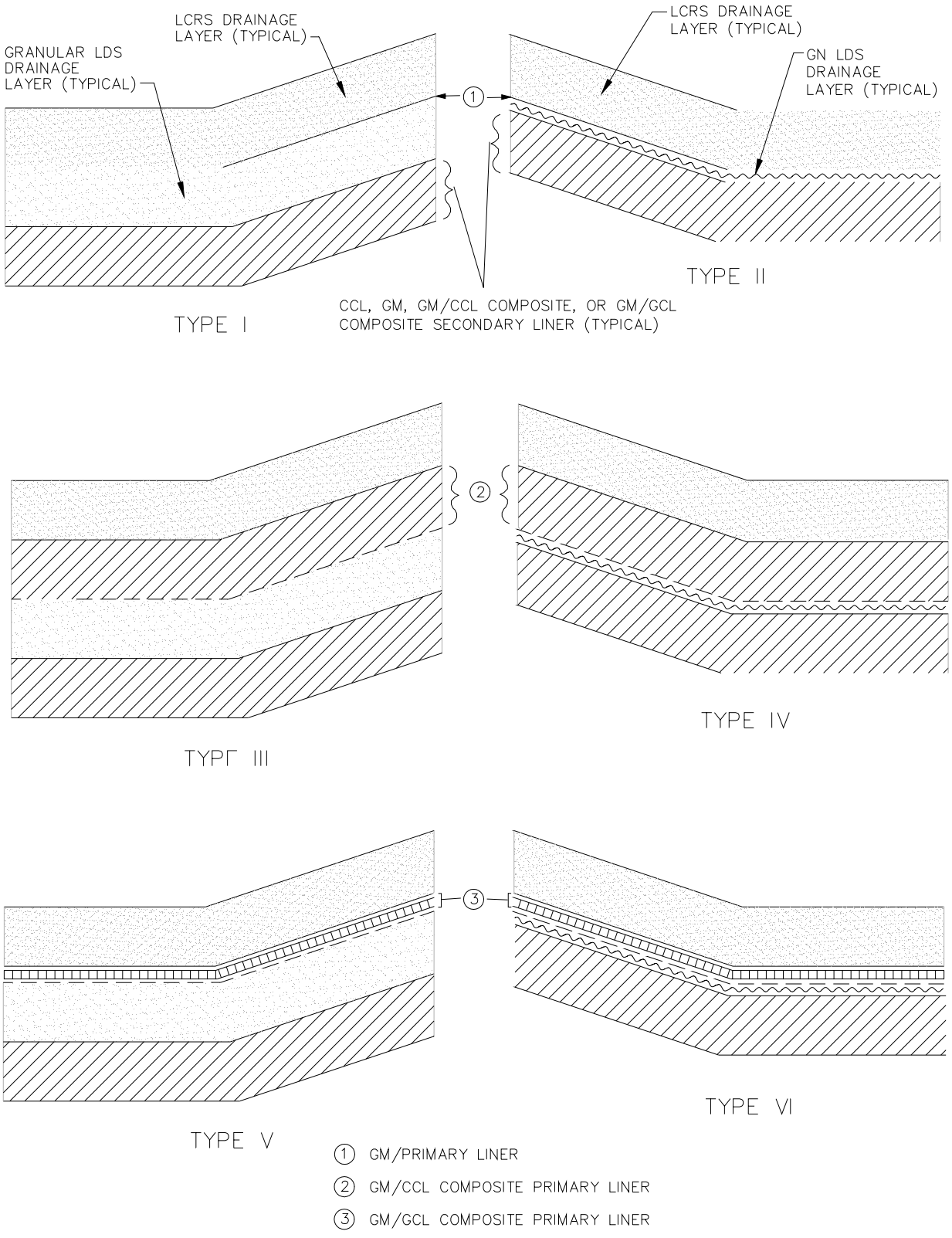

Figure E-1.1. Liner System Types Considered in this Appendix.

Table E-1.1. Definitions of Liner System Types Considered in this Appendix.

Liner System Type	Primary Liner	LDS Material
I	GM	Granular
II		GN
III	Composite GM/CCL or GM/GCL/CCL	Granular
IV		GN
V	Composite GM/GCL	Granular
VI		GN

E-1.3.4 Cover, Daily Cover, Intermediate Cover, and Final Cover System

A *cover* is a barrier placed over material to isolate the material from the surrounding environment. Landfills require daily covers, intermediate covers, or final cover systems, depending on the stage of landfill development.

At most landfills, a *daily cover* is applied to waste to control the spread of insects, rodents, and other burrowing animals, which may use the waste as a food source and to prevent the erosion of waste by wind and surface-water runoff. Daily cover usually consists of a layer of soil, select waste, or other material such as foam or fabric. *Intermediate cover* is often placed on open portions of landfill areas on which waste placement has ceased, either permanently or for an extended period of time. Intermediate cover serves the same purposes as daily cover, but at a higher level. It usually consists of a thicker layer of soil or select waste than daily cover, and may include a temporary GM.

As the active period of operation progresses, the landfill cell is filled with waste, and waste placement ceases. Depending on the landfill, cells may be under intermediate cover for up to several years before a *final cover system* is constructed over the waste. Final cover systems are the only engineered covers on landfill cells. They serve the same purposes as daily and intermediate covers, but are also designed to minimize water infiltration into the waste (i.e., leachate generation), control the migration of gases produced by waste decomposition, and be aesthetically acceptable. As shown in Figure E-1.2, most *final cover systems* constructed today contain (from top to bottom) a vegetated topsoil surface layer, soil protection layer, drainage layer, barrier, gas collection layer (at landfills with wastes that generate gases during decomposition), and a foundation layer (if needed). Final cover systems considered in this appendix primarily have a GM or composite barrier; however, ten cells have a CCL barrier over the entire landfill or the landfill side slopes.

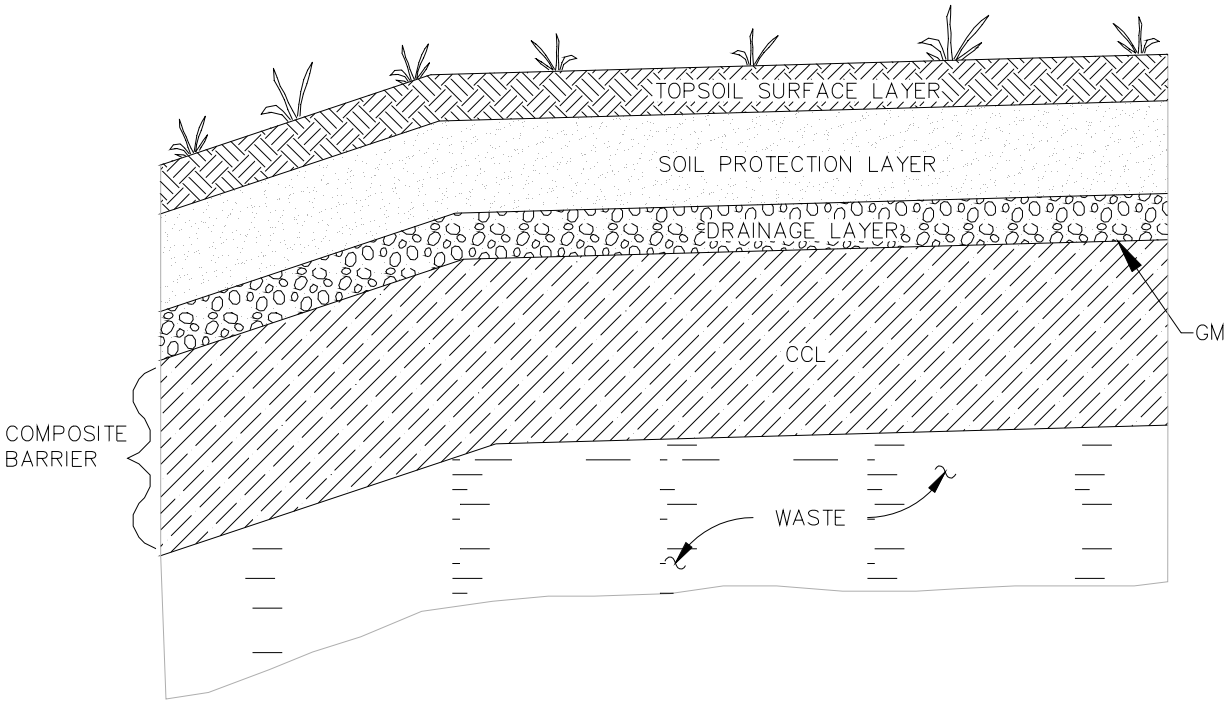

(Note: Gas collection layer and foundation layer are not shown).

Figure E-1.2. Typical Final Cover System for a Modern Landfill.

E-1.3.5 Waste Types in Landfills

The landfill cells in this study are grouped into three categories based on the predominant waste type in a cell:

- MSW;
- HW;
- construction and demolition waste (C&DW);
- ash from MSW combustors (MSW ash); and
- ash from coal-burning power plants (coal ash).

C&DW and coal ash are ISWs.

E-1.3.6 Regions of the United States

The landfills in this study are grouped into three different geographic regions of the U.S.: Northeast U.S. (NE), Southeast U.S. (SE), and West U.S. (W). These regions are outlined in Figure E-1.3 and were chosen because of the climatic differences between these regions (i.e., differences in average annual rainfall, potential evapotranspiration, and days below freezing).

Generally, facilities in the SE receive relatively high rainfall, have relatively high evapotranspiration, and experience few days below freezing annually. Compared to the SE facilities, those in the NE receive slightly lower rainfall, have lower evapotranspiration, and experience a significant number of days below freezing annually. Except for facilities near the northwest coast of the U.S., facilities in the W are in relatively arid climates, with relatively low precipitation and relatively high evapotranspiration, and may or may not experience a significant amount of days below freezing annually (in arid climates this does not markedly affect leachate generation rates).

The climatic differences between regions will have a much larger impact on leachate generation rates at landfills than on LDS flow rates at landfills. LDS flow rates can be affected by climatic differences (higher LCRS flow rates means greater potential for primary liner leakage), but LDS flow rates usually depend more on liner system construction and performance than on climate.

E-1.3.7 LCRS Operational Stages

LCRS flow data for landfills are grouped into three different development stages in the life cycle of a landfill cell: (i) *initial period of operation*; (ii) *active period of operation;* and (iii) *post-closure period*. These stages are defined by characteristics in the LCRS flow rates, as described below and shown for a MSW landfill in Pennsylvania in Figure E-1.4.

Figure E-1.3. Geographic Regions and Locations of Landfills Evaluated in this Study.

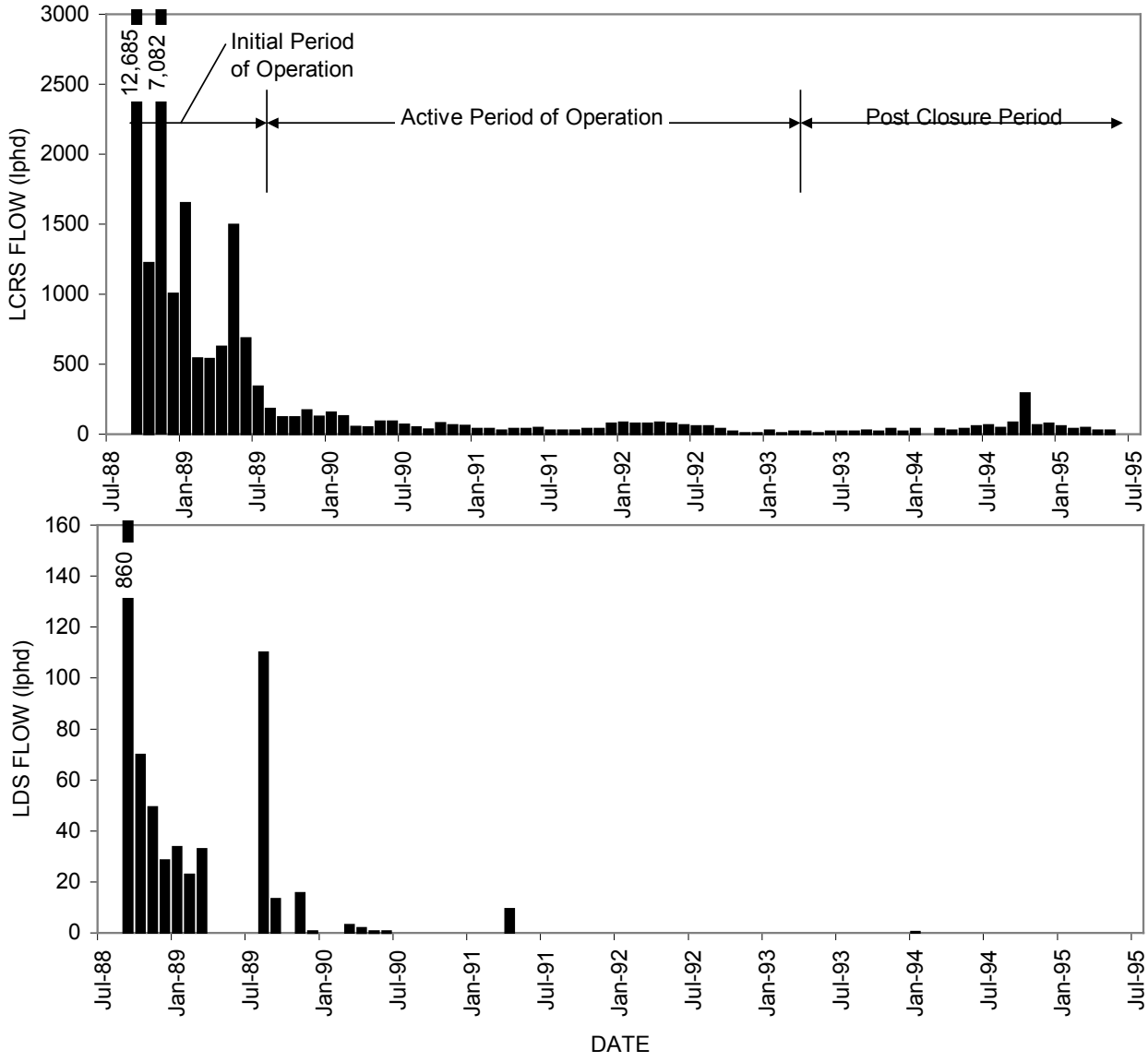

Figure E-1.4. LCRS and LDS flow rates over time at a MSW landfill in Pennsylvania.

The *initial period of operation* occurs during the first few months after the start of waste disposal in a cell. During this stage, there is not sufficient waste in a cell to significantly impede the flow of rainfall into the LCRS. To the extent rainfall occurs during this period, it will rapidly find its way into the LCRS and, unless the LCRS drainage layer has a relatively low permeability (i.e., less than 10^{-4} m/s), to the LCRS sump. LCRS flow rates during this stage are usually controlled by rainfall and can be directly correlated to local climatic conditions. LCRS flow rates are higher at landfills in wetter climates than at those in arid climates. As such, LCRS flow rates during this stage are usually much larger than in later stages and vary widely with the amount of rainfall received.

During the *active period of operation*, the cell is progressively filled with waste and daily and intermediate layers of cover soil. As waste placement continues, more of the rainfall occurring during this stage falls onto the waste and cover soils rather than directly onto the liner system. As a consequence, the LCRS flow rates decrease and eventually stabilize. LCRS flow rates during this stage are generally dependent on rainfall quantity, waste thickness, waste properties (i.e., initial moisture content, field capacity, and permeability), and storm-water management practices. Additional waste reduces LCRS flow rates in two ways:

- it increases the total storage capacity of water within waste in the landfill cell; and
- precipitation falling on cover soil is often directed out of the landfill as surface-water runoff.

During the *post-closure period*, the cell has been closed with a final cover system that further reduces infiltration of rainwater into the waste, resulting in a further reduction in LCRS flow rates.

E-1.3.8 LDS Operational Stages

Similar to LCRS flow data, LDS flow data are also grouped into the same stages in the life cycle of a landfill cell: (i) *initial period of operation*, (ii) *active period of operation*, and (iii) *post-closure period*. During the initial period of operation, most of the LDS flow is usually due to “construction water”. After the active period of operation of a facility, construction water has substantially drained (unless the LDS has a relatively low permeability, i.e., less than $1x10^{-4}$ m/s) and other sources of LDS flow have a stronger influence. Sources of LDS flow are defined in Section E-2.1.1. For simplicity in this appendix, the LCRS and LDS operational stages for a landfill cell are assumed to occur over the same time period.

E-2 Literature Review

E-2.1 Field Performance of Primary Liners

E-2.1.1 Overview

The performance of primary liners at double-lined landfills and surface impoundments has previously been assessed by comparing LDS and LCRS flow rate and chemical constituent data. The first general study of this type, by Gross et al. (1990), identified five potential sources of LDS flow (Figure E-2.1): (i) leakage through the primary liner; (ii) water (mostly rainwater) that infiltrates the LDS during construction and continues to drain to the LDS sump after the start of facility operation ("construction water"); (iii) water that infiltrates the LDS during construction, is held in the LDS by capillary tension, and is expelled from the LDS during waste placement as a result of LDS compression under the weight of the waste ("compression water"); (iv) water expelled into the LDS from the CCL and/or GCL components of a composite primary liner as a result of clay consolidation under the weight of the waste ("consolidation water"); and (v) water that percolates through the secondary liner and infiltrates the LDS ("infiltration water").

Gross et al. (1990) presented the following five-step approach for evaluating the sources of LDS liquid at a specific waste management cell:

- identify the potential sources of flow for the cell based on double-liner system design, climatic and hydrogeologic setting, and cell operating history;
- calculate flow rates from each potential source;
- calculate the time frame for flow from each potential source;
- evaluate the potential sources of flow by comparing measured flow rates to calculated flow rates at specific points in time; and
- compare LCRS and LDS flow chemistry data to further establish the likely source(s) of liquid.

Previously published studies which evaluated the field performance of primary liners in double-lined landfills using LCRS and LDS flow data of are reviewed in this section of the appendix, and the conclusions drawn from the studies are presented. The remainder of this section is organized as follows:

- studies of landfills with GM primary liners are reviewed in Section E-2.1.2; and
- studies of landfills with GM/CCL and GM/GCL primary liners are presented in Section E-2.1.3.

It is noted that the field performance of liners can also be derived from leak location surveys. Several authors (i.e., Darilek et al., 1989; Landreth, 1989; and Peggs, 1990, 1993) have described the use of the electrical leak location method for finding holes in GM liners. Darilek et al. (1989), Laine and Miklas (1989), Laine (1991), Laine and Darilek (1993) and Darilek et al. (1995) reported on the results of electrical leak location

surveys at GM-lined waste containment cells. These results suggest that while GM liners can be constructed with very low hole frequencies (e.g., less than 5 small holes per 10,000 m^2), a number of facilities have been constructed to lower standards resulting in a significantly higher hole frequency, typically as a result of inadequate seaming.

E-2.1.2 GM Primary Liners

E-2.1.2.1 Bonaparte and Gross (1990, 1993)

Bonaparte and Gross (1990, 1993) presented data on LDS flows from several double-lined landfill cells with GM primary liners; the later U.S. Environmental Protection Agency (EPA) sponsored report is an expansion of the 1990 paper. Bonaparte and Gross (1993) presented data for ten landfills containing 25 individually monitored cells. Eighteen of the cells had granular LDSs and seven had GN LDSs. The facilities are located in the Eastern, North-Central, Gulf Coast, and Midwest U.S. Bonaparte and Gross (1993) presented LDS flow rate data for two different time periods: (i) the initial period of cell filling, just after the end of construction; and (ii) the active period of cell filling. They concluded that all landfill cells in their study exhibited LDS flow attributable to primary liner leakage. LDS flow rates averaged over the entire monitored portion of the cell during the active period of cell filling (i.e., LDS flows excluded during the initial period of cell filling) showed that about 40% of the cells with formal Construction Quality Assurance (CQA) programs had LDS flow rates below 50 liters/hectare/day (lphd), 80% below 200 lphd, and all had LDS flow rates below 1,000 lphd. In contrast, 70% of the landfill cells constructed with no formal CQA programs had average active-life LDS flow rates in excess of 1,000 lphd. The landfill cells with no formal CQA programs would not be considered to be constructed to the current standard of practice.

E-2.1.2.2 Maule et al. (1993)

Maule et al. (1993) reported the results of LDS flow rate measurements for three upper midwest landfills, constructed during 1990 and 1991 with formal CQA programs. Each landfill has a GM primary liner and a GN LDS. The three landfills had average LDS flow rates of 10, 11, and 21 lphd over the monitoring periods of up to 17 months. Maximum monthly LDS flow rates during the monitoring periods were 31, 24, and 66 lphd. These LDS flow rates are all very low, at the lower end of the range reported by Bonaparte and Gross (1993) for GN LDSs underlying GM liners (i.e., during the active life period, 0 to 220 lphd).

E-2.1.2.3 Tedder (1997)

Tedder (1997) presented LCRS and LDS flow rate data for 22 cells at eight double-lined landfills located in Florida. All of the cells were constructed with GM primary liners and granular or GN LDSs under formal CQA programs. Data were reported for monitoring periods of 3 to 64 months. Tedder did not specify when cell monitoring was performed

relative to the start of cell operations. Average LCRS flow rates ranged from 1,100 to 91,000 lphd, while average LDS flow rates ranged from 14 to 4,300 lphd. Average LDS flow rates were below 50 lphd for 5 cells (23% of total number of cells), below 200 lphd for 13 cells (59%), and above 1,000 lphd for three cells (14%). These average rates are higher than those reported by Bonaparte and Gross (1990, 1993) for GM liners with CQA. The higher average LDS flow rates in the Tedder study in comparison to the earlier studies may primarily result from the combining of data from the initial period of cell operation (when LDS flow may be in large part attributed to sources other than primary liner leakage) with data from the period of active cell filling. The higher LDS flow rates may also be due to the relatively high LCRS flow rates that occurred in these landfills.

E-2.1.2.4 Conclusions from Previous Studies

Conclusions drawn from the previous studies regarding the hydraulic performance of GM liners are as follows:

- for landfills with GM primary liners, LDS flows during the active period of cell filling is primarily due to primary liner leakage;
- for landfills with GM primary liners constructed using formal CQA programs, average LDS flow rates are typically below 200 lphd and are rarely above 1,000 lphd; and
- average LDS flow rates from landfills with GM primary liners constructed without formal CQA are higher than for landfills with GM primary liners constructed with CQA.

E-2.1.3 Composite Primary Liners

E-2.1.3.1 Bonaparte and Gross (1990, 1993)

Bonaparte and Gross (1990, 1993) presented data on LDS flows from 51 cells at 18 double-lined landfills with composite primary liners; the later 1993 EPA-sponsored report is an expansion of the 1990 paper. The conclusions from their study for these cells are as follows:

- double-lined landfills with GM/CCL composite primary liners almost always exhibited LDS flows due to consolidation water; measured flow rates attributable to consolidation water were in the range of 0 to 1300 lphd;
- LDS flows from landfills with GM/GCL composite primary liners were relatively low and ranged from 0 to 120 lphd during active filling;
- the calculation methods presented by Gross et al. (1990) for estimating consolidation water and construction water flow rates appear reasonable for the facilities reported in this appendix.

Due to the masking effects of consolidation water and the limited available data, Bonaparte and Gross were unable to quantify primary liner leakage rates. The authors did conclude "*the double-liner systems evaluated in this study have performed well. Leakage rates through the primary liners have been low or negligible in most cases*."

E-2.1.3.2 Feeney and Maxson (1993)

Feeney and Maxson (1993) used a methodology similar to that of Bonaparte and Gross (1990) to evaluate LDS flows from 49 double-lined cells at eight HW landfills. The landfills are located in humid, arid, and semi-arid regions of the U.S. All but two of the cells have a GM/CCL composite primary liner on the cell base and a GM primary liner on the cell side slopes (i.e., Category 1 liner system). Two cells have a GM/GCL composite primary liners on both the cell base and side slopes (i.e., Category 2 liner system). All of the cells contain a granular soil/GN LDS on the cell base and a GN LDS on the cell side slopes. All cells were constructed using third-party CQA programs.

For each landfill cell in their study, Feeney and Maxson (1993) reported minimum, maximum, and average LCRS and LDS flow rates. The reporting periods for the 49 cells ranged from 4 to 60 months. At the time of the Feeney and Maxson report, the cells were at different stages of operation, from newly constructed to closed. For 41 of the cells with Category 1 liner systems, average LDS flow rates during the monitoring periods ranged from 0 to 310 lphd. Average LDS flow rates for 27 of the 41 Category 1 cells were less than or equal to 100 lphd. The authors attributed the observed LDS flows primarily to consolidation water. The LDS flow rates reported by Feeney and Maxson (1993) are in the same general range as those reported earlier by Bonaparte and Gross (1990, 1993).

LDS flow rates were temporarily higher for the remaining six Category 1 cells and the two Category 2 cells. Feeney and Maxson indicate that these eight cells initially exhibited similar behavior to the other cells; however, during operations, the primary liner in each cell was damaged, usually by heavy equipment operations in the cell. The primary liner in these cells was subsequently repaired. Average LDS flow rates for the damaged cells were about an order of magnitude higher than the rates for the other cells. The authors do not provide any information on the high frequency of operational damage to the liner systems in their study and whether procedures were developed to prevent similar damage in future cells.

E-2.1.3.3 Workman (1993)

Workman (1993) presented monitoring results for a MSW landfill having a primary liner consisting of a GM on the side slopes and a GM/CCL composite on the base. The LDS consists of a GN drainage layer overlain by a geotextile (GT) filter. The portion of the landfill described by Workman contains three cells constructed between 1989 and 1992. The author does not indicate the level of CQA provided for the construction of each cell. Average LDS flow rates from the three cells initially ranged from 50 to 700 lphd, with

rates at the higher end of the range being associated with the fastest rates of waste disposal. After cell filling ceased, LDS flow rates decreased to 20 to 30 lphd. Workman attributed the observed LDS flows to consolidation of the CCL component of the composite primary liner on the base of the landfill. This conclusion was supported by the concentrations of major ions in the LDS liquids, which were different than the concentrations of major ions in leachate.

Workman (1993) also reported that chemical analyses of the LDS liquids from two of the cells (Cells 1 and 4) revealed the presence of several volatile organic compounds (VOCs), including chloroethane, ethylbenzene, and trichloroethene, at low part-per-billion concentrations, beginning about one year after the start of cell operation. Workman noted that the detected compounds are common constituents of landfill gas and that testing of the gas phase in the LDS indicated methane gas concentrations up to 50% (i.e., up to ≈100% landfill gas). Workman also indicated that landfill gas had not yet been actively removed or passively vented from this landfill at the time of the measurements. He attributed the VOCs to the following source: "*It is believed that methane is impacting the LDS liquids of Cells 1 and 4. No organic constituents have been detected in the Cell 2 LDS. The methane was first detected in Cells 1 and 4 about one year after each cell was placed in operation. This occurred about the same time that the waste reached ground level and totally covered the liner system. Since methane is not actively vented at this time and can accumulate under pressure in the leachate collection system, gradients can occur across the liner system. The sideslopes in this landfill are particularly vulnerable. As methane penetrated the liner and cooled, the gas began to condensate and drain small quantities of liquid to the LDS sump.*"

E-2.1.3.4 Bergstrom et al. (1993)

Bergstrom et al. (1993) presented flow rate and chemical constituent data for the LDSs of five cells at a HW landfill in Michigan. The cells have a GM/CCL composite primary liner, with CCL consisting of a 1.5-m thick layer of compacted clayey till. The LDS consists of a GN drainage layer overlain by a GT filter, with one layer of GN on the cell side slopes and two layers of GN on the cell bases. All cells were constructed using third-party CQA programs.

Average LDS flow rates for the five cells ranged from approximately 200 to 700 lphd during active cell filling and 30 to 60 lphd within one to two years after waste filling ended. Bergstrom et al. (1993) attributed the observed LDS flows primarily to consolidation water. Bergstrom et al. also presented inorganic chemical constituent data obtained from testing of LDS liquid, LCRS liquid, and groundwater. From these data, they concluded that "*each of these water sources has a unique chemical composition and the leachate does not appear to be influencing LDS liquid composition*". The authors reported that VOCs had not been detected in the LDSs of the five cells; however, details of the analyte list, analytical methods, and/or analytical detection limits were not given. They also estimated consolidation water volumes in the LDS using the results of laboratory consolidation testing of the site-specific CCL

material along with records of waste placement in the landfill cells. Estimated consolidation water flow rates were 5 to 60% larger than the observed LDS flow rates.

E-2.1.3.5 Bonaparte et al. (1996)

Bonaparte et al. (1996) analyzed flow rate data for 26 MSW cells at six different landfills containing GM/GCL composite primary liners. These data were collected as part of the ongoing research investigation for the EPA mentioned earlier in this appendix. The authors used the data to calculate average and peak LCRS and LDS flow rates for three distinct landfill development stages: (i) the "initial period of operation"; (ii) the "active period of operation"; and (iii) the "post-closure period". These stages are the same as those used in this appendix and discussed previously in Section E-1.3.7. The mean values calculated by Bonaparte et al. (1996) are presented in Table E-2.1.

Bonaparte et al. (1996) also calculated "apparent" hydraulic efficiencies for the composite primary liners of the 26 landfill cells. They defined liner apparent hydraulic efficiency, E_a as:

$$E_a\,(\%) = (1 - \text{LDS Flow Rate} / \text{LCRS Flow Rate}) \times 100 \qquad \text{(E-1)}$$

The higher the value of E_a, the smaller the flow rate from a LDS compared to the flow rate from a LCRS. The value of E_a may range from zero to 100%, with a value of zero corresponding to a LDS flow rate equal to the LCRS flow rate, and a value of 100% indicating no flow from the LDS. The parameter E_a is referred to as an "apparent" hydraulic efficiency because, as described earlier, flow into the LDS sump may be attributed to sources other than primary liner leakage (Figure E-2.1). The value of E_a is calculated using total flow into the LDS, regardless of source. If the only source of flow into the LDS sump is primary liner leakage, then Equation E-1 provides the "true" liner hydraulic efficiency (E_t). True liner efficiency provides a measure of the effectiveness of a particular liner in limiting or preventing advective transport across the liner. For example, if a primary liner is estimated to have an E_t value of 99%, the rate of leakage through the primary liner would be assumed to be 1% of the LCRS flow rate.

For the landfill cells with GM/GCL composite primary liners and sand LDSs, Bonaparte et al. (1996) found that the E_a is lowest during the initial period of operation (E_{am} = 98.60%; where E_{am} = mean apparent efficiency) and increases significantly thereafter (E_{am} = 99.58% during the active period of operation and E_{am} = 99.89% during the post-closure period). The lower E_{am} during the initial period of operation was attributed to LDS flow from construction water. Bonaparte et al. (1996) stated that for cells with sand LDSs, "*calculated AE (E_a) values during the active period of operation and the post-closure period may provide a reasonably accurate indication of true liner efficiency for the conditions at these units during the monitoring periods.*"

For six cells with GN LDSs, the calculated value of E_{am} for the initial period of operation was 99.96%. This value is higher than the E_{am} for composite liners underlain by sand LDSs for the same facility operational period (i.e., 98.60%). This higher apparent

Table E-2.1. Mean LCRS and LDS Flow Rates in lphd for 26 MSW Landfill Cells with GM/GCL Composite Primary Liners (from Bonaparte et al., 1996).

(a) LCRS	Number of Units	Average Flow Rate		Peak Flow Rate	
		m	σ	m	σ
Initial Period of Operation	25	5,350	3,968	14,964	11,342
Active Period of Operation	18	276	165	752	590
Post-Closure Period	4	124	-	266	-

(b) LDS	Number of Units	Average Flow Rate		Peak Flow Rate	
		m	σ	m	σ
Initial Period of Operation	26	36.6	68.5	141.8	259.9
Active Period of Operation	19	0.7	1.1	7.7	13.7
Post-Closure Period	4	0.2	-	2.3	-

Notes: (1) m = mean value; σ = standard deviation.

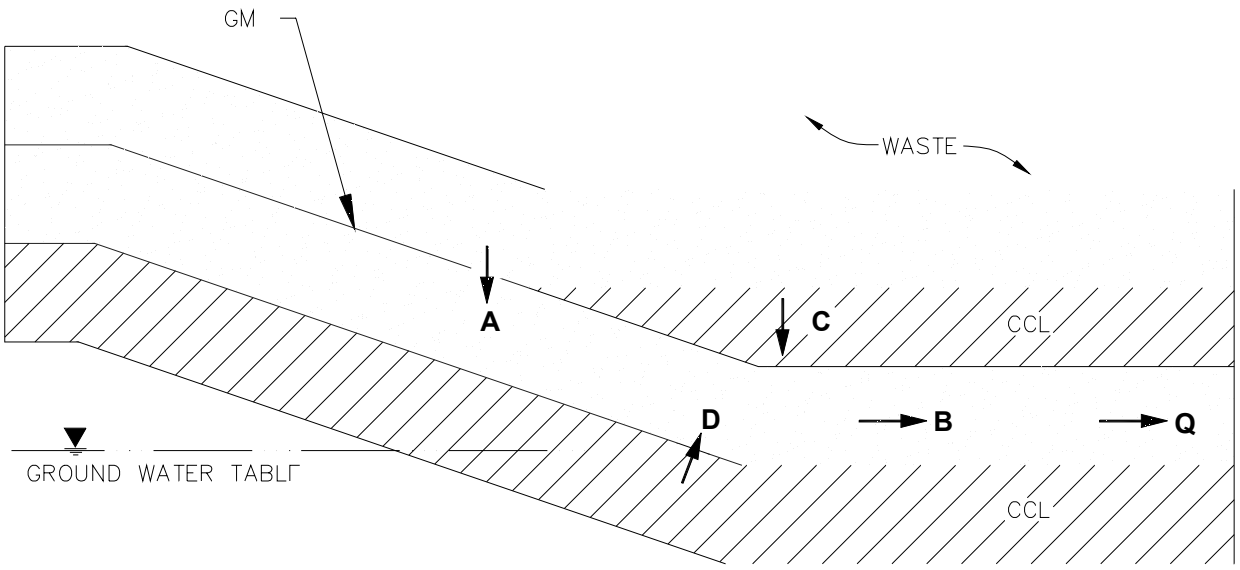

Q = TOTAL FLOW
Q = A+B+C+D

SOURCES:

A = PRIMARY LINER LEAKAGE
B = CONSTRUCTION WATER AND COMPRESSION WATER
C = CONSOLIDATION WATER
D = INFILTRATION WATER

Figure E-2.1. Sources of Flow from LDSs (from Bonaparte and Gross, 1990).

efficiency can be attributed to the differences in liquid storage capacity and hydraulic transmissivity between sand and GN drainage materials. A granular drainage layer can store a much larger volume of construction water and releases this water more slowly during the initial period of operation than does a GN drainage layer. This suggests that, during the initial period of operation, the main source of flow in a sand LDS underlying a GM/GCL composite primary liner is construction water.

Bonaparte et al. (1996) concluded that *"LDS flows attributable to* [primary] *liner leakage vary from 0 to 50 lphd, with most values being less than about 2 lphd. These flow rates are very low. The data shown in Table 4* [not included] *suggest that the true hydraulic efficiency of a composite liner incorporating a GCL may be greater than 99.90 percent. A liner with this efficiency, when appropriately used as part of an overall liner system, can provide a very high degree of liquid containment capability."*

E-2.1.3.6 Conclusions from Previous Studies

The following conclusions are drawn from the previous studies regarding the hydraulic performance of composite liners.

- LDSs underlying GM/CCL composite liners almost always exhibit flow due to consolidation water. Measured LDS flow rates attributable to consolidation water are in the range of 0 to 1,000 lphd, with most values being less than 200 lphd. LDS flow rates attributable to consolidation water are a function of the characteristics of the CCL and the rate of waste placement in the overlying cell. Typically, the rate of flow decreases with time during the later portion of the active period of operation and the post-closure period. LDS flow rates in the range of 0 to 100 lphd have been reported within one to two years of the completion of active filling of cell.
- LDS flow attributable to leakage through GM/CCL primary liners was not quantified in the previous studies due to the masking effects of consolidation water, the very low anticipated flow rates from this source, the limited available database on the chemical constituents in LCRS and LDS liquids, and the relatively long breakthrough times for advective transport through the CCL component of the liner.
- Flow rates from the LDSs of cells with GM/GCL composite primary liners are usually very low. LDS flow rates attributable to leakage through this type of primary liner typically varied from 0 to 50 lphd, with most values being less than about 2 lphd. The true hydraulic efficiency of GM/GCL composite liners may often exceed 99.9%.
- Average LDS flow rates may increase by an order of magnitude, or more, due to liner system damage induced by heavy equipment operations in the cell. Engineering and operational measures should be used to prevent this type of occurrence.

E-2.2 Leachate Generation Rates

E-2.2.1 Overview

Few published studies are available on leachate generation rates at modern landfills. None of these studies included detailed comprehensive evaluations of the rates of landfill leachate generation and how these rates vary with the landfill life cycle, landfill waste type, geographic location, or cover condition for a large number of landfill cells. However, the few published studies present valuable data on leachate flow rates at a limited number of landfills. The findings of these studies are summarized in this section.

E-2.2.2 Feeney and Maxson (1993)

Feeney and Maxson (1993) presented LCRS flow rate data for 41 double-lined landfill cells. Four of the 41 cells are located in arid regions, one is located in a semi-arid region, and 36 are located in humid regions. The average monthly flow rates for the 41 cells ranged from 0 to 33,000 lphd. Nine of the 41 cells (22% of total number of cells) had LCRS flow rates less than 100 lphd, six (15%) had LCRS flow rates between 100 and 1,000 lphd, 17 (41%) had LCRS flow rates between 1,000 and 10,000 lphd, and nine (22%) had LCRS flow rates greater than 10,000 lphd. The four cells located in arid regions had LCRS flow rates between 10 and 70 lphd. Feeney and Maxson noted that 15 of the 41 cells (37%) had received final cover systems during the monitoring periods considered in their paper. The final cover systems consisted of, from bottom to top: high-density polyethylene (HDPE) GM/CCL barrier overlain by a GN drainage layer; and soil protection and surface layer. For six of these closed cells, which were at one landfill, average monthly LCRS flow rates decreased from approximately 1,400 lphd to 470 lphd within six months after closure. Over the next two years, flows decreased further to 90 lphd. The mean LCRS flow rate for all 15 closed cells decreased from approximately 3,740 lphd just before closure to 370 lphd within several months after closure.

E-2.2.3 Maule et al. (1993)

Maule et al. (1993) presented LCRS flow rate and precipitation data from three active upper midwest landfills for monitoring periods between 10 and 20 months. Site A received primary and secondary wastewater treatment sludge dewatered to approximately 35% solids, along with smaller quantities of dry boiler ash, lime mud, and wood waste. Site B received both dry boiler ash and a combined primary and secondary sludge dewatered to an average of 30% solids. Waste disposed in Site C was baled MSW. The LCRS flow rates for Sites A and B varied between 850 lphd and 43,300 lphd. During a 15-month monitoring period for Site A and an eight-month monitoring period for Site B, precipitation at the site averaged approximately 25,000 lphd and LCRS flow rates averaged approximately 22,000 lphd for site A and 18,000 lphd for Site B. Therefore, LCRS flow rates were on average 88 and 72% of precipitation for sites A and B, respectively. Site C had more uniform LCRS flow rates

that averaged approximately 7,000 lphd over a 20-month monitoring period. On average LCRS flows accounted for 32% of precipitation. Maule et al. (1993) attribute the lower LCRS flow rates in Site C than in Sites A and B to the use of soil and synthetic intermediate cover materials over a significant portion of Site C and to the absorptive capacity of the baled MSW. The differences in the wastes moisture contents at disposal time may also have caused the observed differences in leachate generation rates.

E-2.2.4 Haikola et al. (1995)

Haikola et al. (1995) presented LCRS flow rate data for ten HW cells located at a landfill in the NE. Three of these cells are double-lined. Nine of the ten cells have received a final cover system with a GM/CCL composite barrier. Flow rates from the LCRSs of the cells averaged from 7,800 to 15,100 lphd while the cells were open, and from 220 to 1,870 lphd after the cells were closed. The LCRS flow rates decreased from an average of 1,150 lphd during the year prior to closure to five times less after one year of closure and to 40 to 60 times less after ten years of closure. While the cells were open, LCRS flow rates were approximately 60% of annual precipitation at the site. After ten years of closure, LCRS flows accounted for less than 1% of annual precipitation.

E-2.2.5 Bonaparte et al. (1996)

Bonaparte et al. (1996) presented LCRS flow rate data for 25 MSW cells at six different landfills. Mean values of average and peak LCRS flow rates for the cells are presented in Table E-2.1. The mean average flow rates were 5,350 lphd during the initial period of operation, 276 lphd during the active period of operation, and 124 lphd after closure. These LCRS flow rates are significantly lower than those reported in prior studies. The mean LCRS flow rates are controlled by very low LCRS flow rates at 16 cells at one landfill (i.e., cells AX1-16 of this study). The authors of this Appendix attribute the low-LCRS flow rates at this landfill to surface-water management practices implemented at the landfill. Much of the storm water falling onto a cell is diverted away from the cell as clean water.

E-2.2.6 Tedder (1997)

Tedder (1997) presented LCRS flow rate data for 16 active MSW landfill cells located in Florida for monitoring periods of 3 to 64 months. Average LCRS flow rates for 15 of these 16 cells ranged from 1,100 lphd to 24,600 lphd. The remaining cell had a very high average LCRS flow rate of 90,800 lphd. Approximately 70% of the cells had average LCRS flow rates less than 9,000 lphd.

E-2.2.7 Conclusions from Previous Studies

Based on the previous studies of landfill leachate generation rate, the following conclusions are drawn.

- Open landfills (i.e., landfills without a final cover system) located in relatively humid regions have average leachate generation rates that are typically below 20,000 lphd.
- Average reported leachate generation rates for open landfills located in relatively humid regions can be up to 90% of precipitation that occurs at the landfill sites. This ratio is related to: (i) the type of waste and its initial moisture content; and (ii) waste placement and covering practices. The ratio is lower for MSW landfills than for HW or ISW landfills and for wastes with low hydraulic conductivity daily and intermediate covers than for uncovered wastes.
- Open landfill cells located in arid regions have average leachate generation rates that are much lower (i.e., less than 100 lphd) than cells in humid regions.
- Leachate generation rates decrease significantly after cell closure (i.e., after a final cover system is placed on the waste). From the published studies, LCRS flow rates decrease by approximately one to three orders of magnitude within one year after closure, and by up to two orders of magnitude after ten years of closure.

E-2.3 Leachate Chemistry

E-2.3.1 Overview

This section summarizes published information on leachate chemistry for landfills in the U.S. Leachate chemistry is primarily dependent on waste type. Thus, this section is organized by waste type as follows:

- MSW landfill leachate chemistry is discussed in Section E-2.3.2;
- HW landfill leachate chemistry is discussed in Section E-2.3.3; and
- ISW landfill (i.e., coal ash or C&DW landfill) leachate chemistry is discussed in Section E-2.3.4.

For the purposes of the discussions on leachate chemistry presented in this appendix, MSW ash landfill leachate is grouped with leachate from ISW landfills. This grouping is considered appropriate because MSW ash landfill leachate is typically nonhazardous and has chemical characteristics that are more similar to leachate from ISW landfills that to leachates from MSW or HW landfills.

While the focus of this section is on the chemistry of leachate from newer landfills (i.e., landfills that began operation in the 1980's or 1990's), the chemistry of leachate from older landfills is also presented for comparison purposes. There are numerous technical papers containing information on the chemistry of leachate at older MSW or HW landfills in the U.S. (e.g., Sabel and Clark, 1984; Brown and Donnelly, 1988; Tharp, 1991). However, in many of these studies, poorly-defined co-disposal of wastes occurred, the leachate had been diluted by ground water, or the samples were not taken from controlled collection points since the older landfills did not have LCRSs. In addition, the leachate was almost always analyzed for indicator parameters (e.g.,

specific conductance, total suspended solids (TSS), and chemical oxygen demand (COD)) and major cations and anions (e.g., calcium and sulfate), but less frequently analyzed for trace amounts of potentially toxic inorganic and synthetic organic chemicals (i.e., arsenic and benzene) (hereafter referred to as “trace chemicals”) that may be present. These studies, with potentially-significant co-disposal effects, leachate diluted by ground water, leachate sampled from an unknown or uncontrolled collection points, and/or few data on trace chemicals, were excluded from the data summary presented herein. Consequently, most of the information on leachate from older MSW and HW landfills presented in this appendix is from EPA-sponsored studies (i.e., Bramlett et al., 1987; NUS Corporation (NUS), 1988; Gibbons et al., 1992).

With the federal solid waste regulations promulgated in the 1980's and early 1990's, it is expected that the quality of landfill leachate would have improved over time (i.e., the amount of trace chemicals would have decreased). A brief summary of these regulations and the anticipated effect of the regulations on landfill leachate chemistry are presented below.

Prior to 1980, federal regulations for landfilling of solid waste were limited to the guidelines for land disposal of solid waste in 40 CFR § 241 and the criteria for classification of solid waste disposal facilities and practices in 40 CFR § 257. These regulations applied to MSW and ISW, but not to HW and other excluded wastes because of "*the lack of sufficient information on which to base recommended procedures*". While HW was disposed of in designated HW landfills, the regulations allowed HW and other excluded wastes to be disposed of in MSW and ISW landfills under certain circumstances. Following the promulgation of the 1980 federal HW regulations (i.e., Resource Conservation and Recovery Act (RCRA) Subtitle C regulations) that specifically defined "HW" (40 CFR § 261) and the 1982 federal regulations that governed disposal of HW in landfills (40 CFR § 264 Subpart N), landfilled HW was essentially required to be disposed of in specially designed and constructed HW landfills. Only small quantity generators could dispose of HW in MSW and ISW landfills. With the passage of the 1980 and 1982 regulations, less HW was disposed of in MSW and ISW landfills and the amount of trace chemicals in leachate from these landfills would be expected to have decreased. In addition, as the public became more aware of HWs after the passage of regulations and communities instituted voluntary household HW programs, the amount of trace chemicals entering the MSW waste stream would be expected to have decreased.

The Land Disposal Restrictions (LDR) (i.e., 40 CFR § 268) required by the Hazardous and Solid Waste Amendments (HSWA) to the RCRA were promulgated in 1984 and prohibited the disposal of all listed and characteristic HWs and polychlorinated biphenyls (PCBs) in landfills, except under limited circumstances or unless the HWs met the treatment standards of 40 CFR § 268.40 and the PCB waste met the maximum concentration requirement of 40 CFR § 268.32. With the treatment standards, the chemical concentrations in an extract of the waste or of the treatment residue of the waste must not exceed certain values. The chemicals that were covered under this regulation were incrementally added to the list of restricted chemicals from 1986 to 1994 as EPA developed treatment standards for the wastes. The LDR would be expected to

result in a decrease in the amounts of trace chemicals in HW landfill leachate. Small quantity generators of HW are not subject to the LDR; however, the cut-off weight for small quantity generator HW was reduced from that in the 1980 regulations. Thus, this regulation may also have reduced the amount of trace chemicals in leachate from MSW and ISW landfills.

To provide additional assurance that regulated HW and PCB waste were being excluded from MSW landfills, the RCRA Subtitle D regulations (40 CFR § 258) for MSW landfills, promulgated in 1991, included procedures in 40 CFR § 258.20 for detecting and preventing disposal of these wastes. The procedures may have reduced the amount of trace chemicals in leachate from MSW landfills.

E-2.3.2 MSW

E-2.3.2.1 Introduction

Published information on leachate chemistry for MSW landfills in the U.S. is summarized below. A study of leachate chemistry for five Canadian MSW landfills by Rowe (1995) is also included because this study contains more data on the change in leachate chemistry with time than the other studies. It is expected that the same trends would be observed at landfills in the U.S., though the specific constituents and constituent concentrations may be significantly different due to differences in landfill disposal regulations in the U.S. and Canada. Select leachate chemistry data for the landfills are presented in Table E-2.2. The listed parameters were selected based on availability of parameters between studies, frequency of detection, and concentration.

It should be noted that in some of the older MSW landfills, ISW and HW was co-disposed with MSW. For example, in a study of 20 Wisconsin "MSW" landfills by McGinley and Kmet (1984), the principal waste types were MSW for six landfills, MSW and ISW for 11 landfills, and MSW, ISW, and HW for three landfills. The McGinley and Kmet (1984) data are included in the study by NUS (1988). When the data for MSW landfills are separated from the data for co-disposal landfills, such as in the Gibbons et al. (1992) study, the co-disposal landfill data are not included in this appendix.

E-2.3.2.2 NUS (1988)

Under contract to EPA, NUS (1988) summarized leachate chemistry data for 83 MSW landfills from six sources: (i) the Wisconsin Department of Natural Resources (McGinley and Kmet, 1984); (ii) NUS (NUS, 1986,1987a); (iii) the Trade Association (EPA, 1988); (iv) Sobotka & Co., Inc. (NUS, 1986); (v) K.W. Brown and K.C. Donnelly of Texas A&M University (Brown and Donnelly) (NUS, 1986); and (vi) Waste Management, Inc. (Baker, 1987). The purpose of the study was to evaluate which chemicals were present in MSW leachate, the chemical concentrations, and the effect of the 1980 Subtitle C regulations on the chemistry of MSW leachate (i.e., did leachate from newer MSW landfills contain less trace chemicals). The leachate chemistry data for the landfills are not complete: organic chemical, inorganic chemical, and indicator parameter data are

Table E-2.2. Summary of Select Leachate Chemistry Data from Literature.

Waste Type:		MSW						
Start of Operation:		pre-1980	post-1980	pre-1985	post-1985	1978-1989	1979-1993	1995
Location:		U.S.	U.S.	U.S.	U.S.	Florida	Ontario, Canada	Texas
Number of Landfills:		37	9	24	12	6	5	1
Reference:		NUS	NUS	Gibbons et al.	Gibbons et al.	Tedder	Rowe	Hunt and Dollins
Parameter	Units	(1988)	(1988)	(1992)	(1992)	(1992)	(1995)	(1996)
pH	pH units	6.58	6.91			7.07	6.3 - 7.7	6.01 - 7.18
Specific conductance	μmhos/cm	5,540	8,800			7,490		1,640 - 2,880
TDS	mg/l	4,230	7,976			4,645		1,110 - 2,500
TSS	mg/l	264	554			122		NA
COD	mg/l	2,817	4,300			1,731	5,238 - 17,116	50[4]
BOD_5	mg/l	2,600	185			288	3,361 - 12,367	2[4]
TOC	mg/l	810	2,860			103		NA
Alkalinity	mg/l	2,650	3,900			172		642 - 2,000
Chloride	mg/l	550	820			928	851 - 2,247	73 - 137
Sulfate	mg/l	118	260			174		84 - 1,470
Ammonia Nitrogen	mg/l	215	299			481		4 - 14
Calcium	mg/l	284	747			278	322 - 1,643	203 - 460
Magnesium	mg/l	138	412			30.4		27 - 73
Sodium	mg/l	596	817			324		155 - 314
Arsenic	μg/l	15	11	99	ND[4]	36		ND - 30
Barium	μg/l	580	1,000			169		ND - 700
Cadmium	μg/l	18	6.5	55	ND[4]	22	15 - 50	ND
Chromium	μg/l	60	8			56	110 - 390	ND
Lead	μg/l	72	46	205	ND[4]	91	100 - 570	ND
Mercury	μg/l	D(46)	ND	0.5	ND[4]	1.2	0.26 - 5	ND[4]
Nickel	μg/l	164	185			114		ND
Zinc	μg/l	880	335			150	1,320 - 11,000	ND
Acetone	μg/l	320	4,000	D(82)	D(100)[4]			59 - 2,100
Benzene	μg/l	D(56)	ND	65	7	9.9	<3 - 22	ND
Chlorobenzene	μg/l	D(16)	ND	736	D(4)	3.9		ND
Chloroform	μg/l	D(13)	ND	D(3)	D(4)	1		ND
1,1 - Dichloroethane	μg/l	220	4[3]	400	116	5.9		5 - 20
1,2 - Dichloroethane	μg/l	D(9)	ND	D(4)	D(6)	2.0	ND - 10	ND
cis-1,2-Dichloroethylene	μg/l					ND		25 - 28
trans-1,2-Dichloroethylene	μg/l	168	14	492	104			12 - 25
Ethylbenzene	μg/l	D(59)	ND	198	60	27	71 - 170	7 - 20
Methyl ethyl ketone	μg/l	430	9,900	D(65)	D(100)[4]			75[4]
4-Methyl-2-pentanone	μg/l	ND	D(40)	D(50)	D(100)[4]			71 - 85
Methylene chloride	μg/l	1,100	120	898	139	34.8	ND - 3,272	170[4]
Naphthalene	μg/l	D(48)	ND			10		ND[4]
Phenol	μg/l	258	1,700			2,672		ND[4]
Tetrachloroethylene	μg/l	D(24)	ND	D(5)	D(4)	1	ND - 25	ND
Toluene	μg/l	420	590	583	406	84	156 - 1,226	10 - 87
1,1,1 - Trichloroethane	μg/l	D(26)	ND	D(2)	178	12		33[4]
1,1,2-Trichloroethane	μg/l	D(6)	ND	ND	D(1)			ND
Trichloroethylene	μg/l	D(38)	ND	51	71	67	ND - 55	ND
Vinyl chloride	μg/l	D(19)	ND	107	51	19	<13 - 65	10 - 12
Xylenes	μg/l	D(63)	ND	D(20)	NA	38		33 - 38

Table E-2.2. Summary of Select Leachate Chemistry Data from Literature (Continued).

Waste Type:		MSW Ash		Coal Ash		
Start of Operation:		1970 - 1981	1975 - 1988	pre-1978		1974
Location:		U.S.+	U.S.	ash ponds in U.S.	ash extract	U.S.
Number of Landfills:		3+				1
Reference:		NUS	NUS	EPRI	Eisenberg et al.	GeoSyntec
Parameter	Units	(1987b)	(1990)	(1978)	(1986)	(1993)
pH	pH units	7.44 - 8.58	5.2 - 7.4		4.15 - 11.1	10.9 - 11.2
Specific conductance	μmhos/cm	4,200 - >10,000	9,400 - 46,000			1,440 - 2,200
TDS	mg/l	11,300 - 28,900	8,030 - 41,000	404 - 3,328	304 - 1,743	736 - 990
TSS	mg/l			100 - 657		NA
COD	mg/l	<5 - 1,200				NA
BOD_5	mg/l					NA
TOC	mg/l	59 - 636	17 - 420			3 - 4
Alkalinity	mg/l		44 - 744			320 - 419
Chloride	mg/l	1,803 - 18,500	7,700 - 22,000			16 - 29
Sulfate	mg/l	94	14 - 5,080	527 - 2,300	250 - 916	193 - 360
Ammonia Nitrogen	mg/l	1.2 - 36	4 - 35			NA
Calcium	mg/l	21	386 - 8,390	1 - 563	108 - 310	8 - 24
Magnesium	mg/l	NA	15 - 367	20 - 156		ND
Sodium	mg/l	200 - 4,000	1,240 - 3,800	294 - 982		91 - 111
Arsenic	μg/l	5 - 218	ND - 400	15 - 84		12 - 130
Barium	μg/l	1,000	ND - 3,080	300 - 40,000		13 - 73
Cadmium	μg/l	ND - 44	ND - 4	10 - 52	ND - 47	ND - 1
Chromium	μg/l	6 - 1,530	ND - 32	23 - 170	440 - 740	ND - 203
Lead	μg/l	12 - 2,920	ND - 54	24 - 200	ND	ND
Mercury	μg/l	1 - 8	ND	0.2 - 15		NA
Nickel	μg/l	ND - 412	NA	15 - 130	ND - 73	NA
Zinc	μg/l	ND - 3,300	5 - 370	160 - 2,700	ND - 680	NA
Acetone	μg/l	ND	NA			NA
Benzene	μg/l	ND	NA			NA
Chlorobenzene	μg/l	ND	NA			NA
Chloroform	μg/l	ND	NA			NA
1,1 - Dichloroethane	μg/l	ND	NA			NA
1,2 - Dichloroethane	μg/l	ND	NA			NA
cis-1,2-Dichloroethylene	μg/l	ND	NA			NA
trans-1,2-Dichloroethylene	μg/l	ND	NA			NA
Ethylbenzene	μg/l	ND	NA			NA
Methyl ethyl ketone	μg/l	ND	NA			NA
4-Methyl-2-pentanone	μg/l	ND	NA			NA
Methylene chloride	μg/l	ND	NA			NA
Naphthalene	μg/l	ND	ND			NA
Phenol	μg/l	ND	ND - 32			NA
Tetrachloroethylene	μg/l	ND	NA			NA
Toluene	μg/l	ND	NA			NA
1,1,1 - Trichloroethane	μg/l	ND	NA			NA
1,1,2-Trichloroethane	μg/l	ND	NA			NA
Trichloroethylene	μg/l	ND	NA			NA
Vinyl chloride	μg/l	ND	NA			NA
Xylenes	μg/l	ND	NA			NA

Table E-2.2. Summary of Select Leachate Chemistry Data from Literature (Continued).

Waste Type:		C&DW	HW				
Start of Operation:		< 1991	1972 - 1983	pre-1983	pre-1987	post-1987	1969 - 1988
Location:		Texas	U.S.	U.S.	U.S.	U.S.	U.S.
Number of Landfills:		3	13	11	9	3	10
Reference:		Norstrom et al.	Bramlett et al.	NUS	Gibbons et al.	Gibbons et al.	Pavelka et al.
Parameter	Units	(1991)	(1987)	(1988)	(1992)	(1992)	(1994)
pH	pH units	6.5-7.3	8.2	6.9			
Specific conductance	µmhos/cm	2,920 - 6,850	14,690	20,000			
TDS	mg/l	2,412 - 4,270		10,562			
TSS	mg/l	1,000 - 43,000		1,470[3]			
COD	mg/l	3,080 - 11,200	10,217	12,600			
BOD_5	mg/l	100 - 320		13,400			
TOC	mg/l	76 - 1,080	3,097	4,624			
Alkalinity	mg/l	1,710 - 6,520		540[3]			
Chloride	mg/l	125 - 240		2028			
Sulfate	mg/l	<40		399			
Ammonia Nitrogen	mg/l	30 - 184		870[3]			
Calcium	mg/l	148 - 578		72			
Magnesium	mg/l	92 - 192		25.4			
Sodium	mg/l	256 - 1,290		377			
Arsenic	µg/l	17 - 75	13,100	2,780	18,600	NA	13,800
Barium	µg/l	1,500 - 8,000	NA	840			860
Cadmium	µg/l	20 - 30	18.8	600	52,500	NA	430
Chromium	µg/l	100 - 250	281	110			240
Lead	µg/l	220 - 2,130	116	480	405	NA	100
Mercury	µg/l	<2 - 9	5	D( )	82	NA	0.8
Nickel	µg/l		6,420	272			1,800
Zinc	µg/l	1,700-8,630	2,510	536			1,150
Acetone	µg/l		23,200	60,000[3]	D(92)	NA	46,800
Benzene	µg/l		303	D( )	4,030	529	425
Chlorobenzene	µg/l		480	D( )	9,110	156	
Chloroform	µg/l		1,940	D( )	97,500	D(2)	
1,1 - Dichloroethane	µg/l		182	594	33,200	132	135
1,2 - Dichloroethane	µg/l		695	D( )	200,200	4,250	
cis-1,2-Dichloroethylene	µg/l		NA				
trans-1,2-Dichloroethylene	µg/l		166	2,350	1,670	81	
Ethylbenzene	µg/l		334	D( )	152,700	185	
Methyl ethyl ketone	µg/l		13,600		D(82)	NA	59,300
4-Methyl-2-pentanone	µg/l		775		D(80)	NA	41,900
Methylene chloride	µg/l		14,100	7,715	385,400	1,970	39,500
Naphthalene	µg/l		468	D( )			200
Phenol	µg/l		26,100	3,100			32,000
Tetrachloroethylene	µg/l		430	D( )	67,400	112	
Toluene	µg/l		8,340	12,000	79,700	1,670	3,310
1,1,1 - Trichloroethane	µg/l		1,830	D( )	200,600	D(4)	1,900
1,1,2-Trichloroethane	µg/l		21	D( )	39,600	ND	
Trichloroethylene	µg/l		2,040	D( )	95,500	38	4,210
Vinyl chloride	µg/l		ND	D( )	8,960	40,100	
Xylenes	µg/l		1,540		NA	NA	

Table E-2.2. Summary of Select Leachate Chemistry Data from Literature (Continued).

Notes:

(1) Parameter values are given as medians (NUS, 1988) or arithmetic averages (Bramlett et al., 1987; Gibbons et al., 1992; Tedder, 1992; Pavelka et al., 1994) of detected values, ranges of maximum concentrations (EPRI, 1978), ranges of representative peak annual concentrations (Rowe, 1995), or ranges of all concentrations (Eisenberg et al., 1986; NUS, 1987b; NUS, 1990; GeoSyntec, 1993; Hunt and Dollins, 1996).

(2) ND = not detected; NA = not analyzed; D(x) = detected in x% of samples and concentration was not given; " " = not reported.

(3) Based on one detected concentration.

(4) Based on one or two samples.

available for 60 landfills; only inorganic chemical and indicator parameter data are available for 16 landfills; and only organic chemical data are available for seven landfills. In addition, the landfill leachates were not analyzed for the same inorganic and organic chemicals. For example, the leachates in the study by McGinley and Kmet (1984) were analyzed for the 114 organic chemicals on the Priority Pollutant List (PPL). The PPL does not include certain organic chemicals, such as ketones (e.g., acetone, methyl ethyl ketone, 4-methyl-2-pentanone) and xylenes, which are commonly found in MSW landfill leachate. The leachates in the studies by NUS (1986,1987a) were analyzed for the 210 organic chemicals in proposed Appendix IX of 40 CFR § 264, which contained ketones and xylenes. The McGinley and Kmet (1984) , NUS (1986, 1987a), and Baker (1987) studies were based on multiple data sets. Only one data set is available for each of the landfills in the Trade Association (EPA, 1988), Sobotka & Co., Inc. (NUS, 1986), and Brown and Donnelly (NUS, 1986) studies. It is unknown if the data set represented one sampling event or was an average for several events.

NUS divided the leachate chemistry data into three categories: (i) data from 37 landfills that started operation prior to 1980 (pre-1980 landfills); (ii) data from 9 landfills that started operation after 1980 (post-1980 landfills); and (iii) data from 37 landfills whose start of operation date was unknown. From comparison of these three categories of data for MSW landfill leachate and data for HW landfill leachate (discussed in Section 2.3.3.3), NUS found that 89 of the 275 organic chemicals analyzed for and 55 of the 58 inorganic chemicals and indicator parameters analyzed for were detected in MSW leachate. The trace inorganic and organic chemicals detected in more than 60% of the pre-1980 and post-1980 MSW leachate samples are arsenic, barium, boron, cadmium, chromium, copper, lead, manganese, nickel, vanadium, zinc, acetone, methyl ethyl ketone, methylene chloride, phenol, and toluene. Of these chemicals, barium, acetone, methyl ethyl ketone, and phenol were detected at the highest average concentrations. No significant difference in leachate chemistry between the pre-1980 and post-1980 landfills was evident. However, chemicals generally occurred at lower concentrations in MSW landfill leachate than in HW landfill leachate. NUS also found that more that half of the chemicals with federal health-based standards (e.g., maximum contaminant levels (MCLs) for drinking water) were detected in MSW leachate at median concentrations greater than the standards.

E-2.3.2.3 Gibbons et al. (1992)

In their study, Gibbons et al. evaluated the leachate chemistry for 48 MSW, HW, and MSW/HW co-disposal landfills and assessed whether the leachates from these facilities were significantly different. The database included 347 leachate samples from 36 MSW landfills owned or operated by Waste Management of North America (WMNA). Twenty-four of these MSW landfills began operation before 1985 and were considered "old" landfills. Twelve of the landfills began operation in 1985 or later and were considered "new" landfills. The cutoff between the "old" and "new" landfills was based on a WMNA policy implemented in 1985 that limited disposal of liquids in company landfills. Not all samples were analyzed for the same parameters. However, most were analyzed for the 56 PPL volatile organic compounds (VOCs) and some were analyzed for heavy metals.

Gibbons et al. primarily considered the PPL VOCs and four metals, arsenic, cadmium, mercury, and lead, in their evaluation of leachate chemistry.

Gibbons et al. found that MSW leachates in the database were differentiated from HW leachates based on the detection frequencies and concentrations of the considered chemicals (i.e., PPL VOCs and four metals). While aromatic hydrocarbons (e.g., benzene, toluene), arsenic, cadmium, lead, and trans-1,2-dichloroethylene were frequently detected in both MSW and HW leachate samples, certain chemicals, such as chloroform, 1,2-dichloroethane, and tetrachloroethylene, were only found in more than 6% of samples for HW leachate. Other chemicals, such as mercury, trichloroethylene, and vinyl chloride, were primarily detected in HW leachates. Gibbons et al. noted that the difference in chemical detection frequencies between MSW and HW leachates is probably underestimated because the detection limits for HW leachates were generally significantly higher than those for MSW leachates due to sample matrix interference (e.g., for benzene, the average detection limit was about 80 μg/l for MSW leachate and 20,000 μg/l for HW leachate). Thus, a chemical could be present at higher concentrations in HW leachate than in MSW leachate and be reported as "nondetected" in the HW leachate. Of the eight PPL VOCs detected in more than 10% of leachate samples from both old and new MSW landfills, six were found at lower average concentrations in samples from new landfills than in samples from old landfills. However, only benzene was shown to be at a statistically lower concentration in leachate from new MSW landfills. In contrast, almost all chemicals detected in more than 10% of the MSW leachate samples were at significantly lower concentrations in the MSW leachate as compared to old HW landfill leachate. Gibbons et al. also found that the chemistry of leachate from MSW/HW co-disposal landfills was more similar to that of MSW leachate than to HW leachate.

E-2.3.2.4 Tedder (1992)

Tedder summarized leachate chemistry data for six active MSW landfills located in both rural and heavily populated areas in Florida and compared the chemical concentrations to regulatory standards to assess leachate quality. One of the landfills is a co-disposal facility that accepts both MSW and MSW ash. Another landfill is operated as a bioreactor with leachate recirculation. Operation of the landfills began from 1978 to 1989; only one of the landfills was operated prior to 1980. Tedder provided leachate chemistry data for 146 samples collected between January 1987 and February 1992. The suite of parameters that the leachate samples were analyzed for was not given, and each sample was not analyzed for the same parameters.

The trace inorganic and organic chemicals detected at the highest average concentrations are manganese, selenium, pentachlorophenol, and phenol. The detection frequencies for these chemicals were not given. Tedder compared the detected concentrations to regulatory standards and found that the maximum detected chemical concentrations in the leachates were below the toxicity characteristic concentrations for solid waste given in 40 CFR § 261.24. In addition, with the exceptions of ten chemicals (i.e., beryllium, manganese, selenium, methylene bromide,

ethylbenzene, methylene chloride, pentachlorophenol, phenol, trichloroethylene, and vinyl chloride), the average concentrations of detected chemicals were near or below the Florida Department of Environmental Regulation standards or guidance concentrations for drinking water. With the exceptions of four inorganic chemicals (i.e., barium, beryllium, chromium, and selenium) and four phenolics (i.e., 2,4-dimethyl phenol, p-nitrophenol, pentachlorophenol, and phenol), the average concentrations of detected chemicals were near or below the levels reported for MSW leachate in the study by NUS (1988). Tedder concluded that while the concentrations of inorganic chemicals in the Florida landfill leachates were generally similar to those in the NUS study, the concentrations of organic chemicals in the Florida landfill leachates were generally significantly less.

E-2.3.2.5 Rowe (1995)

Rowe presented leachate chemistry data for five MSW landfills in Ontario, Canada and compared the leachate chemistry for these landfills to leachate chemistries for MSW landfills in the U.S. and Europe. Operation of the Canadian landfills began between 1972 and 1983. One landfill was closed in 1988, the remaining four landfills were active in 1993 at the time of the Rowe's study.

Rowe found the representative peak annual chemical concentrations in leachate from the Canadian landfills to be generally consistent with published U.S. and European data. For landfills with sufficient data, the concentration versus time trend for different parameters was investigated. For one active landfill with the most complete data set, chloride, biological oxygen demand (BOD), and COD concentrations and the ratio of BOD to COD increased with time over ten years of operation, though these trends were not monotonic from year to year. The relatively low pH and the relatively high BOD/COD values for the leachate were characteristic of leachate during the acid phase of MSW decomposition. Interestingly, the concentrations of commonly detected VOCs, such as ethylbenzene, methylene chloride, and trichloroethylene, decreased over the same time period. Rowe attributed this trend to degradation of the VOCs. Rowe used the VOC time trends at the landfills along with published information on VOC degradation to estimate half-lives of selected VOCs.

E-2.3.2.6 Hunt and Dollins (1996)

Hunt and Dollins presented leachate chemistry data for a 1.8-ha MSW landfill cell in northcentral Texas that became operational in June 1995. After waste in the cell reached interim grades in September 1995, waste placement in the cell was temporarily ceased. Leachate collected from the cell from June to September was recirculated back into the cell. Leachate chemistry data for five sampling events from June 1995 to June 1996 are summarized in Table E-2.2. The leachate was analyzed for the 62 parameters in Appendix I of 40 CFR § 258 (i.e., detection ground-water monitoring parameters for MSW landfills) for four of the sampling events and the 213 parameters in Appendix II of 40 CFR § 258 (i.e., assessment ground-water monitoring parameters for

MSW landfills) for one of the sampling events. The Appendix I parameters are included in Appendix II. Only 17 of the Appendix II parameters were detected:

- arsenic;
- barium;
- acetone;
- methyl ethyl ketone;
- carbon disulfide;
- chloroethane;
- 1,1-dichloroethane;
- 1,1-dichloroethylene;
- cis-1,2-dichloroethylene;
- trans-1,2-dichloroethylene;
- ethylbenzene;
- 4-methyl-2-pentanone;
- methylene chloride;
- 1,1,1-trichloroethane;
- toluene;
- vinyl chloride; and
- xylenes.

The organic chemicals detected at the highest concentrations were acetone and methylene chloride. Interestingly, the data presented by Hunt and Dollins (1996) also show that leachate pH has been increasing over time from 6.01 in June 1995 to 7.18 in June 1996 and the BOD to COD ratio was very low (i.e., 0.04) when BOD and COD were measured in June 1996, suggesting that waste decomposition has moved from the acid stage to the methane fermentation stage.

E-2.3.2.7 Conclusions from Previous Studies

The published leachate chemistry data show that leachate from MSW landfills is a mineralized, biologically-active liquid containing trace concentrations of heavy metals and synthetic organic chemicals. The limited data on the change in MSW leachate chemical concentrations over time from the Rowe (1995) and Hunt and Dollins (1996) studies are consistent with theory (discussed in Section E-6.2.2). During the active life of a MSW landfill, waste decomposition is primarily in the acid stage. In this stage, BOD to COD ratios are relatively high and pH is relatively low. As waste placement ceases, BOD to COD ratios decrease and pH increases. The trace chemicals were generally found to occur at significantly lower frequencies and concentrations in MSW leachate than in HW leachate. A significant difference between leachate from old and new MSW landfills was not observed in the studies by NUS (1988) and Gibbons et al. (1992), though most trace chemicals were detected at lower concentrations in leachate from new MSW landfills than leachate from old MSW landfills. However, the data set for newer landfills was relatively small and only included one landfill that became

operational after 1989. It is anticipated that the quality of leachate from the post-1990 MSW landfills would be improved over that from pre-1980 MSW landfills.

Table E-2.3 presents a list of the chemicals detected more than once in the U.S. MSW leachate studies and that are also in Appendix II of 40 CFR § 258. Two landfill categories are considered in this table: (i) old MSW landfills (i.e., pre-1980 landfills in NUS (1988) and pre-1985 landfills in Gibbons et al. (1992)); and (ii) new MSW landfills (i.e., post-1980 landfills in NUS (1988), post-1985 landfills in Gibbons et al. (1992), landfills in Tedder (1992), and the landfill in Hunt and Dollins (1996)). In Table E-2.3, chemicals detected more than once are indicated with one check, chemicals detected in at least 30% of the samples are indicated with two checks, and chemicals detected in at least 60% of the samples are indicated with three checks. The Tedder (1992) data could only be used to determine if a chemical has been detected and could not be used to calculate detection frequencies because the number of samples analyzed for a given chemical was not indicated. Appendix II chemicals monitored for but detected once or less are listed in Table E-2.4.

Sixty-one of the Appendix II parameters were detected in MSW leachate more than once, and at least 116 of the parameters were not detected or were detected only once. Nine of the Appendix II inorganic chemicals and four of the Appendix II organic chemicals were detected in more than 60% of the MSW leachate samples analyzed for the constituents. The Appendix II metals detected in the highest concentrations are barium, nickel, and zinc. The four organic chemicals detected with the highest frequency, acetone, methyl ethyl ketone, methylene chloride, and toluene, were also present at higher concentrations than the other Appendix II organic chemicals. These organic chemicals generally have relatively high solubilities. It appears, from Table E-2.3, that certain Appendix II chemicals found in leachate from old MSW landfills were not detected more than once in leachate from new MSW landfills (e.g., 2,4-D, dimethyl phthalate, and 1,1,2-trichloroethane). This effect likely results from the regulations discussed in Section 2.3.1, but may also be partially an artifact of sampling size: there were fewer samples from new MSW landfills analyzed for these chemicals, so it was less likely that the chemicals would be detected.

E-2.3.3 HW

E-2.3.3.1 Introduction

Published information on leachate chemistry for HW landfills in the U.S. is summarized below. Select leachate chemistry data are presented in Table E-2.2. Most of the data are from older landfills or include leachate samples from older landfills, and, thus, do not reflect the improvements in HW landfill leachate chemistry that are expected under the previously-discussed solid waste regulations.

Table E-2.3. Appendix II Chemicals Detected More than Once in Leachate from MSW Landfills.

Constituent	Old Landfills	New Landfills
Antimony	✓✓	
Arsenic	✓✓✓	✓✓✓
Barium	✓✓✓	✓✓✓
Beryllium	✓	
Cadmium	✓✓✓	✓✓✓
Chromium	✓✓✓	✓✓✓
Cobalt	✓✓	
Copper	✓✓✓	✓✓✓
Cyanide	✓✓✓	✓
Lead	✓✓✓	✓✓✓
Mercury	✓	✓
Nickel	✓✓✓	✓✓✓
Selenium	✓✓	✓
Silver	✓✓	✓✓
Thallium	✓✓	
Tin	✓	
Vanadium	✓✓✓	✓✓✓
Zinc	✓✓✓	✓✓✓
Acetone	✓✓✓	✓✓✓
Acetonitrile	✓✓	✓
Benzene	✓✓	✓
Bis(2-ethylhexyl) phthalate	✓	✓
Carbon tetrachloride		✓
Chlorobenzene	✓✓	✓
Chloroethane	✓	✓
Chloroform	✓	✓
p-Cresol	✓✓✓	✓✓
2,4-D	✓✓	
4,4-DDT	✓	✓✓
Di-n-butyl phthalate	✓	✓
o-Dichlorobenzene	✓	
p-Dichlorobenzene	✓	✓
Dichlorodifluoromethane	✓	✓
1,1-Dichloroethane	✓	✓✓
1,2-Dichloroethane	✓	✓
1,1-Dichloroethylene	✓	✓
cis-1,2-Dichloroethylene	No data available	✓✓✓
trans-1,2-Dichloroethylene	✓✓	✓✓
1,2-Dichloropropane	✓	
Diethyl phthalate	✓✓	✓

Table E-2.3. Appendix II Chemicals Detected More than Once in Leachate from MSW Landfills (Continued).

Constituent	Old Landfills	New Landfills
2,4-Dimethylphenol	✓	✓
Dimethyl phthalate	✓	
Ethylbenzene	✓✓	✓✓
2-Hexanone	✓	✓✓
Isophorone	✓✓	✓
Methyl chloride	✓	
Methyl ethyl ketone	✓✓✓	✓✓✓
4-Methyl-2-pentanone	✓✓	✓✓✓
Methylene chloride	✓✓✓	✓✓✓
Naphthalene	✓✓	✓
Nitrobenzene	✓	
Pentachlorophenol	✓	✓
Phenol	✓✓✓	✓✓
Tetrachloroethylene	✓	✓
Toluene	✓✓✓	✓✓✓
1,1,1-Trichloroethane	✓	✓
1,1,2-Trichloroethane	✓	
Trichloroethylene	✓	✓
Trichlorofluoromethane	✓	✓
Vinyl chloride	✓	✓
Xylenes	✓	✓

Notes: (1) ✓ = detected more than once, ✓✓ = detected in at least 30 % of samples, ✓✓✓ = detected in at least 60 % of samples.

Table E-2.4. Appendix II Chemicals Monitored for but Detected Once or Less in Leachate from MSW Landfills .

Acenaphthene	3,3-Dichlorobenzidine	Methyl methanesulfonate
Acenaphthylene	2,4-Dichlorophenol	Methylene bromide
Acetophenone	2,6-Dichlorophenol	2-Methylnaphthalene
2-Acetylanimofluorene	trans-1,3-Dichloropropene	1,4-Naphthoquinone
Acrolein	Dieldrin	1-Naphthylamine
Acrylonitrile	p-(Dimethylamino)azobenzene	2-Naphthylamine
Aldrin	7,12-Dimethylbenz[a]anthracene	m-Nitroaniline
Allyl chloride	3,3-Dimethylbenzidine	o-Nitroaniline
4-Aminobiphenyl	m-Dinitrobenzene	p-Nitroaniline
Anthracene	4,6-Dinitro-o-cresol	o-Nitrophenol
Benzo[a]anthracene	2,4-Dinitrophenol	p-Nitrophenol
Benzo[b]fluoranthene	2,4-Dinitrotoluene	N-Nitrosodi-n-butylamine
Benzo[k]fluoranthene	2,6-Dinitrotoluene	N-Nitrosodiethylamine
Beno[g,h,i]perylene	Dinoseb	N-nitrosodimethylamine
Benzo[a]pyrene	Di-n-octyl phthalate	N-nitrosodiphenylamine
Benzyl alcohol	Diphenylamine	N-nitrosodipropylamine
alpha-BHC	Disulfoton	N-Nitrosomethylethalamine
beta-BHC	Endrin	N-Nitrosopiperidine
gamma-BHC	Endrin aldehyde	N-Nitrosopyrrolidine
Bis(2-chloroethyl) ether	Ethyl methacrylate	Pentachlorobenzene
4-Bromophenyl phenyl ether	Famphur	Pentachloronitrobenzene
Butyl benzyl phthalate	Fluorene	Phenacetin
Carbon disulfide	Heptachlor	Phenanthrene
Chlordane	Heptachlor epoxide	p-Phenylenediamine
p-Chloroaniline	Hexachlorobenzene	Phorate
Chlorobenzilate	Hexachlorobutadiene	Polychlorinated biphenyls
2-Chloronaphthalene	Hexachlorocyclopentadiene	Pronamide
2-Chlorophenol	Hexachloroethane	Pyrene
4-Chlorophenyl phenyl ether	Hexachloropropene	Styrene
Chrysene	Indeno(1,2,3-cd)pyrene	2,4,5-T
m-Cresol	Isobutyl alcohol	1,2,4,5-Tetrachlorobenzene
o-Cresol	Isodrin	1,1,1,2-Tetrachloroethane
4,4-DDD	Kepone	1,1,2,2-Tetrachloroethane
4,4-DDE	Methacrylonitrile	Toxaphene
Dibenz[a,h]anthracene	Methapyrilene	1,2,4-Trichlorobenzene
Dibenzofuran	Methoxychlor	2,4,6-Trichlorophenol
1,2-Dibromo-3-chloropropane	3-Methylcholanthrene	1,2,3-Trichloropropane
1,2-Dibromoethane	Methyl bromide	Vinyl acetate
m-Dichlorobenzene	Methyl iodide	

E-2.3.3.2 Bramlett et al. (1987)

Bramlett et al. presented leachate chemistry data for 13 HW landfills that began operating from 1972 to 1983. The landfills were located in all of the four geographic regions of the U.S. defined by Bramlett et al. and had accepted a variety of HW. Leachate samples were collected from the landfills in 1985 and analyzed for indicator parameters and PPL metals, VOCs, and semivolatile organic compounds (SVOCs).

With the exception of beryllium, which was only detected in leachate from six landfills, all of the PPL metals were detected in leachate from 10 or more landfills. The trace metals detected at the highest average concentrations were arsenic, mercury, and nickel. The most commonly detected organic chemicals were acetone, benzene, 2-hexanone, methyl ethyl ketone, p-cresol, methylene chloride, phenol, and toluene. These chemicals were also generally detected at higher concentrations than other organic chemicals in the leachate.

E-2.3.3.3 NUS (1988)

As part of their study for EPA, NUS abstracted from TRW (1983) select leachate chemistry data for 11 HW landfills. The leachate chemistry data for the HW landfills are not complete: organic and inorganic chemical data are available for nine landfills, only inorganic chemical data are available for one landfill, and only organic chemical data are available for one landfill. The leachate samples were analyzed for 46 indicator parameters and inorganic chemicals and 32 organic chemicals.

The trace metals detected at the most landfills were chromium, copper, and zinc. The metals detected at more than one landfill and at the highest concentrations were arsenic, barium, and zinc. Only the concentrations for nine of the 32 organic chemicals were reported in NUS (1988). Of these, acetone and methylene chloride were detected at the highest concentrations. As described in Section E-2.3.2.2, NUS also compared the leachate chemistry data for the HW landfills and the MSW landfills in the database and found that the inorganic and organic chemicals generally occurred at higher concentrations in HW landfill leachate than in MSW landfill leachate.

E-2.3.3.4 Gibbons et al. (1992)

Gibbons et al. evaluated the chemistry of 945 leachate samples from 12 HW landfills owned by Chemical Waste Management, Inc. Nine of these HW landfills began operation before 1987 and were considered "old" landfills. Three of the landfills began operation in 1987 or later and were considered "new" landfills. The cutoff between the "old" and "new" landfills was based on the start of the LDR and more stringent landfill design requirements. Not all samples were analyzed for the same parameters. However, some were analyzed for trace metals and most were analyzed for the PPL VOCs. Gibbons et al. primarily considered four metals, arsenic, cadmium, mercury, and lead, and the PPL VOCs in their evaluation of leachate chemistry.

Of the four metals, arsenic was detected at the highest frequency (i.e., in 93% of the analyzed samples) and cadmium was detected at the highest concentration. Methylene chloride and toluene were the most frequently detected organic chemicals, found in over 75% of the analyzed samples. The organic chemicals detected at the highest average concentrations were 1,2-dichloroethane, methylene chloride, and 1,1,1-trichloroethane. Gibbons et al. found that most, but not all, of the considered chemicals were detected less frequently and at significantly lower concentrations in leachate from new HW landfills than in leachate from old HW landfills. The two significant exceptions to this are: (i) benzene, which was detected more than twice as frequent and at statistically higher average concentrations in leachate from new landfills than in leachate from old landfills; and (ii) vinyl chloride, which was detected at a statistically higher average concentration in leachate from new landfills than in leachate from old landfills.

E-2.3.3.5 Pavelka et al. (1994)

Pavelka et al. evaluated the leachate chemistry data summarized by EPA (1989) for 18 cells at ten HW landfills in the U.S. The landfills are located in all four of the geographical areas of the U.S. defined by EPA (1989). Three of the 18 cells were reportedly used for co-disposal of MSW and HW, with MSW being the predominant material. Waste disposal began at the landfills between about 1969 and 1988. The EPA report contains leachate chemistry data for one sampling event conducted in 1989. The leachate samples were analyzed for 231 chemicals, including VOCs, SVOCs, and trace metals.

All metals analyzed for were present. The most frequently detected trace metals were arsenic, barium, nickel, and zinc. These metals were also present at the highest concentrations. Twenty-nine of the 72 VOCs and 17 of the 107 SVOCs analyzed for were detected. The three most frequently detected VOCs, acetone, methyl ethyl ketone, and 4-methyl-2-pentanone, also were present at the highest concentrations. The dominant SVOCs were phthalic acid and phenol. Pavelka et al. evaluated the relationship between leachate concentration and chemicals properties and found that that, excluding the alcohols, the organic chemicals detected at the highest concentrations generally had relatively high solubilities. The organic chemicals detected at the lowest concentrations generally had relatively high octanol-water coefficients.

E-2.3.2.6 Conclusions from Previous Studies

Like MSW leachate, HW leachate is a mineralized liquid containing trace concentrations of heavy metals and synthetic organic chemicals. HW leachate may also be biologically active like MSW leachate, though generally to a much lesser degree, depending on the characteristics of the HW. The trace inorganic and organic chemicals detected most frequently and at the highest concentrations in HW leachate were arsenic, barium, nickel, zinc, acetone, methyl ethyl ketone, methylene chloride, phenol, and toluene. The organic chemicals with the highest concentrations have relatively high solubilities. The limited leachate chemistry data from new HW landfills show that most, but not all, of the PPL VOCs and selected metals were detected less frequently and at lower

concentrations in leachate from new HW landfills than in leachate from old HW landfills. Thus, the Subtitle C regulations and the LDR appear to have resulted in improved HW leachate quality. From a comparison of the data for MSW and HW leachate, chemicals are generally present at significantly higher concentrations in HW leachate than in MSW leachate. Also, certain chemicals, such as 1,2-dichloroethane, are detected more often in HW leachate than in MSW leachate. As expected, all of the Appendix II chemicals detected in MSW landfill leachate (Table E-2.3) and analyzed for in HW landfill leachate were found in HW leachate. However, several of the Appendix II chemicals detected once or less in MSW leachate (Table E-2.4) were detected more than once in HW leachate. Of these, acetophenone, o-cresol, 2,4-dichlorophenol, and isobutyl alcohol were detected most frequently in HW leachate.

E-2.3.4 ISW

E-2.3.4.1 Introduction

There are few published studies on the chemistry of leachate from ISW landfills. The primary reasons for this scarcity of information is that: (i) past studies focused on the chemistry of MSW and HW landfills, which historically have resulted in more ground-water contamination problems than ISW landfills; and (ii) ISW landfills have generally been less regulated than MSW and HW landfills, and leachate chemistry data were not typically required to be collected for the ISW landfills. This section summarizes published information on the leachate chemistry for three types of industrial wastes: (i) MSW ash (considered to be an ISW for the discussion of leachate chemistry in this appendix); (ii) coal ash; and (iii) C&DW. Select leachate chemistry data are presented in Table E-2.2.

E-2.3.4.2 MSW Ash

NUS (1987b,1990) conducted two studies to assess the chemical properties of MSW ash leachate. Though their studies included information on the chemistry of ash extracts, leachate from MSW/MSW ash co-disposal landfills, and leachate from MSW ash landfills, only the chemistry of leachate from MSW ash landfills is considered herein.

The first NUS study included a combined summary of leachate chemistry data from publications and for three MSW ash landfills in the U.S. Only limited data on the chemistry of MSW ash landfill leachate were found in publications from the U.S., Canada, Japan, and Europe. These data were collected using a variety of sampling procedures and analytical methods. However, the published data generally fell within the range of values for leachates from three MSW ash landfills in the U.S. These three landfills became operational from 1970 to 1981. Nine leachate samples were collected from the three landfills in 1986 and analyzed for metals, total organic carbon (TOC), organic scan, base neutral extractables (BNAs), PCBs, polychlorinated dibenzo-p-dioxins (PCDDs), and polychlorinated dibenzo-furans (PCDFs). The samples were not analyzed for VOCs because VOCs are combusted during the incineration process and

are not detected in MSW ash. The landfills were resampled for indicator parameters in 1987.

The second NUS study included leachate chemistry data for four MSW ash landfills. The landfills became operational between 1975 and 1988. Thirteen leachate samples were collected in 1988 and 1989 and analyzed for indicator parameters, select metals, Appendix IX SVOCs, and select PCDDs and PCDFs.

The results of the literature survey and chemical analyses indicate that MSW ash leachate can range from acidic to alkaline and has higher levels of specific conductance, total dissolved solids (TDS), sulfate, and chloride and lower levels of COD and TOC than MSW and HW leachates. Of the trace metals listed in Table E-2.2, all were detected in MSW ash leachate at concentrations near or above those for MSW leachate. Only barium, cadmium, and lead were detected at higher concentrations in MSW ash leachate than in MSW or HW leachate. Eleven BNAs were detected in the MSW ash leachate. The most frequently detected BNAs were bis (2-ethylhexyl) phthalate and dimethyl propanediol, both found in leachate from two of the seven landfills described in the NUS reports. Total PCDDs and PCDFs were detected in leachate at very low concentrations, ranging from 0.06-543 μg/l and 0.04-823 μg/l, respectively. NUS hypothesized that suspended solids in the leachate were probably the main contributor of PCDDs and PCDFs since these chemicals have a low water solubility. The maximum detected concentrations of metals in the MSW ash leachate were compared to the toxicity characteristic concentrations for solid waste given in 40 CFR § 261.24 and EPA MCLs and secondary MCLs (SMCLs). While the detected metals concentrations were less than the toxicity characteristic concentrations, most were greater than MCLs and SMCLs.

E-2.3.4.3 Coal Ash

There are few published data on the chemistry of coal ash landfill leachate. Most of the data on coal ash leachate are from ash ponds or chemical extraction tests on ash samples. Ash pond leachate may be more concentrated than landfill leachate due to the relatively long contact time between the ash and water used to sluice the ash. Leachate generated in a laboratory by extraction tests with ash samples may or may not resemble landfill leachate depending on the extraction method. Data on coal ash leachate chemistry for one landfill in the eastern U.S. are presented in this subsection. Chemistry data for ash ponds and coal ash leachate generated in the laboratory are also presented for comparison purposes.

GeoSyntec Consultants (1993) presented leachate chemistry data for a bituminous coal ash landfill that began operating in 1974. Leachate collected in the piping system beneath the ash flows to one of two leachate ponds. Three leachate samples were collected from the inlets to the ponds during 1992 and 1993 and analyzed for indicator parameters and metals. The leachate for this landfill is alkaline (i.e., pH of about 11), which limits the concentrations of dissolved metals in the leachate, and less mineralized than leachates from MSW, HW, and MSW ash landfills. In addition, the concentrations

of trace metals in the coal ash leachate were within the range of values for MSW landfill leachate.

Studies of the chemistry of coal ash leachate (not coal ash landfill leachate) were conducted by the Electric Power Research Institute (EPRI) (1978) and Eisenberg et al. (1986). The EPRI study presented maximum metals concentrations measured in fly ash pond, bottom ash pond, and ash pond leachates. Eisenberg et al. (1986) presented data on the chemistry of three fly ash leachates prepared by extraction tests. The leachates were made by filtering mixtures of fly ashes and dissolved water. All of the fly ashes were produced in plants burning eastern bituminous coal. One of the leachates was alkaline, one had a pH that was nearly neutral, and one was acidic. With the exception of chromium, the acidic leachate had the highest concentrations of metals. Since most of the leachable metals on fly ash are in the form of acid-soluble metal sulfates, a coal ash leachate with a high sulfate concentration generally has high metals concentrations. The coal ash leachates in the EPRI and Eisenberg et al. studies generally contained higher levels of sulfate and metals than the coal ash landfill leachate in the GeoSyntec study.

E-2.3.4.4 C&DW

Norstrom et al. (1991) presented leachate chemistry data for three C&DW landfills located near Houston, Texas. Wastes that are typically allowed at C&DW landfills include brush, grass, lumber, concrete, plaster, asphalt, rock, soil, and metal. Since the landfills did not have LCRSs, leachate was collected from wells installed into the waste. The leachate samples were analyzed for indicator parameters and metals.

Norstrom et al. found that the concentrations of chemicals in the C&DW leachate generally fell within the lower half of the range of concentrations reported for MSW leachate. Barium, lead, and zinc, however, were detected at higher concentrations in C&DW leachate than in MSW leachate.

E-2.3.4.5 Conclusions From Previous Studies

ISW landfill leachate chemistry can vary significantly depending on the type of waste. Leachate from MSW ash landfills can be acidic or alkaline and generally have higher levels of inorganic chemicals than MSW and HW leachates. Of the trace metals analyzed for, all were detected in MSW ash leachate at concentrations near or above those for MSW leachate and barium, cadmium, and lead were detected at concentrations higher than those for HW leachates. Coal ash landfill leachates can also be acidic or alkaline and are generally less mineralized than MSW leachates. Both MSW ash and coal ash leachates have essentially no VOCs and few SVOCs. MSW ash leachates, however, can also contain trace amounts of PCDDs and PCDFs.

C&DW landfill leachate can have lower concentrations of inorganic chemicals than leachate from MSW landfills. However, the trace metals barium, lead, and zinc can be detected at higher concentrations in C&DW leachate than in MSW leachate. C&DW

contains organic chemicals as evidenced by the relatively high TOC and COD levels. Based on the relatively low BOD level for C&DW leachate, these organic chemicals are not readily biodegradable. The specific organic chemicals present in C&DW leachate were not analyzed.

E-3 Data Collection and Reduction

E-3.1 Overview

The LCRS and LDS flow rate and flow chemistry data presented in this appendix were obtained from engineering drawings, project specifications, as-built records, and operation records, and interviews with facility owners, facility operators, design engineers, and regulatory agencies. The data were collected in accordance with a quality assurance project plan, which was reviewed and approved by the EPA. Efforts were made to obtain data from a wide variety of facilities, and to obtain as complete a record of data as possible, from construction of each facility to the time of data collection.

A database was developed that includes information and data for 187 individual landfill cells at 54 double-lined landfills. The data collected includes: (i) general facility information (including location, average annual rainfall, subsurface soil types, ground-water separation distance from bottom of landfill), summarized in Table E-3.1; (ii) general cell information (including cell area, type of waste, height of waste, dates of construction, operation, and closure), summarized in Table E-3.2; (iii) double-liner system design details (including type, thickness, and hydraulic conductivity of each layer), summarized in Table E-3.3; (iv) final cover system design details (including type, thickness, and hydraulic conductivity of each layer) summarized in Table E-3.4; (v) LCRS and LDS flow rate data, summarized in Tables E-3.5 and E-3.6, respectively; and (vi) LCRS and LDS chemical constituent data, summarized in Table E-3.7.

E-3.2 General Description of Cells

The distribution of landfills and cells in the database by waste type and geographic region is shown in Table E-3.8(a). As shown in this table, most of the landfills in the database are located in NE. This is not surprising because: (i) the NE has a relatively dense population; and (ii) double-liner systems are required for MSW landfills in several states in the NE. In addition, the majority of the landfills in the database are used for disposal of MSW. Based on the extent of the database and comparisons of these data with the published data presented in Section E-2, the database appears to adequately characterize conditions for MSW landfills in the NE and SE, HW landfills in the NE and SE, and MSW ash landfills in the NE. The database is quite sparse for landfills in the W, coal ash landfills, and C&DW landfills. Additional data from these facilities should be collected and evaluated.

Table E-3.1. Landfill Site Information.

Landfill Designation	Region of U.S. [1]	Average Annual Rainfall (mm)	Depth to Ground Water (m)	Subsurface Soil Type
A	NE	1120	ND[2]	Silt & Sand
B	NE	1070	3	Coarse Sand
C	SE	1120	2	Sand & Clay
D	SE	1630	2	ND
E	NE	1040	5	ND
F	NE	580	2	Sand
G	NE	910	2	ND
H	NE	1020	0	ND
I	NE	990	1	Silty Clay
J	NE	760	ND	Sand
K	NE	1120	ND	Sand
L	SE	1140	6	Clay
M	SE	1470	ND	ND
N	SE	1520	ND	Sand
O	SE	1500	ND	Sand
P	SE	1500	ND	ND
Q	NE	890	< 2	Glacial Till
R	NE	1040	3	Fine Sand & Silt
S	NE	1040	4	Fine Sand
T	NE	1300	20	Silt & Silty Sand
U	NE	1070	1	ND
V	SE	1730	ND	ND
W	SE	1500	ND	Fine Sand / Clay Layers
X	SE	1020	ND	ND
Y	NE	1190	ND	Glacial Till
Z	NE	1250	ND	Silt & Clay
AA	NE	1140	< 2	Glacial Till
AB	SE	1700	ND	Chalk
AC	W	280	91	Clay / Sandstone
AD	SE	1830	0	Sandy Silt / Clay
AE	NE	1210	3-7	Clay & Silt
AF	NE	1120	2	ND
AG	NE	840	< 2	Clay
AH	NE	840	4	Silty Sand
AI	NE	1140	ND	Sand
AJ	NE	1250	ND	Silt & Clay
AK	NE	760	ND	Silt & Clay
AL	NE	790	3	Sand & Gravel
AM	W	430	14	Silt

Table E-3.1. Landfill Site Information (Continued).

Landfill Designation	Region of U.S. (1)	Average Annual Rainfall (mm)	Depth to Ground Water (m)	Subsurface Soil Type
AN	NE	1120	5	Sand
AO	NE	830	3	Silty Sand
AP	W	380	> 1500	Shale
AQ	NE	970	0	ND
AR	NE	1140	< 2	Clay
AS	SE	1420	1	ND
AT	W	740	3	Clay
AU	NE	1020	3	Clay & Sand
AV	NE	790	3	Silty Clay
AW	SE	1120	2	Silty Sand
AX	NE	1040	1	Sand & Gravel
AY	NE	860	ND	ND
AZ	NE	760	2	Sand
BA	NE	860	14	Silty & Sandy Clay
BB	SE	1090	2	ND

Notes: (1) Region of the U.S. (See Figure E-1.3): NE = northeast, SE = southeast, W = west.
(2) ND = not determined.

Table E-3.2. General Landfill Cell Construction and Operation Information.

Cell No.	Waste Type[1]	Cell Area (ha)	Max. Waste Height (m)	Avg. Liner Base Slope (%)	Final Cover Top/Side Slopes (%)	End of Construct. Date	Waste Placement Start Date	Final Closure Date	3rd Party CQA?		Flow Meas. Methods for LCRS and LDS[2]
									Liner System	Cover System	
A1	C&DW	5.3	79	4.0	NA[3]	1989-90	1989-90	NA	N	NA	ND[3]
A2	C&DW	6.4	79	4.0	NA	Sep-92	Oct-92	NA	N	NA	ND
B1	MSW	3.3	21	2.0	5/25	May-84	May-84	Nov-88	N	Y	5
B2	MSW	3.5	21	2.0	5/25	May-84	May-84	Nov-88	N	Y	5
B3[4]	MSW	6.4	25	2.0	5/25	Jul-87	Jul-87	NA	N	NA	2
B4	MSW	2.9	25	2.0	NA	Apr-91	May-91	NA	N	NA	2
B5	MSW	3.9	25	2.0	NA	May-92	May-92	NA	N	NA	2
C1	MSW	3.2	24	2.5	NA	Apr-90	May-90	NA	Y	NA	2
C2	MSW	3.7	40	2.5	NA	Dec-90	Apr-91	NA	Y	NA	2
C3	MSW	3.6	46	2.5	NA	Mar-91	Aug-91	NA	Y	NA	2
C4	MSW	3.7	46	2.5	NA	Dec-91	Feb-92	NA	Y	NA	2
C5	MSW	2.6	43	3.0	NA	Apr-92	Nov-92	NA	Y	NA	2
C6	MSW	3.6	40	3.0	NA	May-93	Aug-93	NA	Y	NA	2
D1	HW	0.4	7.9	2.0	ND[2]	Sep-85	Oct-85	May-86	Y	ND	6
D2	HW	0.3	7.9	2.0	ND	Sep-85	Jan-86	Mar-88	Y	ND	6
D3	HW	0.3	7.9	2.0	NA	Jun-87	Jul-87	NA	Y	NA	6
D4	HW	0.4	7.9	2.0	NA	Jun-87	Jan-89	NA	Y	NA	6
E1	MSW	2.4	40	1.3	NA	Mar-88	Mar-88	NA	N	NA	6
E2	MSW	2.4	40	1.3	NA	Oct-87	Oct-87	NA	N	NA	6
E3	MSW	1.2	40	1.3	NA	May-90	May-90	NA	N	NA	6
E4	MSW	1.2	40	1.3	NA	Jul-90	Jul-90	NA	N	NA	6
F1	MSW	1.8	ND	5.0	NA	Jul-92	Jul-92	NA	N	NA	ND
G1	MSW	3.0	ND	2.0	NA	May-89	Jun-89	NA	Y	NA	2,3
G2	MSW	1.6	ND	2.0	NA	May-89	Jun-89	NA	Y	NA	2,3
G3	MSW	1.7	ND	2.0	NA	Nov-92	Dec-92	NA	Y	NA	2
H1	HW	0.5	ND	3.0	4/14	1985	1985	1990	Y	ND	ND
H2	HW	1.1	ND	3.0	4/14	1986	1986	NA	Y	NA	ND
H3	HW	0.9	ND	3.0	4/14	1988	Jul-88	NA	Y	NA	ND
H4	HW	1.2	ND	3.0	4/14	1990	Dec-90	NA	Y	NA	ND
H5	HW	0.8	ND	3.0	4/14	1991	Sep-91	NA	Y	NA	ND
H6	HW	1.3	ND	3.0	NA	1992	Nov-92	NA	Y	NA	ND
I1	MSW	3.2/2.7[5]	4.9	2.0	5/33	Aug-87	Aug-87	Oct-94	Y	Y	1
I2	MSW	4.2/2.3[5]	7.9	2.0	5/33	Oct-87	Oct-87	Oct-94	Y	Y	1
I3	MSW	3.4/1.8[5]	7.9	2.0	5/33	Apr-88	Apr-88	Oct-94	Y	Y	1
I4	MSW	4.7	ND	ND	5/33	May-92	May-92	Jul-94	Y	Y	ND
I5	MSW	4.7	ND	ND	5/33	Jul-92	Jul-92	May-94	Y	Y	ND
J1	MSW	1.0	ND	ND	ND	Jul-90	Oct-90	Fall 93	Y	Y	ND
J2	MSW	1.0	ND	ND	ND	Sep-90	Apr-91	Fall 93	Y	Y	ND
J3	MSW	1.0	ND	ND	ND	Aug-91	Nov-91	Fall 93	Y	Y	ND
J4	MSW	1.0	ND	ND	ND	Aug-91	Jul-92	Fall 93	Y	Y	ND
J5	MSW	1.0	ND	ND	NA	Nov-92	Jun-93	NA	Y	NA	ND
J6	MSW	1.0	ND	ND	NA	Nov-92	NA	NA	Y	NA	ND

Table E-3.2. General Landfill Cell Construction and Operation Information (Continued).

Cell No.	Waste Type[1]	Cell Area (ha)	Max. Waste Height (m)	Avg. Liner Base Slope (%)	Final Cover Top/Side Slopes (%)	End of Construct. Date	Waste Placement Start Date	Final Closure Date	3rd Party CQA?		Flow Meas. Methods for LCRS and LDS[2]
									Liner System	Cover System	
K1	MSW	2.7	15	4.5	NA	Oct-89	Dec-89	NA	N	NA	ND
L1	HW	1.5	7.6	2.0	NA	Jun-90	Aug-90	NA	Y	NA	ND
L2	HW	1.5	7.6	2.0	NA	Apr-93	Jan-94	NA	Y	NA	ND
L3	HW	1.5	7.6	2.0	NA	May-90	Jun-90	NA	Y	NA	ND
L4	HW	1.5	7.6	2.0	NA	Oct-91	Feb-92	NA	Y	NA	ND
M1	ASH(M)	4.0	ND	2.0	NA	Late 90	Sep-91	NA	ND	NA	ND
N1	MSW	4.4	ND	2.0	NA	1988	1988	NA	ND	NA	ND
N2	MSW	6.3	ND	2.0	NA	1991	Jan-92	NA	Y	NA	ND
O1	MSW	4.2	7.9	3.2	NA	Aug-88	Mar-88	NA	Y	NA	2
O2	MSW	4.9	7.9	3.2	NA	Feb-89	Mar-89	NA	Y	NA	2
O3	MSW	4.7	ND	3.2	NA	Jan-94	Feb-94	NA	Y	NA	2
P1	ASH(M)	1.8	ND	2.0	NA	1991	1991	NA	Y	NA	ND
P2	ASH(M)	2.4	ND	2.0	NA	1992	Late 92-93	NA	Y	NA	ND
P3	ASH(M)	2.3	ND	2.0	NA	Late 93	Late 93	NA	Y	NA	ND
Q1	MSW	4.5	30	2.0	NA	Mar-90	Mar-90	NA	Y	NA	ND
Q2	MSW	1.8	30	2.0	NA	Dec-93	Mar-94	NA	Y	NA	ND
R1	MSW	2.0	ND	3.5	NA	1993	May-93	NA	N	NA	ND
S1	MSW	2.0	ND	0.5	NA	Sep-90	Sep-90	NA	Y	NA	ND
S2	ASH(M)	1.6	ND	0.5	NA	Aug-90	Aug-90	NA	Y	NA	ND
T1	MSW	3.8	21	2.0	NA	Jan-91	May-91	NA	Y	NA	3
T2	MSW	3.8	21	2.0	NA	Jan-92	Jan-92	NA	Y	NA	3
U1	MSW	1.9	26	2.9	ND	Jul-86	Jul-86	Sep-88	Y	N	1,3
U2	MSW	2.6	26	3.0	ND	Jan-87	Jan-87	Sep-88	Y	N	1,3
U3	MSW	1.5	24	ND	ND	Nov-87	Nov-87	Sep-88	Y	N	1,3
U4	MSW	1.9	23	ND	ND	Mar-88	Mar-88	Oct-88	Y	N	1,3
V1	MSW	4.2	ND	4.0	NA	1989	Jan-90	NA	Y	NA	ND
V2	MSW	3.9	ND	4.0	NA	1989	Jan-90	NA	Y	NA	ND
V3	MSW	4.0	ND	4.0	NA	1990	Nov-90	NA	Y	NA	ND
V4	MSW	3.7	ND	4.0	NA	1990	Dec-90	NA	Y	NA	ND
V5	MSW	3.3	ND	4.0	NA	1993	May-93	NA	Y	NA	ND
W1-2	MSW	15.4	24	1.0	NA	May-92	May-92	NA	Y	NA	ND
X1	MSW	3.0	ND	2.0	NA	1992	Aug-92	NA	Y	NA	ND
Y1	ASH(M)	2.2	ND	5.5	NA	Sep-88	Jan-89	NA	Y	NA	1
Y2	MSW	3.0	ND	5.5	NA	1990	Jan-91	NA	Y	NA	1
Z1	ASH(C)	2.6	23	3.2	NA	Dec-91	Mar-92	NA	N	NA	ND
AA1	MSW	1.8	37	2.0	NA	Oct-90	Oct-90	NA	Y	NA	ND
AA2	MSW	2.6	37	2.0	NA	Jul-90	Jul-90	NA	Y	NA	ND
AA3	MSW	3.4	37	2.0	NA	Sep-91	Mar-92	NA	Y	NA	ND
AB1	HW	3.8	>90	3.0	NA	1986	1987	NA	Y	NA	1
AB2	HW	4.1	>90	3.0	NA	1986	1987	NA	Y	NA	1
AB3	HW	5.0	>90	3.0	NA	Oct-87	Feb-88	NA	Y	NA	1
AB4	HW	5.8	>90	3.0	NA	Apr-89	May-89	NA	Y	NA	1

Table E-3.2. General Landfill Cell Construction and Operation Information (Continued).

Cell No.	Waste Type[1]	Cell Area (ha)	Max. Waste Height (m)	Avg. Liner Base Slope (%)	Final Cover Top/Side Slopes (%)	End of Construct. Date	Waste Placement Start Date	Final Closure Date	3rd Party CQA?		Flow Meas. Methods for LCRS and LDS[2]
									Liner System	Cover System	
AC1	HW	4.6	30	2.0	NA	Feb-87	Mar-87	NA	Y	NA	2
AC2	HW	4.2	30	2.0	NA	Dec-87	Mar-88	NA	Y	NA	2
AC3	HW	4.6	30	2.0	NA	Jun-89	Jun-89	NA	Y	NA	2
AC4	HW	3.8	30	2.0	NA	Jul-89	Jul-89	NA	Y	NA	2
AC5	HW	6.9	ND	ND	NA	Mar-92	Mar-92	NA	Y	NA	2
AC6	HW	6.9	ND	ND	NA	Mar-92	Mar-92	NA	Y	NA	2
AC7	HW	4.0	ND	ND	NA	Dec-93	Jan-94	NA	Y	NA	2
AC8	HW	6.1	ND	ND	NA	Dec-93	Jan-94	NA	Y	NA	2
AD1	HW	0.6	21	2.5	5/20	May-85	May-85	Jul-88	Y	Y	2
AD2	HW	0.6	21	2.5	5/20	Jul-85	Jul-85	Jul-88	Y	Y	2
AD3	HW	0.6	21	2.5	5/20	Nov-85	Nov-85	Jul-88	Y	Y	2
AD4	HW	0.6	21	2.5	5/20	Nov-85	Nov-85	Jul-88	Y	Y	2
AD5	HW	0.5	21	2.5	5/20	Jun-86	Jun-86	Jul-88	Y	Y	2
AD6	HW	0.9	21	2.5	5/20	Jun-86	Jun-86	Jul-88	Y	Y	2
AD7	HW	1.5	24	2.5	5/20	Sep-87	Sep-87	Oct-93	Y	Y	2
AD8	HW	1.5	24	2.5	5/20	Apr-88	Apr-88	Oct-93	Y	Y	2
AD9	HW	1.3	24	2.5	5/20	Dec-88	Dec-88	Oct-93	Y	Y	2
AD10	HW	1.3	24	2.5	5/20	Dec-88	Dec-88	NA	Y	NA	2
AD11	HW	1.1	24	2.5	NA	Aug-89	Aug-89	NA	Y	NA	2
AD12	HW	1.1	24	2.5	NA	Aug-89	Aug-89	NA	Y	NA	2
AD13	HW	1.1	24	2.5	NA	Oct-90	Oct-90	NA	Y	NA	2
AD14	HW	1.1	24	2.5	NA	Oct-90	Oct-90	NA	Y	NA	2
AD15	HW	1.1	24	2.5	NA	Apr-92	Apr-92	NA	Y	NA	2
AD16	HW	1.1	24	2.5	NA	Apr-92	Apr-92	NA	Y	NA	2
AD17	HW	1.7	24	2.5	NA	Mar-94	Mar-94	NA	Y	NA	2
AD18	HW	1.7	24	2.5	NA	Nov-93	Nov-93	NA	Y	NA	2
AE1	MSW	4.5	35	2.0	NA	Apr-88	May-88	NA	Y	NA	ND
AE2	MSW	5.3	35	2.0	NA	Nov-90	Dec-90	NA	Y	NA	ND
AE3	MSW	4.0	35	2.0	NA	Mar-94	May-94	NA	Y	NA	ND
AF1	ASH(M)	2.2	26	2.2	NA	Nov-89	Jan-90	NA	Y	NA	ND
AG1	MSW	8.1	30	5.0	NA	Mar-92	Apr-92	NA	Y	NA	ND
AH1	MSW/ASH(M)	1.2	ND	3.0	NA	Apr-91	Nov-91	NA	Y	NA	ND
AH2	MSW/ASH(M)	1.1	ND	3.0	NA	Apr-91	Nov-91	NA	Y	NA	ND
AH3	MSW/ASH(M)	1.1	ND	3.0	NA	Apr-91	Nov-91	NA	Y	NA	ND
AH4	MSW/ASH(M)	1.1	ND	3.0	NA	Apr-91	Nov-91	NA	Y	NA	ND
AH5	MSW/ASH(M)	1.0	ND	3.0	NA	Apr-91	Nov-91	NA	Y	NA	ND
AI1	C&DW	3.5	49	2.5	NA	Nov-90	Nov-90	NA	N	NA	ND
AI2	C&DW	2.8	49	2.5	NA	Nov-90	Nov-90	NA	N	NA	ND
AJ1	MSW	3.6	ND	2.0	NA	Mar-94	Jun-94	NA	N	NA	2
AK1	MSW	1.4	34	1.0	NA	May-93	Oct-93	NA	Y	NA	2
AK2	MSW	1.6	34	1.0	NA	Oct-94	Oct-94	NA	Y	NA	2
AL1	MSW	14.9	68	1.0	NA	1988-89	1990	NA	Y	NA	3
AM1	MSW	3.2/2.4[5]	27	6.0	NA	Sep-90	Oct-90	NA	Y	NA	ND
AM2	MSW	4.8/2.4[5]	27	6.0	NA	Sep-90	Oct-90	NA	Y	NA	ND

Table E-3.2. General Landfill Cell Construction and Operation Information (Continued).

Cell No.	Waste Type[1]	Cell Area (ha)	Max. Waste Height (m)	Avg. Liner Base Slope (%)	Final Cover Top/Side Slopes (%)	End of Construct. Date	Waste Placement Start Date	Final Closure Date	3rd Party CQA?		Flow Meas. Methods for LCRS and LDS[2]
									Liner System	Cover System	
AN1	ASH(M)	1.2	52	2.5	NA	Jun-91	Jun-91	NA	Y	NA	ND
AN2	ASH(M)	0.5	52	ND	NA	Jun-92	Jun-92	NA	Y	NA	ND
AN3	ASH(M)	0.5	52	ND	NA	Jun-92	Nov-92	NA	Y	NA	ND
AN4	ASH(M)	0.2	52	0.80	NA	Sep-93	Sep-93	NA	Y	NA	ND
AO1	MSW	1.8	23	1.0	NA	Jan-92	Jan-92	NA	Y	NA	2
AO2	MSW	1.8	23	1.0	NA	Jul-92	Jul-92	NA	Y	NA	2
AO3	MSW	1.8	23	1.0	NA	Sep-93	Jun-94	NA	Y	NA	2
AO4	MSW	1.8	23	1.0	NA	Sep-93	Jun-94	NA	Y	NA	2
AP1	HW	1.9	13	2.0	NA	Dec-89	Jul-91	NA	Y	NA	1,4
AQ1	HW	0.6	21	2.0	12/33	Mar-86	Mar-86	Early 90	Y	ND	2
AQ2	HW	0.5	21	2.0	12/33	Mar-86	Mar-86	Early 90	Y	ND	2
AQ3	HW	0.5	21	2.0	12/33	Mar-86	Jul-86	Early 90	Y	ND	2
AQ4	HW	0.6	21	2.0	12/33	Mar-86	Aug-86	Early 90	Y	ND	2
AQ5	HW	0.7	21	2.0	12/33	Sep-86	Apr-87	Mid 91	Y	ND	2
AQ6	HW	0.5	21	2.0	12/33	Sep-86	Apr-87	Mid 91	Y	ND	2
AQ7	HW	0.8	21	2.0	12/33	Sep-86	Apr-87	Mid 91	Y	ND	2
AQ8	HW	0.8	21	2.0	12/33	Sep-86	Jan-89	Mid 91	Y	ND	2
AQ9	HW	0.5	21	2.0	12/33	Sep-86	Jan-89	Mid 91	Y	ND	2
AQ10	HW	0.9	21	2.0	12/33	Sep-86	Jan-89	Mid 91	Y	ND	2
AR1	MSW	9.7	11	2.0	NA	1992	Mar-92	NA	Y	NA	ND
AR2	MSW	2.0	11	2.0	NA	1995	Mar-95	NA	Y	NA	ND
AS1	HW	1.0	9.8	3.0	3/29	Mar-89	Jul-89	Oct-91	Y	Y	ND
AT1	HW	2.6	11	1.5	10/33	Dec-87	Apr-88	Nov-88	Y	Y	ND
AU1	MSW	2.9	23	1.5	NA	Sep-90	Jan-91	NA	Y	NA	ND
AV1	HW	3.1	20	2.0	NA	Sep-86	Sep-86	NA	N	NA	ND
AV2	HW	2.4	20	2.0	NA	Oct-87	Oct-87	NA	N	NA	ND
AV3	HW	2.5	20	2.0	NA	Jun-88	Mar-89	NA	N	NA	ND
AV4	HW	2.0	20	2.0	NA	Oct-89	Nov-89	NA	Y	NA	ND
AV5	HW	2.9	23	2.0	NA	Aug-91	Jan-92	NA	Y	NA	ND
AW1	MSW	2.4	21	2.0	NA	Apr-93	May-93	NA	Y	NA	2
AW2	MSW	2.4	21	2.0	NA	Jul-93	Aug-93	NA	Y	NA	2
AW3	MSW	2.4	21	2.0	NA	May-94	May-94	NA	Y	NA	2
AW4	MSW	2.4	21	2.0	NA	Jun-94	Aug-94	NA	Y	NA	2

Table E-3.2. General Landfill Cell Construction and Operation Information (Continued).

Cell No.	Waste Type[1]	Cell Area (ha)	Max. Waste Height (m)	Avg. Liner Base Slope (%)	Final Cover Top/Side Slopes (%)	End of Construct. Date	Waste Placement Start Date	Final Closure Date	3rd Party CQA?		Flow Meas. Methods for LCRS and LDS[2]
									Liner System	Cover System	
AX1	MSW	2.0	24	2.0	6/33	Jun-88	Jul-88	Feb-91	Y	N	2
AX2	MSW	2.0	24	2.0	6/33	Jun-88	Jul-88	Feb-91	Y	N	2
AX3	MSW	1.7	24	2.0	6/33	Aug-88	Sep-88	Apr-93	Y	N	2
AX4	MSW	1.7	24	2.0	6/33	Aug-88	Sep-88	Apr-93	Y	N	2
AX5	MSW	2.8	24	2.0	6/33	Sep-88	Oct-88	NA	Y	N	2
AX6	MSW	3.9	24	2.0	6/33	Dec-88	Dec-88	NA	Y	N	2
AX7	MSW	2.6	24	2.0	NA/33	Jan-89	Feb-89	NA	Y	N	2
AX8	MSW	3.8	24	2.0	NA/33	Jul-89	Jul-89	NA	Y	N	2
AX9	MSW	3.3	24	2.0	NA/33	Dec-89	Dec-89	NA	Y	N	2
AX10	MSW	3.9	24	2.0	NA/33	Feb-90	Jul-90	NA	Y	N	2
AX11	MSW	3.0	24	2.0	NA/33	Feb-90	Feb-90	NA	Y	N	2
AX12	MSW	4.0	24	2.0	NA/33	Oct-90	Oct-90	NA	Y	N	2
AX13	MSW	3.0	24	2.0	NA/33	Jan-91	Jan-91	NA	Y	N	2
AX14	MSW	2.8	24	2.0	NA	Apr-92	Apr-92	NA	Y	NA	2
AX15	MSW	2.8	24	2.0	NA	May-92	May-92	NA	Y	NA	2
AX16	MSW	4.5	24	2.0	NA	Jan-93	Jan-93	NA	Y	NA	2
AY1	HW	1.3	14	2.0	NA	Jul-94	Oct-94	NA	Y	NA	2
AY2	HW	1.0	14	2.0	NA	Jul-94	Aug-94	NA	Y	NA	2
AY3	HW	1.0	14	2.0	NA	Jul-94	Aug-94	NA	Y	NA	2
AZ1	MSW	3.8	41	2.0	NA	Sep-92	Dec-92	NA	Y	NA	ND
BA1	HW	3.0	27	4.0	NA	Jun-91	Oct-91	NA	Y	Y	ND
BA2	HW	3.2	27	4.0	NA	Nov-93	Apr-94	NA	Y	Y	ND
BB1	MSW	4.0	28	2.0	NA	Dec-90	Feb-91	NA	Y	NA	2
BB2	MSW	2.4	30	2.0	NA	Jan-93	Jan-93	NA	Y	NA	2
BB3	MSW	2.8	30	2.0	NA	Jan-93	Jan-93	NA	Y	NA	2

Notes:

(1) C&DW = construction and demolition waste, MSW = municipal solid waste, HW = hazardous waste. ASH(M) = MSW ash, ASH(C) = coal ash.

(2) Codes for method of flow measurement:
- 1 = Automatic pumping system, liquid volume recorded from accumulating flow meter
- 2 = Periodic pumping if liquid present in sump, volume recorded from accumulating flow meter
- 3 = Periodically measure time to fill a known volume
- 4 = Automatic pumping system from sump to a holding tank, volume transferred from holding tank measured
- 5 = Periodic pumping if liquid present in sump, volume estimated from change in liquid level
- 6 = Automatic pumping system, liquid volume estimated by multiplying pump capacity x time

(3) NA = not applicable, ND = not determined.

(4) Final cover system was installed over 65% of Cell B3 at 65 months after start of waste placement.

(5) Values represent LCRS and LDS areas, respectively.

Table E-3.3. Landfill Double-Liner System Details.

Cell No.	LCRS				Primary Liner				LDS				Secondary Liner			
	Avg. Pipe or Swale Spacing (m)	Pipe or Swale Size (mm or m) & Material	Drainage Layer(s) Material	Drainage Layer(s) Thick. (mm)	Type of Liner[1]	GM Type[2]	GM Thick. (mm)	GCL/CCL Thick. (mm)	Avg. Pipe or Swale Spacing (m)	Pipe or Swale Size (mm or m) & Material	Drainage Layer(s) Material	Drainage Layer(s) Thick. (mm)	Type of Liner[1]	GM Type[2]	GM Thick. (mm)	GCL/CCL Thick. (mm)
A1	17	150 PVC	S	600	GM	HDPE	1.5	NA[3]	17	150 PVC	S	600	GM	PVC	1.5	NA
A2	17	150 PVC	S	600	GM	HDPE	2.0	NA	17	150 PVC	S	600	GM	PVC	1.5	NA
B1-2	38	150 PVC	S	450	GM	CSPE	0.9	NA	38	150 PVC	S	450	GM	PVC	0.8	NA
B3	30	150 PVC	S	450	GM/CCL	CSPE	0.9	600	30	150 PVC	S	450	GM	PVC	0.8	NA
B4-5	ND[3]	ND	S	450	GM/CCL	HDPE	1.5	600	ND	ND	GN	5	GM	HDPE	1.5	NA
C1-5	91	200 PVC	S	600	GM	HDPE	2.0	NA	91	100 PVC	S	450	GM/CCL	HDPE	2.0	300
C6	91	200 HDPE	S	600	GM/GCL	HDPE	2.0	6	91	150 PVC	S	450	GM/CCL	HDPE	2.0	300
D1-4	37	100 HDPE	S	300	GM	HDPE	2.0	NA	37	100 HDPE	S	300	CCL/GM	HDPE	1.0	900
E1-4	46	ND	S	600	GM	CSPE	0.9	NA	46	ND	S	600	GM/CCL	PVC	0.8	600
F1	37	150 PVC	S	600	GM	HDPE	1.5	NA	37	150 PVC	S	300	GM	HDPE	1.5	NA
G1-2	46	150 HDPE	S	600	GM	HDPE	1.5	NA	46	100 HDPE	S	300	GM/CCL	HDPE	1.5	600
G3	23	150 PVC	S/G	600/600	GM/CCL	HDPE	1.5	450	23	100 PVC	S	300	GM/CCL	HDPE	1.5	600
H1-6	46	150 PVC	S	300	GM	PVC	0.8	NA	46	150 PVC	S	300	GM/CCL	PVC	0.8	900
I1-3	30	ND	S	600	GM	HDPE	1.5	NA	30	ND	S	450	GM/CCL	HDPE	1.5	300
I4-5, base	ND	ND	TC/G	150/450	GM/GCL	HDPE	1.5	6	ND	ND	GN	10	GM/CCL	HDPE	1.5	150
I4-5, sides	ND	ND	NA	NA	GM/GCL	HDPE	1.5	6	NA	NA	GN	5	GM/CCL	HDPE	1.5	150
J1-4	ND	PVC	S	600	GM	PVC	1.5	NA	ND	PVC	S	ND	GM	PVC	0.8	NA
J5-6	ND	PVC	S	600	GM	PVC	0.8	NA	ND	PVC	S	ND	GM	PVC	0.8	NA
K1	ND	200 HDPE	S	600	GM	HDPE	2.0	NA	ND	150 HDPE	S/GN	300/5	GM/CCL	LLDPE	1.5	600
L1-4, base	20	ND	S	300	GM/CCL[4]	HDPE	1.5	300	20	ND	S	300	GM/CCL	HDPE	1.5	900
L1-4, sides	NA	NA	S	300	GM	HDPE	1.5	NA	NA	NA	S	300	GM/CCL	HDPE	1.5	900
M1	ND	ND	S	600	GM	HDPE	1.5	NA	ND	ND	S	300	GM	HDPE	1.5	NA
N1	ND	ND	S	600	GM	HDPE	2.5	NA	NA	NA	GN	5	CCL	NA	NA	300
N2	ND	ND	S	600	GM	HDPE	1.5	NA	NA	NA	GN	5	GM/CCL	HDPE	1.5	300
O1-3	NA	NA	G/S	300/300	GM	HDPE	2.0	NA	ND	ND	S/GN	300/5	GM/CCL	HDPE	1.0	150
P1-3, base	NA	NA	S/GN	600/5	GM	HDPE	1.5	NA	ND	ND	GN	5	GM/GCL/CCL	HDPE	1.5	150
P1-3, sides	NA	NA	S/GN	600/5	GM	HDPE	1.5	NA	ND	ND	GN	5	GM/CCL	HDPE	1.5	150
Q1-2	46	100 PVC	S	450	GM	HDPE	1.5	NA	46	100 PVC	S	300	CCL	NA	NA	600
R1	ND	150 HDPE	G	600	GM/CCL	HDPE	1.5	450	ND	150 HDPE	GN	10	GM/CCL	HDPE	1.5	600
S1-2	ND	ND	S/GN	600/5	GM	HDPE	2.0	NA	ND	ND	GN	5	GM/CCL	HDPE	2.0	600
T1-2	30	150 PVC	G/S	150/450	GM	HDPE	1.5	NA	NA	NA	GN	13	GM/CCL	HDPE	1.5	150

Table E-3.3. Landfill Double-Liner System Details (Continued).

Cell No.	LCRS				Primary Liner				LDS				Secondary Liner			
	Avg. Pipe or Swale Spacing (m)	Pipe or Swale Size (mm or m) & Material	Drainage Layer(s) Material	Drainage Layer(s) Thick. (mm)	Type of Liner[1]	GM Type[2]	GM Thick. (mm)	GCL/ CCL Thick. (mm)	Avg. Pipe or Swale Spacing (m)	Pipe or Swale Size (mm or m) & Material	Drainage Layer(s) Material	Drainage Layer(s) Thick. (mm)	Type of Liner[1]	GM Type[2]	GM Thick. (mm)	GCL/ CCL Thick. (mm)
U1	30	100 PVC	S	600	GM	HDPE	1.5	NA	30	100 PVC	GN	5	GM	HDPE	1.5	NA
U2	24	100 PVC	S	600	GM	HDPE	1.5	NA	24	100 PVC	GN	5	GM	HDPE	1.5	NA
U3-4	ND	ND	S	600	GM	HDPE	1.5	NA	ND	ND	GN	5	GM	HDPE	1.5	NA
V1-5	ND	ND	S/GN	600/5	GM	HDPE	1.5	NA	ND	ND	S/GN	300/5	GM/CCL	HDPE	1.5	150
W1-2	91	200 HDPE	S/GN	600/5	GM	HDPE	1.5	NA	NA	NA	GN	5	GM/GCL/CCL	HDPE	1.5	6/150
X1	NA	NA	S	600	GM	HDPE	1.5	NA	ND	ND	GN	5	GM/CCL	HDPE	1.5	150
Y1-2	30	150 PVC	S	600	GM/CCL	HDPE	2.0	450	30	150 PVC	S	300	GM/CCL	HDPE	2.0	600
Z1	35	150 PVC	S	600	GM/CCL	HDPE	1.5	450	ND	150 PVC	S	300	GM/CCL	HDPE	1.5	600
AA1-3	46	150 PVC	S	600	GM/CCL	HDPE	2.0	450	46	150 PVC	S	300	GM/CCL	HDPE	2.0	600
AB1-4, base	ND	ND	G	300	GM/CCL	HDPE	1.5	450	ND	ND	S	300	GM/CCL	HDPE	1.5	900
AB1-4, sides	NA	NA	GN	5	GM/CCL	HDPE	1.5	450	NA	NA	S	300	GM/CCL	HDPE	1.5	900
AC1-4, base	ND	ND	S	300	GM/CCL	HDPE	1.5	450	ND	ND	G/GN	300/5	GM/CCL	HDPE	1.5	900
AC1-4, sides	NA	NA	S	300	GM/CCL	HDPE	1.5	450	NA	NA	GN	5	GM/CCL	HDPE	1.5	900
AC5-8	ND	ND	GN	5	GM/CCL	HDPE	1.5	450	ND	ND	GN	5	GM/CCL	HDPE	1.5	900
AD1-6, base	100	ND	S	300	GM/CCL	HDPE	1.5	900	30	ND	S	300	GM/CCL	HDPE	1.5	900
AD1-6, sides	NA	NA	GN	5	GM/CCL	HDPE	1.5	900	NA	NA	GN	5	GM/CCL	HDPE	1.5	900
AD7-18, base	NA	ND	S	300	GM/CCL	HDPE	1.5	900	53	ND	GN	5	GM/CCL	HDPE	1.5	900
AD7-18, sides	NA	NA	GN	5	GM/CCL	HDPE	1.5	900	NA	NA	GN	5	GM/CCL	HDPE	1.5	900
AE1-3	46	150 HDPE	S	300	GM/CCL	HDPE	2.0	600	46	100 HDPE	S	300	CCL	NA	NA	600
AF1	15	150	S	5	GM/CCL	HDPE	1.5	450	61	150	S	300	GM/CCL	HDPE	2.0	900
AG1	46	150 PVC	G/S	150/300	GM/CCL	HDPE	2.0	450	46	150 PVC	S	300	GM	HDPE	2.0	NA
AH1-5	46	150 PVC	S	450	GM/CCL	HDPE	2.0	450	46	150 PVC	S	300	GM/CCL	HDPE	1.5	600
AI1-2, base	15	150 PVC	S	600	GM/CCL	HDPE	2.0	450	15	150 PVC	S	300	GM/CCL	HDPE	1.5	600
AI1-2, sides	15	150 PVC	S	600	GM	HDPE	2.0	NA	NA	NA	GN	5	GM/CCL	HDPE	1.5	600
AJ1	30	150 PVC	S	600	GM/CCL	HDPE	1.5	450	30	150 PVC	S	300	GM/CCL	HDPE	1.5	600
AK1-2	61	200 HDPE	S/GN	600/5	GM/GCL/CCL	HDPE	1.5	6/600	61	200 HDPE	GN	5	GM/GCL	HDPE	1.5	6
AL1	30	200 PVC	S	600	GM/CCL	HDPE	1.5	900	ND	150 PVC	GN	5	GM/CCL	HDPE	1.5	900
AM1-2	NA	NA	G/S	300/150	GM/CCL	HDPE	2.0	450	NA	NA	GN	5	GM	HDPE	1.5	NA
AN1, base	NA	NA	S/GN	600/5	GM/CCL	LMDPE	2.0	450	ND	ND	GN	5	GM/CCL	HDPE	2.0	600
AN1, sides	NA	NA	S/GN	450/5	GM[5]	LMDPE	2.0	NA	ND	ND	GN	5	GM/CCL	HDPE	2.0	900
AN2-3, base	NA	NA	S/GN	600/5	GM/CCL	HDPE	2.0	450	ND	ND	GN	5	GM/CCL	HDPE	2.0	600
AN2-3, sides	NA	NA	S/GN	450/5	GM	HDPE	2.0	NA	ND	ND	GN	5	GM/CCL	HDPE	2.0	900
AN4	NA	NA	S/GN	600/5	GM	HDPE	2.0	NA	ND	ND	GN	5	GM/CCL	HDPE	2.0	600
AO1-4	61	150 HDPE	S	600	GM/CCL	HDPE	1.5	900	NA	NA	GN	5	GM/CCL	HDPE	1.5	600

Table E-3.3. Landfill Double-Liner System Details (Continued).

Cell No.	LCRS				Primary Liner				LDS				Secondary Liner			
	Avg. Pipe or Swale Spacing (m)	Pipe or Swale Size (mm or m) & Material	Drainage Layer(s) Material	Drainage Layer(s) Thick. (mm)	Type of Liner[1]	GM Type[2]	GM Thick. (mm)	GCL/ CCL Thick. (mm)	Avg. Pipe or Swale Spacing (m)	Pipe or Swale Size (mm or m) & Material	Drainage Layer(s) Material	Drainage Layer(s) Thick. (mm)	Type of Liner[1]	GM Type[2]	GM Thick. (mm)	GCL/ CCL Thick. (mm)
AP1, base	ND	HDPE	S	300	GM/CCL	HDPE	2.0	900	NA	NA	GN	5	GM/CCL	HDPE	2.0	900
AP1, sides	ND	HDPE	GN	5	GM/CCL	HDPE	2.0	1400	NA	NA	GN	5	GM/CCL	HDPE	2.0	900
AQ1-4	61	ND	G/GN	300/5	GM/CCL	HDPE	2.0	450	61	ND	G/GN	300/5	GM/CCL	HDPE	1.5	900
AQ5-10	61	ND	G/GN	300/5	GM/CCL	HDPE	2.0	450	61	ND	G/GN	300/5	GM/CCL	HDPE	2.0	900
AR1-2	46	250 PVC	G/TC	300/450	GM/GCL/CCL	HDPE	1.5	6/300	46	100 PVC	GN	10	GM/CCL	HDPE	1.5	600
AS1, base	NA	NA	GN	5	GM/CCL	HDPE	2.0	900	NA	NA	GN	5	GM/CCL	HDPE	2.0	900
AS1, sides	NA	NA	GN	5	GM/CCL	HDPE	2.0	600	NA	NA	GN	5	GM/CCL	HDPE	2.0	900
AT1, base	122	2.4 x 0.3 G	S	300	GM/CCL	HDPE	1.5	450	122	1.2 x 0.3 G	GN	5	GM/CCL	HDPE	1.5	900
AT1, sides	NA	NA	GN	5	GM/CCL	HDPE	1.5	450	NA	NA	GN	5	GM/CCL	HDPE	1.5	900
AU1-2	30	150 PVC	G	600	GM/CCL	HDPE	1.5	900	NA	NA	GN	6	GM	HDPE	1.5	NA
AV1-4	30	150 HDPE	S	300	GM/CCL	HDPE	2.0	1500	30	ND	GN	10	GM[6]	HDPE	1.5	NA
AV5, base	30	150 HDPE	S	300	GM/CCL	HDPE	2.0	1500	30	25x610 GN	GN	8	GM[6]	HDPE	1.5	NA
AV5, sides	NA	NA	GN	8	GM/CCL	HDPE	2.0	1500	NA	NA	GN	8	GM[6]	HDPE	1.5	NA
AW1-2	91	150 HDPE	S	450	GM/GCL	HDPE	1.5	6	91	150 HDPE	S	300	GM/GCL	HDPE	1.5	NA
AW3-4	91	150 HDPE	S	450	GM	HDPE	1.5	NA	91	150 HDPE	GN	5	GM/GCL/CCL	HDPE	1.5	450
AX1-16, base	30	150 HDPE	G	600	GM/GCL	HDPE	1.5	6	30	100 PVC	G	300	GM/CCL	HDPE	1.5	150
AX1-16, sides	NA	NA	G	600	GM/GCL	HDPE	1.5	6	NA	NA	GN	5	GM/CCL	HDPE	1.5	150
AY1-3	ND	ND	GN	5	GM/GCL	HDPE	1.5	6	ND	ND	GN	5	GM/CCL	HDPE	1.5	900
AZ1	76	150 PVC	S	600	GM/GCL	HDPE	1.5	250	NA	NA	GN	5	GM/CCL	HDPE	1.5	900
BA1-2	12	100 HDPE	S	450	GM/GCL/GM	HDPE	2.0	6	ND	25 GN	GN	5	GM/CCL	HDPE	2.0	900
BB1-3	61	150	S	600	GM/GCL	HDPE	1.5	6	ND	ND	GN	5	GM	HDPE	1.5	NA

Notes: (1) GM = geomembrane, GCL = geosynthetic clay liner, CCL = compacted clay liner
G = gravel, S = sand, GN = geonet, TC = tire chips
(2) HDPE = high-density polyethylene, CSPE = chlorosulfonated polyethylene
PVC = polyvinyl chloride, LLDPE = linear low-density polyethylene
LMDPE = linear medium-density polyethylene
(3) NA = not applicable, ND = not determined
(4) GM and CCL are separated by a geotextile
(5) HDPE GM on upper side slopes
(6) Cells AV1-5 sit on a clay formation

Table E-3.4. Landfill Final Cover System Details.

Cell Number	Protective Soil Thickness (mm)	Drainage Layer(s)		Barrier Layer			
		Type	Thickness (mm)	Type[1]	GM Material[2]	GM Thickness (mm)	Soil Thickness (mm)
B1-2, top	300	S	450	GM	HDPE	1.0	NA
B1-2, sides	300	S	150	CCL	NA[3]	NA	300
D1-2	600	GN/S	5/150	CCL/GM[4]	HDPE	2.0	600
H1, top	690	S	200	GM/CCL	PVC	1.0	600
H1, sides	690	GT	ND[3]	GM/CCL	PVC	1.0	600
I1-5	600	GN	5	GM	HDPE	1.0	NA
J1-4	ND	ND	ND	GM	HDPE	ND	NA
U1-4	600	NA	NA	CCL	NA	NA	300
AD1-6	600	GN	5	GM/CCL	HDPE	1.5	600
AD7-9	600	GN	5	GM/CCL	HDPE	1.5	600
AQ1-10	600	ND	ND	GM/CCL	HDPE	1.5	900
AS1	450	NA	NA	GM/CCL	HDPE	1.5	900
AT1	300	S	200	GM/CCL	HDPE	1.0	600
AX1-4, top	600	GN	5	GM	HDPE	1.0	NA
AX1-4, sides	600	S	150	CCL	NA	NA	300

Notes:
(1) GM = geomembrane, CCL = compacted clay liner, GN = geonet, GT = geotextile, S = sand
(2) HDPE = high-density polyethylene, PVC = polyvinyl chloride.
(3) NA = not applicable, ND = not determined.
(4) Barrier consists of a CCL underlain by a GM.

Table E-3.5. Landfill LCRS Flow Rate Data, Summarized by Landfill Life Cycle Stage.

Cell No.	Waste Type (Region)	Primary Liner/ LDS Type	Initial Period of Operation			Active Period of Operation			Post-Closure Period			Notes
			Time Period[(1)] (mos.)	Avg. Flow (lphd)	Peak Flow (lphd)	Time Period (mos.)	Avg. Flow (lphd)	Peak Flow (lphd)	Time Period (mos.)	Avg. Flow (lphd)	Peak Flow (lphd)	
A1-2	C&D(NE)	I	1-24	ND	ND	25-38	3,108	3,666	NA	NA	NA	Flows are combined for Cells A1 & A2.
						39-42	6,124	8,275				Cell A2 became operational in month 39.
						43-48	2,938	3,221				This caused the elevated flow rates
						Entire Period	3,568	8,275				for months 39-42.
B1	MSW(NE)	I	1-19	ND	ND	20-31	2,245	5,754	55-66	317	670	
						32-43	5,223	6,845	67-78	703	1,877	
						44-54	3,975	7,464	79-90	1,146	1,956	
									91-102	1,306	1,943	
									103-114	510	718	
						Entire Period	3,816	7,464	Entire Period	796	1,956	
B2	MSW(NE)	I	1-19	ND	ND	20-31	2,732	5,393	55-66	493	1,040	
						32-43	3,740	5,707	67-78	337	654	
						44-54	2,337	3,982	79-90	368	1,796	
									91-102	314	855	
									103-114	250	537	
									115-119	442	848	
						Entire Period	2,954	5,707	Entire Period	359	1,796	
B3	MSW(NE)	III	1-4	15,304	24,858	5-16	5,700	8,935	NA	NA	NA	
						17-28	9,272	22,444				
						29-40	7,575	13,978				
						41-52	2,859	6,043				
						53-64	1,189	2,280				
						65-76	403	490				65% of cell was closed after 65 months
						77-88	560	919				of start of waste placement in cell
						89-93	578	648				
						Entire Period	3,748	22,443				
B4	MSW(NE)	IV	1-12	2,930	6,353	13-24	5,315	14,641	NA	NA	NA	
						25-36	4,157	11,675				
						37-47	2,462	3,528				
						Entire Period	4,022	14,641				
B5	MSW(NE)	IV	1-12	8,005	19,521	13-24	5,543	15,567	NA	NA	NA	
						25-35	2,943	4,918				
						Entire Period	4,300	15,567				

Table E-3.5. Landfill LCRS Flow Rate Data, Summarized by Landfill Life Cycle Stage (Continued).

Cell No.	Waste Type (Region)	Primary Liner/ LDS Type	Initial Period of Operation			Active Period of Operation			Post-Closure Period			Notes
			Time Period[(1)] (mos.)	Avg. Flow (lphd)	Peak Flow (lphd)	Time Period (mos.)	Avg. Flow (lphd)	Peak Flow (lphd)	Time Period (mos.)	Avg. Flow (lphd)	Peak Flow (lphd)	
C1	MSW(SE)	I	1-9	ND	ND	10-21	789	1,419	NA	NA	NA	
						22-33	259	780				
						34-45	159	286				
						46-56	103	200				
						Entire Period	332	1,419				
C2	MSW(SE)	I	1-12	1,475	2,585	13-24	435	859	NA	NA	NA	
						25-36	300	610				
						37-45	161	464				
						Entire Period	311	859				
C3	MSW(SE)	I	1-8	3,417	9,558	9-20	311	671	NA	NA	NA	
						21-32	314	752				
						33-41	268	987				
						Entire Period	301	987				
C4	MSW(SE)	I	1-4	14,828	41,331	5-16	937	2,055	NA	NA	NA	
						17-28	438	622				
						29-35	407	686				
						Entire Period	624	2,055				
C5	MSW(SE)	I	1-12	6,419	12,528	13-26	2,513	10,440	NA	NA	NA	
C6	MSW(SE)	V	1-10	3,273	12,155	11-17	393	1,403	NA	NA	NA	
D1	HW(SE)	I	1-7	ND	ND	NA	NA	NA	8-19	ND	ND	
									20-26	ND	ND	
									27-38	376	1,455	
									39-50	715	1,352	
									Entire Period	456	1,455	
D2	HW(SE)	I	1-9	6,803	19,501	10-17	9,940	30,405	28-33	321,768	587,163	Near-liquid waste was disposed of in cell at several different times.
						18-21	224,812	407,523	34-47	40	567	
						22-27	10,862	32,341	Entire Period	96,559	587,163	
						Entire Period	57,997	407,523				
D3	HW(SE)	I	1-12	20,292	51,265	13-24	13,003	44,895	NA	NA	NA	
						25-28	1,010	2,413				
						Entire Period	10,005	44,895				
D4	HW(SE)	I	1-11	31,281	120,527	NA	NA	NA	NA	NA	NA	

Table E-3.5. Landfill LCRS Flow Rate Data, Summarized by Landfill Life Cycle Stage (Continued).

Cell No.	Waste Type (Region)	Primary Liner/ LDS Type	Initial Period of Operation			Active Period of Operation			Post-Closure Period			Notes
			Time Period[1] (mos.)	Avg. Flow (lphd)	Peak Flow (lphd)	Time Period (mos.)	Avg. Flow (lphd)	Peak Flow (lphd)	Time Period (mos.)	Avg. Flow (lphd)	Peak Flow (lphd)	
E1	MSW(NE)	I	1-7	ND	ND	8-19	8,432	19,614	NA	NA	NA	
						20-31	11,521	36,164				
						32-40	6,525	13,075				
						Entire Period	9,035	36,177				
E2	MSW(NE)	I	1-12	ND	ND	13-24	5,821	10,445	NA	NA	NA	
						25-36	4,547	11,014				
						37-45	4,434	6,830				
						Entire Period	4,979	11,014				
E3	MSW(NE)	I	1-12	9,425	25,394	13-14	6,062	9,038	NA	NA	NA	
E4	MSW(NE)	I	1-12	20,148	55,785	NA	NA	NA	NA	NA	NA	
F1	MSW(NE)	I	1-12	14,472	45,010	13-24	9,000	25,450	NA	NA	NA	
						25-30	7,826	10,932				
						Entire Period	8,608	25,450				
G1-2	MSW(NE)	I	1-12	22,371	46,120	13-24	12,893	23,485	NA	NA	NA	Flows are combined for Cells G1 & G2.
						25-36	3,438	11,652				
						37-42	8,356	10,303				
						Entire Period	8,204	23,485				
G1-3	MSW(NE)					43-54	11,774	48,159	NA	NA	NA	Flows are combined for Cells G1, G2,
						55-67	8,690	20,923				& G3 for months 43-67.
						Entire Period	10,170	48,159				
H1-6	HW(NE)	I	ND	ND	ND	ND	ND	ND	ND	ND	ND	
I1	MSW(NE)	I	1-8	ND	ND	9-15	16,224	48,932	85-93*	800	1,794	Cell received intermediate cover
						16-32	ND	ND				approximately 30 months after start
						33-44	7,167	22,020				of waste placement in cell
						45-48	231	332				
						49-54	ND	ND				
						55-66*	624	1,580				*Flows are combined for cells I1, I2, & I3
						67-78*	541	752				during these months.
						79-84*	904	1,827				
						Entire Period	4,149	48,932				

Table E-3.5. Landfill LCRS Flow Rate Data, Summarized by Landfill Life Cycle Stage (Continued).

Cell No.	Waste Type (Region)	Primary Liner/ LDS Type	Initial Period of Operation			Active Period of Operation			Post-Closure Period			Notes
			Time Period[1] (mos.)	Avg. Flow (lphd)	Peak Flow (lphd)	Time Period (mos.)	Avg. Flow (lphd)	Peak Flow (lphd)	Time Period (mos.)	Avg. Flow (lphd)	Peak Flow (lphd)	
I2	MSW(NE)	I	1-7	6,627	13,959	8-24	ND	ND	77-85*	800	1,794	Cell received intermediate cover approximately 28 months after start of waste placement in cell
						25-36	1,030	3,241				
						37-40	427	1,054				
						41-46	ND	ND				
						47-58*	624	1,580				*Flows are combined for cells I1, I2, & I3 during these months.
						59-70*	541	752				
						71-76*	904	1,827				
						Entire Period	728	3,241				
I3	MSW(NE)	I	1-7	11,559	21,081	8-24	ND	ND	77-85*	800	1,794	Cell received intermediate cover approximately 22 months after start of waste placement in cell
						25-36	11,684	26,339				
						37-40	2,464	4,666				
						41-46	ND	ND				
						47-58*	624	1,580				*Flows are combined for cells I1, I2, & I3 during these months.
						59-70*	541	752				
						71-76*	904	1,827				
						Entire Period	3,684	26,339				
I4	MSW(NE)	VI	1-12	4,494	17,251	13-26	2,041	4,282	27-36	567	1,389	
I5	MSW(NE)	VI	1-12	3,938	7,985	13-21	3,108	11,669	22-34	189	779	
J1	MSW(NE)	I	1-3	13,363	16,182	4-6	5,235	5,824	ND	ND	N D	
J1-2	MSW(NE)	I				7-13*	4,813	7,697				*Flows are combined for cells listed; Cells J1-J4 received final closure by month 32. Cells J5 & J6 were not closed.
J1-3	MSW(NE)	I				14-21*	3,904	6,445				
J1-4	MSW(NE)	I				22-32*	3,858	9,880				
J1-5	MSW(NE)	I				33-38*	2,824	5,672				
J1-6	MSW(NE)	I				39-43*	ND	ND				
K1	MSW(NE)	I	1-12	17,808	24,832	13-24	12,929	27,663	ND	ND	ND	
						25-36	10,879	17,683				
						37-48	6,155	11,331				
						49-60	5,952	8,024				
						61-66	9,494	12,245				
						Entire Period	9,036	27,663				

Table E-3.5. Landfill LCRS Flow Rate Data, Summarized by Landfill Life Cycle Stage (Continued).

Cell No.	Waste Type (Region)	Primary Liner/ LDS Type	Initial Period of Operation			Active Period of Operation			Post-Closure Period			Notes
			Time Period[1] (mos.)	Avg. Flow (lphd)	Peak Flow (lphd)	Time Period (mos.)	Avg. Flow (lphd)	Peak Flow (lphd)	Time Period (mos.)	Avg. Flow (lphd)	Peak Flow (lphd)	
L1	HW(SE)	I	1-2	ND	ND	NA	NA	NA	NA	NA	NA	
L1-2	HW(SE)	I	3-7	ND	ND	13-18	2,636	4,293				
			8-12	22,795	51,266							
L1-3	HW(SE)	I				19-25	28,040	68,107				
						26-37	7,649	17,349				
						38-43	7,894	15,145				
						Entire Period	13,417	68,107				
L1-4	HW(SE)	I				44-55	11,132	35,338				
						56-61	8,363	10,954				
						Entire Period	10,209	35,338				
M1	ASH(M)(SE)	I	ND	ND	ND	ND	ND	ND	ND	ND	ND	
N1	MSW(SE)	II	1-12	ND	ND	13-24	ND	ND	NA	NA	NA	
						25-36	ND	ND				
						37-48	ND	ND				
						49-60	1,572	5,601				
						61-72	2,433	17,597				
						73-75	745	888				
						Entire Period	1,862	17,597				
N2	MSW(SE)	II	1-12	ND	ND	13-19	4,547	5,741	NA	NA	NA	
						20-31	2,561	3,460				
						32-34	6,399	7,274				
						35-39	2,741	3,170				
						Entire Period	3,536	7,274				
O1	MSW(SE)	II	1-6	ND	ND	NA	NA	NA	NA	NA	NA	
O1-2	MSW(SE)	II				7-18	4,407	9,826				
						19-30	4,023	13,231				
						31-42	7,089	16,467				
						43-54	6,201	12,561				
						55-64	8,661	15,327				
						Entire Period	5,987	16,467				
O1-3	MSW(SE)	II				65-76	10,691	16,965				
						77-80	11,605	12,766				
						Entire Period	10,920	16,965				

Table E-3.5. Landfill LCRS Flow Rate Data, Summarized by Landfill Life Cycle Stage (Continued).

Cell No.	Waste Type (Region)	Primary Liner/ LDS Type	Initial Period of Operation			Active Period of Operation			Post-Closure Period			Notes
			Time Period[(1)] (mos.)	Avg. Flow (lphd)	Peak Flow (lphd)	Time Period (mos.)	Avg. Flow (lphd)	Peak Flow (lphd)	Time Period (mos.)	Avg. Flow (lphd)	Peak Flow (lphd)	
P1	ASH(M)(SE)	II	1-12	ND	ND	13-34	ND	ND	NA	NA	NA	
						35-39	20,086	45,591				
P2	ASH(M)(SE)	II	1-12	ND	ND	13-22	ND	ND	NA	NA	NA	
						23-27	8,935	12,277				
P3	ASH(M)(SE)	II	1-10	ND	ND	11-15	24,490	60,420	NA	NA	NA	
Q1	MSW(NE)	II	1-7	39,864	111,129	8-19	9,598	16,006	NA	NA	NA	
						20-31	9,290	21,862				
						32-43	4,610	6,761				
						44-48	3,166	5,210				
						Entire Period	7,263	21,862				
Q1-2	MSW(NE)	II				49-58	7,287	16,042	NA	NA	NA	
R1	MSW(NE)	IV	1	ND	ND	13-23	9,323	17,889	NA	NA	NA	
			2-12	11,592	22,266							
S1	MSW(NE)	II	1-10	2,226	5,081	11-22	653	1,220	NA	NA	NA	
						23-28	ND	ND				
						29-40	1,571	4,074				
						41-45	1,086	2,067				
						Entire Period	1,108	4,074				
S2	ASH(M)(NE)	II	1-9	2,185	4,650	10-17	654	1,135	NA	NA	NA	
						18-33	ND	ND				
						34-46	1,255	3,638				
						Entire Period	1,026	3,638				
T1	MSW(NE)	II	1-8	2,137	5,982	ND	ND	ND	NA	NA	NA	
T1-2	MSW(NE)	II	1-8	ND	ND	9-20	2,861	6,804	NA	NA	NA	
						21-25	3,604	5,791				
						26-36	ND	ND				
						37-46	661	2,174				
						Entire Period	1,552	6,804				
U1-4	MSW(NE)	II	ND	ND	ND	ND	ND	ND	ND	ND	ND	

Table E-3.5. Landfill LCRS Flow Rate Data, Summarized by Landfill Life Cycle Stage (Continued).

Cell No.	Waste Type (Region)	Primary Liner/ LDS Type	Initial Period of Operation			Active Period of Operation			Post-Closure Period			Notes
			Time Period[(1)] (mos.)	Avg. Flow (lphd)	Peak Flow (lphd)	Time Period (mos.)	Avg. Flow (lphd)	Peak Flow (lphd)	Time Period (mos.)	Avg. Flow (lphd)	Peak Flow (lphd)	
V1-2	MSW(SE)	II	1-13	13,622	49,828	ND	ND	ND	NA	NA	NA	
V1-3	MSW(SE)	II				11	5,149	5,149	NA	NA	NA	
V1-4	MSW(SE)	II				12-23	14,112	33,926	NA	NA	NA	
						24-35	6,967	18,142				
						36-40	18,045	41,601				
V1-5	MSW(SE)	II				41-52	8,443	31,668	NA	NA	NA	
						53-64	11,683	23,420				
						Entire Period	10,923	41,601				
W1	MSW(SE)	II	1-8	ND	ND	13-24	2,693	6,365	NA	NA	NA	
			9-12	7,492	8,799	25-35	943	1,572				
						Entire Period	1,856	6,365				
W2	MSW(SE)	II	1-8	ND	ND	9-20	4,288	9,389	NA	NA	NA	
						21-32	4,813	10,524				
						33-35	719	2,141				
						Entire Period	4,125	10,524				
X1	MSW(SE)	II	1	111,031	111,031	8-19	5,926	14,315	NA	NA	NA	
			2-7	32,469	104,645	20-33	2,188	5,376				
			Period	43,693	111,031	Entire Period	3,913	14,315				
Y1	ASH(M)(NE)	III	1-12	ND	ND	13-26	19,645	58,673	NA	NA	NA	
						27	ND	ND				
						28-39	20,515	44,593				
						40-51	19,868	34,220				
						52-63	18,177	47,068				
						64-67	47,154	63,832				
						68	ND	ND				
						69-78	8,937	21,355				
						Entire Period	19,319	63,832				
Y2	MSW(NE)	III	1-10	23,368	36,791	11-22	10,353	19,204	NA	NA	NA	
						23-34	11,344	25,308				
						35-46	4,404	6,308				
						47-54	4,397	5,199				
						Entire Period	7,918	25,308				
Z1	ASH(C)(NE)	III	1-12	28,628	49,551	13-24	34,520	68,294	NA	NA	NA	
						25-36	36,866	92,207				
						37-39	32,265	35,763				
						Entire Period	35,312	92,207				

Table E-3.5. Landfill LCRS Flow Rate Data, Summarized by Landfill Life Cycle Stage (Continued).

Cell No.	Waste Type (Region)	Primary Liner/ LDS Type	Initial Period of Operation			Active Period of Operation			Post-Closure Period			Notes
			Time Period[(1)] (mos.)	Avg. Flow (lphd)	Peak Flow (lphd)	Time Period (mos.)	Avg. Flow (lphd)	Peak Flow (lphd)	Time Period (mos.)	Avg. Flow (lphd)	Peak Flow (lphd)	
AA1	MSW(NE)	III	1	ND	ND	9-14	1,065	1,586	NA	NA	NA	
			2-8	4,084	9,261	15-26	3,387	5,503				
						27-31	2,862	4,424				
						32-43	994	1,751				
						45-51	999	3,190				
						Entire Period	1,890	5,503				
AA2	MSW(NE)	III	1-13	14,533	36,777	14-20	3,176	4,781	NA	NA	NA	
AA2-3	MSW(NE)	III				21-34	11,143	21,520	NA	NA	NA	
						35-46	3,719	6,115				
						47-54	2,225	3,509				
						Entire Period	5,870	21,520				
AB1	HW(SE)	III	1-5	479	1,662	6-12	70	200	NA	NA	NA	
						13-24	268	648				
						25-29	301	597				
						30-36	ND	ND				
						37-48	430	724				
						49-53	141	272				
						54-87	ND	ND				
						Entire Period	270	724				
AB2	HW(SE)	III	1-12	878	3,433	13-24	2,371	7,829	NA	NA	NA	
						25-29	2,444	5,197				
						30-36	ND	ND				
						37-48	1,410	2,004				
						49-53	1,162	1,326				
						54-87	ND	ND				
						Entire Period	1,865	7,829				
AB3	HW(SE)	III	1-12	4,050	9,052	13-25	5,800	9,529	NA	NA	NA	
						26-32	ND	ND				
						33-40	3,944	4,569				
						41-74	ND	ND				
						Entire Period	4,971	9,529				
AB4	HW(SE)	III	1-8	ND	ND	14-25	2,114	9,584	NA	NA	NA	
			9-13	7,229	9,558	26-63	ND	ND				

Table E-3.5. Landfill LCRS Flow Rate Data, Summarized by Landfill Life Cycle Stage (Continued).

Cell No.	Waste Type (Region)	Primary Liner/ LDS Type	Initial Period of Operation			Active Period of Operation			Post-Closure Period			Notes
			Time Period[1] (mos.)	Avg. Flow (lphd)	Peak Flow (lphd)	Time Period (mos.)	Avg. Flow (lphd)	Peak Flow (lphd)	Time Period (mos.)	Avg. Flow (lphd)	Peak Flow (lphd)	
AC1	HW(W)	IV	1-13	85	169	ND	ND	ND	NA	NA	NA	
AC2	HW(W)	IV	1	1,429	1,429	7-18	68	217	NA	NA	NA	Cell received intermediate cover
			2-6	40	77	19-30	17	47				approximately 56 months after start
						31-42	8	39				of waste placement in cell
						43-54	3	8				
						55-66	19	72				
						67-78	4	13				
						79-88	2	5				
			Period	272	1,429	Entire Period	18	217				
AC3	HW(W)	IV	1	379	379	13-24	2	13	NA	NA	NA	Cell received intermediate cover
			2-12	11	37	25-36	1	6				approximately 41 months after start
						37-48	1	2				of waste placement in cell
						49-60	1	5				
						61-73	1	4				
			Period	42	379	Entire Period	1	13				
AC4	HW(W)	IV	1-11	51	255	12-23	5	21	NA	NA	NA	Cell received intermediate cover
						24-35	0	1				approximately 40 months after start
						36-47	2	15				of waste placement in cell
						48-59	0	0				
						60-73	1	15				
						Entire Period	2	21				
AC5	HW(W)	IV	1-13	255	977	14-25	82	225	NA	NA	NA	
						26-34	21	44				
						Entire Period	56	255				
AC6	HW(W)	IV	1-10	352	2,990	11-16	534	947	NA	NA	NA	
						17-28	46	101				
						29-34	28	65				
						35-40	345	1,002				
						Entire Period	200	1,002				
AC7	HW(W)	IV	1-12	54	120	13-18	1,925	6,713	NA	NA	NA	
AC8	HW(W)	IV	1-12	67	168	13-18	1,138	4,601	NA	NA	NA	

Table E-3.5. Landfill LCRS Flow Rate Data, Summarized by Landfill Life Cycle Stage (Continued).

Cell No.	Waste Type (Region)	Primary Liner/ LDS Type	Initial Period of Operation			Active Period of Operation			Post-Closure Period			Notes
			Time Period[1] (mos.)	Avg. Flow (lphd)	Peak Flow (lphd)	Time Period (mos.)	Avg. Flow (lphd)	Peak Flow (lphd)	Time Period (mos.)	Avg. Flow (lphd)	Peak Flow (lphd)	
AD1	HW(SE)	III	1-12	ND	ND	13-20	ND	ND	33-44	145	652	
						21-32	373	892	45-51	85	130	
									52-63	3	22	
									64-75	3	42	
									76-87	3	21	
									88-99	1	4	
									100-111	1	2	
									112-121	2	9	
									Entire Period	28	652	
AD2	HW(SE)	III	1-12	ND	ND	13-18	ND	ND	31-42	644	1,152	
						19-30	1,886	3,783	43-54	322	609	
									55-66	213	342	
									67-78	133	410	
									79-90	48	110	
									91-102	60	119	
									103-114	37	106	
									115-119	0	0	
									Entire Period	196	1,152	
AD3	HW(SE)	III	1-14	ND	ND	15-26	1,685	4,197	27-38	321	478	
									39-50	79	209	
									51-62	477	888	
									63-74	399	807	
									75-86	173	555	
									87-98	111	905	
									99-110	61	698	
									111-115	1,226	1,325	
									Entire Period	288	1,325	
AD4	HW(SE)	III	1-14	ND	ND	15-26	1,071	4,523	27-38	465	2,870	
									39-50	66	374	
									51-62	157	478	
									63-74	68	111	
									75-86	13	110	
									87-98	1	9	
									99-110	2	4	
									111-115	586	1,413	
									Entire Period	137	2,870	

Table E-3.5. Landfill LCRS Flow Rate Data, Summarized by Landfill Life Cycle Stage (Continued).

Cell No.	Waste Type (Region)	Primary Liner/ LDS Type	Initial Period of Operation			Active Period of Operation			Post-Closure Period			Notes
			Time Period[1] (mos.)	Avg. Flow (lphd)	Peak Flow (lphd)	Time Period (mos.)	Avg. Flow (lphd)	Peak Flow (lphd)	Time Period (mos.)	Avg. Flow (lphd)	Peak Flow (lphd)	
AD5	HW(SE)	III	1-7	ND	ND	8-19	37,054	115,663	20-31	3,290	5,541	
									32-43	1,166	1,801	
									44-55	683	1,385	
									56-67	444	767	
									68-79	278	1,045	
									80-91	9	58	
									92-103	1	2	
									104-108	0	0	
									Entire Period	792	5,541	
AD6	HW(SE)	III	1-7	ND	ND	8-19	992	1,853	20-31	200	776	
									32-43	114	190	
									44-55	64	86	
									56-67	70	156	
									68-79	37	100	
									80-91	35	125	
									92-103	8	42	
									104-108	0	0	
									Entire Period	71	776	
AD7	HW(SE)	IV	1-12	12,597	26,492	13-24	2,212	2,857	70-81	375	533	Cell received intermediate cover
						25-36	1,539	2,755	82-87	165	334	approximately 12 months after start
						37-48	1,429	2,813				of waste placement in cell
						49-60	249	629				
						61-70	480	614				
						Entire Period	1,206	2,857	Entire Period	305	533	
AD8	HW(SE)	IV	1-8	24,803	39,997	9-20	5,753	10,545	65-76	310	415	Cell received intermediate cover
						21-32	2,747	5,352	77-84	189	315	approximately 12 months after start
						33-44	661	2,393				of waste placement in cell
						45-56	296	1,070				
						57-64	223	355				
						Entire Period	2,058	10,545	Entire Period	261	415	
AD9	HW(SE)	IV	1-9	19,900	42,854	10-21	4,096	8,051	59-60	798	825	Cell received intermediate cover
						22-33	2,417	4,343	61-72	525	797	approximately 12 months after start
						34-45	916	1,680	73-79	463	611	of waste placement in cell
						46-58	227	699				
						Entire Period	1,880	8,051	Entire Period	530	825	

Table E-3.5. Landfill LCRS Flow Rate Data, Summarized by Landfill Life Cycle Stage (Continued).

Cell No.	Waste Type (Region)	Primary Liner/ LDS Type	Initial Period of Operation			Active Period of Operation			Post-Closure Period			Notes
			Time Period[1] (mos.)	Avg. Flow (lphd)	Peak Flow (lphd)	Time Period (mos.)	Avg. Flow (lphd)	Peak Flow (lphd)	Time Period (mos.)	Avg. Flow (lphd)	Peak Flow (lphd)	
AD10	HW(SE)	IV	1-12	20,960	51,425	13-24	7,382	15,064	NA	NA	NA	Cell received intermediate cover approximately 41 months after start of waste placement in cell
						25-36	1,370	9,735				
						37-50	789	2,961				
						51-62	470	867				
						63-74	308	788				1/2 of cell was closed approximately 59 months after start of waste placement in cell
						75-79	154	603				
						Entire Period	1,883	15,064				
AD11	HW(SE)	IV	1-5	11,875	20,518	6-17	3,168	5,974	NA	NA	NA	Cell received intermediate cover approximately 41 months after start of waste placement in cell
						18-29	3,552	5,365				
						30-41	4,305	5,278				
						42-53	4,975	6,246				
						54-65	2,442	6,708				
						66-69	1,255	1,579				
						Entire Period	3,536	6,708				
AD12	HW(SE)	IV	1-13	25,609	55,840	14-25	5,612	19,674	NA	NA	NA	Cell received intermediate cover approximately 41 months after start of waste placement in cell
						26-37	1,362	2,505				
						38-49	1,260	1,605				
						50-61	1,091	1,313				
						62-69	1,064	2,129				
						Entire Period	2,150	19,674				
AD13	HW(SE)	IV	1-12	18,604	86,467	13-18	19,758	51,260	NA	NA	NA	Cell received intermediate cover approximately 41 months after start of waste placement in cell
						19-30	3,287	5,734				
						31-42	2,064	4,942				
						43-55	3,815	8,470				
						Entire Period	5,403	51,260				
AD14	HW(SE)	IV	1-12	20,104	85,939	13-24	10,197	40,684	NA	NA	NA	Cell received intermediate cover approximately 41 months after start of waste placement in cell
						25-36	3,014	5,149				
						37-48	2,023	4,494				
						49-55	1,232	1,480				
						Entire Period	4,452	40,684				
AD15	HW(SE)	IV	1-13	24,664	89,367	14-25	571	1,294	NA	NA	NA	Cell received intermediate cover approximately 41 months after start of waste placement in cell
						26-39	234	549				
						Entire Period	390	1,294				
AD16	HW(SE)	IV	1-12	17,442	84,110	13-24	31,485	153,293	NA	NA	NA	Cell received intermediate cover approximately 41 months after start of waste placement in cell
						25-39	7,080	18,896				
						Entire Period	17,927	153,293				
AD17	HW(SE)	IV	1-12	5,761	10,955	13-16	4,046	6,109	NA	NA	NA	
AD18	HW(SE)	IV	1-12	5,035	15,685	13-19	1,186	3,257	NA	NA	NA	

Table E-3.5. Landfill LCRS Flow Rate Data, Summarized by Landfill Life Cycle Stage (Continued).

Cell No.	Waste Type (Region)	Primary Liner/ LDS Type	Initial Period of Operation			Active Period of Operation			Post-Closure Period			Notes
			Time Period[(1)] (mos.)	Avg. Flow (lphd)	Peak Flow (lphd)	Time Period (mos.)	Avg. Flow (lphd)	Peak Flow (lphd)	Time Period (mos.)	Avg. Flow (lphd)	Peak Flow (lphd)	
AE1	MSW(NE)	III	1-12	ND	ND	13-24	ND	ND	NA	NA	NA	
						25-32	ND	ND				
AE1-2	MSW(NE)	III				33-44	ND	ND	NA	NA	NA	
						45-50	ND	ND				
						51-59	ND	ND				
						60-72	14,000	48,977				
AE1-3	MSW(NE)	III				73-80	21,513	33,542	NA	NA	NA	
						Entire Period	17,705	48,977				
AF1	ASH(M)(NE)	III	1-12	25,383	40,850	13-24	18,257	26,768	NA	NA	NA	
						25-36	22,116	29,973				
						37-48	19,672	41,880				
						49-60	17,809	40,718				
						61-63	ND	ND				
						Entire Period	19,463	41,880				
AG1	MSW(NE)	III	1-12	1,780	5,314	13-24	3,963	12,357	NA	NA	NA	
						25-33	4,022	11,347				
						Entire Period	3,988	12,357				
AH1-5	MSW/ASH(M)(NE)	III	ND	ND	ND	ND	ND	ND	NA	NA	NA	
AI1	C&DW(NE)	III	1-2	ND	ND	13-24	9,952	22,419	NA	NA	NA	
			3-12	15,552	29,341	25-36	11,170	23,200				
						37-50	14,786	29,477				
						Entire Period	12,118	29,477				
AI2	C&DW(NE)	III	1-2	ND	ND	7-18	12,192	20,328	NA	NA	NA	
			3-6	19,613	22,964	19-30	18,026	32,402				
						31-42	17,052	34,159				
						43-50	17,968	28,114				
						Entire Period	16,159	34,159				
AJ1	MSW(NE)	III	1	ND	ND	7-13	4,728	9,936	NA	NA	NA	
			2-6	17,133	24,782							
AK1	MSW(NE)	IV	1-12	9,867	17,983				NA	NA	NA	
AK1-2	MSW(NE)	IV				13-15	2,398	3,130				
AL1	MSW(NE)	IV	1-12	ND	ND	13-29	ND	ND	NA	NA	NA	
						30-41	934	2,085				
						42-54	1,349	5,885				
						Entire Period	1,150	5,885				

Table E-3.5. Landfill LCRS Flow Rate Data, Summarized by Landfill Life Cycle Stage (Continued).

Cell No.	Waste Type (Region)	Primary Liner/ LDS Type	Initial Period of Operation			Active Period of Operation			Post-Closure Period			Notes
			Time Period[1] (mos.)	Avg. Flow (lphd)	Peak Flow (lphd)	Time Period (mos.)	Avg. Flow (lphd)	Peak Flow (lphd)	Time Period (mos.)	Avg. Flow (lphd)	Peak Flow (lphd)	
AM1	MSW(W)	IV	1-9	ND	ND	10-21	270	533	NA	NA	NA	Cell received intermediate cover approximately 5 months after start of waste placement in cell
						22-33	336	329				
						34-45	111	283				
						46-57	20	77				
						58-69	18	21				
						70-81	11	18				
						Entire Period	111	533				
AM2	MSW(W)	IV	1-9	ND	ND	10-21	32	154	NA	NA	NA	Cell received intermediate cover approximately 5 months after start of waste placement in cell
						22-33	35	51				
						34-45	17	45				
						46-57	67	274				
						58-69	64	181				
						70-81	112	136				
						Entire Period	55	274				
AN1	ASH(M)(NE)	IV	1-7	ND	ND	8-12	10,844	13,430	NA	NA	NA	
AN1-2	ASH(M)(NE)	IV				13-17	8,455	21,498				
AN1-3	ASH(M)(NE)	IV				18-31	14,087	30,179				
AN1-4	ASH(M)(NE)	IV				32-34	21,598	23,136				
AO1	MSW(NE)	IV	1-5	ND	ND	6-17	1,984	4,130	NA	NA	NA	
						18-29	1,299	1,577				
						26-36	1,144	1,371				
						Entire Period	1,485	4,130				
AO2	MSW(NE)	IV	1-5	15,881	24,541	6-17	3,027	5,266	NA	NA	NA	
						18-30	1,688	2,383				
						Entire Period	2,331	5,266				
AO3	MSW(NE)	IV	1-8	16,746	53,117	NA	NA	NA	NA	NA	NA	
AO4	MSW(NE)	IV	1-8	20,017	55,470	NA	NA	NA	NA	NA	NA	
AP1	HW(W)	IV	1-12	3,093	10,515	13-24	4,885	15,059	NA	NA	NA	
						25-36	3,353	5,802				
						37-48	4,579	8,260				
						Entire Period	4,272	15,059				

Table E-3.5. Landfill LCRS Flow Rate Data, Summarized by Landfill Life Cycle Stage (Continued).

Cell No.	Waste Type (Region)	Primary Liner/ LDS Type	Initial Period of Operation			Active Period of Operation			Post-Closure Period			Notes
			Time Period[(1)] (mos.)	Avg. Flow (lphd)	Peak Flow (lphd)	Time Period (mos.)	Avg. Flow (lphd)	Peak Flow (lphd)	Time Period (mos.)	Avg. Flow (lphd)	Peak Flow (lphd)	
AQ1	HW(NE)	IV	1-6	10,203	18,944	7-48	ND	ND	59-65	5,835	11,244	Cell final closure date is approximate
						47-58	4,530	10,531	66-77	644	1,011	
									78-89	1,367	3,264	
									90-97	1,615	3,575	
									Entire Period	1,997	11,244	
AQ2	HW(NE)	IV	1-6	13,050	20,721	7-48	ND	ND	59-70	218	717	
						49-58	2,181	6,460	71-82	206	1,082	
									83-94	747	3,040	
									95-97	217	432	
									Entire Period	377	3,040	
AQ3	HW(NE)	IV	1	ND	ND	13-44	ND	ND	55-66	626	2,642	
			2	17,940	17,940	45-54	2,962	13,430	67-78	420	1,038	
			3-12	ND	ND				79-90	721	1,274	
									91-93	1,851	3,167	
									Entire Period	686	3,167	
AQ4	HW(NE)	IV	1	18,970	18,970	13-43	ND	ND	54-57	577	916	Cell final closure date is approximate
			2-12	ND	ND	44-53	1,049	1,622	58-70	4,292	6,345	
									71-82	495	1,210	
									83-92	534	1,141	
									Entire Period	1,779	6,345	
AQ5	HW(NE)	IV	1-12	ND	ND	13-35	ND	ND	51-62	1,040	2,369	
						36-47	11,304	34,353	63-74	603	1,540	
						48-50	5,427	6,692	75-84	561	1,194	
						Entire Period	10,129	34,353	Entire Period	745	2,369	
AQ6	HW(NE)	IV	1-12	ND	ND	13-31	ND	ND	53-64	472	903	
						32-43	2,226	12,072	65-76	504	1,272	
						44-52	3,405	11,119	77-80	551	987	
						Entire Period	2,732	12,072	Entire Period	497	1,272	
AQ7	HW(NE)	IV	1-12	ND	ND	13-30	ND	ND	43-54	35	120	
						31-42	1,256	4,821	55-66	78	211	
									67-79	261	565	
									Entire Period	129	565	
AQ8	HW(NE)	IV	1-12	ND	ND	13-14	ND	ND	27-38	586	1,677	
						15-26	21,329	76,759	39-50	557	1,011	
									51-63	578	1,425	
									Entire Period	573	1,677	

Table E-3.5. Landfill LCRS Flow Rate Data, Summarized by Landfill Life Cycle Stage (Continued).

Cell No.	Waste Type (Region)	Primary Liner/ LDS Type	Initial Period of Operation			Active Period of Operation			Post-Closure Period			Notes
			Time Period[1] (mos.)	Avg. Flow (lphd)	Peak Flow (lphd)	Time Period (mos.)	Avg. Flow (lphd)	Peak Flow (lphd)	Time Period (mos.)	Avg. Flow (lphd)	Peak Flow (lphd)	
AQ9	HW(NE)	IV	1-12	ND	ND	13-14	ND	ND	27-38	275	497	
						15-26	4,579	24,946	39-50	433	1,425	
									51-63	943	2,667	
									Entire Period	561	2,667	
AQ10	HW(NE)	IV	1-9	ND	ND	10-14	ND	ND	27-38	682	2,251	
						15-26	15,933	38,751	39-50	300	1,709	
									51-63	852	1,588	
									Entire Period	618	2,251	
AR1	MSW(NE)	IV	1-11	27,042	65,871	12-23	11,251	23,384	NA	NA	NA	Cell AR1 has four subareas. Waste placement started in months 1, 5, 20, and 26 in subareas 1 through 4, respectively.
						24-36	9,668	26,274				
						Entire Period	10,428	26,274				
AR1-2	MSW(NE)	IV				37-40	5,199	8,156	NA	NA	NA	
AS1	HW(SE)	IV	1-10	ND	ND	11-22	388	1,146	28-39	125	190	
						23-27	186	256	40-51	50	103	
									52-63	32	52	
									64-71	24	61	
						Entire Period	329	1,146	Entire Period	61	190	
AT1	HW(W)	IV	1-5	ND	ND	6-8	1,249	1,964	9-20	88	434	
									21-33	25	107	
									Entire Period	55	434	
AU1	MSW(NE)	IV	1-4	ND	ND	5-20	ND	ND	NA	NA	NA	
						21-32	4,991	11,597				
AV1-4	HW(NE)	IV	1-12	ND	ND	13-40	ND	ND	NA	NA	NA	
						41-52	9,308	19,021				
						53-64	7,907	10,611				
						Entire Period	8,608	19,021				
AV1	HW(NE)	IV				65-76	3,150	7,484				
						77-88	1,715	5,500				
						89-101	1,112	1,468				
						102-104	ND	ND				
						Entire Period	1,821	7,484				

Table E-3.5. Landfill LCRS Flow Rate Data, Summarized by Landfill Life Cycle Stage (Continued).

Cell No.	Waste Type (Region)	Primary Liner/ LDS Type	Initial Period of Operation			Active Period of Operation			Post-Closure Period			Notes
			Time Period[(1)] (mos.)	Avg. Flow (lphd)	Peak Flow (lphd)	Time Period (mos.)	Avg. Flow (lphd)	Peak Flow (lphd)	Time Period (mos.)	Avg. Flow (lphd)	Peak Flow (lphd)	
AV2	HW(NE)	IV				52-63	5,520	12,591	NA	NA	NA	
						64-75	1,829	4,222				
						76-88	1,469	2,638				
						89-91	ND	ND				
						Entire Period	2,682	12,591				
AV3	HW(NE)	IV				35-46	7,964	15,363	NA	NA	NA	
						47-58	3,994	9,294				
						59-71	2,703	5,964				
						72-74	ND	ND				
						Entire Period	4,466	15,363				
AV4	HW(NE)	IV				27-38	3,748	9,778	NA	NA	NA	
						39-50	2,086	4,026				
						51-63	2,787	4,667				
						64-66	ND	ND				
						Entire Period	2,656	9,778				
AV5	HW(NE)	IV	1-12	18,789	44,741	13-24	11,649	27,720	NA	NA	NA	
						25-37	4,215	11,933				
						38-40	ND	ND				
						Entire Period	6,949	27,720				
AW1	MSW(SE)	V	1-12	6,358	20,570				NA	NA	NA	
AW1,3	MSW(SE)	V,II				13-24	1,409	7,031	NA	NA	NA	
AW2	MSW(SE)	V	1-12	3,553	7,480				NA	NA	NA	
AW2,4	MSW(SE)	V,II				13-21	2,330	8,257	NA	NA	NA	
AX1	MSW(NE)	V	1-2	16,718	19,738	3-14	1,128	2,383	34-45	52	75	
						15-26	202	370	46-57	47	56	
						27-33	108	159	58-69	48	75	
									70-83	58	94	
						Entire Period	540	2,383	Entire Period	66	94	
AX2	MSW(NE)	V	1-5	15,521	58,674	6-14	320	570	34-45	248	421	
						15-26	210	421	46-57	142	234	
						27-33	352	480	58-69	109	187	
									70-83	208	300	
						Entire Period	281	570	Entire Period	178	421	

Table E-3.5. Landfill LCRS Flow Rate Data, Summarized by Landfill Life Cycle Stage (Continued).

Cell No.	Waste Type (Region)	Primary Liner/ LDS Type	Initial Period of Operation			Active Period of Operation			Post-Closure Period			Notes
			Time Period[1] (mos.)	Avg. Flow (lphd)	Peak Flow (lphd)	Time Period (mos.)	Avg. Flow (lphd)	Peak Flow (lphd)	Time Period (mos.)	Avg. Flow (lphd)	Peak Flow (lphd)	
AX3	MSW(NE)	V	1-5	3,361	7,985	6-17	188	475	57-68	227	458	Cell received intermediate cover
						18-29	222	692	69-81	187	320	approximately 34 months after start
						30-41	205	692				of waste placement in cell
						42-56	553	1,075				
						Entire Period	307	1,075	Entire Period	206	458	
AX4	MSW(NE)	V	1-12	2,534	12,688	13-17	298	187	57-68	23	37	Cell received intermediate cover
						18-29	67	127	69-81	70	84	approximately 34 months after start
						30-41	42	84				of waste placement in cell
						42-56	42	84				
						Entire Period	75	187	Entire Period	47	84	
AX5	MSW(NE)	V	1-11	1,384	3,394	12-23	106	191	NA	NA	NA	Cell received intermediate cover
						24-35	50	108				approximately 33 months after start
						36-47	32	47				of waste placement in cell
						48-59	44	56				
						60-71	41	65				Cell was partially closed approximately 55
						72-80	65	80				months after start of waste placement in
						Entire Period	56	191				cell
AX6	MSW(NE)	V	1-9	3,759	7,171	10-24	144	655	NA	NA	NA	Cell received intermediate cover
						25-36	132	234				approximately 30 months after start
						37-48	171	196				of waste placement in cell
						49-60	164	224				
						61-72	203	340				Cell was partially closed approximately 53
						73-78	232	355				months after start of waste placement in
						Entire Period	168	655				cell
AX7	MSW(NE)	V	1-10	5,376	12,155	11-22	390	851	NA	NA	NA	Cell was partially closed approximately 51
						23-25	181	309				months after start of waste placement in
						26	ND	ND				cell
						27-38	126	580				
						39-50	206	393				
						51-62	175	281				
						63-76	289	1,412				
						Entire Period	234	851				

Table E-3.5. Landfill LCRS Flow Rate Data, Summarized by Landfill Life Cycle Stage (Continued).

Cell No.	Waste Type (Region)	Primary Liner/ LDS Type	Initial Period of Operation			Active Period of Operation			Post-Closure Period			Notes
			Time Period[1] (mos.)	Avg. Flow (lphd)	Peak Flow (lphd)	Time Period (mos.)	Avg. Flow (lphd)	Peak Flow (lphd)	Time Period (mos.)	Avg. Flow (lphd)	Peak Flow (lphd)	
AX8	MSW(NE)	V	1	21,038	21,038	15-26	545	1,384	NA	NA	NA	Cell was partially closed approximately 46 months after start of waste placement in cell
			2-14	578	6,256	27-38	489	963				
						39-50	352	402				
						51-62	325	626				
						63-71	499	600				
			Period	4,881	21,038	Entire Period	439	1,384				
AX9	MSW(NE)	V	1-9	1,047	3,478	10-21	92	159	NA	NA	NA	Cell was partially closed approximately 41 months after start of waste placement in cell
						22-33	30	75				
						34-45	12	28				
						46-57	30	65				
						58-65	40	70				
						Entire Period	41	159				
AX10	MSW(NE)	V	1-7	2,786	13,698	8-19	330	477	NA	NA	NA	Cell was partially closed approximately 34 months after start of waste placement in cell
						20-31	285	337				
						32-43	342	402				
						44-55	502	645				
						56-59	486	608				
						Entire Period	374	645				
AX11	MSW(NE)	V	1-16	4,675	14,586	17-28	219	300	NA	NA	NA	Cell was partially closed approximately 39 months after start of waste placement in cell
						29-40	112	178				
						41-52	121	337				
						53-62	148	200				
						Entire Period	150	337				
AX12	MSW(NE)	V	1-12	3,494	8,836	13-24	1,376	3,029	NA	NA	NA	Cell may have been partially closed approximately 31 months after start of waste placement in cell
						25-36	711	1,505				
						37-48	493	650				
						49-56	354	500				
						Entire Period	768	3,029				
AX13	MSW(NE)	V	1-7	6,683	14,343	8-19	1,734	3,488	NA	NA	NA	Cell may have been partially closed approximately 28 months after start of waste placement in cell
						20-31	3,058	9,294				
						32-43	250	449				
						44-53	424	1,421				
						Entire Period	1,408	9,294				

Table E-3.5. Landfill LCRS Flow Rate Data, Summarized by Landfill Life Cycle Stage (Continued).

Cell No.	Waste Type (Region)	Primary Liner/ LDS Type	Initial Period of Operation			Active Period of Operation			Post-Closure Period			Notes
			Time Period[1] (mos.)	Avg. Flow (lphd)	Peak Flow (lphd)	Time Period (mos.)	Avg. Flow (lphd)	Peak Flow (lphd)	Time Period (mos.)	Avg. Flow (lphd)	Peak Flow (lphd)	
AX14	MSW(NE)	V	1-11	2,777	6,582	12-23	216	300	NA	NA	NA	
						24-30	324	430				
						31-32	ND	ND				
						33-38	360	449				
						Entire Period	281	449				
AX15	MSW(NE)	V	1-12	5,573	11,809	13-24	277	400	NA	NA	NA	
						25-37	319	561				
						Entire Period	299	2,786				
AX16	MSW(NE)	V	1-10	8,601	17,756	11-22	1,181	5,096	NA	NA	NA	
						23-29	199	393				
						Entire Period	819	5,096				
AY1	HW(NE)	VI	1-9	6,803	12,439	NA	NA	NA	NA	NA	NA	
AY2	HW(NE)	VI	1-11	10,964	23,914	NA	NA	NA	NA	NA	NA	
AY3	HW(NE)	VI	1-11	12,198	32,326	NA	NA	NA	NA	NA	NA	
AZ1	MSW(NE)	VI	1	ND	ND	13-22	4,006	5,054	NA	NA	NA	
			2-12	4,093	5,219	23-25	ND	ND				
						26-31	2,584	3,016				
						Entire Period	3,473	5,054				
BA1	HW(NE)	-[2]	1-14	ND	ND	15-26	5,467	9,440	NA	NA	NA	Cell received intermediate cover approximately 42 months after start of waste placement in cell
						27-38	2,949	4,883				
						39-42	2,406	2,745				
						Entire Period	3,951	9,440				
BA2	HW(NE)	-[2]	1-2	4,979	5,860	3-12	2,190	2,846	NA	NA	NA	
BB1	MSW(SE)	VI	1-6	10,378	22,130	7-18	3,399	5,644	NA	NA	NA	
						19-24	5,127	8,983				
						25-35	3,119	8,343	NA	NA	NA	
						36-47	272	2,621	NA	NA	NA	
						Entire Period	2,494	8,983				
BB2	MSW(SE)	VI	1-11	ND	ND	12-23	5,422	14,042	NA	NA	NA	
BB3	MSW(SE)	VI	1-11	ND	ND	12-23	2,284	7,945	NA	NA	NA	

Notes:

(1) NA = not applicable, ND = not determined.

(2) Cells BA1 and BA2 include a GM/GCL/GM primary liner.

Table E-3.6. Landfill LDS Flow Rate Data, Summarized by Landfill Life Cycle Stage.

Cell No.	Prim. Liner/ LDS Type	Waste Type/ Region	Initial Period of Operation			Active Period of Operation			Post-Closure Period			Notes
			Time Period[1] (mos.)	Avg. Flow (lphd)	Peak Flow (lphd)	Time Period (mos.)	Avg. Flow (lphd)	Peak Flow (lphd)	Time Period (mos.)	Avg. Flow (lphd)	Peak Flow (lphd)	
A1-2	I	C&DW(NE)	1-27	ND	ND	28-38	45	124	NA	NA	NA	Flows are combined for Cells A1 & A2.
						39-50	38	120				Cell A2 became operational in month 39.
						51-58	30	84				Cell A2 became operational
						Entire Period	39	124				in month 39.
B1	I	MSW(NE)	1-19	ND	ND	20-31	266	499	55-66	106	222	
						32-43	424	808	67-78	267	1,134	
						44-54	892	1,426	79-90	279	451	
									91-102	326	612	
									103-114	74	97	
						Entire Period	517	1,426	Entire Period	210	1,134	
B2	I	MSW(NE)	1-19	ND	ND	20-31	404	605	55-66	154	393	
						32-43	996	1,690	67-79	328	514	
						44-54	665	1,102				
						Entire Period	689	1,690	Entire Period	189	514	
B3	III	MSW(NE)	1-4	1,394	4,250	5-16	124	266	NA	NA	NA	
						17-28	101	168				
						29-40	262	803				
						41-52	231	713				
						53-64	45	152				
						65-76	92	133				65% of cell was closed after 65 months
						77-88	102	193				of start of waste placement in cell
						89-93	98	109				
						Entire Period	135	803				
B4	IV	MSW(NE)	1-12	ND	ND	13-24	32	97	NA	NA	NA	
						25-36	1	6				
						37-47	73	100				
						Entire Period	34	100				
B5	IV	MSW(NE)	1-12	11	43	13-24	3	13	NA	NA	NA	
						25-35	16	65				
						Entire Period	9	65				

Table E-3.6. Landfill LDS Flow Rate Data, Summarized by Landfill Life Cycle Stage (Continued).

Cell No.	Prim. Liner/ LDS Type	Waste Type/ Region	Initial Period of Operation			Active Period of Operation			Post-Closure Period			Notes
			Time Period[1] (mos.)	Avg. Flow (lphd)	Peak Flow (lphd)	Time Period (mos.)	Avg. Flow (lphd)	Peak Flow (lphd)	Time Period (mos.)	Avg. Flow (lphd)	Peak Flow (lphd)	
C1	I	MSW(SE)	1-9	ND	ND	10-21	123	304	NA	NA	NA	
						22-33	89	170				
						34-45	27	128				
						46-56	40	227				
						Entire Period	70	304				
C2	I	MSW(SE)	1-12	92	398	13-24	9	31	NA	NA	NA	
						25-36	22	125				
						37-45	7	14				
						Entire Period	13	125				
C3	I	MSW(SE)	1-8	63	268	9-20	2	9	NA	NA	NA	
						21-32	33	276				
						33-41	16	103				
						Entire Period	17	276				
C4	I	MSW(SE)	1-4	178	265	5-16	70	147	NA	NA	NA	
						17-28	51	92				
						29-35	26	29				
						Entire Period	53	147				
C5	I	MSW(SE)	1-12	23	40	13-26	28	115	NA	NA	NA	
C6	V	MSW(SE)	1-10	178	823	11-17	3	15	NA	NA	NA	
D1	I	HW(SE)	1-7	32	80	NA	NA	NA	8-19	102	886	
									20-26	1	10	
									27-38	5	70	
									39-50	64	156	
									Entire Period	41	886	
D2	I	HW(SE)	1-9	0	0	10-17	776	2,426	28-39	9	51	Near-liquid waste was disposed of in cell at several different times.
						18-21	101	122	40-47	1	2	
						22-27	63	133				
						Entire Period	388	2,426	Entire Period	6	51	
D3	I	HW(SE)	1-12	12	56	13-24	7	73	NA	NA	NA	
						25-28	283	341				
						Entire Period	76	341				

Table E-3.6. Landfill LDS Flow Rate Data, Summarized by Landfill Life Cycle Stage (Continued).

Cell No.	Prim. Liner/ LDS Type	Waste Type/ Region	Initial Period of Operation			Active Period of Operation			Post-Closure Period			Notes
			Time Period[1] (mos.)	Avg. Flow (lphd)	Peak Flow (lphd)	Time Period (mos.)	Avg. Flow (lphd)	Peak Flow (lphd)	Time Period (mos.)	Avg. Flow (lphd)	Peak Flow (lphd)	
D4	I	HW(SE)	1-11	233	801	NA	NA	NA	NA	NA	NA	
E1	I	MSW(NE)	1-7	2,144	5,026	8-19	1,436	3,069	NA	NA	NA	
						20-31	1,051	1,915				
						32-40	743	1,015				
						Entire Period	1,107	3,069				
E2	I	MSW(NE)	1	3,518	3,518	13-24	802	2,447	NA	NA	NA	
			2-12	179	536	25-36	685	1,404				
			Period	483	3,518	37-45	596	999				
						Entire Period	703	2,447				
E3	I	MSW(NE)	1-12	1,595	1,951	13-14	1,603	1,758	NA	NA	NA	
E4	I	MSW(NE)	1-12	996	2,362	NA	NA	NA	NA	NA	NA	
F1	I	MSW(NE)	1-12	124	479	13-24	66	83	NA	NA	NA	
						25-30	67	77				
						Entire Period	66	83				
G1	I	MSW(NE)	1-12	ND	ND	13-24	ND	ND	NA	NA	NA	
						25-36	156	238				
						37-42	101	116				
						43-51	121	384				
						52-63	74	139				
						64-67	49	64				
						Entire Period	108	384				
G2	I	MSW(NE)	1-12	197	645	13-24	37	65	NA	NA	NA	
						25-36	35	42				
						37-42	60	100				
						Entire Period	41	100				
G3	III	MSW(NE)	1-12	490	627	13-25	319	384	NA	NA	NA	

Table E-3.6. Landfill LDS Flow Rate Data, Summarized by Landfill Life Cycle Stage (Continued).

Cell No.	Prim. Liner/ LDS Type	Waste Type/ Region	Initial Period of Operation			Active Period of Operation			Post-Closure Period			Notes
			Time Period[1] (mos.)	Avg. Flow (lphd)	Peak Flow (lphd)	Time Period (mos.)	Avg. Flow (lphd)	Peak Flow (lphd)	Time Period (mos.)	Avg. Flow (lphd)	Peak Flow (lphd)	
H1	I	HW(NE)	1-13	ND	ND	14-25	19	65	56-67	3	12	
						26-37	8	21	68-79	0	2	
						38-49	4	7	80-88	0	0	
						50-55	2	5				
						Entire Period	9	65	Entire Period	1	12	
H2	I	HW(NE)	1-12	26	39	13-24	6	9	ND	ND	ND	
						25-29	8	10				
						30-32	ND	ND				
						33-42	108	175				
						43-45	ND	ND				
						46-57*	35	49				*Cell partially closed after month 46
						58-69*	16	25				
						70-76	9	12				
						Entire Period	31	175				
H3	I	HW(NE)	1-11	30	61	12-15	ND	ND	NA	NA	NA	*Cell partially closed after month 31
						16-25	207	415				
						26-28	ND	ND				
						29-30	81	83				
						31-42*	37	62				
						43-54*	32	39				
						55-58*	27	29				
						Entire Period	79	415				
H4	I	HW(NE)	1-9	339	415	10-21*	91	128	NA	NA	NA	*Cell partially closed
						22-29*	58	66				
						Entire Period	78	128				
H5	I	HW(NE)	1-7	197	304	8-20*	97	149	NA	NA	NA	*Cell partially closed
H6	I	HW(NE)	1-6	528	729	ND	ND	ND	NA	NA	NA	

Table E-3.6. Landfill LDS Flow Rate Data, Summarized by Landfill Life Cycle Stage (Continued).

Cell No.	Prim. Liner/ LDS Type	Waste Type/ Region	Initial Period of Operation			Active Period of Operation			Post-Closure Period			Notes
			Time Period[1] (mos.)	Avg. Flow (lphd)	Peak Flow (lphd)	Time Period (mos.)	Avg. Flow (lphd)	Peak Flow (lphd)	Time Period (mos.)	Avg. Flow (lphd)	Peak Flow (lphd)	
I1	I	MSW(NE)	1-5	234	508	6-8	ND	ND	85-93	62	119	Cell received intermediate cover approximately 30 months after start of waste placement in cell
						9-15	5	18				
						16-29	ND	ND				
						30-41	10	44				
						42-48	4	10				
						49-53	ND	ND				
						54-65	2	5				
						66-77	13	42				
						78-84	79	157				
						Entire Period	16	157				
I2	I	MSW(NE)	1-7	31	77	8-24	ND	ND	77-85	2	4	Cell received intermediate cover approximately 28 months after start of waste placement in cell
						25-36	5	35				
						37-40	6	11				
						41-46	ND	ND				
						47-58	8	37				
						59-70	8	23				
						71-76	5	6				
						Entire Period	7	37				
I3	I	MSW(NE)	1-7	37	87	8-24	ND	ND	77-85	3	12	Cell received intermediate cover approximately 22 months after start of waste placement in cell
						25-36	7	23				
						37-40	5	8				
						41-46	ND	ND				
						47-58	4	17				
						59-70	13	55				
						71-76	17	53				
						Entire Period	9	55				
I4	VI	MSW(NE)	1-12	24	70	13-26	26	142	27-36	59	133	
I5	VI	MSW(NE)	1-12	2	11	13-21	11	54	22-34	2	8	
J1	I	MSW(NE)	1-3	24	34	4-15	9	13	33-43	ND	ND	
						16-28	9	12				
						29-32	ND	ND				
						Entire Period	9	13				

Table E-3.6. Landfill LDS Flow Rate Data, Summarized by Landfill Life Cycle Stage (Continued).

Cell No.	Prim. Liner/ LDS Type	Waste Type/ Region	Initial Period of Operation			Active Period of Operation			Post-Closure Period			Notes
			Time Period[1] (mos.)	Avg. Flow (lphd)	Peak Flow (lphd)	Time Period (mos.)	Avg. Flow (lphd)	Peak Flow (lphd)	Time Period (mos.)	Avg. Flow (lphd)	Peak Flow (lphd)	
J2	I	MSW(NE)	1-12	8	13	13-21	8	11	26-36	ND	ND	
						22-25	ND	ND				
J3	I	MSW(NE)	1-7	9	14	8-11	ND	ND	20-21	29	29	
						12-19	19	28	22-30	ND	ND	
J4	I	MSW(NE)	1-7	15	43	8-11	32	44	12-16	13	43	
									17-22	ND	ND	
J5	I	MSW(NE)	1-7	504	786	8-11	139	149	NA	NA	NA	
J6	I	MSW(NE)	1-5	54	236	NA	NA	NA	NA	NA	NA	
K1	I	MSW(NE)	1-12	122	163	13-24	88	180	NA	NA	NA	
						25-36	76	104				
						37-48	514	892				
						49-60	349	495				
						61-66	282	378				
						Entire Period	271	892				
L1	I	HW(SE)	1-3	2,553	3,464	4-15	330	562	NA	NA	NA	
						16-27	134	749				
						28-39	89	409				
						40-51	44	169				
						52-61	143	500				
						Entire Period	148	749				
L2	I	HW(SE)	1-7	301	458	8-20	280	869	NA	NA	NA	
						21-35	21	92				
						36-47	140	702				
						48-59	28	222				
						Entire Period	115	869				
L3	I	HW(SE)	1-5	542	974	6-18	69	537	NA	NA	NA	
						19-30	22	210				
						31-41	0	0				
						Entire Period	31	537				
L4	I	HW(SE)	1-5	105	461	6-18	76	280	NA	NA	NA	

Table E-3.6. Landfill LDS Flow Rate Data, Summarized by Landfill Life Cycle Stage (Continued).

Cell No.	Prim. Liner/ LDS Type	Waste Type/ Region	Initial Period of Operation			Active Period of Operation			Post-Closure Period			Notes
			Time Period[1] (mos.)	Avg. Flow (lphd)	Peak Flow (lphd)	Time Period (mos.)	Avg. Flow (lphd)	Peak Flow (lphd)	Time Period (mos.)	Avg. Flow (lphd)	Peak Flow (lphd)	
M1	I	ASH(M)(SE)	1-12	76	114	13-24	63	93	NA	NA	NA	
						25-36	45	66				
						37-43	49	69				
						Entire Period	53	93				
N1	II	MSW(SE)	1-12	ND	ND	13-24	ND	ND	NA	NA	NA	No GM in bottom liner
						25-36	ND	ND				
						37-48	ND	ND				
						49-60	83	222				
						61-72	183	354				
						73-75	82	108				
						Entire Period	121	354				
N2	II	MSW(SE)	1-12	ND	ND	13-19	113	468	NA	NA	NA	
						20-31	203	669				
						32-34	786	1,058				
						35-39	201	406				
						Entire Period	227	1,058				
O1	II	MSW(SE)	1-6	293	620	7-18	0	3	NA	NA	NA	
						19-30	3	7				
						31-42	0	5				
						43-54	1	6				
						55-64	3	9				
						Entire Period	1	9				
O2	II	MSW(SE)	1-12	6	24	13-24	2	5				
						25-36	1	4	NA	NA	NA	
						37-48	3	11				
						49-59	1	5				
						Entire Period	2	11				
O3	II	MSW(SE)	1-10	359	768	11-16	112	428	NA	NA	NA	
P1	II	ASH(M)(SE)	1-12	ND	ND	13-34	ND	ND	NA	NA	NA	
						35-39	716	2,585	NA	NA	NA	
P2	II	ASH(M)(SE)	1-12	ND	ND	13-22	ND	ND	NA	NA	NA	
						23-27	832	1,220				
P3	II	ASH(M)(SE)	1-10	ND	ND	11-15	1,184	3,179	NA	NA	NA	

Table E-3.6. Landfill LDS Flow Rate Data, Summarized by Landfill Life Cycle Stage (Continued).

Cell No.	Prim. Liner/ LDS Type	Waste Type/ Region	Initial Period of Operation			Active Period of Operation			Post-Closure Period			Notes
			Time Period[1] (mos.)	Avg. Flow (lphd)	Peak Flow (lphd)	Time Period (mos.)	Avg. Flow (lphd)	Peak Flow (lphd)	Time Period (mos.)	Avg. Flow (lphd)	Peak Flow (lphd)	
Q1	II	MSW(NE)	1-3	ND	ND	4-16	23	32	NA	NA	NA	
						17-28	6	11				
						29-40	8	11				
						41-44	6	8				
						Entire Period	12	32				
Q1-2						45-58	43	112	NA	NA	NA	
R1	II	MSW(NE)	1-2	ND	ND	13-18	102	229				
			3-5	154	229	19-20	ND	ND				
			6-8	ND	ND	21-23	110	253				
			9-12	296	475							
			Period	235	475	Entire Period	105	253				
S1	II	MSW(NE)	1-10	12	39	11-22	38	68	NA	NA	NA	
						23-28	ND	ND				
						29-40	8	26				
						41-45	4	7				
						Entire Period	20	68				
S2	II	ASH(M)(NE)	1-9	5	24	10-17	5	24	NA	NA	NA	
						18-33	ND	ND				
						34-46	5	8				
						Entire Period	5	24				
T1	II	MSW(NE)	1-9	ND	ND	10-21	2	19	NA	NA	NA	
						22-32	5	29				
						33-35	ND	ND				
						36	56	56				
						37-41	ND	ND				
						42-46	96	375				
						Entire Period	17	375				
T2	II	MSW(NE)	1	ND	ND	13-24	0	0	NA	NA	NA	
			2-12	0	0	25-27	ND	ND				
						28-31	117	221				
						32	ND	ND				
						33-38	80	414				
						Entire Period	36	414				

Table E-3.6. Landfill LDS Flow Rate Data, Summarized by Landfill Life Cycle Stage (Continued).

Cell No.	Prim. Liner/ LDS Type	Waste Type/ Region	Initial Period of Operation			Active Period of Operation			Post-Closure Period			Notes
			Time Period[1] (mos.)	Avg. Flow (lphd)	Peak Flow (lphd)	Time Period (mos.)	Avg. Flow (lphd)	Peak Flow (lphd)	Time Period (mos.)	Avg. Flow (lphd)	Peak Flow (lphd)	
U1	II	MSW(NE)	1-7	ND	ND	8-19	220	373	NA	NA	NA	
						20-31	170	285				
						32-42	118	181				Side slopes were capped after 24 months
						Entire Period	171	373				
U2	II	MSW(NE)	1	ND	ND	15-26	42	74	NA	NA	NA	
			2-14	218	487	27-36	28	44				
						Entire Period	36	74				Side slopes were capped after 19 months
U3	II	MSW(NE)	1-12	128	187	13-25	147	528	NA	NA	NA	Side slopes were capped after 10 months
U4	II	MSW(NE)	1	ND	ND	9-22	1	14	NA	NA	NA	
			2-8	14	40							Side slopes were capped after 7 months
V1	II	MSW(SE)	1-13	117	153	14-25	51	68	NA	NA	NA	
						26-37	36	58				
						38-49	41	227				
						50-61	39	77				
						62-64	17	18				
						Entire Period	40	227				
V2	II	MSW(SE)	1-13	135	256	14-25	54	70	NA	NA	NA	
						26-37	46	86				
						38-49	37	68				
						50-61	30	33				
						62-64	26	26				
						Entire Period	41	86				
V3	II	MSW(SE)	1	669	669	8-20	118	139	NA	NA	NA	
			2-7	220	258	21-32	75	97				
						33-44	55	73				
						45-54	45	58				
			Period	284	669	Entire Period	76	139				
V4	II	MSW(SE)	1-11	247	573	12-23	102	392	NA	NA	NA	
						24-35	69	197				
						36-47	70	100				
						48-53	68	92				
						Entire Period	79	392				

Table E-3.6. Landfill LDS Flow Rate Data, Summarized by Landfill Life Cycle Stage (Continued).

Cell No.	Prim. Liner/ LDS Type	Waste Type/ Region	Initial Period of Operation			Active Period of Operation			Post-Closure Period			Notes
			Time Period[1] (mos.)	Avg. Flow (lphd)	Peak Flow (lphd)	Time Period (mos.)	Avg. Flow (lphd)	Peak Flow (lphd)	Time Period (mos.)	Avg. Flow (lphd)	Peak Flow (lphd)	
V5	II	MSW(SE)	1-4	300	618	15-24	64	125	NA	NA	NA	
			5-8	2	3							
			9-14	249	432							
			Period	193	618							
W1	II	MSW(SE)	1-8	ND	ND	13-24	34	109	NA	NA	NA	
			9-12	439	765	25-35	19	44				
						Entire Period	27	109				
W2	II	MSW(SE)	1-8	ND	ND	9-20	594	1,826	NA	NA	NA	
						21-32	204	1,217				
						33-35	32	52				
						Entire Period	358	1,826				
X1	II	MSW(SE)	1	364	364	8-19	5	45	NA	NA	NA	
			2-7	4	25	20-33	0	2				
			Period	55	364	Entire Period	2	45				
Y1	III	ASH(M)(NE)	1-6	ND	ND	13-23	242	1,031	NA	NA	NA	
			7-12	381	1,341	24-30	ND	ND				
						31-42	285	643				
						43-54	377	1,157				
						55-66	167	393				
						67-78	98	530				
						Entire Period	230	1,157				
Y2	III	MSW(NE)	1-10	655	1,768	11-22	370	1,993	NA	NA	NA	
						23-34	90	168				
						35-46	70	248				
						47-54	48	56				
						Entire Period	153	1,993				
Z1	III	ASH(C)(NE)	1-12	84	145	13-24	64	107	NA	NA	NA	
						25-36	86	148				
						37-39	104	150				
						Entire Period	78	150				

Table E-3.6. Landfill LDS Flow Rate Data, Summarized by Landfill Life Cycle Stage (Continued).

Cell No.	Prim. Liner/ LDS Type	Waste Type/ Region	Initial Period of Operation			Active Period of Operation			Post-Closure Period			Notes
			Time Period[1] (mos.)	Avg. Flow (lphd)	Peak Flow (lphd)	Time Period (mos.)	Avg. Flow (lphd)	Peak Flow (lphd)	Time Period (mos.)	Avg. Flow (lphd)	Peak Flow (lphd)	
AA1	III	MSW(NE)	1	ND	ND	9-14	1	3	NA	NA	NA	
			2-8	35	57	15-26	93	318				
						27-31	251	794				
						32-43	37	105				
						44-51	39	122				
						Entire Period	73	794				
AA2	III	MSW(NE)	1-3	792	1,021	16-20	92	133	NA	NA	NA	
			4-15	338	560							
			Period	429	1,021							
AA2-3	III	MSW(NE)				21-32	128	251	NA	NA	NA	
						33-44	63	144				
						45-54	63	201				
						Entire Period	87	251				
AB1	III	HW(SE)	1-5	275	518	6-17	55	80	NA	NA	NA	
						18-29	91	337				
						30-41	90	142				
						42-53	66	134				
						54-65	98	209				
						66-77	37	89				
						78-87	17	23				
						Entire Period	66	337				
AB2	III	HW(SE)	1-12	16	33	13-24	20	25	NA	NA	NA	
						25-36	24	36				
						37-48	29	37				
						49-57	30	42				
						58-63	27	35				
						64-75*	64	115				
						76-87*	82	142				
						Entire Period	41	142				

Table E-3.6. Landfill LDS Flow Rate Data, Summarized by Landfill Life Cycle Stage (Continued).

Cell No.	Prim. Liner/ LDS Type	Waste Type/ Region	Initial Period of Operation			Active Period of Operation			Post-Closure Period			Notes
			Time Period[1] (mos.)	Avg. Flow (lphd)	Peak Flow (lphd)	Time Period (mos.)	Avg. Flow (lphd)	Peak Flow (lphd)	Time Period (mos.)	Avg. Flow (lphd)	Peak Flow (lphd)	
AB3	III	HW(SE)	1-12	39	224	13-25	68	232	NA	NA	NA	
						26-32	ND	ND				
						33-44	40	108				
						45-56	21	45				
						57-68	13	21				
						69-74	15	18				
						Entire Period	34	232				
AB4	III	HW(SE)	1-4	ND	ND	14-25	77	107	NA	NA	NA	
			5-13	333	471	26-37	50	98				
						38-49	50	64				
						50-59	35	47				
						60-63	ND	ND				
						Entire Period	54	107				
AC1	IV	HW(W)	1-13	94	206	NA	NA	NA	NA	NA	NA	
AC2	IV	HW(W)	1-6	4	11	7-18	65	107	NA	NA	NA	Cell received intermediate cover approximately 56 months after start of waste placement in cell
						19-30	66	128				
						31-42	96	164				
						43-54	30	40				
						55-66	19	34				
						67-78	12	17				
						79-88	7	13				
						Entire Period	43	164				
AC3	IV	HW(W)	1-12	94	173	13-24	123	159	NA	NA	NA	Cell received intermediate cover approximately 41 months after start of waste placement in cell
						25-36	71	98				
						37-48	47	82				
						49-60	19	26				
						61-73	12	25				
						Entire Period	51	159				

Table E-3.6. Landfill LDS Flow Rate Data, Summarized by Landfill Life Cycle Stage (Continued).

Cell No.	Prim. Liner/ LDS Type	Waste Type/ Region	Initial Period of Operation			Active Period of Operation			Post-Closure Period			Notes
			Time Period[1] (mos.)	Avg. Flow (lphd)	Peak Flow (lphd)	Time Period (mos.)	Avg. Flow (lphd)	Peak Flow (lphd)	Time Period (mos.)	Avg. Flow (lphd)	Peak Flow (lphd)	
AC4	IV	HW(W)	1-11	14	97	12-23	127	495	NA	NA	NA	Cell received intermediate cover approximately 40 months after start of waste placement in cell
						24-35	52	73				
						36-47	42	73				
						48-59	16	25				
						60-73	7	15				
						Entire Period	47	495				
AC5	IV	HW(W)	1-13	1	3	14-25	6	44	NA	NA	NA	
						26-34	1	1				
						Entire Period	4	44				
AC6	IV	HW(W)	1-10	1	5	11-16	54	219	NA	NA	NA	
						17-28	3	9				
						29-34	1	2				
						35-40	2	4				
						Entire Period	12	219				
AC7	IV	HW(W)	1-12	0	0	13-18	0	0	NA	NA	NA	
AC8	IV	HW(W)	1-12	0	3	13-18	2	4	NA	NA	NA	
AD1	III	HW(SE)	1-12	ND	ND	13-20	ND	ND	33-44	24	42	
						21-32	107	603	45-56	26	31	
									57-68	28	45	
									69-80	42	103	
									81-92	23	68	
									93-104	8	46	
									105-116	5	43	
									117-121	6	24	
									Entire Period	21	103	

Table E-3.6. Landfill LDS Flow Rate Data, Summarized by Landfill Life Cycle Stage (Continued).

Cell No.	Prim. Liner/ LDS Type	Waste Type/ Region	Initial Period of Operation			Active Period of Operation			Post-Closure Period			Notes
			Time Period[1] (mos.)	Avg. Flow (lphd)	Peak Flow (lphd)	Time Period (mos.)	Avg. Flow (lphd)	Peak Flow (lphd)	Time Period (mos.)	Avg. Flow (lphd)	Peak Flow (lphd)	
AD2	III	HW(SE)	1-12	ND	ND	13-20	ND	ND	31-42	39	62	
						21-30	258	1,517	43-54	34	45	
									55-66	26	44	
									67-78	14	43	
									79-90	12	28	
									91-102	16	27	
									103-114	11	47	
									115-119	14	25	
									Entire Period	21	62	
AD3	III	HW(SE)	1-16	ND	ND	17-26	231	665	27-38	82	118	
									39-50	96	138	
									51-62	50	148	
									63-74	50	73	
									75-86	29	57	
									87-98	41	72	
									99-110	37	108	
									111-115	0	1	
									Entire Period	52	148	
AD4	III	HW(SE)	1-16	ND	ND	17-26	303	1,517	27-38	56	90	
									39-50	41	51	
									51-62	44	79	
									63-74	34	43	
									75-86	23	44	
									87-98	1	2	
									99-110	2	9	
									111-115	0	1	
									Entire Period	27	90	

Table E-3.6. Landfill LDS Flow Rate Data, Summarized by Landfill Life Cycle Stage (Continued).

Cell No.	Prim. Liner/ LDS Type	Waste Type/ Region	Initial Period of Operation			Active Period of Operation			Post-Closure Period			Notes
			Time Period[1] (mos.)	Avg. Flow (lphd)	Peak Flow (lphd)	Time Period (mos.)	Avg. Flow (lphd)	Peak Flow (lphd)	Time Period (mos.)	Avg. Flow (lphd)	Peak Flow (lphd)	
AD5	III	HW(SE)	1-9	ND	ND	10-19	547	1,417	20-31	56	132	
									32-43	43	68	
									44-55	66	175	
									56-67	94	168	
									68-79	119	244	
									80-91	142	237	
									92-103	155	315	
									104-108	270	486	
									Entire Period	106	486	
AD6	III	HW(SE)	1-9	ND	ND	10-19	763	1,295	20-31	117	173	
									32-43	61	83	
									44-55	41	90	
									56-67	30	38	
									68-79	26	55	
									80-91	12	136	
									92-103	0	2	
									104-108	0	1	
									Entire Period	39	173	
AD7	IV	HW(SE)	1-12	135	1,101	13-24	71	291	70-81	73	157	Cell received intermediate cover
						25-36	96	393	82-87	105	172	approximately 12 months after start
						37-48	17	21				of waste placement in cell
						49-60	33	74				
						61-69	64	112				
						Entire Period	56	393	Entire Period	83	172	
AD8	IV	HW(SE)	1-8	201	554	9-19	108	183	65-76	248	476	Cell received intermediate cover
						20-24	785	1,259	77-84	313	564	approximately 12 months after start
						25-36	82	175				of waste placement in cell
						37-48	46	66				
						49-60	45	131				
						61-64	79	202				
						Entire Period	134	1,259	Entire Period	274	564	

Table E-3.6. Landfill LDS Flow Rate Data, Summarized by Landfill Life Cycle Stage (Continued).

Cell No.	Prim. Liner/ LDS Type	Waste Type/ Region	Initial Period of Operation			Active Period of Operation			Post-Closure Period			Notes
			Time Period[1] (mos.)	Avg. Flow (lphd)	Peak Flow (lphd)	Time Period (mos.)	Avg. Flow (lphd)	Peak Flow (lphd)	Time Period (mos.)	Avg. Flow (lphd)	Peak Flow (lphd)	
AD9	IV	HW(SE)	1-9	157	421	10-21	129	297	59-60	92	135	Cell received intermediate cover
						22-33	27	60	61-72	17	32	approximately 12 months after start
						34-45	23	36	73-79	10	29	of waste placement in cell
						46-58	18	27				
						Entire Period	49	297	Entire Period	22	135	
AD10	IV	HW(SE)	1-12	234	436	13-24	181	404	NA	NA	NA	Cell received intermediate cover
						25-36	67	159				approximately 41 months after start
						37-50	41	64				of waste placement in cell
						51-62*	150	471				
						63-74	124	350				1/2 of cell was closed approximately 59
						75-79	118	237				months after start of waste placement
						Entire Period	111	471				in cell
AD11	IV	HW(SE)	1-5	116	155	6-17	ND	ND	NA	NA	NA	Cell received intermediate cover
						18-29	90	214				approximately 41 months after start
						30-41	81	167				of waste placement in cell
						42-53	88	148				
						54-65	82	197				
						66-69	73	131				
						Entire Period	84	214				
AD12	IV	HW(SE)	1-13	136	369	14-25	84	193	NA	NA	NA	Cell received intermediate cover
						26-37	217	383				approximately 41 months after start
						38-49	120	304				of waste placement in cell
						50-61	102	406				
						62-69	64	98				
						Entire Period	121	406				
AD13	IV	HW(SE)	1-12	72	365	13-18	80	162	NA	NA	NA	Cell received intermediate cover
						19-30	92	237				approximately 41 months after start
						31-42	184	490				of waste placement in cell
						43-55	172	400				
						Entire Period	140	490				

Table E-3.6. Landfill LDS Flow Rate Data, Summarized by Landfill Life Cycle Stage (Continued).

Cell No.	Prim. Liner/ LDS Type	Waste Type/ Region	Initial Period of Operation			Active Period of Operation			Post-Closure Period			Notes
			Time Period[1] (mos.)	Avg. Flow (lphd)	Peak Flow (lphd)	Time Period (mos.)	Avg. Flow (lphd)	Peak Flow (lphd)	Time Period (mos.)	Avg. Flow (lphd)	Peak Flow (lphd)	
AD14	IV	HW(SE)	1-12	61	119	13-24	132	364	NA	NA	NA	Cell received intermediate cover
						25-36	137	329				approximately 41 months after start
						37-48	95	144				of waste placement in cell
						49-55	192	281				
						Entire Period	133	364				
AD15	IV	HW(SE)	1-13	117	277	14-25	134	246	NA	NA	NA	Cell received intermediate cover
						26-39	150	270				approximately 41 months after start
						Entire Period	143	270				of waste placement in cell
AD16	IV	HW(SE)	1-12	188	701	13-24	163	568	NA	NA	NA	Cell received intermediate cover
						25-39	222	459				approximately 41 months after start
						Entire Period	196	568				of waste placement in cell
AD17	IV	HW(SE)	1-12	206	353	13-16	104	119	NA	NA	NA	
AD18	IV	HW(SE)	1-12	131	193	13-19	83	113	NA	NA	NA	
AE1	III	MSW(NE)	1-12	ND	ND	13-24	ND	ND	NA	NA	NA	
						25-35	ND	ND				
						36-47	108	192				
						48-54	83	119				
						55-66	256	1,111				
						67-80	130	166				
						Entire Period	150	1,111				
AE2	III	MSW(NE)	1-8	ND	ND	9-20	205	267	NA	NA	NA	
						21-32	197	241				
						33-44	149	179				
						45-49	101	129				
						Entire Period	174	267				
AE3	III	MSW(NE)	1-11	ND	ND	NA	NA	NA	NA	NA	NA	
AF1	III	ASH(M)(NE)	1-12			13-24	67	95	NA	NA	NA	
						25-36	53	92				
						37-48	27	38				
						49-60	11	23				
						61-63	8	8				
						Entire Period	38	95				

Table E-3.6. Landfill LDS Flow Rate Data, Summarized by Landfill Life Cycle Stage (Continued).

Cell No.	Prim. Liner/ LDS Type	Waste Type/ Region	Initial Period of Operation			Active Period of Operation			Post-Closure Period			Notes
			Time Period[1] (mos.)	Avg. Flow (lphd)	Peak Flow (lphd)	Time Period (mos.)	Avg. Flow (lphd)	Peak Flow (lphd)	Time Period (mos.)	Avg. Flow (lphd)	Peak Flow (lphd)	
AG1	III	MSW(NE)	1-7	85	222	8-19	1	2	NA	NA	NA	
						20-33	0	1				
						Entire Period	1	2				
AH1	III	MSW/ASH(M)(NE)	1-6	8	18	7-18	64	92	NA	NA	NA	
						19-28	63	103				
						Entire Period	64	103				
AH2	III	MSW/ASH(M)(NE)	1-5	10	39	6-13	ND	ND	NA	NA	NA	
						14-25	60	89				
						26-28	70	86				
						Entire Period	62	89				
AH3	III	MSW/ASH(M)(NE)	1-6	8	18	7-12	43	49	NA	NA	NA	
						13-18	5	13				
						19-28	50	78				
						Entire Period	36	78				
AH4	III	MSW/ASH(M)(NE)	1	ND	ND	13-18	2	6	NA	NA	NA	
			2-12	5	17	19-28	43	83				
						Entire Period	28	83				
AH5	III	MSW/ASH(M)(NE)	1-12	18	48	13-24	32	82	NA	NA	NA	
						25-28	26	40				
						Entire Period	31	82				
AI1	III	C&DW(NE)	1-2	ND	ND	13-24	78	220	NA	NA	NA	
			3-6	1,177	1,596	25-36	65	200				
			7-12	359	579	37-50	101	227				
			Period	687	1,596	Entire Period	82	227				
AI2	III	C&DW(NE)	1-2	ND	ND	7-18	97	156	NA	NA	NA	
			3-6	539	893	19-30	46	63				
						31-42	58	98				
						43-50	61	120				
						Entire Period	66	156				
AJ1	III	MSW(NE)	1	ND	ND	7-13	24	47	NA	NA	NA	
			2-6	279	625							
AK1	IV	MSW(NE)	1-12	206	804				NA	NA	NA	
AK1-2	IV	MSW(NE)				11-15	492	1,424	NA	NA	NA	

Table E-3.6. Landfill LDS Flow Rate Data, Summarized by Landfill Life Cycle Stage (Continued).

Cell No.	Prim. Liner/ LDS Type	Waste Type/ Region	Initial Period of Operation			Active Period of Operation			Post-Closure Period			Notes
			Time Period[1] (mos.)	Avg. Flow (lphd)	Peak Flow (lphd)	Time Period (mos.)	Avg. Flow (lphd)	Peak Flow (lphd)	Time Period (mos.)	Avg. Flow (lphd)	Peak Flow (lphd)	
AL1	IV	MSW(NE)	1-12	ND	ND	13-29	ND	ND	NA	NA	NA	
						30-41	221	367				
						42-54	103	183				
						Entire Period	164	367				
AM1	IV	MSW(W)	1-9	ND	ND	10-21	15	64	NA	NA	NA	Cell received intermediate cover
						22-33	10	15				approximately 5 months after start
						34-45	3	14				of waste placement in cell
						46-57	1	1				
						58-69	1	1				
						70-81	5	8				
						Entire Period	6	64				
AM2	IV	MSW(W)	1-9	ND	ND	10-21	9	42	NA	NA	NA	Cell received intermediate cover
						22-33	9	29				approximately 5 months after start
						34-45	3	26				of waste placement in cell
						46-57	0	0				
						58-69	8	13				
						70-81	9	13				
						Entire Period	6	42				
AN1	IV	ASH(M)(NE)	1-7	ND	ND	8-12	13	21	NA	NA	NA	
AN1-2						13-17	46	136				
AN1-3						18-21	65	144				
						22-31	173	368				
						Entire Period	137	368				
AN1-4						32-34	523	580				
AO1	IV	MSW(NE)	1-5	ND	ND	6-17	184	353	NA	NA	NA	
						16-28	96	126				
						29-36	60	102				
						Entire Period	119	353				
AO2	IV	MSW(NE)	1-5	149	191	6-17	110	158	NA	NA	NA	
						18-30	33	64				
						Entire Period	70	158				
AO3	IV	MSW(NE)	1-8	800	1,089	NA	NA	NA	NA	NA	NA	
AO4	IV	MSW(NE)	1-8	385	583	NA	NA	NA	NA	NA	NA	

Table E-3.6. Landfill LDS Flow Rate Data, Summarized by Landfill Life Cycle Stage (Continued).

Cell No.	Prim. Liner/ LDS Type	Waste Type/ Region	Initial Period of Operation			Active Period of Operation			Post-Closure Period			Notes
			Time Period[1] (mos.)	Avg. Flow (lphd)	Peak Flow (lphd)	Time Period (mos.)	Avg. Flow (lphd)	Peak Flow (lphd)	Time Period (mos.)	Avg. Flow (lphd)	Peak Flow (lphd)	
AP1	IV	HW(W)	1-12	43	162	13-24	27	100	NA	NA	NA	
						25-36	24	69				
						37-48	26	58				
						Entire Period	26	100				
AQ1	IV	HW(NE)	1-6	352	569	7-25	255	1,239	59-65	215	246	Cell final closure date is approximate
						26-34	ND	ND	66-77	117	165	
						35-46	197	435	78-89	98	132	
						47-58	116	143	90-97	51	118	
						Entire Period	196	1,239	Entire Period	115	246	
AQ2	IV	HW(NE)	1-12	340	669	13-25	437	1,550	59-70	136	287	
						26-34	ND	ND	71-82	94	168	
						35-46	227	312	83-94	52	71	
						47-58	124	191	95-97	4	12	
						Entire Period	267	1,550	Entire Period	87	287	
AQ3	IV	HW(NE)	1-12	472	2,195	13-21	451	1,390	55-66	179	281	
						22-30	ND	ND	67-78	137	263	
						31-42	287	427	79-90	89	150	
						43-54	161	265	91-93	52	73	
						Entire Period	286	1,390	Entire Period	129	281	
AQ4	IV	HW(NE)	1-3	299	299	14-20	121	220	54-65	151	204	Cell final closure date is approximate
			4	ND	ND	21-29	ND	ND	66-77	96	131	
			5-13	356	642	30-41	195	246	78-89	80	127	
			Period	342	642	42-53	148	278	90-92	69	87	
						Entire Period	160	278	Entire Period	106	204	
AQ5	IV	HW(NE)	1-12	127	688	13-20	ND	ND	51-62	71	131	
						21-32	81	140	63-74	47	99	
						33-44	131	709	75-84	62	112	
						45-50	119	179				
						Entire Period	109	709	Entire Period	60	131	

Table E-3.6. Landfill LDS Flow Rate Data, Summarized by Landfill Life Cycle Stage (Continued).

Cell No.	Prim. Liner/ LDS Type	Waste Type/ Region	Initial Period of Operation			Active Period of Operation			Post-Closure Period			Notes
			Time Period[1] (mos.)	Avg. Flow (lphd)	Peak Flow (lphd)	Time Period (mos.)	Avg. Flow (lphd)	Peak Flow (lphd)	Time Period (mos.)	Avg. Flow (lphd)	Peak Flow (lphd)	
AQ6	IV	HW(NE)	1-12	ND	ND	13-16	ND	ND	53-64	138	227	
						17-28	289	766	65-76	128	197	
						29-40	202	333	77-80	136	166	
						41-52	173	291				
						Entire Period	222	766	Entire Period	134	227	
AQ7	IV	HW(NE)	1-6	38	53	7-15	ND	ND	43-54	56	108	
						16-27	77	160	55-66	42	79	
						28-42	112	488	67-79	45	64	
						Entire Period	97	488	Entire Period	48	108	
AQ8	IV	HW(NE)	1-12	54	118	13-26	111	349	27-38	41	77	
									39-50	44	68	
									51-63	33	75	
									Entire Period	39	77	
AQ9	IV	HW(NE)	1-12	24	75	13-26	126	429	27-38	48	95	
									39-50	112	206	
									51-63	82	179	
									Entire Period	81	206	
AQ10	IV	HW(NE)	1-9	14	32	10-14	26	32	27-38	29	48	
						15-26	48	250	39-50	18	63	
									51-63	24	75	
						Entire Period	42	250	Entire Period	24	75	
AR1	IV	MSW(NE)	1-11	292	705	12-23	181	470	NA	NA	NA	Cell AR1 has four subareas. Waste placement started in months 1, 5, 20, and 26 in subareas 1 through 4, respectively.
						24-36	155	442				
						Entire Period	167	470				
AR1-2						37-40	92	217	NA	NA	NA	
AS1	IV	HW(SE)	1-3	252	283	4-15	51	110	28-39	6	35	
						16-27	17	52	40-51	3	17	
									52-63	2	7	
									64-71	1	4	
						Entire Period	34	110	Entire Period	3	35	
AT1	IV	HW(W)	1-5	ND	ND	6-8	8	15	9-20	0	1	
									21-33	0	0	
									Entire Period	0	1	

Table E-3.6. Landfill LDS Flow Rate Data, Summarized by Landfill Life Cycle Stage (Continued).

Cell No.	Prim. Liner/ LDS Type	Waste Type/ Region	Initial Period of Operation			Active Period of Operation			Post-Closure Period			Notes
			Time Period[1] (mos.)	Avg. Flow (lphd)	Peak Flow (lphd)	Time Period (mos.)	Avg. Flow (lphd)	Peak Flow (lphd)	Time Period (mos.)	Avg. Flow (lphd)	Peak Flow (lphd)	
AU1	IV	MSW(NE)	1-4	ND	ND	5-16	56	274	NA	NA	NA	
						17-29	30	101				
						30-32	ND	ND				
						Entire Period	42	274				
AV1	IV	HW(NE)	1-4	695	1,735	13-24	ND	ND	NA	NA	NA	
			5-12	ND	ND	25-33	ND	ND				
						34-45	156	660				
						46-57	86	114				
						58-69	43	55				
						70-81	54	86				
						82-93	30	55				
						94-104	40	71				
						Entire Period	53	660				
AV2	IV	HW(NE)	1-12	ND	ND	13-20	ND	ND	NA	NA	NA	
						21-32	88	319				
						33-44	59	96				
						45-56	16	49				
						57-68	19	40				
						69-80	13	32				
						81-90	17	29				
						91	ND	ND				
						Entire Period	32	319				
AV3	IV	HW(NE)	1-3	ND	ND	14-25	122	188	NA	NA	NA	
			4-13	409	976	26-34	66	137				
						35-46	7	20				
						47-58	7	12				
						59-71	18	48				
						72-74	ND	ND				
						Entire Period	41	188				

Table E-3.6. Landfill LDS Flow Rate Data, Summarized by Landfill Life Cycle Stage (Continued).

Cell No.	Prim. Liner/ LDS Type	Waste Type/ Region	Initial Period of Operation			Active Period of Operation			Post-Closure Period			Notes
			Time Period[1] (mos.)	Avg. Flow (lphd)	Peak Flow (lphd)	Time Period (mos.)	Avg. Flow (lphd)	Peak Flow (lphd)	Time Period (mos.)	Avg. Flow (lphd)	Peak Flow (lphd)	
AV4	IV	HW(NE)	1	1,767	1,767	6-17	293	323	NA	NA	NA	
			2-5	54	68	18-29	189	372				
						30-41	65	121				
						42-53	38	65				
						54-66	27	52				
			Period	397	1,767	Entire Period	124	372				
AV5	IV	HW(NE)	1-12	180	325	13-24	143	205				
						25-37	60	127				
						38-40	79	136				
						Entire Period	98	205				
AW1	V	MSW(SE)	1-11	131	524				NA	NA	NA	
AW1,3	V,II					12-24	24	127	NA	NA	NA	
AW2	V	MSW(SE)	1-11	290	514				NA	NA	NA	
AW2,4	V,II					12-21	33	83	NA	NA	NA	
AX1	V	MSW(NE)	1-2	0	0	3-14	0	0	34-45	0	0	
						15-26	0	0	46-57	0	0	
						27-33	0	0	58-69	0	0	
									70-83	0	0	
						Entire Period	0	0	Entire Period	0	0	
AX2	V	MSW(NE)	1-5	15	45	3-14	5	21	34-45	0	0	
						15-26	1	2	46-57	0	0	
						27-33	0	0	58-69	0	0	
									70-83	0	0	
						Entire Period	2	21	Entire Period	0	0	
AX3	V	MSW(NE)	1-5	35	151	6-17	6	44	57-68	1	9	Cell received intermediate cover
						18-29	0	1	69-81	1	10	approximately 34 months after start
						30-41	0	0				of waste placement in cell
						42-56	9	47				
						Entire Period	4	47	Entire Period	1	10	

Table E-3.6. Landfill LDS Flow Rate Data, Summarized by Landfill Life Cycle Stage (Continued).

Cell No.	Prim. Liner/ LDS Type	Waste Type/ Region	Initial Period of Operation			Active Period of Operation			Post-Closure Period			Notes
			Time Period[1] (mos.)	Avg. Flow (lphd)	Peak Flow (lphd)	Time Period (mos.)	Avg. Flow (lphd)	Peak Flow (lphd)	Time Period (mos.)	Avg. Flow (lphd)	Peak Flow (lphd)	
AX4	V	MSW(NE)	1-12	101	860	13-17	2	13	57-68	0	0	Cell received intermediate cover
						18-29	1	3	69-81	0	0	approximately 34 months after start
						30-41	1	9				of waste placement in cell
						42-56	0	0				
						Entire Period	1	13	Entire Period	0	0	
AX5	V	MSW(NE)	1-11	37	92	12-23	4	11	NA	NA	NA	Cell received intermediate cover
						24-35	3	37				approximately 33 months after start
						36-47	0	0				of waste placement in cell
						48-59	2	9				
						60-71	0	0				Cell was partially closed approximately 55
						72-80	0	0				months after start of waste placement in
						Entire Period	2	37				cell
AX6	V	MSW(NE)	1-9	53	93	10-21	0	0	NA	NA	NA	Cell received intermediate cover
						22-33	0	0				approximately 30 months after start
						34-45	0	0				of waste placement in cell
						46-57	0	0				
						58-69	0	0				Cell was partially closed approximately 53
						70-78	0	0				months after start of waste placement in
						Entire Period	0	0				cell
AX7	V	MSW(NE)	1-10	34	47	11-22	4	6	NA	NA	NA	Cell was partially closed approximately 51
						23-25	8	9				months after start of waste placement in
						26	ND	ND				cell
						27-38	1	9				
						39-50	3	9				
						51-62	0	0				
						63-76	0	0				
						Entire Period	2	9				

Table E-3.6. Landfill LDS Flow Rate Data, Summarized by Landfill Life Cycle Stage (Continued).

Cell No.	Prim. Liner/ LDS Type	Waste Type/ Region	Initial Period of Operation			Active Period of Operation			Post-Closure Period			Notes
			Time Period[1] (mos.)	Avg. Flow (lphd)	Peak Flow (lphd)	Time Period (mos.)	Avg. Flow (lphd)	Peak Flow (lphd)	Time Period (mos.)	Avg. Flow (lphd)	Peak Flow (lphd)	
AX8	V	MSW(NE)	1-14	48	189	15-26	0	0	NA	NA	NA	Cell was partially closed approximately 46 months after start of waste placement in cell
						27-38	0	0				
						39-50	0	0				
						51-62	0	0				
						63-71	0	0				
						Entire Period	0	0				
AX9	V	MSW(NE)	1-9	1	7	10-21	0	0	NA	NA	NA	Cell was partially closed approximately 41 months after start of waste placement in cell
						22-33	0	0				
						34-45	0	0				
						46-57	0	0				
						58-66	0	0				
						Entire Period	0	0				
AX10	V	MSW(NE)	1-11	0	0	12-23	0	0	NA	NA	NA	Cell was partially closed approximately 34 months after start of waste placement in cell
						24-35	0	0				
						36-47	0	0				
						48-59	0	0				
						60-63	0	0				
						Entire Period	0	0				
AX11	V	MSW(NE)	1-14	0	0	15-26	0	0	NA	NA	NA	Cell was partially closed approximately 39 months after start of waste placement in cell
						27-38	0	0				
						39-50	0	0				
						51-62	0	0				
						Entire Period	0	0				
AX12	V	MSW(NE)	1-12	0	0	13-24	0	0	NA	NA	NA	Cell may have been partially closed approximately 31 months after start of waste placement in cell
						25-36	0	0				
						37-48	0	0				
						49-56	0	0				
						Entire Period	0	0				
AX13	V	MSW(NE)	1-7	0	0	8-19	0	0	NA	NA	NA	Cell may have been partially closed approximately 28 months after start of waste placement in cell
						20-31	0	0				
						32-43	0	0				
						44-53	0	0				
						Entire Period	0	0				

Table E-3.6. Landfill LDS Flow Rate Data, Summarized by Landfill Life Cycle Stage (Continued).

Cell No.	Prim. Liner/ LDS Type	Waste Type/ Region	Initial Period of Operation			Active Period of Operation			Post-Closure Period			Notes
			Time Period[1] (mos.)	Avg. Flow (lphd)	Peak Flow (lphd)	Time Period (mos.)	Avg. Flow (lphd)	Peak Flow (lphd)	Time Period (mos.)	Avg. Flow (lphd)	Peak Flow (lphd)	
AX14	V	MSW(NE)	1-10	0	0	11-22	0	0	NA	NA	NA	
						23-30	0	0				
						31-32*	0	0				
						33-38	0	0				
						Entire Period	0	0				
AX15	V	MSW(NE)	1-12	0	0	13-24	0	0	NA	NA	NA	
						25-37	0	0				
						Entire Period	0	0				
AX16	V	MSW(NE)	1-10	0	0	11-22	0	0	NA	NA	NA	
						23-29	0	0				
						Entire Period	0	0				
AY1	VI	HW(NE)	1-9	0	0	NA	NA	NA	NA	NA	NA	
AY2	VI	HW(NE)	1-11	3	12	NA	NA	NA	NA	NA	NA	
AY3	VI	HW(NE)	1-11	6	28	NA	NA	NA	NA	NA	NA	
AZ1	VI	MSW(NE)	1-2	ND	ND	13-24	3	22	NA	NA	NA	
			3-12	0	0	25-31	0	3				
						Entire Period	2	22				
BA1	-[2]	HW(NE)	1-14	ND	ND	15-26	136	316	NA	NA	NA	Cell received intermediate cover approximately 42 months after start of waste placement in cell
						27-38	73	209				
						39-42	21	30				
						Entire Period	92	316				
BA2	-[2]	HW(NE)	1-2	324	425	3-12	12	39	NA	NA	NA	
BB1	VI	MSW(SE)	1-6	15	65	7-17	13	25	NA	NA	NA	
						18-19	2	5				
						20-23	14	18				
						24-35	1	2				
						36-47	1	4				
						Entire Period	6	25				
BB2	VI	MSW(SE)	1-2	ND	ND	12-23	0	0	NA	NA	NA	
			3-11	1	12							
BB3	VI	MSW(SE)	1-2	ND	ND	12-23	0	1	NA	NA	NA	
			3-11	0	0							

Notes: (1) NA = not applicable, ND = not determined (2) Cells BA1 and BA2 include a GM/GCL/GM primary liner.

Table E-3.7. Select LCRS and LDS Flow Chemistry Data for Landfills.

		MSW LANDFILLS IN NORTHEAST U.S.										
Cell No.		B1-3						F1		G1-3		
System		LCRS1	LDS1	LCRS2	LDS2	LCRS3	LDS3	LCRS	LDS	LCRS/LDS1-3	LCRS/LDS1-2	LDS1-2
Primary Liner\LDS Type			I		I		III		I			I
Waste Placement Dates		5/84-11/88				7/87-5/92		7/92-date		6/89-date		
Liquid Sampling Dates		3/85-1/95	5/85-1/95	3/85-1/95	4/85-1/95	7/87-10/94	7/87-10/94	2/93-6/94	2/93-6/94	1/90-10/94	4/90	4/90
Parameter	Units											
pH	pH units	6.56	6.54	6.42	6.42	6.82	(1)	6.16	7.50	6.68	7.25	7.70
Specific conductance	µmhos/cm	10,972	2,697	9,381	6,821	2,956	1,554	1,833	830	7,683	1,355	470
TDS	mg/l	6,910	1,810	5,991	2,143	4,140	1,148	1,917	544	7,718		
COD	mg/l	10,073	2,037	10,938	2,357	1,912	131	1,747	35	8,267	633	27
BOD_5	mg/l	4,077	484	3,415	1,083	422	88	804	< 3.5(1)	4,056	465	23
TOC	mg/l	3,092	491	3,051	803	554	138	306	10	2,852	197	8
Alkalinity	mg/l							895	408	3,278	373	175
Chloride	mg/l	911	195	894	344	690	148	101	108	1,561	243	25
Sulfate	mg/l	162	43	135	36	131	335	8	40	84	38	59
Calcium	mg/l							278	64	610	100	53
Magnesium	mg/l	298	43	261	69			31	8	111	18	
Sodium	mg/l	727	149	757	292	450	46	65	147	1,115	136	14
Arsenic	µg/l	88	61	68	110		< 24	< 6	< 1	8	< 1	< 1
Cadmium	µg/l	< 17	< 9	< 15	18	< 20	16	8	< 7	7	< 2	< 2
Chromium	µg/l	40	28	53	108	49	3	15	< 28	320	35	< 1
Lead	µg/l	110	< 58	117	< 101	< 44	< 17	< 4	< 4	4	7	< 2
Nickel	µg/l	51	36	38	< 38	102	519	54	< 30	77	< 30	< 30
Benzene	µg/l	< 6	< 5	< 6	< 9	< 5	< 7	< 15	< 1	< 36		
1,1-Dichloroethane	µg/l	< 27	< 56	< 44	< 25	< 40	< 7	114	< 1	55		
1,2-Dichloroethane	µg/l	< 3	< 3	< 3	< 7	< 5	< 6	< 20	< 1	< 35		
cis-1,2-Dichloroethylene	µg/l									< 75		
trans-1,2-Dichloroethylene	µg/l	< 45	< 43	< 34	< 19			< 17	< 1	< 34		
Ethylbenzene	µg/l	14	< 5	< 12	< 8	15	< 6	< 14	< 1	< 37		
Methylene chloride	µg/l	299	< 29	< 186	< 24	< 80	< 17	264	< 1	241		
1,1,1-Trichloroethane	µg/l	< 67	< 112	< 105	< 140	< 107	< 6	269	< 1	< 67		
Trichloroethylene	µg/l	< 104	< 119	< 123	< 123			15	< 1	< 36		
Toluene	µg/l	376	< 178	337	140	< 78	< 9	84	< 1	633		
Vinyl Chloride	µg/l	< 5	< 5	< 5	< 6	< 10	< 12	< 77	< 1	< 53		
Xylenes	µg/l							38	< 1	62		

Table E-3.7. Select LCRS and LDS Flow Chemistry Data for Landfills (Continued).

		MSW LANDFILLS IN NORTHEAST U.S.										
Cell No.		I2		J1-6							K1	
System		LCRS	LDS	LCRS1-6	LDS1-6	LDS1	LDS2	LDS3	LDS4	LDS5	LCRS	LDS
Primary Liner\LDS Type			I		I	I	I	I	I	I		I
Waste Placement Dates		10/87-8/94		10/90-date							12/89-date	
Liquid Sampling Dates		3/88-2/92	5/88-10/93	10/90-4/94	10/90-4/94	10/90-4/94	10/90-4/94	10/90-4/94	10/90-4/94	10/90-4/94	12/91-2/93	12/91-2/93
Parameter	Units											
pH	pH units	6.30	6.65	7.40	6.58	6.73	6.72	6.37	6.52	6.60		
Specific conductance	µmhos/cm	5,332	2,345	1,066	1,257	1,423	1,297	1,035	1,276	985		
TDS	mg/l	3,663									3,820	1,127
COD	mg/l	3,350	< 50	330	55	49	22	84	77	41	1,619	252
BOD_5	mg/l	4,510	< 6								481	459
TOC	mg/l	1,104	96		36	34	26	41	52	26	957	203
Alkalinity	mg/l	1,602	497	503	965	879	813	863	801	410	2,401	898
Chloride	mg/l	356	131	28	18	32	21	12	21	19	341	208
Sulfate	mg/l	29	98	147	9	7	6	14	12	10	118	72
Calcium	mg/l	497	89	66	217	241	201	246	229	170	362	168
Magnesium	mg/l	175	60	159	45	57	54	43	36	32	84	30
Sodium	mg/l	225	46	33	8	7	16	5	5	7	413	69
Arsenic	µg/l	< 10	< 10	47	< 1						17	31
Cadmium	µg/l	10	< 5	< 5	4	2	14	254	4	0.1	< 8	< 4
Chromium	µg/l	< 50	< 50	< 90	5	2	8	258	5		42	28
Lead	µg/l	< 40	< 30		11	17	23	26	4	2	88	< 71
Nickel	µg/l		< 40	< 38							58	< 20
Benzene	µg/l	21	1	< 2	< 1	< 1	< 1	< 1	< 1	< 1	20	14
1,1-Dichloroethane	µg/l	294	110	< 2	7	8	5	4	7	< 1	23	
1,2-Dichloroethane	µg/l	20	< 1	< 1	< 1	< 1	< 1	< 1	< 1	< 1	< 100	< 100
cis-1,2-Dichloroethylene	µg/l			< 1	< 3	8	< 1	< 1	< 1	< 1		
trans-1,2-Dichloroethylene	µg/l		4	< 1	< 1	8	< 1	< 1	< 1	< 1	< 100	< 100
Ethylbenzene	µg/l	85	1	< 1	< 1	< 1	< 1	< 1	< 1	< 1	87	57
Methylene chloride	µg/l	1,303	480	< 1	< 1	6	2	< 1	< 1	< 1	107	85
1,1,1-Trichloroethane	µg/l	84	220	< 2	< 2	4	1	< 1	< 1	< 1	< 100	< 100
Trichloroethylene	µg/l	46	24	< 5	< 1	< 10	< 1	< 1	< 1	< 1	< 100	< 100
Toluene	µg/l	959	5	< 1	7		< 1	< 1	1	27	652	437
Vinyl Chloride	µg/l	< 60	< 1	< 3	< 1	< 1	< 1	< 1	< 1	< 1	< 100	< 100
Xylenes	µg/l	277		< 5	< 1	< 1	< 1	< 1	< 1	< 1	267	179

Table E-3.7. Select LCRS and LDS Flow Chemistry Data for Landfills (Continued).

		MSW LANDFILLS IN NORTHEAST U.S.						
Cell No.		Q1		R1			S3	
System		LCRS/LDS	LDS	LCRS/LDS	LCRS/LDS	LDS	LCRS	LDS
Primary Liner\LDS Type			II			II		II
Waste Placement Dates		3/90-date		5/93-date			2/87-10/92	
Liquid Sampling Dates		2/93-2/94	2/93-2/94	5/93-5/94	5/94	5/94	7/91-4/94	10/91-10/93
Parameter	Units							
pH	pH units	7.00					6.30	6.59
Specific conductance	µmhos/cm	3,148	1,455	2,665	3,240	2,830		
TDS	mg/l	1,648	961	2,041	2,450	2,180	1,533	835
COD	mg/l	199	187	3,742	2,910	2,420	1,499	77
BOD_5	mg/l	9	< 3	1,133	1,500	3	572	38
TOC	mg/l			593	880	720	520	61
Alkalinity	mg/l	1,298	841	973	1,240	1,270		
Chloride	mg/l	299	37	181	240	182	118	22
Sulfate	mg/l	7	66	114	62	< 5	27	
Calcium	mg/l	199	199	231	367	347		
Magnesium	mg/l	70	54	55	70	68		
Sodium	mg/l	211	35	147	189	141	99	92
Arsenic	µg/l	11	< 2	10	16	24		
Cadmium	µg/l	< 2	< 2	< 2	< 2	< 2		
Chromium	µg/l	6	< 3	20	35	38		
Lead	µg/l	< 2	2	6	9	6		
Nickel	µg/l	42	< 12	220	366	579		
Benzene	µg/l						14	< 5
1,1-Dichloroethane	µg/l						239	< 16
1,2-Dichloroethane	µg/l						7	< 5
cis-1,2-Dichloroethylene	µg/l							
trans-1,2-Dichloroethylene	µg/l						16	< 5
Ethylbenzene	µg/l						21	6
Methylene chloride	µg/l						90	8
1,1,1-Trichloroethane	µg/l						18	< 6
Trichloroethylene	µg/l						7	< 8
Toluene	µg/l						264	< 5
Vinyl Chloride	µg/l						9	< 10
Xylenes	µg/l							

Table E-3.7. Select LCRS and LDS Flow Chemistry Data for Landfills (Continued).

		MSW LANDFILLS IN NORTHEAST U.S.						
Cell No.		T1-2			U2		Y2	
System		LCRS1	LCRS2	LDS2	LCRS	LDS	LCRS	LDS
Primary Liner\LDS Type				II		II		III
Waste Placement Dates		5/91-date	1/92-date		7/86-1987/88		1990-date	
Liquid Sampling Dates		6/94-3/95	6/94-3/95	9/94-3/95	1/87-3/87	10/86-3/87	4/91-4/94	4/91-4/94
Parameter	Units							
pH	pH units	6.85	7.10	7.20	6.48	6.55	6.60	7.28
Specific conductance	µmhos/cm	13,035	14,060	11,633	5,063	1,406	5,360	1,583
TDS	mg/l				6,510	1,112	4,939	881
COD	mg/l	5,160	6,188		2,565	34	5,265	50
BOD_5	mg/l				2,760	14	2,076	3
TOC	mg/l			1,263			1,436	11
Alkalinity	mg/l	4,985	6,168		2,127	359	2,520	335
Chloride	mg/l	1,163	1,360	1,263	391	63	628	58
Sulfate	mg/l	< 20	< 15	< 11	23	433	108	231
Calcium	mg/l	583	465	520			1,994	179
Magnesium	mg/l							54
Sodium	mg/l	1,058	1,380				433	46
Arsenic	µg/l				21	18	17	4
Cadmium	µg/l						8	< 2
Chromium	µg/l				100		58	11
Lead	µg/l						5	8
Nickel	µg/l				98		185	25
Benzene	µg/l	< 14	< 15	< 25			10	
1,1-Dichloroethane	µg/l	68	< 15	< 25	209	9	45	
1,2-Dichloroethane	µg/l	< 13	< 15	< 25				
cis-1,2-Dichloroethylene	µg/l	< 80	< 13	< 25				
trans-1,2-Dichloroethylene	µg/l	< 13	< 13	< 25				
Ethylbenzene	µg/l	108	< 18	32			118	
Methylene chloride	µg/l	171	< 17	< 25	969	46	121	
1,1,1-Trichloroethane	µg/l	< 13	< 15	< 25		13		
Trichloroethylene	µg/l	< 84	< 15			3	11	
Toluene	µg/l	1,050	283	330	507		720	7
Vinyl Chloride	µg/l	< 27	< 30	< 50				
Xylenes	µg/l	351	< 88	35			69	

Table E-3.7. Select LCRS and LDS Flow Chemistry Data for Landfills (Continued).

		MSW LANDFILLS IN NORTHEAST U.S.						
Cell No.		AA1-3				AE1	AG1	
System		LCRS1	LDS1	LCRS2-3	LDS2-3	LCRS/LDS	LCRS	LDS
Primary Liner\LDS Type			III		III			III
Waste Placement Dates		10/90-1992		7/90-date		4/88-date	4/92-date	
Liquid Sampling Dates		1994	1994	1994	1994	2/93-12/93	1993	1993
Parameter	Units							
pH	pH units	6.79	6.84	7.20	6.52		7.28	7.35
Specific conductance	µmhos/cm	2,364	1,913	3,405	575		3,098	1,559
TDS	mg/l	8,511	4,588	8,731	1,810		2,510	1,273
COD	mg/l	6,603	939	5,572	114		< 10	32
BOD_5	mg/l	1,778	65	2,534	60	< 2	416	
TOC	mg/l	2,978	648	2,239	20	4	49	31
Alkalinity	mg/l	4,789	3,720	6,810	800		786	181
Chloride	mg/l	1,571	1,039	1,563	70	333	141	18
Sulfate	mg/l	222	77	157	651	1,943	1,376	720
Calcium	mg/l	548	347	374	438			261
Magnesium	mg/l	218	213	163	73		145	72
Sodium	mg/l	415	1,870	1,270	34		23	12
Arsenic	µg/l					< 4	< 2	12
Cadmium	µg/l	1	1	2	< 0.2	< 5	< 2	< 2
Chromium	µg/l					< 10	3	4
Lead	µg/l	10	18	16	< 1	< 3	7	14
Nickel	µg/l					< 37	< 10	< 10
Benzene	µg/l					< 5		
1,1-Dichloroethane	µg/l					< 5		
1,2-Dichloroethane	µg/l					< 5		
cis-1,2-Dichloroethylene	µg/l							
trans-1,2-Dichloroethylene	µg/l							
Ethylbenzene	µg/l					< 5		
Methylene chloride	µg/l					< 5		
1,1,1-Trichloroethane	µg/l					< 5		
Trichloroethylene	µg/l					< 5		
Toluene	µg/l					< 5		
Vinyl Chloride	µg/l					< 10		
Xylenes	µg/l					< 5		

Table E-3.7. Select LCRS and LDS Flow Chemistry Data for Landfills (Continued).

		MSW LANDFILLS IN NORTHEAST U.S.								
Cell No.		AJ1		AK1-2		AL1		AO1-2		
System		LCRS	LDS	LCRS	LDS	LCRS	LDS	LCRS	LDS1	LDS2
Primary Liner\LDS Type			III		IV		IV		IV	IV
Waste Placement Dates		6/94-date		10/93-date		1990-date		1/92-date		
Liquid Sampling Dates		6/94	6/94	12/93-3/95	12/93-3/95	6/91-5/95	12/89-5/95	8/92-6/95	8/92-5/95	8/92-6/95
Parameter	Units									
pH	pH units	6.50	7.30	6.65	7.20	8.09	7.04	7.30	7.17	6.72
Specific conductance	µmhos/cm	597	468	1,592	679	2,707	2,449	6,592	1,132	1,118
TDS	mg/l	480	352			2,892	2,482	2,178	690	722
COD	mg/l	< 10	< 10	1,062	13	860	< 11	618	142	497
BOD_5	mg/l	2	< 1	< 2		1,134	< 2			
TOC	mg/l	407	2	245	4	245	3	414	43	8
Alkalinity	mg/l	384	164	711	331	261	199	1,756	556	558
Chloride	mg/l	5	14	94	4	430	151	862	38	24
Sulfate	mg/l	20	92	45	25	219	1,028	54	44	91
Calcium	mg/l	144	50	387	116	150	465	275	205	196
Magnesium	mg/l	10	10	51	29	98	121	146	66	55
Sodium	mg/l	3	7	64	5	236	38	786	19	8
Arsenic	µg/l	13	10	< 3	< 1	4	< 5	45	7	2
Cadmium	µg/l	< 0.5	1	< 19	< 3	< 11	< 7	< 9	< 1	< 1
Chromium	µg/l	< 50	< 50	< 27	< 2	< 64	< 10	54	< 1	< 1
Lead	µg/l	2	6	< 48	< 5	< 36	< 17	< 32	< 1	< 1
Nickel	µg/l	< 100	< 100	< 50	< 50	57	< 35	108	< 50	< 50
Benzene	µg/l	< 5	< 5	< 5	< 1	< 6	< 2	7	< 1	< 1
1,1-Dichloroethane	µg/l	< 5	< 5	46	< 1	< 8	< 7	15	< 3	< 1
1,2-Dichloroethane	µg/l	< 5	< 5	< 2	< 1	< 6	< 2	< 5	< 1	< 1
cis-1,2-Dichloroethylene	µg/l			< 1	< 1	< 7	< 3	< 6	< 1	< 1
trans-1,2-Dichloroethylene	µg/l			< 1	< 1	< 2	< 2	< 4	< 1	< 1
Ethylbenzene	µg/l	< 5	< 5	< 7	< 1	< 12	< 2	11	< 1	< 1
Methylene chloride	µg/l	< 10	< 10	603	< 5	245	< 77	75	< 5	< 5
1,1,1-Trichloroethane	µg/l	< 5		134	3	< 8	< 4	< 11	< 1	< 1
Trichloroethylene	µg/l			< 1	< 1	< 12	< 2	< 4	< 1	< 1
Toluene	µg/l	< 5	< 5	95	< 1	78	< 7	167	< 86	< 1
Vinyl Chloride	µg/l	< 10	< 10	< 11	< 5	< 11	< 5	< 12	< 7	< 5
Xylenes	µg/l	< 5	< 5	< 30	< 3	< 96	< 5	34	< 3	< 3

Table E-3.7. Select LCRS and LDS Flow Chemistry Data for Landfills (Continued).

		MSW LANDFILLS IN NORTHEAST U.S.								
Cell No.		AR1		AX1-16		AZ1		Unspecified[3]		
System		LCRS	LDS	LCRS	LDS	LCRS	LDS	LCRS/LDS	LCRS/LDS	LDS
Primary Liner\LDS Type			IV		V		VI			III
Waste Placement Dates		3/92-date		7/88-date		12/92-date		5/92-date		
Liquid Sampling Dates		11/92-8/94	11/92-8/94	9/88-12/93	7/88-3/95	9/93-3/95	6/93-3/95	5/92-4/94	4/94	4/94
Parameter	Units									
pH	pH units	6.92	7.00	6.47	6.79	6.14	6.60	7.80	7.52	7.90
Specific conductance	µmhos/cm	5,650	1,368	6,046	2,364	4,810	5,235	2,946	2,500	3,160
TDS	mg/l	3,923	848	3,751		5,200	3,570	1,466	1,328	1,627
COD	mg/l	1,238	22	4,149			154	666	164	145
BOD_5	mg/l	290	5	2,825		2,890		18	35	> 39
TOC	mg/l	333	5	2,016	67	1,009	55	191	40	41
Alkalinity	mg/l	2,075	325	2,828		1,445	1,183	1,106	805	1,640
Chloride	mg/l	1,625	35	493		617	57	319	310	433
Sulfate	mg/l	380	325	104		< 7	1,065	94	280	35
Calcium	mg/l	230	186	602		660	133	197	101	172
Magnesium	mg/l	153	119			106	39	57	43	56
Sodium	mg/l	850	26	366		328	1,102	250	262	348
Arsenic	µg/l	13	< 8	< 18	185	< 12	235	13		
Cadmium	µg/l	< 6	< 7	< 6		< 15	2	< 2	< 2	7
Chromium	µg/l	62	< 10	35		< 37	< 8	10		
Lead	µg/l	< 13	< 9			< 3	8	3	2	4
Nickel	µg/l	< 20	< 100	27		< 132	< 40	40		
Benzene	µg/l	< 100	< 0.5	< 32		< 80	< 2	8		
1,1-Dichloroethane	µg/l	< 100	< 2	73		170	11	< 5		
1,2-Dichloroethane	µg/l	< 100	< 2	< 34		< 80	< 3	< 5		
cis-1,2-Dichloroethylene	µg/l	< 100	< 50	< 53		< 120	< 4	< 5		
trans-1,2-Dichloroethylene	µg/l	< 100	< 2	< 32		< 110	< 4	< 5		
Ethylbenzene	µg/l	< 100	< 2	< 46		< 90	< 3	5		
Methylene chloride	µg/l	< 100	< 2	651		4,150	29	< 5		
1,1,1-Trichloroethane	µg/l	< 100	< 2	< 60		270	< 9	< 5		
Trichloroethylene	µg/l	< 100	< 2	< 29		< 90	< 3	< 5		7
Toluene	µg/l	< 100	< 2	419		275	< 3	9		
Vinyl Chloride	µg/l	< 100	< 4	< 65		< 300	< 8	< 5		
Xylenes	µg/l	< 100	< 4	72		< 170	< 4			

Table E-3.7. Select LCRS and LDS Flow Chemistry Data for Landfills (Continued).

		MSW LANDFILLS IN NORTHEAST U.S.							
Cell No.		Unspecified[1]		Unspecified[1]		Unspecified[1]		Unspecified[1]	
System		LCRS	LDS	LCRS	LDS	LCRS	LDS	LCRS	LDS
Primary Liner\LDS Type			I		IV		VI		III
Waste Placement Dates		3/92-date		3/92-date		6/94-date		4/93-date	
Liquid Sampling Dates		11/92-8/94	11/92-8/94	11/92-8/94	11/92-8/94	1/95	1/95	10/93	10/93
Parameter	Units								
pH	pH units	6.62	7.21		6.85			6.27	
Specific conductance	µmhos/cm	4,290	1,090		302			2,420	2,100
TDS	mg/l	1,200	800	3,100	400	1,310	976	2,300	
COD	mg/l	6,800	56		< 3	49	30	85	< 10
BOD_5	mg/l					< 3	< 3	15	< 4
TOC	mg/l	160	22		3	30	6	24	< 1
Alkalinity	mg/l		505		225	482	783	520	480
Chloride	mg/l	342	19	390	4	206	11	15	38
Sulfate	mg/l	< 34	35	< 34	28	79	146	1,100	1,100
Calcium	mg/l	520	187	470	69	133	222	243	433
Magnesium	mg/l	100	35		23	39	78	35	124
Sodium	mg/l	300	22		17	102	37	19	43
Arsenic	µg/l					< 5	< 5	< 10	< 10
Cadmium	µg/l	1	< 0.2		< 0.2	3	< 2	< 1	< 1
Chromium	µg/l	6	< 1		< 1	49	7	< 25	< 25
Lead	µg/l	36	< 1		< 1	< 3	< 3	< 50	< 50
Nickel	µg/l					< 27	< 27	< 100	115
Benzene	µg/l	19	< 1	17	< 1	< 10	< 10	< 7	< 0.7
1,1-Dichloroethane	µg/l	32	< 1	37	< 1	2	4	18	< 1
1,2-Dichloroethane	µg/l	< 1	< 1	1	< 1	< 10	< 10	< 5	< 0.5
cis-1,2-Dichloroethylene	µg/l	< 3	< 1	8	< 1	< 10	< 10		
trans-1,2-Dichloroethylene	µg/l	< 1	< 1	< 1	< 1	< 10	< 10		< 5
Ethylbenzene	µg/l	17	< 1	28	< 1	< 10	< 10	< 5	< 2
Methylene chloride	µg/l	< 118	< 2	10	< 1	7	6	260	< 5
1,1,1-Trichloroethane	µg/l	< 48	< 1	< 1	< 1	< 10	< 10	27	< 5
Trichloroethylene	µg/l	2	< 1	3	< 1	2	5	< 5	< 1
Toluene	µg/l	375	< 1	740	< 1	< 10	< 10	51	< 2
Vinyl Chloride	µg/l	5	< 1	3	< 1	< 10	< 10	< 10	< 2
Xylenes	µg/l	52	< 3	97	< 3	< 10	< 10	17	

Table E-3.7. Select LCRS and LDS Flow Chemistry Data for Landfills (Continued).

		MSW LANDFILLS IN NORTHEAST U.S.					
Cell No.		Unspecified[1]			Unspecified[1]	Unspecified[1]	Unspecified[1]
System		LCRS/LDS	LCRS	LDS	LCRS/LDS	LCRS/LDS	LCRS/LDS
Primary Liner\LDS Type				III			
Waste Placement Dates		4/88-date			11/92-date	1/85-date	12/92-date
Liquid Sampling Dates		3/92-12/93	12/93	12/93	11/93-2/94	1/85-11/93	1/93-10/93
Parameter	Units						
pH	pH units	7.20	7.08	8.26	6.70	6.73	
Specific conductance	µmhos/cm	3,438		121	2,910	8,388	
TDS	mg/l	2,740	2,005	94		6,858	4,900
COD	mg/l	3,573	5,880	< 2		2,935	4,833
BOD_5	mg/l	1,957	3,340			2,985	> 4,700
TOC	mg/l	947	1,760	24	45	1,962	1,867
Alkalinity	mg/l	1,508	1,580	90	203	2,324	2,567
Chloride	mg/l	199	235	< 1	19	1,237	717
Sulfate	mg/l	95	170	64	750	133	26
Calcium	mg/l	261	397	132	508	331	480
Magnesium	mg/l	115	178	27	62	154	89
Sodium	mg/l	282	487	16	115	875	260
Arsenic	µg/l	9	< 100		< 2	6	7
Cadmium	µg/l	< 1	< 50	< 50	11	< 7	
Chromium	µg/l	< 50	80		32	< 5	
Lead	µg/l	1	< 1	22	1	27	6
Nickel	µg/l	< 50	< 50		202	68	70
Benzene	µg/l				< 10	< 3	
1,1-Dichloroethane	µg/l				54	< 11	84
1,2-Dichloroethane	µg/l				< 10		
cis-1,2-Dichloroethylene	µg/l						
trans-1,2-Dichloroethylene	µg/l						
Ethylbenzene	µg/l				29	< 7	65
Methylene chloride	µg/l				200	< 12	560
1,1,1-Trichloroethane	µg/l				96		
Trichloroethylene	µg/l					< 62	
Toluene	µg/l				290		515
Vinyl Chloride	µg/l				< 10		
Xylenes	µg/l				144	< 20	210

Table E-3.7. Select LCRS and LDS Flow Chemistry Data for Landfills (Continued).

		MSW LANDFILLS IN SOUTHEAST U.S.					MSW LANDFILLS IN WEST U.S.			
Cell No.		C1-6	V1-4	W1-2		AW1-4	AM1-2			
System		LCRS/LDS	LCRS	LCRS/LDS	LDS	LCRS/LDS	LCRS1	LDS1	LCRS2	LDS2
Primary Liner\LDS Type		I	II		III			IV		IV
Waste Placement Dates		5/90-date	12/89-date	5/92-date		5/93-date	10/90-2/91			
Liquid Sampling Dates		4/91-12/94	12/89-11/92	8/92,2/93	8/92	5/93-4/95	4/91-2/95	2/92-12/93	4/91-1/95	2/92-2/95
Parameter	Units									
pH	pH units	6.81	6.51	5.90	5.90	6.40	6.62	6.90	6.60	7.26
Specific conductance	µmhos/cm	5,339	8,983	4,100	340	1,062	2,451	17,250	2,795	17,063
TDS	mg/l	3,302	8,640			893	1,709	14,330	1,413	14,363
COD	mg/l	1,119	804			542	396	184	65	76
BOD_5	mg/l	986	595			361				
TOC	mg/l	401				116	108	116	22	28
Alkalinity	mg/l	2,426				459	1,204	407	867	163
Chloride	mg/l	1,298	2,263			49	183	2,725	332	2,659
Sulfate	mg/l	61	69				18	1,500	9	1,425
Calcium	mg/l	263					376	1,700	319	1,819
Magnesium	mg/l	49				12	95	283	74	299
Sodium	mg/l		333			7	92	1,348	88	1,929
Arsenic	µg/l	7	17	< 10	< 10	< 10	236	< 2	235	< 10
Cadmium	µg/l	< 5		< 5	< 5	< 7	< 20	< 20	< 20	< 10
Chromium	µg/l	< 74	21	< 24	< 10	< 50	< 30	< 30	< 57	< 30
Lead	µg/l	37		< 5	9	< 6	< 2.0		< 7	3
Nickel	µg/l	< 64	27			< 50	< 40	< 40	< 91	< 40
Benzene	µg/l	11		< 25	< 5	< 16	17	< 1	13	< 1
1,1-Dichloroethane	µg/l	< 10		260	150	< 16	172	< 3	136	< 2
1,2-Dichloroethane	µg/l	< 5		< 25	< 5	< 14	6	< 1	< 11	< 1
cis-1,2-Dichloroethylene	µg/l	< 1					324	< 1	547	< 1
trans-1,2-Dichloroethylene	µg/l	< 5				< 1	< 5	< 1	< 8	< 1
Ethylbenzene	µg/l	56		49	< 5	26	57	< 1	29	< 1
Methylene chloride	µg/l	< 123		260	102	43	< 6	3	< 20	< 2
1,1,1-Trichloroethane	µg/l	< 9		35	58	< 19	< 21	< 1	< 16	< 1
Trichloroethylene	µg/l	< 94		< 25	< 5	< 24	3	< 1	< 12	< 1
Toluene	µg/l	< 123		230	20	12	267	< 1	146	< 1
Vinyl Chloride	µg/l	< 7		< 25	< 5	< 18	< 21	< 1	< 11	< 2
Xylenes	µg/l	81		160	< 5	< 33	122	< 1	71	< 2

Table E-3.7. Select LCRS and LDS Flow Chemistry Data for Landfills (Continued).

		MSW ASH LANDFILLS							
Cell No.		M1		P1-2	S2	Y1		AF1	
System		LCRS	LDS	LCRS	LCRS	LCRS	LDS	LCRS	LDS
Primary Liner\LDS Type			I	II			III		III
Waste Placement Dates		9/91-date		1991-date	8/90-date	1/89-date		1/90-date	
Liquid Sampling Dates		4/93-7/94	4/93-7/94	7/91-10/93	7/91-4/94	1/89-4/94	1/89-4/94	7/90-4/95	8/91-4/95
Parameter	Units								
pH	pH units	7.20	8.00	6.76	6.54	7.34	7.34	7.44	7.34
Specific conductance	µmhos/cm	43,383	2,620	17,506		16,709	1,806	10,732	3,108
TDS	mg/l	46,733	2,478	32,638	8,747	10,773	2,628	6,067	672
COD	mg/l				304	355	32	413	14
BOD_5	mg/l				84	61	8	60	8
TOC	mg/l					39	4	109	3
Alkalinity	mg/l					160	8	2,500	740
Chloride	mg/l				10,516	5,848	1,580	2,940	50
Sulfate	mg/l				246	146	148	85	124
Calcium	mg/l					1,332	262	96	154
Magnesium	mg/l						54	113	44
Sodium	mg/l				684	1,994	244	1,460	25
Arsenic	µg/l	5	< 1	< 13		5	< 8	6	< 5
Cadmium	µg/l	< 2	< 2	< 5		< 7	< 6	< 6	< 5
Chromium	µg/l	< 1	1	< 31		< 12	< 8	< 43	< 42
Lead	µg/l	< 6	4	< 29		3	7	24	< 6
Nickel	µg/l					< 40	18	48	< 28
Benzene	µg/l				< 5			< 3	< 3
1,1-Dichloroethane	µg/l				< 33			< 3	< 3
1,2-Dichloroethane	µg/l				< 5			< 3	< 3
cis-1,2-Dichloroethylene	µg/l							< 3	< 3
trans-1,2-Dichloroethylene	µg/l				< 5			< 3	< 3
Ethylbenzene	µg/l				< 7			< 3	< 3
Methylene chloride	µg/l				< 6			< 3	< 3
1,1,1-Trichloroethane	µg/l				< 16			< 3	< 3
Trichloroethylene	µg/l				< 5			< 3	< 3
Toluene	µg/l				< 25			< 3	< 3
Vinyl Chloride	µg/l				< 10			< 3	< 3
Xylenes	µg/l							< 3	< 5

Table E-3.7. Select LCRS and LDS Flow Chemistry Data for Landfills (Continued).

		MSW ASH LANDFILLS			COAL ASH LANDFILLS			
Cell No.		AN1-4	Unspecified[1]		Z1		Unspecified[1]	
System		LCRS/LDS	LCRS	LDS	LCRS	LDS	LCRS1	LCRS2
Primary Liner\LDS Type				III		III		
Waste Placement Dates		6/91-10/94	10/90-date		3/92-date		10/89-date	
Liquid Sampling Dates		3/92-12/93	7/91-10/92	7/91-7/93	3/92-8/93	3/92-8/93	2/93-11/94	2/93-11/94
Parameter	Units							
pH	pH units				7.66	7.85	7.74	7.64
Specific conductance	µmhos/cm				1,144	381	623	2,894
TDS	mg/l	42,000			1,098	495	347	2,563
COD	mg/l	5,607			11	17		
BOD_5	mg/l	15			< 3	6		
TOC	mg/l	40			6	5		
Alkalinity	mg/l	99	5,010	2,130	160	171	220	224
Chloride	mg/l	22,400			21	10		
Sulfate	mg/l	496	3,430	1,380	587	195	178	1,837
Calcium	mg/l	1,271			190	89		
Magnesium	mg/l	420			30	22	15	133
Sodium	mg/l	888	880	105	46	11		
Arsenic	µg/l	< 10	17	< 20	< 9	< 10	62	8
Cadmium	µg/l	49	< 5	< 5	< 9	< 9	< 5	< 10
Chromium	µg/l	< 10	84	14	22	< 11	< 9	< 20
Lead	µg/l	74	3	< 9	< 34	< 3	< 4	< 5
Nickel	µg/l	46	< 24	< 20	38	< 40		
Benzene	µg/l	< 0.5			< 4			
1,1-Dichloroethane	µg/l	< 0.5			< 4			
1,2-Dichloroethane	µg/l	< 0.5			< 4			
cis-1,2-Dichloroethylene	µg/l	< 0.5						
trans-1,2-Dichloroethylene	µg/l	< 0.5			< 1			
Ethylbenzene	µg/l	< 2			< 3			
Methylene chloride	µg/l	< 0.5			< 4			
1,1,1-Trichloroethane	µg/l	< 0.5			< 4			
Trichloroethylene	µg/l	< 0.5			< 4			
Toluene	µg/l	< 0.8			< 2			
Vinyl Chloride	µg/l	< 0.5			< 7			
Xylenes	µg/l	< 0.5			< 4			

Table E-3.7. Select LCRS and LDS Flow Chemistry Data for Landfills (Continued).

		C&DW LANDFILLS					
Cell No.		A1		AI1-2			
System		LCRS	LDS	LCRS1	LDS1	LCRS2	LDS2
Primary Liner\LDS Type			I		III		III
Waste Placement Dates		10/92-date		9/89-date			
Liquid Sampling Dates		3/93-12/93	9/93-12/93	9/91-5/94	9/91-5/94	9/91-5/94	9/91-5/94
Parameter	Units						
pH	pH units			6.58	6.40	6.28	6.20
Specific conductance	µmhos/cm			5,275	800	4,355	830
TDS	mg/l	2,880	216	4,125	803	4,325	515
COD	mg/l	1,139	37	3,293	< 65	4,083	123
BOD_5	mg/l		269	845	4	1,407	20
TOC	mg/l	443	30	1,055	8	1,415	21
Alkalinity	mg/l			2,300	238	2,600	536
Chloride	mg/l	690	40	655	42	687	36
Sulfate	mg/l	463	33	35	113	61	64
Calcium	mg/l	203	36	335	32	428	34
Magnesium	mg/l	202	13				
Sodium	mg/l	324	20	333	104	235	78
Arsenic	µg/l			13	< 2	16	< 2
Cadmium	µg/l	< 5	< 5	< 1	< 1	< 1	< 1
Chromium	µg/l		< 4	37	< 11	40	< 17
Lead	µg/l	< 10	< 10	3	3	3	5
Nickel	µg/l		< 14	< 100	< 100	< 12	< 100
Benzene	µg/l			18	< 1	17	4
1,1-Dichloroethane	µg/l			92	42	108	66
1,2-Dichloroethane	µg/l			2	< 1	3	< 1
cis-1,2-Dichloroethylene	µg/l						
trans-1,2-Dichloroethylene	µg/l						
Ethylbenzene	µg/l			75	< 17	57	32
Methylene chloride	µg/l			382	36	452	252
1,1,1-Trichloroethane	µg/l			44	24	58	39
Trichloroethylene	µg/l			10	< 1	< 11	< 1
Toluene	µg/l			561	9	665	26
Vinyl Chloride	µg/l			11	< 1	6	3
Xylenes	µg/l			251	231	168	480

Table E-3.7. Select LCRS and LDS Flow Chemistry Data for Landfills (Continued).

		HW LANDFILLS			
Cell No.		AQ1&10			
System		LCRS1	LDS1	LCRS10	LDS10
Primary Liner\LDS Type			IV		IV
Waste Placement Dates		3/86-early 1990		late 88-mid 1991	
Liquid Sampling Dates		2/91-11/93	2/91-11/93	2/91-11/93	2/91-11/93
Parameter	Units				
pH	pH units	7.90	7.36	7.20	7.51
Specific conductance	µmhos/cm	23,200	2,582	5,574	4,154
TDS	mg/l				
COD	mg/l				
BOD_5	mg/l				
TOC	mg/l				
Alkalinity	mg/l				
Chloride	mg/l				
Sulfate	mg/l				
Calcium	mg/l				
Magnesium	mg/l				
Sodium	mg/l				
Arsenic	µg/l	189	< 10		< 11
Cadmium	µg/l	< 5	< 5		< 5
Chromium	µg/l	22	12		50
Lead	µg/l	24	31		< 17
Nickel	µg/l	1,190	< 40		84
Benzene	µg/l	< 8	< 4	< 6	< 4
1,1-Dichloroethane	µg/l	14	< 5	135	< 5
1,2-Dichloroethane	µg/l	< 5	< 3	4	< 3
cis-1,2-Dichloroethylene	µg/l				
trans-1,2-Dichloroethylene	µg/l	18	< 2	< 10	< 2
Ethylbenzene	µg/l	< 5	< 5	< 5	< 5
Methylene chloride	µg/l	5	6	< 3	< 3
1,1,1-Trichloroethane	µg/l	9	< 8	36	< 4
Trichloroethylene	µg/l	60	19	5	< 2
Toluene	µg/l	< 5	7	< 13	< 5
Vinyl Chloride	µg/l	13	< 10	< 7	< 10
Xylenes	µg/l				

Table E-3.7. Select LCRS and LDS Flow Chemistry Data for Landfills (Continued).

		HW LANDFILLS							
Cell No.		L1		AD1&7				AS1	
System		LCRS	LDS	LCRS1	LDS1	LCRS7	LDS7	LCRS	LDS
Primary Liner\LDS Type		base III sides I			III		IV		IV
Waste Placement Dates		6/90-date		5/85-late 1989		9/87-9/88, 5/93-6/93		7/89-10/91	
Liquid Sampling Dates		1/91-1/95	1/91	6/85-12/94	6/85-12/94	9/87-12/94	9/87-12/94	12/89-2/95	12/89-3/95
Parameter	Units								
pH	pH units	7.60	7.70	8.72	7.40	9.99	7.45		
Specific conductance	µmhos/cm	12,302	3,477	40,159	1,755	39,036	2,512		
TDS	mg/l								
COD	mg/l								37
BOD_5	mg/l								
TOC	mg/l	7	5	2,006	8	4,471	7		
Alkalinity	mg/l								
Chloride	mg/l	3,783	490	12,709	207	10,759	301		
Sulfate	mg/l	704	1,071	4,428	404	6,105	6,105		
Calcium	mg/l								
Magnesium	mg/l								
Sodium	mg/l	2,514	353	10,394	177	5,549	250		
Arsenic	µg/l	30		125,252	< 13	34,572	< 14		
Cadmium	µg/l			< 410	< 4	< 56	< 3		
Chromium	µg/l			294	29	158	< 12		
Lead	µg/l	55		192	< 29	< 306	< 16		
Nickel	µg/l	285							
Benzene	µg/l			< 184	< 4	555	< 4	18	< 5
1,1-Dichloroethane	µg/l	14		< 138	< 5	< 604	< 6	32	< 5
1,2-Dichloroethane	µg/l			< 67	< 3	< 2,181	< 3	< 17	< 5
cis-1,2-Dichloroethylene	µg/l								
trans-1,2-Dichloroethylene	µg/l			< 48	< 2	< 238	< 3		
Ethylbenzene	µg/l	8		174	< 6	< 850	< 6	< 8	< 5
Methylene chloride	µg/l	32	7	< 292	< 4	< 602	< 3	254	4
1,1,1-Trichloroethane	µg/l	8		< 228	< 4	< 466	< 3	< 20	< 5
Trichloroethylene	µg/l			< 53	< 2	< 240	< 25	< 50	< 5
Toluene	µg/l	12		< 189	< 5	1,042	< 5	< 56	< 5
Vinyl Chloride	µg/l			1,371	< 9	< 7,438	< 9	< 10	< 10
Xylenes	µg/l	9						18	< 5

Notes: (1) " " = not analyzed; ND = all measurements reported as non-detect; < = more than 50% of measurements reported as non-detec

(2) Concentrations are arithmetic averages. Parameters reported as non-detect were taken as one-half the detection limit in calculating the avera

(3) Unspecified landfills were not given a code name due to too few flow rate data to analyze.

Table E-3.8(a). Distribution of LCRS/LDS Flow Rate Data by Waste Type and Geographic Region.

	Geographic Region		
Waste Type	NE	SE	W
MSW	24 landfills 71 cells	8 landfills 26 cells	1 landfill 2 cells
HW	5 landfills 26 cells	5 landfills 31 cells	3 landfills 10 cells
MSW Ash	5 landfills 12 cells	2 landfills 4 cells	-
Coal Ash	1 landfill 1 cell	-	-
C&DW	2 landfills 4 cells	-	-

Table E-3.8(b). Distribution of LCRS/LDS Flow Rate Data by Primary Liner and LDS Types.

	LDS Type	
Primary Liner Type	Sand or Gravel	GN
GM	13 landfills 41 cells	11 landfills 28 cells
GM/GCL Composite	3 landfills 19 cells	4 landfills 9 cells
GM/CCL or GM/GCL/CCL Composite	13 landfills 31 cells	16 landfills 57 cells

Table E-3.8(c). Distribution of LCRS Chemistry Data by Waste Type and Start of Operation Date.

Waste Type	Pre-1990 Start of Operation	Post-1990 Start of Operation
MSW	11 landfills 13 cells	25 landfills 28 cells
HW	3 landfills 5 cells	1 landfill 1 cell
MSW Ash	1 landfill 1 cell	6 landfills 6 cells
Coal Ash	1 landfill 1 cell	1 landfill 1 cell
CADW	1 landfill 2 cells	1 landfill 1 cell

From Table E-3.8(b), most of the cells at most of the landfills have either a GM primary liner (37% of all cells) or a GM/CCL or GM/GCL/CCL primary liner (48%). Fewer cells (15%) have a GM/GCL primary liner. About 48% of the cells have a sand or gravel LDS and 52% have a GN LDS. Based on the distribution of the data, the database appears to be representative of typical double-liner system designs in landfills.

Most of the liquids management data are for open cells; only about 23% of the cells in the database had received a final cover system.

E-3.3 LCRS and LDS Flow Rate Data

All of the landfill cells in the database were operated with a strategy of active liquid removal from both the LCRS and LDS. By federal regulation, MSW, MSW ash, and HW landfills must generally limit the hydraulic head buildup in the LCRS to less than 0.3 m. This is accomplished through design of the LCRS drainage layer with adequate slope and hydraulic conductivity, adequate collection pipe or swale spacing, and regular liquid removal from the LCRS sump. LCRS and LDS flow rate data were reported on either a daily, weekly, or periodic basis, depending on facility. Using this source data, average daily flow rates were calculated for both systems on a monthly basis by dividing the total amount of liquid extracted from the systems during a month by the number of days in the month and the landfill cell areas. The volumes of flow used in the calculations were obtained from landfill operations records, with flow measurements most often obtained using accumulating mechanical flow meters. The reported flow rates should be considered approximate.

Peak and average monthly LCRS and LDS flow rate data are summarized in Tables E-3.5 and E-3.6, respectively. The data are separated into the three operational stages described in Sections E-1.3.7 and E-1.3.8. Both LCRS and LDS flow rate data are available for 170 of the 187 cells. The data set is not complete for the remaining 17 cells: 16 cells do not have available LCRS flow rate data, and one cell does not have available LDS flow rate data.

E-3.4 Landfill Chemistry Data

Leachate chemistry data are available for 59 cells at 50 landfills: 48 cells at 39 landfills from the previously described database (including two cells from one landfill with different waste types) and eleven cells from eleven "unspecified" landfills with too little flow rate data to be given a landfill designation in the database (note that these "undesignated" landfills are in addition to the 54 "designated" landfills in the database). For the purposes of the leachate chemistry evaluation conducted in Section 6 of this appendix, the data are grouped as shown in Table E-3.8(c).

The MSW leachate chemistry data are available for 36 landfills located in all geographic regions of the U.S. This leachate chemistry data are believed to be representative of modern MSW landfills in the U.S. operated without leachate recirculation or other

special activities (e.g., special waste disposal, induced aerobic degradation). While the leachate chemistry data from modern MSW landfills are extensive, they should not be considered to reflect the full range of leachate chemistry associated with the anaerobic decomposition process, from the acid stage to the methane fermentation stage. Moreover, differences will exist from facility to facility based on a variety of climate, site, waste, and operational factors. Additional data are needed from more facilities over a longer time period to better identify the potential range of leachate chemistry characteristics throughout the initial, active, and post-closure operational periods of a facility.

Fewer leachate chemistry data are available for HW and ISW landfills. In addition, the types of wastes placed in HW and ISW landfills are generally more variable between landfills than wastes placed in MSW landfills. With the exception of the leachate chemistry data for MSW ash landfills, it is likely that the data presented in this appendix do not fully characterize the variation in leachate chemistry for HW and ISW landfills. The chemistry data for MSW ash landfill leachate may be representative of modern MSW ash landfills in the U.S. because seven landfills are included in the database and the chemistry of MSW ash is less variable than HW.

Select data from the leachate chemistry database are presented in Table E-3.7. The table summarizes average values for 30 representative chemical parameters: water quality indicator parameters (e.g., pH, specific conductance, TDS, etc.); major inorganic cations and anions (e.g., calcium, chloride, sulfate, etc.); trace metals (e.g., arsenic, chromium, lead, etc.); and VOCs (e.g., benzene, methylene chloride, trichloroethylene, etc.). The specific trace metals and VOCs were chosen for study because these metals and VOCs are sometimes found in leachates from MSW, HW, and ISW landfills. They were also selected based on availability of parameters between landfills, frequency of detection, and concentration. It is recognized that the leachate chemistry database is limited in terms of completeness and duration of monitoring. In addition, key MSW and HW leachate constituents, such as alcohols and ketones, are poorly represented in the database, and, thus, could not be included in the list of select parameters. It is important that these additional data be collected so that our understanding of leachate chemistry can continue to improve. For example, from the literature review in Section 2.3, ketones are found in high concentrations in MSW and HW leachates. However, the majority of leachate samples in the database were not analyzed for ketones. Because of this, there is little benefit in including ketones in the study. The chemical data presented herein are intended to be representative, not comprehensive. The data should not be considered complete for purposes of evaluating potential human health or ecological impacts.

For all landfills in this study, the chemical data were reportedly obtained using sampling and analysis procedures in accordance with EPA protocols (i.e., SW-846 (EPA, 1987b)). EPA protocols contain quality control (QC) standards for both sampling and analysis, including the use of method blanks, matrix spikes, and duplicates. These protocols will provide accurate analytical data for samples obtained from the LCRS and LDS sumps.

However, the potential for VOC volatilization from the sump liquids prior to sampling has not been evaluated. Some of the chemical data reports obtained for the landfills only contained a list of detected chemicals. It was not known for which chemicals the samples were analyzed.

The parameter values given in Table E-3.7 are arithmetic averages of the data for a given sampling point. The arithmetic mean, rather than the geometric mean, was used because more of the data in the literature are based on the arithmetic mean and statistical tests indicated that neither mean was more appropriate. In calculating the average value for each parameter, one-half of the given detection limit was conservatively used for all results reported as non-detect. If more than one-half of the measurements for a parameter were reported as non-detect, the calculated average value given in Table E-3.7 is proceeded by a “<“ symbol. If all of the measurements were reported as non-detect, "ND" is given for the parameter value. As with the flow rate data, the chemical constituent data were obtained from landfill operations records.

E-4 Leakage Rates Through Primary Liners

E-4.1 Overview

The performance of primary liners at double-lined landfills is first assessed in this Subsection in terms of primary liner leakage using the methodology of Gross et al. (1990) described in Section E-2.1.1. Briefly, this method requires the comparison of LDS and LCRS flow rate data to quantify that portion of LDS flow attributable to primary liner leakage as opposed to other sources. The relative performances of the different types of primary liners are then evaluated using the “apparent” liner hydraulic efficiency, E_a, introduced by Bonaparte et al. (1996). If the only source of flow into the LDS is primary liner leakage, then the "apparent" liner hydraulic efficiency is the "true" liner hydraulic efficiency, E_t. The true efficiency of a liner is not constant but rather a function of the hydraulic head in the LCRS and size of the area over which LCRS flow is occurring (the area is larger at high flow rates compared to low flow rates). The true efficiency of a liner is also a function of design: identical liners overlain by different LCRSs or placed on different slopes will exhibit different E_t values. Also, the efficiency of a liner for a given set of hydraulic conditions could change over time if the physical condition of the liner changes. For example, long-term time dependent changes in GMs could result from chemical degradation or brittle stress cracking under certain conditions. Time dependent changes in CCLs or GCLs can result from chemical degradation, consolidation, or other factors. Notwithstanding all of these limitations, the hydraulic efficiency concept is useful in characterizing liner hydraulic performance.

The methodology described above was used to evaluate the hydraulic performance of GM primary liners and GM/GCL composite primary liners. Chemical constituent data were not utilized in the evaluation of these types of liners because the initial hydraulic assessment (i.e., comparing LCRS and LDS flow rates) yielded significant insight into these liners’ true hydraulic efficiencies. However, the situation was found to be more

complicated for GM/CCL and GM/GCL/CCL composite primary liners due the generation of consolidation water by these liners not only during the initial period of operation, but also during the active and post-closure periods. The performance evaluation of these liners included the additional step of comparing the concentrations of select chemical constituents in LDS liquids to concentrations of the same constituents in LCRS liquids. In particular, general water quality characteristics (i.e., major ion, COD, BOD, and TOC concentrations) of the LCRS and LDS liquids were compared to assess whether the liquids had different primary sources (e.g., leachate for LCRS liquids and CCL pore water for LDS liquids). The concentrations of five key chemical constituents (i.e., the inorganic anions sulfate and chloride and the aromatic hydrocarbons benzene, toluene, and xylene) in the LCRS and LDS flows were compared in more detail to further assess whether primary liner leakage had contributed to LDS flows.

It is noted that the presence of chemical constituents in the LDS was evaluated empirically. Therefore, the concentrations of chemicals collected in the LDS were directly compared to concentrations of the same chemicals collected in the LCRS. No fate and transport analysis was performed that accounts for attenuation of the LCRS chemicals migrating through the primary liner CCL. However, to overcome the need to perform such an analysis, the five key chemical constituents evaluated were selected based on their high solubility in water, low octanol-water coefficient, high resistance to hydrolization, and high resistance to anaerobic biodegradation in soil.

E-4.2 Leakage Rates Through GM Primary Liners

E-4.2.1 Description of Data

The performance of 31 of the 69 cells with GM primary liners are assessed in this section. The remaining 38 cells with GM primary liners were excluded from the assessment primarily because they do not have continuous LCRS and LDS flow rate data available for an individual cell from the start of operation and for a significant monitoring period. Cell D2 was excluded because near liquid wastes was disposed in the cell at different times during active filling of the cell. Flow rate data are available for the considered 31 cells at 14 landfills with monitoring periods of up to 114 months. Data from 17 of the 31 cells in this study were included in the previous EPA study by Bonaparte and Gross (1993); however, this study contains additional data for most of these cells. Descriptions of the liner systems installed at these landfills are presented in Table E-4.1. Twenty-five cells have a 1.5- or 2-mm thick HDPE GM primary liner, and the remaining six cells have a 0.9-mm thick chlorosulfonated polyethylene (CSPE) GM primary liner. The LDS consists of a sand layer, a GN, or both. The secondary liner of the double-liner system is a single GM or a GM/CCL composite liner. Formal CQA programs were used in the construction of the liner system for 23 cells, while eight cells were constructed without formal CQA. It is noted that the six cells with CSPE GM primary liners were all constructed without CQA, while only two of the 25 cells with HDPE GM primary liners were constructed without CQA. After the end of their active operation stages, six cells at three landfills received final cover systems with GM or

Table E-4.1. Description of Liner System Components for Considered Landfill Cells with GM Primary Liners.

Cell No.	Type[1] of Waste	LCRS		GM[4] Primary Liner	LDS		Secondary Liner			3rd Party CQA Program (Yes/No?)
		Material[2]	Thickness[3] (mm)	Type (and Thickness (mm))	Material[2]	Thickness (mm)	Geomembrane Type (and Thickness (mm))	Lower Component Material[5]	Lower Component Thickness (mm)	
B1-2	MSW	S	450	CSPE(0.9)	S	450	PVC(0.8)	NA[6]	NA	No
C1-5	MSW	S	600	HDPE(2.0)	S	450	HDPE(2.0)	CCL	300	Yes
D1,3,&4	HW	S	300	HDPE(2.0)	S	300	HDPE(1.0)	CCL	900	Yes
E1-4	MSW	S	600	CSPE(0.9)	S	600	PVC(0.8)	CCL	600	No
F1	MSW	S	600	HDPE(1.5)	S	300	HDPE(1.5)	NA	NA	No
G1-2	MSW	S	600	HDPE(1.5)	S	300	HDPE(1.5)	CCL	600	Yes
I1-3	MSW	S	600	HDPE(1.5)	S	450	HDPE(1.5)	CCL	300	Yes
K1	MSW	S	600	HDPE(2.0)	S/GN	300/5	LLDPE(1.5)	CCL	600	No
N2	MSW	S	600	HDPE(1.5)	GN	5	HDPE(1.5)	CCL	300	Yes
O1-2	MSW	G/S	300/300	HDPE(2.0)	S/GN	300/5	HDPE(1.0)	CCL	150	Yes
S1	MSW	S/GN	600/5	HDPE(2.0)	GN	5	HDPE(2.0)	CCL	600	Yes
S2	ASH	S/GN	600/5	HDPE(2.0)	GN	5	HDPE(2.0)	CCL	600	Yes
V1-2	MSW	S/GN	600/5	HDPE(1.5)	S/GN	300/5	HDPE(1.5)	CCL	150	Yes
W1-2	MSW	S/GN	600/5	HDPE(1.5)	GN	5	HDPE(1.5)	CCL	150	Yes
X1	MSW	S	600	HDPE(1.5)	GN	5	HDPE(1.5)	CCL	150	Yes

Notes: (1) Waste types: MSW = municipal solid waste; HW = hazardous waste; ASH = MSW ash.

(2) LCRS and LDS material types: GN = geonet or geocomposite; S =sand; G = gravel.

(3) All material thicknesses are nominal values.

(4) GM Types: HDPE = high density polyethylene; CSPE = chlorosulfonated polyethylene; PVC = polyvinyl chloride. LLDPE = linear low density polyethylene.

(5) liner lower component material types: CCL = compacted clay liner.

(6) NA = not applicable

GM/CCL barriers. Table E-4.2 contains a summary of the LCRS and LDS flow rate database for the cells with GM primary liners.

E-4.2.2 Analysis of Data

E-4.2.2.1 Interpretation of Data

The interpretation of LDS flow rate data for cells with GM primary liners is relatively straightforward because consolidation water is not a source of LDS flow and, for the facilities included in this study, ground-water infiltration is not occurring. Thus, the only potential sources of LDS flow are construction water, compression water, and primary liner leakage. For cells with GN LDSs, LDS flow should be primarily due to primary liner leakage. For cells with sand LDSs, construction and compression water may be significant sources of LDS flow for a time period of up to one year after cell construction (Gross et al., 1990). Because of this, cells with sand LDSs generally remain in the initial period of operation longer than cells with GN LDSs.

E-4.2.2.2 Summary of Flow Rate Data

LCRS and LDS flow rate data for the 31 cells with GM primary liners are presented in Table E-4.2. Average and peak monthly flow rates are reported for the three landfill operational time periods defined previously. For cells with long periods of active operation and post-closure, data are summarized in approximately twelve-month increments to facilitate the evaluation of temporal changes in flow rate.

From Table E-4.2, average monthly LCRS flow rates ranged from about 1,500 to 43,700 lphd during the initial period of operation, from about 100 to 16,200 lphd during the active period of operation, and from about 320 to 1,300 lphd after closure. Average LDS flow rates for a cell ranged from about 5 to 2,100 lphd during the initial period of operation, 1 to 1,600 lphd during the active period of operation, and 2 to 330 lphd after closure. A review of the data in Table E-4.2 indicates that peak monthly LCRS and LDS flow rates are typically two to four times the average monthly values for individual monitoring periods. This difference becomes larger in the LDS when the flow rates become very low: this is mostly an artifact of the LDS pumping schedule, which becomes infrequent when the flow rate becomes very low. Table E-4.2 shows that between the initial and active periods of operation, LCRS flow rates typically decreased up to about one order of magnitude and LDS flow rates decreased up to about one to two orders of magnitude. LCRS and LDS flow rates continued to decrease after cell closure: for the six cells that were closed, flow rates after closure decreased by up to one order of magnitude compared to flow rates prior to closure.

E-4.2.2.3 Effects of LDS Material and CQA on LDS Flow Rates

Table E-4.3 and Figure E-4.1 present summaries of average LDS flow rates for the 31 cells with GM primary liners during each of the three landfill operational stages. Table E-4.3 has been subdivided to separately report LDS flow rates based on two criteria:

Table E-4.2. Summary of LCRS and LDS Flow Rate Data for Considered Landfill Cells with GM Primary Liners.

Cell No.	Cell Area	Start of Waste Placem.	Final Closure	Initial Period of Operation[1]						Active Period of Operation[2]						Post-Closure Period[3]					
				Time Period	LCRS Flow[4]		LDS Flow		E_a	Time Period	LCRS Flow		LDS Flow		E_a	Time Period	LCRS Flow		LDS Flow		E_a
					Avg.	Peak	Avg.	Peak			Avg.	Peak	Avg.	Peak			Avg.	Peak	Avg.	Peak	
	(ha)	(month-year)	(month-year)	(months)	(lphd)	(lphd)	(lphd)	(lphd)	(%)	(months)	(lphd)	(lphd)	(lphd)	(lphd)	(%)	(months)	(lphd)	(lphd)	(lphd)	(lphd)	(%)
B1	3.3	5-84	11-88	1-19	ND[5]	ND	ND	ND		20-31	2,245	5,754	266	499	88.14	55-66	317	670	106	222	66.48
										32-43	5,223	6,845	424	808	91.87	67-78	703	1,877	267	1,134	62.02
										44-54	3,975	7,464	892	1,426	77.55	79-90	1,146	1,956	279	451	75.64
																91-102	1,306	1,943	326	612	75.01
																103-114	510	718	74	97	85.41
B2	3.5	5-84	11-88	1-19	ND	ND	ND	ND		20-31	2,732	5,393	404	605	85.20	55-66	493	1,040	154	393	68.83
										32-43	3,740	5,707	996	1,690	73.36	67-78	337	654	328	514	2.80
										44-54	2,337	3,982	665	1,102	71.54						
C1	3.2	5-90	NA[5]	1-9	ND	ND	ND	ND		10-21	789	1,419	123	304	84.40	NA	NA	NA	NA	NA	
										22-33	259	780	89	170	65.52						
										34-45	159	286	27	128	83.08						
										46-56	103	200	40	227	61.27						
C2	3.7	4-91	NA	1-12	1,475	2,585	92	398	93.74	13-24	435	859	9	31	98.03	NA	NA	NA	NA	NA	
										25-36	300	610	22	125	92.71						
										37-45	161	464	7	14	95.40						
C3	3.6	8-91	NA	1-8	3,417	9,558	63	268	98.16	9-20	311	671	2	9	99.49	NA	NA	NA	NA	NA	
										21-32	314	752	33	276	89.56						
										33-41	268	987	16	103	94.02						
C4	3.7	2-92	NA	1-4	14,828	41,331	178	265	98.80	5-16	937	2,055	70	147	92.52	NA	NA	NA	NA	NA	
										17-28	438	622	51	92	88.39						
										29-35	407	686	26	29	93.71						
C5	2.6	11-92	NA	1-12	6,419	12,528	23	40	99.64	13-26	2,513	10,440	28	115	98.88	NA	NA	NA	NA	NA	
D1	0.4	10-85	5-86	1-7	ND	ND	32	80		NA	NA	NA	NA	NA		8-19	ND	ND	102	886	
																20-26	ND	ND	1	10	
																27-38	376	1,455	5	70	98.58
																39-50	715	1,352	64	156	91.05
D3	0.3	7-87	NA	1-12	20,292	51,265	12	56	99.94	13-24	13,003	44,895	7	73	99.95	NA	NA	NA	NA	NA	
										25-28	1,010	2,413	283	341	71.97						
D4	0.4	1-89	NA	1-11	31,281	120,527	233	801	99.25	NA	NA	NA	NA	NA		NA	NA	NA	NA	NA	
E1	2.4	3-88	NA	1-7	ND	ND	2,144	5,026		8-19	8,432	19,614	1,436	3,069	82.97	NA	NA	NA	NA	NA	
										20-31	11,521	36,164	1,051	1,915	90.88						
										32-40	6,525	13,075	743	1,015	88.61						

Table E-4.2. Summary of LCRS and LDS Flow Rate Data for Considered Landfill Cells with GM Primary Liners (Continued).

Cell No.	Cell Area	Start of Waste Placem. (month-year)	Final Closure (month-year)	Initial Period of Operation[1]						Active Period of Operation[2]						Post-Closure Period[3]					
				Time Period	LCRS Flow[4]		LDS Flow		E_a	Time Period	LCRS Flow		LDS Flow		E_a	Time Period	LCRS Flow		LDS Flow		E_a
					Avg.	Peak	Avg.	Peak			Avg.	Peak	Avg.	Peak			Avg.	Peak	Avg.	Peak	
	(ha)			(months)	(lphd)	(lphd)	(lphd)	(lphd)	(%)	(months)	(lphd)	(lphd)	(lphd)	(lphd)	(%)	(months)	(lphd)	(lphd)	(lphd)	(lphd)	(%)
E2	2.4	10-87	NA	1-12	ND	ND	483	3,518		13-24	5,821	10,445	802	2,447	86.22	NA	NA	NA	NA	NA	
										25-36	4,547	11,014	685	1,404	84.93						
										37-45	4,434	6,830	596	999	86.56						
E3	1.2	5-90	NA	1-12	9,425	25,394	1,595	1,951	83.08	13-14	6,062	9,038	1,603	1,758	73.56	NA	NA	NA	NA	NA	
E4	1.2	7-90	NA	1-12	20,148	55,785	996	2,362	95.06	NA	NA	NA	NA	NA		NA	NA	NA	NA	NA	
F1	1.8	7-92	NA	1-12	14,472	45,010	124	479	99.14	13-24	9,000	25,450	66	83	99.27	NA	NA	NA	NA	NA	
										25-30	7,826	10,932	67	77	99.15						
G1	3.0	6-89	NA	1-12	22,371	46,120	ND	ND		13-24	12,893	23,485	ND	ND		NA	NA	NA	NA	NA	
										25-36	3,438	11,652	156	238	95.47						
										37-42	8,356	10,303	101	116	98.79						
										43-51	ND	ND	121	384							
										52-63	ND	ND	74	139							
										64-67	ND	ND	49	64							
G2	1.6	6-89	NA	1-12	22,371	46,120	197	645	99.12	13-24	12,893	23,485	37	65	99.71	NA	NA	NA	NA	NA	
										25-36	3,438	11,652	35	42	98.98						
										37-42	8,356	10,303	60	100	99.28						
I1[6]	3.2/2.7[7]	8-87	10-94	1-5	ND	ND	234	508		9-15	16,224	48,932	5	18	99.97	85-93	800	1,794	62	119	92.25
				6-8	ND	ND	ND	ND		16-32	ND	ND	ND	ND							
										33-44	7,167	22,020	10	44	99.86						
										45-48	231	332	4	10	98.49						
										49-54	ND	ND	ND	ND							
										55-66	624	1,580	2	5	99.68						
										67-78	541	752	13	42	97.60						
										79-84	904	1,827	79	157	91.26						
I2[6]	4.2/2.3[7]	10-87	10-94	1-7	6,627	13,959	31	77	99.53	8-24	ND	ND	ND	ND		77-85	800	1,794	2	4	99.71
										25-36	1,030	3,241	5	35	99.52						
										37-40	427	1,054	6	11	98.67						
										41-46	ND	ND	ND	ND							
										47-58	624	1,580	8	37	98.67						
										59-70	541	752	8	23	98.54						
										71-76	904	1,827	5	6	99.49						

Table E-4.2. Summary of LCRS and LDS Flow Rate Data for Considered Landfill Cells with GM Primary Liners (Continued).

Cell No.	Cell Area	Start of Waste Placem. (month-year)	Final Closure (month-year)	Initial Period of Operation[1]						Active Period of Operation[2]						Post-Closure Period[3]					
				Time Period	LCRS Flow[4]		LDS Flow		E_a	Time Period	LCRS Flow		LDS Flow		E_a	Time Period	LCRS Flow		LDS Flow		E_a
					Avg.	Peak	Avg.	Peak			Avg.	Peak	Avg.	Peak			Avg.	Peak	Avg.	Peak	
	(ha)			(months)	(lphd)	(lphd)	(lphd)	(lphd)	(%)	(months)	(lphd)	(lphd)	(lphd)	(lphd)	(%)	(months)	(lphd)	(lphd)	(lphd)	(lphd)	(%)
I3[6]	3.4/1.8[7]	4-88	10-94	1-7	11,559	21,081	37	87	99.68	8-24	ND	ND	ND	ND		77-85	800	1,794	3	12	99.57
										25-36	11,684	26,339	7	23	99.94						
										37-40	2,464	4,666	5	8	99.80						
										41-46	ND	ND	ND	ND							
										47-58	624	1,580	4	17	99.39						
										59-70	541	752	13	55	97.64						
										71-76	904	1,827	17	53	98.14						
K1	2.7	12-89	NA	1-12	17,808	24,832	122	163	99.31	13-24	12,929	27,663	88	180	99.32	NA	NA	NA	NA	NA	
										25-36	10,879	17,683	76	104	99.30						
										37-48	6,155	11,331	514	892	91.64						
										49-60	5,952	8,024	349	495	94.14						
										61-66	9,494	12,245	282	378	97.03						
N2	6.3	1-92	NA	1-12	ND	ND	ND	ND		13-19	4,547	5,741	113	468	97.52	NA	NA	NA	NA	NA	
										20-31	2,561	3,460	203	669	92.08						
										32-34	6,399	7,274	786	1,058	87.72						
										35-39	2,741	3,170	201	406	92.65						
O1[8]	4.2	9-88	NA	1-6	ND	ND	293	620		7-18	4,407	9,826	0	3	99.99	NA	NA	NA	NA	NA	
										19-30	4,023	13,231	3	7	99.93						
										31-42	7,089	16,467	0	5	99.99						
										43-54	6,201	12,561	1	6	99.98						
										55-64	8,661	15,327	3	9	99.97						
O2[8]	4.9	3-89	NA	1-12	4,407	9,826	6	24	99.86	13-24	4,023	13,231	2	5	99.95	NA	NA	NA	NA	NA	
										25-36	7,089	16,467	1	4	99.98						
										37-48	6,201	12,561	3	11	99.96						
										49-59	8,661	15,327	1	5	99.99						
S1	2.0	9-90	NA	1-10	2,226	5,081	12	39	99.45	11-22	653	1,220	38	68	94.18	NA	NA	NA	NA	NA	
										23-28	ND	ND	ND	ND							
										29-40	1,571	4,074	8	26	99.51						
										41-45	1,086	2,067	4	7	99.64						

Table E-4.2. Summary of LCRS and LDS Flow Rate Data for Considered Landfill Cells with GM Primary Liners (Continued).

Cell No.	Cell Area	Start of Waste Placem. (month-year)	Final Closure (month-year)	Initial Period of Operation[1]						Active Period of Operation[2]						Post-Closure Period[3]					
				Time Period	LCRS Flow[4]		LDS Flow		E_a	Time Period	LCRS Flow		LDS Flow		E_a	Time Period	LCRS Flow		LDS Flow		E_a
					Avg.	Peak	Avg.	Peak			Avg.	Peak	Avg.	Peak			Avg.	Peak	Avg.	Peak	
	(ha)			(months)	(lphd)	(lphd)	(lphd)	(lphd)	(%)	(months)	(lphd)	(lphd)	(lphd)	(lphd)	(%)	(months)	(lphd)	(lphd)	(lphd)	(lphd)	(%)
S2	1.6	8-90	NA	1-9	2,185	4,650	5	24	99.78	10-17	654	1,135	5	24	99.20	NA	NA	NA	NA	NA	
										18-33	ND	ND	ND	ND							
										34-46	1,255	3,638	5	8	99.63						
V1[8]	4.2	1-90	NA	1-17	13,622	49,828	117	153	99.14	14-46	ND	ND	40	227		NA	NA	NA	NA	NA	
V2[8]	3.9	1-90	NA	1-17	13,622	49,828	135	256	99.01	14-46	ND	ND	41	86		NA	NA	NA	NA	NA	
W1	15.4	5-92	NA	1-8	ND	ND	ND	ND		13-24	2,693	6,365	34	109	98.72	NA	NA	NA	NA	NA	
				9-12	7,492	8,799	439	765	94.14	25-35	943	1,572	19	44	97.98						
W2	15.4	5-92	NA	1-8	ND	ND	ND	ND		9-20	4,288	9,389	594	1,826	86.15	NA	NA	NA	NA	NA	
										21-32	4,813	10,524	204	1,217	95.76						
										33-35	719	2,141	32	52	95.50						
X1	3.0	8-92	NA	1	111,031	111,031	364	364	99.67	8-19	5,926	14,315	5	45	99.92	NA	NA	NA	NA	NA	
				2-7	32,469	104,645	4	25	99.99	20-33	2,188	5,376	0	2	99.99						

Notes:
(1) "Initial Period of Operation" represents period after waste placement has started and only a small amount of waste has been placed in the cell.
(2) "Active Period of Operation" represents period when waste thickness in cell is significant and/or an effective intermediate cover is placed on the waste.
(3) "Post-Closure Period" represents period after final cover system has been placed on the entire cell.
(4) Flow rates are given in liter/hectare/day.
(5) NA = not applicable; ND = not determined.
(6) LCRS for Cells I1, I2, and I3 are combined after February 1992. Reported flow rates are the average for the three cells.
(7) Values given represent LCRS and LDS areas, respectively.
(8) LCRS flows are combined for Cells O1 and O2 and for Cells V1 and V2. Reported flow rates are the average for the two cells at each landfill.

Table E-4.3. Average LDS Flow Rates in lphd for Considered Cells with GM Primary Liners.

(a) Cells with **Sand** LDS

Constructed **with** Formal CQA				Constructed **without** Formal CQA[1]			
Cell No.	Initial Period of Operation	Active Period of Operation	Post-Closure Period	Cell No.	Initial Period of Operation	Active Period of Operation	Post-Closure Period
C1		70		B1		517	210
C2	92	13		B2		689	241
C3	63	17		E1	2,144	1107	
C4	178	53		E2	483	703	
C5	23	28		E3	1,595	1603	
D1	32		35	E4	996		
D3	12	76		F1	124	66	
D4	233			K1	122	271	
G1		138					
G2	197	41					
I1	234	16	62				
I2	31	7	2				
I3	37	9	3				
O1	293	1					
O2	6	2					
V1	117	40					
V2	135	41					
Number	15	15	4	Number	6	7	2
Range	6-293	1-138	2-62	Range	122-2,144	66-1,603	210-241
Mean	112	37	25	Mean	911	708	226
Median	92	28	19	Median	740	689	

(b) Cells with GN LDS Constructed with Formal CQA

Cell No.	Initial Period of Operation	Active Period of Operation
N2		227
S1	12	20
S2	5	5
W1	439	27
W2		358
X1	55	2
Number	4	6
Range	5-439	2-358
Mean	128	106
Median	34	23

Notes: (1) All Landfill B and E cells have CSPE GM Primary liners while Cells F1 and K1 hav HDPE GM Primary liners. See Section E-4.2 for discussion.

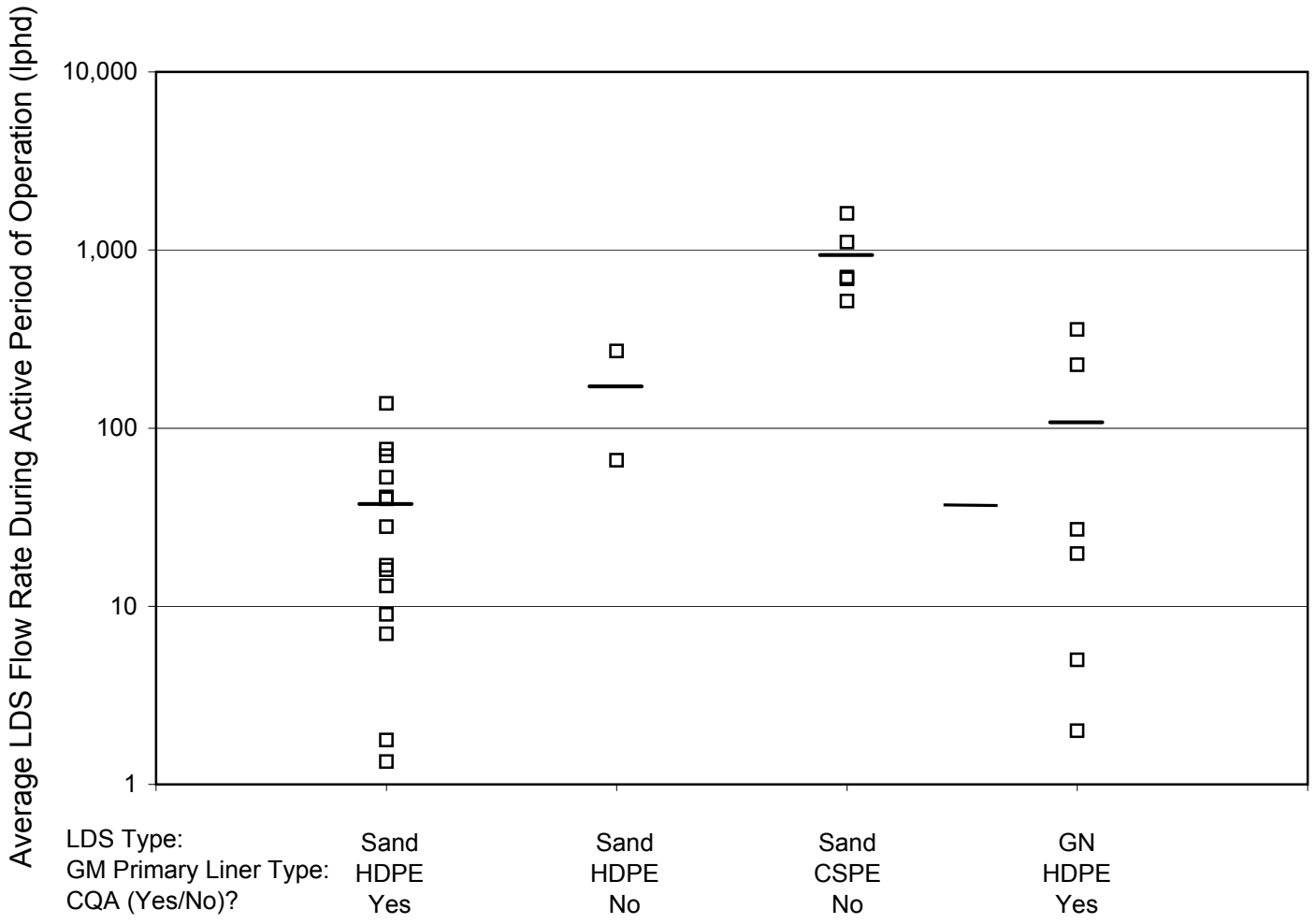

Figure E-4.1. Comparisons of LDS Average Flow Rates During Active Period of Operation for Cells with GM Primary Liners. (Note: Horizontal Line Represents the Mean LDS Flow Rate for Each Group).

(i) type of LDS drainage material (i.e., sand or GN LDS); and (ii) whether or not a formal CQA program was used to construct the cell liner system. These two criteria were selected because of their anticipated influence on LDS flow rates. The type of LDS drainage material is important due to the substantially large potential for cells with sand LDSs to release construction and compression water over time, especially during the initial and early active periods of cell operation. This is in contrast to cells with GN drainage layers, which drain rapidly. As described earlier, the use of CQA can have a significant effect on LDS flow rates for cells with GM primary liners (Bonaparte and Gross, 1990, 1993). Figure E-4.1 presents a graphical demonstration of the effects of LDS type, GM type, and use of CQA on LDS flow rates for the double-lined cells with GM primary liners considered in this appendix. In this figure LDS flow rates are plotted for four groups of data: (i) cells with sand LDSs and HDPE GMs constructed with CQA; (ii) cells with sand LDSs and HDPE GMs constructed without CQA; (iii) cells with sand LDSs and CSPE GMs constructed without CQA; and (iv) cells with GN LDSs constructed with CQA. The effects of LDS material, and CQA on LDS flow rate are discussed below.

Of the 25 cells incorporating sand LDSs, 17 were constructed with a formal CQA program and eight were constructed without CQA. The cells constructed with CQA exhibited average LDS flow rates of about 6 to 290 lphd during the initial period of operation, 1 to 140 lphd during the active period of operation, and 2 to 60 lphd during the post-closure period. The cells constructed without CQA exhibited LDS flow rates of about 120 to 2,140 lphd during the initial period of operation, 70 to 1,600 lphd during the active period of operation, and 210 to 240 lphd during the post-closure period. Mean values of LDS flow rates for all cells are about one order of magnitude lower for cells constructed with formal CQA programs than for cells constructed without CQA. This large difference in mean LDS flow rate is in part attributed to the benefits of CQA. The difference is also attributed to differences in the materials and construction methods associated with the time of cell construction (CSPE GM liners are typically installed using solvent seaming while HDPE GM liners are typically installed using thermal seaming). For example, two of the eight cells without formal CQA programs have HDPE GM primary liners, the same type of GM primary liner used at all of the facilities that had formal CQA (i.e., HDPE). These two cells (F1, K1) had average LDS flow rates during the active period of operation of 66 and 271 lphd respectively. While these flow rates are about two to seven times greater than the mean LDS flow rate for all cells that had formal CQA programs, the flow rates are not statistically different at the 90% confidence level from those cells constructed with CQA. In contrast, the cells with CSPE GM primary liners and no formal CQA exhibited average LDS flow rates in the range of 520 to 1,600 lphd. These flow rates are statistically different than flow rates from cells constructed with CQA.

It is difficult to accurately separate the effects of CQA and GM type (i.e., HDPE vs. CSPE) and construction methods on leakage rates through GM liners for the cells constructed without CQA. The causes of this difficulty are: (i) data are available to the authors for only two cells with HDPE GM primary liners constructed without formal CQA;

and (ii) no data are available for cells with CSPE GM primary liners constructed with formal CQA. Despite these limitations, the available data suggest that both CQA and GM type and construction methods have significant effects on leakage through GMs.

All six cells with GN LDSs in Table E-4.3 were constructed using a formal CQA program. As shown in Table E-4.3, average LDS flow rates for these cells were in the range of 5 to 440 lphd during the initial period of operation and 2 to 360 lphd during the active period of operation. These rates are somewhat higher than LDS flow rates for cells with sand LDSs constructed with CQA; however, the difference between the mean flow rate from these groups is not significant at the 90% confidence level.

Table E-4.4 summarizes LDS flow rates for cells with HDPE GM primary liners constructed with CQA. From this table, it can be seen that of the 18 cells for which initial period of operation data are available, eight exhibited average LDS flow rates of less than 50 lphd, six had average LDS flow rates in the range of 50 to 200 lphd, and four had average LDS flow rates from 200 to 500 lphd. Of the 19 cells for which active period of operation data are available, 13 exhibited average flow rates of less than 50 lphd, four had average flow rates in the range of 50 to 200 lphd, and two had average LDS flow rates in the range of 200 to 500 lphd. Post-closure period data are available for four cells which have undergone CQA: three exhibited average flow rates less than 50 lphd and one had an average flow rate in the range of 50 to 200 lphd.

Table E-4.4. Frequency of Average Measured LDS Flow Rates for Cells with HDPE GM Primary Liners Constructed with CQA.

	Initial Period of Operation	Active Period of Operation	Post-Closure Period
< 50 lphd	8	15	3
50-200 lphd	7	4	1
200-500 lphd	4	2	-

On the basis of the data presented above, it is concluded that LDS flow rates attributable to leakage through properly constructed HDPE GM primary liners that have undergone CQA monitoring will often be less than 50 lphd, but occasionally in excess of 200 lphd. These results are consistent with the findings of Bonaparte and Gross (1990, 1993) discussed earlier in Section E-2.1.2 of this appendix.

E-4.2.2.4 GM Primary Liner Efficiencies

Tables E-4.2 and E-4.5 present calculated E_a values for the GM primary liners. Table E-4.5 has been subdivided to separately report E_a values for the same cell groups as in Table E-4.3 (i.e., grouped based on LDS material type and use of CQA during

Table E-4.5. "Apparent" Hydraulic Efficiencies, E_a, (in %) of GM liners[1].

(a) Cells with **Sand** LDS

Constructed **with** Formal CQA				Constructed **without** Formal CQA[2]			
Cell No.	Initial Period of Operation	Active Period of Operation	Post-Closure Period	Cell No.	Initial Period of Operation	Active Period of Operation	Post-Closure Period
C1		78.92		B1		86.45	73.62
C2	93.74	95.82		B2		76.68	35.82
C3	98.16	94.35		E1		87.75	
C4	98.80	91.51		E2		85.88	
C5	99.64	98.89		E3	83.08	73.56	
D1			94.82	E4	95.06		
D3	99.94	99.24		F1	99.14	99.23	
D4	99.26			K1	99.31	96.20	
G1		97.29					
G2	99.12	99.50					
I1		99.61	92.25				
I2	99.53	99.04	99.71				
I3	99.68	99.76	99.57				
O1		99.98					
O2	99.86	99.96					
V1	99.14						
V2	99.01						
Number	12	13	4	Number	4	7	2
Range	98.16-99.94	78.92-99.98	92.25-99.75	Range	83.08-99.31	73.56-99.23	35.82-73.62
Mean	98.82	97.91[3]	96.59	Mean	94.15	86.54	54.72
Median	99.20	99.14[3]	97.20	Median	97.10	86.45	

(b) Cells with GN LDS Constructed with Formal CQA

Cell No.	Initial Period of Operation	Active Period of Operation
N2		93.58
S1	99.45	97.33
S2	99.77	99.51
W1	94.14	98.55
W2		91.32
X1	99.87	99.95
Number	4	6
Range	94.14-99.87	91.32-99.95
Mean	98.31	96.71
Median	99.61	97.94

Notes: (1) E_a = (1 - LDS Flow / LCRS Flow) x 100 %

(2) All Landfill B and E cells have CSPE GM Primary liners while Cells F1 and K1 have HDPE GM Primary liners. See Section E-4.2 for discussion.

(3) Cell C1 was excluded from calculating mean and median values of Ea for GM liners constructed with formal CQA

construction). The data in Tables E-4.2 and E-4.5 suggest that while LDS flow rates generally decrease with time, E_a values may increase or decrease with time depending on the relative rates of decrease of LCRS flow versus LDS flow. For many of the cells considered in this appendix, E_a values decreased with time due to the faster reduction in LCRS flow rate compared to the reduction in LDS flow rate. For cells with sand LDSs and CQA, E_a values are highest during the initial period of operation (E_{am} = 98.82%; where E_{am} = mean apparent efficiency for all cells) and they decrease thereafter (E_{am} = 97.91% during the active period of operation and E_{am} = 96.59% during the post-closure period). For cells with GN LDSs and CQA, E_{am} values were 98.31 and 96.71%, respectively, for the initial and active periods of operation.

For many of the cells with GM primary liners constructed with CQA, E_a values were very high (i.e., greater than 99%). However, a significant number of the cells showed lower E_a values, in the range of 91 to 99%. Only one cell, C1, had an extremely low E_a value (61.27 to 84.40%). Cell C1 had low LDS flow rates that decreased with time. This suggests low leachate leakage through the GM primary liner. However, because the LCRS flow rates were also very low, calculated E_a values were lower than other cells constructed with CQA and with similar LDS flow rates conditions. Therefore, Cell C1 average LDS flow rate was not included in calculating the E_{am} values presented above for the group of cells with sand LDSs and CQA. The data suggest that GM primary liners constructed with a formal CQA program will have E_t values in the range of about 90 to 100%, with most values being above 95%, and many values being above 99%.

Table E-4.5 also presents calculated E_a values for cells with sand LDSs constructed without formal CQA. From the eight cells in this group, the two which had HDPE GM primary liners had E_a values from about 96% greater than 99%, and the six which had CSPE GM primary liners had E_a values from about 36 to 95%. The calculated E_a values for the CSPE GM primary liners constructed without CQA are much lower than respective values calculated for cells constructed with HDPE GM primary liners and CQA. Again, this data demonstrates the effects of GM material and construction methods and of implementing a formal CQA program to construct GMs.

E-4.2.3 Implications for Landfill Performance

The evaluation results reported above indicate that GM liners can achieve primary liner leakage rates less than 50 lphd and E_t values of 99% or more. This is a very good level of performance. The results also indicate, however, that GM primary liners sometimes will not achieve this performance level and that lower E_t values, in the range of 90 to 99%, are not uncommon. This relatively broad range of E_t values is a consequence of the potential for even appropriately installed GMs to have an occasional small hole, typically due to an imperfect seam, but also potentially due to a manufacturing or construction-induced defect not identified by the CQA program. Leakage can occur, relatively unimpeded, through a GM hole if a low-permeability material such as a CCL or a GCL does not underlie the GM. If a hole occurs at a critical location where a sustained hydraulic head exists, such as a landfill sump, the leakage rate through the

hole can be significant. In contrast, the GCL or CCL component of a composite liner can impede flow through a GM hole, even if it occurs at a critical location. The conclusion to be drawn from the data evaluation is that single liner systems with GMs liners (installed on top of a relatively permeable subgrade) should not be used in applications where E_t values as low as 90% would be unacceptable, even if a thorough CQA program is employed. In these cases, single-composite liner systems or double-liner systems should be utilized. An exception to this conclusion may be made for certain facilities, such as surface impoundments or small, shallow landfill cells, with GM primary liners that can be field tested over the GM sheet and seams using electrical leak location surveys, ponding tests, or other methods. For these facilities, higher efficiencies (i.e., greater than 99%) may be achieved with GM liners by identifying and repairing the GM holes during construction and, especially for surface impoundments, during operation.

E-4.3 Leakage Rates Through Composite Primary Liners

E-4.3.1 Description of Data

The performances of all 28 cells with GM/GCL composite primary liners and 13 of the 88 cells with GM/CCL or GM/GCL/CCL composite primary liners are assessed in this section. The remaining 75 cells with composite primary liners were generally excluded from the assessment because: (i) they did not have continuous LCRS and LDS flow rate data available for an individual cell from the start of operation; or (ii) there were insufficient LCRS and LDS chemical constituent data to evaluate whether primary liner leakage did or did not occur. Flow rate data are available for 41 cells at 16 landfills with monitoring periods of up to 121 months. Data from several of the 41 cells in this study were included in the previous EPA study by Bonaparte and Gross (1993); however, this study contains additional data for most of these cells.

The liner systems for all of the considered cells were constructed under a formal CQA program. Descriptions of the liner systems installed at these landfills are presented in Table E-4.6. The LDS consists of a sand layer, a gravel layer over a GN, or a GN. The secondary liner of the double-liner system is a single GM, a GM/CCL composite, or a GM/GCL composite. Tables E-4.7 and E-4.8 contain a summary of the LCRS and LDS flow rate database for cells with GM/GCL and GM/CCL or GM/GCL/CCL primary liners, respectively. Each of the cells for which post-closure data are available has a final cover system with a GM or GM/GCL composite barrier. For cells with GM/CCL or GM/GCL/CCL composite primary liners, the database also includes LCRS and LDS chemical constituent data. A summary of these data is presented in Table E-4.9. For reasons discussed subsequently, chemical constituent data were not used in the evaluation of GM/GCL primary liners.

Table E-4.6. Description of Liner System Components for Considered Landfills with Composite Primary Liners.

Cell No.	Type[1] of Waste	LCRS		Primary Liner				LDS		Secondary Liner		
		Material[2]	Thickness[3] (mm)	GM[4] Type (and Thickness (mm))	Lower Component			Material[2]	Thickness (mm)	GM Type (and Thickness (mm))	Lower Component	
					Material[5]	Thickness (mm)	Max. Hydraulic Conductivity (m/s)				Material	Thickness (mm)
B3	MSW	S	450	CSPE(0.9)	CCL	600	$1x10^{-9}$	S	450	PVC(0.8)	NA[6]	NA
Y2	MSW	S	600	HDPE(2.0)	CCL	450	$1x10^{-9}$	S	300	HDPE(2.0)	CCL	600
AK1	MSW	S/GN	600/5	HDPE(1.5)	GCL/CCL	6/600	$5x10^{-11}/1x10^{-9}$	GN	5	HDPE(1.5)	GCL	6
AL1	MSW	S	600	HDPE(1.5)	CCL	900	$1x10^{-9}$	GN	5	HDPE(1.5)	CCL	900
AM 1&2	MSW	G/S	300/150	HDPE(2.0)	CCL	450	$1x10^{-8}$	GN	5	HDPE(1.5)	NA	NA
AO 1&2	MSW	S	600	HDPE(1.5)	CCL	900	$5x10^{-10}$	GN	5	HDPE(1.5)	CCL	600
AR1	MSW	G/TC	300/400	HDPE(1.5)	GCL/CCL	6/300	$5x10^{-11}/1x10^{-7}$	GN	10	HDPE(1.5)	CCL	600
AD1 (Base)	HW	S	300	HDPE(1.5)	CCL	900	$1x10^{-9}$	S	300	HDPE(1.5)	CCL	900
(Side slopes)		GN	5	HDPE(1.5)	CCL	900	$1x10^{-9}$	GN	5	HDPE(1.5)	CCL	900
AD7 (Base)	HW	S	300	HDPE(1.5)	CCL	900	$1x10^{-9}$	GN	5	HDPE(1.5)	CCL	900
(Side slopes)		GN	5	HDPE(1.5)	CCL	900	$1x10^{-9}$	GN	5	HDPE(1.5)	CCL	900
AQ1	HW	G/GN	300/5	HDPE(2.0)	CCL	450	$1x10^{-9}$	G/GN	300/5	HDPE(1.5)	CCL	900
AQ10	HW	G/GN	300/5	HDPE(2.0)	CCL	450	$1x10^{-9}$	G/GN	300/5	HDPE(2.0)	CCL	900
AX 1-16	MSW	S	600	HDPE(1.5)	GCL	6	$5x10^{-11}$	S	300	HDPE(1.5)	CCL	200
C6	MSW	S	600	HDPE(2.0)	GCL	6	$5x10^{-11}$	S	450	HDPE(2.0)	CCL	300
AW 1&2	MSW	S	450	HDPE(1.5)	GCL	6	$5x10^{-11}$	S	300	HDPE(1.5)	GCL	6
BB 1-3	MSW	S	600	HDPE(1.5)	GCL	6	$5x10^{-11}$	GN	5	HDPE(1.5)	NA	NA
AZ1	MSW	S	600	HDPE(1.5)	GCL	6	$5x10^{-11}$	GN	5	HDPE(1.5)	CCL	900
AY 1-3	HW	GN	5	HDPE(1.5)	GCL	6	$5x10^{-11}$	GN	5	HDPE(1.0)	GCL	6
I 4-5 (Base)	MSW	TC/G	150/450	HDPE(1.5)	GCL	6	$5x10^{-11}$	GN	10	HDPE(1.5)	CCL	150
(Side slopes)		NA	NA	HDPE(1.5)	GCL	6	$5x10^{-11}$	GN	5	HDPE(1.5)	CCL	150

Notes: (1) Waste Types: MSW = Municipal Solid Waste; HW = Hazardous Solid Waste.

(2) LCRS and LDS Material Types: GN = GN or Geocomposite; TC = Tire Chips; S = Sand; G = Gravel

(3) All material thicknesses are nominal values.

(4) GM Types: HDPE = High Density Polyethylene; CSPE = Chlorosulfonated Polyethylene; PVC = Polyvinyl Chloride.

(5) Liner Lower Component Material Types: CCL = Compacted Clay Liner; GCL = Geosynthetic Clay Liner.

(6) NA = Not Applicable.

Table E-4.7. Summary of Flow Rate Data for Landfill Cells with GM/GCL Composite Primary Liners.

Cell No.	Cell Area	Start of Waste Placem. (month-year)	End of Final Closure (month-year)	Initial Period of Operation[1]					Active Period of Operation[2]					Post-Clo		
				Time Period[6]	LCRS Flow[4]		LDS Flow		Time Period[6]	LCRS Flow		LDS Flow		Time Period[6]	LCRS	
					Avg.	Peak	Avg.	Peak		Avg.	Peak	Avg.	Peak		Avg.	
	(hectare)			(months)	(lphd)	(lphd)	(lphd)	(lphd)	(months)	(lphd)	(lphd)	(lphd)	(lphd)	(months)	(lphd)	
AX1	2.0	7-88	2-91	1-2	16,718	19,738	0	0	3-33	540	2,383	0	0	34-83	66	
AX2	2.0	7-88	2-91	1-5	15,521	58,671	15	45	6-33	281	570	2	21	34-83	178	
AX3	1.7	9-88	4-93	1-5	3,366	7,985	35	151	6-56	307	1,075	4	47	57-81	206	
AX4	1.7	9-88	4-93	1-12	2,534	12,688	101	860	13-56	75	187	1	13	57-81	47	
AX5	2.8	10-88	NA[5]	1-11	1,384	3,394	37	92	12-80	56	191	2	37			
AX6	3.9	12-88	NA	1-9	3,759	7,171	53	93	10-80	168	655	0	0			
AX7	2.6	2-89	NA	1-10	5,376	12,155	34	47	11-76	234	851	2	9			
AX8	3.8	7-89	NA	1-14	4,881	21,038	48	189	15-71	439	1,384	0	0			
AX9	3.3	12-89	NA	1-9	1,047	3,478	1	7	10-65	41	159	0	0			
AX10	3.9	7-90	NA	1-7	2,786	13,698	0	0	8-59	374	645	0	0			
AX11	3.0	2-90	NA	1-16	4,675	14,586	0	0	17-62	150	337	0	0			
AX12	4.0	10-90	NA	1-12	3,494	8,836	0	0	13-56	803	3,029	0	0			
AX13	3.0	1-91	NA	1-7	6,683	14,343	0	0	8-53	1,408	9,294	0	0			
AX14	2.8	4-91	NA	1-11	2,777	6,582	0	0	12-38	281	449	0	0			
AX15	2.8	5-92	NA	1-12	5,573	11,809	0	0	13-37	299	561	0	0			
AX16	4.5	1-93	NA	1-10	8,601	17,756	0	0	11-29	819	5,096	0	0			
C6	3.6	8-93	NA	1-10	3,273	12,155	178	823	11-17	393	1,403	3	15			
AW1	2.4	5-93	NA	1-12	6,358	20,570	131	524								
AW2	2.4	8-93	NA	1-10	3,553	7,480	290	514								
BB1	4.0	2-91	NA	1-6	10,378	22,130	15	65	7-47	2,494	8,983	6	25			
BB2	2.4	1-93	NA	1-11	ND[5]	ND	1	12	12-23	5,422	14,042	0	0			
BB3	2.8	1-93	NA	1-11	ND	ND	0	0	12-23	2,284	7,945	0	1			
AZ1	3.8	12-92	NA	2-12	4,093	5,219	0	0	13-31	3,473	5,054	2	22			

Table E-4.7. Summary of Flow Rate Data for Landfill Cells with GM/GCL Composite Primary Liners (Con

Cell No.	Cell Area	Start of Waste Placem. (month-year)	End of Final Closure (month-year)	Initial Period of Operation[1]					Active Period of Operation[2]					Post-Clo		
				Time Period[6]	LCRS Flow[4]		LDS Flow		Time Period[6]	LCRS Flow		LDS Flow		Time Period[6]	LCRS	
					Avg.	Peak	Avg.	Peak		Avg.	Peak	Avg.	Peak		Avg.	
	(hectare)			(months)	(lphd)	(lphd)	(lphd)	(lphd)	(months)	(lphd)	(lphd)	(lphd)	(lphd)	(months)	(lphd)	
AY1	1.3	10-94	NA	1-9	6,803	12,439	0	0								
AY2	1.0	8-94	NA	1-11	10,964	23,914	3	12								
AY3	1.0	8-94	NA	1-11	12,198	32,326	6	28								
I4	4.7	5-92	7-94	1-12	4,494	17,251	24	70	13-26	2,041	4,282	26	142	27-36	567	
I5	4.7	7-92	5-94	1-12	3,938	7,985	2	11	13-21	3,108	11,669	11	54	22-34	189	

Notes:

(1) "Initial Period of Operation" represents period after waste placement has started and only a small amount of waste has been placed
(2) "Active Period of Operation" represents period when waste thickness in cell is significant and/or an effective intermediate cover is pl
(3) "Post-Closure Period" represents period after final cover system has been placed on the entire cell.
(4) Flow rates are given in liter/hectare/day.
(5) NA = Not Applicable; ND = Not Determined.
(6) Breakthrough time for steady-state saturated flow through GCL component of composite liner is estimated to be 2 months based on using Darcy's equation and a saturated hydraulic conductivity of 5×10^{-11} m/s, hydraulic gradient of 5, and effective porosity of 0.2. calculation, it is assumed that flow through the GM component of the composite liner occurs through small holes and is instantaneo

Table E-4.8. Summary of Flow Rate Data for Landfill Cells with GM/CCL or GM/GCL/CCL Composite Primary Liners.

Cell No.	Cell Area (ha)	Start of Waste Placem. (month-year)	End of Final Closure (month-year)	Initial Period of Operation[1]					Active Period of Operation[2]					E_a (Average for Active Period) (%)	Post-Closure Period[3]					E_a (Average for P-C Period) (%)
				Time Period	LCRS Flow[4]		LDS Flow		Time Period	LCRS Flow		LDS Flow			Time Period	LCRS Flow		LDS Flow		
				(months)	Avg. (lphd)	Peak (lphd)	Avg. (lphd)	Peak (lphd)	(months)	Avg. (lphd)	Peak (lphd)	Avg. (lphd)	Peak (lphd)		(months)	Avg. (lphd)	Peak (lphd)	Avg. (lphd)	Peak (lphd)	
B3[5]	6.4	7-87	NA[6]	1-4	15,304	24,858	1,394	4,250	5-16	5,700	8,935	124	266	97.8						
									17-28	9,272	22,444	101	168	98.9						
									29-40	7,575	13,978	262	803	96.5						
									41-52	2,859	6,043	231	713	91.9						
									53-64	1,189	2,280	45	152	96.2						
									65-76	403	490	92	133	77.3						
									77-88	560	919	102	193	81.8						
									89-93	578	648	98	109	83.0						
Y2	3.0	1-91	NA	1-10	23,368	36,791	655	1,768	11-22	10,353	19,204	370	1,993	96.4						
									23-34	11,344	25,309	90	168	99.2						
									35-46	4,404	6,380	70	248	98.4						
									47-54	4,397	5,199	48	56	98.9						
AK1	1.4	10-93	NA	1-12	9,867	17,986	206	804												
AL1	14.9	1990	NA	1-29	ND[6]	ND	ND	ND	30-41	934	2,085	231	367	75.3						
									42-54	1,349	5,885	103	183	92.4						
AM1	3.2/2.4[7]	10-90	NA	1-9	ND	ND	ND	ND	10-21	270	533	15	64	94.4						
									22-33	236	329	10	15	95.8						
									34-45	111	283	3	14	97.3						
									46-57	20	77	1	1	95.0						
									58-69	18	21	1	1	94.4						
									70-81	11	18	5	8	54.4						
AM2	4.8/2.4[7]	10-90	NA	1-9	ND	ND	ND	ND	10-21	32	154	9	42	71.9						
									22-33	35	51	9	29	74.3						
									34-45	17	45	3	26	82.4						
									46-57	67	274	0	0	100.0						
									58-69	64	181	8	13	87.5						
									70-81	112	136	9	13	92.0						
AO1	1.8	1-92	NA	1-5	ND	ND	ND	ND	6-17	1,984	4,130	184	353	90.7						
									18-29	1,299	1,577	96	126	92.6						
									30-37	1,144	1,371	60	102	94.8						
AO2	1.8	7-92	NA	1-5	15,881	24,541	149	191	6-17	3,027	5,266	110	158	96.4						
									18-31	1,688	2,383	33	64	98.1						
AR1	9.7	3-92	NA	1-11	27,042	65,871	292	705	12-23	11,251	23,384	181	470	98.4						
									24-36	9,668	26,274	155	442	98.4						

Table E-4.8. Summary of Flow Rate Data for Landfill Cells with GM/CCL or GM/GCL/CCL Composite Primary Liners (Continued).

Cell No.	Cell Area (ha)	Start of Waste Placem. (month-year)	End of Final Closure (month-year)	Initial Period of Operation[1]					Active Period of Operation[2]					E_a (Average for Active Period) (%)	Post-Closure Period[3]					E_a (Average for P-C Period) (%)
				Time Period (months)	LCRS Flow[4] Avg. (lphd)	LCRS Flow Peak (lphd)	LDS Flow Avg. (lphd)	LDS Flow Peak (lphd)	Time Period (months)	LCRS Flow Avg. (lphd)	LCRS Flow Peak (lphd)	LDS Flow Avg. (lphd)	LDS Flow Peak (lphd)		Time Period (months)	LCRS Flow Avg. (lphd)	LCRS Flow Peak (lphd)	LDS Flow Avg. (lphd)	LDS Flow Peak (lphd)	
AD1	0.6	5-85	7-88	1-12	ND	ND	ND	ND	13-20	ND	ND	ND	ND		33-44	145	652	24	42	83.4
									21-32	373	892	107	603	71.4	45-51	85	130	26	31	69.5
															52-63	3	22	28	45	-833
															64-75	3	42	42	103	-1300
															76-87	3	21	23	68	-667
															88-99	1	4	8	46	-700
															100-111	1	2	5	43	-400
															112-121	2	9	6	24	-200
AD7	1.5	9-87	10-93	1-12	12,597	26,492	135	1,101	13-24	2,212	2,857	71	291	96.8	70-81	375	533	73	157	80.5
									25-36	1,539	2,755	96	393	93.8	82-87	165	334	105	172	36.3
									37-48	1,429	2,813	17	21	98.8						
									49-60	249	629	33	74	87.0						
									61-69	480	614	64	112	86.6						
AQ1	0.6	3-86	early 90	1-6	10,203	18,944	352	569	7-25	ND	ND	255	1239		59-65	5,835	11,244	215	246	96.3
									26-34	ND	ND	ND	ND		66-77	644	1,011	117	165	81.8
									35-46	ND	ND	197	435		78-89	1,367	3,264	98	132	92.8
									47-58	4,530	10,531	116	143	97.4	90-97	1,615	3,575	51	118	96.8
AQ10	0.9	1-89	mid 91	1-9	ND	ND	14	32	10-14	ND	ND	26	32		27-38	682	2,251	29	48	95.7
									15-26	15,933	38,751	48	250	99.7	39-50	300	1,709	18	63	94.0
															51-63	852	1,588	24	75	97.2

Notes:

(1) "Initial Period of Operation" represents period after waste placement has started and only a small amount of waste has been placed in the cell.

(2) "Active Period of Operation" represents period when waste thickness in cell is significant and/or an effective intermediate cover is placed on the waste.

(3) "Post Closure Period" represents period after final cover system has been placed on the entire cell.

(4) Flow rates are given in liter/hectare/day.

(5) 65 percent of Cell B3 received final cover after 60 months of start of waste placement.

(6) NA = not applicable; ND = not determined.

(7) Values given represent LCRS and LDS areas, respectively.

(8) Estimated breakthrough time for steady-state saturated flow through CCL or GCL/CCL component of composite liner is given in Table E-4.12.

Table E-4.9. Summary of Liquid Chemistry for the LCRS and LDS of Landfills with Composite Primary Liners.

Landfill ID		B (MSW)		Y (MSW)		AK (MSW)		AL (MSW)	
Cell No.-System		B3-LCRS	B3-LDS	Y2-LCRS	Y2-LDS	AK1-LCRS	AK1-LDS	AL1-LCRS	AL1-LDS
Waste Placement Period		07/87-05/92		1990-date		10/93-date		1990 - date	
Liquid Sampling Period		07/87-10/94	07/87-10/94	04/91-04/94	04/91-04/94	12/93-03/95	12/93-03/95	06/91-05/95	12/89-05/95
Parameter	Units								
pH		6.82		6.60	7.28	6.65	7.20	8.09	7.04
Specific Conductance	µmhos/cm	2,956	1,554	5,360	1,583	1,592	679	2,707	2,449
TDS	mg/l	4,140	1,148	4,939	881			2,892	2,482
TSS	mg/l	161	45				60	110	24
COD	mg/l	1,912	131	5,265	50	1,062	13	860	< 11
BOD5	mg/l	422	88	2,076	3	< 2		1,134	< 2
TOC	mg/l	554	138	1,436	11	245	4	245	3
Alkalinity	mg/l			2,520	335	711	331	261	199
Chloride	mg/l	690	148	628	58	94	4	430	151
Sulfate	mg/l	131	335	108	231	45	25	219	1,028
Calcium	mg/l			1,994	179	387	116	150	465
Magnesium	mg/l				54	51	29	98	121
Sodium	mg/l	450	46	433	46	64	5	236	38
Arsenic	µg/l		< 24	17	4	< 3	< 1	4	< 5
Cadmium	µg/l	< 20	16	8	< 2	< 19	< 3	< 11	< 7
Chromium	µg/l	49	3	58	11	< 27	< 2	< 64	< 10
Lead	µg/l	< 44	< 17	5	8	< 48	< 5	< 36	< 17
Nickel	µg/l	102	519	185	25	< 50	< 50	57	< 35
Benzene	µg/l	< 5	< 7	10		< 5	< 1	< 6	< 2
1,1 - Dichloroethane	µg/l	< 40	< 7	45		46	< 1	< 8	< 7
1,2 - Dichloroethane	µg/l	< 5	< 6			< 2	< 1	< 6	< 2
cis- 1,2-Dichloroethene	µg/l					< 1	< 1	< 7	< 3
Trans- 1,2-Dichloroethene	µg/l					< 1	< 1	< 2	< 2
Ethylbenzene	µg/l	15	< 6	118		< 7	< 1	< 12	< 2
Methylene Chloride	µg/l	< 80	< 17	121		603	< 5	245	< 77
1,1,1 - Trichloroethane	µg/l	< 107	< 6			134	3	< 8	< 4
Trichloroethylene	µg/l			11		< 1	< 1	< 12	< 2
Toluene	µg/l	< 78	< 9	720	7	95	< 1	78	< 7
Vinyl Chloride	µg/l	< 10	< 12			< 11	< 5	< 11	< 5
Xylenes	µg/l			69		< 30	< 3	< 96	< 5

Table E-4.9. Summary of Liquid Chemistry for the LCRS and LDS of Landfills with Composite Primary Liners (Continued).

Landfill ID		AM(MSW)				AO (MSW)			AR (MSW)	
Cell No.-System		AM1-LCRS	AM1-LDS	AM2-LCRS	AM2-LDS	AO-LCRS	AO1-LDS	AO2-LDS	AR1-LCRS	AR1-LDS
Waste Placement Period		10/90-02/91		10/90-02/91		01/92-date			03/92-date	
Liquid Sampling Period		04/91-02/95	02/92-12/93	04/91-02/96	02/92-01/96	08/92-06/95	08/92-05/95	08/92-06/95	11/92-08/94	11/92-08/94
Parameter	Units									
pH		6.62	6.90	6.60	7.26	7.30	7.17	6.72	6.92	7.00
Specific Conductance	µmhos/cm	2,451	17,250	2,795	17,063	6,592	1,132	1,118	5,650	1,368
TDS	mg/l	1,709	14,330	1,413	14,363	2,178	690	722	3,923	848
TSS	mg/l					1,310				
COD	mg/l	396	184	65	76	618	142	497	1,238	22
BOD5	mg/l								290	5
TOC	mg/l	108	116	22	28	414	43	8	333	5
Alkalinity	mg/l	1,204	407	867	163	1,756	556	558	2,075	325
Chloride	mg/l	183	2,725	332	2,659	862	38	24	1,625	35
Sulfate	mg/l	18	1,500	9	1,425	54	44	91	380	325
Calcium	mg/l	376	1,700	319	1,819	275	205	196	230	186
Magnesium	mg/l	95	283	74	299	146	66	55	153	119
Sodium	mg/l	92	1,348	88	1,929	786	19	8	850	26
Arsenic	µg/l	236	< 2	235	< 10	45	7	2	13	< 8
Cadmium	µg/l	< 20	< 20	< 20	< 10	< 9	< 1	< 1	< 6	< 7
Chromium	µg/l	< 30	< 30	< 57	< 30	54	< 1	< 1	62	< 10
Lead	µg/l	< 2.0		< 7	3	< 32	< 1	< 1	< 13	< 9
Nickel	µg/l	< 40	< 40	< 91	< 40	108	< 50	< 50	< 20	< 100
Benzene	µg/l	17	< 1	13	< 1	7	< 1	< 1	< 100	< 1
1,1 - Dichloroethane	µg/l	172	< 3	136	< 2	15	< 3	< 1	< 100	< 2
1,2 - Dichloroethane	µg/l	6	< 1	< 11	< 1	< 5	< 1	< 1	< 100	< 2
cis- 1,2-Dichloroethene	µg/l	324	< 1	547	< 1	< 6	< 1	< 1	< 100	< 50
Trans- 1,2-Dichloroethene	µg/l	< 5	< 1	< 8	< 1	< 4	< 1	< 1	< 100	< 2
Ethylbenzene	µg/l	57	< 1	29	< 1	11	< 1	< 1	< 100	< 2
Methylene Chloride	µg/l	< 6	3	< 20	< 2	75	< 5	< 5	< 100	< 2
1,1,1 - Trichloroethane	µg/l	< 21	< 1	< 16	< 1	< 11	< 1	< 1	< 100	< 2
Trichloroethylene	µg/l	3	< 1	< 12	< 1	< 4	< 1	< 1	< 100	< 2
Toluene	µg/l	267	< 1	146	< 1	167	< 86	< 1	< 100	< 2
Vinyl Chloride	µg/l	< 21	< 1	< 11	< 2	< 12	< 7	< 5	< 100	< 4
Xylenes	µg/l	122	< 1	71	< 2	34	< 3	< 3	< 100	< 4

Table E-4.9. Summary of Liquid Chemistry for the LCRS and LDS of Landfills with Composite Primary Liners (Continued).

Landfill ID		AD (HW)				AQ (HW)			
Cell No.-System		AD1-LCRS	AD1-LDS	AD7-LCRS	AD7-LDS	AQ1-LCRS	AQ1-LDS	AQ10-LCRS	AQ10-LDS
Waste Placement Period		05/85 - late '87		09/87 - 09/88, 05-06/93		03/86 - early 90		late 88 - mid 91	
Liquid Sampling Period		06/85-12/94	06/85-12/94	09/87-12/94	09/87-12/94	02/91-10/93	02/91-10/93	02/91-10/93	02/91-10/93
Parameter	Units								
pH		8.72	7.40	9.99	7.45	7.90	7.36	7.20	7.51
Specific Conductance	µmhos/cm	40,159	1,755	39,036	2,512	23,200	2,582	5,574	4,154
TDS	mg/l								
TSS	mg/l								
COD	mg/l								
BOD5	mg/l								
TOC	mg/l	2,006	8	4,471	7				
Alkalinity	mg/l								
Chloride	mg/l	12,709	207	10,759	301				
Sulfate	mg/l	4,428	404	6,105	6,105				
Calcium	mg/l								
Magnesium	mg/l								
Sodium	mg/l	10,394	177	5,549	250				
Arsenic	µg/l	125,252	< 13	34,572	< 14	189	< 10		< 11
Cadmium	µg/l	< 410	< 4	< 56	< 3	< 5	< 5		< 5
Chromium	µg/l	294	29	158	< 12	22	12		50
Lead	µg/l	192	< 29	< 306	< 16	24	31		< 17
Nickel	µg/l					1,190	< 40		84
Benzene	µg/l	< 184	< 4	555	< 4	< 8	< 4	< 6	< 4
1,1 - Dichloroethane	µg/l	< 138	< 5	< 604	< 6	14	< 5	135	< 5
1,2 - Dichloroethane	µg/l	< 67	< 3	< 2,181	< 3	< 5	< 3	4	< 3
cis- 1,2-Dichloroethene	µg/l								
Trans- 1,2-Dichloroethene	µg/l	< 48	< 2	< 238	< 3	18	< 2	< 10	< 2
Ethylbenzene	µg/l	174	< 6	< 850	< 6	< 5	< 5	< 5	< 5
Methylene Chloride	µg/l	< 292	< 4	< 602	< 3	5	6	< 3	< 3
1,1,1 - Trichloroethane	µg/l	< 228	< 4	< 466	< 3	9	< 8	36	< 4
Trichloroethylene	µg/l	< 53	< 2	< 240	< 25	60	19	5	< 2
Toluene	µg/l	< 189	< 5	1,042	< 5	< 5	7	< 13	< 5
Vinyl Chloride	µg/l	1,371	< 9	< 7,438	< 9	13	< 10	< 7	< 10
Xylenes	µg/l								

E-4.3.2 GM/GCL Composite Primary Liners

E-4.3.2.1 Interpretation of Data

The interpretation of LDS flow rate data for cells with GM/GCL primary liners is also relatively straightforward because the potential sources of LDS flow for cells with GM/GCL composite primary liners are construction water, compression water, and primary liner leakage. Ground-water infiltration is not a potential source because all of the facilities are reportedly located above the ground-water table. Consolidation water is a potential source if the GCL hydrates prior to waste filling. While GCL installation procedures are designed to keep the GCL as dry as possible, post-construction changes in moisture content can occur as a result of construction water in the LDS. The GCL components of composite liners will produce little, if any, consolidation water, depending on their moisture content at the start of waste placement. The analysis of these cells has been performed considering only LCRS and LDS flow rate data. LDS chemical constituent data were not considered in the data interpretation because the chemistry data were unavailable for many landfill cells, possibly due to the nonexistent or very low LDS flow rates from these cells.

E-4.3.2.2 Summary of Flow Rate Data

Average and peak monthly flow rates for the 28 landfill cells with GM/GCL primary liners are presented in Table E-4.7 for the three landfill operational time periods described earlier. Average monthly LCRS flow rates ranged from about 1,050 to 16,700 lphd during the initial period of operation, about 40 to 5,420 lphd during the active period, and about 50 to 570 lphd after closure. Average monthly LDS flow rates, excluding Cell I4, ranged from about 0 to 290 lphd during the initial period of operation, 0 to 11 lphd during the active period, and 0 to 2 lphd after closure. Cell I4 was excluded from the data summary because of anomalous LDS flow measurements during the active and post-closure periods. The LDS of this cell exhibited much higher flow rates than any other LDS underlying a GM/GCL composite liner, and also increasing LDS flow rates under conditions of decreasing LCRS flow rates. The reason for this trend in data is unknown. The landfill operator believes the high LDS flow rates are due to surface-water runoff problems around the landfill cell perimeter and direct infiltration of this runoff into both the LCRS and LDS via the liner system anchor trench at the cell perimeter. This hypothesis has not been verified. A review of the data in Table E-4.7 indicates that peak monthly LCRS and LDS flow rates are typically two to five times the average monthly values calculated for the monitoring periods reported in Table E-4.7. This difference becomes larger in the LDS when the flow rates become very low: this is mostly an artifact of the LDS pumping schedule, which becomes infrequent when the flow rate becomes very low. Table E-4.7 shows that between the initial and active periods of operation, LCRS flow rates typically decreased one to two orders of magnitude and LDS flow rates decreased one to three orders of magnitude.

E-4.3.2.3 Liner Efficiencies

Table E-4.10 summarizes calculated E_a values for the GM/GCL composite primary liners. Table E-4.10 has been subdivided to separately report E_a values for cells with sand LDSs and cells with GN LDSs due to the substantially large potential for cells with sand LDSs to generate construction and compression water compared to cells with GN LDSs. For cells with sand LDSs, E_a values are lowest during the initial period of operation (E_{am} = 98.60%) and increase significantly thereafter (E_{am} = 99.53% during the active period of operation and E_{am} = 99.89% during the post-closure period). The lower value of E_{am} during the initial period of operation is attributed to LDS flow from construction water. By conservatively ignoring long-term contributions to LDS flow from construction water, compression water, and consolidation water, E_a values during the active period of operation and the post-closure period can be interpreted to reflect true liner efficiencies (E_t) for the prevailing conditions.

For cells with GN LDSs, E_{am} is 99.96% during the initial period of operation, 99.87% during the active period of operation, and 98.78% during the post-closure period. During the initial period of operation, the E_{am} value for cells with GN LDSs (i.e., 99.96%) is higher than the E_{am} value for cells with sand LDSs (i.e., 98.60%). This higher efficiency can be attributed to the differences in liquid storage capacity and hydraulic transmissivity between sand and GN drainage materials. By conservatively neglecting the potential for consolidation water, E_a values for cells with GN LDSs can be interpreted to reflect E_t.

In summary, from Table E-4.7 (and excluding Cell I4), monthly average LDS flow rates potentially attributable to primary liner leakage vary from 0 to 11 lphd, with many values reported as zero, and most values being less than about 2 lphd. Primary liner leakage rates of this magnitude are very low. The results in Table E-4.10 further indicate that E_t for a GM/GCL constructed to current standards with appropriate CQA will typically be in the range of 99 to 100%, and will frequently be in excess of 99.9%.

E-4.3.3 GM/CCL and GM/GCL/CCL Composite Primary Liners

E-4.3.3.1 Interpretation of Data

The interpretation of flow rate data for cells with GM/CCL or GM/GCL/CCL composite primary liners is more complicated than the interpretation for GM/GCL composite primary liners because of the relatively large contribution of consolidation water to LDS flow. Previous investigations, e.g., Bonaparte and Gross (1990), could not distinguish the occurrence (or lack thereof) of primary liner leakage from the much larger volumes of LDS consolidation water. Also, breakthrough times (i.e., times of travel) for advective transport through the CCL or GCL/CCL component of a composite liner can be quite long, further complicating the evaluation. Both LCRS and LDS flow rate and chemical constituent data were used in this appendix to evaluate GM/CCL and GM/GCL/CCL composite liner performance.

Table E-4.10. "Apparent" Hydraulic Efficiencies, Ea, for GM/GCL Composite Liners (Excluding Cell I4).

Cells with Sand LDS				Cells with GT/GN LDS			
Cell No.	Initial Period of Operation (%)	Active Period of Operation (%)	Post-Closure Period (%)	Cell No.	Initial Period of Operation (%)	Active Period of Operation (%)	Post-Closure Period (%)
AX1	100.00	100.00	100.00	BB1	99.86	99.78	
AX2	99.90	99.33	100.00	BB2		100.00	
AX3	98.97	98.70	99.55	BB3		100.00	
AX4	96.01	98.75	100.00	AZ1	100.00	99.94	
AX5	97.30	96.67		AY1	100.00		
AX6	98.58	100.00		AY2	99.97		
AX7	99.37	99.20		AY3	99.95		
AX8	99.02	100.00		I5	99.95	99.65	98.78
AX9	99.91	100.00					
AX10	100.00	100.00					
AX11	100.00	100.00					
AX12	100.00	100.00					
AX13	100.00	100.00					
AX14	100.00	100.00					
AX15	100.00	100.00					
AX16	100.00	100.00					
C6	94.57	99.29					
AW1	97.94						
AW2	91.84						
Number	19	17	4	Number	7	6	1
Range	91.84 - 100	96.67 - 100	99.55 - 100	Range	99.86 - 100	98.73 - 100	98.78
Mean	98.60	99.53	99.89	Mean	99.95	99.87	98.78
Median	99.90	100.00	100.00	Median	99.95	99.94	98.78

Notes: [1] Apparent Efficiency = (1 - LDS Flow / LCRS Flow) x 100 %

E-4.3.3.2 Analysis of Flow Rate Data

Average and peak monthly flow rate data for the 13 landfill cells with GM/CCL or GM/GCL/CCL composite primary liners are presented in Table E-4.8. Average monthly LCRS flow rates ranged from about 9,900 to 27,000 lphd during the initial period of operation, 10 to 15,900 lphd during the active period of operation, and 1 to 5,800 lphd during the post-closure period. Average monthly LDS flow rates ranged from about 10 to 1,400 lphd during the initial period of operation, 0 to 370 lphd during the active period of operation, and 5 to 210 lphd during the post-closure period. Peak monthly LCRS and LDS flow rates are typically two to five times the reported average monthly value calculated for the reported monitoring period. Between the initial period of operation and later stages of the active period of operation, flow rates for both the LCRS and LDS typically decreased by one to two orders of magnitude. For the active and post-closure periods in particular, LDS flow rates for cells with GM/CCL and GM/GCL/CCL composite primary liners are much higher than those for cells with GM/GCL composite primary liners. These higher flow rates are attributable to consolidation water.

The flow rate data in Table E-4.8 were used to calculate E_a values for GM/CCL and GM/GCL/CCL composite primary liners during the active period of operation and during the post-closure period. E_a values were not calculated for the initial period of operation because leachate breakthrough times for CCL or GCL/CCL components of the primary liners were generally estimated to be greater than the initial period of operation. Calculated E_a values are also presented in Table E-4.8. As can be seen in this table, E_a values ranged from 54.5 to 100.0% during the active period of operation, and from a negative value to 97.2% during the post-closure period. These E_a values are lower than corresponding values for GM/GCL composite primary liners, due to the presence of consolidation water in the LDS. For comparison, E_a values for GM/GCL liners ranged from 96.7 to 100% during the active period and 98.8 to 100% during the post-closure period. Negative E_a values for Cell AD1 imply higher LDS than LCRS flow rates, a consequence of continuing CCL consolidation and/or secondary compression after cell closure. Additional observations with respect to the LDS flow rate data and calculated E_a values for GM/CCL and GM/GCL/CCL composite liners are given below.

- Consolidation water flow rates are dependent on the thickness and hydraulic properties of the CCL and the rate of overlying waste placement. LDS flows from this source may increase or decrease over time depending on the filling schedule for the landfill cell. For most facilities, the filling schedule results in relatively large LDS flow rates early in the active period. Average monthly flow rates during the active period may initially be as high as 200 to 400 lphd, with flows attributed primarily to consolidation water. Average LDS flow rates in the range of 0 to 50 lphd are not uncommon in the latter active life and after closure, although flow rates of more than 100 to 200 lphd are occasionally observed. Continuing low rates of LDS flow after closure are attributed primarily to continuing consolidation or secondary compression of the CCL component of the composite liner.

- While LDS flow rates tend to decrease with time, E_a values may increase or decrease with time depending on the relative rates of decrease of LCRS flow versus LDS flow. For example, E_a values for Cell B3 were initially in the range of 96 to 99%, but decreased to about 80% after 5 to 8 years due to steady LDS flow rates and decreasing LCRS flow rates. For one cell (AD1), E_a values became negative.
- The highest value of E_a was achieved by Cell AM2 at a time period of about four years after the start of cell operations. For this cell, an E_a value of 100% was achieved under a condition of very low rates of LCRS flow (i.e., <100 lphd) during a period when overlying waste placement had ceased. Interestingly, the AM landfill is located in the W in a semi-arid environment. Leachate generation rates at this MSW landfill are, on average, an order of magnitude lower than the rates for the other facilities, all of which are located in the much wetter climate of the eastern U.S.
- The only GM/CCL or GM/GCL/CCL composite primary liner for which primary liner leakage rates and E_t values can be estimated from LDS flow rate data alone is for Cell AM2. For this facility, zero leakage and an E_t value of 100% was achieved for the low LCRS flow rate conditions noted above. Due to the interfering effects of consolidation water, LDS flow data for the other facilities do not alone allow conclusions on E_t values to be drawn. LCRS and LDS chemical constituent data are reviewed below to develop further insight into E_t values for GM/CCL and GM/GCL/CCL composite liners.

E-4.3.3.3 Analysis of Chemical Data

Concentrations of chemical constituents in LDS liquids are compared to concentrations of the same constituents in LCRS liquids for cells with GM/CCL or GM/GCL/CCL composite liners in Table E-4.9. As indicated by the data in Table E-4.9, the general water quality characteristics of LDS liquids are different than the corresponding characteristics for the LCRS liquids. This is due to the different origins of the primary sources of the two liquids, leachate for the LCRS liquids and CCL pore water for the LDS liquids. The different origins of the two liquids are reflected in different major ion chemistries, as well as differences in COD, BOD and TOC concentrations. Figures E-4.2 through E-4.6 present Piper (1944) trilinear diagrams for six of the cells listed in Table E-4.9. These diagrams demonstrate the different primary sources of LCRS and LDS liquids from a given cell. Details for the construction and interpretation of Piper trilinear diagrams can be found in most hydrogeology and geochemistry textbooks.

To further evaluate whether primary liner leakage had contributed to the observed LDS flows, the concentrations of five key chemical constituents in the LCRS and LDS flows were investigated. Several factors were considered in selecting the key constituents: (i) common occurrence in leachate; (ii) high solubility in water and low octanol-water coefficient; and (iii) high resistance to hydrolization and anaerobic biodegradation in soil. Several chemicals that were considered as candidates due to their aqueous solubility characteristics, notably several alcohols and ketones and methylene chloride, could not

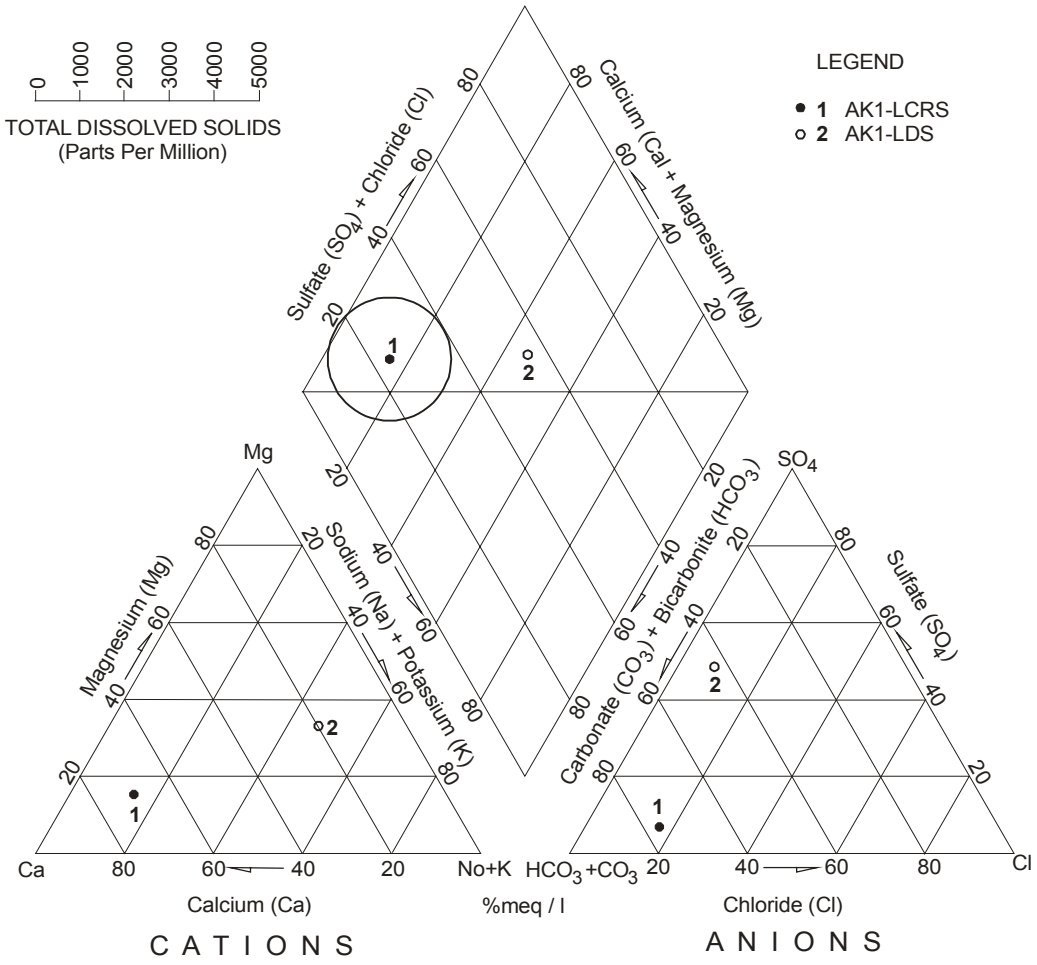

Figure E-4.2. Piper trilinear diagram for cell AK1.

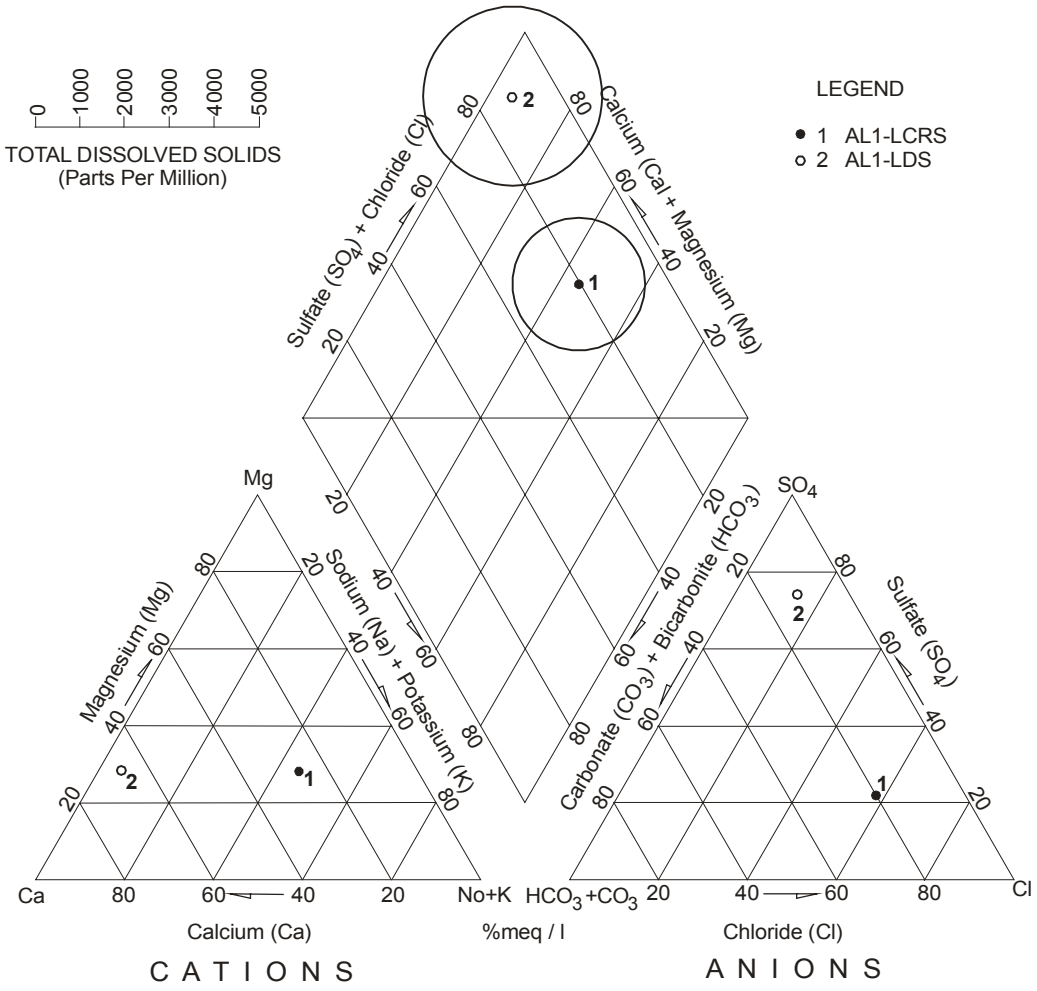

Figure E-4.3. Piper trilinear diagram for cell AL1.

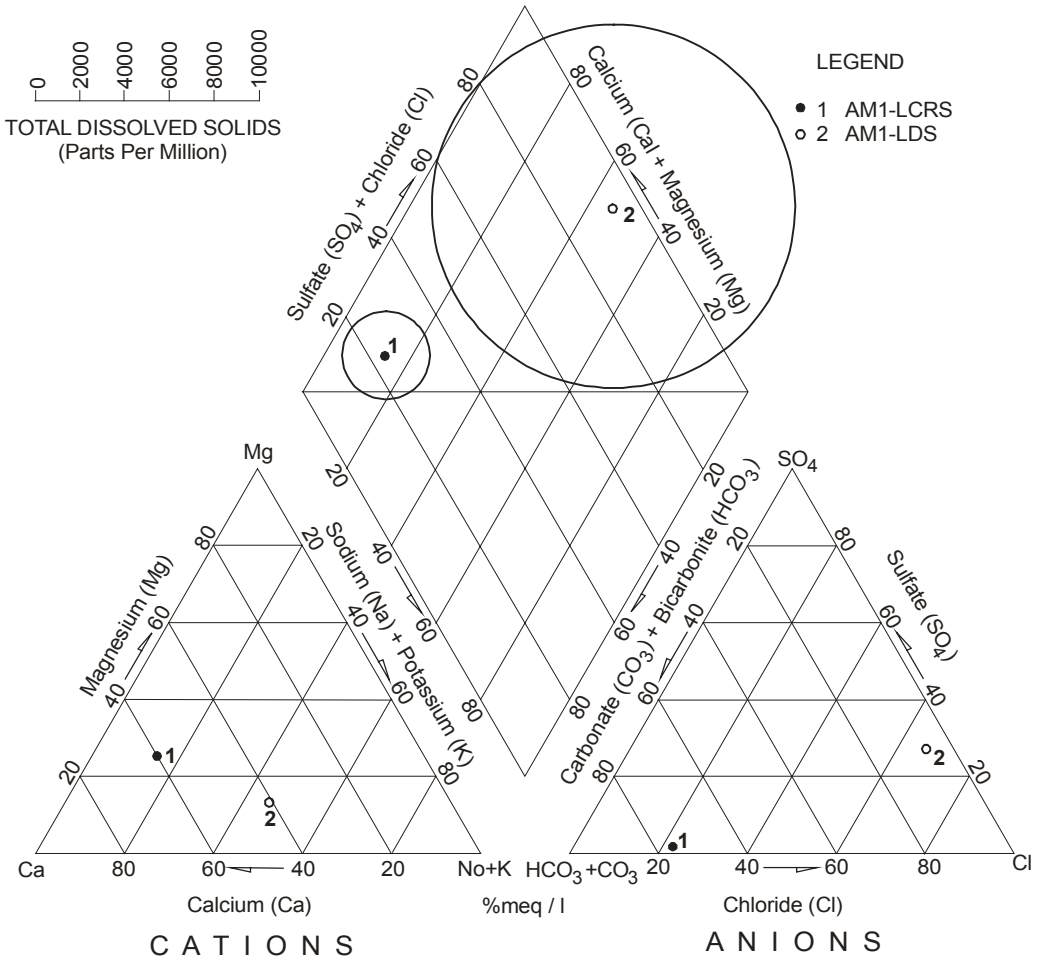

Figure E-4.4. Piper trilinear diagram for cell AM1.

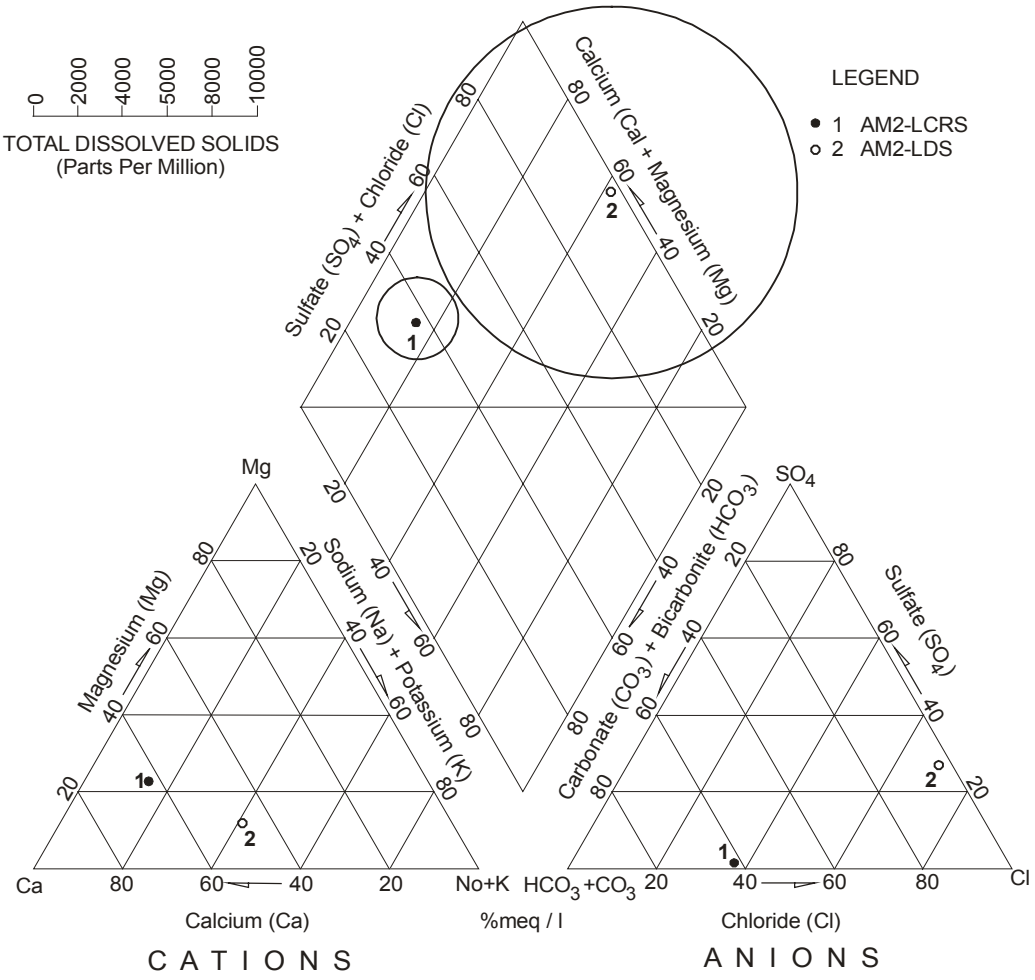

Figure E-4.5. Piper trilinear diagram for cell AM2.

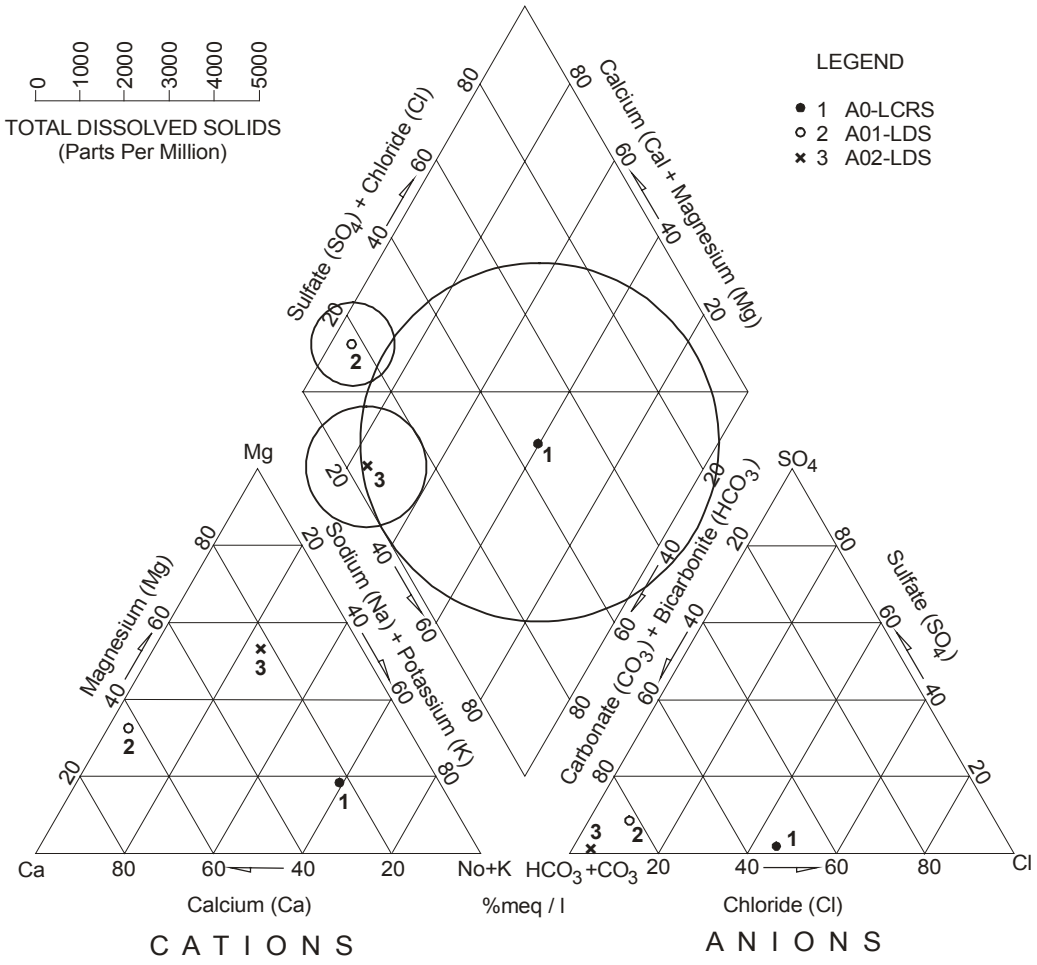

Figure E-4.6. Piper trilinear diagram for cell AO1 and AO2.

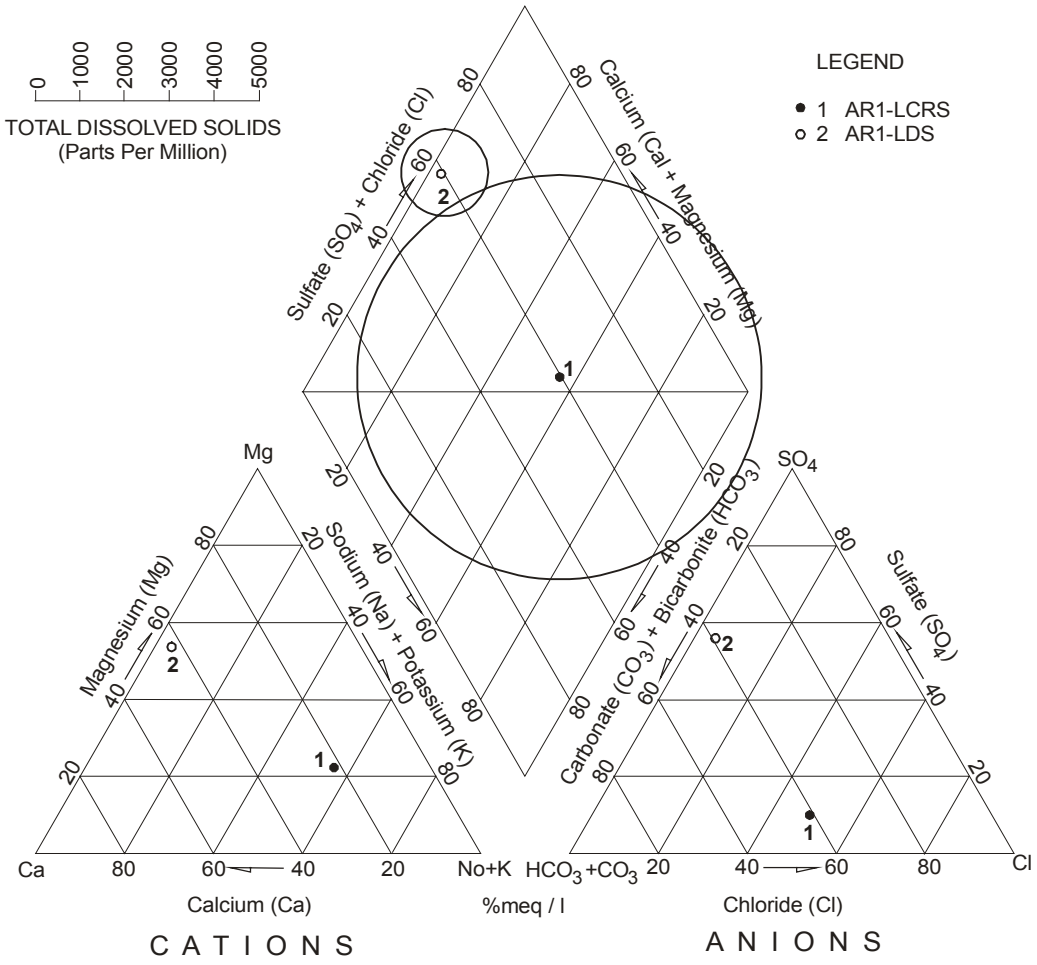

Figure E-4.7. Piper trilinear diagram for cell AR1.

be used due to poor representation in the database or potential for presence in the database as a laboratory contaminant. The five selected key constituents are the inorganic anions sulfate and chloride and the aromatic hydrocarbons benzene, toluene, and xylene. The results of the comparison of key constituents are presented in Tables E-4.11 and E-4.12. Table E-4.11 presents the concentrations of the five key constituents as a function of time period after the start of landfill cell operation. These time periods roughly correspond to the monitoring time periods given in Table E-4.8. Table E-4.12 presents the results of the authors' assessment of the occurrence of key constituent migration through the composite primary liners. This assessment is based on a qualitative comparison of the five key chemical constituents previously identified. Table E-4.12 also presents an estimate of the advective breakthrough time for the CCL or GCL/CCL component of each composite primary liner. The estimated breakthrough times were calculated assuming that the GM component of the composite primary liner has one or more holes through which leachate instantaneously migrates and that leachate migration through the CCL or GCL/CCL component of the composite liner is governed by Darcy's equation assuming one-dimensional steady-state saturated flow. Other assumptions used in the calculations are given in the table. The effect of chemical retardation was not considered in calculating the advective breakthrough times. Retardation of chloride and sulfate should be negligible. Retardation characteristics for benzene, toluene, and xylene will depend on the organic carbon content of the CCL or GCL, redox conditions, and other factors. It is expected, however, that the effective retardation coefficient for these constituents would have been 2 or more. These organic compounds were chosen for analysis notwithstanding their retardation characteristics for a combination of reasons, including relatively widespread occurrence in leachate, and relatively higher concentrations in leachate than other organic compounds. In addition, these three constituents are not known as laboratory contaminants, in contrast to methylene chloride, a constituent that is more mobile but is also a common laboratory contaminant.

The current database is not sufficient to draw definitive conclusions on the performance of GM/CCL and GM/GCL/CCL composite liners. However, using the data and comparisons in Tables E-4.11 and E-4.12, the following observations can be offered with respect to key chemical constituent migration through the composite primary liners:

- Three of the 13 considered landfill cells with GM/CCL or GM/GCL/CCL composite primary liners (i.e., Y2, AQ1, and AQ10) have insufficient chemical data to draw any conclusions on primary liner leakage rates based on the key chemical constituent data. The three cells exhibited average monthly LDS flow rates of 18 to 215 lphd for the active life and post-closure periods, with most values being less than 100 lphd. These flow rates are comparable to rates for the other cells included in the database for similar operational stages (except cells AM1 and AM2, located in a semi-arid climate). Based on this observation, and on calculation results for long-term consolidation and secondary compression (see Gross et al. (1990)), the observed flows are attributed primarily to consolidation water and not primary liner leakage. The potential

Table E-4.11. Average Concentrations of Five Key Chemicals in LCRS and LDS Flows from Landfill Cells with Composite Top Liners.

Cell No.	Time Period (months)	Chemical[1] Sulfate (mg/l)		Chloride (mg/l)		Benzene (µg/l)		Toluene (µg/l)		Xylene (µg/l)	
		LCRS	LDS	LCRS	LDS	LCRS	LDS	LCRS	LDS	LCRS	LDS
B3	1-4	282	95	25	19	<11[2]	<25	150	<25		
	5-16	105	1286	207	173	<1	<1	<1	<1		
	17-28	348		352	241	<1		<1			
	29-40	104	500	580	118	<5	<5	354	<6		
	41-52	47	14	355		8	6	233	24		
	53-64	28	123	899	59	7	<1	101	<1		
	65-76	<127	90	203	58	<5	<5	14	<6		
	77-88	<6	301	998		<5	<5	<5	<4		
	89-93		48	1383		<2	<5	<1	<1		
Y2	1-10	108	231	349	60						
	11-22	108	299	590	25	10		720	7		
	23-34	52	326	876	89						
	35-46										
	47-54										
AK1	1-12	47	16	104	2	<5	<1	88	<1	30	<3
AL1	1-29	300	1030	330	89	<4	<2	133	<1 [3]	540	<1
	30-41	225	900	273	203	1	<1	5	<1	<3	
	42-54	247	1375	400	215	2	<1	2	<1	<3	<1
AM1	1-9	51		77		<21		219		150	
	10-21	<2		120		18	<1	160	2	90	<1
	22-33	<16	1341	159	2260	19	<1	336	<1	121	<1
	34-45	<27	1200	219	2600	18	<1	290	<1	122	<3
	46-57	<12		265		10		199		90	
	58-69	<3		240		13		56		82	
AM2	1-9	96		140		11		22		34	
	10-21	<2		290		17	<1	89	<1	57	<2
	22-33	<13	1032	353	2175	19	<1	266	<1	95	<1
	34-45	<7	1300	326	2600	<18	<1	286	<1	94	<3
	46-57	<2	1730	368	2700	15	<1	148	<1	<115	<2
	58-69	<3	2405	262	2635	7	<1	65	<1	50	<2

Table E-4.11. Average Concentrations of Five Key Chemicals in LCRS and LDS Flows from Landfill Cells with Composite Top Liners (Continued).

Cell No.	Time Period (months)	Chemical									
		Sulfate (mg/l)		Chloride (mg/l)		Benzene (µg/l)		Toluene (µg/l)		Xylene (µg/l)	
		LCRS	LDS	LCRS	LDS	LCRS	LDS	LCRS	LDS	LCRS	LDS
AO1	1-5										
	6-17	49	88	930	58	6	<1	230	<1	59	<3
	18-29	35	41	988	27	10	<1	288	44	45	<3
	30-37	69	2	570	46	<5	<5	77	<5	21	<10
AO2	1-5										
	6-17	49	89	930	16	6	<1	230	<1	59	<3
	18-31	35	93	988	24	10	<1	288	<1	45	<4
AR1	1-11	180	600	1000	49						
	12-23	440	170	2200	8		<1		<2		<4
	24-36	520	265	1650	41	<100	<50	<100	<50	<100	<50
AD1	1-12	6353		3930		492		305			
	13-20	5830		24300	289	429	<4	292	<6		
	21-32	5470	480	10763	210	33	<4	133	<6		
	33-44	4455	498	11590	185	5	<4	60	<6		
	45-51	2223	308	13960	217	35	<4	108	<6		
	52-63		443		240		<4	<300	<6		
	64-75		338		131		<4		<6		
	76-87	1785	456	13900	377		<4		<6		
	88-99	4488	339	14550	137	26	<4	186	<6		
	100-111	3633	296	14075	114	18	<1	<30	<1		
	112-121	3870	369	14800	138	<25	<1	<25	<1		
AD7	1-12	2818	340	3214	109	140	<4	317	<6		
	13-24	3620	683	9550	216	612	<4	892	<6		
	25-36	7361	586	10720	219	1168	<4	1859	<6		
	37-48	8213	954	11535	469	644	<4	2960	<6		
	49-60	6867	1050	14400	418	778	<4	1660	<6		
	61-69	5740	1148	15775	387	687		1288	<6		
	70-81	6998	1168	12875	387	540	<4	906	<1		
	82-87	7480	1132	14267	357	<240	<1	450	<1		

Table E-4.11. Average Concentrations of Five Key Chemicals in LCRS and LDS Flows from Landfill Cells with Composite Top Liners (Continued).

Cell No.	Time Period (months)	Chemical									
		Sulfate (mg/l)		Chloride (mg/l)		Benzene (µg/l)		Toluene (µg/l)		Xylene (µg/l)	
		LCRS	LDS	LCRS	LDS	LCRS	LDS	LCRS	LDS	LCRS	LDS
AQ1	1-58										
	59-65					<5	<4	<5	<10		
	66-77					<8	<4	<5	<6	<5	
	78-89					<12	<4	<5	<14	<8	
	90-97					<5	<4	<5	<5	<5	
AQ10	1-15										
	15-26					<10	<4	<12	<5		
	27-38					<10	<4	<30	<5	190	
	39-50					<6	<4	<6	<5	<7	
	51-63					<5	<4	5	<5	10	

Notes:

(1) Reported concentrations represent average of 1 to 17 individual analysis results (typically on the order of 5) during incremental reporting period.

(2) Data preceded by "<" indicates more than half or more of the measurements for the parameter were reported as non-detects; in calculating average values, half of the test detection limit was conservatively used for all results reported as non-detects.

(3) For Cell AL1, toluene was not detected in nine of ten LDS flow samples obtained during the 1-41 months time period. Toluene was detected at a concentration of 91 µg/l in month 30. This one detection is attributed to sampling or analysis error.

Table E-4.12. Evaluation of Chemical Constituent Migration Through Landfill GM/CCL and GM/GCL/CCL Composite Primary Liners.

Cell No.	Monitor. Period (months)	Estimated Advective Breakthr. Time for GCL/CCL (months)[1]	Chemical					Summary of Observations for Five Key Constituents
			Sulfate	Chloride	Benzene	Toluene	Xylene	
B3	93	46	not diagnostic due to fluctuating C_o[2] in both LCRS and LDS	lower C_o in LDS than in LCRS and trend of decreasing LDS C_o with time not indicative of chloride breakthr.	not diagnostic due to very low C_o in both LCRS and LDS (i.e., C_o almost always below DL[3] of 5 μg/l)	in LCRS, C_o up to 700 μg/l; in LDS, C_o typically below DL of 1 to 10 μg/l; no indication of toluene breakthr.	no data available	no evidence of significant leachate migration into LDS after almost 8 years of cell operation, twice the estimated CCL breakthr. time
Y2	54 (no key chemical data after 34 months)	35	not diagnostic due to high C_o in LDS consol. water	in LCRS, C_o = 170 to 1,160 mg/l with m[2] = 628 mg/l; in LDS, C_o = 8 to 140 mg/l with m = 58 mg/l; no indication of chloride breakthr.	no LDS data available	only one C_o available from each system (at 11-22 months): LCRS C_o = 720 μg/l and LDS C_o = 7 μg/l	no data available	data are insufficient to draw conclusions; monitor. period is about equal to estimated CCL breakthru. time; more chemical data are needed

Table E-4.12. Evaluation of Chemical Constituent Migration Through Landfill GM/CCL and GM/GCL/CCL Composite Primary Liners (Continued).

Cell No.	Monitor. Period (months)	Estimated Advective Breakthr. Time for GCL/CCL (months)(1)	Chemical					Summary of Observations for Five Key Constituents
			Sulfate	Chloride	Benzene	Toluene	Xylene	
AK1	12	48	in LCRS, C_o = 7 to 110 mg/l with m = 47 mg/l; in LDS, C_o = 10 to 51 mg/l with m = 16 mg/l; no indication of sulfate breakthr.	in LCRS, C_o = 2 to 230 mg/l with m = 104 mg/l; in LDS, C_o = 2 to 6 mg/l with m = 4 mg/l; no indication of chloride breakthr.	not diagnostic because C_o is below DL in both LCRS and LDS	in LCRS, C_o = 5 to 300 μg/l with m = 88 μg/l; in LDS, C_o below DL of 1 μg/l; no indication of toluene breakthr.	in LCRS, xylene detected in half of sampling events at C_o up to 79 μg/l; in LDS, C_o below DL of 3 μg/l; no indication of xylene breakthr.	no evidence of significant leachate migration into LDS; however, monitor. period is only about 1/4th of the estimated GCL/CCL breakthr. time; more chemical data are needed
AL1	54	70	not diagnostic due to high C_o in LDS consol. water	increasing LDS C_o with time likely due to decreasing dilution of consol. water by construct. water	not diagnostic because C_o is below DL in both LCRS and LDS	in LCRS, C_o = up to 600 μg/l; in LDS, toluene below DL of 1 μg/l; no indication of toluene breakthr.	not diagnostic because C_o is below DL in LDS and in LCRS too after 29 months	no evidence of significant leachate migration in to LDS; monitor. period somewhat less than estimated CCL breakthr. time; more chemical data are needed

Table E-4.12. Evaluation of Chemical Constituent Migration Through Landfill GM/CCL and GM/GCL/CCL Composite Primary Liners (Continued).

Cell No.	Monitor. Period (months)	Estimated Advective Breakthr. Time for GCL/CCL (months)[1]	Chemical					Summary of Observations for Five Key Constituents
			Sulfate	Chloride	Benzene	Toluene	Xylene	
AM1	58	4	not diagnostic due to high C_o in LDS consol. water	not diagnostic due to high C_o in LDS consol. water	in LCRS, C_o = 12 to 20 μg/l; in LDS, C_o below DL of 1 μg/l; no indication of benzene breakthr.	in LCRS, C_o = 40 to 420 μg/l with m = 267 μg/l; in LDS, C_o below DL of 1 μg/l; no indication of toluene breakthr.	in LCRS, C_o = 71 to 150 μg/l with m = 122 μg/l; in LDS, C_o below DL of 1 to 3 μg/l; no indication of xylene breakthr.	no evidence of significant leachate migration into LDS after almost 5 years of cell operation; monitor. period more than 12 times longer than estimated CCL breakthr. time
AM2	58	4	not diagnostic due to high C_o in LDS consol. water	not diagnostic due to high C_o in LDS consol. water	in LCRS, C_o = 5 to 20 μg/l; in LDS, C_o below DL of 1 μg/l; no indication of benzene breakthr.	in LCRS, C_o = 10 to 400 μg/l with m = 146 μg/l; in LDS, C_o below DL of 1 μg/l; no indication of toluene breakthr.	in LCRS, C_o = 2 to 130 μg/l with m = 71 mg/l; in LDS, C_o below DL of 1 to 3 mg/l; no indication of xylene breakthr.	no evidence of significant leachate migration into LDS after almost 5 years of cell operation; monitor. period more than 12 times longer than estimated CCL breakthr. time

Table E-4.12. Evaluation of Chemical Constituent Migration Through Landfill GM/CCL and GM/GCL/CCL Composite Primary Liners (Continued).

Cell No.	Monitor. Period (months)	Estimated Advective Breakthr. Time for GCL/CCL (months)[1]	Chemical					Summary of Observations for Five Key Constituents
			Sulfate	Chloride	Benzene	Toluene	Xylene	
AO1[4]	37	140	not diagnostic due to similar LCRS and LDS C_o ranges	in LCRS, C_o = 320 to 1300 mg/l with m = 860 mg/l; in LDS, C_o = 7 to 100 mg/l with m = 40 mg/l; no indication of chloride breakthr.	in LCRS, benzene detected in half of the sampling events at C_o = 7 to 12 μg/l; in LDS, C_o below DL of 1 μg/l; no indication of benzene breakthr.	in LCRS, C_o = 10 to 550 μg/l with m = 167 μg/l; in LDS, C_o below DL of 1 μg/l in 2/3 of sampling events; no indication of toluene breakthr.	in LCRS, C_o = 12 to 76 μg/l with m = 34 μg/l; in LDS, C_o below DL of 3 μg/l; no indication of xylene breakthr.	no evidence of significant leachate migration into LDS after 3 years of cell operation; however, monitor. period is only 1/4th of estimated CCL breakthr. time; more chemical data are needed
AO2[4]	31	145	not diagnostic due to similar LCRS and LDS C_o ranges	in LCRS, C_o = 320 to 1,300 mg/l with m = 862 mg/l; in LDS, C_o = 3 to 34 mg/l with m = 24 mg/l; no indication of chloride breakthr.	in LCRS, benzene detected in half of the sampling events at C_o = 7 to 12 μg/l; in LDS, C_o below DL of 1 μg/l; no indication of benzene breakthr.	in LCRS, C_o = 10 to 550 μg/l with m = 167 μg/l; in LDS, C_o below DL of 1 μg/l; no indication of toluene breakthr.	in LCRS, C_o = 12 to 76 μg/l with m = 34 μg/l; in LDS, C_o below DL of 3 μg/l; no indication of xylene breakthr.	no evidence of significant leachate migration into LDS after 3 years of cell operation; however, monitor. period is only 1/4th of estimated CCL breakthr. time; more chemical data are needed

Table E-4.12. Evaluation of Chemical Constituent Migration Through Landfill GM/CCL and GM/GCL/CCL Composite Primary Liners (Continued).

Cell No.	Monitor. Period (months)	Estimated Advective Breakthr. Time for GCL/CCL (months)(1)	Chemical					Summary of Observations for Five Key Constituents
			Sulfate	Chloride	Benzene	Toluene	Xylene	
AR1	36	2	not diagnostic due to similar LCRS and LDS C_o ranges	in LCRS, C_o = 600 to 2700 mg/l with m = 1625 mg/l; in LDS, C_o = 8 to 74 mg/l with m = 35 mg/l; no indication of chloride breakthr.	not diagnostic because C_o is below DL in both LCRS and LDS	not diagnostic because C_o is below DL in both LCRS and LDS	not diagnostic because C_o is below DL in both LCRS and LDS	no evidence of significant leachate migration into LDS; monitor. period is more than 10 times the estimated GCL/CCL breakthr. time; data are not diagnostic; more data are needed
AD1	121	70	in LCRS, C_o = 1,785 to 6,353 mg/l with m = 4,234 mg/l; in LDS, C_o = 296 to 498 mg/l with m = 392 mg/l; no indication of sulfate breakthr.	in LCRS, C_o = 3,930 to 24,300 mg/l, with m = 13,450 mg/l; in LDS, C_o = 114 to 337 mg/l, with m = 204 mg/l; no indication of chloride breakthr.	in LCRS, C_o = <25 to 492 μg/l; in LDS, C_o below DL of 1 to 4 μg/l; no indication of benzene breakthr.	in LCRS, C_o = <25 to 305 μg/l; in LDS, C_o below DL of 1 to 6 μg/l; no indication of toluene breakthr.	no data available	no evidence of significant leachate migration into LDS after 10 years of cell operation and closure, 1.7 times more than the estimated CCL breakthr. time

Table E-4.12. Evaluation of Chemical Constituent Migration Through Landfill GM/CCL and GM/GCL/CCL Composite Primary Liners (Continued).

Cell No.	Monitor. Period (months)	Estimated Advective Breakthr. Time for GCL/CCL (months)(1)	Chemical					Summary of Observations for Five Key Constituents
			Sulfate	Chloride	Benzene	Toluene	Xylene	
AD7	87	70	in LCRS, C_o=2,818 to 8,213 mg/l with m=6,137 mg/l; in LDS, C_o=340 to 1,168 mg/l with m=882 mg/l; increasing LDS C_o after 36 months attributed to decreasing dilution of consol. water by construct. water	in LCRS, C_o=3,214 to 15,775 mg/l with m=11,547 mg/l; in LDS, C_o=109 to 469 mg/l with m=320 mg/l; increasing LDS C_o after 36 months attributed to decreasing dilution of consol. water by construct. water	in LCRS, C_o = <240 to 1,168 μg/l; in LDS, C_o below DL of 1 to 4 μg/l; no indication of benzene breakthr.	in LCRS, C_o = 317 to 2,960 μg/l; in LDS, C_o below DL of 1 to 6 μg/l; no indication of toluene breakthr.	no data available	evidence of possible breakthr. for sulfate & chloride at 12-36 months; authors attribute trend to decreased dilution of consol. water by construct. water; no evidence of organic constituent breakthr.; more chemical data are needed

Table E-4.12. Evaluation of Chemical Constituent Migration Through Landfill GM/CCL and GM/GCL/CCL Composite Primary Liners (Continued).

Cell No.	Monitor. Period (months)	Estimated Advective Breakthr. Time for GCL/CCL (months)(1)	Chemical					Summary of Observations for Five Key Constituents
			Sulfate	Chloride	Benzene	Toluene	Xylene	
AQ1	97	35	no data available	no data available	not diagnostic because C_o is below DL in both LCRS and LDS	not diagnostic because C_o is below DL in both LCRS and LDS	no LDS data available	data are insufficient to draw conclusions; more data are needed
AQ10	63	35	no data available	no data available	not diagnostic because C_o is below DL in both LCRS and LDS	not diagnostic because C_o is below DL in both LCRS and LDS	no LDS data available	data are insufficient to draw conclusions; more data are needed

Notes:

(1) Advective breakthrough times for steady-state saturated flow through CCL or GCL/CCL component of composite liners were calculated using Darcy's equation and specified hydraulic conductivities, hydraulic gradient of 5 for GCLs and 1 for CCLs, and effective porosity of 0 For this calculation, it is assumed that flow through the GM component of the composite liner occurs through small holes and is instantan

(2) C_o = average concentration during incremental reporting period; m = mean concentration for the entire reporting period.

(3) DL = detection limit.

(4) Composite liquid quality samples were collected from the LCRSs of Cells AO1 and AO2; these samples are assumed to represent average conditions at the two cells.

occurrence of primary liner leakage cannot be ruled out, however, because of insufficient chemical data.

- Of the ten remaining landfill cells considered in this study, none exhibited obvious evidence of primary liner leakage. One of these cells (AD7) exhibited a potential indication of primary liner leakage when sulfate and chloride concentrations in LDS flows increased between 12 and 36 months after construction. However, the concentrations of other chemicals did not increase over time. The estimated breakthrough time for the composite primary liner is 70 months, several times greater than the time when sulfate and chloride concentrations increased. The increase in concentration of these anions without an increase in concentration of the organic chemicals would suggest that the source of the LDS flow is not leakage and that the increasing anion concentrations could be attributed to decreasing dilution of consolidation water over time by construction water. However, Cell AD7 has a GN LDS, which should not release much construction water. Also, if construction water was significant, a similar trend would be expected for Cell AD1 from the same facility. Though Cell AD1 has a sand LDS, which can release significant amounts of water during cell operations, a similar trend was not observed. Thus, the reason for the increase in anion concentrations for Cell AD7 is unclear.
- Five of the cells in this study (B3, AD1, AD7, AM1, and AM2) have key constituent data of sufficient completeness and duration to conclude that leachate migration into the LDS at a rate of any engineering significance has not occurred for a time period exceeding the estimated breakthrough time for the CCL component of the composite liner. Cell B3 has a monitoring period of almost 8 years, about twice the estimated CCL breakthrough time. The LDS flow from Cell B3 exhibited a general trend of decreasing chloride concentrations with time while chloride concentrations in the LCRS tended to increase. Also, while toluene concentrations as high as 700 μg/l were detected in LCRS flow, there was no clear indication of toluene breakthrough into the LDS. Cells AM1 and AM2 have a monitoring period of almost 6 years, approximately 17 times longer than the estimated CCL breakthrough time. Concentrations of benzene, toluene, and xylene in the leachate are generally in the 10 to 300 μg/l range throughout the monitoring period; LDS concentrations for these three key constituents are below the detection limit of 1 to 3 μg/l in all cases. Cell AD1 has a monitoring period of 10 years, approximately 70% longer than the estimated CCL breakthrough time. Sulfate, chloride, benzene, and toluene data all exhibit relatively high concentrations in the LCRS of this HW cell, with no indication of breakthrough for any of these constituents. Cell AD7 has a monitoring period of about seven years with no indication of benzene or toluene breakthrough.
- E_t values can be estimated for Cells B3, AM1, AM2, AD1, and AD7 by substituting the flow rate terms in Equation E-1 with constituent mass fluxes from the LCRS and LDS. Mass fluxes were calculated using average flow rates and chemical concentrations for benzene, toluene, and xylene during the active operation and post-closure stages. The precision of this approach is limited by the detection limits of the chemical analytical methods used. For the

calculations, key constituent concentrations were taken as one-half of the reported value where preceded by "<" in Table E-4.11. The approach also assumes that all key constituents are conserved in solution during transport through the composite primary liner and that all of the constituent mass in the LDS is from the LCRS. Using this approach, the Cell B3 composite liner achieved an average E_t of 99.8% through the active and post-closure period, Cells AM1 and AM2 achieved average E_t values in excess of 99.9 and 99.5%, respectively, and Cells AD1 and AD7 achieved average E_t values of 99.1 and greater than 99.9%, respectively.

E-4.3.4 Comparison to Liner Leakage Calculation Results

Giroud and Bonaparte (1989), and Giroud et al. (1992) presented equations for calculating steady-state leakage rates through holes in the GM component of GM/CCL and GM/GCL composite liners, respectively. Input parameters to the equations are the hydraulic head acting on the liner, saturated hydraulic conductivity of the CCL or GCL, number and size (area) of holes in the GM, and average hydraulic gradient across the GM. Calculation results for a range of conditions are given in Table E-4.13. Calculation results are given for two different conditions of contact between the GM and CCL or GCL components of the composite liner: (i) good contact; and (ii) poor contact. These contact conditions are described in Table E-4.13. The calculated leakage rates can be compared to the observed LDS flow rates for cells with composite primary liners summarized above:

- LDS flow rates reported in this appendix for the active life and post-closure period of landfill cells with GM/GCL composite primary liners (except Cell I4) are in the range of 0 to 10 lphd, with most values less than 2 lphd and many values reported as zero (Table E-4.7). From Table E-4.13, calculated steady-state leakage rates for this type of composite liner are in the range of 0.007 to 4 lphd.
- True liner efficiencies (E_t) may exceed 99.9% for GM/CCL and GM/GCL composite liners, particularly at higher LCRS flow rates. This value of E_t would result in composite liner leakage rates of 0.1, 1, and 10 lphd, respectively, for LCRS flow rates of 100, 1,000, or 10,000 lphd. These primary liner leakage rates can be compared to calculated values of 0.05 to 5 lphd for GM/CCL composite liners and 0.007 to 4 lphd for GM/GCL composite liners.

The calculated leakage rates presented in Table E-4.13 are in the same range as the primary liner leakage rates estimated from the data presented in this appendix. These results do not in themselves validate the liner leakage calculation models due to the assumptions and limitations in calculation model development. Also, there is no way to know a priori when a cell liner will have a hole through which leakage can occur and where the hole will be located, e.g., at a critical location such as the sump, or at a less critical location in upgradient portions of the cell. However, the fact that the calculations and monitoring data provide a consistent interpretation of composite liner hydraulic performance is a useful finding.

Table E-4.13. Calculated Steady-State Leakage Rates Through Composite Liners (in lphd).[1]

Composite Liner Type	CCL or GCL Hydraulic Conductivity (m/s)	Hydraulic Head (m)			
		0.01	0.03	0.1	0.3
GM/CCL (Poor contact conditions)[2]	1×10^{-9}	0.3	0.8	2	5
GM/CCL (Good contact conditions)[3]	1×10^{-9}	0.05	0.2	0.4	1
GM/GCL (Poor contact conditions)	5×10^{-11}	0.04	0.1	0.7	4
GM/GCL (Good contact conditions)	5×10^{-11}	0.007	0.03	0.1	0.7

Notes:
(1) Calculations are based on 2.5 GM holes per hectare. Area of each hole assumed to be 10 mm^2. Calculations performed using equations from Giroud and Bonaparte (1989) and Giroud et al. (1992).
(2) Good contact conditions correspond to a GM installed with relatively few wrinkles, placed on top of a CCL that has been adequately compacted and has a smooth surface, or a GCL with a smooth surface.
(3) Poor contact conditions correspond to a GM installed with a certain number of wrinkles, placed on top of a CCL that has not been adequately compacted and does not appear smooth, and/or placed on a GCL that is wrinkled.

E-4.3.5 Implications for Landfill Performance

The evaluation results presented in this section are encouraging with respect to the types of composite liners used widely in landfills throughout the U.S. Leakage rates through these types of composite liners appear to be very low, typically less than 2 lphd for GM/GCL composite liners. Conversely, E_t values appear to be very high. E_t values of 99.9% or more, particularly at higher rates of LCRS flow, are achievable. Coupling this conclusion with that from Section E-4.2 that the frequencies of holes in GMs decrease when third-party CQA programs are employed in landfill cell construction, and also with available guidance for the installation of geosynthetic and natural soil liner components (e.g., Daniel and Koerner (1995)), provides a framework for reliably achieving high levels of composite liner performance.

It is also noteworthy that composite liners with CCL components have advective transport breakthrough times that are long relative to the timeframe for leachate generation in a modern landfill cell operated to: (i) minimize leachate generation; (ii) remove leachate as it is generated; and (iii) "close as you go" using a final cover system that limits the infiltration of precipitation into the landfill. In the U.S., landfill cells are typically operated for periods of one to five years, occasionally longer, and they are promptly covered with a GM or other low-permeability barrier after filling. This operations sequence defines the timeframe for significant leachate generation in a landfill cell that does not contain liquid wastes or sludges and that does not undergo leachate recirculation or moisture addition. For the cells in this study, estimated advective breakthrough times through CCLs, assuming no chemical retardation, were generally calculated to range from about 3 to 12 years. It thus appears that for modern facilities that are properly constructed and operated, GM/CCL and GM/GCL/CCL composite liners can prevent leachate leakage of any engineering significance through the liner over the entire time period of leachate generation. For cells with GM/GCL liners, breakthrough times are anticipated to be faster than for cells with GM/CCL liners.

E-5 Leachate Generation Rates

E-5.1 Overview

The rate of leachate generation in a landfill is expected to be a function of several factors including: (i) the operational stage of the landfill (i.e., initial period of operation vs. active period of operation vs. post-closure period); (ii) the type of waste placed in the landfill (MSW vs. HW vs. ISW); (iii) the condition of the waste at the time of placement (i.e., moisture content and density); (iv) the geographical region of the U.S. in which the landfill is located (i.e., NE vs. SE vs. W); and (v) waste placement practices (i.e., size of the active waste disposal area, characteristics of daily and intermediate covers, and extent of storm water diversion away from the landfill active area). These factors can have significant impacts on the volume of leachate generated from a landfill, and therefore, on potential impacts to the surrounding environment and on the costs of leachate collection and treatment. In this section, leachate generation rates are

evaluated for the landfills included in the current database and some of the factors that influence leachate generation rates are identified. It is noted that a few of the factors mentioned above which may affect leachate generation rates can not be evaluated using the current database (e.g., waste placement practices). Thus, this section concentrates on evaluating the effect of landfill operational stage, waste type, and geographic region on leachate generation rates.

E-5.2 Description of Data

Average and peak monthly LCRS flow rates are provided in Table E-3.5 for the initial and active periods of operation and for the post-closure period. The LCRS flow rates are presented for approximately twelve-month increments. Tables E-5.1 through E-5.5 include summaries of the LCRS flow rates organized by type of waste and region of the landfill. Tables E-5.1 through E-5.4 include data for the initial and active periods of operation for MSW, HW, ash, and C&DW landfills, respectively. Table E-5.5 includes data for the post-closure period for MSW and HW landfills.

Data are available during operation conditions for 73 individually monitored MSW cells from 32 landfills, 56 HW cells from twelve landfills, eight ash cells from six landfills, and three C&DW cells from two landfills. Most of the 50 landfills considered are located in the NE (32 landfills), and only four are located in the W. The available data covers between approximately one and eight years of landfill operation. Almost half of the cells had more than four years of LCRS flow rate data available. Table E-5.5 includes LCRS flow rate data for the post-closure period for eleven MSW cells at three landfills and 22 HW cells at five landfills. The data represents a maximum of six and nine post-closure years for MSW and HW cells, respectively. Half of the eight landfills are located in the NE and only one is located in the W (Landfill AT).

E-5.3 Analysis of Data

Tables E-5.1 through E-5.4 include summaries of data on LCRS flow rates measured during operations of 140 individually monitored cells located at 50 landfills. Average and peak monthly flow rates are reported for the initial and active periods of operation. The ratio (in %) of average LCRS flow rate to historical average annual rainfall is also calculated in these tables. This ratio is referred to herein as the rainfall fraction (RF).

For the 44 MSW cells located in the NE for which initial period of operation data are available, average LCRS flow rates varied between approximately 1,000 lphd and 40,000 lphd. Average LCRS flow rates were less than 10,000 lphd for approximately 60% of these 44 cells and greater than 20,000 lphd for only 14% of these cells. During the active period of operation average LCRS flow rates dropped significantly to a range of approximately 40 lphd to 18,000 lphd. For the 50 cells for which active period of operation data are available, 50% had average LCRS flow rates less than 2,500 lphd, 78% had average LCRS flow rates less than 5,000 lphd, and only 4% had LCRS flow rates greater than 10,000 lphd. Peak monthly LCRS flow rates were typically two to

Table E-5.1. LCRS Flow Rates for MSW Landfills During Operations.

Cell No.	Average Annual Rainfall (mm)	LCRS Flow Rates (lphd) During Operations							
		Initial Period				Active Period			
		Months	Average	Peak	Fraction of Rainfall (%)	Months	Average	Peak	Fraction of Rainfall (%)
(a) Landfills located in the NE									
B1	1,067	1-19	ND	ND		20-54	3,816	7,464	13
B2	1,067	1-19	ND	ND		20-54	2,954	5,707	10
B3	1,067	1-4	15,304	24,858	52	5-93	3,748	22,443	13
B4	1,067	1-12	2,930	6,353	10	13-47	4,022	14,641	14
B5	1,067	1-12	8,005	19,521	27	13-35	4,300	15,567	15
E1	1,041	1-7	ND	ND		8-40	9,035	36,177	32
E2	1,041	1-12	ND	ND		13-45	4,979	11,014	17
E3	1,041	1-12	9,425	25,394	33	13-14	6,062	9,038	21
E4	1,041	1-12	20,148	55,785	71	NA	NA	NA	
F1	584	1-12	14,472	45,010	90	13-30	8,608	25,450	54
G1-2	914	1-12	22,371	46,120	89	13-42	8,204	23,485	33
I1	991	1-8	ND	ND		9-84	4,149	48,932	15
I2	991	1-7	6,627	13,959	24	8-76	728	3,241	3
I3	991	1-7	11,559	21,081	43	8-76	3,684	26,339	14
I4	991	1-12	4,494	17,251	17	13-26	2,041	4,282	8
I5	991	1-12	3,938	7,985	15	13-21	3,108	11,669	11
J1-6	762	1-3	13,363	16,182	64	4-38	4,000	9,880	19
K1	1,118	1-12	17,808	24,832	58	13-66	9,036	27,663	29
Q1	889	1-7	39,864	111,129	164	8-48	7,263	21,862	30
R1	1,041	2-12	11,592	22,266	41	13-23	9,323	17,889	33
S1	1,041	1-10	2,226	5,081	8	11-45	1,124	4,074	4
T1-2	1,295	1-8	2,137	5,982	6	9-46	1,552	6,804	4
Y2	1,194	1-10	23,368	36,791	71	11-54	7,918	25,308	24
AA1	1,143	2-8	4,084	9,261	13	9-51	1,890	5,503	6
AA2-3	1,143	1-13	14,533	36,777	46	14-54	5,870	21,520	19
AE1-2	1,214	1-12	ND	ND		60-80	17,705	48,977	53
AG1	838	1-12	1,780	5,314	8	13-33	3,988	12,357	17
AJ1	1,245	2-6	17,133	24,782	50	7-13	4,728	9,936	14
AK1-2	762	1-12	9,867	17,983	47	13-15	2,398	3,130	11
AL1	787	1-12	ND	ND		30-54	1,150	5,885	5
AO1	826	1-5	ND	ND		6-36	1,485	4,130	7
AO2	826	1-5	15,881	24,541	70	6-30	2,331	5,266	10
AO3	826	1-8	16,746	53,117	74	NA	NA	NA	
AO4	826	1-8	20,017	55,470	88	NA	NA	NA	
AR1	1,143	1-11	27,042	65,871	86	12-36	10,428	26,274	33
AU1	1,016	1-4	ND	ND		21-32	4,991	11,597	18
AX1	1,041	1-2	16,718	19,738	59	3-33	540	2,383	2
AX2	1,041	1-5	15,521	58,674	54	6-33	281	570	1
AX3	1,041	1-5	3,361	7,985	12	6-56	307	1,075	1
AX4	1,041	1-12	2,534	12,688	9	13-56	75	187	0

Table E-5.1. LCRS Flow Rates for MSW Landfills During Operations (Continued).

Cell No.	Average Annual Rainfall (mm)	LCRS Flow Rates (lphd) During Operations							
		Initial Period				Active Period			
		Months	Average	Peak	Fraction of Rainfall (%)	Months	Average	Peak	Fraction of Rainfall (%)
(a) Landfills located in the NE (continued)									
AX5	1,041	1-11	1,384	3,394	5	12-80	56	191	0
AX6	1,041	1-9	3,759	7,171	13	10-78	168	655	1
AX7	1,041	1-10	5,376	12,155	19	11-76	234	851	1
AX8	1,041	1-14	4,881	21,038	17	15-71	439	1,384	2
AX9	1,041	1-9	1,047	3,478	4	10-65	41	159	0
AX10	1,041	1-7	2,786	13,698	10	8-59	374	645	1
AX11	1,041	1-16	4,675	14,586	16	17-62	150	337	1
AX12	1,041	1-12	3,494	8,836	12	13-56	768	3,029	3
AX13	1,041	1-7	6,683	14,343	23	8-53	1,408	9,294	5
AX14	1,041	1-11	2,777	6,582	10	12-38	281	449	1
AX15	1,041	1-12	5,573	11,809	20	13-37	299	561	1
AX16	1,041	1-10	8,601	17,756	30	11-29	819	5,096	3
AZ1	762	2-12	4,093	5,219	20	13-31	3,473	5,054	17
		Number	44	44	44	Number	50	50	50
		Min.	1,047	3,394	4	Min.	41	159	0
		Max.	39,864	111,129	164	Max.	17,705	48,977	54
		Mean	10,227	23,587	39	Mean	3,527	11,308	13
(b) Landfills located in the SE									
C1	1,118	1-9	ND	ND		10-56	332	1,419	1
C2	1,118	1-12	1,475	2,585	5	13-45	311	859	1
C3	1,118	1-8	3,417	9,558	11	9-41	301	987	1
C4	1,118	1-4	14,828	41,331	48	5-35	624	2,055	2
C5	1,118	1-12	6,419	12,528	21	13-26	2,513	10,440	8
C6	1,118	1-10	3,273	12,155	11	11-17	393	1,403	1
N1	1,524	1-12	ND	ND		13-75	1,862	17,597	4
N2	1,524	1-12	ND	ND		13-39	3,536	7,274	8
O1-2	1,499	1-6	ND	ND		7-64	5,987	16,467	15
V1-5	1,727	1-10	13,622	49,828	29	11-64	10,923	41,601	23
W1	1,499	9-12	7,492	8,799	18	13-35	1,856	6,365	5
W2	1,499	1-8	ND	ND		9-35	4,125	10,524	10
X1	1,016	1-7	43,693	111,031	157	8-33	3,913	14,315	14
AW1	1,118	1-12	6,358	20,570	21	ND	ND	ND	
AW2	1,118	1-12	3,555	7,480	12	ND	ND	ND	
BB1	1,092	1-6	10,378	22,130	35	7-47	2,494	8,983	8
BB2	1,092	1-11	ND	ND		12-23	5,422	14,042	18
BB3	1,092	1-11	ND	ND		12-23	2,284	7,945	8
		Number	11	11	11	Number	16	16	16
		Min.	1,475	2,585	5	Min.	301	859	1
		Max.	43,693	111,031	157	Max.	10,923	41,601	23
		Mean	10,410	27,090	33	Mean	2,930	10,142	8

Table E-5.1. LCRS Flow Rates for MSW Landfills During Operations (Continued).

Cell No.	Average Annual Rainfall (mm)	LCRS Flow Rates (lphd) During Operations							
		Initial Period				Active Period			
		Months	Average	Peak	Fraction of Rainfall (%)	Months	Average	Peak	Fraction of Rainfall (%)
(c) Landfills located in the W									
AM1	432	1-9	ND	ND		10-57	111	533	1
AM2	432	1-9	ND	ND		10-81	55	274	0

Table E-5.2. LCRS Flow Rates for HW Landfills During Operations.

Cell No.	Average Annual Rainfall (mm)	LCRS Flow Rates (lphd) During Operations							
		Initial Period				Active Period			
		Months	Average	Peak	Fraction of Rainfall (%)	Months	Average	Peak	Fraction of Rainfall (%)
(a) Landfills located in the NE									
AQ1	965	1-6	10,203	18,944	39	47-58	4,530	10,531	17
AQ2	965	1-6	13,050	20,721	49	49-58	2,181	6,460	8
AQ3	965	1-12	ND	ND		45-54	2,962	13,430	11
AQ4	965	1-12	ND	ND		44-53	1,049	1,622	4
AQ5	965	1-12	ND	ND		36-50	10,129	34,353	38
AQ6	965	1-12	ND	ND		32-52	2,732	12,072	10
AQ7	965	1-12	ND	ND		31-42	1,256	4,821	5
AQ8	965	1-12	ND	ND		15-26	21,329	76,759	81
AQ9	965	1-12	ND	ND		15-26	4,579	24,946	17
AQ10	965	1-9	ND	ND		15-26	15,933	38,751	60
AV1	787	1-13	ND	ND		65-101	1,821	7,484	8
AV2	787	ND	ND	ND		52-88	2,682	12,591	12
AV3	787	ND	ND	ND		35-71	4,466	15,363	21
AV4	787	ND	ND	ND		27-63	2,656	9,778	12
AV5	787	1-12	18,789	44,741	87	13-37	6,949	27,720	32
AY1	864	1-9	6,803	12,439	29	NA	NA	NA	
AY2	864	1-11	10,964	23,914	46	NA	NA	NA	
AY3	864	1-11	12,198	32,326	52	NA	NA	NA	
BA1	864	1-14	ND	ND		15-42	3,951	9,440	17
BA2	864	1-2	4,979	5,860	21	3-12	2,190	2,846	9
		Number	7	7	7	Number	17	17	17
		Min.	4,979	5,860	21	Min.	1,049	1,622	4
		Max.	18,789	44,741	87	Max.	21,329	76,759	81
		Mean	10,998	22,706	46	Mean	5,376	18,175	21
(b) Landfills located in the SE									
D3	1,626	1-12	20,292	51,265	46	13-28	10,005	44,895	22
D4	1,626	1-11	31,281	120,527	70	NA	NA	NA	
L1-3	1,143	8-12	22,795	51,266	73	13-43	13,417	68,107	43
AB1	1,702	1-5	479	1,662	1	6-53	270	724	1
AB2	1,702	1-12	878	3,433	2	13-53	1,865	7,829	4
AB3	1,702	1-12	4,050	9,052	9	13-40	4,971	9,529	11
AB4	1,702	9-13	7,229	9,558	16	14-25	2,114	9,584	5
AD1	1,829	1-12	ND	ND		21-32	373	892	1
AD2	1,829	1-12	ND	ND		19-30	1,886	3,783	4
AD3	1,829	1-14	ND	ND		15-26	1,685	4,197	3
AD4	1,829	1-14	ND	ND		15-26	1,071	4,523	2
AD5	1,829	1-7	ND	ND		8-19	37,054	115,663	74

Table E-5.2. LCRS Flow Rates for HW Landfills During Operations (Continued).

Cell No.	Average Annual Rainfall (mm)	LCRS Flow Rates (lphd) During Operations							
		Initial Period				Active Period			
		Months	Average	Peak	Fraction of Rainfall (%)	Months	Average	Peak	Fraction of Rainfall (%)
(b) Landfills located in the SE (cont.)									
AD6	1,829	1-7	ND	ND		8-19	992	1,853	2
AD7	1,829	1-12	12,597	26,492	25	13-70	1,206	2,857	2
AD8	1,829	1-8	24,803	39,997	49	9-64	2,058	10,545	4
AD9	1,829	1-9	19,900	42,854	40	10-58	1,880	8,051	4
AD10	1,829	1-12	20,960	51,425	42	13-79	1,883	15,064	4
AD11	1,829	1-5	11,875	20,518	24	6-69	3,536	6,708	7
AD12	1,829	1-13	25,609	55,840	51	14-69	2,150	19,674	4
AD13	1,829	1-12	18,604	86,467	37	13-55	5,403	51,260	11
AD14	1,829	1-12	20,104	85,939	40	13-55	4,452	40,684	9
AD15	1,829	1-13	24,664	89,367	49	14-39	390	1,294	1
AD16	1,829	1-12	17,442	84,110	35	13-39	17,927	153,293	36
AD17	1,829	1-12	5,761	10,955	11	13-16	4,046	6,109	8
AD18	1,829	1-12	5,035	15,685	10	13-19	1,186	3,257	2
AS1	1,422	1-10	ND	ND		11-27	329	1,146	1
		Number	19	19	19	Number	25	25	25
		Min.	479	1,662	1	Min.	270	724	1
		Max.	31,281	120,527	73	Max.	37,054	153,293	74
		Mean	15,493	45,074	33	Mean	4,886	23,661	11
(c) Landfills located in the W									
AC1	279	1-13	85	169	1	ND	ND	ND	
AC2	279	1-6	272	1,429	4	7-88	18	217	0
AC3	279	1-12	42	379	1	13-73	1	13	0
AC4	279	1-11	51	255	1	12-73	2	21	0
AC5	279	1-13	255	977	3	14-34	56	255	1
AC6	279	1-10	352	2,990	5	11-40	200	1,002	3
AC7	279	1-12	54	120	1	13-18	1,925	6,713	25
AC8	279	1-12	67	168	1	13-18	1,138	4,601	15
AP1	381	1-12	3,093	10,515	30	13-48	4,272	15,059	41
AT1	737	1-5	ND	ND		6-8	1,249	1,964	6
		Number	9	9	9	Number	9	9	9
		Min.	42	120	1	Min.	1	13	0
		Max.	3,093	10,515	30	Max.	4,272	15,059	41
		Mean	475	1,889	5	Mean	985	3,316	10

Table E-5.3. LCRS Flow Rates for Ash Landfills.

Cell No.	Average Annual Rainfall (mm)	LCRS Flow Rates (lphd) During Operations							
		Initial Period				Active Period			
		Months	Average	Peak	Fraction of Rainfall (%)	Months	Average	Peak	Fraction of Rainfall (%)
(a) Landfills located in the NE									
AF1	1,118	1-12	25,383	40,850	83	13-60	19,463	41,880	64
AN1-4	1,118	1-7	ND	ND		8-34	13,278	30,179	43
S2	1,041	1-9	2,185	4,650	8	10-46	1,026	3,638	4
Y1	1,194	1-12	ND	ND		13-78	19,319	63,832	59
Z1	1,245	1-12	28,628	49,551	84	13-39	35,312	92,207	104
		Number	3	3	3	Number	5	5	5
		Min.	2,185	4,650	8	Min.	1,026	3,638	4
		Max.	28,628	49,551	84	Max.	35,312	92,207	104
		Mean	18,732	31,684	58	Mean	17,680	46,347	55
(b) Landfills located in the SE									
P1	1,499	1-12	ND	ND		13-39	20,086	45,591	49
P2	1,499	1-12	ND	ND		13-27	8,935	12,277	22
P3	1,499	1-10	ND	ND		11-15	24,490	60,420	60
						Number	3	3	3
						Min.	8,935	12,277	22
						Max.	24,490	60,420	60
						Mean	17,837	39,429	43

Table E-5.4. LCRS Flow Rates for C&D W Landfills[(1)].

Cell No.	Average Annual Rainfall (mm)	LCRS Flow Rates (lphd) During Operations							
		Initial Period				Active Period			
		Months	Average	Peak	Fraction of Rainfall (%)	Months	Average	Peak	Fraction of Rainfall (%)
A1-2	1,118	1-24	ND	ND		25-48	3,568	8,275	12
AI1	1,143	3-12	15,552	29,341	50	13-50	12,118	29,477	39
AI2	1,143	3-6	19,613	22,964	63	7-50	16,159	34,159	52
		Number	2	2	2	Number	3	3	3
		Min.	15,552	22,964	50	Min.	3,568	8,275	12
		Max.	19,613	29,341	63	Max.	16,159	34,159	52
		Mean	17,583	26,153	56	Mean	10,615	23,970	34

Notes: (1) All of the landfills in this table are located in the NE of the U.S.

Table E-5.5 LCRS Flow Rates (in lphd) for MSW and HW Landfills During the Post-Closure Period.

Cell No.	Type of Waste	Region	Year 0	Year 1	Year 2	Year 3	Year 4	Year 5	Year 6	Year 7	Year 8	Year 9
B1	MSW	NE	4061.2	568.5	222.5	747.7	1331.0	1174.4	651.1			
B2	MSW	NE	2408.9	500.7	409.1	500.3	242.2	320.9	257.7			
I1	MSW	NE	762.1	675.9								
I2	MSW	NE	762.1	675.9								
I3	MSW	NE	762.1	675.9								
I4	MSW	NE	2114.0	566.6								
I5	MSW	NE	2590.2	204.7	4.9							
AX1	MSW	NE	144.4	64.7	46.0	49.9	120.8	43.0				
AX2	MSW	NE	296.4	292.2	126.2	145.7	240.8	89.8				
AX3	MSW	NE	615.5	254.0	197.7							
AX4	MSW	NE	17.1	61.6	48.1							
D1	HW	SE			480.4	493.3						
AD1	HW	SE	424.0	119.6	145.0	52.5	0.0	5.3	1.4	0.0	0.2	2.6
AD2	HW	SE	2035.3	1141.5	644.0	321.8	213.0	132.7	48.4	60.1	37.1	0.0
AD3	HW	SE	1891.7	652.3	321.5	79.4	476.8	399.1	172.7	111.2	61.2	
AD4	HW	SE	1219.4	326.2	465.3	66.0	156.6	68.4	13.3	1.4	1.8	
AD5	HW	SE	42801.5	8312.2	3288.9	1165.9	682.8	444.2	278.1	9.5	0.6	0.0
AD6	HW	SE	997.0	969.5	200.3	114.2	63.9	70.1	36.6	34.5	8.2	0.0
AD7	HW	SE	450.0	374.6	164.9							
AD8	HW	SE	227.9	309.6	188.7							
AD9	HW	SE	209.9	561.9	549.5							
AQ1	HW	NE	5067.7	477.1	766.7	1766.4	1421.3					
AQ2	HW	NE	1381.4	189.0	205.9	746.8	216.6					
AQ3	HW	NE	2081.1	351.5	419.9	721.4	1850.6					
AQ4	HW	NE	1512.7	4261.8	1982.0	639.0	466.5					
AQ5	HW	NE	9062.3	1406.4	579.8	644.7	490.9					
AQ6	HW	NE	2492.7	3107.9	479.2	532.8	405.7					
AQ7	HW	NE	896.7	40.8	62.9	212.7	360.7					
AQ8	HW	NE	19817.8	498.2	623.1	507.1						
AQ9	HW	NE	3308.8	324.9	286.3	670.9	2111.2					
AQ10	HW	NE	11314.5	521.2	497.4	900.6	774.6					
AS1	HW	SE	329.7	136.0	110.0	38.6	26.1	34.7				
AT1	HW	W	1246.7	87.3	24.5							
Number			32	32	29	22	20	11	8	6	6	4
Avg.			3853.2	897.2	466.9	505.3	582.6	252.9	182.4	36.1	18.2	0.6
S.D.			8151.7	1606.2	660.0	426.4	614.9	342.5	218.8	43.4	25.3	1.3

three times the average monthly flow rates. For the initial period of operation, the peak flow rates ranged between approximately 3,000 lphd and 111,000 lphd, and for the active period of operation, between approximately 160 lphd and 49,000 lphd. Peak rates greater than 10,000 lphd were exhibited by 70% of the cells during the initial period of operation and by 38% of the cells during the active period of operation.

LCRS flow rates measured from the MSW cells located in the SE were in general similar to those from MSW cells located in the NE, as shown in Table E-5.1. However, because rainfall amounts are in general about 20 to 50% greater in the SE than in the NE, calculated RF values are smaller for the SE landfills than for the NE landfills. For example, for the NE MSW landfills during the active period of operation, RF values ranged from 0 to 54%. More than half of the cells had RF values greater than 10% and 25% of the cells had RF values greater than 20%. For the SE MSW Landfills during the active period of operation, RF values ranged from 1 to 23%. Only 25% of the cells had an RF value greater than 10%. It is interesting that the higher rainfall amounts in the SE versus the NE did not yield higher LCRS flow rates for MSW landfills. This may be due to the higher water evaporation rates in the SE (due to the higher temperatures) than in the NE. It may also indicate that rainfall intensity (i.e., amount of rainfall divided by rainfall period) has an impact on leachate generation rates. Rainfall events in the SE are more intense than in the NE. More intense rainfalls have the potential to generate larger surface-water runoffs and less infiltration, and thus less leachate.

Data are only available for two MSW cells located in the W. For these two cells, average and peak LCRS flow rates were very low. Average LCRS flow rates were 111 lphd and 55 lphd for Cells AM1 and AM2, respectively. Peak monthly rates were about five times the average rates. It is noted that Landfill AM receives an average annual rainfall of 432 mm, which is relatively low. The calculated RF values are less than 1%. These RF values are very low in comparison to RF values for landfills in the NE and SE. This indicates that landfills in arid regions that receive average annual rainfalls less than 500 mm may have very low leachate generation rates.

The evaluation of Tables E-5.1 through E-5.4 shows that the MSW landfills produced less leachate than the other types of waste in all three regions of the U.S. The HW landfills had LCRS flow rates during the active period of operation that were 50 to 60% greater than those from the MSW landfills. For the HW cells located in the NE and SE for which initial period of operation data are available, average LCRS flow rates varied between approximately 500 lphd and 31,000 lphd. During the active period of operation, average LCRS flow rates were from approximately 300 lphd to 37,000 lphd. Peak monthly LCRS flow rates were typically two to three times the average monthly flow rates. For the initial period of operation, the peak flow rates ranged between approximately 2,000 lphd and 121,000 lphd, and, for the active period of operation, between approximately 700 lphd and 153,000 lphd. Peak rates greater than 10,000 lphd were exhibited by most of the cells during both the initial and active periods of operation. For the NE HW landfills during the active period of operation, RF values

ranged from 4 to 87% (mean = 21%). For the SE HW landfills during the active period of operation, RF values ranged from 1 to 74% (mean = 1%).

Data are available for ten HW cells located in the W. For these cells, average LCRS flow rates ranged from 40 lphd to 3,000 lphd during the initial period of operation and from 0 lphd to 4,000 lphd during the active period of operation. Peak flows were three times greater than average flows. RF values ranged from 1 to 30% and from 0 to 40% during the initial and active periods of operation, respectively. For most of the cells, RF values were less than 10% during operations.

The limited number of ash and C&DW cells had significantly higher LCRS flow rates than the MSW and HW cells. For the eight ash cells located in the NE and SE, average LCRS flow rates were in the range of approximately 1,000 lphd to 35,000 lphd during operations and the peak flow rates were from approximately 4,000 lphd to 92,000 lphd. The three C&DW landfills located in the NE had average rates during operations from 4,000 lphd to 20,000 lphd, and peak rates from 8,000 lphd to 34,000 lphd. Flow rates from these ash and C&DW cells during the active period of operation were 300 to 600% higher than flow rates from MSW cells. Mean RF values during operations were 52% for the ash cells and 43% for the C&DW cells. The waste characteristics (i.e., initial moisture content, porosity, and permeability) and the waste disposal and covering practices may attribute to these differences in LCRS flows. For example, ash is often sprayed with water to control dust and is not covered with soil as often as MSW.

Tables E-5.1 through E-5.4 show that landfill geographic region (i.e., humid versus arid) has a major impact on LCRS flow rates. Landfills located in the humid NE and SE had much higher LCRS flow rates and RF values than landfills located in the arid W. In particular, almost all of the cells that had historical average annual rainfall less than 500 mm had average LCRS flow rates that are less than 2,000 lphd and peak LCRS flow rates that are less than 7,000 lphd. The RF values for many of these cells were less than 5%. Figures E-5.1 through E-5.4 show the effects of precipitation on LCRS flow rates for the sites considered. These figures show average and peak LCRS flow rates for the initial and active periods of operation plotted as a function of historical average annual rainfalls at the sites. The ranges of average annual rainfalls covered by each of the three regions are also shown on the figures. Though the LCRS flow rates are considerably variable, a general trend can be observed from the four figures. On each figure an envelope was drawn that defines the approximate upper bound of the measured LCRS flow rates. As average annual rainfall increases, the average and peak LCRS flow rates increase. Sites in the W with less than 500-mm average annual rainfall exhibited low LCRS flow rates. In addition, increasing annual rainfall beyond 1,100 to 1,200 mm (which only occurred for sites in the SE in this study) typically does not seem to cause a corresponding increase in leachate generation rates. As previously stated, this may be attributed to differences in waste evaporation rates and rainfall intensities between the SE and the NE.

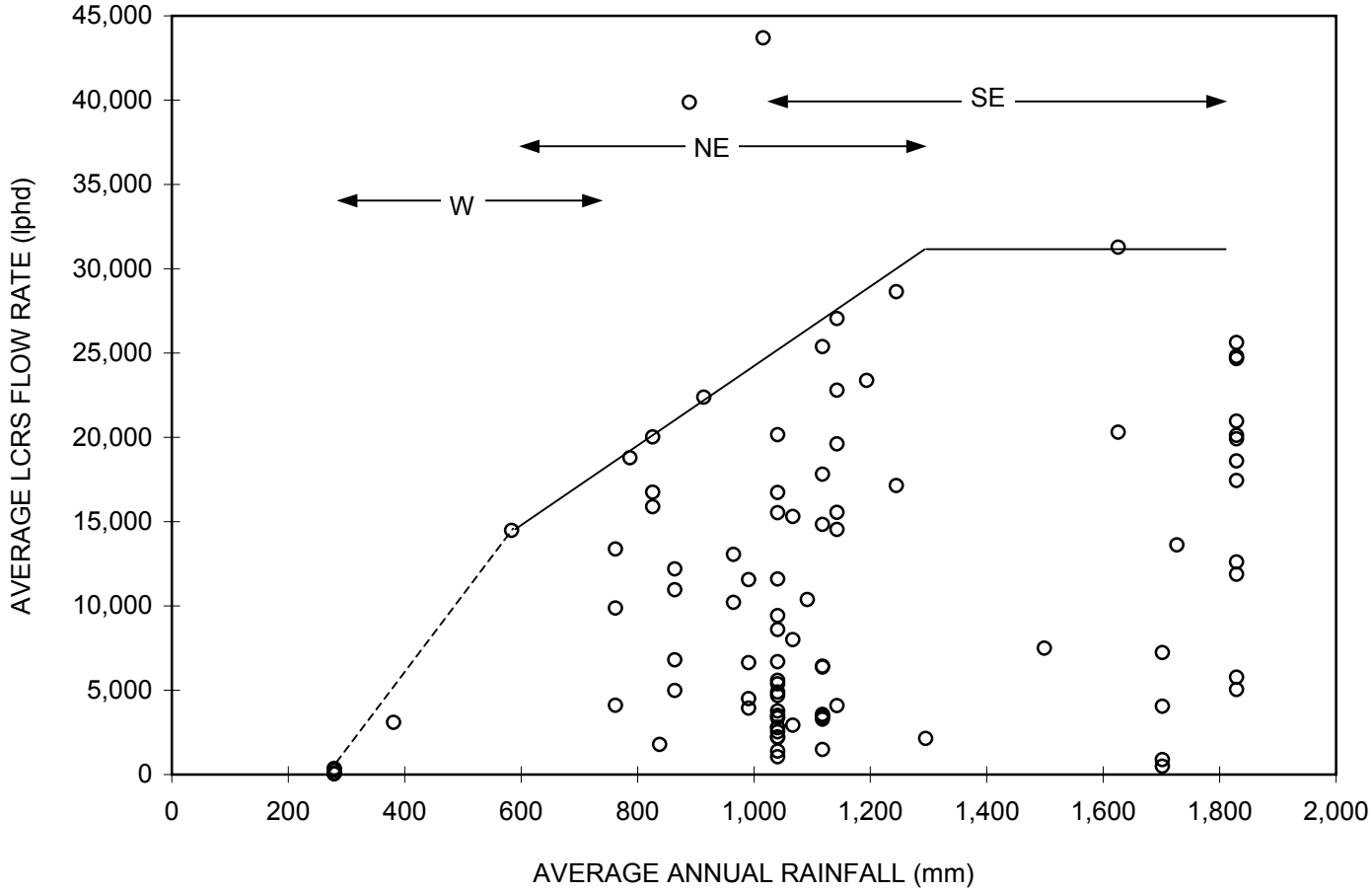

Figure E-5.1. Average LCRS Flow Rate Versus Average Annual Rainfall During the Initial Period of Operation.

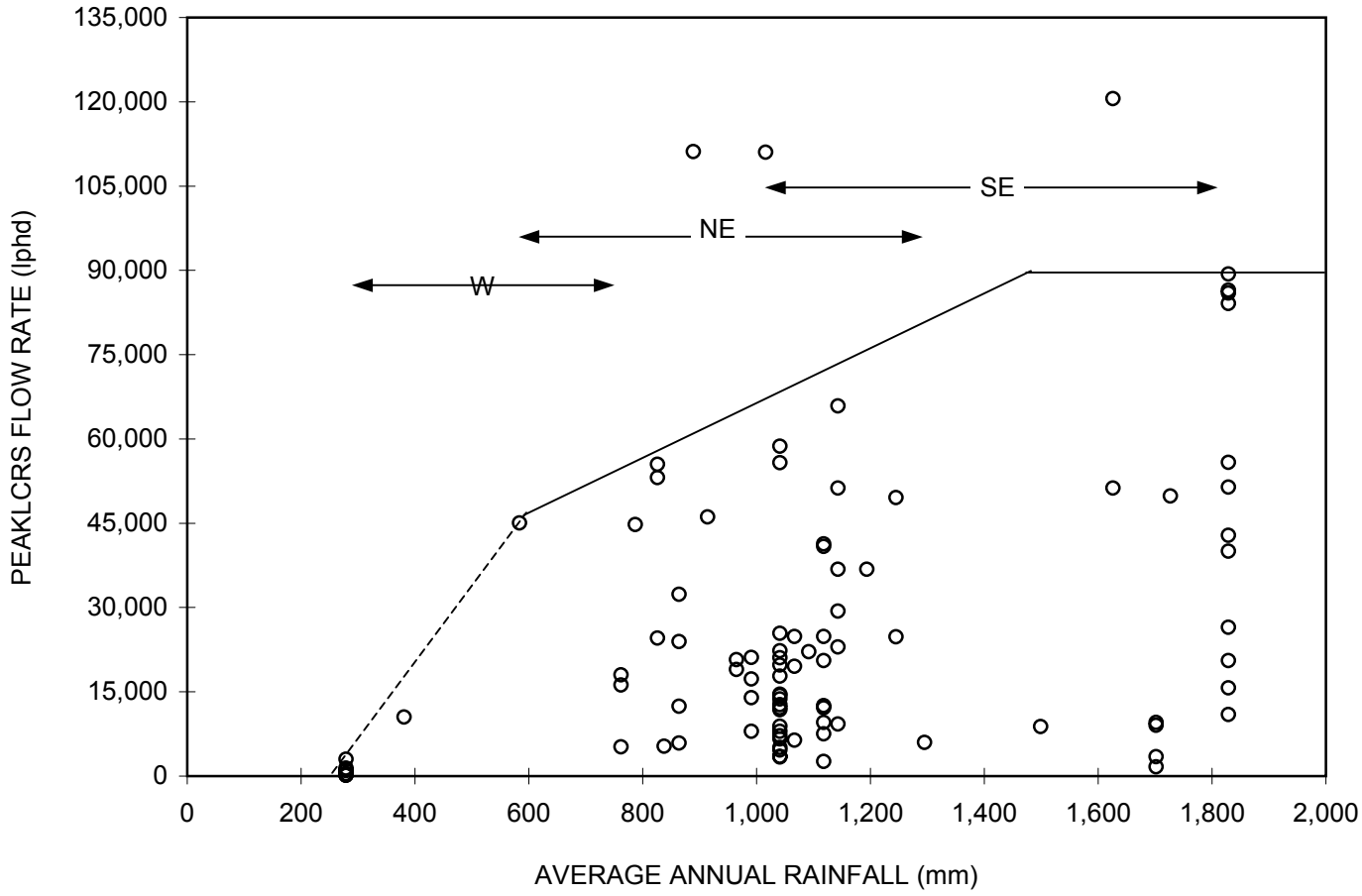

Figure E-5.2. Peak LCRS Flow Rate Versus Average Annual Rainfall During the Initial Period of Operation.

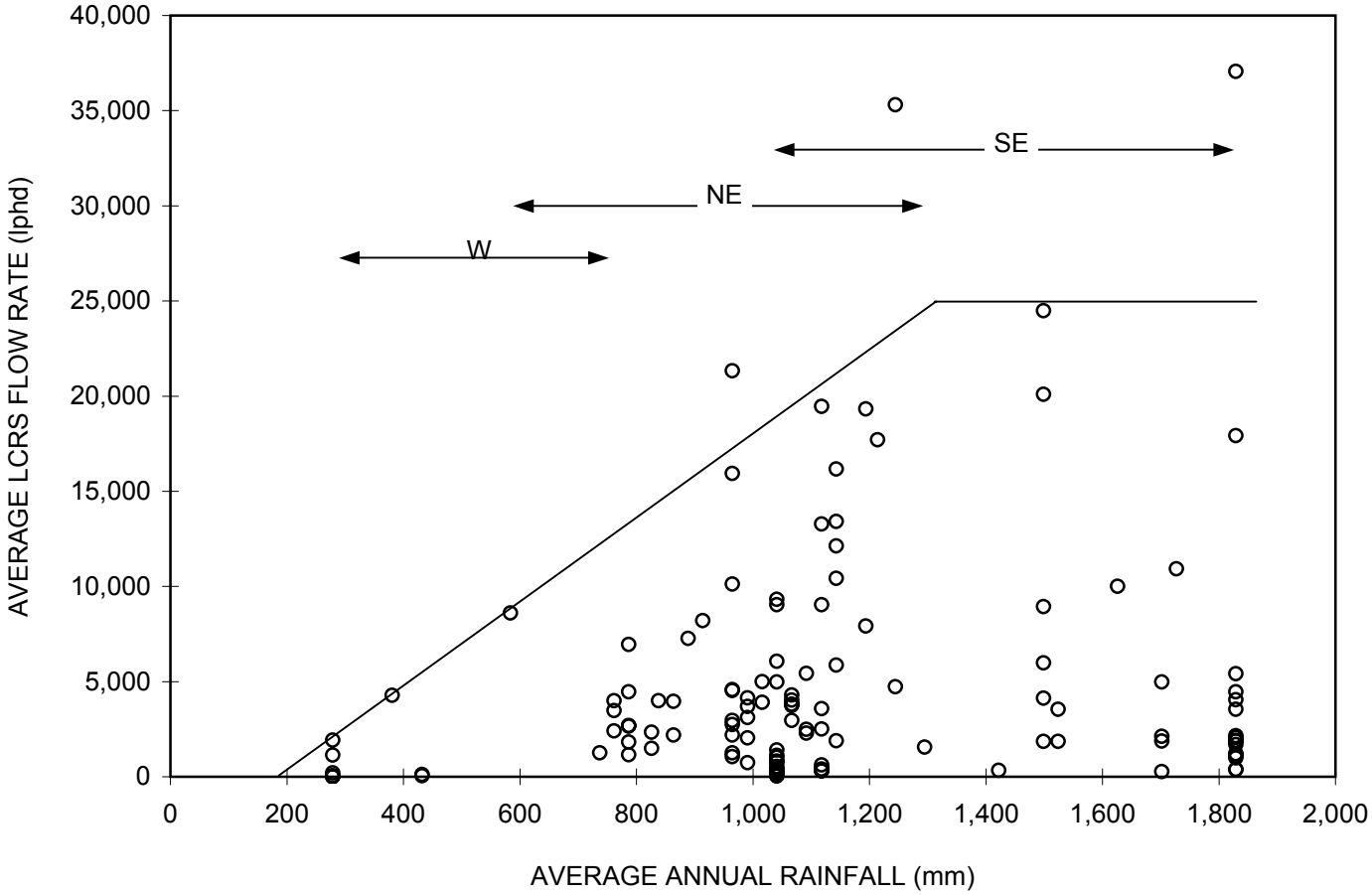

Figure E-5.3. Average LCRS Flow Rate Versus Average Annual Rainfall During the Active Period of Operation.

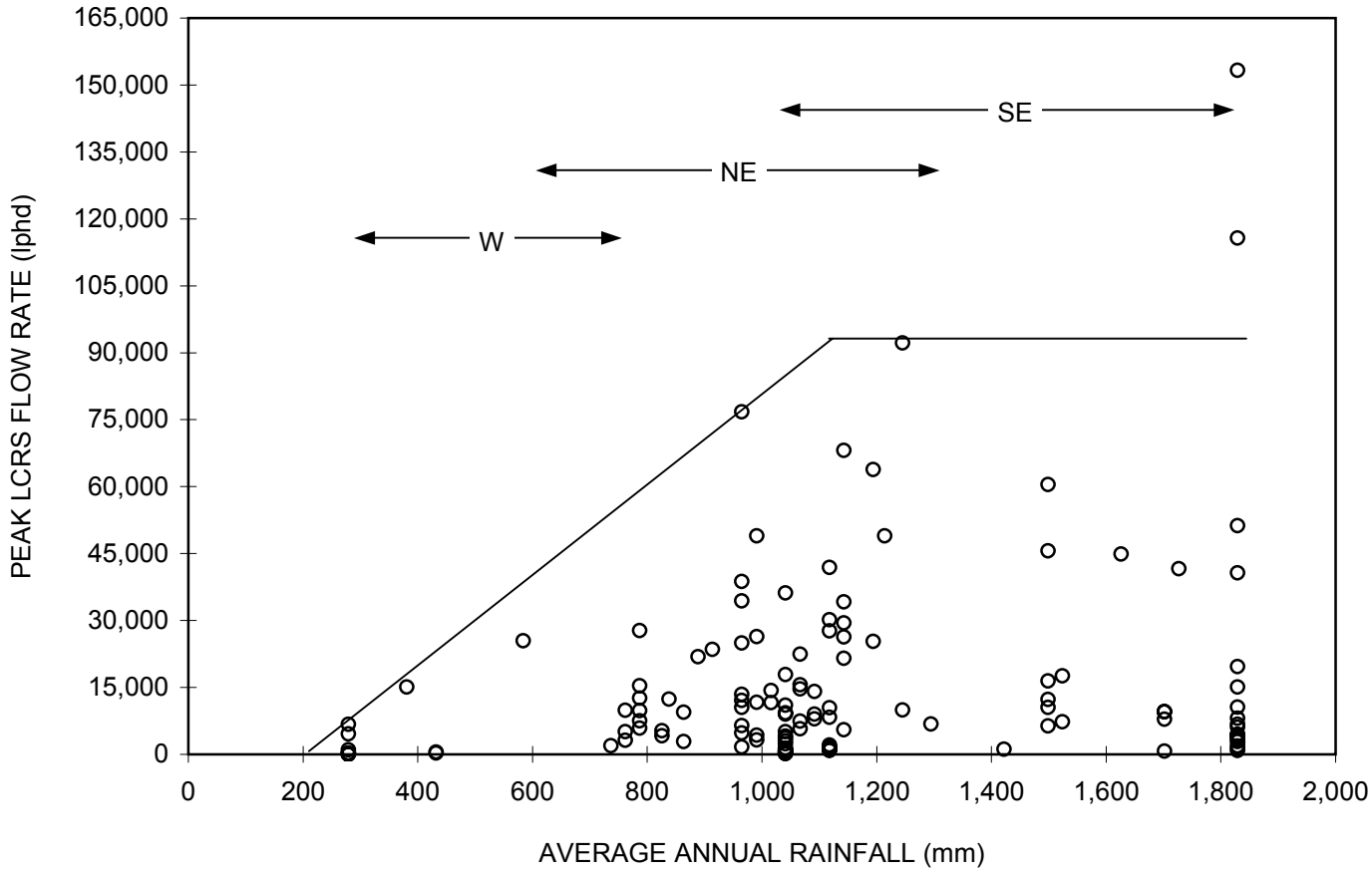

Figure E-5.4. Peak LCRS Flow Rate Versus Average Annual Rainfall During the Active Period of Operation.

Leachate generation rates during the post-closure period for eleven MSW cells and 22 HW cells are summarized in Table E-5.5. The data cover a maximum post-closure period of nine years. The table presents average LCRS flow rates for these cells for the year prior to closure as well as for the years after closure. The mean LCRS flow rate for all of the cells during the year before closure was approximately 3,900 lphd. Within one year after closure, the mean dropped by a factor of four and within two to four years after closure the mean dropped approximately one order of magnitude. After six years of closure, the eight cells for which data are available had LCRS flow rates of approximately 5 to 1,200 lphd (mean of 180 lphd). As shown in Table E-5.5, four of the six cells for which LCRS flow rate data exists for nine years after closure had negligible LCRS flow rates. Figure E-5.5 shows LCRS flow rates for Cell AD5. For this cell, the average LCRS flow rate during the year before closure was 42,800 lphd. After one year of closure, the rate decreased by a factor of five and after two years of closure, the rate decreased an order of magnitude from the pre-closure value. After nine years of closure, the LCRS rate became negligible. This significant decrease in LCRS flow rates demonstrates the ability of well designed and constructed cover systems in minimizing infiltration of rainwater into the waste and thus minimizing leachate generation. Figure E-5.6 shows the average LCRS flow rates measured for the 33 cells under closure. This figure shows that after a cell is closed and a cover system is installed, LCRS flow rates will decrease with time and become negligible after approximately eight to ten years of closure.

E-5.4 Implications for Landfill Performance

The data presented in this section show that for the considered landfills peak monthly LCRS flow rates were typically two to three times the average monthly LCRS flow rates. The data also shows that LCRS flow rates were typically two to three times smaller during the active period of operation than during the initial period of operation. During the initial period of operation, LCRS flow rates will be greatly influenced by rainfall. During the active period of operation, the amount of waste in the cell is greater and daily and intermediate cover soils are placed on the waste, thus minimizing infiltration of rainwater into the waste.

Evaluation of the LCRS flow rate data shows that average and peak LCRS flow rates vary significantly even between similar sites (i.e., sites in the same region and with the same type of waste). For example, for 44 MSW cells located in the NE, the average LCRS flow rate during the initial period of operation varied between approximately 1,000 lphd to 40,000 lphd. Peak monthly LCRS flow rates were even more variable for these 44 cells ranging between approximately 3,000 lphd and 111,000 lphd. Similar results are found for the other types of waste. It is expected based on these results that waste placement practices have a very significant effect on leachate generation rates. Although these effects are not directly quantified in this study, it is expected that a landfill operator can minimize leachate generation rates by using a small active disposal area and implementing effective measures to minimize infiltration of rainwater into the waste and to divert surface water away from the landfill.

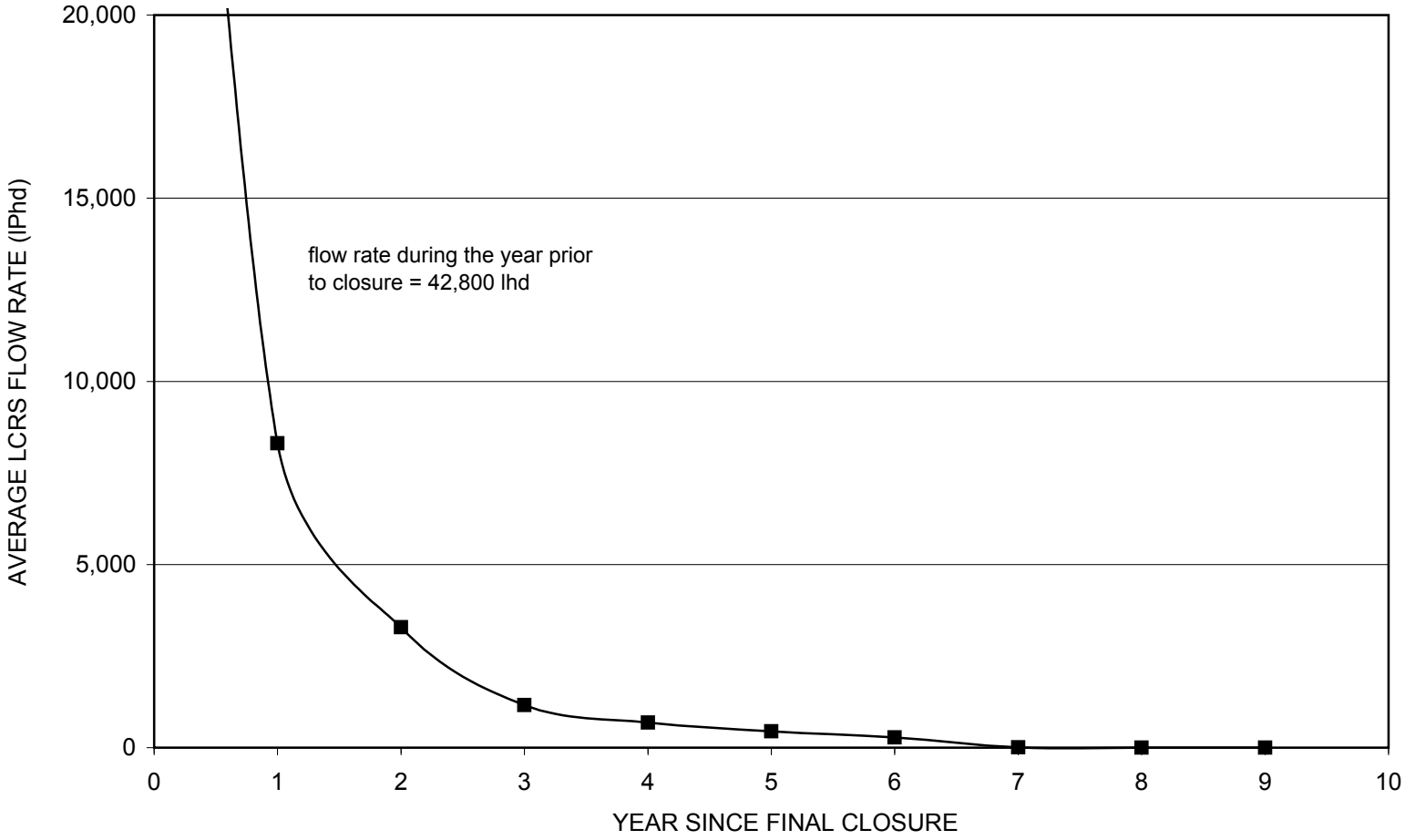

Figure E-5.5. Average LCRS Flow Rates (lhd) After Closure of Cell AD5, a HW Cell Located in the SE.

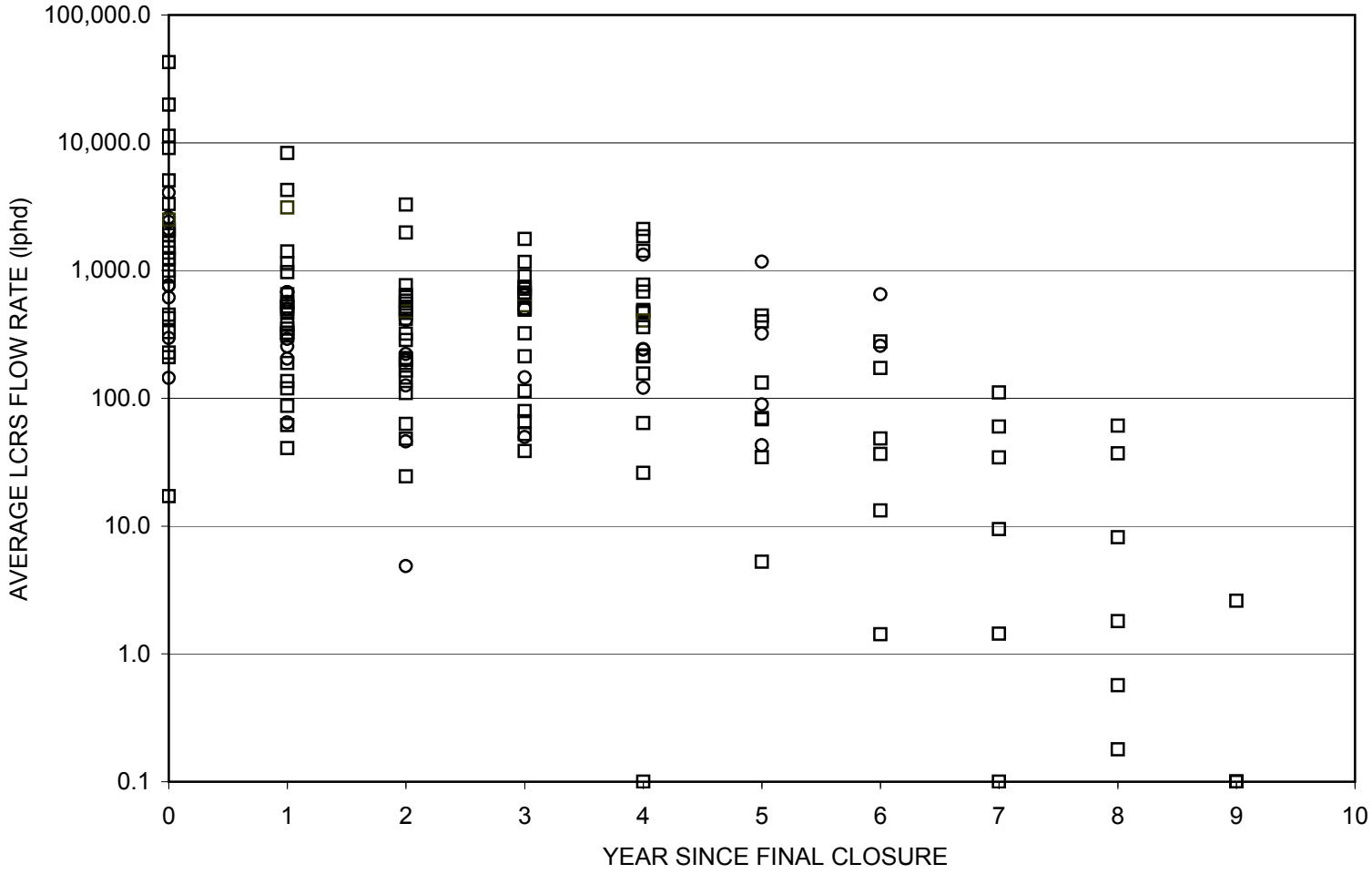

Figure E-5.6. Average LCRS Flow Rates (lhd) After Closure for Eleven MSW Cells (Shown as Circles) and 22 HW Cells (Shown as Squares) (Note: Flow Rates of 0.0 lphd are Shown as 0.1 lphd).

E-6 Leachate Chemistry Data

E-6.1 Introduction

This section presents an evaluation of the available leachate chemistry data presented in Table E-3.7 for 59 cells at 50 landfills. The purpose of this section is to characterize the chemistry of leachate from MSW, HW, and ISW landfills, compare the leachate chemistry data in this appendix to the published data summarized in Section E-2.3, and evaluate the effect of the solid waste regulations discussed in Section E-2.3.1 on leachate quality (i.e., has the amount of trace toxic inorganic and synthetic organic chemicals in leachate decreased). The remainder of this section is organized as follows:

- landfill leachate chemistry is characterized in Section E-6.2;
- the leachate chemistry data are compared to published data in Section E-6.3; and
- the effect of the solid waste regulations on leachate quality is discussed in Section E-6.4.

E-6.2 Characterization of Landfill Leachate Chemistry

E-6.2.1 Introduction

The chemistries of leachates from MSW, HW, and ISW landfills are characterized below in terms of concentrations and relative detection frequencies (i.e., were the chemicals detected in 50% or less of the samples or more than 50% of the samples) of 30 representative chemical parameters. A summary of the average chemical concentrations and the range of average concentrations found in the landfill leachates is given in Table E-6.1. Federal MCLs for community drinking water systems (40 CFR § 141.11, 141.61, 141.62) are available for two of the heavy metals and ten of the VOCs considered in this study, and are also listed in Table E-6.1. The distributions of chemistry data for MSW, HW, and MSW ash landfill cells are shown in Figures E-6.1 through E-6.3, respectively, for the following select parameters and chemicals: BOD, sulfate, chromium, benzene, 1,2-dichloroethane, and toluene. For MSW landfills, the chemical data for older and newer landfills were compared. Older landfills are considered to be those that started operating before 1990 (i.e., pre-1990 landfills). Newer landfills started operating during 1990 or later (i.e., post-1990 landfills). The distributions of chemistry data for pre-1990 and post-1990 MSW landfill cells are shown in Figure E-6.4 for the following select chemicals: chromium, benzene, 1,1-dichloroethane, and toluene. In Figures E-6.1 through E-6.4, non-detected chemicals were graphed at half of their method detection limits.

Leachate chemistry time trends are presented for the one landfill cell (i.e., MSW Cell B1) for which a relatively complete leachate chemistry data set is available for a number of years. Other parameters that may affect leachate chemistry, such as landfill

Table E-6.1. Summary of Landfill Leachate Chemistry Data.

		Waste Type	MSW							
		Number of Landfills	10 Pre-1990				26 Post-1990			
Parameter	Units	MCLs	Average	Minimum	Maximum	No. of Landfills	Average	Minimum	Maximum	No. of Landfills
pH	pH units		6.62	6.30	7.20	8	6.79	5.90	8.09	22
Specific conductance	µmhos/cm		6,588	3,438	8,983	8	3,693	597	13,548	22
TDS	mg/l		5,487	2,740	8,640	9	2,758	480	8,621	21
COD	mg/l		3,878	804	8,267	9	1,939	< 10	6,800	22
BOD_5	mg/l		2,281	< 2	4,510	10	976	< 2	4,700	18
TOC	mg/l		1,509	4	2,852	8	527	24	2,609	21
Alkalinity	mg/l		2,295	1,508	3,278	7	1,536	203	5,800	22
Chloride	mg/l		801	199	2,263	10	463	5	1,625	25
Sulfate	mg/l		274	< 23	1,943	10	205	< 7	1,376	24
Calcium	mg/l		444	261	610	6	398	66	1,994	22
Magnesium	mg/l		153	84	279	6	83	10	191	21
Sodium	mg/l		532	225	1,115	8	282	3	1,219	23
Arsenic	µg/l	50	19	< 4	78	10	23	< 2	236	21
Cadmium	µg/l	5	< 8	< 1	< 17	8	< 7	< 1	< 20	22
Chromium	µg/l	100	68	5	320	10	38	3	90	21
Lead	µg/l		36	1	90	7	15	1	50	22
Nickel	µg/l		56	27	98	9	82	10	220	20
Benzene	µg/l	5	< 17	< 3	< 36	7	< 19	< 2	< 100	21
1,1-Dichloroethane	µg/l		88	< 5	294	8	66	< 2	260	22
1,2-Dichloroethane	µg/l	5	< 33	< 4	< 100	6	< 16	< 1	< 100	20
cis-1,2-Dichloroethylene	µg/l	70	< 64	< 53	< 75	2	< 57	< 1	436	13
trans-1,2-Dichloroethylene	µg/l	100	< 51	< 32	< 100	4	< 18	< 1	< 110	16
Ethylbenzene	µg/l	700	40	< 5	87	7	35	< 1	118	22
Methylene chloride	µg/l		435	< 5	1,303	8	334	< 1	4,150	22
1,1,1-Trichloroethane	µg/l	200	< 68	< 5	100	6	< 55	< 1	270	20
Trichloroethylene	µg/l	5	< 56	< 5	114	7	< 24	< 1	100	19
Toluene	µg/l	1,000	491	< 5	959	7	228	< 1	740	22
Vinyl chloride	µg/l	2	< 49	< 7	< 100	6	< 34	< 3	< 300	20
Xylenes	µg/l	10,000	117	< 5	277	6	83	< 5	220	20

Notes: (1) " " = not analyzed; < = more than 50% of measurements reported as non-detect.

Table E-6.1. Summary of Landfill Leachate Chemistry Data (Continued).

		Waste Type	HW				MSW ASH			
		Number of Landfills	4				7			
Parameter	Units	MCLs	Average	Minimum	Maximum	No. of Landfills	Average	Minimum	Maximum	No. of Landfills
pH	pH units		8.17	7.55	9.36	3	7.06	6.54	7.44	5
Specific conductance	µmhos/cm		22,096	12,302	39,598	3	22,083	10,732	43,383	4
TDS	mg/l						24,493	6,067	46,733	6
COD	mg/l						1,670	304	5,607	4
BOD_5	mg/l						55	15	84	4
TOC	mg/l		1,623	7	3,239	2	62	39	109	3
Alkalinity	mg/l						1,942	99	5,010	4
Chloride	mg/l		7,758	3,783	11,734	2	10,426	2,940	22,400	4
Sulfate	mg/l		2,985	704	5,267	2	881	85	3,430	5
Calcium	mg/l						900	96	1,332	3
Magnesium	mg/l						267	113	420	2
Sodium	mg/l		5,243	2,514	7,972	2	1,181	684	1,994	5
Arsenic	µg/l	50	26,710	30	79,912	3	9	5	17	6
Cadmium	µg/l	5	< 119	< 5	< 233	2	< 12	< 2	49	6
Chromium	µg/l	100	124	22	226	2	< 30	< 1	84	6
Lead	µg/l		109	24	249	3	23	3	74	6
Nickel	µg/l		738	285	1,190	2	< 40	< 24	48	4
Benzene	µg/l	5	< 131	< 7	370	3	< 3	< 1	< 5	3
1,1-Dichloroethane	µg/l		123	< 14	< 371	4	< 12	< 1	< 33	3
1,2-Dichloroethane	µg/l	5	< 382	5	< 1,124	3	< 3	< 1	< 5	3
cis-1,2-Dichloroethylene	µg/l	70					< 2	< 1	< 3	2
trans-1,2-Dichloroethylene	µg/l	100	< 79	< 14	< 143	2	< 3	< 1	< 5	3
Ethylbenzene	µg/l	700	< 133	< 5	< 512	4	< 4	< 2	< 7	3
Methylene chloride	µg/l		161	4	< 447	4	< 3	< 1	< 6	3
1,1,1-Trichloroethane	µg/l	200	< 99	8	< 347	4	< 7	< 1	< 16	3
Trichloroethylene	µg/l	5	< 76	33	< 146	3	< 3	< 1	< 5	3
Toluene	µg/l	1,000	< 173	< 9	616	4	< 10	< 1	< 25	3
Vinyl chloride	µg/l	2	< 1,475	< 10	< 4,405	3	< 5	< 1	< 10	3
Xylenes	µg/l	10,000	14	9	18	2	< 2	< 1	< 3	2

Notes: (1) " " = not analyzed; < = more than 50% of measurements reported as non-detect.

Table E-6.1. Summary of Landfill Leachate Chemistry Data (Continued).

			Waste Type	COAL ASH				C&DW			
			Number of Landfills	2				2			
Parameter	Units	MCLs		Average	Minimum	Maximum	No. of Landfills	Average	Minimum	Maximum	No. of Landfills
pH	pH units			7.70	7.66	7.74	2	6.43	6.43	6.43	1
Specific conductance	µmhos/cm			884	623	1144	2	4815	4815	4815	1
TDS	mg/l			723	347	1098	2	3553	2880	4225	2
COD	mg/l			11	11	11	1	2414	1139	3688	2
BOD_5	mg/l			< 3	< 3	< 3	1	1126	1126	1126	1
TOC	mg/l			6	6	6	1	839	443	1235	2
Alkalinity	mg/l			190	160	220	2	2450	2450	2450	1
Chloride	mg/l			21	21	21	1	681	671	690	2
Sulfate	mg/l			383	178	587	2	255	48	463	2
Calcium	mg/l			190	190	190	1	292	203	382	2
Magnesium	mg/l			22	15	30	2	202	202	202	1
Sodium	mg/l			46	46	46	1	304	284	324	2
Arsenic	µg/l	50		36	< 9	62	2	15	15	15	1
Cadmium	µg/l	5		< 7	< 5	< 9	2	< 3	< 1	< 5	2
Chromium	µg/l	100		< 16	< 9	22	2	39	39	39	1
Lead	µg/l			< 19	< 4	< 34	2	7	3	10	2
Nickel	µg/l			38	38	38	1	< 56	< 56	< 56	1
Benzene	µg/l	5		< 4	< 4	< 4	1	17	17	17	1
1,1-Dichloroethane	µg/l			< 4	< 4	< 4	1	92	92	92	1
1,2-Dichloroethane	µg/l	5		< 4	< 4	< 4	1	3	3	3	1
cis-1,2-Dichloroethylene	µg/l	70									
trans-1,2-Dichloroethylene	µg/l	100		< 1	< 1	< 1	1				
Ethylbenzene	µg/l	700		< 3	< 3	< 3	1	66	66	66	1
Methylene chloride	µg/l			< 4	< 4	< 4	1	417	417	417	1
1,1,1-Trichloroethane	µg/l	200		< 4	< 4	< 4	1	51	51	51	1
Trichloroethylene	µg/l	5		< 4	< 4	< 4	1	< 11	< 11	< 11	1
Toluene	µg/l	1,000		< 2	< 2	< 2	1	613	613	613	1
Vinyl chloride	µg/l	2		< 7	< 7	< 7	1	8	8	8	1
Xylenes	µg/l	10,000		< 4	< 4	< 4	1	210	210	210	1

Notes: (1) " " = not analyzed; < = more than 50% of measurements reported as non-detect.

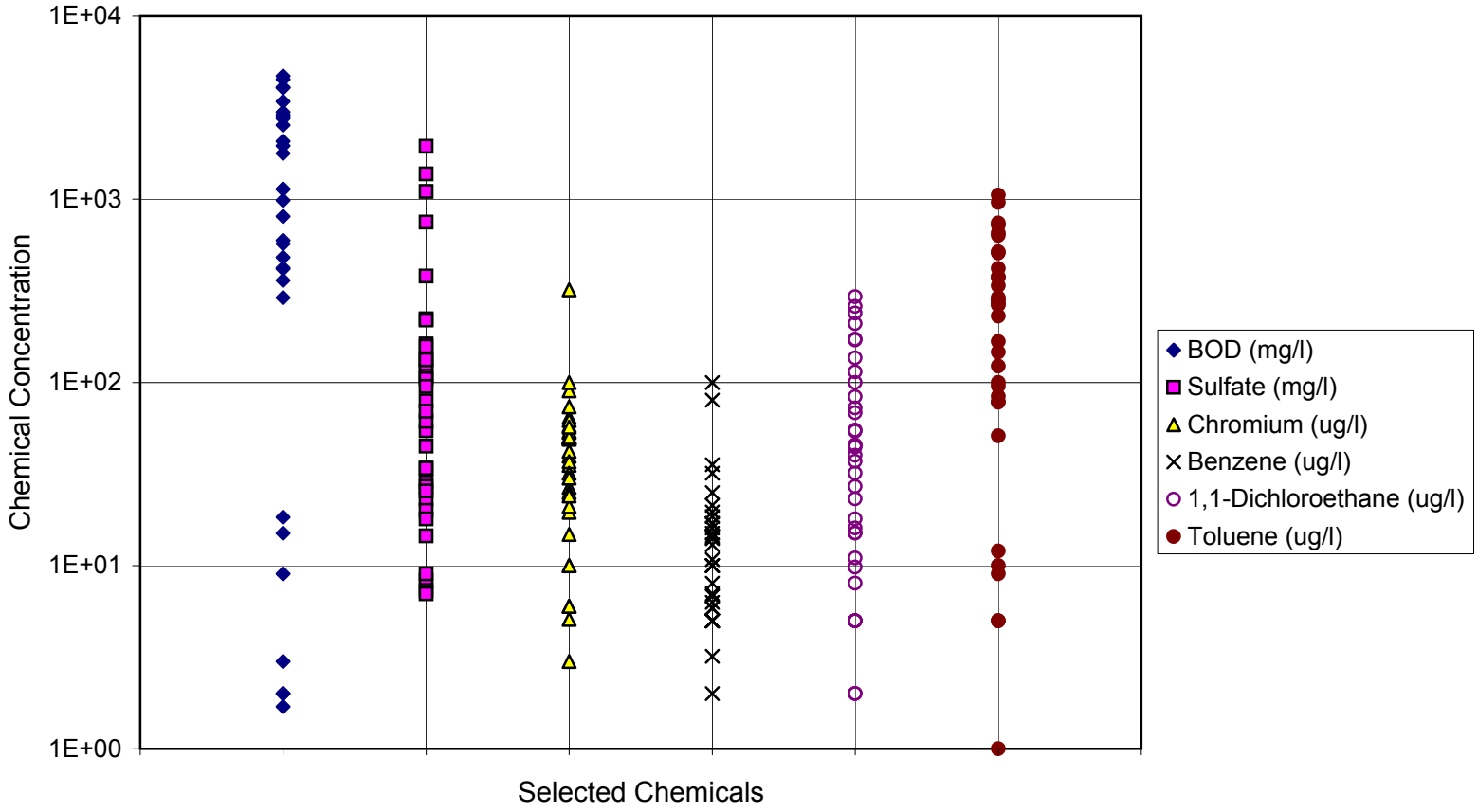

Figure E-6.1. Distribution of Select Chemical Data for MSW Leachate

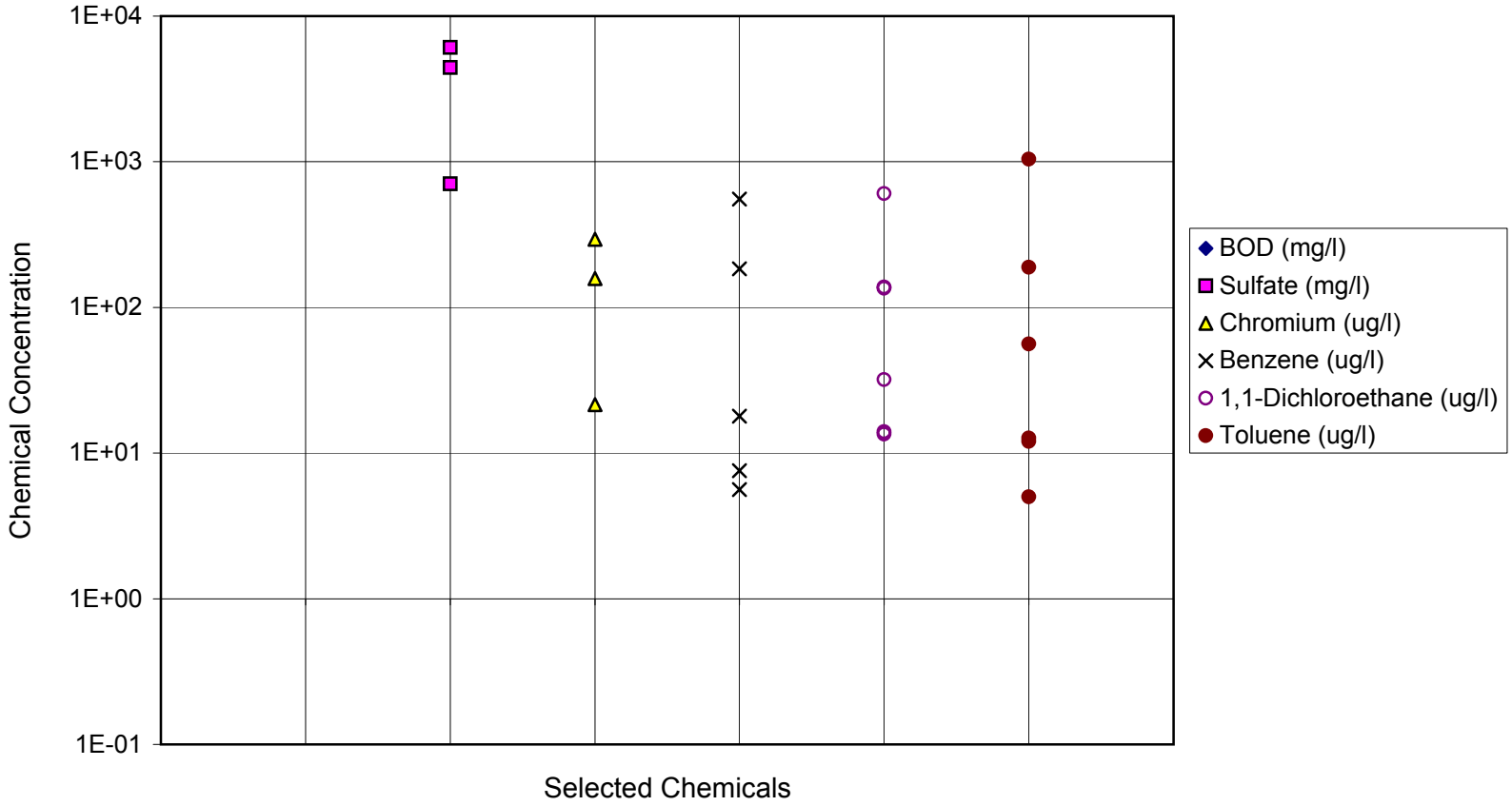

Figure E-6.2. Distribution of Select Chemical Data for HW Leachate

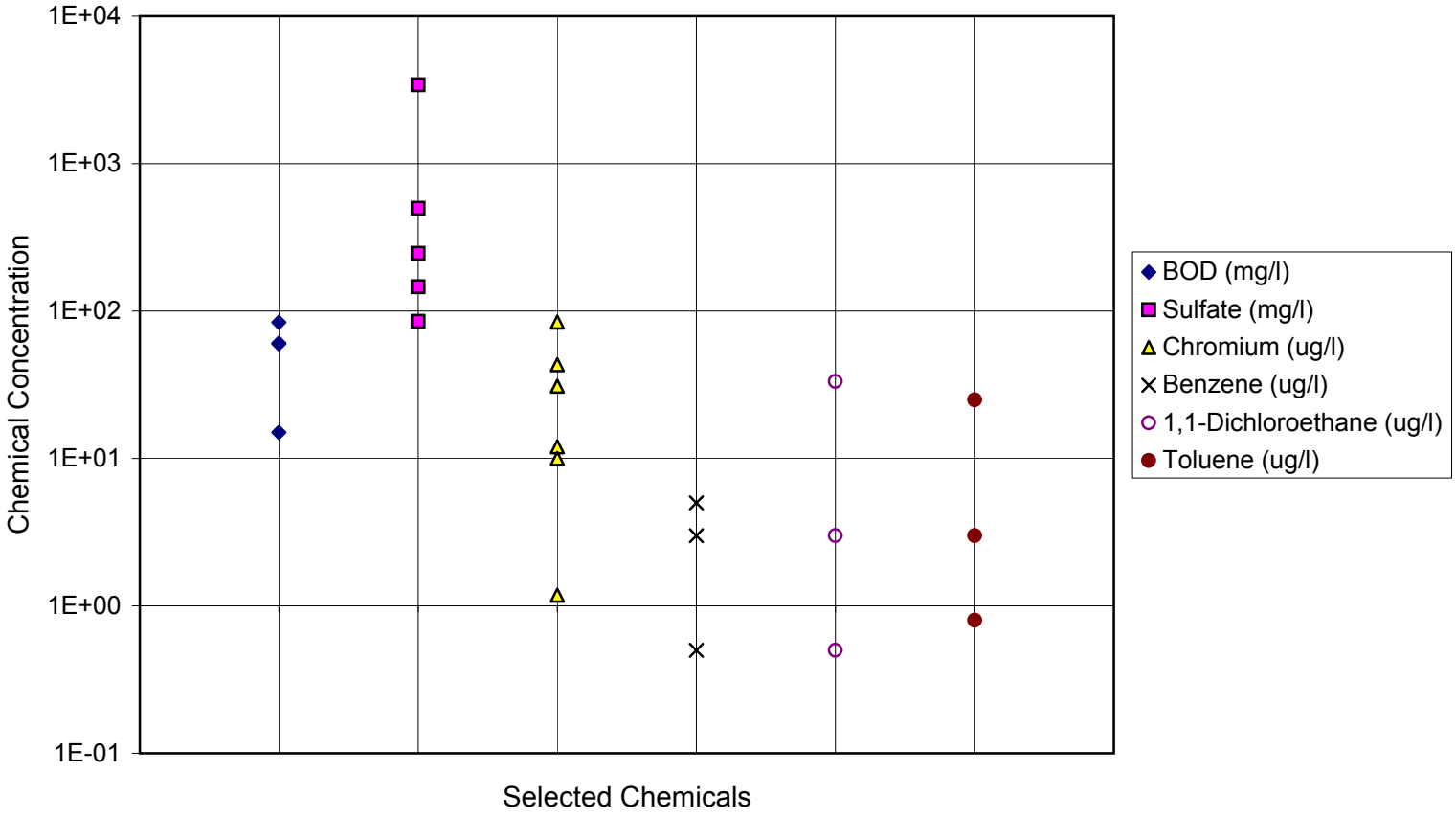

Figure E-6.3. Distribution of Select Chemical Data for MSW Ash Leachate

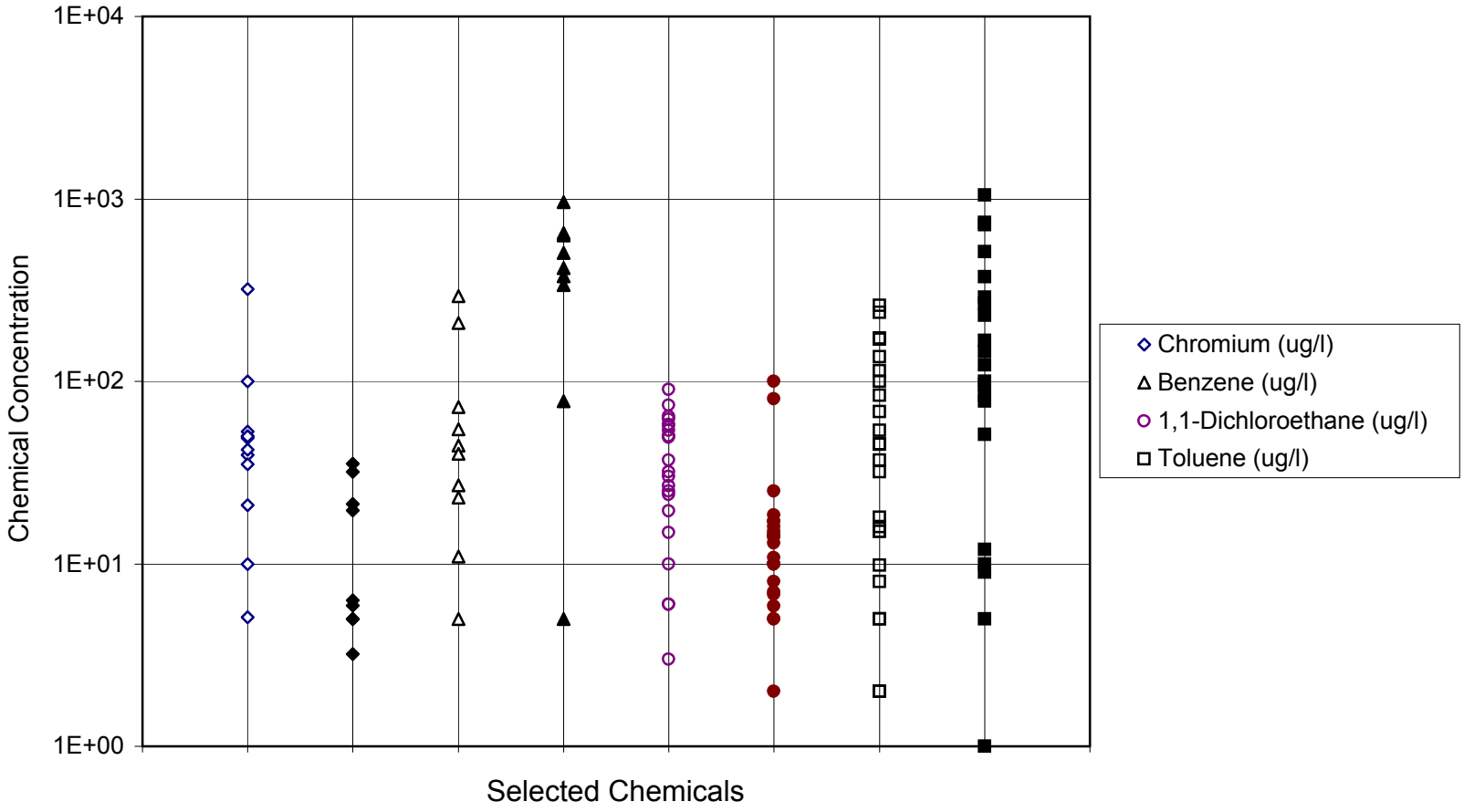

Figure E-6.4. Distribution of Select Chemical Data for MSW Leachates from Pre-1990 and Post-1990 Landfills (Pre-1990 Data have open symbols, Post-1990 data have closed symbols).

geographic location and date of waste placement relative to sample collection date, were also considered. However, there were too few data to draw meaningful conclusions. For example, of the 36 MSW landfills, 31 are located in the NE, four are located in the SE, and one is located in the W. In general, the chemical concentrations for leachate from the SE and W MSW landfills fall within the range of values detected for leachate from the NE MSW landfills. It may be that geographic location has no significant impact on leachate chemistry or it may be that there were too few leachate chemistry data for MSW landfills in the SE and W to observe an effect.

E-6.2.2 MSW

The MSW landfill leachates were found to be mineralized, biologically active liquids with relatively low concentrations of heavy metals and VOCs. Of the trace metals and VOCs in Table E-3.7, chromium, nickel, methylene chloride, and toluene were detected at the highest concentrations. Many of the chemicals exhibited significant concentration variations (e.g., several orders of magnitude difference) between landfills and, sometimes, for a given landfill as shown in Table E-3.7 and Figure E-6.1. Based on the pH values, the MSW landfill leachate was found to be, on average, slightly acidic (i.e., average pH of 6.7). This is expected because carbon dioxide and organic acids are the primary by-products of the first stage (i.e., the acid stage) of anaerobic degradation of organic compounds in MSW landfills. As the MSW in the landfill ages and the placement of fresh MSW ceases, methanogens begin to proliferate in a landfill and the pH begins to approach neutrality as the acids are converted into methane and a bicarbonate buffering system is established (the methane fermentation stage). This increase in pH with time is evident for landfill cell B1 after it was closed, as shown in Table E-6.2. This cell became operational in 1984 and was closed in 1988. In general, a significant increase in pH with time was not observed for active cells receiving fresh MSW. For cell B1, the BOD, COD, and BOD/COD ratios also decreased with time after cell closure. Based on studies of older landfills (i.e., Chian and DeWalle, 1977), the decrease in these parameters was expected. BOD and COD levels decrease as MSW is degraded, but BOD decreases faster than COD. Thus, the BOD/COD ratio also decreases. The BOD/COD ratios for cell B1 are characteristic of a landfill transitioning from the acid stage to the methane fermentation stages. As described by Ehrig and Scheelhaase (1993), the acid stage is characterized by BOD/COD values greater than 0.4, and the methane fermentation stage is characterized by BOD/COD values less than 0.1.

Average chemical concentrations of cadmium, benzene, 1,2-dichloroethane, trichloroethylene, and vinyl chloride in MSW landfill leachates exceeded MCLs. None of the landfills had leachate with average chemical concentrations exceeding the MCLs for ethylbenzene, toluene, or xylenes.

Table E-6.2 Average Concentrations of Select Parameters Over TIme for Cell B1.

Date	pH (pH units)	BOD (mg/l)	COD (mg/l)	BOD/COD	Chloride (mg/l)	Methylene Chloride (μg/l)
1985	6.01	1,180	2,900	0.41		
1986	6.04	2,440	9,650	0.25	359	289
1987	5.93	16,700	38,600	0.43	1,070	898
1988	6.26	3,120	5,780	0.54	1,000	860
1989	6.83	2,065	4,250	0.48	825	560
1990	7.64	730	1,670	0.43	1,180	50
1991	7.47	124	1,850	0.07	4,080	6
1992	7.43	68	572	0.11	1,350	2
1993	7.43	130	1,440	0.09	320	16
1994	7.82	112	1,050	0.11	1,350	8

E-6.2.3 HW

The HW landfill leachates were more mineralized and had a higher organic content than MSW leachates. No COD or BOD data were available for these landfills. All of the HW leachates were alkaline, with pH values ranging from 7.55 to 9.36. One possible explanation for the alkaline pH values is the relatively common practice of solidifying HW with pozzolonic additives prior to disposal. These relatively high pHs decrease the mobility of metals. Even so, the metal concentrations in the HW leachates were relatively high. The average concentrations of the heavy metals were generally several times to several orders of magnitude higher in HW leachate as compared to MSW leachate. The biggest difference occurred for arsenic: the average arsenic concentrations in leachates from HW and MSW landfills were 26,710 and 22 μg/l, respectively. However, the high average arsenic concentration for HW leachate was due to the high arsenic levels in leachate from Landfill AD. Excluding the data from this HW landfill, the average arsenic concentration for HW leachate is 110 μg/l. The HW leachates also had higher average concentrations than MSW leachates of all VOCs except for methylene chloride, toluene, and xylenes. These differences can be seen from comparing the distributions of select chemical data for MSW and HW leachates given in Figures E-6.1 and E-6.2, respectively. Of the heavy metals and VOCs considered in Table E-6.1, arsenic, nickel, 1,2-dichloroethane, and vinyl chloride were detected at the highest concentrations in HW leachates.

Average concentrations of arsenic, cadmium, chromium, benzene, 1,2-dichloroethane, trichloroethylene, and vinyl chloride in HW landfill leachates exceeded MCLs. None of the landfills had leachate with average chemical concentrations exceeding the MCLs for ethylbenzene, toluene, or xylenes.

E-6.2.4 ISW

E-6.2.4.1 MSW Ash

For the purposes of the discussions on leachate chemistry, MSW ash landfill leachate is grouped with leachate from ISW landfills. This grouping is considered appropriate because MSW ash landfill leachate is typically nonhazardous and has chemical characteristics more similar to leachate from ISW landfills than to leachate from MSW or HW landfills. The MSW ash landfill leachates were more mineralized than the MSW leachates, as evidenced by the high specific conductance, TDS, sulfate, and chloride levels of the MSW ash leachates. The concentrations of heavy metals were within the range of those for MSW leachates. Unlike MSW leachates, the COD and BOD values for the MSW ash leachates were very low because most of the organic portion of the MSW had been combusted. As expected, no VOCs were detected. The lower BOD concentration, higher sulfate concentration, and lower VOC concentrations in MSW ash leachate as compared to MSW leachate can be seen by comparing Figures E-6.1 and E-6.3.

Average concentrations of cadmium in the MSW ash landfill leachates exceeded MCLs. None of the landfills had leachate with average chemical concentrations exceeding the MCLs for any considered chemical except cadmium.

E-6.2.4.2 Coal Ash

Leachate chemistry data were obtained for the two coal ash landfills located in the NE. The ash was produced in plants burning eastern bituminous coal. The coal ash leachate was slightly alkaline and contained metals, but no VOCs. This was expected since any VOCs would have been combusted with the coal. In comparison to the MSW, HW, and MSW ash leachates, the coal ash leachate was less mineralized and contained metals at concentrations generally at the lower end of the concentration range for MSW leachates. The relatively low concentrations of metals were expected based on the relatively low levels of sulfate in the leachate.

Average concentrations of cadmium in the coal ash landfill leachates exceeded MCLs. None of the landfills had leachate with average chemical concentrations exceeding the MCLs for any considered chemical except arsenic and cadmium.

E-6.2.4.3 C&DW

The leachates from the two C&DW landfills were similar to MSW leachates in terms of inorganic and organic chemistry. With the exception of benzene, trichloroethylene, and vinyl chloride, the considered heavy metals and VOCs were detected at concentrations below MCLs.

E-6.3 Comparison to Published Data

The leachate chemistry data collected for this study and summarized in Table E-6.1 were compared to the published data presented in Table E-2.2. In general, the leachate chemistry data collected for this study fall within the range of published data. The exception to this are for the ISW landfills, which have not been fully characterized in the literature. Also, the chemistry of ISW landfills is highly variable depending on waste type. Based on published data, the concentrations of metals in MSW ash leachates can be quite high, higher than those for MSW leachates and, sometimes, higher than those for HW leachates. However, the database for MSW ash landfills presented herein does not support this. The concentrations of heavy metals for the MSW ash leachates were within the range of those for MSW leachates. The literature also shows that the heavy metals concentrations in C&DW leachates can be quite high. However, the limited database for C&DW landfills didn't support this. It may be that the total metal content disposed of in landfills has been reduced since the previous studies due to community recycling programs.

E-6.4 Effect of Regulations on Leachate Chemistry

As discussed in Section E-2.3.1, with the solid waste regulations promulgated in the 1980's and early 1990's, it is expected that the quality of landfill leachate would have improved over time. To evaluate whether this has occurred, the MSW and HW leachate chemistry data collected for modern facilities in this appendix were compared to data from older facilities.

The concentrations of the 30 considered constituents in leachates from the older modern MSW landfills constructed prior to 1990 (pre-1990 landfills) and the newer MSW landfills constructed after 1990 (post-1990 landfills) are shown in Table E-6.1. The average concentrations of selected chemicals in the landfill cells are shown in Figure E-6.4. No major differences between the leachate chemistry for the pre-1990 landfills and the post-1990 landfills were apparent. The chemistry data sets had no statistically significant differences in the concentrations of trace metals or VOCs at the 90% confidence level, though average VOC concentrations were generally lower in leachate from the post-1990 landfills. The statistical analysis findings were limited by the data. The limited number of landfills contributing to each data set and the wide range of chemical concentrations led to large confidence intervals for each parameter in the data sets. To further evaluate the differences in leachate chemistry between older and newer MSW landfills, the data for the post-1990 MSW landfills were compared to published leachate chemistry data for 61 older MSW landfills (i.e., pre-1980 landfills in NUS (1988) and pre-1985 landfills in Gibbons et al. (1992)). The distribution of the leachate chemistry data for the older MSW landfills was not known, so the two data sets could not be compared statistically. However, the average concentrations of trace metals and VOCs in leachate from the newer landfills were almost always less than the average concentrations in leachate from the older landfills. Based on the above, it appears that the solid waste regulations have resulted in improved MSW landfill

leachate quality. However, more data are needed to quantify this improvement. From the published information summarized in this report, the regulations may have also reduced the occurrence of certain chemicals. For example, acetonitrile, cyanide, and naphthalene were detected more frequently in leachate from older landfills than in leachate from newer landfills.

Published leachate chemistry data for 33 older HW landfills (i.e., pre-1984 landfills in Bramlett et al. (1987), pre-1983 landfills in NUS (1988), and pre-1987 landfills in Gibbons et al. (1992)) were compared to the data presented for HW landfills in this report (i.e., newer HW landfills). The data set for newer HW landfills is small; only leachate chemistry data for four landfills are available. The concentrations of chemicals in leachate from the newer landfills were found to be within the range of published values for the older landfills. The distribution of the leachate chemistry data for the older HW landfills was not known, so the two data sets could not be compared statistically. However, on average, most heavy metal concentrations and almost all VOC concentrations were lower in leachate from the newer landfills. This reduction in leachate strength is likely a result of the Subtitle C regulations and the Land Disposal Restrictions.

E-7 Conclusions

E-7.1 Primary Liner Leakage Rates and Efficiencies

E-7.1.1 GM Primary Liners

Performance of GM primary liners was evaluated using LCRS and LDS flow rate data from 31 double-lined landfill cells at 14 landfills monitored for periods of up to 114 months. Formal CQA programs were used in the construction of 23 cells that had HDPE GM primary liners. Six of the eight cells that were constructed without a CQA program used CSPE GM primary liners and the remaining two cells used HDPE GM primary liners. The major findings of the evaluation are summarized below:

- LDS flows during the initial period of operation are attributed primarily to construction water and primary liner leakage. LDS flows during the active and post-closure periods are attributed primarily to primary liner leakage.
- Average monthly LDS flow rates for cells constructed with a formal CQA program ranged from about 5 to 440 lphd during the initial period of operation, 1 to 360 lphd during the active period, and 2 to 60 lphd during the post-closure period. Peak monthly flow rates for these cells were typically below 500 lphd and exceeded 1,000 lphd in only two of the 23 cells.
- Based on an analysis of the available data, average monthly active-period LDS flow rates through HDPE GM primary liners constructed with CQA (but without ponding tests or electrical leak location surveys) will often be less than 50 lphd, but occasionally in excess of 200 lphd. These flows are attributable primarily to liner leakage, and, for cells with sand LDSs, possibly construction water.

- The eight cells constructed without a formal CQA program exhibited average monthly LDS flow rates that are about one to two orders of magnitude greater than LDS flow rates for cells constructed with CQA. The average flow rates from the eight cells ranged from 120 to 2,140 lphd during the initial period of operation, 70 to 1,600 lphd during the active period, and, for the two cells for which post-closure data are available, 210 to 240 lphd during the post-closure period. The large differences in LDS flow rates between cells constructed with CQA and cells constructed without CQA are partly attributed to the benefits of CQA and partly due to differences in the GM materials and construction (i.e., seaming) methods. The two cells that had HDPE GM primary liners and no formal CQA had average LDS flow rates that are about two to seven times greater than the mean LDS flow rate for all cells constructed with a formal CQA program. In contrast, the cells with CSPE GM primary liners and no formal CQA exhibited average LDS flow rates that are about one to two orders of magnitude greater than the mean LDS flow rate for all cells that had CQA. There are not sufficient data, however, in this appendix to accurately separate the effects of CQA and GM type (i.e., HDPE vs. CSPE) and construction methods on leakage rates through GM liners.
- Based on an analysis of the available data, GM liners can be constructed to achieve very good hydraulic performance (i.e., E_t values greater than 99%). However, even with a CQA program, GM liners sometimes will not achieve this performance level and lower E_t values, in the range of about 90 to 99%, will occur. This relatively broad range of E_t values is a consequence of the potential for even appropriately installed GMs to have an occasional small hole, typically due an imperfect seam, but also potentially due to a manufacturing or construction-induced defect not identified by the CQA program. Leakage can occur, relatively unimpeded, through a GM hole if the GM is not underlain by a low-permeability material such as a CCL or a GCL. If a hole occurs at a critical location where a sustained hydraulic head exists, such as in a landfill sump, the rate of flow through the hole can be significant. In contrast, the GCL or CCL component of a composite liner can impede flow through a GM hole, even if it occurs at a critical location.

The conclusion to be drawn from the data evaluation is that single-liner systems with GM liners (installed on top of a relatively permeable subgrade) should not be used in landfill applications where E_t values as low as 90% would be unacceptable, even if a thorough CQA program is employed. In these cases, single-composite liner systems or double-liner systems should be utilized. An exception to this conclusion may be made for certain facilities, such as surface impoundments or small, shallow landfill cells, with GM primary liners that can be field tested over the GM sheet and seams using electrical leak location surveys, ponding tests, or other methods. For these facilities, higher efficiencies (i.e., greater than 99%) may be achieved with GM liners by identifying and repairing the GM holes during construction and, especially for surface impoundments, during operation. In all cases, GM liners should be manufactured and installed using formal quality assurance programs.

E-7.1.2 Composite Primary Liners

Performance of composite primary liners was evaluated using LCRS and LDS flow rate and chemical constituent data from 41 double-lined landfill cells monitored for periods of up to 121 months. All 41 of the cells were constructed with formal CQA programs. The major findings are summarized below:

- For cells with composite liners, LDS flows during the initial period of operation are attributed primarily to construction water. LDS flows during the active and post-closure periods are primarily attributed to primary liner leakage and compression water for cells with GM/GCL primary liners or consolidation water (including secondary compression) for cells with GM/CCL or GM/GCL/CCL primary liners.
- LDSs underlying GM/GCL composite liners exhibited average monthly flow rates of 0 to 290 lphd during the initial period of operation, 0 to 11 lphd during the active period, and 0 to 2 lphd (with many values reported as zero) during the post-closure period.
- Average monthly active-period LDS flow rates from cells with GM/GCL primary liners constructed with CQA will often be less than 2 lphd, but occasionally in excess of 10 lphd.
- LDSs underlying composite liners with a CCL or GCL/CCL lower component exhibited average monthly flow rates of about 10 to 1,400 lphd during the initial period of operation, 0 to 370 lphd during the active period of operation, and 5 to 210 lphd during the post-closure period.
- Given the "masking" effects of consolidation water, key chemical constituent data must be used to assess the hydraulic performance of composite primary liners having a CCL or GCL/CCL lower component. This approach was applied to 13 landfill cells. There were insufficient data for three of the cells to draw any conclusions. For the remaining ten cells, key LCRS and LDS chemical constituent data did not reveal obvious indications of primary liner leakage; however, for five of these latter cells, the data were of insufficient completeness and duration to quantify primary liner performance. E_t values were estimated for the remaining five cells. The calculated values range from 99.1 to greater than 99.9%.
- The data in this appendix suggest that GM/GCL, GM/CCL, and GM/GCL/CCL composite liners of the type evaluated in this study can be constructed to achieve E_t values of 99.9% or more. However, E_t values in the range of 99 to 99.9% will also occur. These high efficiencies demonstrate that the low-permeability soil component of a composite liner is effective in impeding leakage through holes in the GM component of the liner.
- Available leakage rate calculation methods for composite liners give leakage rates in the same range as the rates estimated from the data for composite primary liners presented in this appendix. Notwithstanding the uncertainties in both the assumptions used in the calculations and the estimated leakage rates, this is a useful finding.

- In the U.S., landfill cells are typically operated for periods of one to five years, occasionally longer, and they are promptly covered with a GM or other low-permeability barrier after filling. This operations sequence defines the timeframe for significant leachate generation in a landfill cell that does not contain liquid wastes or sludges and that does not undergo leachate recirculation or moisture addition. For the cells in this study, estimated advective breakthrough times through CCLs, assuming no chemical retardation, were generally calculated to range from about 3 to 12 years. It thus appears that GM/CCL and GM/GCL/CCL composite liners are capable of substantially preventing leachate migration over the entire period of significant leachate generation for typical modern landfills.

Finally, it is recognized that the current database for the evaluation of composite liner performance is limited, in terms of both completeness and duration of monitoring. Key constituents, such as alcohols and ketones that could be better organic "tracers" than the aromatic hydrocarbons used in this appendix, are poorly represented in the database. It is important that additional data be collected so that our understanding of the performance characteristics of these systems can continue to improve.

E-7.2 Leachate Generation Rates

Leachate generation rates at 140 individually monitored cells located at 50 modern landfills were evaluated. About 52% of the cells are MSW cells, 40% are HW cells, and only 8% are ash cells and C&DW cells. Most of the landfills (64%) are located in the NE, 28% are located in the SE, and only 8% are located in the W. Leachate generation rates for 33 closed MSW and HW cells, located primarily in the NE and SE, were also evaluated. The monitoring periods were up to 8 years for active operation conditions and up to 9 years for post-closure conditions. The major findings of these evaluations are summarized below.

- LCRS flow rates during operations can vary significantly between landfills located in the same geographic region and accepting similar wastes. Large variations in flow rates (e.g., one order of magnitude difference) can even occur between cells at the same landfill. Differences in waste placement practices may be responsible for these significant variations. Limiting the size of the active disposal area and using effective measures to minimize rainfall infiltration into the waste and to divert surface-water runoff away from the waste will significantly decrease leachate generation rates compared to the rates observed under less controlled conditions.
- Average LCRS flow rates for MSW landfills located in the NE and SE varied between 1,000 lphd and 44,000 lphd during the initial period of operation and between 40 lphd and 18,000 lphd during the active period of operation. For this group of landfills during the initial period of operation, 60% of the cells exhibited average LCRS flow rates less than 10,000 lphd and only 13% had rates greater than 20,000 lphd. For the same group during the active period of operation,

52% of the cells had average LCRS flow rates less than 2,500 lphd, 79% of the cells had average LCRS flow rates less than 5,000 lphd, and only 5% had average LCRS flow rates greater than 10,000 lphd. Only two MSW cells are located in the W. These two cells had very low average LCRS flow rates (i.e., 55 and 110 lphd).

- RF values calculated for the MSW cells in the NE (means of 39% and 13% for the initial and active periods of operation, respectively) were higher than RF values for the SE cells (means of 33% and 8% for the initial and active periods of operation, respectively). It is possible that the higher water evaporation rates and the higher runoff occurring with the shorter duration, more intense rainfall events associated with the SE offset any potential increases in leachate generation rates caused by the higher total amount of rainfall in the SE as compared to the NE. RF values for the two MSW cells that are located at an arid site in the W were less than 1%.
- Average flow rates from HW landfills during the active period of operation were 50 to 60% higher than flow rates from MSW landfills. The reason for these higher leachate generation rates at the HW landfills in this study is unclear, but may, in part, be due to differences in waste characteristics and operational practices. Stabilized HW may be wetter and/or have a lower water storage capacity than MSW. In addition, in comparison to landfills, cover materials are less frequently used in HW landfills to divert clean storm water from the waste. The ten HW cells located in the W had low average flow rates during operations (i.e., less than 4,000 lphd).
- RF values calculated for the HW landfills in the NE (mean = 46% and 21% for the initial and active periods operation, respectively) were higher than RF values for the landfills in the SE (mean = 33% and 11% for the initial and active periods of operation, respectively). Similar to the MSW landfills, the HW landfills in the SE had lower RF values than landfills in the NE. RF values for the HW cells in the W were typically below 10%.
- The limited number of ash and C&DW landfills considered in this study exhibited LCRS flow rates during the active period of operation that were 300 to 600% higher than flow rates from MSW and HW landfills. These average rates during operations were between 1,000 lphd and 35,000 lphd for the ash cells and between 4,000 and 20,000 lphd for the C&DW cells. It is possible that differences in the waste characteristics and disposal practices are responsible for the higher LCRS flow rates for ash and C&DW landfills.
- Mean RF values during operations were about 53% for ash cells and 43% for C&DW cells.
- Peak monthly LCRS flow rates were typically two to three times the average monthly flow rates for all types of waste and regions of the U.S.
- Landfill geographic region has a major impact on LCRS flow rates. For landfill sites with historical average annual rainfall less than 500 mm, average LCRS flow rates were low, typically less than 2,000 lphd. LCRS flow rates increased with increasing rainfall up to a point. In general, for landfill sites with historical

average annual rainfall greater than 1,100 to 1,200 lphd an increase in rainfall did not appear to cause a corresponding increase in leachate generation rate.

- LCRS flow rates were typically two to three times smaller during the active period of operation than during the initial period of operation.
- Leachate generation rates for the closed landfills in this study typically decreased by a factor of four within one year after closure and by one order of magnitude within two to four years after closure. Six years after closure, LCRS flow rates were between 5 and 1,200 lphd (mean of 180 lphd). Nine years after closure, LCRS flow rates were negligible. These data show that well designed and constructed final cover systems can be very effective in minimizing infiltration of rainfall into the waste, thus reducing leachate generation rates to near-zero values.

E-7.3 Leachate Chemistry

Select leachate chemistry data for 59 cells at 50 double-lined landfills are presented and evaluated in this appendix. Most of the data are for MSW landfills: there are 36 MSW landfills, four HW landfills, and eleven ISW landfills in the database. Fewer data are available for HW and ISW landfills. In addition, the types of wastes placed in HW and ISW landfills are generally more variable between landfills than wastes placed in MSW landfills. With the exception of the leachate chemistry data for MSW ash landfills, it is likely that the data presented in this appendix do not fully characterize the variation in leachate chemistry for HW and ISW landfills. The chemistry data for MSW ash landfill leachate may be representative of modern MSW ash landfills in the U.S. because seven landfills are included in the database and the chemistry of MSW ash is less variable than HW.

It is recognized that the database on leachate chemistry is limited in terms of completeness and duration of monitoring. In addition, key MSW and HW leachate constituents, such as alcohols and ketones, are poorly represented in the database. It is important that these additional data be collected so that our understanding of the performance characteristics of composite liners can continue to improve.

From the evaluation of landfill leachate chemistry data presented herein, the following conclusions are drawn:

- For a given waste type, many of the leachate constituents exhibited significant concentration variations (e.g., several orders of magnitude difference) between landfill cells and, sometimes, for a given cell.
- For the leachate types for which data are available for more that two landfills, the average value of pH (pH units), specific conductance (μmhos), COD (mg/l), BOD_5 (mg/l), TOC (mg/l), and chloride (mg/l) were, respectively:
  - MSW leachate: 6.7, 4,470, 2,500, 1,440, 380, and 560;
  - HW leachate: 8.2, 22,100, not available, not available, 1,620, and 7,760; and
  - MSW ash leachate: 7.1, 22,100, 1,670, 55, 62, and 10,400.

- The MSW landfill leachates were mineralized, biologically-active liquids with relatively low concentrations of heavy metals and VOCs. On average, the leachates were slightly acidic (i.e., average pH of 6.7), which is expected because carbon dioxide and organic acids are the primary by-products of the first stage (i.e., the acid stage) of anaerobic degradation of organic compounds in MSW landfills. The chemistry of these leachates changed with time as the organic compounds degraded (see, for example, Table E-6.2). In general, the leachate characteristics for cells receiving waste were more indicative of the acid phase of degradation than the second stage (i.e., the methane fermentation phase) of anaerobic degradation. For closed cells, the leachate pH typically increased with time and the BOD/COD ratio decreased with time, which is expected as the landfill is more fully in the methane fermentation phase of degradation. Of the heavy metals and VOCs considered in Table E-6.1, chromium, nickel, methylene chloride, and toluene were detected at the highest concentrations in MSW leachates. Average concentrations of cadmium, benzene, 1,2-dichloroethane, trichloroethylene, and vinyl chloride in MSW landfills leachates exceeded federal maximum contaminant levels (MCLs) for drinking water. None of the landfills had leachate with average chemical concentrations exceeding the MCLs for ethylbenzene, toluene, or xylenes.
- The HW landfill leachates were more mineralized and had a higher organic content than MSW leachates. All of the HW leachates were alkaline, with pH values ranging from 7.5 to 9.4. One possible explanation for the alkaline pH values is the relatively common practice of solidifying HW with pozzolonic additives prior to disposal. These relatively high pHs decrease the mobility of metals. Even so, the average heavy metals concentrations were generally several times to several orders of magnitude higher in HW leachates as compared to MSW leachates. The HW leachates also had higher average concentrations of all VOCs, except methylene chloride, toluene, and xylenes. Of the heavy metals and VOCs considered in Table E-6.1, arsenic, nickel, 1,2-dichloroethane, and vinyl chloride were detected at the highest concentrations in HW leachates. Average concentrations of arsenic, cadmium, chromium, benzene, 1,2-dichloroethane, trichloroethylene, and vinyl chloride in HW landfill leachates exceeded MCLs. None of the landfills had leachate with average chemical concentrations exceeding the MCLs for ethylbenzene, toluene, or xylenes.
- The chemistry of the ISW landfill leachates was highly variable due to the wide variety of wastes disposed in ISW landfills. The pH values for these leachates ranged from 6.4 to 7.7. The MSW ash leachates, the most mineralized of the ISW landfill leachates, were even more mineralized than the MSW leachates in this study, as evidenced by the high specific conductance, TDS, sulfate, and chloride levels of the MSW ash leachates. Coal ash leachates were the least mineralized. Both the MSW ash and coal ash leachates had low BOD values that were several orders of magnitude less than the BOD values for MSW leachate because most of the organic materials originally in the MSW and coal had been combusted. The average BOD value for C&DW leachate, however,

was within range of values reported for MSW leachate. Heavy metals concentrations in MSW ash and C&DW leachates were similar to those for MSW leachates. Metals concentrations in coal ash leachate were lower, generally at the lower end of the concentration range for MSW leachates. As expected, the MSW ash and coal ash leachates did not contain VOCs. However, published data show that MSW ash leachates can contain trace amounts of base neutral extractables (BNAs), polychlorinated dibenzo-p-dioxins (PCDDs), and polychlorinated dibenzo-furans (PCDFs). The one C&DW landfill for which organic chemistry data are available produced leachate containing VOCs. Average concentrations of cadmium in MSW ash and coal ash landfill leachates and benzene, trichloroethylene, and vinyl chloride concentrations in C&DW landfill leachates exceeded MCLs.

- In general, the leachate chemistry data collected for the study fall within the range of published data.
- With the federal solid waste regulations promulgated in the 1980's and early 1990's, it is expected that the quality of MSW and HW landfill leachates would have improved over time. No statistically significant differences in concentrations of the considered trace metals or VOCs in leachates from older modern MSW landfills constructed prior to 1990 (pre-1990 landfills) and leachates from the newer MSW landfills constructed after 1990 (post-1990 landfills) were observed at the 90% confidence level. However, average VOC concentrations were generally lower in leachate from the post-1990 landfills (Table E-6.1). The statistical analysis findings were limited by the data. The limited number of landfills contributing to each data set and the wide range of chemical concentrations led to large confidence intervals for each parameter in the data sets. To further evaluate the differences in leachate chemistry between older and newer MSW landfills, the data for the post-1990 MSW landfills were compared to published leachate chemistry data summarized in Table E-2.1 for 61 older MSW landfills (i.e., pre-1980 landfills in NUS (1988) and pre-1985 landfills in Gibbons et al. (1992)). The distributions of the leachate chemistry data for the older MSW landfills were not known, so the two data sets could not be compared statistically. However, the average concentrations of trace metals and VOCs in leachate from the newer landfills were almost always less than the average concentrations in leachate from the older landfills. Based on the above, it appears that the solid waste regulations have resulted in improved MSW landfill leachate quality. However, more data are needed to quantify this improvement. From the published information summarized in this report, the regulations may have also reduced the occurrence of certain chemicals. For example, acetonitrile, cyanide, and naphthalene were detected more frequently in leachate from older landfills than in leachate from newer landfills .
- Published leachate chemistry data summarized in Table E-2.1 for 33 older HW landfills (i.e., pre-1984 landfills in Bramlett et al. (1987), pre-1983 landfills in NUS (1988), and pre-1987 landfills in Gibbons et al. (1992)) were compared to the data presented for HW landfills in this report (i.e., newer HW landfills). The data set for newer HW landfills is small; only leachate chemistry data for four

landfills are available. The concentrations of chemicals in leachate from the newer landfills were found to be within the range of published values for the older landfills. The distribution of the leachate chemistry data for the older HW landfills was not known, so the two data sets could not be compared statistically. However, on average, most heavy metal concentrations and almost all VOC concentrations were lower in leachate from the newer landfills.

E-8 References

Baker, J. (1987) personnel communication from J. Baker (WMI) to S. Monney (EPA) concerning MSW landfill leachate data, 1 Dec.

Bergstrom, W.R., Takacs, M.J., and Olson, M.A. (1993) "Behavior of Five Operating Landfill Leak Detection Systems", *Proceedings, Waste Tech '93*, Marina Del Rey, CA, pp. 2.2-2.14.

Bonaparte, R. and Gross, B.A. (1990) "Field Behavior of Double-Liner Systems", *Waste Containment Systems: Construction, Regulation, and Performance*, ASCE Geotechnical Special Publication No. 26, R. Bonaparte, ed., New York, pp. 52-83.

Bonaparte, R. and Gross, B.A. (1993) "*LDCRS Flows from Double-Lined Landfills and Surface Impoundments*", EPA/600/SR-93/070, EPA Risk Reduction Engineering Laboratory, Cincinnati, OH, 65 p.

Bonaparte, R., Othman, M.A., Rad, N.S., Swan, R.H., and Vander Linde, D.L. (1996) "Evaluation of Various Aspects of GCL Performance", Appendix F in *Report of 1995 Workshop on Geosynthetic Clay Liners*, D.E. Daniel and H.E. Scranton, authors, EPA/600/R-96/149, EPA National Risk Management Research Laboratory, Cincinnati, OH, pp. F1-F34.

Bramlett, J., Furman, C., Johnson, A., Ellis, W.D., Nelson, H. and Vick, W.H. (1987) "*Composition of Leachates from Actual Hazardous Waste Sites*", EPA Office of Research and Development, Cincinnati, OH, EPA/600/2-87/043, 113 p.

Brown, K.W. and Donnelly K.C., (1988) "An Estimation of the Risk Associated with the Organic Constituents of Hazardous and Municipal Waste Landfill Leachates", *Hazardous Waste & Hazardous Materials*, Vol. 5, No. 1, pp. 1-30.

Chian, E.S.K. and DeWalle, F.B., (1997) "*Evaluation of Leachate Treatment, Volume I, Characterization of Leachate*", EPA Office of Research and Development, EPA/600/2-77/186a, Cincinnati, OH.

Daniel, D.E. and Koerner, R.M. (1995) "*Waste Containment Systems: Construction Quality Assurance, and Quality Control*", ASCE Press, New York, 354 p.

Darilek, G.T., Laine, D.L., and Parra, J.O. (1989) "The Electrical Leak Location Method for Geomembrane Liners: Development and Applications", *Proceedings, Geosynthetics '89 Conference*, San Diego, CA, Vol. 2, pp. 456-466.

Darilek, G.T., Merizel, R., and Johnson, A. (1995) "Minimizing Geomembrane Liner Damage While Emplacing Protective Soil", *Proceedings, Geosynthetics '95 Conference,* Nashville, Tennessee, Vol. 2, pp. 669-676.

Ehrig, H.J. and Scheelhaase, T. (1993) "Pollution Potential and Long Term Behavior of Sanitary Landfills", Proceedings of the Fourth International Landfill Conference, Sardinia, Italy, pp. 1203-1225.

Eisenberg, S.H., Tittlebaum, M.E., Eaton, H.C., and Soroczak, M.M., (1986) "Chemical Characteristics of Selected Flyash Leachates", *Journal of Environmental Health and Science*, Part A, Vol. 21, No. 4, pp. 383-402.

EPA (1987a) "*Background Document: Proposed Liner and Leak Detection Rule*", EPA/530-SW-87-015, prepared by GeoSyntec Consultants, 526 p.

EPA, (1987b) "*Test Methods for Evaluating Solid Waste, Physical/Chemical Methods*", EPA Publication SW-846, Third Edition, 1986 and Revision I, 1987.

EPA (1988) "*Report to Congress: Solid Waste Disposal in the United States*", Vols. I and II, revised final draft, EPA Office of Solid Waste, Washington, D.C., unpublished.

EPA (1989) "*Cooperative Industry Report, Leachate Treatability Study - Task 1 - Leachate Characterization Analytical Results*", EPA Office of Solid Waste, Washington, D.C.

EPRI (1978) "*The Impact of RCRA (PL 94-580) on Utility Solid Wastes*", EPRI FP-878, EPRI, Palo Alto, California, 133 pp.

Feeney, M.T. and Maxson, A.E. (1993) "Field Performance of Double-Liner Systems", *Proceedings, Geosynthetics '93 Conference*, Vol. 3, Vancouver, B.C., pp. 1373-1387.

GeoSyntec Consultants (1993), Confidential Report on Coal Ash Landfill.

Gibbons, R.D., Dolan, D., Keough, H., O'Leary, K., and O'Hara, R. (1992) "A Comparison of Chemical Constituents in Leachate From Industrial Hazardous Waste & Municipal Solid Waste Landfills", *Proceedings, Fifteenth Annual Madison Waste Conference*, Madison, WI, pp. 251-276.

Giroud, J.P. (1984) "Impermeability: The Myth and a Rational Approach", *Proceedings, International Conference on Geomembranes*, Denver, CO, Vol. 1, pp. 157-162.

Giroud, J.P. and Bonaparte, R. (1989) "Leakage Through Liners Constructed with Geomembranes, Part II: Composite Liners", *Geotextiles and Geomembranes*, Vol. 8, No. 2, pp. 77-111.

Giroud, J.P., Badu-Tweneboah, K., and Bonaparte, R. (1992) "Rate of Leakage Through a Composite Liner Due to Geomembrane Defects", *Geotextiles and Geomembranes*, Vol. 11, No. 1, pp. 1-28.

Gross, B.A., Bonaparte, R., and Giroud, J.P. (1990) "Evaluation of Flow From Landfill Leakage Detection Layers", *Proceedings, Fourth International Conference on Geotextiles*, Vol. 2, The Hague, pp. 481-486.

Haikola, B.M., Loehr, R.C., Daniel, D.E. (1995) "Hazardous Waste Landfill Performance as Measured by Primary Leachate Quantity", *Proceedings, Geoenvironment 2000*, New Orleans, LA , Vol. 1, ASCE Special Topic Paper No. 46, pp. 554-567.

Hunt, W.C. and Dollins, M. (1996) "Continuation of the Study of Leachate Quantity Generation Data Obtained From a Subtitle D Landfill Cell", *Proceedings Texas Solid Waste Management Conference*, Austin, TX, pp. 97-107.

Laine, D.L. (1991) "Analysis of Pinhole Seam Leaks Located in Geomembrane Liners Using the Electrical Leak Detection Method: Case Histories", *Proceedings, Geosynthetics '91 Conference*, Atlanta, GA, Vol. 1, pp. 239-253.

Laine, D.L. and Miklas, M.P. (1989) "Detection and Location of Leaks in Geomembrane Liners Using Electrical Method: Case History", *Proceedings, 10th National Superfund Conference*, Washington, D.C., pp. 35-40.

Laine, D.L., and Darilek, G.T. (1993) "Locating Leaks in Geomembrane Liners of Landfills Covered with Protective Soil", *Proceedings, Geosynthetics '93 Conference*, Vancouver, B.C., Vol. 3, pp. 1403-1412.

Landreth, R.E. (1989) "Locating and Repairing Leaks in Landfill/Impoundment Flexible Membrane Liners", *Proceedings, Geosynthetics '89 Conference*, San Diego, CA, Vol. 2, pp. 467-477.

Maule, J., McCulloch, J., and Lowe, R. (1993) "Performance Evaluation of Synthetically Lined Landfills", *Proceedings, 1993 GRI Seminar*, Philadelphia, PA, pp. 80-90.

McGinley, P.M. and Kmet, P. (1984) "*Formation, Characteristics, Treatment and Disposal of Leachate from Municipal Solid Waste Landfills*", Bureau of Solid Waste Management, Wisconsin Department of Natural Resources, Madison, WI, 288 p.

Norstrom, J. M., Williams, C.E., and Pabor, P.A. (1991) "Properties of Leachate From Construction/ Demolition Waste Landfills", *Proceedings, Fourteenth Annual Madison Waste Conference*, Madison, WI, pp. 357-366.

NUS (1986) "*Determination of Municipal Landfill Leachate Characteristics, Leachate Baseline Report*", EPA Office of Solid Waste, Washington, D.C., unpublished.

NUS (1987a) "*Characterization of Leachates From Municipal Waste Disposal Sites and Codisposal Sites, Volume 6*", EPA Office of Solid Waste and Emergency Response, Washington, D.C.

NUS (1987b) "*Characterization of MWC Ashes and Leachates from MSW Landfills, Monofills, and Co-Disposal Sites*", EPA Office of Solid Waste and Emergency Response, Washington, D.C., EPA/530/SW-87/028A.

NUS (1988) "*Draft Background Document Summary of Data on Municipal Solid Waste Landfill Leachate Characteristics "Criteria for Municipal Solid Waste Landfills" (40 CFR Part 258) Subtitle D of Resource Conservation and Recovery Act (RCRA)*", EPA Office of Solid Waste, Washington, D.C., EPA/530-SW-88-038.

NUS (1990) "*Characterization of Municipal Waste Combustion Ash, Ash Extracts, and Leachates*", EPA and Coalition on Resource Recovery and the Environment.

Pavelka, C., Loehr, R.C., and Haikola, B. (1994), "Hazardous Waste Landfill Characteristics", *Waste Management*, Vol. 13, No. 8, pp. 573-580.

Peggs, I.D. (1990) "Detection and Investigation of Leaks in Geomembrane Liners", *Geosynthetics World*, Vol. 1, No. 2, pp. 7-14.

Peggs, I.D. (1993) "Practical Geoelectric Leak Surveys with Hand-Held, Remote and Water Lance Probes", *Proceedings, Geosynthetics '93 Conference*, Vol. 3, Vancouver, B.C., pp. 1523-1532.

Piper, A.M. (1944) "A Graphic Procedure in the Geochemical Interpretation of Water Analyses", *Transactions of American Geophysical Union*, Vol. 25, pp. 914-923.

Rowe, R.K. (1995) "*Leachate Characteristics for MSW Landfills*", Geotechnical Research Centre Report GEOT-8-95, Department of Civil Engineering, The University of Western Ontario, London, Ont., 19 p.

Sabel, G.V. and Clark, T.P. (1984) "Volatile Organic Compounds as Indicators of Municipal Solid Waste Leachate Contamination", *Waste Management & Research*, No. 2, pp. 119-130.

Tedder, R.B. (1992) "*A Comparison of Florida Landfill Leachate with Regulatory Standards and EPA Landfill Leachate*", Florida Department of Environmental Regulation.

Tedder, R.B. (1997) "Evaluating the Performance of Florida Double-Lined Landfills", *Proceedings, Geosynthetics 97 Conference*, Long Beach, CA, Vol. 1, pp. 425-438.

Tharp, L.D. (1991) "Leachate Characteristics for Missouri Sanitary Landfills", *Proceedings, Fourteenth Annual Madison Waste Conference*, Madison, WI, pp. 313-326.

TRW (1983) "*Compilation of Hazardous Waste Leachate Data*", EPA Office of Solid Waste, Washington, D.C.

Workman, J.P. (1993) "Interpretation of Leakage Rates in Double-Lined Systems", Proceedings, *7th Geosynthetic Research Institute Seminar*, Drexel University, Philadelphia, PA, pp. 91-108.

Appendix F
Waste Containment Systems: Problems and Lessons Learned

by

Beth A. Gross, P.E.
GeoSyntec Consultants
Austin, Texas 70746

Rudolph Bonaparte, Ph.D., P.E.
GeoSyntec Consultants
Atlanta, Georgia 30342

J. P. Giroud, Ph.D.
J. P. Giroud, Inc.
Ocean Ridge, Florida 33435

performed under

EPA Cooperative Agreement Number
CR-821448-01-0

Project Officer

Mr. David A. Carson
United States Environmental Protection Agency
Office of Research and Development
National Risk Management Research Laboratory
Cincinnati, OH 45268

Appendix F
Waste Containment Systems: Problems and Lessons Learned

F-1 Introduction

F-1.1 Appendix Purpose and Scope

This appendix presents the results of an investigation into problems that have occurred in waste containment systems (i.e., liner systems and final cover systems (hereafter referred to as cover systems)) for 69 modern landfill and five modern surface impoundment facilities located throughout the United States (U.S.). The term "modern facility" refers to a facility designed with components substantially meeting current U.S. Environmental Protection Agency (EPA) regulations (e.g., 40 CFR 258 for municipal solid waste (MSW) disposal facilities or 40 CFR 264 for Resource Conservation and Recovery Act (RCRA) hazardous waste (HW) disposal facilities) and constructed and operated to the U.S. state of practice from the mid-1980's forward. The purpose of the study is twofold: (i) to better understand the nature, frequency, and significance of identified problems; and (ii) to develop recommendations to reduce the future occurrence of problems.

This appendix specifically excludes consideration of problems in older waste containment systems not designed and constructed to current standards and practices. These problems include, for example, the leachate collection and removal system (LCRS) and cover system internal drainage layer failures described by Bass (1986), Ghassemi et al. (1986), and Kmet et al. (1988). The appendix also does not address foundation stability problems at older landfills, such as the problems described by Oweis (1985), Dvirnoff and Munion (1986), Richardson and Reynolds (1991), Kenter et al. (1997), Stark and Evans (1997), and Schmucker and Hendron (1997). Problems at older facilities are often not relevant to current standards and practices.

F-1.2 Appendix Organization

This appendix is organized as follows:

- data on waste containment system problems are presented in Subsection F-2;
- the nature, frequency, detection, and remedy of the identified problems are discussed in Subsection F-3;
- the significance of the identified problems is discussed in Subsection F-4;
- conclusions from this study are presented in Subsection F-5;
- recommendations to reduce the future occurrence of the identified problems are presented in Subsection F-6;
- references are provided in Subsection F-7; and
- case histories of the identified problems are presented in Attachment F-A.

F-1.3 Terminology

Waste containment systems consist of liner systems and cover systems (Figure F-1.1). Modern landfills and surface impoundments (hereafter referred to as impoundments) both have liner systems that underlay the wastes placed in them (Figure F-1.2). A liner system consists of a combination of one or more drainage layers and low-permeability barriers (i.e., liners). A landfill single-liner system consists of a liner overlain by an LCRS drainage layer. A landfill double-liner system consists of primary and secondary liners, with a leak detection system (LDS) drainage layer between the two liners and an LCRS drainage layer above the primary liner. Besides drainage layers, the LCRS and LDS may also contain networks of perforated pipes, sumps, pumps, flowmeters, and other flow conveyance and monitoring components. A liner system may also include a protection layer over the LCRS drainage layer to further isolate the liner from the environment (e.g., freezing temperature, stresses from equipment). Impoundment liner systems are similar to those for landfills except that they do not have an LCRS.

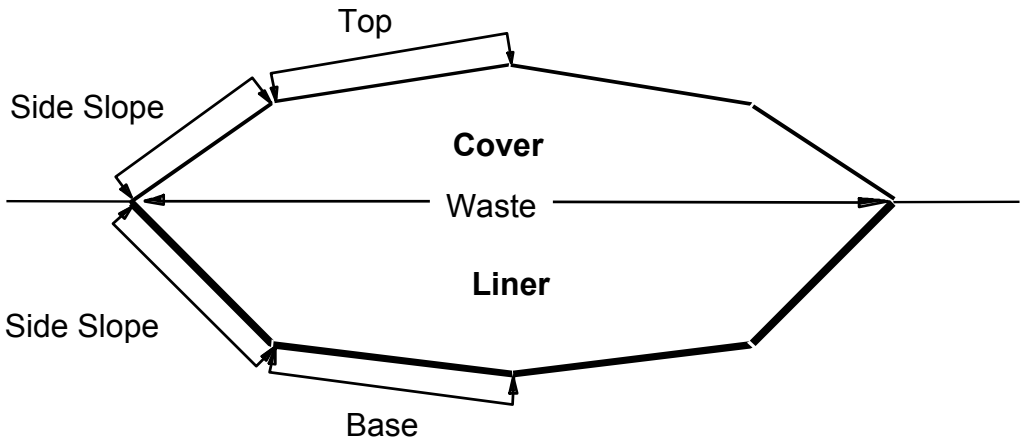

Figure F-1.1. Waste containment systems.

Once an area of a landfill is filled to final grade, a cover system is constructed over the area to contain the waste, minimize the infiltration of water into the waste, and control the emissions of gases produced by waste decomposition or other mechanisms. In contrast to landfills, impoundments are typically clean closed (i.e., the impoundment is removed and the site is reclaimed). A cover system consists of up to six basic components, from top to bottom: (i) surface layer; (ii) protection layer; (iii) drainage layer; (iv) barrier; (v) gas collection layer; and (vi) foundation layer. In some cases, the functions of several adjacent components can be provided by one soil layer. For example, a sand gas collection layer may also serve as a foundation layer.

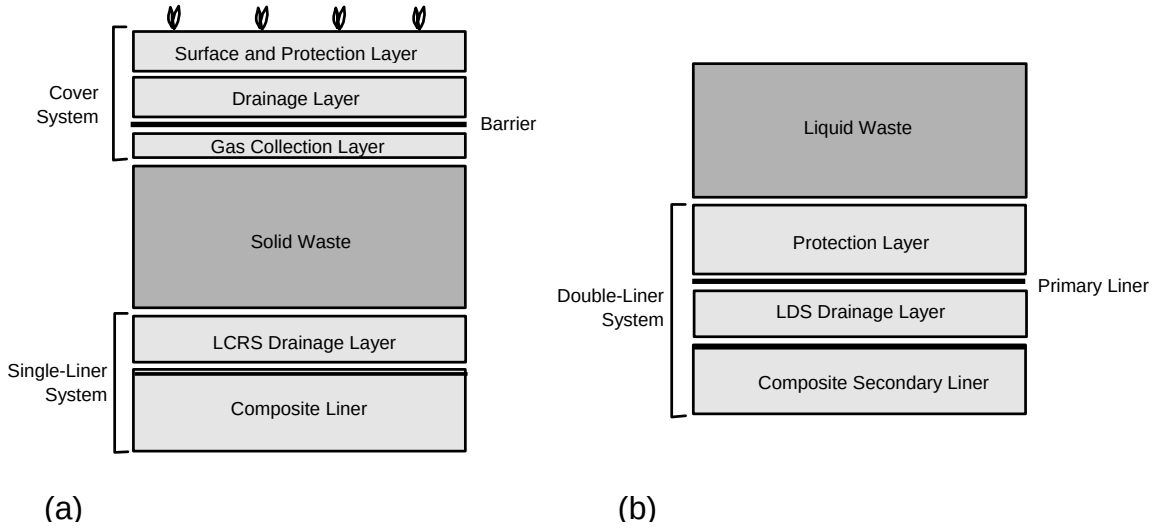

Figure F-1.2. Typical waste containment system components for landfills (a) and impoundments (b).

In general, the materials used to construct liners and barriers in modern waste containment systems are geomembranes (GMs) alone and composites consisting of GMs overlying compacted clay liners (CCLs) or geosynthetic clay liners (GCLs) (i.e., GM/CCL or GM/GCL composites). Drainage layers and gas collection layers are typically constructed with sand, gravel, geonets (GNs), or geotextile (GT)/GN composites (i.e., geocomposites (GCs)). Protection layers typically consist of soil or thick GTs. For landfills, the protection layer over the LCRS drainage layer sometimes consists of select waste. Surface layers for cover systems are typically constructed with vegetated topsoil.

Liner systems for modern MSW landfills and nonhazardous MSW combustor ash (MSW ash) landfills must, based on state-specific implementation of federal RCRA Subtitle D requirements, meet federal minimum design criteria or performance-based design requirements (40 CFR 258.40). The federal minimum design standard for new MSW landfills and MSW ash landfills requires a single-composite liner system that consists of the following, from top to bottom:

- LCRS that limits the head of leachate on the composite liner to 0.3 m or less;
- 0.75-mm thick GM; and
- 0.6-m thick CCL with a maximum hydraulic conductivity of 1×10^{-7} cm/s.

If the GM is made of high-density polyethylene (HDPE), the GM must be at least 1.5 mm thick. While the federal minimum design criteria were adopted by many states, a

few states require that MSW landfills or MSW ash landfills have a double-liner system. The performance standard requires a liner system design that is demonstrated to achieve certain groundwater compliance standards at a specified distance from the landfill. This distance cannot exceed 150 m.

For RCRA HW landfills and impoundments, federal regulations (40 CFR 264) require a double-liner system with at least the following components, from top to bottom:

- for landfills, LCRS that limits the head of leachate on the primary liner to 0.3 m or less;
- GM;
- 0.3-m thick granular LDS drainage layer with a minimum hydraulic conductivity of 1×10^{-2} cm/s or a geosynthetic LDS drainage layer with a minimum hydraulic transmissivity of 3×10^{-5} m^2/s;
- GM; and
- 0.9-m thick CCL with a maximum hydraulic conductivity of 1×10^{-7} cm/s.

Cover systems for modern lined MSW landfills and MSW ash landfills (40 CFR 258.40) must meet federal minimum design criteria or performance-based design requirements (40 CFR 258.60). The cover system meeting federal minimum design criteria consists of the following, from top to bottom:

- 0.15-m thick soil surface layer;
- 0.5-mm thick GM; and
- 0.45-m thick CCL with a maximum hydraulic conductivity of 1×10^{-5} cm/s.

If the GM is made of HDPE, the GM must be at least 1.5 mm thick. The performance-based cover system must perform equivalently to the cover system meeting federal minimum design criteria with respect to reduction in infiltration and erosion protection.

For RCRA HW facilities, EPA gives cover system performance requirements in 40 CFR 264; there are no federal design criteria for cover systems for these facilities. However, EPA guidance (EPA, 1989) recommends that the cover systems for HW facilities consist of the following, from top to bottom:

- 0.6-m thick soil surface and protection layer;
- 0.3-m thick granular drainage layer with a minimum hydraulic conductivity of 1×10^{-2} cm/s or a geosynthetic drainage layer with a minimum hydraulic transmissivity of 3×10^{-5} m^2/s;
- 0.5-mm thick GM; and
- 0.6-m thick CCL with a maximum hydraulic conductivity of 1×10^{-7} cm/s.

For industrial solid waste (ISW) facilities, such as papermill landfills, coal ash landfills, and construction and demolition waste (C&DW) landfills, EPA gives general performance requirements (e.g., "*provide adequate protection to ground and surface waters*") in 40 CFR 241. Currently, there are no federal design criteria for liner systems or cover systems for these facilities.

F-2 Data on Waste Containment System Problems

F-2.1 Data Collection Methodology

The data on waste containment system problems presented in this appendix were obtained from the technical literature and from discussions with facility owners, facility operators, design engineers, and federal and state regulators throughout the U.S. The data were collected in accordance with a quality assurance plan, which was reviewed and approved by the EPA. Efforts were made to obtain information on problems at ISW, MSW, and HW facilities and at facilities with different types of waste containment system components and sites (e.g., facilities constructed on flat terrain, in excavations, and in canyons, and landfills constructed over existing landfills). The investigation focused on landfills, which resulted in more problems being identified at landfills than at impoundments. Based on the broad-based method of data collection for this study, it is believed that the problems in this appendix are representative of those for waste containment systems in landfills nationwide. The study of impoundments was more limited and may not include some of the more common impoundment problems. However, some impoundment problems that have occurred but were not identified in this study may also have occurred at landfills (e.g., operational problems related to the LDS). Thus, the information on landfill problems in this appendix can also be used to identify problems that may have occurred at impoundments.

F-2.2 Detection of Problems

Problems in waste containment systems are typically detected by visual observation or an evaluation of monitoring data. Visual observation is the primary method of detecting problems during construction of liner systems and cover systems. For example, visual observation is used to detect excessive GM wrinkling during construction and uplift of geosynthetics by groundwater. Leak location surveys and other monitoring procedures can also be used to supplement visual observation during construction. For example, leak location surveys are used to detect leaks around pipe penetrations of liners. Common liner system and cover system nonconformities detected during construction quality assurance (CQA) monitoring and repaired in accordance with the CQA plan, however, are generally not problems. These nonconformities, such as CCL lifts not compacted to specification and

defective GM seams, are part of normal construction. During operation and after closure of landfills, liner systems are covered with waste and cannot be visually inspected. Then, evaluation of monitoring data is the primary method of detecting problems. Visual observation is also important, however, for detecting problems that are expressed at the surface of the waste containment system, such as erosion and slope failure.

The waste containment system monitoring data typically collected and evaluated during facility operation and closure are:

- LCRS flow quantity and quality data;
- LDS flow quantity and quality data;
- groundwater quality data (at groundwater monitoring wells); and
- landfill gas quality data (at gas monitoring wells).

LCRS data are used to evaluate: (i) effectiveness of runon controls and other leachate minimization practices; and (ii) treatment requirements for leachate before it may be discharged. LDS data are used to evaluate whether primary liner leakage is occurring. Additional information on LDS flow rates relevant to the evaluation of some of the case histories in this appendix is presented below. Groundwater and gas data are used to evaluate whether migration of contaminants is occurring from waste containment systems.

All liners in modern waste containment systems for HW landfills and for MSW landfills meeting federal design requirements include a GM. In a study of LDS flow rates from double-lined waste containment systems, Bonaparte and Gross (1993) found that all landfill cells with GM primary liners appeared to have exhibited primary liner leakage. Installed GMs typically have a small number of holes (e.g., 1 to 10 per hectare) due to field seaming flaws and construction-related damage. Leakage through GMs primarily occurs by advection through these holes. The leakage rate through a hole increases as hole size and head on top of the hole increase. If the GM is underlain by a low-permeability soil layer (i.e., CCL or GCL) to form a composite liner, the rate of leakage decreases with decreasing hydraulic conductivity of the soil layer. For a given head and hole size, the rate of leakage through a composite liner is approximately 100 to 10,000 times less than that through a GM alone. The head of leachate on liners is usually much smaller on side slopes than on the base. Therefore, all other things being equal, the leakage rate is greater on the base than on the side slopes. But if a composite liner is on the base and GM liner is on the side slopes, the leakage rate is greater on the side slopes.

It is sometimes difficult to use LDS flow rates to evaluate if, and how much, primary liner leakage is occurring because there are potential sources of LDS flow other than leakage (Gross et al., 1990). These sources are:

- water (mostly rainwater) that infiltrates the LDS during construction and continues to drain to the LDS sump after the start of facility operation ("construction water");
- water that infiltrates the LDS during construction, is held in the LDS by capillarity, and is expelled from the LDS as a result of LDS compression under the weight of the waste ("compression water");
- water expelled into the LDS from the CCL component of a composite primary liner as a result of clay consolidation under the weight of the waste ("consolidation water"); and
- water that percolates through the secondary liner and infiltrates the LDS ("infiltration water").

LDS flow quality data can be used and compared to LCRS flow quality data to help in the assessment of primary liner leakage. LDS flow data are used to evaluate whether primary liner leakage is occurring, but do not provide information on the leak location.

F-2.3 Problem Classification

The types of problems identified during the investigation for this appendix are categorized on the basis of two criteria. The first criterion addresses the component or attribute of the landfill liner system, landfill cover system, or impoundment liner system affected by the problem. The specific components and attributes considered in this study are: (i) landfill liner construction; (ii) landfill liner degradation; (iii) landfill LCRS or LDS construction; (iv) landfill LCRS or LDS degradation; (v) landfill LCRS or LDS malfunction; (vi) landfill LCRS or LDS operation; (vii) landfill liner system stability; (viii) landfill liner system displacement; (ix) cover system construction; (x) cover system degradation; (xi) cover system stability; (xii) cover system displacement; (xiii) impoundment liner construction; (xiv) impoundment liner degradation; (xv) impoundment LDS; and (xvi) impoundment liner system stability; and (xvii) impoundment liner system displacement. Specific problems that may affect these components and attributes and the significance of these problems are discussed in Section 4. Other components or attributes not specifically associated with landfill or impoundment integrity were not considered in the investigation. These include landfill daily and intermediate cover components (except for cracking of soil intermediate cover from Northridge earthquake), leachate transmission and treatment components beyond the leachate collection sumps or manholes, and landfill gas extraction and management components.

The second criterion used to categorize the problem addresses the principal human factor contributing to the problem. The principal human factors considered are: (i) design; (ii) construction; and (iii) operation. While a principal human factor has been assigned to each problem, it should be recognized that most problems have complex causes and several contributing factors. Hereafter, the problem classifications are shown as “component or attribute criterion”/”principal human factor criterion” (e.g., landfill liner system stability/design).

F-2.4 Problem Description

This investigation found 74 modern landfill and impoundment facilities that had experienced waste containment system problems. This number of facilities is relatively small in comparison to the total number of modern facilities nationwide. There are approximately 3,900 active MSW and HW landfills and HW surface impoundments nationwide (EPA, 1996; EPA, 1997); based on interviews with regulators, it is estimated that over half of these facilities (i.e., about 2,000) would be considered "modern" using the criteria identified in Section F-1.1. These numbers do not include industrial landfills and surface impoundments. The search for problem facilities for this investigation was not exhaustive, and it is certain that there are other facilities that experienced problems similar to those described in this appendix.

Case histories of the problems are presented in Attachment F-A to this appendix. Each case history includes a summary of the problem, information on how the problem was resolved, and lessons learned for future projects. Landfills with liner system or cover system problems are designated with an “L” or a “C”, respectively (e.g., L-1). Impoundments are designated with an “S”. The classification of the identified problems at each facility, information source, and section of the attachment that describes each problem are given in Table F-2.1. The detailed references for the information sources are listed in Attachment F-A along with each case history. These references are repeated in Chapter F-7 of this appendix. Summaries of the problems are presented in Table F-2.2. In Table F-2.3, the problems are grouped by the classification criteria presented in Section F-2.3.

Table F-2.1. Classification of Identified Problems at Landfill and Impoundment Facilities.

Facility Designation	Information Source	Problem Classification	Attachment Section
L-1	Laine and Darilek (1993)	landfill liner construction/construction	F-A.2.1
L-2	Basnett and Bruner (1993)	landfill liner construction/construction	F-A.3.1
L-3	Darilek et al. (1995)	landfill liner construction/construction	F-A.2.2
L-4	Adams et al. (1997)	landfill liner degradation/operation	F-A.3.2

Table F-2.1. Classification of Identified Problems at Landfill and Impoundment Facilities (Continued).

Facility Designation	Information Source	Problem Classification	Attachment Section
L-5	for F-A.2.3, Silva (1995) and Tedder (1997) for F-A.7.1, unpublished	landfill liner construction/construction landfill LCRS or LDS operation/operation	F-A.2.3 F-A.7.1
L-6	Anderson (1993)	landfill liner construction/operation	F-A.2.4
L-7	Loewenstein and Smrtic (1994)	landfill liner construction/operation	F-A.2.5
L-8	unpublished	landfill liner construction/design	F-A.2.6
L-9	unpublished	landfill liner construction/construction landfill LCRS or LDS malfunction/design landfill liner system displacement/design	F-A.2.7 F-A.5.1 F-A.9.1
L-10	unpublished	landfill LCRS or LDS construction/ construction	F-A.4.1
L-11	unpublished	landfill liner construction/construction landfill liner construction/construction landfill LCRS or LDS malfunction/design landfill liner system displacement/design	F-A.2.8 F-A.2.9 F-A.5.2 F-A.9.2
L-12	unpublished	landfill liner degradation/design landfill LCRS or LDS malfunction/ operation	F-A.3.3 F-A.6.1
L-13	Tisinger et al. (1993) Tisinger et al. (1994)	landfill LCRS or LDS malfunction/ construction	F-A.5.3
L-14	unpublished	landfill liner degradation/operation	F-A.3.4
L-15	unpublished	landfill liner construction/construction landfill LCRS or LDS construction/ construction	F-A.2.10 F-A.4.2
L-16	Bonaparte and Gross (1993)	landfill LCRS or LDS construction/ construction	F-A.4.3
L-17	Bonaparte and Gross (1993)	landfill liner construction/construction	F-A.2.11
L-18	Paulson (1993)	landfill LCRS or LDS malfunction/ construction	F-A.5.4
L-19	unpublished unpublished	landfill liner construction/construction landfill liner construction/construction	F-A.2.12 F-A.2.13
L-20	unpublished	landfill liner degradation/construction	F-A.3.5
L-21	unpublished	landfill liner system stability/design	F-A.8.1
L-22	Koerner et al. (1993)	landfill LCRS or LDS malfunction/ construction	F-A.6.2
L-23	unpublished	landfill LCRS or LDS operation/operation	F-A.7.2
L-24	unpublished	landfill liner system stability/operation landfill liner system displacement/design	F-A.8.2 F-A.9.3
L-25	Mitchell et al. (1990); Seed et al. (1990); Byrne et al. (1992)	landfill liner system stability/design	F-A.8.3

Table F-2.1. Classification of Identified Problems at Landfill and Impoundment Facilities (Continued).

Facility Designation	Information Source	Problem Classification	Attachment Section
L-26	Anderson (1995); Augello et al. (1995); Matasovic et al. (1995); Matasovic and Kavazanjian (1996); Matasovic et al. (1998); Stewart et al. (1994)	landfill liner system stability/design	F-A.8.4
L-27	Anderson (1995); Augello et al. (1995); Chang et al. (1996); Matasovic et al. (1995)	landfill liner system stability/design	F-A.8.5
L-28	unpublished	landfill LCRS or LDS construction/ construction	F-A.4.4
L-29	Koerner et al. (1998)	landfill liner construction/construction	F-A.2.14
L-30	unpublished	landfill LCRS or LDS operation/ construction	F-A.5.5
L-31	unpublished	landfill liner system displacement/design	F-A.9.4
L-32	unpublished	landfill LCRS or LDS construction/ construction	F-A.4.5
L-33	unpublished	landfill LCRS or LDS construction/ construction	F-A.4.6
L-34	unpublished	landfill LCRS or LDS operation/operation	F-A.7.3
L-35	unpublished	landfill LCRS or LDS operation/design	F-A.7.4
L-36	unpublished	landfill LCRS or LDS malfunction/design	F-A.6.3
L-37	unpublished	landfill LCRS or LDS malfunction/ operation	F-A.6.4
L-38	Boschuk (1991); Giroud (1993)	landfill liner system stability/design	F-A.8.6
L-39	Soong and Koerner (1997)	landfill liner system stability/design	F-A.8.7
L-40	Soong and Koerner (1997)	landfill liner system stability/design	F-A.8.8
L-41	Soong and Koerner (1997)	landfill liner system stability/design	F-A.8.9
L-42	Soong and Koerner (1997)	landfill liner system stability/operation	F-A.8.10
L-43	unpublished	landfill liner degradation/construction	F-A.3.6
L-44	unpublished	landfill liner degradation/design	F-A.3.7
L-45	Hullings and Sansone (1996)	landfill liner system stability/operation	F-A.8.11
L-46	unpublished	landfill liner system stability/design	F-A.8.12
C-1	Harris et al. (1992)	cover system degradation/design	F-A.11.1
C-2	unpublished	cover system construction/construction	F-A.10.1
C-3	Paulson (1993)	cover system stability/construction	F-A.12.1
C-4	Bonaparte et al. (1996); Vander Linde et al. (1998)	cover system stability/construction	F-A.12.2
C-5	Boschuk (1991)	cover system stability/design	F-A.12.3
C-6	Boschuk (1991)	cover system stability/construction	F-A.12.4

Table F-2.1. Classification of Identified Problems at Landfill and Impoundment Facilities (Continued).

Facility Designation	Information Source	Problem Classification	Attachment Section
C-7	Boschuk (1991)	cover system stability/construction	F-A.12.5
C-8	Boschuk (1991)	cover system stability/construction	F-A.12.6
C-9	Boschuk (1991)	cover system stability/construction	F-A.12.7
C-10	Boschuk (1991)	cover system stability/construction	F-A.12.8
C-11	Boschuk (1991)	cover system stability/construction	F-A.12.9
C-12	unpublished	cover system degradation/design cover system displacement/design	F-A.11.2 F-A.13.1
C-13	unpublished	cover system stability/design	F-A.12.10
C-14	unpublished	cover system stability/construction	F-A.12.11
C-15	Badu-Tweneboah et al. (1994)	cover system displacement/construction	F-A.13.2
C-16	Calabria and Peggs (1996)	cover system construction/construction	F-A.10.2
C-17	Soong and Koerner (1997)	cover system stability/design	F-A.12.12
C-18	Soong and Koerner (1997)	cover system stability/design	F-A.12.13
C-19	Soong and Koerner (1997)	cover system stability/design	F-A.12.14
C-20	Soong and Koerner (1997)	cover system stability/design	F-A.12.15
C-21	Anderson (1995); Augello et al. (1995); Chang et al. (1996); Matasovic et al. (1995); Stewart et al. (1994)	landfill liner system stability/design	F-A.12.16
C-22	Anderson (1995); Augello et al. (1995); Matasovic et al. (1995); Stewart et al. (1994)	landfill liner system stability/design	F-A.12.17
C-23	Anderson (1995); Augello et al. (1995); Matasovic et al. (1995); Stewart et al. (1994)	landfill liner system stability/design	F-A.12.18
S-1	Peggs et al. (1991)	impoundment liner degradation/ construction	F-A.15.1
S-2	Paulson (1993)	impoundment stability/design	F-A.16.1
S-3	unpublished	impoundment liner construction/ construction	F-A.14.1
S-4	Bonaparte and Gross (1993)	impoundment liner construction/ construction	F-A.14.2
S-5	Bonaparte and Gross (1993)	impoundment liner construction/ construction	F-A.14.3

Table F-2.2. Summary of Identified Problems.

Problem Classification	Facility Designation/ Attachment Section	Problem Summary
landfill liner construction/ construction	L-1/F-A.2.1	leakage through holes in HDPE GM primary liner
landfill liner construction/ construction	L-3/F-A.2.2	leakage through holes in HDPE GM liners
landfill liner construction/ construction	L-5/F-A.2.3	leakage through holes in HDPE GM primary liner
landfill liner construction/ operation	L-6/F-A.2.4	leakage through holes in HDPE GM primary liner
landfill liner construction/ operation	L-7/F-A.2.5	leakage though HDPE GM/CCL composite primary liner at pipe penetration
landfill liner construction/ design	L-8/F-A.2.6	landfill gas migrated beyond liner system and into vadose zone resulting in groundwater contamination
landfill liner construction/ construction	L-9/F-A.2.7	leakage though HDPE GM primary liner at pipe penetration
landfill liner construction/ construction	L-11/F-A.2.8	construction debris in CCL with initially smooth surface protruded from CCL after CCL was left exposed and subsequently eroded
landfill liner construction/ construction	L-11/F-A.2.9	leakage though HDPE GM primary liner at pipe penetration
landfill liner construction/ construction	L-15/F-A.2.10	sand bag under installed GM liner approved by CQA consultant
landfill liner construction/ construction	L-17/F-A.2.11	leakage through holes in HDPE GM primary liner
landfill liner construction/ construction	L-19/F-A.2.12	wind uplifted and tore HDPE GM liner during construction
landfill liner construction/ construction	L-19/F-A.2.13	severe wrinkling of HDPE GM due to thermal expansion during construction
landfill liner construction/ construction	L-29/F-A.2.14	large folded wrinkles in HDPE GM primary liner at two exhumed leachate sumps
landfill liner degradation/ design	L-2/F-A.3.1	desiccation cracking of CCL in exposed HDPE GM/CCL composite liner
landfill liner degradation/ operation	L-4/F-A.3.2	HDPE GM/CCL composite liner damaged by waste fire
landfill liner degradation/ design	L-12/F-A.3.3	leachate extraction well installed in landfill appeared to puncture GM primary liner
landfill liner degradation/ construction	L-14/F-A.3.4	HDPE GM liner damaged by fire believed to be started by lightning strike
landfill liner degradation/ construction	L-20/F-A.3.5	saturation of GCL beneath GM liner when rainwater ponded on tack-seamed patch over GM hole
landfill liner degradation/ construction	L-43/F-A.3.6	water ponded between HDPE GM and CCL components of composite secondary liner and was contaminated from a source other than the landfill

Table F-2.2. Summary of Identified Problems (Continued).

Problem Classification	Facility Designation/ Attachment Section	Problem Summary
landfill liner degradation/ design	L-44/F-A.3.7	landfill gas well punctured GM component of composite liner and extended into CCL
landfill LCRS or LDS construction/construction	L-10/F-A.4.1	rainwater entered LDS through anchor trench
landfill LCRS or LDS construction/construction	L-15/F-A.4.2	sand bags in LCRS drainage layer and debris in LCRS pipe trench approved by CQA consultant
landfill LCRS or LDS construction/construction	L-16/F-A.4.3	rainwater entered LDS through anchor trench
landfill LCRS or LDS construction/construction	L-28/F-A.4.4	excessive needle fragments in manufactured needlepunched nonwoven GT
landfill LCRS or LDS construction/construction	L-32/F-A.4.5	HDPE LCRS pipe separated at joints
landfill LCRS or LDS construction/construction	L-33/F-A.4.6	HDPE LCRS pipe separated at joints
landfill LCRS or LDS degradation/design	L-9/F-A.5.1	erosion of sand LCRS drainage layer on liner system side slopes
landfill LCRS or LDS degradation/design	L-11/F-A.5.2	erosion of sand protection layer on liner system side slopes
landfill LCRS or LDS degradation/construction	L-13/F-A.5.3	polypropylene continuous filament nonwoven GT filter degraded due to outdoor exposure
landfill LCRS or LDS degradation/construction	L-18/F-A.5.4	polypropylene staple-fiber needlepunched nonwoven GT filter degraded due to outdoor exposure
landfill LCRS or LDS degradation/construction	L-30/F-A.5.5	HDPE LCRS pipe crushed during construction
landfill LCRS or LDS malfunction/operation	L-12/F-A.6.1	LCRS pipes were not regularly cleaned and became partially clogged, and LCRS drainage layer may be partially clogged
landfill LCRS or LDS malfunction/design	L-22/F-A.6.2	waste fines clogged needlepunched nonwoven GT filter wrapped around perforated LCRS pipes
landfill LCRS or LDS malfunction/design	L-36/F-A.6.3	waste fines clogged needlepunched nonwoven GT filter around LCRS pipe bedding gravel
landfill LCRS or LDS malfunction/operation	L-37/F-A.6.4	leachate seeped out landfill side slopes in the vicinity of chipped tire layers
landfill LCRS or LDS operation/operation	L-5/F-A.7.1	overestimation of LDS flow quantities due to problems (e.g., clogging) with automated LDS flow measuring and removal equipment
landfill LCRS or LDS operation/operation	L-23/F-A.7.2	valves on LCRS pipes were not opened and leachate could not drain, and waste and leachate flowed over a berm into a new unapproved cell
landfill LCRS or LDS operation/operation	L-34/F-A.7.3	LCRS leachate pump moved air and liquid causing pump airlock and underestimation of leachate quantities

Table F-2.2. Summary of Identified Problems (Continued).

Problem Classification	Facility Designation/ Attachment Section	Problem Summary
landfill LCRS or LDS operation/design	L-35/F-A.7.4	LCRS leachate pumps and flowmeters continually clogged and LDS leachate pumps turned on too frequently and burned out prematurely
landfill liner system stability/design	L-21/F-A.8.1	sliding along PVC GM/CCL interface during construction
landfill liner system stability/operation	L-24/F-A.8.2	sliding along GN/GCL (HDPE GM side) and GCL(bentonite side)/CCL interfaces during operation
landfill liner system stability/design	L-25/F-A.8.3	sliding along HDPE GM/polyester needlepunched nonwoven GT and HDPE GM/CCL interfaces during operation
landfill liner system stability/design	L-26/F-A.8.4	two tears in HDPE GM liner and cracks in soil intermediate cover from Northridge earthquake
landfill liner system stability/design	L-27/F-A.8.5	extensive cracks in soil intermediate cover and further tearing of GT cushion from Northridge earthquake
landfill liner system stability/design	L-38/F-A.8.6	sliding along needlepunched nonwoven GT/HDPE GM primary liner interface after rainfall
landfill liner system stability/design	L-39/F-A.8.7	sliding along needlepunched nonwoven GT/HDPE GM liner interface after rainfall
landfill liner system stability/design	L-40/F-A.8.8	sliding along gravel/HDPE GM liner interface after rainfall
landfill liner system stability/design	L-41/F-A.8.9	sliding along very flexible GM liner/needlepunched nonwoven GT interface after rainfall
landfill liner system stability/operation	L-42/F-A.8.10	sliding along needlepunched nonwoven GT/PVC GM liner interface after a thaw
landfill liner system stability/operation	L-45/F-A.8.11	sliding along needlepunched nonwoven GT/HDPE GM liner interface after erosion of soil anchoring geosynthetics
landfill liner system stability/design	L-46/F-A.8.12	sliding along GN/HDPE GM primary liner interface during construction
landfill liner system displacement/design	L-9/F-A.9.1	uplift of GM by landfill gas after erosion of overlying sand LCRS drainage layer
landfill liner system displacement/design	L-11/F-A.9.2	uplift of geosynthetics by landfill gas after erosion of overlying sand protection layer
landfill liner system displacement/design	L-25/F-A.9.3	uplift of composite liner by surface-water infiltration during construction
landfill liner system displacement/design	L-31/F-A.9.4	uplift of composite liner by surface-water infiltration during construction
cover system construction/ construction	C-2/F-A.10.1	portion of topsoil from off-site source was contaminated with chemicals
cover system construction/ construction	C-16/F-A.10.2	high failure rate of HDPE GM seam samples during destructive testing
cover system degradation/ design	C-1/F-A.11.1	failure of geosynthetic erosion mat-lined downchute on 3H:1V side slope

Table F-2.2. Summary of Identified Problems (Continued).

Problem Classification	Facility Designation/ Attachment Section	Problem Summary
cover system degradation/ design	C-12/F-A.11.2	erosion of topsoil layer on 60 m long, 3H:1V side slope
cover system stability/ construction	C-3/F-A.12.1	sliding along nonwoven GT/GM interface during construction
cover system stability/ design	C-4/F-A.12.2	sliding along topsoil/GCL interface after rainfall
cover system stability/ design	C-5/F-A.12.3	sliding along sand/woven GT interface after rainfall
cover system stability/ design	C-6/F-A.12.4	sliding along sand/GM interface after rainfall
cover system stability/ design	C-7/F-A.12.5	sliding along gap-graded sand/GM interface after rainfall
cover system stability/ design	C-8/F-A.12.6	sliding along gravel/GT interface during construction
cover system stability/ design	C-9/F-A.12.7	sliding along sand/calendered nonwoven GT interface after rainfall
cover system stability/ design	C-10/F-A.12.8	sliding along sand/GM interface after rainfall
cover system stability/ design	C-11/F-A.12.9	sliding along topsoil/nonwoven GT interface during construction
cover system stability/ design	C-13/F-A.12.10	sliding along PVC GM/CCL interface after a thaw
cover system stability/ construction	C-14/F-A.12.11	sliding along geogrid/HDPE GM interface during construction
cover system stability/ design	C-17/F-A.12.12	sliding along sand/CCL interface during rainfall
cover system stability/ design	C-18/F-A.12.13	sliding along sand/CCL interface immediately after rainfall
cover system stability/ design	C-19/F-A.12.14	sliding along sand/CCL interface after rainfall
cover system stability/ design	C-20/F-A.12.15	sliding along sand/CCL interface after rainfall
cover system stability/ design	C-21/F-A.12.16	minor cracks in soil intermediate cover from Northridge earthquake
cover system stability/ design	C-22/F-A.12.17	215-m long crack in soil intermediate cover from Northridge earthquake
cover system stability/ design	C-23/F-A.12.18	minor cracks in soil intermediate cover from Northridge earthquake
cover system displacement/design	C-12/F-A.13.1	cover system settlement caused tearing of HDPE GM boots around gas well penetrations of GM barrier
cover system displacement/construction	C-15/F-A.13.2	localized cover system settlement during construction stretched, but did not damage, PVC GM barrier and opened GCL joints

Table F-2.2. Summary of Identified Problems (Continued).

Problem Classification	Facility Designation/ Attachment Section	Problem Summary
impoundment liner construction/construction	S-3/F-A.14.1	large wrinkles in HDPE GM primary liner at two leachate ponds
impoundment liner construction/construction	S-4/F-A.14.2	leakage through holes in HDPE GM component of composite primary liner
impoundment liner construction/construction	S-5/F-A.14.3	leakage through holes in HDPE GM primary liners at two ponds
impoundment liner degradation/construction	S-1/F-A.15.1	slow crack growth stress cracks and shattering cracks in exposed HDPE GM liner at five ponds
impoundment liner system stability/design	S-2/F-A.16.1	sliding along polypropylene needle-punched nonwoven GT/HDPE GM interface during waste placement

Table F-2.3. Categorization of Identified Problems (Number of Identified Problems is Given)

	Principal Human Factor Contributing to the Problem		
Waste Containment System Component or Attribute	Design	Construction	Operation
Landfill Liner Construction	1	11	2
Landfill Liner Degradation	3	3	1
Landfill LCRS or LDS Construction	0	6	0
Landfill LCRS or LDS Degradation	2	3	0
Landfill LCRS or LDS Malfunction	2	0	2
Landfill LCRS or LDS Operation	1	0	3
Landfill Liner System Stability	9	0	3
Landfill Liner System Displacement	4	0	0
Cover System Construction	0	2	0
Cover System Degradation	2	0	0
Cover System Stability	16	2	0
Cover System Displacement	1	1	0
Impoundment Liner Construction	0	3	0
Impoundment Liner Degradation	1	0	0
Impoundment LDS	0	0	0
Impoundment Liner System Stability	0	1	0
Impoundment Liner System Displacement	0	0	0

From Table F-2.3, there were 85 identified problems at the 74 facilities. The investigation focused on landfill facilities: 94% of the identified problems described

occurred at landfills. Based on the waste containment system component or attribute criterion, the identified problems are distributed as follows:

- landfill liner construction: 17%;
- landfill liner degradation: 8%;
- landfill LCRS or LDS construction: 7%;
- landfill LCRS or LDS degradation: 6%;
- landfill LCRS or LDS malfunction: 5%;
- landfill LCRS or LDS operation: 5%;
- landfill liner system stability: 14%;
- landfill liner system displacement: 5%;
- cover system construction: 2%;
- cover system degradation: 2%;
- cover system stability: 21%;
- cover system displacement: 2%;
- impoundment liner construction: 4%;
- impoundment liner degradation: 1%; and
- impoundment liner system stability: 1%.

No problems were identified under the impoundment LDS and impoundment liner system displacement categories. Therefore, these categories are not discussed further.

Based on the principal human factor contributing to the problem criterion, the identified problems are distributed as follows:

- design: 48%;
- construction: 38%; and
- operation: 14%.

F-3 Evaluation of Identified Problems

F-3.1 Introduction

In this section of the appendix, observations are made on the nature and frequency of the identified problems for each of the 15 waste containment system component or attribute criteria considered in this appendix and listed in Section F-2.3. The methods by which these problems were detected, the time it took to detect the problems after they developed, and the remedy of the problems are also discussed. The most common types of problems for each of the 15 categories and the reasons for these problems are presented.

It should be noted that the problems and remedies described herein are facility specific. It should not be inferred that these problems occur at most facilities or that the specific remedies are appropriate for most facilities.

F-3.2 Landfill Liner Construction

F-3.2.1 Overview

Problems related to construction of landfill liners are one of the most common types of problems identified in this study. This category represents 14 of the 85 problems (i.e., 17%) described herein. The problems in this category were primarily attributed to construction factors. Only one problem was attributed to design and two were attributed to operation. The problems and the number of identified landfills with them are as follows:

- leakage through holes in an HDPE GM primary liner (5 landfills);
- leakage through an HDPE GM primary liner or HDPE GM/CCL composite primary liner at the LCRS pipe penetration of the liner (3 landfills);
- severe wrinkling of an HDPE GM during construction (2 landfills);
- landfill gas migration beyond a liner system and into the vadose zone resulting in groundwater contamination (1 landfill);
- protrusion of construction debris from a CCL with an initially smooth surface after the CCL was left exposed and subsequently eroded (1 landfill);
- presence of a sand bag under a GM liner approved by the CQA consultant (1 landfill); and
- uplift and tearing of a GM by wind during construction (1 landfill).

F-3.2.2 Leakage Through Holes in HDPE GM Primary Liner

The most common problem in this category, leakage through holes (construction- or operation-related) in an HDPE GM primary liner, occurred at landfills L-1, L-3, L-5, L-6, and L-17. Leakage was detected during construction of landfills L-1 and L-3 by the relatively high LDS flow rate (i.e., 2,900 liters/hectare/day (lphd)) that occurred after rainwater ponded in landfill L-1 and by electrical leak location surveys performed as part of CQA of landfill L-3. For both landfills, GM holes were located by electrical leak location surveys and repaired. At landfill L-3, the leak location surveys performed as part of CQA allowed extrusion seaming problems to be identified early and corrected, decreasing the frequency of identified GM holes in subsequent installations. Interestingly, a leak location survey showed that the HDPE GM component of the secondary liner for landfill L-3 was damaged during placement of the overlying gravel layer. Several of the holes were located in the vicinity of the temporary ramps. The HDPE GM primary liner, which was protected by a GT filter overlying a GN LCRS drainage layer, was not damaged during placement of the gravel LCRS drainage layer

on the GT. Thus, the potential for GM damage during placement of a soil layer over a GM can be reduced by protecting the GM.

For the remaining three landfills (i.e., L-5, L-6, and L-17), primary liner leakage was detected during landfill operation. Relatively high LDS flow rates were recorded from landfill L-5. However, due to problems with the LDS flow rate measuring system for about the first three years of operation, the high readings appear to be partially due to measurement error (e.g., flow rates calculated using the number of "pump on" intervals were several times higher than rates calculated using flowmeter readings). By the fourth year of operation, the LDS flow rate measuring system appeared to be functioning adequately, and it was confirmed that the average LDS flow rate was relatively high (i.e., 4,660 lphd). The exact locations of the HDPE GM primary liner holes causing this leakage are unknown. However, it is likely that there is a hole in the sump area because the LDS flow rates decreased significantly (i.e., to about 2,000 lphd) when the “pump on” level in the internal LCRS sump was lowered from 0.6 m to 0.25 m. With respect to the potential for leakage, leachate sumps are generally the most critical locations in landfills with internal sumps. Leachate heads are typically sustained and at higher levels in sumps than at other locations. In addition, GM liners in sumps often have seamed corners to fit the sump geometry. These seams may contain holes. Even one GM hole at a sump can cause relatively high leakage rates due to the relatively high head of leachate in the sump. No other remedial actions beyond lowering the “pump on” level in the sump were implemented for landfill L-5.

At landfills L-6 and L-17, primary liner leakage was detected within several months after start of operation by relatively high LDS flow rates (i.e., average flow rates of 1,200 lphd and 1,030 lphd, respectively) and, for landfill L-17, by the color of and chemical constituents in the LDS liquid. Landfill L-6 has an HDPE GM primary liner on the side slopes and a GM/CCL composite primary liner on the base. With this liner configuration, leakage primarily occurred through the GM primary liner on the side slope. The GM primary liner is overlain only by a GN LCRS drainage layer and a GT filter. There is no soil protection layer on the side slope; waste was placed directly on the GT. It is not known if the GM primary liner was damaged during construction or operation. However, without a thick protection layer, the potential for liner damage during landfill operation increases. GM holes were located in landfill L-6 with a dye test and visual inspection and were repaired.

For landfill L-17, the project specifications only required the inside track of dual track fusion seams be destructively tested. When the HDPE GM liner was inspected for holes shortly after primary liner leakage was detected, liner holes and fusion seam holes were observed at several locations. At the seam holes, the outside track of the seam had separated, allowing leachate to flow through the air channel between the tracks and potentially through the liner if the inside track had holes. Separation of the outside track also increases stress concentrations at the inside track.

For the four landfills where holes were located in GMs, the holes of largest size were found in panels and the majority of holes were found in seams. Based on these five landfills with GM primary liner leakage, and consistent with the study of LDS flow rates from double-lined waste containment facilities conducted by Bonaparte and Gross (1993), construction-related holes in GM liners should be anticipated, even in liners installed with CQA. If there is a head of leachate over a liner hole, leakage occurs. However, as shown for these landfills, GM primary liner holes resulting from construction can be located by ponding tests, leak location surveys, or other methods after liner system construction and be repaired before waste placement.

F-3.2.3 Leakage at Pipe Penetration of Primary Liner

Leakage at pipe penetrations of primary liners occurred at landfills L-7, L-9, and L-11. Leakage was detected during operation of landfill L-7 when the average LDS flow rate increased from about 10 to 400 lphd. This occurred after landfill operations personnel regraded the sand LCRS drainage layer. When the regraded area was inspected, deep tire tracks, made by a rubber-tired loader, were found over the LCRS pipe penetration of the composite primary liner. At the pipe penetration, the pipe was broken and the CCL adjacent to the pipe was rutted. The damage was subsequently repaired.

At landfills L-9 and L-11, leakage at the LCRS pipe penetration of the HDPE GM primary liner was detected during construction after rainwater ponded over the penetration. For landfill L-9, this leakage occurred even though the penetration had two special features to improve the connection integrity: (i) the GM was underlain by a GCL at the penetration; and (ii) the penetration was sealed with two HDPE boots, creating a space between them that could be pressure tested and later filled with foam. Though the pipe penetration at landfill L-9 was inspected twice after construction and a small extrusion seam hole was repaired, the rate of leakage did not decrease substantially. Since the pathway for this leakage could not be identified during construction, this problem was not remedied.

At landfill L-11, leakage at the pipe penetrations in three cells was verified by dye tests. When the GM pipe boots were inspected, the boots in two cells were loose around the pipes and the boot in the third cell appeared adequate, but short. The boots were repaired and the space between the boot and the primary liner was filled with bentonite slurry. Subsequently, leakage decreased.

These case histories demonstrate that it is difficult to construct pipe penetrations to be hole free even when extra measures are taken to enhance the integrity of the connections.

F-3.2.4 Severe Wrinkling of HDPE GM Liner

Severe wrinkling of the smooth HDPE GM liner was identified by visual observation during construction of landfill L-19 and exhumation of two sumps at landfill L-29. At landfill L-19, the large wrinkles were remedied before the liner was covered with an overlying material. The HDPE GM liner for landfill L-19 was deployed and seamed in the winter, when temperatures were near freezing, and not covered with sand until the spring and summer, when temperatures were high and the GM was severely wrinkled. Several thousand linear meters of wrinkles were required to be cut, leading to more GM seams. In addition, the overlying sand layer was placed over the GM at night, when temperatures were cooler and the GM was less wrinkled.

The HDPE GM liner in landfill L-29 also developed large wrinkles. These wrinkles were identified eight years after the liner system was constructed, when expansion of the landfill was underway. Wrinkles were more numerous and larger near the slope toe and near the sump than away from the slope toe and the sump. Some of the wrinkles had folded over, and the GM at the folds had yielded. It is unclear why these large wrinkles were not noticed when the GM was installed. The GM had been covered with a GT, which provided some thermal insulation of the underlying GM. However, it is possible that the GM developed wrinkles after the GT was placed and the wrinkles were hidden. The wrinkled GM was removed when the sumps were reconstructed for the landfill expansion. Both wide width tensile tests (ASTM D 4885) and single point notched constant tensile load tests (ASTM D 5397) were conducted on samples of unwrinkled GM and wrinkled GM at folds to assess the effect of the GM folding on GM integrity. All of the samples had measured properties exceeding the project specifications. While the wrinkled and unwrinkled GM samples had wide width tensile properties that were not significantly different from one another, the wrinkled GM samples had a somewhat lower time to break than the unwrinkled samples.

F-3.2.5 Migration of Landfill Gas Beyond Liner System to Groundwater

Landfill gas migrated beyond the edge of a liner system and into the vadose zone resulting in groundwater contamination at landfill L-8. Volatile organic compounds (VOCs) were detected in shallow groundwater at a monitoring well located 60 m from the downgradient edge of the landfill about four years after waste placement began. This is the only case of groundwater or surface-water contamination by leachate or landfill gas from a facility identified in this study. The migration occurred because landfill gas was not well controlled and a pathway for gas migration was present. Along the perimeter of the landfill, the composite liner was extended horizontally and the GM was secured by covering it with a layer of relatively permeable soil. An asphalt parking lot was constructed on top of a section of the relatively permeable soil layer and natural ground. As waste reached intermediate grades, it was covered with a relatively low-permeability soil intermediate cover layer that graded into the relatively permeable soil layer. The soil intermediate cover layer and the asphalt

served as confining layers, blocking landfill gas moving from the waste from venting to the atmosphere. Instead, some gas migrated through the relatively permeable soil layer and then beyond the limit of the liner system. The remedy consisted of improving source control by installing additional gas extraction wells in the waste, natural biodegradation of the VOCs in groundwater, and continued monitoring.

F-3.2.6 Other Problems

Construction debris protruding from the CCL, a sand bag under a GM liner approved by the CQA consultant, and uplift and tearing of an HDPE GM liner by wind were identified by visual observation during construction of landfills L-11, L-15, and L-19, respectively. These problems were remedied before the liner was covered with an overlying material. At landfill L-11, the contractor constructed the CCL with a soil containing a small amount of construction debris (i.e., about 0.02% by weight). The completed CCL initially had a smooth surface; however, the surface of the CCL eroded when it was left unprotected during the winter and debris protruded from the CCL. The CCL in this state was not suitable for placement of the overlying GM. This problem was remedied by covering the CCL on the base of the landfill with a GCL and covering the CCL on the side slope with a layer of debris-free clay. Landfill L-15 was remedied by removing the sand bag. Landfill L-19 was remedied by replacing the damaged 1.5-mm thick HDPE GM.

F-3.3 Landfill Liner Degradation

F-3.3.1 Overview

Problems related to landfill liner degradation represent 7 of the 85 problems (i.e., 8%) described herein. Three problems in this category were attributed to design factors, three were attributed to construction, and one was attributed to operation. The problems and the number of identified landfills with them are as follows:

- liner damage by fire (2 landfills);
- liner damage during well installation (2 landfills);
- desiccation cracking of a CCL in an exposed HDPE GM/CCL composite liner (1 landfill);
- saturation of a GCL beneath a GM liner when rainwater ponded on a tack-seamed patch over a GM hole (1 landfill); and
- water from the CCL ponded between the HDPE GM and CCL components of a composite secondary liner and was contaminated from a source other than the landfill (1 landfill).

F-3.3.2 Liner Damage by Fire

The liners at landfills L-4 and L-14 were damaged by fire during operation and construction, respectively. The fires were detected by visual observation. The GM liner for landfill L-14 was damaged by fire that is believed to have been started by a lightning strike. Rolls of GC drainage layer lined up on an HDPE GM liner at the top of the side slope caught fire during a thunderstorm. The GM beneath the burnt rolls was rippled and melted in some cases. The damaged GM and GC were replaced. The authors are not aware of other instances where a geosynthetics fire was started by lightning.

At landfill L-4, a chemical reaction of one of the materials disposed of in the landfill caused a waste fire that took about 11 months to contain and extinguish. Based on temperature measurements made near the fire, the temperature in the vicinity of the liner system may have approached 800°C. The liner system in the vicinity of the fire was severely damaged: the liner system geosynthetics were melted and disintegrated and the CCL was desiccated. The damaged materials were replaced.

F-3.3.3 Liner Damage During Well Installation

The liner at landfill L-12 was possibly damaged and the liner at landfill L-44 was definitely damaged during installation of wells in the landfills. The possible liner damage was detected in landfill L-12 by an increase in LDS flow rates; the liner damage in well L-44 was detected when liner system components were observed in auger cutting during well installation. In both cases, the problems were attributed to design factors.

At landfill L-12, a deep, 100-mm diameter leachate extraction well was installed in the double-lined landfill after the LCRS appeared to be clogged. The well design called for the well to extend into the sand LCRS drainage layer over the GM primary liner, but the elevation of the top of the borehole was not surveyed immediately before well installation. Considering waste settlement since the previous survey of the landfill, the target borehole depth may have been too deep. Following well installation, average LDS flow rates increased from about 300 lphd to 400 lphd, and it was suspected that the well had penetrated the GM primary liner. No remedial actions have been implemented because it is not clear if the primary liner was actually punctured and the LDS flow rates have remained relatively low.

During installation of gas extraction wells in a active landfill, one of the 0.9-m diameter boreholes for the wells was advanced into the composite liner. The problem was identified when portions of the liner system were observed in the cuttings from the bucket auger. Upon observing these components in the auger cuttings, field personnel poured bentonite pellets into the bottom of the borehole to create an approximately 0.9-m thick bentonite seal at the borehole base. It was later discovered

that a typographic error had been made on the design drawing for the gas extraction system: the specified borehole depth at the location of the liner damage was greater than the depth to the top of the liner. Though the potential environmental impact from the damage was found to be negligible, the proposed remedy for this problem is repair of the damaged liner system.

F-3.3.4 Other Problems

Saturation of a GCL beneath a GM liner was detected during construction of landfill L-20; desiccation cracking of a CCL in an exposed composite liner and ponding of contaminated water between the GM and CCL components of a composite liner were detected during operation of landfills L-2 and L-43, respectively. At landfill L-20, the GCL component of a composite liner became saturated when rainwater ponded on a tack-seamed patch over a GM hole during construction. This problem was identified by visual inspection after the ponded water was removed. The hydrated GCL had uplifted the GM, and the composite liner was soft in the saturated area. The damaged GCL was replaced.

At landfill L-2, the CCL component of a side slope composite liner for a cell constructed three year earlier was observed to be severely desiccated when it was partially exposed during construction of an adjacent cell. The composite liner, which consisted of an HDPE GM over a CCL, had not been protected from the environment. The design required that the sand LCRS drainage layer be placed incrementally up the side slopes during landfill operation, with the sand advancing ahead of the waste. During construction of the composite liner, water became trapped between the HDPE GM and the CCL near the slope toe. The GM had to be cut so the water could drain. The same phenomenon of trapped water occurred during the construction of the adjacent cell. This occurrence of water was attributed to water vapor thermally driven from the CCL into the space between the GM and CCL during the day as the CCL heated. The water then condensed on the bottom of the GM at night as the GM cooled and flowed downslope to the slope toe. The moisture contents of CCL samples support this hypothesis. The CCL moisture content increased moving downslope from crest to toe. At the crest, the CCL moisture content was significantly less than the average construction moisture content; at the toe, the CCL moisture content was greater than the average construction moisture content. No remedial actions were implemented.

At landfill L-43, water ponded between the HDPE GM and CCL components of the composite secondary liner on the side slope. This landfill has a GM primary liner on the side slope and a GM/CCL composite primary liner on the base; the secondary liner is a GM/CCL composite. By about one year after construction, a large isolated bubble of water developed between the GM and CCL components of the composite secondary liner at the slope toe at a corner of the cell that had not yet received waste. The geosynthetics were cut to remove the water, the water was pumped out, and the

geosynthetics were repaired. The water was chemically analyzed for organic constituents and metals and found to be clean, with a chemistry similar to that of the LDS liquid (i.e., water from the CCL component of the primary liner on the landfill base). A small bubble developed at the same location about one year later and the water was removed, but not chemically analyzed. When bubbles developed at the same location about three years after construction, the bubble water was analyzed and found to contain organic constituents. A testing program to identify the source of the water and contamination is underway. Preliminary results of the study indicate that the source of the water was the CCL. It is believed that the CCL lost the water due to desiccation and consolidation. While the composite primary liner on the base was thermally insulated by a 0.3-m thick sand LCRS drainage layer and the composite secondary liner on the base was thermally insulated by the 0.3 m-thick (each) sand LCRS or LDS drainage layers and the 0.9-m CCL component of the composite primary liner, the composite secondary liner on the side slopes was only overlain by geosynthetics and was not sufficiently thermally insulated. Therefore, the CCL component of the composite liner on the side slopes could potentially lose water by thermal action. Based on a chemical analysis, landfill leachate and groundwater were excluded as the source of the contamination. Surface-water runoff from a nearby former oil facility and fuel from equipment used to construct the liner system are currently considered to be potential sources of the contamination.

F-3.4 Landfill LCRS or LDS Construction

F-3.4.1 Overview

Problems related to landfill LCRS or LDS construction represent 6 of the 85 problems (i.e., 7%) described herein. All of the problems in this category were attributed to construction factors. The problems and the number of identified landfills with them are as follows:

- rainwater entered the LDS through the anchor trench (2 landfills);
- HDPE LCRS pipe was separated at joints (2 landfills);
- sand bags in the LCRS drainage layer and debris in the LCRS pipe trench approved by CQA consultant (1 landfill); and
- excessive needles in a manufactured needlepunched nonwoven GT (1 landfill).

F-3.4.2 Rainwater Entering LDS Through Anchor Trench

Rainwater was found to be entering the LDS through the liner system anchor trench in landfills L-10 and L-16 during construction and operation, respectively. This problem was detected when LDS flow rates from the landfills were higher than expected. When the landfill anchor trenches were inspected, they were found to be full of water. The GC or GN LDS drainage layers in the trenches were conveying water from the trenches into the LDSs. This problem developed for landfill L-10 because its liner

system anchor trench had been backfilled with a sandy soil that allowed significant water to infiltrate and pond on the geosynthetics. To remedy the problem, sections of the back of the anchor trench were excavated to the outside slope of the perimeter berm along the length of the trench, and the ends of the geosynthetics in the trench sections were laid horizontal. The perimeter berm was reconstructed to grade with gravel. This allows water infiltrating the trench to drain to the outside slope of the perimeter berm. To minimize infiltration of rainwater into the anchor trench, a GM was placed over the top of the berm and covered with a 0.3-m thick layer of soil. At landfill L-16, the anchor trench soil was not initially well compacted. Over time, the anchor trench soil settled, and a depression developed over the anchor trench. The depression trapped runoff, which subsequently infiltrated into the trench. The problem for L-16 was remedied by removing, replacing, and regrading the trench soil and grading the soil surface to drain away from the trench.

F-3.4.3 HDPE Pipe Separated at Joints

During the initial video survey of the inside of the HDPE LCRS pipes in active landfills L-32 and L-33, several pipe joints were found to be separated. The separations were typically less than 10 mm in width. The subsequent annual surveys have revealed no further separations in the pipe joints over time. The reason for the separations is unclear. It may be that the pipes were never seamed together during construction or that the quality of some of the pipe seams was so poor that the seams failed during construction. No remedial actions have been taken.

F-3.4.4 Other Problems

Sand bags in the LCRS drainage layer and debris in the LCRS pipe trench approved by the CQA consultant were found in landfill L-15, and excessive broken needle fragments in the manufactured needlepunched nonwoven GT were found in landfill L-28. These problems were detected during construction by visual observation and remedied. For landfill L-15, the sand bags and debris were removed. For landfill L-28, the GT was placed on a GN LCRS drainage layer over a GM/CCL composite liner. By the time the needle problem was discovered, some of the GT had already been covered by a 0.3-m thick soil protection layer. The contractor initially tried to fix the GT that had been deployed and not covered with soil by manually searching for and removing needles. The contractor also tried to locate needles in the GT beneath the soil layer using a metal detector. However, both methods proved to be too time consuming to locate and remove the hundreds of needles. Laboratory tests conducted to evaluate the potential for GM puncture by needles of different lengths and orientations showed that few needles should puncture the GM. The holes caused by these needles would be very small. Nonetheless, the defective GT was removed and replaced with a “needle-free” GT. When the GT was removed, no GM damage from the needles was observed. The manufacturer of the defective GT installed

magnets in the manufacturing plant to remove broken needles from GTs produced in the future.

F-3.5 Landfill LCRS or LDS Degradation

F-3.5.1 Overview

Problems related to landfill LCRS or LDS degradation represent 5 of the 85 problems (i.e., 6%) described herein. Two problems in this category were attributed to design factors and three were attributed to construction. The problems and the number of identified landfills with them are as follows:

- erosion of the sand layer on the liner system side slopes (2 landfills);
- degradation of polypropylene nonwoven GT filters due to outdoor exposure (2 landfills); and
- crushing of HDPE LCRS pipe draining cell during construction (1 landfill).

F-3.5.2 Erosion of Sand Layer on Side Slopes

Progressive erosion of the sand layer on the liner system side slopes was detected at landfills L-9 and L-11 during operation. Landfill L-9 has 100-m long, 4H:1V side slopes, and landfill L-11 has 18-m high, 2.5H:1V side slope segments separated by benches. The erosion caused gullies to develop in the sand layer and the deposition of sand on the base of the landfills. In landfill L-9, the 0.6-m thick sand LCRS drainage layer (specified minimum hydraulic conductivity of 1×10^{-4} m/s) also washed into the exposed gravel around the LCRS pipes and in the sump area. In landfill L-11, the 0.45-m thick sand protection layer (specified minimum hydraulic conductivity of 1×10^{-5} m/s) had eroded down to the liner system geosynthetics in two areas and these areas were subsequently uplifted by landfill gas. The erosion on this landfill was exacerbated by runon from an adjacent MSW landfill. The erosion problem required continual maintenance of both landfills: sand was pushed back up the side slopes numerous times and, in landfill L-9, the gravel in the sump areas was replaced twice. Besides maintenance of the sand layer, the remedy for landfill L-11 also included improvement to the runoff and runon control system. The erosion problem for the landfills will be fully resolved when the sand on the side slopes is covered with waste. However, for these landfills it may be several years before this occurs.

F-3.5.3 Degradation of GT Filter Due to Outdoor Exposure

The polypropylene nonwoven GT filters at landfills L-13 and L-18 degraded due to outdoor exposure. The degradation was detected during construction, and the degraded GTs were replaced. For landfill L-13, the GT was designed assuming it would be exposed to the environment for several months and then covered with a sand protection layer. This strategy was selected because the sand proposed for the

protection layer was very erodable and would require significant maintenance if left exposed. Though a 270 g/m^2 GT met the project specifications, a heavier 540 g/m^2 GT was selected, anticipating that this GT would retain enough strength after several months of exposure to meet the specifications. Due to construction delays, however, the GT was exposed for more than six months. By about 6.7 months of exposure, the GT exhibited significantly reduced strength properties, did not meet the specification for burst strength, and had developed holes in two areas near the side slope crest of one of the perimeter berms. The degraded polypropylene GT was replaced with a 270 g/m^2 polypropylene GT and covered with a sand protection layer soon after installation. Interestingly, a 540 g/m^2 polyester continuous filament nonwoven GT filter was substituted for the polypropylene GT in part of the landfill. While the mechanical properties of the polyester GT decreased with time, the rate of degradation was slower than that for the polypropylene GT. After 14.5 months of exposure, the polyester GT still met the project specifications.

For landfill L-18, the 350 g/m^2 polypropylene staple-fiber needlepunched nonwoven GT component of a GC LCRS drainage layer was exposed on the landfill side slope. A soil protection layer was to be placed incrementally over the GC on the side slopes during filling operations. By about one year after construction, waste had not been placed and the GT component of the GC was falling apart, exposing the GN and underlying GM primary liner. The GT degradation was attributed to exposure to ultraviolet light, sulfuric acid from industrial emissions, water, and high ambient temperature. The problem was remedied by replacing the GC LCRS drainage layer on the side slopes and beginning waste placement in the cell soon afterwards.

F-3.5.4 Other Problems

The pipe draining one cell of landfill L-30 was crushed during construction. However, this problem was not detected until landfill operation began. A valve on the HDPE LCRS pipe that controlled water draining from the cell was kept closed until just before the start of waste placement. During this time, a significant amount of water (i.e., more than meter deep) ponded in the cell. When the valve on the pipe was opened so water could drain, drainage occurred only very slowly. With no other on-site location to dispose of waste, the baled waste was placed in the ponded water. C&DW was placed over the bales to keep the bales from floating. The crushed condition of the pipe was only identified when an attempt was made to flush the pipe to increase the water flow rate from the cell. The C&DW contained relatively high concentrations of sulfate. As the waste decomposed, the sulfate was reduced to hydrogen sulfide gas, which caused gas problems at the landfill. Due to the hydrogen sulfide gas emissions, the landfill was closed early, after only about 1.5 years of filling. A gas extraction system with a flare was installed in the landfill, and gas emissions from the facility are successfully being controlled.

F-3.6 Landfill LCRS or LDS Malfunction

F-3.6.1 Overview

Problems related to landfill LCRS or LDS malfunction represent 4 of the 85 problems (i.e., 5%) described herein. Two problems in this category were attributed to design factors and two were attributed to operation factors. The problems and the number of identified landfills with them are as follows:

- waste fines clogged the needlepunched nonwoven GT filter in the LCRS piping system (2 landfills);
- LCRS pipes were not regularly cleaned and became partially clogged and LCRS drainage layer may be partially clogged (1 landfill); and
- leachate seeped out the landfill side slopes in the vicinity of chipped tire layers (1 landfill).

Interestingly, no problems related to biological clogging of the LCRS or LDS at modern waste facilities were identified. If biological clogging is a major problem at landfills, it is expected that there would be evidence that it was occurring. For example, if the LCRS of a landfill was severely clogged, LCRS flow rates would be relatively low during landfill operation, leachate head would build up in the landfill, and, if the head was high enough, leachate would seep from the landfill side slopes. Since most landfills don't exhibit the "symptoms" of biological clogging, it is currently not affecting landfill operation enough to be noticeable at most landfills.

F-3.6.2 Clogging of GT in LCRS Piping System

Waste fines clogged the needlepunched nonwoven GT filters in the LCRS piping systems of landfills L-22 and L-36. The problems were detected during operation. For landfill L-22, which contained industrial plant waste, lime-stabilized waste, and slurried fines, the 540 g/m^2 needlepunched nonwoven GT filter was wrapped around LCRS perforated pipes bedded in the pea gravel LCRS drainage layer. By about one year after construction, it was apparent that the LCRS was not functioning adequately because: (i) rainwater ponded on the waste surface and did not drain freely into the waste; and (ii) the amount of leachate removed from the LCRS sump was less than expected. When the LCRS was excavated near the sump, the GT wrapping the LCRS pipes was found to be clogged by waste fines at the pipe perforations. As described by Giroud (1996), the purpose of a GT is to retain the material behind the filter, not capture particles in motion. The GT around the pipe serves no purpose. It is not needed to prevent the gravel from falling through the pipe perforations. In fact, this GT proved to be detrimental as it captured waste fines and biological particles at the small flow areas at the pipe perforations. It is not known how this problem was remedied.

For landfill L-36, the needlepunched nonwoven GT around the LCRS pipe bedding gravel is apparently clogged by fines from the incinerated MSW ash placed in the landfill. LCRS flow rates are less than expected. In addition, leachate ponded in the landfill and seeped from the landfill side slopes. When a video camera was run through the LCRS pipes, the pipes were found to be full of ash. The pipes were flushed, but the sump still recharged very slowly even though the landfill was full of leachate. From the gradation of the sand LCRS drainage layer and the apparent opening size of the GT, it is expected that the clogging is most significant in the GT around the pipe bedding gravel. The sand has larger openings than the GT and passes fine ash particles. The owner's proposed remedy for this problem involves installing a leachate collection manhole in the landfill to facilitate leachate removal.

F-3.6.3 Other Problems

At landfill L-12, the LCRS appeared to be partially clogged when LCRS flow rates decreased, but LDS flow rates increased, after soil intermediate cover was placed over the landfilled waste. In addition, the LDS flow rates were higher than those typical of nearly filled landfills in that region of the country. The LCRS drainage layer is a sand with a specified minimum hydraulic conductivity of 1×10^{-5} m/s. The LCRS and LDS pipes in the landfill were not flushed annually as is common practice in the region. Rather than performing maintenance on the LCRS pipes, the landfill owner decided to install a leachate extraction well in the landfill. After the well was installed through the waste, LDS flow rates increased, and it was suspected that the well had penetrated the GM primary liner. Subsequently, the LCRS pipes were cleaned out and are now scheduled to be flushed annually. Insufficient time has past to determine if cleaning the pipes solved the problem or if the LCRS drainage layer may be partially clogged.

After about 1.2 million chipped tires were disposed of in MSW landfill L-37 as part of a site cleanup, leachate was observed to be seeping out the side slopes of the landfill in the vicinity of chipped tire layers. The coarse tire chips have a higher hydraulic conductivity than the MSW and, apparently, promote lateral drainage within the waste. A bucket auger was advanced through the waste to the top of the sand LCRS drainage layer at six locations near the seeps. Perched leachate in the tire chips was found in some of the boreholes at depths of up to 3 m. The boreholes with perched leachate were completed as wells. The wells allow some of the leachate collected in the tire chip layers to readily drain to the LCRS. In addition, leachate levels in the wells are inspected weekly, and the wells are pumped if leachate is present.

F-3.7 Landfill LCRS or LDS Operation

F-3.7.1 Overview

Problems related to landfill LCRS or LDS operation represent 4 of the 85 problems (i.e., 5%) described herein. One problem in this category was attributed to design factors and three were attributed to operation. The problems and the number of identified landfills with them are as follows:

- clogging and other problems with leachate pump or flow rate measuring system (3 landfills); and
- values on LCRS pipes were not opened and leachate could not drain (1 landfill).

F-3.7.2 Malfunction of Leachate Pump or Flow Rate Measuring System

Clogging and other problems with leachate pumps or flow rate measuring systems occurred at landfills L-5, L-34, and L-35. These problems were identified during operation and were primarily remedied by equipment maintenance, repair, and replacement. For landfills L-5 and L-34, the problems also led to overestimation of LDS flow quantities and underestimation of LCRS flow quantities, respectively. At landfill
L-5, there were numerous problems: (i) the control system that measured the liquid levels in the sumps and operated of the pumps was prone to compressor failure and clogging of air lines; (ii) the control system problems caused the LDS sump pump to sometimes stay on even when there was no more liquid to be removed (i.e., it pumped air) and caused pumps to run for too long of an interval, or even continuously, until they burned out; (iii) the mechanical flowmeters frequently clogged and became inoperable; (iv) the venturi flowmeters that replaced the mechanical flowmeters were damaged by an electrical storm; (v) a failed check valve allowed LDS liquid that had been metered to flow back into the LDS of the cell and be remetered; and (vi) the leachate level measurement system in the LCRS sump experienced drift due to the buildup of landfill gas pressures in the sump. These problems were remedied by a program of equipment maintenance, repair, and replacement.

For landfill L-34, the “pump on” time setting at the pump controller tended to drift causing the pump to operate too long and LCRS flow rates to be underestimated. As a result of overpumping, air was pulled into the pump, and the pump tended to become airlocked and shut down. An accumulating flowmeter was installed to provide a better measurement of leachate flow quantities. However, when the air pulled into the pump moved through the flowmeter, the flowmeter overestimated the quantity of leachate removed. Additionally, the pump did not reprime as the leachate levels rose. When the landfill operator noticed this, the pump was removed from the sump and adjusted and the “pump on” time setting was reset. This problem was

resolved by replacing the pumps with self-priming pumps from a different manufacturer.

For landfill L-35, the submersible pumps and magnetic flowmeters in the LCRS continually became clogged with a white precipitate. In addition, the LDS was designed with large, shallow sumps to keep the liquid head in the LDS above the pump intake, but no more than 0.3 m. To accomplish this, the pump cycle was very short. The pump motor overheated from turning on and off so quickly and burned out. The problems for landfill L-35 were resolved by disassembling the LCRS pumps and flowmeters and cleaning them with citric acid about every month. Also, the LDS pumps were replaced with smaller models to increase cycle times.

F-3.7.3 Other Problems

During operation of landfill L-23, it was discovered that valves on the LCRS pipes in two landfill cells were not opened prior to placement of waste in the cells. Consequently, leachate could not drain from the cells. Eventually, the waste became buoyant due to rising leachate levels. After about 1.5 years of operation, a bulldozer operating at the active face sunk in the waste and had to be removed with a crane. In another cell, waste was placed too close to an intercell berm between it and a new cell that had not yet been approved for waste. Sufficient space between the waste and the intercell berm should have been maintained to temporarily store runoff from the waste. After a storm, leachate and waste washed over the berm and into the new cell. A temporary access road made out of waste was constructed over the intercell berm to access the new cell and clean out the waste that had washed into it. At the time, the sand LCRS drainage layer had not been placed over the berm liner system geosynthetics. The waste placed directly on the HDPE GM primary liner damaged the GM. The corrective measures for this landfill have not yet been implemented.

F-3.8 Landfill Liner System Stability

F-3.8.1 Overview

Problems related to landfill liner system stability are one of the most common types of problems identified in this study. This category represents 12 of the 85 problems (i.e., 14%) described herein. The problems in this category were primarily attributed to design factors. Only three problems were attributed to operation. The problems and the number of identified landfills with them are as follows:

- liner system slope failure due to static loading (10 landfills); and
- liner system damage due to an earthquake (2 landfills).

F-3.8.2 Liner System Instability Due to Static Loading

Liner system slope failure due to static loading occurred at landfills L-21, L-24, L-25, L-38, L-39, L-40, L-41, L-42, L-45, and L-46. The slope failures at landfills L-21 and L-46 occurred during construction; the slope failures at the other landfills occurred during operation. All of the failures were detected by visual observation of mass movement of one or more components of the liner system, including cracking of soil layers near the slope crest, and/or tearing, tensioning, or wrinkling of geosynthetics. The primary causes of failure were: (i) using unconservative presumed values for the critical interface shear strength (landfills L-25, L-39, L-41, L-46); (ii) not evaluating the critical condition for slope stability (e.g., liner system with waste at intermediate grades, critical liner system interface) (landfills L-24 and L-38); (iii) not accounting for or underestimating seepage pressures (landfills L-39 and L-40); (iv) not accounting for moisture at the GM/CCL interface (which weakens the interface) due to spraying of the CCL and thermal effects (landfill L-21); (v) not maintaining the drainage layer outlets free of snow and ice, which can lead to increased seepage pressures (landfill L-42); and (vi) not maintaining sufficient thickness of soil layer anchoring geosynthetics (L-45).

During construction of landfill L-21, part of the single-composite liner system on the upper 3.5H:1V side slopes slid downslope along the polyvinyl chloride (PVC) GM/CCL interface. Sliding occurred both after placement of the sand LCRS drainage layer over the PVC GM liner and during placement of the lime-stabilized sludge protection layer over the sand. The slide zone was identified by cracking of the sand layer or stabilized sludge layer near the crest of the side slope and wrinkling of the GM liner near the slope toe. When the GM in the slide zone was exposed, it was taut and, in some cases, torn near the slope crest. The CCL beneath the liner was relatively wet: while it had been constructed with an average measured moisture content of about 2 percentage points wet of standard Proctor optimum, the moisture content measured in the slide zone was about 7 percentage points wet of optimum. The increase in moisture content at the surface of the CCL between compaction and sliding is believed to have resulted from condensation of water on the lower face of the GM due to thermal effects and spraying of the CCL surface to prevent desiccation prior to placement of the GM. A liner system slope stability analysis had not been conducted as part of the landfill design. However, the liner system for another phase of the landfill had been successfully constructed previously using the same liner system components and geometry and similar site soils to construct the CCL. After the failure, the owner conducted direct shear interface tests and slope stability analyses. The owner found that, on the steepest slopes (i.e., 3H:1V), the liner system was just stable after construction. However, the liner system became unstable as the CCL surface became wetter and the strength of the GM/CCL interface decreased. This problem was remedied by: (i) placing a temporary protective cover over the GM liner and CCL in the slide zone to protect the CCL from frost damage until the GM and overlying soil layers could be reconstructed in the spring; (ii) installing a

polypropylene monofilament woven GT reinforcement layer between the GM liner and overlying soils to carry the load of the soils for the liner system constructed on the upper side slopes after the failure occurred; and (iii) developing new construction procedures to reduce the potential for liner system sliding in the future.

At landfill L-24, a liner system slope failure occurred after the intermediate waste slopes in part of the landfill were temporarily increased to about 2.5H:1V, significantly steeper than the maximum slope of 4H:1V specified in the operations plans. Sliding occurred along the GN/GCL (HDPE GM side) and GCL (bentonite side)/CCL interfaces of the single-composite liner. (The GCL consisted of an HDPE GM with a bentonite layer glued to one side of the GM.) The problem was detected when the sand berm at the toe of the waste slope began to heave and the top of the waste slope began to crack. When part of the waste was excavated and the liner system was exposed during the construction of a landfill expansion, the GCL was observed to be folded near the toe of the waste slope and, further back into the waste, the GCL was taut and torn. The stability analysis conducted for design of landfill L-24 was based on presumed interface shear strength values and did not evaluate the liner system with the waste at intermediate grades; there was no regulatory requirement to include this in the permit. When the landfill owner later decided to overfill the cell with waste, the stability of the liner system with the relatively steep waste slopes was not analyzed. This problem was remedied by excavating about 270,000 m^3 of waste, reconstructing the damaged liner system, and regrading the waste slopes to 4H:1V.

At landfill L-25, which has a double-composite liner system, the slope failure was manifested by mass movement of the waste. Cracks were observed on the landfill surface in the early morning and, within about five hours, the waste had slid horizontally up to 11 m and vertically up to 4 m. Around the side slopes, the soil cover over the waste and the waste was cracked and, in some locations, the liner system was torn. Sliding occurred primarily along the HDPE GM/CCL interface of the composite secondary liner on the landfill base and the HDPE GM primary liner/GT interface on the side slopes. Of note, there was no limit on the maximum CCL moisture content in the specifications; the CCL material was compacted at an average moisture content 5 percentage points wet of optimum. The landfill had been designed using presumed interface shear strengths for the liner system. After the failure occurred, interface direct shear and pullout tests were conducted to evaluate the shear strength of critical liner system interfaces, and stability analyses were performed using the actual interface strengths. The results of the laboratory tests showed that only a small amount of displacement (5 mm or less) is required to mobilize the peak shear strength along an interface. At greater displacements, the shear strength decreased and approached the large-displacement value. Assuming that peak shear strengths were mobilized on the landfill base and 3H:1V side slopes and large-displacement shear strengths were mobilized on the 2H:1V side slopes, the calculated factor of safety for the three-dimensional failure surface was 1.08. Thus, the measured interface shear strengths and the rapid decrease in shear strength with

displacement after peak strength has been reached can explain the landfill failure. The problem was remedied by relocating waste into other phases of the facility, repairing the liner system, and refilling the landfill with waste.

At landfill L-38, which has 3H:1V side slopes, a stability analysis conducted during design showed that the sand LCRS drainage layer would not be stable on the underlying HDPE GM primary liner. To keep the sand from sliding downslope, the design engineer added a needlepunched nonwoven GT between the sand and the GM. Apparently, the potential for sliding between the GT and GM was not evaluated. After several rainfall events, the sand drainage layer became wet and the GT began creeping downslope. About one month after sliding started, a relatively heavy rainfall occurred at the site and the liner system slope failed due to excessive creep and tearing of the GT and cracking of the sand layer at the slope crest. At locations where the GT tore and slid downslope, the underlying GM was abraded. Since the failure coincided with rainfall, seepage pressures in the sand probably contributed to the failure. The method of repair was not given.

The slope failures at landfills L-39 and L-40 were also partially attributed to seepage pressures. At landfill L-39, a needlepunched nonwoven GT cushion was placed between a LCRS gravel drainage material and an HDPE GM liner. About one to two years after the liner system was constructed, a portion of the GT tore at the crest of the 3H:1V side slope and slid to the slope toe after a heavy rainfall. A number of successive slides occurred during several subsequent rainfalls. Based on an infinite slope analysis conducted by the authors of this appendix, the GT cushion would have been in tension even without seepage pressures. Information was not available on whether the GT was designed to be in tension. The method of repair was not given.

At landfill L-40, a gravel LCRS drainage layer slid over an HDPE GM liner to the toe of the 3H:1V side slope after a heavy rainfall. After the failure, the gravel was inspected and found to be contaminated with fines. The fines apparently inhibited drainage of water from the gravel and allowed seepage pressures to develop. The method of repair was not given.

At landfill L-41, a very flexible polyethylene GM liner tore at the crest of the 2.5H:1V side slopes and slid downslope over an underlying needlepunched nonwoven GT. The GM was overlain by a sand LCRS drainage layer. Failure occurred after a heavy rain and was attributed to seepage pressures in the sand drainage layer. However, analyses conducted by the authors of this appendix using the method of Giroud et al. (1995) found that seepage pressures above the GM would not significantly affect the stability of the GM/GT interface below the GM. Based on an infinite slope analysis conducted by the authors of this appendix, the liner system was, at best, only marginally stable after construction. Thus, the original design was only marginally stable and the rainfall had the effect of "triggering" the slide. The method of repair was not given.

At landfill L-42, a needlepunched nonwoven GT between a gravel LCRS drainage layer and a PVC GM liner tore at the crest of the 4H:1V side slopes and slid downslope over the GM. The failure occurred after frozen water in the gravel LCRS drainage layer began to melt, but could not freely flow out of the gravel at the slope toe because of ice at the toe. The method of repair was not given.

At landfill L-45, a needlepunched nonwoven GT protection layer slid downslope over an HDPE GM liner after the soil layer anchoring the geosynthetics beyond the crest of the side slope was eroded by landfill traffic. The method of repair was not given.

At landfill L-46, a needlepunched nonwoven GT filter between a soil protection layer and GN tore at the crest of a 3H:1V side slope and the GN separated at its panels and slid downslope over an HDPE GM liner. Slope stability analyses performed as part of the liner system design used assumed interface shear strengths and relied on the GT filter to carry the load of the overlying soil layer and construction equipment. Laboratory interface shear strength testing conducted after the failure gave lower shear strengths than those assumed for design. In addition, the design strength used for the GT was too high and construction loads were underestimated. In areas where the soil protection layer had been placed up the 11-m high slope, the soil was removed and the damaged GT and GN were repaired. The placement of the soil protection layer over the GT was subsequently limited to increase slope stability: the soil layer was required to be placed in 6 m increments along the slope, advancing upslope with waste placement.

Interestingly, the majority of the slides described above occurred along geosynthetic/geosynthetic interfaces. For a number of case histories, the interface friction angle between adjacent liner system components was estimated on the basis of published tested data. This approach should be avoided because there may be significant differences in interface shear strengths between similar materials from different manufacturers and even identical materials from different production lots from the same manufacturer. In fact, only a small error in the estimated interface shear strength may cause slope instability. Because of this, geosynthetic interface shear strengths should not be estimated, they should be measured. Additionally, as more geosynthetics are available on the market, the probability increases that there will be significant differences in properties between geosynthetics that appear to be similar.

F-3.8.3 Liner System Instability Due to an Earthquake

Liner system slope instability due to an earthquake occurred at landfills L-26 and L-27 during operation. The instability was caused by the 17 January 1994 Northridge earthquake (moment magnitude M_w 6.7), which generated estimated rock peak horizontal accelerations at the landfill sites of 0.33g and 0.36g, respectively. The

damage, which was detected by visual inspection, consisted of: (i) tearing of the GM liner at several locations near the side slope crest, parallel to the anchor trench in landfill L-26; (ii) further tearing of the GT cushion above the GM liner on the side slope in landfill L-27; and (iii) surficial cracking of soil intermediate cover, primarily near locations with contrast in seismic response characteristics (e.g., top of waste by canyon walls) at both landfills.

In two canyon fills at landfill L-26, the HDPE GM liner tore on benches above the waste during the earthquake. The tears were located near the side slope crest, parallel to the anchor trench. In one canyon, the GM tear was 4.3 m long and opened up to 0.25 m wide; in the other canyon, there were three parallel tears with a total length of about 23 m. Longitudinal cracks were present in the soil intermediate cover at the top of the waste below the tear. The cracks were up to 0.3 m wide, with vertical offset of 0.15 to 0.3 m. At some locations, the cracks exposed the underlying GM liner. Forensic analyses indicated that the GM tears initiated from locations where GM seam samples were cut for destructive testing. Both the stress concentrations around the hole (which had been patched) and the high pullout capacity of the anchor trench appear to have been factors in the initiation and propagation of the tears. As the GM liner moved during the earthquake, it was constrained at the anchor trench and subsequently tore at locations with concentrated stresses. Furthermore, in these canyons, it appears that the slope stability factor of safety of the waste at intermediate grades was relatively low under the seismic loading of the Northridge earthquake. The seismic-related damage at the landfill was remediated by repairing the damaged GM, securing the liner system above the damaged GM using a soil berm rather than an anchor trench, and regrading and revegetating the cracked soil intermediate cover.

At landfill L-27, tears in the GT cushion above the GM liner appeared to have increased in size as a result of the earthquake. The tears were located on the side slope above the waste. No tears were observed in the GM liner. In addition, extensive cracks were observed in the soil intermediate cover near its contact with the side slope liner system. The cracks, which had up to 25 mm of vertical offset, may have been the result of limited downslope movement of the GT. The damage was remedied by repairing the GT and regrading and revegetating the cracked soil intermediate cover.

F-3.9 Landfill Liner System Displacement

F-3.9.1 Overview

Problems related to landfill liner system displacement represent 4 of the 85 problems (i.e., 5%) described herein. All of the problems in this category were attributed to design factors. The problems and the number of identified landfills with them are as follows:

- uplift of liner system geosynthetics by landfill gas after erosion of the overlying sand layer (2 landfills); and
- uplift of composite liner by surface-water infiltration during construction (2 landfills).

F-3.9.2 Uplift of Liner System Geosynthetics by Landfill Gas

Uplift of liner system geosynthetics by landfill gas occurred during operation of landfills L-9 and L-11, after portions of the overlying sand layer on the liner system side slope eroded. The side slope liner system for both of these landfills was constructed over existing MSW. The designs called for gas beneath the liner system of landfills L-9 and L-11 to be collected in a gravel trench at the crest of the side slope and gas extraction wells, respectively. The designs were not based on site-specific, estimated gas generation rates or field measurements of gas production.

During construction of landfill L-9, an HDPE GM component of a single-composite liner was uplifted after the 0.6-m thick sand LCRS drainage layer began to erode, decreasing the overburden pressure on the liner system. Ten 6-m diameter bubbles developed and uplifted the GM to about 1.5 m. In some areas, the GM yielded. The uplift height was relatively large compared to the diameters of the uplifted areas; consequently, the estimated strain in the GM was relatively large (i.e., 16%). The problem was remedied by cutting the GM at the bubbles, installing temporary gas venting pipes through the liner system and into the underlying waste, and replacing the sand layer.

At landfill L-11, which has a double-liner system, the GC LCRS drainage layer, HDPE GM primary liner, GN LDS drainage layer, and HDPE GM component of the composite secondary liner were uplifted about 0.1 m by landfill gases in two area where the 0.45-m thick sand protection layer had eroded. The diameters of the uplifted areas were about 10 and 20 m. The uplift height was relatively small compared to the diameters of the uplifted areas; consequently, the estimated strain in the GM was relatively small (i.e., less than 0.002%). The GM liner was cut at the two gas bubbles to release the gas, and the liner system was repaired. The sand protection layer was replaced on the side slopes.

F-3.9.3 Uplift of Composite Liner by Surface-Water Infiltration

The GCL/CCL composite liners on the side slopes of landfills L-25 and L-31 were uplifted by surface-water infiltration during construction. This problem was detected by visual observation of ponded water beneath the GCL. For both landfills, the GCL component of the liner consisted of a 1.5-mm thick HDPE GM and a bentonite layer glued to one side of the GM. The GCL was installed with the bentonite side down and was seamed by fusion seaming the GM component of adjacent panels. Also for both landfills, approximately the bottom half of the side slope liner system was constructed in an excavation against native soil (specified maximum hydraulic conductivity of 1 x

10^{-7} m/s) and the upper half was constructed against a more permeable rocky mine spoil berm.

At landfill L-25, the ground surface outside of the berm was graded towards the berm, allowing runoff to pond at the toe of the exterior berm slope. During liner construction, runoff ponded at the toe of the exterior berm slope after rainwater was allowed to evaporate and infiltrate into the soil. Subsequently, water pooled under the GM and saturated the GCL and CCL near the toe of the side slope. When the GM was cut for the water to drain and the damaged GCL was removed, the underlying CCL was very soft. The water appeared to be originating from the interface of the berm mine spoil and the native soil. Apparently, runoff was seeping through the more permeable berm soils into cell. This problem was resolved by dewatering the berm using vertical wells, routing runoff away from the berm toe, constructing a gravel underdrain beneath the liner in the damaged area, and reconstructing the liner.

At landfill L-31, water conveyed in a surface-water diversion ditch located on top of the berm infiltrated into the berm soils, pooled under the GCL, and saturated the GCL and CCL. When the GCL was cut for the water to drain and the damaged GCL was removed, a 0.6-m diameter cavity was found in the berm soils and CCL. The bottom of the cavity was located near the interface of the mine spoil and native soil. Apparently, the relatively high rate of water infiltration through the ditch and into the mine spoil caused erosion of the mine spoil and CCL where the water exited the soil and flowed beneath the GCL. The liner was repaired, and the ditch was lined with clay to reduce infiltration.

F-3.10 Cover System Construction

Problems related to cover systems as they are built represent 2 of the 85 problems (i.e., 2%) described herein. Both problems in this category were attributed to construction factors. The problems and the number of identified landfills with them are as follows:

- portion of topsoil from an off-site source was contaminated with chemicals (1 landfill); and
- high failure rate of HDPE GM seam samples during destructive testing (1 landfill).

The problems related to cover systems construction occurred at landfills C-2 and C-16 and were detected and remedied during construction. At landfill C-2, a portion of the topsoil from an off-site source was contaminated with chemicals. This problem was detected when several truckloads of topsoil brought to the site had an aromatic odor. Samples of the affected soil were analyzed and found to contain unacceptably high concentrations of lead. The problem was resolved by removing the affected material from the site and screening new material brought to the site for contamination.

At landfill C-16, a large proportion of the fusion and extrusion seam samples for a 1-mm thick textured HDPE GM barrier failed destructive testing. The project specifications required that destructive testing of the GM seams be performed by the installer; the CQA consultant was only to monitor the installation. With respect to the fusion seams, initially only the inside track of seam samples was destructively tested in shear and peel by the installer. The project specifications, however, required both tracks of the fusion seam samples be destructively tested. After about 50% of the GM had been approved, based on passing destructive tests, and this GM had been covered with a topsoil layer, the CQA consultant realized that the installer had not tested both seam tracks. Archived fusion seam samples were subsequently obtained and tested. About 60% (i.e., 25 of 42) of the archived seam samples and 49% (i.e., 44 of 90) of the seam samples for the entire GM failed the peel test, primarily due to seam separation exceeding the minimum specified value of 10%. With respect to extrusion seams, 50% (i.e., 6 of 12) of the seam samples taken from GM not covered with topsoil also failed. The installer attributed the high seam sample failure frequency to benzene, toluene, ethylbenzene, and xylenes (i.e., BTEX) in landfill gas being absorbed by the HDPE and inhibiting the formation of good seams. Interestingly, the same installer had placed an HDPE GM barrier over an adjacent section of the landfill about one year earlier and only had about 10% of seam samples failing destructive testing. After laboratory testing was conducted on the seam samples, it was concluded that the primary cause of the poor seam quality was soil in the seams (i.e., inadequate cleaning prior to seaming). Other causes of failure were overheating and, for extrusion seams, inadequate grinding. The BTEX absorbed by the GM had no apparent impact on seam quality. The failed seams were isolated and repaired.

F-3.11 Cover System Degradation

Problems related to cover system degradation represent 2 of the 85 problems (i.e., 2%) described herein. Both problems in this category were attributed to design factors. The problems and the number of identified landfills with them are as follows:

- failure of a geosynthetic erosion mat-liner downchute on 3H:1V side slope (1 landfill); and
- erosion of a topsoil layer on a 60 m long, 3H:1V side slope (1 landfill).

The problems related to cover system degradation occurred at landfills C-1 and C-12 and were detected and remedied during the post-closure period. At landfill C-1, a polyethylene, three-dimensional, grass reinforcement type erosion mat was used experimentally to line one downchute on a landfill cover system. The other downchutes were lined with riprap. The erosion mat-lined downchute had a maximum slope of 3H:1V and conveyed runoff from approximately 2 ha of cover system and 8 ha of adjacent property. The erosion mat was installed and seeded in the fall, when

plant growth is relatively low, resulting in an extended period with poor to no grass cover in the downchute. Within one month after construction, following a series of significant rainfall events, the channel was unserviceable. Soil had raveled along the sides of the downchute, soil had eroded underneath the mat and along mat panel overlaps, and the mat had moved downslope about 2 m. There was little grass in the downchute. The landfill owners concluded that the combination of large drainage area, steep slope, and the inability of grass to sprout quickly in the channel lead to failure of the downchute. The problem was resolved by relining the downchute with riprap and placing topsoil in the eroded areas.

At landfill C-12, the cover system was constructed with 60 m long, 3H:1V unbenched side slopes. Sand diversion berms were located at the top of the cover system and about midway down the side slopes to divert runoff into six downchutes. Within three years after construction, deep gullies had developed on the landfill side slopes in the vicinity of the riprap-lined downchutes and in areas where the sand berms at the side slope crest were breached. Some of the gullies extended through the topsoil and sand drainage layers down to the GM barrier. In several locations, the GM was damaged by punctures and tears, and the subgrade beneath the GM was irregular. The severe erosion was attributed to the following: (i) the sand drainage layer (specified minimum hydraulic conductivity of 1×10^{-5} m/s) in the cover system did not have sufficient capacity; (ii) sand diversion berms and downchutes did not intercept lateral flow in the sand drainage layer; (iii) runoff collected by berms and downchutes could infiltrate through the topsoil layer and enter the drainage layer; and (iv) a lack of access control resulted in unauthorized trafficking of four-wheel drive vehicles or dirt bikes on the landfill. This problem was remedied by adding swales at the top of the cover system to collect runoff and direct it to the downchute, repairing the damaged cover system, and installing a chain link fence around the perimeter of the landfill to limit vehicle access.

F-3.12 Cover System Stability

F-3.12.1 Overview

The most common type of problem identified in this study is related to cover system stability. This category represents 18 of the 81 problems (i.e., 21%) described herein. The problems in this category were primarily attributed to design factors. Only two problem were attributed to construction and one was attributed to operation. The problems and the number of identified landfills with them are as follows:

- cover system slope failure during construction (4 landfills);
- cover system slope failure after rainfall or a thaw (11 landfills); and
- soil cover damage due to an earthquake (3 landfills).

F-3.12.2 Cover System Failure During Construction

Cover system slope failure during construction occurred at landfills C-3, C-8, C-9, and C-14. Slope failure was detected by visual observation of mass movement of the cover system, cracking of soil layers near the slope crest, and wrinkling of geosynthetics at the toe of the cover system slope. The primary causes of failure were: (i) placing soil over the side slope geosynthetics from the top of the slope downward, rather from the toe of the slope upward (landfills C-3 and C-14); using unconservative presumed values for the critical interface shear strength (landfill C-8); and (iii) not considering the effects of variation in the tested geosynthetics, accuracy of test methods, and test conditions on the interface shear strength to use in design (landfill
C-9).

At landfill C-3, the design called for geosynthetic reinforcement to be installed over a nonwoven GT cushion and covered with topsoil. The reinforcement was to be secured on the top of the landfill by covering a length of geosynthetic with soil. Slope stability analyses were conducted assuming topsoil would be placed over the reinforcement from the bottom of the slopes upward. However, this condition was not incorporated into the construction specifications. When construction began, access to the bottom of the side slopes was not available. So the contractor started placing topsoil from the crest of the slope downwards. Shortly afterwards, a section of the soil covered cover system slid along the interface between the GT and an underlying GM barrier. The problem was remedied by repaired by placing new geosynthetic reinforcement and GT layers over the GM barrier, and placing the topsoil over the GT from the bottom of the side slopes upward.

At landfill C-8, a gravel drainage layer placed on a 3H:1V side slope continually slid down the slope, eventually damaging the underlying GM. The contractor had tried to place the gravel by pushing it up the slope with a bulldozer and by placing it on the slope using a clamshell bucket, but neither method worked. The method of repair was not given.

At landfill C-9, as topsoil was being placed over an already-installed sand drainage layer on 3H:1V side slopes, the sand drainage layer slid downslope over a calendered nonwoven GT. Project-specific interface direct shear tests between the sand and GT performed prior to the failure resulted in a secant interface friction angle of about 21°. An infinite slope stability analysis performed with this interface strength shows that the sand should be stable on the 3H:1V slopes. Tilt table tests performed after the failure gave a secant friction angle for the sand/GT interface of about 18°. The differences in secant interface friction angles may be attributed to variation in the tested geosynthetics, accuracy of the test methods, and differences in the test conditions. The cover system was reconstructed with a needlepunched nonwoven GT that had a higher interface shear strength with sand than the calendered GT.

At landfill C-14, the design called for geogrid reinforcement to be installed between an HDPE GM barrier and overlaying soil layers, with the first such layer being a sand drainage layer. The design specified that the reinforcement be secured on the top of the landfill by extending the reinforcement onto the top and covering it with the soil layers. Slope stability analyses were conducted assuming that the soil layers would be placed over the reinforcement from the bottom of the slope upward. However, this condition was not incorporated into the construction specifications. When construction began, not all of the geogrid rolls were secured at the top of the slope because landfill gas wells were in the way. Access to the bottom of the side slopes was limited at some locations due to wetlands near the slope toe. As a consequence of these conditions, the contractor placed a stockpile of sand over the geogrid on the side slope near the crest and began placing the sand from the crest downward. Shortly after sand placement began, the reinforcement snapped at the slope crest beneath the sand stockpile and construction equipment placing the sand. The GM then tore near the slope crest and along outward diagonals down the length of the GM on both sides of the stockpile. The cover system was redesigned without reinforcement and reconstructed successfully.

F-3.12.3 Cover System Failure After Rainfall or a Thaw

Cover system slope failure after rainfall or a thaw occurred at landfills C-4, C-5, C-6, C-7, C-10, C-11, C-13, C-17, C-18, C-19, and C-20 during the post-closure period. Slope failure was detected by visual observation of mass movement of the cover system, cracking of soil layers near the slope crest, and wrinkling of geosynthetics at the toe of the cover system slope. The primary causes of failure appeared to be: (i) not accounting for seepage pressures (landfills C-4, C-5, C-6, C-17, and C-18); (ii) clogging of the drainage system, which can lead to increased seepage pressures (landfills C-7, C-10, C-11, C-19, and C-20); and (iii) not accounting for moisture at the GM/CCL interface (which weakens the interface) due to rain falling on the CCL surface during construction and freeze-thaw effects (landfill C-13).

The cover system slope failures at landfills C-4, C-5, C-6, C-17, and C-18 were primarily attributed to rainfall-induced seepage pressures in soil layers above the failure surface. The cover systems for the landfills have 3H:1V or 2.5H:1V side slopes and are up to about 60 m in slope length. Failure occurred along a topsoil/GCL interface at landfill L-4, a sand drainage layer/woven GT interface at landfill C-5, a sand drainage layer/GM interface at landfill C-6, and a sand layer/CCL interface at landfills C-17 and C-18. The cover system for landfill C-4 has been redesigned with a drainage layer; however, at the time of this appendix, the modified cover system had not been constructed. Landfill C-6 was repaired by reconstructing the cover system with benches and collection pipes that drained water from the sand drainage layer into the benches. The method of repair of landfills C-5, C-17, and C-18 was not given.

For landfills C-7, C-10, C-11, C-19, and C-20, clogging of components of the final system drainage system prohibited the cover systems from draining freely. When significant pore pressures built up in the cover systems after rainfall, the cover systems experienced slope failure. Failure occurred along the sand/GM interface at landfills C-7 and C-10, topsoil/GT interface at landfill C-11, and sand/CCL interface at landfills C-19 and C-20. At landfill C-7, which was constructed with a gap-graded sand drainage layer in the cover system, clogging was caused by fines, presumably washed into the sand from the topsoil and the sand upslope of the failure zone. This problem was remedied by reconstructing the drainage layer with a uniformly graded sand and a GN. At landfills C-10 and C-20, perforated pipes in the sand drainage layer were wrapped with a GT filter. Eventually, fines clogged the GT at the pipe perforations and water became trapped in the drainage layer. At landfill C-10, the pipes were removed and replaced with perforated pipes bedded in gravel wrapped in a GT. The remedy for landfill C-20 was not given. At landfill C-11, the GT beneath the topsoil layer became clogged with soil particles over time and did not drain freely into the underlying gravel. The remedy for landfill C-11 was not given. For landfill C-19, the design called for water collected in the sand drainage layer to drain to the toe, be collected in a gravel toe drain, and exit the cover system through a pipe. An adequate filter system was not established between the topsoil, sand drainage layer, and gravel toe drain. The gravel became very contaminated with fines, which presumably migrated into the gravel from the overlying sand and topsoil. The remedy of landfill C-19 was not given.

The cover system for landfill C-13 was constructed in the fall. During the winter the cover system was covered with snow and the ambient temperature was below freezing until the spring. A few days after the first thaw in spring, a PVC GM slid over a CCL on the 4H:1V side slopes. A forensic investigation showed that water could not exit from the sand drainage layer because the lower end of the drainage layer was blocked by ice and snow. As a result, the cause of the slide was initially assumed to be the seepage pressures that developed when flow started after melting of the ice at the lower end of the drainage layer. However, a subsequent slope stability analysis showed that seepage pressures above a GM have little effect on the factor of safety with respect to a slide that occurs at an interface located beneath the GM. With seepage forces identified as only a minor contributor to the slope failure, an additional investigation was conducted to evaluate the effect of temperature fluctuations on GM/CCL interface shear strength. Interface shear tests simulating the conditions during the winter (-7°C) followed by thaw (+0.5°C) showed that the formation of ice lenses at the GM/CCL interface at below-freezing temperature increased the water content at the GM-CCL interface, resulting in a marked decrease of the interface shear strength after a thaw, compared to the interface shear strength before freezing. With systematic measurements of the water content of the CCL and a slope stability analysis, the slope failure could be explained by the higher CCL water content and lower GM/CCL interface shear strength in the area where the slide occurred than in

other areas. The higher water content was attributed to the heavy rainfall that preceded the installation of the GM in the area where the slide eventually occurred. The fact that a PVC GM had ruptured with an apparently small strain, compared to the typical 300% strain at break of PVC GMs, was also investigated. Tests on the PVC GM showed that, at 0.5°C, the conditions after a thaw, the PVC GM had a yield strain of 9%, which is much less than the strain at break of about 300% at 23°C. This 9% yield strain explains the observed rupture of the GM and is consistent with the observed displacements. The cover system was reconstructed in the slide area without a GM.

F-3.12.3 Soil Cover Damage Due to an Earthquake

Soil intermediate cover damage due to an earthquake occurred at landfills C-21, C-22, and C-23 during operation. The damage was caused by the 17 January 1994 Northridge earthquake (moment magnitude M_w 6.7), which generated estimated rock peak horizontal accelerations at the landfill sites ranging from 0.20g to 0.42g. The damage, which was detected by visual inspection, consisted of surficial cracking of soil intermediate cover occurring primarily near locations with contrast in seismic response characteristics (e.g., top of waste by canyon walls). At landfills C-21 and C-23, the cracking was relatively minor. Cracks at landfill C-23 were up to 100 mm wide. At landfill C-22, one crack near and parallel to the liner system anchor trench was 215 m long, up to 150 mm wide, and vertically offset up to 100 mm. No waste was exposed. At all landfills, the damage was expected and was dealt with as an operation issue through post-earthquake inspection and repair (i.e., regrading and revegetating the cracked soil layers).

F-3.13 Cover System Displacement

Problems related to cover system displacement represent 2 of the 85 problems (i.e., 2%) described herein. One problem in this category was attributed to design factors and one was attributed to construction. The problems and the number of identified landfills with them are as follows:

- cover system settlement caused tearing of HDPE GM boots around gas well penetrations of GM barrier (1 landfill); and
- localized cover system settlement during construction stretched the PVC GM barrier and opened GCL joints (1 landfill).

Problems related to cover system displacement occurred at landfills C-12 and C-15 and were detected during the post-closure period and construction, respectively. At landfill C-12, a cover system, with vertical HDPE gas collection wells that penetrated the HDPE GM barrier, was installed over MSW. At each gas well penetration, an HDPE GM boot was clamped to the well and extrusion seamed to the GM barrier to seal the barrier around the well. By about three years after the cover system was

installed, the MSW had settled up to 0.9 m. When several of the GM boots around the wells were inspected, they were observed to be torn from the GM barrier. The boots were not designed to accommodate settlement of the waste, which would cause downward displacement of the GM barrier relative to the wells. This problem was remedied by replacing the old gas extraction well boots with new expandable boots that can elongate up to 0.3 m. These boots can also be periodically moved down the well to accommodate landfill settlement.

At landfill C-15, a cover system was constructed over saturated, highly compressible paper mill sludge. To facilitate construction of the cover system, a stabilized sludge working surface was spread over the in-place sludge. After the cover system geosynthetics (GC drainage layer, 0.5-mm thick PVC GM barrier, GCL, and GC gas collection layer) were installed, placement of the overlying soil layer began. The repeated trafficking of low-ground pressure bulldozers over portions of the cover system resulted in pumping of the underlying sludge into the stabilized sludge. This pumping progressively reduced the shear strength of the stabilized sludge layer, resulting in localized bulges and, at times, placement of excessive thickness of soil. Eventually, the weakened stabilized sludge layer underwent a localized bearing capacity failure in a 60-m long by 18-m wide area. The measured settlement of the cover system in this area was up to 2.4 m, and the estimated average strain in the geosynthetics where the settlement is 2.4 m is 4.7%. Though none of the geosynthetics appeared to have been damaged by the displacement, the PVC GM was in tension and the GCL seams had separated at two locations along the length of the panels. Adjacent GCL panels had been overlapped 0.15 m along the roll length; however, calculations show that the seam would open if the average strain exceeded 3.2%. The affected area was repaired by removing the cover system materials in this area, restabilizing and regrading the sludge, and reinstalling the cover system with new geosynthetic materials. The bulldozers used to spread the overlying soil layer had ground pressures less than that used previously, and additional grade control measures were implemented to ensure that excess soil was not placed.

F-3.14 Impoundment Liner Construction

F-3.14.1 Overview

Problems related to impoundment liner construction represent 3 of the 85 problems (i.e., 4%) described herein. All problem in this category were attributed to construction factors. The problems and the number of identified landfills with them are as follows:

- leakage through holes in the HDPE GM primary liner or the HDPE GM component of the GM/CCL composite primary liner (2 impoundments); and
- large wrinkles in an HDPE GM primary liner (1 impoundment).

F-3.14.2 Leakage Through Holes in HDPE GM Liner

Leakage through the primary liners of impoundments S-4 and S-5 was detected during operation when LDS flow rates increased unexpectedly after the liquid levels in the impoundments were raised. For impoundment S-5, primary liner leakage was confirmed by the results of chemical analyses of LDS liquid. For impoundment S-4, which has a composite primary liner consisting of a 2.5-mm thick HDPE GM over a 0.45-m thick CCL (specified maximum hydraulic conductivity of 1×10^{-9} m/s), LDS flow rates increased significantly within one month after the liquid level in the pond had reached its highest level of about 3 m. When the pond liquid level was lowered, the LDS flow rates returned to their normal levels. GM holes were located and repaired. However, LDS flow rates increased again when the pond liquid level was raised back to 3 m. The leakage problem for impoundment S-4 was remedied when the GM primary liner was inspected at an elevation corresponding to the maximum liquid level, and holes were found and repaired. In both cases where LDS flow rates increased when the pond liquid level was raised, the flow rate increase occurred over a relatively short time period (less than one month). Presumably at least part of this flow was due to primary liner leakage. It is not clear how leakage entered the LDS in such a short time period given that the primary liner is a composite. The primary liner on the side slope is only protected by “sacrificial” GM; the primary liner is not thermally insulated by a soil protection layer. It may be that the CCL underlying the GM on the side slope has become desiccated due to thermal effects, and the hydraulic conductivity of the CCL has increased by several orders of magnitude.

Impoundment S-5 has two ponds with HDPE GM primary liners. Prior to operation, leak location surveys were performed in both ponds, and identified primary liner holes were repaired. Even so, primary liner leakage was detected in both ponds shortly after start of operation based on LDS flow rates, which increased with increasing pond liquid level, and chemical analysis of the LDS liquid. After about two years of operation, GM primary liner holes were located in the ponds and repaired.

F-3.14.3 Other Problems

The exposed HDPE GM primary liner in two ponds at impoundment S-3 developed large wrinkles after construction. The double-liner system for the ponds was constructed in the winter when temperatures were cooler. At the end of construction, the GM primary liner was noticeably wrinkled, but acceptable to the CQA consultant. By early summer, the ponds had not yet been put into service, and the GM had become more wrinkled under the increasing temperature. Wrinkles were more numerous and larger near the slope toe as they propagated downslope during several months of temperature cycling. (This is sometimes referred to as the “caterpillar effect”.) Wrinkles were, on average, about 100 mm high and several large wrinkles near the slope toe were folded over. This problem will be resolved by cutting out the large wrinkles in the GM and seaming the cuts.

F-3.15 Impoundment Liner Degradation

Problems related to impoundment liner degradation represent 1 of the 85 problems (i.e., 1%) described herein. The problem in this category was attributed to design factors. Slow crack growth (SCG) stress cracks and rapid crack propagation (RCP) shattering cracks developed in the exposed HDPE GM liner in five ponds at impoundment S-1. The problem was detected during operation by visual inspection. One of the pond liners had been installed with compensation panels to allow for liner contraction at low temperatures; designed compensation panels had not been installed in the other pond liners. In general, at temperatures near freezing, the GM on the side slope was taut. All of the GM seams had been constructed by lapping the panels and applying a bead of HDPE extrudate (lap-type extrusion seam). The pond liners were exposed and, therefore, subject to significant thermally induced tensile stresses under the wide range of ambient temperatures at the site (i.e., -30 to 40°C). By four years after installation, the five impoundment liners exhibited relatively short SCG stress cracks in and adjacent to some seams. There were no cracks below water level. The stress cracks generally occurred in the lower GM.

During the winter, record low temperatures appeared to precipitate the cracking of some seams from the side slope crest to toe. These long cracks were surrounded by branching RCP shattering cracks. The liner in the pond containing the fewest visible stress cracks had been installed with compensation panels. There was also some indication that the most seriously damaged liners had been installed at high ambient temperatures and would, therefore, require the largest amount of compensation in order to be stress-free at the lowest operating temperature. The shattering cracks that occurred in the pond liners can be explained by the conjunction of the following (Giroud, 1994a):

- the HDPE resin used in these GMs did not have a low stress-cracking susceptibility;
- tensile stresses caused by thermal contraction;
- strain concentrations caused by the seams;
- decreased allowable yield strain at the low temperatures at which GM shattering occurred; and
- increased crystallinity of the HDPE next to the seam.

Impoundment S-1 was remedied by replacing damaged GM with new GM containing an adequate amount of slackness calculated using the temperature of the GM at the time of the repair. In addition, every third seam in the ponds was cut from the anchor trench to the toe of slope and the GM was allowed to relax. Compensation panels were installed at each cut seam. Stress cracks in seams were repaired using a wide bead extrusion technique developed specifically for this purpose.

F-3.16 Impoundment Liner System Stability

Problems related to impoundment liner system stability represent 1 of the 85 problems (i.e., 1%) described herein. The problem in this category was attributed to design factors. The GT cushion in the double-liner system for sludge impoundment S-2 failed during operation. The failure was detected by visual observation. The failure was attributed to the method of sludge placement: sludge was dumped on the GT cushion at the crest of the 10 m high, 2H:1V impoundment side slopes and allowed to flow to the slope toe. On several occasions, the sludge adhered to a polypropylene needlepunched nonwoven GT cushion layer, which overlies an HDPE GM primary liner. When this occurred, the sludge was pushed downslope by a low-ground pressure bulldozer. Tension developed in the GT, and it eventually tore at the slope crest and slid downslope over the GM. This problem was remedied by replacing the damaged GT and placing a thin GM slipsheet over the GT in the sludge dumping area to facilitate the sliding of sludge downslope.

F-4 Significance of Identified Problems

F-4.1 Introduction

The main impacts of the problems identified in this investigation are interruption of waste containment system construction and operation, increased maintenance, increased costs, and negative public/regulator perception. As discussed in Chapter F-3, almost all of the identified problems were detected during construction or operation, shortly after they occurred. In general, problems detected and repaired during construction have no environmental impact; however, they can delay construction, impact operation (e.g., delay waste placement in a landfill cell), increase construction costs, and reduce public/regulator confidence. Problems detected during operation can potentially have an environmental impact. However, if the problems are detected and remedied soon after they occur, there is less likelihood of environmental impact. Problems that occur during operation are also more likely to interrupt facility operation, increase maintenance, and result in higher costs and greater impact to public/regulator confidence than problems that occur during construction. In addition, problems that occur during operation may be difficult to repair.

Of the problems in this study for which the remedy was identified, six problems were not completely repaired. These problems are classified as landfill liner construction/construction, landfill liner degradation/design, landfill LCRS or LDS construction/construction, and landfill LCRS or LDS malfunction/operation. One problem was detected during construction, and five were detected during operation. These problems are as follows:

- Relatively high leakage rates through the GM primary liner on the base of landfill L-5 were detected shortly after start of operation. However, due to problems with the flow measuring system, leakage rates were not accurately known until about three years after operation began. Leakage rates decreased when the head of leachate in the LCRS sump was reduced; however, the leakage rates were still relatively high. GM primary liner holes have not been located and repaired at this landfill because: (i) there is no anticipated environmental impact of the primary liner leakage given the expected performance capabilities of both the LDS and the composite secondary liner; (ii) repair of liner systems after waste placement would be extremely difficult and expensive; and (iii) additional liner system damage could occur in any attempt to excavate the waste and repair the liner system.
- Leakage at the LCRS pipe penetration of the HDPE GM primary liner for landfill L-9 was detected during construction. The pathway for this leakage could not be identified during construction, and the problem was not remedied. The environmental impact from the leakage, however, is expected to be negligible given that the landfill has a composite secondary liner.
- Severe desiccation cracking of the CCL component of the composite liner for an existing cell at landfill L-2 was detected when a new cell was constructed adjacent to the existing cell which had been constructed three years earlier. The existing cell with the cracked CCL was filled to about 70% of its waste capacity. No actions were required for the older cell by the regulatory agency presumably because: (i) the older cell was almost filled and would be closed shortly afterwards; (ii) the repair would require that the waste be removed from the cell, which is extremely difficult, and costly; (iii) the CCL was only observed to be desiccated on the side slope; all other thing being equal, side slope liner holes are less detrimental than base liner holes because the head of leachate on the side slope is less than the head on the base slope; and (iv) environmental impacts from the potential for increased liner leakage are expected to be negligible given that the liner includes a GM. Two months after construction of the composite liner, the CCL component of the liner on the side slope of the new cell was beginning to crack too, and will likely become more desiccated until the exposed composite liner for the cell is covered with the sand drainage layer.
- Several joints of the HDPE LCRS pipes in active landfills L-34 and L-36 were found to be separated when the inside of the pipes was videotaped. No action has been required by the regulatory agency presumably because: (i) leachate flowing out of the pipe at an open pipe joint can still flow to the leachate sump (though the localized head at the open joint may be somewhat higher that those upgradient and downgradient of the open joint); (ii) the pipe condition has remained unchanged during subsequent annual videos; (iii) repair of LCRS pipes after waste placement would be extremely difficult and expensive; and (iv) environmental impacts from having a localized higher head on the liner at the open pipe joints are expected to be negligible.
- A leachate well installed into landfill L-12 appeared to puncture the GM primary liner in the landfill. No action has been required by the regulatory agency because

it is not clear if the primary liner was actually punctured and the flow rates from the LDS have remained relatively low. Environmental impacts from this possible GM hole are expected to be negligible.

The impacts of the identified problems on the environment; construction, operation, and maintenance, and cost are discussed below.

F-4.2 Environmental Impacts

F-4.2.1 Introduction

The potential consequences of problems associated with landfill liner systems, cover systems, and impoundment liner systems are presented in Tables F-4.1 to F-4.3, respectively. As shown in these tables, the consequences range in severity and potential for environmental impact. The potential environmental impacts are described below. The tables also present methods for potentially preventing the problems. Interestingly, the problems only resulted in an identified environmental impact to groundwater or surface-water quality by leachate or landfill gas at one facility, landfill L-8. At this MSW landfill, groundwater impact by VOCs was attributed to gas migration through a relatively permeable soil layer that secured the edge of the GM liner and extended from the crest of the liner system side slope to beyond the liner system. The problem was resolved by installing additional gas extraction wells in the landfill. Without the measures taken to correct the problems at some of the other facilities, however, adverse environmental impacts could have eventually occurred at these facilities. Furthermore, the mere occurrence of problems, even in the absence of an environmental impact, undermines the confidence that the public holds in the waste management professional community.

F-4.2.2 Landfills Liner Systems

Potential environmental impacts of the problems that can affect landfill liner systems can be ranked as follows, from the most to the least serious:

- major liner breach;
- hole in GM or GCL;
- increased risk of leakage through existing holes;
- increased risk of hole in liner; and
- incorrect monitoring.

Table 4-1. Consequence and Prevention of Landfill Liner System Problems.

PROBLEM TYPE	POSSIBLE CONSEQUENCE	PROBLEM PREVENTION
1. LINER CONSTRUCTION		
• GM holes		
• Seams, Panels	Defect	Specifications, CQA, Ponding test, Leak survey, Conductive GM
• Connections	Defect	Connection design, CQA, Ponding test, Leak survey, Gas tracer test, Conductive GM
• GM condition		
• Wrinkles	Yield (Potential defect)	Installation temperature and method, CQA
• Scratches	Yield (Potential defect)	CQA
• GM uplift by wind	Rupture or yield	Design, Installation method, CQA
• CCL defects		
• Stones, Debris	High permeability, Damage to GM	Specifications, CQA
• Improper compaction	High permeability	Specifications, CQA
• Material in contact with GM		
• Overlying (LCRS or LDS material)	Puncture (Defect)	Cushion, CQA, Ponding test, Leak survey
• Overlying (Waste, no protection layer)	Damage to GM	Cushion, Soil protection layer, Operation QC
• Overlying (Placement of soil protection layer during operations)	Damage to GM	Cushion, CQA, Operation QC
• Underlying (Debris, Sandbags)	Damage to GM	CQA
• Liner system anchor trench/edge covered with a permeable material overlain by a less permeable material	Gas migration over and beyond liner system	Design, CQA
• Contamination of CCL in top liner	Incorrect interpretation of LDS chemistry	Runon control, Equipment maintenance, CQA
2. LINER DEGRADATION		
• GCL outdoor exposure	Hydrated and swollen (Low shear strength, May trigger instability, See "Stability" in 7)	Installation method, CQA
• GM stress cracking	Major liner breach	Resin selection, Protection layer, Minimize tension (Design, Installation temperature and method)
• GM outdoor exposure	Weakening, Embrittlement	GM selection, Protection layer
• CCL outdoor exposure	Cracking, Erosion	Protection layer
• GM/CCL composite outdoor exposure	CCL: Cracking	Protection layer
• Fire	GM: Major breach; CCL: Cracking	Operation
• Advance borehole through liner	Major liner breach	Design, Do not drill in vicinity of liner

Table 4-1. Consequence and Prevention of Landfill Liner System Problems (Continued).

PROBLEM TYPE	POSSIBLE CONSEQUENCE	PROBLEM PREVENTION
2. LINER DEGRADATION (Con.) • GM exposure to chemicals • CCL/GCL exposure to chemicals	Weakening, Permeation, Holes (Defect) Increased permeability	GM selection, Operation (Chemical control) Material selection, Operation (Chemical control)
3. LCRS AND LDS CONSTRUCTION • GT holes due to burning • Drainage layer not sealed in anchor trench • Pipe not connected at joints • Debris in pipe trenches • Sandbags in LCRS or LDS • GT needles	Clogging of drainage layers, pipes, or sumps (See “Clogging” in 5) Water intrusion in LCRS and LDS, Incorrect monitoring Excessive leachate head Potential clogging of pipes or sumps Excessive leachate head Damage to GM	Installation method, CQA Design, CQA CQA CQA CQA Manufacturer QC, GT plant inspection, CQA

4. LCRS AND LDS DEGRADATION
• Soil protection layer outdoor exposure
• GT outdoor exposure
• GN or GC compressive creep
• Pipe failure
  • Pipe crushing
  • Pipe weld separation
	Erosion
	Holes in GT (Clogging of LCRS material, See "Clogging" in 5)
	Excessive leachate head
	Excessive leachate head, Potential GM damage
	Excessive leachate head, Potential GM damage
		Design
		Protection layer
		Design, Testing
		Design, Pipe selection
		Construction method, CQA

5. LCRS AND LDS MALFUNCTION
• GT clogging
  • GT over drainage layer
  • GT around pipe
• Drainage layer clogging
• Pipe clogging
• Water expelled from CCL into LDS
• Leachate lateral seepage
	Delay in leachate collection, Excessive leachate head
	Excessive leachate head
	Excessive leachate head, Incorrect monitoring
	Excessive leachate head, Incorrect monitoring
	Incorrect monitoring
	Leachate migration through cover, Cover uplift
		GT selection, No GT if used to remove moving particles
		No GT around pipe
		Drainage material selection
		Pipe selection, Maintenance
		Design
		Design, Operation

Table 4.1. Consequence and Prevention of Landfill Liner System Problems (Continued).

PROBLEM TYPE	POSSIBLE CONSEQUENCE	PROBLEM PREVENTION
6. LCRS AND LDS OPERATION		
• Leachate generation greater than leachate removal/storage/treatment rate	Excessive leachate head	Design (e.g., temporary storm-water isolation berms)
• Equipment failure		
• Pumps, Cleanout	Excessive leachate head	Design (e.g., sump capacity) , Equipment selection
• Flowmeter, Check valve	Incorrect monitoring	Equipment selection
• Forget to open valves	Excessive leachate head	Operation QC, Simpler design
7. STABILITY (STATIC, HYDRODYNAMIC, SEISMIC)		
• Global (Foundation failure)	Major liner breach	Investigation, Design
• Waste/liner system slide	Major liner breach	Design, Testing, Waste placement sequence
• Liner system slide	Major liner breach	Design, Testing, Construction method
8. DISPLACEMENT		
• Foundation settlement or subsidence	GM: rupture or yield; GCL: open joints	Investigation, Design, Foundation improvement, GM selection
• Differential settlement at connections	GM: rupture or yield	Design, GM selection
• Liner system uplift		
• Water	GM: rupture or yield; GCL: open joints (May trigger instability, See “Stability” in 7)	Underdrain, Protection layer
• Gas	GM: rupture or yield; GCL: open joints (May trigger instability, See “Stability” in 7)	Gas collection system, Protection layer
• Wind	GM: rupture or yield	Design, Installation method, CQA
• Waste settlement		
• Downdrag force on liner	GM: rupture or yield; GCL: open joints	Liner system design, Waste placement (compaction)
• Downdrag force on manhole	Differential settlement (GM: rupture or yield; GCL: open joints)	Manhole foundation design, Manhole-liner connection design

Table 4-2. Consequence and Prevention of Landfill Cover System Problems.

PROBLEM TYPE	POSSIBLE CONSEQUENCE	PROBLEM PREVENTION
1. COVER SYSTEM CONSTRUCTION		
• Periphery sealing	Gas migration	Design
• Contaminated soil used in cover system	Contamination of runoff	Specifications, CQA
• GM holes		
• Seams, Panels	Defect	Specifications, CQA, Leak survey, Conductive GM
• Connections	Defect	Connection design, CQA, Leak survey, Gas tracer survey, Conductive GM
• GM condition		
• Wrinkles	Yield (Potential defect)	Installation temperature and method, CQA
• Scratches	Yield (Potential defect)	CQA
• GM uplift by wind	Rupture or yield	Design, Installation method, CQA
• CCL defects		
• Stones, Debris	High permeability, Damage to GM	Specifications, CQA
• Improper compaction	High permeability	Specifications, CQA
• Material in contact with GM		
• Overlying (Drainage layer material)	Puncture (Defect)	Cushion, CQA
• Underlying (Debris, Sandbags)	Damage to GM	CQA
• GT holes due to burning	Clogging of drainage layers (See “Clogging” in 2)	Installation method, CQA
• Sandbags in drainage layer	Excessive water head (May trigger instability, See “Stability" in 3)	CQA
• GT needles	Damage to GM	Manufacturer QC, GT plant inspection, CQA
COVER SYSTEM DEGRADATION		
• GCL outdoor exposure	Hydrated and swollen (Low shear strength, May trigger instability, See “Stability” in 3)	Installation method, CQA,
• GM stress cracking	Major breach	Resin selection, Protection layer, Minimize tension (Design, Installation temperature and method)
• GM outdoor exposure	Weakening, Embrittlement	GM selection, Protection layer
• GM/CCL composite outdoor exposure	CCL: Cracking	Protection layer
• Surface layer exposure	Erosion (May trigger uplift by gas, See “Displacement” in 4)	Design

Table 4.2. Consequence and Prevention of Landfill Cover System Problems (Continued).

PROBLEM TYPE	POSSIBLE CONSEQUENCE	PROBLEM PREVENTION
2. COVER SYSTEM DEGRADATION (Con.)		
• GT clogging		
◦ GT over drainage layer	Excessive water head (May trigger instability, See "Stability" in 3)	GT selection
◦ GT around pipe	Excessive water head (May trigger instability, See "Stability" in 3)	No GT around pipe
• Drainage layer clogging	Excessive water head (May trigger instability, See "Stability" in 3)	Drainage material selection
3. STABILITY (STATIC, HYDRODYNAMIC, SEISMIC)		
• Surface layer or protection layer slide or cracking of intermediate soil cover during earthquakes	Erosion (May trigger uplift by gas, See "Displacement" in 4); Outdoor exposure of underlying materials	Design, Testing, Construction method
• Cover system slide	Major barrier layer breach	Design, Testing, Construction method
4. DISPLACEMENT		
• Waste settlement or subsidence	GM: rupture or yield; GCL: open joints	Design, GM selection, Construction, Operation
• Differential settlement at connections	GM: rupture or yield	Design, GM selection
• Cover system uplift		
◦ Leachate	GM: yield (May trigger instability, See "Stability" in 3)	Underdrain, Protection layer
◦ Gas	GM: rupture or yield (May trigger instability, See "Stability" in 3)	Gas collection system, Protection layer
◦ Wind	GM: rupture or yield	Design, Installation method, CQA

Table 4-3. Consequence and Prevention of Impoundments Liner System Problems.

PROBLEM TYPE	POSSIBLE CONSEQUENCE	PROBLEM PREVENTION
1. LINER CONSTRUCTION		
• GM holes		
• Seams, Panels	Defect	Specifications, CQA, Ponding test, Leak survey, Conductive GM
• Connections	Defect	Connection design, CQA, Ponding test, Leak survey, Gas tracer test, Conductive GM
• GM condition		
• Wrinkles	Yield (Potential defect)	Installation temperature and method, CQA
• Scratches	Yield (Potential defect)	CQA
• GM uplift by wind	Rupture or yield	Design, Installation method, CQA
• CCL defects		
• Stones, Debris	High permeability, Damage to GM	Specifications, CQA
• Improper compaction	High permeability	Specifications, CQA
• Material in contact with GM		
• Overlying (Soil protection layer)	Damage to GM	Cushion, CQA
• Underlying (Debris, Sandbags)	Damage to GM	CQA
• Contamination of CCL in top liner	Incorrect interpretation of LDS chemistry	Runon control, Equipment maintenance, CQA
2. LINER DEGRADATION		
• GCL outdoor exposure	Hydrated and swollen (Low shear strength, May trigger instability, See "Stability" in 4)	Installation method, CQA
• GM stress cracking	Major liner breach	Resin selection, Protection layer, Minimize tension (Design, Installation temperature and method)
• GM outdoor exposure	Weakening, Embrittlement	GM selection, Protection layer
• CCL outdoor exposure	Cracking, Erosion	Protection layer
• GM/CCL composite outdoor exposure	CCL: Cracking	Protection layer
• Fire	GM: Major breach; CCL: Cracking	Operation
• GM exposure to chemicals	Weakening, Permeation, Holes (Defect)	GM selection, Operation (Chemical control)
• CCL/GCL exposure to chemicals	Increased permeability	Material selection, Operation (Chemical control)
• Wave action	GM: rupture or yield	Protection layer
• Drifting objects or ice	GM: puncture	Protection layer, Operation QC
• Dropped objects	GM: puncture	Protection layer, Operation QC

Table 4-3. Consequence and Prevention of Impoundments Liner System Problems (Continued).

PROBLEM TYPE	POSSIBLE CONSEQUENCE	PROBLEM PREVENTION
3. LDS		
• GT holes due to burning	Clogging of drainage layer, pipes, or sumps (See "Clogging" below)	Installation method, CQA
• Drainage layer not sealed in anchor trench	Water intrusion in LDS, Incorrect monitoring	Design, CQA
• Pipe not connected at joints	Excessive leachate head	CQA
• Debris in pipe trenches	Potential clogging of pipes or sump	CQA
• Sandbags in LDS	Excessive leachate head	CQA
• GT needles	Damage to GM	Manufacturer QC, GT plant inspection, CQA
• Soil protection layer outdoor exposure	Erosion	Design
• Clogging of GT around pipe	Excessive leachate head	No GT around pipe
• Drainage layer clogging	Excessive leachate head	Drainage material selection
• Pipe failure		
• Pipe crushing	Excessive leachate head, Potential GM damage	Pipe selection/Design
• Pipe weld separation	Excessive leachate head, Potential GM damage	Construction method, CQA
• Water expelled from CCL into LDS	Incorrect monitoring	Design
• Equipment failure		
• Pumps, Cleanout	Excessive leachate head	Design (e.g., sump capacity), Equipment selection
• Flowmeter, Check valve	Incorrect monitoring	Equipment selection
4. STABILITY AND DISPLACEMENTS		
• Global stability (Foundation failure)	Major liner breach	Investigation, Design
• Liner system slide	Major liner breach	Design, Testing, Construction method
• Foundation settlement or subsidence	GM: rupture or yield; GCL: open joints	Investigation, Design, Foundation improvement, GM selection
• Differential settlement at connections	GM: rupture or yield	Design, GM selection
• Liner system uplift		
• Water	GM: rupture or yield; GCL: open joints (May trigger instability, See "Stability" above)	Underdrain, Protection layer
• Wind	GM: rupture or yield	Design, Installation method, CQA

Each of these five categories of problems is discussed below. The categories are based on the assumption that the liners have a GM component. Gas migration from an active landfill without a cover system may have a major environmental impact, such as the groundwater contamination by VOCs that occurred at landfill L-8. This problem does not directly affect liner integrity and, therefore, does not fit within the above categories. The gas migration beyond the liner system is believed to be a rare occurrence related to placement of an asphalt layer over the edge of the liner system and inadequate landfill gas control. The problem is not discussed further in this section.

Major breaches in a landfill liner are likely to cause leakage into the ground that may have a significant impact on the environment. Operation of the landfill cell where such a breach occurs must generally be stopped. As indicated in Table F-4.1, major breaches in landfill liners can occur mostly as a result of liner system instability (i.e. slide). Major breaches in landfill liners can also occur as a result of relatively rare events, such as stress cracking, fire, and major mistakes (e.g., advancing a borehole through a liner).

GM or GCL holes can provide a pathway for leachate migration and, therefore, can have a detrimental impact on the environment. As shown by many studies, even properly installed GMs with adequate CQA programs will exhibit a small number of construction holes (i.e., 1 to 10 per hectare). These few holes are mostly due to imperfect seaming and are virtually impossible to eliminate. There have been no identified environmental impacts results from these holes. Nonetheless, every effort should be made to reduce the frequency of seam holes through rigorous control of the seaming and CQA processes. In addition, every effort should be made to eliminate other less frequent causes of GM holes. Many of the holes result from construction activities, and they should be detected during construction. As indicated in Table F-4.1, GM liner holes can occur in landfills due to a variety of causes or as a result of a variety of activities:

- manufacturing holes (a rare occurrence);
- installation holes;
- damage by materials placed in contact (or in the vicinity) of GMs;
- damage during operations (e.g., GM rupture by blade of bulldozer placing soil protection layer); and
- GM tear due to excessive stretching resulting from various types of displacements.

Holes in GCLs can occur due from displacements that result in open GCL joints and from wrinkles or protrusions that cause GCL thinning.

A number of other problems can increase the potential for leakage through the landfill liner. These include problems that result in: (i) an increase of the leachate head on top of the liner; (ii) a CCL constructed with a high hydraulic conductivity due to improper materials or compaction; or (iii) degradation of the GCL or CCL component of a composite liner due to outdoor exposure or exposure to chemicals. As shown in Table

F-4.1, leachate heads in landfills can increase due to problems related to LCRS or LDS installation, degradation, malfunction, and operation, such as:

- unconnected LCRS or LDS pipes;
- clogging of the LCRS or LDS components related to holes in GT filters, debris in the LCRS or LDS, and buildup of sediments, chemical precipitates, or biological mats in the LCRS or LDS;
- pipe failure;
- GN or GC compressive creep;
- failure of leachate pumps or sump liquid level indicator; and
- operation errors.

All problems that result in a weakening of the GM increase the risk of GM holes. As shown in Table F-4.1, these problems include:

- GM installation problems, such as wrinkles and scratches;
- action of materials in contact with the GM that cause scratches on the GM surface or cause the GM to yield;
- exposure of the GM to a variety of agents that weaken or embrittle it (e.g., ultraviolet light, chemicals); and
- displacements that cause yield of the GM.

Problems that result in incorrect monitoring of the leachate quantity removed from a landfill generally do not have a direct impact on the environment. However, it is important to have a properly functioning leachate measuring system, especially for LDSs. As discussed above, LDS flow rates have been used to evaluate whether a liner system is functioning adequately and if liner repairs are necessary. LDS flow chemistry has been used to evaluate whether primary liner leakage occurred.

The problems identified in this study fall in all five of the above categories. With the exception of the problems at landfills L-2, L-5, L-8, L-9, L-12, L-29, and L-36, the problems were detected and remedied shortly after they occurred and did not result in any identifiable environmental impact. Groundwater contamination was found at landfill L-8 and is being remedied. Leakage through the GM primary liner of landfills L-5 and L-12 and leakage at the LCRS pipe penetration of the GM primary liner of landfill L-9 were detected but not remedied. The desiccated CCL component of the single composite liner on the side slopes of landfill L-2 was also not remedied. As previously discussed, the potential for significant environmental impacts from the conditions at landfills L-2, L-5, L-9, and L-12 is expected to be negligible, especially given that landfills L-5, L-9, and L-12 have composite secondary liners. The separated LCRS pipes in landfills L-29 and L-36 were not repaired, but they only result in a small increase in the potential for liner leakage as a result of a localized increase in leachate head on the liners.

F-4.2.3 Cover Systems

Problems that affect cover systems are generally less likely to increase the potential for environmental impacts related to waste containment system integrity than problems that affect liner systems. From Table F-4.2, it appears that, with the exception the problem of using contaminated topsoil as the surface layer, the identified problems that affected landfill cover systems can generally be grouped into two categories based on their potential environmental impact: (i) problems that result in leakage, or increased risk of leakage, through the cover system; and (ii) problems that result in the release of landfill gas to the atmosphere or the ground. These two categories are discussed below. Using contaminated topsoil as the cover system surface layer may contaminate runoff. However, this is a rare occurrence. Though it is not listed in Table F-4.2, sediment and runoff loading from cover systems to offsite properties may also have a potential environmental impact. However, since the impacts from transported sediments and runoff do not affect waste containment system integrity, the focus of this appendix, these impacts are not discussed further.

Problems that result in leakage, or increased risk of leakage, through a landfill cover system are far less critical than problems that result in leakage, or increased risk of leakage, through a liner system for the following reasons: (i) most leakage through the cover system is absorbed by the underlying waste and controlled by the liner system; and (ii) the cover system is exposed and, thus, can be visually inspected for problems and maintained. Therefore, major cover system breaches, which occur mostly as a result of instability, would likely be detected and repaired soon after they occurred. Deformations of the cover system, which could result in holes in the cover system barrier layer, would also be apparent by visual inspection and could be repaired.

From the foregoing discussion it appears that the only impact to the environment of a landfill cover that needs to be considered is the release of gas. The release of gas to the environment is a serious problem, but it is relatively easy to solve. Typical measures are:

- use of a low-permeability barrier layer that includes a GM;
- proper sealing of the cover at its periphery; and
- use of an adequate gas extraction system.

The problems identified in this study fall in both of the above categories. In all cases, the problems were identified and remedied shortly after they occurred and did not result in any detectable environmental impact.

F-4.2.4 Impoundment Liner Systems

Potential environmental impacts of the problems that can affect impoundment liner systems can be ranked as follows, from the most to the least serious:

- major liner breach;
- hole in GM or GCL;
- increased risk of leakage through existing holes;
- increased risk of hole in liner; and
- incorrect monitoring.

Each of these five categories of problems is discussed below.

Major breaches in an impoundment liner system are likely to cause leakage into the ground that may have a significant impact on the environment. Operation of the impoundment where such a breach occurs must generally be stopped, and the impoundment must be emptied for repair. However, emptying an impoundment is relatively easy, as compared to removing waste from a landfill, and the leakage stops as soon as the impoundment is empty. As indicated in Table F-4.3, major breaches in impoundment liners can occur as a result of three principal causes: (i) stress cracking, which has occurred in the past in a number of impoundments, but occurs far less often since progress in GM resin selection has been made; (ii) liner system instability; and (iii) major operational mistakes (e.g., the dropping of a large heavy object on the liner). Major breaches in impoundment liners can also occur as a result of relatively rare events, such as fire.

GM or GCL holes can provide a pathway for leachate migration and, therefore, can have a detrimental impact on the environment. As shown by many studies, even properly installed GMs with adequate CQA programs will exhibit a small number of construction holes (i.e., 1 to 10 per hectare). These few holes are mostly due to imperfect seaming and are virtually impossible to eliminate. There have been no identified environmental impacts results from these holes. Nonetheless, every effort should be made to reduce the frequency of seam holes through rigorous control of the seaming and CQA processes. In addition, every effort should be made to eliminate other less frequent causes of GM holes. Many of the holes result from construction activities, and they should be detected during construction. For example, small leaks can be detected by performing a ponding test, which is relatively easy in the case of an impoundment. As indicated in Table F-4.3, GM liner holes can occur in impoundments due to a variety of causes or as a result of a variety of activities:

- manufacturing holes (a rare occurrence);
- installation holes;
- damage by materials placed in contact (or in the vicinity) of GMs; and
- GM tear due to excessive stretching resulting from various types of displacements.

Holes in GCLs can occur due from displacements that result in open GCL joints and from wrinkles or protrusions that cause GCL thinning.

A number of other problems can increase the potential for leakage through the impoundment liner. These are problems that result in: (i) a CCL constructed with a high hydraulic conductivity due to improper materials or compaction; (ii) degradation of the GCL or CCL component of a composite liner due to outdoor exposure or exposure to chemicals; and (iii) an increase of the leachate head on top of the secondary liner (i.e., problems related to the LDS).

All problems that result in a weakening of the GM increase the risk of GM holes. As shown in Table F-4.3, these problems include:

- GM installation problems, such as wrinkles and scratches;
- action of materials in contact with the GM that cause scratches on the GM surface or cause the GM to yield;
- exposure of the GM to a variety of agents that weaken or embrittle it; (e.g., ultraviolet light, chemicals); and
- displacements that cause yield of the GM.

Problems that result in incorrect monitoring of the liquids in the LDS generally do not have a direct impact on the environment. However, it is important to have a properly functioning liquids measuring system, especially for LDSs. LDS flow rates have been used to evaluate whether a liner system is functioning adequately and if liner repairs are necessary.

The problems identified in this study fall in all five of the above categories. In all cases, the problems were detected and remedied shortly after they occurred and did not result in any identifiable environmental impact.

F-4.3 Construction, Operation, and Maintenance Impacts

The main impacts of the problems in this investigation were interruption of waste containment system construction and operation and increased maintenance. The identified problems that most often disrupted construction and were required to be repaired before construction proceeded were related to:

- holes in GM liners and at pipe penetrations of liners;
- large wrinkles in HDPE GM liners;
- degradation of exposed geosynthetics;
- uplift of constructed liners by groundwater or infiltrating surface water; and
- erosion of unprotected soil layers (CCLs, sand drainage layers, soil protection layers).

Relative to problems that disrupt operation and may require waste relocation, problems that interfere with construction are relatively easy to remedy. In addition, the frequency of these problems can be reduced with good design, construction, and CQA. Holes in

GM liners and at connections can generally be located with leak location surveys, ponding tests, dye, or other nondestructive methods and then repaired. Large wrinkles in HDPE GM liners can be pulled out or cut out or the GM can be allowed to cool during the evening hours and contract. GM wrinkling can also be reduced through development of an adequate strategy for placing and covering the GM for each particular site. Exposed GTs, GCLs, or CCLs that degrade are replaced with new materials or, for CCLs, reconstructed. Eroded soil layers are replaced and/or regraded. Uplift of constructed liners is probably the most complex and time consuming problem because it requires that the water or gas uplifting the liner be controlled before a new liner is constructed.

The identified problems that most often disrupted facility operation and were required to be repaired before operation proceeded were related to:

- holes in GM liners and at pipe penetrations of liners;
- failure of liner system and cover system slopes; and
- clogging of GTs in LCRSs.

Problems that disrupt operation are generally more severe in terms of required repairs than those that interfere with construction and may require waste relocation. Consequently, problems that disrupt operation generally require more time to remedy than problems that are identified and repaired during construction. Problems that involve major breaches of liner systems or cover systems (e.g., failure of landfill liner system slopes) may require months to repair. However, the frequency of these problems can be reduced with good design, construction, CQA, and maintenance.

The identified problems that most often required maintenance were related to:

- erosion of soil layers (sand drainage layers, soil protection layers);
- repair of LCRS or LDS flow rate measuring and removal systems; and
- cracking of soil intermediate cover layers after earthquakes.

Problems that require maintenance may be more severe in terms of required repairs than those that interfere with construction, but are generally less severe than those that interfere with operation. In addition, problems that require maintenance are more likely to be reoccurring. The frequency of these problems, however, can be reduced with good design, construction, CQA, and maintenance.

F-4.4 Cost Impacts

The costs of remedying the problems can be significant. For the identified problems, the costs at the time the remedies were implemented ranged from less than $10,000 for repairs of GM holes identified by leak location surveys during construction to more than several million dollars for repair of a liner system slope failure that occurred during cell

operation. In general, problems that impacted operation were more expensive than those that impacted construction or maintenance. Problems that impacted operation were likely to cause the most damage, require relocation of waste, and result in suspension of waste placement in the containment system. However, certain problems that impact maintenance, such as erosion of soil layers, may ultimately be more costly than other problems if the problems that impact maintenance reoccur.

F-5 Conclusions

Based on the results of the investigation into waste containment system problems presented in Chapters F-2 to F-4 of this appendix, the following conclusions are drawn:

- This investigation identified 74 modern landfill and impoundment facilities (i.e., facilities designed with components substantially meeting current EPA regulations and constructed and operated to the U.S. state-of-practice) that had experienced a total of 85 waste containment system problems. This number of facilities is relatively small in comparison to the over 2,000 modern landfills and surface impoundments nationwide. The search for problem facilities for this study was not exhaustive, and it is certain that there are other facilities with problems similar to those described in this appendix.
- The investigation focused on landfill facilities: 94% of the identified problems occurred at landfills. Among the landfill problems, 70% were liner system related and 30% were cover system related. The ratio of liner system problems to cover system problems is probably exaggerated by the fact that a number of the facilities surveyed were active and did not have a cover system.
- Based on the waste containment system component or attribute criterion, the identified problems were classified as follows, in order of decreasing frequency:
  - cover system stability: 21%;
  - landfill liner construction: 17%;
  - landfill liner system stability: 14%;
  - landfill liner degradation: 8%;
  - landfill LCRS or LDS construction: 7%;
  - landfill LCRS or LDS degradation: 6%;
  - landfill LCRS or LDS malfunction: 5%;
  - landfill LCRS or LDS operation: 5%;
  - landfill liner system displacement: 5%;
  - impoundment liner construction: 4%;
  - cover system construction: 2%;
  - cover system degradation: 2%;
  - cover system displacement: 2%;
  - impoundment liner degradation: 1%; and
  - impoundment liner system stability: 1%.

- Using this criterion, these problems can also be grouped into the following general categories (Figure F-5.1):
  - liner system or cover system slope stability or displacement: 45%;
  - liner, LCRS or LDS, or cover system construction: 28%;
  - liner, LCRS or LDS, or cover system degradation: 17%; and
  - LCRS or LDS malfunction or operation: 10%.

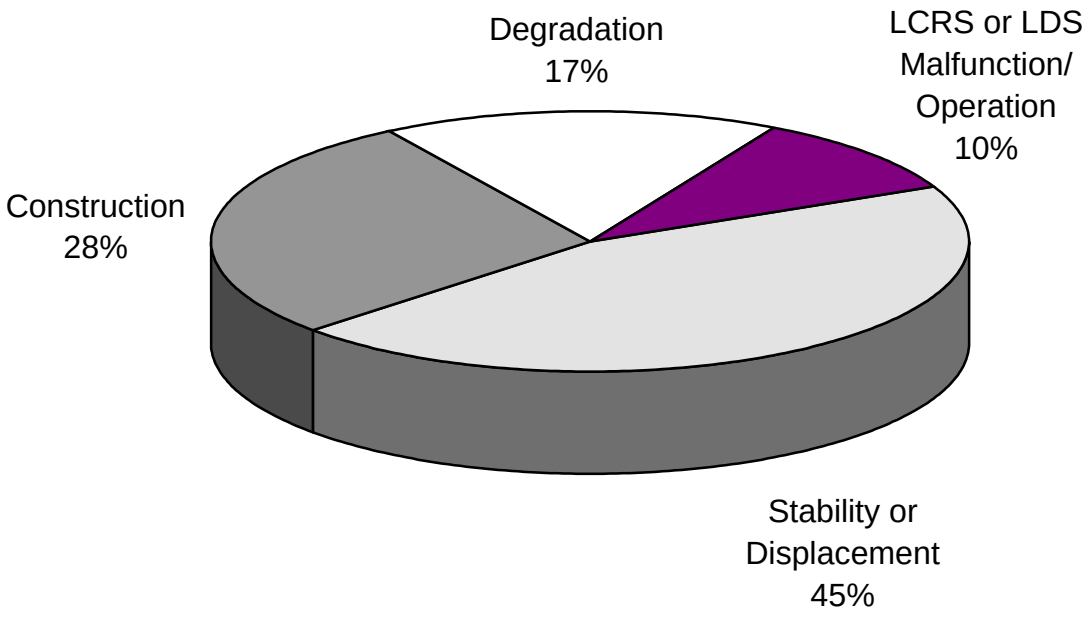

Figure F-5.1. General distribution of problems by waste containment system component or attribute criterion.

- Based on the principal human factor contributing to the problem criterion, the identified problems are classified as follows (Figure F-5.2):
  - design: 51%;
  - construction: 35%; and
  - operation: 14%.

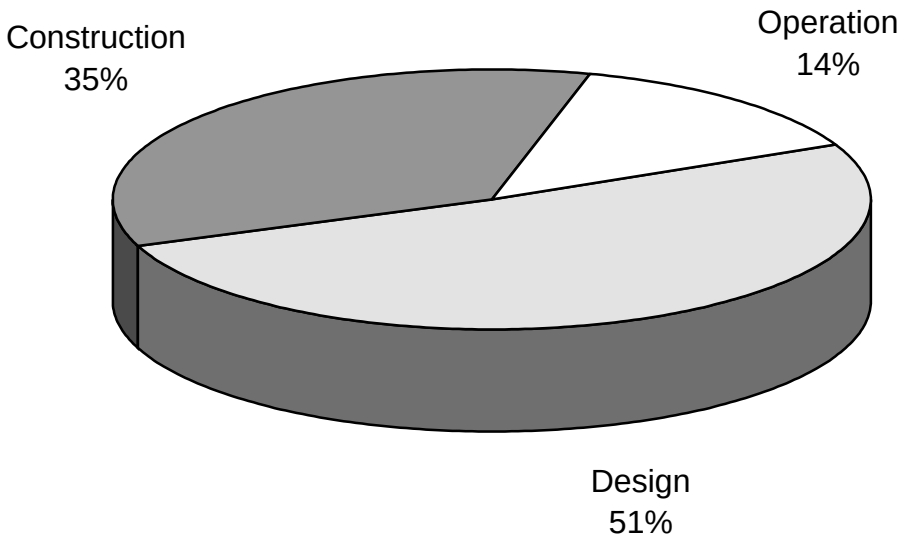

Figure F-5.2. Distribution of problems by principal human factor contributing to the problem criterion.

- Problems that occurred at two or more facilities and the number of facilities at which they occurred are as follows, listed in the order of presentation in Chapter F-3:
  - leakage through holes (construction- or operation-related) in an HDPE GM primary liner (5 landfills);
  - leakage through an HDPE GM primary liner or HDPE GM/CCL composite primary liner at the LCRS pipe penetration of the liner (3 landfills);
  - severe wrinkling of an HDPE GM liner during construction (2 landfills);
  - liner damage by fire (2 landfills);
  - liner damage during well installation (2 landfills);
  - rainwater entered the LDS through the anchor trench (2 landfills);
  - HDPE LCRS pipe was separated at joints (2 landfills);
  - erosion of the sand layer on the liner system side slopes (2 landfills);
  - degradation of polypropylene nonwoven GT filters due to outdoor exposure (2 landfills);
  - waste fines clogged the needlepunched nonwoven GT filter in the LCRS piping system (2 landfills);
  - clogging and other problems with the leachate pump or flow rate measuring system (3 landfills);
  - liner system slope failure due to static loading (10 landfills);
  - liner system damage due to earthquakes (2 landfills);
  - uplift of liner system geosynthetics by landfill gas after erosion of the overlying sand layer (2 landfills);
  - uplift of composite liner by surface-water infiltration during construction (2 landfills);

- cover system slope failure during construction (4 landfills);
- cover system slope failure after rainfall or a thaw (11 landfills);
- soil cover damage due to earthquakes (3 landfills); and
- leakage through holes in the HDPE GM primary liner or the HDPE GM component of the GM/CCL composite primary liner (2 impoundments).

- For problems that occurred at three or more facilities, the principal human factor contributing to the problem criterion, detection of the problem, causes of the problem, and remedy of the problem are described below:
  - *Leakage through holes in an HDPE GM primary liner* occurred at five landfills. In each case, the holes were attributed to construction or, at one landfill, possibly operation factors. At two of the landfills, leakage was first detected during electrical leak location surveys performed as part of CQA and by the relatively high LDS flow rates that occurred after rainwater ponded in a landfill. At the remaining three landfills, leakage was first detected during operation by the relatively high LDS flow rates and the color of and chemical constituents in the LDS liquid. The cause of the leakage was attributed to construction-related holes in the GM. However, at one landfill, where waste was placed directly on liner system geosynthetics (i.e., there is no soil protection layer), the GM may have been damaged during waste placement. The leakage problem was resolved at four landfills by repairing the GM holes; at the remaining landfill, the problem, clearly identified only after the cell had been covered with waste, was partially remedied by lowering the “pump on” liquid level in the LCRS sump.
  - *Leakage through an HDPE GM primary liner or HDPE GM/CCL composite primary liner at the LCRS pipe penetration of the liner* occurred at three landfills. This leakage was attributed to construction factors at two of the landfills and operation factors at the third landfill. At two of the landfills, leakage at the pipe penetration was detected during construction after rainwater ponded over the penetration and LDS flow rates increased. The cause of the leakage was construction defects in the pipe penetration; it is difficult to construct a defect-free pipe penetration, even when extra measures are taken to enhance the integrity of the connection. At the remaining landfill, leakage was detected during operation when the average LDS flow rate increased significantly. For this landfill, the pipe penetration was damaged during operation when a rubber-tired loader trafficked over it. The pipe penetrations were repaired; however, at one landfill where the problem was detected during construction, the repairs did not significantly decrease LDS flow rates; thus there must have existed a penetration defect that was not located.
  - *Clogging and other problems with the leachate pumps or flow rate measuring system* occurred at three landfills. These problems were attributed to design factors at one of the landfills and operation factors at the other two landfills. The problems, which were identified during routine operations, included: (i) clogging of the air lines and failure of the compressor for the control system; (ii) drift of the leachate level measurement system; (iii) drift of the “pump on” time setting; (iv) burn out of pumps due to control system problems; (v) clogging of pumps; (vi)

clogging of mechanical flowmeters; (vii) damage to electrical equipment by electrical storms; (viii) check valve failure; and (ix) inaccurate measurement of LCRS or LDS flow rates due to the above equipment problems. These problems appear to have been primarily caused by: (i) inadequate overall mechanical system design; (ii) using equipment that was less reliable than was needed; (iii) using equipment that was not compatible with the landfill leachate; and (iv) not performing equipment maintenance often enough. These problems were primarily remedied by equipment maintenance, repair, and replacement.

- *Liner system slope failure due to static loading* occurred at ten landfills. These problems were attributed to design factors at seven of the landfills and operation factors at the remaining three landfills. Slope failure occurred during construction at two of the landfills and during operation at the remaining eight landfills. The problem was detected by visual observation of mass movement of the liner system, cracking of soil layers near the slope crest, and tearing, tensioning, or wrinkling of geosynthetics. The primary causes of failure were: (i) using unconservative presumed values for the critical interface shear strength; (ii) not evaluating the critical condition for slope stability (e.g., liner system with waste at intermediate grades); (iii) not accounting for or underestimating seepage pressures; (vi) not accounting for moisture at the GM/CCL interface (which weakens the interface) due to spraying of the CCL with water and thermal effects; and (v) not maintaining the drainage layer outlets free of snow and ice, which can lead to increased seepage pressures. The slope failures were remedied by reconstructing the damaged liner systems, sometimes with different materials, and developing new construction procedures to reduce moisture at the GM/CCL interface.
- *Cover system slope failure during construction* occurred at four landfills. These problems were attributed to design factors at two of the landfills and construction factors at the remaining two landfills. Slope failure was detected by visual observation of mass movement of the cover system, cracking of soil layers near the slope crest, and wrinkling of geosynthetics at the toe of the cover system slope. The primary causes of failure were: (i) placing soil over the side slope geosynthetics from the top of the slope downward, rather from the toe of the slope upward; (ii) not considering the effects of variation in the tested geosynthetics, accuracy of test methods, and test conditions on the interface shear strength to use in design; and (iii) using unconservative presumed values for the critical interface shear strength. The problems were remedied by reconstructing the cover systems using different cover system materials that result in higher interface shear strengths and placing soil over side slope geosynthetics from the toe of the slope upward.
- *Cover system slope failure after rainfall or a thaw* occurred at eleven landfills. At all of these landfills, the failures were attributed to design factors. Slope failure occurred during the post-closure period and was detected by visual observation of mass movement of the cover system, cracking of soil layers near the slope crest, and wrinkling of geosynthetics at the toe of the cover system slope. The

primary causes of failure appeared to be: (i) not accounting for, or underestimating, seepage pressures; (ii) clogging of the drainage system, which can lead to increased seepage pressures; and (iii) not accounting for moisture at the GM/CCL interface (which weakens the interface) due to rain falling on the CCL surface during construction and freeze-thaw effects. In general, the problems were remedied by reconstructing the cover systems with new drainage systems or different materials.

  - *Soil cover damage due to earthquakes* occurred at three landfills. These problems all occurred during operation and were attributed to design factors. The damage, which was detected by visual inspection, consisted of surficial cracking of soil intermediate cover occurring primarily near locations with contrast in seismic response characteristics (e.g., top of waste by canyon walls). The damage was expected and dealt with as an operation issue through post-earthquake inspection and repair (i.e., regrading and revegetating the cracked soil layers).

- Almost all of the problems identified in this investigation were detected shortly after they occurred by visual observation or evaluation of monitoring data.
- Of the problems in this study for which the remedy was identified, six problems were not completely repaired because their environmental impacts were not expected to be significant and because: (i) the source of the problem could not be identified; (ii) the problem was not worsening; (iii) repair of liner systems or LCRS pipes after waste placement would be extremely difficult and expensive; and/or (iv) additional liner system damage could occur in any attempt to excavate the waste and repair the liner system.
- The problems only resulted in an identified environmental impact to groundwater or surface-water quality by leachate or landfill gas at one facility, landfill L-8. At this MSW landfill, groundwater impact by VOCs was attributed to gas migration through a relatively permeable soil layer that secured the edge of the GM liner and extended from the crest of the liner system side slope to beyond the liner system. The problem was resolved by installing additional gas extraction wells in the landfill. Without the measures taken to correct the problems at some of the other facilities, however, adverse environmental impacts could have eventually occurred at these facilities.
- The main impacts of the problems identified in this investigation are interruption of waste containment system construction and operation, increased maintenance, and increased costs.
- The identified problems that most often disrupted construction and were required to be repaired before construction proceeded were related to:
  - holes in GM liners and at pipe penetrations of liners;
  - large wrinkles in HDPE GM liners;
  - degradation of exposed geosynthetics;
  - uplift of constructed liners by groundwater or infiltrating surface water; and
  - erosion of unprotected soil layers (CCLs, sand drainage layers, soil protection layers).

- Problems that disrupt operation are generally more severe in terms of required repairs than those that interfere with construction and may require waste relocation. Consequently, problems that disrupt operation generally require more time to remedy than problems that are identified and repaired during construction. Problems that involve major breaches of liner systems or cover systems (e.g., failure of landfill liner system slopes) may require months to repair. The identified problems that most often disrupted operation and were required to be repaired before operation proceeded were related to:
  - holes in GM liners and at pipe penetrations of liners;
  - failure of one or more components of a liner system or cover system on landfill slopes; and
  - clogging of GTs in LCRSs.
- Problems that require maintenance may be more severe in terms of required repairs than those that interfere with construction, but are generally less severe than those that interfere with operation. In addition, problems that require maintenance are more likely to be reoccurring. The identified problems that most often required maintenance were related to:
  - erosion of soil layers (sand drainage layers, soil protection layers);
  - repair of LCRS or LDS flow rate measuring and removal systems; and
  - cracking of soil intermediate cover after earthquakes.
- The costs of remedying the problems can be significant. For the identified problems, the costs at the times the remedies were implemented ranged from less than $10,000 for repairs of GM holes identified by leak location surveys during construction to more than several million dollars for repair of a liner system slope failure that occurred during cell operation. In general, problems that impacted operation were more expensive than those that impacted construction or maintenance. However, certain problems that impact maintenance, such as erosion of soil layers, may ultimately be more costly than other problems if the problems that impact maintenance reoccur.
- Even though there was only evidence of environmental impact at one of the waste containment systems in this study, the landfill industry should do more to avoid future problems in order to: (i) reduce the potential risk of future environmental impact; (ii) reduce the potential health and safety risk to facility workers, visitors, and neighbors; (iii) increase public confidence in the performance of waste containment systems; (iv) decrease potential impacts to construction, operation, and maintenance; and (v) reduce costs associated with the investigation and repair of problems.
- Importantly, all of the design, construction, and operation problems identified in this investigation can be prevented using available design approaches, construction materials and procedures, and operation practices. It is the responsibility of all professionals involved in the design, construction, operation, and closure of waste containment systems to improve the practice of waste containment system engineering. Owners must be prepared to adequately fund the levels of design and CQA activity necessary to properly design and construct waste containment

systems. Design engineers must improve their practice to avoid the types of problems identified herein. Earthwork contractors, geosynthetics installers, and landfill operators all must be properly trained, supervised, and committed to the "quality goals" necessary to eliminate problems.

F-6 Recommendations to Reduce Incidence of Identified Problems

F-6.1 Introduction

This chapter of the appendix presents general and specific design, construction, and operation measures to reduce the incidence of the waste containment system problems described in this appendix. These measures are not new; they have been used extensively for other engineered structures, such as dams. The measures include widely available design approaches, construction procedures, and operation practices. Many recommendations for landfill liner systems also apply to cover systems and impoundment liner systems, and vice versa. Because of this, the recommendations are grouped to apply to following broad categories:

- general;
- liners and barriers;
- drainage systems;
- surface layers and protection layers;
- liner system and cover system stability; and
- liner system and cover system displacements.

Recommendations for each of these categories are presented below. The designations of the facilities with problems that lead to the recommendations are also listed for each recommendation except those in the general category. It should be noted that the problems and remedies are site specific.

F-6.2 General

General recommendations intended to reduce the occurrence of problems include:

- information dissemination (e.g., this appendix);
- training of design engineers to better understand waste containment system design fundamentals and to avoid the types of design problems described in this appendix;
- training of design engineers to be better prepared to develop waste containment system specifications and CQA plans that are complete and precise, that include the construction-related assumptions made during design, and that require construction and CQA procedures to identify and prevent the kinds of construction problems identified in this appendix;

- training of CQA personnel in standard CQA procedures to avoid the types of construction problems identified in this appendix; for engineering technicians, this training can be demonstrated through the National Institute for Training in Engineering Technologies (NICET) certification program;
- training of contractors to avoid the types of construction problems identified in this appendix;
- development of better construction materials, techniques, and quality control/quality assurance procedures to prevent the kinds of construction problems identified in this appendix;
- development of better operations manuals to describe and provide controls for procedures to be followed by landfill operations personnel;
- training of facility operators to better avoid the types of operation problems identified in this appendix;
- training of facility operators to better detect and quickly report problems occurring during operation; and
- performing periodic independent audits to verify that the specified operation procedures are being practiced.

F-6.3 Liners and Barriers

The following recommendations are made to reduce the frequency of liner and barrier-related problems.

Design

- Resin used to manufacture HDPE GM should be resistant to stress cracking. This is currently evaluated using the notched constant tensile load test (ASTM D 5397). This test should be required in project specifications. (S-1)
- Project specifications should require that both the inner and outer tracks of GM fusion seam samples taken for destructive testing meet the project seam requirements. Failure of one track is generally indicative of overall seaming problems and can results in increased stress concentrations in the adjacent track. In addition, testing both tracks may allow seaming problems to be identified and corrected quicker. (L-17, C-16)
- The potential for GM damage during placement of a soil layer over a GM can be reduced by protecting the GM. Measures for GM protection should be incorporated into the design and specifications. Measures include placing a protection layer (e.g., thick GT cushion or GC drainage layer) over the GM, using a greater initial lift thickness of soil above the GM, and using construction equipment with low ground pressure to place soils over the GM. The protection measures should be selected based on the characteristics of the soil to be placed (e.g., angularity, maximum particle size), the thickness of the soil layer, the type of equipment placing the soil, and whether CQA will be performed during soil placement. If the soil layer is placed during operation without CQA, extra GM protection is necessary. (L-3)

- GMs located in areas subjected to high static and dynamic stresses from construction equipment, such as beneath temporary access roads, require an even higher level of protection than GMs not subjected to high stresses. These protection measures should be incorporated into the design and specifications. (L-3)
- GM should also be protected during waste placement over the GM. Protection measures should be incorporated into the design and specifications. Measures include installing a protection layer (e.g., thick GT cushion, GC drainage layer, or soil layer) over the GM, using spotters to direct equipment operators during placement of waste over the GM, and placing only select waste over the GM. Protection measures should be selected with consideration of waste characteristics and the equipment placing the waste. (L-6)
- Sensitive areas of a liner system (e.g., at pipe penetrations) should be designed to be untraffickable by berms, bollards, or other means to decrease the potential for damage to these areas. (L-7)
- It is difficult to construct pipe penetrations of liners to be defect free. A method that was successful for one landfill (i.e., L-11) was to fill the space between the pipe and pipe boot with bentonite slurry. Until new methods for constructing better connections between GMs and ancillary structures have been developed and tested, designs without pipe penetrations (i.e., designs with internal sumps) should be preferred. (L-9, L-11)
- Internal sumps typically have sustained leachate heads at greater depths than other locations within the landfill and have seamed corners, which may contain holes. To decrease the rate of leakage through GM holes at sumps, the sump design should include additional liner components, such as a GCL, beneath the GM liner in the sump area, even if the GM is already underlain by a CCL. A design with a prefabricated GM sump may also be considered. Bonaparte (1995) provides additional discussion of this design approach. (L-5)
- The potential for landfill gas to migrate over the geosynthetics at the edge of the liner system must be considered in design. The potential for gas migration into the subsurface can be reduced by collecting gas generated in the landfill, using low-permeability soils over the edge of the liner system, and modifying the edge of the liner system so that the liner extends back up to the ground surface (like a reverse anchor trench). (L-8)

Construction

- Construction equipment should be inspected for fuel and oil leaks, and those leaks should be repaired prior to using the equipment in liner system construction to avoid liner and LDS contamination. Runon should be controlled so that it does not contact, and potentially contaminate, the liner and LDS during construction. (L-43)
- Liners and barriers should be constructed in manageable increments that ensure protection of the liner and barrier materials under seasonal weather changes. (L-19)
- CCLs should not be constructed with materials containing construction debris or large particles, even if prior to GM installation the CCL has a smooth surface and

meets the hydraulic conductivity criterion. The debris may adversely impact the hydraulic conductivity of the CCL and/or damage an overlying GM. (L-11)

- CCLs should not be left unprotected for an extended period of time. They can desiccate and crack due to evaporation of water in the CCL, degrade when exposed to freezing and thawing actions, and be eroded by wind and water. (L-11)
- Prior to deploying a GM, all extraneous objects (e.g., tools, sand bags) should be removed from the surface on which the GM is to be placed to avoid GM damage and, for composite liners, promote good contact between the GM and underlying CCL or GCL. (L-15)
- HDPE GMs should be installed so that they are essentially stress-free at their lowest expected temperatures. GMs contract with decreasing temperature. If there is not sufficient slack in the GMs at higher temperatures they may yield and rupture at lower temperatures. (S-1, S-3)
- GMs should be covered with thermal insulation layers at very low temperatures (e.g., -20°C for HDPE GMs or 0°C for PVC GMs) since GM strain at break decreases with decreasing temperature. The effect of temperature on GM strain at break depends on the type of GM polymer. (C-13, S-1)
- The leading edge of an uncovered GM should be secured to prevent wind from flowing beneath the GM and uplifting it. This is typically accomplished by seaming adjacent panels of GM shortly after deployment and placing a row of adjacent sandbags along the edge of the GM. (L-19)
- If sand bags are used to secure GM panels until the panels are seamed, the installer should ensure that the sandbags, and all other extraneous objects, are not trapped beneath the GM after seaming to avoid GM damage and, for composite liners, promote good contact between the GM and underlying CCL or GCL. (L-15)
- For HDPE GMs, fusion seams are preferred over extrusion seams because fusion seams have higher seam integrity and lower stress concentrations at seams. Extrusion fillet seams are preferred over extrusion flat seams because fillet seams have lower stress concentrations at seams. Extrusion seams should be minimized in the field by using prefabricated pipe boots, careful GM installation, etc. (S-1)
- HDPE GM must be thoroughly cleaned along a seam path before the seam is constructed since dirt in the seam adversely impacts seam integrity. To minimize the potential for dirt to accumulate along a seam path, GM should be seamed shortly after deployment. A temporary plastic film may also be placed on the GM edges at the factory and removed from the GM just prior to seaming. (C-16)
- In general, holes in HDPE GM seams should not be repaired by reseaming. This reheating of seams can embrittle the HDPE at the repair and make it more susceptible to stress cracking. (S-1)
- To the extent practicable, holes in GM liners installed over GCLs should be repaired as soon as possible to avoid swelling of the GCL in case of hydration. GCL swelling results in a decrease in GCL shear strength and may impact slope stability. Holes located in areas where rainwater may pond should be patched first. The patches should be sealed with a permanent seam and not only tack welded. (L-20)

- When a GM is placed over a GCL, the GM should be covered with soils as soon as possible to minimize swelling of the GCL in case of hydration. GCL swelling results in a decrease in GCL shear strength and may impact slope stability. (L-20)
- Connections between GMs and ancillary structures should be carefully constructed and inspected to decrease the potential for construction-related GM holes. (L-9, L-11)
- To decrease the potential for construction-related GM holes in sumps, the GM panel layout should be configured to minimize seams in sumps or prefabricated sumps should be used. (L-5)
- With respect to the potential for leakage, pipe penetrations are generally the most critical locations in landfills without internal sumps. If pipe penetrations are used, they should be carefully constructed and inspected.
- Sumps and pipe penetrations of liners should be leak tested by ponding tests, leak location surveys, gas tracer tests, or pressure tests of double pipe boots as part of liner system CQA. Leak testing of the liner system on the facility base (where leachate heads are the highest) or of the entire liner system may also be considered. Identified holes should be repaired. (L-1, L-3, L-6, L-9, L-11)
- The entire installed GM should be inspected for damage and any damage should be repaired prior to placement of overlying materials. (L-3)
- GM should be covered with a soil layer as soon as practicable after installation, but not during the hottest part of the day if the GM is significantly wrinkled, to reduce GM wrinkles, prevent GM uplift by wind, and protect the GM from damage. (L-19, L-29, L-43, S-3)
- Prior to placing soil over a GM, the GM should be inspected for wrinkles. Excessive GM wrinkles and wrinkles that may fold over should be removed by waiting to backfill until the GM cools and contracts during the cooler nighttime and early morning hours, pulling the wrinkles out, or cutting the wrinkles out. The latter method is less desirable than the former methods because it requires intact GM to be cut, and it results in more GM seaming and testing. (L-19, L-29, S-3)
- On long side slopes, it may be preferable to use textured GM rather than smooth GM to decrease the size of GM wrinkles that develop, especially near the slope toe. Interestingly, Giroud (1994b) has shown analytically that GM wrinkles are shorter and spaced closer together when the shear strength between the GM and the underlying material is increased. Therefore, based on analysis, the use of textured, rather than smooth, GM decreases the risk that large wrinkles will form. (L-29)
- Composite liners and barriers constructed with a CCL should be covered with an insulation layer as soon as practicable to prevent CCL desiccation related to heating or freeze-thaw action. (L-2, L-43)

Operation

- Landfill operations manuals should include limitations on the types of equipment that may traffic over the liner system before the first lift of waste is placed to prevent liner

system damage. These limitations are enforced during construction when CQA is implemented; they should also be applied during operation. (L-7)

- Landfill operations personnel should be aware of sensitive areas of a liner system, such as at pipe penetrations or sumps, and should protect these areas from damage. Sensitive areas can be identified with cones, flags, or other markers. They can also be isolated from traffic by berms, bollards, or other means. (L-7)
- Landfills should be operated to minimize the potential for waste fires. Measures to be taken could include not depositing loads of hot waste in a landfill and covering waste with a soil cover to decrease waste access to oxygen. (L-4)
- Care should be taken to not damage the liner system components when drilling into landfilled waste. Settlement of the waste surface must be taken into account when selecting the depth of drilling, and boreholes should not extend close (e.g., within 1 m) to the liner. Also, the limits of waste containment systems should be identified with markers or other means to reduce the potential for liner system or cover system damage by drilling or other invasive activities. (L-12, L-44)

F-6.4 Drainage Systems

The following recommendations are made to reduce the frequency of drainage system-related problems.

Design

- Adjacent materials conveying water should be designed to decrease the clogging potential of the downgradient material using filter criteria calculations and/or laboratory testing. (C-7, C-10, C-11, C-19, C-21)
- If gap-graded soils are used as drainage materials, the effect of particle migration should be evaluated during design using filter criteria calculations and/or laboratory testing. In fact, the effect of particle migration from all granular drainage materials should be evaluated during design, at least qualitatively, since all coarse granular drainage materials have some fines. (C-7)
- Perforated pipes bedded in gravel should not be wrapped with a GT because the GT is useless, and, in some cases, even detrimental because the GT in this location is prone to clogging. This has been discussed by Koerner et al. (1993) and demonstrated by several case histories presented in their paper. Instead, the design should include a GT between the gravel and the surrounding soil or, possibly, no GT. (L-22, C-20)
- Geosynthetic anchor trenches should be backfilled with low-permeability soil and the soil should be well compacted to reduce the potential for water for infiltrate into the trenches and flow into LCRSs or LDSs. If this is not practicable, the anchor trenches should be designed to drain freely and/or covered with a barrier, such as a GM. In addition, the ground surface should be graded away from the trenches to reduce runon from infiltrating into the trenches. (L-10, L-16)

- Project specifications for needlepunched nonwoven GTs should require that the GTs be needle-free and should require a certification from the manufacturer attesting to this. Needles, if present, may damage a nearby GM. (L-28)
- The CQA Plan should require that deployed GTs near GMs be inspected for needles before the GTs are covered with overlying materials. If needles are found, the GT should be rejected. (L-28)
- If a GT is to be exposed to the environment for an extended time period after installation, the potential for degradation of the GT should be evaluated under all the anticipated environmental conditions. EPA recommends that the effect of ultraviolet light on GT properties be evaluated using ASTM D 4355 (Daniel and Koerner, 1993). The test is typically run for 500 hours; however, it can be run for longer time periods to meet project-specific conditions. In any case, prior to covering the GT, the condition of samples of the exposed GT taken from the field should be evaluated by laboratory testing to verify that the exposed GT is still satisfactory. (L-13, L-18)
- If test results indicate that the GT will not have the required properties (typically a specified strength retention) after exposure, the GT should be protected with a sacrificial opaque waterproof plastic tarp, soil layer, or other means. Tisinger et al. (1993) suggest that this may be the best strategy since a heavy degraded GT that meets the specifications is more sensitive to stress concentrations than a new lighter GT that meets the same specifications. (L-13, L-18)
- When the waste in a containment system contains some fine particles that may migrate to the LCRS, the potential for LCRS clogging may be reduced by allowing those fine particles to pass though the LCRS to the leachate collection pipes, which can subsequently be cleaned. The fine particles will pass more easily through the LCRS if no GTs are used in the LCRS or if the LCRS contains relatively thin open nonwoven GTs rather than thicker nonwoven GTs with a smaller apparent opening size. Note that the above does not apply to an LCRS with only a GN drainage layer. Though a GN drainage layer has a high transmissivity, it is thin and is, therefore, generally more susceptible to clogging by sedimentation than a granular drainage layer. (L-36)

Construction

- The drainage system should be kept free of debris that may potentially impede the flow of liquid. In general, all sandbags should be removed from the drainage system. However, if the sand in the bags meets the project specifications for the overlying drainage layer material, the bags can be cut and removed and the sand left in place. (L-15)
- GTs and GCs should be covered as soon as possible after installation to protect them from the environment (e.g., ultraviolet light, water, high temperature, animals). (L-13, L-18)
- The CQA consultant should verify that all connections required for adjacent drainage system pipes have been made. When pipe is connected by butt fusion seaming, the seam should be inspected for defects. (L-32, L-33)

- Care should be taken to not damage drainage system pipes during construction. The contractor should maintain sufficient soil cover between construction equipment and the pipes during construction. Equipment operators should be aware of pipe locations, since pipes can be crushed by trafficking equipment. Also, soil around pipes should be compacted using hand operated or walk-behind compaction equipment. (L-30)
- After construction of a cell with an external sump, the pipe from the cell to the sump should be inspected to verify that the pipe is functioning as designed. The inspection may be performed by surveying the pipe with a video camera, pulling a mandrel through the pipe, flushing the pipe with water, or other means. (L-30)

Operation

- Leachate may seep from landfill side slopes if the leachate can perch on layers of less permeable materials (e.g., daily and intermediate cover materials) within the waste or drain from layers of more permeable materials (e.g., tires) within the waste that are located relatively close to the side slopes. The potential for seepage can be decreased by: (i) not placing layers of the more permeable materials near the side slopes; (ii) sloping layers of the less and more permeable materials away from the side slopes; (iii) distributing the more permeable materials throughout the waste; (iv) constructing leachate chimney drains to the LCRS around these layers; (v) removing perched leachate from wells installed to these layers; and (vi) using alternate daily covers (e.g., foams, tarps) that do not results in layers of less permeable materials in the waste. (L-37)
- Drainage system pipes should be maintained by cleaning the pipes at least annually and more frequently, if warranted. (L-12, L-36)
- Landfills with external sumps may also include riser pipes at the low point of LCRSs as a precautionary measure to allow for leachate removal from the landfill, if necessary. (L-12)
- Leachate flow measurement systems should be calibrated and adjusted as needed at least annually to ensure that the quantities measured are accurate. (L-5, L-34)
- Due to the potential for problems in automated leachate metering and pumping equipment, landfill operations plans should include a verification and contingency method for estimating the quantities of liquid removed from the LCRS and LDS. (L-5, L-34)
- Leachate sump pumps should be self priming so the pumps will not become airlocked and shut down if air is pulled into the pumps. (L-34)
- Leachate sump pumps should be selected to be compatible with sump geometries and anticipated leachate recharge rates so pump cycles are appropriate (e.g., not so short that the pumps turn on and off too frequently and burn out prematurely). (L-35)
- The “pump on” levels in internal sumps should be kept as low as practicable to reduce leakage if there are holes in the GM liner in the sump, especially if the GM is not underlain by a GCL. It is recognized, however, that "pump on" liquid levels in

internal sumps may need to be larger than 0.3 m to achieve efficient sump pump operation. (L-5)

- The potential for clogging of water-level indicators, pumps, and flowmeters must be considered when selecting the types of equipment to use at a facility. For example, the impeller and filter screen in the mechanical flowmeters initially used at landfill L-5 frequently became clogged. After the mechanical flowmeters were replaced with venturi flowmeters, clogging was not a problem. (L-5, L-35)
- Outlets of cover system drainage layers should be kept free of snow and ice so that these layers can drain freely. (L-42)

F-6.5 Surface and Protection Layers

The following recommendations are made to reduce the frequency of surface layer and protection layer-related problems.

Design

- Erosion of soil protection layers on liner system side slopes should be anticipated and dealt with in design. The potential for erosion can be reduced by grading the liner system to avoid concentrated runoff and using a relatively permeable soil in the protection layer. In areas where the potential for erosion is relatively high, erosion control structures (e.g., runoff diversion berms, silt fence) can be used to reduce the need for intensive maintenance of soil protection layers. Protection layers can also be covered with a tarp or temporary erosion control mat. (L-9, L-11)
- When a liner system is constructed on top of an existing landfill (vertical expansion), an exposed GM liner can be uplifted by gases from the underlying landfill. Therefore, in the case of a vertical expansion, unless gases from the underlying landfill are well controlled, GMs must be covered by a soil layer to prevent GM uplift and precautions must be taken to prevent erosion of this soil. (L-9, L-11)
- Better methods for protecting exposed soil layers on liner system side slopes from erosion or alternatives to these soil layers (e.g., sand filled mats, Styrofoam sheets) are needed. A new geosynthetic that will insulate the underlying liner materials could be developed for this purpose. (L-9)
- Post-construction plans should be developed for portions of landfills that may sit idle for an extended period of time. The plans should include procedures describing how the liner system should be maintained prior to operation. (L-9)
- For liner systems where soil protection layers are placed incrementally during landfill operation, a geosynthetic cushion (supercushion) better than the usual thick nonwoven GT needs to be developed to protect the liner system during soil placement.
- Erosion of surface layers on cover system side slopes should be anticipated and dealt with in design. In areas where the potential for erosion is relatively high, erosion control measures (e.g., runoff diversion berms, silt fence, turf reinforcement

and revegetation mat) can be specified to reduce the need for intensive maintenance of soil layers. However, the erosion control measures require maintenance (e.g., periodic removal of soil retained by silt fence). (C-1, C-12)
- The length of cover system slopes between ditches or swales where runoff is collected should be selected to limit erosion to acceptable amounts (e.g., 5 tonnes/ha/yr). At a minimum, the potential for erosion should be evaluated using the universal soil loss equation. As described by EPA (1994), cover system slopes may need to be 4H:1V or less and intercepted by swales at 6-m vertical intervals to meet acceptable erosion levels. (C-12)
- Design flow velocities in drainage channels should be calculated so the appropriate channel lining can be selected. (C-1)

Construction

- Though it may be less costly for the owner to construct several landfill cells at once, this can leave new cells exposed to the environment for a significant time period. These cells will experience more erosion than cells filled sooner and will have more opportunity for liner damage. Additionally, every time an eroded soil layer is pushed back up the side slopes there is an opportunity for the underlying liner system materials to be damaged by construction equipment. (L-9)

F-6.6 Liner System and Cover System Stability

Design

- The stability of liner system and cover system slopes should always be evaluated using rigorous slope stability analysis methods that consider actual shear strengths of materials, anticipated seepage pressures, and anticipated loadings. (L-21, L-24, L-25, L-38 to L-42, L-46, C-3 to C-11, C-17 to C-20, S-2)
- The majority of the slides described herein occurred along geosynthetic/ geosynthetic interfaces. For a number of these cases, the interface shear strengths were estimated on the basis of published tested data. This approach should be avoided because there may be significant differences in interface shear strengths between similar materials from different manufacturers and even identical materials in different production lots from the same manufacturer. Only a small error in the estimated interface shear strength may cause slope instability. Because of this, geosynthetic interface shear strengths should not be estimated, they should be measured. Additionally, as more geosynthetics are available on the market, the probability increases that there will be significant differences in properties between geosynthetics that appear to be similar. (L-21, L-24, L-25, L-38 to L-42, L-46, C-4 to C-11, C-17)
- Interface shear strength test conditions (moisture, stresses, displacement rate, and displacement magnitude) should be representative of field conditions. (L-25)

- The effects of variation in the tested geosynthetics, accuracy of test methods, and test conditions must be considered when selecting the interface shear strength to use in design. (L-25, C-9)
- Freeze-thaw of CCLs can have a significantly detrimental impact on GM/CCL interface shear strength and should be considered when selecting the interface shear strength to use in slope stability analyses. However, freeze-thaw effects on interface strength should not actually be a design consideration, since CCLs should be protected from freezing in the first place. (C-13)
- The effect of construction on moisture conditions at the GM/CCL interface should be considered when developing the specification for CCL construction and selecting the strength of liner system interfaces for slope stability analyses. The CCL construction specification should generally include limitations on maximum compacted moisture content, restrictions on applying supplemental moisture, and requirements for covering the CCL and overlying GM as soon as practical to minimize moisture migration to the GM/CCL interface. If a CCL on a slope becomes desiccated, it should be reworked and not just moistened. (L-21, L-25, C-13)
- Cover systems incorporating a low-permeability barrier layer should include a drainage layer above the barrier when the cover system side slopes are steeper than 5H:1V (EPA, 1994). The purpose of this drainage layer is to prevent the buildup of seepage pressures in the cover system soil layer(s) overlying the barrier layer. (C-4)
- When liner systems or cover systems are constructed over wastes, the potential for the wastes to generate gases that uplifts the liners or barriers must be considered. The gas pressures decrease the shear strength along the bottom interface of the uplifted layer and may lead to slope instability. Gas collection systems, therefore, may be required to prevent the buildup of gas pressures. (L-9, L-11)
- Cover system drainage layers should be designed to handle the total anticipated flow to the drainage layer calculated using a water balance or other appropriate analysis (e.g., Giroud and Houlihan, 1995). Soong and Koerner (1997) recommend using a short-duration intensive storm in the water balance and do not recommend the EPA Hydrologic Evaluation of Landfill Performance (HELP) computer model for this purpose. The drainage layer flow rates output from the HELP model are an average for a 24-hour period and may be much less than the peak flow rates calculated using other methods if the precipitation data used in the HELP model are not carefully selected. (C-4, C-5, C-12, C-17 to C-19)
- Water collected in the drainage layer must be allowed to outlet to prevent the buildup of seepage pressures. (L-42)
- Containment systems should be designed to limit seismic displacements to tolerable amounts. To do this, designs may incorporate predetermined slip surfaces to confine movements to locations where they will cause the least damage (i.e., above the GM liner) and inverted liner system keyways to provide more resistance to movement. For example, a GM with a smooth top surface and a textured bottom

surface could be used in certain liner systems to create a predetermined slip surface above the GM. (L-26, L-27)
- Liner system anchor trenches should be designed to secure geosynthetics during construction, but release the geosynthetics before they are damaged during earthquakes. An alternative is to unanchor the liner system after construction and secure it on a bench with an overlying soil layer. (L-26)
- Stress concentrations at or near the liner system side slope crest should be avoided. Areas with stress concentrations are more problematic when subjected to seismic loading. In particular, GM seams should generally not be sampled near the slope crest. (L-26)

Construction

- Soils should be placed over geosynthetics from the toe of slope upward to avoid tensioning the geosynthetics. Methods of soil placement that are not toe to top should be pre-approved by the engineer who analyzed the stability. (C-3, C-14)
- Geosynthetic reinforcement should be anchored prior to placing the soil layer to be reinforced. (C-14)

Operation

- Outlets of drainage layers should be kept free of snow and ice so these layers can drain freely and prevent the buildup of seepage pressures. (L-42)
- Soils or waste should be placed over geosynthetics from the toe of slope upward to avoid tensioning the geosynthetics. Methods of placement that are not toe to top should be pre-approved by the engineer who analyzed the stability. (S-2)
- Surficial cracking of soil cover layers during seismic loading, especially near locations with contrast in seismic response characteristics (e.g., top of waste by rock canyon walls), should be anticipated and dealt with as an operation issue through post-earthquake inspection and repair. (L-26, L-27, C-21 to C-23)
- Proposed changes to the landfill filling sequence should be reviewed by the design engineer to ensure that these changes will not adversely impact slope stability. (L-24)
- Soil layers anchoring geosynthetics should be maintained during landfill construction and operation. (L-45)

F-6.7 Liner System and Cover System Displacements

The following recommendations are made to reduce the frequency of liner system and cover system displacement-related problems.

Design

- When liner systems or cover systems are constructed over existing wastes, the potential for the wastes to generate gases must be considered. The gases may uplift GMs, causing excessive stresses in the GMs and may impact slope stability. Some landfills may be generating little or no gas at the time of construction and may not need a gas collection system. Other landfills may be generating significant quantities of gas and may require a gas collection system beneath the entire liner system. (L-9, L-11)
- Surface-water runoff should be managed to reduce foundation uplift problems during and after construction. Temporary and permanent surface-water diversion structures located near a cell may need to be lined to reduce infiltration, especially if the structures are located on relatively permeable soils and convey relatively large amounts of water. Runoff should not be allowed to pond near the cell, where it can infiltrate into the cell. (L-25, L-31)
- Liner systems and cover systems constructed over compressible, low shear strength waste materials should be designed to accommodate the anticipated settlements. When GCL is used, seam overlaps should be wider than normal. (C-15)
- Gas extraction well boots should be designed to accommodate the anticipated landfill settlements. (C-12)

Construction

- Cover systems with soil layers placed over compressible, low shear strength waste should use lightweight construction equipment and have good control of the thickness of soil placed over the waste so as not to cause bearing capacity failure of the waste and excessive displacement of the cover system. (C-15)

F-7 References

Adams, F.T., Overmann, L.K., and Cotton, R.L. (1997), "Evaluation and Remediation of a Fire Damaged Geosynthetic Liner System", *Proceedings of Geosynthetics '97*, Long Beach, California, Vol. 1, pp. 379-392.

Anderson, K.A., "Leachate Collection Management at a Hazardous Waste Landfill", *Hydrological Science and Technology*, Vol. 9, No. 1-4, 1993, pp. 30-53.

Anderson, R.L., "Earthquake Related Damage and Landfill Performance", *Earthquake Design and Performance of Solid Waste Landfills*, Yegian, M.K. and Liam Finn, W.D., eds., ASCE Geotechnical Special Publication No. 54, 1995, pp. 1-16.

Augello, A.J., Matasovic, N., Bray, J.D., Kavazanjian, E., Seed, R.B., "Evaluation of Solid Waste Landfill Performance During the Northridge Earthquake", *Earthquake Design and Performance of Solid Waste Landfills*, Yegian, M.K. and Liam Finn, W.D., eds., ASCE Geotechnical Special Publication No. 54, 1995, pp. 17-50.

Badu-Tweneboah, K., Williams, N.D., and Haubeil, D.W., “Assessment of a PVC Geomembrane Used in a Landfill Cover System”, *Proceeding of Fifth International Conference on Geotextiles, Geomembranes and Related Products*, Singapore, 1994, pp. 1029-1032.

Basnett, C.R. and Bruner, R.J., “Clay Desiccation of a Single-Composite Liner System”, *Proceedings of Geosynthetics ’93*, Vancouver, British Columbia, 1993, Vol. 3, pp. 1329-1340.

Bass, J.M., “*Avoiding Failure of Leachate Collection and Cap Drainage Layers*”, EPA/600/2-86/058, EPA Hazardous Waste Engineering Research Laboratory, Cincinnati, Ohio, 1986, 142 p.

Bonaparte, R., "Long-Term Performance of Landfills"' *Proceedings of the ASCE Specialty Conference Geoenvironment 2000*, ASCE Geotechnical Special Publication No. 46, 1995, Vol. 1, pp. 415-553.

Bonaparte, R. and Gross, B.A., “*LDCRS Flow Rates from Double-Lined Landfills and Surface Impoundments*”, EPA/600/SR-93/070, EPA Risk Reduction Research Laboratory, Cincinnati, Ohio, 1993, 65 p.

Bonaparte, R., Othman, M.A., Rad, N.R., Swan, R.H., and Vander Linde, D.L., “Evaluation of Various Aspects of GCL Performance”, Appendix F in *Report of 1995 Workshop on Geosynthetic Clay Liners,* Daniel, D.E. and Scranton, H.B., Editors, EPA National Risk Management Resource Laboratory, Cincinnati, Ohio, EPA/600/R-96/149, 1996, pp. F-1-F-34.

Boschuk, J. Jr., “Landfill Covers An Engineering Perspective”, *Geotechnical Fabrics Report*, IFAI, Mar 1991, pp. 23-34.

Byrne, R.J., Kendall, J., and Brown, S., “Cause and Mechanism of Failure Kettleman Hills Landfill B-19, Phase 1A”, *Stability and Performance of Slopes and Embankments - II*, ASCE Geotechnical Special Publication No. 31, 1992, pp. 1188-1215.

Calabria, C.R. and Peggs, I.D., “Investigation of Geomembrane Seam Failures: Landfill Cover”, *Proceedings of the 10th GRI Conference Field Performance of Geosynthetics and Geosynthetic Related Systems*, Geosynthetic Research Institute, Philadelphia, Pennsylvania, 1996, pp. 234-257.

Chang, S., Bray, J.D., and Seed, R.B., “Engineering Implications of Ground Motions from Northridge Earthquake”, *Bulletin of the Seismological Society of America*, Vol. 86, No. 1, Part B Supplement, 1996, pp. S270-S288.

Daniel, D.E. and Koerner, R.M., “*Technical Guidance Document: Quality Assurance and Quality Control for Waste Containment Facilities*”, EPA/600/R-93/182, EPA Risk Reduction Research Laboratory, Cincinnati, OH, 1993, 305 p.

Darilek, G.T., Menzel, R., and Johnson, A., “Minimizing Geomembrane Liner Damage While Emplacing Protective Soil”, *Proceedings of Geosynthetics ’95*, Nashville, Tennessee, 1995, Vol. 2, pp. 669-676.

Dvirnoff, A.H. and Munion, D.W., "Stability Failure of a Sanitary Landfill", *International Symposium on Environmental Geotechnology*, Lehigh, Pennsylvania, 1986, pp. 25-35.

Environmental Protection Agency, "*Technical Guidance Document: Final Covers on Hazardous Waste Landfills and Surface Impoundments*", EPA/530/SW-89/047, EPA Office of Solid Waste and Emergency Response, Washington, D.C., 1989, 39 p.
Environmental Protection Agency, "*Seminar Publication: Design, Operation, and Closure of Municipal Solid Waste Landfills*", EPA/625/R-94/008, EPA Center for Environmental Research Information, Cincinnati, Ohio, 1994, 86 p.
Environmental Protection Agency, "*List of Municipal Solid Waste Landfills*", EPA/530/R-96/006, EPA Office of Solid Waste and Emergency Response, Washington, D.C., 1996, pp. 1-2.
Environmental Protection Agency, Resource Conservation and Recovery Act Information System (RCRAIS) database, EPA National Oversite Database, Jun 1997.
Ghassemi, M., Crawford, K., and Haro, M., "*Leachate Collection and Gas Migration and Emission Problems at Landfills and Surface Impoundments*", EPA/600/2-86/017, EPA Hazardous Waste Engineering Research Laboratory, Cincinnati, Ohio, 1986, 206 p.
Giroud, J.P., "Lessons Learned From Studying the Performance of Geosynthetics", *Proceeding of Geotextiles-Geomembranes Rencontres 93*, Vol. 1, Joue-les-Tours, France, Sep 1993, pp. 15-31.
Giroud, J.P., "The Mechanics of Geomembrane Stress Cracking", *Computer Methods and Advances in Geomechanics*, Siriwardane, H.J. and Zaman, M.M. (editors), Balkema, Proceedings of the Eighth International Conference on Computer Methods and Advances in Geomechanics, Morgantown, West Virginia, 1994a, Vol. 1, pp. 177-188.
Giroud, J.P., "Quantification of Geosynthetics Behavior", *Proceeding of the Fifth International Conference on Geotextiles, Geomembranes, and Related Products*, Singapore, 1994b, Vol. 4, pp. 1249-1273.
Giroud, J.P., "Granular Filters and Geotextile Filters", *Proceedings of Geofilters '96*, Lafleur, J., and Rollin, A.L., Editors, Montreal, 1996, pp. 565-690.
Giroud, J.P. and Houlihan, M.F., "Design of Leachate Collection Layers", *Proceedings of Fifth International Landfill Symposium*, Sardinia, Italy, Vol. 2, 1995, pp. 613-640.
Giroud, J.P., Bachus, R.C., and Bonaparte, R., "Influence of Water Flow on the Stability of Geosynthetic-Soil Layered Systems on Slopes", *Geosynthetics International*, IFAI, Vol. 2, No. 6, 1995, pp. 1149-1180.
Gross, B.A., Bonaparte, R.B., and Giroud, J.P., "Evaluation of Flow from Landfill Leakage Detection Layers", Proceedings of Fourth International Conference on Geotextiles, Vol. 2, The Hague, The Netherlands, 1990, pp. 481-486.
Harris, J.M., Rivette, C.A., and Spradley, G.V., "Case Histories of Landfill Erosion Protection Using Geosynthetics", *Geotextiles and Geomembranes*, No. 11, 1992, pp. 573-585.
Hullings, D.E. and Sansone, L.J., "Design Concerns and Performance of Geomembrane Anchor Trenches", *Proceedings of the 10th GRI Conference Field Performance of Geosynthetics and Geosynthetic Related Systems*, Geosynthetic Research Institute, Philadelphia, Pennsylvania, 1996, pp. 219-233.
Kenter, R.J., Schmucker, B.O., and Miller, K.R., "The Day the Earth Didn't Stand Still: The Rumpke Landfill", *Waste Age*, Mar 1997, pp. 66-81.

Kmet, P., Mitchell, G., and Gordon, M., “Leachate Collection System Design and Performance - Wisconsin’s Experience”, Proceedings. of *ASTSWMO National Solid Waste Forum on Integrated Municipal Waste Management*, Lake Buena Vista, Florida, 1988.

Koerner, G.R., Koerner, R.M., and Martin, J.P., “Field Performance of Leachate Collections Systems and Design Implications”, *Proceedings of 31st Annual SWANA Conference*, San Jose, California, 1993, pp. 365-380.

Koerner, G.R., Eith, A.W., and Tanese, M., “Properties of Exhumed HDPE Field Waves and Selected Aspects of Wave Management", *Proceedings of the 11th GRI Conference on Field Installation of Geosynthetics*, Geosynthetic Research Institute, Philadelphia, Pennsylvania, 1998, pp. 152-162e.

Laine, D.L. and Darilek, G.T., “Locating Leaks in Geomembrane Liners of Landfills Covered with a Protective Soil”, *Proceedings of Geosynthetics ’93*, Vancouver, British Columbia, 1993, pp. 1403-1412.

Loewenstein, D.L., and Smrtic, M.J., “Primary Liner System Repair Made During Operation of the City of Albany Landfill: A Case History”, *Modern Double Lined Landfill Management Seminar, An Operation and Maintenance Perspective*, sponsored by New York State Association for Solid Waste Management in cooperation with New York State Department of Environmental Conservation Division of Solid Waste, Saratoga Springs, New York, Jan 1994, 6 p.

Matasovic, N. and Kavazanjian, E., Jr., “Observations of the Performance of Solid Waste Landfills During Earthquakes”, *Eleventh World Conference on Earthquake Engineering*, Acapulco, Mexico, Elsevier Science Ltd., 1996, CD-ROM Paper No. 341.

Matasovic, N., Kavazanjian, E., Jr., Augello, A.J., Bray, J.D., and Seed, R.B., “Solid Waste Landfill Damage Caused by 17 January 1994 Northridge Earthquake”, *The Northridge, California, Earthquake of 17 January 1994*, Woods, M.C. and Seiple, W.R., eds., California Department of Conservation, Division of Mines and Geology Special Publication 116, 1995, pp. 221-229.

Matasovic, N., Kavazanjian, E., Jr., and Anderson, R.L., “Performance of Solid Waste Landfills in Earthquakes”, *Earthquake Spectra*, Vol. 13, No. 5, May 1998, pp. 319-334.

Mitchell, J.K., Seed, R.B., and Seed, H.B., “Kettleman Hills Waste Landfill Slope Failure. I: Liner-System Properties”, *Journal of Geotechnical Engineering*, Vol. 116, No. 4, Apr 1990, pp. 647-668.

Oweis, I.S., "Stability of Sanitary Landfills", *Geotechnical Aspects of Waste Management*, seminar sponsored by Metropolitan Section, ASCE, New York, 1985.

Paulson, J.N., “Veneer Stability Case Histories: Design Interactions Between Manufacturer/Consultant/Owner”, *Proceedings of the 7th GRI Seminar Geosynthetics Liner Systems: Innovations, Concerns, and Designs*, Geosynthetic Research Institute, Philadelphia, Pennsylvania, 1993, pp. 235-241.

Peggs, I.D., Winfree, J.P., Giroud, J.P., “A Shattered Geomembrane Liner Case History: Investigation and Remediation”, *Proceedings of Geosynthetics ‘91*, Atlanta, Georgia, 1991, Vol. 2, pp. 495-505.

Richardson, G. and Reynolds, D., "Geosynthetic Considerations in a Landfill on Compressible Clays", *Proceedings of Geosynthetics '91*, Atlanta, Georgia, 1991, Vol. 2, pp. 507-516.

Schmucker, B.O. and Hendron, D.M., "Forensic Analysis of 9 March 1996 Landslide at the Rumpke Sanitary Landfill, Hamilton County, Ohio", *Slope Stability in Waste Systems*, seminar sponsored by ASCE Cincinnati and Toledo Sections, Ohio, 1997.

Seed, R.B., Mitchell, J.K., and Seed, H.B., "Kettleman Hills Waste Landfill Slope Failure. II: Stability Analyses", *Journal of Geotechnical Engineering*, Vol. 116, No. 4, Apr 1990, pp. 669-690.

Silva, M., "Some Landfills Starting to Leak, State Study Says", *Miami Herald*, 18 Jun 1995, p. 6B-7B.

Soong, T.Y. and Koerner, R.M., "*The Design of Drainage Systems Over Geosynthetically Lined Slopes*", GRI Report #19, Geosynthetic Research Institute, Philadelphia, Pennsylvania, 1997, 88 p.

Stark, T.D. and Evans, W.D., "Balancing Act", *Civil Engineering*, Aug 1997, pp. 8A-11A.

Stewart, J.P., Bray, J.D., Seed, R.B., and Sitar, N., "*Preliminary Report on the Principal Geotechnical Aspects of the January 17, 1994 Northridge Earthquake*", Report No. UCB/EERC-94/08, College of Engineering, University of California at Berkeley, Berkeley, California, 1994, 238 p.

Tedder, R.B., "Evaluating the Performance of Florida Double-Lined Landfills", *Proceedings of Geosynthetics '97*, Long Beach, California, 1997, Vol. 1, pp. 425-438.

Tisinger, L.G., Clark, B.S., Giroud, J.P., and Christopher, B.R., "Analysis of an Exposed Polypropylene Geotextile", *Proceedings of Geosynthetics '93*, Vancouver, British Columbia, 1993, pp. 757-771.

Tisinger, L.G., Clark, B.S., Giroud, J.P., and Schauer, D.A., "Performance of Nonwoven Geotextiles Exposed to a Semi-Tropical Environment", *Proceedings of Fifth International Conference on Geotextiles, Geomembranes, and Related Products*, Singapore, 1994, pp. 1223-1226.

Vander Linde, D.L., Luettich, S.M., and Bonaparte, R., "Lessons Learned From the Failure of a Landfill Cover System", *Geosynthetics: Lessons Learned From Failures*, IFAI, to be published in 1998.

Attachment F-A
Case Histories of Waste Containment System Problems

F-A.1 Introduction

The purpose of this attachment to Appendix F is to present case histories of the waste containment system problems described in Chapter F-2 of the appendix. The case histories are divided into 15 categories based on the waste containment system component or attribute criterion affected by the problems: (i) landfill liner construction; (ii) landfill liner degradation; (iii) landfill LCRS or LDS construction; (iv) landfill LCRS or LDS degradation; (v) landfill LCRS or LDS malfunction; (vi) landfill LCRS or LDS operation; (vii) landfill liner system stability; (viii) landfill liner system displacement; (ix) cover system construction; (x) cover system degradation; (xi) cover system stability; (xii) cover system displacement; (xiii) impoundment liner construction; (xiv) impoundment liner degradation; and (xv) impoundment liner system stability. Each of these 15 categories of case histories is presented in a separate section of this attachment (F-A.2 to F-A.16). The case histories are also categorized by the principal human factor contributing to the problem: (i) design; (ii) construction; and (iii) operation. The classification of each case history is shown as "component or attribute criterion"/ "principal human factor criterion" (e.g., landfill liner system stability/design). The nature of the problem in each case history is described. When information is available, the method by which the problem was detected and the remedies, if any, that have been implemented are also presented. Lessons learned for future projects are given.

F-A.2 Landfill Liner Construction

F-A.2.1 L-1

Problem Classification: landfill liner construction/construction
Region of U.S.: unknown
Waste Type: unknown
Reference: Laine, D.L. and Darilek, G.T., "Locating Leaks in Geomembrane Liners of Landfills Covered with a Protective Soil", *Proceedings of Geosynthetics '93*, Vancouver, British Columbia, 1993, Vol. 3, pp. 1403-1412.

Problem Summary: leakage through holes in HDPE GM primary liner

Problem Description: Laine and Darilek (1993) described the results of an electrical leak location survey conducted over the 0.4 ha base of a double-lined landfill cell exhibiting primary liner leakage. The 1.5-mm thick HDPE GM primary liner for the cell was overlain by the following components, from top to bottom:

- 0.3-m thick sand protection layer;
- GT; and

- 0.3-m thick gravel LCRS drainage layer.

The purpose of the survey was to locate GM primary liner holes so they could be repaired prior to placing waste in the cell. The cell had been constructed with third-party CQA and air pressure and vacuum box testing of GM seams. However, primary liner holes were suspected because the flow rate of water from the GN LDS drainage layer into the LDS sump increased to about 2,900 lphd after rainwater ponded over the base of the cell. Laine and Darilek (1993) did not give the height of ponded rainwater. Three small holes were found in the GM primary liner during the survey of the 0.4 ha landfill base. Two holes were located in the GM panels, and one was located in a seam. One of the panel holes was 2.5-mm in diameter. The sizes of the other two holes and the type of seam containing one of the holes (i.e., fusion or extrusion) were not given.

The GM primary liner holes found by Laine and Darilek are not unexpected. In a study of LDS flow rates from double-lined waste containment systems, Bonaparte and Gross (1993) found that all landfill cells with GM primary liners appeared to have exhibited primary liner leakage. The LDS flow rate from the cell surveyed by Laine and Darilek (1993) was higher than the typical LDS flow rates of less than 200 lphd reported by Bonaparte and Gross (1993) for operating landfill cells with GM primary liners constructed with CQA. The relatively high flow rate from this cell as compared to the landfill cells in the study by Bonaparte and Gross (1993) is due to: (i) the relatively high head of rainwater on the holes as compared to the typical head of leachate over holes in a landfill; and/or (ii) the greater size and frequency of the holes as compared to that typical of landfills constructed with CQA. As proposed by Giroud (1984), leakage through a GM hole can be evaluated using Bernoulli's equation for free flow through an orifice. Considering only the 2.5-mm diameter hole, the authors of this appendix found that Bernoulli's equation gives a flow rate of 2,900 lphd through the hole (considering the 0.4 ha cell base) when the head of liquid above the hole is 1.0 m.

Resolution: The identified holes were repaired. The LDS flow rate after the repairs was not given by Laine and Darilek (1993).

Lessons Learned for Future Projects: Based on the available information, the following lessons can be learned from this case history:

- Construction-related holes in GM liners should be anticipated, even in liners installed with CQA. If there is a head of liquid over a liner hole, leakage occurs.
- GM primary liner holes can be located by leak location surveys or other methods even after the LCRS drainage layer and protection layer have been placed. In the case history presented above, the primary liner leakage rate was perceived to be relatively high, and the landfill owner decided to decrease the leakage rate by identifying and repairing GM holes prior to waste placement.
- When water is ponded over a GM primary liner in a landfill, relatively high flow rates can occur through small holes in the GM, depending on the head of water over the

holes. Therefore, these small holes can be easily detected and repaired prior to waste placement if water can be ponded over them.

F-A.2.2 L-3

Problem Classification: landfill liner construction/construction
Region of U.S.: southcentral
Waste Type: HW

Reference: Darilek, G.T., Menzel, R., and Johnson, A., "Minimizing Geomembrane Liner Damage While Emplacing Protective Soil", *Proceedings of Geosynthetics '95*, Nashville, Tennessee, 1995, Vol. 2, pp. 669-676.

Problem Summary: leakage through holes in HDPE GM liners

Problem Description: Darilek et al. (1995) described the results of electrical leak location surveys conducted over the base of three double-lined landfill cells located in southeast Texas. The surveys were performed in addition to normal CQA procedures. For each cell, the following four liner system configurations were surveyed: (i) the 2-mm thick HDPE GM component of the composite secondary liner; (ii) the GM component of the composite secondary liner after placement of the overlying 0.3-m thick pea gravel (maximum particle size about 9 mm) LDS drainage layer; (iii) the 2-mm thick HDPE GM primary liner; and (iv) the GM primary liner after placement of the overlying GN LCRS drainage layer, 440 g/m^2 needlepunched nonwoven GT filter, and 0.3-m thick pea gravel LCRS drainage layer. These configurations allow an assessment of GM damage associated with placing gravel directly on the GM and the degree of protection provided to the GM by the overlying GN and GT.

With respect to the surveys of the six exposed GMs (three GM primary liners and three GM components of secondary liners), the frequency of construction-related holes found during surveys of the bottom GMs in two cells was 33 and 14/ha. An extrusion seaming problem was corrected, and the number of holes located in the bottom GM of the third cell and the top GMs for the three cells dropped to 5/ha or less. Darilek et al. (1995) suggested that the hole frequency might also have decreased due to the GM seaming equipment operators taking more care to avoid seam holes. Most of the located GM holes were in extrusion seams; none were in fusion seams. The four largest holes were punctures or slits in the GM panels. The sizes and possible causes of these holes were not discussed by Darilek et al. One hole was found in the prefabricated HDPE sump structure.

The gravel LCRS and LDS drainage layer material was dumped from the top of the side slopes of the cells onto a sacrificial piece of GM placed over the GM liners. A grader with its blade on a extending boom was used to push the gravel down the slopes until a temporary access ramp could be developed in each cell. Then low ground-pressure

bulldozers pulled the gravel down the ramps and spread it across the cells. The thickness of the gravel between the bulldozers and the GMs was at least 0.3 m. After the gravel was placed, the GMs were resurveyed. The frequency of additional holes detected in the bottom GMs ranged from about 1.3 to 4.8/ha. The holes ranged in size from small punctures to a 60 mm in diameter. Several of the holes were located in the vicinity of the temporary ramps. No additional holes were detected in the GM primary liners, which were separated from the gravel by the GN and GT.

Resolution: The identified GM holes were repaired.

Lessons Learned for Future Projects: Based on the available information, the following lessons can be learned from this case history:

- Construction-related holes in GM liners should be anticipated, even in liners installed with CQA. If there is a head of leachate over a liner hole, leakage occurs. In the case history described above, the performance of electrical leak location surveys during sequential installation of multiple GM liners allowed extrusion seaming problems to be identified early and corrected, decreasing the frequency of identified GM holes in subsequent installations.
- The CQA consultant should be trained in standard CQA practices, such as inspecting the entire installed GM liner for damage prior to placement of overlying materials. In the case history described above, four punctures and slits were found in the GM panels during the leak location survey. If they were visible to a person standing by the hole, the CQA consultant should have identified them.
- The potential for GM damage during placement of a soil layer over a GM can be reduced by protecting the GM. Measures for GM protection include placing a protection layer (e.g., thick GT cushion or GC drainage layer) over the GM, using a greater initial lift thickness of soil above the GM, and using construction equipment with low ground pressure to place soils over the GM. These options are consistent with EPA guidance (Daniel and Koerner, 1993).
- Special care should be taken to protect GMs in areas subjected to high static and dynamic stresses from construction equipment, such as beneath temporary access roads. Measures for GM protection include placing a protection layer over the GM and increasing the thickness of the soil layer over the GM in these sensitive areas.

F-A.2.3 L-5

Problem Classification: landfill liner construction/construction
Region of U.S.: southeast
Waste Type: MSW
References: Silva, M., “Some Landfills Starting to Leak, State Study Says”, *Miami Herald*, 18 Jun 1995, p. 6B-7B.
Tedder, R.B., “Evaluating the Performance of Florida Double-Lined Landfills”, *Proceedings of Geosynthetics ’97*, Long Beach, California, 1997, Vol. 1, pp. 425-438.

Problem Summary: leakage through holes in HDPE GM primary liner

Problem Description: As described by Silva (1995) and Tedder (1997), a survey of LDS flow rates from double-lined MSW landfills in Florida was performed by the Florida Department of Environmental Protection (FDEP). The highest average LDS flow rate was occurring at a landfill cell in Dade County. The cell was constructed in 1991 with a single-composite liner system on the 5.8 ha side slope and double-liner system on the 0.97 ha base. The double-liner system includes a GN LCRS drainage layer, HDPE GM primary liner, GN LDS, and HDPE GM/CCL composite secondary liner. Leachate collected in the LCRS and LDS sumps of the cell was pumped from the sumps when the sump leachate level reached 0.6 m.

Until March 1994, problems with the LCRS and LDS flow measuring system (e.g., flowmeters, check valves) made the measured flows unreliable. From April 1994 to March 1995, the average LDS flow rate from the cell was about 4,660 lphd. All of this flow was attributed to primary liner leakage, rather than other sources, based on chemical constituents in the LDS flow and the fact that the primary liner is a GM and the LDS drainage layer is a GN. Tedder (1997) found that the measured flow rate was greater than the calculated primary liner leakage rate for this cell of about 3,600 lphd for leakage through 2.5 11-mm diameter GM holes/ha under a head of 4 mm (i.e., the thickness of the GN LCRS drainage layer). Interestingly, Tedder showed that, of the 24 landfill cells considered in his survey, only one cell, the cell discussed in this section, exhibited LDS flow rates attributable to primary liner leakage that were greater than calculated primary liner leakage rates.

Tedder calculated the primary liner leakage rate assuming that the head on the liner was 4 mm. However, the head of leachate in the sump area of this cell can be much greater, up to 0.6 m. Using Bernoulli's equation for free flow through an orifice, the authors of this appendix calculated that the observed primary liner leakage rate of 4,660 lphd could be caused by one 5.8 mm diameter GM hole under a 0.6 m head of leachate.

Resolution: In April 1995, the "pump on" level in the LCRS sump was lowered from 0.6 m to 0.45 m, and the LDS flow rates decreased. This decrease was attributed to the reduction of primary liner leakage at the sump. Over a two-month period, the "pump on" level was further decreased, resulting in even lower LDS flow rates. Currently, leachate is pumped from the LCRS sump when the sump leachate level reaches 0.25 m. The average LDS flow rates is now on the order of 2,000 lphd. GM primary liner holes have not been located and repaired at this landfill because: (i) there is no anticipated environmental impact of the primary liner leakage given the expected performance capabilities of both the LDS and the composite secondary liner; (ii) repair of liner systems after waste placement would be extremely difficult and expensive; and (iii) additional liner system damage could occur in any attempt to excavate the waste and repair the liner system.

Lessons Learned for Future Projects: Based on the available information, the following lessons can be learned from this case history:

- With respect to the potential for leakage, leachate sumps are generally the most critical locations in landfills with internal sumps. Leachate heads are typically sustained and at higher levels in sumps than at other locations. In addition, GM liners in sumps often have seamed corners to fit the sump geometry. These seams may contain holes. As described above, even one GM hole at a sump can cause relatively high leakage rates due to the relatively high head of leachate in the sump.
- To decrease the rate of leakage through GM holes at internal sumps, the sump design should include additional liner components, such as a GCL, beneath the GM liner in the sump area, even if the GM is already underlain by a CCL. Bonaparte (1995) provides additional discussion of this design approach. The GM primary liner in the next group of cells constructed at the landfill described above was underlain by a GCL.
- The GM panel layout should be configured to minimize seams in sumps.
- The "pump on" levels in sumps should be kept as low as practicable to reduce leakage if there are holes in the GM liner in the sump, especially if the GM is not underlain by a GCL.

F-A.2.4 L-6

Problem Classification: landfill liner construction/operation
Region of U.S.: southcentral
Waste Type: HW
Reference: Anderson, K.A., "Leachate Collection Management at a Hazardous Waste Landfill", *Hydrological Science and Technology*, Vol. 9, No. 1-4, 1993, pp. 30-53.
Problem Summary: leakage through holes in HDPE GM primary liner

Problem Description: Beginning in March 1990, about six months after the start of waste placement in a new double-lined landfill cell located in Louisiana, average monthly LDS flow rates from the cell increased from less than 140 lphd to up to 1,200 lphd. The relatively high LDS flow rates coincided with high rainfall and high LCRS flow rates. The primary liner for the cell is a 1.5-mm thick HDPE GM on the side slope and a GM/CCL composite on the base. The LDS drainage layer is a GN. Based on the correspondence of LDS flow rates with LCRS flow rates and on the liner system components, the LDS flow from the cell was primarily attributed to leakage through the GM primary liner on the side slope. The GM primary liner on the side slope is overlain only by a GN LCRS drainage layer and a GT filter. There is no soil protection layer on the side slope; waste was placed directly on the GT. It is not known if the GM primary liner was damaged during construction or operation. However, without a thick protection layer, the potential for liner damage during landfill operation increases. After visual inspection of the exposed liner system at the site, the owner concluded that the increased LDS flow was likely due to a GM hole in an area of the cell where runoff from

the waste was collected and pumped out for disposal. This was confirmed after rhodamine dye was added to the impounded leachate and detected in LDS flow less than 24 hours later. Anderson (1993) did not give the depth of leachate that was temporarily impounded in the cell. He did indicate, however, that the leachate was contained on one side of the cell by a 4-m high intermediate berm, and that the leachate level varied.

Resolution: The ponded leachate was pumped out of the cell, waste was excavated from the side slopes of the ponded area, and the liner system was inspected. Four small tears in the GM primary liner were found and patched. After the repairs were made, LDS flow rates decreased to previous levels, less than 140 lphd.

Lessons Learned for Future Projects: Based on the available information, the following lessons can be learned from this case history:

- Holes in GM liners should be anticipated, even in liners installed with CQA. If there is a head of leachate over a liner hole, leakage occurs.
- GM holes can be located during landfill operation using dye or other methods. However, waste relocation may be required to repair these GM holes.
- It is not clear if the GM holes found in the landfill cell described above were caused during construction or operation. A soil protection layer was not placed between the waste and the liner system geosynthetics on the 2.5H:1V side slopes, increasing the chances for the side slope liner system to be damaged by landfill equipment (e.g., a bulldozer) during waste placement. The potential for GM damage can be reduced by installing a protection layer (e.g., thick GT cushion or GC drainage layer) over the GM, using spotters to direct equipment operators during placement of waste over the GM, and placing only select waste over the GM.

F-A.2.5 L-7

Problem Classification: landfill liner construction/operation
Region of U.S.: northeast
Waste Type: MSW
Reference: Loewenstein, D.L., and Smrtic, M.J., "Primary Liner System Repair Made During Operation of the City of Albany Landfill: A Case History", *Modern Double Lined Landfill Management Seminar, An Operation and Maintenance Perspective*, sponsored by New York State Association for Solid Waste Management in cooperation with New York State Department of Environmental Conservation Division of Solid Waste, Saratoga Springs, New York, Jan 1994, 6 p.

Problem Summary: leakage though HDPE GM/CCL composite primary liner at pipe penetration

Problem Description: In March 1992, about four months after waste placement began, the average LDS flow rate from a double-composite lined landfill cell located in New

York increased from about 10 to 400 lphd. At the time, only a small amount of waste had been placed in the cell. The sharp increase in LDS flow rate could not be attributed to leakage through the composite primary liner since flow rates through a composite liner for a landfill should be very small (i.e., less than 1 lphd). It could also not be attributed to water expelled from the CCL component of the primary liner as it compressed under the weight of the overlying waste since little waste had been placed. Shortly before the flow rate increased, landfill operations personnel had been performing minor regrading of the 0.45-m thick sand LCRS drainage layer on the base of the cell. When the base of the cell was inspected in the area of regrading activities, deep tire tracks were observed in the sand over the LCRS pipe penetration of the primary liner at the perimeter berm. The tracks had been caused by a rubber-tired loader. The 150-mm diameter Schedule 80 PVC LCRS pipe was positively projecting into the sand LCRS drainage layer. With this design, the specified separation between the top of the pipe and equipment trafficking on the sand is only 0.3 m.

A closed-circuit television was used to inspect the LDS pipe to evaluate where leachate was entering the pipe. However, due to the sediment buildup in the pipe, it was not clear where leachate was entering. The LDS pipe was flushed and the camera was reintroduced into the pipe. This time, sediment was observed accumulating in the LDS pipe at a distinct location near the pipe penetration of the composite secondary liner. The GM boot at the LCRS pipe penetration of the primary liner was cut so the penetration could be inspected. It was found that the LCRS pipe was broken between the penetration and where it was connected to the boot. Additionally, the CCL component of the composite primary liner was rutted adjacent to the LCRS pipe. The damage at the penetration had allowed leachate to flow out of the broken LCRS pipe within the pipe boot, between the LCRS pipe and the damaged CCL, and into the GC LDS drainage layer.

Resolution: The softened, rutted CCL was removed around the LCRS pipe and replaced with new compacted clay. All cracked or broken LCRS pipe was replaced. Then a new GM boot was constructed around the pipe penetration of the GM primary liner. About one year after the repair, LDS flow rates were approximately 50 lphd.

Lessons Learned for Future Projects: Based on the available information, the following lessons can be learned from this case history:

- Landfill operations manuals should include limitations on the types of equipment that may traffic over the liner system before the first lift of waste is placed. These limitations are enforced during construction when CQA is implemented; they should also be applied during operation.
- Landfill operations personnel should be aware of sensitive areas of a liner system, such as at pipe penetrations or sumps, and should protect these areas. In the case history described above, the loader operator repeatedly trafficked on the sand drainage layer above the pipe penetration until the sand had deep tire tracks. If the operator had been directed to protect this sensitive area, he may have used a

different path over the liner system. Sensitive areas can be identified with cones, flags, or other markers to reinforce this. They can also be isolated from traffic by berms, bollards, or other means.

F-A.2.6 L-8

Problem Classification: landfill liner construction/design
Region of U.S.: southwest
Waste Type: MSW
Reference: unpublished

Problem Summary: landfill gas migrated beyond liner system and into vadose zone resulting in groundwater contamination

Problem Description: A single-composite liner system for a landfill was constructed in 1990 in a canyon underlain by sedimentary marine bedrock and alluvial deposits. Along the perimeter of the landfill, the composite liner was extended horizontally and the GM was secured by covering it with a 0.9-m thick layer of relatively permeable soil. At the toe of the landfill, near the mouth of the canyon, an asphalt parking lot was constructed over the relatively permeable soil layer and natural ground. Upgradient of the landfill, in the upper reaches of the canyon, the shallow aquifer is located about 8 m below ground surface in bedrock. Downgradient of the landfill, near the mouth of the canyon, the shallow aquifer is located about 22 m below ground surface in alluvium and bedrock. Groundwater flow velocities range from less than 0.1 m/yr in the bedrock to about 250 m/yr in the alluvium.

Four years after start of landfill operations, the waste near the toe of the landfill was at intermediate grades and covered with a relatively low-permeability soil intermediate cover layer that graded into the relatively permeable soil layer anchoring the edge of the liner. At this time, several VOCs (i.e., trichlorofluoromethane, dichlorofluoro-methane, benzene, toluene, xylenes, ethylbenzene, and dichlorobenzene) were detected in groundwater from a monitoring well located about 60 m from the downgradient edge of the landfill. The VOCs were generally at concentrations less than EPA maximum contaminant levels (MCLs) for drinking water. Based on groundwater modeling, the VOC plume downgradient of the landfill was estimated to be approximately 60 m wide, 100 m long, and up to 3 m deep in the shallow aquifer. The source of VOCs was thought to be landfill gas for the following reasons: (i) inorganic landfill leachate constituents were not detected in samples from the downgradient well at concentrations above background levels; (ii) the VOCs detected in groundwater were also found in leachate and gas samples; and (iii) relatively high concentrations of methane (i.e., greater than 30%) were detected in the headspace of downgradient groundwater monitoring wells and groundwater subdrains beneath the landfill liner system.

To verify the source of VOCs was landfill gas, a soil gas survey was conducted at 300 m intervals along the perimeter of the landfill. Based on the results of the survey, gas

appeared to be migrating out of the landfill and into the vadose zone near the landfill toe. Here, the asphalt served as a confining layer, blocking landfill gas moving from the waste into the relatively permeable soil layer from venting to the atmosphere. Instead, some gas migrated through the relatively permeable soil layer and then beyond the limit of the liner system. Around the remainder of the landfill, where there was no asphalt, gas migrating into the relatively permeable soil layer essentially vented to the atmosphere and had no observable impact on groundwater. In addition to the soil gas survey, gas samples were collected from the headspace of groundwater monitoring wells, groundwater subdrains, and vadose gas monitoring probes. The chemical signatures of the gas samples indicated that landfill gas was the likely source of the VOCs in groundwater downgradient of the landfill.

Resolution: A fate and transport analysis of the VOC plume was performed that demonstrated the plume would be retarded, primarily by biodegradation, before reaching the property line if gas was controlled. The property line is located about 460 m from the downgradient edge of the landfill. To improve VOC source control, two additional gas extraction wells were installed in the waste near the landfill toe. If these wells do not provide adequate source control, the liner system under the asphalt at the perimeter of the landfill may have to be reconstructed to eliminate the gas migration pathway and a groundwater remedy may need to be implemented.
Lessons Learned for Future Projects: Based on the available information, the following lessons can be learned from this case history:

- Landfill gas may migrate into the vadose zone at the perimeter of a landfill if gas is not well controlled and there is a pathway.
- In the case history described above, the landfill would not have impacted groundwater if the landfill gas had been better controlled, the soil layer anchoring the edge of the liner system had been less permeable, the asphalt parking lot had not been constructed over the edge of the liner system, or the edge of the liner system had been modified so that the end of the liner extended back to the ground surface and into the asphalt. With the latter detail, gas is blocked from moving laterally or vertically into the vadose zone.

F-A.2.7 L-9

Problem Classification: landfill liner construction/construction
Region of U.S.: northeast
Waste Type: MSW
Reference: unpublished

Problem Summary: leakage though HDPE GM primary liner at pipe penetration

Problem Description: After a heavy rainfall that ponded up to 0.5 m of water in the LCRS of three newly constructed cells, one of the cells exhibited primary liner leakage near the LCRS pipe penetration of the primary liner. The LDS flow rate from this cell

was about 250 lphd. The pipe penetration detail had been carefully constructed and had two special features designed to minimize the potential for leakage through the HDPE GM primary liner: (i) the GM primary liner was underlain by a GCL at the penetration; and (ii) the penetration was sealed with two HDPE boots, creating a space that could be pressure tested and later filled with foam. The double-boot system can be described as follows: (i) starting at about 1.5 m into the cell from the LCRS pipe penetration, a 250-mm diameter pipe was placed around the 150-mm diameter LCRS pipe to provide secondary containment of leachate as the LCRS pipe penetrated the secondary liner and the perimeter berm around the landfill; (ii) an HDPE plug was placed at the end of the outer pipe in the cell to prevent inflow of leachate into the annular space between the two pipes; (iii) two prefabricated HDPE GM boots were installed around the outer pipe where the pipe penetrated the primary liner; and (iv) the boots were clamped to the pipe and extrusion seamed to the primary liner. The seams were vacuum tested where there was space for the vacuum box. Then the integrity of the boots was tested by applying an air pressure of about 170 kPa to the space between the boots. This pressure was too high, and the outer boot was overstressed and failed where it was seamed to the primary liner. The outer boot was subsequently reseamed to the liner. The boots were retested at a pressure of 20 kPa and found to hold the air pressure without noticeable leakage. Then the space between the boots was filled with expanding foam sealant. After a heavy rain, which resulted in ponded rainwater at the pipe penetration, primary liner leakage occurred at the penetration, as described above.

Resolution: The pipe bedding gravel around the pipe penetration was removed, and the outer pipe boot was inspected. A small hole at the extrusion seam of the outer boot to the primary liner was found and repaired. Again rainwater ponded at the pipe penetration, and primary liner leakage was observed. The outer boots was uncovered again and inspected, but no obvious GM hole was observed. Since the pathway for this leakage could not be identified during construction, the problem was not remedied. The environmental impact from the leakage, however, is expected to be negligible given that the landfill has a composite secondary liner. Interestingly, at another landfill in the same region, holes in a double-booted pipe penetration of the primary liner were identified during construction using an ammonia colorimetric leak test (ASTM E 1066). The holes were repaired, and the penetration was found to be essentially nonleaking when rainwater ponded around it.

Lessons Learned for Future Projects: Based on the available information, the following lessons can be learned from this case history:

- With respect to the potential for leakage, pipe penetrations are generally the most critical locations within landfills without internal sumps. As demonstrated by the case history described above, even when extra measures are taken to enhance the integrity of the primary liner at the penetration, it is difficult to construct the penetration to be defect free. Methods for constructing better connections between GMs and ancillary structures are needed.

- Since pipe penetrations are critical locations, designs without pipe penetrations should be preferred whenever possible.

F-A.2.8 L-11

Problem Classification: landfill liner construction/construction
Region of U.S.: northeast
Waste Type: MSW ash
Reference: unpublished

Problem Summary: construction debris in CCL with initially smooth surface protruded from CCL after CCL was left exposed and subsequently eroded

Problem Description: During construction of the soil-bentonite CCL component of a composite secondary liner, relatively large pieces of construction debris (e.g., bricks, rebars) were found in the soil delivered to the site for use in the CCL. While the project specifications precluded the contractor from using borrow soil containing "deleterious" material, debris-free soil was not locally available. Additionally, the soil, as delivered to the site, had particles larger than the specified maximum particle size of 19 mm. In spite of being notified by the owner that the soil did not meet specifications, the contractor indicated that the soil would be acceptable after it had been screened. The contractor then proceeded with CCL construction. After the soil had been screened, the total amount of construction debris remaining in the soil was about 0.02% by weight. In addition, laboratory permeability and field Boutwell permeability tests performed on the CCL demonstrated that the CCL met the hydraulic conductivity criterion of the specifications (i.e., hydraulic conductivity no greater than 1×10^{-9} m/s). Construction of the CCL was completed in the fall. At this time, the surface of the CCL was smooth and debris was not visible. The contractor left the CCL unprotected over the winter. When construction resumed the next spring, the surface of the CCL had eroded and some pieces of construction debris were protruding from the CCL. The CCL in this state was not suitable for placement of the overlying GM liner.

Resolution: The state regulatory agency required the CCL on the base of the landfill to be covered with a GCL and the CCL on the side slope to be covered by a 80-mm thick layer of debris-free CCL to protect the overlying GM from puncture by protruding debris. A GCL was not required on the 2.5H:1V side slope due to concerns with the effect of the GCL on liner system slope stability.

Lessons Learned for Future Projects: Based on the available information, the following lessons can be learned from this case history:

- CCLs should not be constructed with materials containing construction debris or large particles, even if prior to GM installation the CCL has a smooth surface and

Figure F-A.2.1. Construction debris in a CCL with an initially smooth surface protruded from the CCL after the CCL was left exposed and subsequently eroded.

meets the hydraulic conductivity criterion. The debris may adversely impact the hydraulic conductivity of the CCL and/or damage an overlying GM. In the case history described above, the constructed CCL had a smooth surface and met the hydraulic conductivity criterion after construction. However, left unprotected, it developed, due to erosion, a surface with some protruding particles.

- CCLs should not be left unprotected for an extended period of time. They can desiccate and crack due to evaporation of water in the CCL, crack when exposed to freezing and thawing actions, and be eroded by wind and water.

F-A.2.9 L-11

Problem Classification: landfill liner construction/construction
Region of U.S.: northeast
Waste Type: MSW ash
Reference: unpublished

Problem Summary: leakage though HDPE GM primary liner at pipe penetration

Problem Description: After rainwater ponded in three newly-constructed landfill cells, the LDS flow rates from the cells were about 200, 200, and 1,000 lphd. These flows were primarily attributed to primary liner leakage since the LDS drainage layer is a GN and the primary liner on the base of the cells is a composite consisting of an HDPE GM over a GCL and structural fill layer. The owner suspected that the leakage was occurring at defects around the LCRS pipe penetrations of the primary liner as it is difficult to construct a defect-free connection between HDPE GM and pipes. To test primary liner integrity at the penetrations, ponding tests were conducted. In each cell, dye added to water ponded in the LCRS around the pipe penetration was rapidly detected in LDS liquid, indicating a direct connection between the LCRS and LDS at the penetration. Subsequently, the LCRS pipe penetrations were inspected to locate the defects. In two cells, including the cell with the highest LDS flow rate, the GM pipe boots were not securely fastened to the pipes; a pencil could be inserted between the boots and the pipes. In the remaining cell, the GM pipe boot appeared adequate though rather short.

Resolution: In the cell with the highest LDS flow rate, the faulty GM boot was reconstructed. Silicon sealant was placed at the intersection of the pipe and GM boot in the other cell with an obvious boot problem. In the remaining cell, a new pipe boot was installed over the old short boot. In each cell, the space between the boot and the primary liner was filled with bentonite slurry. Based on a subsequent ponding test with dye, primary liner leakage into the LDS sumps, if any, was very small and could not be distinguished from earlier primary liner leakage or construction water. By two months after the repairs, the LDS flow rates had dropped to less than 100 lphd for the cell with the reconstructed boot and less than 10 lphd for the other two cells.

Lessons Learned for Future Projects: Based on the available information, the following lessons can be learned from this case history:

- With respect to the potential for leakage, pipe penetrations are generally the most critical locations within landfills without internal sumps.
- Since pipe penetrations are critical locations, designs without pipe penetrations should be preferred whenever possible. If pipe penetrations are used, they should be carefully constructed and inspected.
- The integrity of pipe penetrations can be tested during construction and, if necessary, the penetrations can be improved. In the case history presented above, leakage at a pipe penetration was detected during construction and reduced by filling the space between the boot and the GM primary liner with bentonite slurry.

F-A.2.10 L-15

Problem Classification: landfill liner construction/construction
Region of U.S.: southeast
Waste Type: MSW

Reference: unpublished

Project Summary: sand bag under installed GM liner approved by CQA consultant

Problem Description: About 2 ha of GM liner was installed and inspected by site CQA personnel. The liner was found to be acceptable. Regulatory personnel who subsequently inspected the liner observed a bump beneath the liner on the slope of the LCRS pipe trench. When the liner was cut at a bump, a sand bag was found beneath the liner.

Resolution: The sand bag was removed, and the liner was repaired.

Lessons Learned for Future Projects: Based on the available information, the following lessons can be learned from this case history:

- Prior to deploying a GM, all extraneous objects (e.g., tools, sand bags) should be removed from the surface on which the GM is to be placed. If sand bags are used to secure the GM panels until the panels are seamed, care should be taken by the installer to ensure that the sandbags, and all other extraneous objects, are not trapped beneath the GM after seaming.
- The CQA consultant should be trained in standard CQA practices, such as inspecting the subgrade for extraneous objects and gravel that may damage the liner prior to liner deployment and inspecting the installed liner for underlying objects.

F-A.2.11 L-17

Problem Classification: landfill liner construction/construction
Region of U.S.: northeast
Waste Type: HW
Reference: Bonaparte, R. and Gross, B.A., "*LDCRS Flow Rates from Double-Lined Landfills and Surface Impoundments*", EPA/600/SR-93/070, EPA Risk Reduction Research Laboratory, Cincinnati, Ohio, 1993, 65 p. (Landfill AB)

Problem Summary: leakage through holes in HDPE GM primary liner

Problem Description: Shortly after waste placement began in a double-lined landfill cell, the black color of the LDS liquid and the results of chemical analysis of the liquid indicated that primary liner leakage was occurring. The LDS flow rates at this time were approximately 1,030 lphd. The side slope liner system includes a 0.3-m thick gravel protection layer, GN LCRS drainage layer, HDPE GM primary liner, and GN LDS drainage layer. The base liner system includes an HDPE GM/CCL composite primary liner and a gravel LDS drainage layer. Based on the liner system components, leakage was suspected to be occurring through the GM primary liner on the side slope. Waste was excavated off the side slope where it was present, and the liner system was inspected. Two 10-mm diameter GM holes and five GM fusion seam holes were found

on the side slopes. At the fusion seam holes, the outside track of the dual track seam had separated allowing leachate to flow through the air channel between the tracks and potentially through the liner if the inside track had holes. Though the seam had passed air pressure testing during construction, only the strength of the inside track, which was not visible, had been tested. The project specifications did not require testing of both the inside and outside tracks.

Resolution: The GM holes were repaired. The average LDS flow rate for the next two months after the repairs was about 320 lphd.

Lessons Learned for Future Projects: Based on the available information, the following lessons can be learned from this case history:

- Construction-related holes in GM liners should be anticipated, even in liners installed with CQA. If there is a head of leachate over a liner hole, leakage occurs.
- Frequently, both the inside and outside tracks of a fusion seam are tested in peel and shear. In the case history described above, if the outside track had also been destructively tested, the separation of the outside track after construction may have been avoided. If both tracks are required to have integrity, both tracks should be tested.
- Even though it may not be required for a project, it may be beneficial to test both tracks of the dual track fusion seam to gather more information on overall seam quality. Dual track fusion seaming machines are designed to make high quality seams along two tracks. Holes periodically occurring in one track may also be occurring in the other track. By testing both tracks, seaming problems may be identified and corrected quicker. Also, as shown by Giroud et al. (1995b), the failure of one track of the seam increases the bending strains in the GM next to the adjacent track, simply due to seam geometry. These strain concentrations cause stress concentrations, since stress and strain are linked, and may lead to GM failure under certain conditions. The increase in stress concentrations can be avoided by having two intact seams. Furthermore, the costs associated with destructive testing of both tracks of GM seam samples is small relative to the total cost of CQA.

F-A.2.12 L-19

Problem Classification: landfill liner construction/construction
Region of U.S.: northeast
Waste Type: MSW
Reference: unpublished

Problem Summary: wind uplifted and tore HDPE GM liner during construction

Problem Description: During installation of a 1.5-mm thick HDPE GM liner, the GM installer arrived at the site one morning to find that about 3 ha of GM had been uplifted by wind, torn from the installed GM, and blown into a twisted, folded pile. The wind

uplift occurred even though the GM had been weighted down with sand bags. Interestingly, the GM primarily tore through extrusion seams and along, but outside of, fusion seams.

Resolution: None of the wind-blown GM in the pile could be salvaged because the GM contained too many folds and creases where the yield strain of the HDPE had been exceeded. The damaged GM was replaced with new GM of the same type and thickness.

Lessons Learned for Future Projects: Based on the available information, the following lessons can be learned from this case history:

- The leading edge of an uncovered GM liner should be secured to prevent wind from flowing beneath the GM and uplifting it. This is typically accomplished by seaming adjacent panels of GM liner shortly after deployment and placing a row of adjacent sandbags along the edge of the GM.
- GM liners should be covered with a soil layer as soon as practicable after installation to prevent GM uplift by wind.

F-A.2.13 L-19

Problem Classification: landfill liner construction/construction
Region of U.S.: northeast
Waste Type: MSW
Reference: unpublished

Problem Summary: severe wrinkling of HDPE GM due to thermal expansion during construction

Problem Description: Construction of two 12-ha single-composite lined landfill cells began in the fall. Deployment and seaming of the 1.5-mm thick HDPE GM component of the composite liner were conducted through the winter, when temperatures were near or below freezing. At this time the GM was relatively taut.

Placement of the sand LCRS drainage layer was delayed because the sand initially did not pass the conformance tests. As a result, the GM was left exposed. In the spring and summer, due to the warmer weather, the exposed GM expanded and became very wrinkled. Then, the sand layer could not be placed because of concern that the GM wrinkles would fold over beneath it.

Resolution: Several thousand linear meters of wrinkles were required to be cut and repaired prior to placing the overlying sand LCRS drainage layer. In addition, the sand layer was required to be placed during the cooler nighttime hours, i.e., when GM wrinkles are smaller. Wrinkle repair and sand placement took several months.

Lessons Learned for Future Projects: Based on the available information, the following lessons can be learned from this case history:

- GM liners should be covered with a soil layer as soon as practicable after installation to reduce GM wrinkles and to protect the liner from damage. Placement of the soil layer should not cause the GM wrinkles to fold over; to that end, it may be necessary to place the soil during the cooler nighttime and early morning hours when the wrinkles are smaller.
- Liner systems should be constructed in manageable increments that ensure protection of the liner system materials under seasonal weather changes. In the case history described above, if the expansion had been constructed in several increments, the GM liner constructed in the winter would have likely been covered with the sand LCRS drainage layer by spring and would have been less wrinkled.

F-A.2.14 L-30

Problem Classification: landfill liner construction/construction
Region of U.S.: northeast
Waste Type: MSW
Reference: Koerner, G.R., Eith, A.W., and Tanese, M., "Properties of Exhumed HDPE Field Waves and Selected Aspects of Wave Management", *Proceedings of the 11th GRI Conference on Field Installation of Geosynthetics*, Geosynthetic Research Institute, Philadelphia, Pennsylvania, 1998, pp. 152-162e.

Problem Summary: large folded wrinkles in HDPE GM primary liner at two exhumed leachate sumps

Problem Description: When about 0.4 ha of previously-constructed liner system was exposed at two leachate sumps in an active double-lined landfill during construction of a landfill expansion, the 1.5-mm thick HDPE GM top and secondary liners on the side slope in the vicinity of the sumps were found to have large, folded wrinkles. The GM liners on the side slope were separated by a GN LDS drainage layer. The landfill liner system had been constructed in 1988, approximately eight years prior to the exhumation. GM wrinkles on the landfill side slope above the sumps were orientated diagonal to the crest of the 3H:1V side slope and converged in the sumps. Wrinkles were also more numerous and larger near the slope toe and near the sump than away from the slope toe and the sump. These wrinkles likely began to develop when the GM expanded during the day as temperatures increased and became folded as gravel was placed over the GM. As the wrinkles propagated down the slope during several days of temperature cycling, the wrinkles became more numerous and larger at the slope toe. Koerner et al. (1998) hypothesized that the diagonal wrinkle orientation was due to the original backfilling operation in the sump area. The backfill was placed from the toe of the slope upwards and outwards. They also suggested that the two riser pipes in the sump complicated backfilling and may have contributed to some of the localized GM movement and the resulting wrinkle pattern. The 50 to 800 mm high wrinkles had three

main configurations: (i) a vertically folded prayer wrinkle; (ii) a horizontally folded S-shaped wrinkle; and (iii) a mushroom-shaped wrinkle (i.e., a prayer wrinkle confined laterally and loaded vertically). At some of the wrinkle folds, the GM was observed to be yielding, as evidenced by the change in its color (i.e., it became lighter). These wrinkles were present even though the liner system had been carefully constructed with third-party CQA. The large wrinkles were not noticed prior to placement of a 540 g/m^2 needlepunched nonwoven GT cushion over the GM primary liner on the side slope. Furthermore, the sump and leachate riser pipe bedding gravel and the first 0.3 m of the 0.6-m thick gravel LCRS drainage layer were placed over the GT by a crane with a large bucket (typically used to place concrete) to reduce GM wrinkle development and propagation.

Samples of unwrinkled GM and wrinkled GM at folds were taken for laboratory testing. The wrinkled GM had yielded and was noted to be thinner than adjacent unyielded GM. Both wide width tensile tests (ASTM D 4885) and single point notched constant tensile load tests (ASTM D 5397) were conducted to assess the effect of the GM folding on GM integrity. Interestingly, all of the wrinkled GM samples failed at folds. Both the wrinkled and unwrinkled GM samples had wide width tensile properties at yield that met the project specifications and were not significantly different from one another. Wide width tensile properties at break could not be evaluated due to equipment limitations. All GM samples also had acceptable times to failure (i.e., greater than 200 hours) in the notched constant tensile load test. However, the wrinkled GM samples had a somewhat lower time to break than the unwrinkled samples (i.e., average of 1,033 to >1,823 hours for wrinkled samples and >2,300 hours for all unwrinkled samples).

It should be noted that wrinkling of GM liners may also be caused by downdrag of the GM by waste as it settles. However, the wrinkles associated with downdrag should be shorter and more numerous than those associated with thermal expansion. This can be explained based on wrinkle theory developed by Giroud (1994b). As a result of the bending associated with a GM wrinkle, there are two opposite forces at the base of the wrinkle. These forces must be balanced by the shear force that results from the settling waste and the interface friction between the GM and the material beneath it. For a given amount of GM elongation, as the shear force increases, the wrinkles become shorter and more numerous. The shear forces associated with settling waste (i.e., downdrag and the weight of the GM and waste) are greater that those associated with a GM alone. Thus, the difference in wrinkle appearance between wrinkles associated with thermal expansion (that develop under very small compressive stresses) and the wrinkles that develop under high compressive stresses.

Resolution: The wrinkled GM was removed when the sumps were reconstructed for the landfill expansion. Textured GM was installed on the side slope to increase the interface shear strength between the GM and underlying CCL, for the composite secondary liner, and between the GM and underlying GC LDS drainage layer, for the primary liner. As a result of increasing the interface shear strength, the wrinkles that developed on the side slope were less likely to propagate downslope. Interestingly,

Giroud (1994b) has shown analytically that GM wrinkles are shorter and spaced closer together when the shear strength between the GM and the underlying material is increased, which may result from using a textured GM and/or from increasing the normal stress.

Lessons Learned for Future Projects: Based on the available information, the following lessons can be learned from this case history:

- GM liners should be covered with a soil layer as soon as practicable after installation, but not during the hottest part of the day if the GM is significantly wrinkled, to reduce GM wrinkling as a result of the following two mechanisms: (i) thermal insulation provided by the soil layer reduces GM temperature variations that cause wrinkling; and (ii) the increase in interface shear strength resulting from the weight of the soil layer decreases the size of the wrinkles. A thick GT cushion is generally not sufficient to protect the GM from thermal effects.
- Placement of the soil layer should not cause the GM wrinkles to fold over. Prior to placing soil over a GM, the GM should be inspected for wrinkles. Excessive GM wrinkles and wrinkles that may fold over should be removed by waiting to backfill until the GM cools and contracts during the cooler nighttime and early morning hours, pulling the wrinkles out, or cutting the wrinkles out. The latter method is less desirable than the former methods because it requires intact GM to be cut, and it results in more GM seaming and subsequent testing.
- Using a textured GM on the side slopes has two beneficial effects: (i) it results in wrinkles that are smaller than in the case of a smooth GM; and (ii) it reduces the propagation of wrinkles down the side slopes. These two effects decrease the risk of the formation of very large wrinkles at the toe of side slopes.

F-A.3 Landfill Liner Degradation

F-A.3.1 L-2

Problem Classification: landfill liner degradation/design
Region of U.S.: southeast
Waste Type: MSW
Reference: Basnett, C.R. and Bruner, R.J., "Clay Desiccation of a Single-Composite Liner System", *Proceedings of Geosynthetics '93*, Vancouver, British Columbia, 1993, Vol. 3, pp. 1329-1340.

Problem Summary: desiccation cracking of CCL in exposed HDPE GM/CCL composite liner

Problem Description: Basnett and Bruner (1993) described the severe desiccation cracking of the CCL component of the composite liners for two sections (Section 1 and 2) of a landfill in Florida. The liner systems consist of the following components, from top to bottom:

- 0.6-m thick sand drainage layer;
- 1.5-mm thick HDPE GM liner;
- 0.3-m thick clayey sand CCL (maximum hydraulic conductivity of 1 x 10^{-9} m/s); and
- GT reinforcement layer.

Prior to installing the GM liner, desiccation cracking of the CCL was controlled by spraying it with water. Due to the potential for sliding and erosion of the sand on the 3 horizontal:1 vertical (3H:1V), approximately 14-m high, liner system side slopes, the sand drainage layer was only placed on the landfill base during construction. The design required that sand be placed incrementally up the side slopes during landfill operation, with the sand advancing ahead of the waste.

In 1988, near the end of construction of the Section 1 liner system, water was observed to be trapped between the GM liner and CCL at the slope toe. At that time, the water was attributed to rainwater that had flowed beneath the GM during installation. In 1991, construction of the Section 2 liner system began. When the GM panel in Section 1 was rolled back to allow the Section 2 CCL to be constructed into the CCL in Section 1, the Section 1 CCL on the side slope was observed to be severely desiccated. Cracks were about 25 mm wide and penetrated the full thickness of the CCL. To evaluate whether the desiccation was localized, the Section 1 CCL was inspected at 30 m from Section 2, about 2 m from the slope crest. Here the desiccation was also severe and the bottom surface of the overlying GM was moist. Construction of Section 2 continued and, similar to the Section 1 construction, water became trapped between the GM and CCL near the slope toe. About six weeks after liner installation, the water mounding in Section 2 was so significant that small weep holes were cut in the GM to drain the water. These holes were subsequently patched.

The observed phenomenon can be explained as follows. During the day, as the temperature of the liner system increases, water evaporates from the CCL and the air entrapped between the CCL and the GM becomes saturated with water vapor. During the night, as the temperature decreases, the ability of the entrapped air to contain water vapor decreases. As a result, a fraction of the vapor condenses into water and droplets of water appear against the lower face of GM since the GM is, then the coldest element of the system. If the droplets are small, surface tension prevents them from moving. If the droplets are large (i.e., if the evaporation-condensation mechanism is significant), gravity overcomes surface tension and water migrates downslope and accumulates at the toe of the slope. Therefore, progressively, the CCL moisture content decreases in the upper part of the slope and increases near the toe. To evaluate the mechanism, Basnett and Bruner (1993) collected CCL samples along a transect extending down the side slope in Section 1 and Section 2, and the samples were analyzed for moisture content. The Section 1 CCL, which was constructed with an average moisture content of about 22% along the transect, had average moisture contents of about 7% nearest the slope crest, 11% near midslope, and 24% near the slope toe. The moisture content was also observed to increase with depth at sampling locations on the upper portion of

the slope. Similar effects, though less extreme, were observed for the Section 2 CCL when it was sampled and tested at about two months after construction of the composite liner.

Resolution: At the time of the field study described by Basnett and Bruner (1993), Section 1 was filled to about 70% of its waste capacity, and its composite liner was covered with a sand drainage layer. Section 2 had an exposed liner system and had not yet accepted waste. No actions were required for Section 1 by the regulatory agency presumably because: (i) the older cell was almost filled and would be closed shortly afterwards; (ii) the repair would require that the waste be removed from the cell, which is extremely difficult, and costly; (iii) the CCL was only observed to be desiccated on the side slope; all other thing being equal, side slope liner holes are less detrimental than base liner holes because the head of leachate on the side slope is less than the head on the base slope; and (iv) environmental impacts from the potential for increased liner leakage are expected to be negligible given that the liner includes a GM. Until it is covered and thermally insulated with the sand drainage layer, the Section 2 CCL on the side slopes will likely continue to lose moisture and crack.

Lessons Learned for Future Projects: Based on the available information, the following lesson can be learned from this case history:

- Composite liners constructed with a CCL should be covered to prevent heating and desiccation of the CCL. EPA cautions that temporarily using a GM alone over a CCL may be problematic and indicates that a light-colored GM may be preferable (Daniel and Koerner, 1993).

F-A.3.2 L-4

Problem Classification: landfill liner degradation/operation
Region of U.S.: northeast
Waste Type: HW
Reference: Adams, F.T., Overmann, L.K., and Cotton, R.L., "Evaluation and Remediation of a Fire Damaged Geosynthetic Liner System", *Proceedings of Geosynthetics '97*, Long Beach, California, 1997, Vol. 1, pp. 379-392.

Problem Summary: HDPE GM/CCL composite liner damaged by waste fire

Problem Description: Adams et al. (1997) described the impact of a waste fire on a double-liner system for an active HW landfill containing industrial waste sludges and other chemical manufacturing by-products. The fire was caused by a chemical reaction of one of the materials disposed of in the landfill and located within several meters of the liner system. Based on temperature measurements made near the fire, Adams et al. (1997) concluded that the temperature in the vicinity of the liner system may have approached 800°C. After the fire was discovered, it took about 11 months to contain and finally extinguish it. The fire was controlled by installing hundreds of 50-mm

diameter steel pipes into the affected waste at approximately 0.8 m spacings and recirculating leachate through the pipes to cool the waste.

After the fire was put out, waste was excavated over the portion of the landfill believed to be affected by the fire. About 300 m^2 of liner system on the landfill side slope was obviously damaged based on visual inspection. Nearer the center of the affected area, damage was most severe, as evidenced by the melting and disintegration of the liner system geosynthetics and desiccation cracking of the CCL component of the composite secondary liner. Nearer the boundary of the affected area, the geosynthetics appeared rippled and stretched.

Resolution: The damaged liner system components were identified, removed, and replaced with new materials. The extent of damage to the CCL component of the composite secondary liner was defined by visual inspection and hydraulic conductivity testing of CCL samples. Near the center of the impacted area, the entire 0.9-m thickness of the CCL was desiccated. Here, the hydraulic conductivity of the CCL samples was about two to three orders of magnitude greater than that measured for samples collected during CCL construction. As the distance from the center of the impacted area increased, the thickness of CCL affected by the fire decreased, defining a bowl-shaped region of CCL impact. The desiccated CCL was removed and replaced. With respect to the HDPE GM primary liner and the HDPE GM component of the composite secondary liner, the extent of damage was defined by visual inspection and the results of laboratory testing of GM samples. GM samples were taken along the perimeter of the area that appeared to be damaged and tested for thickness, density, melt flow index, tensile strength at break, and tensile elongation at break. Samples were required to meet the original project specifications for these tests. If a sample did not meet the specifications, another sample was cut near the failing sample, but further from the area with visible damage. The process was repeated until an area bounded by samples that met the specifications could be defined. The GM within this area was removed and replaced.

Lessons Learned for Future Projects: Based on the available information, the following lessons can be learned from this case history:

- Geosynthetics and CCLs can be severely damaged by intense heat. In the case history described above, the estimated maximum liner system temperature of 800°C was high enough to melt the geosynthetics and desiccate the entire thickness of CCL.
- Landfills should be operated to minimize the potential for waste fires. Measures to be taken could include not depositing loads of hot waste in a landfill and covering waste with a soil cover to decrease waste access to oxygen.

A.3.3 L-12

Problem Classification: landfill LCRS or LDS operation/design

Region of U.S.: northeast
Waste Type: MSW
Reference: unpublished

Problem Summary: leachate extraction well installed in landfill appeared to puncture GM primary liner

Problem Description: A deep, 100-mm diameter leachate extraction well was installed in a double-lined landfill after the LCRS appeared to be clogged. The well design called for the well to extend into the sand LCRS drainage layer over the GM primary liner (i.e., extend within 0.3 m of the liner), but the elevation of the top of the borehole was not surveyed immediately before well installation. With waste settlement under its own weight and the weight of the drill rig, the target borehole depth may have been too deep. Following well installation, average LDS flow rates increased from about 300 lphd to 400 lphd, and it was suspected that the well had penetrated the GM primary liner. The well design called for the well to be installed within 0.3 m of the liner, but the elevation of the top of the well boring was not surveyed immediately before well installation. Considering waste settlement (under its own weight and the weight of the drill rig) since the previous survey of the landfill, the target boring depth may have been too deep.

Resolution: No action has been taken with respect to the potential puncture of the GM primary liner because it is not clear if the primary liner was actually punctured and the LDS flow rates have remained relatively low. Environmental impacts from this possible GM hole are expected to be negligible.

Lessons Learned for Future Projects: Based on the available information, the following lessons can be learned from this case history:

- Care should be taken to not damage the liner when drilling into landfilled waste. Settlement of the waste surface must be taken into account when selecting the depth of drilling, and boreholes should not extend close (e.g., within 1 m) to the liner.

F-A.3.4 L-14

Problem Classification: landfill liner degradation/construction
Region of U.S.: northeast
Waste Type: MSW
Reference: unpublished

Problem Summary: HDPE GM liner damaged by fire believed to be started by lightning strike

Problem Description: As the CQA consultant was completing paperwork in a trailer at a landfill construction site, he observed black smoke coming from the landfill. At the time, there was a thunderstorm, and the contractor had left the site. When the CQA

consultant arrived at the landfill, he found rolls of GC drainage layer (HDPE GN and polyester GT) on fire. The GC rolls had been unbagged and were lined up on the installed HDPE GM liner at the top of the side slope, parallel to the slope crest, in preparation for deployment the next day. The fire was attributed to lightning, and presumably propagated from one roll to another. Though there were no eyewitnesses to this, the thunderstorm was large and was said to have more lightning strikes than any previous storm in the area.

Figure F-A.3.1. GC rolls at the top of a liner system side slope caught fire (potentially due to a lightning strike) and damaged the underlying GM.

The authors are not aware of other instances where a geosynthetics fire was started by lightning. Part of this is likely due to the properties of the polymers themselves. Many polymers do not burn easily and some are self-extinguishing.

Resolution: The fire was extinguished and the GM liner and GC rolls were inspected for damage. GC rolls that had caught on fire and GM that was melted, scorched, or rippled was removed and replaced with new materials.

Lessons Learned for Future Projects: Based on the available information, the following lessons can be learned from this case history:

- The igniting of geosynthetics by lightning is a rare occurrence. The authors of this appendix are not aware of other instances of this.
- It is not surprising that the fire spread after the GN ignited. The GN and GM were manufactured from polyethylene, a polymer that burns easily and is not self-extinguishing.

F-A.3.5 L-20

Problem Classification: landfill liner degradation/construction
Region of U.S.: northeast
Waste Type: MSW
Reference: unpublished

Problem Summary: saturation of GCL beneath GM liner when rainwater ponded on tack-seamed patch over GM hole

Problem Description: During construction of a 2.4 ha double-lined landfill cell, water ponded over the GM/GCL composite primary liner on the base of the cell after a significant storm (i.e., more than 50 mm). At one patch, which was tack seamed over a GM hole, water flowed beneath the patch, through the hole, and beneath the GM liner. About 1.4 ha of GCL beneath the GM became saturated. Within this zone of saturation, the GCL was swollen and soft. (Note: a tack seam is intended to hold a patch into place prior to seaming; a tack-seamed patch is only bonded to the GM in some spots and is not sealed at its periphery.)

Resolution: The water was pumped out of the cell, the GM liner was cut to expose the swollen, saturated GCL, and the damaged GCL was removed. New GCL was placed, and the GM primary liner was repaired.

Lessons Learned for Future Projects: Based on the available information, the following lessons can be learned from this case history:

- To the extent practicable, holes in GM liners installed over GCLs should be repaired as soon as possible to avoid hydration of the GCL due to rainfall. Holes located in areas where rainwater may pond should be patched first. The patches should be sealed with a permanent seam and not only tack-seamed.
- When a GM is placed over a GCL, the GM should be covered with soils as soon as possible to minimize swelling of the GCL in case of hydration.

F-A.3.6 L-43

Problem Classification: landfill liner degradation/construction
Region of U.S.: northeast
Waste Type: HW
Reference: unpublished

Problem Summary: water ponded between HDPE GM and CCL components of composite secondary liner and was contaminated from a source other than the landfill

Problem Description: Construction of a 3.0 ha double-lined landfill cell was completed in July 1993. The cell was constructed in an excavation through an approximately 14 m deep glacial till layer and into an approximately 4 m thick clay layer that overlies bedrock. The shallow groundwater table is contained within the glacial till layer, and the excavation had to be dewatered during construction. The constructed cell has approximately 12 m high, 3H:1V side slopes. The cell liner system on the base consists of the following components from top to bottom:

- 0.3-m thick sand LCRS drainage layer;
- HDPE GM/0.9-m thick CCL composite primary liner;
- 0.3-m thick sand layer LDS drainage layer; and
- HDPE GM/3-m thick CCL composite secondary liner.

On the side slopes, the liner system consists of the following components from top to bottom:

- sacrificial GT;
- GC LCRS drainage layer;
- HDPE GM primary liner;
- GN LDS drainage layer; and
- HDPE GM/2-m thick CCL composite secondary liner.

The clay used to construct the CCLs was classified as a CH material in accordance with the Unified Soil Classification System and had a liquid limit in the range of 29 to 31% and a plasticity index in the range of 13 to 15%.

By September 1994, a large isolated bubble of water had developed between the GM and CCL components of the composite secondary liner at the slope toe at the southwest corner of the cell, which had not yet received waste. The bubble was located along the southern exposure of the cell, which receives the most solar radiation throughout the day, and extended about 3 m along the toe. Although the cell base by the bubble was graded inwards towards the center of the cell, the bubble did not extend into the base liner system because of the overburden pressure provided by the soil layers above the secondary liner. The water was pumped from the bubble, chemically analyzed for organic constituents and metals, and found to be clean. About 16,000 L of water were pumped from the bubble, and the liner system perforations made on the side slope to examine the bubble were repaired.

In the spring of 1995, a small water bubble had developed at the same location. About 300 L of water were removed from the bubble, and the liner system was repaired. Since the bubble was relatively small and the water removed the prior year from the

large bubble was clean, the water removed from the small bubble was not chemically analyzed.

By June 1996, a water bubble had developed at the same location as the earlier bubbles and a smaller bubble had developed at the slope toe about 2 m from the first bubble. By this time, about 70% of the cell had been filled with waste and the toe of the intermediate waste slope was located about 3 m from the bubbles. About 4,000 L of water were pumped from the bubbles and chemically analyzed for organic constituents and metals. While the metal concentrations of the bubble water were consistent with those for clean water, the bubble water contained organic constituents, including benzene. Subsequently, an extensive testing program was undertaken to determine the source of the water and the contamination.

Resolution: A testing program was developed to evaluate the following potential sources of the bubble water and/or the contamination:

- leachate from the landfill;
- groundwater;
- surface water;
- fuel from construction equipment; and
- water used to construct the CCL.

Each of these sources is discussed below.

The source of the water and contamination is not leachate from the landfill. The landfill leachate chemistry is different from the bubble water chemistry. The leachate has higher metal concentrations and more organic constituents than the bubble water. Also, the benzene concentration of the bubble water is higher than that of the landfill leachate. Also, no organic constituents have been detected in water from the LDS of the landfill, indicating that leachate has not migrated through the cell primary liner.

Groundwater does not appear to be the source of the bubble water or contamination. The inorganic and organic chemistry of the shallow groundwater collected from three wells installed in the glacial till layer upgradient of the bubbles is different from the bubble water chemistry. The groundwater does not contain organic constituents, so it does not appear to be the source of the organic contamination. Furthermore, when the upper 150-mm of the CCL at the bubble was tested for contamination, the highest degree of contamination was detected in the top 50 mm, and no contamination was found in the bottom 50 mm. This suggests that the contamination is migrating outward rather than inward with groundwater.

Surface-water runoff flowing over the CCL after the CCL was constructed may be a source of the contamination. The organic constituents found in the bubble liquid were also historically present at a nearby former oil facility. However, the pathway for runoff flow from the oil facility to the landfill has not yet been established. If runoff

contaminated the CCL during construction, the contamination was not widespread since the liquid found in the initial bubble in 1994 was clean. The CCL contamination may have been upslope of the bubble area and may have migrated downslope into bubble area over time as the CCL lost water due to thermal effects.

Another possible source of the bubble liquid contamination is fuel from construction equipment. It may be that some fuel from construction equipment or a generator dripped on the CCL upslope of the bubble area during construction or during the repair of the liner system after the first bubble was found. The CCL contamination may have migrated downslope into bubble area over time as the CCL lost water due to thermal effects.

The source of the water in the bubble appears to be from the CCL. As waste was placed on the CCL, the CCL consolidated under the weight of the overlying soil layers and waste, squeezing water from the CCL. Some of this water may have flowed between the GM and CCL along wrinkles to southeast and southwest corners of the cell. Very large 1 m high wrinkles were observed in the GM liner on the cell base at the slope toe prior to placement of the LDS drainage layer. In addition, since the CCL component of the secondary liner on the side slope was not thermally insulated by an overlying soil layer, the CCL may have lost water due to thermal effects. Furthermore, the inorganic chemistry of the LDS liquid and the bubble water are similar, suggesting that source of the bubble water, like the LDS liquid, was the CCL. The consolidation characteristics and pore water chemistry of the CCL component of the composite secondary liner are currently being investigated so that more definitive conclusions on the source of the bubble water can be drawn.

The bubble water was tested in September 1996 and found to be clean. The liner system will be repaired at the conclusion of the investigation.

Lessons Learned for Future Projects: This case history is complex, and there are several conditions that may have contributed to the development of bubbles of contaminated water at the slope toe. Based on the available information, the following lessons can be learned from this case history:

- Composite liners constructed with a CCL should be covered to prevent heating and desiccation of the CCL, which can lead to the ponding of water between the CCL and overlying GM. EPA cautions that temporarily using a GM alone over a CCL may be problematic, and that a light-colored GM may be necessary (Daniel and Koerner, 1993).
- GMs should be covered with soil layers as soon as practicable after installation, but not during the hottest part of the day if the GM is significantly wrinkled, to reduce GM wrinkles.
- During construction of liner systems, runon should be controlled so that it does not contact, and potentially contaminate, the liner.

- Construction equipment should be inspected for fuel and oil leaks, and those leaks should be repaired prior to using the equipment in liner construction to avoid liner contamination.

F-A.3.7 L-44

Problem Classification: landfill liner degradation/design
Region of U.S.: northcentral
Waste Type: MSW
Reference: unpublished

Problem Summary: landfill gas well punctured GM component of composite liner

Problem Description: During installation of gas extraction wells in a active landfill, one of the 0.9-m diameter boreholes for the wells was advanced into the composite liner. At the location of this localized damage, the top of the liner is approximately 18 m below the waste surface. The problem was identified when portions of the liner system were observed in the cuttings from the bucket auger. Based on observations by field personnel, the bucket auger extended through the 0.6-m thick soil protection layer, GC LCRS drainage layer, and 2.0-mm thick HDPE GM liner and into the upper 0.15-m of the 0.9-m thick CCL. Upon observing these components in the auger cuttings, field personnel poured bentonite pellets into the bottom of the borehole to create an approximately 0.9-m thick bentonite seal at the borehole base. The top of the borehole was then temporarily covered with plywood until the potential environmental impact of the liner damage and the need for additional liner remediation could be evaluated. When the cause of the problem was investigated, it was discovered that a typographic error had been made on the design drawing for the gas extraction system: the specified borehole depth at the location of the liner damage was greater than the depth to the top of the liner.

Resolution: An evaluation of the liner damage found the potential environmental impact from the damage to be negligible. The damaged liner is located in an upgradient portion of the cell, and the portion of the LCRS that might drain to this area is very small. Due to the small drainage area and the high transmissivity of the GC LCRS drainage layer, the leachate head on the damaged liner should be small. Also, the damaged area has been filled with low-permeability bentonite and is underlain by a relatively thick natural low-permeability soil layer. Irrespective of this, the landfill owner has proposed to repair the liner system. The proposed remedy for this involves advancing a 3-m diameter steel access shaft to the top of the protection layer over the damaged liner, excavating the waste in the shaft, exposing the damaged portion of the liner system, and repairing each damaged liner system component. This remedy has not yet been implemented.

Lessons Learned for Future Projects: Based on the available information, the following lessons can be learned from this case history:

- Care should be taken to not damage the liner system components when drilling into landfilled waste. To prevent damage, boreholes should not extend close to the liner.

F-A.4 Landfill LCRS or LDS Construction

F-A.4.1 L-10

Problem Classification: landfill LCRS or LDS construction/construction
Region of U.S.: northeast
Waste Type: MSW
Reference: unpublished

Problem Summary: rainwater entered LDS through anchor trench

Problem Description: Flow rates from the LDS of a newly constructed landfill cell ponded with rainwater were higher than expected, on the order of 500 lphd. The double-liner system for the cell includes a GM primary liner on the side slope, GM/GCL composite primary liner on the base, and GC LDS drainage layer on the side slope and base. With these components, the LDS flow from the cell is primarily attributed to leakage through the GM primary liner on the side slope. An electrical leak location survey and a gas tracer leak location survey were performed to locate GM primary liner holes on the base and side slope of the cell, respectively. Several small GM punctures and an approximately 1.1-m long tear were found on the side slopes near the toe. The tear was located under a rubsheet placed beneath the gravel side slope toe drain. The CCL beneath the tear had a 25 to 50 mm deep depression. The large hole is believed to have been caused by a bulldozer blade during construction of the gravel toe drain. The holes were repaired; however, the LDS flow rate did not show significant decrease. Subsequently, the liner system anchor trench at the top of the approximately 9-m high and 4.6-m wide perimeter berm was inspected and found to be full of water. The anchor trench had been backfilled with the sandy site soil, in accordance with the plans. This soil allowed significant water to infiltrate and pond on the geosynthetics, including the GC LDS drainage layer. The GC was conveying water that had infiltrated the anchor trench into the LDS.

Resolution: Sections of the back of the anchor trench were excavated to the outer slope of the perimeter berm at 8 m intervals along the length of the trench, and the ends of the geosynthetics in the trench sections were laid horizontal. The perimeter berm was reconstructed to grade with gravel. This allows water infiltrating the trench to drain to the outside slope of the perimeter berm. To minimize infiltration of rainwater into the anchor trench, a GM was placed over the top of the berm and covered with a 0.3-m thick layer of site soil. After construction of this redesign was complete, the LDS flow rate decreased to less than 100 lphd.

Lessons Learned for Future Projects: Based on the available information, the following lesson can be learned from this case history:

- Geosynthetic anchor trenches should be backfilled with low-permeability soil and the soil should be well compacted. If this is not practicable, the anchor trenches should be designed to drain freely and/or covered with a barrier, such as the GM used in the case history described above. In addition, the ground surface should be graded away from the trenches to reduce runon from infiltrating into the trenches.

F-A.4.2 L-15

Problem Classification: landfill LCRS or LDS construction/construction
Region of U.S.: southeast
Waste Type: MSW
Reference: unpublished

Project Description: sand bags in LCRS drainage layer and debris in LCRS pipe trench approved by CQA consultant

Summary: During construction of a landfill liner system, the contractor used sand bags to secure the GM liner. The sand used to fill the bags met the project specifications for the LCRS drainage layer material. After GM installation was completed, the contractor placed the sand LCRS drainage layer over the sand bags. The contractor also occasionally disposed of debris, such as food waste and aluminum cans, in the LCRS pipe trench gravel. The LCRS was inspected by site CQA personnel and found to be acceptable.

Resolution: Regulatory personnel who inspected the site required the sand bags and debris to be removed from the LCRS.

Lessons Learned for Future Projects: Based on the available information, the following lesson can be learned from this case history:

- CQA personnel should be trained in standard CQA practices, such as keeping the LCRS free of items and debris that may potentially impede the flow of leachate. In the case history described above, the sand in the sand bags met the project specifications for the LCRS drainage layer material. However, the sand was wrapped in a woven bag that may impede flow. In addition, there were numerous bags in the LCRS. While leachate in the LCRS drainage layer can easily flow around one bag, flow may be impeded if there are numerous bags. Consequently, it is good practice to keep sand bags out of the LCRS. Alternatively, if the sand in the bags meets the project specifications for the overlying drainage layer material, the bags can be cut and the sand left in place.

F-A.4.3 L-16

Problem Classification: landfill LCRS or LDS construction/construction
Region of U.S.: southcentral
Waste Type: HW
Reference: Bonaparte, R. and Gross, B.A., "*LDCRS Flow Rate from Double-Lined Landfills and Surface Impoundments*", EPA Risk Reduction Research Laboratory, Cincinnati, OH, EPA/600/SR-93/070, 1993, 65 p. (Landfill cells T-7 and T-8)

Problem Summary: rainwater entered LDS through anchor trench

Problem Description: About two years after construction, the LDS flow rates from two double-lined cells increased from about 30 and 120 lphd to 220 and 840 lphd, respectively. The side slope liner system for the cells includes GN LCRS and LDS drainage layers and a GM primary liner. The base liner system includes a gravel LCRS drainage layer, GN LDS drainage layer, and GM/CCL composite primary liner. Based on the liner system components and the results of chemical analyses of LDS flow, water in addition to that squeezed from the CCL as it compresses appeared to be entering the LDS. The anchor trench for the cells was inspected and found to contain ponded water. The anchor trench was not initially well compacted. Over time, the anchor trench soil settled and a depression developed over the anchor trench. The depression trapped runoff, which subsequently infiltrated into the trench. The GN LDS drainage layer in the anchor trench was conveying this water into the LDS.

Resolution: The anchor trench soil was removed, and the trench was allowed to dry. The soil was recompacted into the trench and graded to drain away from the trench. Shortly afterwards, LDS flow rates for the two cells decreased to 70 and 120 lphd, respectively.

Lessons Learned for Future Projects: Based on the available information, the following lesson can be learned from this case history:

- Geosynthetic anchor trenches should be backfilled with low-permeability soil and the soil should be well compacted. If this is not practicable, the anchor trenches should be designed to drain freely and/or covered with a barrier. In addition, the ground surface should be graded away from the trenches to reduce runon from infiltrating into the trenches.

F-A.4.4 L-28

Problem Classification: landfill LCRS or LDS construction/construction
Region of U.S.: southeast
Waste Type: MSW
Reference: unpublished

Project Summary: excessive needle fragments in manufactured needlepunched nonwoven GT

Problem Description: During construction of an 8 ha single-composite lined landfill cell in 1993, numerous broken needles were found in the needlepunched nonwoven GT filter placed over the GN LCRS drainage layer. The quantity of needle fragments was abnormal (i.e., about 150/ha) and resulted from a GT production problem at the manufacturing plant. Though the project specification for the GT did not require the manufacturer to check for needles, it was the state of practice for manufacturers at the time. By the time the needle problem was discovered by the CQA consultant, about 5 ha of GT had been deployed. About 3 ha of this GT had already been covered by a 0.3-m thick soil protection layer.

Resolution: The contractor initially tried to fix the GT that had been deployed and not covered with soil by manually searching for and removing needle fragments. However, most of this GT was replaced with GT from a different manufacturer because the needle fragment density was very high. The contractor also tried to locate broken needles in the GT beneath the soil layer using a metal detector. However, this method of needle fragment detection proved to be unreliable. At this point the contractor was unsure how to proceed: both removing the soil to expose the defective GT and leaving the defective GT in place could potentially result in GM damage. To evaluate the potential for needle fragments to extend through the GN LCRS and puncture the underlying 1.5-mm thick HDPE GM, laboratory tests were conducted to evaluate GM puncture by needle fragments of different lengths and orientations. Of the ten laboratory tests with 192 needle fragments, only one needle fragment punctured the GM. These results were used, along with the probability distribution of needle fragment sizes and orientations observed in a sample of the GT, to estimate the probability of GM puncture. Based on the results of the analysis, the expected GM holes caused by the needle fragments would be very small and would occur infrequently. The defective GT was left in place beneath the soil layer because it appeared that there was less potential for GM damage by leaving the GT in place than by excavating the overlying soil to remove the GT. The manufacturer of the defective GT installed magnets in the manufacturing plant to remove broken needles from GTs produced in the future.

Lessons Learned for Future Projects: Based on the available information, the following lessons can be learned from this case history:

- Project specifications for needlepunched nonwoven GTs should require that the GTs be needle-free and should require a certification from the manufacturer attesting to this.
- The CQA Plan should require that deployed GTs near GMs be inspected for needles before the GTs are covered with overlying materials.
- Even with excessive needles in the GT, if the GM is separated from the GT by a GN, few needles are expected to puncture the GM.

Figure F-A.4.1. Manually searching for needle fragments in an installed GT.

Figure F-A.4.2. Many needle fragments were found in the deployed GT.

F-A.4.5 L-32

Problem Classification: landfill LCRS or LDS construction/construction
Region of U.S.: southeast
Waste Type: MSW
Reference: unpublished

Problem Summary: HDPE LCRS pipe separated at joints

Problem Description: The condition of the LCRS pipes at an active 19 ha single-lined landfill cell is surveyed for clogging and damage on an annual basis by running a small video camera through the pipes. The pipes are 200-mm diameter smooth wall HDPE. The pipes were supplied in 6.1 m lengths and connected in the field by fusion seaming the ends together. The CQA of the pipe installation consisted primarily of visual inspection. The pipes are bedded in gravel wrapped with a GT filter.

During the initial video conducted after the landfill was constructed, several pipe joints were found to be separated less than 10 mm and one joint appeared to be crushed over a length of about 0.6 m. Two subsequent annual surveys have revealed no further separation in the pipe joints or pipe crushing over time. The reason for this pipe separation is unclear. It may be that the pipes were never seamed together during construction or that the quality of some of the pipe seams was so poor that the seams failed during construction. The crushed pipe may have been damaged by equipment trafficking over it during construction or operation.

Resolution: No action has been required by the regulatory agency presumably because: (i) leachate flowing out of the pipe at an open pipe joint can still flow to the leachate sump (though the localized head at the open joint may be somewhat higher that those upgradient and downgradient of the open joint); (ii) the pipe condition has remained unchanged during subsequent annual videos; (iii) repair of LCRS pipes after waste placement would be extremely difficult and expensive; and (iv) environmental impacts from having a localized higher head on the liner at the open pipe joints are expected to be negligible. The pipes will continue to be surveyed on an annual basis.

Lessons Learned for Future Projects: Based on the available information, the following lesson can be learned from this case history:

- The CQA consultant should verify that all connections required for adjacent LCRS and LDS pipes have been made. When the pipe is connected by butt fusion seaming, the seam should be inspected for holes.

There is little available information for this case history; additional lessons might have been learned if the information had been complete.

F-A.4.6 L-33

Problem Classification: landfill LCRS or LDS construction/construction
Region of U.S.: southeast
Waste Type: MSW
Reference: unpublished

Problem Summary: HDPE LCRS pipe separated at joints

Problem Description: The condition of the LCRS pipes at an active 32 ha single-lined landfill cell is surveyed for clogging and damage on an annual basis by running a small video camera through the pipes. The pipes are 200-mm diameter smooth wall HDPE. The pipes were supplied in 6.1 m lengths and connected in the field by fusion seaming the ends together. The CQA of the pipe installation consisted primarily of visual inspection.

During the initial video conducted after the landfill was constructed, about 10 pipe joints were found to be separated less than 10 mm. Subsequent annual surveys have revealed no additional pipe joint separations over time. The reason for the separation of some pipe segments is unclear. It may be that the quality of some of the pipe seams was so poor that the seams failed during construction.

Resolution: No action has been required by the regulatory agency presumably because: (i) leachate flowing out of the pipe at an open pipe joint can still flow to the leachate sump (though the localized head at the open joint may be somewhat higher that those upgradient and downgradient of the open joint); (ii) the pipe condition has remained unchanged during subsequent annual videos; (iii) repair of LCRS pipes after waste placement would be extremely difficult and expensive; and (iv) environmental impacts from having a localized higher head on the liner at the open pipe joints are expected to be negligible. The pipes will continue to be surveyed on an annual basis.

Lessons Learned for Future Projects: Based on the available information, the following lesson can be learned from this case history:

- The CQA consultant should verify that all connections required for adjacent LCRS and LDS pipes have been made. When the pipe is connected by butt fusion seaming, the seam should be inspected for holes.

There is little available information for this case history; additional lessons might have been learned if the information had been complete.

F-A.5 Landfill LCRS or LDS Degradation

F-A.5.1 L-9

Problem Classification: landfill LCRS or LDS degradation/design
Region of U.S.: northeast
Waste Type: MSW
Reference: unpublished

Problem Summary: erosion of sand LCRS drainage layer on liner system side slopes

Problem Description: Portions of the 0.6-m thick sand LCRS drainage layer on the approximately 100-m long, 4H:1V side slopes of this landfill were progressively eroded by rain. The sand has a specified minimum hydraulic conductivity of 1×10^{-4} m/s and maximum fines content of 5%. Based on the particle size analyses conducted on the sand as part of CQA conformance testing, the areas with the most erosion tended to have been covered with sand containing the most fines (i.e., almost 5%). The erosion has resulted in 0.3-m wide gullies that propagate from the toe of the side slopes upward. Sand has also washed into the exposed gravel around the LCRS pipes and in the sump area. By one year after construction, the sand had been pushed back up the side slopes with low ground-pressure bulldozers more than six times and the gravel in the sump area of two cells that had not yet received waste had been replaced twice. It is anticipated that the two cells will not receive waste for at least another two years.

Resolution: A plastic tarp has been purchased to place over the sand on the approximately 2.4 ha of side slopes in the two inactive cells. However, the tarp has not yet been installed because of concerns with how to anchor the tarp and protect it from uplift by wind. In the meantime, the owner is considering other option: covering the sand with yard compost. Waste has been placed on the side slope of the one active cell, and protection of the sand is not needed.

Lessons Learned for Future Projects: Based on the available information, the following lessons can be learned from this case history:

- Erosion of soil layers on liner system side slopes should be anticipated and dealt with in design. In areas where the potential for erosion is relatively high, erosion control structures (e.g., runoff diversion berms, silt fence) can be used to reduce the need for intensive maintenance of the soil layers. Alternatively, the soil layers can be covered with a tarp or temporary erosion control mat.
- Better methods for protecting exposed soil layers on liner system side slopes or alternatives to these soil layers are needed.
- Though it may be less costly for the owner to construct several landfill cells at once, this can leave new cells exposed to the environment for a significant time period. These cells will experience more erosion than cells filled sooner and will have more opportunity for liner damage. Additionally, every time an eroded soil layer is pushed

back up the side slopes there is an opportunity for the underlying liner system materials to be damaged by construction equipment.

- Post-construction plans should be developed for portions of landfills that may sit idle for an extended period of time. The plans should include procedures describing how the liner system should be maintained prior to operation.

F-A.5.2 L-11

Problem Classification: landfill LCRS or LDS degradation/design
Region of U.S.: northeast
Waste Type: MSW ash
Reference: unpublished

Problem Summary: erosion of sand protection layer on liner system side slopes

Problem Description: Portions of the 0.45-m thick sand protection layer on the side slopes of a landfill liner system were progressively eroded by runon and runoff. The side slopes of the landfill were constructed over an existing MSW landfill; the base slopes were constructed on natural ground. With each significant rainfall, the sand on

Figure F-A.5.1. Erosion of sand protection layer on liner system sideslopes.

the side slopes was eroded by runon from the adjacent existing MSW landfill cover system and runoff at locations on the slopes where flow was concentrated. Runon from the existing landfill occurred because the contractor had not completed or maintained the surface-water drainage system. Runon from the existing landfill also carried topsoil onto the sand protection layer. The 2.5H:1V cell side slopes are broken into approximately 18 m long segments by benches that slope into the landfill. Water collected on a bench primarily infiltrates through the sand protection layer to the GC LCRS drainage layer. However, because the sand hydraulic conductivity is not high enough to allow all of the water to infiltrate (i.e., the specified minimum hydraulic conductivity is 1 $x10^{-5}$ m/s), some of the water also flows across the bench and along the bench to a low point. At this low point, concentrated runoff flows across the bench and down a side slope, and erosion of the sand was most pronounced. In two areas where the protection layer had eroded, the underlying GC LCRS drainage layer, GM primary liner, GN LDS drainage layer, and GM component of the composite secondary liner were uplifted by landfill gases.

Resolution: The remedy developed required: (i) control of runon from the adjacent MSW landfill; and (ii) control of runoff on the side slopes of the landfill under construction. To control runon from the adjacent MSW landfill, small diversion berms were constructed around the landfill side slopes. In addition, hay bales, silt fence, and erosion mat were used to control erosion of cover system soils and subsequent sedimentation and overtopping of runon-control swales. To manage runoff, a riprap-lined downchute was constructed over the sand at the low area on the side slopes where concentrated runoff occurred. The sand protection layer was restored on the side slopes.

Lessons Learned for Future Projects: Based on the available information, the following lessons can be learned from this case history:

- Erosion of soil protection layers on liner system side slopes should be anticipated and dealt with in design. The potential for erosion can be reduced by grading the liner system to avoid concentrated runoff and using a relatively permeable soil in the protection layer. In areas where the potential for erosion is relatively high, erosion control structures (e.g., runoff diversion berms, silt fence) can be used to reduce the need for intensive maintenance of soil protection layers. Alternatively, protection layers can be covered with a tarp or temporary erosion control mat.
- Runon into active waste containment systems from adjacent areas must be controlled. In fact, this is a regulatory requirement for MSW landfills and HW landfills and impoundments.
- When a landfill is constructed on top of an existing landfill (vertical expansion), exposed GM liners can be uplifted by gases from the underlying landfill. Therefore, in the case of a vertical expansion, unless gases from the underlying landfill are well controlled, GMs must be covered by a layer of soil to prevent GM uplift and precautions must be taken to prevent erosion of this soil layer.

F-A.5.3 L-13

Problem Classification: landfill LCRS or LDS degradation/construction
Region of U.S.: southeast
Waste Type: MSW
Reference: Tisinger, L.G., Clark, B.S., Giroud, J.P., and Christopher, B.R., "Analysis of an Exposed Polypropylene Geotextile", *Proceedings of Geosynthetics '93*, Vancouver, British Columbia, 1993, pp. 757-771.
Tisinger, L.G., Clark, B.S., Giroud, J.P., and Schauer, D.A., "Performance of Nonwoven Geotextiles Exposed to a Semi-Tropical Environment", *Proceedings of Fifth International Conference on Geotextiles, Geomembranes, and Related Products*, Singapore, 1994, pp. 1223-1226.

Problem Summary: polypropylene continuous filament nonwoven GT filter degraded due to outdoor exposure

Problem Description: Tisinger et al. (1993, 1994) described the degradation of an exposed 540 g/m^2 polypropylene continuous filament nonwoven GT filter over a GN LCRS drainage layer. The site is located in a semi-tropical environment with high ambient temperatures up to 38°C, humidity, sun, wind, and rain. The design called for the GT to be covered with a sand protection layer just before waste placement. This required the GT to be exposed for at least several months. This strategy was selected because the local sand proposed for the protection layer was very erodable and would require significant maintenance if left exposed. The manufacturer's recommendation for maximum outdoor exposure time of the GT was 500 hours (20 days). Though a 270 g/m^2 GT met the project specifications, a heavier 540 g/m^2 GT was selected, anticipating that this GT would retain enough strength after several months of exposure to meet the specifications.

During construction, it became apparent that waste placement would be delayed and the GT exposure would be on the order of six months or more. Because some deterioration was expected until the sand protection layer could be placed, samples of the GT were periodically tested to verify that the strength properties of the GT still met specifications. Samples tested after 4.5 months of exposure exhibited no significant changes in properties. However, after 6.5 months of exposure, significant degradation of the GT was found. Grab, tear, and puncture strengths had decreased by 22.9, 34.0, and 24.1%, respectively; the change in burst strength was insignificant. Even with this degradation, the GT still met the specifications and approval was given to start placement of the sand protection layer. A few days later, before sand was placed, holes were observed in the GT in two areas near the side slope crest of one of the perimeter berms. The holes ranged in size from 20 to 200 mm. No holes were observed on the side slopes or base. GT samples collected at this time had grab, tear, puncture, and burst strengths that were 62.6, 64.9, 48.2 and 57.4%, respectively, less than their pre-exposure values. The rate of GT degradation had increased substantially, and the GT burst strength of 1,793 kPa did not meet the specified value of 2,000 kPa. Based on

differential scanning calorimetry, infrared spectrophotometry, and microstructural analyses of the GT, GT degradation was attributed to heat and ultraviolet radiation. All possible mechanisms of hole formation were reviewed and it was concluded that the holes had probably developed in the degraded GT due to fiber breakage, removal, and abrasion by wind action since all the holes were on the perimeter berm exposed to the prevailing winds.

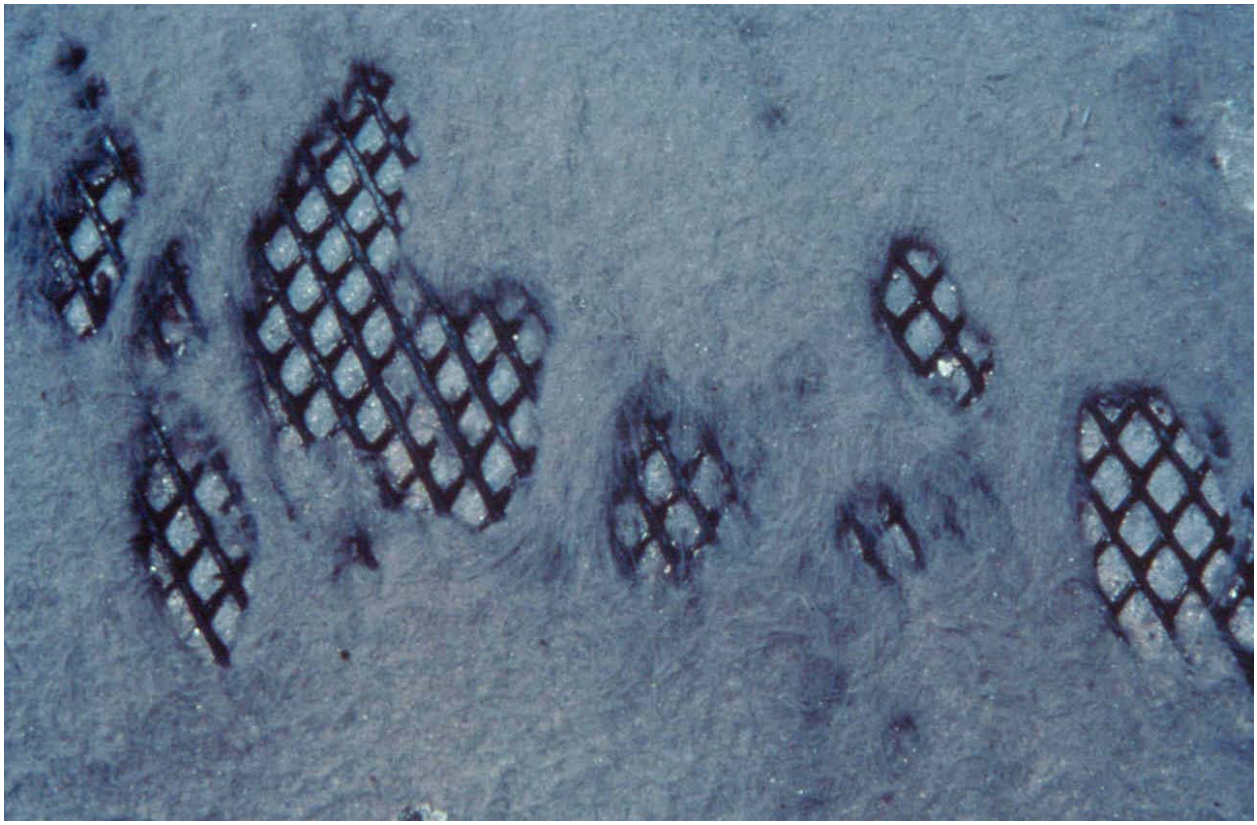

Figure F-A.5.2. Holes developed in a polypropylene GT at the side slope crest after 6.5 months of exposure to the environment.

Interestingly, a 540 g/m^2 polyester continuous filament nonwoven GT filter was substituted for the polypropylene GT in part of the landfill. While the mechanical properties of the polyester GT decreased with time, the rate of degradation was slower than that for the polypropylene GT and appeared to be decreasing with time. After 14.5 months of exposure, samples of the polyester GT had grab, puncture, and burst strengths that were 30.3, 20.1, and 13.0%, respectively, less than their pre-exposure values and a tear strength that was 24.2% greater than its pre-exposure value.

Resolution: The heavily degraded polypropylene GT was replaced with a 270 g/m^2 polypropylene GT and covered with a sand protection layer soon after installation.

Lessons Learned for Future Projects: Based on the available information, the following lessons can be learned from this case history:

- GTs should be covered as soon as possible after installation to protect them from the environment.
- If a GT is to be exposed to the environment for an extended time period after installation, a GT that initially far exceeds the project specifications and will meet the specifications after some degradation can be selected. As shown in the case history presented above, some types of GTs perform better than others. The potential degradation of the selected GT should be evaluated under all the anticipated environmental conditions. EPA recommends that the effect of ultraviolet light on GT properties be evaluated using ASTM D 4355 (Daniel and Koerner, 1993). The test is typically run for 500 hours; however, it can be run for longer time periods to meet project-specific conditions. In any case, prior to covering the GT, the condition of samples of the exposed GT taken from the field should be evaluated by laboratory testing to verify that the exposed GT is still satisfactory.
- If test results indicate that the GT will not have the required properties after exposure (typically a specified strength retention), the GT should be protected with a sacrificial opaque waterproof plastic tarp, soil layer, or other means. Tisinger et al. (1993) suggest that this may be the best strategy since a heavy degraded GT that meets the specifications is more sensitive to stress concentrations than a new lighter GT that meets the same specifications.

F-A.5.4 L-18

Problem Classification: landfill LCRS or LDS degradation/construction
Region of U.S.: southcentral
Waste Type: remediation waste
Reference: Paulson, J.N., "Veneer Stability Case Histories: Design Interactions Between Manufacturer/Consultant/Owner", *Proceedings of the 7th GRI Seminar Geosynthetics Liner Systems: Innovations, Concerns, and Designs*, 1993, pp. 235-241.

Problem Summary: polypropylene staple-fiber needlepunched nonwoven GT filter degraded due to outdoor exposure

Problem Description: Paulson (1993) described the degradation of the 350 g/m^2 polypropylene staple-fiber needlepunched nonwoven GT component of a GC LCRS drainage layer. On the base of the landfill cell, the GC is overlain by a soil protection layer. On the side slopes, the GC was initially exposed; a soil protection layer was to be placed incrementally over the GC on the side slopes during filling operations. Regulatory approval to place waste in the cell was not received on schedule after the cell was constructed, leaving the GC exposed to the environment. By about one year after construction, the GT component of the GC was falling apart, exposing the GN and underlying GM primary liner. Samples of the GT were collected for strength testing, but

could not be tested due to the amount of GT degradation. The GT also had a strong rotten egg-like odor. Paulson noted that the site is locally in a heavy industrial area known locally as having acidic precipitation. He attributed the odor to the fallout of industrial emissions that generated sulfuric acid on the GT. The exposure of the GT to ultraviolet light, sulfuric acid from industrial emissions, water, and high ambient temperature caused its severe degradation.

Resolution: The GC LCRS drainage layer on the side slopes was replaced, and waste placement in the cell began soon afterwards.

Lessons Learned for Future Projects: Based on the available information, the following lessons can be learned from this case history:

- GTs and GCs should be covered as soon as possible after installation to protect them from the environment.
- If a GT is to be exposed for an extended time period after installation, the potential degradation of the GT should be evaluated under all the anticipated environmental conditions. EPA recommends that the effect of ultraviolet light on GT properties be evaluated using ASTM D 4355 (Daniel and Koerner, 1993). The test is typically run for 500 hours; however, it can be run for longer time periods to meet project-specific conditions. In any case, prior to covering the GT, the condition of samples of the exposed GT taken from the field should be evaluated by laboratory testing to verify that the exposed GT is still satisfactory.
- If test results indicate that the GT will not have the required properties after exposure (typically a specified strength retention), the GT should be protected with a sacrificial opaque waterproof plastic tarp, soil layer, or other means.

F-A.5.5 L-30

Problem Classification: landfill LCRS or LDS degradation/construction
Problem Cause: operation
Waste Type: MSW
Reference: unpublished

Problem Summary: HDPE LCRS pipe crushed during construction

Problem Description: The valve on the 150-mm diameter HDPE LCRS pipe draining a newly constructed cell was kept closed until just before the start of waste placement. During this time, a significant amount of water (i.e., more than one meter deep) ponded in the cell. When the valve on the pipe was opened so water could drain, drainage occurred only very slowly. With no other on-site location to dispose of waste, the baled waste was placed in the ponded water. Processed C&DW was placed over the bales to keep the bales from floating. The crushed condition of the pipe was only identified when an attempt was made to flush the pipe to increase the water flow rate from the cell. The location of the pipe damage relative to the landfill cell was not evaluated.

The processed C&DW contained relatively high concentrations of sulfate. As the waste decomposed, the sulfate was reduced to hydrogen sulfide gas. The hydrogen sulfide concentrations were very high, about 2,200 ppm, in the air at the waste surface. Offsite, hydrogen sulfide concentrations were about 2 ppm, and the air had a rotten egg smell.

Resolution: The LCRS pipe was buried under waste and water and was not repaired since it still allowed water to drain, albeit slower than as designed. To control the hydrogen sulfide gas through chemical reaction, hydrogen peroxide was pumped into the waste. However, significant hydrogen sulfide was still formed. Due to the gas problem, the landfill was closed early, after only 1.5 years of filling. A gas extraction system with a flare was installed in the landfill, and gas emissions from the facility are successfully being controlled.

Lessons Learned for Future Projects: Based on the available information, the following lessons can be learned from this case history:

- Care should be taken to not damage leachate pipes during construction. The contractor should maintain sufficient soil cover between construction equipment and the liner system during construction. Equipment operators should be aware of pipe locations, since pipes can be crushed by trafficking equipment. Also, soil around pipes should be compacted using hand operated or walk-behind compaction equipment.
- After construction of a cell with an external sump, the pipe from the cell to the sump should be inspected to verify that the pipe is functioning as designed. The inspection may be performed by surveying the pipe with a video camera, pulling a mandrel through the pipe, flushing the pipe with water, or other means.

F-A.6 Landfill LCRS or LDS Malfunction

F-A.6.1 L-12

Problem Classification: landfill LCRS or LDS malfunction/operation
Region of U.S.: northeast
Waste Type: MSW
Reference: unpublished

Problem Summary: LCRS pipes were not regularly cleaned and became partially clogged and LCRS drainage layer may be partially clogged

Problem Description: As waste was placed into a double-lined landfill and then covered with soil intermediate cover, the LCRS flow rates from the landfill decreased. The LDS flow rates, however, increased from less than 100 lphd to about 300 lphd. Because LDS flow rates did not decrease with decreasing LCRS flow rates and LDS flow rates

were higher than those typical of nearly filled landfills in that region of the country, the LCRS was believed to be partially clogged. The LCRS drainage layer is a sand with a specified minimum hydraulic conductivity of 1 x 10^{-5} m/s. The LCRS and LDS pipes in the landfill were not flushed annually as is common practice in the region. Rather than performing maintenance on the LCRS pipes, the landfill owner decided to install a deep, 100-mm diameter leachate extraction well in the landfill. After the well was installed through the waste, LDS flow rates increased to about 400 lphd, and it was suspected that the well had penetrated the GM primary liner.

Resolution: The LCRS pipes were cleaned out and are scheduled to be flushed annually. Insufficient time has past to determine if cleaning the pipes solved the problem.
Lessons Learned for Future Projects: Based on the available information, the following lessons can be learned from this case history:

- LCRS and LDS pipes should be maintained by cleaning the pipes at least annually and more frequently, if warranted.
- Landfills with external sumps could also include riser pipes at the low point of leachate collection systems as a precautionary measure to allow for leachate removal from the landfill, if necessary.

F-A.6.2 L-22

Problem Classification: landfill LCRS or LDS malfunction/design
Region of U.S.: northeast
Waste Type: industrial
Reference: Koerner, G.R., Koerner, R.M., and Martin, J.P., "Field Performance of Leachate Collections Systems and Design Implications", *Proceedings of 31st Annual SWANA Conference*, San Jose, California, 1993, pp. 365-380.

Problem Summary: waste fines clogged needlepunched nonwoven GT filter wrapped around perforated LCRS pipes

Problem Description: Koerner et al. (1993) described the clogging of a 540 g/m^2 needlepunched nonwoven GT filter wrapped around LCRS pipes perforated with about 20 13-mm diameter holes/m. The pipes are bedded within a 0.3-m thick pea gravel LCRS drainage layer. The gravel is overlain by the same type of GT as that used to wrap the pipe and then a 0.3-m thick sand protection layer. The apparent opening size (AOS) of the GTs is 0.19 mm. The landfill was used for disposal of industrial plant waste, lime-stabilized waste, and slurried fines. About 75% by weight of the slurried fines particles pass the 0.15 mm sieve and about 45% pass the 0.074 mm sieve. Koerner et al. (1993) did not indicate if GT filter design was performed as part of the LCRS design.

By about one year after construction, it was apparent that the LCRS was not functioning adequately. Rainwater ponds developed on the waste surface, grew with time, and required pumping to remove them. In addition, the amount of leachate removed from the LCRS sump was less than expected. The LCRS was excavated near the sump and the following observations were made:

- the LCRS gravel drainage layer was relatively clean and full of leachate;
- based on piezometer measurements, the leachate in the gravel drainage layer near the sump was under pressure indicating it was confined below the waste and not able to freely drain into the pipes;
- the GT wrapping the LCRS pipes was clogged at the pipe perforations; and
- the GT between the sand protection and gravel drainage layers (upper GT) was not clogged.

To evaluate the effect of clogging on the transport of leachate though the GT, permittivity tests were conducted on the following samples: (i) uncleaned upper GT; (ii) cleaned upper GT; and (iii) upper GT conditioned in the laboratory with site-specific slurried fines for six months to model the GT around the pipe. The cleaned upper GT had a permittivity of about 1.8 s^{-1}. The permittivities of uncleaned upper GT and laboratory-conditioned GT about two and five magnitudes lower, respectively. Koerner et al. (1993) concluded that the upper GT was performing well, but the GT around the LCRS pipe had poor performance.

As described by Giroud (1996), the purpose of a GT is to retain the material behind the filter, not capture particles in motion. The upper GT described by Koerner et al. (1993) retains the sand protection layer over the gravel layer. Based on filter design calculations performed by the authors of this appendix, the upper GT also captures some of the slurried fines particles if they move with the leachate. These fines, as well as biological particles, reduced the permittivity of the upper GT. The GT around the pipe serves no purpose. It is not needed to prevent the gravel from falling through the pipe perforations. In fact, this GT proved to be detrimental as it captured fines and biological particles at the small flow areas at the pipe perforations.

Resolution: Koerner et al. (1993) do not indicate how this problem was resolved.

Lessons Learned for Future Projects: Based on the available information, the following lesson can be learned from this case history:

- Perforated pipes bedded in gravel should not be wrapped with a GT because the GT is useless, and, in some cases, even detrimental. Furthermore, EPA recommends that perforated pipes generally not be wrapped with a GT (Bass, 1986).

A.6.3 L-36

Problem Classification: landfill LCRS or LDS malfunction/design
Region of U.S.: southeast
Waste Type: MSW ash
Reference: unpublished

Problem Summary: waste fines clogged needlepunched nonwoven GT filter around LCRS pipe bedding gravel

Problem Description: The LCRS for a single-lined landfill cell consists of a sand drainage layer (specified minimum hydraulic conductivity of 1×10^{-5} m/s) and a piping system. The pipes are bedded in gravel wrapped with a needlepunched nonwoven GT. The specified maximum apparent opening size of the GT is reportedly significantly lower than that necessary to retain the sand. Leachate collected in the pipes drains to an internal sump and is removed by pumping. Significantly less leachate than expected flowed to the sump. In addition, leachate ponded in the landfill and seeped from the landfill side slopes. When a video camera was run through the LCRS pipes, the pipes were found to be full of the incinerated MSW ash placed in the landfill. The pipes were flushed, but the sump still recharged very slowly even though the landfill was full of leachate. Based on this observation, it was concluded that the LCRS is clogged. From the gradation of the sand LCRS drainage layer and the apparent opening size of the GT, it is expected that the clogging is most significant in the GT around the pipe bedding gravel. The sand has larger openings than the GT and passes fine ash particles. The fine particles may have become trapped on and in the GT. However, this does not explain the large quantities of ash in the LCRS pipes. It may be that the GT around the pipe bedding gravel has opened at some locations, allowing leachate to bypass the GT and flow directly into the pipe bedding gravel and the pipe.

Resolution: An underdrain system was constructed around the downgradient edge of the landfill to collect leachate migrating from the landfill. The underdrain consisted of a collection pipe in a gravel-filled trench. The top of the gravel was exposed. Due to the slow draining of leachate to the sump, leachate overtopped the landfill cell and flowed into the underdrain. The leachate carried ash particles that eventually clogged the gravel in the underdrain. Currently, it is proposed that an HDPE manhole be installed on the sand drainage layer on the upgradient side of the landfill to access the landfill leachate. The manhole will be installed on the upgradient side of the landfill because it is anticipated that the clogging will be less severe upgradient and leachate will recharge the manhole faster.

Lessons Learned for Future Projects: Based on the available information, the following lesson can be learned from this case history:

- When the waste in a containment system contains some fine particles that may migrate to the LCRS, the potential for LCRS clogging may be reduced by allowing

those fine particles to pass though the LCRS to the leachate collection pipes, which can subsequently be cleaned. The fine particles will pass more easily through the drainage system if no GTs are used in the drainage system or if the drainage system contains relatively thin open nonwoven GTs rather than thicker nonwoven GTs with a smaller apparent opening size. Note that the above does not apply to an LCRS with only a GN drainage layer. Though a GN drainage layer has a high transmissivity, it is thin and is, therefore, generally more susceptible to clogging by sedimentation than a granular drainage layer.

- Drainage system pipes should be maintained by cleaning the pipes at least annually and more frequently, if warranted.

A.6.4 L-37

Problem Classification: landfill LCRS or LDS malfunction/operation
Region of U.S.: southeast
Waste Type: MSW
Reference: unpublished

Problem Summary: leachate seeped out landfill side slopes in the vicinity of chipped tire layers

Problem Description: As part of a site cleanup, about 1.2 million chipped tires were disposed of in a 3.2 ha MSW landfill cell. The average particle size of the tire chips is about 100 mm. Subsequently, leachate seeped out of the landfill side slopes in the vicinity of chipped tire layers. The coarse tire chips have a higher hydraulic conductivity than the MSW and, apparently, promote lateral drainage within the waste. The LCRS for the single-lined cell consists of a sand drainage layer (specified minimum hydraulic conductivity of 1×10^{-5} m/s) and a piping system. Leachate collected in the pipes drains to an internal sump and is removed by pumping.

Resolution: A 0.9-m diameter bucket auger was advanced through the waste to the top of the sand LCRS drainage layer at six locations near the seeps. Perched leachate in the tire chips was found in several boreholes and several boreholes were dry above the LCRS. The depth of perched leachate was up to 3 m. The boreholes with perched leachate were completed as leachate wells. The wells allow some of the leachate collected in the tire chip layers to readily drain to the LCRS. Leachate levels in the wells are inspected weekly. If there is leachate in a well, the well is pumped.

Lessons Learned for Future Projects: Based on the available information, the following lesson can be learned from this case history:

- Leachate may seep from landfill side slopes if the leachate can perch on less permeable layers within the waste that are relatively close to the side slope. The potential for seepage can be decreased by not placing layers of these less permeable materials near the side slope, sloping less permeable layers away from

the side slopes, distributing the materials throughout the waste, constructing leachate chimney drains to the LCRS around these layers, removing perched leachate from wells installed over these layers, or other means.

F-A.7 Landfill LCRS or LDS Operation

F-A.7.1 L-5

Problem Classification: landfill LCRS or LDS operation/operation
Region of U.S.: southeast
Waste Type: MSW
Reference: unpublished

Problem Summary: overestimation of LDS flow quantities due to problems (e.g., clogging) with automated LDS flow measuring and removal equipment

Problem Description/Resolution: The quantities of liquid pumped from the LCRS and LDS sumps of a MSW landfill cell are monitored by landfill personnel. From 1991, when operation began, to March 1994, problems with the LCRS and LDS flow measuring system made the measured flows unreliable. During 1991, LDS flow rates were estimated by multiplying the time the pump was on by the flow capacity of the pump. However, due to problems with the control system, the pump sometimes stayed on even when there was no more liquid to be removed (i.e., it pumped air), leading to the overestimation of flow rates. The control system that measured the liquid levels in the sumps and operated the pumps was prone to compressor failure and clogging of air lines. This lead to inaccurate measurements of leachate levels in the sumps and caused pumps to run for too long of an interval or even continuously until they burned out. Mechanical flowmeters were installed into the cells in January 1992 to solve the flow rate measurement problem. Flow rates measured using the flowmeters were several times lower than flow rates calculated using the "pump on" time. However, the measured LDS flow rates remained high, and the flow measuring system underwent frequent repair. The impeller and filter screen in the flowmeters frequently became clogged, making the flowmeters inoperable. In March 1994, the mechanical flowmeters were replaced with customized venturi flowmeters that were less prone to clogging. However, these flowmeters were damaged in July 1994 by an electrical storm. The meters were subsequently repaired. In December 1994, it was discovered that a failed check valve in the leachate riser house allowed LDS liquid that had been metered to flow back into the LDS of the cell and be remetered. The check valve was replaced. Even with the above repairs, the measured LDS flow rates were still relatively high. In early 1995, the leachate level measurement system in the LCRS sump experienced drift due to the buildup of landfill gas pressures in the sump, though the gases could passively vent through riser pipes. To correct this problem, the “pump on” levels in the LCRS and LDS sumps were lowered so the gases could vent more freely.

Lessons Learned for Future Projects: Based on the available information, the following lessons can be learned from this case history:

- The potential for clogging of water-level indicators, pumps, and flowmeters must be considered when selecting the types of equipment to use at a MSW landfill. In the case history described above, the venturi flowmeters were less prone to clogging than the mechanical flowmeters with filter screens and impellers.
- Leachate quantity measurement systems should be calibrated and adjusted as needed at least annually to ensure that the quantities measured are accurate.
- Due to the potential for problems in automated leachate metering and pumping equipment, landfill operations plans should include a verification and contingency method for estimating the quantities of liquid removed from the LCRS and LDS.

F-A.7.2 L-23

Problem Classification: landfill LCRS or LDS operation/operation
Region of U.S.: northeast
Waste Type: MSW
Reference: unpublished

Problem Summary: valves on LCRS pipes were not opened and leachate could not drain, and waste and leachate flowed over a berm into a new unapproved cell

Problem Description: An 8 ha landfill expansion was constructed with three single-composite lined cells, separated from each other and from adjacent older cells by intercell berms. Leachate collected in the expansion cells was conveyed to sumps in the adjacent cells by three pipes, each fitted with a valve to be opened prior to placement of waste in the cells. In two of the expansion cells, the valves were not opened before waste placement began and leachate collected in these cells could not drain. Eventually, the waste became buoyant due to rising leachate levels. After about 1.5 years of operation, a bulldozer operating at the active face sunk in the waste and had to be removed with a crane. By this time, about 12 m of waste had been placed over the valves.

The intercell berms had an exposed HDPE GM primary liner. The design called for the sand LCRS drainage layer to be placed incrementally over the 3H:1V berm side slopes, advancing the sand with waste placement. In the one expansion cell with an open valve on the LCRS pipe, waste was placed too close to an intercell berm between it and a new cell that had not yet been approved for waste. Sufficient space between the waste and the intercell berm should have been maintained to temporarily store runoff from the waste. After a storm, leachate and waste washed over the berm and into the new cell. A temporary access road made out of waste was constructed over the GM primary liner on the intercell berm to access the new cell and clean out the waste that had washed into it. The waste placed directly on the GM primary liner damaged the GM.

Resolution: The corrective measures for the above problems have not yet been implemented. However, it is anticipated they will cost on the order of $1,000,000 (about 40% of the original construction cost). It is proposed that the impounded leachate be pumped from the two cells and treated. Then, the waste will be excavated from around the valves, and the valves will be opened. The temporary waste access road will be removed, and the underlying GM liner will be inspected for damage and repaired. The sand LCRS drainage layer will be placed on the berm slopes incrementally with waste placement.

Lessons Learned for Future Projects: Based on the available information, the following lesson can be learned from this case history:

- The procedures to be followed by landfill operations personnel should be documented in an operations manual. Special operation procedures required for a specific design should be emphasized in the manual. Periodically, an audit should be conducted to verify that the specified operation procedures are being practiced.

F-A.7.3 L-34

Problem Classification: landfill LCRS or LDS operation/operation
Region of U.S.: southeast
Waste Type: HW
Reference: unpublished

Problem Summary: LCRS leachate pump moved air and liquid causing pump airlock and underestimation of leachate quantities

Problem Description: The quantity of leachate pumped from the LCRS sump of a 5 ha cell was measured by multiplying the number of times the pump turned on by a fixed "pump on" time. The "pump on" time setting at the pump controller tended to drift causing the pump to operate too long. As a result, air was pulled into the pump, and the pump tended to become airlocked and shut down. The pump did not reprime as the leachate levels rose. When the landfill operator noticed this, the pump was removed from the sump and adjusted and the "pump on" time setting was reset. With the pump coming on longer but less frequent, the quantity of leachate removed from the landfill was underestimated. An accumulating flowmeter was installed to provide a better measurement of leachate quantities. However, when air pulled into the pump moved through the flowmeter, the flowmeter overestimated the quantity of leachate removed. For example, in one month the accumulating flowmeter indicated that the leachate volume removed from the cell was about 1.2 million liters. In comparison, the LCRS flow rates from the adjacent cells of a similar size were about 10 times less.

Resolution: The pumps were replaced with self-priming pumps from a different manufacturer. Leachate flow quantities calculated using the "pump on" counter compared well with quantities measured with the flowmeter.

Lessons Learned for Future Projects: Based on the available information, the following lessons can be learned from this case history:

- Leachate sump pumps should be self priming.
- Leachate quantity measurement systems should be calibrated and adjusted as needed at least annually to ensure that the quantities measured are accurate.
- Due to the potential for problems in automated leachate metering and pumping equipment, landfill operations plans should include a verification and contingency method for estimating the quantities of liquid removed from the LCRS and LDS.

F-A.7.4 L-35

Problem Classification: landfill LCRS or LDS operation/design
Region of U.S.: northeast
Waste Type: MSW
Reference: unpublished

Problem Summary: LCRS leachate pumps and flowmeters continually clogged and LDS leachate pumps turned on too frequently and burned out prematurely

Problem Description: The LCRS and LDS of two landfill cells were designed with large, shallow sumps. State regulations at the time the landfill was permitted required that the head of leachate on the liner system, including in the sump, be no more than 0.3 m. The LCRS drainage layer is sand with a specified minimum hydraulic conductivity of 1×10^{-4} m/s, and the LDS drainage layer is a GN. In the LCRS, the submersible pumps and magnetic flowmeters continually become clogged with a white precipitate. In the LDS, the flow rates into the sumps are less than the capacity of the submersible pumps. To keep liquid levels in the sump less than 0.3 m but above the pump intake, the pump cycle was very short. The pump motor overheated from turning on and off so quickly and burned out.

Resolution: The LCRS pumps and flowmeters are disassembled and cleaned with citric acid about every month. A spare pump is used to pump a sump when a pump is being cleaned. The LDS pumps were replaced with smaller models to increase cycle times.

Lessons Learned for Future Projects: Based on the available information, the following lessons can be learned from this case history:

- Chemicals may precipitate within leachate sump pumps and flowmeters and interfere with their operation. In the case history described above, clogging was only a problem for LCRS pumps and flowmeters. LDS pumps and flowmeters were not

adversely affected by clogging. However, the leachate in the LDS has been diluted by water from consolidation of the CCL component of the primary liner.
- Leachate sump pumps should be selected to be compatible with sump geometries and anticipated leachate recharge rates.

F-A.8 Landfill Liner System Stability

F-A.8.1 L-21

Problem Classification: landfill liner system stability/design
Region of U.S.: northeast
Waste Type: coal ash
Reference: unpublished

Problem Summary: sliding along PVC GM/CCL interface during construction

Problem Description: A single-composite liner system being constructed for a canyon landfill underwent slope failure during construction. The liner system consists of the following components, from top to bottom:

- 0.45 to 0.6-m thick lime-stabilized sludge (28-day compressive strength of about 550 kPa) or bottom ash protection layer;
- 0.3-m thick sand LCRS drainage layer (minimum hydraulic conductivity of 1×10^{-4} m/s);
- 0.75-mm thick PVC GM liner; and
- 0.45-m thick CCL (maximum hydraulic conductivity of 1×10^{-9} m/s).

The inclination of the landfill side slopes are, on average, about 3.5H:1V for the upper 60 m of slope length and 10H:1V for the bottom 90 m of slope length. The maximum side slope inclination is 3H:1V. The compaction criteria for the clay liner were 95% of the standard Proctor maximum dry unit weight and wet of the optimum moisture content. During construction, about 1 ha of the liner system on the upper 3.5H:1V side slopes slid downslope along the GM/CCL interface. The slide zone represented about 50% of the upper slope area that had been covered. Sliding occurred both after placement of the sand drainage layer and during placement of the protection layer. The slide zone was identified by cracking of the sand layer or stabilized sludge layer near the crest of the side slope and wrinkling of the GM liner near the slope toe. When the GM in the slide zone was exposed, it was taut and, in some cases, torn near the slope crest. Analyses of liner system slope stability had not been conducted as part of the landfill design. However, over 30 ha of liner system had been successfully constructed previously using the same liner system components and geometry and similar site soils to construct the CCL.

After sliding of the liner system occurred, a forensic investigation was conducted to identify the cause of this failure. The CCL surface beneath the GM liner in the slide zone was visually inspected and found to be relatively wet. However, this wet zone was only at the surface of the CCL (i.e., in the upper 10 mm). Samples of the CCL material in the slide zone at about 5 mm and 150 mm beneath the top surface of the CCL had measured moisture contents of about 7 and 2 percentage points wet of standard Proctor optimum, respectively. The average moisture contents of two deeper samples of CCL material were equal to the average CCL moisture content measured during construction using a nuclear density gauge and an oven. The average moisture content of the surface sample of CCL material was about 7 percentage points wet of optimum, indicating saturation. The increase in moisture content at the surface of the CCL between compaction and sliding is believed to have resulted from condensation of water on the lower face of the GM due to thermal effects and spraying of the CCL surface to prevent desiccation prior to placement of the GM. The GM liner was placed on the CCL in the fall during days with large diurnal temperature fluctuations. During the day, as the temperature of the liner increased, water evaporated from the CCL and the air entrapped between the CCL and the GM became saturated with water vapor. During the night, as the temperature decreased, the ability of the entrapped air to contain water vapor decreased. As a result, a fraction of the vapor condensed into water and water droplets formed on the lower face of the GM. In the sliding zones, the GM liner and CCL were exposed to these temperature fluctuations for up to two weeks before being covered with the sand drainage layer. In the previous phase of construction, which was completed without incident, the GM liner was placed in the summer when the diurnal temperature fluctuations were less and the GM was only exposed to these fluctuations for about three days before it was covered with soil.

Subsequently, direct shear tests were performed on the GM/CCL interface in accordance with ASTM D 5321 to investigate the effect of CCL moisture content on interface shear strength under low normal stress. When the CCL was compacted at about 2 percentage points wet of its optimum moisture content, the peak and large-displacement secant interface friction angles of the GM/CCL interface were about 19° and 18°, respectively. The peak and large-displacement secant interface friction angles decreased with increasing CCL moisture content and were about 14° and 12°, respectively, when the interface was tested with the CCL at about 7 percentage points wet of optimum. Slope stability analyses performed by the owner indicate that on the steepest 3H:1V portions of the lining system, the liner system is just stable, with a factor of safety of 1.03, for a CCL moisture content 2 percentage points wet of optimum. The liner system is unstable, with a factor of safety of 0.64, for a CCL moisture content 7 percentage points wet of optimum. The owner finds a minimum factor of safety of 1.0 acceptable for the following reasons: (i) most slopes are less steep than 3H:1V and have a factor of safety significantly greater than 1.0 if the 3H:1V slopes have a factor of safety of 1.0; (ii) prior to placement of ash in the landfill, the protection layer will have set and gained strength, increasing the calculated factor of safety to over 1.5; (iii) the ash placed in the landfill will buttress the slopes; and (iv) liner system instability

occurring during construction before the protection layer has gained sufficient strength will be detected and repaired before construction is completed.

Resolution: The following corrective measures were implemented.

- A temporary protective cover was placed over the GM liner and CCL in the slide zone to protect the CCL from frost damage until the GM and overlying soil layers could be reconstructed in the spring.
- A polypropylene monofilament woven GT reinforcement layer was installed between the GM liner and overlying soils to carry the load of the soils for the approximately 1 ha of liner system constructed on the upper side slopes after the failure occurred. The large-displacement secant interface friction angles of the sand/GT and GT/GM interfaces were about 25° and 15°, respectively. The strain measured in the installed GT near the crest of the side slope was less than 2%, which was expected based on the calculated GT tension. Even if the GM/CCL interface is very wet and is the critical interface, i.e., the interface with the lowest strength, slope stability analyses performed by the owner indicate that most of the load associated with the overlying soils will be carried in tension by the GT reinforcement, which is much stiffer than the GM.
- The owner developed new construction procedures to reduce the potential for liner system sliding in the future: (i) the surface of the CCL must not be wet with supplemental moisture (e.g., rain, dew, spraying) when the overlying GM is installed; (ii) the GM liner must be covered with the sand drainage layer within five working days after it is placed to reduce the potential for moisture migration to the GM/CCL interface; and (iii) GT reinforcement must be used if the CCL surface has a moisture content greater than 3 percentage points wet of optimum prior to placement of the sand.

Lessons Learned for Future Projects: Based on the available information, the following lessons can be learned from this case history:

- Liner system slopes should always be evaluated using rigorous slope stability analysis methods that consider the actual shear strengths of the liner system materials. Actual interface strengths can only be assessed by project-specific testing. Such testing is recommended.
- The effect of construction on moisture conditions at the GM/CCL interface should be considered when developing the specification for CCL construction and selecting the strength of liner system interfaces for slope stability analyses. The CCL construction specification should generally include limitations on maximum compacted moisture content, restrictions on applying supplemental moisture, and requirements for covering the CCL and overlying GM as soon as practical to minimize the moisture migration to the GM/CCL interface.

A.8.2 L-24

Problem Classification: landfill liner system stability/operation
Region of U.S.: northeast

Waste Type: MSW
Reference: unpublished
Problem Summary: sliding along GN/GCL (HDPE GM side) and GCL (bentonite side)/CCL interfaces during operation

Problem Description: A single-composite liner system for one cell of a landfill expansion was constructed in a 17-m deep excavation. The cell was shaped like a triangle, with 3H:1V side slopes on one side and the excavation base on the other two sides. The liner system on the base slope consists of the following components, from top to bottom:

- 0.45-m thick sand protection layer;
- nonwoven GT filter;
- GN LCRS drainage layer;
- GCL composed of a 1.5-mm thick HDPE GM (textured on side slopes and smooth on base) and a bentonite layer glued to one side of the GM; and
- 0.9-m thick CCL.

On the side slopes, the GT and GN are replaced by a GC. The GCL was installed with the bentonite side down and was seamed by fusion seaming the GM component of adjacent panels.

When construction of a new adjacent cell began, waste from an old unlined landfill in the footprint of the new cell was required to be relocated to the existing lined active cell. The existing cell did not have adequate capacity for the waste, and was temporarily overfilled to hold the waste. With the additional waste, the height of the waste in the existing cell was about 17 m and the intermediate waste slopes were at about 2.5H:1V, significantly steeper than the maximum slope of 4H:1V specified in the operations plans. The top of the waste extended from the crest of the side slopes up to about 80 m from slopes, in the direction of the apex of the triangular-shaped cell. A 0.9-m high sand berm was located at the toe of the intermediate waste slopes to increase slope stability by providing a buttress for the waste.

As part of the landfill permit, the design engineer conducted a slope stability analysis of the landfill assuming that the secant friction angles for the waste and the weakest liner system interface were 25° and 7°, respectively. No project-specific interface shear strength tests of the liner system interfaces were performed. The stability analysis conducted for design did not consider the liner system with the waste at intermediate grades; there was no regulatory requirement to include this in the permit. The minimum calculated static factor of safety for landfill stability was 1.4. This factor of safety was for

the 3H:1V waste slopes (between benches) at their final grades. The minimum static factor of safety calculated for failure through the liner system, with waste at final grades, was 5.0. When the landfill owner later decided to overfill the cell with waste, the stability of the liner system with the relatively steep waste slopes was not analyzed.

Shortly before the liner system in the active cell was connected to the liner system in the new cell, the sand berm at the toe of the active cell began to heave. A crack on the order of 50 mm wide developed on top of the waste near the slope crest. The crack extended for about 20 m along the crest, on one side of the triangular-shaped cell, and was quasi parallel to the side slope anchor trench. Smaller cracks developed parallel to the larger crack and extended back into the slope from the larger crack. All visible cracks ended by 7 m from the side slope crest As the liner system for the new cell was being tied into that for the old cell, GCL folds were observed near the tie-in. In one instance, about 3 m of GCL was folded into a 1.2-m long section. When the sand was removed from over the LCRS pipe, the pipe popped up out of the ground. Under the moving waste mass, the pipe had bent and doubled-up.

Resolution: About 270,000 m^3 of waste was removed from the failure zone to inspect and repair the damaged liner system. The damaged liner system extended up to about 60 m into the waste, and was defined by the area where the GCL was taut and torn. Within the failure zone, the liner system slid along the hydrated bentonite, tearing the GCL in two locations: (i) four 3-m long parallel tears about 2 m apart and parallel to the toe of the waste slope; and (ii) a 0.15-m long tear parallel to the toe of the waste slope. When waste and liner system materials were removed from over the tears, repairs had to be quickly made since the GCL was so taut that the tears opened further. The GCL on the side of the tear furthest into the waste pulled back into the waste. When GCL samples were cut to define the area of damage, the GCL at the sample locations also tended to split along the cuts. The GM component of the GCL in the samples was generally about 10% thinner than the thicknesses measured during GCL conformance testing and the samples were thinner than the minimum allowable thickness given in the project specifications. However, the samples met the required strength requirements. The GCL was repaired by patching it. Interestingly, no damage to the GT and GN over the GCL was found. These materials moved up to about 3 m less than the GCL due to sliding between the GN and GM component of the GCL. The liner system at the anchor trench has not yet been inspected. To increase the stability of the liner system, the intermediate waste slopes have been regraded to 4H:1V.

The design engineer backanalyzed the stability of the liner system at failure and concluded that with an assumed secant friction angle for the waste of 25°, the minimum secant friction angle for the liner system interfaces at failure was about 2°.

Lessons Learned for Future Projects: Based on the available information, the following lessons can be learned from this case history:

- Liner system slopes should always be evaluated using rigorous slope stability analysis methods that consider the actual shear strengths of the liner system materials. Actual interface strengths can only be assessed by project-specific testing. Such testing is recommended.
- Proposed changes to the landfill filling sequence should be reviewed by the design engineer to ensure that these changes will not adversely affect the landfill.

Figure F-A.8.1. When waste was excavated from the failure zone, large wrinkles in the GCL were evident.

A.8.3 L-25

Problem Classification: landfill liner system stability/design
Region of U.S.: southwest
Waste Type: HW
References: Byrne, R.J., Kendall, J., and Brown, S., "Cause and Mechanism of Failure Kettleman Hills Landfill B-19, Phase 1A", *Stability and Performance of Slopes and Embankments - II*, ASCE Geotechnical Special Publication No. 31, 1992, pp. 1188-1215.

Mitchell, J.K., Seed, R.B., and Seed, H.B., “Kettleman Hills Waste Landfill Slope Failure. I: Liner-System Properties”, *Journal of Geotechnical Engineering*, Vol. 116, No. 4, Apr 1990, pp. 647-668.
Seed, R.B., Mitchell, J.K., and Seed, H.B., “Kettleman Hills Waste Landfill Slope Failure. II: Stability Analyses”, *Journal of Geotechnical Engineering*, Vol. 116, No. 4, Apr 1990, pp. 669-690.

Problem Summary: sliding along HDPE GM/polyester needlepunched nonwoven GT and HDPE GM/CCL interfaces during operation

Problem Description: Landfill B-19 at the Kettleman Hills hazardous waste treatment, storage, and disposal facility, located in Kettleman City, California, is a 15 ha double-composite lined landfill. The landfill was constructed in a 30 m deep excavation. The liner system on the landfill base consists of the following components, from top to bottom:

- 0.3-m thick soil protection layer;
- GT;
- 0.3-m thick granular material/GT/GN LCRS drainage layer;
- 1.5-mm thick HDPE GM/0.45-m thick CCL composite primary liner;
- GT;
- 0.3-m thick granular LDS drainage layer;
- GT;
- 1.5-mm thick HDPE GM/2-m thick CCL composite secondary liner;
- GT/drainage rock/GT/2-mm thick HDPE GM vadose zone monitoring system.

The liner system on the side slopes consists of the following components, from top to bottom:

- 0.6-m thick soil protection layer;
- 1.5-mm thick HDPE GM protection layer (i.e., sacrificial GM);
- GT;
- GN LCRS drainage layer;
- 1.5-mm thick HDPE GM primary liner;
- GT;
- GN LDS drainage layer; and
- 1.5-mm thick HDPE GM/2-m thick CCL composite secondary liner.

The GT in the liner system is a polyester needlepunched nonwoven type. The landfill was designed using presumed interface shear strengths for the liner system. The presumed strengths were based on published information available at the time. The plasticity index of the CCL material ranged from 22 to 46%. On average, the CCL material was compacted to 94% of its Standard Proctor maximum dry unit weight at a moisture content 5 percentage points wet of optimum. There was no limit on the

maximum CCL moisture content in the specifications. Waste placement began in the first landfill cell, Phase IA, in early 1987. This cell occupies about 6 ha and was constructed against the 2H:1V excavation side slopes on the southwest and northwest and the 3H:1V side slopes on the northeast. The southeast side of the cell was constructed on the relatively flat base and separated from the adjacent cell by a berm. By 15 March 1988, up to 27 m of waste had been placed over the liner system. The slope of the waste, dipping toward the southeast, was about 3H:1V.

Around 6:30 am on 19 March 1988, an approximately 10-mm wide crack was observed across the landfill access road at the north corner of the landfill. This access road was used to descend into the cell. By about 9:30 am, a 80 to 100-mm wide crack with a vertical offset of 160 to 200 mm was observed along the top of the waste slopes where they intersected the northwest and southwest side slopes of the landfill. By noon, the cracks in the waste had opened wider to several decimeters. The main failure, with sliding of the waste mass from the northwest to the southeast, occurred by about 1:30 p.m. Horizontal displacements of the waste mass were up to 11 m and vertical displacements along the side slopes were up to 4 m. The vertical riser from the LCRS and LDS sumps, located in the center of the northeast side, also appeared to have translated about 11 m with the waste. Around the side slopes, the soil cover over the waste and the waste was cracked and, in some locations, the liner system was torn. Based on the nature of the movements and the pattern of cracking, it was concluded that the waste moved as a mass and sliding likely occurred within the landfill liner system.

Excavation of waste from Phase IA began in October 1989. As the waste was removed and relocated into other phases of B-19, the condition of the waste and the liner system was mapped. The field investigation revealed that, on the base of the cell, the 3H:1V northeast side slopes, and the lower portions of the 2H:1V northwest and southwest side slopes, sliding occurred along the GM/CCL interface of the secondary liner. The materials above the CCL component of the secondary liner appeared to have moved monolithically with little movement between or within the liner system components. Striations on the surface of the CCL were consistent with the southeastern direction of the slide. There was no evidence of sliding within the CCL, except at the location of the LDS sump. On the northeast side slopes, all of the geosynthetics remained fixed in the anchor trench at the top of the slope and had been pulled along the slope in the direction of sliding. On the northwest and southwest side slopes, the GM primary liner pulled out of the anchor trench and slide downslope with the waste about 8 m and 5 m, respectively, over the underlying GT. Further downslope, the failure surface moved to the GM/CCL interface of the secondary liner and this GM tore. The tear extended across the northwest slopes and into the southwest slopes and was on the order of 8 to 9 m wide. At the toe of the northwest and southwest slopes, the failure mechanism appeared more complex, due to the kinematic constraints posed by the relatively sharp change in orientation of the liner and the changes in liner system components. Immediately upslope of the toe area, wrinkles and folds were observed in some of the geosynthetics. A corresponding pattern of tension tears was found downgradient of the

toe area. Based on relative movements between liner system geosynthetics and striations on the surface of the CCL component of the primary liner, at least some of the sliding at the toe occurred at the GM/CCL primary liner interface.

After the failure occurred, interface direct shear and pullout tests were conducted to evaluate the shear strength of critical liner system interfaces and stability analyses were performed using actual interface strengths. Unconsolidation-undrained triaxial tests, consolidated-undrained triaxial tests, and one-dimensional consolidation tests were also performed to evaluate the shear strength and consolidation characteristics of the CCL. Based on the results of the tests, only a small amount of displacement (5 mm or less) is required to mobilize the peak shear strength along an interface. At greater displacements, the shear strength decreased and approached the large-displacement value. The most critical interfaces with the lowest large-displacement shear strengths are GM/GT, GM/GN, and GM/CCL (saturated). The mean large-displacement secant interface friction angles of the GM/GT and GM/GN interfaces under submerged conditions are about 8°. The mean large-displacement undrained interface shear strength of the GM/CCL interface is 33 kPa with the CCL at its average as-placed moisture content and overburden pressures corresponding to the maximum depth of waste at failure. The undrained interface shear strength decreases with increasing CCL moisture content. At lower stresses, the GM/GT and GM/GN interfaces are more critical; at higher stresses, the GM/CCL interface is more critical. This is generally consistent with the observed Phase IA failure surface.

The two-dimensional and three-dimensional slope stability factors of safety for the landfill cell were calculated by Byrne et al. (1992) using peak and large-displacement shear strengths. Only the three-dimensional analyses are discussed herein because they better represent the complex cell geometry. The factors of safety for the pre-failure cell configuration using peak and large-displacement strengths were 1.25 and 0.85, respectively. From a comparison of the load-displacement curves for the critical interfaces, peak shear strength would not be expected to be simultaneously mobilized at the interfaces. Assuming that peak shear strengths were mobilized on the landfill base and 3H:1V side slope and large-displacement shear strengths were mobilized on the 2H:1V side slopes, the calculated factor of safety was 1.08. Thus, the measured interface shear strengths and the rapid decrease in shear strength with displacement after peak strength has been reached can explain the Kettleman Hills Landfill failure.

Resolution: The waste was relocated into other phases of B-19, the liner system was repaired, and the cell was refilled with waste.

Lessons Learned for Future Projects: Based on the available information, the following lessons can be learned from this case history:

- Liner system slopes should always be evaluated using rigorous slope stability analysis methods that consider the actual shear strengths of the liner system

materials. Actual interface strengths can only be assessed by project-specific testing. Such testing is recommended.

- The effect of displacement on interface shear strength must be considered when selecting the strength to use for design.
- The effect of construction on moisture conditions at the GM/CCL interface should be considered when developing the specification for CCL construction and selecting the strength of liner system interfaces for slope stability analyses. The CCL construction specification should generally include limitations on maximum compacted moisture content, restrictions on applying supplemental moisture, and requirements for covering the CCL and overlying GM as soon as practical to minimize the moisture migration to the GM/CCL interface.

A.8.4 L-26

Problem Classification: landfill liner system stability/design
Region of U.S.: southwest
Waste Type: MSW
References: Anderson, R.L., "Earthquake Related Damage and Landfill Performance", *Earthquake Design and Performance of Solid Waste Landfills*, Yegian, M.K. and Liam Finn, W.D., eds., ASCE Geotechnical Special Publication No. 54, 1995, pp. 1-16.

Augello, A.J., Matasovic, N., Bray, J.D., Kavazanjian, E., Seed, R.B., "Evaluation of Solid Waste Landfill Performance During the Northridge Earthquake", *Earthquake Design and Performance of Solid Waste Landfills*, Yegian, M.K. and Liam Finn, W.D., eds., ASCE Geotechnical Special Publication No. 54, 1995, pp. 17-50.

Geosynthetic Research Institute, "*Evaluation of an High Density Polyethylene Geomembrane Exhumed from Canyon C*", Geosynthetic Research Institute, Drexel University, Philadelphia, Pennsylvania, 29 Apr 1994.

Matasovic, N., Kavazanjian, E., Jr., Augello, A.J., Bray, J.D., and Seed, R.B., "Solid Waste Landfill Damage Caused by 17 January 1994 Northridge Earthquake", *The Northridge, California, Earthquake of 17 January 1994*, Woods, M.C. and Seiple, W.R., eds., California Department of Conservation, Division of Mines and Geology Special Publication 116, 1995, pp. 221-229.

Matasovic, N. and Kavazanjian, E., Jr., "Observations of the Performance of Solid Waste Landfills During Earthquakes", *Eleventh World Conference on Earthquake Engineering*, Acapulco, Mexico, Elsevier Science Ltd., 1996, CD-ROM Paper No. 341.

Matasovic, N., Kavazanjian, E., Jr., and Anderson, R.L., "Performance of Solid Waste Landfills in Earthquakes", *Earthquake Spectra*, Vol. 13, No. 5, May 1998.

Stewart, J.P., Bray, J.D., Seed, R.B., and Sitar, N., "*Preliminary Report on the Principal Geotechnical Aspects of the January 17, 1994 Northridge Earthquake*", Report No. UCB/EERC-94/08, College of Engineering, University of California at Berkeley, Berkeley, California, 1994, 238 p.

Problem Summary: two tears in HDPE GM liner and cracks in soil intermediate cover after Northridge earthquake

Problem Description: The Chiquita Canyon Landfill is located at the western edge of the Santa Clara Valley in Valencia, California. The site is underlain by alluvium, cemented sandstone with interbedded conglomerate and siltstone, poorly to moderately indurated sandstone, siltstone, mudstone, and conglomerate. No active faults are known to cross the site. The landfill is divided into five units: Primary Canyon, and Canyons A, B, C, and D. Canyons A and D are separated by a soil fill wedge. The Primary Canyon is not modern or geosynthetically lined and is not discussed further. Canyons A to D have single liners overlain by a sand LCRS drainage layer on the base and a soil protection layer on the side slope. The liner for Canyons A and D is a 1.5-mm thick HDPE GM on the side slope and a soil-bentonite CCL on the base. Canyon B has a 1.5-mm thick HDPE GM on the side slope and western base and a soil-bentonite CCL on the eastern base. Canyon C has a single composite liner on the base and a 1.5-mm thick HDPE GM liner on the side slopes. The liner system side slope inclinations range from 2.5H:1V to 1.5H:1V.

The 17 January 1994 Northridge earthquake (moment magnitude M_w 6.7) occurred on a blind thrust fault at a depth of approximately 15 km at the northern end of the San Fernando Valley in the greater Los Angeles area. The Chiquita Canyon Landfill is located about 12 km from the zone of energy release (i.e., the fault plane). Strong motion stations located on rock outcrops in the area recorded peak horizontal accelerations on the order of 0.4g. The estimated rock peak horizontal acceleration at the landfill resulting from the earthquake is 0.33g. At the time of the Northridge earthquake, Canyon B was inactive and awaiting closure, Canyons A and D were partially filled and used only for landfilling in wet weather, and Canyon C was active.

After the earthquake, GM liner tears were found in Canyons C and D on benches above the waste. The tears were located near and parallel to liner system anchor trenches. The GM tear located in Canyon C was 4.3 m long and opened up to 0.25 m wide. Longitudinal cracks were present in the soil intermediate cover at the top of the waste below the tear. The cracks were up to 0.3 m wide, with vertical offset of 0.15 to 0.3 m and extended along the entire side slope. In Canyon D, there were three parallel GM tears with a total length of about 23 m. Longitudinal cracks in the soil intermediate cover at the top of the waste below the tears and across the side slope were about 0.3 m wide with 0.2 m of vertical offset. At some locations, the cracks exposed the underlying GM liner. The subgrade beneath the GM at both tear locations did not appear to have been impacted. Forensic analyses indicated that the GM tears initiated from locations where GM seam samples were cut for destructive testing. In fact, the tears appear to have occurred from a corner of the rectangular hole left where the seam was cut out. Both the stress concentrations around the hole (which had been patched) and the high pullout capacity of the anchor trench appear to have been factors in the initiation and propagation of the tears. As the GM liner moved during the earthquake, it was constrained at the anchor trench and subsequently tore at locations with

concentrated stresses. Furthermore, in Canyons C and D, it appears that the slope stability factor of safety of the waste at intermediate grades was relatively low under the seismic loading of the Northridge earthquake. Cracks in the soil intermediate cover were also observed in Canyon A near the contact of the landfill and the soil fill wedge and in Canyon B along the perimeter of the side slope liner system. The cracks in Canyon A were about 0.15 m wide with 0.13 m of vertical offset. At some locations, waste was exposed. The soil intermediate cover in Canyon B had some minor cracking with no waste exposed.

Figure F-A.8.2. Longitudinal cracks in soil intermediate cover at Chiquita Canyon Landfill after the Northridge earthquake.

Resolution: The GM tears were patched. The liner system anchor trenches in Canyons C and D above the GM tears were abandoned. The GM liner was removed from trenches, laid horizontal over the side slope bench, and covered with a soil berm. The cracked soil intermediate cover on the entire landfill was regraded and revegetated.

Lessons Learned for Future Projects: Based on the available information, the following lessons can be learned from this case history:

- Composite liner systems on both base and side slopes, if properly designed and constructed, can sustain relatively strong earthquake shaking without experiencing significant damage.
- Liner system anchor trenches should be designed to secure geosynthetics during construction, but release the geosynthetics before they are damaged during earthquakes. For example, the liner system anchor may be designed with a relatively low factor of safety that is greater than 1.0 under static loading, but less than 1.0 under seismic loading that would damage an anchored liner system. An alternative is to unanchor the liner system after construction and secure it on a bench with an overlying soil layer.
- Stress concentrations at or near the liner system side slope crest should be avoided. In particular, GM seams should generally not be sampled near the slope crest.
- Seismic design of composite liner systems can not prevent seismic displacements. However, good seismic design should limit seismic displacements to tolerable amounts. To do this, designs may incorporate predetermined slip surfaces to confine movements to locations where they will cause the least damage (i.e., above the GM liner), soil covers that will resist cracking, and inverted liner system keyways.
- Surficial cracking of soil cover layers during seismic loading, especially near locations with contrast in seismic response characteristics (e.g., top of waste by rock canyon walls), should be anticipated and dealt with as an operation issue through post-earthquake inspection and repair.

F-A.8.5 L-27

Problem Classification: landfill liner system stability/design
Region of U.S.: southwest
Waste Type: MSW
References: Anderson, R.L., "Earthquake Related Damage and Landfill Performance", *Earthquake Design and Performance of Solid Waste Landfills*, Yegian, M.K. and Liam Finn, W.D., eds., ASCE Geotechnical Special Publication No. 54, 1995, pp. 1-16.

Augello, A.J., Matasovic, N., Bray, J.D., Kavazanjian, E., Seed, R.B., "Evaluation of Solid Waste Landfill Performance During the Northridge Earthquake", *Earthquake Design and Performance of Solid Waste Landfills*, Yegian, M.K. and Liam Finn, W.D., eds., ASCE Geotechnical Special Publication No. 54, 1995, pp. 17-50.

Chang, S., Bray, J.D., and Seed, R.B., "Engineering Implications of Ground Motions from Northridge Earthquake", *Bulletin of the Seismological Society of America*, Vol. 86, No. 1, Part B Supplement, 1996, pp. S270-S288.

Matasovic, N., Kavazanjian, E., Jr., Augello, A.J., Bray, J.D., and Seed, R.B., "Solid Waste Landfill Damage Caused by 17 January 1994 Northridge Earthquake", *The Northridge, California, Earthquake of 17 January 1994*, Woods, M.C. and Seiple, W.R., eds., California Department of Conservation, Division of Mines and Geology Special Publication 116, 1995, pp. 221-229.

Problem Summary: further tearing of GT cushion and extensive cracks in soil intermediate cover from Northridge earthquake

Problem Description: The Bradley Avenue Landfill is located in a former gravel quarry in the San Fernando Valley in southern California. The site is underlain by alluvium, which overlies crystalline and metamorphic basement complex rocks. The older alluvium consists of silty, subangular sand, cobbles and boulders. These deposits, which are more than 150 m deep, are crudely horizontally stratified, unweathered, and contain less than 1% clay. The more recent 15 to 23 m thick alluvial deposits are mainly accumulations of subangular boulders, gravels, and sands. The deposits are uncemented but are tightly packed and stand at slopes of 1H:1V or steeper. The landfill is divided into three units: Bradley East, Bradley West, and Bradley West Extension. Bradley East and Bradley West are not modern or geosynthetically lined and are not discussed further. Bradley West Extension has a single composite liner system on the base and up to 1H:1V side slopes. The liner system consists of the following components, from top to bottom:

- gravel LCRS drainage layer;
- nonwoven GT cushion;
- 1.5-mm thick HDPE GM liner; and
- CCL.

The 17 January 1994 Northridge earthquake (moment magnitude M_w 6.7) occurred on a blind thrust fault at a depth of approximately 15 km at the northern end of the San Fernando Valley of the greater Los Angeles area. The Bradley Avenue Landfill is located about 11 km from the zone of energy release (i.e., the fault plane). Peak horizontal accelerations recorded at nearby rock stations ranged from 0.2g to 0.4g. The estimated rock peak horizontal acceleration at the landfill resulting from the earthquake is 0.36g. At the time of the Northridge earthquake, the Bradley West Extension was receiving waste.

After the earthquake, extensive cracks were observed in the soil intermediate cover near its contact with the side slope liner system. The cracks, which had up to 25 mm of vertical offset, may have been the result of limited downslope movement of the GT cushion over the GM liner or the GM liner over the CCL. No tears were observed in the GM liner. However, GT tears reportedly initiated prior to the earthquake appeared to have increased in size as a result of the earthquake strong shaking.

Resolution: The GT tears were repaired. The cracked soil intermediate cover was regraded and revegetated.

Lessons Learned for Future Projects: Based on the available information, the following lessons can be learned from this case history:

- Seismic design of composite liner systems can not prevent seismic displacements. However, good seismic design should limit seismic displacements to tolerable amounts. To do this, designs may incorporate predetermined slip surfaces to confine movements to locations where they will cause the least damage (i.e., above the GM liner), soil covers that will resist cracking, and inverted liner system keyways.
- Surficial cracking of soil cover layers during seismic loading, especially near locations with contrast in seismic response characteristics (e.g., top of waste by rock canyon walls), should be anticipated and dealt with as an operation issue through post-earthquake inspection and repair.

F-A.8.6 L-38

Problem Classification: landfill liner system stability/design
Region of U.S.: northeast
Waste Type: MSW
Reference: Boschuk, J. Jr., "Landfill Covers An Engineering Perspective", *Geotechnical Fabrics Report*, IFAI, Mar 1991, pp. 23-34.
Giroud, J.P., "Lessons Learned From Studying the Performance of Geosynthetics", *Proceeding of Geotextiles-Geomembranes Rencontres 93*, Vol. 1, Joue-les-Tours, France, September 1993, pp. 15-31.

Problem Summary: sliding along needlepunched nonwoven GT/HDPE GM primary liner interface after rainfall

Problem Description: Boschuk (1991) and Giroud (1993) described the slope stability failure of a double-lined landfill cell. The liner system consists of the following components, from top to bottom:

- 0.6-m thick sand LCRS drainage layer (specified minimum hydraulic conductivity of 1×10^{-5} m/s);
- 200 g/m^2 needlepunched nonwoven GT;
- 1.5-mm thick HDPE GM primary liner;

- 0.3-m thick granular LDS drainage layer; and
- 1.5-mm thick HDPE GM/0.6-m thick CCL composite secondary liner.

The 3H:1V side slopes of the cell were up to 30 m long. Project-specific interface direct shear testing was not performed. After analyzing the stability of the liner system side slope, the design engineer added the GT between the sand LCRS drainage layer and the HDPE GM primary liner. The stability analyses showed the sand drainage layer would be unstable if it were placed over the GM, but stable if placed over a needlepunched nonwoven GT layer. Apparently, the potential for sliding between the GT and GM was not evaluated.

After several rainfall events, the sand drainage layer became wet and the GT began creeping over the GM on the side slopes. About one month after sliding started, a relatively heavy rainfall occurred at the site and the liner system slopes failed due to excessive creep and tearing of the GT and cracking of the sand layer at the slope crest. When the rain ended, the liner system was inspected and the sand at the toe of the slope was saturated. At locations where the GT tore and slid downslope, the underlying GM was abraded. In several areas, higher "ridges" in the GM, which was not installed perfectly flat, were sanded off. Since the failure coincided with rainfall, seepage pressures in the sand probably contributed to the failure.

An infinite slope analysis was conducted by the authors of this appendix. In this analysis, the secant friction angle for the nonwoven GT/GM interface was assumed to be 10°, which is within the range of friction angles reported for this interface in the technical literature. The calculated slope stability factors of safety are 0.52 and 0.25 without and with full seepage pressures in the sand layer, respectively. These values do not take into account tension in the geosynthetics, and, being an infinite slope stability analysis, do not take into account the toe buttressing effect.

Resolution: The liner system was repaired at a cost of over $800,000. The method of repair was not given by Boschuk.

Lessons Learned for Future Projects: Based on the available information, the following lesson can be learned from this case history:

- Liner system slopes should always be evaluated using rigorous slope stability analysis methods that consider the anticipated seepage pressures in the liner system and the actual shear strengths of the liner system materials assessed by project-specific testing. Such testing is recommended.

There is little available information for this case history; additional lessons may have been learned if the information was complete.

F-A.8.7 L-39

Problem Classification: landfill liner system stability/design
Region of U.S.: unknown
Waste Type: MSW
Reference: Soong, T.Y. and Koerner, R.M., "*The Design of Drainage Systems Over Geosynthetically Lined Slopes*", GRI Report #19, Geosynthetic Research Institute, Philadelphia, PA, 1997, 88 p.

Problem Summary: sliding along needlepunched nonwoven GT/HDPE GM liner interface after rainfall

Problem Description: Soong and Koerner (1997) described the slope stability failure of a liner system on a 45 m long, 3H:1V side slope that occurred in 1992. The liner system consists of the following components, from top to bottom:

- 0.45-m thick AASHTO #57 crushed limestone LCRS drainage layer (average particle size of 15 mm);
- needlepunched nonwoven GT cushion; and
- HDPE GM liner.

Soong and Koerner (1997) do not indicate if project-specific interface direct shear testing or slope stability analyses were performed.

About one to two years after the liner system was constructed, a portion of the GT tore at the crest of the slope and slid to the slope toe after a heavy rainfall. A number of successive slides occurred during several subsequent rainfalls. Soong and Koerner do not indicate if the GM liner was damaged by the slides. They attributed the failure to seepage pressures that developed in the drainage layer during heavy rainfall after it had become contaminated with fines. The source of the fines was not discussed.

An infinite slope analysis was conducted by the authors of this appendix. In this analysis, the secant friction angle for the nonwoven GT/GM interface was assumed to be 10°, which is within the range of friction angles reported for this interface in the technical literature. The calculated slope stability factors of safety are 0.52 and 0.25 without and with full seepage pressures in the sand layer, respectively. These values do not take into account tension in the geosynthetics, and, being an infinite slope stability analysis, do not take into account the toe buttressing effect. Based on these factors of safety, the GT cushion would have been in tension even without seepage pressures. Soong and Koerner do not indicate whether the GT was designed to be in tension.

Resolution: The method of repair was not given by Soong and Koerner (1997).

Lessons Learned for Future Projects: Based on the available information, the following lesson can be learned from this case history:

- Liner system slopes should always be evaluated using rigorous slope stability analysis methods that consider the anticipated seepage pressures in the liner system and the actual shear strengths of the liner system materials assessed by project-specific testing. Such testing is recommended.

There is little available information for this case history; additional lessons might have been learned if the information had been complete.

F-A.8.8 L-40

Problem Classification: landfill liner system stability/design
Region of U.S.: unknown
Waste Type: MSW
Reference: Soong, T.Y. and Koerner, R.M., "*The Design of Drainage Systems Over Geosynthetically Lined Slopes*", GRI Report #19, Geosynthetic Research Institute, Philadelphia, PA, 1997, 88 p.

Problem Summary: sliding along gravel/HDPE GM liner interface after rainfall

Problem Description: Soong and Koerner (1997) described the slope stability failure of a liner system on a 30 m long, 3H:1V side slope that occurred in 1993. The liner system consists of the following components, from top to bottom:

- 0.45-m thick AASHTO #3 crushed gravel LCRS drainage layer (average particle size of 37 mm); and
- HDPE GM liner.

Soong and Koerner (1997) do not indicate if project-specific interface direct shear testing or slope stability analyses were performed.

About three to four years after the liner system was constructed, the gravel slid over the GM to the slope toe. Soong and Koerner do not indicate if the GM liner was damaged by the slides. They attributed the failure to seepage pressures that developed in the gravel layer during heavy rainfall after the gravel had become contaminated with fines. The source of the fines was not discussed. The fines apparently inhibited drainage of water from the gravel and allowed the seepage pressures to develop.

An infinite slope analysis was conducted by the authors of this appendix. In this analysis, the secant friction angle for the gravel/GM interface was assumed to be 18°, which is within the range of friction angles reported for this interface in the technical literature. The calculated slope stability factors of safety are 0.97 and 0.47 without and with full seepage pressures in the gravel layer, respectively. Being an infinite slope stability analysis, these values do not take into the toe buttressing effect. Based on these factors of safety, the liner system was probably, at best, only marginally stable after construction.

Resolution: The method of repair was not given by Soong and Koerner (1997).

Lessons Learned for Future Projects: Based on the available information, the following lesson can be learned from this case history:

- Liner system slopes should always be evaluated using rigorous slope stability analysis methods that consider the anticipated seepage pressures in the liner

system and the actual shear strengths of the liner system materials assessed by project-specific testing. Such testing is recommended.

There is little available information for this case history; additional lessons might have been learned if the information had been complete.

F-A.8.9 L-41

Problem Classification: landfill liner system stability/design
Region of U.S.: unknown
Waste Type: MSW
Reference: Soong, T.Y. and Koerner, R.M., "*The Design of Drainage Systems Over Geosynthetically Lined Slopes*", GRI Report #19, Geosynthetic Research Institute, Philadelphia, PA, 1997, 88 p.

Problem Summary: sliding along very flexible GM liner/needlepunched nonwoven GT interface after rainfall

Problem Description: Soong and Koerner (1997) described the slope stability failure of a liner system on a 20 m long, 2.5H:1V side slope that occurred in 1994. The liner system consists of the following components, from top to bottom:

- 0.3-m thick sand LCRS drainage layer;
- very flexible polyethylene GM liner; and
- needlepunched nonwoven GT.

Soong and Koerner (1997) do not indicate if project-specific interface direct shear testing or slope stability analyses were performed.

About two to six months after the liner system was constructed, the GM tore along about 30 m of the slope crest and slid downslope over the GT after a light rainfall. Soong and Koerner attributed the failure to seepage pressures that developed in the sand layer during the rainfall.

An infinite slope analysis was conducted by the authors of this appendix. In this analysis, the secant friction angle for the GM/GT interface was assumed to be 18°, which is within the range of friction angles reported for this interface in the technical literature. The calculated slope stability factor of safety is 0.81 without and with full seepage pressures in the sand layer. This value does not take into account tension in the GM, and, being an infinite slope stability analysis, does not take into account the toe buttressing effect.

Thus, the authors found that seepage pressures above the GM would not significantly affect the stability of a failure surface along the GM/ GT interface below the GM. This effect can be explained as follows (Giroud et al., 1995a). The slope stability factor of

safety equals the shear strength divided by the shear stress. The shear stress acting above the GM is the same as that acting below the GM, with or without seepage above the GM. The shear strength of an interface is dependent on the interface adhesion, interface friction angle, and effective normal stress at the interface. The effective normal stress at an interface decreases as the seepage pressures at that interface increase. With seepage pressures above a GM, the effective stress on top of the GM decreases and, consequently, the shear strength at the interface above the GM decreases. This decrease in shear strength leads to a decrease in the slope stability factor of safety. Seepage pressures above a GM, however, do not impact the effective stresses at the interface below the GM. Thus, the shear strength of this interface and the slope stability factor of safety are unchanged with these seepage pressures.

Based on the infinite slope analysis conducted by the authors of this appendix, the liner system was, at best, only marginally stable after construction and the rainfall had the effect of "triggering" the slide. The light rain described by Soong and Koerner (1997) may have increased the weight of the overlying sand, which increased the tension in the underlying GM.

Resolution: The method of repair was not given by Soong and Koerner (1997).

Lessons Learned for Future Projects: Based on the available information, the following lesson can be learned from this case history:

- Liner system slopes should always be evaluated using rigorous slope stability analysis methods that consider the anticipated seepage pressures in the liner system and the actual shear strengths of the liner system materials assessed by project-specific testing. Such testing is recommended.

There is little available information for this case history; additional lessons might have been learned if the information had been complete.

F-A.8.10 L-42

Problem Classification: landfill liner system stability/operation
Region of U.S.: unknown
Waste Type: MSW
Reference: Soong, T.Y. and Koerner, R.M., "*The Design of Drainage Systems Over Geosynthetically Lined Slopes*", GRI Report #19, Geosynthetic Research Institute, Philadelphia, PA, 1997, 88 p.

Problem Summary: sliding along needlepunched nonwoven GT/PVC GM liner interface after a thaw

Problem Description: Soong and Koerner (1997) described the slope stability failure of a liner system on 30 m long, 4H:1V side slope segments between benches that

occurred in 1995. The liner system consists of the following components, from top to bottom:

- 0.45-m thick crushed gravel LCRS drainage layer (average particle size of 25 mm);
- needlepunched nonwoven GT; and
- PVC GM liner.

Soong and Koerner (1997) do not indicate if project-specific interface direct shear testing or slope stability analyses were performed.

About one to two years after the liner system was constructed, the GT tore and slid downslope, exposing approximately 3 ha of GM. Soong and Koerner attributed the failure to seepage pressures that developed in the gravel layer as frozen water in the gravel melted. The water could not flow freely out of the gravel at the toe of the slope because of the ice at the toe.

An infinite slope analysis was conducted by the authors of this appendix. In this analysis, the secant friction angle for the GT/GM interface was assumed to be 18°, which is within the range of friction angles reported for this interface in the technical literature. The calculated slope stability factors of safety are 1.30 and 0.62 without and with full seepage pressures in the gravel layer. These values do not take into account tension in the GT, and, being an infinite slope stability analysis, do not take into account the toe buttressing effect.

Resolution: The method of repair was not given by Soong and Koerner (1997).

Lessons Learned for Future Projects: Based on the available information, the following lesson can be learned from this case history:

- Liner system slopes should always be evaluated using rigorous slope stability analysis methods that consider the anticipated seepage pressures in the liner system and the actual shear strengths of the liner system materials assessed by project-specific testing. Such testing is recommended.
- Outlets of drainage layers should be kept free of snow and ice.

There is little available information for this case history; additional lessons might have been learned if the information had been complete.

F-A.8.11 L-45

Problem Classification: landfill liner system stability/operation
Region of U.S.: unknown
Waste Type: unknown
Reference: Hullings, D.E. and Sansone, L.J., “Design Concerns and Performance of Geomembrane Anchor Trenches", *Proceedings of the 10th GRI Conference Field*

Performance of Geosynthetics and Geosynthetic Related Systems, Geosynthetic Research Institute, Philadelphia, PA, 1996, pp. 219-233.

Problem Summary: sliding along needlepunched nonwoven GT/HDPE GM liner interface after erosion of soil anchoring geosynthetics

Problem Description: Hullings and Sansone (1996) described the slope stability failure of a liner system after the 0.5-m thick soil layer anchoring the geosynthetics beyond the slope crest was eroded by landfill traffic. The runout length of the geosynthetics beyond the crest was 3 m. At the time of the failure the 1.5-mm thick HDPE GM liner on the side slope was only covered by a needlepunched nonwoven GT protection layer. Assuming the secant interface friction angle was 10° between the GT and underlying GM and 15° between the GM and underlying soil, Hullings and Sansone concluded that the anchorage resistance provided by the soil layer was greater for the GM than for the GT.

During the wet winter months, landfill traffic traveled over the anchored geosynthetics, rather than over an adjacent muddy road. The soil layer covering the geosynthetics quickly began to erode and, eventually, was not thick enough to anchor the geosynthetics. The GT and the overlying soil layer slid downslope over the GM.

Resolution: The method of repair was not given by Hullings and Sansone (1996).

Lessons Learned for Future Projects: Based on the available information, the following lesson can be learned from this case history:

- Soil layers anchoring geosynthetics should be maintained during landfill construction and operation. The limits of liner system can be identified with cones, flags, or other markers and can also be isolated from traffic by berms, bollards, or other means.

There is little available information for this case history; additional lessons might have been learned if the information had been complete.

F-A.8.12 L-46

Problem Classification: landfill liner system stability/operation
Region of U.S.: northwest
Waste Type: MSW
Reference: unpublished

Problem Summary: sliding along GN/HDPE GM primary liner interface during construction

Problem Description: A double-composite liner system underwent slope failure during construction. The side slope liner system consists of the following components, from top to bottom:

- 0.3-m thick soil protection layer;
- needlepunched nonwoven GT filter;
- GN LCRS drainage layer;
- 1.5-mm thick HDPE GM primary liner;
- GN LDS drainage layer;
- 1-mm thick HDPE GM secondary liner; and
- 0.6-m thick CCL.

The side slopes are 11 m high and have an inclination of 3H:1V. Project-specific interface direct shear testing was not conducted. Slope stability analyses performed as part of the liner system design used assumed interface shear strengths and relied on the strength of the GT to carry part of the load of the overlying soil layer. The critical interface for slope stability was assumed to occur between the GN LCRS drainage layer and GM primary liner. The secant friction angle for this interface was taken as 11°. For the analyses, it was also assumed that the GT mobilized its wide-width tensile strength at 10% strain. The resulting factors of safety against tearing of the GT and sliding along the GN/GM primary liner interface were 2.0 and 1.6, without and with construction loads, respectively. The designer concluded that even if the strain were greater, the GM should not tear "*because of its ability to elongate 750% before tearing*". The effect of the strain in the GT and GN LCRS drainage layer on the hydraulic properties of these materials was not considered.

As the soil protection layer was being placed in the cell, the soil layer began to crack near the slope crest. A small test pit was excavated through the soil layer to inspect the geosynthetics. The GT was torn in this area and the GN was stretched and damaged. The cause of this damage was initially unclear and was considered to be potentially caused by slope instability or construction equipment. Subsequently, a slope failure initiated at the excavation area and expanded laterally as it progressed downslope. The GT tore near the slope crest and the GN panels separated and both slid downslope over the GM in a localized area of the cell, approximately 15 m wide and 9 m long. The sides of the slide zone ran along sewn seams of GT. The GN panel separations along the slope were about 5 cm. Compression ridges in the soil protection layer were present near the slope toe. Construction ceased until the case of the failure could be investigated. About three months later, after a significant precipitation event reportedly deposited several decimeters of wet snow at the site, several more slides occurred. The original slide zone moved further downslope, and slides similar in character to the original one occurred in three new areas. The slide zones covered approximately 75% of the north slope of the cell, the only slope covered with the soil protection layer. The original slide zone moved 6 to 9 m further downslope. The other three slide zones, ranging from about 15 to 30 m wide, slid from 6 to 18 m downslope. At one location near the slope crest, the GN was observed to have slide along the GM and GN panels

were separated along the slope by about 0.2 m. In general, the slide zones appeared to have moved somewhat diagonal across the slope, perhaps sliding parallel to the top ridge of the GN. Tears in the GM liner were not observed.

A forensic investigation was conducted to evaluate the cause of the slope failure. The investigation including performing interface shear strength tests and reviewing the slope stability analyses conducted by the design engineer. The measured secant friction angle for the GN/HDPE GM interface was about 8°, significantly lower than the assumed value of 11°. In addition, the strengths of the GT used in the original analyses were too high: the GT secant modulus at 10% strain rather than the GT strength at 10% strain was used in the calculations. Further, the low ground pressure bulldozer actually placing the soil protection layer weighed about twice as much as that used in design. Using the measured critical interface shear strength, the GT strength at 10% strain, and the actual weight of the construction equipment, the investigators calculated factors of safety of 0.63 and 0.48 without and with construction loads, respectively. The investigators also indicated that GT filters probably should not be used to carry significant tensile loads since they have very low tensile moduli and, thus, require significant strain to mobilize moderate strengths.

Resolution: In areas where the soil protection layer had been placed, the soil was removed and the damaged GT and GN were repaired. The placement of the soil protection layer over the GT was subsequently limited to increase slope stability: the soil layer was required to be placed in 6 m increments along the slope, advancing upslope with waste placement.

Lessons Learned for Future Projects: Based on the available information, the following lesson can be learned from this case history:

- Liner system slopes should always be evaluated using rigorous slope stability analysis methods that consider the anticipated seepage pressures in the liner system and the actual shear strengths of the liner system materials assessed by project-specific testing. Such testing is recommended.

F-A.9 Landfill Liner System Displacement

F-A.9.1 L-9

Problem Classification: landfill liner system displacement/design
Region of U.S.: northeast
Waste Type: MSW
Reference: unpublished

Problem Summary: uplift of HDPE GM by landfill gas after erosion of overlying sand LCRS drainage layer

Problem Description: During construction of a landfill liner system over the side slopes of an existing active MSW landfill, the GM component of the single-composite liner was uplifted by gas emanating from the waste. The liner system on the approximately 4H:1V 25-m high side slopes was underlain by a 0.3-m thick structural fill foundation layer. The foundation layer was not permeable enough to freely convey gas beneath the liner system, and a gas collection layer was not provided. Instead, the design called for gas beneath the liner system to be collected in an approximately 0.3 m wide by 1.5 m high gravel-filled trench located at the crest of the side slopes. This design required the gas to migrate through the existing landfill waste or liner system foundation layer to the trench and ultimately to a flare. The design was not based on site-specific considerations, rather it was based on designs that had been used successfully at other landfills. Landfill gas generation rates beneath the liner system were not estimated, and field measurements of gas production beneath the side slopes were not made.

Prior to construction of the liner system, the existing waste slope was regraded. The exposed waste was wet and contained pockets of gas that subsequently vented. Landfill gas was smelled by residents up to approximately 2 km from the existing landfill. The liner system was subsequently constructed over the waste. As the HDPE GM was seamed on the side slopes, gas emitted from the waste periodically ignited; one seamer was injured. After a 0.6-m thick sand LCRS drainage layer was placed over the GM, there were no more gas problems until the sand began to erode after a rainfall. At the eroded areas there was less overburden pressure on the liner system, allowing bubbles of gas to form beneath the GM. Ten 6-m diameter gas bubbles developed over the 3.6 ha landfill side slopes and uplifted the GM to about 1.5 m. In some areas the GM was observed to be yielding, as evidenced by the change in its color (i.e., it became lighter). When the GM was subsequently cut to release the gas, the yielded GM appeared thinner than adjacent GM. The biaxial strain in the uplifted GM was calculated by the authors of this appendix to be about 16%, assuming that the uplifted area has a spherical curved shape. In comparison, the biaxial yield strain of HDPE GMs is on the order of 10%.

Resolution: The GM liner was cut at the ten gas bubbles, and temporary gas venting pipes were installed through the liner system and into the underlying waste. These gas vents will be removed and the liner repaired before waste is placed over the liner system in these areas.

Lessons Learned for Future Projects: Based on the available information, the following lessons can be learned from this case history:

- When liner systems (or cover systems) are constructed over existing waste, the potential for the waste to generate gas must be considered. Calculation methods are available to estimate the gas generation rates for MSW landfills, based on the age of waste and other factors. Some landfills may be generating little or no gas at the time of construction of an overlying liner system. For these landfills, a gas collection layer may not be needed. Other landfills, like the one described above,

may be generating significant quantities of gas. For these landfills, a gas collection layer may be required beneath the entire liner system.
- When a landfill is constructed on top of an existing landfill (vertical expansion), exposed GM liners can be uplifted by gases from the underlying landfill. Therefore, in the case of a vertical expansion, unless gases from the underlying landfill are well controlled, GMs must be covered by a layer of soil to prevent GM uplift and precautions must be taken to prevent erosion of this soil layer.
- Uplift of a GM liner by landfill gas may generate a GM strain that exceeds the yield strain of the GM, which may weaken the GM, thereby reducing its ability to withstand subsequent stresses.

F-A.9.2 L-11

Problem Classification: landfill liner system displacement/design
Region of U.S.: northeast
Waste Type: MSW ash
Reference: unpublished

Problem Summary: uplift of geosynthetics by landfill gas after erosion of overlying sand protection layer

Problem Description: A landfill double-liner system was constructed over the slopes of an existing unlined MSW landfill. On the 2.5H:1V side slopes of the existing landfill, the double-liner system was underlain by a 0.15-m thick foundation layer. The foundation layer was not permeable enough to freely convey gas beneath the liner system, and a gas collection layer was not provided. Instead, the design called for gas beneath the liner system to be collected in the gas extraction wells for the existing landfill.

Portions of the 0.45-m thick sand protection layer on the side slopes were progressively eroded by runon and runoff. In two areas where the protection layer had eroded, the underlying GC LCRS drainage layer, HDPE GM primary liner, GN LDS drainage layer, and HDPE GM component of the composite secondary liner were uplifted about 0.1 m by landfill gases. The diameters of the uplifted areas were about 10 and 20 m. The biaxial strain in the uplifted GM was calculated by the authors of this appendix to be about very small (i.e., less than 0.002%), assuming that the uplifted area has a spherical curved shape. In comparison, the biaxial yield strain of HDPE GM is on the order of 10%.

Resolution: The GM liner was cut at the two gas bubbles to release the gas and the liner system was repaired. The sand protection layer was replaced on the side slopes.

Lessons Learned for Future Projects: Based on the available information, the following lessons can be learned from this case history:

- One waste containment system problem can lead to a number of other problems. In the case history described above, erosion of the sand protection layer led to uplift of the unballasted liner system geosynthetics by landfill gas. Erosion of the protection layer could have also lead to damage of the underlying geosynthetics by construction equipment replacing the protection layer over the liner system and by exposure to the environment (e.g., ultraviolet light, freezing temperatures).
- In the case of a vertical expansion, unless gases from the underlying landfill are well controlled, GMs must be covered by a layer of soil to prevent GM uplift and precautions must be taken to prevent erosion of this soil layer.
- From the viewpoint of gas uplift, erosion of the soil protection layer is generally less detrimental if it occurs over a large area than if it occurs over a small area because the GM strain is likely to be larger if the uplifted area is limited.

F-A.9.3 L-25

Problem Classification: landfill liner system displacement/design
Region of U.S.: northeast
Waste Type: MSW
Reference: unpublished

Problem Summary: uplift of composite liner by surface-water infiltration during construction

Problem Description: A single-composite liner system for two cells of a landfill expansion was constructed with 16.7-m high side slopes. The bottom 7.6 m of the side slope liner system was constructed in an excavation against native soil having a specified maximum hydraulic conductivity of 1×10^{-7} m/s. The upper 9.1 m of the side slope liner system was constructed against a more permeable rocky mine spoil berm. The ground surface outside of the berm was graded towards the berm, allowing runoff to pond at the toe of the exterior berm slope. Prior to construction of the liner and after rainfall, portions of the excavation base near the toe of the side slopes seemed soft and moist. The soft native soil was removed and replaced with compacted mine spoil. After several days, this mine spoil became moist. However, it did not soften as much material as the native soil and was considered acceptable for liner installation. The liner for the cells consists of the following components, from top to bottom:

- GCL composed of a 1.5-mm thick HDPE GM and a bentonite layer glued to one side of the GM; and
- 0.9-m thick CCL.

The GCL was installed with the bentonite side down and was seamed by fusion seaming the GM component of adjacent panels.

As the liner was being constructed, there were several storms that left runoff ponded at the toe of the exterior berm slope. This water was not removed by the contractor, but

was left to evaporate and infiltrate into the soil. Subsequently, water pooled under the GM and saturated the GCL and CCL near the toe of the side slope. When the GM was cut for the water to drain and the damaged GCL was removed, the underlying CCL was very soft. From inspection of the cell side slopes, the water appeared to be originating about halfway up the side slopes at the interface of the berm mine spoil and the native soil. Apparently, runoff was seeping through the more permeable berm soils into cell.

Resolution: Prior to reconstructing the damaged liner, the runoff infiltration problem was resolved as follows:

- Three vertical wells were installed into the berm to drain the water. The wells were pumped for about one week before construction resumed. Pumping continued at a lower rate throughout construction.
- The ground outside of the berm was regraded so that runoff did not collect at the toe of the berm slope.
- A gravel underdrain was constructed beneath the liner in the wet areas. Water collected in the underdrain flows through a water collection pipe that penetrates the berm.

The damaged liner was reconstructed.

Lessons Learned for Future Projects: Based on the available information, the following lesson can be learned from this case history:

- Surface-water runoff should be managed to reduce foundation problems during and after construction. Runoff should not be allowed to pond near the cell, where it can infiltrate into the cell.

F-A.9.4 L-31

Problem Classification: landfill liner system displacement/design
Region of U.S.: northeast
Waste Type: MSW
Reference: unpublished

Problem Summary: uplift of composite liner by surface-water infiltration during construction

Problem Description: A single-composite liner system for one cell of a landfill expansion was constructed with 16.7-m high side slopes. The bottom 7.6 m of the side slope liner system was constructed in an excavation against native soil having a specified maximum hydraulic conductivity of 1×10^{-7} m/s. The upper 9.1 m of the side slope liner system was constructed against a more permeable rocky mine spoil berm. The liner consists of the following components, from top to bottom:

- GCL composed of a 1.5-mm thick HDPE GM and a bentonite layer glued to one side of the GM; and
- 0.9-m thick CCL (specified maximum hydraulic conductivity of 1 x 10^{-9} m/s).

The GCL was installed with the bentonite side down and was seamed by fusion seaming the GM component of adjacent panels.

A surface-water diversion ditch was located in the mine spoil on top of the berm. The ditch was used to convey runoff and rainwater that ponded in the cell during construction. Some of the water collected in the ditch infiltrated into the mine spoil berm, pooled under the GCL, and saturated the GCL and CCL. When the GCL was cut for the water to drain and the damaged GCL was removed, a 0.6-m diameter cavity was found in the berm soils and CCL. The bottom of the cavity was located near the interface of the mine spoil and native soil. Apparently, the relatively high rate of water infiltration through the ditch and into the mine spoil caused erosion of the mine spoil and CCL where the water exited the soil and flowed beneath the GCL.

Resolution: The liner was repaired, and the ditch was lined with clay to reduce infiltration.

Lessons Learned for Future Projects: Based on the available information, the following lessons can be learned from this case history:

- Surface-water runoff must be managed to reduce foundation problems during and after construction. Temporary and permanent surface-water diversion structures located near a cell may need to be lined to reduce infiltration, especially if the structures are located on relatively permeable soils and convey relatively large amounts of water.
- Elementary geotechnical engineering principles must be followed for the design of berms. For example, adequate filters should be used to prevent internal erosion ("piping") in berms.

F-A.10 Cover System Construction

F-A.10.1 C-2

Problem Classification: cover system construction/construction
Region of U.S.: northeast
Waste Type: MSW
Reference: unpublished

Problem Summary: portion of topsoil from off-site source was contaminated with chemicals

Problem Description: During placement of the topsoil surface and protection layer for a landfill cover system, several truckloads of topsoil brought to the site by the contractor had an aromatic odor. The project specification for topsoil prohibited deleterious material in the topsoil, so topsoil hauling was ceased until the affected soil could be tested. Samples of the affected soil were collected and analyzed for VOCs and metals. Based on the results of the testing, the soil was found to contain unacceptably high concentrations of lead.

Resolution: Topsoil that smelled aromatic or contained chemicals ionized by a photoionization meter was removed from the site. Each truckload of topsoil subsequently brought to the site was screened using the above criteria.

Lessons Learned for Future Projects: Based on the available information, the following lessons can be learned from this case history:

- EPA recommends that soil borrow sources be investigated by the owner unless the materials are supplied by a commercial materials company (Daniel and Koerner, 1993). In the case history described above, topsoil was excavated by the contractor from an off-site property. If the owner had required that testpits be excavated so the topsoil could be inspected prior to construction, the topsoil contamination may have been identified earlier. The soil contamination also might have been identified earlier if the contractor had been required to submit chemical analyses on samples of the topsoil brought to the site.
- On-site CQA personnel should be trained to identify signs of soil contamination.

F-A.10.2 C-16

Problem Classification: cover system construction/construction
Region of U.S.: northeast
Waste Type: MSW
Reference: Calabria, C.R. and Peggs, I.D., "Investigation of Geomembrane Seam Failures: Landfill Cover", *Proceedings of the 10th GRI Conference Field Performance of Geosynthetics and Geosynthetic Related Systems*, Geosynthetic Research Institute, Philadelphia, PA, 1996, pp. 234-257.

Problem Summary: high failure rate of HDPE GM seam samples during destructive testing

Problem Description: A 1-mm thick textured HDPE GM barrier was installed over an MSW landfill between November 1994 and March 1995. The project specifications required that destructive testing of the GM seams be performed by the installer; the CQA consultant was only to monitor the installation. Initially, only the inside track of fusion seam samples was destructively tested in shear and peel by the installer. The project specifications, however, required both tracks of the fusion seam samples be destructively tested. After about 50% of the GM had been approved, based on passing

destructive tests, and this GM had been covered with a topsoil surface and protection layer, the CQA consultant realized that the installer had not tested both seam tracks. Archived fusion seam samples were subsequently obtained and tested. About 60% (i.e., 25 of 42) of the archived seam samples and 49% (i.e., 44 of 90) of the seam samples for the entire GM failed the peel test, primarily due to seam separation exceeding the minimum specified value of 10%. Most of the failures were associated with four of nine seaming machines and two of nine operators. Fifty percent (i.e., 6 of 12) of the extrusion seam samples taken from the section of GM not covered with topsoil also failed. These failure frequencies for fusion and extrusion seam samples do not include samples collected and tested to isolate poor quality seams. The installer attributed the high seam sample failure frequency to BTEX in landfill gas being absorbed by the HDPE and inhibiting the formation of good seams. However, after the installer sent a new supervisor to the site, the failure rate for extrusion seams dropped. In the section of GM covered with topsoil, only about 7% (i.e., two of 30) of the extrusion seam samples failed destructive testing. Interestingly, the same installer had placed an HDPE GM barrier over an adjacent section of the landfill about one year earlier and only had about 10% of seam samples failing destructive testing.

Calabria and Peggs (1996) described their investigation to determine if the amount of BTEX absorbed by the HDPE GM impacted the seam quality at the site. The investigation included obtaining archived seam samples for destructive testing and microstructural examination and analyzing GM from the site for BTEX constituents. They also exposed site-specific GM samples to BTEX, seamed them, and tested them in peal and shear. Calabria and Peggs found that most of the archived fusion seam samples showed rippling along the seam tracks and extensive warping. They attributed the ripples to GM overheating from setting the seaming machine temperature too high and speed too low. They attributed the warp to manual adjustment of the seaming machine to change its direction. They also noted that the GM at the outer edge of the seam tracks was notched, creating a location where stresses could be concentrated, which could potentially lead to stress cracking. Over 50% of the archived portions of seam samples that had previously failed destructive testing failed the peel test when tested by Calabria and Peggs. Some of these seams had linear features oriented along the length of the seam in areas of the seams where the GM was shiny and not heated sufficiently to melt its surface. Calabria and Peggs attributed these linear features to soil particles being dragged along the seam by the hot wedge of the seaming machine. A number of the extrusion seam samples could be separated by hand. Some of the these samples contained soil particles in the extrusion seams. Others showed evidence of GM overheating and lack of bonding of the extruded bead to the top or bottom GM.

Selected seam samples from the installed GM were collected and analyzed for BTEX constituents and subjected to peel testing. None of the constituents was detected at a concentration greater than 1 mg/L. No relationship was found between constituent concentration and seam failure rate. Site-specific GM samples exposed to BTEX, seamed, and then tested them in peal were found to have good quality seams. Only four of 50 individual samples tested in peel did not meet the project specification.

Calabria and Peggs noted that these few failures appeared to be related to the cleanliness of the GM in the area being seamed.

Based on their investigation, Calabria and Peggs concluded that the high failure rate for GM seam samples was predominantly caused by soil in the seams (i.e., inadequate cleaning prior to seaming). Other causes of failure were overheating and, for extrusion seams, inadequate grinding. The BTEX absorbed by the GM had no apparent impact on seam quality.

Resolution: The failed seams were isolated and repaired.

Lessons Learned for Future Projects: Based on the available information, the following lessons can be learned from this case history:

- It is important to store archive portions of GM seam samples taken for destructive testing.
- The absorption of relatively low concentrations of BTEX by HDPE GM does not appear to affect the quality of seams subsequently constructed.
- HDPE GM must be thoroughly cleaned along a seam path before the seam is constructed since dirt in the seam adversely impacts seam integrity.
- Dual track fusion seaming machines are designed to make high quality seams along two tracks. Both tracks should be destructively tested since failure of one track is generally indicative of overall seaming problems, and failure of one track can increase the stress concentrations in the adjacent track. In addition, seaming problems may be identified and corrected quicker.

F-A.11 Cover System Degradation

F-A.11.1 C-1

Problem Classification: cover system degradation/design
Region of U.S.: northcentral
Waste Type: MSW
Reference: Harris, J.M., Rivette, C.A., and Spradley, G.V., "Case Histories of Landfill Erosion Protection Using Geosynthetics", *Geotextiles and Geomembranes*, No. 11, 1992, pp. 573-585.

Problem Summary: failure of geosynthetic erosion mat-lined downchute on 3H:1V side slope

Problem Description: Harris et al. (1992) described the failure of a geosynthetic erosion mat-lined downchute on the cover system of a landfill in Missouri. An erosion mat was used to line one downchute that conveyed runoff from approximately 2 ha of cover system and 8 ha of adjacent property; riprap was used to line the remaining three downchutes that drained a total of about 10 ha. The erosion mat was a polyethylene,

three-dimensional, grass reinforcement type (i.e., turf reinforcement and revegetation mat (TRM)). The mat-lined downchute was installed on the top slope about 3 m from the slope crest, down the side slope, and along a perimeter section of the landfill. At the start, the downchute slope is about 5%, and runoff is diverted into the downchute by small diversion berms. The downchute grade increases to 33% on the side slope. Near the slope toe, the downchute has a more gentle inclination of about 8%. Riprap was placed in the downchute at this transition for energy dissipation. Mat was supplied in rolls that were typically 1.5 m wide and 30 m long. Adjacent rolls were overlapped at least 75 mm and secured to the underlying soil with 0.2 m long staples installed at 0.75 m spacings. Roll ends overlapped a minimum of 0.45 m and were shingled downward. Mat was also anchored in 0.3 m deep trenches at the top of each roll and along the sides of the downchute. After the mat was placed, it was seeded and covered with about 13 mm of topsoil. Within one month after construction, following a series of significant rainfall events, the channel was unserviceable. Soil had raveled along the sides of the downchute, soil had eroded underneath the mat and along mat panel overlaps, and the mat had moved downslope about 2 m. Failure of the mat appeared to have started at the top of the slope and progressed downward. Though grass was becoming established across the cover system by this time, there was little grass in the downchute at the time of failure.

The most severe damage to the downchute is believed to have occurred after a peak rainfall intensity of about 64 mm/hr, estimated to represent the peak rainfall from a 1-hr storm with a 5-year recurrence interval. The peak runoff from this storm in the downchute on the side slope was estimated by Harris et al. (1992) to be 1.33 m^3/s. The corresponding peak velocity in the downchute was calculated to be 2.9 m/s. A design chart used by Harris et al. (1992) indicated that limiting velocities in bare and fully grassed mat-lined channels were about 3 and 5 m/s, respectively, for a flow duration of 1 hour. Subsequently, a detailed laboratory testing program was conducted to evaluate the relationship between flow velocity and erosion of a mat-lined surface for a simulated flow duration of 0.5 hr. The results of the study indicated that fully-grassed mat-lined channels had noticeable erosion at flow velocities of about 5 m/s. However, without grass, the velocity required to develop noticeable erosion was about 3 m/s. Harris et al. (1992) concluded that the combination of large drainage area, steep slope, and the inability of grass to sprout quickly in the channel lead to failure of the downchute.

Resolution: The downchute was relined with riprap, and topsoil was replaced in the eroded areas.

Lessons Learned for Future Projects: Based on the available information, the following lessons can be learned from this case history:

- Flow velocities in drainage channels under the design storm should be calculated so the appropriate channel lining can be selected. If an erosion mat is selected for a channel and the erosion mat cannot withstand the design flow velocities until grass

is established, significant maintenance and/or failure of the downchute should be anticipated.

- If the downchute had been constructed earlier, within the plant growing season, the grass may have become established faster and erosion of the downchute may have been less severe. The erosion mat was installed and seeded in the fall, when plant growth is relatively low, resulting in an extended period with poor to no grass cover in the downchute. The average plant growing season at the site starts in April and ends in October, the month in which construction of the downchute was completed.

F-A.11.2 C-12

Problem Classification: cover system degradation/design
Region of U.S.: northeast
Waste Type: MSW
Reference: unpublished

Problem Summary: erosion of topsoil layer on 60 m long, 3H:1V side slope

Problem Description: A 16 ha landfill cover system was constructed with 60 m long, 3H:1V side slopes that were unbenched. The design called for sand berms to divert surface-water runoff from the top of the landfill to six riprap-lined downchutes on the side slopes. Sand diversion berms were also located about midway down the side slopes on the east side of the landfill and near the toe of the side slopes on the west side of the landfill. The cover system consists of the following components, from top to bottom:

- vegetated topsoil layer, 0.2 m thick on top slopes and 0.3 m thick on side slopes;
- sand drainage layer with a specified minimum hydraulic conductivity of 1×10^{-5} m/s, 0.2 m thick on top slopes and 0.4 m thick on top slopes; and
- 1-mm thick HDPE GM barrier.

Within three years after construction, about 0.8 ha of the cover system was severely eroded and 0.07 ha of cover system soils had slid downslope. Sixteen deep gullies developed on the landfill side slopes in the vicinity of the riprap-lined downchutes and in areas where the sand berms at the side slope crest were breached. Gullies typically started near the slope crest and propagated downslope. The gullies extended through the topsoil and sand drainage layers down to the GM barrier. In several locations, the GM was damaged by punctures and tears, and the subgrade beneath the GM was irregular. EPA HELP model simulations conducted after the erosion was observed indicated that the sand drainage layer on the landfill top slopes and side slopes had insufficient capacity to convey surface-water infiltration from the 25-year, 24-hour storm. Under this condition, the lateral drainage that could not be conveyed within the drainage layer flowed through the overlying topsoil layer and as surface flow. Seepage pressures in the sand drainage layer and topsoil layer increase surface erosion. Other project details that contributed to the development of erosion and gullies at the site include: (i)

sand diversion berms and downchutes did not intercept lateral flow in the sand drainage layer; (ii) runoff collected by berms and downchutes could infiltrate through the topsoil layer and enter the drainage layer; and (iii) a lack of access control resulted in unauthorized trafficking of four-wheel drive vehicles or dirt bikes on the landfill.

In two areas, the cover system topsoil moved downslope, causing longitudinal cracks through the topsoil layer and into the sand drainage layer at the crest of the slide areas and compression ridges at the toe of the areas. The GM beneath the slide areas was undamaged. The slides are attributed to the development of high seepage pressures in the sand drainage layer. One area of sliding was located near the top of the east side slope and was approximately 20 m wide x 3 m long; the other area was located near the middle of the west side slope and was about 45 m wide x 15 m long.

Resolution: The following corrective measures were implemented:

- vegetated swales, underlain by HDPE GM, were constructed along the side slope crest to collect runoff and water in the sand drainage layer at the top of the landfill and direct it to the downchutes;
- the cover system soils were replaced and the damaged GM was repaired within the gullies and slide areas; and
- a chain link fence was installed around the perimeter of the landfill to limit vehicle access.

Lessons Learned for Future Projects: Based on the available information, the following lessons can be learned from this case history:

- The surface-water runoff management strategy for this landfill, which did not effectively divert the flow of water from the top of the landfill to the downchutes and allowed uninterrupted sheet flow over the 60-m long, 3H:1V side slopes, proved inadequate to prevent erosion. A design that incorporated runoff interceptors on the side slopes, such as benches or swales, would likely have been more effective in limiting erosion.
- Cover system drainage layers should be designed to handle the total anticipated flow. Hydraulic requirements for the drainage layer should be evaluated using water balance calculations or other appropriate analyses (e.g., Giroud and Houlihan, 1995). Soong and Koerner (1997) recommend using a short-duration intensive storm in the water balance and do not recommend the EPA HELP computer model for this purpose. The drainage layer flow rates output from the HELP model are an average for a 24-hour period and are less than the peak flow rates. Thus, the HELP model values are somewhat unconservative.

F-A.12 Cover System Stability

F-A.12.1 C-3

Problem Classification: cover system stability/construction
Region of U.S.: northeast
Waste Type: MSW
Reference: Paulson, J.N., "Veneer Stability Case Histories: Design Interactions Between Manufacturer/Consultant/Owner", in *Proceedings of the 7th GRI Seminar Geosynthetics Liner Systems: Innovations, Concerns, and Designs*, Geosynthetic Research Institute, Philadelphia, PA, 1993, pp. 235-241.

Problem Summary: sliding along nonwoven GT/GM interface during construction

Problem Description: Paulson (1993) described a cover system slope failure. The cover system consists of the following components, from top to bottom:

- topsoil surface and protection layer;
- geosynthetic reinforcement;
- nonwoven GT cushion; and
- GM barrier.

The side slopes are about 9 to 27 m long; the slope inclination was not given by Paulson. The design specified that the geosynthetic reinforcement be secured on the top of the landfill by extending the reinforcement onto the top and covering it with a 0.9-m thick topsoil layer. Slope stability analyses were conducted assuming topsoil would be placed over the reinforcement from the bottom of the slopes upward. However, this condition was not incorporated into the construction specifications. When construction began, access to the bottom of the side slopes was not available. So the contractor started placing topsoil from the crest of the slope downwards. Shortly afterwards, about a 50 m wide by 20 m long section of soil covered cover system slid along the GT/GM interface.

Resolution: The cover system in the failed area was repaired by placing new geosynthetic reinforcement and GT layers over the GM barrier, and placing the topsoil over the GT from the bottom of the side slopes upward.

Lessons Learned for Future Projects: Based on the available information, the following lessons can be learned from this case history:

- EPA recommends that soil layers on side slope geosynthetics generally be placed from the toe of slope upward to avoid tensioning the geosynthetics (Daniel and Koerner, 1993). If the construction specifications for the cover system described above had included this requirement, the cover system may not have slid.

- The construction-related assumptions made during design should be incorporated into the construction specifications.
- All anticipated loads should be considered and incorporated into the design.

F-A.12.2 C-4

Problem Classification: cover system stability/design
Region of U.S.: southeast
Waste Type: MSW
References: Bonaparte, R., Othman, M.A., Rad, N.R., Swan, R.H., and Vander Linde, D.L., "Evaluation of Various Aspects of GCL Performance", Appendix F in *Report of 1995 Workshop on Geosynthetic Clay Liners,* Daniel, D.E. and Scranton, H.B., Editors, EPA National Risk Management Resource Laboratory, Cincinnati, OH, EPA/600/R-96/149, 1996, pp. F-1-F-34.
Vander Linde, D.L., Luettich, S.M., and Bonaparte, R., "Lessons Learned From the Failure of a Landfill Cover System", *Geosynthetics: Lessons Learned From Failures*, IFAI, to be published in 1998.

Problem Summary: sliding along topsoil/GCL interface after rainfall

Problem Description: Bonaparte et al. (1996) and Vander Linde et al. (1998) described the slope stability failure of a cover system in northern Georgia that occurred shortly after construction. The cover system consisted of the following components:

- 0.3-m thick silty sand topsoil surface and protection layer (hydraulic conductivity in the range of 10^{-6} to 10^{-5} m/s); and
- stitch-bonded reinforced GCL barrier.

The 3H:1V cover system side slopes are up to 54 m long. During design, the slope stability factor of safety for the cover system was calculated to be greater than 1.3 assuming no seepage pressures in the topsoil layer and a topsoil/GCL secant interface friction angle of 24°. This interface shear strength was selected by the engineer based on information provided by the GCL manufacturer.

Within three months after construction, the cover system experienced two major episodes of downslope movement of the topsoil layer over the GCL. The first major slide occurred about one month after the end of construction; the movement occurred after a three-day rainfall of 58 mm. The slide was limited to a relatively small area on the bottom half of the side slopes. The design engineer believed that the movement was the result of erosion. Consequently, the contractor was directed to repair the area, but reportedly was not able to complete the work due to the wet/soft condition of the cover system. The next major slide occurred about six weeks later, after a 41 mm rainfall occurred at the site over a two-day period. Numerous slides occurred on the upper and lower portions of the side slopes. (A slide was characterized by a section of topsoil moving monolithically over the GCL.) Horizontal cracks through the topsoil layer

and parallel to the slope crest were apparent near the top of the section and compression ridges, up to about 0.45 m high, were present at the bottom of the section. The total downslope movement during these two episodes exceeded 1 m at some locations. By the end of these two sliding episodes, the topsoil on about 50% of the landfill side slopes had slid downslope.

Figure F-A.12.1. Cover system at the end of the second sliding episode.

A forensic investigation was conducted to identify the cause of the cover system failure. The topsoil was removed in part of the slide zone and the GCL was inspected. Though the GCL was hydrated and under a low overburden stress, the bentonite in the GCL was not visibly extruded through the upper GT. The GCL was intact and did not appear to have moved. The soil over the GCL was saturated and did not drain freely. A back analysis of the cover system slope stability was conducted which accounted for the effect of rainfall-induced seepage pressures. The hydraulic heads of water in the topsoil layer during the two episodes of downslope movement were estimated by several different calculation methods to range from 0.15 to 0.3 m. These heads were used to

calculate seepage pressures in the topsoil layer. The back analysis was initially conducted using secant interface friction angles of 20°, 24°, and 26° for the topsoil/GCL interface. A slope stability analysis was conducted and the following results were obtained using the equations presented by Giroud et al. (1995a):

		Factor of Safety	
Friction Angle	Head = 0 m	Head = 0.1 m	Head = 0.2 m
20°	1.09	0.84	0.60
24°	1.35	1.04	0.73
26°	1.47	1.13	0.80

Shear strength tests performed on the topsoil/GCL interface after the completion of the back analyses resulted in peak and large-displacement secant friction angles of 23° and 21°. Based on these results and on the calculated slope stability factors of safety presented above, the episodes of cover system sliding were primarily attributed to seepage pressures in the topsoil.

Resolution: The cover system was redesigned to consist of the following components:

- 0.6-m thick topsoil surface and protection layer;
- GC drainage layer; and
- HDPE GM barrier.

This redesign has not yet been approved by the landfill owner and may be modified. As of almost three years since the failure, no improvements have been made to the cover system.

Lessons Learned for Future Projects: Based on the available information, the following lessons can be learned from this case history:

- Cover system slopes should always be evaluated using rigorous slope stability analysis methods that consider the anticipated seepage pressures in the cover system and the actual shear strengths of the cover system materials and interfaces. Both of these considerations probably contributed to the cover system failure described above. The hydraulic head of water in the topsoil layer should be evaluated using water balance calculations or other appropriate analysis method (e.g., Giroud and Houlihan, 1995). Soong and Koerner (1997) recommend using a short-duration intensive storm in the water balance and do not recommend the EPA HELP computer model for this purpose. The drainage layer flow rates output from the HELP model are an average for a 24-hour period and may be much less than the peak flow rates calculated using other methods if the precipitation data used in the HELP model are not carefully selected.
- Cover systems incorporating a low-permeability barrier layer should include a drainage layer above the barrier. A drainage layer is typically included when the

cover system side slopes are steeper than 5H:1V (EPA, 1994). For the case history described above, cover system failure would likely have been prevented if the cover system design had included an adequate drainage layer.

- The hydraulic head of rainwater in the cover system topsoil layer is a function of drainage path length. A design that incorporated topsoil seepage interceptors, such as benches or swales, on the 54 m long, 3H:1V side slopes would likely have reduced the potential for slope failure.
- Though the topsoil/GCL interface shear strength assumed for design was within the range of strengths reported in the technical literature, it was higher than the strength measured in the laboratory after the failure. An error or one or two degrees on the interface friction angle can have a significant impact on the factor of safety. Actual interface strengths can only be assessed by project-specific testing. Such testing is recommended.

F-A.12.3 C-5

Problem Classification: cover system stability/design
Region of U.S.: northeast
Waste Type: MSW
Reference: Boschuk, J. Jr., "Landfill Covers An Engineering Perspective", *Geotechnical Fabrics Report*, IFAI, Mar 1991, pp. 23-34.

Problem Summary: sliding along sand/woven GT interface after rainfall

Problem Description: Boschuk (1991) described a cover system slope failure. The cover system consists of the following components, from top to bottom:

- topsoil surface and protection layer;
- medium-coarse sand drainage layer;
- woven GT reinforcement layer; and
- GM barrier.

Project-specific interface direct shear testing was not performed. For design, the sand/GT interface secant friction angle was assumed to be 24°. After a significant rainfall, the soil layers slid off the GT on the 3H:1V side slopes.

Boschuk (1991) did not indicate if a slope stability analysis was performed as part of the cover system design. Since the failure appeared to coincide with rainfall, seepage pressures in the cover system soils probably contributed to the failure. An infinite slope analysis was conducted by the authors of this appendix. Using the assumed sand/GT interface friction angle of 24°, which is at the lower end of the range of secant friction angles reported for this interface in the technical literature, the calculated slope stability factor of safety is 1.34 with no seepage pressures in the cover system, 0.98 with seepage in the sand layer, and 0.63 with full seepage in the sand and topsoil layers.

Resolution: The method of repair was not given by Boschuk.

Lessons Learned for Future Projects: Based on the available information, the following lessons can be learned from this case history:

- Cover system slopes should always be evaluated using rigorous slope stability analysis methods that consider the anticipated seepage pressures in the cover system and the actual shear strengths of the cover system materials. Both of these considerations probably contributed to the cover system failure described above.
- Cover system drainage layers should be designed to handle the total anticipated flow. Hydraulic requirements for the drainage layer should be evaluated using water balance calculations or other appropriate analysis method (e.g., Giroud and Houlihan, 1995). Soong and Koerner (1997) recommend using a short-duration intensive storm in the water balance and do not recommend the EPA HELP computer model for this purpose. The drainage layer flow rates output from the HELP model are an average for a 24-hour period and may be much less than the peak flow rates calculated using other methods if the precipitation data used in the HELP model are not carefully selected. It is not clear if the drainage layer hydraulic requirements were evaluated for the cover system described above.

There is little available information for this case history; additional lessons might have been learned if the information had been complete.

F-A.12.4 C-6

Problem Classification: cover system stability/design
Region of U.S.: northeast
Waste Type: MSW
Reference: Boschuk, J. Jr., "Landfill Covers An Engineering Perspective", *Geotechnical Fabrics Report*, IFAI, Mar 1991, pp. 23-34.

Problem Summary: sliding along sand/GM interface after rainfall

Problem Description: Boschuk (1991) described a cover system slope failure. The cover system consists of the following components, from top to bottom:

- topsoil surface and protection layer;
- sand drainage layer (specified minimum hydraulic conductivity of 1×10^{-4} m/s); and
- GM barrier.

The 3H:1V cover system side slopes are over 60 m long. After three days of rainfall, the lower portions of the slopes became saturated and the soil layers slid downslope along the sand/GM interface.

Boschuk (1991) did not indicate if interface direct shear testing or a slope stability analysis were performed as part of the cover system design. Since the failure appeared

to coincide with rainfall, seepage pressures in the cover system soils probably contributed to the failure. An infinite slope analysis was conducted by the authors of this appendix. In this analysis, the secant friction angle for the sand/GM interface was assumed to be 20°, which is within the range of friction angles reported for this interface in the technical literature. The calculated slope stability factor of safety is 1.09 with no seepage pressures in the soil layers and about 0.80 with full seepage in the sand layer. Being an infinite slope stability analysis, these values do not take into account the toe buttressing effect.

Resolution: The cover system was reconstructed with benches, so that the maximum 3H:1V cover system slope length was reduced. At each bench, collection pipes were installed to drain the water from the sand drainage layer onto the bench. It is not known if a slope stability analysis or drainage layer design calculations were performed for this redesign.

Lessons Learned for Future Projects: Based on the available information, the following lessons can be learned from this case history:

- Cover system slopes should always be evaluated using rigorous slope stability analysis methods that consider the anticipated seepage pressures in the cover system drainage layers and the actual shear strengths of the cover system materials. Both of these considerations probably contributed to the cover system failure described above.
- Cover system drainage layers should be designed to handle the total anticipated flow. Hydraulic requirements for the drainage layer should be evaluated using water balance calculations or other appropriate analysis method (e.g., Giroud and Houlihan, 1995). Soong and Koerner (1997) recommend using a short-duration intensive storm in the water balance and do not recommend the EPA HELP computer model for this purpose. The drainage layer flow rates output from the HELP model are an average for a 24-hour period and may be much less than the peak flow rates calculated using other methods if the precipitation data used in the HELP model are not carefully selected. It is not clear if the drainage layer hydraulic requirements were evaluated for the cover system described above.
- The hydraulic head of rainwater in the cover system topsoil layer is a function of drainage path length. A design that incorporated topsoil seepage interceptors, such as benches or swales, on the over 60 m long, 3H:1V side slopes would likely have reduced the potential for slope failure.

There is little available information for this case history; additional lessons might have been learned if the information had been complete.

F-A.12.5 C-7

Problem Classification: cover system stability/design
Region of U.S.: northeast

Waste Type: MSW
Reference: Boschuk, J. Jr., "Landfill Covers An Engineering Perspective", *Geotechnical Fabrics Report*, IFAI, Mar 1991, pp. 23-34.

Problem Summary: sliding along gap-graded sand/GM interface after rainfall

Problem Description: Boschuk (1991) described a cover system slope failure that appeared to be related to clogging of the sand drainage layer. The cover system consists of the following components, from top to bottom:

- topsoil surface and protection layer;
- gap-graded sand drainage layer (specified minimum hydraulic conductivity of 1×10^{-4} m/s); and
- GM barrier.

The cover system side slopes are about 50 to 90 m long. In less than one year after construction, the entire lower third of the cover system slope slid downslope along the sand/GM interface over several rainfall events. The sand drainage layer in the slide zone contained significant fines, presumably washed into the sand from the topsoil layer and the sand in the upper two-thirds of the side slope.

Boschuk (1991) did not indicate if filter design calculations or laboratory tests were performed to evaluate whether the topsoil would be retained by the sand. He also did not indicate if a slope stability analysis or interface direct shear testing were performed as part of the cover system design. Since the failure appeared to coincide with clogging of the sand drainage layer and rainfall and since failure occurred at the upper interface of the GM, seepage pressures in the cover system soils probably contributed to the failure. An infinite slope analysis was not conducted by the authors of this appendix because the slope inclination was not given by Boschuk.

Resolution: The cover system drainage layer on the side slope was reconstructed with an improved drainage layer consisting of, from top to bottom:

- uniformly-graded sand drainage layer;
- GT filter; and
- GN drainage layer.

No information is available on the method used to design the improved drainage layer.

Lessons Learned for Future Projects: Based on the available information, the following lessons can be learned from this case history:

- Gap-graded soils are more prone to migration of finer-sized particles (i.e., internal instability) than continuously-graded soils. As shown in the case history described above, this particle migration may result in clogging of the soil. Therefore, if gap-

graded soils are used as drainage materials, the effect of particle migration should be evaluated during design. For example, filter design can be performed to assess if the coarser particles will retain the finer particles or laboratory tests can be performed to assess the effect of particle migration on hydraulic conductivity.

- In the case history described above, the sand should act as a filter for the overlying topsoil. Filter layers should be designed to be compatible with the upgradient soil using filter criteria and/or laboratory testing. It is not clear if this was done for the cover system described above.
- Cover system slopes should always be evaluated using rigorous slope stability analysis methods that consider the anticipated seepage pressures in the cover system drainage layers and the actual shear strengths of the cover system materials. Both of these considerations probably contributed to the cover system failure described above.

There is little available information for this case history; additional lessons might have been learned if the information had been complete.

F-A.12.6 C-8

Problem Classification: cover system stability/design
Region of U.S.: northeast
Waste Type: MSW
Reference: Boschuk, J. Jr., "Landfill Covers An Engineering Perspective", *Geotechnical Fabrics Report*, IFAI, Mar 1991, pp. 23-34.

Problem Summary: sliding along gravel/GM interface during construction

Problem Description: Boschuk (1991) described a cover system that could not be constructed due to slope failure. The cover system, as designed, consisted of the following components, from top to bottom:

- topsoil surface and protection layer;
- pea gravel drainage layer; and
- GM barrier.

During construction, the gravel placed on the 3H:1V side slope continually slid down the slope, eventually damaging the GM. The Contractor had tried to place the gravel by pushing it up the slope with a bulldozer and by placing it on the slope using a clamshell bucket, but neither method worked. The length of the side slope was not given by Boschuk.

Boschuk (1991) did not indicate if interface direct shear testing or a slope stability analysis were performed as part of the cover system design. However, from an infinite slope analysis, the cover system would be unstable if the secant friction angle for the

gravel/GM interface was less than the slope angle, or 18.4°. This value is within the range of friction angles reported for a gravel/GM interface in the technical literature.

Resolution: The method of repair was not given by Boschuk.

Lessons Learned for Future Projects: Based on the available information, the following lesson can be learned from this case history:

- Cover system slopes should always be evaluated using rigorous slope stability analysis methods that consider the actual shear strengths of the cover system materials.

There is little available information for this case history; additional lessons might have been learned if the information had been complete.

F-A.12.7 C-9

Problem Classification: cover system stability/design
Region of U.S.: northeast
Waste Type: MSW
Reference: Boschuk, J. Jr., "Landfill Covers An Engineering Perspective", *Geotechnical Fabrics Report*, IFAI, Mar 1991, pp. 23-34.

Problem Summary: sliding along sand/calendered nonwoven GT interface during construction

Problem Description: Boschuk (1991) described a cover system slope failure. The cover system consists of the following components, from top to bottom:

- topsoil surface and protection layer;
- sand drainage layer;
- calendered nonwoven GT cushion; and
- GM barrier.

Project-specific interface direct shear tests between the sand and GT resulted in a secant interface friction angle of about 21°. These tests were reportedly conducted at confining stresses significantly greater than those representative of field conditions. As topsoil was being placed over the already-installed sand drainage layer on 3H:1V slopes, the cover system slid along the sand/GT interface.

Boschuk (1991) did not indicate if a slope stability analysis was performed as part of the cover system design. However, he noted that tilt table tests subsequently performed at low stresses representative of those at failure gave an secant friction angle for the sand/GT interface of about 18°. The differences in secant interface friction angles may be attributed to variation in the tested geosynthetics, accuracy of the test methods, and

differences in the test conditions. An infinite slope analysis was conducted by the authors of this appendix. For an interface secant friction angles of 18°and 21°, the calculated slope stability factors of safety are 0.98 and 1.15, respectively, with no seepage forces. Being an infinite slope stability analysis, these values do not take into account the toe buttressing effect.

Resolution: The calendered nonwoven GT was replaced with a needlepunched nonwoven GT. The results of tilt table tests between the sand and needlepunched nonwoven GT indicated that the needlepunched GT would be suitable.

Lessons Learned for Future Projects: Based on the available information, the following lessons can be learned from this case history:

- Cover system slopes should always be evaluated using rigorous slope stability analysis methods that consider the actual shear strengths of the cover system materials.
- Actual interface shear strengths can only be assessed by project-specific testing. The effects of variation in the tested geosynthetics, accuracy of test methods, and test conditions must be considered when selecting the interface shear strength to use in design.

There is little available information for this case history; additional lessons might have been learned if the information had been complete.

F-A.12.8 C-10

Problem Classification: cover system stability/design
Region of U.S.: northeast
Waste Type: MSW
Reference: Boschuk, J. Jr., "Landfill Covers An Engineering Perspective", *Geotechnical Fabrics Report*, IFAI, Mar 1991, pp. 23-34.

Problem Summary: sliding along sand/GM interface after rainfall

Problem Description: Boschuk (1991) described a cover system slope failure. The cover system consists of the following components, from top to bottom:

- topsoil surface and protection layer;
- sand drainage layer; and
- GM barrier.

Perforated pipes wrapped with a nonwoven GT filter were installed in the sand drainage layer to drain the collected water out of the cover system. Eventually, fines clogged the GT at the pipe perforations and water became trapped in the drainage layer. Pore pressures increased in the soils, and the soils slid downslope. Failure occurred at the

sand/GM interface, primarily on the lower third of the slope. After the failure, the pipes were dry and the surrounding sands were saturated.

Boschuk (1991) did not indicate if filter design, interface direct shear testing, or a slope stability analysis were performed as part of the cover system design. The GT should have been designed to be compatible with the sand using filter criteria calculations and/or laboratory testing. Hydraulic gradients tests performed on the sand and GT after the slope failure found that the sand fines clogged the GT. A thinner, more open nonwoven GT that let the fines pass but retained the sand, would have performed better. An infinite slope analysis was conducted by the authors of this appendix. In this analysis, the secant friction angle for the sand/GM interface was assumed to be 20°, which is within the range of friction angles reported for this interface in the technical literature. The slope stability factor of safety is 1.09 with no seepage pressures in the soil layers and about 0.80 with full seepage in the sand layer. Being an infinite slope stability analysis, these values do not take into account the toe buttressing effect.

Resolution: The pipes were removed and replaced with perforated pipes bedded in gravel wrapped in a GT. The cover system was reconstructed in the failed areas. Boschuk did not indicate if the same type of GT was used. If it was, clogging of the GT may occur again.

Lessons Learned for Future Projects: Based on the available information, the following lessons can be learned from this case history:

- GT filters should be designed to be compatible with the upgradient soil using filter criteria calculations and/or laboratory testing.
- Cover system slopes should always be evaluated using rigorous slope stability analysis methods that consider the anticipated seepage pressures in the cover system drainage layers and the actual shear strengths of the cover system materials. Both of these considerations probably contributed to the cover system failure described above.

There is little available information for this case history; additional lessons might have been learned if the information had been complete.

F-A.12.9 C-11

Problem Classification: cover system stability/design
Region of U.S.: northeast
Waste Type: MSW
Reference: Boschuk, J. Jr., “Landfill Covers An Engineering Perspective”, *Geotechnical Fabrics Report*, IFAI, Mar 1991, pp. 23-34.

Problem Summary: sliding along topsoil/nonwoven GT interface after rainfall

Problem Description: Boschuk (1991) described a cover system slope failure. The cover system consists of the following components, from top to bottom:

- topsoil surface and protection layer;
- nonwoven GT filter;

- gravel drainage layer; and
- GM barrier.

Over time, the GT became clogged by the topsoil and rainwater infiltrating the topsoil did not drain freely into the underlying gravel. After rainfall, pore pressures increased in the topsoil layer, and the topsoil slid downslope over the GT. Failure occurred primarily on the lower third of the slope.

Boschuk (1991) did not indicate if filter design, interface direct shear testing, or a slope stability analysis were performed as part of the cover system design. The GT should have been designed to be compatible with the topsoil using filter criteria calculations and/or laboratory testing. Compatibility between a soil and a GT is more of a concern when the soil is topsoil rather than clean sand because topsoil generally has a lower degree of internal stability than clean sand. Internally unstable soils are likely have a large amount of finer particles that move through the soil and may result in clogging of downgradient filters. Topsoil is sometimes susceptible to this piping of fines because it generally has a significant amount of fines and it is placed loose. However, this effect may be counterbalanced by the cohesiveness of topsoils. Soils with cohesive fines are more likely to be internally stable. An infinite slope analysis was conducted by the authors of this appendix. In this analysis, the secant friction angle for the topsoil/GT interface was assumed to be 24°, which is within the range of friction angles reported for this interface in the technical literature. The slope stability factor of safety is 1.34 with no seepage pressures in the topsoil layer and about 0.63 with full seepage in the topsoil layer. Being an infinite slope stability analysis, these values do not take into account the toe buttressing effect.

Resolution: The method of repair was not given by Boschuk.

Lessons Learned for Future Projects: Based on the available information, the following lesson can be learned from this case history:

- Cover system slopes should always be evaluated using rigorous slope stability analysis methods that consider the anticipated seepage pressures in the cover system drainage layers and the actual shear strengths of the cover system materials. Both of these considerations probably contributed to the cover system failure described above.
- When a filter layer is used, the filter should be designed to be compatible with the upgradient soil using filter criteria calculations and/or laboratory testing.

There is little available information for this case history; additional lessons might have been learned if the information had been complete.

F-A.12.10 C-13

Problem Classification: cover system stability/operation
Region of U.S.: northeast
Waste Type: MSW
Reference: unpublished

Problem Summary: sliding along PVC GM/CCL interface after a thaw

Problem Description: A landfill cover system was constructed in the fall. It consisted of the following components, from top to bottom:

- 0.1-m thick topsoil surface layer;
- 0.2-m thick sand protection layer;
- needlepunched nonwoven GT filter;
- 0.3-m thick sand drainage layer;
- 0.75-mm thick PVC GM barrier; and
- 0.45-m thick CCL.

The side slope grade is 3H:1V in some areas and 4H:1V in other areas.

During the winter, the cover system was covered with snow and the ambient temperature was below freezing temperature until the spring. In April, a slide occurred at the GM/CCL interface, on a 4H:1V slope, but no failure occurred in the 3H:1V slope and in other parts of the 4H:1V slope. The slide area was approximately 26 m long in the slope direction and 60 m wide. Rupture of the GM occurred about 2 m downslope of the slope crest, and the GM slid about 3 m downslope from the tear. Above the tear, the GM remained secured in an anchor trench. When the soil layers were removed from the GM in the slide area so the GM could be inspected, the upper 6 m of GM was torn into strips that covered only about 50% of the underlying CCL surface (i.e., there were spaces between the strips). The middle 6 m of GM in the slide zone was flat and not in tension. The lower 14 m of GM, near the slope toe, was very wrinkled, occupying a slope length of only 9 m. Based on the coverage of the GM strips in the upper 6 m of the slope, the average GM strain at failure in this portion of the slope was less than 100%. The average GM strain in slide area was 12%.

Temperature records showed that the slide occurred a few days after a first thaw following the winter. The investigation showed that water could not exit from the sand drainage layer because the lower end of the drainage layer was blocked by ice and snow accumulated at the edge of the road located at the toe of the landfill cover slope. As a result, the cause of the slide was assumed to be the seepage pressures that

developed when flow started after melting of the ice at the lower end of the drainage layer. However, slope stability analyses showed that seepage pressures above a GM have little effect on the factor of safety with respect to a slide that occurs at an interface located beneath the GM (Giroud et al., 1995a). This can be explained as follows. The slope stability factor of safety equals the shear strength divided by the shear stress. The shear stress acting above the GM is the same as that acting below the GM, with or without seepage above the GM. The shear strength of an interface is dependent on the interface adhesion, interface friction angle, and effective normal stress at the interface. The effective normal stress at an interface decreases as the seepage pressures at that interface increase. With seepage pressures above a GM, the effective stress on top of the GM decreases and, consequently, the shear strength at the interface above the GM decreases. This decrease in shear strength leads to a decrease in the slope stability factor of safety. Seepage pressures above a GM, however, do not impact the effective stresses at the interface below the GM. Thus, the shear strength of this interface and the slope stability factor of safety are unchanged with these seepage pressures.

With seepage forces identified as only a minor contributor to the slope failure, an additional investigation was conducted to evaluate the effect of temperature fluctuations on GM/CCL interface shear strength. Interface shear tests simulating the conditions during the winter (-7°C) followed by thaw (+0.5°C) showed that the formation of ice lenses at the GM/CCL interface at below-freezing temperature increased the water content at the GM-CCL interface, resulting in a marked decrease of the interface shear strength after a thaw, compared to the interface shear strength before freezing. Slope stability calculations showed that the cover system on a 4H:1V slope at the site would be unstable if the initial water content of the CCL was greater than 23%. Systematic measurements of the water content of the CCL showed that this condition was met by the CCL water content in the area where the slide occurred, and showed that the CCL water content was greater in the area where the slide occurred than in other areas. This was attributed to the heavy rainfall that preceded the installation of the GM in the area where the slide eventually occurred. The analyses also showed that the conditions for a slide to occur in the 3H:1V slope were not met. The softening of the toe of the soils overlying the GM resulted in a decrease of the factor of safety due to partial loss of toe support. This effect was evaluated and was found to be less significant than the effect of the decrease in interface shear strength.

The fact that a PVC GM had ruptured with an apparently small strain, compared to the typical 300% strain at break of PVC GMs, was investigated. Tests on the PVC GM at 23°C showed that the PVC GM after six months in the ground was identical to the original GM, and tensile tests conducted at 0.5°C showed that, under the conditions after a thaw, the PVC GM had a yield strain of 9%, which is much less than the strain at break at 23°C. This 9% yield strain explains that the observed rupture of the GM is consistent with the observed displacements.

Resolution: In the slide area, the cover soil and the GM were removed. The CCL was reworked, and covered by soil layers and GT as in the original design. However, no GM

was used in the repair of the slide area. This decision was made by the owner and the reason for this decision is not documented.

Lessons Learned for Future Projects: Based on the available information, the following lessons can be learned from this case history:

- Seepage forces, even when they exist, should not be considered responsible for all slope stability failures. Seepage forces may have a marked effect on slides that occur along an interface located above the GM; however, they generally have no significant effect on slides that occur on interfaces located below the GM.
- Freeze-thaw of CCLs can have a significantly detrimental impact on GM/CCL interface shear strength.
- Excessive CCL water content, due for example to rainfall prior to GM placement, can have a detrimental impact on interface shear strength. The CCL construction specification should generally include limitations on maximum compacted moisture content and restrictions on applying supplemental moisture.
- Outlets of drainage layers should be kept free of snow and ice.
- At low temperatures, PVC GMs may break at a low strain (e.g., on the order of 10%).

F-A.12.11 C-14

Problem Classification: landfill liner system stability/construction
Region of U.S.: unknown
Waste Type: MSW
Reference: unpublished

Problem Summary: sliding along geogrid/HDPE GM interface during construction

Problem Description: During the construction of a cover system over a landfill with approximately 32 m long, 3H:1V side slopes, a portion of the cover system failed. The cover system consists of the following components, from top to bottom:

- 0.15-m thick topsoil protection layer;
- 0.45-m thick sand drainage layer;
- geogrid reinforcement layer;
- smooth HDPE GM barrier;
- GN gas venting layer; and
- sand bedding layer.

The design specified that the reinforcement be secured on the top of the landfill by extending the reinforcement onto the top and covering it with the 0.6-m thick topsoil and sand layers. Slope stability analyses were conducted assuming that the soil layers

would be placed over the reinforcement from the bottom of the slope upward. However, this condition was not incorporated into the construction specifications.

When construction began, not all of the geogrid rolls were secured at the top of the slope because landfill gas wells were in the way. Where the gas wells interfered with geogrid installation, the geogrid was only tied to adjacent geogrid on the side slope and did not extend far beyond the slope crest. Access to the bottom of the side slopes was limited at some locations due to wetlands near the slope toe. As a consequence of these conditions, the contractor placed a stockpile of sand over the geogrid on the side slope near the crest and began placing the sand from the crest downward. Shortly after sand placement began, the reinforcement snapped at the slope crest beneath the sand stockpile and construction equipment placing the sand. The GM then tore near the slope crest and along outward diagonals down the length of the GM on both sides of the stockpile. Several rolls of geogrid in the slide area had not been anchored. The torn GM was subsequently inspected and found to have been damaged by the GN. The GN abraded the GM and in some areas broke through it.

Resolution: The cover system was redesigned and reconstructed successfully. The redesigned cover system consists of the following components, from top to bottom:

- 0.6-m thick gravel surface and protection layer (specified maximum particle size of 50 mm);
- GT cushion;
- geogrid reinforcement layer;
- textured HDPE GM barrier;
- GC gas venting layer; and
- sand bedding layer.

Lessons Learned for Future Projects: Based on the available information, the following lessons can be learned from this case history:

- EPA recommends that soil layers on side slope geosynthetics generally be placed from the toe of slope upward to avoid tensioning the geosynthetics (Daniel and Koerner, 1993). If the construction specifications for the cover system described above had included this requirement, the cover system may not have slid.
- The construction-related assumptions made during design should be incorporated into the construction specifications. In the case history presented above, the specifications should have required that the geogrid reinforcement be anchored prior to placing the soil layer to be reinforced.

F-A.12.12 C-17

Problem Classification: cover system stability/design
Region of U.S.: unknown

Waste Type: MSW
Reference: Soong, T.Y. and Koerner, R.M., "*The Design of Drainage Systems Over Geosynthetically Lined Slopes*", GRI Report #19, Geosynthetic Research Institute, Philadelphia, PA, 1997, 88 p.

Problem Summary: sliding along sand/CCL interface during rainfall

Problem Description: Soong and Koerner (1997) described the slope stability failure of a cover system on a 40 m long, 2.5H:1V side slope that occurred in 1995. The cover system consists of the following components, from top to bottom:

- 0.75-m thick silty sand surface and protection layer (approximate hydraulic conductivity of 1 x 10^{-5} m/s); and
- CCL barrier.

Soong and Koerner (1997) do not indicate if slope stability analyses were performed for design. About two to three years after the cover system was constructed, the sand slid downslope over the CCL during a storm. The slide was relatively small and localized. Soong and Koerner attributed the failure to seepage pressures that developed in the sand layer.

An infinite slope analysis was conducted by the authors of this appendix. In this analysis, the friction angle for the sand was assumed to be 30°. The calculated slope stability factors of safety are 1.44 and 0.66 without and with full seepage pressures in the sand layer. Being an infinite slope stability analysis, these values do not take into account the toe buttressing effect.

Resolution: The method of repair was not given by Soong and Koerner (1997).

Lessons Learned for Future Projects: Based on the available information, the following lesson can be learned from this case history:

- Cover system slopes should always be evaluated using rigorous slope stability analysis methods that consider the anticipated seepage pressures in the cover system drainage layers.
- Cover system drainage layers should be designed to handle the total anticipated flow. Hydraulic requirements for the drainage layer should be evaluated using water balance calculations or other appropriate analysis method (e.g., Giroud and Houlihan, 1995). Soong and Koerner (1997) recommend using a short-duration intensive storm in the water balance and do not recommend the EPA HELP computer model for this purpose. The drainage layer flow rates output from the HELP model are an average for a 24-hour period and may be much less than the peak flow rates calculated using other methods if the precipitation data used in the HELP model are not carefully selected. It is not clear if the drainage layer hydraulic requirements were evaluated for the cover system described above.

There is little available information for this case history; additional lessons might have been learned if the information had been complete.

F-A.12.13 C-18

Problem Classification: cover system stability/design
Region of U.S.: unknown
Waste Type: MSW
Reference: Soong, T.Y. and Koerner, R.M., "*The Design of Drainage Systems Over Geosynthetically Lined Slopes*", GRI Report #19, Geosynthetic Research Institute, Philadelphia, PA, 1997, 88 p.

Problem Summary: sliding along sand/CCL interface immediately after rainfall

Problem Description: Soong and Koerner (1997) described the slope stability failure of a cover system on a 50 m long, 3H:1V side slope that occurred in 1996. The cover system consists of the following components, from top to bottom:

- 0.6-m thick topsoil surface and protection layer;
- 0.3-m thick sand drainage layer (approximate hydraulic conductivity of 1×10^{-4} m/s); and
- CCL barrier.

Soong and Koerner (1997) do not indicate if slope stability analyses were performed for design. About five to six years after the cover system was constructed, the sand slid downslope over the CCL immediately after a storm. At least four localized slides occurred. Soong and Koerner attributed the failure to relatively high seepage pressures that developed in the cover system because the drainage layer hydraulic conductivity was too low.

An infinite slope analysis was conducted by the authors of this appendix. In this analysis, the friction angle for the sand was assumed to be 30°. The calculated slope stability factors of safety are 1.73 and 1.40 without and with full seepage pressures in the sand layer. With seepage pressures in the sand and topsoil layers (i.e., the sand drainage layer has insufficient capacity to convey all infiltration), the calculated factor of safety is 0.77. Being an infinite slope stability analysis, these values do not take into account the toe buttressing effect.

Resolution: The method of repair was not given by Soong and Koerner (1997).

Lessons Learned for Future Projects: Based on the available information, the following lesson can be learned from this case history:

- Cover system slopes should always be evaluated using rigorous slope stability analysis methods that consider the anticipated seepage pressures in the cover system drainage layers.
- Cover system drainage layers should be designed to handle the total anticipated flow. Cover system drainage layers should be designed to handle the total anticipated flow. Hydraulic requirements for the drainage layer should be evaluated using water balance calculations or other appropriate analysis method (e.g., Giroud and Houlihan, 1995). Soong and Koerner (1997) recommend using a short-duration intensive storm in the water balance and do not recommend the EPA HELP computer model for this purpose. The drainage layer flow rates output from the HELP model are an average for a 24-hour period and may be much less than the peak flow rates calculated using other methods if the precipitation data used in the HELP model are not carefully selected. It is not clear if the drainage layer hydraulic requirements were evaluated for the cover system described above.

There is little available information for this case history; additional lessons might have been learned if the information had been complete.

F-A.12.14 C-19

Problem Classification: cover system stability/design
Region of U.S.: unknown
Waste Type: MSW
Reference: Soong, T.Y. and Koerner, R.M., "*The Design of Drainage Systems Over Geosynthetically Lined Slopes*", GRI Report #19, Geosynthetic Research Institute, Philadelphia, PA, 1997, 88 p.

Problem Summary: sliding along sand/CCL interface after rainfall

Problem Description: Soong and Koerner (1997) described the slope stability failure of a cover system on a 45 m long, 3H:1V side slope that occurred in 1996. The cover system consists of the following components, from top to bottom:

- 0.75-m thick topsoil surface and protection layer;
- 0.3-m thick sand drainage layer; and
- CCL barrier.

The design called for water collected in the sand drainage layer to drain to the toe, be collected in a gravel toe drain, and exit the cover system through a pipe. The gravel toe drain was not wrapped with a GT. Soong and Koerner (1997) do not indicate if filter design of the topsoil, sand, and gravel or slope stability analyses were performed for design.

By about five to six years after the cover system was constructed, a number of localized slides of the sand over the CCL had occurred. When the gravel toe drain was exhumed, the gravel was found to be very contaminated with fines, which presumably migrated into the gravel from the overlying sand and topsoil. Soong and Koerner attributed the failure to relatively high seepage pressures that developed in the cover system after the gravel toe drain became clogged.

An infinite slope analysis was conducted by the authors of this appendix. In this analysis, the friction angle for the sand was assumed to be 30°. The calculated slope stability factors of safety are 1.73 and 1.45 without and with full seepage pressures in the sand layer. With seepage pressures in the sand and topsoil layers (i.e., the sand drainage layer has insufficient capacity to convey all infiltration), the calculated factor of safety is 0.76. Being an infinite slope stability analysis, these values do not take into account the toe buttressing effect.

Resolution: The method of repair was not given by Soong and Koerner (1997).

Lessons Learned for Future Projects: Based on the available information, the following lesson can be learned from this case history:

- Adjacent soils conveying water should be designed to be compatible with the upgradient soil using filter criteria and/or laboratory testing.
- Cover system slopes should always be evaluated using rigorous slope stability analysis methods that consider the anticipated seepage pressures in the cover system drainage layers.
- Cover system drainage layers should be designed to handle the total anticipated flow. Cover system drainage layers should be designed to handle the total anticipated flow. Hydraulic requirements for the drainage layer should be evaluated using water balance calculations or other appropriate analysis method (e.g., Giroud and Houlihan, 1995). Soong and Koerner (1997) recommend using a short-duration intensive storm in the water balance and do not recommend the EPA HELP computer model for this purpose. The drainage layer flow rates output from the HELP model are an average for a 24-hour period and may be much less than the peak flow rates calculated using other methods if the precipitation data used in the HELP model are not carefully selected. It is not clear if the drainage layer hydraulic requirements were evaluated for the cover system described above.

There is little available information for this case history; additional lessons might have been learned if the information had been complete.

F-A.12.15 C-20

Problem Classification: cover system stability/design
Region of U.S.: unknown
Waste Type: MSW

Reference: Soong, T.Y. and Koerner, R.M., "*The Design of Drainage Systems Over Geosynthetically Lined Slopes*", GRI Report #19, Geosynthetic Research Institute, Philadelphia, PA, 1997, 88 p.

Problem Summary: sliding along sand/CCL interface after rainfall

Problem Description: Soong and Koerner (1997) described the slope stability failure of a cover system on a 45 m long, 2.5H:1V side slope sections between benches that occurred in 1996. The cover system consists of the following components, from top to bottom:

- 0.6-m thick topsoil surface and protection layer;
- 0.2-m thick sand drainage layer; and
- CCL barrier.

The design called for water collected in the sand drainage layer to drain to the toe, be collected in a gravel toe drain, and exit the cover system through a pipe. The pipe was wrapped with a GT. Soong and Koerner (1997) do not indicate if filter design or slope stability analyses were performed for design.

By about four to five years after the cover system was constructed, a number of small localized slides of the sand over the CCL had occurred. When the gravel toe drain was exhumed, the GT was found to be clogged with fines at pipe perforations. The fines presumably migrated to the GT from the sand and topsoil. Soong and Koerner attributed the failure to relatively high seepage pressures that developed in the cover system after the GT around the pipe became clogged.

An infinite slope analysis was conducted by the authors of this appendix. In this analysis, the friction angle for the sand was assumed to be 30°. The calculated slope stability factors of safety are 1.44 and 1.24 without and with full seepage pressures in the sand layer. With seepage pressures in the sand and topsoil layers (i.e., the sand drainage layer has insufficient capacity to convey all infiltration), the calculated factor of safety is 0.63. Being an infinite slope stability analysis, these values do not take into account the toe buttressing effect.

Resolution: The method of repair was not given by Soong and Koerner (1997).

Lessons Learned for Future Projects: Based on the available information, the following lesson can be learned from this case history:

- Perforated pipes bedded in gravel should not be wrapped with a GT because the GT is useless, and, in some cases, even detrimental (Giroud, 1996). Furthermore, EPA recommends that perforated pipes generally not be wrapped with a GT (Bass, 1986).

- Cover system slopes should always be evaluated using rigorous slope stability analysis methods that consider the anticipated seepage pressures in the cover system drainage layers.
- Cover system drainage layers should be designed to handle the total anticipated flow. Cover system drainage layers should be designed to handle the total anticipated flow. Hydraulic requirements for the drainage layer should be evaluated using water balance calculations or other appropriate analysis method (e.g., Giroud and Houlihan, 1995). Soong and Koerner (1997) recommend using a short-duration intensive storm in the water balance and do not recommend the EPA HELP computer model for this purpose. The drainage layer flow rates output from the HELP model are an average for a 24-hour period and may be much less than the peak flow rates calculated using other methods if the precipitation data used in the HELP model are not carefully selected. It is not clear if the drainage layer hydraulic requirements were evaluated for the cover system described above.

There is little available information for this case history; additional lessons might have been learned if the information had been complete.

F-A.12.16 C-21

Problem Classification: cover system stability/design
Region of U.S.: southwest
Waste Type: MSW
References: Anderson, R.L., "Earthquake Related Damage and Landfill Performance", *Earthquake Design and Performance of Solid Waste Landfills*, Yegian, M.K. and Liam Finn, W.D., eds., ASCE Geotechnical Special Publication No. 54, 1995, pp. 1-16.

Augello, A.J., Matasovic, N., Bray, J.D., Kavazanjian, E., Seed, R.B., "Evaluation of Solid Waste Landfill Performance During the Northridge Earthquake", *Earthquake Design and Performance of Solid Waste Landfills*, Yegian, M.K. and Liam Finn, W.D., eds., ASCE Geotechnical Special Publication No. 54, 1995, pp. 17-50.

Chang, S., Bray, J.D., and Seed, R.B., "Engineering Implications of Ground Motions from Northridge Earthquake", *Bulletin of the Seismological Society of America*, Vol. 86, No. 1, Part B Supplement, 1996, pp. S270-S288.

Matasovic, N., Kavazanjian, E., Jr., Augello, A.J., Bray, J.D., and Seed, R.B., "Solid Waste Landfill Damage Caused by 17 January 1994 Northridge Earthquake", *The Northridge, California, Earthquake of 17 January 1994*, Woods, M.C. and Seiple, W.R., eds., California Department of Conservation, Division of Mines and Geology Special Publication 116, 1995, pp. 221-229.

Stewart, J.P., Bray, J.D., Seed, R.B., and Sitar, N., "*Preliminary Report on the Principal Geotechnical Aspects of the January 17, 1994 Northridge Earthquake*", Report No. UCB/EERC-94/08, College of Engineering, University of California at Berkeley, Berkeley, California, 1994, 238 p.

Problem Summary: minor cracks in soil intermediate cover from Northridge earthquake

Problem Description: The Lopez Canyon Landfill is located in the foothill region of the San Gabriel Mountains, approximately 50 km northwest of downtown Los Angeles. The site is underlain by siltstones, sandstones, and conglomerates. Terrace deposits are present locally near the southeastern boundary of the property. Three known faults are located to the northwest and through the southeast corner of the site. The landfill is divided into four units: Areas A, B, AB+, and C. Areas A, B, and AB+ are not modern or geosynthetically lined and are not discussed further. Area C has a single composite liner system on the base and the 1.5H:1V to 1H:1V side slopes. The side slope liner system consists of the following components, from top to bottom:

- soil protection layer;
- nonwoven GT filter;
- GN LCRS drainage layer; and
- 2-mm thick HDPE GM liner (textured on one side, textured side down);
- GCL.

The side slope liner system was constructed over a reinforced concrete veneer. The predetermined liner system slip surface on the side slope is at the GN/GM interface.

The 17 January 1994 Northridge earthquake (moment magnitude M_w 6.7) occurred on a blind thrust fault at a depth of approximately 15 km at the northern end of the San Fernando Valley of the greater Los Angeles area. The Lopez Canyon Landfill is located about 8 km from the zone of energy release (i.e., the fault plane). Strong motion stations located on rock outcrops in the area recorded peak horizontal accelerations on the order of 0.4g to 0.45g. The estimated rock peak horizontal acceleration at the landfill resulting from the earthquake is 0.42g. At the time of the Northridge earthquake, Area C was active. Phase I of Area C was fully lined and filled to a height of about 30 m. Phase II was fully lined across the base, but only partially lined on the side slope.

Post-earthquake damage inspection was carried out immediately after the earthquake. There was no sign of permanent relative displacement between the waste and liner system in Area C. However, minor cracking was observed in the soil intermediate cover. At one location on side slope of Phase II where the composite liner was not completed (i.e., GN LCRS drainage layer was just placed and anchored at the top of the slope with sand bags), it appeared that the GN had slid up to +/- 20 mm over the underlying GM liner during the earthquake. This sliding occurred at the predetermined slip surface. The GN was not damaged.

Resolution: Portions of the soil intermediate cover with the widest cracks (i.e., 100 mm) were regraded.

Lessons Learned for Future Projects: Based on the available information, the following lessons can be learned from this case history:

- Surficial cracking of soil cover layers, especially near locations with contrast in seismic response characteristics (e.g., top of waste by side slopes), should be anticipated and dealt with as an operation issue through post-earthquake inspection and repair.

F-A.12.17 C-22

Problem Classification: cover system stability/design
Region of U.S.: southwest
Waste Type: MSW
References: Anderson, R.L., "Earthquake Related Damage and Landfill Performance", *Earthquake Design and Performance of Solid Waste Landfills*, Yegian, M.K. and Liam Finn, W.D., eds., ASCE Geotechnical Special Publication No. 54, 1995, pp. 1-16.
Augello, A.J., Matasovic, N., Bray, J.D., Kavazanjian, E., Seed, R.B., "Evaluation of Solid Waste Landfill Performance During the Northridge Earthquake", *Earthquake Design and Performance of Solid Waste Landfills*, Yegian, M.K. and Liam Finn, W.D., eds., ASCE Geotechnical Special Publication No. 54, 1995, pp. 17-50.
Matasovic, N., Kavazanjian, E., Jr., Augello, A.J., Bray, J.D., and Seed, R.B., "Solid Waste Landfill Damage Caused by 17 January 1994 Northridge Earthquake", *The Northridge, California, Earthquake of 17 January 1994*, Woods, M.C. and Seiple, W.R., eds., California Department of Conservation, Division of Mines and Geology Special Publication 116, 1995, pp. 221-229.
Stewart, J.P., Bray, J.D., Seed, R.B., and Sitar, N., "*Preliminary Report on the Principal Geotechnical Aspects of the January 17, 1994 Northridge Earthquake*", Report No. UCB/EERC-94/08, College of Engineering, University of California at Berkeley, Berkeley, California, 1994, 238 p.

Problem Summary: 215-m long crack in soil intermediate cover from Northridge earthquake

Problem Description: The Calabasas Landfill is a canyon fill located in the Santa Monica Valley in Agoura, California. The site is underlain by landslide deposits, interbedded sandstone and shale, and interbedded sandstone and conglomerate. Three inactive faults have been identified on site. The landfill is divided into a number of lined and unlined cells. The lined cells have a CCL or a single-composite liner system.

The 17 January 1994 Northridge earthquake (moment magnitude M_w 6.7) occurred on a blind thrust fault at a depth of approximately 15 km at the northern end of the San Fernando Valley of the greater Los Angeles area. The Calabasas Landfill is located about 23 km from the zone of energy release (i.e., the fault plane). The estimated rock peak horizontal acceleration at the landfill resulting from the earthquake is 0.20g. At the time of the Northridge earthquake, the landfill had only one geosynthetically-lined cell (Cell P). Cell P was partially constructed and receiving waste.

After the earthquake, a 215-m long crack in the soil intermediate cover was observed near and parallel to the liner system anchor trench in Cell P. The crack was up to 150 mm wide and vertically offset up to 100 mm. No waste was exposed.

Resolution: The cracked soil intermediate cover was regraded and revegetated.

Lessons Learned for Future Projects: Based on the available information, the following lesson can be learned from this case history:

- Surficial cracking of soil cover layers, especially near locations with contrast in seismic response characteristics (e.g., top of waste by side slopes), should be anticipated and dealt with as an operation issue through post-earthquake inspection and repair.

F-A.12.18 C-23

Problem Classification: cover system stability/design
Region of U.S.: southwest
Waste Type: MSW
References: Anderson, R.L., "Earthquake Related Damage and Landfill Performance", *Earthquake Design and Performance of Solid Waste Landfills*, Yegian, M.K. and Liam Finn, W.D., eds., ASCE Geotechnical Special Publication No. 54, 1995, pp. 1-16.
Augello, A.J., Matasovic, N., Bray, J.D., Kavazanjian, E., Seed, R.B., "Evaluation of Solid Waste Landfill Performance During the Northridge Earthquake", *Earthquake Design and Performance of Solid Waste Landfills*, Yegian, M.K. and Liam Finn, W.D., eds., ASCE Geotechnical Special Publication No. 54, 1995, pp. 17-50.
Matasovic, N., Kavazanjian, E., Jr., Augello, A.J., Bray, J.D., and Seed, R.B., "Solid Waste Landfill Damage Caused by 17 January 1994 Northridge Earthquake", *The Northridge, California, Earthquake of 17 January 1994*, Woods, M.C. and Seiple, W.R., eds., California Department of Conservation, Division of Mines and Geology Special Publication 116, 1995, pp. 221-229.
Stewart, J.P., Bray, J.D., Seed, R.B., and Sitar, N., "*Preliminary Report on the Principal Geotechnical Aspects of the January 17, 1994 Northridge Earthquake*", Report No. UCB/EERC-94/08, College of Engineering, University of California at Berkeley, Berkeley, California, 1994, 238 p.

Problem Summary: minor cracks in soil intermediate cover from Northridge earthquake

Problem Description: The Simi Valley Landfill is a canyon fill located in Ventura County, California. The site is underlain by alluvium, which overlies crystalline and metamorphic basement complex rocks. The landfill has a single-composite liner system.

The 17 January 1994 Northridge earthquake (moment magnitude M_w 6.7) occurred on a blind thrust fault at a depth of approximately 15 km at the northern end of the San Fernando Valley of the greater Los Angeles area. The Simi Valley Landfill is located about 22 km from the zone of energy release (i.e., the fault plane). The estimated rock peak horizontal acceleration at the landfill resulting from the earthquake is 0.21g. At the time of the Northridge earthquake, the landfill had two lined cells, one active and one inactive.

After the earthquake, minor cracking of the soil intermediate cover was reported.

Resolution: The cracked soil intermediate cover was regraded and revegetated.

Lessons Learned for Future Projects: Based on the available information, the following lesson can be learned from this case history:

- Surficial cracking of soil cover layers, especially near locations with contrast in seismic response characteristics (e.g., top of waste by side slopes), should be anticipated and dealt with as an operation issue through post-earthquake inspection and repair.

F-A.13 Cover System Displacement

F-A.13.1 C-12

Problem Classification: cover system displacement/design
Region of U.S.: northeast
Waste Type: MSW
Reference: unpublished

Problem Summary: cover system settlement caused tearing of GM boots around gas well penetrations of GM barrier

Problem Description: A landfill cover system with a 1-mm thick HDPE GM barrier was constructed in 1991 and 1992. By late 1992, a gas collection system, including vertical HDPE gas collection wells that penetrated the GM barrier, had been installed in the landfill. At each penetration, an HDPE GM boot was clamped to the well and extrusion seamed to the GM barrier to seal the barrier around the well.

When several of the GM boots around the wells were inspected in 1995, the boots were observed to be torn from the GM barrier. The boots were not designed to accommodate settlement of the waste, which would cause downward displacement of the GM barrier relative to the wells. Since the cover system had been constructed, the landfill top had settled from 0.3 to 0.9 m and the side slopes had settled less than 0.3 m.

Resolution: The gas extraction well boots were replaced with new expandable boots that can elongate up to 0.3 m. These boots can also be periodically moved down the well to accommodate landfill settlement.

Lessons Learned for Future Projects: Based on the available information, the following lesson can be learned from this case history:

- Gas extraction well boots should be designed to accommodate the anticipated landfill settlements.

F-A.13.2 C-15

Problem Classification: cover system displacement/construction
Region of U.S.: northeast
Waste Type: paper mill sludge
Reference: Badu-Tweneboah, K., Williams, N.D., and Haubeil, D.W., "Assessment of a PVC Geomembrane Used in a Landfill Cover System", *Proceeding of Fifth International Conference on Geotextiles, Geomembranes and Related Products*, Singapore, 1994, pp. 1029-1032.

Problem Summary: localized cover system settlement during construction stretched, but did not damage, PVC GM barrier and opened GCL joints

Problem Description: A cover system was constructed over saturated, highly compressible paper mill sludge. The cover system consisted of the following components, from top to bottom:

- 0.75-m thick soil surface and protection layer;
- GC drainage layer;
- 0.5-mm thick PVC GM barrier;
- GCL; and
- GC gas collection layer.

To facilitate construction, a 3 to 6-m thick stabilized sludge working surface with a minimum undrained shear strength of 24 kPa was spread over the in-place sludge. After the geosynthetics were installed, they were covered with a soil layer. The soil was hauled from the perimeter of the landfill and spread over the geosynthetics by low-ground pressure bulldozers. The specifications required that the ground pressure of this equipment be less than 34 kPa.

The repeated trafficking of bulldozers over portions of the cover system resulted in pumping of the underlying sludge into the stabilized sludge. This pumping progressively reduced the shear strength of the stabilized sludge layer, resulting in localized bulges and, at times, placement of excessive thickness of soil. When subjected to the stresses of this excess soil, the weakened stabilized sludge layer underwent a localized bearing

capacity failure in a 60-m long by 18-m wide area. Tests pits dug to the top of the cover system geosynthetics showed that they had been subjected to settlements of 0.1 to 2.4 m. Based on calculations performed by the authors of this appendix, if the geosynthetics within this trough have a circular curved shape across the width of the trough, the average strain in the geosynthetics in the case where the settlement is 2.4 m is about 4.7%.

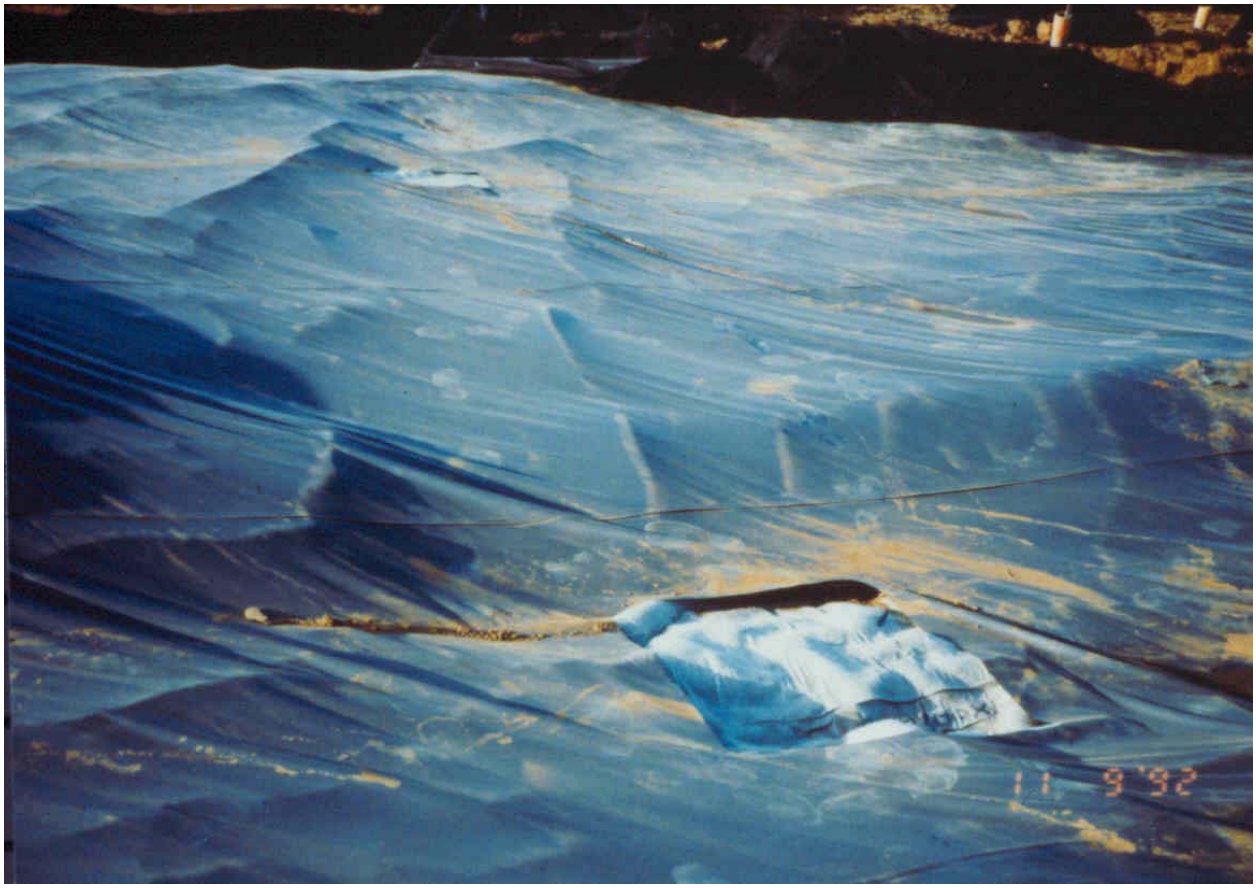

Figure F-A.13.1. Localized bearing capacity failure of stabilized sludge caused a depression in the liner system.

The soil was removed from over the geosynthetics in the affected area. None of the geosynthetics appeared to have been damaged by the straining, though the GCL seams had separated at two locations along the length of the panels. Adjacent GCL panels had been overlapped 0.15 m along the roll length; however, based on calculations by the authors of this appendix, the seam would open if the average strain exceeded 3.2%. The GM showed some lateral wrinkling, indicating it was in tension in the other direction. However, it had no tears, scratches, or separated seams, except for the few locations damaged by the backhoe excavating the soil off of the geosynthetics. Samples of the GM panels and seams taken from the affected area and tested in the laboratory indicated that the GM still met the project specifications and was not

adversely affected. This is not surprising given that the PVC GM underwent a relatively low level of strain as calculated above. In comparison, the strain at break of a PVC GM is on the order of 300% at normal temperature.

Resolution: The affected area was repaired by removing the cover system materials in this area, restabilizing and regrading the sludge, and reinstalling the cover system with new geosynthetic materials. The bulldozers used to spread the soil surface and protection layer had ground pressures less than that used previously. Additional grade control measures were implemented to ensure that no more than 0.75 m of soil was placed over the geosynthetics.

Lessons Learned for Future Projects: Based on the available information, the following lessons can be learned from this case history:

- PVC GMs are acceptable for construction over very compressible, low shear strength waste materials, since they can stretch (if the temperature is above 0° C).
- Cover systems with soil layers placed over compressible, low shear strength waste should use lightweight construction equipment and have good control of the thickness of soil placed over the waste
- When GCL is used over soft subgrade, seam overlaps should be wider than normal.

F-A.14 Impoundment Liner Construction

F-A.14.1 S-3

Problem Classification: impoundment liner construction/construction
Region of U.S.: southeast
Waste Type: MSW leachate
Reference: unpublished

Problem Summary: large wrinkles in HDPE GM primary liner at two leachate ponds

Problem Description: Two double-lined leachate ponds were constructed during the winter. The liner system for the ponds consists of the following components, from top to bottom:

- 1.5-mm thick HDPE GM primary liner;
- GN drainage layer;
- 1.5-mm thick GM secondary liner; and
- 0.15-m thick CCL.

The ponds have 3H:1V side slopes and are about 3 m deep. At the end of construction, the GM primary liner in the ponds was noticeably wrinkled. However, the ponds seemed acceptable to the CQA consultant. As temperatures increased before the ponds were put into service, the GM became more wrinkled. On the side slope,

wrinkles were oriented parallel to the slope crest. Wrinkles became more numerous and larger near the slope toe as they propagated down the slope during several months of temperature cycling. By the following summer, wrinkles were, on average, about 100 mm high. In both cells there were several large wrinkles, located near the slope toe, that folded over.

Resolution: The wrinkles in the GM will be cut out, and the GM will be seamed.

Lessons Learned for Future Projects: Based on the available information, the following lesson can be learned from this case history:

- During construction, excessive GM wrinkles and wrinkles that may fold over should be removed by waiting to backfill until the GM cools and contracts during the cooler nighttime and early morning hours, pulling the wrinkles out, or cutting the wrinkles out. The latter method is less desirable than the former methods because it requires intact GM to be cut, and it results in more GM seaming and subsequent testing.
- Enough slack should be left in GMs so they are essentially stress-free at their lowest expected temperatures.
- GM liners should be covered with a soil layer or insulated by other means as soon as practicable after installation, but not during the hottest part of the day if the GM is significantly wrinkled, to reduce GM wrinkling.

F-A.14.2 S-4

Problem Classification: impoundment liner construction/construction
Region of U.S.: southwest
Waste Type: HW
Reference: Bonaparte, R. and Gross, B.A., "*LDCRS Flow Rates from Double-Lined Landfills and Surface Impoundments*", EPA Risk Reduction Research Laboratory, Cincinnati, OH, EPA/600/SR-93/070, 1993, 65 p. (Impoundment C-2)

Problem Summary: leakage through holes in HDPE GM component of composite primary liner

Problem Description: A double-composite lined pond was placed into service in September 1986 and slowly filled with waste. The primary liner for the pond consists of a 2.5-mm thick HDPE GM over a 0.45-m thick CCL (specified maximum hydraulic conductivity of 1×10^{-9} m/s). The LDS drainage layer is a GN on the side slope and a gravel layer over a GN on the base. The GM component of the primary liner is protected on the side slope by a GM that is tack seamed to it. The primary liner is not protected by a soil protection layer.

After seventeen months of operation, when the liquid level in the pond had reached its highest level of about 3 m, monthly LDS flow rates increased from 0 to 250 lphd to 520 to 1,380 lphd. The pond liquid level was allowed to drop by evaporation, and the GM

protection layer was inspected for holes along the pond perimeter at an elevation corresponding to the maximum liquid level. One small hole was found in the GM protection layer and primary liner. The holes were repaired and the pond was slowly filled with liquid again. At thirty months after operation, again the liquid level in the pond again reached a level of about 3 m and monthly LDS flow rates increased from 0 to 50 lphd to 800 to 1,020 lphd.

In both cases where LDS flow rates increased when the pond liquid level was raised to 3 m, the increase occurred over a relatively short time period (less than one month). Presumably at least part of this flow was due to primary liner leakage. It is not clear how leakage entered the LDS in such a short time period given that the primary liner is a composite. It may be that the CCL underlying the GM on the side slope has become desiccated due to thermal effects. This desiccation would be worst in the upper portion of the side slope, where the primary liner is not insulated from ambient temperature cycling by the pond liquid. The hydraulic conductivity of a desiccated CCL may be several orders of magnitude greater than that of a protected CCL.

Resolution: When the protection layer was removed and the GM primary liner was inspected at an elevation corresponding to the maximum liquid level, a GM patch previously seamed over an old tear was found to have failed at the seam. A new patch was seamed over the tear, and the pond was slowly filled to a liquid level of about 3 m. Monthly LDS flow rates remained relatively low, in the range of 0 to 130 lphd.

Lessons Learned for Future Projects: Based on the available information, the following lessons can be learned from this case history:

- Holes in GM liners installed with CQA should be anticipated. If there is a head of leachate over a hole, primary liner leakage can occur.
- Primary liner leakage can occur in impoundments with GM/CCL primary liners that are not insulated from the environment with a soil protection layer or other material.
- It can be difficult to locate primary liner holes in operating impoundments without taking the pond out of service and inspecting the primary liner components.

F-A.14.3 S-5

Problem Classification: impoundment liner construction/construction
Region of U.S.: northeast
Waste Type: HW
Reference: Bonaparte, R. and Gross, B.A., "*LDCRS Flow Rates from Double-Lined Landfills and Surface Impoundments*", EPA Risk Reduction Research Laboratory, Cincinnati, OH, EPA/600/SR-93/070, 1993, 65 p. (Impoundments H-2 and H-3)

Problem Summary: leakage through holes in HDPE GM primary liners at two ponds

Problem Description: Two double-lined shallow ponds (H-2 and H-3) became operable in November 1988. The ponds have a 2-mm thick HDPE GM primary liner. The LDS drainage layer is a GN on the side slopes and sand on the base. The ponds are designed to have a maximum liquid level of 1.4 m. Prior to operation, leak location surveys were performed in both ponds, and identified primary liner holes were repaired.

Chemical analyses of LDS flows from ponds H-2 and H-3 indicated that primary liner leakage was occurring by seven and one months, respectively, after start of operation. LDS flow rates from the ponds also increased with increasing pond liquid level. The average LDS flow rates from the ponds H-2 and H-3 from seven to 25 months of operation were 310 and 5,150 lphd, respectively. It is unclear why the LDS flow rates from pond H-3 are so high, given that a leak location survey was performed prior to pond operation. Since primary liner leakage was evident shortly after filling started, a primary liner hole was probably located on the base or near the slope toe of this pond.

Resolution: After 25 months of operation, GM primary liner holes were located in the ponds and repaired. No information is available on the size or location of the holes. The average LDS flow rates from the ponds H-2 and H-3 from 26 to 31 months of operation were 400 and 440 lphd, respectively. For pond H-2, the LDS flow rates increased after the repairs when the liquid level in the pond was increased.

Lessons Learned for Future Projects: Based on the available information, the following lessons can be learned from this case history:

- Holes in GM liners should be anticipated, even in liners installed with CQA. If there is a head of leachate over a liner hole, leakage occurs.
- It can be difficult to locate primary liner holes in operating impoundments without taking the pond out of service and inspecting the primary liner.

F-A.15 Impoundment Liner Degradation

F-A.15.1 S-1

Problem Classification: impoundment liner degradation/construction
Region of U.S.: northcentral
Waste Type: process water, ash, and other
Reference: Peggs, I.D., Winfree, J.P., Giroud, J.P., "A Shattered Geomembrane Liner Case History: Investigation and Remediation", *Proceedings of Geosynthetics '91*, Atlanta, 1991, Vol. 2, pp. 495-505.

Problem Summary: slow crack growth stress cracks and shattering cracks in exposed HDPE GM liner at five ponds

Problem Description: Peggs et al. (1991) described the shattering of HDPE GM liners in five of thirteen ponds at a coal-fired power plant facility. These liners were exposed

and, therefore, subject to significant thermally induced tensile stresses under the wide range of ambient temperatures at the site (i.e., -30 to 40°C). At temperatures near freezing, the GM on the side slope was taut. By four years after installation, the five pond liners exhibited relatively short (i.e., 20 mm) slow crack growth (SCG) stress cracks in and adjacent to some seams. There were no cracks below water level. All of the seams had been constructed by lapping the panels and applying a bead of HDPE extrudate (extrusion flat seam). The stress cracks generally occurred in the lower GM.

During the winter, record low temperatures appeared to precipitate the cracking of some seams from the side slope crest to toe, a length of about 22 m. The maximum crack opening occurred at mid-slope and was about 0.2 m. These long cracks were surrounded by branching rapid crack propagation (RCP) shattering cracks. The shattering cracks propagated into the GM panels at an angle to the long crack (upward in the top half of the slope and downward in the bottom half of the slope). Shattering cracks also extended from some of the short stress cracks into the GM panels, fracturing the GM. The mechanics of shattering crack development have been described by Giroud (1994a). The liner in the pond containing the fewest visible stress cracks had been installed with compensation panels to allow for liner contraction at low temperatures; designed compensation panels had not been installed in the other pond liners. There was also some indication that the most seriously damaged liners had been installed at high ambient temperatures and would, therefore, require the largest amount of compensation in order to be stress-free at the lowest operating temperature.

Subsequent laboratory studies conducted by Peggs et al. (1991), which included examination of microtome sections and measurement of mechanical and physical properties, found that many stress cracks were initiated where the original seam had been repaired with an extruded fillet bead. Other stress cracks were initiated where there was evidence of overheating during seaming. A few stress cracks initiated where there was no visible cause for initiation. Peggs et al. (1991) also showed that the shattering cracks were all initiated at stress cracks located along seams. They concluded that if stress cracks are not present in HDPE GM, shattering cracks will not occur. Peggs et al. (1991) hypothesized that the observed stress cracks were caused primarily by heating of the HDPE during seaming. However, Giroud (1994b) later concluded that normal heating during seaming does not seem to make HDPE GMs more susceptible to stress cracking. Rather, HDPE GM stress cracks are primarily associated with stress concentrations caused by seams. The shattering cracks that occurred in the pond liners can be explained by the conjunction of the following:

- the HDPE resin used in these GMs did not have a low stress-cracking susceptibility;
- tensile stresses caused by thermal contraction;
- stress concentrations caused by the seams;
- decreased allowable yield strain at the low temperatures at which GM shattering occurred; and
- increased crystallinity of the HDPE next to the seam.

Resolution: Seams and panels were visually inspected for cracks. Panels and seams with shattering cracks were replaced with new GM containing an adequate amount of slackness calculated using the temperature of the GM at the time of the repair. The new panels were installed during the coolest time of the day so the minimum amount of slackness would be required. In addition, every third seam was cut from the anchor trench to the toe of slope and the GM was allowed to relax. Compensation panels, typically 1 m wide, were installed at each cut seam. Stress cracks in seams were repaired using a wide (i.e., 100 mm) bead extrusion technique developed specifically for this purpose.

Lessons Learned for Future Projects: Based on the available information, the following lessons can be learned from this case history:

- Resin used to manufacture HDPE GM should be resistant to stress cracking. This is currently evaluated using the notched constant tensile load test (ASTM D 5397). This test was not performed for the GM in the case history described above.
- HDPE GMs should be installed so that they are essentially stress-free at their lowest expected temperatures. This is consistent with EPA guidance (Daniel and Koerner, 1993).
- For HDPE GMs, fusion seams are preferred over extrusion seams because fusion seams have higher seam integrity and lower stress concentrations at seams (Giroud, 1994b). Extrusion fillet seams are preferred over extrusion flat seams because fillet seams have lower stress concentrations at seams. In the case history described above, stress cracking may have been less severe if fusion seams, rather than extrusion flat seams, had been used.
- In general, holes in HDPE GM seams should not be repaired by seaming over the hole. This reheating of seams can embrittle the HDPE at the repair and make it more susceptible to stress cracking.
- In general, GMs should be covered with a thermal insulation layers at very low temperatures (e.g., -20°C for HDPE GMs) since GM strain at break decreases with decreasing temperature.

F-A.16 Impoundment Liner System Stability

F-A.16.1 S-2

Problem Classification: impoundment liner system stability/design
Region of U.S.: unknown
Waste Type: HW
Reference: Paulson, J.N., "Veneer Stability Case Histories: Design Interactions Between Manufacturer/Consultant/Owner", *Proceedings of the 7th GRI Seminar Geosynthetics Liner Systems: Innovations, Concerns, and Designs*, Geosynthetic Research Institute, Philadelphia, PA, 1993, pp. 235-241.

Problem Summary: sliding along polypropylene needlepunched nonwoven GT/HDPE GM interface during waste placement

Problem Description: Paulson (1993) described the slope stability failure of components of a sludge impoundment liner system that occurred during sludge placement. The double-liner system consists of the following components, from top to bottom:

- 530 g/m^2 polypropylene needlepunched nonwoven GT cushion layer;
- HDPE GM primary liner;
- GN LDS drainage layer;
- GM secondary liner; and
- CCL.

The 2H:1V side slopes are about 10 m high. Sludge was placed in the impoundment by dumping it on the GT cushion at the slope crest and allowing it to flow down the GT to the slope toe. On several occasions when the sludge adhered to the GT, a low-ground pressure bulldozer was used to push the sludge downslope. This method of sludge placement caused tension to develop in the GT. Eventually, the GT progressively tore at the slope crest and slid over the GM to the slope toe.

Paulson (1993) does not indicate if slope stability analyses or interface direct shear testing were performed as part of the lining system design. An infinite slope analysis was conducted by the authors of this appendix. In this analysis, the secant friction angle for the polypropylene GT/HDPE GM interface was assumed to be 10°, which is within the range of friction angles reported for this interface in the technical literature. The slope stability factor of safety thus calculated is 0.35 with no seepage pressures. Based on this factor of safety, the GT would be in tension if sludge were placed on it. Paulson (1993) does not indicate whether the GT was designed to be in tension.

Resolution: The damaged GT was replaced. Additionally, a thin GM slipsheet was placed over the GT in the sludge dumping area to facilitate the sliding of sludge down the slope.

Lessons Learned for Future Projects: Based on the available information, the following lessons can be learned from this case history:

- Liner system slopes should always be evaluated using rigorous slope stability analysis methods that consider the actual shear strengths of the liner system materials and the method of waste placement. Both of these considerations probably contributed to the liner system failure described above.
- Waste should generally be placed over geosynthetics from the toe of slope upward to avoid tensioning the geosynthetics. Methods of waste placement that are not toe to top must be pre-approved by the engineer who analyzed the stability.

F-A.17 References

Bass, J.M., "*Avoiding Failure of Leachate Collection and Cap Drainage Layers*", EPA/600/2-86/058, EPA Hazardous Waste Engineering Research Laboratory, Cincinnati, Ohio, 1986, 142 p.

Bonaparte, R., "Long-Term Performance of Landfills"' *Proceedings of the ASCE Specialty Conference Geoenvironment 2000*, ASCE Geotechnical Special Publication No. 46, 1995, Vol. 1, pp. 415-553.

Bonaparte, R. and Gross, B.A., "*LDCRS Flow Rate from Double-Lined Landfills and Surface Impoundments*", EPA/600/SR-93/070, EPA Risk Reduction Research Laboratory, Cincinnati, OH, 1993, 65 p.

Daniel and Koerner "*Technical Guidance Document: Quality Assurance and Quality Control for Waste Containment Facilities*", EPA/600/R-93/182, EPA Risk Reduction Research Laboratory, Cincinnati, OH, 1993, 305 p.

Environmental Protection Agency, "*Seminar Publication: Design, Operation, and Closure of Municipal Solid Waste Landfills*", EPA/625/R-94/008, EPA Center for Environmental Research Information, Cincinnati, Ohio, 1994, 86 p.

Giroud, J.P., "Impermeability: The Myth and a Rational Approach", *Proceedings of International Conference on Geomembranes*, Denver, Colorado, Vol. 1, 1984, pp. 157-162.

Giroud, J.P., "Lessons Learned From Studying the Performance of Geosynthetics", *Proceeding of Geotextiles-Geomembranes Rencontres 93*, Vol. 1, Joue-les-Tours, France, Sep 1993, pp. 15-31.

Giroud, J.P., "The Mechanics of GM Stress Cracking", *Computer Methods and Advances in Geomechanics*, Siriwardane, H.J. and Zaman, M.M. (editors), Balkema, Proceedings of the Eighth International Conference on Computer Methods and Advances in Geomechanics, Morgantown, West Virginia, USA, 1994a, Vol. 1, pp. 177-188.

Giroud, J.P., "Quantification of Geosynthetics Behavior", *Proceeding of the Fifth International Conference on Geotextiles, Geomembranes, and Related Products*, Singapore, 1994b, Vol. 4, pp. 1249-1273.

Giroud, J.P., "Granular Filters and Geotextile Filters", *Proceedings of Geofilters '96*, Lafleur, J., and Rollin, A.L., Editors, Montreal, 1996, pp. 565-690.

Giroud, J.P. and Houlihan, M.F., "Design of Leachate Collection Layers", *Proceedings of Fifth International Landfill Symposium*, Sardinia, Italy, Vol. 2, 1995, pp. 613-640.

Giroud, J.P., Bachus, R.C., and Bonaparte, R., "Influence of Water Flow on the Stability of Geosynthetic-Soil Layered Systems on Slopes", *Geosynthetics International*, IFAI, Vol. 2, No. 6, 1995a, pp. 1149-1180.

Giroud, J.P., Tisseau, B., Soderman, K.L., and Beech, J.F., "Analysis of Strain Concentrations Next to Geomembrane Seams", *Geosynthetics International*, IFAI, Vol. 2, No. 6, 1995b, pp. 1049-1097.

Soong, T.Y. and Koerner, R.M., "*The Design of Drainage Systems Over Geosynthetically Lined Slopes*", GRI Report #19, Geosynthetic Research Institute, Philadelphia, Pennsylvania, 1997, 88 p.

Appendix G
Long-Term Landfill Management

by

Rudolph Bonaparte, Ph.D., P.E.
GeoSyntec Consultants
Atlanta, GA 30342

David E. Daniel, Ph.D., P.E.
University of Illinois
Urbana, IL 61801

Robert M. Koerner, Ph.D., P.E.
Drexel University
Philadelphia, PA 19104

performed under

EPA Cooperative Agreement Number
CR-821448-01-0

Project Officer

Mr. David A. Carson
United States Environmental Protection Agency
Office of Research and Development
National Risk Management Research Laboratory
Cincinnati, OH 45268

DISCLAIMER

The ideas presented in this appendix are the authors' and do not represent EPA policy. EPA considers some of these approaches developmental. If the Agency initiates any changes with respect to post-closure, it will be noticed in the Federal Register and only after review and discussions with the stakeholders involved.

Appendix G
Long-Term Landfill Management

G-1 Introduction

The performance data for operating landfills presented in this research report demonstrate that landfills can be designed, constructed, and operated/maintained to achieve very high levels of leachate and landfill gas containment and collection. The report has also demonstrated that design, construction, and operation/maintenance issues and problems persist at many landfills. In Chapter 6, the authors attempted to provide guidance to design engineers on how to avoid the most significant issues and problems that may typically arise. Information on the anticipated service lives of the various engineered components of a landfill waste containment system was also given.

The ultimate degradation of any individual waste containment system component of a landfill after the completion of that component's useful service life may or may not lead to a release of leachate or gas and contamination of groundwater. Furthermore, a release may, or may not, result in a significant environmental impact. In evaluating the consequences of ultimate degradation, the design engineer must consider a wide range of factors including: the climatological and hydrogeologic setting; the composition, age, and level of degradation of the waste; the potential for leachate and gas generation after the component has completed its service life; the potential to maintain, rehabilitate, or install other systems to achieve leachate and gas containment; and collection, cost, and social and institutional factors. These various factors should be considered within an overall decision-making framework, herein referred to as a long-term landfill management strategy.

G-2 Strategies for Long-Term Landfill Management

Seven strategies originally developed by Bonaparte (1995) for long-term landfill management are summarized in Table G-1 and presented below. In this report, the discussions of the strategies are focused towards municipal solid waste (MSW) landfills. Each strategy has implications for long-term landfill maintenance and monitoring (with advantages and disadvantages). It is noted that variations on the strategies described in this report are possible and alternative strategies could also be developed.

Strategy 1 - Standard Landfill with Perpetual Post-Closure Period: This approach embodies the original United States Environmental Protection Agency (EPA) "liquids management strategy". With this approach, waste is disposed of at its' "as received" moisture content, and efforts are made to minimize the ingress of moisture into the landfill. This type of landfill does not receive supplemental moisture through, for example, leachate recirculation or water addition. Liquid/gas containment and collection during the active life of this type of landfill are achieved through operation of the liner system and liquid and gas removal systems. Ideally, the leachate collection and removal system (LCRS) should be

Table G-1. Summary of Strategies for Long-Term Landfill Management (from Bonaparte, 1995).

Strategy	Landfill Classification	Moisture Conditions	Requirements for Long-Term Protection of Groundwater and Air	Advantages	Disadvantages
1	Standard Landfill – Perpetual Post-Closure Period	No supplemental moisture addition	Containment and collection systems must be maintained for as long as leachate and gas are generated and through the post-closure period. Final cover system must be maintained in perpetuity.	• This strategy can prevent significant gas and leachate migration in perpetuity, assuming adequate maintenance • This strategy complies with regulations and is consistent with EPA's liquids management strategy • Capital costs are lower than for other strategies • This strategy may be applied to virtually all sites, including sensitive sites	• Final cover system must be maintained, and monitoring must be performed in perpetuity • This strategy results in perpetual maintenance and monitoring costs • Waste retains a latent potential to generate leachate and gas and release pollutants
2	Standard Landfill – Limited Post-Closure Period	No supplemental moisture addition	Containment and collection systems must be maintained for as long as leachate and gas are generated and through the post-closure period. Impacts of any leachate or gas generated after the post-closure period must be within acceptable limits.	• This strategy has the same advantages as Strategy 1, except that, due to limited post-closure period, this strategy may not be acceptable for sensitive sites	• Limited gas or leachate migration could occur in the long term, after the post-closure period • The design must consider the potential for long-term migration, and it must be established that potential migration rates are within acceptable limits
3	Standard Landfill – Clean Closure	No supplemental moisture addition	Containment and collection systems must be maintained until clean closure.	• Clean closure eliminates contaminant source • Concerns about long-term performance of landfill waste containment system are eliminated • Waste is used as a resource	• Clean closure is not presently cost effective for most projects • Environmental impacts of clean closure operations must be addressed • Waste residuals must be managed
4	Recirculation Landfill – Perpetual Post-Closure Period	Supplemental moisture is added to the landfill	Containment and collection systems must be maintained for as long as leachate and gas are generated and through the post-closure period. Final cover must be maintained in perpetuity. An enhanced liner system may be required to gain regulatory approval. Recirculation hardware is needed.	• This strategy has the same advantages as Strategy 1, except that the capital costs are higher • Recirculation improves gas generation • Biostabilized waste has a lower latent potential to pollute groundwater and air than Strategies 1 and 2 • Post-closure maintenance costs are lower than dry landfill strategies	• This strategy has the same disadvantages as Strategy 1, except that the waste retains a lower latent potential to pollute groundwater and air • Recirculation hardware and operations result in additional capital and operations costs; if required, an enhanced liner system will results in additional capital costs • Design and operational experience with recirculation is currently limited
5	Recirculation Landfill – Limited Post-Closure Period	Supplemental moisture is added to the landfill	Containment and collection systems must be maintained for as long as leachate and gas are generated, and through the post-closure period. An enhanced liner system may be required to gain regulatory approval. Recirculation hardware is needed. Impacts of any leachate or gas generated after the post-closure period must be within acceptable limits.	• This strategy combines the advantages of Strategies 2 and 4 • This strategy may be suitable for the great majority of sites, including sensitive sites	• This strategy has the same disadvantages as Strategy 4, except that perpetual care of the final cover system is not required • The design must consider the potential for long-term migration, and it must be established that potential migration rates are within acceptable limits

Table G-1. Summary of Strategies for Long-Term Landfill Management (from Bonaparte, 1995) (cont.).

Strategy	Landfill Classification	Moisture Conditions	Requirements for Long-Term Protection of Groundwater and Air	Advantages	Disadvantages
6	Recirculation Landfill – Clean Closure	Supplemental moisture is added to the landfill	Containment and collection systems must be maintained until clean closure. An enhanced liner system may be required to meet regulations. Recirculation hardware is needed.	• This strategy combines the advantages of Strategies 3 and 4, except that capital costs are higher • May be able to reuse liner system after clean close a cell	• This strategy has the same disadvantages of Strategies 3 and 4, except that long-term maintenance and monitoring is not required
7	Inward-Gradient Landfill	This strategy may be developed with or without supplemental moisture addition	Inward gradient design must not allow leachate diffusion through liner system. Depending upon the design strategy, inward gradient must be maintained in perpetuity, for a limited post-closure period, or until clean closure.	• An inward gradient provides active (not passive control of contaminant advection and diffusion • An inward gradient approach can be incorporated into the framework of Strategies 1 to 6	• This strategy is not compatible with current U.S. regulations • Inward gradient will not exist in unsaturated zone above water table, unless an engineered hydraulic control system (e.g., a double-liner system) is constructed • Large liquid volumes must likely be collected from LCRS and treated

designed to allow rapid removal of leachate generated by the landfill. In this way, the potential for significant advective or diffusive transport through the liner system can essentially be eliminated. Both transport mechanisms require time periods on the order of years for leachate breakthrough of modern geomembrane/compacted clay liner (GM/CCL) composite liners. Rapid leachate removal can be achieved by having a highly permeable, adequately sloped LCRS that precludes both a leachate head buildup on the liner and a sustained leachate head on the liner.

After closure of such a landfill, the final cover system (which will typically contain a GM to satisfy present-day federal regulations) will essentially eliminate infiltration into the landfilled waste. Consequently, over time, leachate and gas generation will progressively decrease and eventually cease. A nominal stabilization of waste (i.e., partial conversion of the decomposable organic constituents and leaching or fixation of hazardous waste constituents) will probably occur by the end of the post-closure period, although this process will be incomplete due to a deficit of moisture in the landfill (Tchobanoglous et al., 1993). The waste will retain a latent capacity to generate leachate and gas and release pollutants should moisture be reintroduced into the landfill in the future. The goal with this strategy is to prevent a reoccurrence of leachate or gas generation in the future. This goal can be achieved through perpetual maintenance of the final cover system. In a modern landfill with no supplemental moisture addition, leachate and gas generation will eventually cease and, thus, the need for ongoing maintenance of systems other than the final cover system will, in the long term, not be necessary.

Strategy 2 - Standard Landfill with Limited Post-Closure Period: This strategy is the same as Strategy 1, except it is assumed that the post-closure maintenance period will be of limited duration. After the post-closure period, requirements for ongoing maintenance and monitoring are suspended. This approach is consistent with current regulations that prescribe a minimum post-closure period of 30 years. For this strategy to be effective in the long term, events that occur after the end of the post-closure period must not result in unacceptable groundwater or air pollution. These events may include degradation of the final cover system, renewed leachate and gas generation, accumulation of leachate and gas in the unit, and, eventually, migration of these waste by-products from the unit. An assessment of the eventual impacts requires evaluation of: (i) the potential for long-term degradation of the final cover system; (ii) water infiltration through the final cover system in its long-term condition; (iii) leachate and gas generation resulting from the water infiltration; (iv) the potential for long-term degradation of the liner system; (v) gas migration through the final cover system in its' long-term condition and leachate and gas migration through the liner system in its' long-term condition; and (vi) impacts to groundwater resulting from the leachate and gas migration and impacts to air resulting from gas migration. Evaluations of the type just

described have been performed by Rowe and Fraser (1993a,b) considering the potential for groundwater contamination for several hypothetical landfill scenarios.

Potential groundwater impacts associated with this type of strategy depend on a variety of factors. Any impacts may be acceptable if long-term contaminant migration rates are low and/or if the landfill is located in a favorable hydrogeologic setting. Conversely, if anticipated contaminant migration rates are high and the landfill is in a vulnerable hydrogeologic setting, the long-term consequences of this strategy may not be acceptable. In the future, when regulators and design engineers assess the need to extend the post-closure period of a particular landfill beyond the 30-year regulatory minimum, they will need to perform an assessment of the type described in the preceding paragraph. The authors recommend that, for new landfills, this assessment process be included at the initial design stage, within the framework of a long-term management strategy.

Strategy 3 - Standard Landfill with Clean Closure: This strategy is one that has post-closure care until, at some future date, the landfill will undergo clean closure. Clean closure would involve mining the landfilled waste and subjecting it to one or more resource recovery operations, possibly including materials recovery and waste-to-energy. Landfill mining has been tried at a few locations on a small scale (Nutting, 1994). However, regulatory, economic, and technology constraints make broad-based application of this strategy infeasible at the present time. Future technology advancements and changing markets may change this situation to a degree where resource recovery and clean closure become viable. The advantages of this strategy include removal of the contaminant source (i.e., clean closure) and beneficial use of waste materials. Since the landfill is clean closed, concerns about the long-term performance of landfill waste containment system components are also eliminated. The disadvantages of this strategy include cost, potential environmental impacts associated with resource recovery operations, and the need to redispose of waste residuals.

Strategy 4 - Recirculation Landfill with Perpetual Post-Closure Period: The fourth strategy is similar to Strategy 1, except that, instead of avoiding supplemental moisture addition, leachate recirculation (or another form of moisture addition) is implemented for purposes of enhancing gas generation and waste stabilization. With this technique, the landfill is viewed as an anaerobic bioreactor that both accelerates the "biostabilization" of waste and the treatment of the recirculated leachate (Pohland and Harper, 1986; Pohland et al. 1992). Leachate recirculation has been a technique under development for twenty years. Reinhart (1993) reports that full-scale recirculation landfills are presently in operation or under construction in twelve states, and that state regulations allow for the use of recirculation in all but

seven states. Information on leachate recirculation and landfill bioreactor design has been summarized by EPA (EPA, 1995).

The advantages of leachate recirculation include enhanced/accelerated gas production and waste stabilization and removal or biofixation of leachable constituents. Pohland and Harper (1986) have suggested that leachate recirculation reduces the time period for landfill stabilization from several decades to a few years. This technique involves higher initial capital costs (e.g., recirculation hardware and, possibly, an enhanced liner system beneath the landfill), but cost advantages are gained by having less need for post-closure maintenance. This technique also results in a waste mass having a much lower "latent" threat of pollution than the waste mass in a dry landfill. While this strategy requires perpetual care, it is reasonable to assume that the necessary level of care will be less than with Strategy 1. A current disadvantage of all of the recirculation strategies is the limited long-term and large-scale field experience with this technique. This situation will improve in the coming years.

Strategy 5 - Recirculation Landfill with Limited Post-Closure Period: This strategy is similar to the preceding one except that the landfill has a limited post-closure care period (e.g., 30 years). The same factors that affect the long-term effectiveness of Strategy 2 apply to this strategy. However, this strategy has an advantage in that recirculation results in more complete conversion of decomposable organic materials than occurs in a standard landfill, as well as less potential for the leaching of hazardous constituents should renewed infiltration occur after the end of the post-closure period. It is envisioned that with leachate recirculation and adequate design of the landfill liner and final cover systems, Strategy 5 will be acceptable in most hydrogeologic settings and it will not be necessary to implement Strategy 4 (i.e., perpetual post-closure care).

Strategy 6 - Recirculation Landfill with Clean Closure: This strategy is similar to Strategies 4 and 5, except that after the waste has undergone biostabilization, it is removed from the landfill and processed as with Strategy 3. Processing may involve recovery of any recyclable materials and incineration or land application of stabilized waste residuals. The main advantages this option are the same as with Strategy 4, plus the benefits of resource recovery and clean closure of a site. Disadvantages include higher capital costs and any potential health risks associated with clean closure.

One intriguing aspect of this strategy is that after the waste is mined, the liner system can be inspected and remediated if necessary and the site re-permitted to accept new waste materials. Even further, by proper sequencing of a large site, a perpetual placement/mining/replacement scheme can be envisioned, see Figure G-1. Some countries with critical shortage of space are discussing this concept.

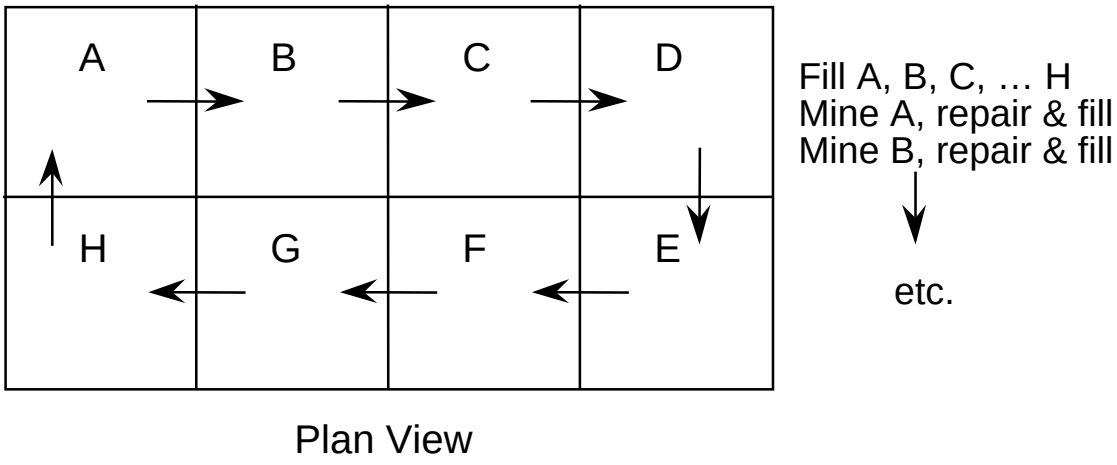

Figure G-1. Sequential mining of individual waste cells to provide for a perpetual landfill of a given footprint area.

Strategy 7 - Inward-Gradient Landfill: The seventh strategy can be similar to any of the preceding six, except that an inward hydraulic gradient is included across all, or a portion of, the liner system. Inward gradients can be maintained by creating a hydraulic pressure in the leak detection system (LDS) of a double-liner system (Rowe and Fraser, 1993a,b) or triple-liner system (Giroud, 1984b), or by installing a single-liner system in an excavation below the groundwater table. This latter type of facility was used in the early 1980s at landfills in the northcentral U.S., prior to the time when U.S. regulations mandated the use of GMs. Inward gradient landfills have also been termed "zone of saturation landfills" (Oakley, 1987).

The inward gradient design concept may be used with CCLs, but the concept is not directly applicable to GM/CCL composite liners (which is the typical configuration used in modern U.S. landfills). Inward gradient landfills appear to be of growing interest in Canada, but the regulatory framework in the U.S. precludes their use in this country in most situations. Inward gradient facilities can be designed such that inward flow velocities through the liner exceed outward chemical diffusion rates (Rowe and Fraser, 1993a, b). However, the goal of preventing significant chemical diffusion can also be achieved without an inward gradient by using a composite liner and by designing the LCRS above the composite liner to rapidly convey leachate to a sump, thereby preventing the buildup of leachate head on the liner and a sustained leachate head on the liner. It would be prudent to consider a GM/CCL/GM three-component barrier system for a liner system with an inward gradient design.

The main advantage of this strategy is that it provides an inward gradient that prevents leakage or diffusion out of the unit. It may also provide a setting in which long-term maintenance of final cover systems, liquid collection systems, etc., is unnecessary. Disadvantages include the difficulty in gaining regulatory acceptance for this type of unit, the need to use an engineered (rather than natural) hydraulic control system at many sites, uncertainly associated with long-term groundwater levels (at sites with natural hydraulic control systems), and the need to manage/treat the large volume of liquid likely to require removal from the LCRS.

Each management strategy described above has minimum requirements for providing short- and long-term protection of groundwater quality. These minimum requirements are summarized in Table G-1. The strategies all require that for at least some period of time, engineered systems be used for the containment and collection of landfill leachate and gas. The strategies vary, however, in the required service lives of the various systems and in detailed design performance criteria (e.g., contaminant transport rates, breakthrough times, mass fluxes, etc.).

G-3 Incorporating Management Strategies into Design

The authors believe that insufficient attention is given to defining a long-term management strategy during the permitting and design stages of most new landfills. Both regulators and designers typically focus their efforts on achieving regulatory compliance, developing an adequate detailed design, and developing specifications and a construction quality assurance (CQA) plan to achieve satisfactory initial construction. Rarely do the project participants raise questions such as *"what is our strategy for long-term management of this facility, what are the design, construction, operating, monitoring, and maintenance actions required to implement the strategy, and what funding should be set aside at the beginning of the project to enable implementation?"* These questions should receive more attention during the landfill design and permitting process. Each new facility should have a well-defined management strategy, a well-defined set of design and performance criteria that will achieve the strategy objectives, and financial assurances consistent with the strategy. Figure G-2 provides a flow chart, developed by Bonaparte (1995), that indicates the manner that long-term landfill management planning can be incorporated into the landfill permitting and design process.

G-4 Landfill Maintenance, Monitoring, and Response Actions

Long-term maintenance is also a critical element of many of the landfill management strategies described previously. Thus, any plan for new landfill development should contain the following elements: (i) a program for long-term maintenance that is consistent with the requirements of the long-term management strategy (the maintenance program will need to account for each waste containment system

component that contributes to achieving the objectives of the landfill management strategy); (ii) financial funding mechanisms for long-term maintenance consistent with the requirements of the strategy; and (iii) provisions for quality control and quality assurance of required maintenance operations.

The monitoring programs for a landfill should also be developed to be consistent with the long-term management strategy for that facility. For example, for Strategy 1, a program should be established to monitor the final cover system on a permanent basis. As another example, if a strategy assumes that leachate generation will cease after a certain period of time, monitoring should be used to confirm this aspect of system performance. As a final example, if the strategy involves a recirculation landfill designed to obtain a high degree of biostabilization of the waste mass, leachate and gas quantities and compositions should be monitored during the recirculation process to confirm that this objective is being achieved. Monitoring results should be compared to design-phase analysis and modeling information to confirm that the behavior of the facility is as predicted.

Groundwater monitoring wells will continue to be a necessary element of landfill monitoring programs, if for no other reasons than to meet the requirements of existing regulations and the customs of most practicing professionals. Depending on the management strategy, other types of monitoring should also be considered, including: (i) vadose zone moisture, chemistry or pressures, for the early detection of a release of either leachate or gas; (ii) LCRS and LDS flow rates and liquid quality; (iii) liquid heads in LCRS sumps; (iv) LCRS and LDS hydraulic conductivities, which may be assessed by injecting a tracer through a test pipe and monitoring the travel time to a detection point (i.e., sump); (v) liner or final cover material integrity, using test coupons or other means; and (vi) gas extraction system flow, pressure, and temperature. Finally, monitoring programs should also describe response actions, or at least steps to be taken to establish appropriate response actions, should monitoring results reveal a problem. As indicated in Figure G-2, potential response actions should be evaluated during the initial design phase of a landfill project. Design details should be developed to enable their implementation should the need for response actions ever arise.

G-5 Conclusion

Landfill containment and control systems must perform satisfactorily during the entire period of significant leachate and gas generation. This period may be different for different types of facilities and for facilities in different climatic and hydrogeologic settings. In addition, standard landfills will retain a “latent” capacity to generate leachate or gas for long periods of time.

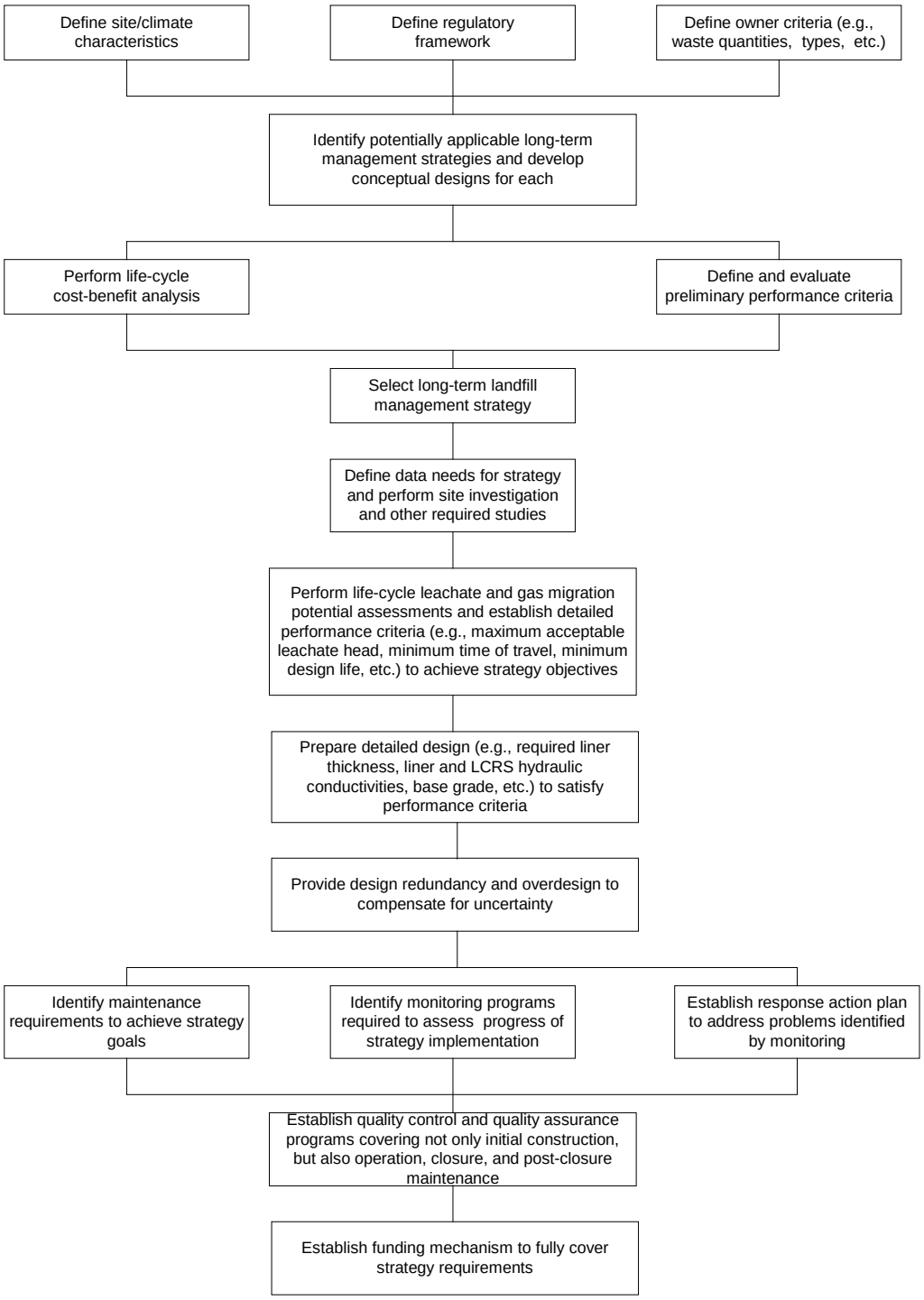

Figure G-2. Flow chart for incorporating long-term management strategy into landfill permitting and design process (from Bonaparte, 1995).

Seven strategies for addressing long-term landfill management were described in this appendix. These strategies provide a framework for assessing the time periods for leachate and gas generation, and the resulting minimum requirements for long-term groundwater quality protection. Conservative designs, developed within the framework of an appropriate long-term management strategy, can prevent both short- and long-term leachate and gas impacts to groundwater. Achievement of these objectives is also dependent on the use of appropriate quality control and assurance of not only landfill construction, but also landfill operations, closure, and post-closure maintenance. It is recommended that new landfills be designed and permitted within the framework of a long-term management strategy. The flow chart presented in this appendix (Figure G-2) can be used for this purpose.

G-6 References

Bonaparte, R. (1995), "Long-Term Performance of Landfills," *Proceedings of the ASCE Specialty Conference Geoenvironment 2000,* ASCE Geotechnical Special Publication No. 46, Y.B. Acar and D.E. Daniel, eds., Vol. 1, pp. 514-553.

EPA (1995), "*Seminar Publication, Landfill Bioreactor Design and Operation*," EPA/600/R-95/146, Office of Research and Development, Washington, DC, 230 p.

Giroud, J. P. (1984b), "Impermeability: The Myth and a Rational Approach," *Proceedings International Conference on Geomembranes,* Vol. 1, Denver, pp. 157-162.

Nutting, L. M. (1993), "The Economics of Landfill Mining and Reclamation," *Proceedings Waste Tech '93,* National Solid Waste Management Association, Marina Del Ray, 17 p.

Oakley, R. E. (1987), "Design and Performance of Earth-Lined Containment Systems," *Geotechnical Practice for Waste Disposal '87,* Geotechnical Special Publication No. 13, R. D. Woods, ed., pp. 117-136.

Pohland, F. G., Cross, W. H., Gould, J. P. and Reinhart, D. R. (1992), "*Behavior and Assimilation of Organic and Inorganic Priority Pollutants Codisposed with Municipal Waste*," Report for cooperative agreement CR-812158, EPA Risk Reduction Research Laboratory, Cincinnati, 197 p.

Pohland, F. G. and Harper, S. R. (1986), "*Critical Review and Summary of Leachate and Gas Production from Landfills*," EPA/600/2-87/044, EPA Hazardous Waste Engineering Research Laboratory, Cincinnati, 186 p.

Reinhart, D. R. (1993), "Wet vs. Dry Landfilling: Does it Really Make a Difference," *Proceedings Waste Tech '93,* National Solid Waste Management Association, Marina Del Ray, 9 p.

Rowe, R. K. and Fraser, M. J. (1993a), "Long-Term Behavior of Engineered Barrier Systems," *Proceedings, IV International Landfill Symposium,* Sardinia, pp. 397-406.

Rowe, R. K. and Fraser, M. J. (1993b), "Service Life of Barrier Systems in the Assessment of Contaminant Impact," *Geotechnical Research Center Report,* GEOT-5-93, The University of Western Ontario, 8 p.
Tchobanoglous, G., Theisen, H. and Vigil, S. (1993), "*Integrated Solid Waste Management*," McGraw-Hill, Inc., New York, 978 p.